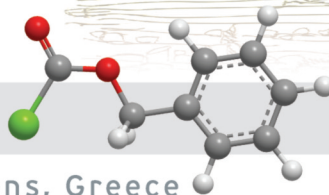




32EPS



2-7 September 2012, Athens, Greece

PEPTIDES 2012

Proceedings of the
Thirty-Second European Peptide Symposium

Edited by:
George Kokotos
Violetta Constantinou-Kokotou
John Matsoukas



THE EUROPEAN
PEPTIDE SOCIETY



PEPTIDES 2012

Proceedings of the
Thirty-Second European Peptide Symposium
September 2-7, 2012 – Athens, Greece

Edited by

George Kokotos

Violetta Constantinou-Kokotou

John Matsoukas



PEPTIDES 2012

Proceedings of the
Thirty-Second European Peptide Symposium
September 2-7, 2012 – Athens, Greece

Edited by

George Kokotos

*Department of Chemistry
University of Athens, Greece
gkokotos@chem.uoa.gr*

Violetta Constantinou-Kokotou

*Department of Sciences
Agricultural University of Athens, Greece
vikon@aua.gr*

John Matsoukas

*Department of Chemistry
University of Patras, Greece
imats@chemistry.upatras.gr*

Editorial Assistant

Victoria Magrioti

*Department of Chemistry
University of Athens, Greece
vmagriot@chem.uoa.gr*

European Peptide Society

ISBN 978-960-466-121-3

Copyright ©2012 the European Peptide Society

All rights reserved. No part of the material protected by this copyright notice may be reproduced or utilized in any form or by any means, electronic or mechanical, including photocopying, recording or by any information storage and retrieval system, without written permission from the copyright owner.

Published by the University of Athens, Laboratory of Organic Chemistry.

Preface

The Thirty-Second European Peptide Symposium (32EPS) was held in Athens, Greece on September 2-7, 2012. The symposium was organized in the Megaron conference center, located downtown in the city.

In September 1958, a small group from various European centers met in Prague to discuss methods of peptide synthesis. This is considered to be the beginning of the European Peptide Symposia. That gave the sparkle and in subsequent years, meetings have been held in Munich, Basle, Moscow and Oxford. In 1963, the 6th European Peptide Symposium took place in Athens, Greece organized by Leonidas Zervas, who was Professor of Organic Chemistry at the University of Athens at that time. Around 70 researchers participated in that symposium. After almost 50 years, we were delighted to host again the European Peptide Symposium in Athens. In 2012, the number of participants reached 700 hundred, coming from both academia and industry and from 46 different countries.

The symposium covered the most recent, cutting-edge research on a broad range of topics in the area of Peptide Science, including synthetic chemistry of amino acids and peptides, peptide synthesis technology, peptide mimetics, conjugates and peptide nucleic acids, macromolecular peptide assemblies, peptide biochemistry and biology, peptide receptors, ligands and signaling, peptide therapeutics, neuropeptides, peptide hormones and immunological peptides, antimicrobial peptides, glycopeptides and lipopeptides, prodrugs, targeting and uptake with peptides, chemical biology, proteomics and peptide bioinformatics, nanotechnology, bioimaging and analytical techniques, peptide materials and catalysts. We have been delighted by the quality of the abstracts submitted for consideration and we would like to thank the Scientific Committee for their assistance in assembling such a high quality program of speakers.

The opening ceremony on Sunday begun with the welcome address by George Kokotos, Chairman of the Symposium and with the introduction by Ferenc Hudecz, the Chairman of the European Peptide Society. This was followed by the presentation of the Leonidas Zervas Award, sponsored by the University of Athens, to Prof. Knud J. Jensen (University of Copenhagen, Denmark) and the Josef Rudinger Memorial Lecture Award, sponsored by Polypeptide Group, to Prof. David J. Craik (The University of Queensland, Australia). In subsequent days, nine plenary and invited lectures as well as 85 oral presentations were presented, accompanied by two poster sessions with 400 poster presentations. We trust that the present symposium was an excellent forum to exchange views on recent scientific developments, meet old friends and build new relationships.

ESCOM Science Foundation sponsored the Dr. Bert L. Schram Young Investigators' Mini Symposium that took place before the opening ceremony. Two awards were given to young investigators for the best presentations of this mini symposium at the closing ceremony. In addition, five awards were given for the best poster presentations: two sponsored by the ESCOM Science Foundation, while the others by the University of Athens, the Agricultural University of Athens and the Royal Society of Chemistry.

In addition to the scientific program, the symposium provided a superb opportunity to visit Athens, which is the largest city and capital of Greece. From this town the light of democracy, civilization and science has been bequeathed to the whole world. It is not accidental that Athens is widely referred as the cradle of Western civilization. Three thousand years old cultural riches are housed in approximately fifty museums, including the new Acropolis museum.

The Chairman would like to thank each of the sponsors and exhibitors for their financial support which contributed to the success of the symposium.

Special thanks are due to the members of the Organizing Committee for their contribution and in particular to the University of Athens T-shirt volunteers who guided the participants during the symposium with kindness and enthusiasm.

It was a great honor and experience for us to organize the 32nd European Peptide Symposium and to host so many distinguished colleagues in Athens. We hope you enjoyed your stay in this historic city and left keeping pleasant memories of our city, our country and its people.

George Kokotos
Chairman of the
32nd European Peptide Symposium



Professor George Kokotos (left), Chairman of the 32nd European Peptide Symposium, Professor Kurt Wuthrich (center), Nobel Prize Laureate 2002, and Professor Ferenc Hudecz (right), Chairman of the European Peptide Society.



Members of the Organizing Committee together with the University of Athens T-shirt volunteers.

32nd EUROPEAN PEPTIDE SYMPOSIUM

September 2-7, 2012

Athens, Greece

Chairman

Prof. George Kokotos (*University of Athens, Greece*)

Honorary Chairman

Prof. Paul Cordopatis (*University of Patras, Greece*)

Scientific Committee

Prof. Kleomenis Barlos (*University of Patras, Greece*)

Prof. Ettore Benedetti (*University of Naples "Federico II", Italy*)

Prof. Ernest Giralt (*Institute for Research in Biomedicine, Barcelona, Spain*)

Prof. Ferenc Hudecz (*Eötvös Loránd University, Hungary*)

Prof. Knud Jensen (*University of Copenhagen, Denmark*)

Prof. Yoshiaki Kiso (*Nagahama Institute of Bio-Science and Technology, Japan*)

Prof. Solange Lavielle (*University Pierre et Marie Curie, Paris, France*)

Prof. Jean Martinez (*University of Montpellier, France*)

Prof. John Matsoukas (*University of Patras, Greece*)

Prof. Luis Moroder (*Max Planck Institute of Biochemistry, Martinsried, Germany*)

Prof. Paolo Rovero (*University of Florence, Italy*)

Prof. Maria Sakarellos-Daitsiotis (*University of Ioannina, Greece*)

Prof. Ivanka Stoineva (*Bulgarian Academy of Sciences, Bulgaria*)

Prof. John C. Vederas (*University of Alberta, Canada*)

Prof. Helma Wennemers (*ETH Zurich, Switzerland*)

Organizing Committee

Prof. Violetta Constantinou-Kokotou (*Agricultural University of Athens*)

Assoc.Prof. Dimitrios Gatos (*University of Patras*)

Assis. Prof. Dimitrios Georgiadis (*University of Athens*)

Dr. Leondios Leondiadis (*NCSR Demokritos, Athens*)

Lect. Victoria Magrioti (*University of Athens*)

Assoc. Prof. Thomas Mavromoustakos (*University of Athens*)

Assoc. Prof. Panagiota Moutevelis-Minakakis (*University of Athens*)

Assis. Prof. George Pairas (*University of Patras*)

Assis.Prof. Theodore Tselios (*University of Patras*)

Major Sponsor



Gold Sponsors



Silver Sponsor



Bronze Sponsors



AMINOLOGICS

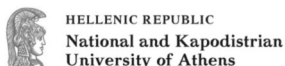
Contributors



HECHENG®



Thermo SCIENTIFIC



Municipality of Halandri

Media Partners



PepGene



European Peptide Symposia

Symposium	Year	Location
1 st	1958	Prague, Czechoslovakia
2 nd	1959	Munich, GFR
3 rd	1960	Basel, Switzerland
4 th	1961	Moscow, Russia
5 th	1962	Oxford, UK
6 th	1963	Athens, Greece
7 th	1964	Budapest, Hungary
8 th	1966	Noordwijk, The Netherlands
9 th	1968	Orsay, France
10 th	1969	Abano Terme, Italy
11 th	1971	Vienna, Austria
12 th	1972	Reinhardsbrunn, GDR
13 th	1974	Kiryat Anavim, Israel
14 th	1976	Wepion, Belgium
15 th	1978	Gdansk, Poland
16 th	1980	Helsingor, Denmark
17 th	1982	Prague, Czechoslovakia
18 th	1984	Djuronaset, Sweden
19 th	1986	Porto Carras, Greece
20 th	1988	Tubingen, GFR
21 st	1990	Barcelona, Spain
22 nd	1992	Interlaken, Switzerland
23 rd	1994	Braga, Portugal
24 th	1996	Edinburgh, UK
25 th	1998	Budapest, Hungary
26 th	2000	Montpellier, France
27 th	2002	Sorrento, Italy
28 th	2004	Prague, Czech Republic
29 th	2006	Gdansk, Poland
30 th	2008	Helsinki, Finland
31 st	2010	Copenhagen, Denmark
32 nd	2012	Athens, Greece

The Josef Rudinger Award

2012 David J. Craik

The University of Queensland, Australia

2010 Stephen B. H. Kent

University of Chicago, USA

2008 Horst Kessler and Manfred Mutter

Technical University of Munich, Germany and

University of Lausanne, Switzerland

2006 Ettore Benedetti and Claudio Toniolo

University of Napoli "Frederico II", Italy and

University of Padova, Italy

2004 Luis Moroder

Max-Planck-Institute für Biochemie, Martinsried, Germany

2002 Sándor Bajusz and Kálmán Medzihradzky

IVAX-Institute of Drug Research, Budapest, Hungary and

Department of Organic Chemistry, Eötvös L. University, Budapest, Hungary

2000 Bernard P. Roques

INSERM, CNRS, Paris, France

1998 Shumpei Sakakibara

Peptide Institute, Osaka, Japan

1996 Ralph Hirschmann

University of Pennsylvania, Philadelphia, USA

1994 Robert C. Sheppard

MRC, Cambridge, United Kingdom

1992 Viktor Mutt

Karolinska Institute, Stockholm, Sweden

1990 R. Bruce Merrifield

The Rockefeller University, New York, USA

1988 Erich Wunsch

Max-Planck-Institut für Biochemie, München, Germany

1986 Robert Schwyzler

ETH Zürich, Switzerland

The Leonidas Zervas Awards

2012 Knud J. Jensen

University of Copenhagen, Denmark

2010 Helma Wennemers

University of Basel, Switzerland

2008 Anna Maria Papini

University of Florence, Italy

2006 Carlos García-Echeverría

Novartis Institutes for BioMedical Research, Basel, Switzerland

2004 Helene Gras-Masse

Institut Pasteur de Lille, France

2002 Thomas W. Muir

Rockefeller University, New York, USA

2000 Antonello Pessi

Istituto di Ricerche di Biologica Molecolare P. Angeletti, Rome, Italy

1998 Annette G. Beck-Sickinger

ETH Zürich, Switzerland

1996 Morten Meldal

Carlsberg Laboratory, Valby, Denmark

1994 Ernest Giralt and Fernando Albericio

University of Barcelona, Barcelona, Spain

1992 Günther Jung

University of Tübingen, Tübingen, Germany

1990 Michal Lebl and Jean Martinez

*Czechoslovak Academy of Sciences, Prague and
CNRS, Montpellier, France*

1988 Alex Eberle

University of Basel, Basel, Switzerland

Young Investigators' Awards

Dr. Bert L. Schram Oral Presentation Awards

Dr. V. Pattabiraman (*ETH Zürich, Switzerland*): “Chemoselective α -ketoacid-hydroxylamine (KAHA) ligation with 5-oxaproline for chemical protein synthesis”.

Dr. F. Mende-Thomas (*University of Bristol, UK*): “De novo designed heterodimeric coiled coils – Useful tools for the development of new biomaterials”.

Dr. Bert L. Schram Poster Presentation Awards

I. Valverde (*University of Basel, Switzerland*): “Click-peptides: Novel 1,2,3-triazole backbone-modified peptidomimetics for tumor targeting”.

S. Cujova (*Czech Academy of Sciences, Czech Republic*): “Panurgines, novel antimicrobial peptides from the venom of wild bee *Panurgus calcaratus* and their interaction with phospholipids vesicles”.

University of Athens Poster Presentation Award

E. Thinon (*Imperial College, UK*): “Targeting N-myristoyl transferase-1 in cancer using peptide microarrays”.

Agricultural University of Athens Poster Presentation Award

M. Lefrancois (*Université de Sherbrooke, Canada*): “Binding, signaling and in vivo efficacy of novel peptidic CXCR4 agonists”.

Royal Society of Chemistry Poster Presentation Award

P. Giannelou (*University of Athens, Greece*): “Identification of a novel amyloidogenic peptide in the sequence of the highly amyloidogenic human calcitonin”.

**Proceedings of the
Thirty-Second European Peptide Symposium
September 2-7, 2012
Athens, Greece**

Contents

Discovery and applications of cyclotides	
<i>D. J. Craik</i>	2
From microwave heating to control of nano-scale self-assembly in peptide science	
<i>K. J. Jensen</i>	4
The multiple fully-extended (2.0₅-helix) peptide conformation	
<i>C. Toniolo</i>	6
Tumor targeting with peptides in four decades – from initial concepts to an array of highly sophisticated methods	
<i>A. N. Eberle</i>	8
D-Amino acid adhesion peptides by combinatorial selection: Control of cellular growth on inert surfaces	
<i>M. Meldal, B. Wu, F. Diness, T. Nielsen</i>	10
Ion Mobility- and Affinity- Mass Spectrometry: New tools for elucidating structures and pathways of “misfolding” - aggregating proteins	
<i>M. Przybylski, K. Lindner, C. Vlad, N. Pierson, C. Karreman, S. Schildknecht, M. Leist, N. Tomczyk, J. Langridge, T. Ciossek, A. Petre, M. Gross, B. Hengerer, D. Clemmer</i>	12
De novo design of artificial peptides that specifically interact with HIV-1 gp41 to inhibit viral-cell membrane fusion and infection	
<i>K. Liu, L. Cai, W. Shi, C. Wang, K. Wang</i>	14
From aberrant N-glycosylation to alpha actinin 1 as a new candidate autoantigen of an antibody mediated form of Multiple Sclerosis	
<i>S. Pandey, E. Peroni, I. Dioni, P. Rovero, A. M. Papini</i>	16
N-Amino-imidazolin-2-one turn mimics	
<i>C. Proulx, S. H. Bouayad-Gervais, Y. García-Ramos, W. D. Lubell</i>	18
Bis(2-sulfanylethyl)amido native peptide ligation and novel tools for protein total synthesis	
<i>N. Ollivier, L. Raibaut, E. Boll, J. Dheur, R. Mhidia, O. Melnyk</i>	20
From simple to complex to ultra complex and back to simple	
<i>M. Lebl</i>	22
NPPS: A new integrated method for solid phase synthesis of peptides on nanoparticles	
<i>G. Byk, V. Machtey, A. Weiss, R. Khandadash</i>	24
Rational design and synthesis of linear and cyclic myelin epitope peptides: New directions in the immunotherapy of Multiple Sclerosis	
<i>G. Deraos, T. Tselios, P. Katsougraki, P. Plotas, M.-E. Androutsou, J. Matsoukas</i>	26
Preventing failure in difficult sequences: An improved resin matrix, its properties and application	
<i>W. Rapp, M. Beyermann, P. Henklein, R. Pipkorn, S. Rawer, S. Rothmund</i>	28
SNARE analogous peptides for membrane fusion	
<i>A. Lygina, K. Meyenberg, G. van den Bogaart, R. Jahn, U. Diederichsen</i>	30
Total synthesis of marine cyclopeptide scytonemin A	
<i>J. Liu, L. Wang, Z. Xu, T. Ye</i>	32
Development of a series of diketopiperazine vascular targeting anticancer agents based on microtubule depolymerization activity	
<i>Y. Hayashi, Y. Yamazaki, F. Yakushiji, M. Sumikura, H. Tanaka, K. Muguruma,</i>	

<i>H. Yasui, T. Chinen, T. Usui, S. Neuteboom, B. Potts, M. Palladino, G. K. Lloyd</i>	34
Branched diketopiperazines as a universal scaffold for preparation of orally active small peptide derivatives	
<i>V. Deigin</i>	36
Glycan targets of the anti-cancer peptide NK-2	
<i>S. Gross, J. Andrä</i>	38
Design, synthesis and analysis of anti-tuberculosis peptides	
<i>Z. Amso, C. Miller, R. O'Toole, V. Sarojini</i>	40
Cardioprotective peptides to fight ischemia/reperfusion injury in mouse hearts	
<i>P. Boisguerin, A. Franck, A. Covinhes, S. Barrère-Lemaire, B. Lebleu</i>	42
Lead optimization of allophenylnorstatine-containing inhibitors as therapeutic drug and application to peptidomimic protease probe	
<i>K. Hidaka, M. Adachi, R. Kuroki, S. Tokai, K. Akaji, Y. Tsuda, Y. Kiso</i>	44
Enhancing peptide activity and structure by synthetic constraint of beta-turns and beta-sheets: CLIPS and anti-CD40L phylomers	
<i>S. R. Stone, R. Hopkins, P. T. Cunningham, M. Kerfoot, Y.-F. Tan, W. Schaaper, N. Dailly, P. Timmerman</i>	46
Development of a unique peptide synthetic method AJIPHASE® using anchor support molecules to suppress alkylation in final cleavage step	
<i>D. Takahashi, T. Inomata</i>	48
Mixed ion-exchange centrifugal partition chromatography: An efficient solution for peptide separation	
<i>N. Amarouche, L. Boudesoque, P. Lameiras, J.-M. Nuzillard, M. Giraud, A. Butte, F. Quattrini, R. Kapel, I. Marc, J.-H. Renault</i>	50
Conformation and biological activity of cyclolinopeptide A analogs modified within tetrapeptide fragment Pro-Pro-Phe-Phe	
<i>J. Katarzyńska, K. Kierus, J. Olejnik, K. Huben, J. Artym, M. Zimecki, J. Zabrocki, S. Jankowski</i>	52
Solid state reaction peptides and proteins with spillover hydrogen	
<i>Y. A. Zolotarev, A. K. Dadayan, A. T. Kopylov, I. V. Nazimov, E. V. Bocharov, B. V. Vaskovsky, Y. A. Borisov, N. F. Myasoedov</i>	54
Insight into Aβ misfolding and aggregation	
<i>S. Lovas, Y. Zhang, Y. L. Lyubchenko</i>	56
Isotope labeling strategies for solution NMR studies of high-molecular-weight protein drug-targets	
<i>G. A. Spyroulias, C. T. Chasapis, A. Argyriou, D. Bentrop</i>	58
Delivering the native structures of peptides from computer simulations and predicted NMR proton chemical shifts	
<i>P. Thévenet, Y. Shen, J. Maupetit, F. Guyon, A. Padilla, P. Derreumaux, P. Tufféry</i>	60
Computational prediction of bioactive peptides	
<i>C. Mooney, K. O'Brien, N. J. Haslam, R. J. Edwards, N. E. Davey, F. J. Duffy, K. Golla, I. Stavropoulos, N. Khaldi, A. J. Chubb, F. Lombardi, T. Holton, V. Vijay, M. Devocelle, N. Moran, D. C. Shields</i>	62

Peptides as a new emerging class of medical biomarkers	
<i>V. T. Ivanov, R. H. Ziganshin, V. M. Govorun</i>	64
Peptide self-assembled monolayers as a new tool for nanotechnology	
<i>M. Venanzi, M. Caruso, E. Gatto, F. Formaggio, C. Toniolo, A. M. Textera, J. C. Rodriguez-Cabello</i>	66
Engineering pro-angiogenic peptides using stable disulfide-rich cyclic scaffolds	
<i>L. Y. Chan, S. Gunaekera, S. T. Henriques, N. F. Worth, S. J. Le, R. J. Clark, J. H. Campbell, D. J. Craik, N. L. Daly</i>	68
Folding landscape exploration by circular permutation and capping β structures	
<i>B. Kier, A. Byrne, M. Scian, J. Anderson, N. Andersen</i>	70
Lasso peptides: From linear to interlocked structures	
<i>Y. Li, S. Zirah, R. Ducasse, A. Blond, C. Goulard, E. Lescop, E. Guittet, J.-L. Pernodet, S. Rebuffat</i>	72
IANUS peptide array as a tool to screen for protein antagonists	
<i>M. Malešević, F. Erdmann, E. Prell, G. Jahreis, G. Fischer</i>	74
Comprehensive peptide microarrays for histone research	
<i>K. Schnatbaum, J. Zerweck, T. Knaute, C. Tersch, N. Pawlowski, J. Seznec, D. Wildemann, H. Wenschuh, M. Schutkowski, C. Wilczek, D. Shechter, U. Reimer</i>	76
The antimicrobial peptide M33. An example of drug development	
<i>J. Brunetti, C. Falciani, S. Bindi, S. Scali, B. Lelli, L. Lozzi, L. Bracci, A. Pini</i>	78
Synthesis of cyclic lipo-octapeptide derivatives of burkholdines and its antifungal activity	
<i>H. Konno, Y. Otsuki</i>	80
Peptides labeled by quaternary ammonium salts for sensitive detection by electrospray mass spectrometry	
<i>R. Bączor, M. Rudowska, M. Cydzik, D. Wojewska, A. Kluczyk, P. Stefanowicz, Z. Szewczuk</i>	82
How hydrophobicity dictates the size of self-replicating self-assembling macrocycles	
<i>M. Malakoutikhah, M. Colomb-Delsuc, J. J.-P. Peyralans, M. C. A. Stuart, S. Otto</i>	84
Protein-fragment complementation and semi-rational design: Engineering specific antagonists of protein-protein interactions	
<i>T. Rao, N. Acerra, R. O. Crooks, N. M. Kad, J. M. Mason</i>	86
Food protein fragments are regulatory oligopeptides	
<i>A. A. Zamyatnin, O.L. Voronina</i>	88
On the way to synthetic peptide vaccine against hepatitis C	
<i>E. Kolesanova, A. Moisa, N. Pyndyk, V. Prozorovsky, S. Funikov, X. Thomas, J. Dubuisson, A. Dadayan, Y. Zolotarev</i>	90
A synthetic heparin sulfate-mimetic peptide conjugate to a mini CD4 displays very high anti-HIV activity	
<i>B. Connell, F. Baleux, Y.-M. Coïc, P. Clayette, D. Bonnaffé, H. Lortat-Jacob</i>	92
Branched neurotensin specifically binds a highly selective tumor cell marker, which is not neurotensin receptor 1	
<i>C. Falciani, J. Brunetti, B. Lelli, N. Ravenni, L. Lozzi, L. Depau1, A. Pini, L. Bracci</i>	94

Anticancer drug delivery systems containing GnRH-III as a targeting moiety <i>M. Manea, U. Leurs, E. Orbán, V. N. Schreier, L. Pethő, P. Schlage, Á. Schulcz, B. Kapuvári, J. Tóvári, G. Halmos, G. Mező</i>	96
Bivalent ligands for the chemokine receptor CXCR4 dimer and their function <i>W. Nomura, T. Tanaka, H. Aikawa, T. Narumi, H. Tamamura</i>	98
Azapeptide calpain inhibitors <i>Z. Bánóczy, L. E. Dókus, Á. Tantos, P. Tompa, P. Friedrich, F. Hudecz</i>	100
Production and characterization of matrix metalloproteinases implicated in multiple sclerosis <i>S. Amar, G. B. Fields</i>	102
Receptor and blood-brain barrier characterization of opioid peptides in drug research & early development <i>M. Verbeken, S. Stalmans, E. Wynendaele, N. Bracke, B. Gevaert, K. Peremans, I. Polis, C. Burvenich, B. De Spiegeleer</i>	104
Selective cell signaling study of GPCR via PWR spectroscopy <i>M. Cai, H. Zhang, M. M. Dedek, S. Saavedra, V. J. Hruby</i>	106
PEGylation of the endogenous peptide Neuromedin U yields a promising candidate for the treatment of obesity and diabetes <i>P. Ingallinella, A. M. Peier, A. Pocai, A. Di Marco, K. Desai, K. Zytko, Y. Qian, X. Du, A. Cellucci, E. Monteagudo, R. Laufer, E. Bianchi, D. J. Marsh, A. Pessi</i>	108
Design, synthesis and binding assays of sialic acid and sialyl-saccharide conjugates to lectins and influenza H1N1 virus <i>M. Sakarellos-Daitsiotis, S. Zevgiti, J. G. Zabala, A. Darji, U. Dietrich, E. Panou-Pomonis</i>	110
The ghrelin receptor: New potent ligands for a functional selectivity <i>A.-L. Blayo, A. Moulin, L. Demange, C. M'Kadmi, D. Gagne, S. Mary, J. Marie, M. Damian, S. Denoyelle, J.-L. Banères, J. Martinez, J.-A. Fehrentz</i>	112
Nanoparticles-based peptide subunit vaccines against group A Streptococcus <i>M. Skwarczynski, A. A. H. Ahmad Fuaad, M. Zaman, Z. Jia, J. Kowapradit, L. Rustanti, Z. M. Ziora, M. J. Monteiro, M. R. Batzloff, M. F. Good, I. Toth</i>	114
Bioportides <i>S. Jones, M. Lukanowska, J. Howl</i>	116
Transduction of peptides, proteins and nucleotides into live cells by cell penetrating peptides <i>A.-A. Keller, R. Breitling, P. Hemmerich, F. Mussbach, B. Schaefer, S. Lorkowski, S. Reissmann</i>	118
SS14-Based radiopeptides: Synthesis & biology <i>A. Tatsi, T. Maina, B. Waser, R. Cescato, E. P. Krenning, M. de Jong, J.-C. Reubi, P. Cordopatis, B. A. Nock</i>	120
Efficient identification of peptide ligands for proteins via high-throughput screening of combinatorial peptide libraries <i>S. S. Lee, J. Lim, Y. L. Ang, J.-E. Jee, J. Oon</i>	122
Chemical synthesis and in vitro and in vivo evaluation of a bombesin peptide analog linked to a cytotoxic drug for the targeting of bombesin receptor-positive tumors <i>S. M. Okarvi</i>	124

Novel approaches to the design of novel multivalent ligands for the detection and treatment of cancer	
<i>V. J. Hrubby, N. Brabez, J. Josan, C. DeSilva, J. Vagner, G. Chassaing, D. Morse, R. J. Gillies, S. Lavielle</i>	126
Chemical synthetic glycopeptide vaccine for cancer therapy	
<i>H. Cai, Z.-H. Huang, L. Shi, Z.-Y. Sun, H. Kunz, Y.-M. Li</i>	128
Engineering of proteinaceous orally active bradykinin peptide antagonists	
<i>J. P. Tam, C. T. T. Wong, Y. Qiu</i>	130
Chemoselective α-ketoacid-hydroxylamine (KAHA) ligation with 5-oxaproline for chemical protein synthesis	
<i>V. R. Pattabiraman, A. O. Ogunkoya, J. W. Bode</i>	132
Recognition pliability is coupled to structural heterogeneity	
<i>M. Nagulapalli, G. Parigi, J. Yuan, J. Gsponer, G. Deraos, V. V. Bamm, G. Harauz, J. Matsoukas, M. R. R. de Planque, I. P. Gerotheranassis, M. Madan Babu, C. Luchinat, A. G. Tzakos</i>	134
Biofunctionalization of biopolymers with peptide conjugated dendrons	
<i>P. Fransen, D. Pulido, R. Seelbach, A. Mata, D. Eglin, M. Royo, F. Albericio</i>	136
Membrane thickness and the mechanism of action of the short peptaibol trichogin GA IV	
<i>S. Bobone, Y. Gerelli, M. De Zotti, G. Bocchinfuso, A. Farrotti, B. Orion, A. Palleschi, F. Sebastiani, E. Latter, J. Penfold, R. Senesi, F. Formaggio, C. Toniolo, G. Fragneto, L. Stella</i>	138
Mild chemoselective alkylation of aza-sulfurylglycyl peptides	
<i>S. Turcotte, T. Havard, W. D. Lubell</i>	140
Direct and specific detection of intact sulfated peptides using MALDI-TOF MS reflectron positive ion mode	
<i>S. Cantel, L. Brunel, C. Enjalbal, J. J. Vasseur, J. Martinez, M. Smietana</i>	142
Alanine scan of Limnonectin peptides on the Overture™ robotic peptide library synthesizer	
<i>J. P. Cain, M. A. Onaiyekan, C. A. Chantell, M. Menakuru</i>	144
Antimicrobial activity of new analogues of Chrysopsin-1	
<i>E. Tsoumani, A. Niarchos, R. Exarchakou, Z. Zagoriti, V. Mertziani, N. L. Assimomytis, K. Poulas, P. Cordopatis, V. Magafa</i>	146
Antimicrobially active peptides isolated from fleshfly larvae	
<i>T. Neubauerová, T. Macek, M. Šanda, Z. Vobůrka, M. Macková</i>	148
Conformational properties of the spin-labeled tylopeptin B and heptaibin peptaibiotics based on PELDOR spectroscopy data	
<i>M. Gobbo, B. Biondi, M. De Zotti, A. D. Milov, Y. D. Tsvetkov, A. G. Maryasov, F. Formaggio, C. Toniolo</i>	150
De novo design of short peptides with antimicrobial activity and the effect of acyl conjugation	
<i>A. Macůrková, R. Ježek, G. Kroneislová, P. Lovecká, T. Macek, M. Macková</i>	152
Design and synthesis of amphipathic α-helical peptide models for the development of new antimicrobial agents	
<i>A. Marianou, A. Balliu, M. Sakka, A.-I. Koukkou, M. Sakarellos-Daitsiotis, E. Panou-Pomonis</i>	154

Development of human Cathelicidin LL-37-derived short antimicrobial peptides with prokaryotic selectivity, LPS-neutralizing activity and protease stability <i>S. Y. Shin, Y. H. Nan, J.-K. Bang</i>	156
Enhanced anti-staphylococcal activity of an analog derived from the 107-115 human lysozyme fragment <i>N. B. Iannucci, R. González, F. Guzmán, O. Cascone, F. Albericio</i>	158
Enhancement of bacterial outer membrane binding action of the antimicrobial peptide magainin 2 by minimal amino acid substitution <i>S. Fukuoka, L. Heinbockel, Y. Kaconis, J. Andrä, M. Rössle, T. Gutschmann, K. Brandenburg</i>	160
Interaction of the antimicrobial peptide gomesin with model membranes <i>T. M. Domingues, B. Mattei, J. Seelig, K. R. Perez, K. A. Riske, A. Miranda</i>	162
Lipopeptides – synthesis and their properties <i>M. Kukowska, K. Dzierzbicka, Ł. Nowicki, M. Samsel</i>	164
Membrane-perturbing effects of antimicrobial peptides: A systematic spectroscopic analysis <i>D. Roversi, L. Giordano, M. De Zotti, G. Bocchinfuso, A. Farrotti, S. Bobone, A. Palleschi, Y. Park, K.-S. Hahm, F. Formaggio, C. Toniolo, L. Stella</i>	166
Metanicins, peptaibol antibiotics from the ascomycetous fungus CBS 597. 80 <i>A. Kimonyo, H. Brückner</i>	168
“Minimum bias” molecular dynamics simulations to determine peptide orientation in membranes <i>G. Bocchinfuso, A. Farrotti, A. Palleschi, B. Bechinger, L. Stella</i>	170
Internalisation by translocations and endocytosis of cell penetrating peptide (CPP) by a reductionist approach <i>P. Lecorché, A. Walrant, S. A. Bode, M. Thévenin, C. Bechara, S. Bregant, I. D. Alves, S. Lavielle, G. Chassaing, S. Sagan, F. Burlina</i>	172
Panurgines, novel antimicrobial peptides from the venom of wild bee <i>Panurgus calcaratus</i> and their interaction with phospholipids vesicles <i>S. Čujová, L. Monincová, J. Slaninová, L. Bednářová, V. Čerňovský</i>	174
Peptaibiotic folding and bioactivity: Role of backbone endothioamide linkages <i>M. De Zotti, B. Biondi, C. Peggion, M. De Poli, H. Fathi, S. Oancea, F. Formaggio, C. Toniolo</i>	176
Structure and biological activity of Aurein 1.2 and dimeric analogues <i>E. N. Lorenzóna, L. G. Nogueirab, T. M. Bauabb, E. M. Cillia</i>	178
Studies on the properties and mode of action of a synthetic Hemocidin derived from α-Hemoglobin <i>L. A. C. Carvalho, C. Remuzgo, M. T. Machini</i>	180
Sviceucin, a lasso peptide from <i>Streptomyces sviceus</i>: Isolation and structural analysis <i>R. Ducasse, Y. Li, A. Blond, S. Zirah, E. Lescop, C. Goulard, E. Guittet, J.-L. Pernodet, S. Rebuffat</i>	182
Synthesis of PAF, an antifungal protein from <i>Penicillium chrysogenum</i> by native chemical ligation <i>G. Váradi, G. Batta, L. Galgóczi, Z. Kele, G. K. Tóth</i>	184

Synthesis of glycated and glycosylated peptides to detect autoantibodies in diabetic patients' sera	
<i>C. Rentier, O. Monasson, F. Nuti, P. Traldi, A. Lapolla, M. Larregola, P. Rovero, M. Chorev, A. M. Papini</i>	186
Synthesis, structure-activity relationship study and antimicrobial activity of a new tigerinins analog	
<i>F. Bédard, T. T. A. Nguyen, I. Kukavica-Ibrullj, H. Maaroufi, R. C. Lévesque, E. Biron</i>	188
The study of defensins of biomedical importance isolated from arthropods	
<i>V. Čeršovský, B. El Shazely, V. Fučík, Z. Voburka, J. Žďárek, J. Slaninová, T. Chrudimská, L. Grubhoffer</i>	190
Trichogin GA IV and selected analogs as new antitumor agents: Synthesis, conformational analysis and cytotoxicity evaluation	
<i>M. De Zotti, B. Biondi, R. Tavano, C. Peggion, M. Crisma, F. Formaggio, E. Papini, C. Toniolo</i>	192
A convenient post-screening ring-opening approach for the decoding of one-bead-one-compound cyclic peptide libraries	
<i>A. Girard, E. Biron</i>	194
Design and synthesis of biotinylated peptidyl phosphonate probe for the isolation of single chain Fv with hydrolyzing activity	
<i>H. Taguchi, Y. Fujita, Y. Tsuda</i>	196
The identification of advanced glycation sites in proteins by isotopic labeling with ¹³C₆ glucose	
<i>M. Kielmas, M. Kijewska, P. Stefanowicz, Z. Szewczuk</i>	198
Elimination of partial cleavage of acid labile groups during removal of Mtt protection	
<i>Z. Flegelova, M. Flegel, M. Lebl</i>	200
New methods for fluorescent labeling of peptide hormones and enzyme substrates	
<i>K. Hoogewijs, D. Buyst, J. Martins, A. Madder</i>	202
A new producer and new 19- and 20-residue peptaibiotics: suzukacillin-related hypophellins	
<i>C. R. Röhrich, A. Iversen, W. M. Jaklitsch, H. Voglmayr, A. Vilcinskas, K. F. Nielsen, U. Thrane, H. Brückner, T. Degenkolb</i>	204
Rapid alkalization factors in grape <i>Vitis vinifera</i>	
<i>A. A. Zamyatnin</i>	206
Screening the natural habitat: New peptaibiotics from specimens and pure cultures of the fungicolous fungus <i>Hypocrea pulvinata</i>	
<i>C. R. Röhrich, A. Iversen, W. M. Jaklitsch, H. Voglmayr, A. Berg, H. Dörfelt, A. Vilcinskas, K. F. Nielsen, U. Thrane, H. Brückner, T. Degenkolb</i>	208
Targeting <i>N</i>-myristoyl transferase in cancer using peptide arrays	
<i>E. Thinon, D. Mann, E. W. Tate</i>	210
<i>Bis</i>(2-sulfanylethyl)amido peptide chemistry enables a one-pot three segments ligation strategy for protein chemical synthesis	
<i>N. Ollivier, J. Vicogne, H. Drobecq, R. Desmet, B. Leclercq, O. Melnyk</i>	212

Molecular dynamics of amylin 10-29 amyloid formation: Parallel, antiparallel and bent structures	
<i>D. Lapidus, S. Ventura, C. Czaplewski, A. Liwo, I. Liepina</i>	214
Odd-even effect in the induced plasmonic CD band of peptide-capped gold nanoparticles	
<i>E. Longo, A. Orlandin, F. Mancin, C. Toniolo, A. Moretto</i>	216
Scope and limitations of bis(2-sulfanylethyl)amino (SEA) native peptide ligation	
<i>L. Raibaut, E. Lissy, O. Melnyk</i>	218
Binary switch activity of the Tat peptide: From membrane penetration to lytic action	
<i>S. Piantavigna, M. E. Abdelhamid, A. P. O'Mullane, C. Zhao, X. Qu, B. Graham, L. Spiccia, L. L. Martin</i>	220
Encapsulation and radiolabeling approaches of potential peptide-type biomarkers for assessment of amyloid plaques related to the Alzheimer's disease	
<i>F. R. Cabral, C. R. Nakaie, O. P. Martins, A. C. Tedesco, L. Malavolta</i>	222
Generation of silver nanoparticles in the presence of oligoproline derivatives	
<i>P. Feinšügge, H. Wennemers</i>	224
Simultaneous determination of aspartame, alitame, neotame and advantame by HILIC-ESI-MS/MS	
<i>M. G. Kokotou, C. G. Kokotos, N. S. Thomaidis</i>	226
Stability studies on MMP-2 specific peptides for the preparation of molecular probes	
<i>A. Radulska, S. Ait-Mohand, V. Dumulon-Perreault, R. Lebel, R. Zriba, B. Guérin, W. Neugebauer, M. Lepage</i>	228
Charting the antiproliferative activity of [Arg⁸]vasopressin analogues against cancer cell lines	
<i>V. Kounnis, E. Elia, A. Tzakos, E. Briasoulis, L. Borovičková, J. Slaninová, P. Cordopatis, V. Magafa</i>	230
Computer modeling of human μ-opioid receptor	
<i>T. Dzimbova, F. Sapundzhi, N. Pencheva, P. Milanov</i>	232
Detection of antibodies against synthetic peptides mimicking ureases fragments in atherosclerotic patients sera	
<i>B. Kolesińska, J. Fraczyk, I. Relich, I. Konieczna, M. Kwinkowski, W. Kaca, Z. J. Kamiński</i>	234
Determination of in vitro T-cell stimulating activity of Dsg3 peptide antigens on PBMC from patients with pemphigus vulgaris	
<i>K. Uray, H. Szabados, P. Silló, S. Kárpáti, S. Bősze</i>	236
Direct antiproliferative effect on breast cancer cells of [Mpa¹, D-Tyr(Et)²] or [Mpa¹, D-1-Nal²] oxytocin analogues containing β-(2-thienyl)-Alanine in position 3 or 7	
<i>V. Magafa, E. Giannopoulou, G. Pairas, R. Exarchakou, N. L. Assimomytis, E. Tsoumani, L. Borovičková, J. Slaninová, H. P. Kalofonos, P. Cordopatis</i>	238
JMV 2009, a potent neurotensin antinociceptive analog	
<i>A. René, P. Tétreault, N. Beudet, P. Sarret, J. Martinez, F. Cavalier</i>	240
Neuroprotective peptide Colivelin and labeled derivatives: Structural, in vitro and in vivo evaluation	
<i>M. Kostomoiri, C. Zikos, D. Benaki, M. Paravatou-Petsotas, T. Tsotakos, C. Triantis, I. Pirmettis, M. Papadopoulos, M. Pelecanou, E. Livaniou</i>	242

New bradykinin analogues modified in their C-terminus with D-pipecolic acid <i>M. Śleszyńska, D. Sobolewski, I. Born, B. Lammek, A. Prah</i>	244
Phylogenetic diversity of C-terminally expressed hepta-peptide unit in opioid precursor polypeptide proenkephalin A <i>A. Magyar, E. Bojnik, E. Boynik, M. Corbani, F. Babos, A. Borsodi, S. Benyhe</i>	246
Searching diagnosable disease using plasma kisspeptin levels as a biomaker <i>F. Katagiri, M. Nomizu</i>	248
Synthesis and biological activity of cyclic peptides from cyanobacteria <i>F. Boyaud, I. Bonnard, B. Banaigs, A. Witczak, F. Gattacceca, N. Inguibert</i>	250
Synthesis and biological studies of 2-naphthylalanine modification of Cyclolinopeptide A <i>M. Kinas, K. Kierus, K. Huben, M. Zimecki, S. Jankowski, J. Zabrocki</i>	252
Synthesis and conformational analysis of linear, dimeric and cyclic analogues of the C-terminal hexapeptide of Neurotensin <i>C. Potamitis, P. Zoumpoulakis, R. Exarchakou, V. Karageorgios, V. Mertziani, A. Spyridaki, G. Liapakis, P. Cordopatis, V. Magafa</i>	254
Aggregation and cytotoxic properties of hIAPP17-29 and rIAPP17-29 fragments: A comparative study with the respective full-length parent polypeptides <i>F. M. Tomasello, A. Sinopoli, F. Attanasio, T. Campagna, G. Pappalardo</i>	256
Analogues of SFTI-1 as the potential inhibitors of the 20S proteasome <i>D. Dębowski, A. Mizeria, A. Lesner, A. Łęgowska, K. Rolka</i>	258
Angiotensin I metabolism in various kinds of fat tissue- ex vivo study in rat model of obesity and insulin resistance <i>B. Bujak-Giżycka, M. Suski, J. Madej, B. Bystrowska, Š. Zorad, L. Gajdošechova, K. Krskova, R. Olszanecki, R. Korbut</i>	260
Assessment of angiotensinogen metabolism in aorta and heart of hypertensive rats <i>B. Bujak-Giżycka, B. Bystrowska, K. Kuś, R. Olszanecki, R. Korbut</i>	262
Design, synthesis and biological evaluation of linear peptide analogs of the A2 subunit (sequence 558-565) of the Factor VIII of blood coagulation <i>C. Anastasopoulos, Y. Sarigiannis, G. Stavropoulos</i>	264
Design, synthesis and biological evaluation of cyclic peptide analogs of the A2 subunit (sequence 558-565) of the Factor VIII of blood coagulation <i>C. Anastasopoulos, Y. Sarigiannis, G. Stavropoulos</i>	266
Development of potent and specific PACE4 inhibitors <i>I. Małuch, A. Kwiatkowska, C. Levesque, S. Routhier, R. Desjardins, F. D'Anjou, W. Neugebauer, B. Lammek, A. Prah, R. Day</i>	268
DNA topoisomerases inhibition by peptides from <i>E.coli</i> ParE toxin <i>L. C. B. Barbosa, S. S. Garrido, L. N. Santos, M. Pons, R. Marchetto</i>	270
Ex vivo assessment of angiotensin metabolism in retroperitoneal and periaortic fat tissue of hypertensive rats <i>B. Bujak-Giżycka, M. Suski, J. Madej, K. Kuś, Š. Zorad, R. Olszanecki, R. Korbut</i>	272
Hydrophobic α-amino acids favour the inhibition of human GIIA phospholipase A₂ by 2-oxoamides <i>S. Vasilakaki, E. Barbayianni, T. M. Mavromoustakos, M. H. Gelb, G. Kokotos</i>	274

<i>In vitro</i> efficacy of CcdB toxin peptide analogues mediated by drug delivery systems formulation	
S. S. Garrido, R. Marchetto, S. Barbosa, P. Ciancaglini	276
HslVU, an ancestral form of the 26S proteasome as a potential target for the treatment of parasitoses due to protozoa (<i>Leishmania</i>, <i>Trypanosoma</i>)	
K. Samanta, N. M. Kebe, V. Apicella, V. Lisowski, A. Kajava, N. Payrot, M. Pagès, J. Martinez, P. Bastien, O. Coux, J.-F. Hernandez	278
N- or C-terminal biotinylated citrullin containing filaggrin epitope peptides: The effect of biotinylation on the antibody recognition in Rheumatoid Arthritis	
F. Babos, E. Szarka, G. Nagy, Z. Majer, G. Sármay, A. Magyar, F. Hudecz	280
New neutrophil serine proteases substrates optimized in prime positions using the combinatorial approach	
J. Popow, M. Wysocka, A. Lesner, K. Rolka	282
Peptides in <i>Xenorhabdus</i> and <i>Photorhabdus</i> spp	
F. I. Nollmann, C. Dauth, D. Reimer, Q. Zhou, H. B. Bode	284
Study on the application of furan crosslinking at the protein-DNA interface	
L. G. Carrette Lieselot, M. Gattner, J. Van den Begin, T. Carell, T. Morii, A. Madder	286
Transmembrane channel formation induced by the peptaibol paracelsin from <i>Trichoderma reesei</i> (<i>Hypocrea jecorina</i>)	
S. Gelfert-Peukert, G. Boheim, G. Jung, H. Brückner	288
Analgesic effects of novel modified with β2-tryptophan hexapeptide analogues as nociceptin receptor ligands	
A. I. Bocheva, H. H. Nocheva, N. D. Pavlov, M. Calmès, J. Martinez, P. T. Todorov, E. D. Naydenova	290
Binding, signaling and <i>in vivo</i> efficacy of novel peptidic CXCR4 agonists	
M. Lefrançois, M.-R. Lefebvre, P. Boulais, J. Cabana, C. Mona, É. St-Louis, P. Lavigne, R. Leduc, N. Heveker, E. Escher	292
New structural and functional insights in SOCSs/kinases interaction	
P. Brandi, D. Marasco, I. De Paola, R. Pastore, A. Angelastro, P. L. Scognamiglio	294
Elucidation of the structure-activity relationships of Apelin: Influence of unnatural amino acids on binding, signaling and plasma stability	
A. Murza, A. Parent, E. Besserer-Offroy, N. Beaudet, P. Sarret, E. Marsault	296
Fluorescence spectroscopy as a tool for studying protein-peptide interactions: Evaluation of talin affinity for β_3 integrin derived peptides	
A. Gkesouli, P. Stathopoulos, A. Psillou, A. S. Politou, V. Tsikaris	298
Functionalized oligoprolines as multivalent scaffolds in tumor targeting	
P. Wilhelm, C. Kroll, H. Mäcke, H. Wennemers	300
Heterofunctional dimer of endothelin ET_A antagonist and ET_B agonist “clicked” N-terminally on resin with second peptide component in solution	
W. A. Neugebauer, M. Houde, J. Labonté, G. Bkaily, P. D’Orléans-Juste	302
Medicinal chemistry approach for solid phase synthesis of peptide mimetics of viperistatin disintegrin as lead compounds for α1/α2 integrin receptors	
T. Momic, J. Katzhendler, C. Marcinkiewicz, J. A. Eble, P. Lazarovici	304

New antagonists of VEGFR-1: Design, synthesis and biochemical evaluation <i>W.-Q. Liu, S. Broussy, L. Wang, N. Eilstein, M. Reille, F. Huguenot, M. Vidal</i>	306
New polypeptide azemiopsin from <i>Azemiops feae</i> viper venom is a selective ligand of nicotinic acetylcholine receptor <i>M. N. Zhmak, Y. N. Utkin, C. Weise, I. E. Kasheverov, T. V. Andreeva, E. V. Kryukova, V. G. Starkov, D. Bertrand, V. I. Tsetlin</i>	308
Novel neutrophil-activating cryptides hidden in mitochondrial cytochrome c <i>Y. Hokari, T. Seki, H. Nakano, Y. Matsuo, A. Fukamizu, E. Munekata, Y. Kiso, H. Mukai</i>	310
N-Terminal modifications of highly potent bradykinin agonists and antagonists for structure activity relationship and cell imaging studies <i>L. Gera, C. Roy, M.-T. Bawolak, X. Charest-Morin, R. S. Hodges, F. Marceau</i>	312
Peptide based artificial receptors for carbohydrate anthrose detection <i>A. Jakas, P. Cudic, N. Bionda, J. Suć, K. Vlahoviček-Kahlina, M. Cudic</i>	314
Pharmacological activity of new cyclic endomorphin analogs <i>R. Perlikowska, J. Piekielna, J. Fichna, J. C. do-Rego, A. Janecka</i>	316
Conformational properties and energetic analysis of Aliskiren in solution and receptor site <i>A. Politi, G. Leonis, H. Tzoupis, D. Ntountaniotis, M. G. Papadopoulos, S. Golic Grdadolnik, T. Mavromoustakos</i>	318
Recognition of adamantyl-anchored mannosylated-tripeptides on liposome surface by Concanavaline A <i>A. Štimac, S. Šegota, M. Dutour Sikirić, R. Ribić, L. Frkanec, V. Svetličić, S. Tomić, B. Vranešić, R. Frkanec</i>	320
Synthesis and biological activity of endomorphin-2 analogues containing isoproline, oxopiperadine or oxopyrrolidine ring in position 2 <i>A. Ambo, M. Tanaka, M. Minamizawa, Y. Sasaki</i>	322
Synthesis of novel modified with β2-tryptophan hexapeptide analogues as NOP receptor ligands <i>N. Pavlov, P. Todorov, J. Martinez, M. Calmès, E. Naydenova</i>	324
Tumor cell binding of bombesin-like peptides <i>C. Zikos, C. C. Liolios, C.-E. Karachaliou, E. A. Fragogeorgi, M. Durkan, A. D. Varvarigou, M. Paravatou-Petsotas, E. Livaniou</i>	326
Adapting to substrate requirements: Peptide catalyzed 1,4-addition reactions to α,β-disubstituted nitroolefins <i>J. Duschmalé, H. Wennemers</i>	328
Complex modified silaffin peptides: Versatile tools for efficient enzyme immobilization <i>C. C. Lechner, C. F. W. Becker</i>	330
Novel ureas based on dipeptide analogues as organocatalysts for the asymmetric aldol reaction <i>P. Revelou, C. G. Kokotos, P. Moutevelis-Minakakis</i>	332
Synthesis and a preliminary binding study to a metal surface of peptides characterized by the helicogenic, cyclic disulfide-containing α-amino acid Adt <i>K. Wright, E. Longo, E. Gatto, M. Venanzi, M. Crisma, F. Formaggio, C. Toniolo</i>	334

Polymer-supported thiourea catalysts for enantioselective Michael reaction <i>S. Fotaras, N. Ferderigos, G. Kokotos</i>	336
Primary amine-thioureas based on dipeptides as efficient organocatalysts for Michael reactions <i>D. Linnios, D. Spanou, C. G. Kokotos, G. Kokotos</i>	338
Primary amino acids as organocatalysts for the asymmetric α-amination of aldehydes <i>A. Theodorou, G. N. Papadopoulos, C. G. Kokotos</i>	340
A concise synthesis, docking studies and biological evaluation of <i>N</i>-substituted 5-butylimidazole analogues as potent Angiotensin II receptor blockers <i>G. Agelis, A. Resvani, S. Durdagi, T. Tümová, J. Slaninová, P. Giannopoulos, K. Spyridaki, G. Liapakis, D. Vlahakos, T. Mavromoustakos, J. Matsoukas</i>	342
AZT-systemin conjugate translocation throughout tomato plant <i>M. Dobkowski, P. Rekowski, P. Mucha</i>	344
Click-peptides: Novel 1,2,3-triazole backbone-modified peptidomimetics for tumor targeting <i>I. E. Valverde, A. Bauman, C. Kluba, A. Mascarin, S. Vomstein, M. Walter, T. L. Mindt</i>	346
Synthesis, biological and structural evaluations of cyclic enkephalins with a diversely substituted guanidine bridge <i>Y. Touati-Jallabe, E. Bojnik, B. Legrand, E. Mauchauffée, M.-C. Averlant-Petit, N. N. Chung, P. W. Schiller, S. Benyhe, J. Martinez, J.-F. Hernandez</i>	348
Design and synthesis of non peptide mimetics of the immunodominant 83-99 myelin basic protein epitope (MBP₈₃₋₉₉) <i>V. Tsoulougian, I. Friligou, E. Mantzourani, T. Tselios</i>	350
Design and synthesis of small BACE1 inhibitor peptides <i>Y. Hamada, H. D. Tagad, Y. Kiso</i>	352
Design and synthesis of 3'-peptidyl-tRNA analogues – new tools for investigation of the ribosome function <i>A. G. Tereshchenkov, A. V. Golovin, A. V. Shishkina, N. V. Sumbatyan, A. A. Bogdanov</i>	354
Design, synthesis and antinociceptive activity of novel Endomorphin-2 and Morphiceptin analogues <i>K. Georgiev, T. Dzimbova, H. Nocheva, A. Bocheva, T. Pajpanova</i>	356
Facile and efficient syntheses of structurally modified <i>E</i>-urocanic acid analogs as potent Angiotensin II receptor blockers <i>A. Resvani, G. Agelis, C. Nikolis, G. Liapakis, D. Vlahakos, C. Koukoulitsa, D. Ntountaniotis, T. Mavromoustakos, J. Matsoukas</i>	358
First synthesis of suitably protected PG-Phe-Ψ[P(S)(OX)CH₂]-Gly-PG' as Thiophosphinyl Dipeptide Isoester (TDI) analog and comparative study for selective deprotection <i>S. Vassiliou</i>	360
Fluorescent analogues of SFTI-1 - synthesis and application <i>A. Legowska, M. Wysocka, A. Lesner, M. Filipowicz, A. Sieradzan, M. Pikula, P. Trzonkowski, K. Guzow, K. Rolka</i>	362
Functional mimicry of protein binding sites: Using CLIPS technology in combination with oxime ligation for the reconstruction of <i>discontinuous</i> epitopes <i>L. E. J. Smeenk, H. Hiemstra, J. H. van Maarseveen, P. Timmerman</i>	364

Synthesis and purification of enantiomerically pure <i>N</i>-amino-imidazolin-2-one dipeptide <i>Y. García-Ramos, C. Proulx, C. Camy, W. D. Lubell</i>	366
In vitro assessment of the cytotoxic effects of novel RGD-mimetics <i>K. Georgiev, A. Balacheva, E. Peycheva, M. Georgieva, T. Dzimbova, L. Georgiev, I. Iliev, R. Detcheva, G. Miloshev, T. Pajpanova</i>	368
Microwave assisted solid phase synthesis of urea and urea/amide based foldamers <i>K. Pulka, C. Douat-Casassus, G. Guichard</i>	370
Peptide mediated bacterial drug delivery A mechanistic study of uptake and resistance towards novel antibiotics <i>K. M. Olsen, T. Bentin, P. E. Nielsen</i>	372
Synthesis of oxytocin-steroid chimeric molecule and its visualization on the rat uterus slices <i>M. Jurasek, P. Skopek, M. Flegel, Z. Flegelova, P. Drasar, M. Lebl, T. Kraus, S. Hynie, V. Klenerova</i>	374
Rational design, efficient synthesis and biological evaluation of new <i>N,N'</i>-symmetrically bis-substituted butylimidazole analogs as potent Angiotensin II receptor blockers <i>A. Resvani, G. Agelis, C. Koukoulitsa, A. Afantitis, G. Melagraki, A. Siafaka, E. Gkini, T. Tũmová, K. Spyridaki, D. Kalavrizioti, M.-E. Androutsou, J. Slaninová, G. Liapakis, D. Vlahakos, T. Mavromoustakos, J. Matsoukas</i>	376
Structure activity relationship study of (+)-negamycin with readthrough-promoting activity for duchenne muscular dystrophy chemotherapy <i>A. Taguchi, M. Shiozuka, Y. Yamazaki, F. Yakushiji, R. Matsuda, Y. Hayashi</i>	378
Studies on a reverse-turn scaffold containing a thiourea functionality <i>M. Zervou, K. Paschalidou, S. Fotaras, V. Constantinou-Kokotou, G. Kokotos</i>	380
Synthesis and characterization of modified peptidic nucleic acids (PNAs) toward the production of patterned gold surfaces to assist cellular migration <i>V. Corvaglia, R. Marega, R. Vulcano, D. Bonifazi</i>	382
Synthesis of conjugates of muramyl dipeptide and nor-muramyl dipeptide derivatives with adenosine as potential immunosuppressants <i>M. Samsel, K. Dzierzbicka, P. Trzonkowski</i>	384
Synthesis of CXCR4 specific agonists: SAR studies on the agonist-antagonist transition <i>C. Mona, M. Lefrançois, A. Osborne, M.-R. Lefebvre, N. Heveker, É. Marsault, E. Escher</i>	386
Synthesis of new inhibitors of STAT1 mRNA as attractive compounds in treatment of atherosclerosis <i>M. Wojciechowska, M. Alenowicz, J. Ruczyński, M. Szeląg, K. Sikorski, J. Wesoly, H. Bluijssen, P. Rekowski</i>	388
Synthesis of 4-aminotetrolic acid – a part of triazolic nucleic acid monomers <i>M. Dobkowski, M. Pieszko, P. Rekowski, P. Mucha</i>	390
Synthesis, pharmacological evaluation and conformational investigation of Endomorphin-2 hybrid analogues <i>A. Silvani, F. Airaghi, G. Balboni, E. Bojnik, A. Borsodi, T. F. Murray, G. Lesma, S. Salvadori, T. Recca, A. Sacchetti</i>	392

Targeting pre-miRNA by PNAs: A new strategy to interfere in the miRNA function <i>C. Avitabile, M. Saviano, L.D.D' Andrea, N. Bianchi, E. Fabbri, E. Brognara, R. Gambari, A. Romanelli</i>	394
Tetrahydro-β-carboline-based spirocyclic lactam as potential type II' β-turn somatostatin mimetic <i>G. Lesma, R. Cecchi, F. Meneghetti, M. Musolino, A. Sacchetti, A. Silvani</i>	396
The analogues of SFTI-1 modified in the P₁ position by β- and γ-amino acids and N-substituted β-alanines <i>A. Legowska, R. Lukajtis, M. Filipowicz, M. Legowska, D. Debowski, M. Wysocka, A. Lesner, K. Rolka</i>	398
Transdermal delivery: New approach in anti-hypertensive therapy <i>M. Michalidou, M.-E. Androutsou, T. Tselios, A. Resvani, P. Katsougraki, G. Agelis, D. Vlahakos, J. Matsoukas</i>	400
Trehalose conjugated β-sheet breaker peptides as stabilizers of Aβ monomers <i>F. Attanasio, I. Naletova, V. Muronetz, A. Giuffrida, M. L. Giuffrida, F. M. Tomasello, F. Caraci, A. Copani, G. Pappalardo, E. Rizzarelli</i>	402
Use of substituted oxamide structure in designing pseudo-symmetric HIV protease inhibitors to employ multiple bridging water molecules <i>K. Hidaka, Y. Toda, M. Adachi, R. Kuroki, Y. Kiso</i>	404
Optimization of the PNA-synthesis using different bases for Fmoc-deprotection <i>S. Rawer, K. Braun, R. Pipkorn</i>	406
Alkoxyphenylthio: Novel reducing agent labile cysteine protecting groups <i>T. M. Postma, M. Giraud, F. Albericio</i>	408
Fast and efficient microwave-assisted monitoring of difficult peptide sequences <i>F. Rizzolo, C. Testa, D. Lambardi, M. Chorev, M. Chelli, P. Rovero, A. M. Papini</i>	410
Highly efficient infrared (IR) heating method for SPPS in multiple reactors on the Tribute® UV-IR peptide synthesizer <i>J. P. Cain, M.A. Onaiyekan, C. A. Chantell, C. Donat, A. S. Waddell, R. W. Hensley, M. Menakuru</i>	412
In-water solid-phase peptide synthesis using nanoparticulate Fmoc-amino acids with microwave irradiation <i>K. Hojo, A. Hara, M. Onishi, H. Ichikawa, Y. Fukumori</i>	414
Novel Liquid Phase Peptide Synthesis (LPPS) technology: Elongation using Organic Solvent Nanofiltration (OSN) <i>W. Chen, M. Cristau, A. G. Livingston</i>	416
Return of cotton as a carrier for solid phase synthesis <i>M. Lebl, Z. Flegelova</i>	418
Simplifying native chemical ligation with an N-acylsulfonamide linker <i>F. Burlina, C. Morris, R. Behrendt, P. White, J. Offer</i>	420
Solid phase synthesis and biological evaluation of novel bifunctional opioid agonist – neurokinin-1 antagonist peptidomimetics <i>K. Guillemyn, I. Van den Eynde, A. Keresztes, E. Varga, J. Lai, F. Porreca, E. Miclet, I. Correia, N. N. Chung, C. Lemieux, J. Vanden Broeck, P. W. Schiller, D. Tourwé, S. Ballet</i>	422

A combined biological and theoretical study of prolyl peptides as inhibitors of angiotensin I converting enzyme	
<i>B. Yakimova, M. Rangelov, D. Petkova, B. Tchorbanov, I. Stoineva</i>	424
A platform technology for the emergency response to outbreaks of novel enveloped viruses	
<i>A. Pessi, A. Langella, E. Capitò, S. Ghezzi, E. Vicenzi, G. Poli, T. Ketas, C. Mathieu, B. Horvat, A. Moscona, M. Porotto</i>	426
A stable gonadotropin releasing hormone analogue for the treatment of endocrine disorders and prostate cancer	
<i>T. Katsila, E. Balafas, G. Liapakis, P. Limonta, M. M. Marelli, K. Gkountelias, T. Tselios, N. Kostomitsopoulos, J. Matsoukas, C. Tamvakopoulos</i>	428
Anti-peptide antibodies to synthetic fragments of alpha7-subunit acetylcholine receptor or prion protein protect cells against beta-amyloid toxicity	
<i>A. V. Kamynina, K. M. Holmstrom, D. O. Koroev, O. M. Volpina, A. Y. Abramov</i>	430
Autoantibodies to N-glycosylated peptide sequons in Rett syndrome: The first insight to disclose an autoimmune mechanism	
<i>F. Nuti, F. Real-Fernandez, G. Rossi, S. Pandey, G. Sabatino, C. Tiberi, M. Larregola, S. Lavielle, J. Hayek, C. De Felice, P. Rovero, A. M. Papini</i>	432
Synthesis and formulation design of PEGylated vasoactive intestinal peptide derivative with high metabolic stability	
<i>S. Onoue, M. Kato, T. Matsui, T. Mizumoto, B. Liu, L. Liu, S. Yamada</i>	434
Design and synthesis of potent linear and cyclic Dirucotide analogues	
<i>K. Mavridaki, G. Deraos, S. Deraos, P. Katsougraki, P. Plotas, T. Tselios, A. Mouzaki, J. Matsoukas</i>	436
Design of CXCR4 ligands for diagnostic and therapeutic applications	
<i>O. Demmer, I. Dijkgraaf, E. Gourni, M. Schottelius, A. O. Frank, F. Hagn, L. Marinelli, S. Cosconati, R. Brack-Werner, S. Kremb, U. Schumacher, H.-J. Wester, H. Kessler</i>	438
Development of new anti-prostate cancer agents through SAR studies of potent PACE4 inhibitor	
<i>A. Kwiatkowska, C. Levesque, F. Couture, R. Desjardins, S. Routhier, X.-W. Yuan, F. D'Anjou, W. Neugebauer, R. Day</i>	440
Development of the first orally active NPFF-R antagonist capable of reversing opioid-induced hyperalgesia in rodents	
<i>F. Bihel, S. Schneider, M. Schmitt, J. P. Humbert, K. Elhabazi, E. Laboueyras, G. Simonnet, E. Schneider, B. Petit-Demouliere, F. Simonin, J. J. Bourguignon</i>	442
Enhanced stability and biological properties of rationally designed cyclic analogues of Luteinizing Hormone – Releasing Hormone	
<i>D. Laimou, T. Katsila, J. Matsoukas, A. Schally, K. Gkountelias, G. Liapakis, C. Tamvakopoulos, T. Tselios</i>	444
Enhancement of the antiplatelet activity of novel synthetic peptides in animals receiving low doses of aspirin, in an experimental model of arterial thrombosis	
<i>V. Moussis, C. V. Englezopoulos, K. Rousouli, N. D. Papamichael, V. D. Roussa, C. S. Katsouras, K. K. Naka, A. D. Tselepis, L. K. Michalis, V. Tsikaris</i>	446

HIV-1 epitopes localizing to the membrane proximal external region (MPER) of gp41 and to the V3 loop of gp120: Synthesis and immunization assays <i>I. Kostoula, M. Zhou, M. Hertje, E. Panou, U. Dietrich, M. Sakarellos-Daitsiotis</i>	448
Identification of novel anti-thrombotic cadherin derived peptides <i>K. Golla, I. Stavropoulos, D. C. Shields, N. Moran</i>	450
Improved antiproliferative activity of desmopressin analogs assessed by Ala-scanning <i>M. Pastrian, F. Guzmán, G. Ripoll, J. Garona, M. Pifano, O. Cascone, G. Ciccìa, F. Albericio, D. Gómez, D. Alonso, N. Iannucci</i>	452
Kinetic investigations on amide analogues of isoform 3 of antistasin <i>R. Raykova, D. Danalev, D. Marinkova, L. Yotova, S. Tchaoushev, N. Mahmoud</i>	454
Lebetin peptides: Chemical synthesis, biological activity and structure activity relationships <i>A. Mosbah, N. Marrakchi, M. J. Ganzalez, E. Giralt, M. El Ayeb, D. Bertin, M. Baudy-Floc'h, D. Gímes, H. Darbon, K. Mabrouk</i>	456
Ligands that stabilize the amyloid β-peptide in a helical conformation reduces Aβ toxicity <i>J. Maity, D. Honcharenko, P. P. Bose, J. Johansson, R. Strömberg</i>	458
Novel non-covalent staple peptides <i>R. Z. Vázquez, J. T. Puche, F. Albericio</i>	460
On the mechanism of degradation of oxytocin and its analogues in aqueous solutions - part II <i>K. Wiśniewski, J. Finnman, M. Flipo, R. Galyean, C. D. Schteingart</i>	462
Peptide inhibitors of integrin $\alpha_{\text{m}}\beta_3$ activation <i>V. Moussis, K. Kiouptsi, A. Gourogíanni, V. Koloka, M. Egot, C. Bachelot-Loza, E. Panou-Pomonis, M. Sakarellos-Daitsiotis, D. C. Tsoukatos, V. Tsikaris</i>	464
A proteomic approach to investigate the mechanism of action of anticancer peptides <i>F. Genovese, A. Gualandi, L. Taddia, M. Caselli, G. Ponterini, S. Ferrari, G. Marverti, R. Guerrini, M. Pelà, G. Pavesi, C. Trapella, M.P. Costi</i>	466
Ribavirin-Cell Penetrating Peptides hybrid molecules a promising alternative as inhibitors of multienzyme systems <i>R. Raykova, D. Danalev, L. Yotova, N. Lubin-Germain, J. Uziel, N. Mahmoud, B. Hristova</i>	468
Sequences of ACE-inhibitory precursor peptides from bacterial fermented milk of <i>Camelus dromedarius</i> <i>O. A. Alhaj, H. Brückner, A. S. Al-Khalifa</i>	470
Short bioactive peptides against <i>Plasmodium gallinaceum</i> <i>A. F. Silva, C. Maciel, M. L. Capurro, A. de Miranda, V. X. de Oliveira Junior</i>	472
Synthesis and anticancer activity of new analogs of Vapreotide and RC-121 <i>S. Staykova, E. Naydenova, D. Wesselinova, L. Vezenkov</i>	474
Synthesis and biological evaluation of creatinyl amino acids <i>S. Burov, M. Leko, M. Dorosh, O. Veselkina</i>	476
Synthesis and evaluation of SARS 3CL protease inhibitors using the serine template <i>D. Takanuma, K. Akaji, H. Konno</i>	478
The influence of N-terminal extremity in the antiplasmodial activity of Angiotensin II <i>M. Der Torossian Torres, A. Farias Silva, M. Chamlian, A. J. Barros, C. R. Nakaie, A. Miranda, M. L. Capurro, V. X. de Oliveira Junior</i>	480

Analog of RGD as anti-angiogenic compounds	
<i>T. Thi Phan, S. Abbour, F. Jouan, Y. Arlot-Bonnemains, M. Baudy-Floc'h</i>	482
[¹¹¹In/¹⁷⁷Lu]JMV4168 in the diagnosis and therapy of GRPR-positive tumors	
<i>T. Maina, P.J. Marsouvanidis, L. M. van der Graaf, J. A. Fehrentz, B. Hajjaj, L. Brunel, B. A. Nock, E.P. Krenning, J. Martinez, M. de Jong</i>	484
[¹¹¹In]AT5S & [¹¹¹In]AT6S: Two novel bis-disulfide bridged SS-14 radiopeptides with diverging biological profiles	
<i>A. Tatsi, R. Cescato, T. Maina, B. Waser, E. P. Krenning, M. de Jong, J.-C. Reubi, P. Cordopatis, B. A. Nock</i>	486
Amantadine and rimantadine analogues with peptidomimetics	
<i>K. Chuchkov, R. Georgiev, A. S. Galabov, I. G. Stankova</i>	488
Chemical stability of esters of acyclovir with amino acid and cholic acids	
<i>K. Chuchkov, R. Chayov, I. G. Stankova</i>	490
Comparative evaluation of [¹¹¹In-DOTA]GRP analogs as candidates for GRPR⁺-tumor imaging: Preclinical results	
<i>P. I. Marsouvanidis, T. Maina, E. P. Krenning, M. de Jong, B. A. Nock</i>	492
Synthesis of a cyclic CPP by on-resin side chain-to-side chain cyclisation via CuAAC click chemistry	
<i>F. Reichart, I. Neundorff</i>	494
Neurotensin and oligo-branched peptides decorating liposomes for selective doxorubicin delivery	
<i>D. Tesauro, A. Accardo, C. Falciani, I. Brunetti, B. Lelli, L. Bracci, G. Morelli</i>	496
Non-toxic delivery of siRNA by amphiphilic peptides and silencing of hTERT	
<i>M. Fujii, S. Fujiki</i>	498
Botulinum enzyme retargeted using SNARE protein stapling is capable of selectively silencing neuroendocrine cells	
<i>J. Arsenault, E. Ferrari, D. Niranjana, B. Davletov</i>	500
Short-chain fatty acid acylated daunorubicin-GnRH-III bioconjugates with enhanced cellular uptake, in vitro and in vivo antitumor activity	
<i>R. Hegedüs, M. Manea, E. Orbán, I. Szabó, É. Sipos, G. Halmos, B. Kapuvári, Á. Schulcz, J. Tóvári, G. Mező</i>	502
Stability and biodistribution of three ¹¹¹In-labeled CCK2R-targeting peptides – A comparative study in mice	
<i>A. Kaloudi, P.J. Marsouvanidis, A. Tatsi, E. P. Krenning, M. de Jong, B. A. Nock, T. Maina</i>	504
Synthesis and characterization of a ^{99m}Tc-labeled rhodamine-conjugated angiotensin peptide as a potential cardiac function imaging agent	
<i>S. M. Okarvi</i>	506
Synthesis and <i>in vitro</i> antitumor activity of new GnRH-II conjugates	
<i>I. Szabó, E. Orbán, S. Bősze, B.G. de la Torre, D. Andreu, G. Mező</i>	508
Synthesis and <i>in vitro</i> characterization of peptide conjugates containing new drug candidates effective against <i>Mycobacterium tuberculosis</i> H₃₇Rv	
<i>Z. Baranyai, K. Horváti, N. Szabó, G. Mező, D. Schnöller, C. Péntzes, É. Kiss, F. Hudecz, S. Bősze</i>	510

Synthesis of GSH-linked tyrosinase-activated melanoma prodrugs <i>P. Ruzza, A. Calderan, A. Nassi, L. Quintieri</i>	512
Synthesis, <i>in vitro</i> and <i>in vivo</i> evaluation of new ^{99m}Tc-labeled cyclic RGDfK peptide monocationic complexes <i>A. Calderan, C. Bolzati, B. Biondi, F. Refosco, N. Morellato, N. Salvatore, P. Ruzza</i>	514
The influence of HIV-1 Tat protein sequences on platelet activation <i>P. Stathopoulos, A. A. Dimitriou, E. Malisiova, V. G. Chantzichristos, A. Gatsiou, A. D. Tselepis, V. Tsikaris</i>	516
<i>trans</i>-4-Hydroxyproline analogues of cyclolinopeptide A: Synthesis, conformation and biology <i>J. Katarzyńska, A. Wyczałkowska, K. Huben, M. Zimecki, S. Jankowski, J. Zabrocki</i>	518
An NMR method to discriminate between the 2₀-helix and the 3₁₀-helix of a spacer peptide <i>C. Peggion, M. Crisma, F. Formaggio, C. Toniolo</i>	520
Anti-Freeze Peptides for potential applications in the food industry: Molecular modelling, chemical synthesis and analytical studies <i>H. Z. Kong, C. Evans, C. Perera, V. Sarojini</i>	522
Conformational analysis of liposomal Aβ1-15 derived lipopeptides by Attenuated Total Reflectance Infrared (ATR-IR) spectroscopy <i>M. P. Lopez Deber, D. Mlaki, D. T. Hickman, P. Reis, A. Pfeifer, A. Muhs</i>	524
Conformational similarities and differences of Angiotensin II (AII): AII acetate vs AII TFA salt in solution <i>C. Potamitis, E. Kritsi, A. Resvani, M.-E. Androutsou, P. Plotas, P. Katsougraki, G. Agelis, M. Zervou, P. Zoumpoulakis, J. Matsoukas</i>	526
Consequence of Pro→Ala point mutations for peptide structure and flexibility based on the SAA protein (86-104) fragment mutants <i>M. Maszota, P. Czaplewska, N. Karska, M. Spodzieja, J. Ciarkowski, S. Rodziewicz-Motowidło</i>	528
How ionic liquids interact with peptides <i>C. Mrestani-Klaus, A. Richardt, F. Bordusa</i>	530
Short-chain fatty acid acylated daunorubicin-GnRH-III bioconjugates with enhanced cellular uptake, <i>in vitro</i> and <i>in vivo</i> antitumor activity <i>R. Hegedüs, M. Manea, E. Orbán, I. Szabó, É. Sipos, G. Halmos, B. Kapuvári, Á. Schulcz, J. Tóvári, G. Mező</i>	532
Investigating the structural determinants of neuropeptide 26RFa required for the activation of the receptor GPR103 <i>A. Marotte, L. Guilhaudis, Ganesan, C. Neveu, B. Lefranc, J. Leprince, H. Vaudry, I. Ségalas-Milazzo</i>	534
Local control of the peptide backbone geometry using trifluoromethylated pseudoproline <i>D. Feytens, G. Chaume, G. Chassaing, S. Lavielle, T. Brigaud, J. B. Byun, K. Y. Kang, M. Emeric</i>	536
Model of angiotensin II bound to the AT1 receptor in the lipid bilayer environment <i>M.-T. Matsoukas, T. Tselios</i>	538
Molecular modeling of the Kyotorphin analogues, containing unnatural amino acids <i>N. Dodoff, T. Dzimbova, T. Pajpanova</i>	540

Monitoring peptide folding in membrane-active peptides: A time-resolved spectroscopic study	
<i>E. Gatto, S. Lopez, L. Stella, G. Bocchini, A. Palleschi, C. Serpa, F. Formaggio, C. Toniolo, M. Venanzi</i>	542
Pharmacophore model of cysteine-based $\alpha\beta 1$ integrin ligands based on conformational solution studies	
<i>M. Zervou, C. Potamitis, P. Zoumpoulakis, C. Fotakis, E. Papadimitriou, P. Cordopatis, V. Magafa</i>	544
Probing alpha-synuclein molecular binding sites and their effects on aggregation by NMR spectroscopy	
<i>A. Byrne, M. Bisaglia, L. Bubacco, N. Andersen</i>	546
Synthesis and <i>in vitro</i> activity examinations of 1,4-disubstituted-[1,2,3]triazolyl-containing cyclopeptides, analogs of MT-II, obtained via i to i+5 intramolecular side chain to side chain azide-alkyne cycloaddition	
<i>C. Testa, D. D'Addona, M. Scrima, A. M. D'Ursi, M. L. Dirain, M. Chorev, C. Haskell-Luevano, P. Rovero, A. M. Papini</i>	548
Scaffold discovery by phylomers: A novel CD40L specific scaffold derived from glycyI tRNA synthetase	
<i>S. R. Stone, K. Hoffmann, N. Milech, P. T. Cunningham, M. Kerfoot, S. Winslow, Y.-F. Tan, M. Anastasas, C. Hall, M. Scobie, P. Watt, R. Hopkins</i>	550
Structural studies of nucleophosmin 1 helical peptides	
<i>C. Di Natale, L. De Rosa, M. Leone, P. L. Scognamiglio, L. Vitagliano, D. Marasco</i>	552
Structurally diverse cyclisation linkers impose different backbone conformations in bicyclic peptides	
<i>S. Chen, J. Morales-Sanfrutos, A. Angelini, B. Cutting, C. Heinis</i>	554
Study of peptide structural modifications induced by controlled gamma ray irradiation experiments	
<i>R. F. F. Vieira, D. T. Nardi, N. Nascimento, J. C. Rosa, C. R. Nakaie</i>	556
Temperature dictates the conformational preference of "RGD" in peptide sequence "RIPRGDMP" from kistrin and selects the bio-active conformation	
<i>S. K. Upadhyay, D. Writer, Y. U. Sasidhar</i>	558
The crystal structure of the 14-residue peptaibol trichovirin at atomic resolution	
<i>R. Gessmann, D. Axford, R. L. Owen, H. Brückner, K. Petratos</i>	560
The fully-extended peptide conformation as a molecular bridge: A fluorescence investigation	
<i>F. Formaggio, M. Crisma, G. Ballano, C. Peggion, M. Venanzi, C. Toniolo</i>	562
Vasopressin and vasotocin - NMR studies in a membrane-mimicking environment	
<i>E. A. Lubecka, E. Sikorska, F. Kasprzykowski, D. Sobolewski, J. Ciarkowski</i>	564
β-Phenylproline: Effect of the β-phenyl substituent on the β-turn propensity and pyrrolidine puckering	
<i>P. Fatás, A. I. Jiménez, M. I. Calaza, C. Cativiela</i>	566
4-Methoxybenzyloxymethyl group as a thiol protecting group for cysteine to suppress base-catalyzed racemization in Fmoc chemistry	
<i>H. Hibino, Y. Nishiuchi</i>	568

Synthesis of various peptides using DIC/HOBt and preactivation on the Overture™ robotic peptide library synthesizer <i>J. P. Cain, C. A. Chantell, M. A. Onaiyekan, M. Menakuru</i>	570
A convenient [2+2] cycloaddition-cycloreversion reaction for the synthesis of colorful peptides as new imaging chromophores <i>N. Kramer, R. M. J. Liskamp, D. T. S. Rijkers</i>	572
Access to all β-phenylproline stereoisomers in enantiomerically pure form <i>P. Fatás, A. M. Gil, A. I. Jiménez, M. I. Calaza, C. Cativiela</i>	574
Access to cyclic or branched peptides using bis(2-sulfanylethyl)amido side-chain derivatives of Asp and Glu <i>E. Boll, J. Dheur, H. Drobecq, O. Melnyk</i>	576
Unprecedented side reactions in the SPSS of Cys-containing peptides <i>P. Stathopoulos, S. Papas, C. Pappas, V. Mousis, N. Sayyad, A. Tzakos, V. Tsikaris</i>	578
Amides of antiviral drug oseltamivir with antioxidant active aminoacids: Synthesis and biological activities <i>M. Chochkova, G. Ivanova, A. Galabov, T. Milkova</i>	580
An expedient synthesis of guanidine-bridged cyclopeptides <i>X. Yang, H. Lin, D. Wang</i>	582
Aryl hydrazine resin as a tool in the synthesis of C-terminal modified peptides – optimization of oxidation conditions <i>I. Małuch, A. Walewska, A. Kwiatkowska, B. Lammek, R. Day, A. Prahł</i>	584
Catalytic conversion of tertiary amides of amino acids to amines <i>E. Barbayanni, G. Kokotos</i>	586
Chemical stability and structure – activity relationship studies of novel cyclic NGR peptides <i>G. Mező, K. Enyedi, A. Czajlik, I. Szabó, R. Hegedüs, Z. Majer, E. Lajkó, L. Kőhidai, A. Perczel</i>	588
Clickable peptides and their attachment to oligonucleotides <i>M. Hocharenko, M. Alvira, P. Steunenber, R. Strömberg</i>	590
Comparison of alternative deprotection reagents to piperidine for the synthesis of a poly-alanine peptide on the Tribute® peptide synthesizer <i>M. A. Onaiyekan, J. P. Cain, C. A. Chantell, M. Menakuru</i>	592
Cyclolinopeptide A analogs modified with pipercolic acid <i>J. Olejnik, P. Kossakowska, K. Huben, J. Artym, M. Zimecki, J. Zabrocki, S. Jankowski</i>	594
Synthesis of the first Multivalent Epitope containing N^ε-(1-deoxy-d-fructosyl)lysyl as diagnostic tool for diabetes <i>O. Monasson, F. Rizzolo, P. Traldi, A. Lapolla, M. Chorev, P. Rovero, A. M. Papini</i>	596
Enantiopure trifluoromethylated pseudoprolines: Synthesis and incorporation in small peptides <i>J. Pytkowicz, J. Simon, N. Lensen, E. Chelain, G. Chaume, T. Brigaud</i>	598
FastBoc synthesis of ACP (65-74) using preactivation on the Overture™ robotic peptide library synthesizer <i>J. P. Cain, C. A. Chantell, M. A. Onaiyekan, M. Menakuru</i>	600

Resin via click chemistry to apply in SPPS	
<i>V. Castro, H. Rodriguez, F. Albericio</i>	602
Fully automated click cyclization of a cancer-targeting peptide on the Prelude® peptide synthesizer	
<i>J. P. Cain, M. A. Onaiyekan, C. A. Chantell, M. Menakuru</i>	604
Manufacture of optically active D-allo-threonine from L-threonine by ARCA technology	
<i>E. S. Jeong, J. Maeng, Y. S. Ahn, M. Kim, K. M. Kim, H. Yoon, H. Lee</i>	606
Methodological study of the peptide coupling of N-deactivated proline surrogate trifluoromethylated pseudoprolines	
<i>G. Chaume, D. Feteyns, P. Lesot, E. Miclet, S. Lavielle, G. Chassaing, T. Brigaud</i>	608
New functionalized aza-β³-amino acids for click-chemistry	
<i>S. Abbour, M. Baudy-Floc'h</i>	610
N-Oligoethyleneglycol cyclic peptides	
<i>A. I. Fernández-Llamazares, J. Spengler, F. Albericio</i>	612
Peptidyl-vinylketones as a novel class of inhibitors of the cysteine protease caspase-3	
<i>K. Holland-Nell, J. Rademann</i>	614
Ring-closing metathesis of astressin-derived peptides as novel corticotropin releasing factor antagonists	
<i>A. H. K. Al Temimi, R. M. J. Liskamp, D. T. S. Rijkers</i>	616
Simple and efficient solid-phase preparation of azido-peptides	
<i>M. B. Hansen, T. H. M. van Gulp, J. C. M. van Hest, D. W. P. M. Löwik</i>	618
SPPS of N-glycosylated Multivalent Epitopes to detect autoantibodies in Multiple Sclerosis patients' sera	
<i>C. Tiberi, G. Sabatino, M. Di Pisa, G. Rossi, P. Rovero, A. M. Papini</i>	620
Synthesis and preliminary characterization of a nitronyl nitroxide α-amino acid	
<i>K. Wright, J. Scola, A. Toffoletti, F. Formaggio, C. Toniolo</i>	622
Synthesis of a protected derivative of (2R,3R)-β-hydroxyaspartic acid suitable for Fmoc-based solid phase peptide synthesis	
<i>F. Boyaud, B. Viguiet, N. Inguibert</i>	624
First synthesis of both pure diastereomeric N⁶-(1,2-dithiolane-(3R or S)-pentanoyl)-N²-Fmoc-L-Lys-OH for Fmoc/tBu SPPS	
<i>C. Rentier, F. Nuti, M. Chelli, G. Pacini, P. Rovero, C. Selmi, A. M. Papini</i>	626
Synthesis and polymerization of silaproline targeting PPII structure	
<i>C. Martin, J. Martinez, F. Cavelier</i>	628
Design and synthesis of cross-linked peptide probes for the development of an in vitro diagnostics for Coeliac Disease	
<i>M. Di Pisa, G. Sabatino, S. Pascarella, M. Chelli, P. Rovero, A. M. Papini</i>	630
Synthesis of O-glycopeptides using N, N²-isopropylidene dipeptide derivatives	
<i>H. Kobayashi, T. Inazu</i>	632
Synthetic approaches for the development of cell penetrating conjugates linked through thioether or disulfide bond	
<i>E. Sereti, S. Papas, A. Dimitriou, C. Papadopoulos, V. Moussis, A. D. Tselepis, V. Tsikaris</i>	634

Synthetic study of Callipeltin B analogues and its cytotoxicity <i>M. Kikuchi, Y. Watanabe, M. Tanaka, K. Akaji, H. Konno</i>	636
Templating cyclic β-tripeptides: Combination of inhibitor and recognition motifs with fluorescence labeling and cell penetrating units <i>H. Radzey, F. Stein, U. Diederichsen</i>	638
Three-component synthesis of neoglycopeptides using a Cu(II)-triggered aminolysis of peptide hydrazide resin and azide-alkyne cycloaddition sequence <i>J.-P. Ebran, N. Dendane, O. Melnyk</i>	640
Total chemical synthesis of calstabin 2 protein <i>M. Jullian, O. Melnyk, G. Ferry, J. A. Boutin, L. Ronga, K. Puget</i>	642
Statistical analysis of amino acid fingerprint to characterize protein binders in works of art <i>G. Sabatino, F. Di Pisa, M. Potenza, L. Rosi, L. Dei, A. M. Papini</i>	644
Use of internal references for the quantitative HPLC-UV analysis of solid-phase reactions <i>J. Spengler, A. I. Fernández-Llamazares, F. Albericio</i>	646
β_2-Microglobulin: A “difficult” protein <i>S. Abel, M. Beyermann</i>	648
A synthetic 83 amino acid long peptide corresponding to the minimal metacaspase catalytic domain induces cell death in <i>Leishmania major</i> <i>C. Servis, H. Zalila, I. Gonzalez, L. Lozano, N. Fasel</i>	650
Condensation of peptides with dienophiles <i>L. Sklyarov, I. Nazimov, R. Ziganshin, V. Zaikin, S. Andreev</i>	652
Development of a novel structural vaccinology strategy for epitope discovery for the <i>Burkholderia pseudomallei</i> OppA antigen <i>A. Gori, C. Peri, R. Longhi, G. Colombo</i>	654
Development and validation of a UPLC- MS analytical method for the control of the conjugation of [Lys-Gly]₅-MOG₃₅₋₅₅ with mannan <i>M.-E. Androutsou, I. Friligou, J. Matsoukas, T. Tselios</i>	656
Cell-Penetrating Peptide mimetics with 1,2-fused isoxazoles and phthalazines as anchor heterocycles of α- or β-peptide sequences <i>P. G. Tsoungas, G. N. Pairas, P. Cordopatis</i>	658
Keratin and collagen models as a tool in the deterioration of works of art <i>E. Fotou, I. Kostoula, S. Zevgiti, E. Panou-Pomonis, G. Panagiaris, M. Sakarellos-Daitsiotis</i>	660
New biphasic solvent systems for the purification of non-ionic synthetic hydrophobic peptides by Centrifugal Partition Chromatography <i>N. Amarouche, L. Boudesoque, M. Giraud, A. Butte, F. Quattrini, J.-H. Renault</i>	662
Spectroscopic investigation of the interaction of curcumin with the β-amyloid peptide of Alzheimer’s disease <i>D. Benaki, K. Stamatakis, L. Leondiadis, E. Mikros, M. Pelecanou</i>	664
Synthesis and anticancer activities of lipophilic somatostatin derivatives <i>H. Inazumi, T. Suyama, D. Takami, K. Hidaka, A. Miyazaki, T. Yokoi, I. Kuriyama, H. Yoshida, Y. Mizushima, Y. Tsuda</i>	666

Synthesis of an anthraquinone type compound conjugated to the immunodominant 35-55 myelin oligodendrocyte glycoprotein (MOG₃₅₋₅₅)	
<i>I. Friligou, A. Tapeinou, J. Matsoukas, T. Tselios</i>	668
Design and synthesis of N-methyl derivatives of urotensin-II	
<i>F. Merlino, S. Di Maro, A.M. Yousif, P. Campiglia, S. Meini, P. Santicioli, C. A. Maggi, E. Novellino, P. Grieco</i>	670
Peptide-epitope mapping and reactivity of the autoantigen Aquaporin-4	
<i>H. Alexopoulos, E. I. Kampylafka, H. M. Moutsopoulos, M. C. Dalakas, A. G. Tzioufas</i>	672
Spectroscopic studies and in vitro functional effect of the chiral complexes of dinuclear rhodium	
<i>Z. Majer, G. Szilvagy, T. Sipocz, N. Szoboszlai, E. Orban, S. Bosze</i>	674
Chiroptical spectroscopic investigation on diamide peptide models	
<i>K. Knapp, M. Gorecki, M. Hollosi, E. Vass, Z. Majer</i>	676
Role of cation-pi interaction in the photolysis of disulphide bridge containing cyclic model peptides	
<i>E. Illyes, K. Knapp, G. Csik, Z. Majer</i>	678
Antimicrobial peptides as novel delivery vehicles for genetic antibiotics	
<i>G. Bonke Seigan, H. Franzyk, P. E. Nielsen</i>	680
Solid-phase syntheses of galanins [GALs] and their fragments with different strategies, analytical controls, conformations and new biological studies	
<i>L. Balaspiri, J. Toth, G. Blazso, Z. Majer, G.K. Toth, E. Lajko, L. Kohidai, I. Szabo, G. Mezo, L. Virag, G. Papp, A. Varro</i>	682

**Proceedings of the
Thirty-Second European Peptide Symposium
September 2-7, 2012
Athens, Greece**

Table 1: Examples of grafted cyclotides

Cyclotide	Bioactive epitope	Disease indication	Reference
kalata B1	anti-angiogenic	cancer	2008 [9]
MCoTI-II	protease inhibitor	infectious disease	2008 [10]
MCoTI-II	protease inhibitors	inflammatory conditions	2009 [11]
kalata B1	angiogenic	wound healing	2011 [12]
kalata B1	bradykinin antagonist	inflammatory pain	2012 [13]

In addition to recent advances in the use of the cyclotides as pharmaceutical grafting frameworks, substantial advances have also been made in understanding the mode of action of naturally occurring cyclotides. Briefly, cyclotides exert their insecticidal actions by binding to membranes. Recent studies show that they bind to phosphatidylethanolamine containing lipids specifically and subsequently insert into membranes, leading to pore formation and membrane disruption. Although much remains to be discovered about cyclotides, the studies described herein on natural and ‘grafted’ cyclotides provide a foundation for future applications in medicine and agriculture.

Acknowledgments

Work in my laboratory on cyclotides is supported by grants from the Australian Research Council (DP0984390) and the National Health and Medical Research Council (APP1009267 and APP1026501). I sincerely thank my students, staff and colleagues for their invaluable contributions to the studies described in the cited references and the European Peptide Society for the Rudinger Memorial Award associated with this presentation.

References

- [1] Craik D J: *Science*, **2006**, *311*, 1561.
- [2] Gruber C W, Elliot A, Ireland D C, Delprete P G, Dessein S, Göransson U, Trabi M, Wang C K, Kinghorn A B, Robbrecht E F, Craik D J: *The Plant Cell*, **2008**, *20*, 2471.
- [3] Craik D J, Daly N L, Bond, T, Waine C: **1999**, 294, 1327.
- [4] Henriques S T, Craik D J: *Drug Discovery Today* **2010**, *15*, 57.
- [5] Barbata B L, Marshall A T, Gillon A D, Craik D J, Anderson M A: *PNAS* **2008**, *105*, 1221.
- [6] Gran L: *Lloydia* **1973**, *36*, 174.
- [7] Gustafson K R, Sowder R C I, Henderson L E, Parsons I C, Kashman Y, Cardellina J H I, McMahon J B, Buckheit R W J, Pannell L K, Boyd M R: *J Amer. Chem. Soc.* **1994**, *116*, 9337.
- [8] Tam J P, Lu Y A, Yang J L, Chiu K W: *PNAS* **1999**, *96*, 8913.
- [9] Gunasekera S, Foley F M, Clark R J, Sando L, Fabri L J, Craik D J, Daly N L: *J. Med. Chem.* **2008**, *51*, 7697.
- [10] Chan L Y, Gunasekera S, Worth N F, Le S-J, Clark R J, Campbell J H, Craik D J, Daly N L: *Blood* **2011**, *118*, 6709.
- [11] Thongyoo P, Roque-Rosell N, Leatherbarrow R J, Tate E W: *Org & Biomol. Chem.*, **2008**, *6*, 1462.
- [12] Thongyoo P, Bonomelli C, Leatherbarrow R J, Tate E W: *J Med. Chemistry Letts.* **2009**, *52*, 6197.
- [13] Wong C T T, Rowlands D K, Wong C H, Lo T W C, Nguyen G K T, Li H Y, Tam J P: *Angewandte Chemie* **2012**, *51*, 5620.

From microwave heating to control of nano-scale self-assembly in peptide science

Knud J. Jensen

University of Copenhagen, Faculty of Science, Department of Chemistry

E-mail: kjj@chem.ku.dk

Introduction

In recent years my research group has followed several different lines of research which, however, are interconnected and mutually enabling. This combines synthetic methodology, including new reagents[1] and the use of microwave heating, with chemical biology and medicinal chemistry, and finally the study of self-assembly at the nano-scale and application of nano-scale phenomena for detection of biological recognition. Here I wish to highlight three of these projects.

Results and Discussion

Microwave instruments offer the prospect of fast and precise heating in solid-phase synthesis. However, for this to be widely adapted, there is a need not only for well-documented applications but also for systematic studies.[2] In reality, peptide synthesis is often performed in dilute solutions of water, as DMF and NMP are very hygroscopic. This fact appears to have been underappreciated, at least in academic peptide chemistry. Very recently, we addressed the questions what the stabilities of *coupling reagents* are as a function of residual water and what the stabilities of their *activated esters* are as a function of residual water and temperature.[3] For example, we found that COMU is more labile than HBTU and HATU, and that the half-life of Oxyma esters decreases significantly with increasing temperature. However, when this is taken into consideration, COMU and the resulting Oxyma esters can be very useful in peptide synthesis. Another question is how the balance between the main reaction and possible side-reactions is affected by an increase in temperature. We have shown that the formation of the lactam of Fmoc-Arg(Pbf)-OH becomes a dominant side-reaction reaction at higher temperatures.[4]

Site-selective strategies for post-translational modification of peptides and proteins are essential tools for many areas of research in the life sciences, yet remain a chemical challenge due to the multiplicity of functional groups present. There are powerful chemoselective reactions, however, they aim at introducing only one functionality at each reaction site. We have developed a one-pot, three-component dual-functionalization of peptides or proteins based on a 1,3-dipolar cycloaddition between a functionalized maleimide, an N-hydroxylamine and a peptide or protein with an N-terminal serine residue at the N-terminus, which is selectively oxidized to an aldehyde.[5] Many common moieties for labeling, e.g. fluorophores and PEG-chains, are commercially available as maleimides. Nitrones were easily obtained by condensation of peptide aldehydes and primary N-hydroxylamines under aqueous conditions. The chemoselective 1,3-dipolar cycloaddition reaction between the peptide nitron, and a functionalized maleimide proceeded in aqueous solution at room temperature or with gentle heating, which provided the stable

isoxazolidine product. We envision that this 'one site - two functions' method can be used widely to introduce two separate moieties.

Self-assembly of peptides and proteins mediated by metal ions is ubiquitous in nature. Novel strategies for direct control of self-assembly by an abiotic metal ion ligand in a peptide or protein offers the prospect of selectivity over side-chain driven self-assembly. Insulin binds Zn^{II} to form a hexamer, which is important for its function. We have re-engineered an insulin variant to control its self-assembly by covalent attachment of 2,2'-bipyridine. The use of Fe^{II} provided chemoselective binding over the native site, forming a homo-trimer in a reversible manner, which was easily followed by the characteristic color of the Fe^{II} complex. This provided the first well-defined insulin trimer and the first insulin variant where self-assembly can be followed visually.[6] We are currently expanding this for the construction of higher-ordered structures. In a separate strategy, we have used the abiotic self-segregation of perfluorous groups to direct insulin's self-assembly in a manner that depended on the size of the perfluoroalkyl moiety appended to insulin.[7]

Acknowledgments

A rewarding aspect of scientific research is the opportunity to collaborate with gifted people from around the world. I would like to acknowledge my talented co-workers, as well as my collaborators and my former mentors for their contributions and inspiration over the years. I am also very appreciative of Professor George Kokotos' dedicated work in organizing the successful 32nd European Peptide Symposium, where the Zervas award was presented.

References

- [1] Review: Boas, U.; Brask, J.; Jensen, K. J. *Chem. Rev.*, **2009**, *109*, 2092.
- [2] Review: Pedersen, S. L.; Tofteng, A. P.; Malik, L.; Jensen, K. J. *Chem. Soc. Rev.*, **2012**, *41*, 1826.
- [3] Tofteng, A. P.; Pedersen, S. L.; Staerk, D.; Jensen, K. J. *Chem. Eur. J.*, **2012**, *18*, 9024.
- [4] Roodbeen, R.; Pedersen, S. L.; Hosseini, M.; Jensen, K. J. *Eur. J. Org. Chem.*, in 2012, *in press*.
- [5] Munch, H. K.; Rasmussen, J. E.; Popa, G.; Christensen, J. B., Jensen, K. J. *submitted*.
- [6] Munch, H. K.; Heide, S. T.; Christensen, N. J.; Hoeg-Jensen, T.; Thulstrup, P.W.; Jensen, K. J. *Chem. Eur. J.*, **2011**, *17*, 7198.
- [7] Malik, L.; Nygaard, J.; Høiberg-Nielsen, R.; Arleth, L.; Hoeg-Jensen, T.; Jensen, K. J. *Langmuir*, **2011**, *28*, 593.

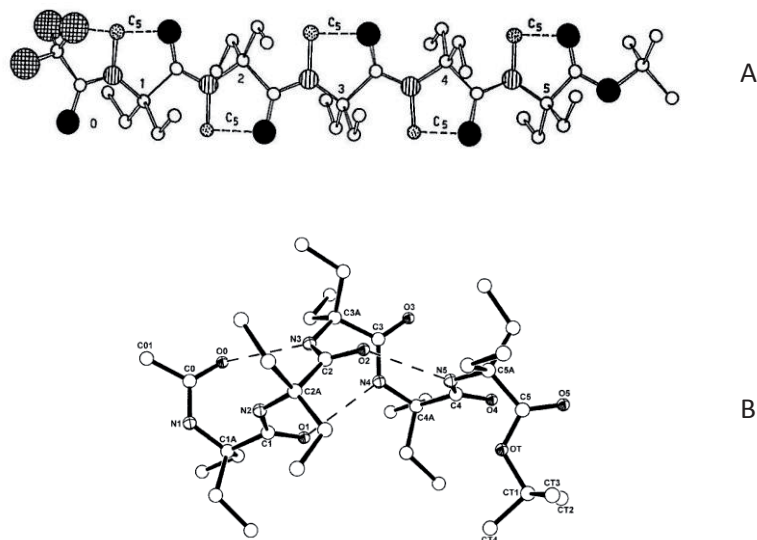


Fig. 1. X-Ray diffraction structures of : (A) Tfa-(Deg)₅-OtBu [9] and (B) Ac-(Deg)₅-OtBu [10]. The intramolecular C=O...H-N H-bonds are represented as dashed lines.

References

- [1] Toniolo, C.; Crisma, M.; Formaggio, F.; Peggion, C. *Biopolymers (Pept. Sci.)* **2001**, *60*, 396.
- [2] Crisma, M.; Formaggio, F.; Moretto, A.; Toniolo, C. *Biopolymers (Pept. Sci.)* **2006**, *84*, 3.
- [3] Tanaka, M.; Imawaka, N.; Kurihara, M.; Suemune, H. *Helv. Chim. Acta* **1999**, *82*, 494.
- [4] Imawaka, N.; Tanaka, M.; Suemune, H. *Helv. Chim. Acta* **2000**, *83*, 2823.
- [5] Crisma, M.; Moretto, A.; Peggion, C.; Panella, L.; Kaptein, B.; Broxterman, Q. B.; Formaggio, F.; Toniolo, C. *Amino Acids* **2011**, *41*, 629.
- [6] Formaggio, F.; Crisma, M.; Peggion, C.; Moretto, A.; Venanzi, M.; Toniolo, C. *Eur. J. Org. Chem.* **2012**, 167.
- [7] Formaggio, F.; Crisma, M.; Ballano, G.; Peggion, C.; Venanzi, M.; Toniolo, C. *Org. Biomol. Chem.* **2012**, *10*, 2413.
- [8] Peggion, C.; Crisma, M.; Toniolo, C.; Formaggio, F. *Tetrahedron* **2012**, *68*, 4429.
- [9] Benedetti, E.; Barone, V.; Bavoso, A.; Di Blasio, B.; Lelj, F.; Pavone, V.; Pedone, C.; Bonora, G. M.; Toniolo, C.; Leplawy, M. T.; Kaczmarek, K.; Redlinski, A. *Biopolymers* **1988**, *27*, 357.
- [10] Crisma, M.; Formaggio, F.; Toniolo, C., manuscript in preparation.

Tumor targeting with peptides in four decades – from initial concepts to an array of highly sophisticated methods

Alex N. Eberle

*Department of Biomedicine, University Hospital and University Children's Hospital Basel,
University of Basel and Collegium Helveticum, ETH Zurich, Switzerland*

E-mail: Alex.N.Eberle@unibas.ch

Introduction

The first steps towards tumor targeting with peptides date back to the early 1970s when biologically active radiopeptides containing tritium were prepared and tested for specific (receptor-mediated) accumulation in tumors [1]. It took almost two more decades to understand expression, structure and function of receptors and to design novel targeting peptide ligands containing diagnostic or therapeutic agents with which the specificity needed for medical application could be obtained [2, 3]. In the meantime radiopeptides have become routine tools in nuclear oncology not only for tumor localization and staging (e.g. by PET) [4], but also for treatment, particularly of certain neuroendocrine tumors [5].

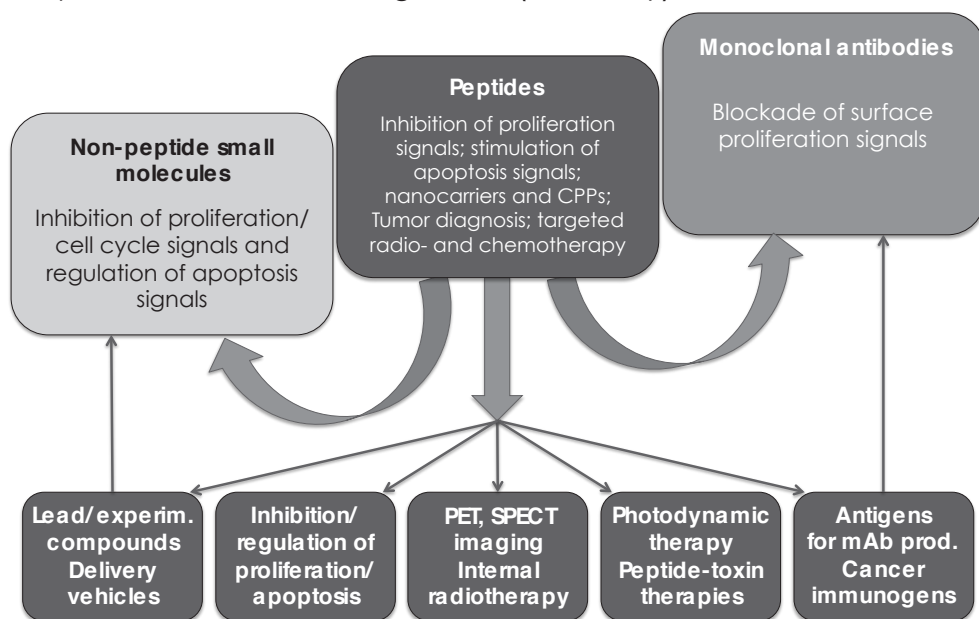
In analogy to immunotoxins, peptide-toxin conjugates for cancer treatment also have a long history with many preclinical and clinical trials but with slow progress towards clinical application; however, the recently reported D-Lys⁶-LHRH-doxorubicin appears to become a promising candidate for therapy of ovarian and endometrial cancers [6]. These and other studies with monomeric peptide conjugates have been complemented by an array of sophisticated chemical multimeric constructs and carriers in the past decade, with the aim of increasing the targeting specificity and potency ("magic bullet") or sensitivity (imaging): peptide multimers with fluorophores or other diagnostic or therapeutic principles, nanoparticle-peptide and liposome-peptide complexes with specific (programmable) characteristics. All these approaches require carefully designed synthetic peptides.

Results and Discussion

A large number of peptides conjugated to chelators (e.g. DOTA or NOTA; MAG₃, GSCG or HYNIC) for radiometals (e.g. ¹¹¹In, ⁶⁴Cu, ⁶⁸Ga, or ¹⁷⁷Lu; ^{99m}Tc) suitable for receptor-mediated tumor targeting have become available for (potential) diagnostic use in specialized clinics. By contrast, application of therapeutic radionuclides (e.g. ⁹⁰Y or ¹⁷⁷Lu; ^{186/188}Re) remains restricted to specialized centers. The disadvantages of therapeutic radiopeptides are the extremely long approval/registration procedures, their non-specific accumulation in healthy tissues (kidneys, liver, intestinal tract), and the insufficient residence time of radioisotopes in tumor cells which may partly be solved by a dual targeting approach [7].

At present, approved (non-radioactive) drugs for clinical use in tumor therapy are in their majority small molecules (for intracellular targets) or monoclonal antibodies (for cell surface targets). Specific delivery of peptides targeting intracellular signalling molecules in tumor tissues is more complex and requires selective cell-penetrating peptides or other vehicles. A greater potential for peptides in cancer treatment lies in their use as vehicles for extra- or intracellular delivery of toxins or sensitizers for, e.g., photodynamic therapy.

Peptides in cancer management (summary)



In conclusion, several hundred peptides have been identified as potential candidates for tumor targeting, although to date only a fraction thereof has been tested in vitro or in vivo in animal models. Apart from peptides for tumor diagnosis and targeted radio- and chemotherapy, they include peptides that inhibit proliferation signals or stimulate apoptosis signals, or serve as antigens for the generation of specific anti-tumor antibodies or as lead structures for small molecules. In the next few years, particular attention will be drawn to multifunctional nanoparticle-based ‘theranostics’ but also to suitable in vivo test systems that should reflect the human situation of metastasis and cellular heterogeneity of tumors.

Acknowledgments

The author wishes to thank the Swiss National Science Foundation and the Swiss Cancer League for their longstanding support.

References

- [1] Eberle, A.N.; Froidevaux, S. *J. Mol. Recognit.* **2003**, *16*, 248-254.
- [2] Eberle, A.N.; Mild, G. *J. Recept. Signal. Transd.* **2009**, *29*, 1-37.
- [3] Fani, M.; Mäcke, H.R. *Eur. J. Nucl. Med. Mol. Imaging* **2012**, *39* Suppl., S11-S30.
- [4] Breeman, W.A.; de Blois, E.; Sze Chan, H.; Konijnenberg, M.; Kwekkeboom, D.J.; Krenning, E.P. *Semin. Nucl. Med.* **2011**, *41*, 14-21.
- [5] Reubi, J.C.; Mäcke, H.R.; Krenning, E.P. *J. Nucl. Med.* **2005**, *46* Suppl. 1, 67S-75S.
- [6] Engel, J.B.; Schally, A.V.; Buchholz, S.; Seitz, S.; Emons, G.; Ortmann, O. *Arch. Gynecol. Obstet.* **2012**, *286*, 437-432.
- [7] Kluba, C.A.; Bauman, A.; Valverde, I.E.; Vomstein, S.; Mindt, T.L. *Org. Biomol. Chem.* **2012**, *10*, 7594-7602.

D-Amino acid adhesion peptides by combinatorial selection: Control of cellular growth on inert surfaces

Morten Meldal, Boqian Wu, Frederik Diness, Thomas Nielsen

Nano Science Center, Department of Chemistry, University of Copenhagen, Denmark

E-mail: meldal@nano.ku.dk

Introduction

Adhesion of cells to surfaces through natural adhesion molecules that interact specifically with cell surface receptors have been investigated by many groups.[1] We were interested in developing adhesion directly through non-invasive interaction directly with the lipids of the cell membrane and in this manner provide a metabolically stable support for cellular proliferation and growth. In order to provide biological stability to the adhesion molecules we selected D-amino acids as building blocks and employed combinatorial assembly of a D-amino acid hexapeptide library on non-adhesive PEGA resin.

Results

U2OS cells were seeded on the peptide split mix library and beads adhering cells were isolated and characterized. HEK293 suspension cell culture was seeded on the hits and the best adhesion peptides for HEK293 cells were identified by amino acid sequencing. When a hexapeptide L-amino acid library was used as control a significantly reduced number of active adhesion molecules were isolated, probably due to proteolytic cleavage of surface accessible peptides by membrane bound or excreted proteases from the cells. The active substances showed some sequence similarity and a x-basic-lipo.-basic-hydro.-basic sequence e.g. arirqr. The adhesion was significant but not completely stable to mechanical agitation. Therefore a second library was synthesized which was representing all amino acid combinations from the active structures in the first library (55.000 compounds). HEK293 cells, constitutively expressing GFP were seeded and adhesion was observed to most of the PEGA₁₉₀₀ beads of the library. The library with fluorescent cells attached was agitated by stirring with two magnets in a sample cup of a COMPAS bead sorter (Union Biometrica) to impose a shear force to the attached cells. After 5 min of stirring cells on most beads had detached and sorting was initiated to isolate only those beads with extreme adhesion. The beads were rinsed and cells detached through treatment with 2% aq. TFA. The peptides were cleaved off the beads and analyzed by ESI MS-MS. The presence of many positive charges resulted in multi-charged ions preventing direct structure readout. To this end software was developed which constructed the virtual library of 55000 compounds and their fragmentation spectra. A least squares fitting of the observed to the virtual fragmentation pattern combined with accurate mass determination allowed us to identify all the isolated compounds. The consensus pattern was now quite clear and the best compounds were k l h/y r i/v r; i.e. different from the results of the first screen.

The peptide H-k l h r i r a-OH was modeled by molecular dynamics using MOE (CCG) in water. A clear picture emerged from the modeling in which two arginines and one lysine

are stabilized by histidine on one side of the molecules while the leucine and isoleucine residues interact and form a lipophilic patch on the other side.

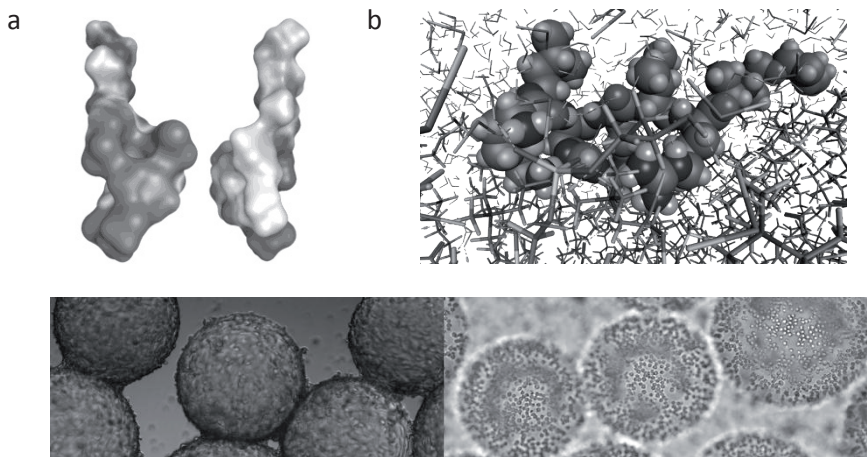
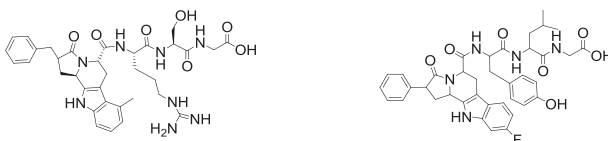


Figure 1. Molecular modeling in water (removed) of the D-amino acid adhesion peptide k l h r i r a. a) Hydrophilic patch stabilized by histidine and hydrophobic patch. b) The peptide was docked into the lipid membrane showing main interaction between phosphate diester head groups and basic side chains. The lipophilic sidechains did not insert in the lipid. Several cell lines including HEK293, Jurkat, and E. Coli (not shown) adhered to these beads.

The adhesion molecules were used in a cells-on-beads assay for cells expressing GPCR's. Initial studies used melanocortin-4 receptor and e-YFP by a dual vector transfection. Cells were active for a 3 week period, by which time they lost most fluorescence upon activation. Transfected cells were seeded on beads that carried a library of 34.500 different small molecules derived through intermolecular cascade reactions of peptide aldehydes as previously reported.[2] Sub- μ M MCR4 ligands were isolated and resynthesized and studied in solution on MC4R, e. g. the ligands below.



References

- [1] Alpin, E. A., Howe, A. K., and Juliano, R. L. (1999). *Current Opinion in Cell Biology*, 11, 737-744.
- [2] Nielsen, T. E.; Meldal, M. *J. Org. Chem.*, **2004**, 69, 3765-3773.

Ion Mobility- and Affinity- Mass Spectrometry: New tools for elucidating structures and pathways of “misfolding” - aggregating proteins

**Michael Przybylski¹, Kathrin Lindner¹, Camelia Vlad¹, Nick Pierson²,
Christiaan Karreman¹, Stefan Schildknecht¹, Marcel Leist¹, Nick
Tomczyk³, James Langridge³, Thomas Ciossek⁴, Alina Petre^{1,5}, Michael
Gross⁵, Bastian Hengerer⁴, David Clemmer²**

¹Departments of Chemistry and Biology, University of Konstanz, 78457 Konstanz, Germany; ²Indiana University, Department of Chemistry, Bloomington, IN, USA; ³Waters Ltd., Micromass Atlas Park, Manchester, UK; ⁴Boehringer Ingelheim Pharma GmbH, ZNS Research, Biberach, Germany; ⁵Department of Chemistry, Washington University St. Louis, St. Louis, USA

Introduction

A large variety of cellular processes are based on the formation and dynamics of multi- and supramolecular protein assemblies, and several diseases, previously thought to be unrelated, such as cancer and neurodegenerative diseases, are characterised by “misfolded” protein aggregates. Chemical structures and reaction pathways of pathophysiological aggregates are only poorly characterised and understood at present. “Soft-ionisation” mass spectrometry (MS), such as HPLC-electrospray-MS, is often unsuitable to direct analysis of reaction pathways and intermediates in aggregation. Recently, *ion mobility- MS* (IM-MS) has been emerging as a new tool for analysis of protein oligomerization- aggregation [1, 2] due to its concentration-independent gas phase separation capability.

Results and Discussion

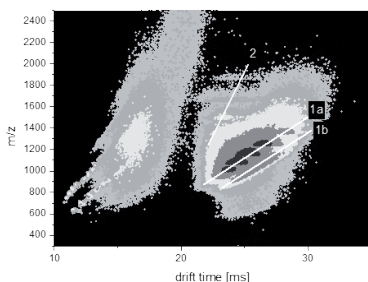
First applications of IM-MS to *in vitro* oligomerization products of α -synuclein (α Syn), a key protein for Parkinson’s Disease (PD), enabled hitherto unknown degradation and aggregation products to be identified. Studies of the *in vitro* oligomerization- aggregation of α Syn provided the first identification of specific autoproteolytic fragments, previously observed by gel electrophoresis but not identified [1]. A highly aggregating fragment, α Syn(72-140), formed by cleavage in the central aggregation domain of α Syn, was prepared by chemical synthesis and recombinant expression and showed substantially faster oligomerization and aggregation, and increased neurotoxicity compared to the intact protein. IM-MS Drift time profiles provide the analysis of conformationally different forms upon α Syn incubation *in vitro* (Fig. 1). Recently, the development and application of combined online affinity-MS [3] enabled the direct structure identification of α Syn polypeptides from brain material. These results indicate ion mobility- MS and affinity- MS as powerful tools for the molecular elucidation of structures and intermediates involved in polypeptide aggregation. Moreover, they provide a basis for (i), the detailed study of oligomerization- aggregation pathways, and (ii), the design of peptides capable of inhibiting or modifying aggregation.

Acknowledgments

This work has been supported by EU-Marie Curie IRSES Grant “MSLife”.

References

- [1] Vlad, C.; Lindner, K.; Karreman, C.; Schildknecht, S.; Leist, M.; Tomczyk, N.; Rontree, J.; Langridge, J.; Danzer, K.; Ciossek, T.; Petre, A.; Gross, M.L.; Hengerer, B.; Przybylski, M. *ChemBiochem.* **2011**, *12*, 2740.
- [2] Vlad, C.; Iurascu, M.I.; Slamnoiu, S.; Hengerer, B.; Przybylski, M. In: *Experimental Tools for the Analysis of Intrinsically Disordered Proteins, Vol. I* (Eds. VN Uversky and AK Dunker), Humana Press, **2012**, 357.
- [3] Dragusanu, M.; Petre, B.A.; Slamnoiu, S.; Vlad, C.; Tu, T.; Przybylski, M. *J. Am. Soc. Mass Spectrom.* **2010**, *21*, 1643.

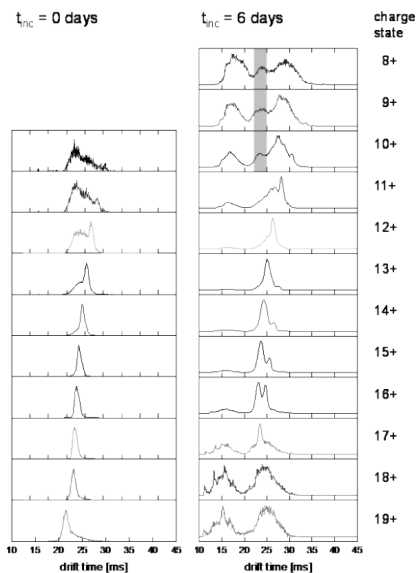


A

Figure 1. IM-MS Drift time separation of *in vitro* incubation mixture of α -Synuclein wild type (α Syn wt): After 6 days incubation in sodium phosphate buffer (pH 7.5) [1] at 37°C three protein ion series were observed with differing conformational and charge states.

A: Ion series 1 corresponds to wt- α Syn with partially folded conformation (1a) and elongated conformation (1b), while ion series 2 corresponds to a modified α Syn species (molecular mass, 14868 Da).

B: Drift time profiles of α Syn before (left) and after 6 days (right) incubation. Before incubation α Syn shows a typical correlation between charge states and drift time, with dominant elongated conformation. Right: After 6 days of incubation α Syn-wt shows two conformational states, partially folded (ion series 1a) and elongated conformation (1b), and formation of non- α Syn-wt species.



B

De novo design of artificial peptides that specifically interact with HIV-1 gp41 to inhibit viral-cell membrane fusion and infection

Keliang Liu*, Lifeng Cai, Weiguo Shi, Chao Wang, Kun Wang

Beijing Institute of Pharmacology & Toxicology, Beijing 100850, China

E-mail: keliangliu@yahoo.com

Introduction

Human immunodeficiency virus type 1 (HIV-1) gp41 plays key role in virus-cell membrane fusion and infection [1]. The ectodomain of gp41 contains functional domains such as fusion peptide (FP), N-terminal heptad repeat (NHR), C-terminal heptad repeat (CHR) and membrane proximity external region (MPER). The formation of a coiled coil six helical bundle (6HB) of NHR and CHR provides energy for virus-cell membrane fusion and HIV-1 infection. Peptides derived from gp41 CHR (C-peptide) are highly potent fusion inhibitors (Fig. 1), including T20 (Fuzeon, enfuvirtide), the first approved fusion inhibitor for clinical use, C34 [2], CP32 [3] and other engineered C-peptides [4, 5]. They act by interaction with gp41 NHR to prevent fusogenic 6HB formation [2]. Though highly efficient to drug-naive patients, C-peptide HIV fusion inhibitors suffer from short *in vivo* half time and inefficiency to emerging drug-resistant HIV isolates. These drawbacks call for a new generation of fusion inhibitors with improved antiviral and pharmacokinetic profiles [6].

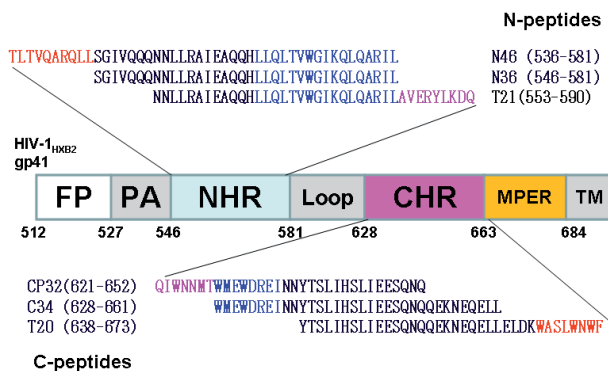


Fig. 1 HIV-1 gp41 functional domains and peptide fusion inhibitors.

Results and Discussion

Structure-function relationship analysis showed that peptide fusion inhibitors contain three functional domains, a pocket binding domain (PBD) with a Trp-Trp-Ile motif that specific interacts with deep pocket of gp41 NHR, a helix area that makes extensive contact with NHR groove, and a lipid binding domain (LBD) that helps the fusion inhibitor inserting into viral membrane to promote binding (Fig. 2) [6].

We first designed novel artificial heptad repeat peptide sequence $(X_1EE X_2X_3KK)_n$ as a universal template^[7], where the solvent exposed EE/KK residues were designed as double salt bridge in order to stabilize the helical structure, while the X_1 , X_2 and X_3 residues that directly contact with gp41 NHR target were subjected to optimization. Highly potent peptide fusion inhibitors with little homology to known protein and peptide sequences were identified, by optimization of X_1 , X_2 and X_3 residues to make specific interaction with gp41 NHR, using computational modeling based on crystal structure of the HIV-1 gp41 core^[2]. Second, we designed peptide conjugates by replacing the PBD or LBD domains with small molecule moieties or cholesterol groups, respectively. Highly potent peptide conjugates with shorter peptide sequences were identified by selecting proper small molecule moieties and suitable linkers.

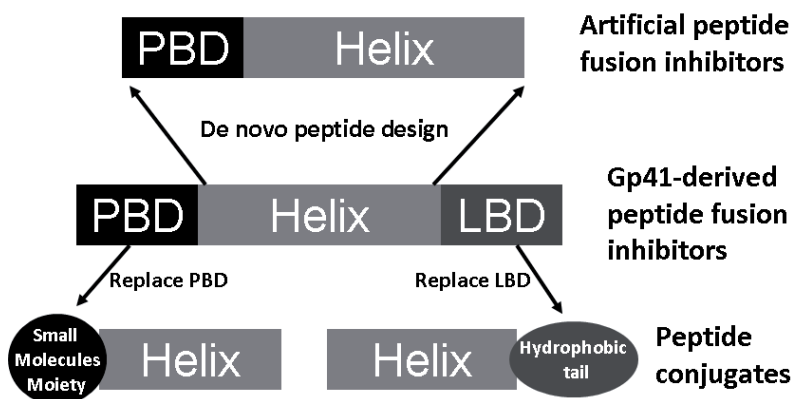


Fig. 2 Novel fusion inhibitor design

The designed peptide fusion inhibitors showed high anti-HIV activities as evaluated by using a HIV-1 gp41 mediated cell-cell fusion assay. They specifically interact with HIV-1 gp41 NHR to form typical 6HB. The strategies reported here can be used for next generation fusion inhibitor design against HIV-1, as well as other virus use class I fusion proteins as virus-cell membrane fusion machinery.

Acknowledgments

This research is supported by grants from National Science Foundation of China (30973617, 81072581, 81173098), Nature Science Foundation of Beijing (7102123), and National Science and Technology Major Project of China (2012ZX09301003).

References

- [1] Eckert, D.M. and P.S. Kim, *Ann. Rev. Bioch.*, 2001. 70: 777-810.
- [2] Chan, D.C., et al., *Cell*, 1997. 89: 263-273.
- [3] He, Y.X., et al., *J. Virol.*, 2008. 82(13): 6349-6358.
- [4] Dwyer, J.J., et al., *Proc. Natl. Acad. Sci. USA*, 2007. 104: 12772-12777.
- [5] Otaka, A., et al., *Angew. Chem.-Int. Ed.*, 2002. 41: 2938-2940.
- [6] Cai, L.F. and S.B. Jiang, *Chemmedchem*, 2010. 5(11): p. 1813-1824.
- [7] Qi, Z., et al., *J. Biol. Chem.*, 2008. 283(44): p. 30376-30384.

From aberrant N-glycosylation to alpha actinin 1 as a new candidate autoantigen of an antibody mediated form of Multiple Sclerosis

**S. Pandey,^{1,2} E. Peroni,^{1,3} I. Dioni,^{1,4} P. Rovero,^{1,4}
A. M. Papini^{1,2,3}**

¹Laboratory of Peptide & Protein Chemistry & Biology - PeptLab - www.peptlab.eu;

²Department of Chemistry "Ugo Schiff", Via della Lastruccia 3/13, Polo Scientifico e Tecnologico, University of Florence, I-50019 Sesto Fiorentino, Italy; ³SOSCO – EA4505, University of Cergy-Pontoise, Neuville-sur-Oise, 95031 Cergy-Pontoise, France;

⁴Department of Pharmaceutical Sciences, Via Ugo Schiff 6, Polo Scientifico e Tecnologico, University of Florence, I-50019 Sesto Fiorentino, Italy

E-mail: annamaria.papini@unifi.it

Introduction

Multiple sclerosis (MS) is an inflammatory demyelinating disease of the central nervous system (CNS) whose pathogenesis has not been yet elucidated, even if an autoimmune mechanism against myelin antigens is thought to contribute to its etiopathogenesis. However, in spite of extensive research efforts, a clear-cut identification of the native autoantigen(s) has not been accomplished. The most extensively studied putative autoantigens are components of normal CNS myelin, and special attention has been devoted to the role of post-translational modifications. In spite of this uncertainty, immunological characterization of autoantibodies circulating in patients' sera as disease biomarkers has been strongly pursued, aiming at the development of simple and reliable diagnostic/prognostic tools, a still largely unmet medical need.

We have previously described a family of synthetic glycopeptides¹ that serve as probes for the detection of disease-related autoantibodies present in the serum of MS patients. These probes are capable of identifying and measuring MS-related autoantibodies whose levels are correlated with clinical assessment of MS activity and magnetic resonance imaging (MRI) profile of brain lesions.² Furthermore, glycopeptide affinity-purified autotantibodies from MS serum specifically stained myelin and oligodendrocyte antigens in human brain histological specimens.¹ These peptides represents an unconventional approach since their structure is completely unrelated to myelin oligodendrocyte glycoprotein or any other myelin derivative and is not linked to any particular pathogenetic hypothesis.³

Given this background we wondered whether affinity-purified antibodies from MS patients' sera, could be useful in back-tracking CNS antigens implicated in the MS-related autoimmune response.

Results and Discussion

In this report we describe the identification of putative antigens based on their recognition by autoantibodies isolated from MS patient's serum. In a previous work from this laboratory we have shown that an N-glycosylated β -turn peptide probe, named

CSF114(Glc), specifically identifies serum autoantibodies in a subset of MS patients, representing approximately 30% of the patients' population. The autoantibodies, purified from MS patients' sera, through CSF114(Glc) affinity chromatography, detected three immunoreactive protein bands present in the rat brain. Proteomic analysis of the immunoreactive bands, involving MALDI and MS/MS techniques, revealed the presence of four proteins distinguishable by their mass: alpha fodrin, alpha actinin 1, creatine kinase, and CNPase.

The immunoreactive profile of these rat brain proteins was compared with that of commercially available standard proteins by challenging against either CSF114(Glc) purified MS autoantibodies, or monoclonal antibodies. Further discrimination among the rat brain proteins was provided by the following procedure: whereas monoclonal antibodies recognize all rat brain proteins, isolated MS specific antibodies recognize only alpha actinin 1. In fact, alpha actinin 1 displayed a robust immunoreactive response against all MS patients' sera examined, whereas the other three bands were not consistently detectable. Thus, alpha actinin 1, a cytoskeleton protein implicated in inflammatory/degenerative autoimmune diseases (lupus nephritis and autoimmune hepatitis) might be regarded as a novel MS autoantigen, perhaps a prototypic biomarker for the inflammatory/degenerative process typical of the disease.

It is of interest that the use of autoantibodies isolated by CSF114(Glc), which is not linked to any particular pathogenetic mechanism, discloses antigens undetected by conventional approaches, e.g. alpha actinin 1. It appears that the "a priori" designation of a specific pathogenetic autoimmune model for MS, poses limitations as it reveals antigens confined to that specific mechanism.

Although it is difficult to assess, at this point, what is the role of alpha actinin 1 in the pathogenesis of MS, its detection in several autoimmune diseases, underscoring its involvement in inflammatory/degenerative pathologies, warrants further investigations.

Acknowledgments

We thank for the financial support by Ente Cassa di Risparmio di Firenze and the ANR Chaire d'Excellence 2009-2013 PepKit (France) to AMP.

References

- [1] Lolli F., Mulinacci B., Carotenuto A., Bonetti B., Sabatino G., Mazzanti B., D'Ursi A.M., Novellino E., Pazzagli M., Lovato L., Alcaro M.C., Peroni E., Pozo-Carrero M.C., Nuti F., Battistini L., Borsellino G., Chelli M., Rovero P., and Papini A.M., *Proc. Natl. Acad. Sci.* **2005**, 102, 10273-10278.
- [2] Lolli F., Mazzanti B., Pazzagli M., Peroni E., Alcaro M.C., Sabatino G., Lanzillo R., Brescia Morra V., Santoro L., Gasperini C., Galgani S., D'Elia M.M., Zipoli V., Sotgiu S., Pugliatti M., Rovero P., Chelli M., and Papini A.M. *J. Neuroimmunol.* **2005**, 167(1-2), 131-137.
- [3] Papini A.M., *J. Pept. Sci.* **2009**, 15 621-628.

N-Amino-imidazolin-2-one turn mimics

Caroline Proulx, Samir H. Bouayad-Gervais, Yésica García-Ramos,
William D. Lubell

Département de Chimie, Université de Montréal, C.P. 6128, Succursale Centre-Ville,
Montréal, Québec H3C 3J7

E-mail: william.lubell@umontreal.ca

Introduction

Heterocycle scaffolds are valuable for making constrained secondary structures. For example, so-called Freidinger-Veber lactams induce β -turns by covalent restriction of amino acid ψ - and ω -torsion angles in α -amino- γ -lactams [1]. Azapeptides possess semicarbazide moieties, which restrict ϕ - and ψ -dihedral angles, respectively, due to the electronic lone pair-lone pair repulsion of adjacent nitrogen and the planarity of the urea obtained from replacement of an amino acid CH α by nitrogen [2]. Combining the covalent and electronic constraint of Freidinger lactams and azapeptides, 4- and 5-methyl *N*-amino-imidazolin-2-ones have been designed and synthesized for use as backbone- and side-chain-restricted turns (Figure) [3].

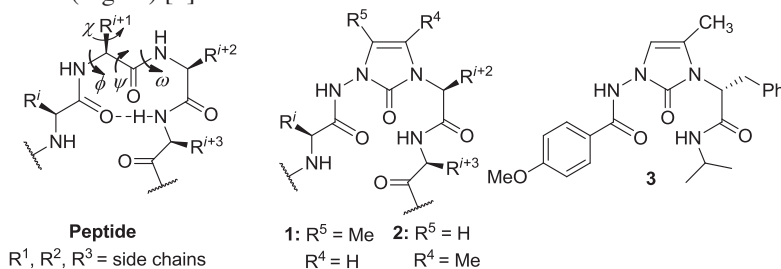


Figure. 4- and 5-methyl *N*-amino-imidazolin-2-one turn mimics.

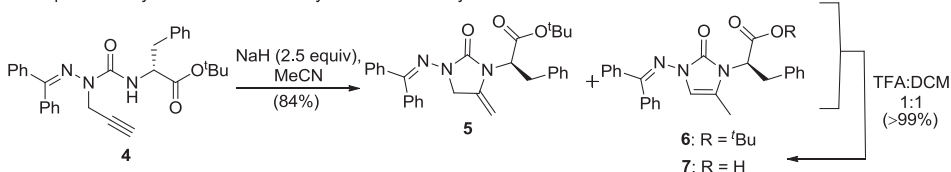
Results and Discussion

We reported recently the synthesis and conformational analysis of 4-methyl *N*-amino imidazol-2-one mimic **3**, which was observed to adopt turn conformers by X-ray crystallography and NMR spectroscopy [3]. Key for the synthesis of **3** was a NaH-promoted 5-*exo-dig* cyclization of the urea nitrogen onto the side chain of aza-propargylglycine ester **4** (Scheme); however, attempts to induce cyclization using a cationic gold catalyst failed. Moreover, a variety of aromatic side-chains were installed at the 4-position of the imidazolinone by performing a Sonogashira cross-coupling prior to the cyclization reaction [3].

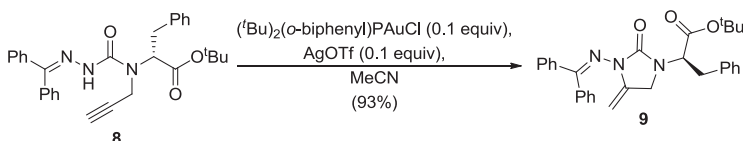
Substituents at the 4- and 5-positions would in principle occupy different regions in chi-space [4]. Although 4-position substituents may mimic amino acid side chains, the 5-position appears more suited for orienting substituents in a more natural geometry. Considering a related 5-*exo-dig* cyclization of the hydrazone nitrogen onto the acetylene group of aza-glycinyl-*N'*-propargyl ester **8** would provide the related 5-methyl *N*-amino imidazolin-2-one **9**, we have prepared aza-dipeptide **8** to test this hypothesis.

N-Propargylation of *D*-phenylalanine *tert*-butyl ester, followed by coupling to *p*-nitrophenyl benzylidene carbamate provided aza-dipeptide **4** [5]. In contrast to aza-dipeptide **4**, under mild homogeneous gold catalysis conditions, the electron-deficient semicarbazone nitrogen reacted onto the acetylene to afford imidazolin-2-one **9** in 93% yield (Scheme). In the case of **5**, the acid conditions for removing the *tert*-butyl ester caused olefin migration to afford the thermodynamically favored endocyclic double bond in imidazol-2-one **7**.

Base-promoted cyclization of **1** for the synthesis of 4-methyl amino-imidazolin-2-one **4**:



Gold-catalyzed cyclization of **5** for the synthesis of 5-methyl amino-imidazolin-2-one **8**:



Scheme. Synthesis of 4- and 5-substituted imidazolin-2-one heterocyclic scaffolds.

N-Amino-imidazolin-2-ones possessing 4- and 5-position substituents have been synthesized to serve as turn inducing scaffolds, which orient side chains in different parts of chi-space. Elaboration of this chemistry to other side chains, as well as exploration of the influence of substituent positioning on the conformation and activity of biologically relevant peptides are now under study.

Acknowledgments

This research was supported by NSERC of Canada and the CIHR grant #TGC-114046. CP is grateful to NSERC and Boehringer Ingelheim for graduate student fellowships.

References

- [1] (a) Freidinger, R. M.; Veber, D. F.; Perlow, D. S.; Brooks, J. R.; Saperstein, R. *Science*. **1980**, *210*, 656. (b) Jamieson, A. G.; Boutard, N.; Beauregard, K.; Bodas, M. S.; Ong, H.; Quiniou, C.; Chemtob, S.; Lubell, W. D. *J. Am. Chem. Soc.* **2009**, *131*, 7917-7927. (c) Boutard, N.; Jamieson, A. G.; Ong, H.; Lubell, W. D. *Chem. Biol. Drug. Des.* **2010**, *75*, 40-50.
- [2] Proulx, C.; Sabatino, D.; Hopewell, R.; Spiegel, J.; Garcia Ramos, Y.; Lubell, W. D. *Future Med. Chem.* **2011**, *3*, 1139-1164.
- [3] Proulx, C.; Lubell, W. D. *Org. Lett.* **2012**, *14*, ASAP.
- [4] Hruby, V. J.; Li, G.; Haskell-Luevano, C.; Shenderovich, M. D. *Biopolymers (Pept. Sci.)*. **1997**, *43*, 219-266.
- [5] (a) Buysse, K.; Farard, J.; Nikolaou, A.; Vanderheyden, P.; Vauquelin, G.; Sejer Pedersen, D.; Tourwé, D.; Ballet, S. *Org. Lett.*, **2011**, *13* (24), 6468-6471. (b) Bourguet, C. B.; Proulx, C.; Kloczek, S.; Sabatino, D.; Lubell, W. D. *J. Pept. Sci.* **2010**, *16*, 284-296.

Bis(2-sulfanylethyl)amido native peptide ligation and novel tools for protein total synthesis

N. Ollivier, L. Raibaut, E. Boll, J. Dheur, R. Mhidia, O. Melnyk

UMR CNRS 8161, Univ Lille Nord de France, Pasteur Institute of Lille, France

Oleg.Melnyk@ibl.fr

Introduction

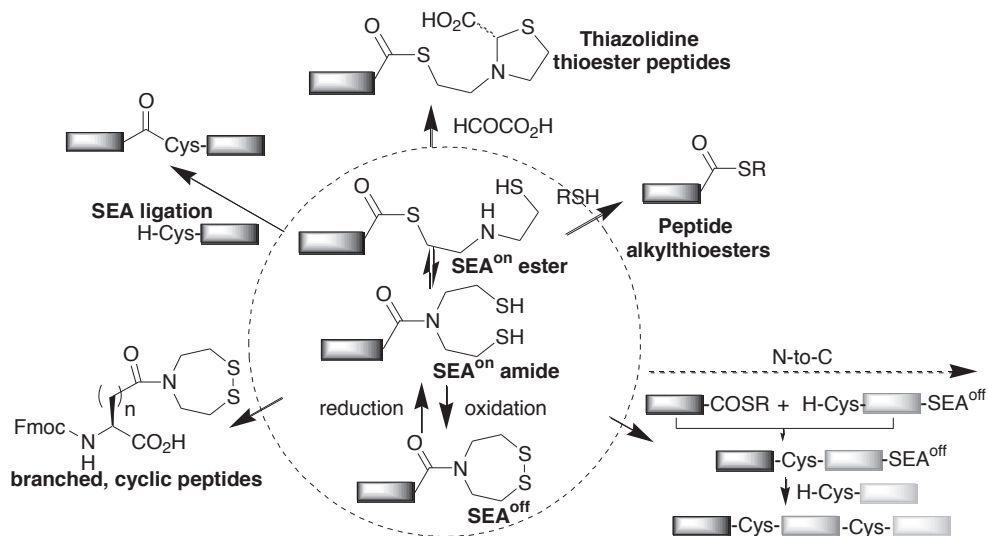
The discovery of native peptide ligation methods and the design of chemical tools enabling the total synthesis of complex peptide scaffolds or the expedited and simple access to medium sized proteins is a challenging and important goal. This paper discusses the interest of *bis*(2-sulfanylethyl)amido (called SEA^{on}) group for the design of novel amide bond forming reactions,[1] for the synthesis of peptide thioesters which are key building blocks in Native Chemical Ligation-based chemistries,[2,3] for the synthesis of branched or cyclic peptides,[4] or for the design of N-to-C sequential native peptide ligation strategies.[5,6]

Results and Discussion

Our studies on *N,S*-acyl shift systems[7] led us to the discovery of the synthetic potential of SEA^{on} group. SEA^{on} amide form equilibrates with SEA^{on} thioester form in water. The later can be trapped *in situ* by a Cys peptide as in NCL to give a native peptide bond.[1] The *N,S*-acyl shift is the rate limiting step of this reaction called SEA ligation. Moreover, SEA ligation is acid catalyzed, making the reaction significantly faster at pH 5.5 than at neutral pH. Alternately, SEA^{on} thioester form can be exchanged by an alkylthiol at mild acidic pH, giving a simple access to C-terminal peptide thioesters.[2] Another possibility is to trap SEA^{on} thioester form by making a thiazolidine with glyoxylic acid. Such thioesters react much faster than conventional alkylthioesters in NCL, and constitute a potential solution to the formation of difficult junctions.[3]

What certainly distinguishes SEA^{on} group from other *N,S*-acyl systems is the presence of two thiol groups within its structure, thereby enabling its inactivation by formation of a cyclic disulfide called SEA^{off}. SEA^{off} is compatible with conventional Fmoc SPPS, and can be installed for example on the side-chain of Asp or Glu amino acids for the synthesis of branched or cyclic peptide scaffold using intermolecular or intramolecular SEA ligation respectively.[4] In another application, it can serve as a masked thioester surrogate during NCL *in the absence of TCEP*, a strong reducing agent which activates SEA^{off} into SEA^{on}. This property enables to ligate sequentially in a one-pot procedure three peptide segments in the N-to-C direction, and thus the straightforward synthesis of small protein domains.[5,6]

In conclusion, SEA chemistry allows a vast array of methodologies to be designed for solving important synthetic challenges. New developments are in progress to extent the limits of protein total synthesis and will be reported in due course.



Acknowledgments

We acknowledge financial support from Cancéropôle Nord-Ouest, Région Nord Pas de Calais, ANR grant "click-unclick" and the European Community.

References

- [1] Ollivier, N.; Dheur, J.; Mhida, R.; Blanpain, A.; Melnyk, O. *Org. Lett.* **2010**, *12*, 5238.
- [2] Dheur, J.; Ollivier, N.; Vallin, A.; Melnyk, O. *J. Org. Chem.*, **2011**, *76*, 3194.
- [3] Dheur, J.; Ollivier, N.; Melnyk, O. *Org. Lett.*, **2011**, *13*, 1560.
- [4] Boll, E.; Dheur, J.; Drobecq, H.; Melnyk, O. *Org. Lett.* **2012**, *14*, 2222.
- [5] Ollivier, N.; Vicogne, J.; Vallin, A.; Drobecq, H.; Desmet, R.; El Mahdi, O.; Leclercq, B.; Goormachtigh, G.; Fafeur, V.; Melnyk, O. *Angew. Chem. Int. Ed.*, **2012**, *51*, 209.
- [6] Raibaut, L.; Ollivier, N.; Melnyk, O. *Chem. Soc. Rev.*, in press, **2012**, DOI:10.1039/C2CS35147A
- [7] Ollivier, N.; Behr, J. B.; El-Mahdi, O.; Blanpain, A.; Melnyk, O. *Org. Lett.* **2005**, *7*, 2647.

From simple to complex to ultra complex and back to simple

Michal Lebl

Spyder Institute Praha, Czech Republic

E-mail: michallebl@gmail.com

Introduction

Attempts to automate peptide and DNA synthesis can be traced back to the invention of solid phase synthetic methodology. We have participated in this endeavor for the last three decades and we have developed multitudes of synthesizers based on different concepts starting from single channel bromophenol blue monitored synthesizer through parallel synthesizers, library synthesizers, synthesizers based on centrifugation or tilted centrifugation, or continuous synthesizers on cotton substrate. We pushed the limit of parallel solid phase synthesis with two generations of DNA synthesizers performing up to several millions couplings per day [1,2]. Even though these synthesizers are quite impressive, their realization in multiple laboratories is limited due to their size and cost. Recently our efforts are focused on development of synthesizers which could be used even in laboratories with very limited budgets.

Results and Discussion

The ultra-high throughput synthesizer [2] is based on a concept of a continuous synthesis [3] on a linearly arranged substrate where at any moment all steps of the synthesis are performed at the same time at a different location.

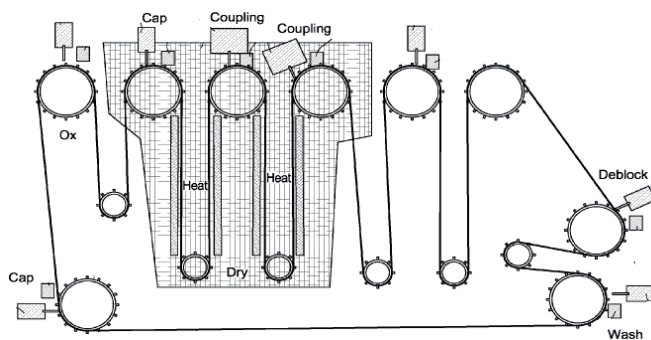


Figure 1. Scheme of the ultra-high throughput synthesizer.

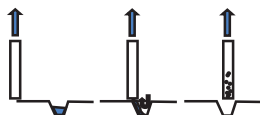


Figure 2. Non-contact evacuation concept.

The substrate was a polypropylene belt with imprinted depressions in an arrangement of the 384-well microtiterplate. Each depression was about 2 mm deep and contained controlled pore glass (CPG) functionalized with universal linker. CPG was attached to the bottom of the depression [4]. Liquid reagents are added on the fly and removed by non-contact surface suction illustrated in Figure 2. Vacuum nozzles placed in close proximity to the moving belt remove completely the liquids in milliseconds and the next reagent can be added almost immediately. Reactions are controlled by camera system evaluating the completeness of the deprotection in every step [5]. This system allows for synthesis of tens of thousands hundredmers in one day.

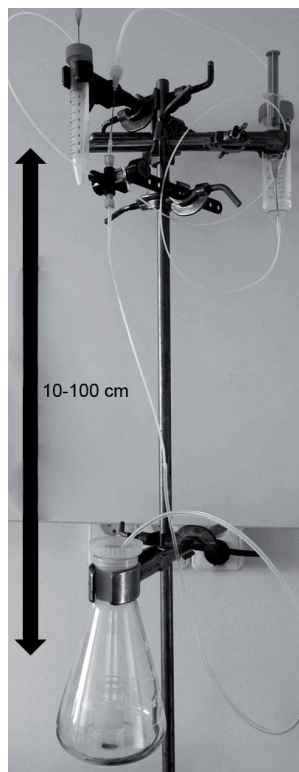


Figure 3. Synthesizer with gravity driven liquid delivery.

The capacity of the described synthesizer can be utilized only by companies with extremely high demand for number of individual oligomers. Another problem is the high cost of the instrument of this type. The synthesizer which can be implemented without any investment in any chemical laboratory is shown in Figure 3. It is composed of a selection valve connected to the vials with DMF, piperidine/DMF, and to the luer lock connected syringe with activated amino acid. The opening leading down from this valve is connected to the tubing tightly filled with activated cotton thread. The difference in the liquid levels of the containers at the top of the system and end of this tubing is defining the speed of the flow through the cotton carrier. The operator of this synthesizer just turns the valve in appropriate intervals and replaces the activated amino acids solutions. We have shown the feasibility of this synthesizer on manual synthesis of model peptides, but the complete automation based on timed rotation of motorized valve is easily imaginable. The major advantage of this system is elimination of any pumping – liquid is delivered by combination of the gravity and capillary forces.

For the parallel synthesis of up to 24 peptides we have utilized the centrifugal synthesizer described earlier [6] which was modified for the use of cotton as the solid support. Due to the physical shape of a cotton thread the construction of the rotor could be simplified, and the filtration or concept of tilted centrifugation was not needed in this case. The simple wells with side narrow opening were holding the cotton thread pieces during the whole operation.

Acknowledgments

Author is indebted to the company Illumina, Inc. where the development of the ultra-high throughput DNA synthesizers could be realized by experienced team of mechanical and software engineers in collaboration with group of excellent chemists.

References

- [1] Heiner, D.; Jones, A. C.; Fambro, S. P.; Nibbe, M. J.; Burgett, S. R.; Ellman, B. M.; Lebl, M. USA 7,914,739, Mar 29, 2011.
- [2] Lebl, M.; Perbost, M.; DeRosier, C. F.; Nibbe, M.; Burgett, S. R.; Heiner, D. USA 20110178285, Jul 21, 2011.
- [3] Lebl, M.; Eichler, J. *Peptide Res.* 1989, 2 (4), 297-300.
- [4] Ellman, B.; Lebl, M.; Jones, A.; Fambro, S.; Heiner, D. USA 8,022,013, Sep 20, 2011.
- [5] Heiner, D. L.; Fambro, S. P.; Kotseroglou, T.; Lebl, M. USA 7,887,752, Feb 15, 2011.
- [6] Lebl, M.; Pistek, C.; Hachmann, J. P.; Mudra, P.; Pesek, V.; Pokorny, V.; Poncar, P.; Zenisek, K. *Int. J. Pept. Res. Ther.* **2007**, 13 (1-2), 367-375.

NPPS: A new integrated method for solid phase synthesis of peptides on nanoparticles

Gerardo Byk,¹ Victoria Machtey,¹ Aryeh Weiss,² Raz Khandadash¹

¹Laboratory of Nano-Biotechnology, Dept. of Chemistry; ²School of Engineering, Bar Ilan University 52900-Ramat Gan, Israel
E-mail:Gerardo.byk@biu.ac.il

Introduction

Introduction of biological signals into nanoparticles is critical for many applications ranging from cell sensing to drug delivery. While most synthetic monomers allow creating and engineering nanoparticles with carefully tuned structures and desired matrix properties, synthetic bio-compatible polymers lack any biologically recognized functionality, and at best, facilitate non-specific interactions that can be exploited with limited control. Thus, there is a great deal of interest in the development of strategies to tether biological signals or therapeutic molecules on nanometric systems. The currently available nanoparticle/nanohydrogel modifications include conjugation with a single molecule such as proteins, antibodies, or enzymes, followed by a tedious process of dialysis or ultra-centrifugation for repeated washings. In the context of our efforts for synthesizing and using substituted nanospheres for live cell applications, we have designed and synthesized nanoparticle hydrogels (NPHG's) so that they can be functionalized with biological signaling molecules by a novel Merrifield multistep reaction approach. The process has been automated using a multiple organic synthesis robot for parallel synthesis bringing about a novel dimension for Merrifield synthesis where the synthesized peptides are used for biological applications while linked to nanoparticles. We called the approach NPPS, Nano-Particle-Peptide-Synthesis.

Results and Discussion

Cross-linked monodispersed PEG nanohydrogels of different sizes were obtained by free radical dispersion polymerization using mixtures containing low molecular weight PEG-diamine substituted with mono and diacrylamide and N-isopropylacrylamide (NIPAAM) that nucleates growth for the polymerization and formation of the nanospheres thanks to its low critical solution temperature (LCST) [1]. Thus, NPHG's sized 20, 50, 80, 100, 130, 250, 300 nm were obtained.

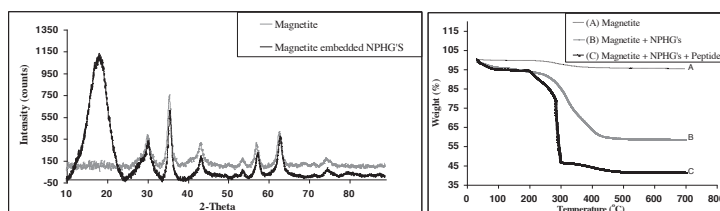


Fig. 1. Left panel: XRD analysis of magnetite (grey) and magnetite-embedded NPHG's (black). Right panel: Thermo-gravimetric analysis of magnetite (A), magnetite embedded NPHG's (B) and magnetite embedded NPHG's after peptide synthesis (C).

In order to allow the Merrifield synthesis, nanohydrogels were embedded into magnetite and magnetic susceptibility was used for repeated reactions and washings. Magnetite was generated as previously shown [2] but in the presence of the NPHG's that were thus embedded into the magnetic matrix. XRD and TGA analyses of magnetite and magnetite-embedded NPHG's demonstrated the embedment of the particles (see figure 1, left panel). As proof of feasibility, we have synthesized a nuclear localization sequence (NLS) peptide PKKKRKV [3]. This and similar peptides have been shown to penetrate into cells and localize in the nuclei. The cell penetration process can be observed if the synthesized NLS-modified NPHG's include a fluorescent label that allows intracellular tracking after incubation with cells using microscopy. An Advanced ChemTech 496MOS robot was adapted to the NPPS by placing cylindrical magnets (N50) on both sides of each reaction well well so that the magnetic matrix adheres to the walls of the reaction well permitting the contact of solvents and reagents with the matrix and appropriate evacuation of solvents/reagents through the filter (see figure 2).

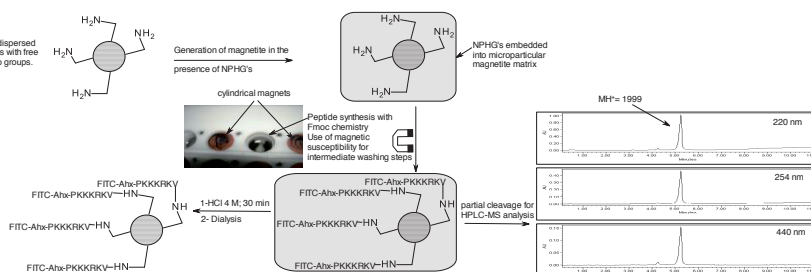


Fig. 2. Nanoparticle peptide synthesis of FITC-Ahx-KKKRKV nuclear localization sequence.

Peptides were synthesized using Fmoc chemistry with coupling reagent BOP/HOBT. At the N-terminal position an amino-hexanoyl (Ahx) spacer was placed and reacted with FITC to give the final labeled NLS-NPHG's. The linker HMBA allowed partial cleavage of the peptide by hydrolysis of the ester bond for HPLC-MS analysis of the fully protected peptide. The product was compared to the crude obtained using the same chemistry but on conventional solid supports and was of high quality (see figure 2). Thermo-gravimetric analysis of the magnetite embedded NPHG's with the peptide disclosed a substantially different pattern than that observed for magnetite or magnetite embedded unmodified NPHG's (see figure 1, right panel). Finally the FITC-NLS-NPHG's were recovered from the matrix after treatment with HCl for 30 min. followed by addition of EDTA, neutralization to pH=7 and single dialysis process to remove iron-EDTA soluble complex.

Acknowledgments

This research was financed by the ISF grant 830/11, the Israel Council for Higher Education and the "Marcus Center for Medicinal Chemistry".

References

- [1] Leobandung, W., Ichikawa, H., Fukumori, Y., Peppas, N.A. *J. Appl. Polym. Sci.* **2003**, 87, 1678.
- [2] Zhiya, M.A., Yueping, G., Huizhou, L. *J. Polym. Sci. A: Polym. Chem.* **2005**, 43, 3433.
- [3] Kaihatsu, K., Huffman, K.E.; Corey, D.R. *Biochemistry* **2004**, 43, 14340.

Rational design and synthesis of linear and cyclic myelin epitope peptides: New directions in the immunotherapy of Multiple Sclerosis

Georgios Deraos^{1,3}, Theodore Tselios¹, Pigi Katsougraki¹, Panagiotis Plotas^{2,3}, Maria-Eleni Androutsou^{1,3}, John Matsoukas^{1,3}

¹Department of Chemistry, University of Patras, Patras, Greece; ²School of Medicine, University of Patras, Greece; ³Eldrug S.A., Pharmaceutical Company, GR-26504, Platani, Patras, Greece

E-mail: imats@upatras.gr

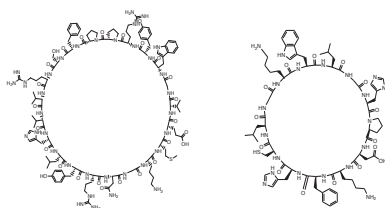
Introduction

Therapeutic approaches for multiple sclerosis, involve the design and use of peptide analogues of disease-associated myelin epitopes to induce peripheral T cell tolerance or the use of immunotherapeutic techniques to develop Th1/Th2 responses followed by release of appropriate cytokines. There is gathering evidence that analogues of disease-associated epitopes can inhibit disease through the activation of antigen-specific regulatory T cells or by the release of appropriate cytokines. It has been demonstrated that vaccination with BV8S2 protein (a regulator proVa protein shown to cross react with MBP) in mice induced specific T cells that inhibited MBP-reactive T cell proliferation and encephalitogenic activity *in vitro*. The inhibition was a result of Th2 cytokine release by T cells. It was evident that the IL-4, IL-10, and to a lesser extent, IFN-gamma and TGF-beta, were the major regulatory cytokines responsible for inhibiting encephalitogenic activity, proliferation, and IFN-gamma secretion of MBP-reactive Th1 cells. These results indicate that cytokine regulation is the major mechanism through which TCR specific CD4⁺ T cells regulate encephalitogenic and potentially other bystander Th1 cells. The ability to alter the cytokine secretion of auto-reactive T cell lines through peptide or mimetic treatment even in longstanding autoimmune disease indicates that cytokine therapy might have therapeutic benefits by switching the function of myelin reactive T cells such that they are non-pathogenic.

Results and Discussion

Our study with Myelin epitope analogues is targeting 1. Inhibition of trimolecular MBPpeptide-MHC-TCR complex implicated in MS, 2. Diverse of cytokine secretion from pathogenic Th1 to therapeutic Th2 and 3. Immunoregulation of disease by vaccination. The use of antagonist peptides derived from the myelin sheath constitutes a promising therapeutic approach for multiple sclerosis (MS). Furthermore cyclization of peptide analogues is of great interest, since the limited stability of linear peptides restricts their potential as therapeutic agents. A number of studies by us and others have used mutated peptides, whereby mutations of amino acids have been made at TCR contact residues, in order to alter immune responses from Th1 to Th2 or inhibit experimental autoimmune encephalomyelitis (EAE), an animal model of MS. In previous studies by our group, mutated peptide analogues of MBP83-99, along with the linear and cyclic agonist MBP83-

99, conjugated to reduced mannan, were tested for their ability to induce T cell responses. Mannosylation of MBP 83-99 (Ala⁹¹, Ala⁹⁶) resulted in diversion of Th1 response to Th2. [1] The use of reduced mannan to further divert immune responses to Th2 when conjugated to MBP peptides constitutes a novel strategy for immunotherapy of the disease. A double mutation of the agonist PLP139–151 peptide, in which both of the TCR binding sites were replaced with L or R ([L144, R147]PLP139–151), was able to antagonize PLP-specific T cell clones in vitro. The mutated analog inhibited EAE and prevented clinical disease progression when administrated in the early stage of EAE induction. [2]



Cyclic(35-55)MOG35-55 Cyclic(139-151)PLP139-151

In areas of inflammation in MS, antibodies against the minor protein MOG have been demonstrated. Thus, we now know that antibodies do play a role in MS, and cooperate with antigen presenting cells in myelin destruction. Blocking the effects of these MOG antibodies with secondary antibodies or non-peptide mimetics might be an important avenue for future therapy.

Interestingly, replacement of Arg (providing a stable conformation) with citrulline (disorganizing the conformation of Myelin) leads to Th1 secretion, indicating a mechanism of disease and the importance of Arginine to stabilize conformation. [3]

Currently, we are investigating linear and cyclic analogues conjugated to mannan in oxidized (OM) or reduced (RM) forms via Lys–Gly bridge. Specific analogues in a number of preliminary vaccination and therapeutic protocols have shown interesting properties as potential vaccine drugs in the treatment of Multiple Sclerosis

Acknowledgments

This work is financially supported by the “Cooperation” program 09SYN-609-21, (O. P. Competitiveness & Entrepreneurship (EPAN II). We are grateful to VIANEX S.A. for supporting this work.

References

- [1] Katsara M, Yuriev E, Ramsland PA, Deraos G, Tselios T, Matsoukas J, Apostolopoulos V. *J Neuroimmunol.* 2008 Aug 30;200(1-2):77-89.
- [2] Katsara M, Deraos G, Tselios T, Matsoukas MT, Friligou I, Matsoukas J, Apostolopoulos V. *J Med Chem.* 2009 Jan 8;52(1):214-8.
- [3] Deraos G, Chatzantoni K, Matsoukas MT, Tselios T, Deraos S, Katsara M, Papathanasopoulos P, Vynios D, Apostolopoulos V, Mouzaki A, Matsoukas J. *J Med Chem.* 2008 Dec 25;51(24):7834-42.

Preventing failure in difficult sequences: An improved resin matrix, its properties and application

Wolfgang Rapp¹, Michael Beyermann², Petra Henklein³, Ruediger
Pipkorn⁴, Stephan Rawer⁵, Sven Rothemund⁶

¹Rapp Polymere GmbH, 72072 Tübingen, Germany; ²Leibnitz-Institute for Molecular
Pharmacology, 13125 Berlin, Germany; ³Humboldt Universität Berlin, Institute for
Biochemistry, 13347 Berlin, Germany; ⁴Deutsches Krebsforschungszentrum, 69120
Heidelberg, Germany; ⁵Life Technologies GmbH, 64293 Darmstadt, Germany;

⁶Universität Leipzig, 04103 Leipzig, Germany

E-mail: rapp-polymere@t-online.de

Introduction

So called difficult sequences are still a major problem in SPPS. Novel resins like TentaGel, Chematrix resin or PEGA were developed and chaotropic salts, magic mixtures, elevated temperature and microwave assisted synthesis were used to improve the yield of the peptides. PEGA, SPOC and Chematrix resins are polar resins having a high PEG content. Other than polystyrene or TentaGel which are crosslinked by DVB they are crosslinked by polymeric crosslinking molecules. These polymeric crosslinkers give those resins the extraordinary high swelling volume. The central question to us was: what happens to a well established commercial available resin like the PEGylated polar TentaGel resin and the unpolar polystyrene resin if one increases the swelling of these matrices to that extent that the final resin shows a comparable swelling to PEGA and Chematrix resins. A further question was whether the synthesizer itself has to be considered as parameter for the success of the synthesis.

Results and discussion

Based on this we want to keep the polymeric system of polystyrene or TentaGel constant but changing the crosslinking to achieve the goal for a comparable swelling to the other polymeric systems PEGA or Chematrix [1].

resin	solvent [ml/g]				
	water	MeOH	DMF	DCM	MeCN
Polystyrene	1,6	1,6	5,6	8,3	3,2
Polystyrene HS	1,6	1,6	7	14,6	2
PEGA	16	13	11,5	13	-
Chematrix resin	8,2	9	8	11,5	6,3
TentaGel HS	4	10	13,2	19	9
TentaGel	3,6	3,6	4,7	6,3	4,2

Fig.1 Swelling of 1g resin in different solvents at RT

Summarized in Fig.1 the new resins polystyrene HS and TentaGel HS (HS stands for “high swelling”) show very comparable swelling volumes to Chematrix and PEGA.

Ala₁₀Lys was chosen as a model system to investigate the impact of this change of the physico chemical property to peptide quality. To see if the agitation/mixing also influence the peptide yield and purity the sequence was synthesized on 4 different synthesizers.

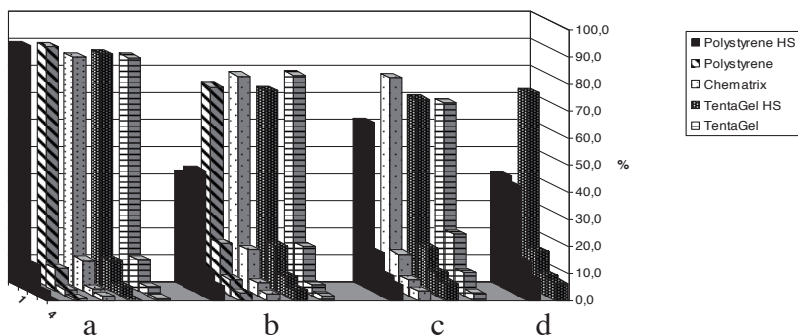


Fig 2. A₁₀K with a) vortexing, b) continuous flow, c) gently shaking, d) no mixing. The bars represent A₁₀K and the n-1, n-2, n-3 and n-4 failure sequence

Vortexing gave the best results independent from the used resin. All other systems gave almost the same results with the exception of polystyrene HS. This very soft matrix obviously collapses during the synthesis conditions b and d (where the resin is not moved), partially with c but not with a. The very strong mechanical forces during vortexing prevent the peptide from aggregation. This peptide-peptide interaction ends up in an additional physical crosslinking which results in the collapse of the resin.

The sequence PNA₄-peptide₁₅-PNA₁₁ was synthesized by vortexing on the resins listed in Tab 1. The polystyrene resin (entry 1) was 1 % crosslinked with DVB. With the high swelling resins (soft gels) significant better results were achieved compared to the more rigid 1% crosslinked polystyrene resin.

resin	yield [%]	Tab.1 Purified yield of PNA ₄ -peptide ₁₅ -PNA ₁₁
Polystyrene	0	
Chematrix	20	
Polystyrene HS	28	
TentaGel HS	32	

References

- [1] Garcia-Martin, F., Quintanar-Audelo, M., Garcia-Ramos, Y., Cruz, L.J., Gravel, C., Furic, R., Cote, S., Tulla-Puche, J., Albericio, F. *J.Comb. Chem.* **8**, 213-220 (2006)

SNARE analogous peptides for membrane fusion

**Antonina Lygina¹, Karsten Meyenberg¹, Geert van den Bogaart²,
Reinhard Jahn², Ulf Diederichsen¹**

¹*Institute for Organic and Biomolecular Chemistry, Georg-August-University Göttingen,
Tammannstraße 2, 37077 Göttingen, Germany;* ²*Department of Neurobiology, Max Planck
Institute for Biophysical Chemistry, Am Faßberg 11, 37077 Göttingen, Germany*

E-mail: udieder@gwdg.de

Introduction

Membrane fusion in case of synaptic transmission is triggered by fusion proteins like the SNARE (Soluble N-ethylmaleimide-Sensitive Factor Attachment Protein Receptor) proteins.[1] Fusion of lipid bilayers is initiated by formation of a coiled-coil four-helix bundle between SNARE proteins syntaxin-1A and SNAP-25 residing in the plasma membrane and the SNARE protein synaptobrevin residing in the membrane of synaptic vesicles. Formation of the tetrameric SNARE complex forces the two merging membranes in close proximity. The precise mechanism of SNARE mediated membrane fusion is still under debate. Especially, the zipper-like recognition forming the SNARE complex and the role of synaptobrevin (Syb) and syntaxin-1A (Sx) transmembrane domains for the fusion event need to be mechanistically elucidated. Therefore, fusion was investigated using vesicles reconstituted with artificial model systems mimicking the SNARE *in vitro* fusion process. Thereby, the SNARE assembly reaction was provided with analogs of reduced complexity allowing systematic structural variations.[2] Two SNARE analogous model systems based on transmembrane peptides and covalently linked recognition motifs like coiled-coil forming peptides or peptide nucleic acids were synthesized and elucidated with respect to vesicle fusion.[3,4] The fusion efficiency turned out to be dependent on length, orientation, and terminal charge of the transmembrane domains. Furthermore, it was indicated that the transmembrane helices are actively participating in the fusion process.

Results and Discussion

SNARE models with α -peptide coiled-coil recognition motif were prepared based on the transmembrane/linker region of Sx and Syb (VAMP2) and peptide recognition sequences G(EIAALEK)₃ (E3) and WWG(KIAALKE)₃ (K3), respectively (Fig. 1A).[3] With these artificial peptides it was possible to induce membrane fusion of vesicles as indicated by fluorescence based assays detecting the mixing of donor and acceptor labeled vesicles. Evidence for fusion was also derived from content mixing assays of a calcein or sulforhodamine B filled vesicles with empty vesicles. No fusion was observed when the recognition motifs were blocked or between vesicles with only one kind of SNARE analog. The E3-VAMP3 and K3-syntaxin system was further used to study the influence of linker modifications e.g. exchanging a charged amino acid for a neutral one close to the lipid head group region. Furthermore, the linker was extended by about 1.5 helical turns. In both cases, liposome fusion was of comparable efficiency as with the unmodified variants.

SNARE models with peptide nucleic acid (PNA) recognition motif were investigated as second set of analogs (Fig. 1B). Syb and Sx TMD/linker constructs were combined with

Total synthesis of marine cyclopeptide scytonemin A

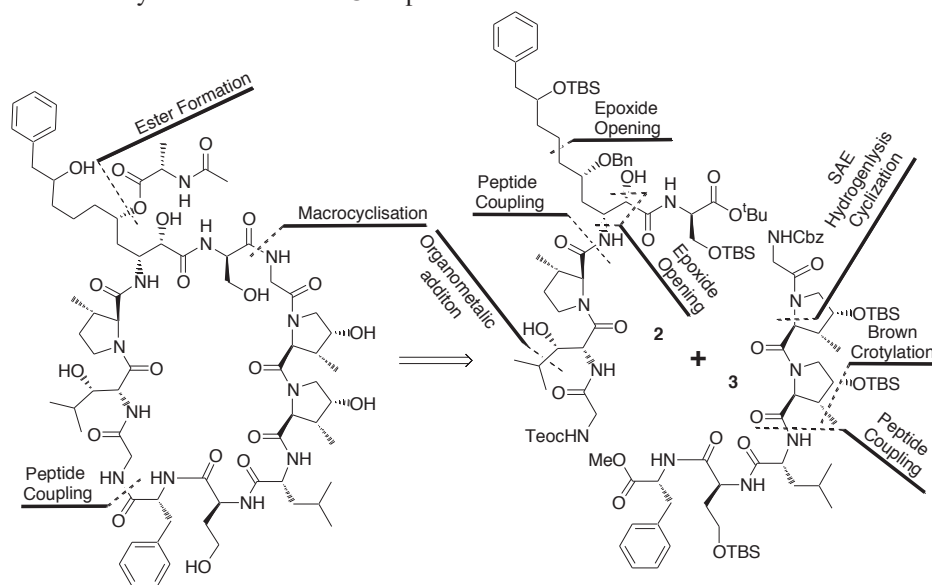
Junyang Liu,^a Lei Wang,^a Zhangshuang Xu,^{a,b} Tao Ye^{a,b}

^aLaboratory of Chemical Genomics, Peking University Shenzhen Graduate School, Shenzhen, China, 518055; ^bDepartment of Applied Biology and Chemical Technology, The Hong Kong Polytechnic University, Hung Hom, Kowloon, Hong Kong

E-mail: bctaoye@inet.polyu.edu.hk

Introduction

Scytonemin A, a 34-membered cyclic undecapeptide with potent calcium-antagonistic activity, was isolated from a *Scytonema* sp. (strain U-3-3) by Moore and coworkers in 1988.¹ The structure of the scytonemin A was determined by interpretation of spectral data, chemical degradation, and evaluation of the amino acids obtained by acid hydrolysis. However, the absolute configuration of one of the stereogenic centers presented within the side chain was not assigned. As part of our program on the synthesis of marine secondary metabolites², we were interested in synthetic approaches toward the total synthesis of scytonemin A and establishing of its absolute chemistry. Herein we describes stereocontrolled strategies for the preparation of all unique amino acids and the total synthesis of scytonemin A and its C-9 epimer.



Results and Discussion

The synthesis commenced with the preparation of various unnatural amino acid fragments. Two stereogenic centers of Ahda side chain were derived from chirality pool, while the other two stereogenic centers were constructed *via* a regio-selective SN₂ reaction of *cis*-epoxide with sodium azide. The *syn* stereochemistry of HyLeu unit was established by the substrate-controlled addition of isopropyl Grignard reagent to Garner's aldehyde. HyMePro

unit was prepared by a sequence of reactions including Brown's asymmetric crotylation, Wittig reaction, Sharpless asymmetric epoxidation and an intramolecular epoxide-opening process. A modified Hofmann-Löffler-Freytag reaction was developed for the construction of MePro by the use of a protected isoleucine as the starting material. Both key fragments **2** and **3** were constructed using standard protection/deprotection and activation/coupling sequences. Assembly of those two key fragments led to a linear undecapeptide which served as the advanced precursor. Simultaneous removal of *tert*-butyl ester and Boc-group with 1 M TiCl₄ at room temperature gave the corresponding amino acid, which was then treated with HATU at a low concentration (0.5×10^{-3} M) to afford the desired macrocycle. Finally, global deprotection of silyl protecting groups with aqueous hydrochloride in THF provided scytonemin A. The total synthesis of scytonemin A was accomplished in a longest linear sequence of 31 steps with an overall yield of 0.42%. Both synthetic samples, (9S)-scytonemin A and (9R)-scytonemin A, were compared with an authentic sample of the natural product kindly provided by Dr. Gregory L. Helms. By careful NMR analysis of synthetic scytonemin A containing either (9R)-Ahda or (9S)-Ahda side chain, we have established that the natural product contains a (9R)-Ahda subunit. Further confirmation came from the identity of the Chiral HPLC studies of synthetic scytonemin A with the authentic sample of natural scytonemin A. Co-injection of (9R)-scytonemin A and the natural sample resulted in a single peak observed by chiral-HPLC. The total synthetic studies thus fully established the stereochemistry of scytonemin A without ambiguity.

Acknowledgments

We would like to thank for the financial support from the Hong Kong Research Grants Council (Projects: PolyU 5040/10P; PolyU 5037/11P; PolyU 5020/12P)

References

- [1] Helms, G. L.; Moore, R. E.; Niemczura, W. P.; Patterson, G. M. L. *J. Org. Chem.* **1988**, *53*, 1298–1307.
- [2] (a) Dai, L.; Chen, B.; Lei, H.; Wang, Z.; Liu, Y.; Xu, Z.; Ye, T., *Chem. Commun.* **2012**, *48*, 8697–8699.; (b) Wang, M.; Feng, X.; Cai, L.; Xu, Z.; Ye, T., *Chem. Commun.* **2012**, *48*, 4344–4346.; (c) Liu, J.; Ma, X.; Liu, Y.; Wang, Z.; Kwong, S.; Ren, Q.; Tang, S.; Meng, Y.; Xu, Z. Ye, T., *Synlett*, **2012**, *19*, 783–787.; (d) Wang, L.; Xu, Z.; Ye, T., *Org. Lett.* **2011**, *13*, 2506–2509.; (e) Liu, H.; Liu, Y. Q.; Xu, Z. S.; Ye, T. *Chem. Commun.* **2010**, *46*, 7486–7488.; (f) Gao, X. G.; Liu, Y. Q.; Kwong, S. Q.; Xu, Z. X.; Ye, T. *Org. Lett.* **2010**, *12*, 3018–3021.; (g) Li, S.; Chen, Z.; Xu, Z.S.; Ye, T. *Chem. Commun.* **2010**, *46*, 4773–4775.; (h) Chen, Z.; Song, L.; Xu, Z. S.; Ye, T. *Org. Lett.* **2010**, *12*, 2036–2039.; (i) Jin, Y.; Liu, Y. Q.; Wang, Z.; Kwong, S.; Xu, Z. S.; Ye, T. *Org. Lett.* **2010**, *12*, 1100–1103.; (j) Liang, S.; Xu, Z. S.; Ye, T. *Chem. Commun.* **2010**, *46*, 153–155.; (k) Chen, B.; Dai, L.; Zhang, H.; Tan, W.; Xu, Z. S.; Ye, T. *Chem. Commun.* **2010**, *46*, 574–576. (l) Li, S.; Liang, S.; Tan, W. F.; Xu, Z. S.; Ye, T. *Tetrahedron* **2009**, *65*, 2695–2702.; (m) Li, S.; Liang, S.; Xu, Z. S.; Ye, T. *Synlett* **2008**, 569–574.; (n) Ren, Q.; Dai, L.; Zhang, H.; Tan, W.; Xu, Z. S.; Ye, T. *Synlett* **2008**, 2379–2383.; (o) Chen, Z. Y.; Ye, T. *New J. Chem.* **2006**, *30*, 518–520.; (p) Pang, H. W.; Xu, Z. S.; Chen, Z. Y.; Ye, T. *Lett. Org. Chem.* **2005**, *2*, 699–702.; (q) Pang, H. W.; Xu, Z. S.; Ye, T. *Lett. Org. Chem.* **2005**, *2*, 703–706.; (r) Chen, H. L.; Xu, Z. S.; Ye, T. *Tetrahedron* **2005**, *61*, 11132–11140. (s) Chen, Z. Y.; Deng, J. G.; Ye, T. *ARKIVOC* **2003**, Part VII, 268–285.; (t) Peng, Y. G.; Pang, H. W.; Ye, T. *Org. Lett.* **2004**, *6*, 3781–3784.; (u) Xu, Z. S.; Peng, Y. G.; Ye, T. *Org. Lett.* **2003**, *5*, 2821–2824.

Development of a series of diketopiperazine vascular targeting anticancer agents based on microtubule depolymerization activity

Yoshio Hayashi¹, Yuri Yamazaki¹, Fumika Yakushiji¹, Makiko Sumikura², Hironari Tanaka¹, Kyouhei Muguruma¹, Hiroyuki Yasui², Takumi Chinen³, Takeo Usui³, Saskia Neuteboom⁴, Barbara Potts⁴, Michael Palladino⁴, G. Kenneth Lloyd⁴

¹Department of Medicinal Chemistry, Tokyo University of Pharmacy and Life Sciences, Tokyo 192-0392, Japan; ²Department of Analytical and Bioinorganic Chemistry, Kyoto Pharmaceutical University, Kyoto 607-8414, Japan; ³Graduate School of Life and Environmental Science, University of Tsukuba, Tsukuba, Ibaraki 305-8572, Japan; ⁴Nereus Pharmaceuticals, San Diego, CA 92121, USA
E-mail: yhayashi@toyaku.ac.jp

Introduction

Anti-microtubule agents such as microtubule stabilizing taxanes and microtubule depolymerizing vinca alkaloids have been used as effective chemotherapies for a variety of cancers. By contrast, a microtubule depolymerizing agent colchicine has not been approved as an anticancer drug due to its extreme toxicity. However, over the past decade, various agents possessing colchicine-like tubulin depolymerizing activities (*e.g.*, combretastatin A-4 [CA-4], ZD6126, AVE8062 and ABT-751) have been recognized to act as both cytotoxic and vascular disrupting agents (VDAs) [1]. The latter class of molecules induces the collapse of established tumor vasculature via rapid microtubule depolymerization. This leads to a loss of blood supply and eventual contraction of the tumor. Hence, the microtubule-depolymerizing agents represent a promising new class of anti-cancer drugs.

Results and Discussion

Plinabulin (**1**, NPI-2358/KPU-2, Fig. 1), which we developed, is a potent anti-microtubule agent derived from the natural diketopiperazine (DKP) Phenylahistin [2] with a colchicine-like tubulin depolymerization activity. **1** was developed as a VDA in 2006 [3], and is now in clinical trials as an anticancer drug in four countries including the United States. We further modified the phenyl group and 5-position of the imidazole ring on **1**, and evaluated their cytotoxic and tubulin-binding activities. One of the derivatives (**2**, KPU-105, Fig. 1), which possess a benzophenone, *m*-benzoyl derivative, was more potent than the original structure [4]. The vascular disrupting activity of **2** as evaluated with human vascular endothelial cells (HuVECs) was 10- and 3-fold more potent than that of CA-4 and **1**, respectively. This result indicated that **2** was a valuable anti-microtubule and vascular disrupting agent. In further modification, a series of potent diketopiperazine-type anti-microtubule agents with a benzophenone structure was designed and synthesized. Then, a SAR study was performed, which indicated that we had developed a potent 4-fluorobenzophenone derivative, **3a** (R₃ = F, R₁, R₂, R₄ = H), possessing subnanomolar IC₅₀

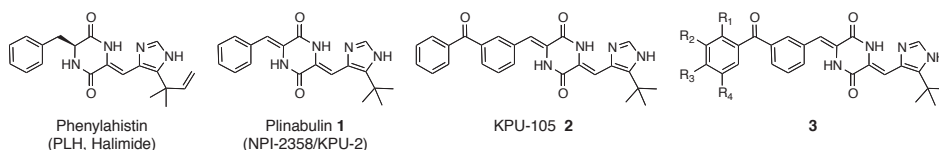


Fig. 1. Structure of anti-microtubule diketopiperazines

values against HT-29 cells [5]. In general, modifications at the 4-position of the benzophenone structure were well tolerated with respect to activity. Moreover, our data suggested that the non-planar conformation of the benzophenone was crucial to effective tubulin binding and potent cytotoxicity. Next, the effects on mitotic spindles were evaluated in HeLa cells. Treatment with 3 nM of **3a** partially disrupted the interphase microtubule network, whereas treatment with CA-4 at the same concentration had almost no effect, indicating that **3a** had more potent anti-mitotic activity than CA-4. As a result, we developed a highly potent compound, which has 30-times higher cytotoxicity than **1**, would be a promising candidate for the next-generation drug.

We have also studied the tubulin-binding site of these DKPs using photoreactive chemical probes to understand the precise mechanism of microtubule depolymerization [6]. Moreover, since the water solubility of **1** was very low (<0.1 mg/mL), a water-soluble prodrug was developed to improve the pharmaceutical value, based on the skeletal transformation to monolactim and click chemistry to conjugate the serine-type water-solubilizing moiety [7]. The prodrug showed a 64,000-fold higher water-solubility (6.8 mg/mL) than **1** and completely reproduce **1** by esterase hydrolysis without any side reaction.

Acknowledgments

This research was supported by grants from the Ministry of Education, Culture, Sports, Science and Technology (MEXT) of Japan, including a Grant-in-aid for Young Scientists (B) 23790143 and a Grant-in-aid for Scientific Research (B) 23390029.

References

- [1] Daenen, L. G. M.; Roodhart, J. M. L.; Shaked, Y.; Voest, E. E. *Curr. Clin. Pharmacol.* **2010**, *5*, 178.
- [2] a) Kanoh, K.; Hayashi, Y. *et al. Bioorg. Med. Chem.* **1999**, *7*, 1451; b) Hayashi, Y. *et al. J. Org. Chem.* **2000**, *65*, 8402.
- [3] Nicholson, B. *et al. Anti-Cancer Drugs* **2006**, *17*, 25.
- [4] Yamazaki, Y.; Hayashi, Y. *et al. J. Med. Chem.* **2012**, *55*, 1056.
- [5] Yamazaki, Y.; Hayashi, Y. *et al. Bioorg. Med. Chem.* **2012**, *20*, 4279.
- [6] a) Yamazaki, Y.; Hayashi, Y. *et al. ChemBioChem* **2008**, *9*, 3074; b) Yamazaki, Y.; Hayashi, Y. *et al. Bioorg. Med. Chem.* **2010**, *18*, 3169; c) Yamazaki, Y.; Hayashi, Y. *et al. ibid.* **2011**, *19*, 595.
- [7] a) Yakushiji, F.; Hayashi, Y. *et al. Chem. Eur. J.* **2011**, *17*, 12587; b) Yakushiji, F.; Hayashi, Y. *et al. Chem. Pharm. Bull.* **2012**, *60*, 877.

Branched diketopiperazines as a universal scaffold for preparation of orally active small peptide derivatives

Vladislav Deigin

*Shemyakin & Ovchinnikov Institute of Bioorganic Chemistry Russian Academy of Sciences,
Moscow, Russia
E-mail: vdeigin@gmail.com*

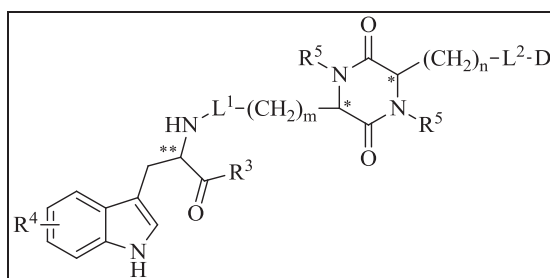
Introduction

One of the main challenges of peptide-based drugs is their low enzymatic stability and hence limited potential for oral administration. This limitation is narrowing the introduction of peptides in medical practice. [1].

Our work in 1980s on separation of the biologically active peptide L-Glu-L-Trp from the calf thymus extracts gave rise to the structure-functional studies of peptide families containing this dipeptide. The influence of optical and chemical isomers on biological activity of various Glu-Trp analogs has been studied in vitro and in vivo [2]. The data obtained pointed to a link between the biological activity and the chemical and optical structures for each of the twelve possible isomers. [2]. Three approved pharmaceutical preparations: Thymogen (L-Glu-L-Trp-ONa), Thymodepressin (D-Glu-(D-Trp)-ONa) and Stemokine (L-Ile-L-Glu-L-Trp-ONa) had been developed as a result of these studies. [3].

Results and Discussion

One of the possible ways of stabilizing the dipeptides is converting them into 2,5-diketopiperazine derivatives (DKP). Among the Glu-Trp peptides, biological activity was exhibited by isomers with gamma peptide bond between Glu and Trp residues. These compounds do not form DKP and require an alternative approach to stabilization. We have developed a new chemical platform based on branched diketopiperazines for creating orally available biologically active peptidomimetic and other “chimerical” compounds. In this case we have synthesized DKP derivative containing a third amino acid attached to the NH₂- group of the Glu residue (both L- and D- configurations). This new DKP-derivative became a novel scaffold for the family of cyclo-{(X-Glu)-Trp} (Fig.1) analogs. [4].



L¹, L² – linkers; R^x – substitutes; D – bioactive molecules; m, n, - 1,2, 3;

Fig.1. General formula of 2,5-diketopiperazine derivatives containing a built-in Glu-Trp fragment.

The platform technology we have developed, called Cyclotechnology, allows taking a small peptide with a particular biological activity and creating a new orally available compound that possesses the same type of activity (Fig.1). Using the conventional solution method, we have synthesized a number of dually functional compounds that combine a diketopiperazine scaffold and known small molecule pharmacophores, such as fatty acids, carbohydrates, antibiotics and non-steroid anti-inflammatory molecules. This approach has been applied to molecules whose mass ranges from 300 to 1000 Daltons. Results of oral activity for some immune- and hemoregulatory compounds are listed in Tables 1 and 2.

Table 1: Comparison of Thymodepressin and cyclo-immune- and hemosuppressors

Structure	CFU-8-S per 10 ⁵ cells	% suppression
Control	11.2± 0.4	-
γDGlu-DTrp (Thymodepressin) (i/p)	6.3±0.6*	55
cyclo-DAla-DGlu-(DTrp-ONa) (per os)	6.0±0.7*	58
cyclo-LAla-LGlu-(LTrp-ONa) (i/p)	11.7± 0.8	0
cyclo-DPhe-DGlu-(DTrp-ONa) (per os)	8.1± 0.4*	48

** Significance was calculated relative to this group,

* P < 0.05

Table 2: Comparison of Stemokine and novel cyclic peptides of hemostimulation

Irradiation Dose	Peptide	Dose, µg/kg	CFU-8-S per 10 ⁵ cells M ± m	% stimulation
-	-	-	11.9 ± 0.4	100
1 Gy	-	-	6.2 ± 0.6**	0
1 Gy	Stemokine (IM)	10	11.6 ± 0.8*	97.5
1 Gy	Stemokine (per/os)	100	6.7 ± 0.5	0
1 Gy	cyclo-[L-Glu(L-Ile)-L-Glu(L-Trp)] (per/os)	100	11.7±0.6*	98.3
1 Gy	Cyclo-LAla-LGlu-(LTrp-ONa) (per/os)	100	8.9 ± 0.5*	74.8

** Significance was calculated relative to this group,

* P < 0.05

References

- [1] Antosova, Z; Mackova, M; Kral,V.; Macek, T. *Trends in Biotechnology*, **2010**, 27, N 11, 628.
- [2] Deigin, V.I.; Semenets T.N.; et.al. *Int. Immunopharmacology*, **2007**, 7, 375.
- [3] Deigin, V.I, Poverenny, A, Semina, O.; Semenets, T. *Proc. of American Peptide Symposia*, **2002**, V. 6, Part 14, 626.
- [4] Deigin, V.I; *Australian patent - AU2007280995*; Patent pending: **WO 2008/014613 -1 - CT/CA2007/001357**; worldwide priority: 60/835,428 04.08.06 US.

Glycan targets of the anti-cancer peptide NK-2

Stephanie Gross, Jörg Andrä

*Hamburg University of Applied Sciences, Department of Biotechnology, Lohbrügger
Kirchstr. 65, D-21033 Hamburg, Germany*

E-mail: joerg.andrae@haw-hamburg.de

Introduction

NK-2 is a synthetic peptide of 27 amino acid residues in length [1] and represents the cationic core region of NK-lysin, a protein with anti-cancer activity, which has been originally identified in porcine NK-cells [2]. NK-2 has a positive net charge and adopts an amphipathic α -helical secondary structure upon interaction with negatively charged lipid membranes [1, 3, 4]. We and others have comprehensively studied the activity and mode of action of NK-2 and of derivatives thereof against model membranes [3-7], bacteria [3, 7, 8], bacterial endotoxin [9, 10], protozoa [11, 12], and against normal as well as transformed human cells (Table 1) [13-15]. The peptide turned out to be a potent antimicrobial at the same time exhibiting low cytotoxicity to normal human cells such as erythrocytes. Bacterial killing is a rapid process. Initial binding of the peptide to the bacterial membrane is followed by effective membrane permeabilization and accompanied by dramatic morphological changes of attacked cells [8]. The selectivity of NK-2 for bacteria could be linked to the preference of the peptide to interact with negatively charged bacterial membrane components, i.e. phosphatidylglycerol [5, 7] and lipopolysaccharide [8]. The human cell surface is normally devoid of anionic lipids, however, phosphatidylserine may be dislocated from the inner membrane leaflet to the cell surface during various pathophysiological processes including cancer [13, 16, 17] and thus rendering also human cells sensitive to the action of cationic peptides such as NK-2 [13]. Besides phosphatidylserine, in particular sialic acids have been discussed as potential targets for cationic peptides on cancer cells.

Results and Discussion

We followed the hypothesis that sialic acids are potential target structure of cationic peptides on cancer cells. Hence, we enzymatically removed cell surface sialic acids from PC-3 human prostate cancer cells. Surprisingly, this treatment had virtually no effect on NK-2-mediated changes in cell metabolism, cell membrane permeabilisation, cell killing rate, as well as cell killing kinetics [15]. To identify hitherto unidentified carbohydrate target structures of NK-2, a glycan microarray screen with fluorescently labeled peptides has been performed. Among 465 mammalian glycan structures on the chip, more than 20 different sulphated glycans were detected as preferred binding partners of peptide NK-2. In contrast, the amount of NK-2 which was bound to sialic acid containing oligosaccharides was close to background level. This finding was consistent with microcalorimetric experiments revealing high and low binding enthalpies of peptides to sulphated carbohydrates and to sialic acid, respectively. Moreover, cytotoxicity of NK-2 was drastically impaired by competitive inhibition by chondroitin sulphate, but not by sialic acid and sialylated fetuin. Conclusively, we suggest that sulphated glycans rather than sialic

acids are the primary carbohydrate targets of peptide NK-2 and related peptides on cancer cells.

Table 1

Activity of peptide NK-2 against human cancer cell lines and primary cells		
Human cells	IC ₅₀ (µg/ml)	References
PC-3 prostate cancer	10 - 13	[15]
LAN-1 neuroblastoma	6 - 10	[13]
HaCaT keratinocytes	25 - 32	[1, 14]
Primary lymphocytes	>> 300	[13]
Erythrocytes	> 150	[14]

IC₅₀, concentration at which the viability of a cell population was reduced by 50%

Acknowledgements

The glycan array analysis was performed by core H of the Consortium for Functional Glycomics (CFG). This project was supported by a grant of the German Science Foundation (Deutsche Forschungsgemeinschaft, DFG, AN301/5-1).

References

- [1] Andrä, J.; Leippe, M. *Med. Microbiol. Immunol.* **1999**, *188*, 117.
- [2] Andersson, M.; Gunne, H.; Agerberth, B.; Boman, A.; Bergman, T.; Sillard, R.; Jörnvall, H.; Mutt, V.; Olsson, B.; Wigzell, H.; Dagerlind, A.; Boman, H. G.; Gudmundsson, G. H. *EMBO J.* **1995**, *14*, 1615.
- [3] Andrä, J.; Monreal, D.; Martinez de Tejada, G.; Olak, C.; Brezesinski, G.; Sanchez Gomez, S.; Goldmann, T.; Bartels, R.; Brandenburg, K.; Moriyon, I. *J. Biol. Chem.* **2007**, *282*, 14719.
- [4] Olak, C.; Muentner, A.; Andrä, J.; Brezesinski, G. *J. Pept. Sci.* **2008**, *14*, 510.
- [5] Schröder-Borm, H.; Willumeit, R.; Brandenburg, K.; Andrä, J. *Biochim. Biophys. Acta* **2003**, *1612*, 164.
- [6] Willumeit, R.; Kumpugdee, M.; Funari, S. S.; Lohner, K.; Pozo Navas, B.; Brandenburg, K.; Linsler, S.; Andrä, J. *Biochim. Biophys. Acta* **2005**, *1669*, 125.
- [7] Andrä, J.; Goldmann, T.; Ernst, C. M.; Peschel, A.; Gutschmann, T. *J. Biol. Chem.* **2011**, *286*, 18692.
- [8] Hammer, M.; Brauser, A.; Olak, C.; Brezesinski, G.; Goldmann, T.; Gutschmann, T.; Andrä, J. *Biochem. J.* **2010**, *427*, 477.
- [9] Andrä, J.; Koch, M. H. J.; Bartels, R.; Brandenburg, K. *Antimicrob. Agents Chemother.* **2004**, *48*, 1593.
- [10] Brandenburg, K.; Garidel, P.; Fukuoka, S.; Howe, J.; Koch, M. H.; Gutschmann, T.; Andrä, J. *Biophys Chem* **2010**, *150*, 80.
- [11] Jacobs, T.; Bruhn, H.; Gaworski, I.; Fleischer, B.; Leippe, M. *Antimicrob. Agents Chemother.* **2003**, *47*, 607.
- [12] Gelhaus, C.; Jacobs, T.; Andrä, J.; Leippe, M. *Antimicrob. Agents Chemother.* **2008**, *52*, 1713.
- [13] Schröder-Borm, H.; Bakalova, R.; Andrä, J. *FEBS Lett.* **2005**, *579*, 6128.
- [14] Drechsler, S.; Andrä, J. *J. Bioenerget. Biomem.* **2011**, *43*, 275.
- [15] Gross, S.; Andrä, J. *J. Biol. Chem.* **2012**, *393*, 817.
- [16] Utsugi, T.; Schroit, A. J.; Connor, J.; Bucana, C. D.; Fidler, I. J. *Cancer Res.* **1991**, *51*, 3062.
- [17] Riedl, S.; Rinner, B.; Asslaber, M.; Schaidler, H.; Walzer, S.; Novak, A.; Lohner, K.; Zwegyick, D. *Biochim. Biophys. Acta* **2011**, *1808*, 2638.

Design, synthesis and analysis of anti-tuberculosis peptides

Zaid Amso¹, Chris Miller², Ronan O'Toole², Vijayalekshmi Sarojini^{1,*}

¹School of Chemical Sciences, The University of Auckland, Private Bag 92019, Auckland, New Zealand; ²School of Biological Sciences, Victoria University of Wellington, Wellington, New Zealand

*E-mail: v.sarojini@auckland.ac.nz

Introduction

The evolution of multidrug resistant strains of *Mycobacterium tuberculosis* threatens the effectiveness of current therapies [1]. New drugs are thus needed to treat drug resistant and latent forms of TB. Antimicrobial peptides are attractive alternatives to conventional antibiotics in this regard. Incorporation of non-protein amino acids in designed antimicrobial peptides is widely used to overcome the short half-life of these, otherwise, attractive molecules as drugs. Because of the beneficial effects of selenium containing micronutrient supplementation in pulmonary tuberculosis, selenopeptides hold promise for tuberculosis therapy. Chemical library screening under nutrient deprived conditions by Miller *et. al.* identified the non-protein amino acid Se-methylselenocysteine (MeSeCys) as a potent inhibitor of *Mycobacterium smegmatis* [2]. It is hypothesised to be cleaved by a selenocysteine lyase encoded by mycobacteria producing toxic methylselenol accounting for the observed anti-mycobacterial activity. In an analogous process, derivatives of a closely related amino acid, selenomethionine, has been reported to produce methanethiol significantly higher than the parent compound selenomethionine [3]. No literature data is available on the anti-mycobacterial activity of selenomethionine (SeM) but it is hypothesized that selenomethionine containing peptides could induce toxicity to mycobacteria through the production of methylselenol. Preliminary studies to test this hypothesis have been carried out using a small number of SeM dipeptides and derivatives. Results from these studies are presented here.

Results and Discussion

The SeM peptides were prepared by manual Fmoc solid-phase peptide synthesis and purified to homogeneity using reversed-phase High Performance Liquid Chromatography. Resazurin reduction microtitre assay was used to evaluate the *in vitro* anti-mycobacterial activity of the selenopeptides on *M. tuberculosis* H37Ra in comparison to isoniazid. Bioassay results are summarised in table 1. SeM showed good activity against the bacterial strain with an MIC of 32 μ M. Three different dipeptides of the sequence Ala-SeM, SeM-Ala and SeM-Arg were also tested in this assay. It was hypothesized that conjugating alanine to SeM could facilitate easy entry into the cells through the hydrophobic lipid bilayer increasing bacterial uptake leading to better activity. Based on the work of Ferchichi *et. al.* on *Brevibacterium linens* that showed significant increase in the production of methanethiol from L-Met-NH₂ in comparison to L-Met itself, it was also hypothesized that the amidated versions of SeM and Ala-SeM could augment the production of methylselenol leading to enhanced anti-mycobacterial activity. SeM-Arg was included in the bioassay because of the beneficial effects reported for arginine as an adjuvant treatment in tuberculosis therapy [4]. Unfortunately, all compounds tested showed diminished anti-

mycobacterial activity in comparison to SeM itself indicating that the observed activity of SeM is sensitive to structural modifications. The diminished activity of the tested compounds could indicate reduced affinity to the lyase enzyme resulting in poor metabolism to the toxic methylselenol product. Even though the synthetic peptides did not show improved anti-mycobacterial activity as speculated, this study was useful to gain knowledge on the structure-activity relationships (SAR) of this class of compounds. A sequence dependence of anti-mycobacterial activity amongst the tested compounds could be observed. The four-fold difference in MIC observed between the two alanyl dipeptides indicate that the bioactivity is very sequence dependent even at the dipeptide stage. The detrimental effect on anti-mycobacterial activity was much less pronounced for SeM-Arg which showed an MIC of 125 μM , 8 X that of its alanyl counterpart. Favourable electrostatic interactions between arginine and the negatively charged groups on the bacterial cell membrane is clearly facilitating better targeting of SeM to bacterial cells. Our results (SeM vs SeM-NH₂) also indicate that the carboxylic acid group at the C-terminus could be vital for prodrug recognition and cleavage.

Sensitivity of the anti-mycobacterial activity of SeM towards structural modifications is apparent from the results presented in this paper. However, these preliminary observations will need to be verified further using larger selenopeptide libraries to fully understand the SAR of selenopeptides and evaluate their potential as potential anti-tuberculosis agents. This is currently being investigated in our laboratories.

Table 1. The minimal inhibitory concentration (MIC) of selenopeptides against *M.tuberculosis* H37Ra

Compound	Isoniazid	SeM	SeM-NH ₂	SeM-Ala	Ala-SeM	Ala-SeMNH ₂	SeM-Arg
MIC (μM)	3.13	32	125	1000	250	250	125

References

- [1] Blanchard, J.S. *Annual review of biochemistry* **1996**, 65, 215-239.
- [2] Miller, C. H.; Nisa, S.; Dempsey, S.; Jack, C.; O'Toole, R. *Antimicrob. Agents Chemother.* **2009**, 53, 5279-5283.
- [3] Ferchichi, M., D. Hemme, M. Nardi, and N. Pamboukdjian. **1985**. *J. Gen. Microbiol.* 131, 715-723.
- [4] Schon, T.; Elias, D.; Moges, F.; Melese, E.; Tessema, T.; Stendahl, O.; Britton, S.; Sundqvist, T. *Eur. Res.pir. J* **2003**, 21, 483-8.

Cardioprotective peptides to fight ischemia/reperfusion injury in mouse hearts

Prisca Boisguerin^{1,3}, Alicia Franck², Aurélie Covinhes², Stéphanie Barrère-Lemaire², Bernard Lebleu¹

¹UMR 5235 CNRS, Université Montpellier 2, Place Eugène Bataillon, 34095 Montpellier cedex 5, France; ²Institut de Génomique Fonctionnelle, UMR 5203, U661, Université Montpellier 1, 2 ; 141 rue de la Cardonille, 34094 Montpellier cedex 5, France; ³IMI, Charité Universitätsmedizin Berlin, Hessische Strasse 3-4, 10115 Berlin, Germany

E-mail: prisca.boisguerin@univ-montp2.fr

Introduction

Acute myocardial infarction (AMI) is a frequent and disabling disease, and infarct size is a major determinant of myocardial functional recovery and mortality. Prompt revascularization of AMI by reperfusion (using thrombolysis or primary coronary angioplasty) has improved myocardial function and increased patient survival dramatically [1, 2]. However, reperfusion is a double edge sword inducing deleterious effects called ischemia-reperfusion (IR) injury. Many pathological conditions are associated with IR injury: cardiac surgery, organ transplantation, trauma and resuscitation or - in the case of ischemic cardiovascular disease - acute coronary syndrome and stroke. The prevention of apoptosis during myocardial IR is thought to be promising for myocardial protection in cardiac surgery.

Proteins of the apoptosis cascade generally interact over large surfaces lacking well-defined pockets. Therefore, inhibitory peptides are optimal biomolecules to target these large protein surfaces. They are often more selective to their target than conventional small organic molecules and they can be tailored for optimal affinity or desired metabolic property. Since peptides do not cross freely biological membranes, they are generally administered in association with cell penetrating peptides (CPPs).

Results and Discussion

As a first *in vivo* approach, we made use of the already known BH4 peptidic inhibitor of the mitochondrial apoptotic pathway, which showed cardioprotective properties in a murine model of AMI after a single bolus of intravenous administration [1].

Interestingly, the BH4 peptide is efficiently internalized and inhibits apoptosis in primary cardiomyocytes significantly when conjugated to the Tat CPP. This differs from our previous data with Tat conjugated to peptide nucleic acid (PNA) or phosphorodiamidate morpholino oligonucleotide (PMO) showing low efficiency in the absence of endosomolytic agents.[4] At the optimal concentration of 1 mg/kg, Tat-BH4 and Pip2b-BH4 conjugates gave rise to a reduction in infarct size of 45% to 48%, which was not observed for the control Tat-scrBH4 construct after 24 h reperfusion. Furthermore, the cardioprotective effects of both conjugates were correlated to apoptosis as monitored by specific DNA fragmentation measurements revealing a strong decrease in apoptosis by comparing the ratio of soluble nucleosomes detected in the ischemic (I) versus non

ischemic (NI) part of the left ventricle [3]. In agreement with the *in vitro* data, Pip2b-BH4 was as efficient as Tat-BH4 to inhibit IR-induced DNA fragmentation at 24 h reperfusion (Tat-BH4: 55.8%; Pip2b-BH4: 66.0%) and this was not observed with negative controls.

Additionally, we have screened SPOT peptide libraries for new apoptosis inhibitors and coupled them to the Tat CPP. Biological activity was tested *in vitro* as the ability to protect primary mouse cardiomyocytes from death induced by staurosporine. Cardioprotection was achieved upon systemic low dose administration in C57BL/6J mice submitted to an I/R protocol [3]. First results will be shown and discussed [5].

In general, a peptidic strategy is considered as a disadvantage due to its fast degradation by seric proteins. In the case of IR injuries, peptides represent particularly well-suited drugs since the anti-apoptotic agent only needs to be present over a short time-window and should preferably be degraded and rapidly eliminated thereafter minimizing side effects (i.e. immunogenicity). Our data show that our CPP constructs are rapidly degraded upon incubation with mouse serum (*in vitro*) [3, 5] and are cleared by hepatic and renal elimination (as seen by *in vivo* SPECT scan imaging in mice).

More importantly, similar peptidic strategies and tools are likely to be adaptable to many other situations in which cells have to be protected from apoptosis such as stroke or organ transplantation.

Acknowledgments

This work was supported by the Agence Nationale pour la Recherche (ANR-08-Genopat-031) and by the CNRS.

References

- [1] Braunwald, E. *Circulation* **1989**, 79, 441.
- [2] McGovern, P.G., Pankow, J.S., Shahar, E., Doliszny, K.M., Folsom, A.R., Blackburn, H., Luepker, R.V. *N. Engl. J. Med.* **1996**, 334, 884.
- [3] Boisguerin, P., Clouet-Redt, C., Franck, A., Licheheb, S., Barrere-Lemaire, S., Nargeot, J., Lebleu, B. *J. Control. Release.* **2011**, 156, 117.
- [4] Richard, J.P., Melikov, K., Brooks, H., Prevot, P., Lebleu, B., Chernomordik, L.V. *J. Biol. Chem.* **2005**, 280, 15300.
- [5] Boisguerin, P., Redt-Clouet, C., Franck-Miclo, A., Vincent, A., Covinhes, A., Lattuca, B., Piot, C., Nargeot, J., Lebleu, B., Barrère-Lemaire, S. submitted to *Circulation* **2012**.

Lead optimization of allophenylnorstatine-containing inhibitors as therapeutic drug and application to peptidomimic protease probe

Koushi Hidaka¹, Motoyasu Adachi², Ryota Kuroki², Satoko Tokai³,
Kenichi Akaji³, Yuko Tsuda¹, Yoshiaki Kiso^{1,4}

¹Faculty of Pharmaceutical Sciences, Kobe Gakuin University, Kobe, Japan; ²Molecular Structural Biology Group, Japan Atomic Energy Agency, Tokai, Japan; ³Department of Medicinal Chemistry, Kyoto Pharmaceutical University, Kyoto, Japan; ⁴Peptide Science Laboratory, Nagahama Institute of Bio-Science and Technology, Nagahama, Japan

E-mail:khida@pharm.kobegakuin.ac.jp

Introduction

Allophenylnorstatine (Apns) is *alpha*-hydroxy-*beta*-amino acid which has hydroxymethylcarbonyl moiety to mimic substrate transition state tetrahedral diol in hydrolysis mechanism of aspartic protease. Apns-containing peptidomimetics are known to bind tightly to aspartic proteases such as HIV protease and malarial plasmepsin (Plm), potential drug targets against HIV infection and malaria, respectively. The hydrogen bonding interactions between hydroxymethylcarbonyl and two catalytic Asp residues of HIV protease were recently disclosed by neutron crystallography [1]. In the HIV protease inhibitor study, we faced a problem of much difference in activity of a compound with 2,6-dimethylphenoxyacetyl moiety against the enzyme and the virus. The protease inhibitory potency was plateau because of the limited structural modifications. Therefore, we shifted to modify the property such as reduction of the hydrophobicity. During the struggles, amino substitution succeeded in improving the water solubility to enhance the anti-HIV activity and with the sustained protease inhibitory activity [2]. This result stimulated us to modify the Apns-containing inhibitors for the development of therapeutic drug and to utilize them as aspartic proteases probes.

Results and Discussion

Apns-containing Plm inhibitor study was in the similar situation that a small peptidic Plm inhibitor KNI-10006 possesses highly potent activity against Plms but with low anti-malarial activity (Plm II K_i 0.5 nM, EC_{50} 6.8 μ M, Fig. 1) [3]. As derived from Apns-containing HIV protease inhibitors, KNI-10006 possesses the same 2,6-dimethylphenoxyacetyl moiety at the *N*-terminal, suggesting the hydrophobic problem above mentioned. Along with the modification on HIV protease inhibitors, we searched substituted amino group to attach at the 2,6-dimethylphenoxyacetyl moiety to enhance anti-malarial activity. The series with amino substituents resulted in ten-fold increased potency including KNI-10538 (K_i 10 nM, EC_{50} 0.3 μ M, Fig. 1) [4]. Interestingly, these compounds maintained the nanomolar Plm II inhibitory activity. We roughly estimate the activity gap ratio, EC_{50}/K_i , was changed from 13600 (KNI-10006) to 30 (KNI-10538) with the amino substituent.

Enhancing peptide activity and structure by synthetic constraint of beta-turns and beta-sheets: CLIPS and anti-CD40L phylomers

**Shane R. Stone¹, Richard Hopkins^{1,2}, Paula T. Cunningham¹, Maria
Kerfoot¹, Yew-Foon Tan¹, Wim Schaaper³, Nicolas Dailly³,
Peter Timmerman³**

*¹Drug Discovery Technology Unit, Telethon Institute for Child Health Research, 100
Roberts Road, Subicaco, 6008, Western Australia; ²Phylogica Pty Ltd, 100 Roberts Road,
Subiaco, 6008, Western Australia; ³Pepsan, Zuidersluisweg 2, 8243 RC, Lelystad, The
Netherlands*

E-mail: sstone@ichr.uwa.edu.au

Introduction

The CD40-CD40L pathway plays a number of important roles within the immune system and has been a subject in the potential treatment of the autoimmune diseases rheumatoid arthritis and systematic lupus erythematosus [1]. The CD40-CD40L pathway has also been the focus of antibody-based treatments for a variety of cancers [2] but with varying degrees of success due to complications arising from Fc effector functions [3]. It is believed that small protein and peptide-based inhibitors of this pathway may provide more attractive therapeutic alternatives to antibodies [3]. In this paper we present, as a case study, our results from targeting CD40L using phylomer libraries [4] and our attempts to enhance structure and potency using Pepsan's CLIPS technology [5] to stabilize β -turns and promote β -sheet conformation.

Results and Discussion

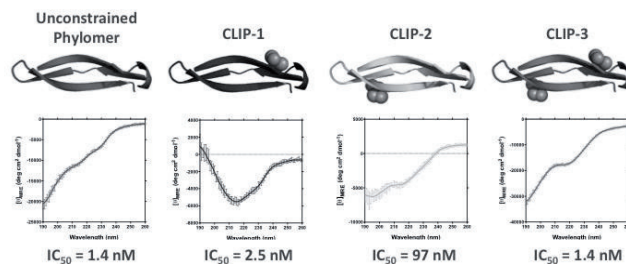
Biopanning of phylomer phage display libraries against human CD40L yielded a cluster of six, highly specific, overlapping peptide fragments corresponding to the conserved catalytic domain from the G α 2 β 2 family of Glycyl tRNA synthetases. Structural analysis of the Glycyl tRNA synthetase family showed that the overlapping peptide fragments described a scaffold consisting of a central β -sheet, comprising 4 anti-parallel β -strands, flanked by N- and C-terminal α -helices, and this was confirmed by Circular Dichroism of a recombinant phylomer.

Further analysis of the overlapping hits indicated that the minimum interaction sequence comprised the 41 amino acids encoding the 3 N-terminal β -strands of the larger conserved motif. Further it appeared that two highly conserved β -turns and the conserved location of several hydrophobic residues were critical for activity by ensuring correct folding to a β -sheet containing structure. With this in mind we hypothesized that the β -sheet structure was key for binding and activity and that by stabilizing the conserved β -turns we could enhance β -sheet content and thus potency. To achieve this we utilized Pepsan's CLIPS technology

to synthetically constrain the β -turns by substitution of certain residues with cysteine and using small molecule linkers to join the proximal residues.

Circular Dichroism spectra of the unconstrained and three CLIPs phylomers showed that the CLIPs do have an effect on the conformation. Strikingly, the unconstrained phylomer did not recapitulate the strong β -sheet conformation seen for the original 4-stranded motif. The CLIP-1 peptide, which linked strands 1 and 2 had the most pronounced impact, effectively restoring β -sheet conformation seen for the full four-stranded motif. The CLIP-2 phylomer, which linked strands 2 and 3, and the CLIP-3 phylomer, linking strands 1 and 2, and 2 and 3, both showed shifted random coil but with small minima at ~ 218 nm, suggestive of some β -sheet content.

Figure 1. Circular Dichroism spectra and CD40L/CD40 Alphascreen IC₅₀s for the unconstrained Phylomer and the three CLIPs-variants



In terms of activity, the most potent phylomers were the unconstrained 3-stranded phylomer and the doubly constrained CLIP-3, which were equipotent. Constraining strands 2 and 3 for CLIP-2 resulted in a 70-fold reduction in potency but with no clear concomitant conformational change. The strongly β -sheet CLIP-1 was 2-fold less potent than the control. That there is conformational discrepancy between almost equipotent phylomers suggests that our initial hypothesis that the structure of the 3-stranded phylomer is vital for binding is incorrect. Rather, the data indicates that these fragments are likely to binding via an induced-fit mechanism.

In conclusion, we established that phylomer β -sheet content in solution did not necessarily correlate with increased potency but that the use of CLIPS could significantly stabilize β -turns and induce β -sheet conformation. Other results (not shown) also highlighted the importance of the CLIPS positioning in the sequence and structure, and their chemical properties and linker length.

References

- [1] Daoussis, D., Andonopoulos, A.P., Liossis, S.N., *Clin. Diag. Lab. Immun.* **2004**,11 (4): 635-41
- [2] Elgueta, R., Benson, M.J., de Vries, V.C., Wasiuk, A., Guo, Y., Noelle, R.J., *Immun. Rev.* **2009**, 229 (1): 152-72
- [3] Deambrosis, I., Lamorte, S., Giarretta, F., Tei, L., Biancone, L., Bussolati, B., Camussi, G., *J. Mol. Med.*, **2009**, 87 (2): 181-97
- [4] Watt, P.M., *Nature Biotech.*, **2006**, 24 (2): 177-83
- [5] Timmerman P, Puijk WC, Melen RH., *J. Mol. Recognit.* **2007**, 20, 283-299

Development of a unique peptide synthetic method AJIPHASE[®] using anchor support molecules to suppress alkylation in final cleavage step

Daisuke Takahashi, Tatsuji Inomata

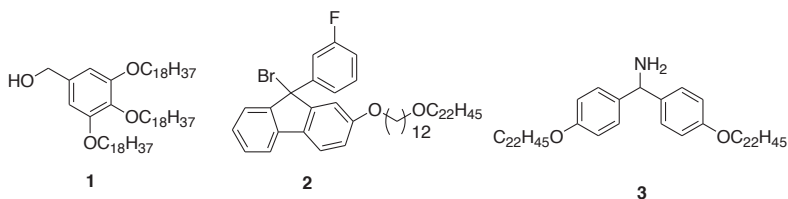
Research Institute for Bioscience products and Fine chemicals, AJINOMOTO Co., Inc.,
1730 Hinaga Yokkaichi Mie 510-0885 Japan

E-mail: daisuke_takahashi@ajinomoto.com

Introduction

In recent years, development of peptide drugs has increasingly expanded and the need for peptide synthesis has increased accordingly. The peptide synthesis methods are roughly divided into liquid-phase peptide synthesis (LPPS) and solid-phase peptide synthesis (SPPS) techniques. Both methods have strong points and weak point respectively. Tamaki et al. reported an efficient LPPS protocol with a benzyl alcohol derivative bearing three long alkoxy chains **1**. Recently, we have also developed and reported new peptide synthetic method AJIPHASE[®] which combined the advantages of SPPS and LPPS, by using anchor support compounds bearing long aliphatic chain as a protecting group at C-terminal **2, 3**.

In traditional peptide synthesis, alkylated by-products have been generated by alkyl cation in the final deprotection step of protecting groups. Similar to the traditional peptide synthesis, alkylated peptide was observed in our synthesis, leading to significantly decrease of the yield of targeted peptide.

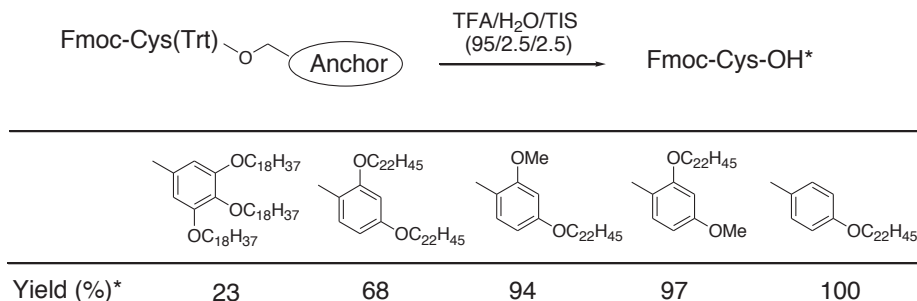


Results and Discussion

We developed a soluble anchor support molecule, possessing a benzyl alcohol/amine scaffold substituted by a long alkoxy chain and methoxy groups. This anchor molecule is applicable to Fmoc chemistry to prepare free form peptides, peptide amides and protected peptide acids. Long alkoxy chain works as the more efficient electron donating group compared to methoxy group. Undesirable alkylations in final deprotection step using TFA were suppressed by this modified anchor molecule which has one long alkoxy groups and methoxy groups instead of two or more long alkoxy chains. This concept was attempted and confirmed in the test of exposing Fmoc-Cys(Trt) loaded on to various type of anchor support molecules under TFA condition. This developed anchor support compounds allows the synthesis of various types of peptides with negligible amount of alkylation and good yield. The usefulness of the reported anchor support molecules for LPSS is demonstrated by the successful synthesis of peptides with more than 40 amino acid residues or with

difficult sequenced peptides. Their yields and purities were higher than ones using SPPS. That work was applied the patents for WO2011/078295.

Table. Evaluation of the recovery yield of Fmoc-Cys-OH from Fmoc-Cys(Trt) loaded onto various type anchor support compounds under TFA condition.



*recovery yield are total value of Fmoc-Cys-OH + Fmoc-Cys(Trt)-OH

Acknowledgments

We would like to thank Mr. Tatsuya Fukui and Mrs. Ai Nitta for help with experiments.

References

- [1] Tamiaki, H; Obata, T; Toma, K., *Peptide Science* **1998**, 125-128.
- [2] Takahashi, D.; Yamamoto, T. *Tetrahedron Letters*. **2012**, 53, 1936-1939.
- [3] Takahashi, D.; Fukui, T; Tatsuya, Y. *Organic Letters*. **2012**, in Press.

Mixed ion-exchange centrifugal partition chromatography: An efficient solution for peptide separation

Nassima Amarouche^a, Leslie Boudesoque^a, Pedro Lameiras^a, Jean-Marc Nuzillard^a, Matthieu Giraud^b, Alessandro Butte^b, Francesca Quattrini^b, Romain Kapel^c, Ivan Marc^c, Jean-Hugues Renault^{a*}

^aICMR UMR CNRS 7312, SFR Cap-Santé Université de Reims Champagne-Ardenne, Bât. 18, Moulin de la Housse, B.P. 1039, 51687 Reims cedex 2, France; ^bLonza AG, Valais Works, Rottenstrasse 6, 3930 Visp, Switzerland; ^cLaboratoire de Réactions et Génie des Procédés, UPR CNRS 3349, Institut National Polytechnique de Lorraine Nancy, France

E-mail: jh.renault@univ-reims.fr

Introduction

Centrifugal Partition Chromatography (CPC) is a support-free chromatographic technique, which was particularly developed in the field of phytochemistry [1]. The introduction of the so-called displacement mode expanded the field of CPC applications by allowing an easiest access to ionic or ionizable compounds. Ion-exchange CPC (IXCPC) purification of cationic molecules requires the presence of an exchanger in the organic stationary phase, namely a lipophilic anionic extraction agent.

During sample injection, the analytes and the exchanger must preferentially form ion pairs in the organic stationary phase. Then, the displacer-containing aqueous mobile phase is pumped through the stationary phase, and performs the displacement process of the hydrophilic analytes in the mobile phase, thus allowing them to progress in the CPC column as an isotactic train [2] (Fig. 1). In this framework, we have developed a preparative purification method devoted to peptide purification and based on strong and/or weak ion-exchange CPC. This method uses a lipophilic cation-exchanger: diethylhexylphosphoric acid (DEHPA), partially deprotonated by triethylamine (TEA) and a couple of displacers: Ca^{2+} and H^+ (fig. 1). To define the optimal operating conditions, a model mixture of five dipeptides was initially studied [3].

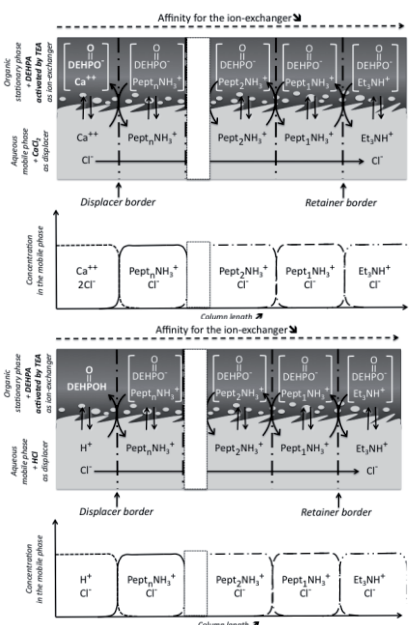


Fig. 1 : Isotactic train A: in the strong ion-exchange mode, B: in the weak ion-exchange mode.

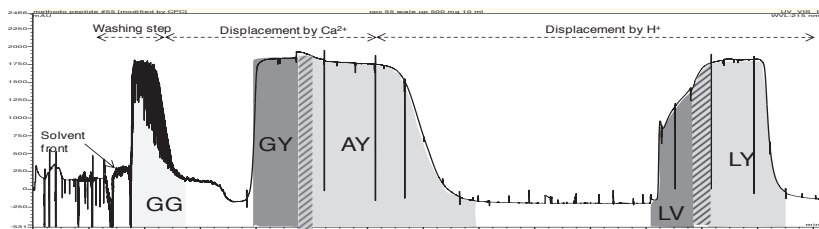


Fig. 2. MIXCPC chromatogram for the purification of 100 mg of each dipeptide. Biphasic solvent system: MtBE/CH₃CN/*n*-BuOH/water (2:1:2:5, v/v); stationary phase: upper organic phase + DEHPA (75 mM) with 30 % (25 % of the column volume) then 2.15% of TEA (75 % of the column volume); mobile phase: aqueous phase + CaCl₂ 7.2 mM, then HCl 12.5 mM; rotation speed: 1200 rpm; flow rate: 2 mL/min.

Results and Discussion

A model mixture of five dipeptides - GG, GY, AY, LV and LY - was chosen in order to study the potential of ion exchange CPC for peptide purification. These peptides have very close isoelectric points that range from 6.08 to 6.1, so that they are electrically charged in the same way at the same pH. Nevertheless, they cover a large polarity range, from the very polar GG to the quite apolar LV and LY. Both GY and AY have an intermediate polarity, and are structurally very close. The model mixture we chose thus allowed us to investigate the chromatographic process selectivity in a non-trivial case. Indeed, this mixture is not resolved by the previous published methods using CPC [3]. After optimization of the different experimental parameters, IX CPC, using the quaternary biphasic solvent system MtBE/CH₃CN/*n*-BuOH/water (2:1:2:5, v/v), was successfully applied to the purification of dipeptides within a five component model mixture as shown by the Fig. 2. The optimal separation conditions relied on a Mixed Ion eXchange CPC (MIXCPC) mode, which combined a strong displacer, calcium, and a weak displacer, proton. Moreover, the column was segmented in two parts, in which the exchanger was activated by triethylamine at two different concentrations (see caption of Fig. 2). Secondly, the ion exchange process we developed during this study succeeded to polish a synthetic peptide, the dirucotide, which was longer than those already purified by means of a similar strategy. Dirucotide, a 17-aminoacid peptide, analog of the 82-98 sequence of the myelin basic protein, is a drug candidate for the treatment of multiple sclerosis. The high purity (about 98%) of the obtained dirucotide fractions after IXCPC demonstrated the high selectivity of our process, since most of critical impurities were eliminated in our conditions, although they usually were co-eluted with all the previously tested methods. The presented results strongly suggest that IXCPC will be a very easy-to-use promising alternative to conventional peptide purification protocols.

References

- [1] Pauli, G.F.; Pro, S.M.; Friesen, J.B. *J. Nat. Prod.* **2008**, 71, 1489.
- [2] Maciuk, A.; Renault, J.-H.; Margraff, R.; Trébuchet, P.; Zèches-Hanrot, M. and Nuzillard, J.-M. *Anal. Chem.* **2004**, 76, 6179.
- [3] Boudesocque, L.; Lameiras, P.; Amarouche, N.; Giraud, M.; Quattrini, F.; McGarrity, J.; Nuzillard, J.-M.; Renault, J.-H.; *J. Chromatogr. A* **2012**, 1236, 115.

Conformation and biological activity of cyclolinopeptide A analogues modified within tetrapeptide fragment

Pro-Pro-Phe-Phe

Joanna Katarzyńska¹, Krzysztof Kierus¹, Jadwiga Olejnik¹, Krzysztof Huben¹, Jolanta Artym², Michał Zimecki², Janusz Zabrocki^{1,3},
Stefan Jankowski¹

¹Institute of Organic Chemistry, Faculty of Chemistry, Lodz University of Technology, Żeromskiego 116, 90-924 Łódź, Poland; ²Institute of Immunology and Experimental Therapy, Polish Academy of Sciences, R. Weigla 12, 53-114 Wrocław, Poland; ³Peptaderm Inc., Krakowskie Przedmieście Str.13, Warsaw, Poland

E-mail: stefan.jankowski@p.lodz.pl

Introduction

Cyclolinopeptide A (CLA) was isolated from linseed oil and identified as nonapeptide c(-Pro-Pro-Phe-Phe-Leu-Ile-Ile-Leu-Val), possessing a strong immunosuppressive activity comparable in low doses with cyclosporine A [1]. We focused on structure – activity studies of CLA analogues, modified within the tetrapeptide unit Pro-Pro-Phe-Phe, important for CLA activity. Different activities in several immunological models (proliferative response of mouse splenocytes to mitogens, humoral immune response *in vitro*, toxicity, modification of suppressive activity of MTX) were observed when β -prolines [2], β^3 -phenylalanine [3], homophenylalanine [4] or ethylene bridge between phenylalanine nitrogen atoms [5] were incorporated into CLA molecule.

Results and Discussion

Recently we applied new modifications within CLA molecule by introducing hydroxyproline (Hyp), pipercolic acid (Pip) or 2-naphthylalanine (Nal). The obtained peptides were characterized by means of NMR spectroscopy in CDCl₃ or/and DMSO solutions at 700 MHz.

For a CLA analogue, containing 4-hydroxyproline in position 1 (CLA-Hyp¹), only one isomer was found with the same *cis* geometry between proline residues as in native CLA. All peptide bonds in cyclopeptides containing 4-hydroxyproline in position 2 (CLA-Hyp²) or pipercolic acid in position 1 (CLA-Pip¹) were found to be *trans*. CLA analogues with two 4-hydroxyprolines (CLA-Hyp^{1,2}) or pipercolic acid in position 2 (CLA-Hyp²) exist as a mixture of two isomers due to *cis/trans* isomerization of Pro-Hyp or Pip-Pip peptide bonds. For CLA analogues with 2-naphthylalanine, the conformational analysis was not completed. ¹H NMR spectra of CLA-Nal in CDCl₃ analogues exhibit broad signals, similar to spectra recorded for unmodified CLA and characteristic for conformational flexibility of the peptide. The presence of 2-naphthylalanine in position 3 as in CLA-Nal³ and CLA-Nal^{3,4}

did not cause changes of chemical shifts of the γ protons of Pro². This can be interpreted as a much smaller shielding effect of Nal aromatic system in comparison to the phenyl ring of Phe in CLA.

The new peptides exhibited moderate anti-proliferative and anti-inflammatory properties as evaluated in the model of proliferation of human peripheral blood mononuclear cells (PBMC) stimulated with phytohemagglutinin A and in the lipopolysaccharide-induced production of tumor necrosis factor alpha in the human whole blood culture. Importantly, the peptides were devoid of toxicity up to 100 μ g/mL with regard to PBMC except of CLA-Hyp¹. CLA-Pip¹ was additionally tested for growth inhibition of L-1210 lymphatic leukemia and was found to strongly inhibit the cell growth even at low concentration (63% inhibition at 5 μ g/ml). Considering the range and degree of TNF α inhibition and lack of toxicity, CLA-Nal³ peptide might be interesting for further research in the *in vivo* models of inflammation. In conclusion, small modifications of the active sequence (Pro-Pro-Phe-Phe) within CLA molecule may result in appearance of new properties of potential therapeutic utility.

Acknowledgments

This project was supported by National Science Centre grant N N405 424239 .

References

- [1] Kaufmann, H. R.; Tobschirbel, A. *Chem. Ber.* **1959**, *92*, 2805.
- [2] Katarzyńska, J.; Mazur, A.; Bilska, M.; Adamek, E.; Zimecki, M.; Jankowski, S.; Zabrocki, J. *J. Pept. Sci.* **2008**, *14*, 1283.
- [3] Kaczmarek, K.; Farina, B.; Zubrzak, P.; Jankowski, S.; Zimecki, M.; Suder, P.; Benedetti, E.; Fattorusso, R.; Saviano, M. Zabrocki, *J. Pept. Sci.* **2009**, *15*, 166.
- [4] Drygała, P., Olejnik, J.; Mazur, A.; Kierus, K.; Jankowski, S.; Zimecki, M.; Zabrocki, J. *Eur. J. Med. Chem.* **2009**, *44*, 3731.
- [5] Katarzyńska, J.; Mazur, A.; Rudzińska, E.; Artym, J.; Zimecki, M.; Jankowski, S.; Zabrocki, J. *Eur. J. Med. Chem.* **2011**, *46*, 4608.

Solid state reaction peptides and proteins with spillover hydrogen

Yurii A. Zolotarev¹, Alexander K. Dadayan¹, Arture T. Kopylov², Igor V. Nazimov³, Eduard V. Bocharov³, Boris V. Vaskovsky³, Yurii A. Borisov⁴, Nikolay F. Myasoedov¹

¹Institute of Molecular Genetics, Russian Academy of Sciences, Moscow, Russia; ²Institute of Biomedical Chemistry, RAMS, Moscow, Russia; ³Shemyakin–Ovchinnikov Institute of Bioorganic Chemistry, RAS, Moscow, Russia; ⁴Nesmeyanov Institute of Organoelement Compounds, RAS, Moscow, Russia

E-mail: zolya@img.ras.ru

Introduction

This report summarizes data on the theoretical and experimental investigation of high temperature solid state catalytic isotope exchange (HSCIE) that takes place in organic compounds under the action of spillover hydrogen (SH) [1]. The HSCIE reaction has been shown to proceed on Brønsted-type acidic centers formed under the action of SH. The new one-center synchronous mechanism of hydrogen substitution at the saturated carbon atom under the action of H_3O^+ has been studied. The HSCIE reaction proceeds in virtually complete absence of racemization, making this reaction a valuable preparative method used for the production of evenly tritium or deuterium labeled peptides.

Results and Discussion

Analysis of the kinetic isotopic effects (K_{IE}) of the HSCIE reaction were conducted for the first time. To analyze the substitution degree of hydrogen for hydrogen isotopes in glycine and alpha-isobutyric acid (Aib), resulting from the HSCIE reaction, labeled amino acids were transformed to their phenylthiocarbonyl derivatives. For Gly, the activation energies of the exchange reaction of hydrogen for deuterium and tritium, 13.6 and 13.7 kcal/mol, respectively were established. For Aib, the activation energies of the exchange reaction of hydrogen for deuterium and tritium, 15.3 and 15.4 kcal/mol, respectively were established. The difference of the activation energies for the exchange reaction of hydrogen for deuterium and tritium equals 0.1 kcal/mol in these amino acids. To accomplish theoretical analysis of isotope effects for the solid state hydrogen exchange reaction, Hartree-Fock quantum-chemical calculations in the 6-31G* basis of the transition stage structure for the one-center hydrogen exchange mechanism were used. Calculations of the exchange in Gly and Aib showed the energy activation differences for the exchange reaction of hydrogen for deuterium and for tritium to be 0.19 and 0.12 kcal/mol, respectively. K_{IE} for reactions with Gly, Aib and the methyl group of alanine was equal to 1.42, 1.32 and 1.23 (HF 6-31G*, 450 K), respectively. It was shown that the kinetic isotopic effect of solid state reaction of hydrogen exchange with SH is 1.2 – 1.4, which is several times lower than that of liquid state reactions of protium and deuterium transfer equal to 3 to 30. Good agreement was observed between our experimental data and the results of quantum chemical calculations

of hydrogen exchange on model acidic centers type $H^+(H_2O)_n$. The yielded data indicate that in HSCIE reaction hydrogen isotopes react at virtually the same rate.

Use of evenly tritium labeled peptides for the pharmacokinetics studies and binding assay is discussed. By reaction HSCIE it was received deuterium-labeled octapeptide bradykinin with 5.5 atoms of deuterium and labeled hexapeptide dalargin (TyrDAlaGlyPheLeuArg) with 14 atoms of deuterium (Fig. 1).

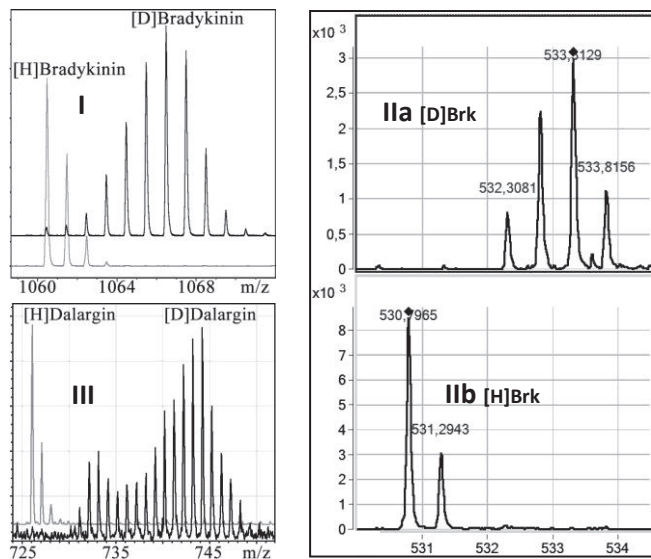


Fig. 1. MS analysis of $[G-^2H]$ bradykinin with MALDY (I); MS-MS analysis mixture of $[^1H]$ bradykinin / $[G-^2H]$ bradykinin with Q-TOF (II) and MS analysis of $[G-^2H]$ dalargin with ESI TOF (III).

Possible employment of evenly labeled peptides for the quantitative MS analysis was estimated. For this purpose, a matrix mixture of peptides was prepared by protein fraction trypsinolysis of the *Calu* line cell culture and it was mixed with equal amounts of light- and heavy bradykinin in 1/5, 1/10, 1/100/1/500 and 1/1000 ratios. The obtained samples were analyzed by HPLC on a Zorbax-SB-300 column (C18, 150 mm x 75 μ m. 5 μ m, 300 A) in acetonitrile linear gradient in the presence of 0.08% formic acid and 0.007% heptafluorobutyric acid. MS and MS-MS analysis was carried out on an Agilent Q-TOF 6530 quadrupole TOF high resolution mass spectrometer in the nano flux regime. The scanning range in the tandem regime of MS/MS was 200-1000 m/z, the scanning rate in the MS/MS regime 4.23 spectra/sec. The ion isolation mode was no more than 1.3 m/z units. It has been shown that the isotope label was distributed over the whole molecule $[^2H]$ bradikinin, allowing the monitoring to be possible to be carried out in all the fragments formed during its proteolysis with the use of mass spectrometry.

The influence of polypeptides' three-dimensional organization on their fragments' reactivity in HSCIE has been studied. Considerable decrease in the ability to exchange hydrogen for SH in the contact area of protein subunits has been demonstrated. The HSCIE reaction can be used not solely for the preparative production of tritium labeled proteins (such as insulin, interferon and hemoglobin) but also for identification of the contact area during complex formation in proteins.

References

[1] Zolotarev, Yu.A.; Dadayan, A.K.; Borisov, Yu.A.; Kozik, V.S. *Chem. Rev.* **2010**, *110*, 5425-5446.

Insight into A β misfolding and aggregation

Sándor Lovas^a, Yuliang Zhang^b, Yuri L. Lyubchenko^b

^a*Department of Biomedical Sciences, Creighton University, Omaha, NE 68178;*

^b*Department of Pharmaceutical Sciences, University of Nebraska Medical Center, Omaha, NE 68198, USA*

slovas@creighton.edu

Introduction

Misfolding and self-assembly of amyloid beta (A β) peptide into different oligomeric states could lead to the development of Alzheimer's disease. The solution structure of A β is known, but the molecular mechanism of the oligomerization is still not well understood. Using single molecule atomic force microscopy, the high stability of A β dimers was revealed [1] but the mechanism of dimer formation and its structure is still unknown. We combined molecular dynamics (MD) simulations and AFM to characterize misfolding and aggregation of A β (1-40) and its 13-23 (HHQKLFFFAED) fragment. His¹³ was replaced with Cys to use as an anchor for a site specific immobilization of the peptide in AFM experiments. MD simulations of structures of A β (1-40) and [Cys¹³]A β (13-23)-NH₂ monomers and dimers were performed using the GROMACS 4.5.4 package. To analyze the stability of the structure of the dimer of A β (13-23), steered MD (SMD) simulation was used to examine its force-induced dissociation. The dimer was pulled apart by applying external forces to the center of mass of Cys¹³ of monomer A at a constant rate of 5 nm/ns. Umbrella sampling simulations were used to calculate the free energy of binding ($\Delta G_{\text{bindA,B}}$) between monomers.

Results and Discussion

The AFM experiments demonstrate that A β (13-23), in 100 μ M solution, forms fibrils of different lengths but rather uniform heights. Dynamic force spectroscopy analysis revealed that the peptide develops stable dimers with a lifetime of 1.06 ± 0.95 s. Similar lifetime ranges were observed for A β (1-40) [1] and α -synuclein [2], suggesting that this long lifetime for transient dimers is common for amyloid proteins.

MD simulations of the dimer structure of A β (1-40) were started from two different initial structures. The initial parallel β -sheet structure, which was obtained from solid-state NMR measurements [3], was stable during 750 ns simulation. Although one of the chains partially unfolded refolded so that it wrapped around the other chain in a β -harpin conformation. When the randomly dimerized solution NMR structure (pdb id. 2lfm [4]) of A β (1-40) was simulated for 1.4 μ s, neither antiparallel nor parallel β -sheet structures were observed, although, the chains assumed antiparallel orientation. On the basis of our long-time MD simulations, in agreement with previous AFM results [1], A β (1-40) in solution can most probably form a stable dimer in antiparallel orientation.

MD simulations reveal that monomers of Ac-[Cys¹³]A β (13-23)-NH₂ form β -turn/bend structures. When two monomers interact, they refold to an antiparallel β -sheet conformation and form a stable dimer (Figure 1A). The assembled dimers are stabilized by inter-chain hydrogen bonds, salt bridges and weakly polar interactions. Steered MD

simulation showed that individual peptide chains under the applied force, as during the AFM experiments, undergo structural transition which is accompanied by sharp rupture of the dimer (Figure 1B).

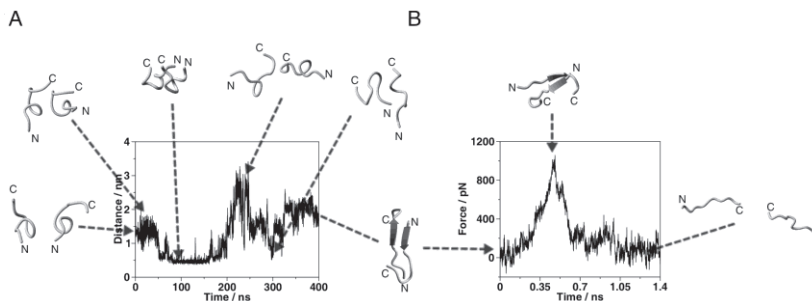


Figure 1. **A.** Distance between the center of mass of Cys¹³ of chain A and the center of mass of Cys¹³ of chain B during 400 ns MD simulation of the dimer structure Ac-[Cys¹³]A β (13-23)-NH₂. Snapshots of the dimer backbone structures from the trajectory are placed inside the plot. **B.** Force curve acquired at 5 nm/ns pulling rate from steered MD simulation. Snapshots of the simulation show the dissociation of the dimers.

Umbrella sampling simulations indicate strong interaction between monomers, with $\Delta G_{\text{bindA,B}}$ of -85.45 kJ/mol. Our results suggest that the formation of A β dimer is the key initial step of the oligomerization and the dimers are the building blocks of A β aggregates.

Acknowledgments

The work was supported in part by grants DE-FG02-08ER64579 (DOE), 1 R01 GM096039-01A1 (NIH), EPS-004094 (NSF) to YLL and NIH grants 5P20RR016469 and 8P20GM103427 to SL.

References

- [1] Kim, B. H.; Palermo, N. Y.; Lovas, S.; Zaikova, T.; Keana, J. F.; Lyubchenko, Y. L. *Biochemistry* **2011**, *50*, 5154.
- [2] Yu, J.; Malkova, S.; Lyubchenko, Y. L. *J. Mol. Biol.* **2008**, *384*, 992.
- [3] Petkova, A. T.; Yau, W. M.; Tycko, R. *Biochemistry* **2006**, *45*, 498.
- [4] Vivekanandan, S.; Brender, J.R.; Lee, A.Y; Ramamoorthy, A. *Biochem. Biophys. Res. Comm.* **2011**, *411*, 312.

Isotope labeling strategies for solution NMR studies of high-molecular-weight protein drug-targets

Georgios A. Spyroulias¹, Christos T. Chasapis¹, Aikaterini Argyriou¹,
Detlef Bentrop²

¹Department of Pharmacy, University of Patras, GR-26504, Patras, Greece; ²Institute of Physiology II, University of Freiburg, D-79104 Freiburg, Germany
E-mail:G.A.Spyroulias@upatras.gr

Introduction

Pentameric ligand-gated ion channels from the Cys-loop family are of special importance for the rapid chemo-electrical transduction, and a significant class of drug targets. Recently the X-ray structures of two prokaryotic homologues of the LGIC family most studied member, the nicotinic acetylcholine receptor (nAChR) have been determined; (a) the bacterial *Gloeobacter violaceus* pentameric LGIC homologue (GLIC) studied at 2.9 Å resolution in an apparently open conformation [1] and (b) the bacterium *Erwinia chrysanthemi* (ELIC) pentamer, studied at 3.3 Å resolution defining a closed conformation of the channel [2].

The methodologies of the incorporation of stable isotopes in proteins play a key role on the NMR-based conformational studies of proteins or macromolecular complexes and drug design efforts. Application of various schemes of uniform or selective isotope labeling schemes on the extracellular domain (ECD) of a subunit from the *Gloeobacter violaceus* pentameric Ligand-Gated-Ion-Channel (LGIC), in our lab, resulted to the complete NMR characterization of the 200-residue ECD polypeptide chain.

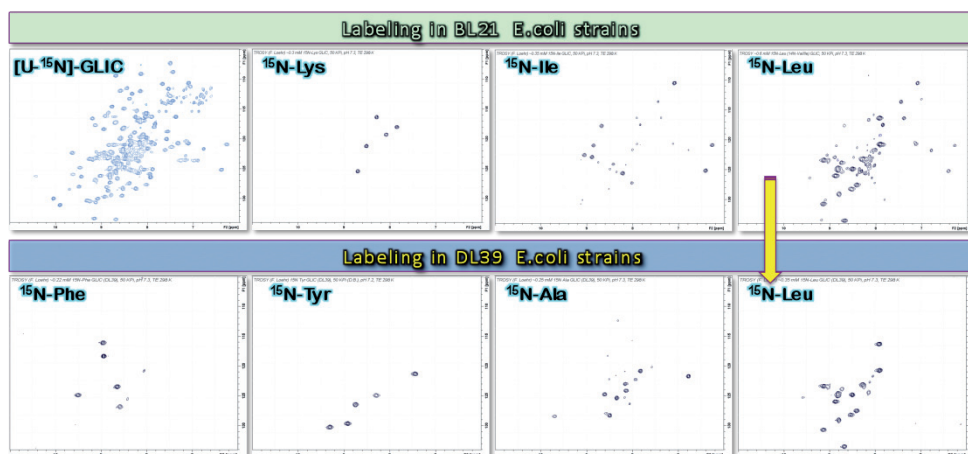


Figure. ¹H-¹⁵N HSQC spectra of ¹⁵N-uniformly labeled GLIC and selectively labeled ¹⁵N-Lys/Ile/Leu/Ala/Phe/Tyr GLIC in *E.coli* prototrophs and auxotrophs.

Results and Discussion

The 200-residue extracellular domain of GLIC (193 residues + 7 residues as His-tag & cloning artifact; 11 Prolines) was cloned and expressed in high yields in *E. coli*. The ^1H - ^{15}N HSQC exhibits signal dispersion typical for polypeptides with mainly beta structure. The triple labeled $^2\text{H}/^{13}\text{C}/^{15}\text{N}$ GLIC ECD, and the acquired triple-resonance NMR spectra resulted to the identification of >50% (~110 residues) of the GLIC ECD backbone resonances. To corroborate and extend this assignment amino acid selective ^{15}N labeling and/or reverse labeling (“unlabeling” of a ^{15}N protein) was applied for 12 amino acids (Ala, Leu, Ile, Val, Phe, Tyr, Asn, His, Lys, Arg, Asp and Glu) according to known or modified strategies. Efficient unlabeleding of ^{15}N -GLIC_{ECD} was performed for Arg, Lys, His, and Asn in *E. coli* BL21(DE3). Successful selective ^{15}N -labeling in *E. coli* BL21(DE3) was achieved for Lys, Val and Ile (in the presence of ^{14}N -amino acids in order to avoid cross-labeling; **Figure**). Efficient selective ^{15}N -labeling of GLIC_{ECD} with Leu, Ala, Phe, Tyr, Asp, and Glu was obtained in the auxotrophic strain *E. coli* DL39 (**Figure**).

The ^{15}N -selective labeling approach described above yielded around 40 more unambiguously assigned HN resonances. Experiments carried out in higher Temperature, T=308K, have also significantly contributed to the identification of residues that belong to the protein regions that undergo a conformational exchange process. Applying a variety of selective labeling protocols we managed to unambiguously identify almost the 80% (~150 residues) of GLIC residues and to study the dynamic behavior of the protein in ps-ns time scale, through R1, R2 and hetero-NOE measurements. H/D experiments were also carried out and data were consistent with relaxation data. According to the ^{15}N -relaxation measurements the GLIC ECD is found to be in monomeric state in solution. This study provided finally, an atomic-level insight for the conformational dynamics of the GLIC ECD, while it reveals the segments that undergo a conformational exchange process. These segments are parts of the subunit-subunit interaction interface of the protein, when it is found in its 5mers (entire polypeptide chain) or in 6mers (ECD). In solution GLIC ECD is found as a monomer and these segments are in equilibrium between different conformational states [3].

Overall, selective labeling techniques applied for the ^{15}N -aminoacid labeling (or the reverse ^{14}N -labeling) of GLIC, facilitating thus the identification of the backbone nuclei resonances for >80% of the non-proline GLIC residues and the study of GLIC dynamics in solution. This technique is particularly useful for the NMR study of protein-ligand interaction and drug design efforts since it does not require neither the complete analysis of numerous NMR data sets nor the structure determination of the drug-target protein.

Acknowledgments

EU FP7-INFRA “EAST-NMR” (nr. 228461) & FP7-HEALTH “Neurocypres” (nr. 202088)

References

- [1] Bocquet N, Nury H, Baaden M, Le Poupon C, Changeux JP, Delarue M, Corringier PJ. *Nature* **2009**, 457, 111
- [2] Hilf RJ, Dutzler R. *Nature* **2009**, 457, 115
- [3] Chasapis C, Argyriou AI, Corringier PJ, Bentrop D, Spyroulias GA. *Biochemistry* **2011**, 50, 9681

Delivering the native structures of peptides from computer simulations and predicted NMR proton chemical shifts

P. Thévenet,^{a,b} Y. Shen,^{a,b} J. Maupetit,^{a,b} F. Guyon,^{a,b} A. Padilla,^c
P. Derreumaux,^{b,c,d} Pierre Tufféry^{*,a,b}

^a INSERM, U973, F-75205 Paris, France ; ^b Univ. Paris Diderot, Sorbonne Paris Cité, F-75205 Paris, France; ^c Laboratoire de Biochimie Théorique, UPR 9080 CNRS, Institut de Biologie Physico Chimique, Paris, France; ^d Institut Universitaire de France, Paris, France; ^e Centre de Biochimie Structurale, CNRS UMR 5048 - UM 1 - INSERM UMR 1054, Montpellier, France

E-mail: pierre.tuffery@univ-paris-diderot.fr

Introduction

Fast peptide structure identification remains an every day's concern in a context where complete genome scans or proteomics pipelines produce a large amount of peptide sequences. In the recent years, we introduced PEP-FOLD [1,2] a *de novo, in silico* approach to the identification of peptide structures from L-amino acid sequences at neutral pH. Originally restricted to linear peptides of length varying between 9 to 25 amino acids, we recently extended it up to 50 amino acids, and implemented disulfide bond management [3]. PEP-FOLD is available online at: <http://bioserv.rpbs.univ-paris-diderot.fr/PEP-FOLD/>. Free of any experimental data and using a benchmark of 56 peptides, we found PEP-FOLD and ROSETTA [4] have similar accuracy for β and α/β peptides, but PEP-FOLD shows higher accuracy for α -helical peptides.

Simulations can, however, benefit from experimental information, and in particular NMR measurements. Recently, using backbone chemical shift restraints (N, $C\alpha$, C, $C\beta$, HA, HN), high-resolution models were generated either with molecular fragment approach and sequence homology information[5] or molecular dynamics (MD) simulations[6]. Proton chemical shifts (CS) are particularly appealing for synthetic peptides, since no isotope enrichment is needed, proton signal has high sensitivity, and is easily available from 2D NMR studies. The sensitivity of HA CS to secondary structures [7] and the relationship between HN CS and backbone conformations through H-bonding [8] have long been known, but it is still difficult to accurately decipher all contributing factors. In this study, we considered the possibility to enhance PEP-FOLD performances by using the information of the predicted NMR proton chemical shifts. We used SPARTA+ [9] to predict the chemical shift values from PEP-FOLD 3D models, and we analyzed if the predicted values can be used to assist the identification of native structure.

Results and Discussion

We have considered a collection of 23 (resp. 20) peptides in solution of size between 25-52 amino acids, with structures deposited in the Protein Data Bank (PDB), solved by NMR at neutral pH (more than 5.5), and for which the experimental information of the HN (resp. Ha) CSs is available from the BMRB [10]. Each peptide was subject to 200 PEP-FOLD simulations. Considering PEP-FOLD alone, we find the average TM-score [11] of PEP-

FOLD 5 best returned models – a total of 114 models - is of 0.40. Introducing CS information, we could not derive any significant correlation between (i) the RMS deviation between the predicted and observed HA and HN CSs and (ii) model quality (TM-score). However, analyzing the HN-CS predicted error values provided by SPARTA+, we observed that large deviations between consecutive residues could be used to filter the models. Using the maximal standardized HN error value over the residues of the model (δ_1) and the maximal standardized HN error difference between two consecutive residues (δ_2) we have setup a simple procedure that first selects for each protein, the models of the 10 best ranked PEP-FOLD clusters having HA CS RMS, HN CS RMS, δ_1 and δ_2 values less than 2. SD, 0.2 SD, 2 SD and 2 SD, respectively and selects a maximal number of 5 models. These values can be progressively relaxed, if necessary, until at least one model is detected or maximum values are reached. Doing so, we identified a subset of 69 models for all 23 targets leading to a mean TM-score of 0.43. Over the 23 peptides, PEP-FOLD was able to generate native structures for 20 of them. Interestingly, no model passed the CS filter for the 3 incorrectly predicted peptides and a small number of models were returned for the other peptides. These results suggest it should be possible to use the predicted backbone hydrogen CSs with PEP-FOLD to drive the identification of the native structure.

Acknowledgments

The authors thank INSERM and CNRS for recurrent funding and RPBS for providing access to the calculation resource.

References

- [1] Maupetit, J.; Derreumaux, P.; Tufféry, P. *J Comput Chem.* **2010**, *31*, 726-38.
- [2] Maupetit, J.; Derreumaux, P.; Tufféry, P. *Nucleic Acids Res.* **2009**, *37*, W498-503.
- [3] Thévenet, P.; Shen, Y.; Maupetit, J.; Guyon, F.; Derreumaux, P.; Tufféry, P. *Nucleic Acids Res.* **2012**, *40*:W288-93.
- [4] Das, R., Baker, D.; *Annu. rev. Biochem.* 2008, *77*, 363-382.
- [5] Shen, Y.; Vernon, R.; Baker, D.; Bax, A. *J Biomol NMR.* 2009, *43*, 63-78.
- [6] Robustelli, P.; Kohlhoff, K.; Cavalli, A.; Vendruscolo, M. *Structure* 2010, *18*, 923-933.
- [7] (a) Wang, Y.; Jardetzky, O. *J. Am. Chem. Soc.* 2002, *124*, 14075-14084. (b) Wishart, D.S.; Sykes, B.D.; Richards, F.M. *Biochemistry* 1992, *31*, 1647-1651.
- [8] Asakura, T.; Taoka, K.; Demura, M.; Williamson, M.P. *J Biomol NMR.* 1995, *6*, 227-236
- [9] Shen, Y.; Bax, A. *J Biomol NMR.* **2010**, *48*, 13-22.
- [10] Ulrich, E.L.; Akutsu, H.; Doreleijers, J.F.; Harano, Y.; Ioannidis, Y.E.; Lin, J.; Livny, M.; Mading, S.; Maziuk, D.; Zachary Miller, Z. Et al., *Nucleic Acids Res.* **2007**, *36*, D402-D408.
- [11] Xu, J.; Zhang, Y. *Bioinformatics* 2010, *26*, 889-895.

Computational prediction of bioactive peptides

Catherine Mooney^{a,b}, Kevin O'Brien^{a,b}, Niall J Haslam^{a,b}, Richard J Edwards^c, Norman E Davey^d, Fergal J Duffy^{a,b}, Kalyan Golla, Ilias Stavropoulos^{a,b}, Nora Khaldi^{a,b}, Anthony J. Chubb^{a,b}, Federica Lombardi^{a,b}, Therese Holton^{a,b}, Vaishnavi Vijay^{a,b}, Marc Devocelle^e, Niamh Moran^f, Denis C. Shields^{a,b}

^aComplex and Adaptive Systems Laboratory (UCD-CASL), and ^bSchool of Medicine and Medical Science, University College Dublin, Ireland; ^cCentre for Biological Sciences, University of Southampton, UK; ^dEMBL Heidelberg, Germany; ^eMolecular and Cellular Therapeutics and ^fPharmaceutical and Medicinal Chemistry, Royal College of Surgeons in Ireland, Dublin, Ireland

E-mail:denis.shields@ucd.ie

Introduction

The discovery of short peptide regions that are bioactive, either as part of a largely disordered sequence environment, or as a cleaved oligopeptide, has the potential to be greatly accelerated by the large-scale accumulation of genome sequencing and mass spectrometry based proteomics. We demonstrate the rationale for, and provide implementations of, separate methods and work-flows for the computational prediction of both intracellular and extracellular peptidic regions based on combinations of machine learning¹, relative conservation and motif-overrepresentation^{2,3} rules.

Results and Discussion

We developed a bioactivity prediction program, PeptideRanker¹, which was trained on a combined dataset of primarily extracellular antimicrobial, peptide hormone, and toxin/venom peptides. It carries out separate predictions for short and long (>20 residue) peptides. We demonstrate that it has good predictive power compared to existing antimicrobial predictors (AntiBP2 & CAMP), but is more generalisable across peptide classes (Fig 1), showing a better Matthew's correlation coefficient (MCC). Intracellular potentially bioactive peptides can correspond to known linear motifs with protein binding properties. We trained a separate predictor, SLiMPred², which predicts such regions in both disordered and ordered contexts. It is trained on shorter regions than the ANCHOR method, which focuses on protein binding regions of disordered proteins. Conservation also provides a useful tool to identify motifs embedded within disordered contexts, and a motif identification method SLiMPrints³ identified 23 previously validated motifs among 122 most significant human conserved motifs (p<0.00001). Web servers for motif and bioactive peptide prediction are at <http://bioware.ucd.ie>. Systematic searches for over-represented motifs in man provides a large dataset of over-represented motifs of potential function⁴. Our experimental validation of bioactive peptide discovery focuses on platelet signalling⁵ and on the integrin adhesome and cadherin adhesome complexes, combining both linear and cyclised⁶ peptide (Fig. 2) approaches to target signalling.

Figure 1 Comparison of bioactive peptide predictors on different peptide types

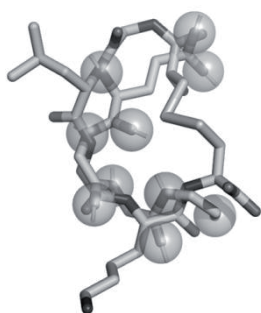
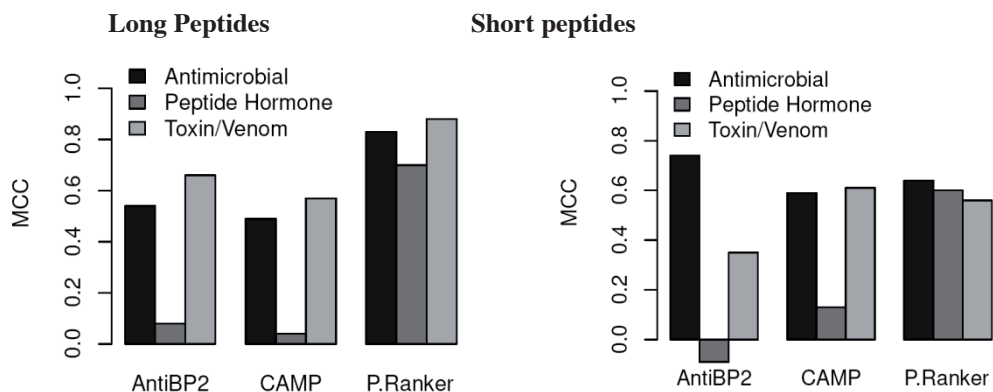


Figure 2. Pharmacophore matching of a cyclic peptide from an *in silico* library⁶ with a cadherin tail region.

Acknowledgments

This work is funded by SFI grant no. 08/IN.1/B1864.

References

- [1] Mooney C, Pollastri G, Shields DC, Haslam NJ *J Mol Biol* **2012**, *415*, 193-204.
- [2] Mooney CM, Haslam NJ, Pollastri G, Shields DC *PLOS One* **2012** in press.
- [3] Davey, N; Cowan, J.; Shields, D.; Gibson, T.; Coldwell, M.; Edwards, R *Nucleic Acids Res*, **2012** in press.
- [4] Edwards RJ, Davey NE, O'Brien K, Shields DC. *Mol Biosyst.* **2012** *8*, 282-95.
- [5] Edwards RJ, Moran N, Devocelle M, Kiernan A, Meade G, Signac W, Foy M, Park SDE, Dunne E, Kenny D, Shields DC *Nature Chemical Biology* **2007** *3*, 108-112
- [6] Duffy FJ, Verniere M, Devocelle M, Bernard E, Shields DC, Chubb AJ. *J Chem Inf Model.* **2011** *51*, 829-36.

Peptides as a new emerging class of medical biomarkers

V. T. Ivanov, R. H. Ziganshin, V. M. Govorun

Shemyakin & Ovchinnikov Institute of Bioorganic Chemistry, Russian Academy of Sciences, Moscow, Russia

E-mail: ivavt@ibch.ru

Introduction

It is generally accepted that biological tissues, fluids, cells, etc. contain *in vivo* rich sets of peptides resulting from proteolytic degradation of endogenous proteins. Moreover, composition of those sets depends on the physiological state of the organism from which the sample was taken, providing thereby biochemical ground for application of peptidomic analysis to medical diagnostics (see [1] and references therein). Search for potential human peptide biomarkers has been carried out in a number of laboratories in the past decade (for example see [2-9]). However, these attempts have not yet produced practically applicable protocols due to extreme complexity of blood peptidome, as well as formidable technical difficulties, such as rather poorly reproducible *ex vivo* peptide formation in blood samples (especially blood serum) and tight binding of peptides to huge excesses of major blood proteins. Below we present our recent results in that area.

Results and Discussion

Blood serum was used as a test material. Samples were taken from three groups of patients (with ovarian cancer, colorectal cancer and syphilis, average group size 157 patients) and from a control group of 343 healthy women. All samples were treated according to the standard robotic protocol described in [10] by weak cation exchange magnetic beads. Peptides were desorbed from the eluted blood proteins by heating for 15 min. at 95°C and the resultant material was subjected to mass-spectral analysis. Bioinformatic treatment of the MALDI-TOF profiles revealed clearly expressed, statistically reproducible differences between the four groups of spectra which allowed to build disease *vs.* norm classification models with excellent (92-100%) sensitivity and selectivity indicators. However, in the disease *vs.* disease cross-validation analysis respective parameters dropped considerably, in some cases below 40%. Such result demonstrates the limited applicability of peptide profiling (“finger print” or “bar code” approach) to straightforward diagnostics of studied tumors.

The same material provided rich structural information on its peptide composition after RPLC-ESI-QTOF-MS/MS analysis. As shown in the diagram, each group of blood samples contains a large group of unique peptides, not present in three other groups. This result provides a firm ground for further development of the described structural approach to medical diagnostics based on peptide markers.

Other than blood biological fluids (saliva, urine, liquor) have by far simpler molecular composition than blood and therefore favorably lend themselves for similar analysis. For example, in our study of meningitis associated peptides we found that liquors taken from the patients with the viral form of meningitis carry 37 unique peptides not present in the

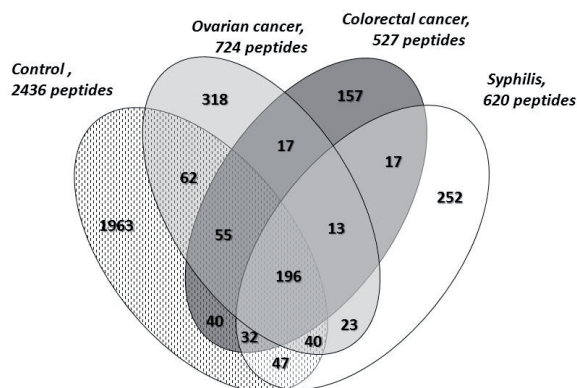


Figure 1. Number of individual peptide sequences identified in the four test groups of blood serum. Each figure inside the oval indicates the number of identified peptides present in a single or, depending on the overlap, in several test groups

liquor of patients with bacterial meningitis, while the latter have 380 such peptides. Peptide based diagnosis will make in this case no problem.

Acknowledgments

This work is supported by a grant of the Presidium of the Russian Academy of Sciences (Program “Molecular and Cellular Biology” 10P)

References

- [1] Ivanov, V.T.; Yatskin, O.N. *Expert Rev. Proteomics* **2005**, *2*, 463.
- [2] Petricoin, E.F.; Ardekani, A.M.; Hitt, B.A.; Levine, P.J.; Fusaro, V.A.; Steinberg, S.M.; Mills, G.B.; Simone, C.; Fishman, D.A.; Kohn, E.C.; Liotta, L.A. *Lancet* **2002**, *359*, 57.
- [3] Robbins, R.J.; Villanueva, J.; Tempst. *J. Clin. Oncology* **2005**, *23*, 4835.
- [4] Diamandis, E.P.; van der Merwe, D.E. *Clin. Cancer Res.* **2005**, *11*, 963.
- [5] Liotta, L.A.; Petricoin, E.F. *J. Clin. Invest.* **2006**, *116*, 25.
- [6] Villanueva, J.; Shaffer, D.R.; Philip, J.; Chaparro, C.A.; Erjument-Bromage, H.; Olshen, A.B.; Fleisher, M.; Lilja, H.; Brogi, E.; Boid, J.; Sanches-Carbayo, M.; Holland, E.C.; Cordon-Cardo; Scher, H.I.; Tempst, P. *J. Clin. Invest.* **2006**, *116*, 271.
- [7] Villanueva, J.; DeNoyer, P.J.; Tempst, P. *Nat. Protoc.* **2007**, *2*, 588.
- [8] Ueda, K.; Saichi, N.; Takami, S.; Kang, D.; Toyama, A.; Daigo, Y.; Ishikawa, N.; Kohno, N.; Namura, K.; Shuin, T.; Nakayama, M.; Sato, T.-A.; Nakamura, Y.; Nakagawa, H. *PLoS ONE* **2011**, *6*, e18567
- [9] Yang, Y.; Song, Y.-C.; Dang, C.-X.; Song, T.-S.; Liu, Z.-G.; Guo, Y.-M.; Li, Z.-F.; Huang, C. *Clinical and Experimental Medicine* **2012**, *12*, 79.
- [10] Ziganshin, R.; Arapidi, G.; Azarkin, I.; Zaryadieva, E.; Alexeev, D.; Govorun, V.; Ivanov, V. *J. Proteomics* **2011**, *74*, 595

Peptide self-assembled monolayers as a new tool for nanotechnology

Mariano Venanzi¹, Mario Caruso¹, Emanuela Gatto¹, Fernando Formaggio², Claudio Toniolo², Ana Maria Textera³, José Carlos Rodriguez-Cabello³

¹Department of Chemical Sciences and Technologies, University of Rome "Tor Vergata", 00133 Rome, Italy; ²ICB, Padova Unit, CNR, Department of Chemistry, University of Padova, 35131 Padova, Italy; ³Department of Physics of Condensed Matter, E.T.S.I.I./University of Valladolid, 47002 Valladolid, Spain

E-mail:venanzi@uniroma2.it

Introduction

Peptide-based self-assembled monolayers (SAMs) have been attracting more and more interest for their versatility and possible applications as enantioselective sensors, biocompatible platforms for tissue engineering, and smart elements in hybrid devices for microelectronics. In particular, peptide SAMs formed by helical peptide building blocks, have shown unique electronic conduction properties over large distances (>100 nm), promoting directional electron transfer (ET) from the C- to the N-terminus of the peptide helix [1]. In this contribution, we report on the photochemical properties of peptide SAMs containing optically active groups and linked to a gold surface via Au-S interaction. Results on two different peptide SAMs will be presented: (1) Bicomponent peptide SAMs formed by two conformationally constrained oligopeptides, functionalized with a pyrene (Py) or a tryptophan (W) group at the N- and C-terminus, respectively. The W-containing peptide was linked to the gold surface through the disulfide group of a lipoic acid, while the Py-functionalized peptide has been embedded into the W-peptide SAM. (2) Elastin-mimicking polypeptides functionalized by azobenzene units and chemisorbed on a gold surface via a Cys residue. Photocurrent generation through the polypeptide SAM has been investigated as a function of the photoinduced *cis-trans* isomerization of the azobenzene group.

Results and Discussion

(1) A novel method to build bicomponent peptide SAMs has been developed, by exploiting helix···helix macrodipole interactions [2]. Specifically, a Py-containing octapeptide, [Z-Aib-Api(Py)-(αMe)Nva-Aib-(αMe)Nva-(αMe)Nva-Aib-Api(Boc)-NHtBu, A8Py, where Api is 4-aminopiperidine-4-carboxylic acid and (αMe)Nva is C^α-methylnorvaline], and a hexapeptide, functionalized at the N-terminus with a lipoic acid (Lipo) for binding to gold substrates [Lipo-(Aib)₄-Trp-Aib-OtBu, SSA4WA] via Au-S linkages, have been employed. Both peptides, being almost exclusively formed by strongly folding inducer C^α-tetrasubstituted α-amino acids, have been shown to attain a helical structure.

The two peptides form a densely packed bicomponent peptide monolayer, where A8Py is embedded into the SSA4WA palisade in an antiparallel arrangement stabilized by helix···helix macrodipole interactions. The composition of the peptide film has been

investigated by spectroscopic and electrochemical methods, while the morphology of the monolayer has been analyzed by ultra high-vacuum scanning tunnelling microscopy.

Photocurrent generation experiments have provided important information on the molecular mechanism governing the ET process. In particular, we have shown that it is possible: (i) to modulate the ET efficiency by functionalizing the peptide scaffold with a suitable chromophore (*antenna effect*); (ii) to open additional ET pathways, involving side-by-side interchain interactions in bicomponent SAMs, and (iii) to tune coupling between the photoactive layer and the conductive substrate by changing the nature of the metal/organic layer interface (covalently linked or physically adsorbed, *junction effect*).

(2) As a second case study, we have analyzed a new photosensitive polypeptide mimicking elastin (AzoGlu15). The structure of AzoGlu15 corresponds to a triblock polymer with the following peptide sequence: C-[VPGVG)₂(VPGE_{pho0.5}G)(VPGVG)₂]₁₅. The acronym E_{pho0.5} stands for 50% of glutamic acid residues, side-chain functionalized with azobenzene units *via* amide bond formation. The N-terminal Cys residue allows for a stable linking of the polypeptide to the gold surface.

Azobenzene is well-known to give rise to a *trans*→*cis* photoisomerization upon visible irradiation ($\lambda=455$ nm) and to a *cis*→*trans* conversion upon UV excitation ($\lambda=370$ nm). The *trans* isomer is more stable by approximately 50 kJ/mol, and the barrier to photoisomerization is approximately 200 kJ/mol. We have found that under dark conditions a *cis*→*trans* relaxation of the supported layer does take place very slowly (~24h). Cyclic voltammetry experiments have shown that AzoGlu15 forms a densely packed film on a gold electrode, inhibiting the discharge of K₃[Fe(CN)₆] in solution almost completely.

When the peptide layer is irradiated between 260 and 500 nm, the azobenzene moiety gives rise to ET from its excited state to the surface Fermi level of the gold electrode. Subsequently, the donor triethanolamine transfers an electron to the azobenzene group, thus producing a net, anodic electronic current. Photocurrent experiments performed before and after 15 minutes of UV light irradiation at 370 nm, have allowed us to separate the contributions of the *trans* and *cis* isomers to the electronic current, as clearly revealed by the action spectra, *i.e.* the photocurrent response *vs* the excitation wavelength, of the monolayer in the *cis* and *trans* conformations.

These findings have paved the way to the design of optoelectronic devices based on electroactive units driven by electromagnetic excitation, the response of which can be finely tuned by modification of the metal surface properties by the functionalized peptide SAMs.

Acknowledgments

The financial support (PRIN 2008, 20088NTBKR) of the Italian Ministry for University and Research (MIUR) is acknowledged.

References

- [1] Gatto, E.; Caruso, M.; Porchetta, A.; Toniolo, C.; Formaggio, F.; Crisma, M.; Venanzi, M. *J. Pept. Sci.* **2011**, *17*, 124.
- [2] Gatto, E.; Porchetta, A.; Scarselli, M.; De Crescenzi, M.; Formaggio, F.; Toniolo, C.; Venanzi, M. *Langmuir* **2012**, *28*, 2817.

Engineering pro-angiogenic peptides using stable disulfide-rich cyclic scaffolds

L. Y. Chan¹, S. Gunaekera¹, S. T. Henriques^{1,2}, N. F. Worth³, S. J. Le³,
R. J. Clark^{1,4}, J. H. Campbell³, D. J. Craik¹, N. L. Daly^{1,5}

¹The University of Queensland, Institute for Molecular Bioscience, Brisbane, Australia;

²Instituto de Medicina Molecular, Faculdade de Medicina da Universidade de Lisboa,

Lisbon, Portugal; ³the Australian Institute for Bioengineering and Nanotechnology,

Brisbane, Australia, ⁴The University of Queensland, School of Biomedical Sciences,

Brisbane, Australia; ⁵Queensland Tropical Health Alliance, James Cook University,

Cairns, Australia

E-mail: norelle.daly@jcu.edu.au

Introduction

Pro-angiogenic compounds have significant potential in the treatment of conditions such as wound healing and cardiac ischemia.¹ However, problems with compound stability have hindered previous attempts to develop therapeutic agents.² An alternative approach for the development of novel drug leads involves grafting small peptides with potent activity into stable cyclic peptide scaffolds.

The peptides chosen for grafting in the current study are regions from the extracellular matrix proteins laminin and osteopontin, referred to as LAM and OPN. These peptides are six and seven residues in length respectively and have been shown to promote potent angiogenic activity. Their small size makes them ideal candidates for grafting into disulfide-rich cyclic peptide scaffolds. In the current study we have used the plant-derived peptides MCoTI-II and SFTI-1 as stable scaffolds. Both MCoTI-II and SFTI-1 are potent trypsin inhibitors, but MCoTI-II is a 34 amino acid peptide with three disulfide bonds,³ and SFTI-1 contains only a single disulfide bond and 14 amino acids.⁴ Grafting the bioactive peptide sequences into the cyclic peptide scaffolds resulted in stable and potent angiogenic agents with promising potential in the design of drug leads for therapeutic angiogenesis.⁵

Results and Discussion

The sequences of SFTI-1 and MCoTI-II, and the grafted peptides are given in Figure 1. The grafted peptides are labeled with the scaffold name first followed by the code for the linear sequence (e.g. SFTI-OPN). The angiogenic activity was assessed with an *in vitro* endothelial cell sprouting assay and an *in vivo* CAM assay. The CAM assay provided more reproducible results and all grafted peptides showed a significant increase in angiogenic activity compared to the linear sequences. SFTI-OPN was the most active compound inducing angiogenic effects at nanomolar concentrations, followed by MCo-OPN, SFTI-LAM, and MCo-LAM. All of the grafted peptides had enhanced stability in human serum compared to the linear bioactive sequences. Interestingly, SFTI-OPN, although more stable than the linear peptides, was less stable than the other grafted analogues. The grafted loop in SFTI-OPN is disordered in solution and this may account for both the enhanced bioactivity

and decreased stability in serum. A similar result was observed when an anti-angiogenic peptide sequence was grafted into a related cyclic peptide, kalata B1. More structural disorder was observed in the peptide with the greatest bioactivity compared to the other grafted peptides.⁶

In summary, we have used naturally occurring cyclic peptide scaffolds to design a peptide that is stable in human serum, induces endothelial cell sprouting *in vitro*, and induces angiogenesis *in vivo* at nanomolar concentration. This is the first study using these cyclic peptide scaffolds for the design of angiogenic agents and represents a promising approach for promoting angiogenesis for therapeutic uses.



Figure 1: Sequences of cyclic peptides SFTI-1 and MCoTI-II, and grafted analogues. The grafted sequences are highlighted in bold. The disulfide bond connectivity is shown at the top of sequences and the cyclic backbone represented by the thicker line connecting the termini.

Acknowledgments

This work was supported by a grant from the National Health and Medical Research Council (NHMRC) Grant ID: 401600. STH is a Marie Curie International Outgoing Fellow (PIOF-GA-2008-220318). D.J.C. is an NHMRC Professorial Research Fellow. R.J.C. and N.L.D are Australian Research Council Future Fellows.

References

- [1] (a) Carmeliet, P., *Nature* **2005**, *438*, 932-6; (b) Simons, M.; Ware, J. A., *Nat Rev Drug Discov* **2003**, *2*, 863-71.
- [2] Zachary, I.; Morgan, R. D., *Heart* **2010**, *97*, 181-9.
- [3] Hernandez, J. F.; Gagnon, J.; Chiche, L.; Nguyen, T. M.; Andrieu, J. P.; Heitz, A.; Trinh Hong, T.; Pham, T. T.; Le Nguyen, D., *Biochemistry* **2000**, *39*, 5722-5730.
- [4] Luckett, S.; Garcia, R. S.; Barker, J. J.; Konarev, A. V.; Shewry, P. R.; Clarke, A. R.; Brady, R. L., *J. Mol. Biol.* **1999**, *290*, 525-33.
- [5] Chan, L. Y.; Gunasekera, S.; Henriques, S. T.; Worth, N. F.; Le, S. J.; Clark, R. J.; Campbell, J. H.; Craik, D. J.; Daly, N. L., *Blood* **2011**, *118*, 6709-17.
- [6] Gunasekera, S.; Foley, F. M.; Clark, R. J.; Sando, L.; Fabri, L. J.; Craik, D. J.; Daly, N. L., *J. Med. Chem.* **2008**, *51*, 7697-7704.

Folding landscape exploration by circular permutation and capping β structures

B. Kier, A. Byrne, M. Scian, J. Anderson, N. Andersen*

Chemistry Department, University of Washington, Seattle, WA 98195, U.S.A.

E-mail: andersen@chem.washington.edu

Introduction

Circular permutation consists of cutting a protein chain and stitching together the former termini; effectively shifting the position of the termini without otherwise altering the sequence. It is an effective technique for decoupling sequence order from structure, yet until the present report this technique has been applied only to proteins of medium size (e.g., SH3 domains) and larger. Though smaller miniproteins are necessarily stabilized by highly compact networks of interactions, we predicted that strategically located cut-points could afford stable circular permutants. We have now demonstrated circular permutation with retention of the fold topology for multiple miniproteins: the Trp-cage, the Villin Headpiece domain, and a WW domain.

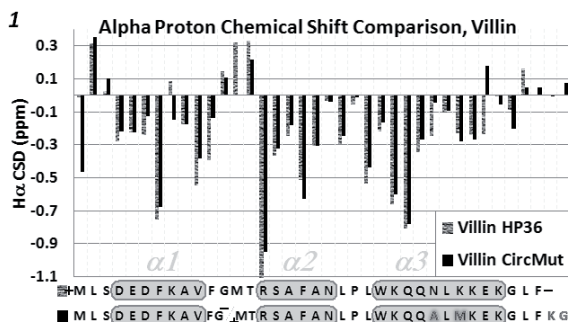
Results and Discussion

Two cases will be presented in preliminary form herein: villin and a WW domain.

The C-terminal fragment of the Villin Headpiece domain (Villin HP36) is a highly stable, ultra-fast-folding [1] non-standard 3-helix bundle stabilized primarily by core packing of 3 Phe residues. A 21 residue fragment consisting of helices 1 and 2 was shown to possess considerable stability in isolation [2]. This

fragment contains all essential Phe residues, and the linker between these two essential helices is thought to be the folding nucleation site. To investigate the importance of these local Phe/Phe interactions, we chose to circularly permute Villin HP36 by cutting the nucleating turn between helices 1 and 2. We hypothesized that this circular permutation should fold considerably slower than wild-type due to the extreme changes in contact order, yet the structural features could be preserved. Expecting some loss in stability, we chose the hyperstable N28A / K30M mutant as our starting point [3].

The resulting circular permutant was remarkably stable; it exhibited CSDs (NMR Chemical Shift Deviations) nearly identical to wild-type (Fig. 1), and a strong helical CD signature with a T_M of 45°C, vs. 90°C for the analogous normal-topology N28A K30M mutant.



Our circular permutation strategy for the Pin1 WW domain also utilized a cut that moved a key tertiary structure feature from a local interaction to the termini. Specifically, the fold-nucleating turn of the $\beta 1/\beta 2$ hairpin [4] was excised, leaving the $\beta 1/\beta 2$ sheets at opposing termini. The inclusion of β -capping units [5] was key to stabilizing the resulting fold. With a β -cap, β -sheet structure can persist even when the strands are connected by long flexible linker sequences. For example, peptide RWITVTI(GGGGKK)₃IRVWE is 75% folded at 280K ($\Delta G_F = -2.5$ kcal) – stable, yet very slow-folding ($\sim 100\mu s$) presumably due to the long loop-search times required for terminal strand association. If a long, unstructured linker can be used to connect two capped β -strands, then one might assume that a *structured* linker (the remainder of the WW domain, the $\beta 2/\beta 3$ hairpin and structured former termini, plus a short loop connecting the two former termini) would produce even better results.

The resulting circular permutant was shown to be *more* stable than the WT Pin1 WW domain (T_M 63 °C, vs. 59 °C for WT), though it compared less favorably vs. the non-circularly permuted control (T_M 94 °C) incorporating the same stabilizing mutations as the circular permutant. (Fig. 2, mutations shown in gray italics.)

These constructs were too stable for kinetics studies, but a shorter version (+RWFYFNRTGKRQ-FERPKGLVKGWWEKRWD-; T_M 52 °C vs. 74 °C for an analogously truncated WT) have proven viable. Though studies are still underway, we can report a $\sim 35\mu s$ folding rate for the circular permutant, vs. $\sim 10\mu s$ for the analogous “wild type”.

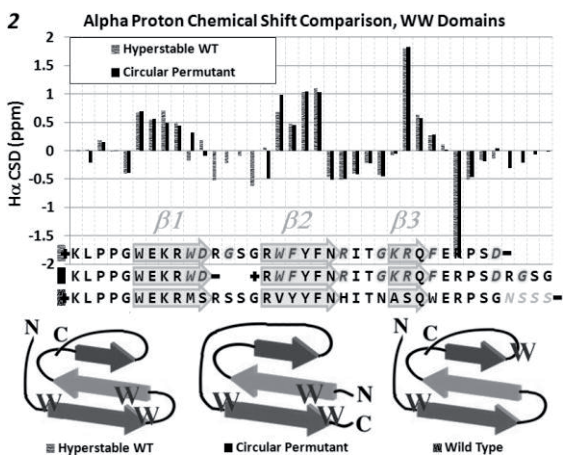
Fragments and alternate cut-points of these constructs are currently being examined. It appears that circular permutation of mini-proteins will be a powerful method for investigating protein folding landscapes.

Acknowledgments

These studies were supported by grants from the U.S. National Institutes of Health (GM-059658 and GM99889) as well as the NSF (CHE0650138 and CHE1152218).

References

- [1] Kubelka, J.; Chiu, T.; Davies, D.; Eaton, W.; Hofrichter, J. *J. Mol. Biol.* **2006** *359*, 546-553
- [2] Tang, Y.; Goger, M.; Raleigh, D. *Biochemistry* **2006** *45*, 6940-6946
- [3] Xiao, S.; Bi, Y.; Shan, B.; Raleigh, D. *Biochemistry* **2009** *48*, 4607-4616
- [4] Fuller, A. et al. *Proc. Natl. Acad. Sci.* **2009** *106*, 11067-11072
- [5] Kier, B.; Shu, I.; Eidenschink, L.; Andersen, N. *Proc. Natl. Acad. Sci.* **2010** *107*, 10466-10471



Lasso peptides: From linear to interlocked structures

Yanyan Li,¹ Séverine Zirah,¹ Rémi Ducasse,¹ Alain Blond,¹ Christophe Goulard,¹ Ewen Lescop,² Eric Guittet,² Jean-Luc Pernodet,³ Sylvie Rebuffat¹

¹ Muséum National d'Histoire Naturelle, CNRS, Laboratoire Molécules de Communication et Adaptation des Microorganismes, UMR 7245, CP 54, 57 rue Cuvier, 75005 Paris, France; ² CNRS, Centre de Recherche de Gif, Institut de Chimie des Substances Naturelles, UPR 2301, Avenue de la Terrasse, 91198 Gif-sur-Yvette, France; ³ Université Paris Sud, CNRS, Institut de Génétique et Microbiologie, UMR 8621, Orsay, France

E-mail: yanyanli@mnhn.fr

Introduction

Lasso peptides form a group of fascinating cyclized peptides, which have an interlocked topology. They possess an 8 or 9-residue macrolactam ring at the N-terminus and a C-terminal tail that loops back and is threaded through the ring. Such a lasso fold is compact and generally very stable. Lasso peptides are either enzyme inhibitors or receptor antagonists leading to diverse biological activities. They are recently considered promising molecular scaffolds for drug development. To date it is still impossible to obtain lasso folds by synthetic methods. Therefore understanding their biosynthetic mechanisms is the key for peptide engineering purposes. The archetype of lasso peptides is microcin J25 (MccJ25), an antibacterial peptide produced by *Escherichia coli* whose biosynthesis has been extensively studied. MccJ25 is synthesized ribosomally from a linear 58-AA precursor peptide that has a 37-AA leader sequence N-terminal to the MccJ25 structural sequence. The gene cluster contains four genes encoding the precursor peptide (McjA), two maturation enzymes (McjB and C) and one ABC transporter (McjD) for export of MccJ25 and self-immunity. Reconstitution *in vitro* unambiguously confirmed that McjB and C are sufficient to convert the linear McjA to MccJ25 [1]. McjB features a C150-H182-E186/D194 triad at the C-terminal region which is typical of cysteine proteases, while McjC shows significant homology to asparagine synthetases B by conserving residues involved in ATP binding (e. g. D203 and D302). Substitution of these active site residues in McjB and McjC to Ala, respectively, led to abortion of their functions *in vivo* [2]. Therefore it was proposed that McjB functions as a protease that cleaves off the leader peptide and McjC is a lactam synthetase involved in the cyclization step. The maturation reaction would require a pre-folding step of the linear peptide to form the β -hairpin structure before ring closure, because the lasso topology is sterically blocked. In this work we characterized the precise role of each maturation enzyme *in vitro* [3], providing important insights into the molecular mechanism of the maturation process.

Results and Discussion

Recombinant McjB and McjC were produced in *E. coli* ArcticExpress (DE3) and purified by one-step Ni²⁺-affinity chromatography. Although they were co-purified with chaperons, this did not affect subsequent activity assays. Inactive mutants of McjB and McjC, namely McjB[C150A/H154A] and McjC[D302A], were obtained by site-directed mutagenesis on

corresponding genes. Maturation reactions were carried out in the presence of recombinant McjA, ATP and MgCl₂ at 30 °C for 3 hours. When wild-type McjB and McjC were used, a minor product having a triply charged [M+3H]³⁺ ion at m/z 709 was detected in addition to MccJ25 by HPLC-MS analysis. This corresponded to linear MccJ25 (l-MccJ25), an intermediate released after cleavage of the leader peptide. This allowed us for the first time to directly probe the proteolytic step. Interestingly, in the absence of McjB or McjC, neither the linear nor the mature MccJ25 was produced, indicating that the two enzymes are functionally interdependent. To prove the protease activity of McjB, the double substituted mutant [C150A/H154A] was used with McjC and no products could be observed. On the contrary, when McjC[D302A] was incubated with McjB, only l-MccJ25 was produced, confirming the role of McjC as a lactam synthetase. Moreover, in the presence of McjB or McjB[C150A/H154A], McjC was able to mature l-MccJ25 with the leader peptide provided *in trans*, albeit with a very low yield.

We reasoned that a proposed pre-folding step would require energy. Since the N-terminal domain of McjB displayed weak similarity to human adenosine kinases, it is likely that McjB can perform ATP hydrolysis to provide the required energy. Thus we next performed maturation assays in the presence of non-hydrolysable ATP analogues. Interestingly, we observed that the protease activity of McjB was significantly reduced when ATP was omitted or replaced by adenosine 5'-(β, γ-imido)triphosphate (AMP-PNP). In contrast, α, β-methyleneadenosine 5'-triphosphate (AMP-CPP) did not affect McjB proteolytic activity. The opposite effects of AMP-PNP and AMP-CPP suggest that ATP hydrolysis to ADP and phosphate, and not nucleotide binding, is essential for McjB protease function.

In summary, these experiments characterized unambiguously McjB as a novel ATP-dependent cysteine protease and McjC as a lactam synthetase. They function in a concerted manner while having distinct functions, and possibly form a structural complex that we termed MccJ25 synthetase. Current model of MccJ25 biosynthesis is shown in Figure 1.

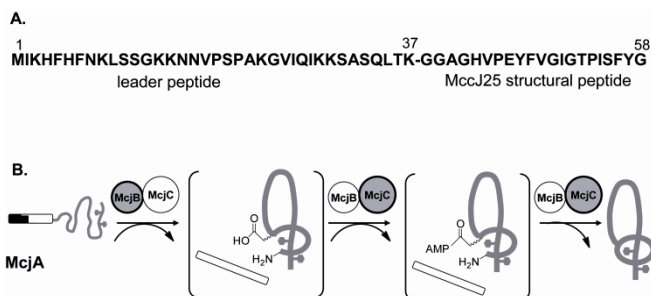


Figure 1. A) Sequence of McjA. B) Biosynthesis of MccJ25. Empty bar represents the leader peptide; functional enzyme in each step is in bold and in gray.

Acknowledgments

This work was supported by ANR (grant no. BLAN-NT09-692063). We thank the mass spectrometry platform at MNHN for access to the ESI-Qq-TOF mass spectrometer.

References

- [1] Duquesne, S.; Destoumieux-Garzón, D.; Zirah, S.; Goulard, C.; Peduzzi, J.; Rebuffat, S. *Chem. Biol.* **2007**, *14*, 793-803.
- [2] Pan, S. J.; Rajniak, J.; Maksimov, M. O.; Link, A. J. *Chembiochem* **2012**, *48*, 1880-1882.
- [3] Yan, K.-P.; Li, Y.; Zirah, S.; Goulard, C.; Knappe, T.; Marahiel, M. A.; Rebuffat, S. *Chembiochem* **2012**, *13*, 1046-1052.

IANUS peptide array as a tool to screen for protein antagonists

**Miroslav Malešević, Frank Erdmann, Erik Prell, Günther Jahreis,
Gunter Fischer**

*Max Planck Research Unit for Enzymology of Protein Folding, Weinbergweg 22, 06120
Halle/Saale, Germany*

E-mail: Malesevic@enzyme-halle.mpg.de

Introduction

The IANUS (Induced orgANization of strUcture by matrix-assisted togethernesS) peptide array is a low-resolution method to study protein-protein interactions for biopolymers that are still unreachable by modern recombinant techniques [1]. In this array the architecture of protein-protein interaction surfaces is revealed through template-assisted peptide-peptide interactions [2]. In contrast to standard spot array technology [3], each spot in the IANUS peptide array contains a trifunctional template with two peptides that are derived from corresponding interacting proteins. In such a way a full scan through both protein sequences that cover all possible peptide pair combinations can be made. The main obstacles of the array are library size and identification of template-assisted intramolecular interactions of peptide pairs. However, if these issues are solved, the array will provide at least two advantages over standard microarray technology: (i) no soluble protein probe or selective antibodies are needed, because solely amino acid sequences are sufficient for successful protein-protein binding analysis, and (ii) the binding regions of both interacting proteins can be analyzed in a single experiment. Up to date this array has been successfully used to analyze protein-ligand [2] and protein-protein [1] interactions but not to develop an enzyme antagonist. Herein, we applied the IANUS peptide array to screen for selective inhibitors of the interaction between calcineurin (CaN) and the nuclear factor of activated T cells (NFAT).

Results and Discussion

The Ca²⁺/calmodulin-activated phosphatase CaN is able to trigger gene expression by dephosphorylation of several phosphoserine residues of NFAT. Dephosphorylated NFAT then undergoes conformational changes and translocates into the nucleus, where it binds to specific regulatory DNA elements and triggers the gene transcription of different subsets of cytokines and chemokines. This process can be interrupted by the well-known immunosuppressive drugs cyclosporin A (CsA) and FK-506. Both CsA and FK-506 are powerful but not monofunctional CaN inhibitors. Probably as a consequence of interference with other pathways, severe side effects, like nephrotoxicity or hypertension, are observed upon treatment with these immunosuppressive drugs. A significant step toward development of selective immunosuppressive agents is the rational analysis of the interacting interfaces of both CaN and NFAT proteins. To this end the fluorescence resonance energy transfer (FRET) coupled IANUS peptide array was applied.

At first, the cellulose membrane was functionalized with an orthogonally (Fmoc and Alloc) protected trimesic acid derivative [4]. Using a standard spot technique [3], overlapping 12-

mer peptides spanning the entire catalytic subunit A and regulatory subunit B of CaN were synthesized on the Fmoc side of the template. The *N*-termini of each peptide were then capped with dansyl chloride. To screen all possible peptide combinations of both protein sequences an excessive number of peptide pairs would have been needed. Instead, after cleavage of the Alloc protective group, the SGPSPRIEITPSH peptide from the regulatory domain of NFAT, which is crucial for interaction with CaN, was synthesized as second peptide chain in all spots and subsequently labeled with 5(6)-carboxyfluorescein. Upon cleavage of all side-chain protecting groups, the membrane was irradiated with UV light at 312 nm; the resulting fluorescence emission was filtered at 520 nm and recorded. As expected, the resulting membrane image presented spots with different fluorescence intensity. Because of membrane heterogeneity and the lack of an internal standard for distance calculations in the IANUS peptide array, a comparison of relative spot fluorescence intensities was used to identify interacting peptide pairs. The interacting peptide pairs are expected to have higher spot fluorescence intensity because of FRET effects caused by interaction-induced chain proximity. Two or more consecutive spots with fluorescence intensity higher than the standard deviation from average fluorescence intensities were considered as indicative for the peptide-peptide interaction. Several such spot regions with strong fluorescence signal were detected by densitometric analysis. Seven peptides from spot regions that fulfill this predefined conditions for peptide-peptide interactions were synthesized and tested for their ability to inhibit (i) the NFAT dephosphorylation by CaN, (ii) the NF κ B dephosphorylation by CaN, and (iii) the CaN phosphatase activity. The peptide Ac-MAGPHPVIVITGPHEE-NH₂ [5] was used as positive control and the peptide Ac-HGGLSPEINTLD-NH₂, derived from a spot with fluorescence intensity lower than average, as a negative control. Most of the selected peptides from IANUS positive spots could considerably reduce the NFAT-driven reporter gene expression (only one false positive hit was observed) while negative control showed no activity in any of the used assays. Two peptides were even better CaN antagonists than the reference Ac-MAGPHPVIVITGPHEE-NH₂ peptide. More importantly, two of the tested peptides did not significantly inhibit CaN-dependent dephosphorylation of other substrates, i.e. NF κ B and RII phosphopeptide, and thus appeared to be selective. Also confocal laser scanning microscopy was used to visualize the influence of best hit and negative control peptides on the translocation of a green fluorescent protein-NFAT fusion protein (GFP-NFAT) into the nucleus upon stimulation. Indeed the translocation of GFP-NFAT into the nuclei was completely inhibited only with best hit peptide, thus confirming the potency of IANUS peptide array for identification of selective enzyme inhibitors.

References

- [1] Malešević, M.; Poehlmann, A.; Alvarez, B. H.; Diessner, A.; Träger, M.; Rahfeld, J. U.; Jahreis, G.; Liebscher, S.; Bordusa, F.; Fischer, G.; Lücke, C. *Biochemistry* **2010**, *49*, 8626.
- [2] Yu, C.; Malešević, M.; Jahreis, G.; Schutkowski, M.; Fischer, G.; Schiene-Fischer, C. *Angew. Chem. Int. Ed.* **2005**, *44*, 1408.
- [3] Frank, R. *Tetrahedron* **1992**, *48*, 9217.
- [4] Malešević, M.; Lücke, C.; Jahreis, G. *Peptides 2004, Proceedings of the Third International and Twenty-Eighth European Peptide Symposium*, Kenes International, Israel **2005**, 391.
- [5] Aramburu, J.; Yaffe, M. B.; Lopez-Rodriguez, C.; Cantley, L. C.; Hogan, P. G.; Rao, A. *Science* **1999**, *285*, 2129.

Comprehensive peptide microarrays for histone research

Karsten Schnatbaum¹, Johannes Zerweck¹, Tobias Knaute¹, Christoph Tersch¹, Nikolaus Pawlowski¹, Janina Seznec¹, Dirk Wildemann¹, Holger Wenschuh¹, Mike Schutkowski², Carola Wilczek³, David Shechter³, Ulf Reimer¹

¹JPT Peptide Technologies, Berlin, Germany; ²Martin-Luther-Universität Halle-Wittenberg, Germany; ³Albert Einstein College of Medicine, NY

E-mail: reimer@jpt.com

Introduction

Histones are important regulators of key processes including DNA replication, transcription, and DNA repair in healthy and diseased cells. Their regulation is mainly based on posttranslational modifications (PTMs), such as methylation, acetylation, phosphorylation, etc. Despite their importance, studying the complex dynamic effects of histone modifications is difficult i.a. because of the high number of potential PTM sites and sequence variants, as well as new PTMs that are continuously identified.^{1,2}

High-density peptide microarrays are ideal tools for the parallel presentation and examination of peptides. Their value has been proven in numerous applications, e.g. the investigation of humoral immune response, biomarker discovery, enzyme/antibody profiling and the identification of enzyme substrates.

Results and Discussion

We developed protocols for the high throughput synthesis of posttranslationally modified histone peptides and prepared building blocks for the synthesis of new PTMs. This enabled us to obtain a peptide microarray that contains peptide scans with posttranslational modifications at all potential sites in histones H2A, H2B, H3 and H4, including all available sequence variants from protein databases, as well as all combinations of reported PTMs (Fig. 1).

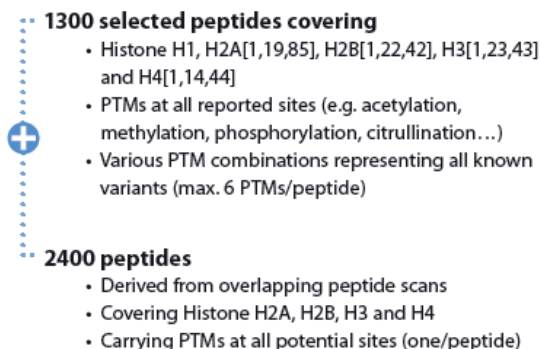


Figure 1: Overview about the histone code peptide microarray content.

The microarray can be used to identify the binding specificity of PTM-directed antibodies and histone interaction partners as well as the substrate specificity of histone modifying enzymes.

We will present experimental data from different applications. As an example, Fig. 2 shows the specificity testing for two commercial antibodies directed against H4R3Me1.

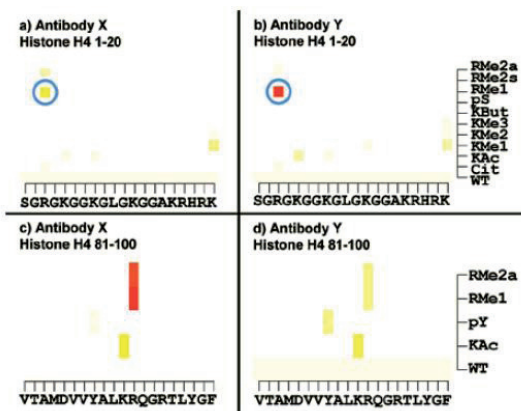


Figure 2: Specificity testing for two commercial antibodies directed against H4R3Me1 (blue circle). Shown are the results for two different H4 peptides. Dark colour represents strong specific signals, shades show weaker signals. Antibody X exhibits undesired strong binding to H4R92Me1 and also cross-reacts with the RMe2a modification (c). Antibody Y is specific for H4R3Me1 without cross-reactivity (b).

References

- [1] Dhall, A.; Chatterjee, C. *ACS Chem. Biol.* **2011**, *6*, 987–999.
- [2] Suganuma, T.; Workman, J. L. *Annu. Rev. Biochem.* **2011**, *80*, 473–499.

The antimicrobial peptide M33. An example of drug development

Jlenia Brunetti¹, Chiara Falciani², Stefano Bindi², Silvia Scali²,
Barbara Lelli², Luisa Lozzi², Luisa Bracci², Alessandro Pini²

¹SetLance srl, via Fiorentina 1, Siena, Italy; ²Department of Medical Biotechnologies,
University of Siena, Italy

E-mail:pinia@unisi.it

Introduction

The synthetic peptide M33 was obtained by random selection from a home-made phage-display peptide library panned against *E. coli* cells and a successive optimization phase for biological activity, synthesis and purification procedures [1-5]. The M33 sequence (KKIRVRLSA) is amphipathic and cationic, which is typical for AMPs, but did not show any sequence homology with known AMPs of natural or non-natural origin. M33 was synthesized in tetra-branched form, proving resistant to proteolytic degradation and very active in vitro against clinical isolates of several Gram-negative pathogens, including MDR strains of *Pseudomonas aeruginosa*, *Acinetobacter baumannii*, *Klebsiella pneumoniae* and *Escherichia coli*, while being less active against the Gram-positive pathogen *Staphylococcus aureus*. The peptide also protected mice lethally infected with multi-resistant clinical isolates of *P. aeruginosa* and *E. coli* [3] (Fig. 1).

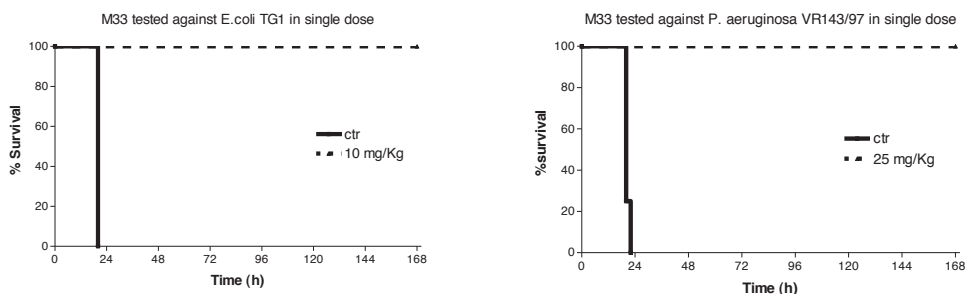


Figure 1. Left, Balb-c mice were injected with a lethal amount of *E. coli*. Continuous line (Ctr) indicates mice only injected with bacteria and no M33. Broken line indicates mice injected with bacteria and a single injection of M33. Right, Balb-c mice were injected with a lethal amount of *P. aeruginosa* cells. Continuous line (Ctr) indicates mice which only received bacteria; broken line indicates mice which received bacteria and a single dose of M33.

Results and Discussion

The mechanism of action of peptide M33 has been characterized for membrane interaction, pore formation, biofilm eradication, DNA binding and LPS neutralization [1-5]. Neutralization of LPS, demonstrated as a reduction in TNF- α production by macrophages, is a crucial aspect because it suggests that in vivo the peptide is involved not only in the direct killing of bacteria but possibly also in the reduction of cytokines that generate inflammation. This aspect, along with the low MIC shown by M33 against clinical isolates of *P. aeruginosa* from patients with Cystic Fibrosis or sepsis, increases the interest of this molecule as a new drug for diseases where inflammation triggered by bacterial infection is a major element of pathology progression.

The current preclinical development of peptide M33 consists of efficacy experiments in animal models of sepsis, pneumonia and skin infection along with toxicity and PK evaluation. These studies are in their final steps and M33 is running to start its clinical trials within the next future.

Acknowledgments

This research was financed by the Italian Foundation for Cystic Fibrosis (project FFC#24/2011 adopted by FFC delegations from Legnago, Varese, Reggio Emilia and Assistgroup), the Tuscan Regional Administration (Project SPAC: POR CRo FESR 2007–2013) and PROGETTO PRIN (2008KCLR7M_004).

References

- [1] Pini, A.; Giuliani, A.; Falciani, C.; Runci Y.; Ricci C.; et al. *Antimicrob Agents Chemother* **2005**, *49*, 2665.
- [2] Pini, A.; Giuliani, A.; Falciani, C.; Fabbrini, M.; Pileri, S.; et al. *J Pept Sci* **2007**, *13*, 393.
- [3] Pini, A.; Falciani, C.; Mantengoli, E.; Bindi, S.; Brunetti, J.; et al. *FASEB J* **2010**, *24*, 1015
- [4] Pini, A.; Lozzi, L.; Bernini, A.; Brunetti, J.; Falciani, C.; et al. *Amino Acids* **2012**, *43*, 467
- [5] Falciani, C.; Lozzi, L.; Pollini, S.; Luca, V.; Carnicelli, V.; et al. *PLoS ONE* **2012**, *7*, e46259.

Synthesis of cyclic lipo-octapeptide derivatives of burkholdines and its antifungal activity

Hiroyuki Konno and Yusuke Otsuki

Department of Biochemical Engineering, Graduate School of Science and Technology,
 Yamagata University, Yonezawa, Yamagata 992-8510, Japan

E-mail: konno@yz.yamagata-u.ac.jp

Introduction

Burkholdines (Bk) are potent antifungal cyclic lipopeptides isolated from a culture of *Burkholderia ambifaria* 2.2N by Schmidt's group in 2010.¹ Bk-1097 (**1**) and Bk-1229 (**2**) show potent antifungal activities of 1.6 and 0.4 µg/mL by the MIC, respectively against the yeast *Saccharomyces cerevisiae*. These compounds, which are more potent than amphotericin B, are cyclic octapeptides contained with L-threo-β-hydroxyasparagine (β-HAsn), β-hydroxytyrosine (β-HTyr), and a new fatty acyl amino acid (FAA). Although the stereochemistry of β-HTyr and FAA have not been determined, it would be difficult to prepare all of possible stereoisomers for the comparison of spectroscopic data.

We planned design, synthesis, and evaluation of simplified Bk analogues toward the determination of absolute stereochemistry and elucidation of the essential motif for antifungal activities (Fig. 1).

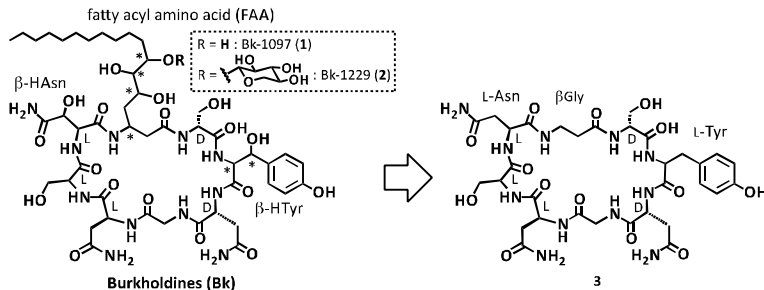
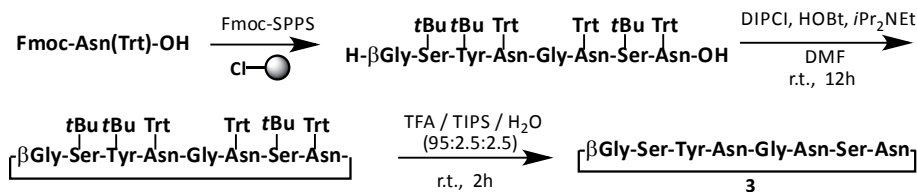


Fig. 1. Structures of Bk-1097 (**1**) and 1229 (**2**), and simplified analogue (**3**).

Results and Discussion

We firstly designed and synthesized the cyclic octapeptides composed of usual L- and/or D-amino acids as the most simplified analogues. The synthetic route for cyclic octapeptides is shown in Scheme 1. Designed linear peptides were prepared by Fmoc-based



Scheme 1. Synthesis of *cyclo*(-L-βGly-L-Ser-L-Tyr-L-Asn-Gly-L-Asn-L-Ser-L-Asn-) (**3**)

SPPS with 2-chlorotrityl chloride resin. The octapeptide resins were treated with HFIP followed by the intra-molecular cyclization and final deprotection with TFA/TIPS/H₂O to give the desired cyclic octapeptide (**3**) (Scheme 1). The antifungal activities of all of the synthetic cyclic peptides against *Saccharomyces cerevisiae* were extremely weak.

Next, the entry of simplified fatty acyl amino acid (sFAA) prepared by the coupling of L- or D-Fmoc-Asp^(Bu)-OH and dodecylamine was attempted to expect the increase of antifungal activity. Designed lipo-octapeptides with sFAA residues were similarly prepared without any problems as Scheme 1. As the assay results, *cyclo*(-L-sFAA-D-Ser-L-Tyr-D-Asn-Gly-L-Asn-L-Ser-L-Asn-) (**8**) and *cyclo*(-L-sFAA-D-Ser-D-Tyr-D-Asn-Gly-L-Asn-L-Ser-L-Asn-) (**9**) were shown to have antifungal activities of 50 and 25 μg/mL, respectively (Fig. 2). For more potent antifungal activity, replacement with L-sFAA instead of β-Gly or D-sFAA gave the antifungal compounds. In contrast, comparison of L-Tyr and D-Tyr produced no significant difference of antifungal activities.

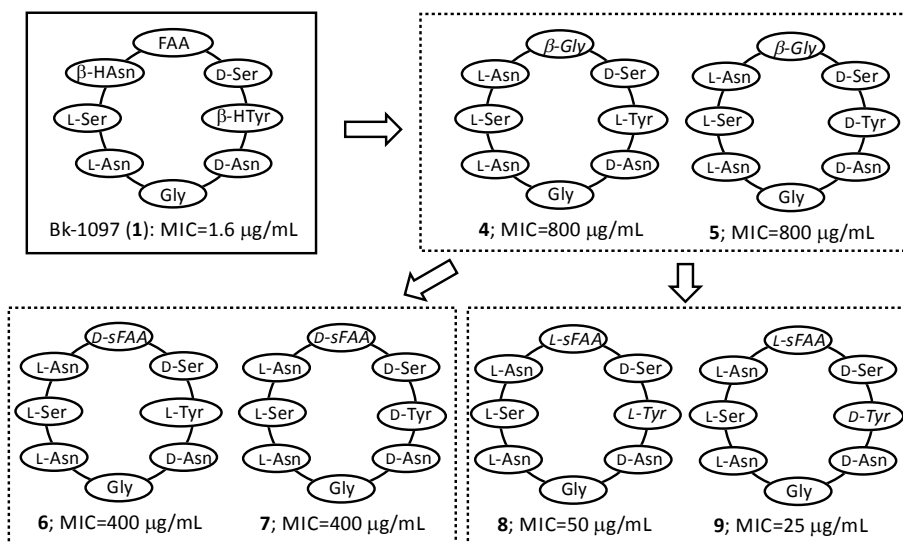


Fig. 2. Structure activity relationship study of Bk analogues.

Although these results suggest that the stereochemistry of β-position of FAA was likely to L-form, we must elucidate still more structure activity relationships. Synthetic study of all possible diastereoisomers of β-hydroxytyrosine and the Bk analogues including these unusual amino acids is currently underway in our laboratory.

Acknowledgments

We thank Dr. Kazuto Nosaka (Hyogo College of Medicine) for useful discussion. This work was supported in part by a grant from Yamagata University Research Institute.

References

- [1] Tawfik, K.; Jeffs, P.; Bray, B.; Dubay, G.; Falkinham, J. O. III; Mesbah, M.; Youssef, D.; Khalifa, S.; Schmidt, E. W. *Org. Lett.* **2010**, *12*, 664-666.

Peptides labeled by quaternary ammonium salts for sensitive detection by electrospray mass spectrometry

Remigiusz Bąchor, Magdalena Rudowska, Marzena Cydzik, Dominika Wojewska, Alicja Kluczyk, Piotr Stefanowicz, Zbigniew Szewczuk

Faculty of Chemistry, Wrocław University, Wrocław, Poland

E-mail: zbigniew.szewczuk@chem.uni.wroc.pl

Introduction

Split-and-mix technique has become an important tool in preparation of one-bead-one-compound (OBOC) peptide libraries [1,2]. The advantage of this technique is that thousands or even millions of compounds can be synthesized rapidly and screened for their biological activity. The main problem of OBOC peptide library analysis is the small amount of compound obtained from a single resin bead and insufficient ionization efficiency of some peptides for standard electrospray ionization mass spectrometry analysis (ESI-MS).

Recently, we developed an efficient and straightforward method for quaternary ammonium salts (QAS) formation on solid support [3]. This derivatization increases ionization efficiency and reduces the detection limit, allowing for ESI-MS/MS analysis of trace amounts of compounds. The fragmentation pathways of QAS-peptides were also analyzed, with the aid of deuterium-labeled analogs [4]. The hydrogen/deuterium exchange at α -carbon atom in peptides derived with *N,N,N*-trialkylglycine was also investigated [5]. The exchange reaction is strongly base catalyzed and is dramatically slow at lower pH, therefore introduced deuterons are not back-exchanged during LC-MS analysis with mobile phase containing 0.1% HCOOH. Increased ionization efficiency, provided by fixed positive charge on QAS group, as well as the deuterium labeling, enables analysis of trace amount of peptides.

We developed an application of a new linker containing QAS group for high-throughput analysis of single resin beads from OBOC libraries using high resolution ESI-MS/MS [6].

Results and Discussion

A small 16-member training library of α chymotrypsin substrates was designed and synthesized on TentaGel resin. The N-terminal amino groups were capped by the reaction with acetic anhydride. QAS in a form of *N,N,N*-triethylglycine were efficiently prepared on solid support after the peptide library synthesis and the Mtt-group removal from the ϵ -amino group of lysine residue by 1% TFA in DCM.

Proteolysis of peptide bonds by α chymotrypsin results in formation of free amino groups, which are known to yield a purple color (Ruhemann's purple) in the presence of ninhydrin. This allows for positive beads identification by observation of color change, and enables selection of beads containing chymotrypsin substrates (Figure 1). Each bead was treated independently by cyanogen bromide in formic acid for 18 h, releasing peptides combined with the linker bearing QAS group.

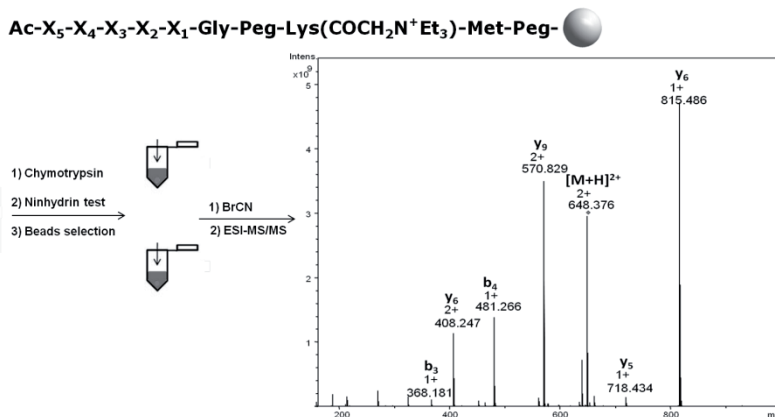


Figure 1. Schematic representation of high-throughput analysis of OBOC QAS peptide library. Gray ball indicates single resin bead. Less than 10% of the peptide obtained from a single resin bead was sufficient for the sequencing by ESI-MS/MS.

The analysis of peptides obtained from single resin beads confirmed that even a small portion of peptides derivatized by QAS cleaved from a single resin bead is sufficient for sequencing by HR ESI-MS/MS experiments.

The obtained results confirm the applicability of the proposed method in combinatorial chemistry.

Acknowledgments

This work was supported by a grant No. N N204 180040 from the Ministry of Science and Higher Education of Poland.

References

- [1] Lam, K.S.; Salmon, S.E.; Hersh, E.M.; Hruby, V.J.; Kazmierski, W.M.; Knapp, R.J. *Nature* **1991**, *354*, 82-84.
- [2] Furka, A.; Sebastyen, F.; Asgedom, M.; Dibo, G. *Int. J. Pept. Protein Res.* **1991**, *37*, 487-493.
- [3] Cydzik M, Rudowska M, Stefanowicz P, Szewczuk Z. *J. Pept. Sci.* **2011**, *17*, 445-453.
- [4] Cydzik, M.; Rudowska, M.; Stefanowicz, P.; Szewczuk, Z. *J. Am. Soc. Mass Spectrom.* **2012**, *22*, 2103-2107.
- [5] Rudowska, M.; Wojewska, D.; Kluczyk, A.; Bąchor, R.; Stefanowicz, P.; Szewczuk, Z. *J. Am. Soc. Mass Spectrom.* **2012**, *23*, 1024-1028.
- [6] Bąchor, R.; Cydzik, M.; Rudowska, M.; Kluczyk, A.; Stefanowicz, P.; Szewczuk, Z. *Mol. Diversity* **2012**, *16*, 613-618.

How hydrophobicity dictates the size of self-replicating self-assembling macrocycles

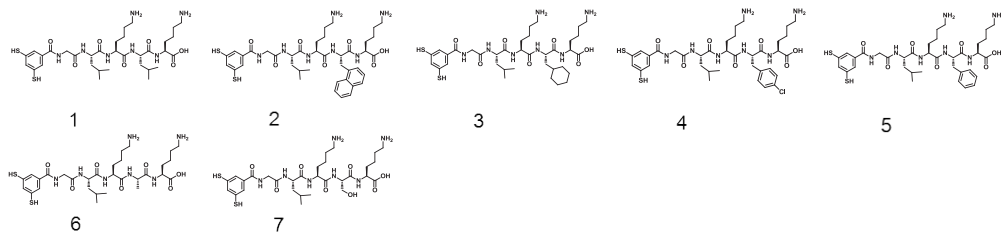
Morteza Malakoutikhah,¹ Mathieu Colomb-Delsuc,¹ Jerome J.-P. Peyralans,¹ Marc C. A. Stuart,^{1,2} Sijbren Otto^{*1}

¹University of Groningen, Centre for Systems Chemistry, Stratingh Institute, Nijenborgh 4, 9747 AG Groningen, the Netherlands; ²Groningen Biomolecular Sciences and Biotechnology Institute, University of Groningen, Nijenborgh 4, 9747 AG Groningen, the Netherlands

E-mail: s.otto@rug.nl

Introduction

How did life start? This is one of the most challenging unanswered questions in science. Self-replicating molecules might have had an important role in the origin of life. We have investigated how self-replicating molecules can emerge spontaneously from a network of interconverting molecules based on dynamic combinatorial chemistry. It was recently reported by our group that oxidizing a stirred solution of peptide **1** (XGLKLK, X: 3,5-dimercaptobenzoic acid) initially gave rise to an equilibrium mixture of many different disulfide macrocycles. After some time, the cyclic heptamer suddenly grew to become the dominant product. Surprisingly, when the mixture was agitated by shaking a different product appeared: the cyclic hexamer. Without any agitation only trimer and tetramer but no hexamer or heptamer was obtained. A number of detailed studies established that the formation of hexamer or heptamer is the result of autocatalysis. The hexamer or heptamer self-associates to form long fibers (observable by cryo-TEM) through β -sheet formation (proved by circular dichroism, thioflavin T and Congo red assays) that grow from their two ends.^[1] To discover further self-replicating peptides and explore the effect of the strength of peptide-peptide interaction on the self-replication process a library of six peptides was designed. The new peptide sequences were designed to be either less or more hydrophobic than peptide **1**, by substituting the C-terminal leucine (Leu) of peptide **1** with more hydrophobic amino acids such as 1-naphthylalanine (1-Nal in **2**), cyclohexylalanine (Cha in **3**), para-chlorophenylalanine (*p*-Cl-Phe in **4**) and phenylalanine (Phe in **5**) or less hydrophobic amino acids like alanine (Ala in **6**) and serine (Ser in **7**). Our expectation was that a more hydrophobic sequence would give rise to more stable β -sheets, so that fibre formation (and concomitant self-replication) becomes feasible for a reduced macrocycle size. Conversely, a less hydrophobic peptide should give fibres assembled from larger macrocycles.



Results and Discussion

Peptide self-assembly. Three solutions (3.8 mM) were prepared for each peptide in borate buffer (50 mM, pH 8.2), and then each solution was kept under different conditions namely stirred, shaken and non-agitated. Oxidation of thiol groups by oxygen from air produced macrocycles of different ring sizes. Appearance of these species as a function of time was monitored using HPLC and HPLC-MS. Peptide **2** as the most hydrophobic peptide in the group produced cyclic trimer and tetramer in all samples. Cyclic trimer was also the main product in the non-agitated solution of peptide **3**, while in the agitated samples cyclic hexamer grew to become the dominant species. Peptide **4** formed cyclic pentamer and hexamer in the non-agitated and agitated samples respectively. In all three samples of peptide **4** for the first several days different macrocycles coexisted following by the growth of cyclic pentamer, mostly at the expense of the cyclic trimer. While in the non-agitated sample the pentamer kept growing to become the dominant species, in the stirred and shaken solutions the amount of the pentamer decreased because the hexamer started growing by consuming the cyclic pentamer and eventually becoming the major product. In the case of peptide **5** initially, non-agitated and agitated samples, showed comparable behavior. However, after several days, the behavior of the samples diverged. The ones subjected to shear stress (shaking or stirring) showed a rapid exponential growth of cyclic hexamer at the expense of all other species. In sharp contrast, the library that was not agitated showed only a slow increase in the amount of hexamer while trimer and tetramer continued to dominate the mixture over the time-course of the experiment. Similar experiments were set up starting from peptides **6** and **7**. In the absence of agitation a mixture composed mostly of cyclic trimer and tetramer was obtained. However, repeating the experiment with agitation resulted in the rapid and nearly quantitative formation of octameric macrocycles for both peptides.

Fiber characterization. The self-assembly properties of the macrocycles to form fibers were evaluated by cryo-TEM. Cryo-TEM images show that all peptides formed fibers. Peptide **2**, which produced trimer and tetramer, formed twisted fibers even in the non-agitated sample. Fiber formation for this peptide implies that the hydrophobic interaction between peptide molecules is strong enough to form fiber even with the trimer and tetramer. Peptide **3** formed non-twisted fibers. Peptide **4** also formed twisted fibers in the non-agitated and agitated samples. Peptides **5**, **6** and **7** only formed fibers in the agitated samples. Analysis of the peptide solutions by circular dichroism (CD) and thioflavin T fluorescence assay suggested that the fibers are formed through β -sheet formation. These results confirm our hypothesis that the size of macrocycles can be tuned by peptide hydrophobicity.

Self-replication. Self-replicating properties of macrocycles were confirmed by seeding experiments where the addition of small amount of pre-existing fibres clearly induced the formation of the respective macrocycles.

Acknowledgments

This work has been supported by a postdoctoral fellowship from the Marie Curie Actions.

References

- [1] Carnall, J. M. A., Waudby, C. A.; Belenguer, A. M.; Stuart, M. C.A.; Peyralans, J. J. P.; Otto, S. *Science* **2010**, *327*, 1502.

Protein-fragment complementation and semi-rational design: Engineering specific antagonists of protein-protein interactions

**Tara Rao, Nicola Acerra, Richard O. Crooks, Neil M. Kad,
Jody M. Mason**

*School of Biological Sciences, University of Essex, Wivenhoe Park, Colchester, U.K.
CO43SQ*

E-mail: jmason@essex.ac.uk

Introduction

There has been a recent surge in interest for peptide-based antagonists of protein-protein interactions implicated in disease pathways. Therapeutic peptides are interesting since they are capable of bringing large surface areas into close contact. Interactions can consequently form across surfaces lacking well defined binding pockets that traditionally suit small molecules. In addition, the high specificity and low toxicity of peptides offers a viable alternative to the small molecule. To this end our two primary interests have centered on the design screening and selection of peptide antagonists that target two disease relevant protein-protein-interaction systems with both high affinity and specificity: **i**) the oncogenic transcriptional regulator, Activator Protein-1 (AP-1). Numerous oncogenic signalling pathways converge on AP-1 in different tissues ultimately controlling gene expression patterns and resulting in tumor formation, progression and metastasis (1, 2). **ii**) beta-amyloid and alpha-synuclein, the primary proteins implicated in Alzheimer's disease (AD) (3) and Parkinson's disease (PD) pathology (4,5).

Results and Discussion

We have designed and generated a range of peptide antagonists capable of inhibiting protein-protein interactions with high affinity and specificity. The forces that drive protein stability are increasingly well understood, however much less is known about those directing specificity. To this end, we have employed an intracellular selection system using Protein-fragment Complementation Assays (PCAs (6, 7)) for antagonist selection. In addition, we have undertaken Competitive And Negative Design Initiatives (CANDI (8)) to improve the specificity of PCA. CANDI works by expressing proteins that may otherwise result in undesirable off-target interactions with PCA selected antagonists. For example, target homologues can be expressed during protein during selection to ensure that target specific antagonists are selected. Further characterizations include folding pathway analysis to extract the underlying target-antagonist association/dissociation rates and the role of key residues in directing interaction (9, 10). These experiments suggest that electrostatic contacts in the AP-1 coiled coil enhance stability predominantly by decreasing the unfolding rate. This has major implications for future antagonist design whereby kinetic rules could be applied to increase the residency time of the antagonist-peptide complex, and therefore significantly increase the efficacy of the antagonist. More recently, iterations of Truncation, Randomization and Selection (TRaSe (11)) have also been employed using

PCA to identify the smallest functional units within peptide sequences that are required for effective binding to the target. Lastly, introduction of peptide mimetics (12) are also being investigated to bring additional stability and interaction affinity to the molecules.

Acknowledgments

JMM is the recipient of a Cancer Research UK Career Establishment Award (C29788/A11738) and a Wellcome Trust Project Grant (WT090184MA). JMM thanks Alzheimer's Research UK for a pilot project grant (ART/PPG2008B/2) and AgeUK for a New Investigator Award (#304). JMM and NMK also thank Parkinson's UK for awarding a PhD Studentship (H-1001).

References

- [1] Eferl, R., and Wagner, E.F. *Nat. Rev. Cancer* **2003**, 3, 859-68.
- [2] Ozanne, B.W., Spence, H.J., McGarry, L.C., and Hennigan, R.F. *Oncogene* **2007**, 26, 1-10.
- [3] Masters C.L., and Selkoe, D.J. *Cold Spring Harb Perspect Med.* **2012**, 2, a006262
- [4] Breydo L., Wu J.W., Uversky V.N., *Biochim Biophys Acta.* **2012**, 1822, 261-85.
- [5] Cookson, M.R., *Mol Neurodegener.* **2009**, 4:9.
- [6] Mason, J. M., Schmitz, M. A., Muller, K. M., and Arndt, K. M. *Proc Natl Acad Sci USA* **2006**, 103, 8989-8994.
- [7] Mason, J. M., Hagemann, U. B., and Arndt, K. M. *Biochemistry* **2009**, 48, 10380-10388.
- [8] Mason, J. M., Muller, K. M., and Arndt, K. M. *Biochemistry* **2007**, 46, 4804-4814.
- [9] Mason, J. M., Hagemann, U. B., and Arndt, K. M. *J Biol Chem* **2007**, 282, 23015-23024.
- [10] Mason, J. M. *FEBS J* **2009**, 276, 7305-7318.
- [11] Crooks, R. O., Rao, T., and Mason, J. M. *J Biol Chem* **2011**, 286, 29470-29479.
- [12] Mason, J. M. *Future Med Chem* **2010**, 2, 1813-1822.

Food protein fragments are regulatory oligopeptides

Alexander A. Zamyatnin^{1,2}, Olga L. Voronina¹

¹A.N.Bach Institute of Biochemistry, Russian Academy of Sciences, 119071 Moscow, Russian Federation; ²Departamento de Informática, El Centro Científico Tecnológico de Valparaíso, Universidad Técnica Federico Santa María, 110-V, Valparaíso, Chile

E-mail: aaz@inbi.ras.ru; alexander.zamyatnin@usm.cl

Introduction

Along with endogenous proteins, exogenous proteins are also present in a living organism. They enter regularly with food. These proteins are exposed to proteases in the gastrointestinal tract, resulting in their successive breakdown into smaller and smaller fragments down to amino acids. Until recent time they were viewed mainly as one of the sources of energy as well as essential and nonessential amino acids necessary for protein synthesis, as well as serving as precursors for many vital biomolecules. However, we assumed earlier [1] that fragments of food proteins could also carry out regulatory functions. This work provides a theoretical basis for such assumption. The first proteolytic enzyme to be encountered by a food protein is pepsin, which is secreted in the human stomach. That is why significant attention is given to this enzyme in our work. Proteins present in bovine muscles and cows' milk were used as substrates.

Results and Discussion

Investigations were conducted by comparing primary structures of protein fragments with amino acid sequences of natural regulatory oligopeptides known to date *in silico*. Primary structures of proteins were taken from the UniProtKB/SwissProt database (<http://uniprot.org>), and the data on natural regulatory oligopeptides was taken from the specialized EROP-Moscow database (<http://erop.inbi.ras.ru>) [2]. We used also data about the possibility of cleavage of all possible combination of amino acid residues at pH 1.0, 2.5, and 4.0 by porcine pepsin [3]. By normalizing these data, the possibilities of cleavage of all variants (400) of peptide bonds by pepsin at three pH values were calculated. Repeated participation of the enzyme in substrate cleavage is characterized by its turnover rate, which is 0.5 sec⁻¹ for pepsin [4]. This value characterizes the fact that the events of interaction of a single enzyme molecule with substrate molecules occur approximately every 2 sec. Then the probability of accumulation of an uncleaved fragment of the selected protein was calculated. For this, the probabilities of cleavage by pepsin of peptide bonds surrounding the fragment in the protein and the probabilities of non-cleavage of peptide bonds inside the fragment were calculated. The kinetic curves were obtained (see Figure).

It is shown that fragments formed as a result of animal food protein cleavage by proteolytic enzymes can exist in the gastrointestinal tract for a long time. Many of them are enzyme inhibitors, regulators of nervous, endocrine, and immune system, and possess antimicrobial and other activities. It has also been shown that the lifetime of fragments before their cleavage in the gastrointestinal tract could be enough for performing corrective functions.

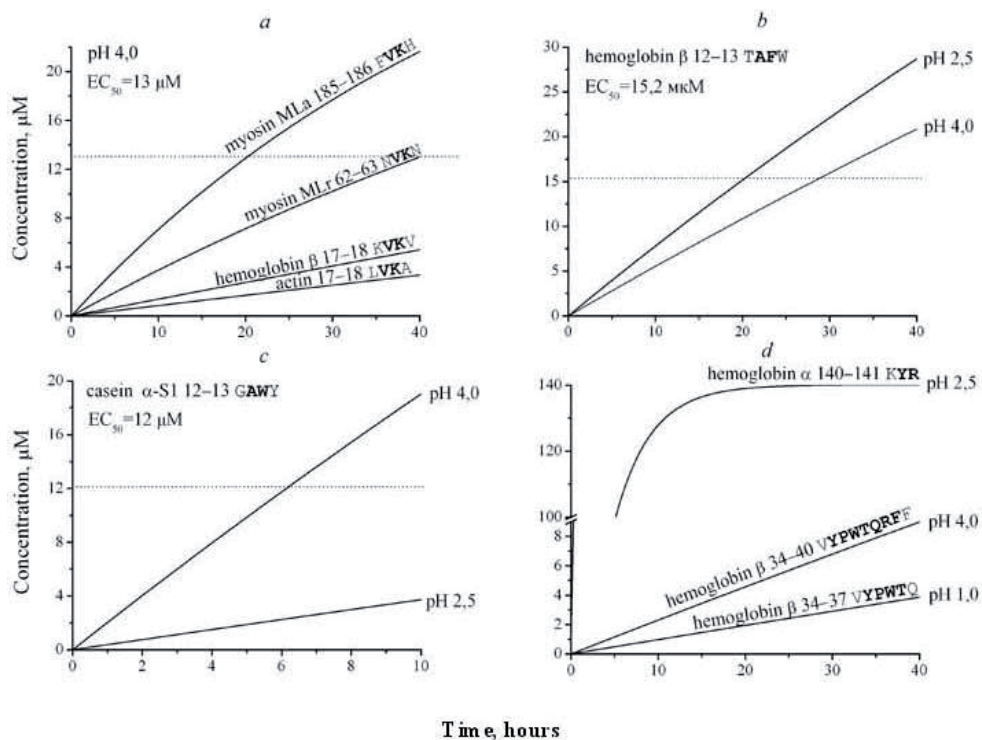


Figure. Kinetics of fragments formation from food proteins. a) Enzyme inhibitor **VK** formed from different proteins. b) Enzyme inhibitor **AF**. c) Enzyme inhibitor **AW**. d) Neuropeptide **YR** ($IC_{50}=0.69\mu\text{M}$), **YWTQRF** ($2.9\mu\text{M}$), and **YPWT** ($45.2\mu\text{M}$). Amino acid residues of a fragment are shown in bold, surrounding residues are in normal font. Dashed lines correspond to EC_{50} .

Thus, as a result of food protein fragmentation a dynamic pool of exogenous regulatory oligopeptides with functions changing as shorter fragments are generated may form. The detection of an endogenous–exogenous pool of regulatory molecules expands the significance and content of the hypothesis on a functional continuum of natural oligopeptides [5].

Acknowledgments

The authors are grateful to E. Zárata for help in carrying out calculations.

References

- [1] Zamyatnin, A. A. *Biochemistry (Moscow)*, **2009**, *74*, 201.
- [2] Zamyatnin, A. A.; Borchikov, A. S.; Vladimirov, M. G.; Voronina, O. L. *Nucl. Acids Res.* **2006**, *34*, D261.
- [3] Palashoff, M. H. *Determining the Specificity of Pepsin for Proteolytic Digestion*, *Chemistry Master's Theses*, **2008**, Paper 1, <http://hdl.handle.net/2047/d10016636>.
- [4] Stenesh, J. *Biochemistry*, Plenum Press, N. Y., **1998**, p. 89.
- [5] Ashmarin, I. P.; Obukhova, M. F. *Biochemistry (Moscow)*, **1986**, *51*, 531.

On the way to synthetic peptide vaccine against hepatitis C

Ekaterina Kolesanova¹, Alexandr Moisa¹, Nadezhda Pyndyk¹, Vladimir Prozorovsky¹, Sergei Funikov¹, Xavier Thomas², Jean Dubuisson², Alexandr Dadayan³, Yuri Zolotarev³

¹*Orekhovich Institute of Biomedical Chemistry, RAMS, Moscow, Russia;* ²*Center of Infection and Immunity of Lille, Universite Lille Nord de France/Institut Pasteur de Lille, Lille, France;* ³*Institute of Molecular Genetics, RAS, Moscow, Russia*

E-mail: ekaterina.kolesanova@ibmc.msk.ru

Introduction

Hepatitis C virus (HCV) exhibits extremely high genetic variability and therefore employment of the traditional approach for vaccine development based on attenuated or inactivated virus strain or full-size viral proteins is ineffective in the case of HCV [1]. Hence nontraditional approaches are needed for the development of anti-HCV vaccines, in order to overcome a possible isolate specificity of immune response and virus escape from the host response [1]. We have focused our attention on the development of peptide immunogenic constructs composed solely of conserved fragments of HCV envelope proteins, with one part representing a B-epitope, the second representing a widely specific T-helper epitope, and a short linker between them.

Results and Discussion

Search for putative T-helper epitope motifs in HCV envelope proteins with the help of SYFPEITHI Database revealed at least two conserved T-helper epitopes, broadly specific to Human Leukocyte Antigen (HLA) allele products, in E2 protein. Six artificial peptide constructs were made using one of the fragments (CR2; fragment designation as in [2]) as a Th-epitope and three fragments of E2, responsible for the binding to heparan-sulfates [3], as B-epitopes, with diglycine linker. The corresponding peptides were synthesized by Fmoc-SPPS, purified by reverse-phase HPLC and tested for the immunogenicity in rats (table 1).

Table 1. Artificial peptide constructs made from E2 HCV protein fragments and their immunogenicity testing results.

Peptide	Antibody titer*		
	Against peptide	Against E2 protein	Against E1E2 heterodimer
CR2-GG-CR3	1:32000	1:50-1:100 (3)	1:50-1:100 (3)
CR3-GG-CR2	1:8100	1:50-1:100 (3)	1:50-1:100 (3)
PRR1-GG-CR2	1:900	1:50 (1)	1:50 (1)
CR2-GG-PRR1	1:9200	1:50(2)	1:50(2)
CHR-GG-CR2	1:5600	1:50 (2)	1:50 (2)
CR2-GG CHR	1:2700	1:50 (1)	1:50 (1)
Mixture of 6	1:2000-1:24000 depending on peptide	1:150 (3)	1:100 (3)

* Numbers in brackets show the number of antisera samples containing corresponding antibodies. Number of rats in experimental groups – 5 (4 in the last group).

The constructs were highly immunogenic in the absence of any carrier besides Freund's adjuvant and able to elicit antibodies that interacted with full-size envelope proteins. The equivalent mixture of all six constructs showed the comparable immunogenicity and enhanced ability in eliciting anti-HCV envelope protein antibodies (table 1).

Antibodies raised against five of six constructs as well as against the mixture of constructs were capable of binding HCV from patient plasma (fig. 1).

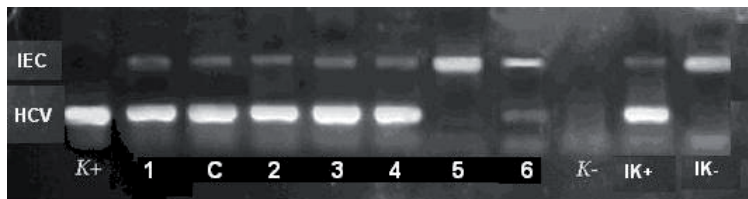


Figure 1. HCV binding to antibodies elicited by artificial peptide constructs, PCR detection. Nos. of the constructs used for the immunization (see table 1) shown in the line below, C – mixture of all 6 constructs. K+ and K- - positive and negative controls; IK+ and IK- - internal controls; IEC – internal control PCR product; HCV – HCV-derived PCR product.

High immunogenicity of the designed peptide immunogens could be explained by their ability to form oligomers with average particle sizes of about 10 nm, as it was shown by the laser correlometry measurements of particle sizes in peptide construct water solutions at physiological pH (data not shown).

Despite of the ability of binding HCV particles from patient sera, all antibody preparations did not reveal significant HCV-neutralizing activity in the tests of hepatoma cell infection with cell culture-produced HCV particles [4]. The lack of virus-neutralizing activity can be explained either by too low concentration of HCV-specific antibodies in antipeptide antibody preparations or by a somewhat improper presentation of HCV-specific B-epitopes in peptide constructs, or both. Nevertheless, the development of highly immunogenic peptide constructs composed of highly conserved fragments of HCV envelope protein shows the way to the creation of an anti-HCV vaccine. The ability of peptides to form oligomers with the enhanced immunogenicity points to the fact that the constructs can be incorporated into phospholipid micelles or liposomes with an amendment of their presentation as HCV-specific antigens.

Acknowledgments

The research was supported by joint RFBR-CNRS grant No.10-04-91054a. HCV-infected patient sera were provided by Dr. O.B. Kovalyov (Russian State Medical University, Moscow, Russia).

References

- [1] Gal-Tanamy, M., Walker, C., Foug, S., Lemon, S.M. In: *Vaccines for Biodefence and Emerging and Neglected Diseases*, A.T. Barrett and L.R. Stanberry (Eds.). Academic Press, **2009**, 413.
- [2] Sobolev, B.N., Poroikov, V.V., Olenina, L.V., Kolesanova, E.F., Archakov, A.I. *J. Viral Hepat.*, **2000**, *7*, 368.
- [3] Olenina, L.V., Kuzmina T.I., Sobolev B.N., Kuraeva T.E., Kolesanova, E.F., Archakov, A.I. *J. Viral Hepat.*, **2005**, *12*, 584.
- [4] Vieyres, G., Thomas, X., Descamps, V., Duverlie, G., Patel, A.H., Dubuisson, J. *J. Virol.* **2010**, *84*, 10159.

A synthetic heparin sulfate-mimetic peptide conjugate to a mini CD4 displays very high anti-HIV activity

Bridgette Connell¹, Françoise Baleux², Yves-Marie Coïc², Pascal Clayette³, David Bonnaffé⁴, Hugues Lortat-Jacob¹

¹*IBS, UMR5075, Grenoble;* ²*Institut Pasteur, UMR3523, Paris;* ³*Bertin Pharma, Fontenay aux roses;* ⁴*ICMMO, UMR8182, Orsay, France*

E-mail: francoise.baleux@pasteur.fr

Introduction

Tremendous progress has been made in the development of antiviral drugs to treat HIV infection, but despite the availability of some 25 approved antiretroviral compounds the virus continues to be a major concern and remains one of the leading causes of death worldwide. To overcome the emergence of resistant viral strains and the strong adverse side effects associated with long-term exposure necessitate the development of new drugs that target a different virus cycle step. Inhibition of HIV-1 entry, a process based on sequential interaction of the viral glycoprotein (gp120) with the cell surface CD4 and either one of the two chemokine receptors CCR5 or CXCR4, acting as a coreceptor, has become a compelling target for controlling viral replication. We actually develop bi-functional conjugates that simultaneously blocked the CD4 and coreceptor binding sites on gp120. Based on miniCD4 peptide covalently linked to polyanionic compounds, we generate a first conjugate, mCD4-HS12, that established the proof of concept of our approach[1].

Results and Discussion

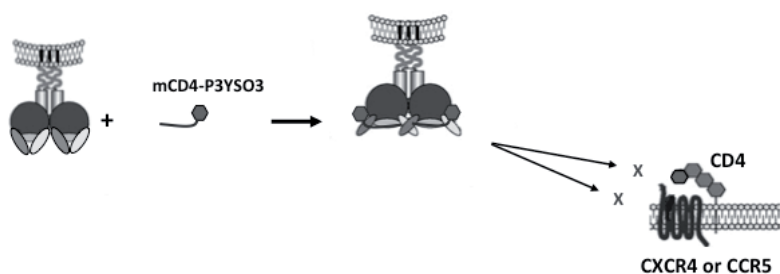
Sulfated oligosaccharides synthesis is notoriously difficult. To overcome this problem, sulfotyrosine containing peptides were evaluated as heparin sulfate (HS) mimics. As a first approach, a tridecapeptide of general sequence SXDXSXDXSXDXS, was selected. X stands for sulfotyrosine (YSO3) or tyrosine (Y). Aminosuberic acid (Asu) and paracarboxymethyl phenylalanine (pF) were also evaluated as sulfotyrosine isostere. A polyglutamate peptide (E13) was used as full polyanionic peptide. All peptides were synthesized by Fmoc SPPS, purified by C18 RP-HPLC with linear gradients of ammonium or triethylamine acetates buffers in acetonitrile. A thiol function was introduced at the N-terminus of each peptide by SATP coupling. After hydroxylamine deprotection, the polyanionic peptides were coupled to maleimide-activated mCD4 affording five conjugates.

Antiviral activity was then evaluated in PBMC infected with HIV Lai (X4) or Ba-L (R5) strains. Among the five conjugates, the sulfotyrosine one (mCD4-P3YSO3) turned out to be the more effective in blocking HIV replication with EC₅₀ in the low nanomolar range (0,5-1,3 nM) and was more active than mCD4-HS12. These results also emphasize the importance of the presence of a sulfate group and of the aromatic moiety in the polyanionic peptidic part. As for mCD4-HS12, the antiviral results confirmed the synergetic effect obtained by covalent linkage of mCD4 and the polyanionic part. More interestingly, mCD4-P3YSO3 was also effective on more relevant clinical isolates of different clades. Among them, a clade C virus was inhibited with an EC₅₀ of 29 nM [2]. Clade C viruses account for half of the circulating viruses in the world. These encouraging results confirm

that the HS12, bearing 18 sulfates groups, can be advantageously replaced by a tridecapeptide containing only 6 sulfates groups. The synthesis of sulfotyrosines peptides is less complex than HS12 one. This finding opens the way to more readily accessible structure/function studies on the importance on the number and position of sulfate groups for HIV inhibition.

As mCD4-P3YSO3 will be evaluated in first intention as microbicide gel in macaque, stability at pH 4 (vaginal pH) was analyzed by HPLC and LCMS. The compound turned out to be stable over 48hours at 37°C.

Although relatively limited in MW (5,500 da), the mCD4-P3YSO3 bi-functional molecule has the remarkable property to target simultaneously two critical and conserved regions of gp120, i.e the CD4 and coreceptor binding sites:



mCD4-P3YSO3 displays very high anti-HIV-1 activity independently of coreceptor usage. The compound is non-toxic up to 1 μM .

Acknowledgments

This work was supported by the Agence Nationale de la Recherche sur le Sida (ANRS).

References

- [1] Baleux, F., Loureiro-Morais, L., Hersant, Y., Clayette, P., Arenzana-Seisdedos, F., Bonnaffe, D. & Lortat-Jacob, H. *Nat Chem Biol* **2009**, *5*, 743-8.
- [2] Connell, B. J., Baleux, F., Coic, Y. M., Clayette, P., Bonnaffe, D. & Lortat-Jacob, H. *Chemistry & Biology*, **2012**, *19*, 131-9.

Branched neurotensin specifically binds a highly selective tumor cell marker, which is not neurotensin receptor 1

Chiara Falciani^{1,2}, Jlenia Brunetti¹, Barbara Lelli¹, Niccolò Ravenni¹,
Luisa Lozzi¹, Lorenzo Depau¹, Alessandro Pini¹, Luisa Bracci^{1,2}

¹ Department of Biotechnology, University of Siena, Italy; ² Istituto Toscano Tumori (ITT),
Siena, Italy

E-mail: chiarafalciani@unisi.it

Introduction

In the last few decades, peptides have been increasingly considered as a promising new class of tumor selective targeting agents. The rationale for the use of peptides for selective targeting of cancer cells was provided years ago, with the finding that different endogenous peptides are over-expressed by many human tumors, together with their own receptors [1]. This observation suggested the possibility to target novel tumor antigens, through a peptide receptor strategy. In previous works, we synthesized tetra-branched NT peptides (NT4) conjugated to different functional units, for selective imaging and killing of cancer cells [2] and we demonstrated that NT4 can efficiently discriminate between tumor and healthy tissue in human surgical samples from colon and pancreas adenocarcinoma in a high number of patients, with good statistical significance, whereas monomeric NT cannot [3]. Moreover, we proved that NT4 can efficiently and selectively deliver functional units or liposomes [4] for cell imaging or therapy to different human cancer cells. Besides, by using NT4 conjugated to methotrexate or 5FdU we obtained reduction of tumor growth in mice by respectively 60 and 50% [2]. Since multimeric binding, together with the chemical modification caused by coupling to the branched core, might have affected selectivity of receptor recognition by NT4, we have analyzed receptor selectivity of branched NT peptides compared with that of native NT.

Results and Discussion

NT4 peptide, binds to membrane receptors on both HT29 and TE671 cell lines. Since TE671 cells do not express NTR1, NT4 peptide seems to bind additional receptors beyond the high affinity NTR1 (Figure 1).

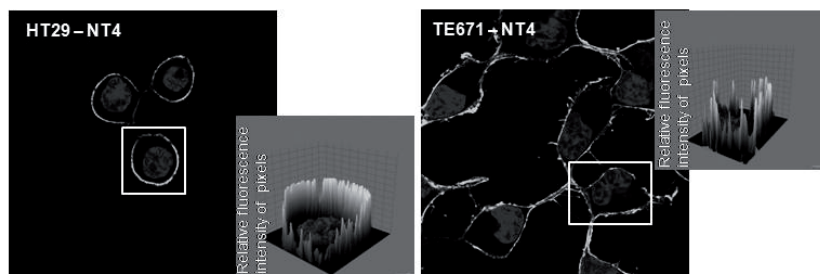


Figure 1. Binding of NT4 on HT29 and TE671 cell lines. Relative quantification was assessed by fluorescence surface plot (grey panels).

NTR1 is involved in the release of intracellular Ca^{2+} , we then measured Ca^{2+} release induced by NT branched and monomeric peptides in HT29 cells and in TE671 cells.

The COOH terminal group of NT sequence, and of its C-terminal functional fragment NT(8-13), was reported to have a crucial role in peptide binding to both NTR1 G-protein coupled receptor and to sortilin (27, 28). In our NT4 tetra-branched peptides, the C-terminal carboxyl group is actually missing, being engaged in the coupling to the three lysines core. A NT tetra-branched peptide was synthesized by chemoselective ligation, where the coupling to the three lysine core was obtained via the N-terminus of NT sequence, obtaining a branched peptide with a free C-terminus (NT4-COOH). NT4-COOH binding to membrane receptors on both HT29 and TE671 cell lines, is much lower in intensity compared to that of NT4 (not shown).

In HT29 cells, monomeric native NT as well as NT4-COOH peptides induced strong Ca^{2+} release, proving to be both full agonists. As expected, considering that TE671 cells do not express NTR1 (or NTR2), no Ca^{2+} release was detected in these cells when incubated with any NT peptide (not shown). On the other side, NT4, lacking the free C-terminal COOH, induced a much lower Ca^{2+} release, as well as a monomeric NT sequence carrying a C-terminal amide (Figure 2, left).

We tested the ability of the specific NTR1 antagonist SR48692, to inhibit peptide induced Ca^{2+} release, in order to confirm that the event was actually caused by NTR1 receptor binding. In fact, SR48692 completely inhibited intracellular Ca^{2+} release induced by all NT peptides. Even the much lower Ca^{2+} release induced by peptides lacking the free C-terminal COOH, is completely inhibited by SR48692, indicating that the Ca^{2+} release is always induced by stimulation of NTR1 (Figure 2, right).

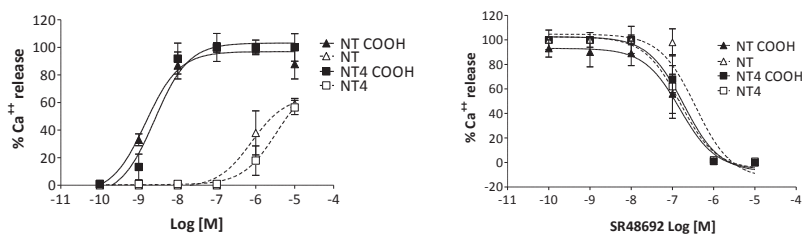


Figure 2. HT29 endocellular Ca^{2+} release

We demonstrate that the much higher binding of NT4 in respect to native NT to either cancel cell lines or human cancer surgical samples, as well as the higher selectivity toward human cancer tissues, is due to additional membrane receptors that are more selectively expressed in human cancer tissues, than NTR1 receptors.

Acknowledgments

This study was undertaken with the financial support of AIRC and ITT.

References

- [1] Reubi, J.C., Mäcke, H.R., Krenning, E.P., *J. Nucl. Med.* **2005** *46*, 67S-75S.
- [2] Falciani, C., et al. *Mol. Cancer Ther.* **2007**, *6*, 2441-2448.
- [3] Falciani, C., et al. *Curr. Cancer Drug Targets.* **2010**, *10*, 695-704.
- [4] Falciani, C., et al. *ChemMedChem.* **2011**, *6*, 678-685.

Anticancer drug delivery systems containing GnRH-III as a targeting moiety

Marilena Manea^{1,2}, Ulrike Leurs^{1,3}, Erika Orbán⁴, Verena Natalie Schreier¹, Lilla Pethő⁴, Pascal Schlage^{1,5}, Ákos Schulcz⁶, Bence Kapuvári⁶, József Tóvári⁶, Gábor Halmos⁷, Gábor Mező⁴

¹Laboratory of Analytical Chemistry and Biopolymer Structure Analysis, Department of Chemistry, University of Konstanz, 78457 Konstanz, Germany; ²Zukunftskolleg, University of Konstanz, 78457 Konstanz, Germany; ³Department of Drug Design and Pharmacology, Faculty of Health and Medical Sciences, University of Copenhagen, 2100 Copenhagen, Denmark; ⁴Research Group of Peptide Chemistry, Hungarian Academy of Sciences, Eötvös Loránd University, 1117 Budapest, Hungary; ⁵Institute of Cell Biology, ETH Zürich, 8093 Zürich, Switzerland; ⁶National Institute of Oncology, 1122 Budapest, Hungary; ⁷Department of Biopharmacy, Medical and Health Science Center, University of Debrecen, 4032 Debrecen, Hungary

E-mail: marilena.manea@uni-konstanz.de

Introduction

Targeted cancer chemotherapy is a modern oncological approach developed in order to overcome the drawbacks associated with the application of free anticancer drugs. Tumor targeting can be achieved by attaching a chemotherapeutic agent to a targeting moiety, which recognizes tumor-specific or highly expressed receptors on cancer cells [1]. Considering that receptors for gonadotropin-releasing hormone (GnRH-Rs) are expressed on a variety of human cancer cells with relatively limited expression in normal tissues, they represent important molecular targets for cancer therapy [1]. In our work, lamprey GnRH-III (<EHWSHDWKPG-NH₂; <E is pyroglutamic acid) was employed as a targeting moiety to which anticancer drugs such as daunorubicin and methotrexate were covalently coupled. GnRH-III was selected as a targeting moiety based on its binding to the GnRH-Rs, its antiproliferative effect on various cancer cells and lower hormonal effect than human GnRH [2]. To enhance the antitumor activity of anticancer drug-GnRH-III derivative bioconjugates, several strategies were employed, e.g. different chemical linkages between the anticancer drug and targeting moiety, modification of the GnRH-III peptide sequence and incorporation of more than one anticancer drug in a bioconjugate.

Results and Discussion

The anticancer drug-GnRH-III derivative bioconjugates were prepared by a combination of solid phase peptide synthesis and chemical ligation strategies. Daunorubicin (Dau) was attached to GnRH-III through different linkages such as hydrazone, amide or oxime bonds (either directly or by insertion of a GFLG tetrapeptide spacer known to be cleaved by Cathepsin B). Except for the amide bond-linked bioconjugate, all the other compounds exerted *in vitro* cytostatic effect on MCF-7 human breast and HT-29 human colon cancer cells, with IC₅₀ values in low μM range. From the hydrazone bond containing bioconjugate, free Dau was released within several minutes at pH 5; also at pH 7.4, Dau was released

after 2 h. The oxime bond-linked compounds were chemically stable under acidic and neutral conditions; furthermore, they were stable in human serum for at least 24 h. They were degraded in the presence of rat liver lysosomal homogenate; however, no free Dau was released. H-Lys(Dau=Aoa)-OH and Dau=Aoa-Gly-OH were the smallest drug containing metabolites identified by mass spectrometry, which were able to bind to the DNA *in vitro*. On the basis of the *in vitro* results, oxime bond-linked bioconjugates were selected for further *in vivo* studies. Both compounds exerted a significant tumor growth inhibitory effect on murine C26 and human HT-29 colon carcinoma bearing mice; moreover, they were not toxic on healthy mice [3-5]. A possible approach to enhance the antitumor effect of the bioconjugates is the modification of the GnRH-III sequence. In our work, replacement of Ser⁴ by Lys(Ac) resulted in a compound with enhanced enzymatic stability, cellular uptake and antitumor activity both *in vitro* (on MCF-7, HT-29 and LNCaP cell lines) and *in vivo* (on C26 colon carcinoma bearing mice) [6]. However, its binding to the GnRH receptors on the pituitary cells and prostate cancer specimen was not significantly higher than that of the parent bioconjugate. The effect of GnRH-III[⁴Lys(Ac), ⁸Lys(Dau=Aoa)] (Aoa is aminooxyacetyl) on the protein expression profile of human HT-29 colon cancer cells was investigated by proteomics approaches. Several proteins (e.g., metabolism-related proteins, molecular chaperons, proteins involved in signaling etc) were found to be present in a lower or higher amount after chemotherapeutic treatment. Another strategy that might result in compounds with enhanced antitumor activity is the attachment of more than one anticancer drug, identical or different, to the same GnRH-III based targeting moiety. We have design, synthesized and biochemically characterized compounds containing two Dau molecules or one Dau and one methotrexate coupled to GnRH-III derivatives. These multifunctional bioconjugates exerted higher *in vitro* cytostatic effect than the compounds containing only one anticancer drug [7,8]. Taken together, our results lead to the conclusion that targeted chemotherapy is a promising approach for the treatment of cancer.

Acknowledgments

This work was supported by grants from the University of Konstanz (Zukunftskolleg - Project 879/08; Young Scholar Fund - Projects 435/11 and 462/12) and the Hungarian National Science Fund (OTKA NK 77485).

References

- [1] Schally, A.V.; Nagy, A. *Eur. J. Endocrinol.* **1999**, *141*, 1.
- [2] Lovas, S.; Pályi, I.; Vincze, B.; Horváth, J.; Kovács, M.; Mező, I.; Tóth, G.; Teplán, I.; Murphy, R.F. *J. Pept. Res.* **1998**, *52*, 384.
- [3] Orbán, E.; Mező, G.; Schlage, P.; Csík, G.; Kulic, Ž.; Ansorge, F.; Fellingner, E.; Möller, H.; Manea, M. *Amino Acids* **2011**, *41*, 469.
- [4] Schlage, P.; Mező, G.; Orbán, E.; Bösze, Sz.; Manea, M. *J. Control. Release* **2011**, *156*, 170.
- [5] Manea, M.; Tóvári, J.; Tejada, M.; Schulcz, Á.; Kapuvári, B.; Vincze, B.; Mező, G. *Anti-Cancer Drugs* **2012**, *23*, 90.
- [6] Manea, M.; Leurs, U.; Orbán, E.; Baranyai, Zs.; Öhlschläger, P.; Marquardt, A.; Schulcz Á.; Tejada, M.; Kapuvári, B.; Tóvári, J.; Mező, G. *Bioconjug. Chem.* **2011**, *22*, 1320.
- [7] Leurs, U.; Mező, G.; Orbán, E.; Öhlschläger, P.; Marquardt, A.; Manea, M. *Biopolymers Pept. Sci.* **2012**, *98*, 1.
- [8] Leurs, U.; Lajkó, E.; Mező, G.; Orbán, E.; Öhlschläger, P.; Marquardt, A.; Köhida, L.; Manea, M. *Eur. J. Med. Chem.* **2012**, *52*, 173.

Bivalent ligands for the chemokine receptor CXCR4 dimer and their function

**Wataru Nomura, Tomohiro Tanaka, Haruo Aikawa, Tetsuo Narumi,
Hirokazu Tamamura**

*Institute of Biomaterials and Bioengineering, Tokyo Medical and Dental University,
Chiyoda-ku, Tokyo 101-0062, Japan*

E-mail: tamamura.mr@tmd.ac.jp

Introduction

G protein-coupled receptors (GPCRs), which are attractive drug targets, the targets of 40% of commercially available drugs. It has been difficult however to obtain structural information pertaining to GPCR which is necessary for drug development. To date, a few structures of GPCRs have been solved by X-ray crystallography. The chemokine receptor CXCR4 belongs to the GPCR family. Interaction of CXCR4 with its endogenous ligand stromal-cell derived factor-1 (SDF-1)/CXCL12 induces various physiological functions. Recently, a ligand-independent homodimerization of CXCR4 was revealed by BRET analysis and X-ray crystallography. However, information obtained from these analyses is limited due to the mutation. Furthermore, it is also difficult to estimate the precise distance between CXCR4s that form a dimer structure. In this study, we designed and synthesized novel CXCR4 bivalent ligands that linked two FC131 [1,2] analogues [*cyclo*-(D-Tyr-Arg-Arg-Nal-D-Cys-)], which is a highly potent CXCR4 antagonist, with a polyproline or PEGylated polyproline linker to sustain a constant distance between two ligands (Figure 1). We applied our bivalent ligands to estimate the distance between the binding sites of CXCR4 in the dimer form by evaluating binding affinity of these ligands with various lengths of linkers.

Results and Discussion

The binding affinity was evaluated in a competitive binding assay against [¹²⁵I]-CXCL12. The results showed that the binding affinity of these bivalent ligands is clearly dependent on the linker lengths. It is noteworthy that the maximum increase in binding affinity was observed for both of the linker types of similar length (ca. 5.5-6.5 nm) [3]. Based on the increased binding affinity of linker-optimized bivalent ligands, ligands were applied as probes specific to CXCR4 on the cell surface because the receptors are overexpressed in several kinds of malignant cells. The dimer formation of the receptor should depend on the expression level, thus higher population of dimers should be observed on the surface of malignant cells. Accordingly, the ligand with the highest binding affinity was labeled with tetramethylrhodamine (TAMRA), which was designated as compound **1**, and applied to the imaging of CXCR4. To obtain merge images of CXCR4 and ligands, the EGFP gene was fused to the C-terminus of the CXCR4 gene and the plasmid was transiently transfected. The increase in binding affinity of the bivalent ligand **1** was clearly reflected in the imaging of the cell surface CXCR4. When a TAMRA-labeled monomer ligand was utilized, only a trace of binding was observed. The CXCR4 recognition by the ligands showed clear

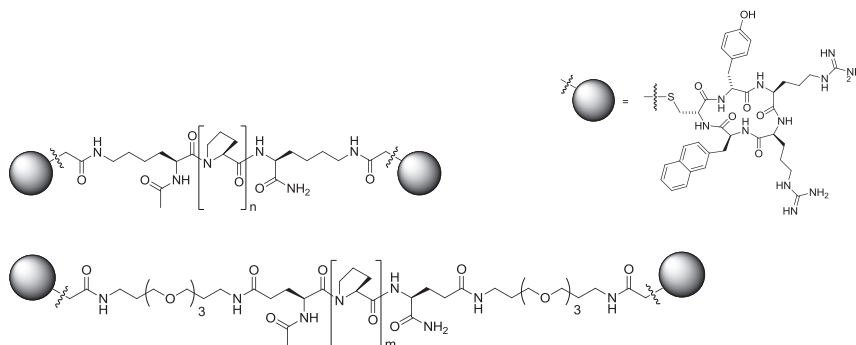


Figure 1. Design of bivalent ligands against CXCR4. As a CXCR4 binding moiety, D-Cys FC131 (shown as a gray circle) was prepared. Poly-proline (upper, $n = 6-27$) and PEG-conjugated poly-proline (lower, $m = 3-18$) with D-Cys FC131 on both ends were synthesized.

dependence on the expression of CXCR4. To further evaluate the binding specificity, FACS analyses utilizing Jurkat, K562, and HeLa cells were performed. The variable levels of CXCR4 expression of the cells are Jurkat > HeLa > K562. The binding was evaluated by changes of mean fluorescent intensity (MFI) of these cells. The bivalent ligand **1** showed intense binding to Jurkat cells, which highly express CXCR4, in a dose-dependent manner. For binding to HeLa cells, MFI was increased to 2.4-fold by binding of ligand at 1 μM , although no significant increase of MFI was observed at 25 or 250 nM of **1**. Meanwhile, the monovalent ligand at 2 μM showed similar binding to Jurkat and HeLa cells. Thus, it is difficult to distinguish the expression level of CXCR4 by molecular imaging using the monovalent ligand. In addition, the binding of both CXCR4 ligands would be responsible to CXCR4 because no binding of both ligands to K562 cells, which express a trace of CXCR4, was observed. Taken together, the ligand could distinguish cancerous cells with high CXCR4 expression and normal cells such as endothelial cells. This information would be useful for the design of bivalent ligands of any GPCR with the advantages that the ligand can directly capture dimeric forms of GPCRs.

Acknowledgments

T.T. was supported by JSPS Research Fellowships for Young Scientists. This research was supported in part by New Energy and Industrial Technology Development Organization (NEDO).

References

- [1] Tamamura, H.; Xu, Y.; Hattori, T.; Zhang, X.; Arakaki, R.; Kanbara, K.; Omagari, A.; Otaka, A.; Ibuka, T.; Yamamoto, N.; Nakashima, H.; Fujii, N. *Biochem. Biophys. Res. Commun.* **1998**, *253*, 877.
- [2] Fujii, N.; Oishi, S.; Hiramatsu, K.; Araki, T.; Ueda, S.; Tamamura, H.; Otaka, A.; Kusano, S.; Terakubo, S.; Nakashima, H.; Broach, J. A.; Trent, J. O.; Wang, Z.; Peiper, S. C. *Angew. Chem., Int. Ed.* **2003**, *42*, 3251.
- [3] Tanaka, T.; Nomura, W.; Narumi, T.; Masuda, A.; Tamamura, H. *J. Am. Chem. Soc.* **2010**, *130*, 15899.

Azapeptide calpain inhibitors

Z. Bánóczy¹, L.E. Dókus¹, Á. Tantos², P. Tompa², P. Friedrich²,
F. Hudecz^{1,3}

¹Research Group of Peptide Chemistry, Hungarian Academy of Sciences, Eötvös L. University, Pázmány P. s. 1/A, H-1117 Budapest, Hungary; ²Institute of Enzymology, Biological Research Center, Hungarian Academic of Sciences, Karolina út 29, H-1113 Budapest, Hungary; ³Department of Organic Chemistry, Eötvös L. University, POB 32, H-1518 Budapest 112, Hungary

e-mail:banoczy@elte.hu

Introduction

Calpains are intracellular cysteine proteases and are of considerable interest due to their implication in numerous physiological events. Besides these functions, they could play a key role in some well-studied pathological processes. The overactivation of calpains, which is resulted in by the disorder in Ca²⁺ homeostasis, increases the degradation of the enzyme substrates and could contribute to the development of the Alzheimer and/or Huntington diseases and also to death of nervous cells caused by traumatic brain injury, spinal cord injury [1]. Thus the inhibition of calpain may be important in blocking of calpain overactivation. This claim requires more selective inhibitors, with proper cell-membrane permeability.

Results and Discussion

Our aim is to develop peptide based calpain inhibitors, using the sequence of substrate (TPLKSPPPSPR) which was identified by us [2]. In the new inhibitor family, the Lys residue after which the calpain cleaves the substrate was replaced with azaglycine [3]. Different number of amino acids, derived from the preference matrix [2], at *N*- and *C*-terminal was also included. The azapeptides were built up on MBHA resin using Boc/Bzl strategy. The azaglycine moiety was incorporated into the sequence using carbonyl-diimidazole and Boc-hydrazide.

The inhibitory effect of azapeptides was examined against *m*- and μ -calpain and papain using Suc-LY-AMC as substrate and was characterized by K_i values. Table 1 summarizes only azapeptides with *m*-calpain inhibitory effect. Azapeptides with shorter *C*- and *N*-terminus (*Ac*-TPLAglySP-NH₂, *Ac*-PLAglySPPPS-NH₂, *Ac*-LAGlySPPPS-NH₂, *Ac*-AglySPPPS-NH₂) had no inhibition at 100 μ M concentration. If Leu at P₂ position was replaced by Thr or Val, the azapeptides did not show inhibitory activity. These results are in accordance with literature, namely Leu is very much preferred at this site. We obtained the same results if a) serine at P₁' was replaced by Thr or Arg and b) proline at P₂' position was substituted by Ser or Gln. Only the replacement of Pro at P₂ position resulted in azapeptides with inhibitory activity (**5** and **6**). The selection of amino acids for replacement in a given position was based on the preference matrix [2].

Table 1 Inhibitory activity of azapeptides against different cysteine proteases.

Code	Azapeptide sequence	K_i (μM) ^a (sd)		
		m-calpain	μ -calpain	papain
1	<i>H</i> -TPLAglySPPPSPR- <i>NH</i> ₂	20.3 (1.32)	169.9 (13.4)	3.0 (1.3)
2	<i>Ac</i> -TPLAglySPPPSPR- <i>NH</i> ₂	7.2 (2.2)	13.3 (4.7)	4.1 (2.1)
3	<i>Ac</i> -TPLAglySPPPS- <i>NH</i> ₂	8.7 (0.12)	16.0 (7.8)	8.6 (1.2)
4	<i>Ac</i> -TPLAglySPP- <i>NH</i> ₂	89.8 (54.0)	42.9 (12.9)	8.4 (6.2)
5	<i>Ac</i> -TWLAglySPPPS- <i>NH</i> ₂	5.8 (0.37)	3.9 (1.9)	5.5 (1.7)
6	<i>Ac</i> -TSLAglySPPPS- <i>NH</i> ₂	3.5 (0.062)	14.0 (5.3)	14.5 (3.1)

^a Enzyme kinetic data were analyzed by the MicroCal Origin data analysis software to determine the initial slope of fluorescence change.

The inhibitory azapeptides on m-calpain was studied on both μ -calpain and papain. All compounds inhibited both enzymes. In case of μ -calpain only compound **1** showed significantly lower inhibitory activity and therefore higher selectivity. The azapeptides inhibited the papain with the same or better activity than inhibited m-calpain.

These results indicate that the replacement of lysine residue in the substrate sequence with azaglycine (TPLAglySPPPSPR) results in an inhibitor molecule. This compound bind to m-calpain better than the substrate, as its K_i value is lower than the K_M value of substrate ($K_M = 93 \mu\text{M}$). This suggests that the elimination of the side chain of lysine does not weaken the m-calpain binding of azapeptides. To prove this idea we have prepared several azapeptides to study the effect of amino acids at the C- and N- terminus and at different positions on the inhibitory activity. We have identified a sequence, as optimal in which the amino acid at P₃ position (e.g. Trp or Leu) could be varied without an essential loss of function. Based on these observations we conclude that azapeptides described in this communication might be useful tools to study the amino acid preference of m-calpain at different binding sites (e.g. analysis of the enzyme interaction at P and P') and also to develop more potent and selective calpain inhibitors.

Acknowledgments

This study was supported by grants: OTKA K-68285, OTKA PD-83923 and GVOP-3.2.1-2004-04-0352/3.0. Bánóczy, Z. acknowledges the support of Bolyai János Scholarship (Hungarian Academy of Sciences).

References

- [1] Saez, E. M. et al. *Drug Discov. Today*. **2006**, *11*, 917.
- [2] Tompa, P. et al. *J. Biol. Chem.* **2004**, *279*, 20775.
- [3] Bánóczy, Z. et al. Peptides 2010, Proceedings of 31st European Peptide Symposium, 606 (2010).

Production and characterization of matrix metalloproteinases implicated in multiple sclerosis

S. Amar and G. B. Fields

Torrey Pines Institute for Molecular Studies, Port St. Lucie, FL, USA

E-mail: gfields@tpims.org

Introduction

Breakdown of the blood-brain barrier (BBB), perivascular infiltration of inflammatory auto-reactive T cells in the central nervous system, and demyelination are characteristic of the initial phase of multiple sclerosis (MS). The roles of specific matrix metalloproteinases (MMPs) in MS are beginning to be revealed. The ability of MMPs to degrade components of the extracellular matrix, including collagen, as well as myelin indicates a crucial role in the active stage of MS. MMP-9 levels are elevated in MS serum and cerebrospinal fluid, particularly in patients with active disease. Injection of MMP-9 into the brain causes disruption of the basement membrane and is associated with breakdown of the BBB [1]. MMP-25 efficiently cleaves all myelin basic protein isoforms and inactivates crystalline $\alpha\beta$, a suppressor of MS [2]. In highly active demyelinating MS lesions, macrophages were strongly immunoreactive for MMP-19 [3]. MMP-28 protein expression is increased within demyelinated human MS lesions compared to surrounding normal tissue [4]. Most prior studies focused on the characterization of MMP-19, MMP-25, and MMP-28 have considered only the catalytic domain of these enzymes. The present study has sought to produce full-length MMP-19, MMP-25, and MMP-28. The use of full-length MMPs procures the advantage of considering the roles of secondary binding sites (exosites) in enzymatic activity. Production of recombinant MMPs utilizing bacterial systems is a convenient and a relatively fast method to obtain higher yields as compared to the use of mammalian cells. This will ultimately allow for the characterization of proteolytic activities relevant to MS.

Results and Discussion

Full-length MMP-19 and MMP-25 have been expressed using the pET28b vector and produced in *E. coli* strain Rosetta(DE3)pLysS. MMP-28 constructs were found to encode for two variants, V1 and V2. The variants differ due to an alternative splicing in exon 8, which contains a premature stop codon. V2 was obtained by site directed mutagenesis and possesses a shorter hemopexin (HPX)-like domain than V1. All recombinant MMPs contained a *N*-terminal His-tag and were purified from inclusion bodies under denaturing condition using a HisTrap column and gel filtration followed by a 3 step dialysis to ensure proper refolding. Proteolytic activation of MMP-19, MMP-25 and MMP-28V2 (via trypsin-3 or furin) resulted in enzymes that catalyzed the degradation of single-stranded synthetic substrates. The refolding of MMP-28 was a limiting step and so far only MMP-28V2 has demonstrated enzymatic activity. This is probably due to its shorter HPX domain, which facilitates refolding of the protein. The amount of active MMP-19 and MMP-25 was determined by titration with recombinant tissue inhibitor of metalloproteinase (TIMP)-2 and TIMP-3. MMP-19 showed a higher level of inactive enzyme as compared to MMP-25.

Aggregation of MMP-19 occurred during the refolding step and after freezing/thawing. MMP-19 tended to self-activate and autodegrade, which can explain a lower yield.

A fluorescence resonance energy transfer (FRET) triple-helical peptide (fTHP) was utilized to determine whether the recombinant MMPs were able to hydrolyze collagen triple-helical structure [5]. FRET was achieved via incorporation of the 5-carboxyfluorescein (5-Fam) fluorophore and the 4-[4-(dimethylamino)phenylazo]-benzoic acid (Dabcyl) quencher within the same peptide chain. MMP-25 showed greater fTHP hydrolysis activity compared to MMP-19, while incubation with MMP-28 did not lead to any significant increase of fluorescence (Figure 1). The specificity of MMP-25 for this particular fTHP may be due to distinct substrate conformational features interacting with protease exosites. The fTHP may therefore be a useful tool to identify non-active site binding MMP-25 selective inhibitors.

Type IV collagen is a major component of the basement membrane, an important functional and structural element of blood vessels. Since invasion of the BBB is a critical step in MS, analysis of MMP-19, MMP-25, and MMP-28 cleavage sites in type IV collagen will provide significant insight into the respective roles of these specific proteases in the disease. Establishing the cleavage sites will also enable the design of selective substrates and inhibitors. Human type IV collagen was digested with MMP-19 or MMP-25 for 48 h and cleaved fragments were separated by SDS-PAGE. One challenge for type IV collagen coverage is 5-hydroxylysine glycosylation, which may impact trypsin digestion and MS analysis. Deglycosylation prior to analysis is being pursued. A recent report has indicated several type IV collagen cleavage sites by MMP-25 [6].

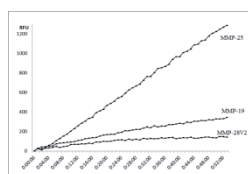


Figure 1: 1.5 μ M of fTHP was incubated with 30 nM MMP-25, 1.5 μ M MMP-19, or approximately 3 μ M MMP-28V2. Fluorescence was monitored over time using $\lambda_{\text{excitation}} = 490$ nm and $\lambda_{\text{emission}} = 520$ nm in a 384 well plate. The fTHP [(GPO)₅GPK(5-Fam)GPQG~LRG-Q(Dabcyl)GVR(GPO)₅, where O = 4-hydroxy-L-proline] incorporated a consensus types I-III collagen sequence described previously [5]. MMP-25 hydrolysis of types I and II collagen has been reported [6].

Acknowledgments

We thank Dr. Rafi Fridman for providing the human MMP-25 cDNA. This work was supported by NIH grant CA98799 and the Multiple Sclerosis National Research Institute.

References

1. Sobel, R. A.; Ahmed, A. S., *J. Neuropathol. Exp. Neurology* **2001**, *60*, 1198.
2. Shiryayev, S. A.; Savinov, A. Y.; Cieplak, P.; Ratnikov, B. I.; Motamedchaboki, K.; Smith, J. W.; Strongin, A. Y., *PLoS One* **2009**, *4*, e4952.
3. van Horsen, J.; Vos, C. M.; Admiraal, L.; van Haastert, E. S.; Montagne, L.; van der Valk, P.; de Vries, H. E., *Neuropathol. Applied Neurobiology* **2006**, *32*, 585.
4. Werner, S. R.; Dotzlaw, J. E.; Smith, R. C., *BMC Neuroscience* **2008**, *9*, 83.
5. Minond, D.; Lauer-Fields, J. L.; Cudic, M.; Overall, C. M.; Pei, D.; Brew, K.; Visse, R.; Nagase, H.; Fields, G. B., *J. Biol. Chem.* **2006**, *281*, 38302.
6. Starr, A. E.; Bellac, C. L.; Dufour, A.; Goebeler, V.; Overall, C. M., *J. Biol. Chem.* **2012**, *287*, 13382.

Receptor and blood-brain barrier characterization of opioid peptides in drug research & early development

Mathieu Verbeken¹, Sofie Stalmans¹, Evelien Wynendaele¹, Nathalie Bracke¹, Bert Gevaert¹, Kathelijne Peremans², Ingeborg Polis², Christian Burvenich², Bart De Spiegeleer¹

¹Faculty of Pharmaceutical Sciences, Ghent University, Harelbekestraat 72, 9000 Ghent, Belgium; ²Faculty of Veterinary Medicine, Ghent University, Salisburylaan 133, 9820 Merelbeke, Belgium

E-mail: bart.despiegeleer@UGent.be

Introduction

The opioid receptors (ORs) are known to be distributed widely in the central nervous system (CNS) and in peripheral sensory and autonomic nerves. Activation of ORs by endogenous and exogenous ligands results in a multitude of physiological functions and behaviors, e.g. pain and analgesia, stress and social status, tolerance and dependence, learning and memory, eating and drinking, and many more [1]. Due to this widespread pharmacological profile of ORs, opioid peptides are becoming key players in the pharmaceutical industry, more specifically in research and development of pain modulating agents. Among the opioid receptor subtypes, the μ -opioid receptor subtype is the main target due to its essential contribution to control pain (*i.e.* narcotic analgesics used in clinic are all agonists of the μ -opioid receptor subtype) [2]. For analgesics to target ORs in the CNS and exert medical activity, opioid peptides should penetrate the blood–brain barrier (BBB), with limited efflux behavior, have a favorable receptor-subtype selectivity and sufficient metabolic stability.

Results and Discussion

The opioid receptor-subtype selectivity can be assessed not only by the classic radioligand binding methods, but also by novel techniques such as SAW (surface acoustic wave) measuring the binding kinetics. Pharmacokinetics include metabolic stability, brain influx and efflux characteristics, as well as brain capillary retention. Metabolic stability is evaluated *i.a.* by *in vitro* kinetic studies using different target tissues. Using *in vivo* mouse models, the influx transfer constant from serum into mouse brain is determined by multiple time regression, while the efflux kinetics are investigated with the intra-cerebroventricular injection technique. Furthermore, the brain parenchyma/capillary distribution is evaluated by the capillary depletion method. Finally, the *in vivo* antinociceptive activity can be quantified in a mouse model.

During these initial research and discovery phase, the peptide quality and its stability characteristics are often neglected, possibly leading to misinterpretation of biological results, and thus are important factors to avoid false functionality conclusions [3].

Results evaluating the requested and labeled (supplier's certificate of analysis) *versus* the experimentally determined quality of 46 peptides from one supplier were problematic. The quality of more than 30% of the evaluated peptides was below 90% compared to the

requested 95% purity. This confirms a previous study where the quality of one peptide from different suppliers was also found to be problematic [7]. Moreover, these impurities do influence the functionality, as demonstrated by the observed baseline contraction of guinea pig ileum longitudinal smooth muscle in a tissue organ bath test which was due to the impurities and not to the peptide INSL6[151-161] itself [3].

The stability of peptides during *ex vivo* experiments was also evaluated, demonstrating that some remained stable but others were chemically and/or physically (adsorption to tissue/glass) unstable and thus unable to exert their full functionality.

In order to have a good antinociceptive activity, the BBB characteristics of opioid peptides should be favorable. Information about the BBB behavior of peptides, including the opioids, is scattered throughout the literature, with a wide variety of different study protocols being used. Therefore, the currently available BBB-data are collated in the database Brainpeps, which can *i.a.* be used for QSPR analyses [4]. Moreover, the CNS-functional drugability of a set of opioid peptides was comparatively scored using a Derringer's desirability function combining the different drugability requirements into a single figure-of-merit [5]. The overall *in vivo* antinociceptive effect of these opioid peptides was also investigated using a tail-flick mouse model [6]: the obtained *in vivo* results correlated well with the ranking from the desirability criterion.

Acknowledgments

This research is partially funded by the "Institute for the Promotion of Innovation through Science and Technology in Flanders (IWT Vlaanderen)" (IWT 50164 and IWT 73402) and by the Special Research Fund of Ghent University (BOF 01J22510).

References

- [1] Henriksen, G.; Willoch, F, *Brain* **2008**, *131*, 1171-96.
- [2] Mizoguchi, H.; Watanabe, C.; Sakurada, T.; Sakurada, S., *Curr Opin Pharmacol* **2011**, *12*, 87-91.
- [3] Verbeken, M.; Wynendaele, E.; Lefebvre, R. A.; Goossens, E.; Spiegeleer, B. D., *Anal Biochem* **2012**, *421* (2), 547-55.
- [4] Van Dorpe, S.; Bronselaer, A.; Nielandt, J.; Stalmans, S.; Wynendaele, E.; Audenaert, K.; Van De Wiele, C.; Burvenich, C.; Peremans, K.; Hsuchou, H.; De Tre, G.; De Spiegeleer, B., *Brain Struct Funct* **2012**, *217* (3), 687-718.
- [5] Van Dorpe, S.; Adriaens, A.; Vermeire, S.; Polis, I.; Peremans, K.; De Spiegeleer, B., *J Pept Sci* **2011**, *17* (5), 398-404.
- [6] Novoa, A.; Van Dorpe, S.; Wynendaele, E.; Spetea, M.; Bracke, N.; Stalmans, S.; Chung, N. N.; Lemieux, C.; Cooper, M. A.; Zuegg, J.; Tourwé, D.; De Spiegeleer, B.; Schiller, P. W.; Ballet, S., *J Med Chem* **2012**, *submitted*.
- [7] De Spiegeleer, B.; Vergote, V.; Pezeshki, A.; Peremans, K.; Burvenich, C., *Anal Biochem* **2008**, *376*, 229-234.

Selective cell signaling study of GPCR via PWR spectroscopy

**Minying Cai, Han Zhang, Matt M. Dedek, S, Scott. Saavedra,
Victor. J. Hruby**

Department of Chemistry, University of Arizona, Tucson, Arizona 85721, USA
Email: mcai@email.arizona.edu

Introduction

The Melanocortin system is involved in various physiological functions including regulation of blood pressure and heart rate, skin pigmentation, erectile function, feeding behavior, obesity etc[1]. These multifaceted functions have great potential for medical application for a wide range of symptoms. Despite the central importance of the medical applications of the melanocortin system, few of the melanotropins have been successful in clinical trials due to lack of understanding of the mechanisms of ligand induced down regulation which may cause the side effects. Melanocortin (MC) receptors belong to the rhodopsin I group of the GPCR family. Five melanocortin receptor subtypes with different patterns of tissue expression in the brain and in the periphery have been cloned and characterized. The latest studies have demonstrated that GPCR activated ensembles of signaling pathways are organized as integrated networks. In addition to the heterotrimer G-proteins, GRKs and β -arrestins are also considered to be G protein independent signaling transducers. Each of them can activate different cascades in cellular signaling. Therefore, the study of selective cell signaling with biased ligands is a great opportunity for the discovery of new drugs with fewer side effects. Fluorescence spectroscopy, NMR, and crystallography have been used for selective cell signaling studies, nevertheless, all of these techniques can only provide the indirect information. Plasmon Wave-guided Resonance Spectroscopy (PWR), a state of the art new technology which was developed at the University of Arizona can provide direct evidence of the ligand induced GPCR conformation changes which will be favorable for G proteins, GRKs and β -arrestins binding [2], therefore leading to the different cellular cascade responses that have clinical relevance.

Results and Discussion

The human melanocortin 4 receptor (hMC4R) is a GPCR representative to be purified for this study. The hMC4R is believed to be related to obesity, diabetes and sexual dysfunction. Melanotan II (MTII) (**Figure 1**), a synthetic cyclized melanotropin with a lactam bridge which is derived from the naturally occurring melanocortin peptide hormone, α -melanocyte stimulate hormone, is a super potent nonselective agonist of the melanocortin system and is in clinical trials for the control of feeding behavior and erectile dysfunction [3]. β -Arrestin 2 (β Arr2), a ubiquitous multi-functional scaffold protein, is a major cytosolic transducer to be studied in this work. In the living cellular system, when the hMC4R is activated by MTII, it will recruit to the receptor, forms a hMC4R/ β Arr complex and decouples hMC4R from $G\alpha$, thereby **desensitizing** the receptor to prevent further stimulation [4]. In this study, purified β -arrestin2 is also applied for in vitro study of MTII activated β -arrestin2 binding towards the hMC4R. **Figure 2** shows that purified solubilized hMC4R was incorporated in the Egg PC and the binding capability with purified β -

arrestin2 was tested. The receptor was pre-treated with MTII. Angular PWR established and characterized by the author was used to monitor the binding activity of hMC4R in the work. In this study, purified hMC4 receptor pre-treated with MTII and without treatment of MTII shows different binding affinities. Hence, we are able to directly track agonist activated receptor conformational changes from the PWR spectrum.

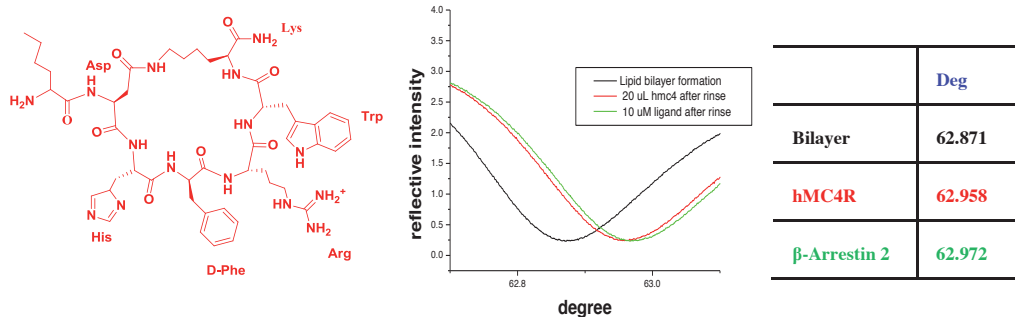


Figure1.Left: MTII **Figure 2.** Right: PWR data of human melanocortin receptor pretreated with MTII is able to bind with β -arrestin 2

G protein-coupled receptors (GPCRs), a superfamily represents the most successful targets of modern drug therapy, with proven efficaciousness in the treatment of a broad range of human conditions and disease processes. It is now appreciated that β -arrestins, once viewed simply as negative regulators of traditional GPCR-stimulated G protein signaling, act as multifunctional adapter proteins that regulate GPCR desensitization and trafficking and promote distinct intracellular signals in their own right. Moreover, several GPCR biased agonists, which selectively activate these divergent signaling pathways, can be directly identified using PWR.

Acknowledgments

Supported by Grants from the USPHS, DK17420. EB 007047.

References

- [1] Cone, R.D., Ed., The Melanocortin Receptors, Humana Press, 2000, pp 551.
- [2] Al-Obeidi, F.; Hadley, M.E.; Pettitt, B.M.; Hruby, V.J. *J. Amer. Chem. Soc.* 1989, 111, 3413-3416.
- [3] Alves, I.D.; Ciano, K.A.; Boguslavsky, V.; Varga, E.; Salamon, Z.; Yamamura, H.I.; Hruby, V.J.; Tollin, G. *J. Biol. Chem.*, 2004, 279, 44673-44682
- [4] Cai, M.; Stankova, M.; Pond, S.J.K.; Mayorov, A.V.; Perry, J.W.; Yamamura, H.I.; Trivedi, D.; Hruby, V.J. *J. Am. Chem. Soc.* 2004, 126, 7160-7161.

PEGylation of the endogenous peptide Neuromedin U yields a promising candidate for the treatment of obesity and diabetes

Paolo Ingallinella,^{1,3} Andrea M. Peier,² Alessandro Pocai,² Annalise Di Marco,^{1,4} Kunal Desai,² Karolina Zytka,¹ Ying Qian,² Xiaobing Du,² Antonella Cellucci,^{1,4} Edith Monteagudo,^{1,4} Ralph Laufer,^{1,4} Elisabetta Bianchi,^{1,4} Donald J. Marsh,¹ Antonello Pessi^{1,5}

¹IRBM P. Angeletti, Pomezia (RM) Italy; ²Merck Research Laboratories, Rahway, NJ, USA; ³Current address: DiaSorin, Gerenzano (VA) Italy; ⁴Current address: IRBM Science Park, Pomezia (RM) Italy; ⁵Current address: PeptiPharma, Pomezia (RM) Italy

E-mail: donald_marshall@merck.com; a.pessi@peptipharma.it

Introduction

Neuromedin U (NMU) is a 25-aa endogenous peptide with a well-documented role in the regulation of feeding and energy homeostasis [1]. Two NMU receptors have been identified: NMUR1, expressed primarily in the periphery, and NMUR2, expressed predominantly in the brain. We recently demonstrated that acute peripheral administration of NMU exerts potent anorectic activity and improves glucose homeostasis [1]. However, the half-life of the peptide after subcutaneous (sc) injection is < 5 min, precluding its use as a therapeutic. Therefore, we set out to develop a metabolically stable analog of NMU, based on conjugation to the native peptide of poly(ethylene) glycol ("PEGylation").

Results and Discussion

We explored variables including PEG size, structure, site of attachment, and PEGylation chemistry (Figure 1). We initially selected branched 40 kDa PEG (PEG40), which was conjugated either by reaction of the peptide with PEG40 N-hydroxysuccinimide, taking advantage of the absence of any amine other than the N-terminal one (PEG40-NMU), or by introduction of an extra-Cys and reaction with maleimido-PEG40 [C(PEG40)-NMU]. Both PEGylated derivatives were full agonists of the human NMUR1/NMUR2 receptors, with comparable functional EC₅₀s (Table 1).

Table 1. *In vitro* and *in vivo* activity of selected NMU analogues.

Peptide	EC ₅₀ (nM)		% Food intake reduction ¹		
	hNMUR1	hNMUR2	day 1	day 2	day 3
hNMU	2.3±1.1	1.4±0.7	45	-	-
PEG40-NMU	125±16	147±21	51	57	22
C(PEG40)-NMU	36±16	109±35	57	62	23
C(PEG20)-NMU	20±80	37±18	99	65	-
C(PEG5)-NMU	5.8±1.1	12±2.3	79	-	-

¹Single sc administration at 10 mg/kg. All peptides were tested at equimolar doses

Shortening of the sequence starting from the N-terminus, and PEGylation at internal positions were then explored, the latter by mutating the amino acid at positions 4, 8, 12 and 16 into cysteine for reaction with maleimido-PEG40. In both cases, moving PEG towards the C terminus caused a progressive considerable decrease in potency.

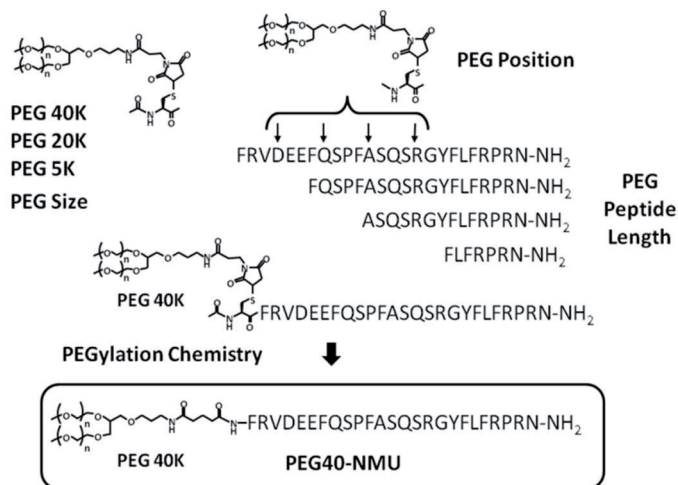


Figure 1. Optimization of PEGylated NMU. The chosen compound PEG40-NMU is framed.

Having established the N-terminus as the best site for PEGylation, we then explored PEG of different sizes. As expected, the smaller the PEG, the lower the steric hindrance; however, prolonged *in vivo* efficacy required larger-size PEG (Table 1).

Overall, the above data indicated that N-terminal derivatization of NMU with 40 kDa PEG was the most appropriate to achieve metabolic stability and prolonged duration of action. For further characterization, PEG40-NMU was preferred over C(PEG40)-NMU because of the potential of cys-maleimide derivatives for slow drug release in plasma [2].

PEG40-NMU showed an excellent pharmacokinetic profile, with 47% sc bioavailability, a half-life of 25 h, and a clearance of 0.03 mL/min/kg. When dosed sc at 3 and 10 mg/kg in DIO C57BL/6 mice every other day for 10 days, sustained body weight loss was observed throughout the study, with a cumulative reduction of 2.4% and 7.6%, respectively, primarily due to a decrease in fat mass. Moreover, PEG40-NMU at 0.1 and 1 mg/kg markedly improved glucose tolerance during an oral (OGTT) and intra-peritoneal glucose tolerance test (IPGTT). Notably, the minimal efficacious dose for glucose was significantly lower than what was required for body weight loss, suggesting an independent mechanism.

In conclusion, PEG40-NMU represents a promising candidate for the treatment of obesity and diabetes. Future work will be directed at better understanding its mechanism of action, and ensuring that no adverse effects become apparent upon chronic treatment.

References

- [1] Peier, A. M.; Desai, K.; Hubert, J.; Du, X.; Yang, L.; Qian, Y.; Kosinski, J. R.; Metzger, J. M.; Poci, A.; Nawrocki, A. R.; Langdon, R. B.; Marsh, D. J., *Endocrinology* 2011, 152, 2644.
- [2] Alley, S. C.; Benjamin, D. R.; Jeffrey, S. C.; Okeley, N. M.; Meyer, D. L.; Sanderson, R. J.; Senter, P. D., *Bioconj. Chem.* 2008, 19, 759.

Design, synthesis and binding assays of sialic acid and sialyl-saccharide conjugates to lectins and influenza H1N1 virus

**Maria Sakarellos-Daitsiotis,¹ Stella Zevgiti,¹ Juliana Gonzalez Zabala,^{2,3}
Ayub Darji,^{2,3} Ursula Dietrich,⁴ Eugenia Panou-Pomonis¹**

¹*Section of Organic Chemistry and Biochemistry, Department of Chemistry, University of Ioannina, Greece;* ²*Centre de Recerca en Sanitat Animal (CRESA), UAB Campus de la Universitat Autònoma de Barcelona, 08193 Bellaterra, Barcelona, Spain;* ³*Institut de Recerca I Tecnologia Agroalimentaries (IRTA), Barcelona, Spain;* ⁴*Georg-Speyer-Haus, Institute for Biomedical Research, Paul-Ehrlich-Str. 42-44, 60596 Frankfurt, Germany*

E-mail: msakarel@uoi.gr

Introduction

Human and avian influenza A viruses differ in their recognition of host cell receptors: the former preferentially recognize receptors with saccharides terminating in sialic acid- α 2,6-galactose (SA α 2,6Gal), whereas the latter prefer those ending in SA α 2,3Gal. It is the receptor-binding site of haemagglutinin HA protein that recognizes SA α 2,3Gal or SA α 2,6Gal on the host cell surface and initiates the virus attachment [1]. A conversion from SA α 2,3Gal to SA α 2,6Gal recognition is thought to be one of the changes that must occur before avian influenza viruses can replicate efficiently in humans and acquire the potential to cause a pandemic.

Our objective is to design, synthesize and use models of the terminal segment of the receptor to validate their binding to different lectins as well as to appropriate influenza viruses. For this purpose, sialic acid (SA), 3'-sialyllactose (3'SL) and 6'-sialyllactose (6'SL) were linked independently, in two and four copies, to SOC₄, a synthetic carrier developed in our laboratory, which is formed by having four repeats of the tripeptide unit Lys-Aib-Gly in tandem. The obtained glyco-conjugates were tested in a biotin/avidin-mediated assay for their binding to lectins, whereas the attachment of H1N1 virus to the immobilized SOC₄-saccharides onto nitrocellulose membrane in an immune blot experiment was investigated.

Results and Discussion

Solid phase peptide synthesis was carried out manually following the Fmoc/tBu methodology on a Rink Amide AM resin (0.67 mmol/g). The protected fragment of the SOC₄ carrier, was synthesized by coupling each Fmoc-amino acid (3 mol equiv.) in the presence of HBTU/HOBt/DIEA (2.9/3/6 molar ratio) in a DMF/DCM mixture. Lysines were introduced either as Fmoc-Lys(Ac)-OH or as Fmoc-Lys(Mtt)-OH. The Mtt groups were removed by 1.8% TFA/DCM, before coupling the Boc-aminooxy acetic acid to the Lys-N^εH₂ groups when needed.

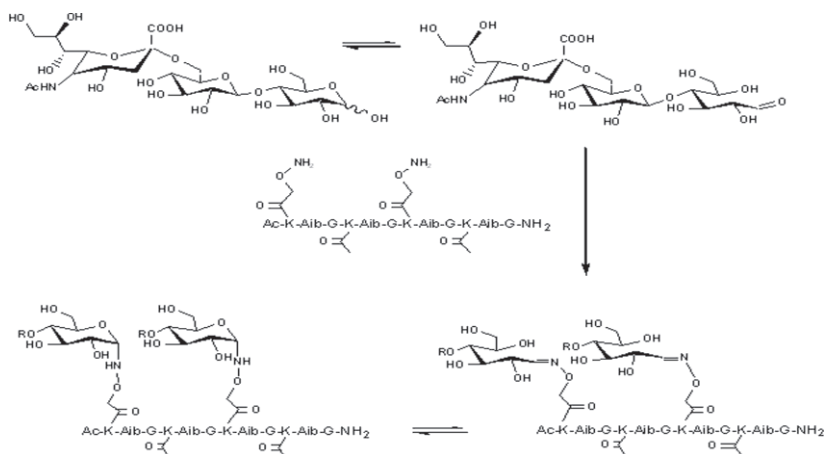


Figure 1: Coupling of α 2,6-sialyllactose to SOC₄.

SOC₄-glyco-conjugates (shown below) were synthesized in the liquid phase using the chemoselective ligation approach [2], which leads to the formation of an oxime bond between each aminoxy group of the SOC₄ carrier and the corresponding saccharide moiety: H-SOC₄(Aoa)₄-NH₂ **1**, Ac-SOC₄[(Ac)₂(Aoa)₂]-NH₂ **2**, H-SOC₄(SA-Aoa)₄-NH₂ **3**, Ac-SOC₄[(Ac)₂(SA-Aoa)₂]-NH₂ **4**, Ac-SOC₄[(Ac)₂(3'SL-Aoa)₂]-NH₂ **5** and Ac-SOC₄[(Ac)₂(6'SL-Aoa)₂]-NH₂ **6** (Aoa is the amino-oxycetyl group and SA sialic acid (Figure 1). All glyco-conjugates were purified by semi-preparative HPLC and characterized by analytical HPLC and by ESI-MS.

The binding of lectins, which are usually used to differentiate the functional properties of saccharides, to SOC₄-glyco-conjugates showed that only compound **6** bearing two copies of 6'-sialyllactose in specifically recognized in a dose dependent manner by SNA lectin. Preliminary immune blot assays showed that the SOC₄-glyco-conjugates **5** and **6** are both well recognized by H1N1 virus onto nitrocellulose membrane, while the acetylated SOC₄ carrier is not recognized. These findings indicate that the virus binds both α 2,6 and α 2,3Gal bonds contrary to lectins. The shift of specificity towards to compound **5** could be due to the form of virus propagation as initially it was obtained from allantoic cavity of SPF eggs [3].

It is concluded that the SOC₄-glyco-conjugates can be used as mimics of the receptor for easy screening of binding and inhibition assays of virus-receptor interactions.

References

- [1] Li, M.; Wang, B. *Biochem. Biophys. Res. Commun.* **2006**, *347*, 662-668.
- [2] Zevgiti, S.; Zabala, J.G.; Darji, A.; Dietrich, U.; Panou, E.; Sakarellos-Daitsiotis, M. *J. Pept. Sci.* **2012**, *18*, 52-58.
- [3] Ferraz, N.; Carnevia, D.; Nande, G.; Rossoti, M.; Miguez, M.; Last, J.; Gonzalez-Sapienza, G. *Anal. Bioanal. Chem.* **2007**, *389*, 2195.

The ghrelin receptor: New potent ligands for a functional selectivity

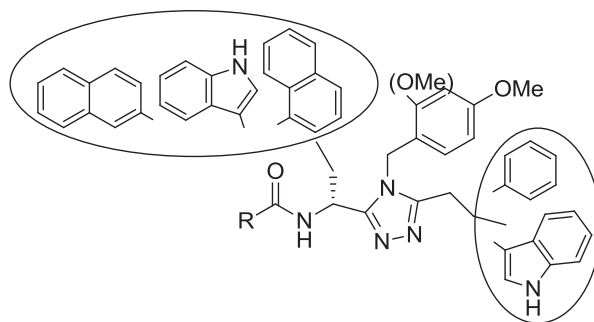
**Anne-Laure Blayo, Aline Moulin, Luc Demange, Céline M'Kadmi,
Didier Gagne, Sophie Mary, Jacky Marie, Marjorie Damian, Séverine
Denoyelle, Jean-Louis Banères, Jean Martinez, Jean-Alain Fehrentz**

*Institut des Biomolécules Max Mousseron, CNRS UMR 5247, Université Montpellier 1 & 2,
Faculté de Pharmacie, 15 avenue Charles Flahault 34093 Montpellier cedex 05, France*

E-mail: jean-alain.fehrentz@univ-montp1.fr

Introduction

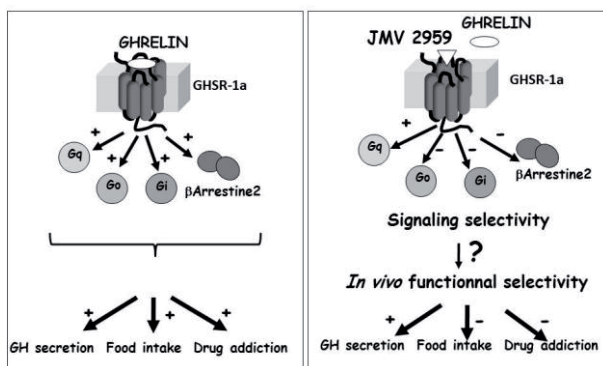
Ghrelin is a neuroendocrine peptide hormone that acts through its cognate GPCR (GHS-R1a) to control diverse physiological processes such as growth hormone secretion, food intake, or reward-seeking behaviors. We recently described potent ligands of the ghrelin receptor which structures are based on a 3,4,5-trisubstituted 1,2,4-triazole moiety [1-3]. Changing one single atom in these structures can lead to toggle an agonist compound into an antagonist derivative. A structure-activity relationship study was performed on about 500 compounds that led us to a consensus general structure to obtain affine ligands where the R group drives the affinity toward the GHS-R1a and controls the agonist / antagonist character.



Results and Discussion

Some of our compounds are able in vivo to totally inhibit food intake elicited by an agonist without altering growth hormone secretion induced by the same agonist. In order to try to understand the functional selectivity of these compounds, we decided to deeply study their effect on the different signalling pathways triggered by the ghrelin receptor. Two models were used for this study; with the first one, the purified ghrelin receptor assembled into lipid discs and labeled with a fluorescent probe [4], we analyzed how ligands and signaling proteins affect the receptor conformational repertoire. Our data suggest that ligand efficacy and functional selectivity are directly related to the ability of the compounds to stabilize different receptor conformations. Of importance, we also bring evidence indicating that distinct effector proteins (G proteins, arrestins, μ -AP2) may affect the conformational landscape of the ghrelin receptor in different manners [5]. These results are to be correlated

with those obtained with the second model, HEK393T cells expressing the ghrelin receptor. Using this model, we delineated how our compounds activate and/or recruit the effector proteins associated to the different signaling pathways. By doing so, we showed that full agonists (ghrelin, MK-0677, JMV 1843) are able to trigger both β -arrestin recruitment and activation of Gq, Gi1, Gi2, Gi3, GoA and GoB. Unexpectedly, by measuring inositol phosphate production we demonstrate that the high level of constitutive activity of GHS-R1a may conceal the partial agonist properties of some ligands that were previously identified as antagonists based on calcium flux assay. Moreover, unlike full agonists, these partial agonists at Gq are neither able to activate Gi/Go nor to trigger recruitment of β -arrestin 2, so that these compounds can be considered as Gq-biased ligands. Even more interestingly, we identified new biased GHS-R1a ligands that selectively activate Gq but antagonize ghrelin-mediated Gi/Go activation (for example JMV 2959 compound). Overall, our work allowed us to both identify a new series of biased ghrelin receptor ligands and provide new insights into the molecular mechanisms underlying ligand-directed selectivity of the ghrelin receptor. All this may have implications for designing new drugs with higher selectivity and, therefore, limited side effects.



Acknowledgments

This work was supported by Universities Montpellier 1 & 2, CNRS and Agence pour la Recherche Contract PCV08_323163.

References

- [1] Demange, L.; Boeglin, D.; Moulin, A.; Mousseaux, D.; Ryan, J.; Bergé, G.; Gagne, D.; Heitz, A.; Perrissoud, D.; Locatelli, V.; Torsello, A.; Galleyrand, J.-C.; Fehrentz, J.-A.; Martinez, J. *J. Med. Chem.* **2007**, *50*, 1939.
- [2] Moulin, A.; Demange, L.; Bergé, G.; Gagne, D.; Ryan, J.; Mousseaux, D.; Heitz, A.; Perrissoud, D.; Locatelli, V.; Torsello, A.; Galleyrand, J.-C.; Fehrentz, J.-A.; Martinez, J. *J. Med. Chem.* **2007**, *50*, 5790.
- [3] Moulin, A.; Demange, L.; Ryan, J.; Mousseaux, D.; Sanchez, P.; Berge, G.; Gagne, D.; Perrissoud, D.; Locatelli, V.; Torsello, A.; Galleyrand, J.-C.; Fehrentz, J.-A.; Martinez, J. *J. Med. Chem.* **2008**, *51*, 689.
- [4] Damian, M.; Marie, J.; Leyris, J.-P.; Fehrentz, J.-A.; Verdié, P.; Martinez, J.; Banères, J.-L.; Mary, S. *J. Biol. Chem.* **2012**, *287*: 3630.
- [5] Mary, M.; Damian, M.; Louet, M.; Floquet, N.; Fehrentz, J.-A.; Marie, J.; Martinez, J.; Banères, J.-L. *PNAS* **2012**, *109*, 8304.

Nanoparticles-based peptide subunit vaccines against group A Streptococcus

M. Skwarczynski,^a A. A. H. Ahmad Fuaad,^a M. Zaman,^a Z. Jia,^b J. Kowapradit,^a L. Rustanti,^a Z. M. Ziora,^a M. J. Monteiro,^b M. R. Batzloff,^c M. F. Good,^c I. Toth^{*a}

^aThe University of Queensland, School of Chemistry and Molecular Biosciences, Brisbane QLD 4072, Australia; ^bThe University of Queensland, Australian Institute for Bioengineering and Nanotechnology (AIBN), Brisbane QLD 4072, Australia; ^cInstitute for Glycomics, Griffith University, Southport QLD 4215, Australia

E-mail:m.skwarczynski@uq.edu.au

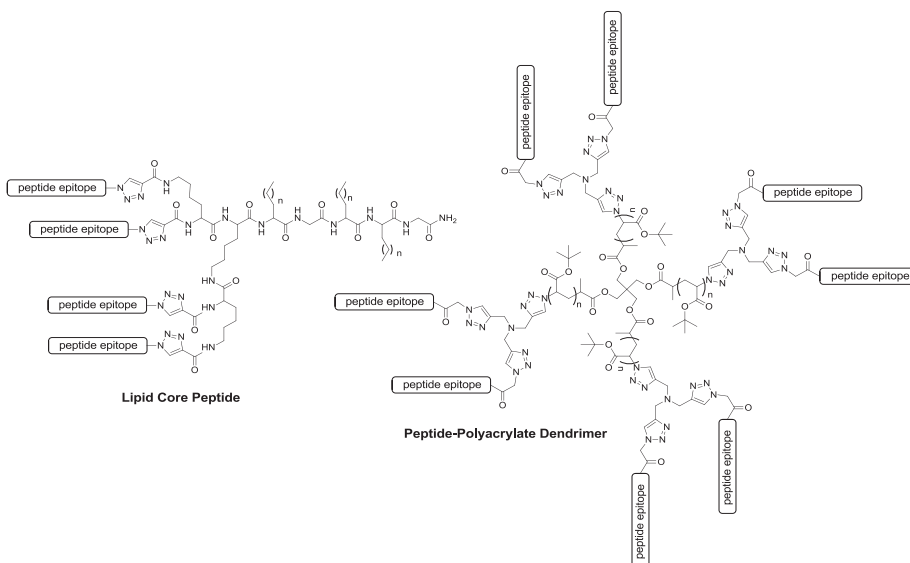
Introduction

According to the recent estimations as much as 70 million individuals worldwide currently have Rheumatic Heart Disease (RHD) which results in 1.4 million deaths per year from RHD and its complications [1]. RHD often develops after illness with rheumatic fever (RF). RF and RHD are autoimmune diseases caused by a group A streptococcal (GAS) infection. Therefore the development of save and affective vaccine against GAS is considered as one of the most promising approaches toward eradication of RHD.

Protein-based vaccines have significant drawbacks including the cost of recombinant protein production, stability and purity problems. A foreign protein may cause autoimmune responses, which is well illustrated in the case of the challenges to develop a vaccine against group A streptococcal (GAS) infection. The use of peptide epitopes for development of subunit vaccines allows greatly reduced or elimination of the risk of autoimmune responses. Since it has been revealed that not only the bio/chemical composition of immunogens but also their morphological properties and particle size play a role in such vaccine efficacy [2], we have developed nanoparticulate peptide-based subunit vaccine candidates against GAS.

Results and Discussion

We have developed promising vaccine delivery systems, lipid core peptide (LCP) system, which is able to induce strong immune response to the incorporated peptide epitopes without help of additional adjuvant [3]. Recently, we designed new delivery system-based on the polyacrylate polymer and novel LCP nanoparticles [4-7]. We have designed several constructs using different delivery systems to incorporate and display J14 GAS epitope in optimal manner for immune system recognition. The use of copper wires in azide alkyne Huisgen cycloaddition (click) reaction allowed us to obtain desired product in highly pure form without tedious purification. Constructs were examined toward particle formation under aqueous conditions and conformation of peptide epitopes was determined. We demonstrated that our delivery systems were able to induce native helical conformation of J14 peptide required for proper epitope recognition and form nanoparticle in aqueous environment. The constructs alone elicited high-levels of antibody titers comparable to that



of positive control (J14 + Complete Freund's Adjuvant) after subcutaneous administration in mice. We have shown also that immune responses induced against J14 were dependant on particle size and polymeric nanoparticle with diameter of 20 nm induced production of the highest antibody titers among examined constructs.

Interestingly, even intranasal administration of polymer nanoparticulate construct without additional adjuvant induced J14-specific IgG, [8] which was also capable of in vitro opsonization of GAS, highlighting the potential of self-adjuvanting polyacrylate nanoparticle-based construct as a peptide vaccine delivery platform that may afford promising opportunities for treating GAS infection and preventing RHD.

Acknowledgments

We gratefully acknowledge support from The National Health and Medical Research Council (program grant 496600).

References

- [1] Paar, J. A.; Berrios, N. M.; Rose, J. D.; Caceres, M.; Pena, R.; Perez, W.; Chen-Mok, M.; Jolles, E.; Dale, J. B. *Am. J. Cardiol.* **2010**, *105*, 1809.
- [2] Skwarczynski, M.; Toth, I. *Curr. Drug Delivery* **2011**, *8*, 282.
- [3] Zhong, W.; Skwarczynski, M.; Toth, I. *Aust. J. Chem.* **2009**, *62*, 956.
- [4] Skwarczynski, M.; Parhiz, B. H.; Soltani, F.; Srinivasan, S.; Kamaruzaman, K. A.; Lin, I.-C.; Toth, I. *Aust. J. Chem.* **2012**, *65*, 35.
- [5] Skwarczynski, M.; Kamaruzaman, K. A.; Srinivasan, S.; Zaman, M.; Lin, I. C.; Batzloff, M. R.; Good, M. F.; Toth, I. *Curr. Drug Delivery* **2012**, accepted (2012.06.12).
- [6] Skwarczynski, M.; Ahmad Fuaad, A. A. H.; Rustanti, L.; Ziora, Z. M.; Aqil, M.; Batzloff, M. R.; Good, M. F.; Toth, I. *Drug Deliv. Lett.* **2011**, *1*, 2.
- [7] Skwarczynski, M.; Zaman, M.; Urbani, C. N.; Lin, I. C.; Jia, Z. F.; Batzloff, M. R.; Good, M. F.; Monteiro, M. F.; Toth, I. *Angewandte Chemie-International Edition* **2010**, *49*, 5742.
- [8] Zaman, M.; Skwarczynski, M.; Malcolm, J. M.; Urbani, C. N.; Jia, Z. F.; Batzloff, M. R.; Good, M. F.; Monteiro, M. J.; Toth, I. *Nanomed.-Nanotechnol. Biol. Med.* **2011**, *7*, 168.

Bioportides

Sarah Jones, Monika Lukanowska, John Howl

*Molecular Pharmacology Group, Research Institute in Healthcare Science, University of
Wolverhampton, Wulfruna Street, Wolverhampton, WV1 1LY, UK*

E-mail: S.Jones4@wlv.ac.uk

Introduction

The study and exploitation of Cell Penetrating Peptides (CPPs) now extends into a third exciting decade. Moreover, it is now apparent these mostly cationic sequences have enormous potential in biomedicine and drug discovery. Thus, a range of inert CPPs have proven utility for the efficient intracellular delivery of highly active cargoes designed to influence intracellular targets. Pharmacokinetic modulators, including common sequences such as Tat, Penetratin and Transportan 10, markedly enhance the intracellular delivery of small drugs, peptides and proteins. Cell-selective targeting of CPPs can also be facilitated by the chimeric combination of a CPP and an appropriate homing peptide (recently reviewed in [1]).

The intracellular internalisation of CPP vectors may be accompanied by undesirable actions upon cellular physiology (reviewed in [2]). Not surprisingly, many of these reported side-effects may be a consequence of detrimental actions upon plasma membrane integrity that consequentially compromise cellular viability. CPP-induced Ca^{2+} -influx into mast cells may also induce the receptor-independent secretion of inflammatory mediators from mast cells *in vivo*. Moreover, the intrinsic biological activities of some CPPs prompted our current endeavours to identify cell penetrant sequences that possess physiologically useful bioactive profiles. More recently we have introduced the term bioportide [3] to distinguish this class of bioactive CPP from the more commonly employed inert vector peptides.

Results and Discussion

The many bioportides now reported in the scientific literature conform to two general types of molecular topography. Synchologically-organised bioportides comprise an inert CPP vector conjugated to an impermeable bioactive peptide. Strategically, the CPP provides an *address* function whilst the bioactive cargo, often a protein mimetic sequence, is the *message*. It is not always necessary to covalently combine CPP and cargo as many peptide vectors can deliver proteins and oligonucleotides as non-covalent complexes and nanoparticles. Conversely, rhegnylogic bioportides are monomeric peptides presenting pharmacophores for internalization and bioactivity that are discontinuously distributed within the primary sequence. Indeed, it is most likely that the amine and guanadinium functions of Lys and Arg respectively will contribute to both cellular penetration and the biological functions of rhegnylogically-organised bioportides [3].

The capability to predict candidate CPPs [4] within the primary sequences of proteins has supported the identification of a sub-set of bioportides within cytochrome *c* [5] and, more recently, leucine rich repeat kinase 2 (LRRK2). We have also characterised in greater detail [3] the potent anti-angiogenic properties of nosangiotide, a rhegnylogic bioportide derived from endothelial nitric oxide synthase (eNOS⁴⁹²⁻⁵⁰⁷). Significantly, nosangiotide inhibits

features of both *in vitro* and *in vivo* angiogenesis in the nanomolar concentration range [3] and may be acting as a specific modulator of RhoGEF 16.

Our more recent endeavours have focussed upon the identification of novel bioportides within LRRK2. This relatively massive protein is of significant current interest since some known mutations are believed to be the most common genetic cause of familial Parkinson's disease. With >5000 probable CPPs spanning the entire 2527 amino acid multi-domain architecture of LRRK2, we have selected 33 candidate bioportides that, collectively, map to all predicted domains and include known mutated residues and phosphorylation sites. Initial observations have confirmed that a majority of these are CPPs are rapidly internalised with varying degrees of efficacy. We are currently identifying LRRK2-derived bioportides that specifically localise with the intracellular kinase and others that modulate its phosphorylation status and stability. Very recently, LRRK2 has been reported to sequester the transcription factor nuclear factor of activated T-cells (NFAT) within the cytoplasm and LRRK2 deficiency enhances both translocation of NFAT to the nucleus and a susceptibility to experimental colitis [6]. We therefore hope to establish LRRK2-derived bioportides that modulate NFAT translocation. Thus far some of our candidate bioportides include; the LRRK2 localising peptide LRRK2¹⁵⁴⁶⁻¹⁵⁶⁴, which reduces both serine phosphorylation at LRRK2⁹³⁵ and NFAT translocation and the highly cell-penetrant peptide LRRK2¹³²²⁻¹³⁴⁰, which localises with the LRRK2 protein and prevents NFAT translocation.

We now intend to further characterise *stapled* analogues of LRRK2-derived helical bioportides that are likely to display improved pharmacokinetic and pharmacodynamic parameters [7].

We conclude that bioportides represent a novel class of bioactive agent with tremendous potential as both research tools and for clinical development as therapeutic agents.

Acknowledgments

We are pleased to acknowledge that the Michael J Fox Foundation, New York, provided financial support for our studies with LRRK2-derived bioportides.

References

- [1] Svensen, N.; Walton, J.G.A.; Bradley, M. *Trends Pharmacol. Sci.* **2012**, *33*, 186.
- [2] Verdurmen, W.P.R.; Brock, R. *Trends Pharmacol. Sci.* **2011**, *32*, 116.
- [3] Howl, J.; Matou-Nasri, S.; West, D.C.; Farquhar, M.; Slaninová, J.; Östenson, C-G.; Zorko, M.; Östlund, P.; Kumar, S.; Langel, Ü.; McKeating, J.; Jones, S. *Cell. Mol. Life Sci.* **2012**, *69*, 2951.
- [4] Hällbrink, M.; Kilk, K.; Elmquist, A.; Lundberg, P.; Jiang, Y.; Pooga, M.; Soomets, U.; Langel, Ü. *Int. J. Peptide Res. Ther.* **2005**, *11*, 249.
- [5] Jones, S.; Holm, T.; Mäger, I.; Langel, Ü.; Howl, J. *Chem. & Biol.* **2010**, *17*, 735.
- [6] Liu, Z.; Lee, J.; Krummey, S.; Lu, W.; Cai, H.; Lenardo, M.J. **2011**, *12*, 1063.
- [7] Guo, Z.; Mohanty, U.; Noehre, J.; Sawyer, T.K.; Sherman, W.; Krilov, G. *Chem. Biol. Drug Des.* **2010**, *75*, 348.

Transduction of peptides, proteins and nucleotides into live cells by cell penetrating peptides

Andrea-Anneliese Keller¹, Reinhard Breitling³, Peter Hemmerich²,
Franziska Mussbach¹, Buerk Schaefer³, Stefan Lorkowski¹,
Siegmond Reissmann¹

¹Friedrich-Schiller-University Jena, Biological and Pharmaceutical Faculty; ²Leibniz
Institute of Age Research; ³Jena Bioscience GmbH
E-mail:siegmond.reissmann@uni-jena.de

Introduction

Cell membranes are permeable only for small hydrophobic compounds. While *in-vitro* transfection studies can be performed with viral factors, electroporation, magneto-fection or application of lipid detergents the internalization of cargos for medically relevant purposes requires more gentle methods such as use of nano-particles or cell-penetrating peptides (CPPs). Especially the formation and internalization of non-covalent complexes between CPPs and cargos meets the requirements for application in diagnosis and therapy.

Results and Discussion

We were interested in consolidating knowledge about the very easy and convenient to handle types of CPPs, which are able to form non-covalent complexes with different cargos. We studied relationships between amphiphilicity and proteolytic stability of these CPPs, properties of the cargos and of the cell types on the one hand and transport efficiency into live cells as well as cytotoxicity on the other site. As cargos we used enzymes, fluorescently labeled antibodies, bovine serum albumin and nucleoside triphosphates. Cells differ in their membrane properties regarding lipid, protein and glycan composition, surface-bound proteases as well as in signal pathways and metabolic activities. Cargos can also strongly differ in molecular size, surface charge and other chemical properties. Only certain structural types of CPPs are able to form sufficiently stable non-covalent complexes with cargos. Thus, for each cell type and cargo the right CPP has to be estimated with respect to uptake efficiency and cytotoxicity. Cocktails of CPPs provide a more universal approach for internalization of cargos through compatibility with numerous cell types and various membrane structures, triggering different mechanisms of transduction and allowing complexation with structural different cargos.

For our studies we used *cells* from different sources, having different properties: HeLa-, COS-7 and NIH 3T3 as adherent cells and Jurkat, NB-4 and Kasumi-1 as suspension cells [2,3]. Additionally we investigated the behavior of the protozoa *Leishmania tarentolae* [4]. As *CPPs* we used the following peptides and proteins: HIV-TAT (YGRKKRRQRR), histon H2A from calf, penetratin (RGIKWFGNRRM-KWKK), pentapeptide CPPP-2 (KLPVM), MPG α (AcGALFLAFLAAALSLMGLWSQPKKKRKV-NH-CH₂-CH₂-SH), MPG β (Ac-GALFLGFLGAAGSTMGAWSQPKKKRKV-NH-CH₂-CH₂-SH) and CAD-2 (GLWRALWRLRLSLWRLWKA-NH-CH₂-CH₂-SH). The latter three peptides were particularly developed for formation of non-covalent complexes [1]. All cells have surface-

bound *proteolytic activities* and hydrolyze the CPPs. Thus, intact HeLa-, NIH 3T3-cells and Leishmania degrade penetratin completely within 60 minutes [4]. The used CPPs are differently hydrophobic and show different *proteolytic stabilities*. CAD-2 is the most hydrophobic peptide and is more resistant to proteolytic degradation than other used CPPs [4]. We also found a *cargo-dependent uptake*. Thus, the CPPs trigger the uptake of the high molecular weight enzyme β -galactosidase into HeLa-cells in the following rank order: Proteoducin > MPG α \geq MPG β > CAD-2 >> CPPP-2. For the uptake of the fluorescently labeled nucleotide ATTO488-dUTP into HeLa-cells we found another order: CAD-2 > MPG α \geq MPG β > penetratin >> CPPP-2 [2,3]. Due to different membrane properties and the transport mechanisms the *uptake efficiency* is cell-dependent [4]. CPPs are in many cases able to transduce even very difficult to transfect cells such as Kasumi-1 cells [3]. *Leishmania tarentolae* can be transduced with β -galactosidase and with ATTO488-BSA [4]. CPPs can have special localization sequences. Thus, MPG α , H2A and MPG β are able to transport the fluorescent protein ATTO488-BSA into the nucleus and the kinetoplast of Leishmania. *Quantitative uptake efficiencies* were estimated by fluorescence measurements and with calibrated SDS-PAGE. Intracellular amounts depend on the cell volume and can reach the amole range. Intracellular concentrations come to the low micromolar range [3,4]. *Cytotoxic effects* depends on the cell-type and CPP used [2,3,4].

Quantitative Uptake Efficiencies

Amount of added complex per 1.6 ml serum-free medium	Internalized amount (0.3×10^6 HeLa-cells per well)	
	amol per cell	Intracellular concentration in μ M
ATTO488-deoxyuridine triphosphate into HeLa-cells		
1 μ g + JBS-Nucleoducin, charge by charge 1:4	1.1	0.1
ATTO488-bovine serum albumin into HeLa-cells		
10 μ g + JBS-Proteoducin, molar ratio 1:10	20	
25 μ g + JBS-Proteoducin, molar ratio 1:10	50	4.3
FITC-antibody (secondary) into HeLa-cells		
5 μ g + JBS-Proteoducin, molar ratio 1:10	0.4	
25 μ g + JBS-Proteoducin, molar ratio 1:10	4.3	0.6
ATTO488-bovine serum albumin into <i>Leishmania tarentolae</i>		
5 μ g + MPG α , molar ratio 1:10	1.7×10^{-2}	0.1
10 μ g + MPG α , molar ratio 1:10	3.3×10^{-2}	0.2

CPPs and cocktails of them allow cellular uptake of kinases, phosphatases, deacetylases, proteases, small GTPases, activity modulators and as well as substrates and inhibitors of enzymes as tools for signal pathway studies and for therapeutically use. Internalized antibodies act more specifically than inhibitors of kinases or mono-valent ligands for protein binding domains and can compete with RNA silencing techniques.

References

- [1] Deshayes, S., Morris, M., Heitz, F., Divita, G. *Adv. Drug Deliv. Rev.* **2008**, 60, 537.
- [2] Mussbach, F.; Pietrucha, R.; Schaefer, B.; Reissmann, S. *Meth. Mol. Biol.* **2011**, 683, 375.
- [3] Mussbach, F.; Franke, M.; Zoch, A.; Schaefer, B.; Reissmann, S. *J. Cell. Biol.* **2011**, 112, 3824.
- [4] Keller, A.-A. et al., *Pharmaceuticals*, **2012**, Issue: "Cell-penetrating Peptides", submitted.

SS14-Based radiopeptides: Synthesis & biology

Aikaterini Tatsi^{a,b}, Theodosia Maina^a, Beatrice Waser^c, Renzo Cescato^c,
 Eric P. Krenning^d, Marion de Jong^d, Jean-Claude Reubi^c,
 Paul Cordopatis^b, Berthold A. Nock^a

^aMolecularRadiopharmacy, IRRP, NCSR “Demokritos”, Athens, Greece; ^bDepartment of Pharmacy, University of Patras, Greece; ^cInstitute of Pathology, University of Bern, Bern, Switzerland; ^dDepartment of Nuclear Medicine, Erasmus MC, Rotterdam, The Netherlands

E-mail: ktatsi19@gmail.com

Introduction

Multi sst-subtype expression has been manifested in various human cancers, such as neuroendocrine tumors [1-3]. Thus, radioligands with an expanded sst₁₋₅ affinity profile (pansomatostatins) will bind to more binding sites on such tumors increasing sensitivity and broadening the clinical indications of currently available sst₂-preferring analogs. For this purpose, we have synthesized twelve cyclic tetradecapeptide analogs (ATXS) of somatostatin-14 (SS14) undergone the structural modifications shown in Table 1. The effects of these interventions on several biological parameters of ATXS and the respective ¹¹¹In-radiotracers, [¹¹¹In]ATXS, are reported.

Results and Discussion

The twelve ATXS were synthesized on the solid support and MS data confirmed their formation (Table 1). The affinity profile of ATXS to the five human sst₁₋₅ studied by receptor autoradiography competition assays against the universal radioligand [¹²⁵I]LTT-SS-28 is summarized in Table 2 [4,5]. Reduction of the ring size was found to cause a gradual decrease of sst₁₋₅ affinity, with the 6-member ring analogs (X: 3, 5, 7) having totally lost affinity to all receptor subtypes.

Table 1: Formulae, # of ring AAs and MS data for ATXS, X: 1-12

Code - Sequence	# ring AA	m/z; found/Calc
AT1S: [DOTA ⁰]SS14	12	1013.7/1013.1
AT2S: [DOTA ⁰ ,DTrp ⁸]SS14	12	1013.4/1013.1
AT3S: [DOTA ⁰ ,Nle ³ ,Cys ⁶ ,Tyr ⁷ ,DTrp ⁸ ,Cys ¹¹ ,Gly ¹⁴]SS14	6	958.9/959.0
AT4S: [DOTA ⁰ ,Nle ³ ,Cys ⁵ ,DTrp ⁸ ,Cys ¹² ,Gly ¹⁴]SS14	8	990.8/990.7
AT5S: [DOTA ⁰ ,Cys ⁶ ,DTrp ⁸ ,Cys ¹²]SS14	6, 12	967.3/968.1
AT6S: [DOTA ⁰ ,Cys ⁵ ,DTrp ⁸ ,Cys ¹¹]SS14	8, 12	1007.4/1007.6
AT7S: [DOTA ⁰ ,Nle ³ ,Cys ⁶ ,DTrp ⁸ ,Cys ¹¹ ,Gly ¹⁴]SS14	6	950.7/951.0
AT8S: [DOTA ⁰ ,Arg ⁴ ,DTrp ⁸ ,DCys ¹⁴]SS14	12	1026.9/1027.1
AT9S: [DOTA ⁰ ,Nle ³ ,DCys ⁵ ,DTrp ⁸ ,Cys ¹² ,Gly ¹⁴]SS14	8	990.4/990.6
AT10S: [DOTA ⁰ ,PEG ₂ ^{1,2,3} ,Gly ⁴ ,Cys ⁵ ,DTrp ⁸ ,Ser ¹² ,Cys ¹³ ,desCys ¹⁴]SS14	9	878.2/878.4
AT11S: [DOTA ⁰ ,PEG ₂ ^{1,2,3} ,Arg ⁴ ,Cys ⁵ ,DTrp ⁸ ,Ser ¹² ,Cys ¹³ ,desCys ¹⁴]SS14	9	927.8/928.0
AT12S: [DOTA ⁰ ,PEG ₁ ^{1,2} ,Arg ⁴ ,DTrp ⁸ ,Cys ¹² ,desSer ¹³ ,desCys ¹⁴]SS14	10	919.3/919.5

Labeling of ATXS with ¹¹¹In was straightforward following a published protocol [4].

Table 2: ATXS (X: 1-12) $hsst_{1-5}$ affinity profile (IC_{50} in nM, mean \pm SEM, n= 3)

Code, ring size	$hsst_1$	$hsst_2$	$hsst_3$	$hsst_4$	$hsst_5$
SS14 (12)	2.1 \pm 0.4	0.6 \pm 0.1	3.9 \pm 1.3	1.9 \pm 0.6	11.0 \pm 3.5
AT1S (12)	5.1 \pm 1.4	2.8 \pm 0.3	1.8 \pm 0.6	2.5 \pm 0.6	17 \pm 3
AT2S (12)	14 \pm 2.4	1.5 \pm 0.3	2.4 \pm 0.5	3.7 \pm 0.7	12 \pm 2.0
AT3S (6)	> 1000	946 \pm 148	> 1000	> 1000	> 1000
AT4S (8)	33 \pm 3.5	11 \pm 0.9	16 \pm 4.4	4.0 \pm 0.8	50 \pm 21
AT5S (6/12)	> 1000	616 \pm 148	> 1000	> 1000	> 1000
AT6S (8/12)	12 \pm 3.3	6.3 \pm 0.6	9.7 \pm 3.6	5.4 \pm 0.8	26 \pm 7.0
AT7S (6)	> 1000	> 1000	> 1000	> 1000	> 1000
AT8S (12)	38 \pm 18	1.6 \pm 0.5	16 \pm 6.2	2.8 \pm 0.3	25 \pm 11
AT9S (8)	18 \pm 3.8	50 \pm 19	98 \pm 40	5.4 \pm 1.4	37 \pm 13
AT10S (9)	795 \pm 358	1.0 \pm 0.2	18 \pm 7.9	1.2 \pm 0.3	58 \pm 19
AT11S (9)	171 \pm 75	0.76 \pm 0.1	24 \pm 9.8	0.9 \pm 0.5	16 \pm 4.0
AT12S (10)	274 \pm 136	59 \pm 18	408 \pm 193	2.1 \pm 0.7	286 \pm 200

By injection of [111 In]ATXS in Swiss albino mice and analyzing the blood collected 5 min later by RP-HPLC, the *in vivo* stability of [111 In]ATXS was found to progressively increase as the ring sized decreased [4,6]. The most striking effect on metabolic stability was observed in the 6-member ring analogs (X: 3, 5, 7) [6] as well as in [111 In]AT6S where a second disulfide bridge has been introduced between Cys⁵ and Cys¹¹ [7].

On the other hand, sst_2 -mediated internalization of [111 In]ATXS in AR4-2J cells was affected by sst_2 -affinity and ring size being more pronounced for the 12- (X: 1, 2, 8) and 9-member analogs (X: 10, 11) (Fig. 1; A). Uptake in sst_2^+ AR4-2J tumors in SCID mice was a combined result of sst_2^+ -affinity, internalization capacity and metabolic stability (Fig. 2).

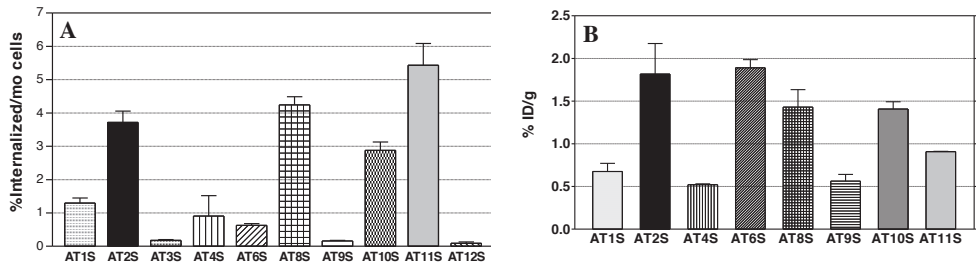


Figure 1: (A) Comparative internalization of [111 In]ATXS (X: 1-4, 6-12) in sst_2^+ AR4-2J cells in 1 h at 37°C and (B) Comparative tumor uptake of [111 In]ATXS in SCID mice bearing AR4-2J tumors at 4 h pi (%ID/g, mean \pm sd, n= 4); data for non- sst_2^+ -affine [111 In]ATXS (X: 3, 5, 7, 12) is not shown.

References

- [1] Patel, Y. C.; Greenwood, M. T.; Panetta, R.; et al. *Life Sci.* **1995**, *57*, 1249.
- [2] Patel, Y. C. *Front. Neuroendocrinol.* **1999**, *20*, 157.
- [3] Reubi, J. C.; Waser, B.; Schaer, J. C.; Laissue, J. A. *Eur. J. Nucl. Med.* **2001**, *28*, 836.
- [4] Tatsi, A.; Maina, T.; Cescato, R.; et al. *Eur. J. Nucl. Med. Mol. Imaging Res.* **2012**, *2*, 25.
- [5] Cescato, R.; Schulz, S.; Waser, B.; et al. *J. Nucl. Med.* **2006**, *47*, 502.
- [6] Guo, H.; Yang, J.; Gallazzi, F.; Miao, Y. *J. Nucl. Med.* **2010**, *51*(3), 418.
- [7] Tatsi, A.; Cescato, R.; Maina, T.; et al. *J. Pept. Sci.* **2012**, *18*(S1), S151, P258.

Efficient identification of peptide ligands for proteins via high-throughput screening of combinatorial peptide libraries

Su Seong Lee, Jaehong Lim, Yi Li Ang, Joo-Eun Jee, Jessica Oon

Institute of Bioengineering and Nanotechnology, 31 Biopolis Way, The Nanos,
Singapore 138669

E-mail: sslee@ibn.a-star.edu.sg

Introduction

Combinatorial one-bead-one-compound (OBOC) peptide libraries are widely used for affinity screening against various biomolecules such as proteins. A high-throughput screening platform was developed by integrating automatic peptide synthesizer, bead sorter and MALDI-MS-based peptide sequencing.[1] A semi-automatic sequencing algorithm based on MS/MS spectra was developed by implementing existing knowledge of amino acid chemistry and a new strategy for differentiating isobaric pairs of amino acids. It was clearly validated in comparison with Edman degradation sequencing.[2] However, this novel tool still requires improvement in terms of time and labor. In particular, most of negatively charged peptides produced sodium adducts dominantly in their MS spectra, which are extremely challenging to identify the correct parent mass. Herein, we introduce an OBOC peptide library of a novel structure that is designed for rapid and reliable peptide sequencing. This novel library was successfully applied to identifying a group of hexamer ligands of good binding affinity for C-reactive protein (CRP).

Results and Discussion

There are four major problems involved in *de novo* peptide sequencing via MALDI-TOF/TOF experiments, which are i) weak ionization of certain types of peptides, ii) adverse formation of sodium adducts of certain types of peptides that often contain negatively charged residues, iii) overlapping of parent masses with matrix clusters causing difficult identification of correct parent masses in MS spectra, and iv) identification of fragmented mass peaks for peptide sequencing in MS/MS spectra. A novel OBOC library was designed to solve these problems as shown in Figure 1.

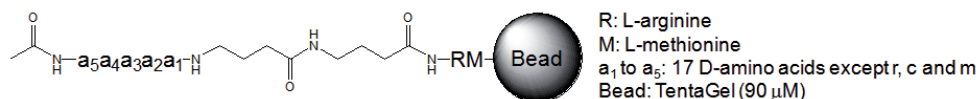


Figure 1. Structure of the novel peptide library

An arginine that appends positively charged guanidine group is adopted to enhance ionization tendency of most peptides for good signal to noise ratio. In addition, this particular functionality turned out significantly suppressing the formation of sodium adducts. Typically, arginine tends to lose ammonia (17 amu) from all fragments in a MS/MS spectrum exhibiting a characteristic series of doublet mass peaks, which facilitate visual identification for sequencing. In this novel library, arginine needs to be opted out from the diversity region to maintain only one arginine per peptide for easier peptide sequencing. Two repetitive units of γ -aminobutyric acid (GABA) moiety were inserted as a

spacer between the ionization promoter (arginine) and the diversity region (peptide i) to increase the overall masses of the cleaved peptide and its truncates to solve the “overlap problem”, and ii) to minimize the participation of arginine in screening.

With these beneficial features integrated in the structure, this novel library was proven to enhance sequencing protocol and accuracy by easy identification of y ion peaks in MS/MS spectra of peptides. Figure 2 demonstrates one example of peptide sequencing. In addition to the abovementioned advantages in sequencing, the new peptide library was also found to minimize non-specific bindings between the ligand and the target object by excluding arginine from the peptide diversity region. Arginine in many cases accounts for major source of electrostatic interactions with negatively charged fluorescence dye in screening. These beneficial effects improved the overall quality of screening through suppressing the generation of false hit sequences originated from non-specific bindings.

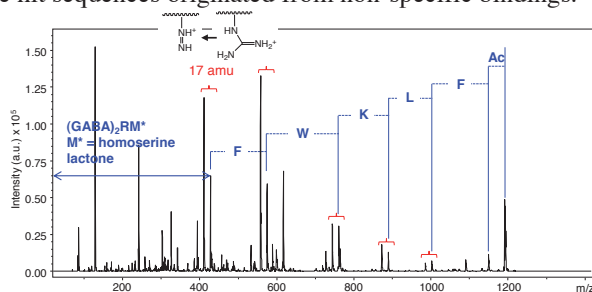


Figure 2. One example of sequencing of a peptide (fwklf).

A series of hexamer peptide ligands for CRP were successfully identified using the novel library, associated with the efficient sequencing protocol. Figure 3 shows surface plasmon resonance (SPR) sensorgrams of the two representative hexamer peptide ligands (lyfrw and lrfrwf) that exhibit a few micromolar K_D values as the binding affinity.

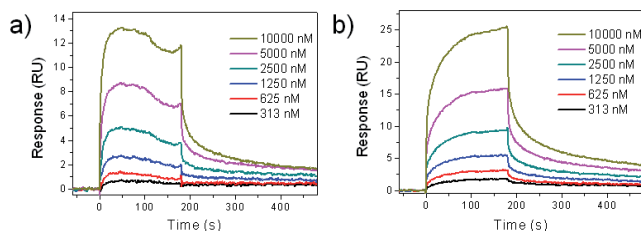


Figure 3. SPR sensorgrams of a) lyfrw and b) lrfrwf for CRP (protein immobilization level = 2,000 RU).

Acknowledgments

This work was supported by the Institute of Bioengineering and Nanotechnology (Biomedical Research Council, Agency for Science, Technology and Research, Singapore).

References

- [1] Cha, J.; Lim, J.; Zheng, Y.; Tan, S.; Ang, Y. L.; Oon, J.; Ang, M. W.; Ling, J.; Bode, M.; Lee, S. *S. J. Lab. Auto.* **2012**, 17, 186.
- [2] Lee, S. S.; Lim, J.; Tan, S.; Cha, J.; Yeo, S. Y.; Agnew, H. D.; Heath, J. R. *Anal. Chem.* **2010**, 82, 672.

Chemical synthesis and *in vitro* and *in vivo* evaluation of a bombesin peptide analog linked to a cytotoxic drug for the targeting of bombesin receptor-positive tumors

Subhani M. Okarvi

Cyclotron and Radiopharmaceuticals Department, King Faisal Specialist Hospital
and Research Centre, PO Box 3354, Riyadh 11211, Saudi Arabia

E-mail: sokarvi@kfshrc.edu.sa

Introduction

Among the most clinically-relevant peptide receptor systems, bombesin (BN) peptide receptors are of great interest, because of the overexpression of their receptors on various important human cancers including prostate and breast cancer. The high expression in cancer cells and low expression in normal tissues makes BN peptides attractive for tumor targeting [1, 2]. These features also provide the possibility to link anti-cancer drugs to BN peptides for site-specific delivery of cytotoxic drugs into tumor cells [3]. Cytotoxic peptide conjugates are hybrid molecules, composed of a peptide carrier, which binds to receptors on tumor cells, and a cytotoxic moiety. Such conjugates are designed to deliver cytotoxic drugs more specifically to the cancer cells for efficient targeting of tumors [2, 3]. In an effort to develop a cytotoxic-peptide conjugate for the efficient targeting of BN peptide receptor-expressing tumors (i.e., breast and prostate), we have prepared a novel BN analog, derived from the universal sequence of BN peptide and coupled to a widely-characterized anticancer agent, methotrexate (MTX), which is chemically suitable for conjugation to peptides. The high affinity of the universal BN peptide to all the BN receptor subtypes makes this hybrid molecule a potential candidate for the targeting of BN receptor-positive tumors. MTX is an important anticancer agent for the treatment of a variety of malignant tumors including acute leukemia, osteogenic sarcoma and breast cancer. The benefit of labeling MTX-BN analog with ^{99m}Tc may allow us to initially diagnose the disease non-invasively, which may lead to the appropriate treatment and ultimate cure of these BN receptor-expressing tumors.

We prepared MTX-BN conjugate (Fig. 1) by solid-phase peptide synthesis using Fmoc/HBTU chemistry. At the end of synthesis, MTX was manually attached to the peptide via Lys residue to form MTX-BN conjugate. Radiolabeling with ^{99m}Tc was achieved via Gly-Gly-Cys chelating sequence. *In vitro* tumor cell binding and cellular internalization studies were performed on MDA-MB-231, MCF-7, T47-D breast and PC-3 prostate cancer cell lines. *In vivo* biodistribution studies and clearance kinetics were conducted on balb/c mice and *in vivo* tumor targeting capacity was determined in nude mice (n=3-4; 1 and 4 h post-injection) bearing human tumor xenografts.

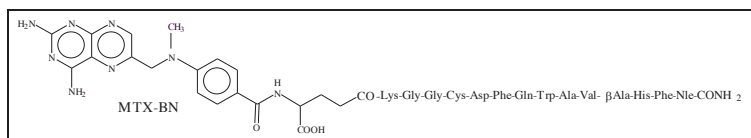


Figure 1. Structure of MTX-BN conjugate.

Results and Discussion

The MTX-BN conjugate was prepared conveniently and successfully using standard Fmoc/HBTU chemistry. MTX-BN was labeled efficiently with ^{99m}Tc (>75% labeling efficiency) via stannous-tartrate method. ^{99m}Tc -MTX-BN exhibited a good chemical stability against cysteine transchelation and a high *in vitro* metabolic stability in human plasma. *In vitro* cell-binding and internalization on MDA-MB-231, MCF-7, T47-D and PC-3 cell lines demonstrated the high affinity and specificity of ^{99m}Tc -MTX-BN towards both human breast and prostate cancers (binding affinities in low nanomolar range). In addition, the radioconjugate displayed a significant internalization (values ranged between 19–35%) into the tumor cells – an important characteristic for radionuclide therapy. *In vivo* biodistribution and clearance kinetics in Balb/c mice are characterized by an efficient clearance from the blood with moderate uptake in the major organs. The radioconjugate with low lipophilicity cleared mainly through the renal pathway, with some elimination via the hepatobiliary system.

In vivo tumor uptake in nude mice bearing MDA-MB-231 cells was $2.70 \pm 0.44\%$ ID/g at 1 h (see Fig. 2). The radioactivity in the tumors was always higher than the radioactivity in the blood and muscle, with good tumor retention and good tumor-to-blood and tumor-to-muscle uptake ratios. The accumulation/retention in the major organs was low to moderate (<6% ID/g) in both healthy and tumor-bearing mice. However, the uptake/retention in the kidneys was rather high (up to 11% ID/g), which is of a concern, particularly for radionuclide therapy. Receptor blocking studies in which $\sim 100\ \mu\text{g}$ dose of unlabeled BN peptide was injected 30 min prior to the administration of ^{99m}Tc -MTX-BN reduced the uptake in the target organs, tumor and pancreas, indicating the receptor-specificity of the radioconjugate.

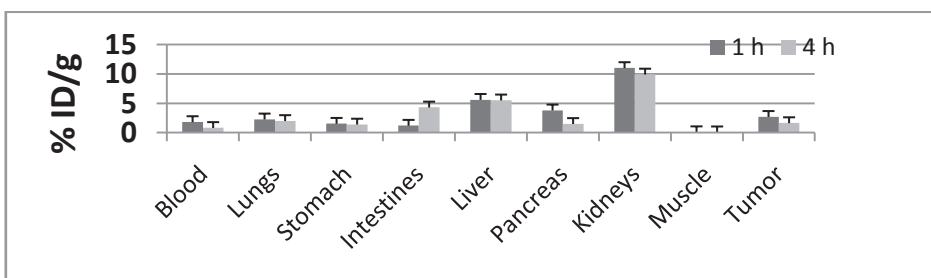


Figure 2. Biodistribution of ^{99m}Tc -MTX-BN in MDA-MB-231 bearing nude mice at 1 and 4 h post-injection. Data are expressed as % injected dose per gram (% ID/g).

In conclusion, this study demonstrates that the cytotoxic BN analog under investigation has certain favorable *in vitro* and *in vivo* properties, which may make it an attractive candidate for targeting of BN receptor-expressing tumors. The present data provide useful insight for designing and developing new cytotoxic peptide conjugates for targeting tumors that overexpress specific receptors for the peptides.

References

- [1] Okarvi, S. M. *Cancer Treat Rev.* **2008**, *34*, 13.
- [2] Okarvi, S. M. *Nucl. Med. Biol.* **2010**, *37*, 277.
- [3] Schally, A. V.; Nagy, A. *Life Sci.* **2003**, *72*, 2305.

Novel approaches to the design of novel multivalent ligands for the detection and treatment of cancer

V. J. Hraby¹, N. Brabez^{1,2}, J. Josan¹, C. DeSilva¹, J. Vagner¹,
G. Chassaing², D. Morse³, R.J. Gillies³, S. Lavielle²

¹Department of Chemistry and Biochemistry, University of Arizona, Tucson, AZ 85721 U.S.A.; ²Université Pierre et Marie Curie, UMR7203, Laboratoire des BioMolécules, UPMC Paris 06 – CNRS – ENS and FR 2769, Chimie Moléculaire; ³Departments of Radiology and Cancer Imaging and Metabolism, H.L. Moffitt Cancer Center & Research Institute, Tampa, FL, 33612, U.S.A.

E-mail: hruby@email.arizona.edu

Introduction

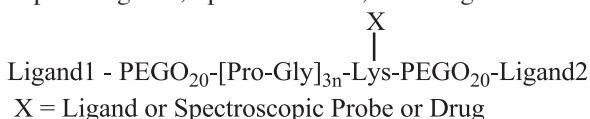
From comparative genomics and proteomics it has become clear that cancer results from numerous changes in the expressed genome of a cell (tens to hundreds). We have suggested [1] that advantage can be taken of these changes in the expressed genome to target 2 or more cell surface protein changes that distinguish cancers from normal cells. Such an ability would provide an opportunity to selectively deliver imaging or therapy to cancers with little off-target effects. Since the binding pockets on two membrane proteins are expected to be 25 Å to 100 Å or more apart in 3D space, it is necessary to design scaffolds that can place pharmacophore ligands for these proteins (receptors, enzymes, etc.) at those distances as well as reporter groups (fluorescent, phosphorescent, radiolabeled, etc.) that can be used to detect binding interactions *in vivo* and *in vitro*. The use of multivalency is expected to lead to synergies in binding affinities.

Results and Discussion

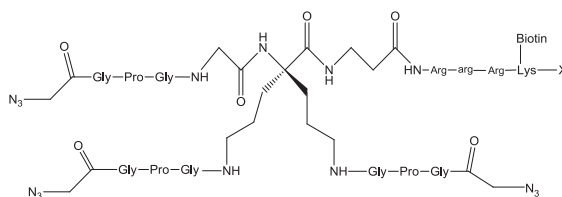
A critical first goal in this research is to establish suitable scaffolds that will allow maximum flexibility in spacing of ligands and reporter groups, and still retain biocompatible properties for *in vivo* delivery. As shown in Figure 1, we have designed

Figure 1. Two Scaffolds Designed to Be Biocompatible, Non-toxic, and Suitable for Attachment of Peptide and Non-Peptide Ligands, Spectral/Probes, and Drugs.

I. Linear Branched Scaffold:



II. Dendrimer Scaffold:



X=Bead, OH, NH₂, arg=D-Arg

several scaffolds (2 are shown), for attaching suitable ligands for multivalent interaction with cancer cells but not normal cells [2-4]. Syntheses of scaffolds **1** and **2** have been optimized so that purified constructs can be obtained with overall yields of 40-55%.

Both Receptors	Binding Affinity (nM)
1. Scaffold I- α -MSH(7)- Monovalent	240
2. Scaffold I- α -MSH(7)-Bivalent	3
3. Scaffold I- NH-CCK6-Ala-c-Monovalent	120
4. Scaffold I- NH-CCK6-Ala-c-Bivalent	120

To evaluate our hypothesis, we have prepared a variety of homomultimeric and heteromultimeric ligands, a few examples of which are given in Table **1**. This is particularly instructive because it demonstrates a very interesting observation we have made with heterobivalent ligands and then binding interaction with cells that have both receptors on their cell surfaces. Very excellent synergy is seen for the heterobivalent ligand binding to the hMC4R but not to the CCK2R. Note that CCK2 receptor (CCK2R) is present in greater amounts (about 10 fold) than the melanocortin 4 receptor (MC4R). We have seen, by imaging experiments of bivalent ligands with a fluorescent probe, that agonist ligands lead to rapid internalization of the multivalent ligands (e.g. 4).

Using the dendrimer homovalent and heteromultivalent ligand, we have made similar observations and seen synergies up to over 300 fold in some cases [5]. Interestingly, the ligands prefer no or very minimal spacers on the basic dendrimer structure (Figure 1).

In vivo studies on mice and rats bearing tumors showed in many cases, strong bonding (presumably nonspecific) to the liver and to a lesser extent, the kidney, in addition to the tumor containing the receptors for the multivalent ligands, which is imaged. However after 8-24 hours labeling of the liver and kidney is greatly diminished, but this is not the case for the tumor. Approaches to minimize the non-specific labeling, especially at the liver and kidney are being investigated.

Acknowledgments

This work was supported in part by grants from the U.S. Public Health Service, National Institutes of Health, CA097300 and CA 123547. NB acknowledges CNRS for a doctoral fellowship.

References

- [1] Gillies, R.J.; Hruby, V.J. *Expert Opinion Ther. Targets*. **2003**, *7*, 137.
- [2] Vagner, J.; Xu, L.; Handl, H.L.; Josan, J.S.; Morse, D.L.; Mash, E.A.; Gillies, R.J.; Hruby V.J. *Angew. Chem. Intl. Ed.* **2008**, *47*, 1685.
- [3] Brabez, N.; Lynch, R.M.; Xu, L.; Gillies, R.J.; Chassing, G.; Lavielle, S.; Hruby, V.J. *J. Med. Chem.* **2011**, *54*, 7375.
- [4] Josan, J.S.; Vagner, J. Handl, H.L.; Sankaranarayanan, R.; Gillies, R.J.; Hruby, V.J. *Int. J. Pept. Res. Ther.* **2008**. *14(4)*, 293.
- [5] Sharma, S.D.; Jiang, J.; Hadley, M.E.; Bentley, D.L.; Hruby, V.J. *Proc. Natl. Acad. Sci. U.S.A.*; **1996**, *93*, 13715.

Chemical synthetic glycopeptide vaccine for cancer therapy

**Hui Cai¹, Zhi-Hua Huang¹, Lei Shi¹, Zhan-Yi Sun¹, Horst Kunz²,
Yan-Mei Li^{1,*}**

¹*Key Lab of Bioorganic Phosphorus Chemistry & Chemical Biology (Ministry of Education), Department of Chemistry Tsinghua University Beijing 100084, P.R.China;*

²*Institute of Organic Chemistry, Johannes Gutenberg University of Mainz, Duesbergweg 10-14, 55128 Mainz, Germany*

E-mail: liym@tsinghua.edu.cn

Introduction

Cancer is one of the most dangerous diseases over the world. Traditional therapies including surgery, chemotherapy and radiotherapy have serious side-effect or may lead to metastasis. So tumor vaccines were considered as a more effective and safer therapy.

There are several kinds of vaccines. Gene vaccine, a plasmid containing target protein motif, can express protein in vivo in patient cells and elicit immune system. Dendritic cell vaccine, which is extracted from patient and loaded antigen in vitro, can elicit directly immune system after injected back to patient. Peptide vaccine is short peptides antigen.

In contrast, chemical synthetic glycopeptide vaccine is a kind of vaccines bearing tumor-associated carbohydrate antigens (TACAs) on peptide sequence, which is synthesized by total chemical approach. This kind of vaccines target peptide antigen and also carbohydrate modification. And the quality control and standardization are easily processed. But as small peptide from self-tissue, the immunogenicity of these glycopeptides are low, so the point of chemical synthetic glycopeptide vaccine is to find effective glycopeptide antigen and to construct effective systems.

MUC1 is a member of transmembrane protein family, mucin, which has 20-mer variable numbers of tandem repeats (VNTR) in its extracellular domain. In VNTR, there are five Ser/Thr sites which can be glycosylated. Compared to normal cells, MUC1 is over-expressed on all surfaces and glycosylated by TACAs. So MUC1 are wildly used as the targets of tumor vaccine development.

Bovine Serum Albumin and Tetanus Toxoid were used as a carrier protein to increase the immunogenicity of glycopeptides [1]. But carrier proteins are high immunogenic, which elicited high level of anti-carrier protein antibody. So improved vaccines consist of B-cell epitope and T-cell epitope are developed [2] Also Toll-like receptors (TLRs) ligand was constructed in vaccine to assist immune response [3,4].

Results and Discussion

In our research, we used different system to construct different kinds of vaccines.

The first kind of vaccines is conjugates of glycopeptides and BSA proteins. Tn, T, Sialyl-Tn and Sialyl-T antigens were used as TACAs. This kind of vaccine elicited high level of immune response [5,6].

Then we screened several T-cell epitopes from Tetanus Toxoid to construct B-T two-component vaccines, one of which helped to elicit high level of immune response.

Also we used Cu-catalyzed click reaction to synthesize multivalent vaccines containing B-cell epitope and lipopeptide of TLR2 ligand [7].

Next, we constructed three-component vaccine of B-cell epitope, T-cell epitope and lipopeptide by thioether method. These signals combined and highly stimulated immune system.

In our design, T-cell epitope is necessary to activate helper T cell, which is fundamental in T-cell dependent pathway. And TLR ligand can activate TLR to stimulate innate system. A basic logic to design vaccine is to combine different signals to increase the effect.

As a new design, we built a self-assembly small peptide to B-cell epitope. The kind of vaccines aggregated into fibers in neutral condition and elicited immune response without adjuvant [8].

Self-assembly systems can spontaneously aggregate into particles, vesicles or fibers with large scale and multivalent antigen, which may benefit for immune response. Meanwhile, aggregates will dissociate into monomers and be easily cleaned.

Acknowledgments

This work was supported by the Major State Basic Research Development Program of China (973 Program) (2012CB821600), the National Natural Science Foundation of China (20825206 and 21028004) and by the Sino-German Center for Research Promotion (GZ561).

References

- [1] Kaiser, A.; Gaidzik, N.; Westerlind, U.; Kowalczyk, D.; Hobel, A.; Schmitt, E.; Kunz, H. *Angew. Chem.-Int. Edit.* 2009, *48*, 7551-7555.
- [2] Westerlind, U.; Hobel, A.; Gaidzik, N.; Schmitt, E.; Kunz, H. *Angew. Chem. Int. Ed.* 2008, *47*, 7551-7556.
- [3] Ingale, S.; Awolfert, M.; Gaekwad, J.; Buskas, T.; Boons, G. J. *Nat. Chem. Biol.* 2007, *3*, 663-667.
- [4] Wilkinson, B. L.; Day, S.; Malins, L. R.; Apostolopoulos, V.; Payne, R. J. *Angew. Chem. Int. Ed.* 2011, *50*, 1635-1639.
- [5] Cai, H.; Huang, Z. H.; Shi, L.; Zou, P.; Zhao, Y. F.; Kunz, H.; Li, Y. M. *Eur. J. Org. Chem.* 2011, 3685-3689.
- [6] Cai, H.; Huang, Z. H.; Shi, L.; Sun, Z. Y.; Zhao, Y. F.; Kunz, H.; Li, Y. M. *Angew. Chem. Int. Ed.* 2012, *51*, 1719-1723.
- [7] Cai, H.; Huang, Z. H.; Shi, L.; Zhao, Y. F.; Kunz, H.; Li, Y. M. *Chem. Eur. J.* 2011, *17*, 6396-6406.
- [8] Huang, Z. H.; Shi, L.; Ma, J. W.; Sun, Z. Y.; Cai, H.; Chen, Y. X.; Zhao, Y. F.; Li, Y. M. *J Am Chem Soc* 2012, *134*, 8730-3.

Engineering of proteinaceous orally active bradykinin peptide antagonists

James P. Tam, Clarence T. T. Wong, Yibo Qiu

*School of Biological Sciences, Nanyang Technological University, 60 Nanyang Drive,
Singapore 637551*

jptam@ntu.edu.sg

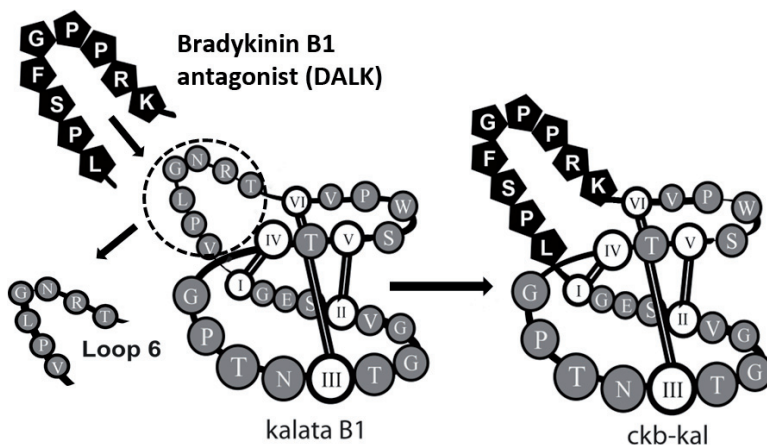
Introduction

Proteinaceous therapeutics have an advantage over the small-molecule drugs due to their large foot prints which confer high affinity and specificity to drug targets. However, they are also hindered by their metabolic lability and tissue impermeability. Overcoming these two limitations has been the central issue in developing orally active peptide therapeutics. To address these limitations, we have developed a protein engineering approach based on grafting a bioactive epitope into an ultra-stable cyclotide scaffold which is resistant to heat and enzymatic degradation.

Cyclotides are naturally-occurring peptides in many medicinal plants, possessing peptide-like size and protein-like structure. They are macrocyclic cystine-rich peptides with three interlocking disulfide bonds in a cysteine knot^[1]. As such, they represent an exceptionally promising scaffold for our grafting strategy for engineering orally active therapeutics. Furthermore, cyclotides are diverse in sequences and tolerant to amino acid substitutions. Here, we show a potential therapeutic application for engineering edible analgesics by grafting a bradykinin (BK) B1 receptor antagonist into a cyclotide kalata B1, aiming to target chronic pain management. Chronic pain is a universal health issue associated with numerous medical conditions, such as after severe burns or following major surgery^[2]. Compelling evidence suggests that bradykinin receptor antagonists could be useful in treating chronic pain and inflammatory pain^[3]. Thus, a rational engineering of bradykinin receptor antagonists using the cyclotide-grafting strategy will likely improve the half-lives and oral availability.

Results and Discussion

A novel orally active BK-peptide analgesics ckb-kal was designed by grafting bradykinin B1 receptor antagonists, des-Arg10-[Leu9]-kallidin (DALK) into the kalata B1 scaffold, the prototypic cyclotide. The engineered peptide ckb-kal was prepared by a stepwise solid-phase peptide synthesis using Boc chemistry to afford their unprotected thioester precursors. Under thia-zip cyclization, their backbones were cyclized with the C- and N-termini joined as an amide^[4]. The oxidative folding of engineered BK antagonists was performed in the presence of reduced (GSH) and oxidized glutathione (GSSG) to afford a folded peptide. The disulfide connectivity was confirmed by a partial reduction and S-alkylation strategy followed by MS/MS sequencing. The serum stability and analgesic effects of the engineered peptide ckb-kal showed >350 folds improvement in the half-life and 42% inhibition of pain response through oral delivery whereas its linear analogs showed no inhibition^[5].



Acknowledgments

This research was supported by Biomedical Research Council (BMRC 09/1/22/19/612) and National Research Foundation (NRF-CRP001-109) in Singapore.

References

- [1] Craik, D. J.; Daly, N. L.; Bond, T.; Waine, C. *Journal of Molecular Biology* **1999**, *294*, 1327–1336.
- [2] Marceau, F.; Regoli, D. *Nat Rev Drug Discov* **2004**, *3*, 845–852.
- [3] Stewart, J. M. *Peptides* **2004**, *25*, 527–532.
- [4] Tam, J. P.; Lu, Y. A.; Yu, Q. T. *Journal of the American Chemical Society* **1999**, *121*, 4316–4324.
- [5] Wong, C. T. T., Rowlands, D. K., Wong, C.-H., Lo, T. W. C., Nguyen, G. K. T., Li, H.-Y., and Tam, J. P. *Angewandte Chemie International Edition* **2012** *51*, 5620-5624

Chemoselective α -ketoacid–hydroxylamine (KAHA) ligation with 5-oxaproline for chemical protein synthesis

Vijaya R. Pattabiraman, Ayodele O. Ogunkoya, Jeffrey W. Bode*

Laboratorium für Organische Chemie, ETH Zürich, 8093 Zürich, Switzerland

E-mail: bode@org.chem.ethz.ch

Introduction

Total chemical synthesis of proteins is an important method for accessing both natural and modified proteins for applications in biology, medicine and materials. For chemical protein synthesis, native chemical ligation (NCL) is at the forefront of the available methods, albeit with its own boundaries.[1] Inspired by native chemical ligation, we have developed the α -ketoacid–hydroxylamine (KAHA) ligation for the synthesis of medium-sized peptides and small molecules. [2] Our initial attempts to extend it for the synthesis of proteins was impeded by the reduced performance of the α -ketoacid and *O*-unsubstituted hydroxylamine ligation in aqueous medium, which is typically required for solubilizing large protein segments. A detailed mechanistic study of the α -ketoacid and *O*-unsubstituted hydroxylamine ligation suggested that water could be detrimental to the ligation rates and efficiency.[2c] This prompted us to identify a hydroxylamine derivative that is stable to the synthesis and handling steps, but would readily undergo ligation in water with a α -ketoacid.

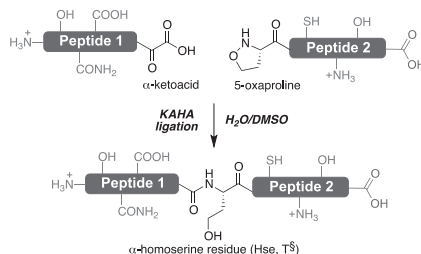
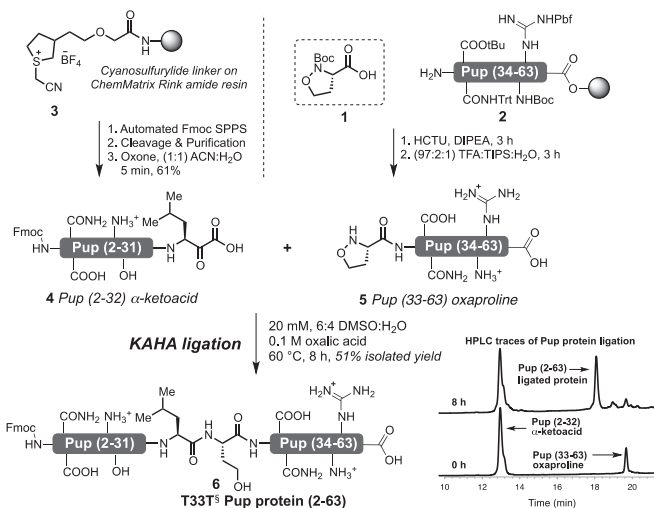


Figure 1: KAHA ligation with 5-oxaproline

Results and Discussion

We were pleased to identify 5-oxaproline, as a stable *N*-hydroxyamino acid that undergoes ligation with fully unprotected peptide α -ketoacid in water to give unnatural α -homoserine at the ligation site (Figure 1). Boc protected 5-oxaproline **1** suitable for use in solid-phase peptide synthesis can be easily prepared in >20 g scale by a short synthetic sequence.[3a] To investigate the suitability of the 5-oxaproline for protein synthesis, we undertook the total chemical synthesis of prokaryotic ubiquitin-like protein (Pup), a 64 amino acid protein from *Mycobacterium tuberculosis*. We began with the synthesis of the oxaproline segment **2** by automated Fmoc-SPPS on Wang resin up to residue 34. *N*-Boc-5-oxaproline **1** was coupled to the *N*-terminal amine on-resin using HCTU and NMM for 3 h. This was followed by cleavage and purification, to give Pup (33-63) oxaproline segment **5** with no degradation of the oxaproline moiety (Scheme 1). We prepared the Pup (2-32)- α -ketoacid segment **4** starting from cyanosulfurylide resin using our established method.[3b] With both the Pup protein segments **4** & **5** in hand, a brief optimization studies indicated that the ligation works better with increasing amount of water in the ligation mixture. With this information, we performed the preparative scale Pup ligation in 6:4 DMSO/H₂O containing 0.1M oxalic acid at 60 °C. The ligated Pup protein **6** was isolated by preparative HPLC in



Scheme 1: Synthesis of Pup protein by KAHA ligation with 5-oxaproline

unrelated to Pup protein sequence, we chose to prepare cspA protein. The α -ketoacid segment of cspA **7** and the cspA oxaproline segment **8** were prepared using the methods described above. The ligation between **7** and **8** in 8:2 DMSO/H₂O at 60 °C gave synthetic cspA protein **9** in 53% isolated yield (Scheme 2). Importantly, the CD spectrum of the synthetic cspA protein **9** matched well with literature data.

In summary, we have established the KAHA ligation with 5-oxaproline as a highly suitable method for chemical protein synthesis. The 5-oxaproline monomer can be prepared in >20 g scale in few easy steps. We are currently applying the KAHA ligation with 5-oxaproline for the preparation of a variety of proteins and concurrently, we are designing new hydroxylamine monomers.

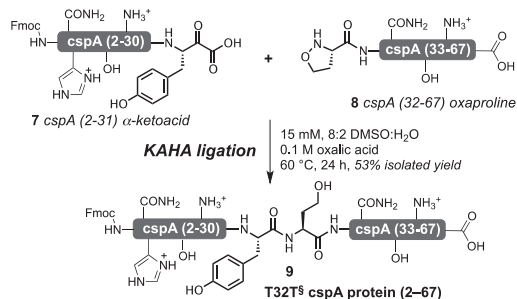
Acknowledgments

This work was supported by the Swiss National Science Foundation (200021_131957) and an ETH Fellowship to V.R.P. (ETH FEL 06-10-1).

References

- [1] a) Dawson, P. E.; Muir, T. W.; Clarklewis, I.; Kent, S. B. H. *Science* **1994**, *266*, 776. b) Kent, S. B. H. *Chem. Soc. Rev.* **2009**, *38*, 338.
- [2] a) Bode, J. W.; Fox, R. M.; Baucom, K. D. *Angew. Chem. Int. Ed.* **2006**, *45*, 1248. b) Wu, J.; Ruiz-Rodriguez, J.; Comstock, J. M.; Dong, J. Z.; Bode, J. W. *Chem. Sci.* **2011**, *2*, 1976. c) Pusterla, I.; Bode, J. W. *Angew. Chem. Int. Ed.* **2012**, *51*, 513.
- [3] a) V. R. Pattabiraman, A. O. Ogunkoya, J. W. Bode, *Angew. Chem. Int. Ed.* **2012**, *51*, 5114. b) Ju, L.; Bode, J. W. *Org. Biomol. Chem.* **2009**, *7*, 2259.

51% yield and fully characterized by FTMS and MS/MS analysis. CD spectroscopic data of the synthetic Pup protein showed the presence of α -helical regions as proposed for the natural pup protein. This implies that the α -homoserine introduced by the ligation does not interfere in the ability of the synthetic Pup protein to adopt the expected tertiary structure. To examine KAHA ligation with 5-oxaproline for the synthesis of a protein



Scheme 2: Synthesis of cspA protein by KAHA ligation with 5-oxaproline

Recognition pliability is coupled to structural heterogeneity

**Malini Nagulapalli¹, Giacomo Parigi¹, Jing Yuan¹, Joerg Gsponer,^{2,3}
George Deraos,⁴ Vladimir V. Bamm,⁵ George Harauz,⁵ John
Matsoukas,⁴ Maurits RR de Planque,⁶ Ioannis P. Gerothanassis,⁷ M.
Madan Babu,² Claudio Luchinat,¹ Andreas G. Tzakos⁷**

¹*Magnetic Resonance Center (CERM), University of Florence, Italy;* ²*MRC Laboratory of Molecular Biology, Cambridge, UK;* ³*Centre for High-Throughput Biology, University of British Columbia, Vancouver;* ⁴*Department of Chemistry, University of Patras, Patras, Greece;* ⁵*Department of Molecular and Cellular Biology, University of Guelph, Canada;* ⁶*Biomembrane Structure Unit, University of Oxford, UK;* ⁷*Department of Chemistry, University of Ioannina, Greece*
E-mail: atzakos@upatras.gr

Introduction

Protein interactions within regulatory networks should adapt in a spatiotemporal dependent dynamic environment, in order to process and respond to diverse and versatile cellular signals. However, the principles governing recognition pliability in protein complexes are not well understood. We have investigated a region of the intrinsically disordered protein myelin basic protein (MBP₁₄₅₋₁₆₅) that interacts with calmodulin, but that also promiscuously binds other biomolecules (membranes, modifying enzymes). To characterize this interaction, we implemented an NMR spectroscopic approach that calculates, for each conformation of the complex, the maximum occurrence based on recorded pseudocontact shifts and residual dipolar couplings. We found that the MBP₁₄₅₋₁₆₅-calmodulin interaction is characterized by structural heterogeneity. Quantitative comparative analysis indicated that distinct realms of spatial heterogeneity are sampled for different calmodulin-target complexes. Such structural heterogeneity in protein complexes could potentially explain the way that transient and promiscuous protein interactions are optimized and tuned in complex regulatory networks.

Results and Discussion

On the basis of recently established algorithms that allow prediction of disordered binding regions in proteins a specific binding regions undergoing a disorder-to-order transition (disordered binding regions) using PONDR® located a binding site at the C-terminus of the 18.5 kDa isoform of MBP (residues 145-165 in the 170-residue human protein) that overlaps with a region that is susceptible to post-translational modifications (citrullination, serine and threonine phosphorylation). The MBP₁₄₅₋₁₆₅ peptide was synthesized and CD was used to verify its intrinsically disordered nature. The Ca₄CaM - MBP₁₄₅₋₁₆₅ interaction was studied by solution NMR spectroscopy and isothermal titration calorimetry (ITC). The binding site with the highest affinity to the MBP peptide is characterized by a dissociation constant (K_d) of $7.7 \pm 0.2 \mu\text{M}$. The chemical shift perturbation between free Ca₄CaM and in the presence of 2.25 equivalents of MBP₁₄₅₋₁₆₅ peptide indicated that the residues for which chemical shifts differ most in the two forms are located mainly in the C-terminal domain of CaM. From the titration, a dissociation constant of $10 \mu\text{M}$ was estimated for the Ca₄CaM -

MBP₁₄₅₋₁₆₅ interaction that is in consensus with the relevant value obtained from ITC. The conformational space sampled by domain reorientations in CaM upon MBP epitope binding was explored by using a novel approach based on the exploitation of residual dipolar couplings (rdc) and pseudocontact shifts (pcs), after substitution of a paramagnetic lanthanide ion for one diamagnetic calcium ion of the N60D CaM variant. This approach involves calculating for each protein conformation the maximum occurrence (MO) consistent with the collected pcs and rdc data, and studying the conformations with the largest MO. The MO of a given conformation is defined as the percent of time that the system can spend in that conformation which can reproduce the experimental data. Through this approach CaM was found to adopt a large ensemble of conformations in its adduct with the MBP₁₄₅₋₁₆₅, similarly to what observed for the protein free in solution and in the frame of CaM recognition by another intrinsically disordered protein, α -synuclein. Having a collective view of the largest MO values sampled by free CaM, a rigid CaM-DAPk peptide complex, the CaM- α -synuclein complex and the CaM-MBP₁₄₅₋₁₆₅ complex presented here, we performed a quantitative global comparative analysis of recognition heterogeneity induced in CaM upon interaction with different targets. Intriguingly, it was found that the complex CaM- MBP145-165 confers conformational heterogeneity, which differs from other CaM-complexes, to provide the plasticity necessary to interact with a large number of different targets. The recorded disorder in this complex could provide an additional understanding of how intrinsically disordered protein binding regions transmit and realize their multiple functions within complexes. Functional coupling of structural heterogeneity and recognition pliability in protein complexes could be envisioned as a mechanism enabling the fine-tuning a system's response to various cellular events. Such disorder information within the complex level should be employed in the future to develop new strategies for the discovery of new drugs.

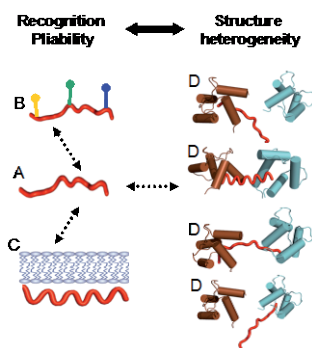


Figure 1. Functional coupling of structure heterogeneity and recognition pliability.

References

- [1] Bertini, I., Gupta, Y.K., Luchinat, C., et al., *J Am Chem Soc* (2007) 129, 12786-12794.
- [2] Bertini, I., Giachetti, A., Luchinat, C., et al., *J Am Chem Soc* (2010) 132, 13553-13558.
- [3] Nagulapalli M, Parigi G, Yuan J, et al., *Structure* (2012) 20, 522-33.

Biofunctionalization of biopolymers with peptide conjugated dendrons

Peter Fransen¹, Daniel Pulido², Ryan Seelbach³, Alvaro Mata³, David Eglin⁴, Miriam Royo², Fernando Albericio¹

¹IRB Barcelona, Barcelona, Spain; ²Unitat de Química Combinatòria/Parc Científic de Barcelona, Barcelona, Spain; ³Nanotechnology Platform/Parc Científic de Barcelona, Barcelona, Spain; ⁴AO Research Institute Davos, Davos, Switzerland

E-mail: peter.fransen@irbbarcelona.org

Introduction

Dendrimers are highly branched, monodisperse and symmetrical macromolecules of nanodimensions. The architecture of these molecules can be engineered precisely, and also the external terminal functional groups can be modified to meet varying requirements of different applications in drug delivery, gene delivery, sensors and biomaterials.

In this study, we present the synthesis of PEG-based dendrons which are functionalized with peptides to serve as biofunctionalization platforms for biopolymer hydrogels. The polymer, hyaluronic acid, which forms the hydrogel scaffold, is modified through click chemistry with the aforementioned peptide conjugated dendrons together with the polymer NIPAM. The resulting material is thermoresponsive and can potentially be injected into load bearing joints to serve as a tissue engineering approach for repair of damaged articular cartilage.

Results and Discussion

The dendrons consist of a diethylene triamine pentaacetic acid (DTPA)-derived branching unit, to which a single azide-functionalized PEG-chain of exact length was incorporated at the focal point and four Boc-protected amine-functionalized PEG-chains of identical length were introduced in the other carboxylic acid functions. The Boc-groups were eliminated by means of acidic treatment to yield the dendrons with four amines available for further peptide conjugation.

Diverse peptides such as RGDS, RSGD, YPVHPST, HRGYPLDG, and LPLGNSH were selected to serve as biosignaling entities which play a role in promoting specific tissue growth [1,2].

Using the copper catalyzed azide-alkyne 1,3 cycloaddition, the functionalized dendron, together with NIPAM, can be grafted onto alkyne-functionalized hyaluronic acid [3].

Preliminary results show that peptide conjugated dendrons introduce the biofunctionality of the formed thermoresponsive hydrogel. Hydrogels grafted with PEG-based dendrons exhibited good cell viability. Furthermore, excretion of extracellular matrix proteins was significantly higher in hydrogels grafted with RGDS peptide dendrons compared to those which were grafted with control RSGD dendrons or those which were not grafted at all.

These results are the proof of concept that peptide conjugated dendrons can serve as tuneable, modular platforms for the biofunctionalization of polymer hydrogels. Consequently, these platforms can successfully provide the biochemical environment needed for cell proliferation and differentiation in the tissue engineering scaffold.

Further experiments with the other peptide conjugated dendrons are planned for the short-term future.

Acknowledgements

This work was supported financially by the Spanish Ministry of Science and Innovation, (CTQ2009-07758, CTQ2008-00177, EUI2008-00174), the Spanish Ministry of Economy (SAF2011-30508-C02-01), the Generality de Catalunya (2009SGR 1024), the AO Foundation, the LaCaixa social program and the Spanish Network for Biomedical Research in Bioengineering, Biomaterials and Nanomedicine (CIBER-BBN).

References

- [1] Liu, S.Q.; Ee, P.L.; Ke C.Y.; Hedrick J.L.; Yang Y.Y. *Biomaterials*. **2009**, 30, 1453-1461
- [2] Garvican, E.R.; Vaughan-Thomas A.; Innes J.F.; Clegg P.D. *Vet J*. **2010**, 185, 36-42
- [3] Mortison, D.; Peroglio, M.; Alini, M.; Eglin, D. *Biomacromolecules*. **2010**. 11, 1261-72

Membrane thickness and the mechanism of action of the short peptaibol trichogin GA IV

S. Bobone¹, Y. Gerelli², M. De Zotti³, G. Bocchinfuso¹, A. Farrotti¹, B. Orioni¹, A. Palleschi¹, F. Sebastiani², E. Latter⁴, J. Penfold⁴, R. Senesi⁵, F. Formaggio³, C. Toniolo³, G. Fragneto², L. Stella¹

¹*University of Rome "Tor Vergata", Department of Chemical Sciences and Technologies, 00133 Rome, Italy;* ²*Institut Laue-Langevin, 38000 Grenoble, France;* ³*University of Padova, ICB, Padova Unit, CNR, Department of Chemistry, 35131 Padova, Italy;* ⁴*ISIS, STFC, Rutherford Appleton Laboratory, Chilton, Didcot, OXON, OX11 0QX, UK;* ⁵*University of Rome "Tor Vergata", Department of Physics, 00133 Rome, Italy*
E-mail: stella@stc.uniroma2.it

Introduction

Antimicrobial peptides (AMPs) are small molecules with antibiotic properties, which are produced by most of the organisms as a first defense against infections. AMPs mainly act by perturbing the bacterial cell membranes. This effect makes the membrane permeable, which in turn leads the cell to death. Because of their membranolytic mechanism of action, the rise of bacterial resistance is unlikely.

Trichogin GA IV (TGAIV) is an antimicrobial peptide belonging to the peptaibol family, the most extensively studied member of which is alamethicin. For this latter peptide, it has been convincingly demonstrated that it forms transmembrane pores according to the barrel-stave mechanism. TGAIV and alamethicin share similar 3D-structural and physico-chemical features. Moreover, experimental evidence supporting a barrel-stave mechanism for TGAIV has been reported [1,2]. However, while the alamethicin length (32 Å) is comparable to the hydrophobic thickness of a biological membrane, TGAIV is only 16 Å long [3]. This latter value is too low for TGAIV to span the normal thickness of a bilayer. .

In this work, we report both experimental and computational data which indicate that trichogin GAIV causes a significant membrane thinning and support the possibility for this peptaibol to form barrel-stave channels.

Results and Discussion

Neutron reflectivity experiments were performed on a POPC bilayer in the presence of increasing amounts of TGAIV, using the contrast variation methodology. Measurements were carried out on a chain-hydrogenated POPC bilayer (to which partially deuterated TGAIV was added) and on a chain-deuterated POPC bilayer (to which hydrogenated TGAIV was added). Data analysis of the reflectivity profiles showed that TGAIV addition causes a significant thinning of the POPC hydrophobic thickness, which decreases from 28 to 21 Å (Figure 1). Furthermore, we determined that the peptide was located exclusively in the tail region of the bilayer.

Molecular dynamics simulations were also carried out to shed light on the effects of TGAIV on the bilayer when inserted in a transmembrane orientation. During the simulation

time, strong interactions between the phospholipid headgroup moieties and the peptide N- and C-termini were detected. Due to these interactions, the polar headgroups in proximity of the peptide molecules were forced to insert within the hydrophobic core of the membrane. As a consequence, a thinning of the lipid bilayer in the region where the peptide was located was observed.

Membrane leakage experiments showed that the TGAIV activity is dramatically dependent on the hydrophobic thickness of the membrane. In particular, when the bilayer thickness becomes comparable to the trichogin length, the peptide activity is found to be similar to that of alamethicin, while in thicker membranes alamethicin exhibits a significantly higher activity (Figure 2).

Overall, these data indicate that a barrel-stave mechanism of pore formation might be possible for TGAIV and similarly short peptaibols despite their relatively small size.

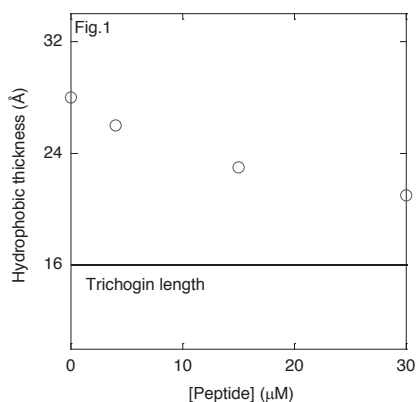


Fig.1: Bilayer's hydrophobic thickness as a function of peptide concentration. The continuous line represents the length of TGAIV.

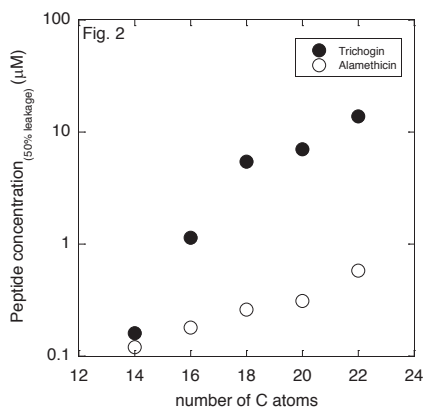


Fig.2: TGAIV and alamethicin activity as a function of the bilayer thickness.

References

- [1] Stella, L.; Mazzuca, C.; Venanzi, M.; Palleschi, A.; Didoné, M.; Formaggio, F.; Toniolo, C.; Pispisa, B. *Biophys. J.* **2004**, *86*, 936.
- [2] Mazzuca C.; Stella, L.; Venanzi, M.; Formaggio, F.; Toniolo, C.; Pispisa, B. *Biophys. J.* **2005**, *88*, 3411.
- [3] Toniolo, C.; Peggion, C.; Crisma, M.; Formaggio, F.; Shui, X.; Eggleston, D.S. *Nat. Struct. Biol.* **1994**, *12*, 908.

Mild chemoselective alkylation of aza-sulfurylglycinyl peptides

Stéphane Turcotte, Thierry Havard, William D. Lubell*

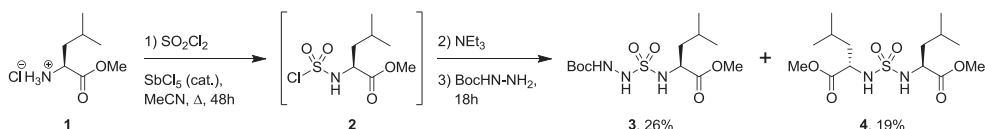
Département de chimie, Université de Montréal, C.P. 6128, Succursale Centre-Ville,
Montréal, Québec, H3C 3J7, Canada

E-mail: william.lubell@umontreal.ca

Introduction

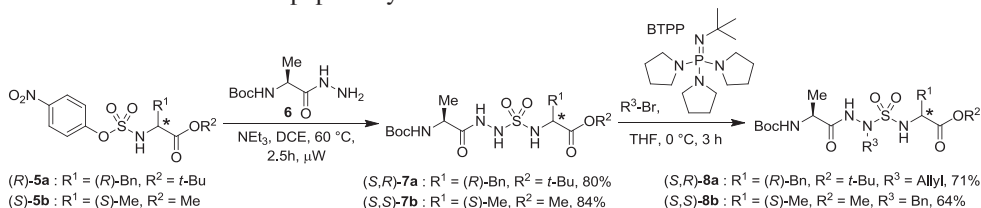
Mimics of the tetrahedral transition states common in enzyme-catalyzed reactions, such as phosphoramidates [1] and silanediols [2], have served as enzyme inhibitors. In this vein, the analogous α -aminosulfonamido peptide would offer potential; however, such α -aminosulfonamides were found to rapidly decompose [3]. On the contrary, reasonable stability has been exhibited by *N*-aminosulfamido peptides, in which a nitrogen and a sulfonyl group replace respectfully both the CH α and the carbonyl of an amino acid residue. To the best of our knowledge, prior to our research, only one method had been reported for constructing acyclic *N*-aminosulfamides [4]. This method suffered, however, from sluggish couplings leading to formation of symmetric sulfamides, due to the use of sulfonyl chloride and catalytic amounts of antimony pentachloride to combine the hydrazide and amine components (Scheme 1) [4]. Moreover, *N*-alkyl hydrazide synthesis was required for the introduction of side chains onto the *N*-aminosulfamide residue.

Scheme 1. Symmetric sulfamide formation competes with *N*-aminosulfamide synthesis.



We reported recently a three-step method for the synthesis of *N*-aminosulfamides [5]. In the first step, a crystalline 4-nitrophenyl sulfamidate **5** is produced by acylation of the amino acid component with 4-nitrophenyl chlorosulfate. Sulfamidate **5** provides an effective means for preventing formation of symmetric sulfamide during *N*-aminosulfamide synthesis, such that in the second step, reaction with hydrazide **6** under microwave irradiation at 60°C gives selectively aza-sulfamido tripeptide **7**. Although side chains may be introduced by employment of *N*-alkyl hydrazides, we have also shown that chemoselective alkylation of aza-sulfurylglycinamides **7** can be accomplished to install effectively *N*-alkyl side-chains, using the phosphazene base BTPP (Scheme 2).

Scheme 2. Aza-sulfamido peptide synthesis .



Results and Discussion

Alkylation of aza-sulfurylglycinamide **7** provides an effective method for adding diverse side chains to expand the scope of aza-sulfamido peptide diversity; however, the expense of BTTP as base may be prohibitive. Exploring alternative bases, we have found that the inexpensive and milder base, NEt₄OH can be effectively used to achieve the desired chemoselective alkylation (Table 1).

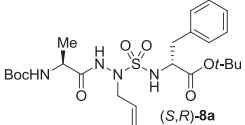
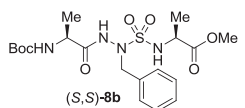
Product	Yield (BTTP, 0 °C, 3h)	Yield (Et ₄ NOH, 40 °C, 3h)
 (<i>S,R</i>)- 8a	71%	81%
 (<i>S,S</i>)- 8b	64%	40%

Table 1. Head-to-head comparison of BTTP with Et₄NOH.

In the alkylation of *N*-(Boc)alaninyl-aza-sulfurylglycinyl-D-phenylalanine *tert*-butyl ester [(*S,R*)-**7a**] with allyl bromide, NEt₄OH at 40°C gave superior yield of (*S,R*)-**8a** over BTTP at 0°C after 3h in THF. On the other hand, the alkylation of aza-sulfurylglycinamide (*S,S*)-(**7b**) with benzyl bromide was less successful using the NEt₄OH conditions, likely due to competing methyl ester hydrolysis. To ascertain if epimerization occurred during the alkylation of **7** using Et₄NOH, the diastereoisomeric ratio of (*S,R*)- and (*S,S*)-**8a** were compared in MeOD. Observation of the respective *tert*-butyl ester signals at 1.41 ppm and 1.47 ppm in the ¹H NMR spectra revealed that no epimerization occurred.

In conclusion, NEt₄OH has been used as an inexpensive milder replacement for the costly base BTTP in the chemoselective alkylation of aza-sulfurylglycinyl peptides.

Acknowledgments

This research was supported by the Natural Sciences and Engineering Research Council of Canada (NSERC) and the Canadian Institutes of Health Research (CIHR) grant No. TGC-114046. S.T. thanks the FQRNT for a graduate student fellowship.

References

- [1] Hirschmann, R.; Yager, K. M.; Taylor, C. M.; Witherington, J.; Paul, A. S.; Phillips, B. W.; Moore, W.; Smith III, A. B. *J. Am. Chem. Soc.* **1997**, *119*, 8177.
- [2] Chen, C. A.; Sieburth, S. M.; Glekas, A.; Hewitt, G. W.; Trainor, G. L.; Erickson-Viitanen, S.; Garber, S. S.; Cordova, B.; Jeffry, S.; Klabe, R. M. *Chem. Biol.* **2001**, *8*, 1161.
- [3] Gilmore, W. F.; Lin, H. J. *J. Org. Chem.* **1978**, *43*, 4535.
- [4] Cheeseright, T.; Edwards, A.; Elmore, D.; Jones, J.; Raissi, M.; Lewis, E. *J. Chem. Soc., Perkin Trans. 1* **1994**, 1595.
- [5] Turcotte, S.; Bouayad-Gervais, S. H.; Lubell, W. D., *Org. Lett.* **2012**, *14*, 1318.

Direct and specific detection of intact sulfated peptides using MALDI-TOF MS reflectron positive ion mode

**S. Cantel, L. Brunel, C. Enjalbal, J.J. Vasseur, J. Martinez,
M. Smietana**

*IBMM – UMR 5247, Institut des Biomolécules Max Mousseron, Universités Montpellier 1
et 2, Place Eugene Bataillon, CC1703, 34095 Montpellier Cedex 5, FRANCE
E-mail:scantel@univ-montp2.fr*

Introduction

Tyrosine sulfation has been shown to be an essential post-translational modification (PTMs) in the regulation of biological activity. A better understanding of the biological roles of sulfated proteins requires the use of tools able to provide efficient and rapid structural information.

Whereas mass spectrometry has become the method of choice for the analysis of PTMs, intact sulfated peptides are still difficult to detect by soft ionization methods like ESI or MALDI due to several factors like the lability of sulfate-ester bond limiting the analysis in positive ionization mode and leading generally to spectra dominated by totally desulfated species. MALDI linear mode is thus preferred since less fragmentation occurs compared to the reflectron mode. A variety of methods devoted to the analysis of sulfated peptides have been established over the years, but the intrinsic nature of sulfated proteins slowed-down considerably the exploration of the sulfoproteome.

Results and Discussion

Prompted by results involving the use of pyrenemethylguanidium (pmg) as an efficient derivatizing agent for MALDI-TOF detection of highly acidic biomolecules such as DNA or sulfated polysaccharides [1], we decided to evaluate the effect of pmg as a derivatizing agent and ionization enhancer for MALDI-TOF analysis of sulfated peptides in reflectron positive ion mode through the formation of stable salt-bridges with sulfated tyrosine residues. We generated a library of CCK-8 analogues, as nonsulfated monosulfated, disulfated, and phosphorylated derivatives.

MALDI positive and negative ion spectra of monosulfated peptide H-Asp-Tyr(SO₃H)-Nle-Gly-Trp-Nle-Asp-Phe-NH₂ were generated in both linear and reflectron modes. As expected the intact sulfated peptide could only be detected in negative mode with partial loss of the sulfate moiety whereas it was quantitatively lost in positive mode. Same results were obtained in the presence of pmg thus demonstrating that it did not affect the ionization of the peptide in both the linear and the reflectron negative ionization modes. However, we could observe a different profile in the positive modes (linear and reflectron modes) (fig.1a). Two other peaks separated by a mass difference of 353.1 Da were clearly identified. The highest m/z value (at 1702.8) corresponded to the intact sulfated peptide complexed with 2 pmg. This mass difference related to a specific SO₃-pmg cleavage.

When pmg was added to the disulfated analogue, we observed specific peaks that directly related to the number of sulfate groups (fig.1b). Three peaks separated by a 353.1 amu were clearly observed, corresponding to two consecutive losses of the pmg-SO₃ pair. The degree

of sulfation of the analytes could therefore be deduced from the number of observed species having a 353.1 amu difference.

Another issue was the isobaric nature existing between sulfated and phosphorylated peptides causing their MALDI-MS differentiation often fastidious. The reflectron positive ion mode MALDI analysis of phosphorylated peptides in the presence of pmg revealed a different behaviour compared to their disulfated analogues (fig.1c), with the unique formation of a non-specific pmg adduct (273.1 amu difference,) which demonstrated the ability of this method to differentiate easily phosphorylated and sulfated peptides.

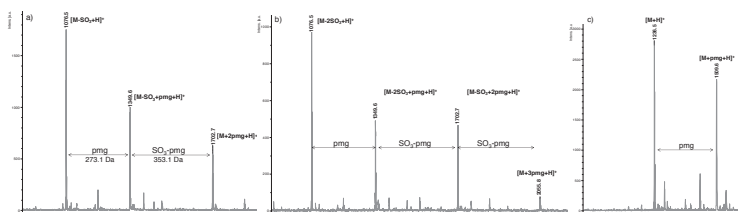


Figure 1: MALDI-mass spectra of a) monosulfated peptide H-Asn-Tyr(SO₃H)-Nle-Gly-Trp-Nle-Asp-Phe-NH₂; b) disulfated peptide H-Asn-Tyr(SO₃H)-Tyr(SO₃H)-Gly-Trp-Nle-Asp-Phe-NH₂; c) diphosphorylated peptide H-Asn-Tyr(PO₃H₂)-Tyr(PO₃H₂)-Gly-Trp-Nle-Asp-Phe-NH₂ in reflectron positive ion mode in the presence of pmg.

Finally, we demonstrated the general applicability of our method through the analysis of a tryptic digest of CCK-33, leading to the formation of two main fragments (M₁ and M₂ fig.2). Without pmg we could only detect the fragment of interest (M₂ fig.2a) under its desulfated form. In the presence of pmg, we could recover the information, detecting easily the intact fragment, carrying its sulfate-ester trapped by pmg (fig.2b).

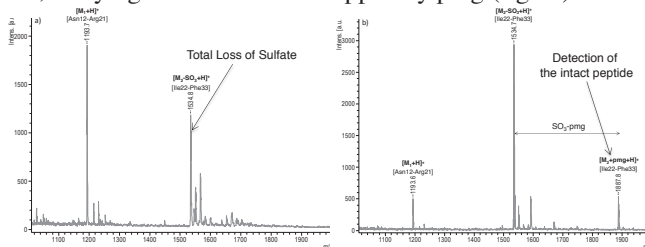


Figure 2: Reflectron positive ion MALDI-mass spectra of CCK-33 tryptic digest a) in the absence and b) in the presence of pmg.

In summary, we have developed a reliable strategy allowing direct detection of intact sulfated peptides by MALDI-MS positive reflectron mode using a non-covalent stabilizing agent / ionization enhancer. This technique can be performed in a routine mode and does not require any chemical treatment. Moreover, this methodology allows determination of the degree of sulfation and is discriminating over phosphopeptides [2]. It will certainly contribute to ongoing investigations of the sulfoproteome.

References

- [1] a) Ohara, K.; Jacquinet, J.C.; Jouanneau, D.; Helbert, W.; Smietana, M.; Vasseur J.J. *J. Am. Soc. Mass Spectrom.* **2009**, *20*, 131-137. b) Ohara, K.; Smietana, M.; Vasseur J.J. *J. Am. Soc. Mass Spectrom.* **2006**, *17*, 283-291.
- [2] Cantel, S.; Brunel, L.; Ohara, K.; Enjalbal, C.; Martinez, J.; Vasseur, J.J.; Smietana, M. *Proteomics*, **2012**, *12*, 2247-2257.

Alanine scan of Limnonectin peptides on the Overture™ robotic peptide library synthesizer

**James P. Cain, Michael A. Onaiyekan, Christina A. Chantell,
Mahendra Menakuru**

Protein Technologies, Inc. Tucson, Arizona, 85714

E-mail: info@ptipep.com

Introduction

The limnonectins are a newly discovered class of antimicrobial peptides found in the skin secretions of the frog *Limnonectes fujianensis* [1]. Two 16-mer peptides have been identified to date, but no structure-activity data has yet been published for these compounds. The Overture™ robotic peptide library synthesizer features extremely powerful and flexible peptide library design tools for generating overlapping peptide libraries, alanine-scan libraries, positional-scan libraries, combinatorial n-positional scan libraries, truncation libraries, T-cell truncated libraries and scrambled libraries.

We have performed an alanine scan on one of the peptides identified thus far, Limnonectin-1Fa (SFPFFPPGICKRLKRC-OH), using the library generation tools available with the Overture™. The results of the synthesis are shown. Other methods, such as truncation or positional scanning, may be useful in future studies.

Results and Discussion

All of the designed peptides were successfully synthesized, as indicated by LC-MS analysis (data not shown). Species with two, three, and four charges are most abundant in the mass spectra; unsurprising given that the native sequence contains four basic residues. The analytical HPLC traces of most of the peptides showed only one major peak with an average purity of 80.3% (Figure 1). In some cases a minor peak with retention time approximately four minutes after the main peak was found, but the impurity was not identified. The native form of the peptide contains a disulfide bridge between cysteines 10 and 16.

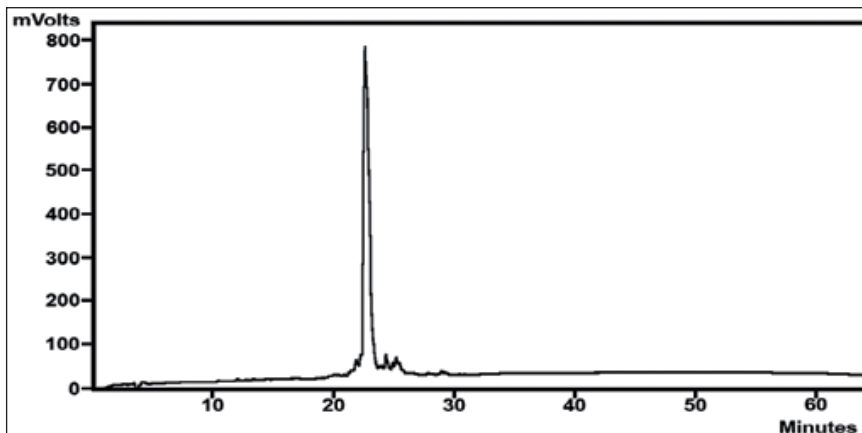


Fig. 1. Example crude HPLC trace: SIA analog.

We have synthesized an alanine-scan library of limonectin-1Fa analogs with an average crude purity of 80.3% on the Overture™ robotic peptide library synthesizer. This library was designed using the tools provided with the Overture™ Windows Utility software. The results of assays for antimicrobial activity could provide important new information regarding the structure-activity relationships for this series of compounds.

References

- [1] Wu Y *et al.* *Biochimie*, **2011**, 93, 981.

Antimicrobial activity of new analogues of Chrysopsin-1

Eleftheria Tsoumani¹, Athanassios Niarchos², Revekka Exarchakou¹,
Zoi Zagoriti², Vassiliki Mertziani¹, Nikos L. Assimomytis¹,
Konstantinos Poulas², Paul Cordopatis¹, Vassiliki Magafa¹

¹Laboratory of Pharmacognosy and Chemistry of Natural Products, Department of Pharmacy, University of Patras, GR-26500 Patras, Helas; ²Laboratory of Molecular Biology and Immunology, Department of Pharmacy, University of Patras, GR-26500 Patras, Hellas

E-mail: magafa@upatras.gr

Introduction

Antimicrobial peptides (AMPs) are an important component of innate immune system of most living organisms. They have recently gained much attention as new anti-infective drugs with new modes of actions and few or no side effects. Their antimicrobial spectrum covers Gram⁺ and Gram⁻ bacteria as well as fungi and certain viruses [1]. Fish have proven to be a rich source of antimicrobial peptides. Three *chrysopsin* peptides (*chrysopsin-1*, -2, -3) have been identified in the gills of the red sea bream, *Chrysophrys major*, which are all bactericidal to pathogenic bacteria at low concentrations [2]. They are cationic α -helical peptides, rich in histidine residues and all end in an unusual RRRH motif. However, in addition to its high antimicrobial potency, *chrysopsins* have considerable hemolytic activity. The development of new analogues which would preserve high antimicrobial potency, but would lack the undesired hemolytic activity, could be a useful tool with possible commercial and clinical applications. In the present study, we synthesized *chrysopsin-1*, *chrysopsin-1(ΔC)*, where the C-terminal RRRH sequence of *chrysopsin-1*, was deleted and two new analogues of *chrysopsin-1*, *chrysopsin-1(A)* and *chrysopsin-1(B)* with different ratios of Lys and His residues. For comparison purposes we have also synthesized *omiganan* (a 12-residue, peptide analogue of indolicidin). The antimicrobial properties of the above peptide analogues are currently testing in three Gram⁺ (*S. aureus*, *S. epidermidis*, *E. faecium*) and two Gram⁻ (*E. coli*, *P. aeruginosa*) bacteria. The goal is to identify the bacteriostatic activity of the analogues, by determining the minimum inhibitory concentrations (MIC), as well as the hemolytic or cytotoxic activity of the peptides.

Results and Discussion

All analogues were synthesized manually on the Rink Amide MBHA resin or the Sieber Amide as solid support by using standard coupling procedures and Fmoc/Bu^t strategy. The synthetic procedure did not present significant complications. The overall yield of the syntheses was in the range 55-68% (calculated on the amount of linker initially coupled to the resin). Higher yields were obtained using the Sieber Amide resin as solid support. ESI mass spectrometry confirmed that the purified products were indeed the desired peptides and analytical HPLC revealed a purity of over than 98% for the synthetic analogues. The physicochemical properties of the analogues are summarized in Table 1. All five peptides were active against the Gram⁻ *E. coli*. In detail, MICs of *Chrysopsin-1*, *Chrysopsin-1(A)*, *Chrysopsin-1(B)* and *Omiganan* peptides against *E. coli* were 6.25 μM, 10.0 μM, 12.5 μM

and 12.5 μM , respectively, while it exhibited a decreased susceptibility to truncated *Chrysopsin-1*(ΔC) peptide (MIC=50 μM) (Table 2). On the other hand, the Gram⁺ *S. aureus* was intermediately susceptible to *Chrysopsin-1* peptide, only (MIC=25 μM).

Table 1: Physicochemical properties of the synthesized analogues of *chrysopsin-1*.

	Analogues	HPLC*	TLC**	
			t_R (min)	R _{fA}
<i>Chrysopsin-1</i>	H-Phe ¹ -Phe ² -Gly ³ -Trp ⁴ -Leu ⁵ -Ile ⁶ -Lys ⁷ -Gly ⁸ -Ala ⁹ -Ile ¹⁰ -His ¹¹ -Ala ¹² -Gly ¹³ -Lys ¹⁴ -Ala ¹⁵ -Ile ¹⁶ -His ¹⁷ -Gly ¹⁸ -Leu ¹⁹ -Ile ²⁰ -His ²¹ -Arg ²² -Arg ²³ -Arg ²⁴ -His ²⁵ -CONH ₂	12.99	0.28	0.31
<i>Chrysopsin-1</i>(ΔC)	H-Phe ¹ -Phe ² -Gly ³ -Trp ⁴ -Leu ⁵ -Ile ⁶ -Lys ⁷ -Gly ⁸ -Ala ⁹ -Ile ¹⁰ -His ¹¹ -Ala ¹² -Gly ¹³ -Lys ¹⁴ -Ala ¹⁵ -Ile ¹⁶ -His ¹⁷ -Gly ¹⁸ -Leu ¹⁹ -Ile ²⁰ -His ²¹ -CONH ₂	12.55	0.22	0.25
<i>Chrysopsin-1</i>(A)	H-Phe ¹ -Phe ² -Gly ³ -Trp ⁴ -Leu ⁵ -Ile ⁶ -Lys ⁷ -Gly ⁸ -Ala ⁹ -Ile ¹⁰ -Lys ¹¹ -Ala ¹² -Gly ¹³ -Lys ¹⁴ -Ala ¹⁵ -Ile ¹⁶ -Lys ¹⁷ -Gly ¹⁸ -Leu ¹⁹ -Ile ²⁰ -Lys ²¹ -Arg ²² -Arg ²³ -Arg ²⁴ -Lys ²⁵ -CONH ₂	12.46	0.20	0.23
<i>Chrysopsin-1</i>(B)	H-Phe ¹ -Phe ² -Gly ³ -Trp ⁴ -Leu ⁵ -Ile ⁶ -Lys ⁷ -Lys ⁸ -Ala ⁹ -Ile ¹⁰ -Lys ¹¹ -Ala ¹² -Lys ¹³ -Lys ¹⁴ -Ala ¹⁵ -Ile ¹⁶ -Lys ¹⁷ -Lys ¹⁸ -Leu ¹⁹ -Ile ²⁰ -Lys ²¹ -Arg ²² -Arg ²³ -Arg ²⁴ -Lys ²⁵ -CONH ₂	12.34	0.19	0.21
<i>Omiganan</i>	H-Ile ¹ -Leu ² -Arg ³ -Trp ⁴ -Pro ⁵ -Trp ⁶ -Trp ⁷ -Pro ⁸ -Trp ⁹ -Arg ¹⁰ -Arg ¹¹ -Lys ¹² -CONH ₂	7.28	0.36	0.41

* Linear gradient from 5 to 85% acetonitrile (0.1% TFA) for 30 min, Nucleosil 100 C₁₈ column

** A) butan-1-ol/water/acetic acid/pyridine (4/1/1/2, v/v), B) butan-1-ol/water/acetic acid (4/5/1 v/v, upper phase)

Table 2: Minimum Inhibitory Concentration (MIC) of synthetic peptides against pathogenic bacteria. MICs of peptides are given in μM .

Minimum Inhibitory Concentration (μM)					
Bacteria	Analogues				
	<i>Chrysopsin-1</i>	<i>Chrysopsin-ΔC</i>	<i>Chrysopshin-1</i> (A)	<i>Chrysopshin-1</i> (B)	<i>Omiganan</i>
<i>E. coli</i>	6.25	50.0	10.0	12.5	12.5
<i>S. aureus</i>	25	R*	R*	R*	R*

* Bacteria were considered resistant (R) if no inhibition was observed.

More detailed experiments are in progress to study the effect of synthesized peptides on all mentioned bacteria. Preliminary results showed that *Chrysopsin-1*(ΔC) is, also, active against *S. epidermidis* (MIC=25 μM) and *E. faecium* (MIC=12.5 μM).

References

- [1] Hancock, R. E.; Scott, M. G. *Proc. Natl. Acad. Sci. USA* **2002**, *97*, 8856.
- [2] Iijima, N.; Tanimoto, N.; Emoto, Y.; Morita, Y.; Uematsu, K.; Murakami, T.; Nakai, T. *Eur. J. Biochem.*, **2003**, *270*, 675.

Antimicrobially active peptides isolated from fleshfly larvae

T. Neubauerová^a, T. Macek^a, M. Šanda^b, Z. Vobůrka^b, M. Macková^a

^a Institute of Chemical Technology Prague, Faculty of Food and Biochemical Technology, Department of Biochemistry and Microbiology, Prague, Czech Rep., ^bInstitute of Organic Chemistry and Biochemistry, Czech Academy of Sciences, Prague, Czech Rep.

E-mail:neubauet@vscht.cz

Introduction

The resistance of microbial pathogens has increased in the last years and represents a great problem for public health. There are very low chances to cure the multiresistant infections by existing antibiotics. This lead to development of new classes of antimicrobials with different mechanism of action and low toxicity. We focus on natural molecules of peptide nature.

Insects are a widespread and numerous class on the Earth due to the AMPs - quick defense mechanism of innate immunity. Approximately half of antimicrobial peptides were isolated from insects. Mapping of immunity of fruitfly *Drosophila melanogaster* (*Diptera*) revealed several AMPs with antibacterial and/or antifungal activity. We chose larvae of the fleshfly *Neobellieria bullata* from the same order to isolate the new AMPs.

Antimicrobial peptides (AMPs) are produced as a part of innate immunity in each organism – microorganisms, plants, invertebrates and also vertebrates. These peptides show broad spectrum of activity. They act against bacteria, yeasts, molds and some viruses. Most of them are small, cationic peptides. The activity depends on amphipaticity of secondary structure including α -helixes and β -sheets. These structures interact with cell membranes and cause pore forming or destruction. Some peptides can also attack submolecular structures (RNA, DNA) and cause cell death. Some AMPs of bacterial origin are well known food preservative nisin and antibiotic bacitracin. Several of the AMPs isolated from invertebrates are already at trials.

Results and Discussion

Fractions with antimicrobial activity were during chromatography eluted from 25 to 80% of acetonitrile. These fractions showed antibacterial (fractions 1 to 3) and also antifungal activity (fractions 4 to 6). For antimicrobial assay we used diffusion test.

Tricine electrophoresis showed the presence of low molecular peptides which were confirmed with MALDI-TOF analysis.

We isolated six active peptide fractions from haemolymph of larvae of the fleshfly and proved the presence of low molecular peptides with molecular masses between 2 and 16 kDa with antibacterial and antifungal activity. Edmann degradation provided unique N-terminal sequences (tab. 1). N-terminal sequencing exhibited similarity with odourant binding proteins 56d and 99c from *Drosophila melanogaster*, but their antimicrobial activity were not proved yet. Although some odourant-binding proteins 99b and 99c were found in antimicrobially active fractions earlier. [2] One sequence revealed similarity with predicted liver-expressed antimicrobial peptide 2-like from *Danio rerio* (zebrafish). Further characterization and complete sequencing is needed.

Tab. 1 Characterization of antimicrobially active fraction

	ACTIVITY	MW [kDa]	N-TERMINAL SEQUENCE
1	G+	2,17; 5,455	KKKTRKRTLPKN
2	G+	4,807, 6,507, 7,619	SRDDXPVQQVPFXXP
			SRAANXPVQDKKFN
3	G+	3,711, 9,621	AIAMAR
		4,060 6,820	DAGTVAKHPS
			DLSVGRFLHPEZENK
4	G+, fungi, (G-)	4,060; 4,478; 6,820 9,748	DHYEXGXNXESX (antimicrobial peptide 2- like <i>Danio rerio</i>) DVXTEG DLSVGRFLHPEYENK
5	G+, fungi	6 820, 13,223, 16,018	ANPQLSDEQKAV(K)E ANTIQLSDEQKAK (Obp 56d <i>Drosophila</i> <i>melanogaster</i>) EDEWTVKNGEQIKQI (Obp 99c - <i>Drosophila melanogaster</i>)
6	G+, fungi, (G-)	9,339	DAPASNPIDDLATI IKNAAG

Acknowledgements

Acknowledgements: this work was sponsored by the grants GAČR 305/09/H008, 522/09/1693.

References

- [1] Wang, P., Lyman, R. F., Shabalina S. A., Mackay T. F., Anholt R. R. *Genetics* **2007**, *177*, 1655.
- [2] Ciencialová, A., Neubauerová, T., Šanda, M., Šindelka, R., Cvačka, J., Vobůrka, Z., Buděšinský, M., Kašička, V., Sázelová, P., Šolínová, V., Macková, M., Koutek, B., Jiráček, J. *J Pept Sci* **2008**, *14*, 670.

Conformational properties of the spin-labeled tylopeptin B and heptaibin peptaibiotics based on PELDOR spectroscopy data

Maria Gobbo¹, Barbara Biondi¹, Marta De Zotti¹, Alexander D. Milov²,
 Yuri D. Tsvetkov², Alexander G. Maryasov², Fernando Formaggio¹,
 Claudio Toniolo¹

¹ICB, Padova Unit, CNR, Department of Chemistry, University of Padova, 35131 Padova,
 Italy; ²Institute of Chemical Kinetics and Combustion, 630090 Novosibirsk, Russian
 Federation

E-mail: barbara.biondi@unipd.it

Introduction

Information about the aggregation ability and 3D-structure of peptaibiotics, obtained by different spectroscopic methods (FTIR absorption, CD, FRET, NMR), is important to study the molecular mechanism of drug action and ion channel formation in detail. Here, pulsed electron-electron double resonance (PELDOR) spectroscopy, combined with site-directed spin labeling, was chosen as an effective method to determine the structural parameters of peptaibiotics under different conditions. PELDOR allows one to measure distances between spins in the 1.5-8 nm range. The method of double peptide labeling also provides information on a number of additional issues: distance distribution between labels, peptide conformation, onset of peptide aggregates, number of particles in the aggregate, peptide/membrane interactions, and peptide channels in membranes [1].

Results and Discussion

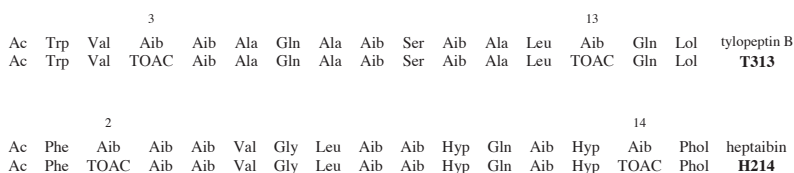
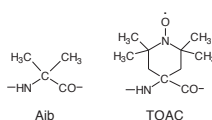


Fig. 1. Chemical structures of the Aib and TOAC residues and amino acid sequences of tylopeptin B, heptaibin, and the two double TOAC-labeled analogs synthesized and investigated in this work.

In this work, we extracted 3D-structural information on newly synthesized, medium-length, double spin-labeled peptaibiotics using PELDOR spectroscopy. In particular, we

investigated the magnetic dipole-dipole interactions between spin labels and the orientation selectivity effects. Specifically, the medium-length peptaibiotics tylopeptin B [2,3] and heptaibin [4], double spin-labeled with the nitroxyl probe TOAC (4-amino-1-oxyl-2,2,6,6-tetramethylpiperidine-4-carboxylic acid) (Figure 1), were investigated by means of X-Band PELDOR spectroscopy. This study was conducted on tylopeptin B labeled at positions 3 and 13 (**T313**) and heptaibin labeled at positions 2 and 14 (**H214**) in frozen glassy methanol solutions at 77 K. PELDOR data analysis was carried out using the theory developed for short interspin distances [1].

The distance distribution functions between spin labels for **T313** (maximum at 1.78 nm, half-width of 0.08 nm) and **H214** (maximum at 2.30 nm, half-width of 0.05 nm) were determined. The intramolecular distances observed between the labels allowed us to assign an essentially α -helical conformation to **T313** and a largely prevailing 3_{10} -helical structure to **H214** (Figure 2) under the aforementioned experimental conditions.

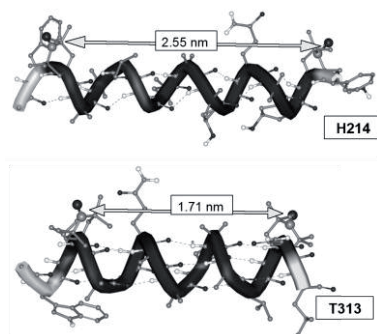


Fig. 2. Molecular models of **H214** in the 3_{10} -helical conformation and **T313** in the α -helical conformation. Intramolecular C=O...H-N H-bonds are indicated by dashed lines. The intramolecular, nitroxyl N...N distances are indicated.

References

- [1] Tsvetkov, Yu.D.; Milov, A.D.; Maryasov, A.G. *Russian Chem. Rev.* **2008**, *77*, 487.
- [2] Gobbo, M.; Poloni, C.; De Zotti, M.; Peggion, C.; Biondi, B.; Ballano, G.; Formaggio, F.; Toniolo, C. *Chem. Biol. Drug Des.* **2010**, *75*, 169.
- [3] Gobbo, M.; Merli, E.; Biondi, B.; Oancea, S.; Toffoletti, A.; Formaggio, F.; Toniolo, C. *J. Pept. Sci.* **2012**, *18*, 37.
- [4] De Zotti, M.; Biondi, B.; Peggion, C.; Park, Y.; Hahm, K.-S.; Formaggio, F.; Toniolo, C. *J. Pept. Sci.* **2011**, *17*, 585.

***De novo* design of short peptides with antimicrobial activity and the effect of acyl conjugation**

**Anna Macůrková, Rudolf Ježek, Gabriela Kroneislová, Patra Lovecká,
Tomáš Macek, Martina Macková**

*Institute of Chemical Technology, Prague, Faculty of Food and Biochemical Technology,
Department of Biochemistry and Microbiology, Technická 3, 166 28 Prague, Czech
Republic*

anna.macurkova@vscht.cz

Introduction

Animals and plants have coexisted with microbes throughout their evolution, sometimes to their mutual benefit, often in open war. Gene-encoded antimicrobial peptides (AMPs) are an ancient and pervasive component of the innate defense mechanisms they have developed to control the natural flora and combat pathogens [1,2]. Nosocomial infections have drawn much attention from the medical and scientific communities. Therefore the development of new and more effective antimicrobials which use novel mechanisms of action is urgently needed. The alternative is mediated by AMPs, many of these peptides appears to act via the same mechanism like antibiotics, but many of them act via a specific, but non receptor-mediated, permeabilization of microbial membranes. They fold into a variety of secondary structures such as α -helices, β -sheets or they may form cycles and hairpin loops. Despite their diversity, most AMPs share common features that include a net positive charge and an amphipathic character [3,4]. Certain AMPs show affinities not only to bacteria but also to higher eukaryotic cells [5]. Structure-activity relationship studies with these peptides indicate that changes in the amphipathicity could be used to dissociate the antimicrobial activity from the haemolytic activity and toxicity [6].

In this study we report on the *de novo* designed synthetic cationic peptides and the effect of N-terminal acylation on possible antimicrobial activity and toxicity. We designed three synthetic hexapeptides (SHPs) with amphipathic character and a positive net charge. Design of peptides was primarily based on relative frequency of occurrence of amino acids in antimicrobial peptides with requested properties such as length, activities or conformation. This selection was based on statistical data gained from databases [7,8]. The helical peptides are generally more active, the sequence of amino acids was built to form peptide with helical conformation. Many sources demonstrated C-terminal amidation [9] or N-terminal acylation to increase of activity [10]. Our study was further focused on description of biological properties such as antimicrobial and haemolytic activity or toxicity, and their changes resulted from subsequent modifications.

Results and Discussion

The most perspective sequences appeared to be LVKRA -NH_2 (SHP-1.1), LVKGAR -NH_2 (SHP-2.1) and GVLKRA -NH_2 (SHP-3.1). For testing of possible increase of antimicrobial activity N-terminal acylation were chosen palmitic acid (SHP-x.2) and lithocholic acid (SHP-x.3). SHPs were synthesized by SPPS methodology on Rink amide MBHA resin using Fmoc amino acids. N-terminal acylation was the final synthetic step. Crude peptides

were purified by RP-HPLC in gradient of ACN containing 0.1% TFA. Identification of fractions was carried out by MALDI-TOF MS.

All prepared synthetic hexapeptides displayed antimicrobial activity against the tested microorganisms, Gram-positive, Gram-negative bacteria and fungi. Minimal inhibitory concentration (MIC) was determined by spectrophotometric measurement of growth of treated and untreated microbial cells. The highest activity was detected against Gram-positive bacteria, especially against *Staphylococcus aureus*, *Bacillus subtilis* and *Micrococcus luteus*. Unmodified SHPs displayed only low level of activity, MIC values were higher than 1 mg.ml⁻¹. The peptides with N-terminal acylation provided more interesting results. In most cases active concentrations decreased under 100 µg.ml⁻¹. MIC values of these peptides were determined ranging from 7 to 80 µg.ml⁻¹. In case of bacteria acylation by palmitic acid and lithocholic acid had the same result. In case of Fungi, acylation by palmitic acid had no effect, while peptides with lithocholic acid proved to be active against *Candida tropicalis* with MIC value in range 30-60 µg.ml⁻¹. Different activities may be explained by different composition of the membrane of prokaryotic and eukaryotic cells.

Haemolytic activity of the prepared SHPs was not demonstrated in concentration equal to MIC value. Toxicity assay, realized by measurement of electrical impedance across interdigitated micro-electrodes integrated on the bottom of tissue culture, of peptides with lithocholic acid demonstrated negative effect against human liver hepatocellular carcinoma cell line (HepG2) and human embryonic kidney (Hek293T) cells cultivated *in vitro*. Growth inhibition effect of SHPs-x.3 in concentrations ranging from 50 to 200 µg.ml⁻¹ was in average equal to 25%, resp. 60%.

The first screening for mechanism of antimicrobial action of acylated SHPs, based on measurement of inhibition effect on metabolizing and nonmetabolizing cells, showed for two of the prepared peptides relationship to metabolism, one peptide probably act via pore formation. These assumptions will be subject to further investigation.

Acknowledgements

This project is supported by projects GACR 522/09/1693 and 305/09/H008, from specific university research MSMT no. 21/2012 and from IGA project no. A2_FPBT_2012_037

References

- [1] Andreu, A.; Rivas, L. *Biopolymers* **1998**, *47*, 415-433.
- [2] Boman, H. G. *Ann. Rev. Immunol.* **1995**, *13*, 61-92.
- [3] Hancock, R. E. W. *Drugs* **1999**, *57*, 469-473.
- [4] Oren, Z.; Shai, Y. *Biopolymers* **1998**, *47*, 451-463.
- [5] Hwang, P. M.; Vogel, H. J. *Biochem. Cell. Biol.* **1998**, *76*, 235-246.
- [6] Kondejewski, L. H.; Farmer, S. W.; Wishart, D. S.; Kay, C. M.; Hancock, R. E. W.; Hodges, R. S. *J. Biol. Chem.* **1996**, *271*, 25261-25268.
- [7] Wang, G.; Li, X.; Wang, Z. *Nucleic Acids Res.* **2009**, *37*, D33-D937.
- [8] Tossi, A.; Tarantino, C.; Romeo, D. *Eur. J. Biochem.* **1997**, *250*, 549-558.
- [9] Dos Santos Cabrera, M.P.; Arcisio-Miranda, M.; Broggio Costa, S.T.; Konno, K.; Ruggiero, J.R.; Procopio, J.; et al. *J. Pept. Sci.* **2008**; *14*, 661-669.
- [10] Radzishewsky, S.I.; Rotem, S.; Zaknoon, F.; Gaidukov, L.; Dagan, A.; Mor, A. *Antimicrob. Agents Chemother.* **2005**, *49*, 2412-2420.

Design and synthesis of amphipathic α -helical peptide models for the development of new antimicrobial agents

Asimina Marianou, Alexandra Balliu, Marianna Sakka, Anna-Irini Koukkou, Maria Sakarellos-Daitsiotis, Eugenia Panou-Pomonis

*Peptide Chemistry Research Laboratory, Section of Organic Chemistry and Biochemistry,
Department of Chemistry, University of Ioannina, 45110 Ioannina, Greece*

E-mail: minamarianou@gmail.com

Introduction

The widespread use of antibiotics led to the development of antibiotic-resistant microbial strains, resulting in an urgent need for new antimicrobial agents. Cationic antimicrobial peptides (AMPs) are considered one reasonable alternative for conventional antibiotics, hence bacterial target of the peptides is the cytoplasmic membrane [1]. Synthetic cationic peptides are a class of positively charged small peptides with amphipathic conformation. AMPs have broad-spectrum of action against both Gram-negative and Gram-positive bacteria as well as fungi, and viruses.

Our approach is based on the design, synthesis and study of cationic helical peptides of the following type:

X-RWLRLLLRLLRL-NH₂, X-RWLRL-2-Atd-LRLLRL-NH₂

where X = H-, Ac-, td- (tetradecanoic-)

X-RWLRLWRFLRL-NH₂, X-RWLRLWRRFLRL-NH₂, X-RWLKLLWRFLKL-NH₂,
X-KWLKLLWKFLKL-NH₂ where X = H-, Ac-, Ahx- (aminohexanoic-)

in order to develop new antibiotics.

The above peptides were tested for their antimicrobial activity against Gram- negative bacteria, Gram-positive bacteria and fungi. The peptides were also tested for their hemolytic activity and proteolytic stability. The conformational characteristics of the peptide models were evaluated by circular dichroism spectroscopy (CD).

Results and Discussion

The synthesis of the peptides was carried out by the stepwise solid-phase synthesis procedure, SPPS on a Rink Amide AM resin using the Fmoc methodology. Fmoc groups were removed using 20% piperidine in dimethyl - formamide (DMF). The coupling reactions were performed using a molar ratio of Fmoc-amino acid/HBTU/HOBt/DIEA/resin 3/3/3/6/1. Crude linear peptides were purified by RP-HPLC while the purity of the peptides was checked by analytical HPLC. The correct molecular masses were confirmed by electrospray ionization mass spectrometry (ESI-MS).

➤ Antimicrobial activity

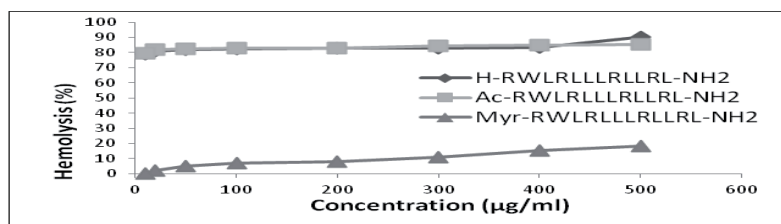
The peptides were tested for their antimicrobial activity against Gram-negative bacteria: *Escherichia coli* DH5a, *Pseudomonas aeruginosa* PAO, *Zymomonas mobilis* ATCC 10988

and Gram-positive bacteria: *Mycobacterium smegmatis* mc²155, *Bacillus subtilis* DELTA. The antimicrobial activities were expressed as the minimum inhibitory concentration (MIC) at which 100% inhibition of growth was observed.

Table 1. Antimicrobial activity: minimal inhibitory concentration (MIC) (µg/ml).

AMPs	Microorganisms	Gram (-)		Gram (+)			Fungi
		<i>E.coli</i> DH5a	<i>P. Aeruginosa</i> PAO	<i>Z. Mobilis</i> ATCC 10988	<i>B. Subtilis</i> DELTA	<i>M. Smegmatis</i> mc ² 155	<i>Candida parapsilosis</i>
	H-Arg-Trp-Leu-Arg-Leu-Leu-Leu-Arg-Leu-Leu-NH ₂	100	30	50	-	100	300
	Ac-Arg-Trp-Leu-Arg-Leu-Leu-Leu-Arg-Leu-Leu-NH ₂	200	50	100	200	400	400
	H-Arg-Trp-Leu-Lys-Leu-Leu-Trp-Arg-Phe-Leu-Lys-Leu-NH ₂	150	100	20	200	40	100

➤ Hemolytic assay



➤ Proteolytic stability

The enzymatic degradation with trypsin was carried out at 37°C for 4 h, proteolysis stopped by adding an appropriate trypsin inhibitor at different time points and the samples were tested for their residual antimicrobial activity.

➤ Conformational studies

CD spectra of peptides (10⁻⁴M) in PBS (pH 7), TFE/H₂O (50/50), 8 mM SDS and 5 mM C₁₄PC indicate that the peptides adopt helical characteristics.

➤ Conclusions

Almost all peptides exhibited antimicrobial activity against Gram (-) bacteria *P. aeruginosa* PAO and *Z. mobilis* ATCC 10988. The peptide H-Arg-Trp-Leu-Arg-Leu-Leu-Leu-Arg-Leu-Leu-Arg-Leu-NH₂ exhibited MIC (30 µg/ml) against Gram (-) bacterium *P. aeruginosa* PAO and the peptide H-Arg-Trp-Leu-Lys-Leu-Leu-Trp-Arg-Phe-Leu-Lys-Leu-NH₂ exhibited MIC (20 µg/ml) against Gram (-) bacterium *E. coli* DH5a. The last one was also stable to proteolysis and it was not toxic at MIC value.

References

1. Powers, J.P.; Hancock, R. *Peptides*. **2003**, *24*, 1681–1691.

Development of human Cathelicidin LL-37-derived short antimicrobial peptides with prokaryotic selectivity, LPS-neutralizing activity and protease stability

Song Yub Shin,^{a,*} Yong Hae Nan,^a Jeong-Kyu Bang^b

^a*Department of Cellular and Molecular Medicine, School of Medicine Chosun University, Gwangju 501-759, Republic of Korea;* ^b*Division of Magnetic Resonance, Korea Basic Science Institute, Chungbuk 363-883, Republic of Korea*

**E-mail: syshin@chosun.ac.kr*

Introduction

LL-37 is the only antimicrobial peptide (AMP) of the human cathelicidin family.¹ In addition to potent antimicrobial activity, LL-37 is known to have the potential to inhibit lipopolysaccharide (LPS)-induced endotoxic effects.¹ In this study, to develop LL-37-derived short AMPs with prokaryotic selectivity and LPS-neutralizing activity, a series of amino acid-substituted analogs (Table 1) based on IG-19 (residues 13-31 of LL-37) were synthesized. To provide the stability to proteolytic digestion of the designed peptides, we synthesized the diastereomeric peptides (a4-W1-D and a4-W2-D) with D-amino acid substitution at positions 3, 7, 10, 13 and 17 of a4-W1 and a4-W2, respectively and their enantiomeric peptides (a4-W1-E and a4-W2-E) composed D-amino acids.

Results and Discussion

Analog a4 showed the highest prokaryotic selectivity, but much lower LPS-neutralizing activity compared to LL-37. The analogs, a5, a6, a7 and a8 with higher hydrophobicity displayed LPS-neutralizing activity comparable to that of LL-37, but much lesser prokaryotic selectivity. These results indicated that the proper hydrophobicity of the peptides is crucial to exert the amalgamated property of LPS-neutralizing activity and prokaryotic selectivity. To increase LPS-neutralizing activity of the analog a4, we synthesized Trp-substituted analogs (a4-W1 and a4-W2), in which Phe⁵ or Phe¹⁵ of a4 is replaced by Trp. Despite their same prokaryotic selectivity, a4-W2 displayed much higher LPS-neutralizing activity compared to a4-W1. This result suggested that the effective site for Trp-substitution when designing novel AMPs with higher LPS-neutralizing activity, without a remarkable reduction in prokaryotic selectivity, is the amphipathic interface between the end of the hydrophilic side and the start of the hydrophobic side rather than the central position of the hydrophobic side in their α -helical wheel projection. The diastereomeric peptides (a4-W1-D and a4-W2-D) exhibited the best prokaryotic selectivity and effective protease stability, but no or less LPS-neutralizing activity. In contrast, D-enantiomeric peptides (a4-W1-E and a4-W2-E) of a4-W1 and a4-W2 possessed not only more improved prokaryotic selectivity and retained LPS-neutralizing activity compared to a4-W2 but also protease stability (Table 1 and Fig. 1). Taken together, D-enantiomeric peptides (a4-W1-E and a4-W2-E) can serve as promising templates for the development of therapeutic agents for the treatment of endotoxic shock and bacterial infection.

Table 1. Prokaryotic selectivity and LPS-neutralizing activity of the peptides.

Peptides	Amino acid sequences	GM ^a (μ M)	MHC ^b (μ M)	TI ^c	% TNF- α Inhibition ^d
LL-37	LLGDFFRKSKEKIGKEFKR IVQRIKDFLRNLVPRTES	6.7	6.7	1.0	83.3 \pm 1.8
IG-19	IGKEFKRIVQRIKDFLRNL	7.3	21.6	2.9	47.7 \pm 4.9
a1	IGKKFKRIVQRIKDFLRNL	4.3	13.8	3.2	38.4 \pm 0.9
a2	IGKKFKRIVQRIKKFLRNL	5.3	11.2	2.1	9.1 \pm 1.7
a3	IGKKFKRIVQRIKKFLRKL	4.7	23.7	5.0	9.9 \pm 3.1
a4	IGKKFKRIVKRIKKFLRKL	4.7	33.2	7.1	33.5 \pm 1.4
a5	IGKLFKRIVQRIKKFLRNL	6.0	3.0	0.5	82.8 \pm 1.2
a6	IGKLFKRIVQRILKFLRNL	6.3	1.2	0.2	69.6 \pm 0.7
a7	IGKLFKRIVKRILKFLRKL	5.0	1.1	0.2	74.9 \pm 2.4
a8	ILKLFKRIVKRILKFLRKL	6.7	1.6	0.2	79.8 \pm 1.6
a4-W1	IGKKWKRIVKRIKKFLRKL	3.3	9.2	2.8	26.1 \pm 3.5
a4-W2	IGKKFKRIVKRIKKWLRKL	3.0	8.4	2.8	69.8 \pm 3.0
a4-W1-D	IGKKWKRIVKRIKKFLRKL	3.3	100 <	60.6	20.4 \pm 2.7
a4-W2-D	IGKKFKRIVKRIKKWLRKL	2.7	100 <	74.1	10.7 \pm 3.4
a4-W1-E	igkkwkrivkrikkflrkl	3.3	11.6	3.5	66.1 \pm 1.4
a4-W2-E	igkkfkrivkrikkwlrkl	3.3	10.8	3.3	72.6 \pm 0.7

Small letter indicates D-amino acids.

^aThe geometric mean (GM) of the MIC values against six bacterial strains.

^bMHC (minimal hemolytic concentration) is the concentration that induces 10% hemolysis.

^cTherapeutic index (prokaryotic selectivity): The ratio of the MHC (μ M) to the GM (μ M).

^dThe percent inhibition of TNF- α release at the peptide concentration of 5.0 μ M.

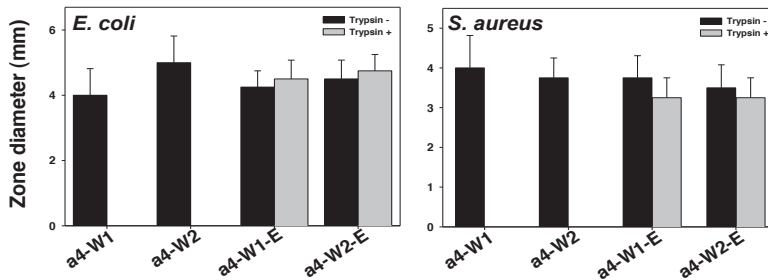


Fig. 1. Inhibition of antimicrobial activity of the peptides by tryptic digestion assessed using the radial diffusion assay

Acknowledgments

This work was supported by the grant from the Korea Research Foundation (KRF-2011-0009039).

References

- [1] Durr, U. H.; Sudheendra, U. S.; Ramamoorthy, A. *Biochim. Biophys. Acta* **2006**, 1758, 1408-1425.

Enhanced anti-staphylococcal activity of an analog derived from the 107-115 human lysozyme fragment.

Nancy B. Iannucci^{1,2}, Rodrigo González¹, Fanny Guzmán³,
Osvaldo Cascone¹, Fernando Albericio^{4,5,6}

¹School of Pharmacy and Biochemistry, University of Buenos Aires, Argentina.

²Therapeutic Peptides Research and Development Laboratory, Chemo-Romikin, Buenos Aires, Argentina. ³Biotechnology Nucleus, Pontifical University of Valparaiso, Chile.

⁴Institute for Research in Biomedicine, Barcelona Science Park, Spain. ⁵CIBER-BBN, Networking Centre on Bioengineering, Biomaterials and Nanomedicine, Barcelona Science Park, Spain. ⁶Department of Organic Chemistry, University of Barcelona, Spain

E-mail: iannucci@ffyb.uba.ar

Introduction

Original practical approaches for the discovery of new anti-infective drugs are well-regarded by the pharmaceutical industry in order to overcome the advance of microbial resistance. Antimicrobial peptides (AMPs) are inspiring molecules for the rational design of new antibiotic compounds [1]. In our previous work, we introduced a new compound derived from the 107-115 human lysozyme (hLz) fragment with 4- and 20-fold increase in antimicrobial activity against *Escherichia coli* ATCC 25922 and *Staphylococcus aureus* ATCC 29213, respectively. This analog was developed by a straightforward approach involving the sequential Ala-substitution by activity-relevant amino acids in the lead peptide. Peptide safety was assessed by hemolytic activity, resulting significant at 10-fold its minimal anti-staphylococcal concentration [2]. In order to determine the effectiveness of this peptide, the activity against a drug-resistant strain, methicillin-resistant *Staphylococcus aureus* (MRSA) ATCC 43300, was assayed. Furthermore, the bactericidal power of the peptide was experimentally confirmed against both *Staphylococcus aureus* strains.

Results and Discussion

107-115 hLz and the improved analog, [K¹⁰⁸W¹¹¹] 107-115 hLz sequences are shown:

107

115

RA**W**V**A****W****R****N****R** 107-115 hLz

RK**W**V**W****R****N****R** [K¹⁰⁸W¹¹¹] 107-115 hLz

The additional positive charge near the *N* terminus (108) and the extra hydrophobic residue at the centre of the molecule (111) determines an amphiphilic balance in the novel peptide which might enhance the anti-staphylococcal activity through the interaction with the plasma membrane. This amino acidic constellation in cationic AMPs is in agreement with other reports [3].

Minimal inhibition concentrations (MICs) values obtained for both peptides against *E. coli* ATCC 25922, *S. aureus* ATCC 29213, and *MRSA* ATCC 43300 are compared in the following table:

Peptide	MIC <i>E. coli</i> [μ M]	MIC <i>S. aureus</i> [μ M]	MIC <i>MRSA</i> [μ M]
107-115 hLz	412	206	412
[K ¹⁰⁸ W ¹¹¹]107-115 hLz	90	11	22

The increase in the anti-staphylococcal activity of [K¹⁰⁸W¹¹¹]107-115 hLz against *S. aureus* ATCC 29213 was conserved against *MRSA* 43300 (20-fold compared to 107-115 hLz). Bacterial plasma membrane might be the AMP target since its enhanced activity was maintained against both Gram positive bacteria, despite its sensitivity to methicillin, a classic antibiotic with an intracellular target. Its bactericidal effect confirms this hypothesis because the damage at the plasma membrane might be lethal.

Bactericidal activity results showed irreversible inhibition growth when samples were incubated with 0,1 mg/mL of [K¹⁰⁸W¹¹¹] 107-115 hLz at 37°C for 1 h. Afterwards, pellets were extensively washed, resuspended, and cultivated in Muller Hinton plates at 37°C for 21h. Washing controls were included.

Since the antimicrobial activity of [K¹⁰⁸W¹¹¹]107-115 hLz might be mediated through the interaction with the bacterial plasma membrane, it was conserved against the *MRSA* strain. *MRSA* display resistance through the modification of the methicillin intracellular target, the penicillin binding protein. This resistance mechanism resulted useless against peptide [K¹⁰⁸W¹¹¹]107-115 hLz, thus being an effective anti-staphylococcal agent. This result encourages further investigation for the development of an active pharmaceutical ingredient.

Acknowledgments

NBI and OC are researchers from CONICET. Authors thank Chemo Romikin peptide synthesis facilities.

References

- [1] Iannucci N.; González R.; Cascone O.; Albericio F. In: *Science against microbial pathogens: communicating current research and technological advances*. A. Méndez-Vilas (Ed) **2011**, 2, 961.
- [2] González R.; Albericio F.; Cascone O.; Iannucci NB. *J. Pept. Sci.* **2010**, 16, 424.
- [3] Ibrahim HR, Thomas U, Pellegrini A. *J. Biol. Chem.* **2001**; 276: 43767.

Enhancement of bacterial outer membrane binding action of the antimicrobial peptide magainin 2 by minimal amino acid substitution

Satoshi Fukuoka,¹ Lena Heinbockel,² Yani Kaconis,² Jörg Andrä,^{2,3}
Manfred Rössle,⁴ Thomas Gutschmann,² Klaus Brandenburg²

¹National Institute of Advanced Industrial Science and Technology (AIST), Takamatsu, 761-0395, Japan; ²Forschungszentrum Borstel, Leibniz-Zentrum für Medizin und Biowissenschaften, D-23845 Borstel, Germany; ³Hamburg University of Applied Sciences, Department of Biotechnology, D-21033 Hamburg, Germany; ⁴European Molecular Biology Laboratory EMBL, c/o DESY, D-22603 Hamburg, Germany

E-mail: fukuoka-s@aist.go.jp

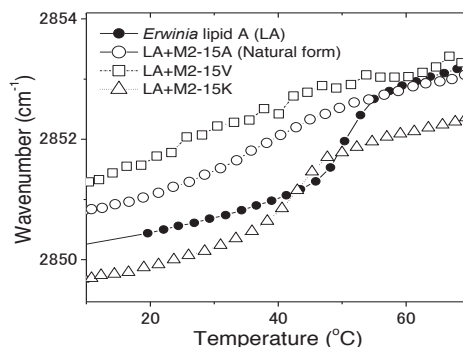
Introduction

The neutralization of endotoxins (lipopolysaccharide, LPS) by suitable compounds has been shown to be a key step in the treatment of infectious diseases, in particular in the case of Gram-negative bacteria. The active endotoxic center of LPS is lipid A (LA), its lipophilic part. An effective antimicrobial peptide against Gram-negative bacteria is magainin 2 (M2, GIGKFLHSAKKFGKAFVGEIMNS-NH₂), which was originally found in the skin of an African frog [1]. Here, we studied the interaction of hexa-acyl bisphosphoryl lipid A [2] prepared from *Erwinia carotovora* LPS with M2 and magainin two synthetic variants of M2 with selected substitutions in the amino acid pattern (A15V, A15K). By using Fourier-transform infrared spectroscopy, the gel to liquid crystalline phase transition of the acyl chains of lipid A [3], as well as the profile of the secondary structure [4] of the peptides was investigated.

Results and Discussion

The gel to liquid crystalline phase transition of LA aggregates was affected by magainin 2 amide M2 and its amino acid substituted analogues. (Fig. 1) The sharpness of the phase transition at T_m decreased in the presence of V-substituted peptide. Among the peptides tested, the most effective substituting position was at position 15. Furthermore, the K-substituted peptide exhibited similar phase transition curve to that of lipid A with a slight lower shift of the T_m value.

Fig. 1 Gel to liquid crystalline phase transition behavior of lipid A in the presence of M2 or its analogues as measured by FTIR. Lipid A and peptides (20 mM, 1:1 by molar ratio) were dispersed in 20 mM HEPES buffer (pH 7.0) and sonicated. FTIR measurements were performed by placing the sample in between CaF₂ crystals.



The FTIR-ATR spectra in the range of amide band I and II (Fig. 2) indicates that the native M2 peptide adopts an α -helical structure (peak around 1680 cm^{-1}), whereas the V-substituted peptide adopt a β -sheet like structure (main peak around 1620 to 1630 cm^{-1}). The change in secondary structure may explain the different effect on the phase transition behavior of lipid A. The K-substituted peptide which has an additional positive charge, binds stronger to the negatively charged part of the lipid A. This interaction seems to be resulted in the dominant α -helix structure (Fig. 2C).

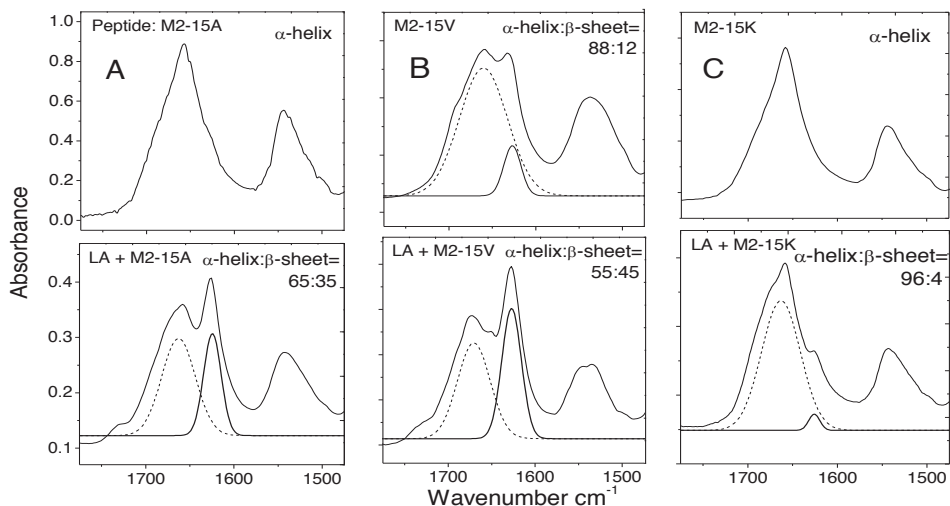


Fig. 2 Amide I band peak splitting of the M2-substituted analogues (top) and lipid A-peptide mixtures (bottom). A, magainin 2 natural form (15A); B, 15V; C, 15K; ----, α -helix; —, β -sheet. The underlying secondary structures were analyzed by band shape analysis.

Conformation alteration by differences in secondary structures - different hydrogen bonding - correlates with differences of the peptide binding to lipid A, which goes along with changes in biochemical and biophysical parameters.

Acknowledgments

The authors are indebted to the German ministry BMBF (project 01GU0824) for financial support. Part of this work was supported by FY2010 Researcher Exchange Program between JSPS and DAAD, Japan-Germany Research Cooperative Program, and Grant-in-Aid for Scientific Research (KAKENHI 21550168).

References

- [1] Zasloff, M. *Proc. Natl. Acad. Sci. U S A* **1987**, *84*, 5449.
- [2] Fukuoka, S.; Brandenburg, K.; Müller, M.; Lindner, B.; Koch, M. H. J.; Seydel, U. *Biochim. Biophys. Acta* **2001**, *1510*, 185.
- [3] Fukuoka, S.; Howe, J.; Andrä, J.; Gutsmann, T.; Rössle, M.; Brandenburg, K. *Biochim. Biophys. Acta* **2008**, *1778*, 2051.
- [4] Tiewsiriri, K.; Fischer, W. B.; Angsuthanasombat, C. *Arch. Biochem. Biophys.* **2009**, *482*, 17.

Interaction of the antimicrobial peptide gomesin with model membranes

T. M. Domingues¹, B. Mattei¹, J. Seelig², K. R. Perez¹, K. A. Riske¹, A. Miranda¹

¹*Departamento de Biofísica, Universidade Federal de São Paulo, São Paulo, Brazil;*

²*Biozentrum, University of Basel, Div. of Biophysical Chemistry, Basel, Switzerland*

tmdomingues@unifesp.br

Introduction

Antimicrobial peptides are present in the immune system of flora and fauna, and have attracted attention due to their great potential of lytic action against membranes of a wide range of microorganisms. Here we study the interaction of the antimicrobial peptide gomesin (Gm), isolated from the Brazilian spider *Acanthoscurria gomesiana* [1,2], with large unilamellar vesicles (LUVs) composed of palmitoyl oleoyl phosphatidylcholine (POPC) and palmitoyl oleoyl phosphatidylglycerol (POPG) (1:1 mol:mol). Former studies with optical microscopy of giant vesicles indicated that gomesin disrupts the membrane via the carpet model [3]. In the present work, isothermal titration calorimetry (ITC) is used to measure the reaction heat from the binding of gomesin to LUVs. In parallel, light scattering and optical microscopy are used to assess peptide-induced vesicle aggregation. The ability of gomesin to alter membrane permeability is examined with fluorescence spectroscopy measurements of leakage of carboxyfluorescein (CF) entrapped in the inner volume of LUVs. LUVs coated with PE-PEG lipids are also used to study the influence of peptide-induced vesicle aggregation in the lytic activity of gomesin.

Results and Discussion

We show that the interaction of gomesin with charged LUVs (1:1 POPC:POPG) is an exothermic process accompanied by vesicle aggregation (Figure 1). ITC data has a sigmoidal behavior (Figure 1a, continuous line) and exhibits a decrease in the magnitude of the heat per injection (Figure 1b) with the increase of the lipid-to-peptide molar ratio, because less peptide is available for binding after each injection. The sum of the heat obtained during the whole process gives the total enthalpy, $\Delta H = -9.9$ kcal/mol of peptide. Figure 1a also displays the intensity of 90° light scattering obtained as gomesin is titrated with LUVs (dotted line). The light scattering increases substantially at the beginning of each injection, indicating a large extent of vesicle aggregation, followed by a steady decrease in light scattering, which is explained by the sedimentation of the micrometer-sized aggregates formed (see optical micrograph of the lipid dispersion with gomesin in Figure 2a). Addition of 3 mol% PE-PEG to the membrane virtually abolishes peptide-induced vesicle aggregation, as seen in Figure 2b. ITC data shows that the presence of 3 mol% PE-PEG causes a change in the calorimetric profile: the exothermic reaction heat exhibits a steeper dependence with the lipid-to-peptide molar ratio, indicating a much higher affinity of gomesin to coated surfaces, and the appearance of an additional small endothermic component at the end of the process, whose origin remains unclear. The total

enthalpy change decreases to -8.4 kcal/mol of peptide in the presence of 3 mol% PE-PEG, due to the appearance of the endothermic contribution.

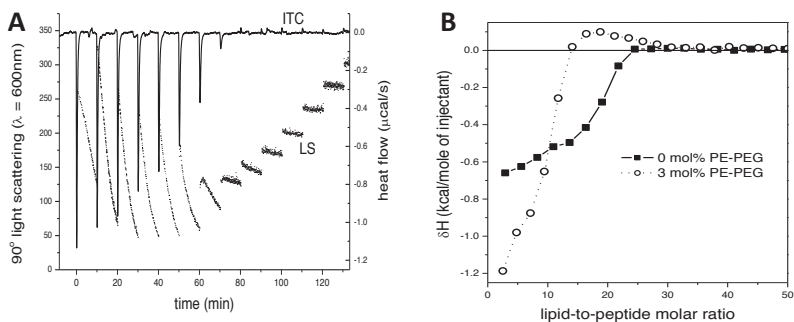


Figure 1. a) Heat flow measured with ITC (continuous line), and intensity of 90° light scattering ($\lambda = 600\text{ nm}$) (dotted line). 5 μL -Aliquots of a dispersion of 11.7 mM 1:1 POPC:POPG LUVs (buffer HEPES 30 mM with 100 mM NaCl) were injected into 15 μM gomesin every 10 minutes. b) Integrated heat per injection as a function of the lipid-to-peptide molar ratio measured with ITC. 1:1 POPC:POPG LUVs with 0 (straight line) and 3 mol% PE-PEG (dashed line).

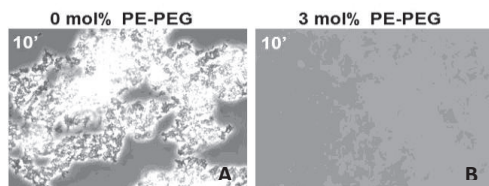


Figure 2. Phase contrast optical microscopy images of 37 μM 1:1 POPC:POPG with a) 0 and b) 3 mol% PE-PEG LUVs in the presence of 15 μM gomesin (buffer HEPES 30 mM with 100 mM NaCl).

Fluorescence spectroscopy of initially entrapped carboxyfluorescein shows that gomesin induces substantial vesicle leakage (> 77% at 10 mol/mol lipid-to-peptide). The lytic activity was stronger against vesicles with 3 mol% PE-PEG (98%) than without PE-PEG (77%), probably due to a higher affinity of gomesin to coated membranes.

We conclude that binding of gomesin to negatively charged membranes is mainly an exothermic process accompanied by vesicle aggregation and membrane perturbation. Surface coating with PE-PEG largely attenuates vesicle aggregation and increases the affinity of gomesin to the membrane surface. Since the enthalpic contribution changes only slightly when PE-PEG is added, the increase in affinity is explained by a different entropic contribution in the presence and absence of PE-PEG.

Acknowledgments

This work was supported by FAPESP, CNPq, CAPES and INCT-FCx.

References

- [1] Silva, P.I.; Daffre, S.; Bulet, P. *J. Biol. Chem.* **2000**, *275*, 33464-70.
- [2] Fazio, M.A.; Oliveira, V.X.; Bulet, P.; Miranda, M.T.M.; Daffre, S.; Miranda, A. *Biopolymers* **2006**, *84*, 205-18.
- [3] Domingues, T.M.; Riske, K.A.; Miranda, A. *Langmuir* **2010**, *26*, 11077-84.

Lipopeptides – synthesis and their properties

**Monika Kukowska¹, Krystyna Dzierzbicka¹, Łukasz Nowicki²,
Monika Samsel¹**

¹ *Department of Organic Chemistry, Chemical Faculty, Gdansk University of Technology, 11/12 G. Narutowicza Street, 80-233 Gdansk, Poland;* ² *PERLAN TECHNOLOGIES Sp. z o.o., 303 Puławska Street, 02-785 Warsaw*
E-mail: m-kukowska@wp.pl

Introduction

Glycyl-L-Histidyl-L-Lysine (GHK) is a short amino acid sequence of natural origin, localized in the α -II-chain of human collagen, released during its hydrolysis in the inflammation and wound healing processes. It is known to be involved in several processes in the skin, such as stimulation of collagen and elastin synthesis, proteoglycan and glycosaminoglycan (GAG) production, formation of extracellular cement between cells [1-3].

Its palmitoyl analogue has been successfully investigated as an agent in skin disease therapy or skin care products. Fatty acid linked to peptide has given promising results in penetration process [4-7]. In last few years it become a model in design new peptidic compounds.

Prediction of the permeability of the molecule is very important information for the rational design of bioactive compounds. The distribution coefficient at physiological pH ($\log D^{7.4}$) is well correlated with a transport across the lipid barrier of the skin. The knowledge of the parameter and the lipophilicity profile will be helpful in optimization of the penetration process [8-9].

Results and Discussion

In our further studies, we designed a series of Gly-His-Lys analogues containing Gly-X-Y fragment (where X = Met, Hyp, Hyp-Met, Gly-Hyp and Y = Lys or D-Lys). Continuing our work, we decided to synthesize the analogues modified with the fatty acid. All lipopeptides **1-5a**, **1b**, **1c** (Table 1) were obtained by the solid phase using Fmoc strategy. The method of elongation of the peptide chain was based on two-step procedure involving deprotection (25% piperidine/DMF) and coupling (using DIC and HOBt in a mixture of DMF, DCM, NMP) until the peptide sequence was built up. The acylation with the fatty acid was carried out on the *N*-termini of the peptide-resin using TBTU, HOBt in presence of DIPEA, in addition 1% triton. Finally, the liberation of the lipopeptide from the resin and simultaneous deprotection of Boc group from the lysine side chain was achieved using TFA cocktail.

The final products were purified by RP-SPE to obtain highly pure lipopeptides (greater than 98% on HPLC) with the yield (>50%) and were characterized by RP-HPLC, MS and elemental analysis.

For the determination of the distribution coefficient $\log D^{7.4}$ we used traditional shake flask technique. Peptide in concentration 100-200 $\mu\text{g/ml}$ was used to extraction in octanol/buffer phosphate system (1:1, 1:2, 2:1, v/v). On the basis of the HPLC analysis the $\log D^{7.4}$ were calculated.

The results indicated that the modification with the fatty acids improves the affinity of the analogues to the lipid barrier of the skin. The $\log D^{7.4}$ value for compounds **1b**, **1c**, **3a**, **5a** is ranged from 0 to 3 suggesting a good affinity to the lipid membrane. Acylation with a longer fatty acid should be done in case compounds **2a**, **4a**. It is noticeable that tripeptide **5a** with D-Lys has even the higher value than compound **1a**, the same correlation was observed for unmodified analogues. We compared the $\log D^{7.4}$ values determined experimentally with the values calculated by I-LAB 2.0 software product. The values determined experimentally are in good correlation with that calculated from I-LAB 2.0. For the modified analogues the values were rather lower, whereas for the unmodified analogues were higher. The good results we obtained for tripeptide **3a** or **1a** and **1b** when we compared $\log D$ I-LAB2.0 values with a model tripeptide palmitoyl-Gly-His-Lys. We also determined the distribution profile for modified analogues (shake flask $\log D$ vs. $pH=2-11$). Modification the *N*-termini of peptides with fatty acid caused that diprotonated fraction of peptides does not exist. Three different fraction (protonated, the fraction of neutral net, deprotonated) exist over the whole range of measured pH . The knowledge of the dissociation constants of ionizable groups ($pK_{a1}(\epsilon-NH_2-Lys)$, pK_{a2} (C-terminal)) determined by pH -metric measurements were used to calculate the percentage of the fraction of the species at different pH and then the lipophilicity parameters for the species ($\log P^C$, $\log P^A$, $\log P^Z$; C-cation, A-anion, Z-zwitterion). The zwitterionic fraction exists over the whole range of measured pH with its maximum percentage in pH 6-8. It suggest that it is more lipophilic than its singly charged cation or anion. The results help to understand different mechanism of skin penetration for modified analogues.

Number	Peptide sequence
1a	Lauroyl-Gly-Hyp-Lys
1b	Palmitoyl-Gly-Hyp-Lys
1c	Stearoyl-Gly-Hyp-Lys
2a	Lauroyl-Gly-Gly-Hyp-Lys
3a	Lauroyl-Gly-Met-Lys
4a	Lauroyl-Gly-Hyp-Met-Lys
5a	Lauroyl-Gly-Hyp-D-Lys

Table 1. Gly-His-Lys analogues modified with fatty acids

References

- [1] Lupo, P. M. *Dermatol Surg* **2005**, *31*, 832.
- [2] Mazurowska, L.; Mojski, M., *Talanta* **2007**, *72*, 650.
- [3] Kukowska, M.; Dzierzbicka, K. *Wiad. Chem.* **2010**, *64*, 630.
- [4] Namjoshi, S.; Benson, H. A. E., *Biopolymer (J. Pept. Sci.)* **2010**, *94(5)*, 673.
- [5] Namjoshi, S.; Caccetta, R.; Benson, H. A. E., *J. Pharm. Sci.* **2008**, *97*, 2524.
- [6] Venillez, F.; Deshusses, J.; Buri, P., *Eur. J. Pharm. Biopharm.* **1999**, *48*, 21.
- [7] Chirita, R. I.; Chaimbault, P.; Archambault, J. Ch.; Robert, I.; Elfakir, C., *Anal. Chim. Acta* **2009**, *641*, 95.
- [8] Smith, D. A.; Van der Waterbeemd, H.; Walker, D. K. *Pharmacokinetics and Metabolism in Drug Design*, 2nd ed.; Wiley-VCH: Weinheim, Germany, 2006; pp 2-17.
- [9] Corner, J.; Tam, K. Lipophilicity Profiles: Theory and measurement. In *Pharmacokinetic Optimization in drug research: Biological, Physicochemical and Computational strategies*; Testa, B.; Van der Waterbeemd, H.; Folkers, G.; Guy R.; Wiley-VCH: Weinheim, Germany, 2007; pp 275-304.

Membrane-perturbing effects of antimicrobial peptides: A systematic spectroscopic analysis

**D. Roversi¹, L. Giordano¹, M. De Zotti², G. Bocchinfuso¹, A. Farrotti¹,
S. Bobone¹, A. Palleschi¹, Y. Park³, K.-S. Hahm⁴, F. Formaggio²,
C. Toniolo², L. Stella^{1,*}**

¹University of Rome “Tor Vergata”, Department of Chemical Sciences and Technologies, 00133 Rome, Italy; ²University of Padova, ICB, Padova Unit, CNR, Department of Chemistry, 35131 Padova, Italy; ³Chosun University, Department of Biotechnology, 501759-Gwangju, Korea; ⁴BioLeaders Corporation, 305500-Daejeon, Korea; ⁵University of Rome “Tor Vergata”, Department of Physics, 00133 Rome, Italy
E-mail: stella@stc.uniroma2.it

Introduction

Antimicrobial peptides (AMPs) are part of the innate immune system of many organisms, including man, and are active against a wide range of microorganisms. Many AMPs kill bacteria mainly by perturbing the permeability of their membranes through the formation of pores. However, AMPs effects on membrane properties probably extend beyond pore-formation. For instance, the “sand in a gearbox” model proposes that AMPs perturb the structural and dynamical features of the bacterial membrane, and, as a consequence, disrupt the proper function of the membrane-bound protein complexes [1]. Here we report a systematic spectroscopic study of the effects on membrane dynamics of two very different AMPs: the cationic PMAP-23, which creates pores according to the “carpet” model [2], and alamethicin, which forms “barrel-stave” channels [3].

Results and Discussion

We determined the range of peptide concentrations causing leakage of carboxyfluorescein from POPC/POPG (2:1) vesicles ([lipid]=50 μ M). Alamethicin is significantly more active and cooperative than PMAP-23 (Figures 1 and 2).

Peptide effects on the fluidity of the membrane were determined by measuring the steady-state and time-resolved fluorescence anisotropy of probes located at different depths from the membrane center: NBD-PE and DPH. Fluorescence anisotropy measures the rotational mobility of the probe, and as such it is an indication of the local viscosity of the membrane. Surprisingly, PMAP-23 decreased the mobility of probes located at all depths (data for DPH are shown in Figure 1), indicating an overall peptide-induced rearrangement of the bilayer. By contrast, alamethicin did not induce any significant perturbation in membrane dynamics in the concentration range where it forms pores (Figure 2).

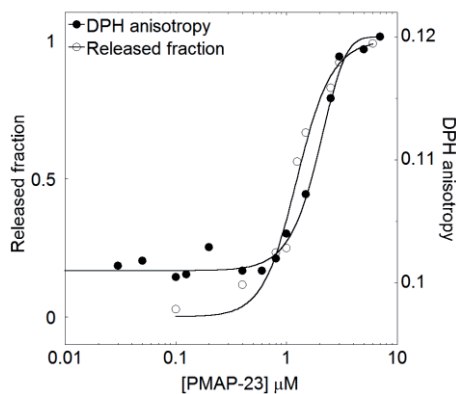


Fig.1: PMAP-23: fraction of liposomes contents release induced by the peptide in 20', and DPH fluorescence anisotropy.

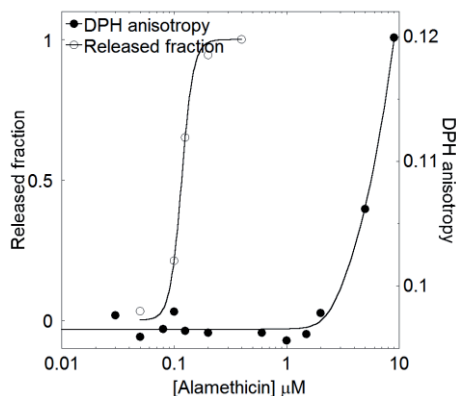


Fig.2: Alamethicin: fraction of liposomes contents release induced by the peptide in 20', and DPH fluorescence anisotropy.

The PMAP-23-induced membrane stiffening was also confirmed by the reduction of water penetration into the double layer, demonstrated by the spectral shift of the membrane probe Laurdan. Liposomes containing the probe pyrene allowed us to analyze peptide effects on the lipid lateral mobility, confirming once again a PMAP-23-induced reduction in the mobility of the probe (data not shown).

In conclusion, in all cases the most significant peptide-induced effect is a surprising reduction in membrane fluidity, lateral lipid mobility and water penetration, probably induced by a tightening of the bilayer driven by peptide-lipid interactions. Indeed, the observed effects are similar to those previously reported for the Ca^{2+} -membrane interaction [4]. However, while for PMAP-23 all membrane-perturbing effects are correlated with the vesicle leakage process, alamethicin does not significantly influence membrane dynamics at the concentrations in which it forms pores. Only at considerably higher alamethicin concentrations effects similar to those of PMAP-23 were observed. We suggest this distinction as a clear-cut criterion to discriminate between peptides acting according to the carpet or barrel-stave models.

References

- [1] Pag, U., Oedenkoven, M., Sass, V., Shai, Y., Shamova, O., Antcheva, N., Tossi, A., Sahl, H.-G. *J. Antimicrob. Chemother.* **2008**, *61*, 341-352.
- [2] Orioni, B.; Bocchinfuso, G.; Kim, J.Y.; Palleschi, A.; Grande, G.; Bobone, S.; Park, Y.; Kim, J. I.; Hahm K.-S.; Stella, L. *Biochim. Biophys. Acta* **2009**, *1788*, 1523-1533..
- [3] Stella, L.; Burattini, M.; Mazzuca, C.; Palleschi, A.; Venanzi, M.; Baldini, C.; Formaggio, F.; Toniolo, C.; Pispisa, B. *Chem. Biodivers.* **2007**, *4*, 1299-1312.
- [4] Szekely, O., Steiner, A., Szekely, P., Amit, E., Asor, R., Tamburu, C., Raviv, U. *Langmuir* **2011**, *27*, 7419-7438.

Metanicens, peptaibol antibiotics from the ascomycetous fungus CBS 597.80

Anastase Kimonyo¹ and Hans Brückner²

¹Kigali Institute of Science and Technology (KIST), Kigali 3900, Rwanda (present address);

²Research Center for BioSystems, Land Use and Nutrition (IFZ), Department of Food Sciences,
University of Giessen, 35392 Giessen, Germany

E-mail: hans.brueckner@ernaehrung.uni-giessen.de

Introduction

Filamentous fungi such as *Trichoderma/Hypocrea* are abundant sources of a particular group of antimicrobial polypeptides containing α -aminoisobutyric acid (Aib) and for which the acronyms peptaibols/peptaibiotics became established [1]. We had investigated a mixture of 20-residue peptaibols named **metanicin** (MTC) [2,3], isolated from a fungus received as entomopathogenic *Metarhizium anisopliae* v. *anisoplia* strain CBS 597.80 (CBS = Centralbureau voor Schimmelcultures, Utrecht, The Netherlands). However, due to unusual shaped conidia and based on RNA sequencing of its internal transcribed spacer regions, the genus *Metarhizium* became questioned by CBS. We became informed that this ascomycete is still in the CBS culture collection but has been withdrawn from the public strain collection. This strain is under taxonomic reinvestigation.

Results and Discussion

Fermentation of the fungus and isolation of the peptaibol mixture from the fermentation broth of CBS 597.80 using XAD, Sephadex LH-20 and silica gel chromatography and sequence data have been described previously [2]. Analyses of total hydrolysates of individual MTC-peptides using a conventional amino acid analyzer, HPLC after derivatization with *o*-phthaldialdehyde/isobutyl-L-cystein (OPA/IBLC), and GC-MS of *N*-pentafluoropropionyl-*O*-1-propyl esters on Chirasil-ValTM revealed the amino acid stoichiometry and chirality of components and the absence of isoleucine. The presence and *C*-terminal position of D-isovaline in MTC B and D was determined by EDMAN-sequencing of isolated *C*-terminal polypeptides resulting from selective trifluoroacetylation of the peptides. The sequences of MTC A-D and the FAB-MS of MTC-B as example are shown in Figure 1. Amino acid exchange positions in peptides are indicated in bold letters. Note the correct amino acids in positions 9 and 12 in metanicin components B and D, correctly assigned in [3] but misprinted in a previous report [2].

(A) Ac-Aib-Ala-Aib-Ala-Aib-**Ala**-Gln-Aib-Val-Aib-Gly-Leu-Aib-Pro-Val-Aib-**Aib**-Gln-Gln-Pheol

(B) Ac-Aib-Ala-Aib-Ala-Aib-**Ala**-Gln-Aib-Val-Aib-Gly-Leu-Aib-Pro-Val-Aib-**Iva**-Gln-Gln-Pheol

(C) Ac-Aib-Ala-Aib-Ala-Aib-**Aib**-Gln-Aib-Val-Aib-Gly-Leu-Aib-Pro-Val-Aib-**Aib**-Gln-Gln-Pheol

(D) Ac-Aib-Ala-Aib-Ala-Aib-**Aib**-Gln-Aib-Val-Aib-Gly-Leu-Aib-Pro-Val-Aib-**Iva**-Gln-Gln-Pheol

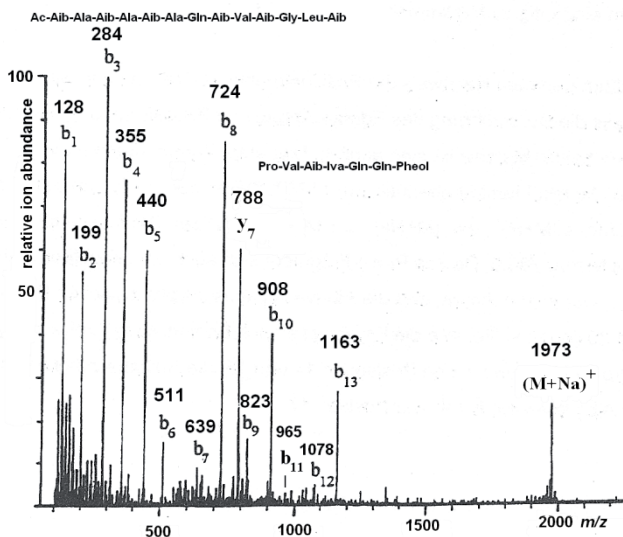


Figure 1. Sequences of metanicin (MTC) A-D (above) and FAB-MS of MTC-B (below) showing the diagnostic series (nominal masses) of acylium ions of the series b_1 - b_{13} , and the sodium adduct of the molecular ion at m/z 1973. The y_7 fragment ion at m/z 788 represents the C-terminal, protonated prolylheptapeptide. Ac = acetyl; Pheol = L-phenylalaninol, Iva = D-isovaline; chiral protein amino acids are of the L-configuration;

References

- [1] Toniolo, C.; Brückner, H. (Eds.) Topical Issue Peptaibiotics. *Chem. Biodivers.* **2007**, 6(4), 1021-1412.
- [2] Brückner, H., Kimonyo A., In Peptides 1994, Proceedings of the Twenty-Third European Peptide Symposium; Maia, H. L. S., Ed.; ESCOM, Leiden, 1995, p. 429.
- [3] Kimonyo, A., Dissertation, University of Hohenheim at Stuttgart, Germany, 1997.

“Minimum bias” molecular dynamics simulations to determine peptide orientation in membranes

G. Bocchinfuso^a, A. Farrotti^a, A. Palleschi^a, B. Bechinger^b, L. Stella^{a,*}

*^aDepartment of Chemical Sciences and Technologies, University of Rome “Tor Vergata”,
00133 Rome, Italy; ^bUniversité de Strasbourg/Centre National de la Recherche
Scientifique, Institut de Chimie, F-67000 Strasbourg, France
E-mail: stella@stc.uniroma2.it*

Introduction

The rise in multiple drug-resistant microbes caused an urgent need for the development of novel antibacterial drugs. Antimicrobial peptides (AMPs) exhibit a strong bactericidal activity, mainly due to the perturbation of bacterial membranes. Therefore, in order to improve the pharmacologic properties of AMPs, a detailed understanding of their interaction with phospholipid membranes is needed.

Molecular dynamics (MD) simulations can provide atomistic details on peptide-membrane systems, which are very difficult to obtain with other techniques. However, simulations starting from a preformed bilayer suffer from sampling problems. By contrast, the “minimum-bias” approach starts from a random mixture of peptide, lipids and water molecules that self-assemble during the simulation^{1,2}. The high fluidity of the system during the first steps of this process ensures that the peptide can find its minimum free energy configuration in a reasonable simulation time.

In this work we test the ability of “minimum bias” MD simulations to determine the orientation in a lipid bilayer of a peptide called LAH4. This 26 amino acids long AMP comprises 4 His residues that change their protonation state with pH (their pKa values are 5.4, 5.8, 5.9 and 6.0)³. Solid-state NMR experiments demonstrated that at pH values where the His residues are charged this peptide is always located on the membrane surface, while when they are neutral, the peptide inserts in a transmembrane orientation³. Therefore, simulations of this peptide in different protonation states provide a very stringent test of the reliability of the MD methods.

Results and Discussion

We performed a total of four all-atoms simulations (two for neutral and two for charged His LAH4) at 300 K, starting from a box containing the peptide, 128 lipids (POPC) and 7500 water molecules, for a cumulative trajectory length of about 1 μ s.

In both simulations with neutral His residues we observed the formation of a defect-free bilayer, with the peptide in the expected transmembrane orientation (Figures 1a and 1b). This arrangement was stabilized by interactions between phosphorus atom of the lipids headgroups and nitrogen atom of Lys side-chains. The helical structure of LAH4 was retained during the simulations.

In simulations with charged His residues we were not able to obtain a defect-free bilayer (Figures 1c and 1d). In addition, the helical structure of the peptide was partially disrupted,

as observed in NMR experiments in micelles (pdb-code: 2KJN). The difficulty to attain a perfect bilayer could be due to the destabilizing effects of the peptide itself. This would agree with the much higher activity of LAH4 at acidic pH with respect to neutral conditions⁴. However, it is also possible that the system did not reach equilibrium, due to insufficient sampling. Further simulations will be performed to overcome this problem, including the use of coarse-grained force-fields.

In conclusion, the “minimum bias” approach was able to predict the correct orientation of peptides in a bilayer when an equilibrium conformation was reached, as in the case of LAH4 with neutral His residues. On the other hand, for LAH4 simulations with charged His side-chains, the systems might be trapped in local free-energy minima. Overall the present study confirms that MD simulations represent a useful tool to study AMP/bilayer interactions at the molecular level, if they are carefully validated by comparison with experimental data. In this context, the LAH4 peptide, with its different modes of membrane interaction, represents a challenging test of the simulation conditions.

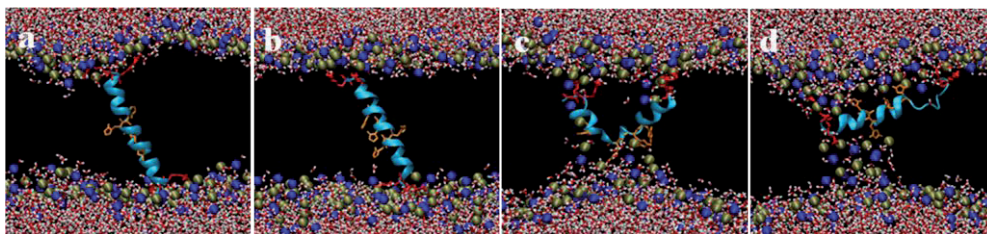


Figure 1: Final structures of LAH4 simulations with neutral (a,b) and charged (c,d) His residues. Water molecules are shown as sticks with oxygen and hydrogen atoms in red and white, respectively. LAH4 is represented as a ribbon in cyan, with Lys and His side-chains in red and orange respectively. Lipid chains are not displayed for clarity, while POPC nitrogen and phosphorus atoms are shown as blue and golden spheres.

References

- [1] Esteban-Martin, S.; Salgado, S. *Biophys. J.* **2007**, *92*, 903-912.
- [2] Bocchinfuso, G.; Palleschi, A.; Orioni, B.; Grande, G.; Formaggio, F. Toniolo, C.; Park, Y.; Hahn, K.S.; Stella, L. *J. Pept. Sci.* **2009**, *15*, 550-558.
- [3] Bechinger, B. *J. Mol. Biol.* **1996**, *263*, 768-775.
- [4] Vogt, T.C.B.; Bechinger, B. *J. Biol. Chem.* **1999**, *41*, 29115-29121.

Internalisation by translocations and endocytosis of cell penetrating peptide (CPP) by a reductionist approach

P. Lecorché, A. Walrant, S. A. Bode, M. Thévenin, C. Bechara, S. Bregant, I. D. Alves, S. Lavielle, G. Chassaing, S. Sagan, F. Burlina

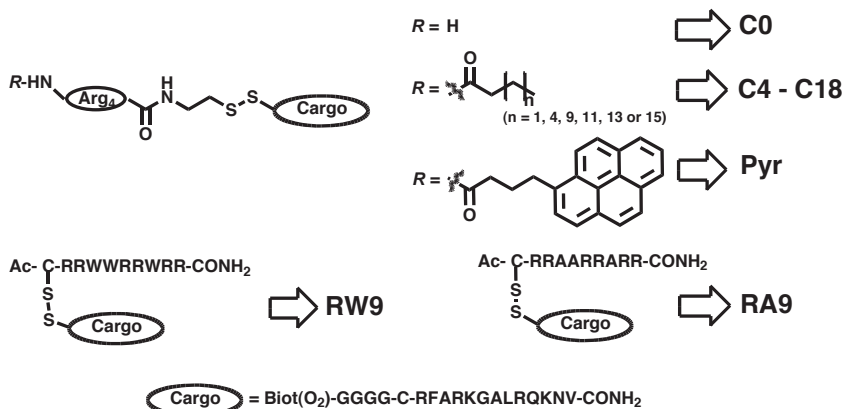
Laboratoire des BioMolécules, UPMC Univ Paris 06, UMR 7203, LBM, CNRS, UMR 7203, LBM, Ecole Normale Supérieure, UMR 7203., Dpt Chimie ENS 24, Rue Lhomond F-75005, Paris, France

fabienne.burlina@upmc.fr

Introduction

It is become rather consensual that internalisations of CPP occur by two competitive processes: translocations and endocytosis¹. The large diversity of CPP structures corresponding to various origins and structures (fragment of proteins, structurally constrained synthetic peptides, orthogonal high-throughput screening of peptide libraries² or dendrimers) hampered the identification of general rule(s). We have developed a reductionist approach based on the restriction of atoms and functions (amide and guanidinium) in order to modulate the amphiphilic properties: 1) the primary amphiphilic properties *via* lipopeptides constituted of tetraarginines coupled to fat acids of different chain lengths or 2) secondary amphiphilic properties *via* a periodic sequence constituted of alanines and arginines³. These CPPs were linked by a disulfide to a peptide cargo, corresponding to a peptidic inhibitor of protein kinase C (PKCi).

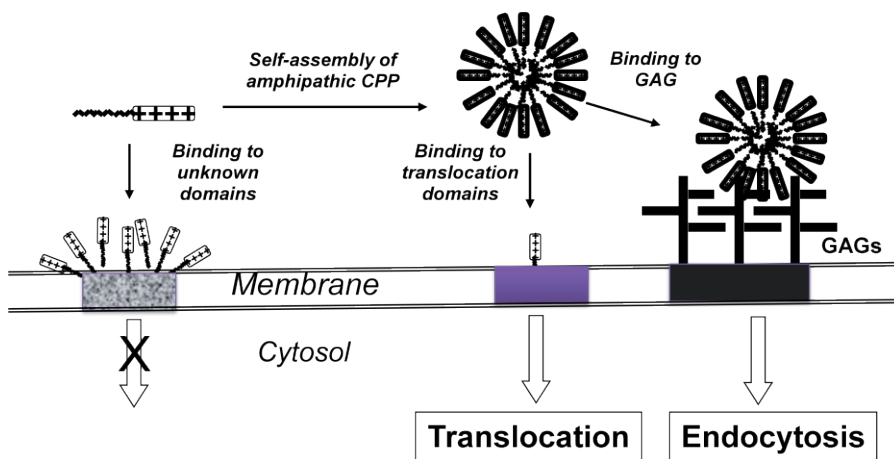
Results and Discussion



Mass spectrometry quantification. The analysis of the relative contributions in the internalisation processes was based on the rigorous determinations of the conjugates by quantification of the amounts of: i) the PKCi bound on cell surface of CHO-K1 and CHO-pgsA745 (glycoaminoglycan-deficient cells), ii) the internalized cargo (PKCi) calculated from the amounts of protected PKCi towards trypsin degradation on both CHO-K1 cell at

4°C and 37°C and CHO-pgsA745 cell (GAG-deficient). By confocal microscopy, the biotinylated intracellular PKCi peptide was revealed by rhodamine-labelled avidin after quenching the membrane-associated species with unlabelled avidin, followed by cell fixation with paraformaldehyde and permeabilisation as described.

Dynamic light scattering (DLS) experiments. DLS showed that conjugates with the longest fatty chains C12 to C18 were able to self-assemble in the conditions used for the uptake experiments (concentration and culture medium).



Independently of their efficiency internalisation, all these conjugated peptides bind strongly to unknown external domains. A small part of bound peptides cross the cell membrane *via* glycosaminoglycan, between 0.3 to 3% of the total amount of cell associated peptides. A smallest part binds to unidentified lipid partner and translocates into the cells. It appears that the internalisation efficiency increases more strongly with the enhancement of the primary hydrophobicity than with the secondary hydrophobicity.

References

- [1] Jiao, CY.; Delaroche, D.; Burlina, F.; Alves, ID.; Chassaing, G.; Sagan, S. *J. Biol. Chem.* **2009**, *284*, 33957-33965.
- [2] Marks, J.R.; Placone, J.; Hristova, K.; Wimley, WC. *J. Am. Chem. Soc.*, **2011**, *133*, 8995-9004.
- [3] Lecorché, P.; Walrant, A.; Burlina, F.; Dutot, L.; Sagan, S.; Mallet, JM.; Desbat, B.; Chassaing, G.; Alves, ID.; Lavielle, S. *Biochim Biophys Acta Biomembranes*, **2012**, *1818*, 448-457.
- [4] S. A. Bode, M. Thévenin, C. Bechara, Sarah Bregant, S. Lavielle, S. Sagan, G. Chassaing, F. Burlina (2012) *Chemical Communications*, *48*, 7179-7181.

Panurgines, novel antimicrobial peptides from the venom of wild bee *Panurgus calcaratus* and their interaction with phospholipids vesicles

Sabína Čujová,^{1,2} Lenka Monincová,^{1,2} Jiřina Slaninová,¹ Lucie Bednářová,¹ Václav Čerovský¹

¹Institute of Organic Chemistry and Biochemistry, Academy of Sciences of the Czech Republic, Flemingovo nám. 2, Prague 6, 166 10 Czech Republic; ²Charles University of Prague, Department of Biochemistry, Hlavova 8, Prague 2, 120 00 Czech Republic

E-mail: cujova@uochb.cas.cz

Introduction

Antimicrobial peptides (AMPs) are important components of an innate defense system of all forms of life. Common features of these peptides include a positive net charge under physiological conditions, amphipathic secondary structure upon interaction with biological membranes, and rapid killing of bacteria. Although their exact mechanism of action is not well understood, it is generally accepted that it resides in the disruption of bacterial cytoplasmic membrane [1]. Remarkable category of AMPs has been identified in the venom of stinging insect (Hymenoptera). In our laboratory we have isolated several novel AMPs from the venom of different wild bees [2].

Liposomes are useful model for the study of AMPs action mechanism on membrane level. They are defined as spherical vesicles with membrane composed of phospholipid bilayer [3]. Liposomes are spontaneously formed when phospholipids are dispersed in aqueous medium. The interactions of AMPs with liposomes are usually studied by observing the leakage of fluorescent dye (calcein) entrapped inside those vesicles upon disruption of the liposomal membrane by AMP.

Results and Discussion

We isolated three novel peptides from the venom extract of the wild bee *Panurgus calcaratus* by RP-HPLC (Figure 1) and named them panurgines. These are: one α -helical amphipathic dodecapeptide LNWGAILKHIK-NH₂ (PNG-1) and two cyclic peptides containing 25 amino acid residues and two intramolecular disulfide bridges of the pattern C8-C23 and C11-C19 that have almost identical sequence established as LDVKKIICVACKIXPNPACKKICPK-OH (X=K, PNG-K and X=R, PNG-R). The peptides were synthesized using the standard protocol of N⁹-Fmoc SPPS chemistry on Rink Amide MBHA resin or 2-chlorotriyl chloride resin and then were purified by RP-HPLC. Panurgines exhibited antimicrobial activity against Gram-positive bacteria and Gram-negative bacteria, antifungal activity and low hemolytic activity. We prepared 11 analogues of PNG-1 with the aim to increase its antimicrobial activity and decrease the hemolytic activity, and linear analogues of PNG-K and PNG-R to elucidate the importance of disulfide bridges for their activity. From the series of PNG-1 analogues, the LNWGKILKHIK-NH₂ analogue had improved antimicrobial activity especially against *S. aureus* and *P.aeruginosa* (MIC, 8.7 μ M, 20.8 μ M, respectively) and lower hemolytic

activity ($LC_{50} >140$, μM) than the parent compound (MIC, 10.6 μM , 51.7 μM , LC_{50} , 119 μM). The cyclic disulfide bridges containing PNG-K and PNG-R peptides exhibited strong antimicrobial activity against sensitive Gram-positive *M. luteus* and *B. subtilis*, weak activity against *E. coli* but both peptides were inactive against pathogenic *S. aureus* and *P. aeruginosa* and were not hemolytic. Their linear analogs having all four Cys residues replaced by Abu were inactive against all bacteria tested with the exception of weak activity against the most sensitive *M. luteus*. CD-spectra of PNG-1 and its analogues measured in the presence of SDS showed α -helical structure with increasing trend of helical content upon increasing the concentration of SDS correlating with their biological activities and permeabilization of liposomes. CD spectra of PNG-K and PNG-R indicate the mixture of α -helical and β -sheet structure.

We studied the effect of panurgines on the disruption of artificially made membrane by observing the leakage of fluorescence dye (calcein) entrapped in phospholipids large unilamellar vesicles. Specifically, we investigated membrane interactions of panurgines on negatively charged 1:2 dioleoyl-phosphatidylcholine (DOPC)/ dipalmitoyl-phosphatidylglycerol (DPPG) and 1:2 DOPC/ dioleoyl-phosphatidylglycerol (DOPG) liposomes as a general model of bacteria and 15:80:5 DOPC/DOPG/ cardiolipin (CL) as a possible model for *Bacillus subtilis*. The uncharged DOPC liposomes were used as potential model for erythrocytes. Results indicate that panurgines and their analogues have stronger disrupting activity against bacteria-mimicking anionic liposomes than against liposomes made solely from DOPC. This correlates well with their biological activity.

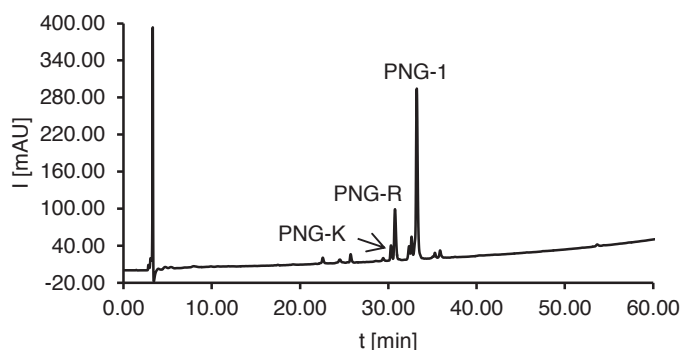


Fig. 1. RP-HPLC profile of *Panurgus calcaratus* venom extract at 220 nm. An elution gradient of solvents from 5% to 70% of acetonitrile in water/0.1% TFA was applied for 60 min at 1 ml/min flow rate.

Acknowledgments

This work was supported by the Grant Agency of the Charles University, grant No. 645012 and by research project RVO 61388963 of the Institute of Organic Chemistry and Biochemistry, Academy of Sciences of the Czech Republic.

References

- [1] Wimley, W.C.; Hristova, K. *J. Membrane Biol.* **2011**, *239*, 27.
- [2] Monincová, L.; Slaninová, J.; Fučík, V.; Hovorka, O.; Voburka, Z.; Bednářová, L.; Maloň, P.; Štokrova, J.; Čeřovský, V. *Amino Acids.* **2012**, *43*, 751
- [3] Sharma, S.; Sharma, N.; Kumar, S.; Gupta, G.D. *J. Pharm. Res.* **2009**, *2*, 1163.

Peptaibiotic folding and bioactivity: Role of backbone endothioamide linkages

Marta De Zotti¹, Barbara Biondi¹, Cristina Peggion¹, Matteo De Poli¹,
Haleh Fathi¹, Simona Oancea², Fernando Formaggio¹,
Claudio Toniolo¹

¹ICB, Padova Unit, CNR, Department of Chemistry, University of Padova, 35131 Padova,
Italy; ²Department of Biochemistry and Toxicology, University "Lucian Blaga", 550012
Sibiu, Romania

E-mail: barbara.biondi@unipd.it

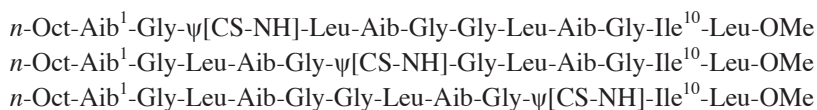
Introduction

A common tool to bias the conformation of linear peptides is the insertion of side-chain modified amino acids or side-chain/main-chain conformationally restricted building blocks. An alternative approach is a simple backbone modification. In this latter connection, backbone amide replacements with (almost) isosteric surrogates were extensively used [1]. These modifications may impart resistance to enzymatic degradation and better bioavailability to the peptides, but also influence their secondary structure.

A thioamide (ψ [CS-NH]) is perhaps the closest structural mimic of an amide [2-4]. However, it possesses different and attractive features: (i) Its NH group forms stronger hydrogen bonds, being more acidic than that of the amide. (ii) Its C-N bond undergoes *cis/trans* isomerization by irradiation at 260 nm ($\pi \rightarrow \pi^*$ transition). (iii) It may act as a "minimalist" fluorescence quencher.

Results and Discussion

For all these reasons, we started a project aimed at exploring how the endothioamide bond affects peptide folding and bioactivity. In this communication, we describe the synthesis, and preliminary conformational and biophysical results on the three mono-thionated analogs of the membrane-active, 10-mer lipopeptaibiotic [Leu¹¹-OMe] trichogin GA IV [5] listed below:



where *n*-Oct is *n*-octanoyl, Aib is α -aminoisobutyric acid, and OMe is methoxy.

The syntheses of the three peptides were accomplished in solution according to a segment condensation approach. Appropriate thioamide-containing tri- or tetrapeptides were prepared by treating the corresponding all-amide precursors with the Lawesson reagent. The RP-HPLC profiles of the final products are shown in Figure 1.

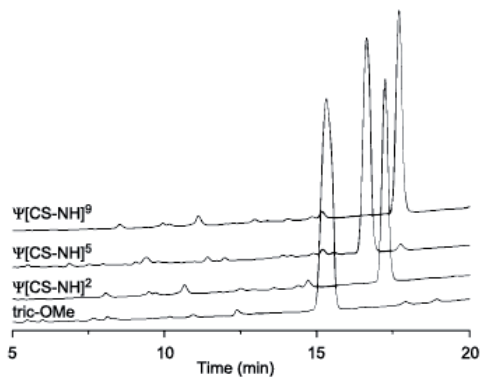


Fig. 1 RP-HPLC profiles obtained for [Leu¹¹-OMe] trichogin GA IV (tric-OMe) and its ψ [CS-NH]², ψ [CS-NH]⁵, and ψ [CS-NH]⁹ analogs.

FT-IR absorption, 2D-NMR and CD conformational investigations on the three analogs were conducted in comparison with [Leu¹¹-OMe] trichogin GA IV. The results show that a single thioamide linkage is well tolerated in the overall helical conformation of the lipopeptaibiotic [6]. Moreover, all of them maintain the capability to interact with the DOPE/DOPG model phospholipid membranes and exhibit a comparable bioactivity against the Gram-positive bacterial strain *S. aureus*.

References

- [1] Spatola, A. F. In *Chemistry and Biochemistry of Amino Acids, Peptides and Proteins*; Weinstein, B., Ed.; Dekker: New York, **1983**; pp 267–357.
- [2] La Cour, T. F. M.; Hansen, H. A. S.; Clausen, K.; Lawesson, S.-O. *Int. J. Pept. Protein Res.* **1983**, *22*, 509.
- [3] La Cour, T. F. M. *Int. J. Pept. Protein Res.* **1987**, *30*, 564.
- [4] De Zotti, M.; Biondi, B.; Peggion, C.; De Poli, M.; Fathi, H.; Oancea, S.; Toniolo, C.; Formaggio, F. *Beilstein J. Org. Chem.* **2012**, *8*, 1161.
- [5] Toniolo, C.; Crisma, M.; Formaggio, F.; Peggion, C.; Monaco, V.; Goulard, C.; Rebuffat, S.; Bodo, B. *J. Am. Chem. Soc.* **1996**, *118*, 4952.
- [6] Peggion, C.; Formaggio, F.; Crisma, M.; Epand, R.F. ; Epand, R.M. ; Toniolo, C. *J. Pept. Sci.* **2003**, *9*, 679.

Structure and biological activity of Aurein 1.2 and dimeric analogues

E. N. Lorenzón^a, L. G. Nogueira^b, T. M. Bauab^b, E. M. Cilli^a

^a*Institute of Chemistry, Unesp - Univ. Estadual Paulista, Araraquara, São Paulo, Brazil;*

^b*Faculty of Pharmaceutical Sciences, Unesp - Univ. Estadual Paulista, Araraquara, São Paulo, Brazil*

E-mail:estebanlorenzonzon@hotmail.com

Introduction

Antibiotic resistant bacterial strains represent a global health problem. Antimicrobial peptides (AMPs) have been proposed as a potential new class of antimicrobial agents because they displayed little or no resistance effects. AMPs are found in animals, plants, insects, and microorganisms [1]. Most of them disrupt the plasma membrane of microbes via three general mechanisms. The shorter peptides remain tightly bound to the membrane interface until reach a threshold concentration when promote bilayer damage via carpet-like mechanism. On the other hand, the longer peptides form transmembrane pores. In the “barrel-stave” pore model, the peptides adopt a helical conformation and aggregate into a barrel-like structure that spans the membrane with the peptides lying perpendicular to the plane of the membrane. In “toroidal pore” mechanism, the peptides are tightly bound to the polar lipid groups of the membrane, promoting the bending of the bilayer [2]. It is well know that charge, amphipathicity, hydrophobicity and helicity correlates directly with the antimicrobial activity of AMPs [3]. In addition, the aggregation of molecules of AMPs, either before or after binding to the membrane surface, is a prerequisite for pore formation. The synthesis of dimeric peptides is the simplest way to mimic this aggregation. Several bioactive sequences were dimerized obtaining enhanced antimicrobial activity [4]. However, the effect of this modification is unclear since dimeric versions of some AMPs lost antimicrobial activity or gained toxicity [5]. Here, we used the AMP Aurein 1.2 (AU) to study the effects of dimerization on its structure and biological activity.

Results and Discussion

AU and two dimeric versions were synthesized manually by solid-phase peptide synthesis (SPPS) using the standard Fmoc (9-fluorenylmethyloxycarbonyl) protocols on a Rink-MBHA resin. As the linker units, lysine was used for the C-terminal dimer (AU)₂K, while glutamic acid was used for the N-terminal dimer E(AU)₂. Microbiological tests were performed using the broth microdilution method. The data showed that both N- and C-terminal dimerization led to inactive molecules. However, dimeric peptides promoted the aggregation of *C. albicans* cells. This may be due to the interaction of the peptides with yeast cell-wall carbohydrates. To evaluate the citotoxicity of the peptides, the hemolysis test was performed. The results showed that the hemolytic activity of the dimeric peptides seems to be not concentration dependent. Carboxyfluorescein release from vesicles composed of DPPA/DPPC (1,2-dipalmitoyl-sn-glycero-3-phosphatidic acid:1,2-dipalmitoyl-sn-glycero-3-phosphatidylcholine) (5:95, ratio) showed that all peptides have

permeabilization activity. The loss of antimicrobial activity and the permeabilization activity can be explained in terms of interactions between peptides and cell wall carbohydrates. Previous studies have shown that dimeric peptides may be inhibited from passing through the cell walls of prokaryotic cells, while in vesicle experiments, without a cell wall, dimers can act directly on the membrane mimetic [6]. Using circular dichroism, we have found that dimeric peptides have defined structures in aqueous solution. (AU)₂K showed a typical α -helix spectrum while E(AU)₂ a "coiled-coil" one. However, AU displayed mainly random coil structures. For all the peptides, an α -helical structure was induced by the non-polar environment of LPC micelles. Because of the lack in antimicrobial activity of the dimeric versions, we suggest that the unstructured-state of AU may be a requisite to cross the cell wall and reach the membrane.

In conclusion, we found that the antimicrobial activity of AU decrease with dimerization. It may be due to the structure modification promoted by dimerization and the interactions between peptides and cell wall carbohydrates. In addition, the ability to aggregate yeast cells could make dimeric versions of AU great candidates to prevent *C. albicans* adhesion to biological targets and medical devices, preventing disease caused by this fungus.

Acknowledgments

The authors are grateful to Conselho Nacional de Desenvolvimento Científico e Tecnológico (CNPq) and Fundação ao Amparo a Pesquisa do Estado de São Paulo (FAPESP) for financial support.

References

- [1] Cespedes, G. F.; Lorenzón, E. N.; Vicente, E. F.; Mendes-Giannini, M. J.; Fontes, W.; Castro, M. S.; Cilli, E. M. *Protein Pept Lett* **2012**, 19 (6), 596-603.
- [2] Ambroggio, E. E., F. Separovic, J. H. Bowie, G. D. Fidelio, and L. A. Bagatolli. *Biophys J.*, **2005**, 89:1874-1881.
- [3] Huang, Y., J. Huang, and Y. Chen. *Protein Cell*, **2010**, 1:143-152.
- [4] Liu, S., L. Zhou, R. Lakshminarayanan, and R. Beuerman. *Int J Pept Res Ther*, **2010**, 16:199-213.
- [5] Lorenzón, E. N., Cespedes, G.F., Vicente, E.F., Nogueira, L.G., Bauab, T.M., Castro, M.S., Cilli, E.M. *Antimicrob. Agents Chemother*, **2012**, 56:3004-3010.
- [6] Jiang, Z. Q., A. I. Vasil, L. Gera, M. L. Vasil, and R. S. Hodges. *Chem Biol Drug Des*, **2011**, 77:225-240.

Studies on the properties and mode of action of a synthetic hemocidin derived from α -hemoglobin

L. A. C. Carvalho,¹ C. Remuzgo,² M. T. Machini^{1*}

¹Department of Biochemistry, Institute of Chemistry, University of São Paulo; ²Special Laboratory of Pain and Signalling, Butantan Institute; São Paulo; Brazil
*mtmachini@iq.usp.br

Introduction

Candidemia has become a major problem in tertiary-care hospital worldwide as it causes morbidity and mortality in hospitalized patients, especially in the immunocompromised [1]. In Brazil, this is a large problem because the incidence rates of candidemia is 2-10 times higher than those documented in USA and Europe.

Hb40-61a (**KTYFPHFDSLHGSQAQVKGHGAK-NH₂**) is an amidated N-terminally truncated analogue of fragment 33-61 of bovine α -hemoglobin (**Hb**), the first antimicrobial peptide generated *in vivo* and isolated from the gut contents of the cattle tick *Boophilus microplus* [2]. Previously, we showed that both peptides are equally lethal to *Candida albicans* MDM8 and practically not active on human erythrocytes [3]. To better examine the anticandidal/anticandidacid activity and investigate the mode of action of Hb40-61a, in the present work we synthesized it, the all D-analog (D-Hb60-41a) and the fluorescently labeled analogue (FAM-Hb40-61a).

Stepwise solid-phase peptide synthesis was performed manually at 60°C using conventional heating and customized protocols [4,5]. The crude peptides were characterized by LC-ESI/MS and purified by RP-HPLC. The overall purities of the final products, evaluated by RP-HPLC and confirmed by LC-ESI/MS, were higher than 95%. Their peptide contents were obtained by full hydrolysis followed by amino acid analysis of the hydrolyzates. Their anticandidal, anticandidacid and hemolytic activities were measured as described earlier [3,6]. The potential of the fluorescently labeled analogue to damage the fungal cells was also verified by fluorimetry, confocal microscopy and FACS analysis.

Results and Discussion

Hb40-61a and D-Hb40-61a were 2-fold more active than FAM-Hb40-61a. All of them were able to kill the *Candida* strains tested (**Table 1**) and caused low hemolysis. On the other hand, these synthetic hemocidins were inactive against *Escherichia coli* ATCC 25922 and *Staphylococcus aureus* ATCC 25923.

Apparently, Hb40-61a targets the plasma membrane because, at the half of its MIC, FAM-Hb40-61a accumulates on it (**Fig. 1A**); at its MIC, the peptide penetrates into the cell and causes death (**Fig. 1B**). Indeed, at such concentration, 97% of the fluorescently labeled peptide incubated with the fungal cell was found into it.

Table 1. Minimum Inhibition Concentrations and Minimum Fungicidal Concentrations of the peptides studied at pH 5.5.

Peptide	MIC (μM)			MFC (μM)		
	<i>C. albicans</i> ATCC 90028	<i>C. krusei</i> ATCC 6258	<i>C. parapsilosis</i> ATCC 22019	<i>C. albicans</i> ATCC 90028	<i>C. krusei</i> ATCC 6258	<i>C. parapsilosis</i> ATCC 22019
Hb40-61a	6.25-12.5	25.0-50.0	6.25-12.5	12.5	50.0	12.5
D-Hb40-61a	6.25-12.5	25.0-50.0	6.25-12.5	12.5	50.0	12.5
FAM-Hb40-61a	12.5-25.0	50.0-100.0	25.0-50.0	25.0	100.0	50.0



Figure 1. Confocal microscopy analysis of the fungal cells treated with 12.5 μM FAM-Hb40-61a (A) and 25 μM FAM-HB40-61a (B).

Membrane permeabilization assays using Hb40-61a confirmed progressive membrane damage associated with the increase of peptide concentration. Additional experiments employing bis-(1,3-dibutylbarbituric acid) trimethine oxonol [DiBAC₄(5)] and 1,6-diphenyl-1,3,5-hexatriene (DPH) revealed that Hb40-61a induces the fungal plasma membrane depolarization and alters its dynamics, leading to cell death.

Acknowledgments

The authors are grateful to FAPESP (grant 2008/11695-1 to MTM), CAPES (fellowship to LACC), Prof. Dr. Iolanda M. Cuccovia (Department of Biochemistry, IQ-USP) and Prof. Dr. Katia R. Perez (Department of Biophysics, UNIFESP-SP).

References

- [1] Colombo, A. L.; Janini, M.; Salomão, R.; Medeiros, E. A. S.; Wey, S. B.; Pignatari, A. C. C. *Annals of the Brazilian Academy of Sciences*, **81**, 571-587 (2009).
- [2] Fogaça, A. C.; Silva, P. I.; Miranda, M. T. M.; Bianchi, A. G.; Miranda, A.; Tibolla, P. E.; Daffre, S. *Journal of Biological Chemistry*, **274**, 25330-25334, (1999).
- [3] Machado, A.; Sforça, M. L.; Miranda, A.; Daffre, S.; Pertinhez, T. A.; Spisni, A.; Miranda, M. T. M. *Biopolymers*, **88**, 413-426, (2007).
- [4] Souza, M.P.; Tavares, M. F. M.; Miranda, M. T. M. *Tetrahedron* **60**, 4671-4681 (2004).
- [5] Remuzgo, C.; Andrade, G. F. S.; Temperini, M. L. A.; Miranda, M T. M. *Biopolymers* **92**, 65-75 (2009).
- [6] Fehlbaum P.; Bulet, P.; Michaut, L.; Lagueux, M.; Broekaert, W. F.; Hetru, C.; Hoffman, J. A. *J. Biol. Chem.* **269**, 33159-33163 (1994).

Sviceucin, a lasso peptide from *Streptomyces sviceus*: Isolation and structural analysis

Rémi Ducasse,¹ Yanyan Li,¹ Alain Blond,¹ Séverine Zirah,¹ Ewen Lescop,² Christophe Goulard,¹ Eric Guittet,² Jean-Luc Pernodet,³ Sylvie Rebuffat¹

¹Muséum National d'Histoire Naturelle, CNRS, Laboratoire Molécules de Communication et Adaptation des Microorganismes, UMR 7245, CP 54, 57 rue Cuvier, 75005 Paris, France; ²CNRS, Centre de Recherche de Gif, Institut de Chimie des Substances Naturelles, UPR 2301, Avenue de la Terrasse, 91198 Gif-sur-Yvette, France; ³Université Paris Sud, CNRS, Institut de Génétique et Microbiologie, UMR 8621, Orsay, France
 E-mail: rebuffat@mnhn.fr

Introduction

Lasso peptides form a growing class of 16- to 21-residue ribosomally-synthesized and post-translationally modified peptides produced by bacteria. They share a rigid and compact interlocked structure consisting of a macrolactam ring at the N-terminus and a C-terminal tail that loops back and is threaded through the ring, forming a typical [1]rotaxane [1,2]. The macrolactam is formed by condensation of an Asp8 or Glu9 side-chain with the free amino group of a Gly1 or Cys1. The lasso fold is stabilized by steric hindrance assumed by bulky amino acid side-chains and/or by disulfide bridges. Lasso peptides are subdivided into three classes depending on the absence (type II) or presence of one (type III) or two (type I) disulfide bridges (Table 1). Given their unique knotted topology, they display a high stability against proteolytic and chemical degradation. They are biologically active on various protein targets, which confer them in some cases an interesting antimicrobial activity. These characteristics make the lasso scaffold a promising tool for biotechnological application in the development of bioactive peptides. In this study, we isolated and characterized the structure of a novel type I lasso peptide produced by *Streptomyces sviceus* that we called sviceucin.

Table 1: Type-I lasso peptides. The macrolactam ring and disulfide bridges are shown above and below the amino acid sequence, respectively. The conserved amino acids are shown in bold.

Name	Sequence	Producing bacteria
Siamycin 1 (or MS-271 or NP-06)		<i>Streptomyces</i> sp.
Siamycin 2		<i>Streptomyces</i> sp.
RP 71955 (or aborycin)		<i>Streptomyces</i> sp., <i>Streptomyces griseoflavus</i>
Sviceucin		<i>Streptomyces sviceus</i>

Results and Discussion

We discovered a gene cluster of a putative type I lasso peptide, termed svuceucin, in the genome of *S. svuceus* DSM 924. Heterologous expression of the biosynthetic gene cluster in *Streptomyces coelicolor* led to high production of the peptide (5 mg peptide / L culture). The structure of svuceucin was characterized by NMR at 600 MHz in d_3 -MeOH at 298 K. The ^1H spectra showed a significant chemical shift dispersion, which testifies that the peptide is highly structured. The NOESY spectrum revealed correlations between the macrolactam ring and residues of the C-terminal tail, indicative of the lasso fold, and permitted to assign the disulfide bridge pattern. A total of 163 interproton distances and 12 Φ angles was used as constraints to calculate the three-dimensional structure of the peptide (Figure 1). The structure is close to that reported for RP-71955 [5,6] (Table 1), which displays antibacterial and anti-HIV activities. Svuceucin has a bulky residue below the ring (Trp17), which could participate in the steric entrapping of the tail in the macrolactam ring.

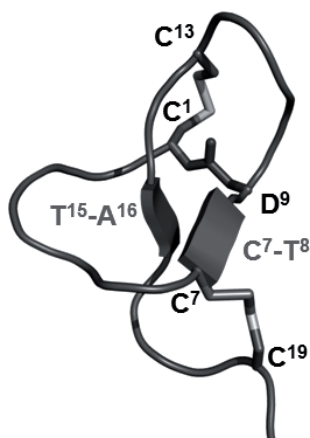


Figure 1: Three-dimensional structure of svuceucin.

Acknowledgments

The ANR (grant LASSO, BLAN-NT09-692063) and the TGE RMN THC Fr3050 are gratefully acknowledged for financial support for conducting the research. We thank the mass spectrometry platform (MNHN, Paris) for access to the ESI-Qq-TOF mass spectrometer.

References

- [1] Rebuffat, S.; Blond, A.; Destoumieux-Garzón, D.; Goulard, C.; Peduzzi, J. *Curr. Protein Pept. Sci.* **2004**, *5*, 383-91.
- [2] Maksimov, M. O.; Pan, S. J.; Link, J. A. *Nat. Prod. Rep.* **2012**, *29*, 996-1006.
- [3] Helynck, G.; Dubertret, C.; Mayaux, J. F., Leboul, J. *J. Antibiot.* **1993**, *46*, 1756-7.
- [4] Fréchet, D.; Guittou, J. D.; Herman, F.; Faucher, D.; Helynck, G.; Monegier du Sorbier, B.; Ridoux, J. P.; James-Surcouf, E.; Vuilhorgne, M. *Biochemistry* **1994** ; *33*, 42-50.

Synthesis of PAF, an antifungal protein from *Penicillium chrysogenum* by native chemical ligation

Györgyi Váradi¹, Gyula Batta², László Galgóczi³, Zoltán Kele¹,
Gábor K. Tóth¹

¹Department of Medical Chemistry, University of Szeged, Dóm tér 8, 6720 Szeged, Hungary; ²Department of Organic Chemistry, University of Debrecen, Egyetem tér 1, 4010 Debrecen, Hungary; ³Department of Microbiology, University of Szeged, Közép fasor 52, 6726 Szeged, Hungary

E-mail: varadi.gyorgyi@med.u-szeged.hu

Introduction

The *Penicillium chrysogenum* antifungal protein (PAF) is a cysteine-rich, cationic 55-mer protein that inhibits the growth of a variety of filamentous fungi [1, 2]. It has no toxic effects on mammalian cells [3], therefore, PAF may be a promising candidate for the development of new antifungal drugs [4]. The structure of PAF is stabilized by three disulfide bridges that are essential for the biological activity [5]. NMR investigations suggested two possible disulfide bond patterns for PAF: *abcabc* or *abbacc* [6]. Based on homology to other cysteine-rich antifungal proteins, the *abcabc* topology is more feasible (Fig. 1).



Fig. 1. Sequence and supposed disulfide bond pattern of PAF.

We aimed the chemical synthesis of PAF for the unambiguous determination of the disulfide bond pattern and for establishing a way for preparing analogues. All these efforts can lead to a better understanding of the striking differences between the mode of action of highly homologous antifungal proteins like PAF and AFP.

Results and Discussion

The first attempt for the synthesis of PAF was a stepwise synthesis on the solid-phase using either Fmoc or Boc chemistry. Different coupling methods were tested, but none of the Fmoc-based syntheses led to the desired product. Applying Boc chemistry, the yield of the synthesis was only 3% for the unfolded protein. The failure of stepwise synthesis prompted us to use native chemical ligation [7]. The two parts of PAF were successfully synthesized on the solid phase using Boc chemistry. One of the crucial points of native chemical ligation is the preparation of the thioester. A new method has been worked out which used the sulfhydryl group of a cysteine residue as thiol component in the thioester. Native chemical ligation of the purified fragments was conducted in a pH 7.5 buffer in the presence of thiophenol in 4-5 hours providing unfolded PAF.

Two strategies were tested for folding of PAF: selective and non-selective protection of the cysteine residues. When selective protection was applied, pairs of cysteines were protected

by Mbzl, Acn and Fm groups. In parallel to the cleavage from the solid support, Mbzl groups were removed, allowing the formation of the first disulfide bridge right after the chemical ligation in a pH 7.5 buffer by stirring oxygen to the solution. Then, iodine easily cleaved the acetamidomethyl groups and formed the second S-S bridge in a one-pot reaction. Nevertheless, basic treatment triggered rearrangement of the previously formed disulfide bonds during the cleavage of Fm groups and resulted in misfolding of the protein. When non-selective protection was used, most of the oxidative folding methods led to unnatural disulfide bridge pattern. The only method that produced native PAF was intensive stirring of oxygen into a solution of the synthetic “linear” PAF in a pH 7.5 buffer in the presence of catalytic amount of cysteine [8].

Synthetic PAF was characterized by analytical HPLC, MS, NMR and *in vitro* broth microdilution antifungal susceptibility test. To determine disulfide bond pattern, the peptide was digested using a mixture of trypsin and chymotrypsin. The fragments were separated by HPLC and analyzed by MS. MS-Bridge program at <http://prospector.ucsf.edu/prospector/mshome.htm> was applied for the determination of disulfide linked fragments. Several different NMR techniques (¹H-NMR, ¹³C-HSQC and 2D-NOESY) were used for investigating the 3D structure of PAF. These measurements prove that the structures of synthetic and native PAF are identical. The minimal inhibitory concentrations determined to *Aspergillus nidulans* FGSC26, *Aspergillus niger* SZMC 601 and *Trichoderma longibrachiatum* UAMH 7955 indicate that the *in vitro* antifungal activity of synthetic PAF on filamentous fungi is similar to which is exerted by native PAF [9].

Acknowledgements

This work was supported by TÁMOP 4.2.1/8-09/1/KONV-2010-0005 and 4.2.1/B-09/KONV-2010-0007 grants and by the Hungarian Scientific Research Fund OTKA CK 77515. László Galgóczi holds a postdoctoral fellowship from the Hungarian Scientific Research Fund (OTKA; PD83355).

References

- [1] Marx, F.; Haas, H.; Reindl, M.; Stoffler, G.; Lottspeich, F.; Redl, B. *Gene* **1995**, *167*, 167.
- [2] Marx, F. *Appl Microbiol Biotechnol* **2004**, *65*, 133.
- [3] Hegedűs, N.; Szigeti, G. P.; Pál, B.; Rusznák, Z.; Szűcs, G.; Rajnavölgyi, É.; Balla, J.; Balla, G.; Nagy, E.; Leiter, É.; Pócsi, I.; Marx, F.; Csernoch, L. *Naunyn-Schmiedeberg's Arch. Pharmacol.* **2005**, *371*, 122.
- [4] Marx, F.; Binder, U.; Leiter, É.; Pócsi, I. *Cell. Mol. Life Sci.* **2008**, *65*, 445.
- [5] Campos-Olivas, R.; Bruix, M.; Santoro, J.; Lacadena, J.; Delpozo, A. M.; Gavilanes, J. G.; Rico, M. *Biochemistry* **1995**, *34*, 3009.
- [6] Batta, G.; Barna, T.; Gáspári, Z.; Sándor, S.; Kövér, K. E.; Binder, U.; Sarg, B.; Kaiserer, L.; Chhillar, A. K.; Eigentler, A.; Leiter, É.; Hegedűs, N.; Pócsi, I.; Lindner, H.; Marx, F. *FEBS Journal* **2009**, *276*, 2875.
- [7] Dawson, P. E.; Muir, T. W.; Clark-Lewis, I.; Kent, S. B. H. *Science* **1994**, *266*, 776.
- [8] Szabó, I.; Schlosser, G.; Hudecz, F.; Mező, G. *Peptide Science* **2006**, *88*, 20.
- [9] Galgóczy, L., Kovács, L., Vágvolgyi, C., p 550-559. In Méndez-Vilas A (ed), *Current Research, Technology and Education Topics in Applied Microbiology and Microbial Biotechnology* Vol. 1, Microbiology Book Series-Number 2. Formatex, Bajadóz, Spain, 2010

Synthesis of glycated and glycosylated peptides to detect autoantibodies in diabetic patients' sera

C. Rentier,^{1,2,3} O. Monasson,^{1,3} F. Nuti,^{1,2} P. Traldi,⁴ A. Lapolla,⁵ M. Larregola,^{1,3} P. Rovero,^{1,6} M. Chorev,^{7,8} A. M. Papini^{1,2,3}

¹Laboratory of Peptide & Protein Chemistry & Biology - PeptLab - www.peptlab.eu;

²Department of Chemistry "Ugo Schiff", Via della Lastruccia 3/13, Polo Scientifico e Tecnologico, University of Florence, I-50019 Sesto Fiorentino, Italy; ³SOSCO – EA4505, University of Cergy-Pontoise, Neuville-sur-Oise, 95031 Cergy-Pontoise, France; ⁴CNR ISTM, Corso Stati Uniti 4, I-35127 Padua, Italy; ⁵University of Padua, Dipartimento Sci. Med. & Chirurg., Via Giustiniani 2, I-35128 Padua, Italy; ⁶Department of Pharmaceutical Sciences, Via Ugo Schiff 6, Polo Scientifico e Tecnologico, University of Florence, I-50019 Sesto Fiorentino, Italy; ⁷Laboratory for Translational Research, Harvard Medical School, One Kendall Square, Building 600, Cambridge, MA 02139 USA; ⁸Department of Medicine, Brigham and Women's Hospital, 75 Francis Street, Boston, MA 02115, USA

E-mail:cedric.rentier@gmail.com

Introduction

Diabetes is characterized by abnormal concentration of glucose in blood (hyperglycemia). Two different mechanisms for possible aberrant post-translational modifications of proteins by sugars: a non-enzymatic mechanism (i.e., glycation) initiated by Schiff base formation followed by an Amadori rearrangement and elaborated to form advanced glycation endproducts (AGEs) [1] and an enzymatic mechanism (i.e., glycosylation), giving rise to N- or O-glycosylation patterns. Glycation and AGEs are believed to play a critical role in diabetic vascular complications. We speculate that hyperglycemia may generate a higher concentration of glycated/glycosylated peptides in the bodily fluids of diabetic patients as compared to healthy individuals.

We previously demonstrated that incorporating a glycosylated side chain in a type I' β -turn peptide (i.e., CSF114) provides an optimal presentation of the minimal glycosylated epitopes. These can be used in the solid-phase (SP)-ELISA to recognize, capture with high affinity, and specific autoantibodies related to immune-mediated diseases [2,3]. Thus, we propose to use glycated and glucosylated peptides in SP-ELISA for the potential detection of disease-related autoantibodies in sera of diabetic patients (types I and II).

Results and Discussion

We synthesized the [N^c-(1-deoxyfructopyranosyl)Lys⁷]CSF114 (**I**), using *N*^α-Fmoc-*L*-Lys(N^c-2,3:4,5-di-O-isopropylidene-1-deoxy- β -D-deoxyfructopyranosyl,N^c-Boc)-OH as a building-block in the SPPS, e.g. [4], and the unglycated peptide [Lys⁷]CSF114 (**II**) as a control. The MW-assisted SPPS of peptide **I** by Fmoc/tBu strategy, was performed on a Biotage SyroWave system starting from Fmoc-Lys(Boc)-Wang resin (0.7 mmol/g) using Fmoc-protected amino acids, TBTU (5 eq) in 0.5M DMF solution, and DIPEA (5 eq) in 1M NMP. Coupling of *N*^α-Fmoc-*L*-Lys(N^c-2,3:4,5-di-O-isopropylidene-1-deoxy- β -D-

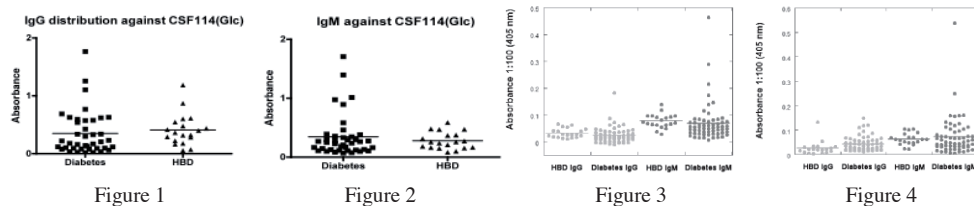
deoxyfructopyranosyl, N^{ϵ} -Boc)-OH (2.5 eq) was performed with TBTU (5 eq) and DIPEA (5eq). MW-coupling conditions were 5 min at 75°C and 20W. Because of possible Met oxidation, the cleavage was performed following the protocol previously reported by Taboada *et al.* [5], which is based on a one-pot cleavage-reduction.

Peptide **II** was obtained by manual SPPS using Fmoc/tBu strategy, starting from Fmoc-Lys(N^{ϵ} -Boc)-Wang resin (0.7 mmol/g) and coupling the amino acids with TBTU in DMF (4 eq) and NMM (5 eq). CSF114(Glc) was synthesized following the previously reported method [3]. Characterizations are summarized in the following table:

Peptide	HPLC R_f (min)	ESI/MS (m/z) [M+3H] ³⁺	MALDI (m/z) [M+H] ⁺
[(1-deoxyfructopyranosyl)Lys ⁷]CSF114 (I)	3.99 ^a	874.78 (calc. 874.13)	2620.443 (calc. 2620.370)
[Lys ⁷]CSF114 (II)	2.61 ^b	820.76 (calc. 820.11)	2458.436 (calc. 2458.318)
CSF114(Glc)	2.64 ^b	870.19 (calc. 869.44)	2606.321 (calc. 2606.318)

RP-HPLC, Phenomenex Jupiter C18 250x5mm, MeCN/0.1% TFA in H₂O/0.1% TFA in 5 min at ^a0.6 mL/min, 20-70%, ^b 30-60%
MALDI were performed with a Bruker Daltonics flexAnalysis on HCCA matrix.

We tested peptides **I**, **II**, and CSF114(Glc) on 40 diabetes sera (type-1 and type-2 patients) and 20 healthy blood donors (HBD). In Figures 1-4 we report the IgG and IgM Ab titers (measured at 405 nm) as obtained by SP-ELISA using as antigens CSF114(Glc) (Fig. 1 and 2), [N^ε-(1-deoxyfructopyranosyl)Lys⁷]CSF114 (**I**) (Fig. 3), and [Lys⁷]CSF114 (**II**) (Fig. 4).



We do not observe any statistically significant differences between Ab titer in sera of HBDs and type-1 and type-2 diabetes patients, using both peptides **I** and **II**.

However, in the case of the CSF114(Glc), diabetes samples (5/40, 12%) present higher Ab titers compared to HBD. All 5 positive sera are clinically defined as type-1 diabetes.

We continue to screen diabetic and normal individuals' sera in order to reach statistical significance of these interesting preliminary results.

Acknowledgments

ANR Chaire d'Excellence PeptKit 2009-2013 (AMP) is gratefully acknowledged for its financial support.

References

- [1] Ulrich, P.; *et al. Recent Prog. Horm. Res.* **2001**, *56*, 1–21.
- [2] a) Papini, A.M. *J. Pept. Sci.*, **2009**, *15*, 621-628. b) Carotenuto, A. ; *et al. J. Med. Chem.* **2006**, *49*, 5072-5079. c) Carotenuto, A. ; *et al. J. Med. Chem.* **2008**, *51*, 5304-5309.
- [3] Lolli, F. *et al. PNAS*, **2005**, *102*(29), 10273-10278.
- [4] Carganico, S. *et al. J. Pept. Sci.* **2009**; *15*, 67–71.
- [5] Taboada, L. *et al. Tetrahedron Lett.*, **2001**, *42*, 1891-1893.

Synthesis, structure-activity relationship study and antimicrobial activity of a new tigerinins analog

François Bédard^a, Thi Thuy An Nguyen^b, Irena Kukavica-Ibrullj^b,
Halim Maaroufi^b, Roger C. Lévesque^b, Eric Biron^{a*}

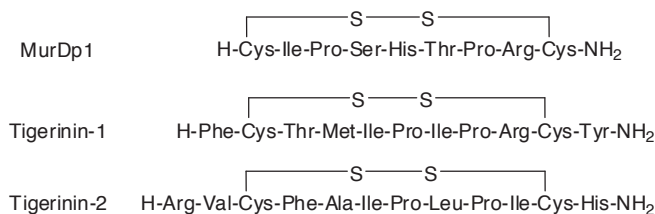
^aFaculty of Pharmacy, Université Laval and Laboratory of Medicinal Chemistry, CHUQ Research Center, CHUL Section, Quebec (QC), Canada; ^bFaculty of Medicine, Université Laval and Institut de Biologie Intégrative et des Systèmes (IBIS), Quebec (QC), Canada
E-mail: eric.biron@pha.ulaval.ca

Introduction

The worldwide spread of antibiotic resistance among emerging and re-emerging bacterial pathogens has promoted the development of structurally new antibacterials with novel modes of action. Antimicrobial peptides (AMP) play an important role in innate immunity in several species. Intracellular targets have been reported for some AMP but for most of them act by membrane disruption [1]. The bacterial cell wall biosynthesis pathway represents an attractive antibacterial target source since it encodes essential enzymes whose inhibition gives a lethal phenotype. Many clinically useful antibiotics interfere with the late cell wall synthesis step but few antibacterial agents inhibit the early cytoplasmic steps of the pathway. In order to discover MurD inhibitors, phage display libraries were screened with the purified *Pseudomonas aeruginosa* MurD to identify peptide inhibitors [2]. From the 60 peptides identified, the MurDp1 peptide H₂N-[CIPSHTPRC]-CONH₂ showed ATPase inhibition activity with an IC₅₀ of 4 μM. Based on this good activity, we were interested to identify natural AMP with sequence similarities to MurDp1 and to evaluate their antimicrobial activity and MurD inhibition activity.

Results and Discussion

Natural bioactive peptides with similarities to MurDp1 were looked up in the «Antimicrobial Peptide Database» (<http://aps.unmc.edu/AP/main.html>). This search brought to light Tigerinin-1 and Tigerinin-2. Tigerinins are 11 to 12 residue AMP isolated from the Indian frog *Rana tigerina* [3]. With reported MIC ranging from 10 to 50 μg/ml against different bacterial strains, these peptides are characterized by a disulfide-bridged loop composed of 9 amino acids. Tigerinins represent the smallest non-helical cationic AMP from amphibians. Their mode of action is believed to be by membrane disruption but has not been clearly elucidated [3,4]. Based on the inhibitory activity of MurDp1 on the MurD enzyme and its important similarity with tigerinins, the next step was to investigate if the enzyme MurD could be an intracellular target for the tigerinins.



Peptides MurDp1, Tigerinin-1 and Tigerinin-2 were prepared on Rink Amide resin by standard Fmoc solid phase peptide synthesis. After their release from the resin with a TFA cleavage cocktail, the peptides were cyclized in solution with 20% DMSO in water. The peptides were purified by HPLC and characterized by LC-MS (ESI). Antimicrobial activity of MurDp1 and Tigerinin-2 was then evaluated. To do so, bacterial cells (*E. coli* strain MC1061) in the midlogarithmic phase of growth (10^5 CFUs) were incubated with different concentrations of MurDp1 and Tigerinin-2. Aliquots were taken after incubation for 2 h and plated on Mueller Hinton agar. CFUs were determined after 24 h at 37°C. The results showed that the antibacterial activity of MurDp1 is comparable to Tigerinin-2. *In silico* studies were performed with the model structure of MurD from *P. aeruginosa* and the studied peptides using Modeller, AutoDock and PatchDock. The results obtained suggested a greater stability for the MurD/Tigerinin-2 complex than for Tigerinin-1. We also noted that Cys3 and His12 of Tigerinin-2 form H-bonds with MurD Arg39, Asp190, Asp355, and Arg380. On the other hand, Phe433 which interact with D-Glu in the natural substrate is involved in cation- π interactions with Arg1 of Tigerinin-2. This interaction is also observed with the MurDp1 peptide.

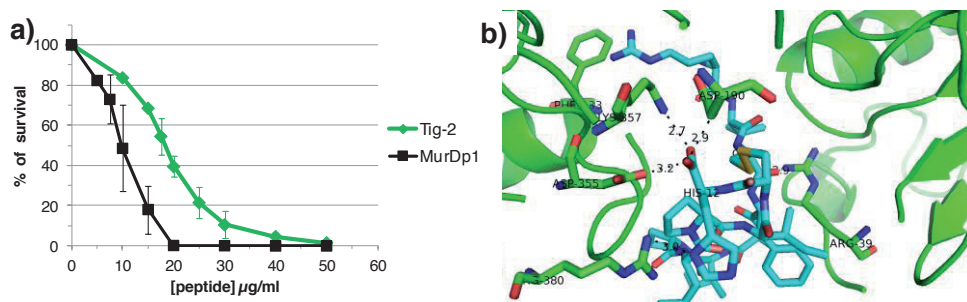


Fig. 1. Antimicrobial activity of and *in silico* studies: a) Kinetics of killing of bacteria by MurDp1 and Tigerinin-2; b) MurD-Tigerinin-2 complex.

In summary, the peptide MurDp1, isolated by phage display, is a MurD enzyme inhibitor showing good antimicrobial activity. Database mining for homologous natural AMP has allowed us to identify the Tigerinins. *In silico* studies suggested that Tigerinin-2 could be a potential MurD enzyme inhibitor and that MurD could be an intracellular target. Enzymatic assays on purified MurD with MurDp1, Tigerinin-1 and Tigerinin-2 as well as X-ray crystallography analyses of MurD/Tigerinin-2 complex are underway.

Acknowledgments

We gratefully acknowledge the NSERC of Canada and FRQS of Quebec for financial support. F.B. thanks the NSERC of Canada for undergraduate Scholarships.

References

- [1] Brogden, K. A. *Nature Rev. Microbiol.* **2005**, *3*, 238-250.
- [2] Paradis-Bleau, C.; Beaumont, M.; Boudreault, L.; Lloyd, A.; Sanschagrin, F.; Bugg, T. D. H.; Lesvesque, R. C. *Peptides* **2006**, *27*, 1693-1700.
- [3] Sai, K. P.; Jagannadham, M. V.; Vairamani, M.; Raju, N. P.; Devi, A. S.; Nagaraj, R.; Sitaram, N. *J. Biol. Chem.* **2001**, *276*, 2701-2707.
- [4] Sitaram, N.; Sai, K.P.; Singh, S.; Sankaran, K.; Nadaraj, R. *Antimicrob. Agents Chemother.* **2002**, *46*, 2279-2283.

The study of defensins of biomedical importance isolated from arthropods

Václav Čerovský,¹ Baydaa El Shazely,¹ Vladimír Fučík,¹ Zdeněk Voburka,¹ Jan Žďárek,¹ Jiřina Slaninová,¹ Tereza Chrudimská,²
Libor Grubhoffer²

¹Institute of Organic Chemistry and Biochemistry, Academy of Sciences of the Czech Republic, Flemingovo nám. 2, 16610 Prague, Czech Republic; ²Faculty of Science, University of South Bohemia, Branišovská 31, 37005 České Budějovice, Czech republic

E-mail: cerovsky@uochb.cas.cz

Introduction

Defensins are the most widespread antimicrobial peptides (AMPs) characterized in arthropods. These are cyclic peptides of the size 4-6 kDa folded into hairpin-like β -sheets or α -helical/ β -sheet mixed structures. They share a common conserved motif of three intramolecular disulfide bridges with a connectivity Cys1-Cys4, Cys2-Cys5 and Cys3-Cys6. They display multifunctional properties with implications as potential therapeutic agents. They have ability to kill preferentially Gram-positive bacteria and some fungi, but not Gram-negative bacteria. During recent period we have identified several novel AMPs in arthropods including defensins [1-3]. Here we report isolation and characterization of two defensins identified in medicinal larvae of the flies *Lucilia sericata* [1] and *Lucilia cuprina*, and one defensin identified in European tick *Dermacentor marginatus* [3]. Larvae of *L. sericata* and *L. cuprina* flies are routinely used in hospitals for the treatment of non-healing infected wounds during the procedure known as maggot therapy.

Lyme disease is a serious human illness caused by spirochetes of the complex *Borrelia burgdorferi* sensu lato, being transmitted to human by certain tick species. In contrast, European ticks of the genus *Dermacentor* are incompetent to serve as vectors of this disease. Furthermore, they are able to effectively eliminate spirochetes from their body using humoral factors of innate immunity. We presume that defensin involved in the immune responses of *Dermacentor marginatus* might possess a borreliacidal activity.

Results and Discussion

Lucifensin, 40 amino acid residues AMP identified formerly in our laboratory [1] in the medicinal maggots of *L. sericata*, was synthesized by Fmoc protocol of SPPS. Oxidative folding of linear precursor was achieved through an air-mediated oxidation of pre-purified linear peptide resulting in a single peptide product of the molecular mass (4113.5) identical to natural peptide. In antimicrobial assays, lucifensin showed activity preferentially against Gram-positive bacteria and was not hemolytic [2]. To confirm the importance of disulfide bridges for its activity and structure we synthesized three lucifensin analogs cyclized through one native disulfide bridge in different positions (Cys3-Cys30, Cys16-Cys36, Cys20-Cys38) and having the remaining four cysteines substituted by alanine. The analog cyclized through the Cys16-Cys36 disulfide bridge showed weak antimicrobial activity, while the other two analogs containing one disulfide bridge in other positions were inactive

[2]. Weak antimicrobial activity of shortened lucifensin analog Luc[des1-10, Ala30] indicates the importance of the N-terminal part of the molecule for maintaining the lucifensin conformation which is a prerequisite for the lucifensin action mechanism [2].

Lucifensin II was isolated from the hemolymph of *L. cuprina* larvae using an improved purification protocol. It included two ultrafiltration steps of the hemolymph extract (50% acetonitrile containing 0.5% TFA), which resulted in removal of redundant high and low molecular weight compounds. In the subsequent step utilizing RP-HPLC (C18, 250 x 4.6 mm column, 20 consecutive runs) the antimicrobial activity was detected in one tiny fraction. This fraction was further subjected to size-exclusion HPLC resulting in well separated peak of lucifensin II. Its final re-purification by RP-HPLC gave sufficient amount of pure lucifensin II for the elucidation of its primary structure by Edman degradation and by mass spectrometry. Lucifensin II (determined molecular mass 4127.9) sequence differs from that of lucifensin by only one amino acid residue; that is by Ile instead of Val at position 11. As confirmed by NMR study, the side chain of Val¹¹ in lucifensin is exposed to the solvent and does not directly participate to the interactions required for stabilizing of the peptide core [4]. Predicted structural effect of the alteration of Val at this position for Ile in lucifensin II will be minimal, as the change does not require a major rearrangement of the adjacent residues. We anticipate that the difference represented by an extra methyl moiety will be not reflected in its biological activity.

D.m.-defensin was purified from the extract of the hemolymph of blood sucking tick *Dermacentor marginatus* (*D.m.*) using similar purification procedure as above, but omitting the size exclusion chromatography step. Its determined exact monoisotopic molecular mass 4222.90 was in good agreement with the calculated value 4222.89 based on the sequence of defensin determined by Edman degradation: Gly-Phe-Gly-X-Pro-Leu-Asn-Gln-Gly-Ala-X-His-Asn-His-X-Arg-Ser-Ile-Arg-Arg-Arg-Gly-Gly-Tyr-X-Ser-Gly-Ile-Ile-Lys-Gln-Thr-X-Thr-X-Tyr-Arg-Asn (assuming that the undetermined amino acid residues (X) were cysteines forming three disulfide bridges). The sequence of isolated *D.m.*-defensin is identical with the sequence which was already determined in our laboratory by the methods of molecular biology [3], and shows no homology to the sequence of above mentioned lucifensins. By SPPS prepared linear precursor of *D.m.*-defensin was pre-purified by RP-HPLC and then subjected to oxidative folding under the open air. The linear peptide was straightforwardly folded into cyclic one which was identical to that of native peptide. In antimicrobial assay using a set of different bacteria, the *D.m.*-defensin shows activity preferentially against Gram-positive bacteria including *Staphylococcus aureus* (MIC values: 0.25 μ M, *Micrococcus luteus*; 0.25 μ M, *Bacillus subtilis*; 2.0 μ M, *Staphylococcus aureus*) but is inactive against Gram-negative bacteria and *Candida albicans*.

Acknowledgments

This work was supported by the Czech Science Foundation, Grants Nos. P302/11/1901, 203/08/0536 and by the research project RVO 61388963 of the Institute of Organic Chemistry and Biochemistry, Academy of Sciences of the Czech Republic.

References

- [1] Čerovský, V.; Žďárek, J.; Fučík, V. et al. *Cell. Mol. Life Sci.* **2010**, *67*, 455.
- [2] Čerovský, V.; Slaninová, J.; Fučík, V. et al. *ChemBioChem* **2011**, *12*, 1352.
- [3] Chrudimská, T.; Chrudimský, T.; Golovchenko, M. et al. *Vet. Parasitol.* **2010**, *167*, 298.
- [4] Nygaard, M.K.E.; Andersen A.S.; Kristensen, H.-H. et al. *J. Biomol. NMR* **2012**, *52*, 277.

Trichogin GA IV and selected analogs as new antitumor agents: Synthesis, conformational analysis and cytotoxicity evaluation

Marta De Zotti¹, Barbara Biondi¹, Regina Tavano², Cristina Peggion¹,
Marco Crisma¹, Fernando Formaggio¹, Emanuele Papini²,
Claudio Toniolo¹

¹ICB, Padova Unit, CNR, Department of Chemistry, University of Padova, 35131 Padova, Italy; ²C.R.I.B.I. and Department of Biomedical Sciences, University of Padova, 35121 Padova, Italy

E-mail: barbara.biondi@unipd.it

Introduction

Trichogin GA IV, isolated from the fungus *Trichoderma longibrachiatum* [1], is the prototype of lipopeptaibols, a sub-class of short-length peptaibiotics exhibiting membrane-modifying properties. Its primary structure is as follows: *n*-Oct-Aib¹-Gly-Leu-Aib-Gly-Gly-Leu-Aib-Gly-Ile¹⁰-Lol, where *n*-Oct is *n*-octanoyl, Aib is α -aminoisobutyric acid, and Lol is the 1,2-amino alcohol leucinol.

This 10-mer peptaibol is predominantly folded in a mixed 3₁₀-/ α -helical conformation with a clear, albeit modest, amphiphilic character [2]. In this work, we synthesized by solution and solid-phase methodologies a set (**A**) of trichogin GA IV analogs in which the four Gly residues, lying on the poorly hydrophilic face of the helical structure, are substituted by one (or more) strongly hydrophilic Lys residues [3]. Moreover, we synthesized another set (**B**) of analogs where one (or more) Aib residues are replaced by Leu [4]. The complete list of the peptides prepared and investigated is given below.

- A**
- n*-Oct-Aib-**Lys**-Leu-Aib-Gly-Gly-Leu-Aib-Gly-Ile-Lol
 - n*-Oct-Aib-Gly-Leu-Aib-**Lys**-Gly-Leu-Aib-Gly-Ile-Lol
 - n*-Oct-Aib-Gly-Leu-Aib-Gly-**Lys**-Leu-Aib-Gly-Ile-Lol
 - n*-Oct-Aib-Gly-Leu-Aib-Gly-Gly-Leu-Aib-**Lys**-Ile-Lol
 - n*-Oct-Aib-**Lys**-Leu-Aib-**Lys**-Gly-Leu-Aib-Gly-Ile-Lol
 - n*-Oct-Aib-Gly-Leu-Aib-**Lys**-**Lys**-Leu-Aib-Gly-Ile-Lol
 - n*-Oct-Aib-**Lys**-Leu-Aib-**Lys**-Gly-Leu-Aib-**Lys**-Ile-Lol
 - n*-Oct-Aib-**Lys**-Leu-Aib-**Lys**-**Lys**-Leu-Aib-**Lys**-Ile-Lol
- B**
- n*-Oct-**Leu**-Gly-Leu-Aib-Gly-Gly-Leu-Aib-Gly-Ile-Lol
 - n*-Oct-Aib-Gly-Leu-**Leu**-Gly-Gly-Leu-Aib-Gly-Ile-Lol
 - n*-Oct-**Leu**-Gly-Leu-Aib-Gly-Gly-Leu-**Leu**-Gly-Ile-Lol

Results and Discussion

The conformational preferences of these analogs were assessed by X-ray diffraction, CD, and 2D-NMR techniques [3,4]. We also tested the role played by the substitutions on the peptide bioactivity, *e.g.* protease resistance, cytotoxicity, and hemolysis. In particular, cytotoxicity was examined using two *in vitro* cell-based assays: (i) mortality of separate sub-populations of human blood leukocytes; (ii) cell mortality in three tumor-derived stable cell lines (HeLa, A541, and A431). Our data show that a few of our trichogin analogs are active against tumor cells, while being less toxic towards leukocyte cells. We are currently trying to understand if dissimilar biological behaviors can be ascribed to different peptide conformations, such as those observed for instance for the Leu-analogs (Figure 1).

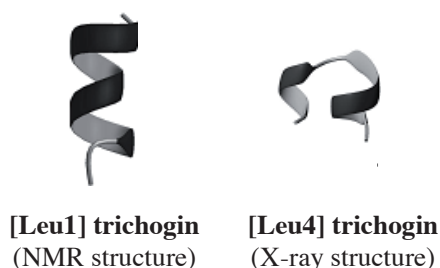


Fig. 1. Example of the relevant influence of residue replacements on peptide folding.

References

- [1] Auvin-Guette, C.; Rebuffat, S.; Prigent, Y.; Bodo, B. *J. Am. Chem. Soc.* **1992**, *114*, 2170.
- [2] Peggion, C.; Formaggio, F.; Crisma, M.; Epand, R.F.; Epand, R.M.; Toniolo, C. *J. Pept. Sci.* **2003**, *9*, 679.
- [3] De Zotti, M.; Biondi, B.; Peggion, C.; Formaggio, F.; Park, Y.; Hahm, K.-S.; Toniolo, C. *Org. Biomol. Chem.* **2012**, *10*, 1285.
- [4] De Zotti, M.; Biondi, B.; Park, Y.; Hahm, K.-S.; Crisma, M.; Toniolo, C.; Formaggio, F. *Amino Acids* **2012**, in press, DOI: 10.1007/s00726-012-1261-7.

A convenient post-screening ring-opening approach for the decoding of one-bead-one-compound cyclic peptide libraries

Anick Girard and Eric Biron

Faculty of Pharmacy, Université Laval and Laboratory of Medicinal Chemistry, CHUQ
Research Center, CHUL Section, Quebec (QC), Canada
E-mail: eric.biron@pha.ulaval.ca

Introduction

Cyclic peptides are useful tools in chemical biology and medicinal chemistry. The great degree of molecular diversity that can be accessed by simple changes in their sequence has prompted their use in combinatorial chemistry. The one-bead-one-compound (OBOC) approach, in which each bead carries many copies of a unique compound, has become a powerful tool in drug discovery [1]. However, its use with cyclic peptides has been limited by difficulties in sequencing hit compounds after the screening. Lacking a free N-terminal amine, Edman degradation sequencing cannot be used and complicated fragmentation patterns are obtained by MS/MS. In this regard, Pei group used a one-bead-two-compound approach on topologically segregated bilayer beads in which the cyclic peptide is exposed on the surface and its linear counterpart is found inside as a tag for sequencing [2]. More recently, Lim group reported a ring-opening strategy on cyclic peptoids to reduce the need for encoding [3]. The strategy involved the introduction of a cleavable alkylthioaryl bridge in the cycle to allow linearization of the molecule by oxidation and hydrolysis to generate a sequenceable linear peptoid. Based on this strategy, our objective was to develop a simple and efficient approach to prepare OBOC cyclic peptide libraries that would allow fast sequence determination after simultaneous macrocycle opening and release from the resin.

Results and Discussion

Our strategy was based on the incorporation of a cleavable residue within the cycle and as a linker (Fig. 1). Amongst the different linkers and cleavable residues readily available, we were particularly interested in methionine (Met). Being an amino acid, Met can be used in standard solid phase peptide synthesis and its impact on the conformation will be limited compared to extended aromatic residues. Moreover, Met is stable in acidic, basic or reductive conditions used to remove protecting groups. Finally, the reaction conditions used to cleave Met are very selective and compatible with free amino acid side chains.

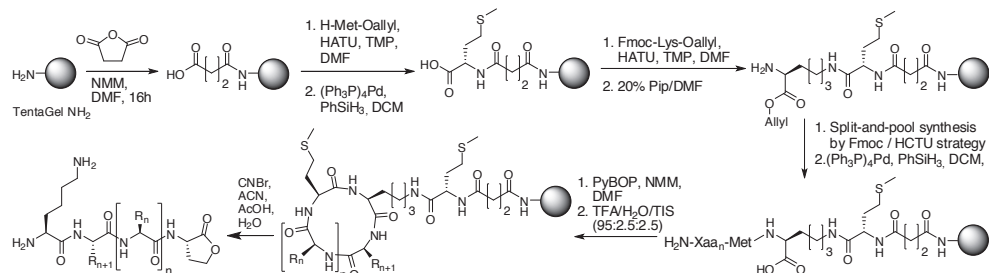


Fig. 1. Synthesis of OBOC cyclic peptide libraries on a reverse Met handle.

Met has been widely used as a linker in OBOC peptide libraries and can be selectively cleaved upon treatment with CNBr to yield a C-terminal homoserine lactone. In the proposed approach, the cleavable residue can be incorporated as the first or as the last amino acid during peptide synthesis. As reported by Simpson and Kodadek with cyclic peptoids [4], we observed incomplete cyclization when Met was the N-terminal amino acid. Moreover, when Met was the first amino acid, the MS/MS fragmentation patterns were difficult to analyse in the presence of two C-terminal homoserine lactones. To overcome these drawbacks, the Met in the cycle was introduced first and the Met linker was inverted to eliminate one C-terminal homoserine lactone (Fig.1). To do so, H-Met-OAll was coupled to the carboxylic acid derived resin **1** and following allyl ester cleavage, Fmoc-Lys-OAll was anchored to resin **2** via its side chain. After standard Fmoc solid phase synthesis, head-to-tail cyclization was performed on resin **3** and the side chains deprotected to yield the Lys side chain anchored cyclic peptides **4**. The introduction of a Met residue directly after the side chain anchored lysine in the cyclic peptide allowed a simultaneous ring-opening and cleavage from the resin upon treatment with a CNBr solution to yield a linear peptide bearing a single C-terminal homoserine lactone and an N-terminal lysine **5** (Fig. 1). The generated peptides were analyzed by MALDI-TOF/TOF and showed very clear MS/MS fragmentation patterns, allowing a rapid and accurate sequence determination (Fig. 2).

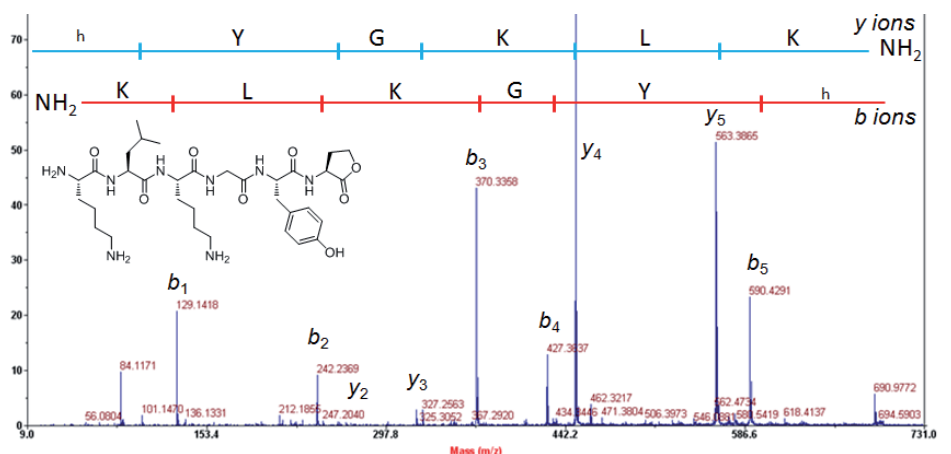


Fig. 2. MS/MS spectrum of peptide H_2N -KLKGYh.

In summary, the described procedure allows the simultaneous linearization of cyclic peptides and their release from the resin. This approach can be applied to prepare and decode OBOC cyclic peptide libraries without using bead encoding.

Acknowledgments

We gratefully acknowledge the NSERC of Canada and FRQS of Quebec for financial support. A.G. thanks the FER of Université Laval for postgraduate Scholarships.

References

- [1] Lam, K.S.; Krchnak, V.; Lebl, M. *Chem. Rev.* **1997**, *97*, 411.
- [2] Joo, S. H.; Xiao, Q.; Ling, Y.; Gopishetty, B.; Pei, D. *J. Am. Chem. Soc.* **2006**, *128*, 13000.
- [3] Lee, J. H.; Meyer, A. M.; Lim, H. S. *Chem. Comm.* **2010**, *46*, 8615.
- [4] Simpson, L. S.; Kodadek, T. A. *Tet. Lett.* **2012**, *53*, 2341.

Design and synthesis of biotinylated peptidyl phosphonate probe for the isolation of single chain Fv with hydrolyzing activity

Hiroaki Taguchi¹, Yoshio Fujita¹, Yuko Tsuda^{2,3}

¹Faculty of Pharmaceutical Sciences, Suzuka University of Medical Science, Suzuka, Japan;

²Faculty of Pharmaceutical Sciences, Kobe Gakuin University, Kobe, Japan;

³Cooperative Research Center of Life Sciences, Kobe Gakuin University, Kobe, Japan

taguchi@suzuka-u.ac.jp

Introduction

Some antibodies (Abs) and Ab L chains catalyze the hydrolysis of amyloid β peptides ($A\beta$), VIP and the HIV coat proteins gp41 and gp120. Diisopropylfluorophosphate, serine protease inhibitor, consistently inhibits the catalytic Abs and a serine protease-like catalytic triad in a model proteolytic Ab L chain has previously been deduced from site-directed mutagenesis studies. In principle, probes that can specifically recognize the active site of Abs with hydrolyzing activity could be applied for the isolation of Abs with hydrolyzing activity from display libraries.

Accumulation of $A\beta$ in the brain is one of the pathological hallmarks of Alzheimer's disease (AD) and has been considered to play a crucial role in the neurodegenerative events underlying AD. Catalytic Abs capable of binding and hydrolyzing $A\beta$ are candidates as immunotherapeutic agents for AD due to their ability to inactivate multiple $A\beta$ molecules per Ab molecule. We have reported that Abs with $A\beta$ hydrolyzing activity inhibited $A\beta$ aggregation and protected neuronal cells from $A\beta$ -induced toxicity [1]. However, homogeneous Abs with catalytic rate constants sufficient for therapy have not been generated until now. Here, we present synthesis of a novel probe (**1**) that was designed with the aim of isolating $A\beta$ hydrolyzing single chain Fv (scFv) or Fab clones from phage libraries. The probe **1** displayed the ability to inhibit hydrolyzing activity of trypsin and to bind anti- $A\beta$ monoclonal Ab specifically (Figure 1).

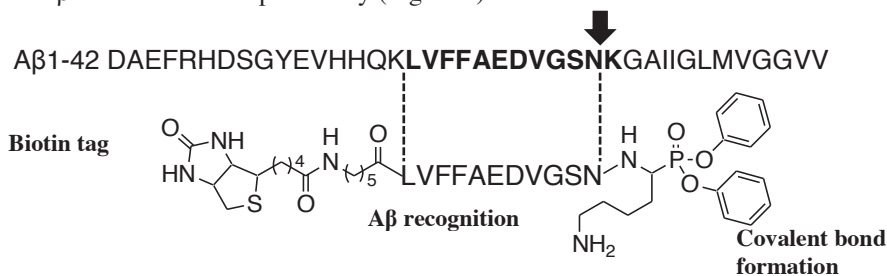


Figure 1. Structure of biotinylated $A\beta$ 17-27- Lys^P -(OPh)₂ (**1**)

Results and Discussion

Peptidyl (α -aminoalkyl) phosphonate esters, a class of inhibitors, that have been used to investigate serine protease and shown to be very stable and specific irreversible inhibitors of trypsin-like enzymes. Diphenyl amino(4-aminobutyl)methanephosphonate derivatives

are active site-directed irreversible inhibitors of trypsin-like enzymes, forming the covalent enzyme-inhibitor adducts by phosphorylating the active site Ser residue. The positively charged amino group adjacent to the phosphonate diester group serves as an analogue of Lys28 of A β . The Lys28–Gly29 bond is the major specific cleavage target by Abs because; 1) most natural proteolytic Abs cleave Lys/Arg–X bonds (X represents an amino acid residue); 2) hydrolyzing this bond lead to inhibition of forming A β aggregates and protection of neuronal cells from A β -induced toxicity.

Phosphonate diester analogue mimicking Lys was synthesized by Oleksyszyn reaction. Protected peptide fragment corresponding to A β 17–27 was synthesized by conventional Fmoc SPPS. The protected peptide fragment was coupled with phosphonate analogue with the aid of HATU followed by TFA treatment to remove the protecting group. The crude material was purified by HPLC and structure was confirmed by ESI-MS.

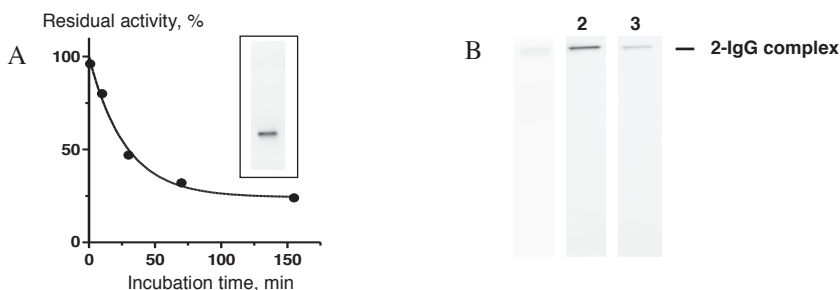


Figure 2. Irreversible inhibition of trypsin by **1** (A) and specific covalent binding of **1** by IgG (B). Inset, streptavidin-peroxidase-stained blot of SDS gel showing trypsin treated with **1**. B, streptavidin-peroxidase-stained blots of SDS gels showing **1** adducts formed by treatment with IgG to active protein C (lane 1) and IgG to A β in the absence of A β 1–40 (lane 2) or presence of A β 1–40 (lane 3)

The probe **1** irreversibly inhibited *N*-tert-butoxycarbonyl- γ -benzyl-Glu-Ala-Arg-7-amino-4-methylcoumarin hydrochloride hydrolysis by trypsin. Formations of a covalent adduct of **1** and trypsin was evident by denaturing SDS-PAGE. Labeling of trypsin by **1** was inhibited by pretreatment of phosphonate diester analogue without peptide region that is an active site-directed serine protease inhibitor. Thus, the phosphonate diester group at the C terminus formed the complex with active site serine residue. To evaluate peptide moiety, substrate specificity of **1** was tested by formation of the covalent complex with A β specific Abs. The probe **1** specifically formed the covalent complex with monoclonal antibody to A β , which was blocked by presence of A β 1–40. Those findings suggest that **1** has preferable property for isolation of A β hydrolyzing scFv or Fab clones from phage libraries.

Acknowledgments

This work was supported in part by an AstraZeneca VRI research grant and a Grant-in-Aid for Scientific Research (C) (No. 24590151).

References

- [1] Taguchi, H.; Planque, S.; Nishiyama, Y.; Symersky, J.; Boivin, S.; Szabo, P.; Friedland, R. P.; Ramsland, P. A.; Edmundson, A. B.; Weksler, M. E.; Paul, S. *J. Biol. Chem.* **2008**, 283, 4714.

The identification of advanced glycation sites in proteins by isotopic labeling with $^{13}\text{C}_6$ glucose

**Martyna Kielmas, Monika Kijewska, Piotr Stefanowicz,
Zbigniew Szewczuk**

Faculty of Chemistry, University of Wrocław, Wrocław, Poland

E-mail: piotr.stefanowicz@chem.uni.wroc.pl

Introduction

The Maillard reaction is a complex process that involves reducing-sugars and proteins, giving a multitude of end products that are known as AGEs (Advanced glycation end products). AGEs are formed by a modification of the lysine and/or arginine side chains and may contain variable number of carbon atoms [1]. They are a diverse class of compounds formed under oxidative or carbonyl stress [2].

It has been shown that the formation of AGEs *in vivo* contributes to several pathophysiological events associated with aging and diabetes mellitus, such as chronic renal insufficiency, Alzheimer's disease, nephropathy, neuropathy and cataract [3, 4].

Because the structures of AGEs are diverse, currently there is no general procedure for detection of this class of compounds [2].

In this study we combined ^{13}C isotopic labeling [5, 6, 7, 8] with LC-MS allowing detection of AGEs. The glycation was performed on a well studied protein - hen egg lysozyme at model conditions [8].

Results and Discussion

Samples of hen egg lysozyme were modified by an equimolar mixture of [$^{12}\text{C}_6$]glucose and [$^{13}\text{C}_6$]glucose. Then the glycated protein was subjected to reduction of the disulfide bridges followed by tryptic hydrolysis. LC-MS method was used for analysis of the obtained mixture of peptides.

Early and advanced end glycation products were identified on the basis of characteristic isotopic patterns resulting from the use of isotopically labeled D-glucose (a doublet signal in MS scan presented in **Fig. 1**). The intensity of MS signals corresponding to the two forms of the peptide labeled with both glucose isotopomers was practically the same (**Fig. 1**). The analysis of data was performed automatically using an in-house-developed program written in JAVA. To confirm the obtained results we used additional criteria: an identical retention time for chromatographic peaks of [$^{12}\text{C}_6$]AGEs and [$^{13}\text{C}_6$]AGEs and a difference of molecular mass between the detected compound and a possible tryptic lysozyme peptide. Although the error accepted in the search was under 10 ppm, more than 95% of identified glycated peptides corresponded to the calculated masses with the error below 5 ppm.

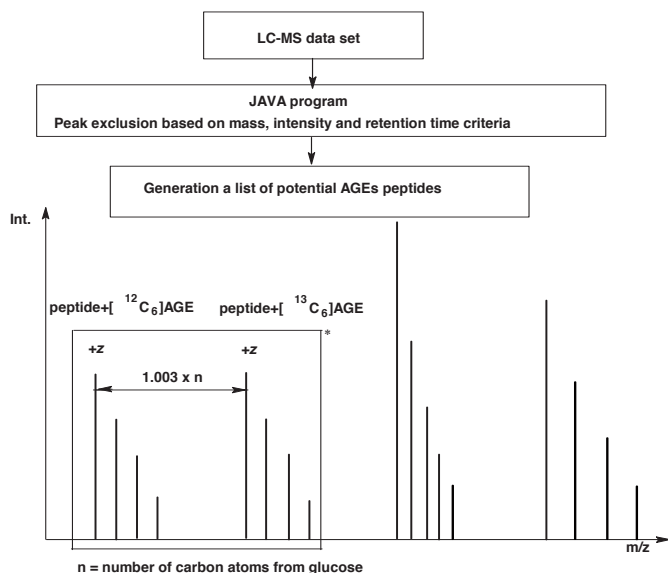


Fig.1 The scheme of selective identification of AGEs peptides in the mixture of peptides obtained by the enzymatic hydrolysis of proteins glycosylated with an equimolar mixture of [$^{12}\text{C}_6$]glucose and [$^{13}\text{C}_6$]glucose.

We found the group of possible advanced glycation end products (four types of AGEs reported in the literature). The majority of AGEs are located on the arginine residues. Their molecular masses correspond to the imidazolone A. These modifications probably occurred indirectly, e.g. in the reaction of the guanidine group with 3-deoxyglucosone.

Although all the end products detected in our experiment contained all six carbon atoms from glucose, the same procedure may be useful for the detection of any glycation product, disregarding the number of glucose derived carbon atoms. In view of this we presented a general method suitable for the model studies on proteins glycation. In addition this approach may potentially result in discovering new AGEs and establishing their structures.

References

- [1] Cho, S.J.; Roman, G.; Yeboah, F.; Y. Konishi, Y. *Curr. Med. Chem.* **2007**, *14*, 1653.
- [2] Smit, A.J.; Lutgers, H.L. *Curr. Med. Chem.* **2004**, *11*, 2767.
- [3] Zhang, Q.; Ames, J.M.; Smith, R.D.; Baynes, J.W.; Metz, T.O. *J. Proteome Res.* **2009**, *8*, 754.
- [4] Misciagna, G.; De Michele, G.; Trevisan, M. *Curr. Pharm. Des.* **2007**, *13*, 3688.
- [5] Stefanowicz, P.; Kijewska, M.; Kluczyk, A.; Szewczuk, Z. *Anal. Biochem.* **2010**, *400*, 237.
- [6] Priego-Capote, F.; Scherl, A.; Muller, M.; Waridel, P.; Lisacek, F.; Sanchez, J.-C. *Mol. Cell. Proteomics* **2010**, *9*, 579.
- [7] Zhang, J.; Zhang, T.; Jiang, L.; Hewitt, D.; Huang, Y.; Kao, Y.; Katta, V. *Anal. Chem.* **2012**, *84*, 2313.
- [8] Kielmas, M.; Kijewska, M.; Stefanowicz, P.; Szewczuk, Z. DOI: 10.1016/j.ab.2012.08.026

Elimination of partial cleavage of acid labile groups during removal of Mtt protection

Zuzana Flegelova¹, Martin Flegel², Michal Lebl¹

¹Spyder Institute Prague, Czech Republic; ²Institute of Organic Chemistry and Biochemistry, Czech Academy of Sciences, Prague, Czech Republic
E-mail:michallebl@gmail.com

Introduction

Lys(Mtt) is an important building block for construction of complex branched or multicyclic peptides [1,2]. It was shown earlier that Mtt cleavage by 1% TFA in presence of various scavengers leads to a loss of Trt protecting groups and also to a loss of peptide from the Wang and Rink resin [3]. Multiple exposure to diluted TFA solution was recommended as an optimal method [4]. During the synthesis of several peptides requiring Lys(Mtt) deprotection, we have found either incomplete cleavage of Mtt or unacceptable loss of peptide chain from the Rink amide resin. We decided to study this reaction and find optimal conditions for the Mtt removal.

Results and Discussion

As a model peptide we prepared Fmoc-Tyr(But)-Gly-Lys(Mtt)-RinkResin. We compared the following conditions (i) 1%TFA/DCM, (ii) 1%TFA/1%MeOH/DCM, and (iii) 1%TFA/1%TIS/DCM. Protected peptide resin (15 mg) was prewashed (60sec) with the TFA solution (0.5 ml) and exposed to the particular solution (5 ml) for a given time, resin was quickly washed with DCM, DMF, 5%DIEA/DMF and acetylated by Ac₂O/DIEA/DMF solution. Samples were cleaved by 95% TFA/5% Water and analyzed by HPLC. Peak 1 is Fmoc-Tyr-Gly-Lys-NH₂ – result of total deprotection and cleavage by 95% TFA without previous removal of Mtt and acetylation, peak 2 is Fmoc-Tyr-Gly-Lys(Ac)-NH₂ – Mtt deprotection, acetylation and total deprotection and cleavage, and peak 3 is Fmoc-Tyr(Ac)-Gly-Lys(Ac)-NH₂ – Mtt and But deprotection, acetylation and total deprotection and cleavage.

We have found that addition of small amount of MeOH into the cleavage solution prevents formation of typical yellow color and we speculated that Mtt cation is very effectively quenched. However, the fact that cleavage of Mtt is dramatically slower may be the reason of no coloration. We have also found that even after 1h, tert-butyl protection from tyrosine is cleaved in 1%TFA without any additives as well as in the presence of triisopropylsilane. After 16 hour exposure the tBu cleavage was substantial (see Figure 1). Presence of MeOH completely prevented this undesirable side reaction. Preliminary experiments let us believe that the premature cleavage from the Rink amide resin was prevented as well.

Surprisingly, we have found that cleavage of Mtt by 10% TFE / 20% HFIP / 70% DCM, complete in 16 h, leads also to partial cleavage of tBu type groups. Eventhough the extent of this cleavage is substantially lower than in the case of 1% TFA solution (2% vs. 15%), it can also be prevented by addition of 1% MeOH.

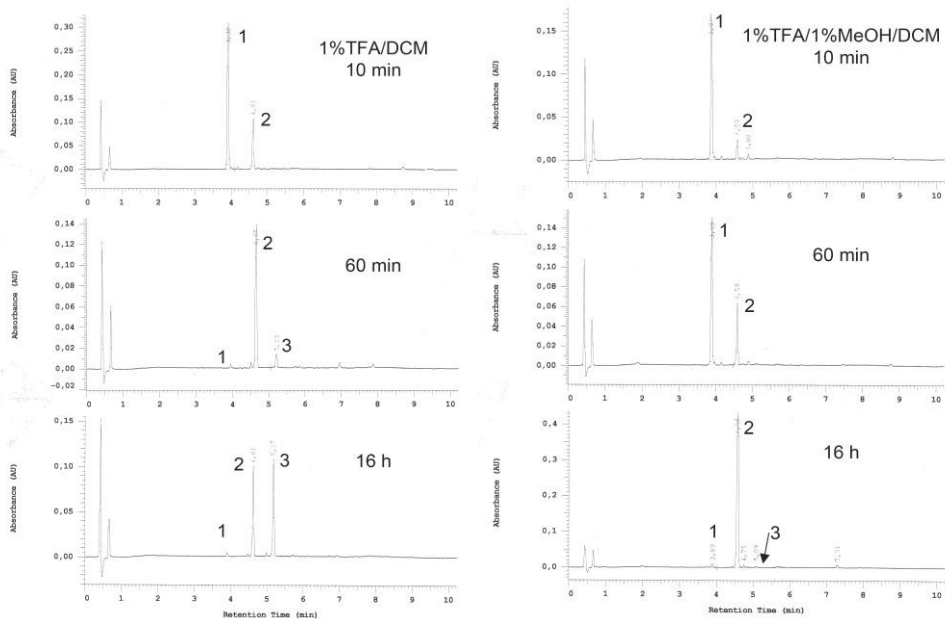


Figure 1. HPLC traces of model peptide Fmoc-Tyr-Gly-Lys.

Our tentative conclusion is that methanol may be an additive of choice for selective removal of Mtt group.

References

- [1] Aletras, A.; Barlos, K.; Gatos, D.; Koutsogianni, S.; Mamos, P. *Int. J. Peptide Prot. Res.* 1995, 45, 488-496.
- [2] Hoogerhout, P.; Stittelaar, K. J.; Brugghe, H. F.; Timmermans, J. A. M.; ten Hove, G. J.; Jiskoot, W.; Hoekman, J. H. G.; Roholl, P. J. M. *J. Pept. Res.* 1999, 54 (5), 436-443.
- [3] Bourel, L.; Carion, O.; Gras-Masse, H.; Melnyk, O. *J. Peptide Sci.* 2000, 6 (6), 264-270.
- [4] Li, D.; Elbert, D. L. *J. Pept. Res.* 2002, 60, 300-303.

New methods for fluorescent labeling of peptide hormones and enzyme substrates

Kurt Hoogewijs^a, Dieter Buyst^b, José Martins^b, Annemieke Madder^{*a}

^a University of Ghent, Laboratory for Organic and Biomimetic Chemistry, Ghent, Belgium;

^b NMR and Structure Analysis, Ghent, Belgium

*E-mail: annemieke.madder@ugent.be

Introduction

Modern chemical biology oriented research frequently relies on the ability to site-selectively label macromolecules such as peptides, carbohydrates and oligonucleotides with fluorophores. Although most strategies make use of the nucleophiles naturally present in the biomolecules, the introduction of an electrophile in the biomolecule would allow a more selective and orthogonal labeling. However, the introduction of selectively modifiable electrophiles, such as carbonyl moieties, into biomolecules is not always straightforward. Generally, internal or C-terminal aldehyde functionalities are generated through use of building blocks that require lengthy syntheses and/or making use of orthogonal protection schemes. Recently, our group published a method for the labeling of peptides by generation of a reactive aldehyde in the sequence. In this approach, a non-natural amino acid containing a furan moiety has been incorporated into the peptide.¹ By selective oxidation the furan moiety is then converted into an alpha,beta-unsaturated aldehyde. Next, a simple reductive amination facilitates the introduction of the desired fluorophore (figure 1).² This promising strategy seems especially convenient for the preparation of doubly labeled peptides such as FRET-probes.

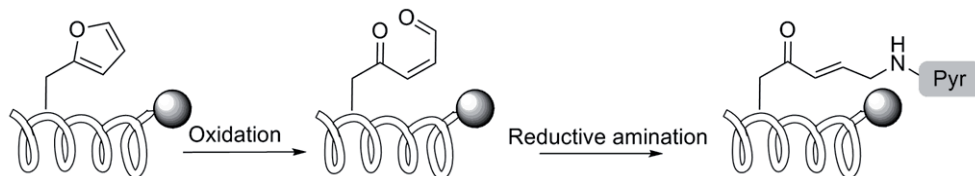


Figure 1: Oxidation of the furan moiety leads to an alpha, beta unsaturated aldehyde, the fluorophore is introduced by reductive amination.

Results and Discussion

Peptide **1** was synthesized by automated peptide synthesis using the Fmoc/tBu strategy with HBTU as coupling reagent (figure 2). Oxidation with N-bromosuccinimide in THF/acetone/H₂O (5:4:2; 5h) generated an alpha,beta-unsaturated aldehyde which was subsequently labeled by reductive amination with aminopyrene, NaCNBH₃ and AcOH in THF/H₂O (peptide **2**). The Fmoc group on the lysine side chain was removed using 20% piperidine in DMF. Using only a small excess of Dabsyl-Cl and triethylamine in DCM, the amine was completely converted to the Dabsyl sulfonamide (peptide **3**). Deprotection and cleavage from the resin with TFA/TIS/H₂O (95:2,5:2,5) gave a Paal-Knorr type pyrrole formation and resulted in the crude peptide **4**.

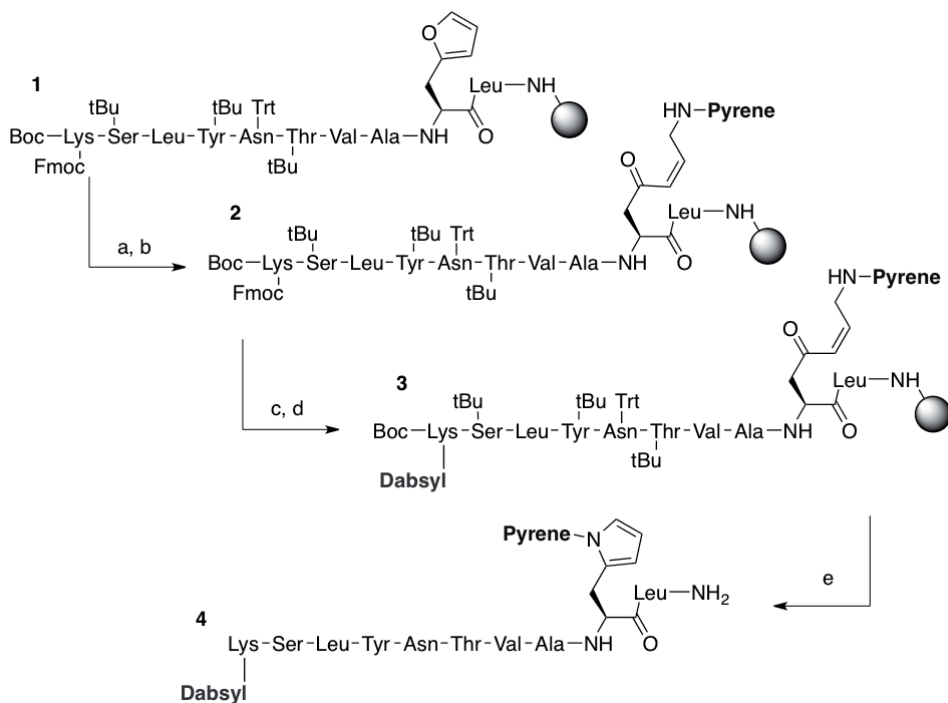


Figure 3: (a) NBS in THF/acetone/H₂O (5:4:2; 5h); (b) aminopyrene, NaCNBH₃, AcOH in THF/H₂O (1h); (c) 20% piperidine in NMP (2', 5' and 15'); (d) Dabsyl-Cl, TEA in DCM (1h); (e) TFA/TIS/H₂O (95:2.5:2.5) (2h)

Using our previously published furan oxidation-reduction strategy, we here present a straightforward method for the synthesis of fluorescent peptides, and doubly labeled peptides for FRET-probes in particular. We expect more strategies based on furan reactivity will emerge in the near future and will continue to explore the reactivity of furan moieties for peptide and protein labeling.

Acknowledgments

This research was supported by the Bijzonder Onderzoeksfonds of Ghent University. Celina Bermúdez, Debbie Lauwers, Wannes Libbrecht are gratefully acknowledged for their preliminary work leading to these results.

References

- [1] Hoogewijs, K.; Deceuninck, A.; Madder, A., *Organic & Biomolecular Chemistry* **2012**, 10 (20), 3999-4002.
- [2] Deceuninck, A.; Madder, A., *Chem. Commun.* **2009**, (3), 340-342.

A new producer and new 19- and 20-residue peptaibiotics: Suzukacillin-related hypophellins

Christian R. Röhrich^{1*}, Anita Iversen^{2*}, Walter M. Jaklitsch³, Hermann Voglmayr³, Andreas Vilcinskas^{1,4}, Kristian Fog Nielsen², Ulf Thrane², Hans Brückner^{5,6}, Thomas Degenkolb^{2,4}

¹Fraunhofer Institute for Molecular Biology and Applied Ecology (IME), Bioresources Project Group, 35394 Giessen, Germany; ²Dept. of Systems Biology, Center for Microbial Biotechnology, Technical University of Denmark, 2800 Kgs. Lyngby, Denmark; ³Dept. of Systematic and Evolutionary Botany, Faculty Centre of Biodiversity, University of Vienna, 1030 Vienna, Austria; ⁴Institute of Phytopathology and Applied Zoology, Dept. of Applied Entomology, IFZ, Justus-Liebig University Giessen, 35392 Giessen, Germany; ⁵Institute of Nutritional Science, Dept. of Food Sciences, IFZ, Justus-Liebig University Giessen, 35392 Giessen, Germany; ⁶Visiting Professor at the Department of Food Sciences and Nutrition, College of Food Sciences and Agriculture, King Saud University, Riyadh 11451, Kingdom of Saudi Arabia; *equal contribution

E-mail: thomas.degenkolb@ernaehrung.uni-giessen.de

Introduction

Recently, the fungicolous fungus *Hypocrea phellinicola* was described as a new species growing on its natural host, the Rusty Porecrust (*Phellinus ferruginosus*) [1]. Species of *Hypocrea* and its *Trichoderma* anamorphs are rich sources of peptaibiotics, a particular group of non-ribosomally biosynthesised antibiotic polypeptides, which contain the non-proteinogenic marker amino acid α -aminoisobutyric acid (Aib). As peptaibiotics are well-known to form ion channels in biological membranes [2], the producing fungus could benefit from these bioactive polypeptides by using them for colonisation and defence of its natural habitat. However, reports on the occurrence of peptaibiotics in the natural environment of the producer(s) have sparsely been published so far [3,4].

Results and Discussion

The specimen of *H. phellinicola* could be identified as a prolific source of 20-residue peptaibiotics of the suzukacillin-type [5], using a peptaibiomics approach [6]. Their structures were independently confirmed by analysing the 19-residue peptaibiotics (Δ [Ala/Aib]⁶) of an agar plate culture of *H. phellinicola* CBS 119283 (*ex-type*) grown under laboratory conditions. Major sequence variations are displayed in Figure 1 and HPLC elution profiles of peptides in Figure 2. Two minor components of the 19-residue peptaibols are hypothesized to carry a novel C-terminal residue, tentatively assigned as tyrosinol (Tyrol). Notably, twenty-four of the 30 sequences from *H. phellinicola* are new and were thus named **hypophellins**. Thus, *H. phellinicola* can be attributed as a potent producer of long-chain peptaibiotics in its natural habitat. Release of Aib-containing fungal polypeptides in the environment [7] – in this case: the host fungus – is evident. Structural analogies of the hypophellins particularly with other biocidal 18-, 19-, and 20-residue

peptaibiotics suggest that hypophellins may synergistically act with cell wall-degrading enzymes [8] and could thus support the hypothesis of a parasitic life style of their fungicolous producer *H. phellinicola*.

Residue																				
1	2	3	4	5	6	7	8	9	10	11	12	13	14	15	16	17	18	19	20	
Ac	Aib	Ala	Aib	Ala	Aib	Ala	Gln	Aib	Vxx	Aib	Gly	Lxx	Aib	Pro	Vxx	Aib	Aib	Gln	Gln	Pheol
	Aib				Aib				Aib							Vxx	Glu			

Residue																				
1	2	3	4	5	6	7	8	9	10	11	12	13	14	15	16	17	18	19	20	
Ac	Aib	Ala	Aib	Ser	Aib	-	Gln	Aib	Lxx	Aib	Gly	Lxx	Aib	Pro	Vxx	Aib	Vxx	Gln	Gln	Pheol
	Vxx	Ala	Ala	Ala											Aib	Vxx	Aib	Glu		Tyrol
	Lxx			Vxx																

Fig. 1: Sequence variations of major hypophellins detected in extracts of *H. phellinicola* from the natural habitat (above) and from potato dextrose agar plate cultures (below).

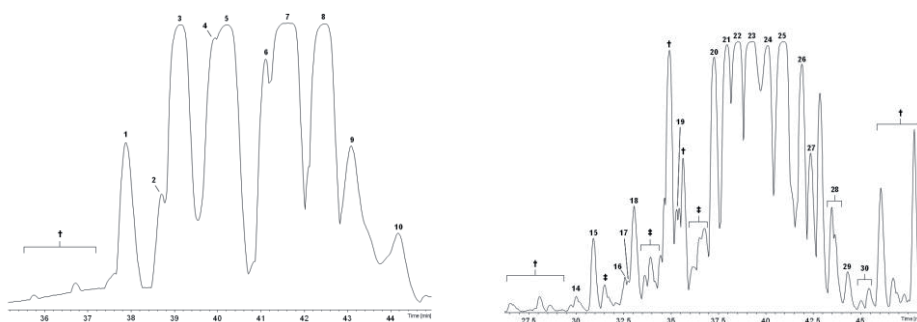


Fig. 2: Base-peak chromatograms of hypophellins, detected in the specimen (left) and in agar plate cultures (right) of *H. phellinicola* CBS 119283 (ex-type). † - no peptaibiotic, ‡ - coeluting peptaibiotics, not sequenced.

References

- [1] Jaklitsch, W. M. *Fungal Divers.* **2011**, *48*, 1.
- [2] Degenkolb, T.; Brückner H. *Chem. Biodivers.* **2008**, *5*, 1817.
- [3] Lehr, N.-A.; Meffert, A.; Antelo, L.; Sterner, O.; Anke, H.; Weber, R. W. S. *FEMS Microbiol. Ecol.* **2006**, *55*, 105.
- [4] Neuhof, T.; Berg, A.; Besl, H.; Schwecke, T.; Dieckmann, R.; von Döhren, H. *Chem. Biodivers.* **2007**, *4*, 1103.
- [5] Krause C.; Kirschbaum, J.; Jung, G.; Brückner, H. *J. Pept. Sci.* **2006**, *12*, 321.
- [6] Degenkolb, T.; Gräfenhan, T.; Berg, A.; Nirenberg, H. I.; Gams, W.; Brückner, H. *Chem. Biodivers.* **2006**, *3*, 593.
- [7] Brückner, H.; Becker, D.; Gams, W.; Degenkolb, T. *Chem. Biodivers.* **2009**, *6*, 38.
- [8] Lorito, M.; Farkas, V.; Rebuffat, S.; Bodo, B.; Kubicek, C. P. *J. Bacteriol.* **1996**, *178*, 6382.

Rapid alkalization factors in grape *Vitis vinifera*

Alexander A. Zamyatnin^{1,2}

¹Departamento de Informática, El Centro Científico Tecnológico de Valparaíso, Universidad Técnica Federico Santa María, 110-V, Valparaíso, Chile; ²A. N. Bach Institute of Biochemistry, Russian Academy of Sciences, 119071 Moscow, Russian Federation

E-mail: alexander.zamyatnin@usm.cl; aaz@inbi.ras.ru

Introduction

More than 1000 oligopeptides with different types of functional activity have been described for many plants (<http://erop.inbi.ras.ru/>). One only grape oligopeptide with antimicrobial function was extracted and characterized before [1] whereas information on numerous grape uncharacterized proteins has to be found in public protein databases. Several years ago the oligopeptide possessing new functional property was discovered in common tobacco leaves [2]. It consisted of 49 amino acid residues and induced a rapid alkalization of the culture medium of tobacco suspension-cultured cells and a concomitant activation of an intracellular mitogen-activated protein kinase. It was named as rapid alkalization factor (RALF). After this a family of RALF was elucidated in many plants, but not in grape. Thereupon the aim of the current study was an identification of unknown grape (*Vitis vinifera*) RALF oligopeptide structures.

Results and Discussion

GenBank database (<http://www.ncbi.nlm.nih.gov/sites/entrez>) primary structures of unrecognized grape proteins (named as hypothetical proteins or unnamed protein products) were compared with sequences of all EROP-Moscow rapid alkalization factors EROP-Moscow database (<http://erop.inbi.ras.ru/>) [3]. The identity in the amino acid residue sequences was equal or more than 30%. Multiple sequence program ClustalW2 (<http://www.ebi.ac.uk/Tools/clustalw2/index.html>) was used for alignment procedure performance.

This method revealed several new structures of potentially active rapid alkalization factors in grape after alignment procedure. Nineteen grape hypothetical proteins and unnamed protein products (potential RALF precursors) were found homologous to known regulatory oligopeptides isolated from different sources. All of them were characterized by a conserved C terminal motif containing four cysteine residues forming potentially two disulfide bridges. As a result unrecognized proteins formed structural family (RALF1-RALF7) containing seven new different putative oligopeptide structures not described before. They consisted of from 49 to 57 amino acid residues and their similarity with other plant RALF primary structures was from 54.4 to 89.8%.

RALF, common tobacco AT-KKYISYGALQKNSVPCSRRGASYYNCKP-GAQANPYSRGCSAITRC-RS
RALF, native tobacco AT-KKYISYGALQKNSVPCSRRGASYYNCKP-GAQANPYSRGCSAITRC-RS
RALF, mouse-ear cress AT-KKYISYGALQKNSVPCSRRGASYYNCKP-GAQANPYSRGCSAITRC-RS
RALF, tomato AT-KKYISYGALQKNSVPCSRRGASYYNCKP-GAQANPYTRGCSAITRC-RS
RALF, garden pea AT-TKYISYGALQRNTVPCSRRGASYYNCRP-GAQANPYSRGCSAITRC-RS
RALF1, grape AT-SKYISYGALQRNSVPCSRRGASYYNCKP-GAQANPYNRGCSTITRC-RS
RALF, barrel medic AT-TKYISYGALQRNTVPCSRRGASYYNCRP-GAQANPYSRGCSAITRC-RG
RALF1, poplar AT-TKYISYGALQRNNVPCSRRGASYYNCKP-GAQANPYSRGCSAITRC-RS
RALF2, poplar AT-SRYVSYGALQKNNVPCSRRGASYYNCKN-GAQANPYSRGCSAITRC-RG
RALF, poplar AT-SSYVSYGALQKNNVPCSRRGASYYNCKN-GAQANPYSRGCSAITRC-RG
RALF, ice plant AT-NSYISYGALNKNRVPCSRRGASYYNCRP-GAQANPYSRGCSAITRC-RP
RALF33, mouse-ear cress AT-TKYISYGALRRNTVPCSRRGASYYNCRP-GAQANPYSRGCSAITRC-RR
RALF22, mouse-ear cress AQ-KKYISYGAMRRNSVPCSRRGASYYNCKP-GAQANPYSRGCSTITRC-RR
RALF, soybean AG-RSYISYGALRRNTVPCSRRGASYYNCRP-GAQANPYSRGCSAITRC-RR
RALF2, grape AS-KRYISYGALSRNSVPCSRRGASYYNCRP-GAQANPYTRGCSAITRC-RR
RALF3, grape AT-TQYISYGALQRNTVPCSRRGASYYNCKP-GAEANPYNRGCSTITRC-RS
RALF23, mouse-ear cress AT-RRYISYGALRRNTI PCSRRGASYYNCRP-GAQANPYSRGCSAITRC-RRS
RALF1, mouse-ear cress AT-TKYISYQSLKRNSVPCSRRGASYYNCKN-GAQANPYSRGCSTIARC-RS
RALF, cotton QT-TRYISYGALQRNTVPCSRRGASYYNCKP-GAQANPYNRGCSTITRC-RG
RALF, maize YGG-GYISYGALRRDNVPCSRRGASYYNCRP-GGQANPYHRGCSAITRC-RG
RALF, sorghum Y-GNGYISYGALRRDNVPCSRRGASYYNCRP-GGQANPYHRGCSAITRC-RG
RALF, barley Q-GRGYISYGALRRGTVP CNRRGASYYNCRP-GAQANPYHRGCSAITRC-RG
RALF, rice QGGSGYIGYDALRRDSVPCSRRGASYYNCKP-GAEANPYSRGCSAITQC-RG
RALF, wheat QDGSYIGYDALRRDNVPCSRRGASYYNCKP-GAEANPYSRGCSAITQC-RG
RALF, cryptomeria AT-TQYISYGALRADSVPCSKSGT SYYNCGSSG-QANPYSKSCTQITRCARDTS
RALF4, grape AQGGKFISYGALKKNVPCNRRGR.SYYNCRK-GGRANPYQRGCSTITHCARYTN
RALF6, grape AQRRRYISYGALRRNQVPCNRRGR.SYYNCRK-GGRANPYRRGCSVITKCHRFTD
RALF5, grape AQRSRFISYGALKKNVPCNRRGN.SYYNCRSG-KANPYRRGCSAITHCQRYS
RALF, pine AG-RTYISYKSLAADSVPCSKRGT SYYNCRST-QANPYQRGCSTQITRCARSTS
RALF7, grape VMQKKYISYETLKKDMI PCARPGASYYNCRASG-EANPYNRGCSEVITGCARGVRDINS
CONSENSUS * ** * ***** ***** * * * *

The amino acid residue sequences of seven found grape RALF oligopeptides compared with twenty three primary structures is shown in Figure. The homology in primary structure found among widely divergent plant species suggests that the RALF primary sequence has been highly conserved over millions of years and that RALF has a role of fundamental importance in many plant families.

Acknowledgments

We thank Eric Zarate for technical assistance. This work has been supported by Chilean National Science and Technology Research (Grant No. 1080504).

References

- [1] De Beer, A.; Vivier, M.A. Doe, J.; Johnson, G.; Smith, K. *BioMed Central Plant Biol.* **2008**, *8*, 75.
- [2] Pearce, G.; Morua, D.S.; Stratmann, J.; Ryan, C.A. Jr. *Proc. Natl Acad. Sci. USA*, **2001**, *98*, 12843.
- [3] Zamyatnin, A.A.; Borchikov, A.S.; Vladimirov, M.G.; Voronina, O.L. *Nucl. Acids Res.* **2006**, *34*, D261.

Screening the natural habitat: New peptaibiotics from specimens and pure cultures of the fungicolous fungus

Hypocrea pulvinata

Christian R. Röhrich^{1*}, Anita Iversen^{2*}, Walter M. Jaklitsch³, Hermann Voglmayr³, Albrecht Berg⁴, Heinrich Dörfelt⁵, Andreas Vilcinskas^{1,6}, Kristian Fog Nielsen², Ulf Thrane², Hans Brückner^{7,8}, Thomas Degenkolb^{2,6}

¹Fraunhofer Institute for Molecular Biology and Applied Ecology (IME), Bioresources Project Group, 35394 Giessen, Germany; ²Dept. of Systems Biology, Center for Microbial Biotechnology, Technical University of Denmark, 2800 Kgs. Lyngby, Denmark; ³Dept. of Systematic and Evolutionary Botany, Faculty Centre of Biodiversity, University of Vienna, 1030 Vienna, Austria; ⁴Dept. of Biomaterials, Innovent e.V., 07745 Jena, Germany; ⁵Dept. of Microbial Communication, Institute of Microbiology, Friedrich Schiller University Jena, 07743 Jena, Germany; ⁶Institute of Phytopathology and Applied Zoology, Dept. of Applied Entomology, IFZ, Justus-Liebig University Giessen, 35392 Giessen, Germany; ⁷Institute of Nutritional Science, Dept. of Food Sciences, IFZ, Justus-Liebig University Giessen, 35392 Giessen, Germany; ⁸Visiting Professor at the Department of Food Sciences and Nutrition, College of Food Sciences and Agriculture, King Saud University, Riyadh 11451, Kingdom of Saudi Arabia; *equal contribution

E-mail: Thomas.degenkolb@ernaehrung.uni-giessen.de

Introduction

Reports on the occurrence of peptaibiotics, a particular group of non-ribosomally biosynthesised polypeptide antibiotics which contain the non-proteinogenic marker amino acid α -aminoisobutyric acid (Aib), in the natural environment of the producer(s) have sparsely been published so far. In order to investigate the potential significance of these peptide antibiotics for the producing organism(s) in the natural habitat, we screened specimens of the fungicolous fungus *Hypocrea pulvinata*, the Ochre Cushion, growing on its specific hosts, the Birch Bracket (*Piptoporus betulinus*) and the Red Banded Polypore (*Fomitopsis pinicola*) [1]. The present study is aimed at the question as to whether peptaibiotics formation under the conditions of the natural habitat of the producer(s) is either a rather infrequent or a more common phenomenon. If the latter is true, peptaibiotics might play a decisive role in antibiotic-assisted colonisation and defence of the substrate.

Results and Discussion

Using a peptaibiomics approach [2], we detected predominant 19-residue peptide (Δ [Aib/Ala]⁶) sequences in the specimens analysed by (U)HPLC/HR-ESI-QqTOF-MS. Structures of peptaibiotics found were independently confirmed by analysing the peptaibiome of pure agar cultures, which was again dominated by 19-residue peptides although 20-residue are also present (Figure 1). Remarkably, 26 of the 28 peptaibiotics

sequenced (Figure 2) are new and were thus named **hypopulvins**. Notably, *H. pulvinata* was identified as a potent producer of long-chain peptaibiotics in its natural habitat. Release of Aib-containing polypeptides in the environment is evident [3]. Structural analogies of the hypopulvins particularly with other biocidal 18-, 19-, and 20-residue peptaibiotics suggest that hypopulvins may synergistically act with cell wall-degrading enzymes [4] and could thus support the hypothesis of a parasitic life style of *H. pulvinata*, which is a common, widespread fungicolous species of Europe, North America, Japan, and Russia [1].

		Residue																		
		1	2	3	4	5	6	7	8	9	10	11	12	13	14	15	16	17	18	19
Ac	Aib	Ala	Ala	Ala	Aib	–	Gln	Aib	Lxx	Aib	Gly	Lxx	Aib	Pro	Vxx	Aib	Aib	Gln	Gln	–
			Ser	Ser	Ala					Ala	Ala	Vxx				Vxx			Pheol	
					Vxx					Ser										Lxxol

		Residue																			
		1	2	3	4	5	6	7	8	9	10	11	12	13	14	15	16	17	18	19	20
Ac	Aib	Ala	Ala	Ser	Aib	–	Gln	Aib	Lxx	Aib	Gly	Lxx	Aib	Pro	Vxx	Aib	Aib	Gln	Gln	Pheol	
			Aib	Ala		Aib			Vxx		Ser				Lxx			Glu			
											Ala										

Fig. 1: Sequence variations of major hypopulvins detected in extracts of *H. pulvinata* from the natural habitat (above) and from potato dextrose agar plate cultures (below).

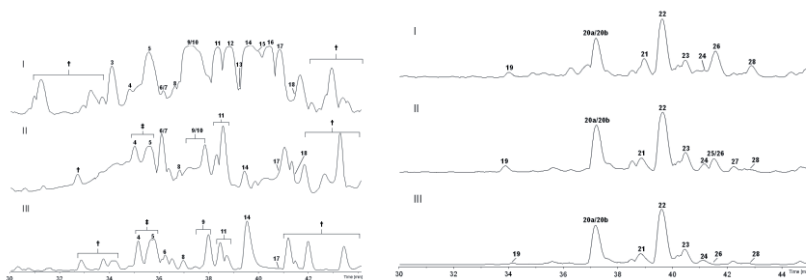


Fig. 2: Base-peak chromatograms I-III of hypopulvins, novel peptaibiotics detected in methanol/dichloromethane extracts of specimens (left) and agar plate cultures (right) of *H. pulvinata*; † - no peptaibiotic, ‡ - co-eluting peptaibiotics, not sequenced.

References

- [1] Jaklitsch, W. M. *Fungal Divers.* **2011**, *48*, 1.
- [2] Degenkolb, T.; Gräfenhan, T.; Berg, A.; Nirenberg, H. I.; Gams, W.; Brückner, H. *Chem. Biodivers.* **2006**, *3*, 593.
- [3] Brückner, H.; Becker, D.; Gams, W.; Degenkolb, T. *Chem. Biodivers.* **2009**, *6*, 38.
- [4] Lorito, M.; Farkas, V.; Rebuffat, S.; Bodo, B.; Kubicek, C. P. *J. Bacteriol.* **1996**, *178*, 6382.

Targeting *N*-myristoyl transferase in cancer using peptide arrays

Emmanuelle Thion¹, David Mann², Edward W. Tate¹

¹Department of Chemistry or ²Department of Life Sciences, Imperial College London,
Exhibition Road, SW7 2AZ London, UK

E-mail: e.thion09@imperial.ac.uk

Introduction

Protein *N*-myristoylation is the irreversible attachment of a C14 saturated fatty acid to the N-terminal glycine of a target protein. This modification is catalysed by myristoyl CoA: protein *N*-myristoyl transferase (NMT) [1] (Fig. 1.).

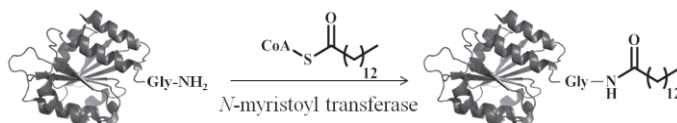


Fig. 1. Myristoylation of a protein substrate

Humans possess two distinct NMT enzymes, NMT1 and NMT2, and it has been suggested that they possess distinct but overlapping substrate specificity and function. It has been reported that NMT is upregulated in several cancers [1]. Also, RNA interference experiments in a mouse xenograft model suggested that some cancer cells may be reliant on NMT1 but not NMT2 for tumour growth [3]. These data suggest that specifically targeting NMT1 may be a novel therapeutic route. However, selective inhibitors are not yet available. Preliminary experiments with a non-selective inhibitor in cancer cells showed that NMT inhibition led to cell growth arrest after 1 day and cell death after 7 days [2]. Here we present a method to identify peptide substrates of NMT1 and/or NMT2. Peptide libraries can be prepared on a cellulose membrane and screen for activity using a labeling technology. If peptide substrates specific to a particular NMT could be identified, they may provide a basis for peptidomimetic inhibitors to validate a specific NMT as a new therapeutic target for cancer.

Results and Discussion

Peptides made of the first 15 amino acids at the N-terminus of known or predicted myristoylated proteins were synthesized on an amino-functionalised cellulose membrane using standard solid phase peptide synthesis. As negative controls, peptides which were reported not to be myristoylated were also included.

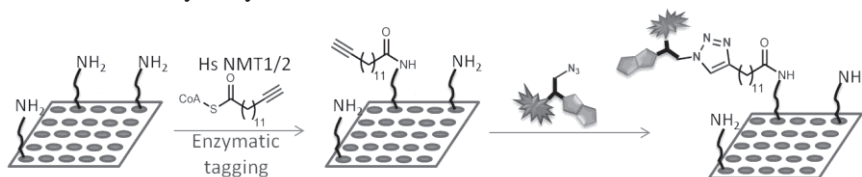


Fig. 2. Detection of NMT1/2 peptide substrates on a cellulose membrane

Peptides were exposed to recombinant NMT1 and/or NMT2 and an alkyne-tagged analogue of myristoyl CoA (Fig. 2.). Only peptide substrates modified by the enzyme would bear an alkyne tag. Subsequent azide-alkyne “click” cycloaddition was then used to allow visualisation of the myristoylated substrates either directly via fluorescence of the associated TAMRA fluorophore or indirectly by chemiluminescence after incubation with Neutravidin HRP and visualisation using a chemiluminescent HRP substrate (Fig. 3.). Attempts to visualise the spots via fluorescence were unsuccessful due to high background.

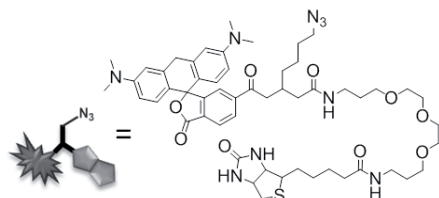


Fig. 3. Capture reagent

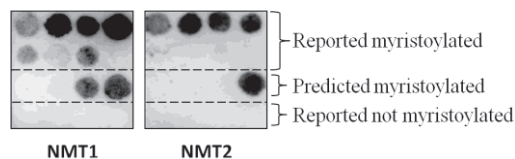


Fig. 4. Peptides on a cellulose membrane screened using NMT1 or NMT2

To circumvent this problem, membranes were therefore blocked with BSA, probed with Neutravidin HRP and visualised using a chemiluminescent HRP substrate (Fig. 4.). No signals were detected for the peptides corresponding to proteins that have been shown not to be myristoylated, demonstrating that the method does not give unspecific background. Signals were detected for some peptides which had been reported or predicted to be substrates of NMT1 and/or NMT2. Interestingly a different pattern was obtained for NMT1 and NMT2. Peptides were re-synthesised individually and their ability to be myristoylated verified using a solution based assay [5], confirming the peptide array data.

We have shown that it is possible to myristoylate and detect NMT1/NMT2 peptide substrates on a cellulose membrane. However, the use of cellulose membranes presents some limitations. Fluorescence, which provides a rapid readout, could not be used to detect the substrates on a cellulose membrane due to background problems. Moreover, peptides which were reported to be myristoylated were not all detected using this method, perhaps due to synthesis issues on the membrane. Future work will focus on the preparation and screening of peptide libraries functionalised with a biotin moiety at the C-terminus to allow immobilisation on an avidin-functionalised glass plate.

Acknowledgments

This work was supported by Cancer Research UK (Grant C29637/A10711).

References

- [1] Wright, M.H.; Heal, W.P.; Mann, D.J.; Tate, E.W. *J. Chem. Biol.* **2010**, *3*, 19-35.
- [2] Manuscript in preparation
- [3] Ducker, C.E.; Upson, J.J.; French, K.J.; Smith, C.D. *Mol. Cancer Res.* **2005**, *3*, 463-76.
- [4] Heal W.P.; Wright, M.H.; Thinon, E.; Tate, E.W. *Nat. Protoc.* **2011**, *1*, 105-17.
- [5] Goncalves, V.; Brannigan, J.A.; Thinon, E.; Olaleye, T.O.; Serwa, R.; Lanzarone, S.; Wilkinson, A.J.; Tate, E.W.; Leatherbarrow, R.J. *Anal Biochem.* **2012**, *421*, 342-4

Bis(2-sulfanylethyl)amido peptide chemistry enables a one-pot three segments ligation strategy for protein chemical synthesis

**Nathalie Ollivier, Jérôme Vicogne, Hervé Drobecq, Rémi Desmet,
Bérénice Leclercq, Oleg Melnyk**

UMR CNRS 8161, Univ Lille Nord de France, Pasteur Institute of Lille, France

Oleg.Melnyk@ibl.fr

Introduction

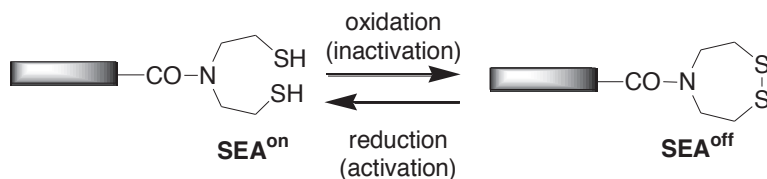
Total protein chemical synthesis requires a case by case design and optimization which is governed by factors such as the solubility of the individual peptide segments, their primary sequence and in particular the presence of “difficult” amino acid residues at ligation junctions such as proline or the location of cysteines. Usually, a subset of chemical tools is selected among a vast array of methodologies to match the specificities of the target protein. In this context, methods enabling the assembly of three peptide segments in the N-to-C and C-to-N direction play a central role and must be considered as complementary as they can be selected for building subdomains of the target protein. To date, most of the proteins were assembled in the C-to-N direction. Only few methods are available for the N-to-C sequential assembly of proteins, whose design is highly challenging [1].

We have recently reported that SEA ligation, that is the reaction of a *bis*(2-sulfanylethyl)amido group (called SEA^{on}) with a cysteinyl peptide, allows the formation of a native peptide bond in water and at neutral pH [2]. SEA belongs to the family of *N,S*-acyl shift systems [3].

We report here that Native Chemical Ligation and the unique chemical properties of SEA group [4], [5] can be combined in order to design a highly efficient one-pot three segments protein assembly procedure, working in the N-to-C direction [6].

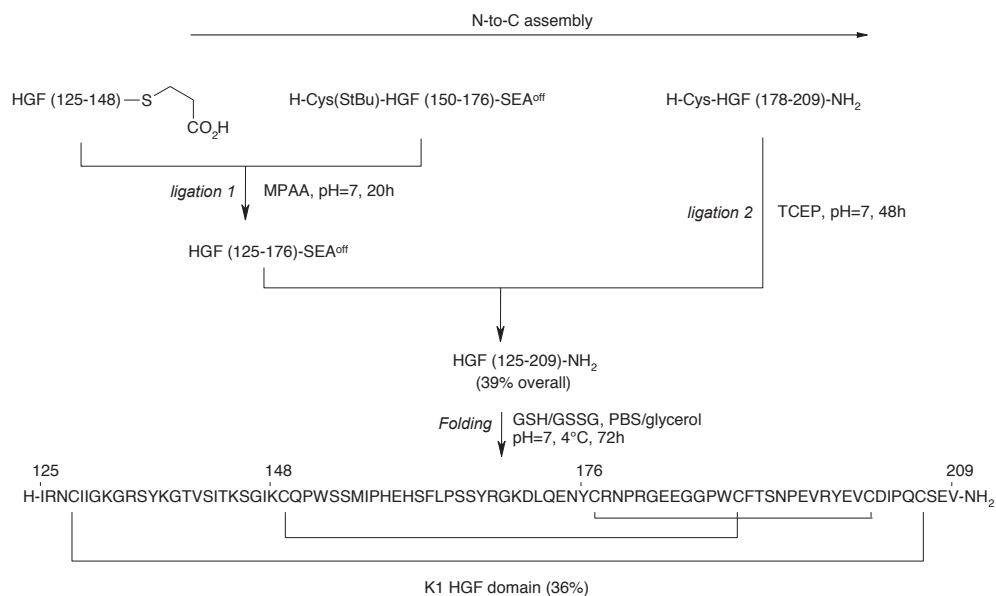
Results and Discussion

Oxidation of SEA^{on} results in a cyclic disulfide called SEA^{off}, which is a self-protected form of SEA^{on}. SEA^{off} and SEA^{on} can be easily interconverted by reduction/oxidation as shown below.



Sequential ligation of three peptide segments A-CO-X, Cys-B-CO-Y and Cys-C in the N-to-C direction involves first the reaction of A-CO-X with Cys-B-CO-Y to give AB-CO-Y.

CO-Y must be activated into CO-Y* to permit the second ligation step with Cys segment C. Ideally, CO-Y must be inert during the first ligation in order to avoid oligomerization or cyclization of Cys-B-CO-Y. Advantageously, activation should be carried out in situ after the first ligation using reagents compatible with ligation 2 to permit a one-pot process. SEA^{on/off} concept is a solution to this difficult problem. Indeed, we found that SEA^{off} is stable and unreactive using the standard conditions for Native Chemical Ligation (NCL) *in the absence of TCEP*, that is at pH 7 in the presence of an aryl thiol catalyst such as 4-(mercaptophenyl)acetic acid (MPAA). This allowed us to design a sequential assembly process in which CO-X is a thioester, CO-Y is SEA^{off} and CO-Y* SEA^{on}. The method is illustrated below with the synthesis of the first kringle (K1) domain of Hepatocyte Growth Factor (HGF), the high affinity ligand of MET tyrosine kinase receptor. The folded protein was found to be biologically active in an in vitro MET phosphorylation assay.



Acknowledgments

We thank CNRS, Région Nord-Pas-de-Calais, Institut Pasteur de Lille and Cancéropôle Nord-Ouest for financial support. We acknowledge CSB platform (<http://csb.ibl.fr>) for technical support.

References

- [1] Raibaut, L.; Ollivier, N.; Melnyk, O. *Chem. Soc. Rev.*, in press, **2012**, DOI:10.1039/C2CS35147A
- [2] Ollivier, N.; Dheur, J.; Mhidia, R.; Blanpain, A.; Melnyk, O. *Org. Lett.* **2010**, *12*, 5238.
- [3] Ollivier, N.; Behr, J.B.; El-Mahdi, O.; Blanpain, A.; Melnyk, O. *Org. Lett.* **2005**, *7*, 2647.
- [4] Dheur, J.; Ollivier, N.; Vallin, A.; Melnyk, O. *J. Org. Chem.*, **2011**, *76*, 3194.
- [5] Dheur, J.; Ollivier, N.; Melnyk, O. *Org. Lett.*, **2011**, *13*, 1560.
- [6] Ollivier, N.; Vicogne, J.; Vallin, A.; Drobecq, H.; Desmet, R.; El Mahdi, O.; Leclercq, B.; Goormachtigh, G.; Fafeur, V.; Melnyk, O. *Angew. Chem. Int. Ed.*, **2012**, *51*, 209.

Molecular dynamics of amylin 10-29 amyloid formation: parallel, antiparallel and bent structures

**Dmitrijs Lapidus¹, Salvador Ventura², Cezary Czaplewski³,
Adam Liwo³, Inta Liepina¹**

¹*Latvian Institute of Organic Synthesis, Latvia;* ²*Institut de Biotecnologia i de Biomedicina,*
Universitat Autònoma de Barcelona, Spain; ³*University of Gdansk, Poland*

E-mail: inta@osi.lv

Introduction

Amylin is one of the most amyloidogenic peptides, its fibrils are responsible for causing type II diabetes. Amyloid formation mechanism is investigated both to find amyloid inhibitors as potential medical drugs, and to use amyloids as potential self-assembling biomaterials [1]. Amyloid formation of amylin 10-29, its reverse analogue β -sheets and β -sheet stacks, as well as the bent amylin 10-29 β -sheet, was studied by molecular dynamics (MD), Amber 9.0, f99 force field.

Results and Discussion

MD revealed that for amylin 10-29 and its reverse analogue both the parallel and antiparallel β -sheet and β -sheet stack structures are stable suggesting that this could explain the high tendency of amylin to form amyloid fibrils. Parallel amylin 10-29 β -sheet stacks are kept together by two hydrophobic cores [1], while for the antiparallel system the dominating is the backbone hydrogen bonding between neighbor strands. Also the bent form of the amylin 10-29 β -sheet is stable for 412 ns of MD run (*Fig.1*). This is in concordance with transmission electron microscopy (TEM) experiments stating that all three peptides, amylin 10-29, its reverse and designed analogues, exhibited significant fibrillar polymorphism [2].

During the 412 ns MD simulation the bend form of the amylin 10-29 β -sheet has lost one of the side strands, which partly turned to α -helix, and one half of the other side strand has tendency to obtain α -helix (*Fig.1*), showing that the amylin 10-29 peptide can easily come from one structure to another. The α -helical structure is amylin 10-29 solution structure.

The amylin 10-29 bent β -sheet structure is kept together both by strong H-bonding and by hydrophobic cores similarly as for the other amyloidogenic peptides [3]. The H-bonding is characteristic also for the bend region. The two hydrophobic cores which bind together extended parallel amylin 10-29 β -sheet, in the bent form of the amylin 10-29 β -sheet are hydrophobically interacting stabilizing the bend structure. Residues Leu 27 (i strand) are interacting with residues Phe15 of neighboring strands (i-1) and (i-2) (*Fig. 1c*). Residues Phe15 of the neighboring strands interact via sandwich type π - π stacking. The nearby Val17 of neighboring strands interaction contribute to the stability of the hydrophobic core. Residues Phe23 of the neighboring strands, placed at the bend, has their benzene rings in parallel displacement and T-shaped orientation.

We can conclude that the bent amylin 10-29 parallel β -sheet is stable and could exist, however it is more probable that such the bent structure exists for longer peptides. Amylin 10-29 peptide could exist as antiparallel β -sheet or β -sheet stack, parallel β -sheet or β -sheet stack and bent β -sheet, that could explain the fibrillar polymorphism detected by TEM [2].

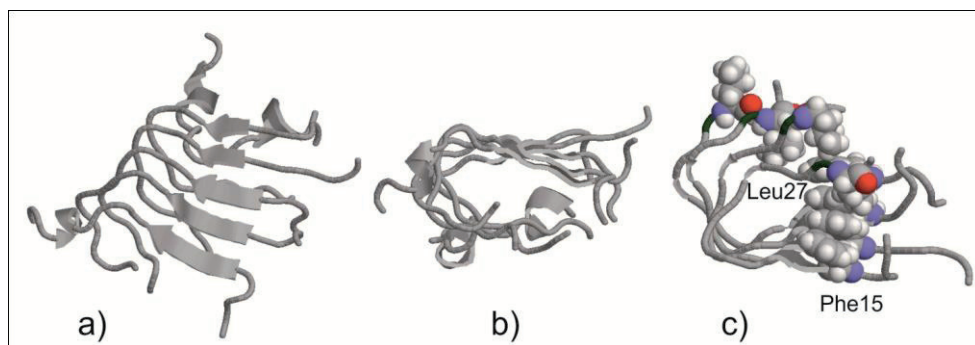


Fig. 1. Amylin 10-29 bent form at 412 ns of MD run: a) front view, b) side view, c) the Phe15-Leu27 interactions stabilizing the bend.

Acknowledgments

Supported by ESF project 2009/0197/1DP/1.1.1.2.0/ 09/ APIA/VIAA/014, Gdansk Academic Computer Center TASK.

References

- [1] Valle-Delgado, J.J.; Liepina, I.; Lapidus, D.; Sabaté, R.; Ventura, S.; Samitier, J.; Fernández-Busquets, X. *Soft Matter* **2012**, *8*, 1234-1242.
- [2] Sabaté, R., Alba Espargaró, Natalia S. de Groot 1, Juan José Valle-Delgado, Xavier Fernández-Busquets and Salvador Ventura. *Journal of Molecular Biology* **2010**, *40*, 337-352.
- [3] Lapidus, D.; Duka, V., Czaplowski, C.; Liwo, A.; Ventura, S. and Liepina I. *Biopolymers. Peptide Science*. Accepted manuscript online: 24 SEP 2012 05:52AM EST | DOI: 10.1002/bip.22161

Odd-even effect in the induced plasmonic CD band of peptide-capped gold nanoparticles

Edoardo Longo, Andrea Orlandin, Fabrizio Mancin, Claudio Toniolo,
Alessandro Moretto

Department of Chemistry, University of Padova, 35131 Padova, Italy

E-mail: alessandro.moretto.1@unipd.it

Introduction

Nucleotides and α -amino acids are crucial building blocks for living organisms. These chiral molecules are the biosynthetically precursors of two of the most important classes of biopolymers, DNA and proteins, respectively. The 3D-structures of biomolecules are currently studied using a variety of techniques, while helical handedness is routinely detected by means of light pulses of opposite circular polarization. The difference in the UV absorption of these two circularly polarized pulses is called electronic circular dichroism (ECD). In Nature, biomolecules explore a wide range of conformations with intrinsically strong ECD signals in the 200-300 nm region, but these signals are essentially absent in the visible. Nanomaterials such as metallic nanoparticles (depending on their size) display absorptions in the visible region but are achiral. As a result, when biomolecules are co-assembled with nanomaterials their chirality is transferred to create a plasmon-induced ECD signal in the visible region [1].

Results and Discussion

In this work, we present our results which underscore the occurrence of moderately strong ECD bands in the 300-550 nm range resulting from a series of appropriately thiol-functionalized peptide oligomers (based on alternating Ala and Aib (α -aminoisobutyric acid) residues, Figure 1) [2] covalently anchored to 2.0-2.4 nm sized Au nanoparticles (Np) (Table 1).

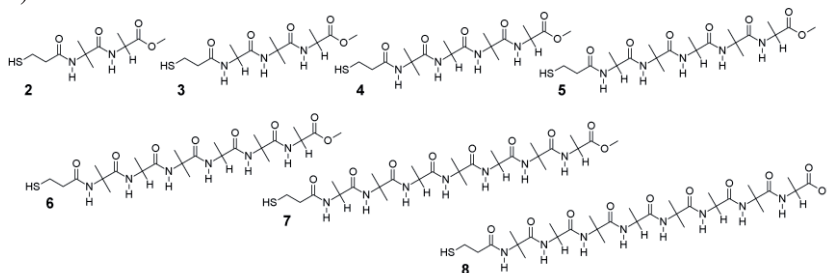


Fig 1. Chemical structures for: 2, *mpr*-Aib-Ala-OMe; 3, *mpr*-Ala-Aib-Ala-OMe; 4, *mpr*-(Aib-Ala)₂-OMe; 5, *mpr*-Ala-(Aib-Ala)₂-OMe; 6, *mpr*-(Aib-Ala)₃-OMe; 7, *mpr*-Ala-(Aib-Ala)₃-OMe; 8, *mpr*-(Aib-Ala)₄-OMe. *Mpr* stands for mercaptopropionic acid and *OMe* for methoxy.

We related the (positive or negative) signs of the ECD plasmonic signal to the length of the oligopeptide, that in turn is strictly associated with their secondary structure. This latter

property was simultaneously monitored *via* ECD in the 200-250 nm range. We believe that in our systems a peptide-to-metallic surface chirality transfer would take place.

Table 1. Structural data for the peptide-capped AuNp(2-8) synthesized in this work

Entry	Core <i>d</i> (nm) ^[a]	Au atoms for AuNp ^[b]	Pept. chains for AuNp	Footprint (nm ²)
AuNp2	2.0	247	126	0.10
AuNp3	2.2	329	138	0.11
AuNp4	2.3	376	119	0.14
AuNp5	2.0	247	55	0.23
AuNp6	2.3	376	54	0.31
AuNp7	2.4	427	33	0.45
AuNp8	2.4	427	27	0.68

^[a]*d* = diameter. Calculated by averaging over 200 Np. ^[b]Calculated assuming a spherical model.

Acknowledgments

We thank University of Padova (“Progetto Strategico” HELIOS 2008, prot. STPD08RC and PRAT 2011) for financial support.

References

- [1] *Circular Dichroism: Principles and Application*; Berova, N.; Nakanishi, K.; Woody, R. W., Eds.; Wiley-VCH: New York, **2000**.
- [2] Longo, E.; Moretto, A.; Formaggio, F.; Toniolo, C. *Chirality* **2011**, 23, 756.

Scope and limitations of *bis*(2-sulfanylethyl)amino (SEA) native peptide ligation

L. Raibaut, E. Lissy, O. Melnyk

UMR CNRS 8161, Univ. Lille Nord de France, Pasteur Institute of Lille, France

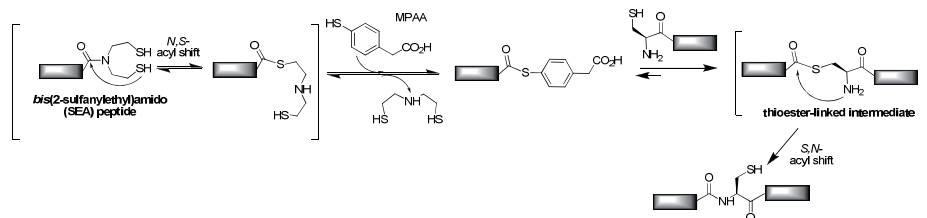
Oleg.Melnyk@ibl.fr

Introduction

The total chemical synthesis of native or modified proteins is gaining increase importance in the study of protein function, but also in the development of protein therapeutics. It is usually achieved by assembling in water unprotected peptide segments using native peptide ligation methods^[1].

Recently, our group has developed a novel native peptide ligation method based on a peptide featuring a *bis*(2-sulfanylethyl)amido (SEA)^[2] group on its C-terminus in reaction with a cysteinyl peptide in water (Scheme 1).

Here, we report a kinetic study of SEA ligation by using a series of SEA peptides featuring all the possible proteinogenic amino acids at the C-terminus. We will present also experiments intended to clarify the mechanism of SEA ligation such as the ability of the transient thioester SEA form produced by in situ *N,S*-acyl shift to participate in thiol-thioester exchange.



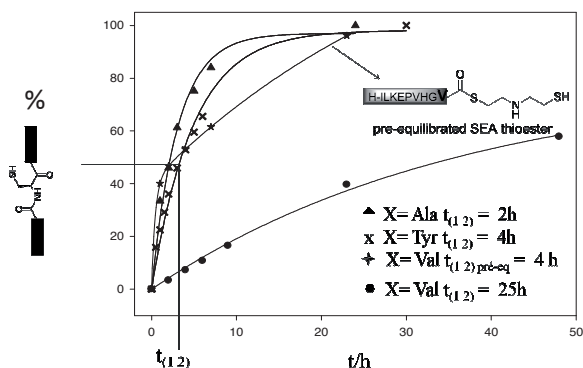
Scheme 1 *Bis*(2-sulfanylethyl)amido native peptide ligation (SEA ligation)^[2]

Results and Discussion

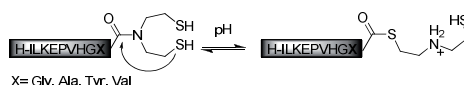
A library of SEA peptides H-ILKEPVHGX-SEA (X is any of the 20 proteinogenic amino acids) was synthesized by using *bis*(2-sulfanylethyl)amino polystyrene resin and standard Fmoc-SPPS. Then SEA ligations were performed using the model N-terminal Cys peptide H-CILKEPVHGV-NH₂. The progress of the ligations was monitored by RP-HPLC.

The data fit with a first order kinetic law (scheme 2a). Interestingly, SEA ligation kinetic rate order (Ala $t_{1/2}$ = 2h, Tyr $t_{1/2}$ = 4h, Val $t_{1/2}$ = 25h) can be correlated with a previous study^[3] (scheme 2b), which determined *N,S*-acyl shift kinetic rate for different amino acids (Ala $t_{1/2}$ = 1.4h, Tyr $t_{1/2}$ = 3h, Val $t_{1/2}$ = 6h). Moreover, other experiments (scheme 2a) show that

SEA ligation proceeds much faster when *N,S*-acyl shift is carried out prior to the ligation step (Val $t_{1/2}$ pre-equil= 4h).



Scheme 2a SEA ligation kinetic rate



Scheme 2b *N,S*-acyl shift equilibrium^[3]

According to these results the *N,S*-acyl shift seems to be the rate determining step in SEA native peptide ligation. Not surprisingly, the ranking of the different amino acids as determined by the half-life of model SEA ligations differs significantly from what is observed in NCL with Cys peptides, for which the thiol-thioester exchange of the alkylthioester with the exogenous arylthiol is rate determining.

Acknowledgments

This work was supported financially by Cancéropôle le Nord-Ouest, SIRIC OncoLille, Région Nord-pas-de-Calais and by the European Community.

References

- [1] L. Raibaut, N. Ollivier, O. Melnyk, *Chem. Soc. Rev.* **2012**, in press, DOI: 10.1039/C2CS35147A.
- [2] N. Ollivier, J. Dheur, R. Mhida, A. Blanpain, O. Melnyk, *Org. Lett.* **2010**, *12*, 5238.
- [3] J. Dheur, N. Ollivier, A. I. Vallin, O. Melnyk, *J. Org. Chem.* **2011**, *76*, 3194.

Binary switch activity of the Tat peptide: From membrane penetration to lytic action

Stefania Piantavigna,¹ Muhammad E. Abdelhamid,¹ Anthony P. O'Mullane,² Chuan Zhao,³ Xiaohu Qu,¹ Bim Graham,⁴ Leone Spiccia,¹ Lisandra L Martin¹

¹*School of Chemistry, Monash University, Clayton, Victoria 3800, Australia;* ²*School of Applied Sciences, RMIT University, Melbourne, Victoria 3000, Australia;* ³*School of Chemistry, The University of New South Wales, Sydney, NSW 2052, Australia;* ⁴*Monash Institute of Pharmaceutical Sciences, Monash University, Parkville, Victoria 3052, Australia*

E-mail: Lisa.Martin@monash.edu

Introduction

Cell penetrating peptides (CPP) possess the ability to cross the plasma membrane of eukaryotic cells. Among these peptides, the Tat peptide has been subject to intensive studies [1]. The amino acid sequence of Tat includes the basic RNA-binding domain of the HIV-1 Tat protein (YGRKKRRQRRR) that is responsible for its translocation across the cell membrane [2]. However, the mechanism by which these CPP enter the cell still remains unclear.

Quartz Crystal Microbalance with Dissipation monitoring (QCM-D) has been employed to elucidate the mechanism in which the Tat (44-57 and 49-57) peptides (Ac-GISYGRKKRRQRRR-NH₂ and Ac-RKKRRQRRR-NH₂) interact with supported lipid bilayers (SLBs) [3]. The artificial membrane can be composed to mimic either eukaryotic or prokaryotic plasma membranes. In addition, Scanning Electrochemical Microscopy (SECM) was employed to measure changes in the permeability of the membrane to a redox active mediator hence, report on the interaction of these Tat peptides.

Results and Discussion

Typically, the QCM technique monitors the temporal variation in frequency (Δf) and in Dissipation (ΔD), in real time. These parameters correlate with the changes in mass and viscoelasticity due to binding events [4]. In this case, the Tat peptides bind to a membrane coated layer, which consists of 6-mercaptohexanoic acid (MHA) modified gold sensor. In the presence of DMPC/Cholesterol (7:3 v/v) bilayer, an eukaryotic mimetic membrane, Tat (49-57) (10 μ M) bound to the membrane (Fig.1a, black line). This appears to be a trans-membrane insertion as the mass uptake is similar for a series of harmonics $n = 3, 5, 7$ and 9 , where every harmonic probes various depths within the membrane layer (data not shown). In contrast, using the DMPC/DMPG (2:1 v/v), a prokaryotic mimetic membrane, a two stage process occurs; the Tat peptides insert into the membrane followed by a rapid removal of lipid (Fig.1a, grey line). The same behavior was observed also for Tat (44-57).

Fig.1b and c show the SECM approach curves revealing the change in the permeability of the various membrane layers measured with a Pt microelectrode of 10 μ m diameter. The

effect of the interaction with the Tat peptides is shown as an increase in permeability of the $[\text{Fe}(\text{CN})_6]^{3-/4-}$ redox-active mediator. In Fig.1b and c approach curves correspond to: *i.* the theoretical conducting response, *ii.* the theoretical insulating response, *iii.* MHA on gold surface, *iv.* lipid layer on MHA, *v.* after the addition of Tat (44-57) 10 μM on the lipid layer. Similar SECM data were observed for Tat (49-57).

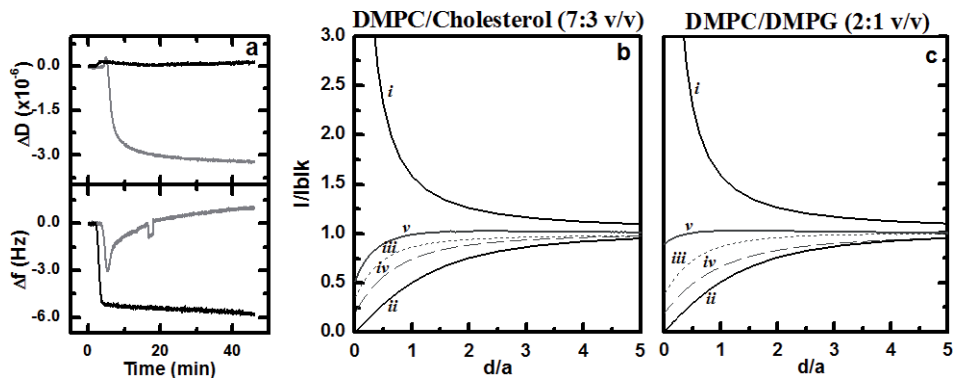


Figure 4: (a) QCM traces of Tat (49-57) and (b and c) SECM approach curves of Tat (44-57) interacting with biomimetic membrane.

In summary, the combination of QCM and SECM data reveals that the Tat peptides translocate across the membrane in a facile and passive way. This finding is contrary to some literature in which it is reported that the translocation of Tat peptides through the cell membrane requires active transport [5]. Of particular note in our study, it has been showed that these peptides act specifically and differently towards prokaryotic or eukaryotic biomimetic membranes.

Acknowledgments

The authors thank George McCubbin for discussions in the early stages of this work.

References

- [1] Trehin, R.; Merkle, H. P. *Eur. J. Pharm. Biopharm.* **2004**, *58* (2), 209.
- [2] Herce, H. D; Garcia, A. E. *Proc. Natl. Acad. Sci. USA* **2007**, *104* (52), 20805.
- [3] Piantavigna, S.; McCubbin, G.A; Boehnke, S.; Graham, B.; Spiccia, L.; Martin, L.L; *Biophys. Biochem. Acta – Biomembranes*, **2011**, *1808*(7), 1811.
- [4] Mechler, A; Praporski, S.; Piantavigna, S.; Heaton, S. M.; Hall, K. N.; Aguilar, M.-I.; Martin, L. L., *Biomaterials* **2009**, *30* (4), 682.
- [5] Green, I; Christison, R.; Voyce, C. J.; Bundell, K. R.; Lindsay, M. A., *Trends Pharmacol. Sci.* **2003**, *24* (5), 213.

Encapsulation and radiolabeling approaches of potential peptide-type biomarkers for assessment of amyloid plaques related to the Alzheimer's disease

F.R. Cabral¹, C.R. Nakaie², O.P. Martins³, A.C. Tedesco³, L. Malavolta⁴

¹*Instituto do Cerebro/Instituto Israelita Albert Einstein, Sao Paulo, Brazil;* ²*Universidade Federal de Sao Paulo, Sao Paulo, Brazil;* ³*Universidade de Sao Paulo, Ribeirão Preto, Brazil;* ⁴*Faculdade de Ciências Médicas da Santa Casa de Sao Paulo, Sao Paulo, Brazil*

luciana.quaglio@fcmsantacasasp.edu.br

Introduction

Considerable efforts have been made to design new peptide-carrier macrostructures which allow a stable and controlled release form of peptides in the organism [1-2]. In this regard, one of the main challenges to be overcome refers to an efficient peptide delivery in the blood-brain barrier. Recent findings demonstrate that the use of nanotechnology and molecular imaging methods have been used to assess diagnostic data of the central nervous system (CNS) [3,4]. Following with previous report [5], the present work presents results obtained with an alternative peptide encapsulation and radiolabeling approaches applicable for monitoring fibril formation induced by peptide aggregation process, responsible for some types of brain disorders.

Results and Discussion

Based upon the (1-42) A β -amyloid peptide present in Alzheimer's disease, the VHHQKLFFFAED (12-24) fragment and also the (36-42) and (16-20) but attaching a His residue at their C-terminal positions (VGGVVIAH and KLVFFH, respectively), were synthesized, purified and tested as potential biomarkers. The microspheres using the biodegradable polymer PLGA (poly-lactic-co-glycolic acid) were used as the support for inducing controlled biomarkers releasing system. The nanoparticles (Np) were prepared using the method of double emulsification and solvent evaporation [6] and exhibited a spherical shape with an average diameters varying in the 230-250 nm range.

The incorporation of peptides within this type of nanoparticles seemed to be a promising approach as it protects the peptide structure from degradation in the bloodstream. It was also verified that all peptides were efficiently entrapped by PGLA nanoparticles, applying the water/oil/water double-emulsion/solvent evaporation strategy. Higher encapsulation efficiency was verified in the order KLVFFH (72.3%) > VGGVVIAH (69.8%) > VHHQKLFFFAED (51.6%) These results showed that the encapsulation degree of the larger (12-24) segment was less effective than the others thus stressing the importance of the peptide length to this internalization process.

Visualization of the penetration in the hippocampus of mice with confocal microscope was carried out by testing both the PLGA and PLGA polymers derived with phthalocyanine probe. The Np were administered by injection directly into the brain (positive control) and through the tail vein of mice (n =4 for each type of Np, 2mg/mL). The analyses of the images obtained in the *in vivo* experiments (Fig. 1) showed clearly that the nanoparticles

with PLGA-phthalocyanine were able to cross the blood brain barrier, thus suggesting improved bioavailability and uptake for Np delivery into the brain.

In regard to the radiolabeling approach, the ^{99m}Tc radioisotope was used to label the peptide sequences at His residues, as previously described [7]. Stable metal-peptide complexes were obtained in 10^{-5} - 10^{-6} M peptide concentration range. Noteworthy, higher metal labeling yield was achieved with peptide segments bearing His residues at peptide C-terminal position, thus pointing to a position-dependent effect for the ^{99m}Tc coupling reaction.

In conclusion, these findings indicate potentials for the proposed encapsulation and radiolabeling strategies applicable for *in vitro* and *in vivo* diagnostic using this type of peptides.

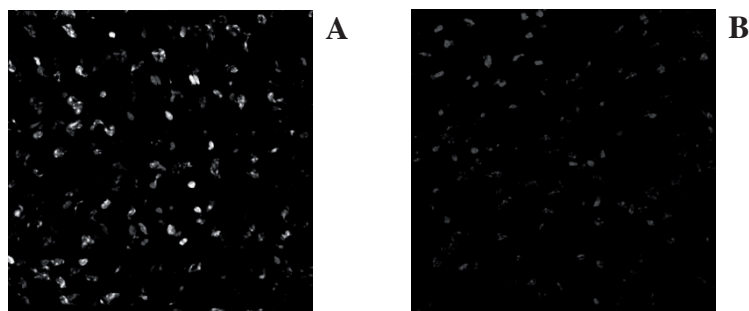


Fig. 1. Pictures of a representative mouse brain slides obtained with a confocal microscope with dual excitation band DAPI (gray spots) and phthalocyanine (white spots). In the pictures A and B were injected, through the tail vein, fluorescent nanoparticles and nanoparticles without probe as a control, respectively. (x 250 Magnification).

Acknowledgments

Grants from the Brazilian FAPESP and CNPq agencies are gratefully acknowledged.

References

- [1] Degim, T.; Celebi, N. *Curr. Pharm. Design* **2007**, *13*, 99-117.
- [2] Malavolta, L.; Cabral, F.R. *Neuropeptides* **2011**, *45*, 309-316.
- [3] Malavolta, L.; Cabral, F.R.; Conterras, L.F.G.; Ringheim, A.M.; Bressan, R.A. *Rev. Bras. Psiq.* **2009**, *31*, 300-302.
- [4] KulKarni, P.V. et al. *Rev. Nanomed. Nanobiotechnol.* **2010**, *2*, 35-47.
- [5] Malavolta L.; Nakaie, C.R. *Neur.Sci.* **2011**, *32*, 1123-1127.
- [6] Simioni, A.R. et al. *J. Nanosci. Nanotechnol.* **2006**, *6*, 2413-2415.
- [7] Waibel, R. et. al. *Nat. Biotechnol.* **1999**, *17*, 897-901.

Generation of silver nanoparticles in the presence of oligoproline derivatives

P. Feinäugle and H. Wennemers*

*Laboratory of Organic Chemistry, ETH Zürich, Wolfgang-Pauli Strasse 10,
CH - 8093 Zürich, Switzerland*

E-mail: Wennemers@org.chem.ethz.ch

Introduction

In the last years, the generation of silver nanoparticles (AgNPs) attracts, due to their unusual physical and chemical properties, more and more attention. AgNPs offer great opportunities for applications in molecular electronics, catalysis, imaging and as antimicrobial coatings. [1] The properties depend on their shape and size which are still challenging to control. [1] Many efforts have been made to optimize the generation process which typically involves the chemical reduction of a silver salt in the presence of an additive. The additive is influencing the formation process as well as the stability of the resulting nanoparticles. Thus many attempts have been carried out to modify these additives to achieve the desired size, shape and stability of the AgNPs. [2] Typical additives are polymers and surfactants. [3] Other promising candidates as additives are peptides, because of their large structural and functional diversity. [4]

Results and Discussion

The Wennemers group is following two different approaches to investigate the generation process of AgNPs using peptides as additives. One approach is the identification of suitable peptides in a colorimetric on-bead screening of split-and-mix libraries. Here we take advantage of the plasmon surface resonance which result in different colours of the AgNPs depending on their size and shape and allow for the identification of the additive peptide on bead. [5] The library contained the amino acids serine (Ser), aspartic acid (Asp), histidine (His) and tyrosine (Tyr) that were connected with either rigid or flexible linker. [5] Peptidic additives that act successfully as additives were identified after complexation of the library with Ag^+ and using either light or sodium ascorbate to reduce silver ions and generate AgNPs. In the screening using sodium ascorbate, differently sized AgNPs were found on different beads bearing different peptides. The size difference was reflected in different coloured beads, what was confirmed by scanning electron microscopy. For example, the AgNPs on beads bearing the peptide His-Ahx-Asp were approximately 50nm in size and agglomerated to sizes of $\leq 200\text{nm}$, whereas the AgNPs on the beads bearing peptides with the sequence Ser-Ahx-Tyr were approximately 10nm in diameter. This showed that peptides are not only suitable additives for the generation of AgNP but moreover that different peptides are able to control the size depending on their sequence. [5]

The second approach for the investigation of the generation of AgNPs is based on the rational design of peptides that are able to act as additives. The idea is to decorate a rigid and defined peptidic scaffold with functional groups able to act as additives in the AgNP generation. Towards this goal recently introduced oligoprolines, containing azidoproline

were used. These peptides adopt in an aqueous environment a highly symmetric polyproline type II helix, where every third residue is stacked on top of each other. They can easily be functionalized *via* the azido function in defined spatial distances of for example ~ 1 nm. [6]

The scaffold was functionalized with aldehyde moieties that can participate in a Tollens reaction (Figure 1). Ag^+ is reduced to $\text{Ag}(0)$ and at the same time the aldehyde is oxidized to a carboxylic acid that can bind to the $\text{Ag}(0)$ and stabilize the generated AgNPs. This reaction was carried out using the aldehyde functionalized oligoprolines with different lengths. The size of the resulting AgNPs directly correlated with the length of the additive in an almost perfect linear fashion (Figure 1). [7]

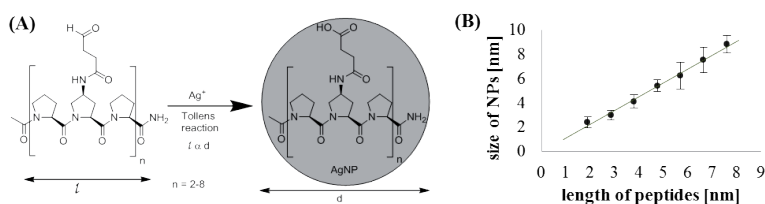
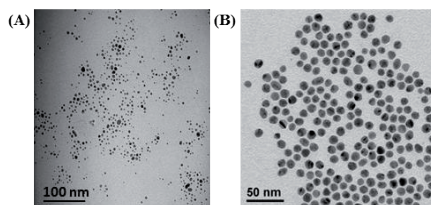


Figure 1: (A) Reaction scheme of Tollens reaction (B) Size of AgNPs with used peptides

These studies showed that the rigid backbone of the additive is very important for controlling the size of the AgNPs. We are now investigating different ligands on proline based peptides that can coordinate to Ag^+ and to $\text{Ag}(0)$ for their ability to act as additives in the generation of AgNPs.

To study this further, we designed oligoproline based peptides, bearing functional groups that allow for binding to both the silver ions and the AgNPs. To test their ability to act as an additive in the generation of AgNPs, an external reducing agent like sodium ascorbate was used. The new peptides differ in the influence on the resulting AgNPs (Figure 2). Differently sized nanoparticles were obtained depending on the nature of the ligand, but not on the length of the peptide. To examine the influence of the ligand on the size of the AgNPs, further studies are carried out.



References

- [1] Chen, C.-L., Rosi, N. L. *Angew. Chem. Int. Ed.* **2010**, *49*, 1924.
- [2] Rycenga, M., Cobley, C. M., Zeng, J., Li, W., Moran, C. H., Zhang, Q., Qin, D., Xia, Y., *Chem. Rev.*, **2011**, *111*, 3669
- [3] Zeng, J., Zheng, Y., Rycenga, M., Tao, J., Li, Z.-Y., Zhang, Q., Zhu, Y., Xia, Y., *J. Am. Chem. Soc.*, **2010**, *132*, 8552
- [4] Dickerson, M., B., Sandhage, K., H., Naik, R., R., *Chem Rev.*, **2008**, *108*, 4935
- [5] Belser, K., Slenters, T., V., Pfumbidzai, C., Upert, G., Mirolo L., Fromm, K., M., Wennemers, H., *Angew. Chem. Int. Ed.*, **2009**, *48*, 3661
- [6] a) Nagel, Y., A., Kuemin, M., Wennemers, H., *Chimia*, **2011**, *65*, 264; b) Kuemin, M., Sonntag, L.-S., Wennemers, H., *J. Am. Chem. Soc.*, **2007**, *129*, 466
- [7] Upert, G., Bouillère, F., Wennemers, H., *Angew. Chem. Int. Ed.*, **2012**, *51*, 4231

Simultaneous determination of aspartame, alitame, neotame and advantame by HILIC-ESI-MS/MS

Maroula G. Kokotou,¹ Christoforos G. Kokotos,²
Nikolaos S. Thomaidis¹

¹Laboratory of Analytical Chemistry, Department of Chemistry, University of Athens, Athens 15784, Greece; ²Laboratory of Organic Chemistry, Department of Chemistry, University of Athens, Athens, Greece

E-mail: ntho@chem.uoa.gr

Introduction

The wide application of aspartame (each year 16.000 t for worldwide consumption) as an artificial sweetener in low caloric products led to the discovery of new sweet dipeptides, namely alitame, neotame and most recently advantame [1]. Alitame, neotame and advantame are 2000, 6000 and 37000 sweeter than sucrose, respectively [2]. Such sweeteners are used in food products and beverages and they can help in managing body weight and disorders like obesity and diabetes [3]. In this work, the simultaneous determination of aspartame, alitame, neotame and advantame by negative and positive electrospray ionization (ESI), under Hydrophilic Interaction Chromatography (HILIC), is presented. HILIC is a normal phase chromatography technique, where the mobile phase consists of a high percentage of organic solvent (>80%) and a low percentage of an aqueous/polar solvent. At least 3% of aqueous solvent is needed for the hydration of static phase particles [4].

Results and Discussion

The structures of the analytes are shown in Figure 1. The synthesis of neotame and advantame is also depicted in Figure 1. The key-step for their synthesis was the reductive amination of H-Asp(OBu^t)-Phe-OMe with 3,3-dimethylbutanal and 3-(3-hydroxy-4-methoxyphenyl)propanal, respectively.

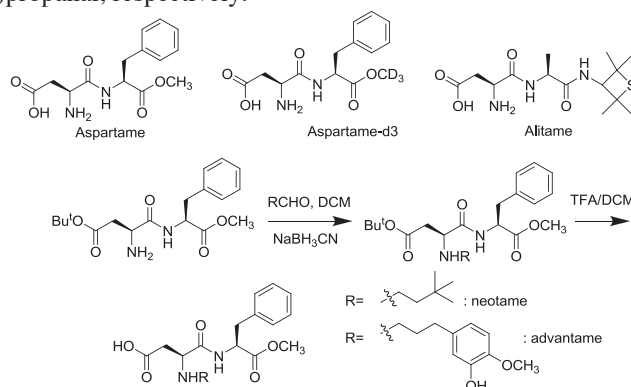


Figure 1. Structures of aspartame, aspartame-d3, alitame and synthesis of neotame and advantame

Measurements were performed with a Thermo TSQ Quantum Access system with triple quadrupole. The data acquisition was carried out with XCalibur Data System software (version 2.0.6). The chromatographic behavior of the artificial sweetener dipeptides was studied on two HILIC columns: Kinetex HILIC (a fused core silica column) and ZIC-HILIC column (a zwitterionic sulfoalkylbetaine column). The separation of dipeptides was achieved on Kinetex HILIC using 5 mM ammonium formate buffer pH 3.5 / methanol / acetonitrile (15/10/75), with a flow rate of 100 μ L/min at 50 $^{\circ}$ C column oven temperature. The best signal for the sweeteners dipeptides and the deuterated standard was achieved under (+) ESI, as shown in Figure 2. At this pH, silica is neutral and the dipeptides are in positively charged form. The retention mechanism of all analytes seems to be partition to the water layer as well as hydrogen bonding [5].

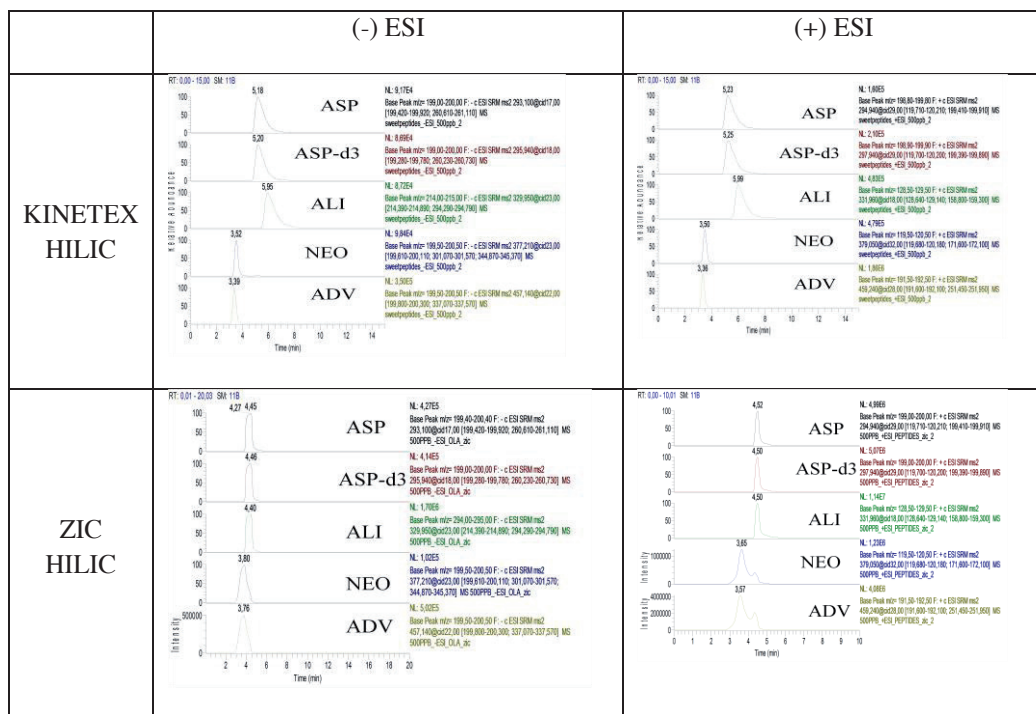


Figure 2. Simultaneous determination of sweetener dipeptides on KINETEX HILIC and ZIC HILIC columns.

References

- [1] Otabe, A.; Fujieba, T.; Masuyama, T.; Ubukata, K.; Lee, C. *Food Chem. Toxicol.* **2011**, *49*, S2-S7.
- [2] Kokotou, M. G.; Asimakopoulos, A. G.; Thomaidis, N. S. "Sweeteners" in *Food Analysis by HPLC*, ed. L. M. L. Nolle and F. Toldra, Third Edition, CRC Press: Boca Raton, FL, **2012**, in press.
- [3] Kokotou M. G.; Asimakopoulos, A. G.; Thomaidis, N. S. *Anal. Methods* **2012**, *4*, 3057.
- [4] Alpert, A. J. *Chromatogr. A* **1990**, *499*, 177.
- [5] Kokotou, M. G.; Thomaidis, N. S. *Chromatographia* **2012**, *75*, 457.

Stability studies on MMP-2 specific peptides for the preparation of molecular probes

Adrianna Radulska,^a Samia Ait-Mohand,^a Veronique Dumulon-Perreault,^a Rejean Label,^a Rriadh Zriba,^a Brigitte Guérin,^a Witold Neugebauer,^b Martin Lepage^a

^a*Département de médecine nucléaire et radiobiologie, Centre d'imagerie moléculaire de Sherbrooke,* ^b*Département de pharmacologie, Université de Sherbrooke, Sherbrooke, QC, Canada*

E-mail: Martin.Lepage@USherbrooke.ca

Introduction

Plasma and in vivo stability is an essential requirement for the successful development of potential drug candidates and diagnostic imaging probes. Rapid degradation of compounds in plasma may result in insufficient concentration to produce the desired pharmacological activity or to be used as a diagnostic agent. MMPs are zinc-dependent endopeptidases able to degrade the extracellular matrix (ECM) and are involved in cancer progression. We have previously reported on probes which specifically detect matrix metalloproteinase-2 (MMP-2) activity with magnetic resonance and optical imaging [1, 2]. The main goal of this work was to modify this specific peptide sequence to improve its stability while preserving enzyme activity. Specific MMP-2 substrates [3] (325 and Ka15) were selected and their stability was evaluated in three different conditions: in plasma, in plasma with a MMP inhibitor and in a MMP-2 solution. The samples were analyzed by HPLC to detect the degradation pattern and by LC-MS to determine the molecular mass of peptide fragments. These results show that peptide 325 was specific for MMP-2 but not stable in plasma, while Ka15 was found to be very stable in plasma, but was cleaved by MMP-2 at a lower rate. Peptides were modified either by substituting the most unstable residues by L-, D- amino acids or by non-natural amino acids (to improve stability) or by modifying their cleavage site (to improve MMP-2 digestion).

Results and Discussion

The starting point for this study was peptide 325 (Figure 1a), which was found to be specific for MMP-2 [1, 2] compared with MMP-9, -3 and -7. The LC/MS data suggested that the most unstable residues were: Ala and Ser (bold letters on Figure 1). Instead of Ser residue, D-Ser and Gly residues were introduced, but no beneficial impact was noted. On the other hand, Gly modification allowed a 10% MMP-2 hydrolysis increase (Figure 1a). Replacement of Ala with D-Ala inhibited the cleavage by MMP-2, but did not improve plasma stability. In the next iteration (peptide 325D-aa), all residues were replaced by D-amino acids except for the Tyr residues bordering the cleavage site. This completely inhibited digestion by MMP-2. Non-natural amino acid such as Abu (L- α -aminobutyric acid) in position P2 reduced the peptide hydrolysis by MMP-2 and increased plasma stability. Two additional sequences from Ref 3 were tested and found to be sensitive to MMP-2 [3] (346 and Ka11/14). Peptide 346 was efficiently digested (100%) by MMP-2, with a moderate 50% stability in plasma. Introducing its cleavage side (Ala in position P1

and Leu in P1') in the 325GAbu sequence resulted in similar results (peptide 346GAbu). The 325 series sequences are completely degraded in plasma and assays with the plasma/MMP-inhibitor reduced this degradation by 20-30%, suggesting that most unspecific degradation is caused by enzymes other than MMPs and occurs near the cleavage site. Modifications introduced in the 325 sequence were not sufficient. Non-natural and D- amino acids increase the stability but decrease the sensitivity to the enzyme.

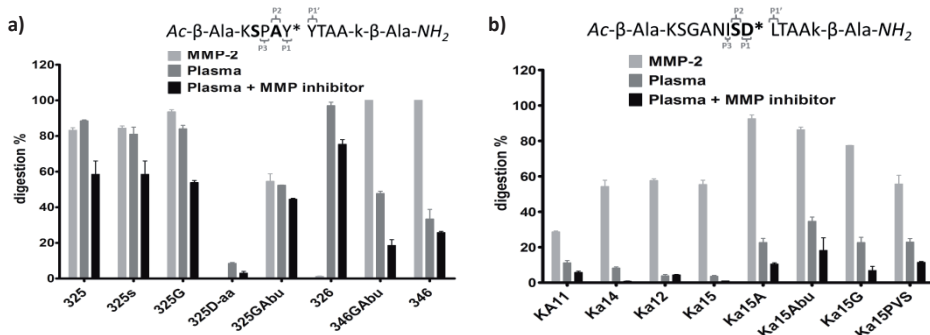


Figure 1. Plasma stability and MMP-2 digestion series a) 325 and b) Ka, * indicates the MMP-2 cleavage site.

The second sequence was tested in two versions: Ka14 and a shorter version termed Ka11. Both sequences were found to be very stable in plasma (85%), but also show lower sensitivity to MMP-2 (55%), especially Ka11. Its acetylated and amidated version (Ka12/15) had a similar sensitivity to MMP-2 and improved plasma stability (95%) (Figure 1b). Peptide Ka15 was incorporated in a solubility switchable probe with radiolabelled (⁶⁸Ga)-DOTA. Its *in vivo* stability was estimated to 30 minutes (100%), making it a suitable candidate for further *in vivo* investigations (in progress). To improve its specificity to MMP-2, Ala, Abu or Gly were introduced at position P1. These modifications yielded higher MMP-2 cleavage rate, but with reduced plasma stability (Figure 1b). Ka15A modifications results in the largest influence, improving the cleavage efficiency by MMP-2 from 55% to 93% and decreasing its stability in plasma to 75%. Addition of MMP-inhibitor slowed its degradation rate by 60%, suggesting that much unspecific degradation is caused by MMPs naturally present in the plasma. The LC/MS data showed that degradation occurs mostly near Ser (P2). Introducing a small, hydrophobic residue in position P1 (instead of Asp) decreased its plasmatic stability. Perspective: This residue will be modified to further increase the plasma stability of this sequence.

Acknowledgments

Martin Lepage is the Canada Research Chair in Magnetic Resonance Imaging. This study was funded by the Canadian Institutes of Health Research.

References

- [1] Lebel, R.; Jastrzebska, B.; Therriault, H.; Cournoyer, M.-M.; McIntyre, J.; Escher, E.; Neugebauer, W.; Paquette, B.; Lepage, M. *Magn. Reson. Med.* **2008**, *60*, 1056-1065.
- [2] Lebel, R.; Bonin, M.-A.; Zriba, R.; Radulska, A.; Neugebauer, W.; Paquette, B.; Lepage, M. *Contrast Media Mol. Imaging*, **2012**, *7*, 328-337.
- [3] Chen, E.; Kridel, J.; Howard, E.; Li, W.; Godzik, A.; Smith, J., *J. Biol. Chem.* **2002**, *8*, 4485-4491.

Charting the antiproliferative activity of [Arg⁸]vasopressin analogues against cancer cell lines

Valentinos Kounnis¹, Elena Elia¹, Andreas Tzakos^{1,2}, Evangelos Briasoulis¹, Lenka Borovičková³, Jiřina Slaninová³, Paul Cordopatis⁴, Vassiliki Magafa⁴

¹*Cancer Biobank Center of the University of Ioannina, GR-45110 Ioannina, Hellas;*
²*Department of Chemistry, University of Ioannina, GR-45110 Ioannina, Hellas;*³*Institute of Organic Chemistry and Biochemistry, Academy of Sciences of Czech Republic, Prague 6, Czech Republic;*⁴*Department of Pharmacy, University of Patras, GR-26500 Patras, Hellas*

E-mail: magafa@upatras.gr

Introduction

The posterior pituitary hormone Arginine Vasopressin (AVP) is a cyclic nonapeptide [c(Cys¹-Tyr²-Phe³-Gln⁴-Asn⁵-Cys⁶)-Pro⁷-Arg⁸-Gly⁹-NH₂]. The primary physiological role of AVP involves regulation of cardiovascular smooth muscle, via V1a receptor, and antidiuretic actions on the kidney (blood osmolality regulation), via V2 receptor [1]. Binding of AVP on the V1a receptor subtype also stimulates glycogenolysis in the liver and promotes platelet aggregation. In addition activation of the V1b receptor causes adrenocorticotrophic hormone release from the anterior pituitary. In addition to its well-known antidiuretic activity, AVP appears to have several peripheral effects, most of which are still unknown. Recent studies suggest that vasopressin may be involved in cell growth and proliferative mechanisms in different types of cancer cells. Vasopressin receptors have been found on the cell surface of pulmonary, pancreatic and breast cancers [2]. In a continuation of our previous work [3] and in order to study the effect of modifications with non natural amino acids in various positions of the peptide sequence of AVP, we synthesized a series of analogues containing mercapto propionic acid [Mpa] or S-salicylic acid [Sal] in position 1, Tyrosine(O-Methyl) [Tyr(Me)] or 2-Naphtylalanine [2-Nal] in position 2, L- α -t-butylglycine [Gly(Bu^t)] or L- β -(2-thienyl)-alanine [Thi] in positions 4 or 9, respectively. The effect of the relevant peptides on cell proliferation and cytotoxicity in MCF7, BxPC-3 and MIA PaCa-2 cancer cell lines was monitored in real-time using electronic cell sensor array technology (xCELLigence Systems).

Results and Discussion

The AVP analogues were synthesized by Fmoc/Bu^t solid phase methodology [4] utilizing the Rink Amide MBHA and the 2-chlorotrityl-chloride resin to provide the C-terminal amide and carboxylic acid, respectively. The cyclization was performed in DMSO/H₂O (2:8, v/v) for 24-36h. The physicochemical properties of the AVP analogues are summarized in Table 1. The effect of AVP and its analogue 8 on the proliferation of the cell lines studied here was assessed with the xCELLigence system. Cells were seeded at an initial concentration of 5000 cells per well in xCELLigence DP system's E-plates. Cells were allowed to adhere and enter the log-phase of proliferation. At 48h post seeding cells were exposed to compounds at 200 μ M, 100 μ M and 50 μ M concentrations. Compounds

were diluted in DMSO in order that the final DMSO concentration would be at 0.1% w/w which was previously assessed and found to be non-toxic for the cell lines mentioned above. Proliferation rate of control *versus* exposed cells was monitored in real time from the time cells were seeded until they had reached a growth plateau (100% confluence). All experiments have been carried in duplicates.

Table 1. Physicochemical properties of AVP analogues.

	AVP Analogues	Yield (%)	HPLC* <i>t_R</i> (min)	TLC**	
				<i>R_{f(A)}</i>	<i>R_{f(B)}</i>
1.	[Mpa ¹ , Tyr(Me) ² , Gly(Bu ⁹) ⁹] AVP	73	21.19	0.64	0.70
2.	[Mpa ¹ , 2-Nal ² , Gly(Bu ⁹) ⁹] AVP	62	21.87	0.59	0.63
3.	[Mpa ¹ , Thi ⁴] AVP	68	18.28	0.57	0.60
4.	[Sal ¹ , Thi ⁴] AVP	65	17.82	0.56	0.59
5.	[Mpa, Tyr(Me) ² , Gly(Bu ⁹) ⁹]-COOH AVP	68	20.27	0.55	0.57
6.	[Mpa ¹ , 2-Nal ² , Gly(Bu ⁹) ⁹]-COOH AVP	64	21.01	0.52	0.55
7.	[Mpa ¹ , 2-Nal ² , Thi ⁹]-COOH AVP	77	19.71	0.48	0.52
8.	[Sal ¹ , 2-Nal ² , Thi ⁹]-COOH AVP	70	20.19	0.52	0.54

*Linear gradient from 5 to 85% acetonitrile (0.1% TFA) for 30 min, Nucleosil 100 C₁₈ column

**A) butan-1-ol/water/acetic acid/pyridine (4/1/1/2, v/v) B) butan-1-ol/water/acetic acid (4/1/15 v/v, upper phase)

AVP compound seems to increase the proliferation rate of only BxPC-3 cell line by 28%, 29% and 10% for the concentrations used (200µM, 100µM and 50µM respectively). In contrary when MIA PaCa-2 cells are exposed to AVP, Cell Index (CI, a dimensionless parameter derived from xCELLigence System as a relative change in measured electrical impedance to represent cell status) shows a transient reduction by 21%, 25% and 11% for the three concentrations used, whereas on MCF7 cells AVP didn't seem to have any significant effect. Analogue 8 illustrate a similar profile on pancreatic cell lines where it shows the highest inhibitory growth effect at the intermediate concentration of 100µM lowering MIA PaCa-2 and BxPC-3 CI by 26% and 27% respectively, while MCF-7 cells are exposed to 200µM of analogue show to have a reduced proliferation rate by 41%. The monitored effect of these analogues on cancer cell lines provides further evidence on the diverse therapeutic areas that can be targeted by these moieties. Detailed mechanism of their action as also determination of the bio-profile of the remaining molecules is currently underway in our labs.

Acknowledgments

The authors thank the University of Patras for the K. Karatheodoris Research Grant (to V. Magafa_2010_D.156). Part of this research has been co-financed by the European Union (European Social Fund – ESF) and Greek national funds through the Operational Program "Education and Lifelong Learning" of the National Strategic Reference Framework (NSRF) - Research Funding Program: Heracleitus II. Investing in knowledge society through the European Social Fund.

References

- [1] Berberis, C.; Mouillac, B.; Durroux, T. *Endocrinol.* **1998**, *156*, 229.
- [2] North, W.G. *Exp. Physiol.* **2000**, *85*, 27S.
- [3] Magafa, V.; Pappa, E.; Borovičková, L.; Pairas, G.; Manessi-Zoupa, E.; Slaninová, J.; Cordopatis, P. In *"Peptides 2008"* (H. Lakinen, Ed.), pp. 350-351.
- [4] Fields, B. G., Noble, L., R. *Int J Pept. Prot. Res.* **1990**, *35*, 161.

Computer modeling of human μ -opioid receptor

Tatyana Dzimbova¹, Fatima Sapundzhi², Nevena Pencheva²,
Peter Milanov^{2,3}

¹Institute of Molecular Biology, Bulgarian Academy of Sciences, Bulgaria, 1113 Sofia;

²South-West University "Neofit Rilski", Bulgaria, 2700 Blagoevgrad; ³Institute of
Mathematics and Informatics, Bulgarian Academy of Sciences, Bulgaria, 1113 Sofia

E-mail: tania_dzimbova@abv.bg

Introduction

The μ -opioid receptor (MOR) is an important target in the search for novel analgesics. Numerous MOR selective ligands have been identified since determination of the structure of morphine in 19th century. Most of opioid alkaloids and their derivatives have μ -opioid affinity. Morphine is still the drug of choice for treating severe pain caused by cancer or surgical operation but its side effects are the reason for the searching and development of new selective MOR agonists, which analgesic effects are distinct from the effects of addiction.

The aim of the presented work is to find the relationship between structure and activity of the selective ligands of MOR in order to develop a reliable approach for design of new active analogues.

In the present work the following software is used in order to perform computational studies on a series of enkephalin analogues, designed to be selective for MOR: - crystal structure of the MOR was obtained from RCSB² (PDB id: 4dkl); - ligand preparation was done with Avogadro (an open-source molecular builder and visualization tool - Version 1.0.3)²; - docking studies were performed by using GOLD 5.1 (Genetic Optimization for Ligand Docking)³, run on Scientific LINUX 5.5 operating system; - for generation figure Molegro Molecular Viewer⁴ was used.

Thirteen peptides ([Cys(O₂NH₂)²-Leu⁵]-enk, [Cys(O₂NH₂)²-Met⁵]-enk, Dalargin, Dalarginamide, Dalarginethylamide, DAMGO (MOR selective ligand), [D-Phe⁴]-Dalarginamide, [L-Ala²]-Dalargin, [Leu⁵]-enkephalin, [Met⁵]-dalargin, [Met⁵]-enkephalin, N-Me-[D-Phe⁴]-Dalarginamide, and N-Me-[L-Phe⁴]-Dalarginamide) were chosen for docking with receptor. All of them were synthesized, *in vitro* biologically tested, and already published^{5,6}. GOLD uses generic algorithm and considers full ligand conformational flexibility and partial protein flexibility. From literature⁷, the binding site for MOR was defined as residues within 10Å radius of aspartic acid of third TM domain, which is involved in the most crucial interaction. In the case of MOR this is Asp147. ChemScore algorithm was used and scoring function (presented as Score from Docking data) was calculated for each ligand. The conformations of the ligands with best scoring functions were selected and parameters of the scoring functions were use in order to find correlations between them and *in vitro* results, presented in the Table 1.

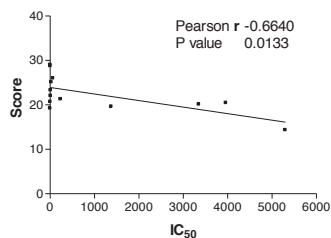
Table 1. The inhibitory effect (IC₅₀, nM) on evoked contractions of the isolated guinea-pig ileum^{5,6} and scoring function of dalargin, its analogues, [Leu⁵]-enkephalin, [Met⁵]-enkephalin and DAMGO.

Ligands	IC ₅₀ (nM)	Score
N-Me-[L-Phe ⁴]-Dalarginamide	0.57±0.08	20.08
DAMGO	5.8±0.4	29.02
Dalarginamide	5.8±0.7	20.67
Dalarginethylamide	6.0±0.7	28.75
[Met ⁵]-dalargin	11.9±1.7	23.27
Dalargin	12.3±1.7	22.05
[Met ⁵]-enkephalin	28.6±8.4	25.11
[Leu ⁵]-enkephalin	65.3±8.2	25.95
[L-Ala ²]-Dalargin	234±46	21.28
[Cys(O ₂ NH ₂) ² -Met ⁵]-enk	1378±245	19.6
N-Me-[D-Phe ⁴]-Dalarginamide	3350±850	19.17
[Cys(O ₂ NH ₂) ² -Leu ⁵]-enk	3960±740	20.44
[D-Phe ⁴]-Dalarginamide	5300±408	14.31

The values are the means ± SEM of 4-6 observations. The Krebs solution contained the following peptidase inhibitors: bestatine 10 µM, thiorphan 3 µM, capropril 10 µM and Leu-Leu 2 µM.

Results and Discussion

Docking was performed with MOR and all 13 ligands. The results of docking studies of ligands are presented in Table 1. All of the ligands bind to the receptor by forming many H-bonds. Very important residue in the receptor sequence is Asp147, which forms salt bridge with NH₃⁺ of the ligand's molecule. All 13 ligands interact with MOR with their terminal NH₃⁺. Key part of the ligands structure is phenolic hydrogen group (Tyr residue). In all cases it binds to different residues in the receptor structure.



Correlations of docking data and *in vitro* experiments results are performed with GraphPad Prism 3.0. Good Pearson's correlation was obtained between Scoring function from GOLD docking procedure with IC₅₀ value in Guinea-pig myenteric plexus. The correlation between *in vitro* data and scoring function is significant. Lower value of the scoring function corresponds to lower inhibitory effect.

Acknowledgments

This work was supported by NFSR of Bulgaria projects: MY-FS-13/07, DVU 01/197/16.12.2008 and DO 02-135/31.07.2009.

References

- [1] <http://www.rcsb.org/pdb/home/home.do>
- [2] <http://avogadro.openmolecules.net/>.
- [3] Jones, G., Willett, P., Glen, R.C., Leach, A.R., Taylor, R., *J.Mol.Biol.*, **267**, 727-748 (1997).
- [4] <http://molegro.com/index.php>
- [5] Pencheva, N., Pospišek, J., Hauzerova, L., Barth, T., Milanov, P. *Br. J. Pharmacol.* **128**, 569-576 (1999).
- [6] Pencheva, N., Vezenkov, L., Naydenova, E., Milanov, P., Pajpanova, T., Malamov, S., Bojkova, L. *Bul. Chem. Comm.* **33**, 47-58 (2001).
- [7] Befort, K., Tabbara, L., Bausch, S., Chavkin, C., Evans, C., Kieffer, B. *Mol.Pharmacol.* **49**, 216-223 (1996).

Detection of antibodies against synthetic peptides mimicking ureases fragments in atherosclerotic patients sera

Beata Kolesińska,^a Justyna Fraczyk,^a Inga Relich,^a Iwona Konieczna,^b
Marek Kwinkowski,^b Wiesław Kaca,^b Zbigniew J. Kamiński^a

^aInstitute of Organic Chemistry, Technical University of Lodz, Poland, ^bDepartment of Microbiology, Institute of Biology, Jan Kochanowski University, Kielce, Poland
e-mail: zbigniew.kaminski@p.lodz.pl

Introduction

Atherosclerosis is a chronic disorder leading to narrowing of the blood vessels lumen. There are suggestions that atherosclerosis may have autoimmune background [1]. Probably, infectious agents are involved in disease progress and atherosclerosis plaques may be place of bacterial colonization [2]. Especially, infections caused by *Helicobacter pylori* was connected with atherosclerosis occurrence [3, 4]. This bacteria produce large amount of urease, a protein catalyzing hydrolysis of urea to ammonia and carbon dioxide. The aim of this study was to investigate the level and specificity of antibodies binding to the synthetic peptides corresponding to the bacterial ureases “flap” region sequences in the atherosclerosis patients sera.

Results and Discussion

For these investigations peptide with amino-acid sequences derived from “flap” region of different ureases immobilized on a cellulose membrane were used. The peptide were synthesized directly on the support using 4-(4,6-dimethoxy-1,3,5-triazin-2-yl)-4-methylmorpholinium tetrafluoroborate (DMT/NMM/BF₄) as coupling reagent [3]. Five oligopeptides corresponding flap region of ureases from different organisms were tested: BK-61A: SIKEDVQF and BK-61B: CHHLDKSIKEDVQFADSR – characteristic for *Helicobacter pylori*;

BK-65B: MLMVCHHLDPSSIPEDVA – characteristic for *Proteus* sp.;

BK-65C: MVMITHHLNASIPEDIA – characteristic for *Staphylococcus* sp.,

BK-65D: MLMVCHHLNREIPEDIA – similar to *Canavalia ensiformis*

The level and specificity of antibodies recognizing synthetic peptides were analyzed by quantitative dot blot method using 25 sera from atherosclerosis patients (AP) with mean age 60±12 years and 26 sera from volunteer blood donors (VBD) with mean age 50±4.5 years. In all sera reaction with all analyzed peptides were observed. However, in AP sera the level of bound antibodies was higher (Fig.1).

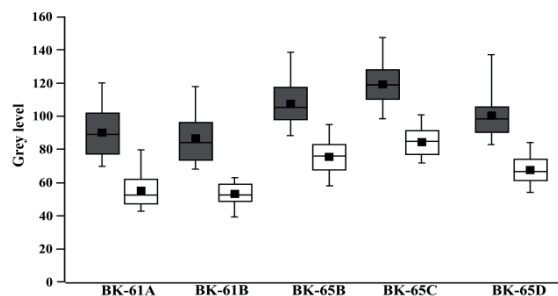


Figure1. Statistical graph of the level of antibodies recognizing synthetic peptides in AP sera (grey bars) and VBD control sera (white bars); black squares mark a mean of reactions, lines in bars – a median.

The differences between level of antibodies recognizing ureases flap fragment in AP versus VBD sera were statistically significant ($p < 0.001$; one way ANOVA) for each analyzed synthetic peptide. We performed assay to determine specificity of antibodies in AP and VBD sera. In first step, antibodies in sera were adsorbed using *H.pylori* BK-61A peptide. In earlier studies we revealed that adsorption of anti-BK-61A antibodies from AP serum results by decrease the level of antibodies recognizing BK-61B peptide in this serum [4]. In present work we show that level of antibodies bounding to BK-65B (nonadecapeptide characteristic for *P. mirabilis* urease) is also statistically lower (Fig.2).

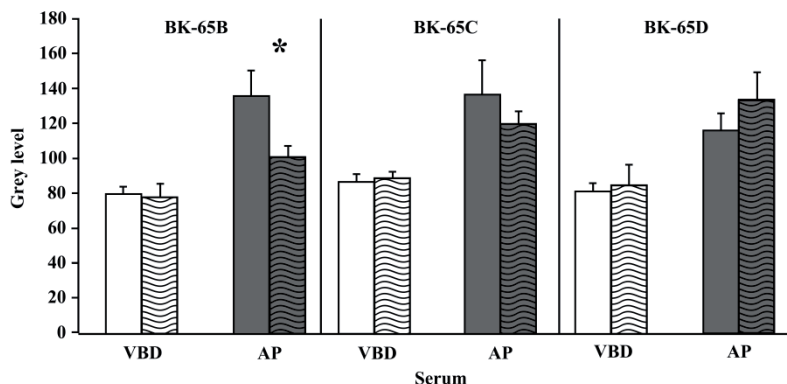


Figure 2. The differences in level of antibodies bound to synthetic peptides in adsorbed (bars with lines) and non-adsorbed (bars without lines) VBD and AP sera. Asterisk mark statistically significant differences.

In conclusion: immune system of atherosclerosis patients may produce a spectrum of antibodies recognizing not only a specific epitope but also a set of peptides with similar sequence. These results support the theory that atherosclerosis is an autoimmune process. Moreover, synthetic peptides analyzed by us could be useful probe for investigation of AP pathogenesis.

Acknowledgments

This work was supported by Ministry of Science and Education, Poland Grant NN304 044639 and Grant N N405 669540.

References

- [1] Mandal K., Jahangiri M., Xu Q. *Autoimmun. Rev.*, **2004**, 3, 31-37.
- [2] Ott S.J., El Mokhtari N.E., Musfeldt M., Hellmig S., Freitag S., Rehman A., Kühbacher T., Nikolaus S.; Namsolleck P., Blaut M., Hampe J., Sahly H., Reinecke A., Haake N., Günther R., Krüger D., Lins M., Herrmann G., Fölsch U.R., Simon R., Schreiber S. *Circulation*, **2006**, 113, 929-937.
- [3] Shmueli H., Passaro D.J., Vaturi M., Sagie A., Pitlik S., Samra Z., Niv Y., R. Koren, Harell D., Yahav J. *Atherosclerosis*, **2005**, 179, 127-132.
- [4] Arabski M., Konieczna I., Sołowiej D., Rogoń A., Kolesińska B., Kamiński Z., Kaca W. *Clin. Biochem.*, **2010**, 43, 115-123.
- [5] Kamiński, Z. J.; Kolesińska, B.; Kolesińska, J.; Sabatino, G.; Chelli, M.; Rovero, P.; Błaszczyk, M.; Głowska, M. L.; Papini, A. M. *J. Am. Chem. Soc.* **2005**, 127; 16912.

Determination of in vitro T-cell stimulating activity of Dsg3 peptide antigens on PBMC from patients with pemphigus vulgaris

Katalin Uray¹, Hajnalka Szabados¹, Pálma Silló², Sarolta Kárpáti², Szilvia Bősze¹

¹ *Research Group of Peptide Chemistry, Hungarian Academy of Sciences, Eötvös L. University, Budapest, Hungary;* ² *Department of Dermato-Venereology and Skin Oncology, Semmelweis University, Budapest, Hungary*

E-mail:uray@elte.hu

Introduction

Pemphigus vulgaris (PV), an autoimmune bullous skin disease, is a rare, but life-threatening disorder. It is characterized by autoreactive antibodies directed against adhesion molecules of the epidermis [1,2]. In the pathogenesis of PV, autoreactive T-cell response also plays a crucial role. T-cells recognize epitopes from desmoglein 3 (Dsg3) protein [3-5], producing different cytokines, e.g. interferon- γ (IFN- γ).

Based on previous epitope mapping studies [5,6] four potential T-cell epitope regions (Dsg3/189-205, 206-222, 342-358 and 763-777) within the protein Dsg3 were selected for further analysis using synthetic oligopeptides. The peptides and their *N*-terminally truncated derivatives were used to stimulate the peripheral blood mononuclear cells (PBMC) of PV patients and healthy controls.

Detailed analysis of T-cell epitope regions of Dsg3 protein has outstanding importance in the immunopathological research of PV in order to design and develop novel synthetic antigens as future diagnostic tools.

Results and Discussion

Peptides were synthesized by solid phase peptide synthesis method using Fmoc/tBu chemistry on Rink amide MBHA resin. After cleavage from the resin the peptides were RP-HPLC purified, then characterized by ESI-MS and amino acid analysis.

PBMC from the heparinized whole peripheral blood of three healthy donors (D1-3) and three patients diagnosed with PV (PV1-3) were isolated using density gradient centrifugation based separation [7]. PBMC were incubated with Dsg3 peptides at 0.025 mM concentration [8]. After 20 hrs of incubation, supernatants were collected. IFN- γ content was measured by sandwich ELISA.

PBMC of healthy donors produced less IFN- γ than those of PV patients. PBMC of healthy donors showed activity only to some peptides (e.g. D1 – Dsg3/763-777, Figure 1; threshold: 50 pg/mL IFN- γ). The Dsg3 derived peptides caused increased IFN- γ release on the PBMC of all PV patients to a different extent. Figure 1 illustrates a pattern of IFN- γ production representative for the difference between healthy donors and PV patients on the example of region Dsg3/763-777. In case of the other regions similar IFN- γ production

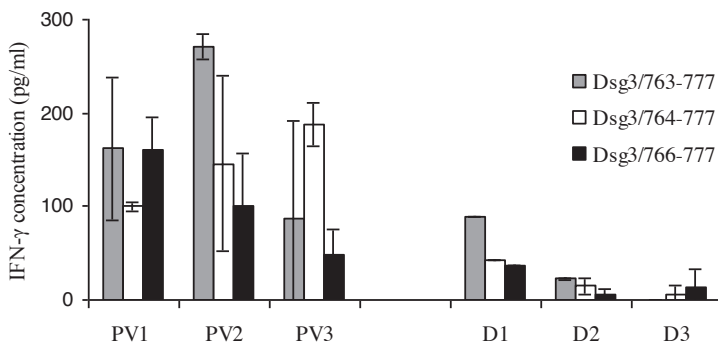


Figure 1. IFN- γ production of PBMC of PV patients (PV1-3) and healthy donors (D1-3) after 20h stimulation with 0.025 mM Dsg3/763-777 peptide and its truncated derivatives.

pattern was observed (data not shown). More than 50 pg/mL IFN- γ concentration was measured in case of at least one peptide from all four regions studied. In case of region 189-205 truncated peptides proved to be more stimulatory than the original peptides, while in region 206-222 mostly the longest peptides reacted with the PBMC (data not shown).

Peptides from region 342-358 had no stimulatory effect on the PBMC of patient PV2, but on those of the other two patients marked IFN- γ production was observed (data not shown).

Three peptides (Dsg3/192-205, 342-358 and 764-777, Figure 1) were able to stimulate the PBMC of all patients and neither of those of healthy controls. Although the other peptides could not distinguish so conclusively, the pattern of stimulatory activity also showed marked difference in their case.

We showed that IFN- γ production of healthy donors and PV patients may be distinguished using *in vitro* PBMC stimulation with synthetic peptides representing T-cell epitope regions.

Acknowledgments

These studies were supported by OTKA K61518, NKTH-OTKA 68358.

References

- [1] Hertl, M. *Int Arch Allergy Immunol*; **2000**, *122*, 91-100.
- [2] Hertl, M.; Eming, R.; Veldman, C. *J Clin Invest*. **2006**, *116*, 1159-1166.
- [3] Amagai, M.; Klaus-Kovtun, V.; Stanley, J.R. *Cell* **1991**, *67*, 869-877.
- [4] Kárpáti, S.; Amagai, M.; Prussick, R.; Cehrs, K.; Stanley, J.R. *J Cell Biol*. **1993**, *122*, 409-415.
- [5] Veldman, C.M.; Gebhard, K.L.; Uter, W.; Wassmuth, R.; Grötzinger, J.; Schultz, E.; Hertl, M. *J Immunol* **2004**, *172*, 3883-3892.
- [6] Wucherpfennig, K.W.; Yu, B.; Bhol, K.; Monos, D.S.; Argyris, E.; Karr, R.W.; Ahmed, A.R.; Strominger, J.L. *Proc. Natl. Acad. Sci. USA* **1995**, *92*, 11935-11939.
- [7] Jurcevic, S. et al; *Clin Exp Immunol* **1996**, *105*, 416-421.
- [8] Bősze, Sz.; Caccamo, N.; Majer, Zs.; Mező, G.; Dieli, F.; Hudecz, F. *Biopolymers (Peptide Science)* **2004**, *76*, 467-476.

Direct antiproliferative effect on breast cancer cells of [Mpa¹, D-Tyr(Et)²] or [Mpa¹, D-1-Nal²] oxytocin analogues containing β -(2-thienyl)-Alanine in position 3 or 7

Vassiliki Magafa^{1*}, Efstathia Giannopoulou², George Pairas¹, Revekka Exarchakou¹, Nikos L. Assimomytis¹, Eleftheria Tsoumani¹, Lenka Borovičková³, Jiřina Slaninová³, Haralabos P. Kalofonos², Paul Cordopatis¹

¹Department of Pharmacy, University of Patras, GR-26500 Patras, Hellas; ²Clinical Oncology Laboratory, Division of Oncology, Department of Medicine, University of Patras, GR-26504 Patras, Hellas; ³Group of Peptide Biochemistry, Institute of Organic Chemistry and Biochemistry, Academy of Sciences of Czech Republic, Flemingovo square 2, Prague 6, CZ-166-10, Czech Republic

E-mail: magafa@upatras.gr

Introduction

Oxytocin (OT) is a cyclic nonapeptide [cyclo(Cys-Tyr-Ile-Gln-Asn-Cys)-Pro-Leu-Gly-NH₂] hormone of hypothalamus that is released into the circulation from the posterior lobe of the pituitary gland. Its major physiological roles are: a) to induce uterine contractions and b) milk ejection. Beside these actions, OT is involved in several other functions, such as vascular and cardiac regulation and sexual, maternal and social behavior [OT receptors (OTR) are widespread distributed also in the brain] [1]. OT antagonists may not only be studied as promising inhibitors of preterm labor but may also prove useful in the treatment of dysmenorrhea, benign prostatic hyperplasia and psychiatric illnesses such as anxiety, sexual dysfunctions, eating disorders etc. [2]. Several tumor types have been reported to express OT receptors (OTRs): primary breast cancers, endometrial carcinomas, neuroblastomas, glioblastomas. The effect of oxytocin on the proliferation of cancer is cell type dependent with reports of increased proliferation, decreased proliferation or no effect [3]. Based on literature data and in continuation of our previous work [4], we compared activities of OT and its eight analogues (Table 1), in the rat uterotonic *in vitro* test, in the rat pressor assay and in the binding affinity test using human OT receptors and [³H]OT. In parallel, the analogues were tested for their ability to inhibit proliferation of human hormone-dependent and -independent breast cancer cells MCF-7, MDA-MB-231 and MDA-MB-468, respectively.

Results and Discussion

The analogues were synthesized by Fmoc solid phase methodology utilizing Sieber Amide resin as solid support to provide the peptide amide and diisopropylcarbodiimide/1-hydroxybenzotriazole (DIC/HOBt) as coupling reagents. The cyclization was performed in dimethylsulfoxide (DMSO)/water (1:4, v/v) for 24-36h [4]. The identification of the analogues was performed by ESI mass spectrometry. Uterotonic and pressor activities as well binding affinity were determined as previously described [4]. The physicochemical properties and biological evaluation of the analogues are summarized in Table 1.

Table 1: Physicochemical Properties and Biological Activity of the Oxytocin Analogues

	Analogues	HPLC* t _r (min)	TLC R _{f(A)} **	Activity		
				Uterotonic in vitro (pA ₂)	Pressor (pA ₂)	Binding Affinity IC ₅₀ (nM)
I	[Mpa ¹ , D-Tyr(Et) ²]OT	22.26	0.67	7.82 ± 0.07	0	148 ± 26
II	[Mpa ¹ , D-1-Nal ²¹]OT	22.41	0.62	7.92 ± 0.21	0	34.6 ± 2.9
III	[Mpa ¹ , D-Tyr(Et) ² , Thi ³]OT	26.42	0.69	7.09 ± 0.13	0	212 ± 18
IV	[Mpa ¹ , D-Tyr(Et) ² , D-Thi ³]OT	23.52	0.68	0	0	>10000
V	[Mpa ¹ , D-1-Nal ² , Thi ³]OT	26.41	0.65	8.50 ± 0.24	6.10	5.2 ± 0.7
VI	[Mpa ¹ , D-1-Nal ² , D-Thi ³]OT	28.14	0.64	6.17 ± 0.22	0	3226 ± 93
VII	[Mpa ¹ , D-Tyr(Et) ² , Thi ⁷]OT	25.92	0.62	8.50 ± 0.30	0	111 ± 29
VIII	[Mpa ¹ , D-1-Nal ² , Thi ⁷]OT	25.85	0.60	8.22 ± 0.30	0	138 ± 25

* Linear gradient from 5 to 85% acetonitrile (0.1% TFA) for 30 min, Nucleosil 100 C₁₈ column,

** A) butan-1-ol/water/acetic acid/pyridine (4/1/1/2, v/v)

As can be seen (Table 1), substitution of Ile³ or Pro⁷ by Thi influenced biological activities significantly. Analogues with L-stereoisomer of Thi³ exhibited higher inhibitory potency in comparison to analogues with D-stereoisomer of Thi³. Analogues having in position 7 Thi retain the oxytocin antagonistic potency. Furthermore analogues with D-stereoisomer of Thi³ showed significantly low binding affinity to the OT receptor. Initially, OT was tested on cell proliferation of MCF-7, MDA-MB-231 and MDA-MB-468 [5]. We found that OT did not affect cell number in any cell line, although all cell lines express OTR. Further, we selected MDA-MB-468 cells to test the effect of selected analogues because these cells express the higher levels of calcium channels, a target of OTR. Analogues with D-Tyr(Et) in position 2 have a dual effect in MDA-MB-468 cells proliferation 48 and 72h after cells treatment. These analogues inhibited cell proliferation when cells were treated with serum supplemented medium but increased cell proliferation when medium without serum was used. In addition the same analogues were tested to MCF-7 cells with low levels of calcium channels and we did not find any effect of the analogues in cell number. These results suggest that the antiproliferative effect of analogues with D-Tyr(Et) in position 2 might implicate a mechanism dependent on levels of calcium channels and this effect is modulated by serum presence. More studies are needed to elucidate the activated pathways and the role of serum environment.

Acknowledgments

The authors thank the University of Patras for the K. Karatheodoris Research Grant (to V. Magafa_2010_D.156).

References

- [1] Gimpl, G.; Fahrenholz, F. *Physiol. Rev.* **2001**, *81*, 629.
- [2] Borthwick, A. D. *Ann. Rep. Med. Chem.* **2006**, *41*, 409.
- [3] Reversi, A.; Cassoni, P.; Chini, B. *J. Mamm. Gland. Biol. Neopl.* **2006**, *10*, 221.
- [4] Magafa, V.; Borovičková, L.; Slaninová, J.; Cordopatis, P. *Amino Acids* **2009**, *38*, 1549.
- [5] Peters, A. A.; Simpson, P. T.; Bassett, J. J.; Lee, J. M.; Da Silva, L.; Reid, L. E.; Song, S.; Parat, M. O.; Lakhani, S. R.; Kenny, P. A.; Roberts-Thomson, S. J.; Monteith, G. R. *Mol Cancer Ther.* **2012**, *11*, doi: 10.1158/1535-7163.

JMV 2009, a potent neurotensin antinociceptive analog

Adeline René¹, Pascal Tétreault², Nicolas Beudet², Philippe Sarret²,
Jean Martinez¹, Florine Cavalier*¹

¹IBMM, UMR-CNRS 5247, Universités Montpellier I et II, UM II, Place Eugène Bataillon, 34095 Montpellier cedex 05, France; ²Département de Physiologie et Biophysique, Faculté de Médecine et des Sciences de la Santé, Université de Sherbrooke, 3001, 12^{ème} Avenue Nord, Sherbrooke, Québec, J1H 5N4 Canada

E-mail: florine@univ-montp2.fr

Introduction

Neurotensin (NT) is a tridecapeptide, which is widely distributed in the brain and in the gastrointestinal tract. This peptide exerts a variety of physiological effects including hypothermia, analgesia and antipsychotic-like properties. As an antinociceptive agent, NT was found to be even more potent than morphine without having opioids-related adverse effects.

Structure-activity relationship (SAR) studies showed that the C-terminal hexapeptide fragment NT(8-13) corresponds to the minimal active sequence. This lead compound needs modifications to improve blood-brain barrier (BBB) crossing and resistance to enzymatic degradation.

Here, we studied the substitution of proline in position 10 by a silylated analog, silaproline (Sip) [1], in terms of physico-chemical characteristics, affinity and activity.

Results and Discussion

Starting from the NT(8-13) sequence, replacement of arginines by lysines does not affect affinity. Indeed, H-Lys-Lys-Pro-Tyr-Ile-Leu-OH (JMV 438) has almost the same affinity and activity than NT(8-13). Silaproline was introduced in position 10 of JMV 438 to afford compound JMV 2009 (Figure 1).

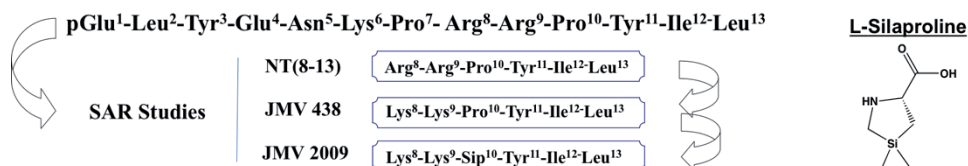


Figure 1. Sequence of NT analogues.

The synthesis was performed on solid phase following a Fmoc strategy (Figure 2).

Neuroprotective peptide Colivelin and labeled derivatives: Structural, in vitro and in vivo evaluation

**Myrta Kostomoiri,¹ Christos Zikos,² Dimitra Benaki,¹ Maria
Paravatou-Petsotas,² Theodoros Tsotakos,² Charalambos Triantis,²
Ioannis Pirmettis,² Minas Papadopoulos,² Maria Pelecanou,¹
Evangelia Livanidou²**

*Institutes of ¹Biology and ²Radioisotopes & Radiodiagnostic Products, NCSR
"Demokritos", 153 10 Athens, Greece
e-mails: pelmar@bio.demokritos.gr; livanlts@rrp.demokritos.gr*

Introduction

Colivelin (CL, SALLRSIPAPAGASRLLLLTGEIDL^P) is a 26-amino acid hybrid peptide first reported in 2005 as the most potent member of the Humanin (HN) family of peptides. CL consists of the activity-dependent neurotrophic factor ADNF-9 (SALLRSIPA) C-terminally attached to the bioactive modified core of the neuroprotective HN sequence (PAGASRLLLLTGEIDL^P). CL exhibits in vitro and in vivo rescuing action at femtoM level offering hope in the fight against neurodegenerative diseases [1-2]. The exact mechanism through which CL exerts its neuroprotective action remains elusive. In the current work we present (a) the investigation through CD spectroscopy of the direct interaction of CL with the β -amyloid peptide β -AP(1-40) considered to play a central role in the development of Alzheimer's disease (AD) pathology, and (b) the synthesis and initial evaluation of three CL derivatives to be used as molecular tools in the investigation of the mode of action of CL with in vitro and in vivo experiments.

Results & Discussion

The aggregation of β -AP(1-40) either in soluble oligomers or in higher order insoluble fibrillar forms is implicated in the pathogenesis of AD. In order to investigate whether the presence of CL intervenes in the aggregation process, 50 μ M solutions of β -AP(1-40) in phosphate buffered-saline (PBS) were incubated with in-house prepared, synthetic CL at 1:1 and 1:2 molar ratios. The aggregation process was monitored by obtaining CD spectra every 12 to 24 h for a period of one month and comparing them to the behavior of solutions of plain CL and of β -AP(1-40). The spectra of plain CL show an unordered structure that remains stable in time while those of plain β -AP(1-40) present a transition from random coil to β -sheet accompanied by a gradual reduction in signal intensity due to precipitation of insoluble aggregates. However, in the spectra of their mixture a quick reduction of CD intensity is observed that provides strong and direct evidence of interaction of the two peptides in solution that speeds up precipitation.

To investigate the effect of CL in more complex systems three new derivatives of CL (Fig.1) were designed bearing labeling moieties, i.e. (a) the fluorescent molecule FITC, (b) the streptavidin-counterpart biotin, and (c) the ^{99m}Tc-radiometal chelating unit dimethylGly-Ser-Cys (*dm*GSC). These derivatives will be used as molecular probes in various biological assays.

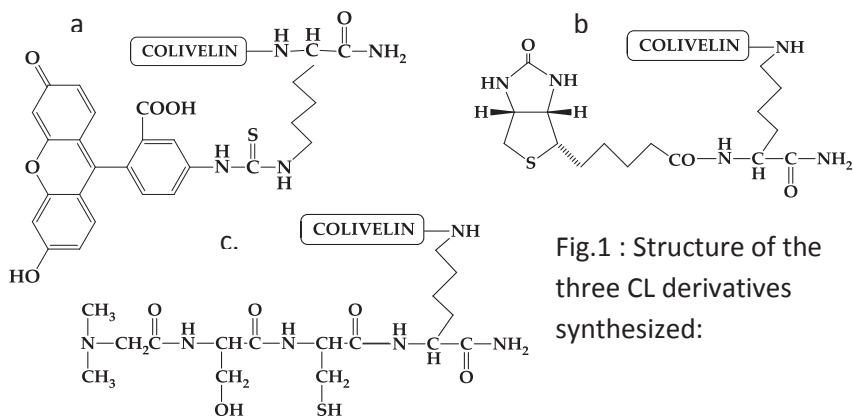


Fig.1 : Structure of the three CL derivatives synthesized:

The derivatives were synthesized manually according to the Fmoc-solid phase peptide synthesis strategy, purified with semi-preparative RP-HPLC, and characterized with analytical RP-HPLC and ESI-MS. The tag molecule (FITC, biotin, *dmGSC*) and the parental peptide (CL) were coupled/built up through the N^α and N^ε amino groups of a “bifunctional” Fmoc-Lys(Dde)-OH anchored on the resin.

The NMR spectra of aqueous solutions of biotin-Lys(CL) and *dmGSC*-Lys(CL) were completely assigned using the sequential assignment strategy in 2D TOCSY and NOESY experiments. Comparison with the parent molecule CL, revealed minor chemical shift changes in the direct vicinity of the added groups. Based on the NMR data, the attached moieties have not induced changes to the bioactive CL structure. The study of the CL-FITC derivative is more challenging due to its low solubility.

Finally, the *dmGSC*-Lys(CL) derivative was successfully radiolabeled with ^{99m}Tc and the stability of the ^{99m}Tc complex was assessed over time in its synthesis reaction mixture and in plasma. The ^{99m}Tc-radiolabeled derivative was subsequently administered to Swiss Albino mice in order to determine the biodistribution of CL in the living organism and its route of excretion. Our results demonstrated that the radiolabeled peptide was rapidly cleared from the blood pool and was excreted via the urinary system, whereas brain uptake was about 0,6% injected dose/g at 2 min post injection, which is an interesting result for a labeled peptide and merits further investigation.

References

- [1] Chiba, T.; Yamada, M.; Hashimoto, Y.; Sato, M.; Sasabe, J.; Kita, Y.; Terashita, K.; Aiso, S.; Nishimoto, I.; Matsuoka, M. *J. Neurosci.* **2005**, *25*, 10252.
- [2] Chiba, T.; Nishimoto, I.; Aiso, S.; Matsuoka, M. *Mol. Neurobiol.* **2007**, *35*, 55.

New bradykinin analogues modified in their C-terminus with D-pipecolic acid

Małgorzata Śleszyńska¹, Dariusz Sobolewski¹, Ilona Born²,
Bernard Lammek¹, Adam Prahl¹

¹Institute of Organic Synthesis, Faculty of Chemistry, University of Gdańsk, Gdańsk, Poland; ²Institute of Biochemistry and Biotechnology, Martin-Luther University, Halle-Wittenberg, Germany

E-mail: bernard@chem.univ.gda.pl

Introduction

Kinins, such as the nonapeptide bradykinin, are important mediators of various physiological and pathophysiological responses including inflammatory disease, asthma, rhinitis, cell division, pain, vascular permeability, allergic reactions, pathogenesis of septic and endotoxic shock. There are two types of receptors for kinins, known as B₁ and B₂. B₂ receptors are constitutively expressed in wide variety of cells and required entire BK sequence for recognition, while B₁ receptors have normally very limited expression and respond to [desArg⁹]BK. B₁ receptors gene is turned on following either tissue damage or inflammation [1, 2]. Accumulated evidence indicates that most of the clinically relevant effects of BK are functions of B₂ receptors this being the reason why research on their antagonists is a topic of great interest.

In our previous study we described the synthesis and some pharmacological properties of four new analogues of bradykinin (BK), designed by substitution of position 7 or 8 of the known [D-Arg⁰,Hyp³,Thi^{5,8},D-Phe⁷]BK antagonist with L-pipecolic acid (L-Pip) (both analogues were also prepared in N-acylated form with 1-adamantaneacetic acid (Aaa)) [3]. Our results showed that presence of L-Pip in position 7 slightly increased antagonistic potency in the blood pressure test, but it turned the analogue into an agonist in the rat uterus test. Replacement of Thi by L-Pip in position 8 also enhanced antagonism in the rat pressure test but preserved the antagonism in the rat uterus test.

Results and Discussion

In the present study we continue our previous investigations to find structural requirements which in the case of BK analogues result in high B₂ antagonistic activity. Several new bradykinin analogues modified in their C-terminus with D-pipecolic acid were synthesized. All the peptides were obtained by the solid-phase method on a Symphony Multiple Peptide Synthesizer (Protein Technologies Inc., USA) using the Fmoc-strategy and starting from Fmoc-Arg(Pbf)-Wang resin (capacity 0.4 mmol/g, 25 µmol scale). The crude peptides were desalted on a Sephadex G-15 column, and purified by RP-HPLC. The purity of the peptides was checked using analytical HPLC. MALDI TOF mass spectrometry (molecular ion) was used to confirm the identity of the pure products. Biological activity of the compounds was assessed in the *in vitro* rat uterus test [4] and the *in vivo* rat blood pressure test [5]. Pharmacological data of four previously synthesized (III-VI) and four new analogues (VII-X) together with those of Stewart's antagonist and its acylated version (I, II - used as a positive controls) are summarized in Table 1.

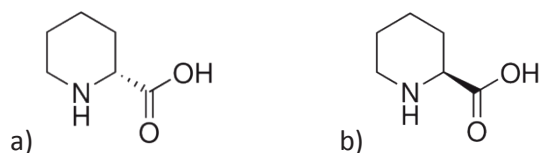


Figure 1. Structures of *L*-pipecolic acid (*L*-Pip) - (a) and *D*-pipecolic acid (*D*-Pip) - (b).

Analogue	pA ₂ or % of BK activity	pressure test	
		ED ₂₀ [μg/min]	ED ₅₀ [μg/min]
[D-Arg ⁰ , Hyp ³ , Thi ^{5,8} , D-Phe ⁷]-BK (I)	6.88±08	1.73±0.4	124.00±27.00
Aaa[D-Arg ⁰ , Hyp ³ , Thi ^{5,8} , D-Phe ⁷]-BK (II)	7.43±0.11	0.84±0.09	13.94±1.69
[D-Arg ⁰ , Hyp ³ , Thi ^{5,8} , L-Pip ⁷]-BK (III)	18.3 (%)	0.23±0.04	44.98±0.64
Aaa[D-Arg ⁰ , Hyp ³ , Thi ^{5,8} , L-Pip ⁷]-BK (IV)	0.45 (%)	1.30±0.46	4456.38±1575.57
[D-Arg ⁰ , Hyp ³ , Thi ⁵ , D-Phe ⁷ , L-Pip ⁸]-BK (V)	7.43 ± 0.26	0.10±0.02	11.35±1.76
Aaa[D-Arg ⁰ , Hyp ³ , Thi ^{5,8} , D-Phe ⁷ , L-Pip ⁸]-BK (VI)	7.99 ± 0.25	0.16±0.03	28.99±6.15
[D-Arg ⁰ , Hyp ³ , Thi ^{5,8} , D-Pip ⁷]-BK (VII)	1.1 (%)	week antagonist	
Aaa[D-Arg ⁰ , Hyp ³ , Thi ^{5,8} , D-Pip ⁷]-BK (VIII)	0.09 (%)	week antagonist	
[D-Arg ⁰ , Hyp ³ , Thi ⁵ , D-Phe ⁷ , D-Pip ⁸]-BK (IX)	0	4.36±1.92	2343.98±31.27
Aaa[D-Arg ⁰ , Hyp ³ , Thi ⁵ , D-Phe ⁷ , D-Pip ⁸]-BK (X)	0	1.32±0.13	3960.14±200.27

Table 1. Pharmacological data of BK analogues

In the rat uterus test, the analogues did not display antagonistic activity. Nevertheless, their agonistic potency (related to the activity of BK) is reduced from 1,1% (analogue VII) to 0% (analogues – IX, X). In the blood pressure assay, our compounds exhibited weak (analogues VII, VIII) or moderate (analogues IX, X) antagonistic activity, but only in lower doses. What is interesting all the new compounds inhibited the vasodepressor response in the rat blood pressure test (antagonistic activity) and in the same time they are completely inactive in the rat uterus test. In comparison to analogues modified with L-Pip its antagonistic activity against blood vessels is much lower.

Acknowledgments

This work was supported by the University of Gdańsk (DS/8453-4-0169-2).

References

- [1] Bhoola, K.D.; Figueroa, C.D.; Worthy, K. *Pharmacol. Rev.* **1992**, *44*, 1.
- [2] Regoli, D., Barabe, J. *Pharmacol. Rev.* **1980**, *32*, 1.
- [3] Śleszyńska, M.; Sobolewski, D.; Kwiatkowska, A.; Wierzba, T.; Slaninová, J.; Zabrocki, J.; Katarzyńska, J.; Prah, A. *Acta. Biochim. Pol.* **2009**, *56*, 641.
- [4] Holton, P. *Br. J. Pharmacol.* **1948**, *3*, 328.
- [5] Labudda, O.; Wierzba, T.H.; Sobolewski, D.; Śleszyńska, M.; Slaninová, J.; Prah, A. *Acta Biochim. Pol.* **2007**, *54*, 193.

Phylogenetic diversity of C-terminally expressed heptapeptide unit in opioid precursor polypeptide proenkephalin A

A. Magyar¹, E. Bojnik², E. Boynik³, M. Corbani⁴, F. Babos¹,

A. Borsodi², S. Benyhe²

¹*Research Group of Peptide Chemistry, Hungarian Academy of Sciences, Eötvös L. University, Pázmány P. s. 1/A, H-1117 Budapest, Hungary;* ²*Institute of Biochemistry, Biological Research Centre, HAS, Szeged, Hungary;* ³*University of Prishtina, Department of Mathematics and Informatics, Prizren, Kosovo;* ⁴*Institut of Functional Genomics, University of Montpellier, Montpellier, France*

e-mail:magyar@chem.elte.hu

Introduction

The heptapeptide, Met-enkephalin-Arg6-Phe⁷ (MERF) with the sequence of YGGFMRF is a potent endogenous opioid located at the C-terminus of proenkephalin-A (PENK), the common polypeptide precursor of Met- and Leu-enkephalin. Our systematic bioinformatic survey revealed considerable sequence polymorphism at the heptapeptide region of different PENK prepeptides among 56 vertebrate animals.

The aim of the study was therefore to collect all currently available PENK encoded C-terminal heptapeptide sequences from various species. The bioinformatically identified sequence variants were chemically synthesized and studied further in biochemical pharmacological assays. Here we describe and compare the bioactivity pattern of four distinct peptides that occur naturally in vertebrates and correspond to the most common mammalian heptapeptide enkephalin sequence MERF.

Results and Discussion

Peptides were synthesized by automated SPPS equipment (SYRO, Multisynth), using Fmoc/tBu strategy on 2-chloro-trityl resin with double-coupling protocol. The crude products were purified by RP-HPLC. The structure of the peptides was proved by electron spray ionization (ESI) mass spectrometry.

Inbred Wistar rats (250–300 g body weight) and guinea pigs (R9 strain) were housed in the local animal house of the Biological Research Center (BRC, Szeged, Hungary). All binding assays were performed at 25 °C for 30 min in 50 mM Tris-HCl buffer (pH 7.4) in a final volume of 1 ml, containing 1 mg BSA and 0.2–0.4 mg/ml membrane protein. Rat brain membrane fractions (~10 µg of protein/sample) were incubated at 30°C for 60 min in Tris-EGTA buffer (50 mM Tris-HCl, 1 mM EGTA, 3 mM MgCl₂, 100 mM NaCl, pH 7.4) containing [³⁵S]GTPγS (0.05 nM) and increasing concentrations (10⁻⁹ to 10⁻⁵ M) of the compounds tested in the presence of 30 µM GDP in a final volume of 1 ml. Total binding was measured in the absence of the test compound, non-specific binding was determined in the presence of 10 µM label free GTPγS and subtracted from total binding to calculate the specific binding.

Ligand-regulated internalization of hMOP-EGFP receptors stably were expressed in HEK293 cells. Each compound was added at the dose of 1 μ M for 1 h at 24 °C. The MOPr-EGFP was revealed by imaging with Olympus Cell-R fluorescent microscopy (objective 20x) and appeared to be concentrated in endogenous vesicles following internalization.

All data were expressed as means \pm standard error of the mean of n experiments. Curve fitting was performed using PRISM 4.0 (GraphPad Software Inc., San Diego, U.S.A.).

Four orthologous heptapeptides with single or double amino acid replacements were identified among 15 animal species, such as YGGFMGY (zebrafish), YGGFMRY (newt), YGGFMKF (hedgehog tenrek) and YGGFMRI (mudpuppy). Each novel heptapeptide, together with the mammalian consensus MERF sequence and Met-enkephalin, were subjected to functionality studies, using radioligand binding competition and G-protein activation assays in rat brain membranes. Equilibrium binding affinities changed from good to modest as measured by receptor type selective [³H]opioid radioligands. The relative affinities of the heptapeptides reveal slight mu-receptor (MOP) preference over the delta-receptors (DOP). [³⁵S]GTP_S assay, which measures the agonist-mediated G-protein activation, has demonstrated that all the novel heptapeptides were also potent in stimulating the regulatory G-proteins. All peptides were effective in promoting the agonist induced internalization of the green fluorescence protein-tagged human mu-opioid receptor (hMOP-EGFP) stably expressed in HEK293 cells. Thus, the C-terminally processed PENK heptapeptide orthologs exhibited satisfactory bioactivities, moreover they represent further members of the so called „natural combinatorial neuropeptide library” emerged by evolution [1].

Phylogenetic neuropeptide libraries, defined here as a collection of mutationally different species variants of orthologous and paralogous peptide sequences, represent the natural molecular diversity of the neuropeptides. Such libraries can provide a wide range of structural information establishing comparative functional analyses. Since DNA sequencing data are rapidly increasing, more development in the natural peptide library approach is expected.

Acknowledgments

This work was supported by grants from the National Scientific Research Fund Hungary (OTKA CK-78566) and A. Magyar is grateful for the support from the Foundation for Hungarian Peptide and Protein Research, Budapest, Hungary.

References

- [1] Bojnik, E.; Boynik, E.; Corbani, M.; Babos, F.; Magyar, A.; Borsodi, A.; Benyhe, S. *Neuroscience* **2011**, *178*, 56–67.

Searching diagnosable disease using plasma kisspeptin levels as a biomaker

Fumihiko Katagiri, Motoyoshi Nomizu

Tokyo University of Pharmacy and Life Sciences, Hachioji, Japan

E-mail:katagiri@toyaku.ac.jp

Introduction

Kisspeptin (metasitin), the product of the *KiSS1* gene, is an endogenous ligand for orphan receptor GPR54 [1]. *KiSS1* is highly expressed in human brain, placenta, testis, kidney, pancreas and intestine. Kisspeptin was reported to inhibit the lung metastasis of GPR54-overexpressed melanoma cells [1]. Today, reports about several cancers are there that investigate relationship between *KiSS1* expression and clinical state or prognosis. Peripheral administration of kisspeptin strongly promotes gonadotropin secretion [2]. Kisspeptin is thought to play important role for GnRH secretion. Furthermore, plasma kisspeptin levels increase with progression of pregnancy, and decline to the nonpregnant level by parturition [3]. The purpose of this study is that we identify diagnosable disease by plasma kisspeptin levels as a biomarker.

Results and Discussion

Subjects were patients affected diseases that were thought to be related with kisspeptin (*e.g.* some cancers, perinatal complication, hypogonadism). We measured their plasma kisspeptin-like immunoreactive substance (LI) levels using enzyme immunoassay [4], and analyzed the relationship between clinical findings and plasma kisspeptin-LI levels. We measured plasma kisspeptin-LI levels in 33 pancreatic cancer patients, 26 pregnancy-induced hypertension (PIH) patients, 6 gestational diabetes mellitus (GDM) patients, 76 polycystic ovary syndrome (PCOS) patients, 70 infertile (IF) patient, 3 hypogonadism patients, 2 organic brain disorder patient, 2 adolescent boys, a male menopause, and healthy subjects.

Plasma kisspeptin-LI levels in pancreatic cancer patients were significantly high compared with healthy subjects ($P<0.001$). Among the pancreatic cancer patients, the plasma kisspeptin-LI levels in patients whose tumor was invaded out of pancreas and in unresectable case were high. Considering that kisspeptin has anti-metastasis activity [1] and that *KiSS1* expression in pancreatic cancer is lower than normal tissue [5], the excess kisspeptin in pancreatic cancer patients may secret not from tumor, but from somewhere normal tissue. Plasma kisspeptin-LI levels in healthy pregnant women (HPW) ($P<0.001$, $R^2=0.165$) and PIH ($P=0.023$, $R^2=0.206$) were positively correlated with gestation week. Plasma kisspeptin-LI levels in 3rd trimester HPW were significantly higher than 1st or 2nd trimester ($P<0.001$). It is suggested that kisspeptin is produced at syncytiotrophoblast participates in suppression of villous cell proliferation in placental villus. At early gestation, villous cells proliferation is active, while not at late gestation. The plasma kisspeptin-LI levels were indicated to be correlated negatively with villous cells proliferation. Serum kisspeptin levels in PIH were significantly lower than those in HPW ($P<0.001$). Farina *et*

al. reported that the expression of circulating mRNA for *KiSS1* gene of PIH patients was decreased [6], supporting the results in this study. Although plasma kisspeptin-LI levels in GDM were not significantly correlated with gestation week ($P=0.518$, $R^2=0.025$), they were significantly higher than those in HPW ($P<0.001$). Plasma kisspeptin-LI levels those in IF were significantly lower than HW ($P<0.001$), and those in PCOS were significantly lower than HW ($P<0.001$) and IF ($P=0.020$). At the upstream of kisspeptin neuron, leptin, which is related to feeding, obesity, and suppression of follicular growth, plays important role [7]. Plasma kisspeptin-LI levels in all case of central nervous system dysfunction were in the normal range (4.0-16.5 fmol/mL), before any treatment. The plasma follicle stimulation hormone (FSH) and luteinizing hormone (LH) in the two congenital hypogonadism patients were not detected before treatment. Several hormone-loading tests (thyroid releasing hormone, gonadotropin-releasing hormone (GnRH), corticotropin-releasing hormone gonadotropin-releasing factor, human chorionic gonadotropin, *etc.*) indicated the hypothalamic hypogonadism. The plasma kisspeptin levels represented low value at all times. The hCG+hMG therapy (human chorionic gonadotropin, 150 IU; human menopausal gonadotropin, 5,000 IU /weekly s.c.) made plasma sex steroid concentration recovery, but no change in their plasma kisspeptin-LI levels.

Plasma kisspeptin levels are different kinetics depending on kinds of cancer (*e.g.* hepatic, breast, bladder, esophageal, and pancreatic cancer). Setting the threshold levels can screen for early diagnosis. The plasma kisspeptin levels are expected to be a good biomarker for perinatal complication, however, may be difficult to use for central nervous system dysfunction such as hypogonadism. GnRH cannot be a biomarker for the hypogonadism, because GnRH is subject to degradation, and generally does not exist in circulating blood. Kisspeptin is there in circulating blood, and stably measurable by our enzyme immunoassay. The kisspeptin is expected to be a biomarker, replaced with GnRH.

Acknowledgments

This study was supported by Grant-in-Aid for Scientific research from the Ministry of Education, Culture, Sports, Science and Technology of Japan (22790172).

References

- [1] Ohtaki, T.; Shintani, Y.; Honda, S.; Matsumoto, H.; Hori, A.; Kanehashi, K.; Terao, Y.; Kumano, S.; Takatsu, Y.; Masuda, Y.; Ishibashi, Y.; Watanabe, T.; Asada, M.; Yamada, T.; Suenaga, M.; Kitada, C.; Usuki, S.; Onda, H.; Nishimura, O.; Fujino, M. *Nature* **2001**, *411*, 613-617.
- [2] Matsui, H.; Takatsu, Y.; Kumano, S.; Matsumoto, H.; Ohtaki, T. *Biochem. Biophys. Res. Commun.* **2004**, *320*, 383-388.
- [3] Horikoshi, Y.; Matsumoto, H.; Takatsu, Y.; Ohtaki, T.; Kitada, C.; Usuki, S.; Fujino, M. *J. Clin. Endocrinol. Metab.* **2003**, *88*, 914-919.
- [4] Katagiri, F.; Tomita, K.; Oishi, S.; Takeyama, M.; Fujii, N. *J. Pept. Sci.* **2007**, *13*, 422-429.
- [5] Masui, T.; Doi, R.; Mori, T.; Toyoda, E.; Koizumi, M.; Kami, K.; Ito, D.; Peiper, S. C.; Broach, J. R.; Oishi, S.; Niida, A.; Fujii, N.; Imamura, M. *Biochem. Biophys. Res. Commun.* **2004**, *315*, 85-92.
- [6] Farina, A.; Sekizawa, A.; Purwosunu, Y.; Rizzo, N.; Banzola, I.; Concu, M.; Morano, D.; Giommi, F.; Bevini, M.; Mabrook, M.; Carinci, P.; Okai, T. *Prenat. Diagn.* **2006**, *26*, 1115-1120.
- [7] Hausman, G. J.; Barb, C. R. *Endoc. Dev.*, **2010**, *19*, 31-44.

Synthesis and biological activity of cyclic peptides from cyanobacteria

**F. Boyaud, I. Bonnard, B. Banaigs, A. Witczak, F. Gattacceca,
N. Inguibert**

*Laboratoire de Chimie des Biomolécules et de l'Environnement-EA4215 Centre de
Phytopharmacie, 58 avenue Paul Alduy 66860 Perpignan*

E-mail: nicolas.inguibert@univ-perp.fr

Introduction

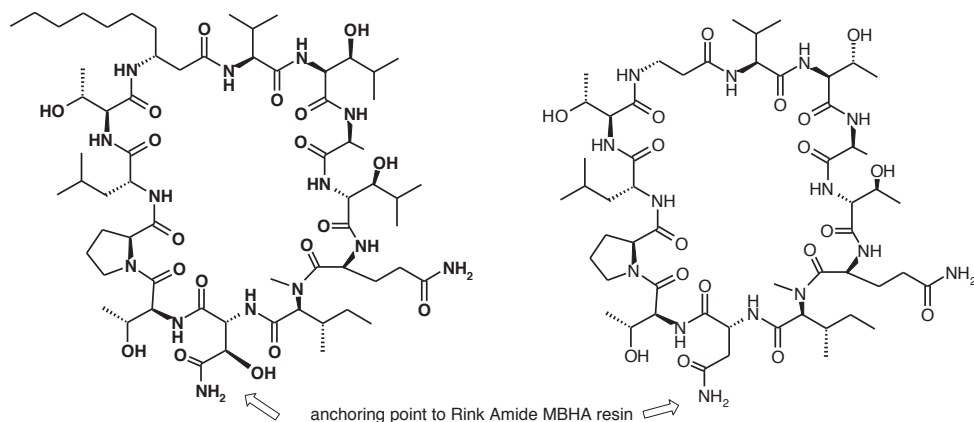
The marine environment contains a wide variety of organisms that produce many secondary metabolites, including cyclic peptides. Our team has isolated several cyclic lipopeptides from the cyanobacteria *Anabaena torulosa* known as laxaphycins [1]. The structural originality of those peptides lies on the presence of five non-proteinogenic amino acids: hydroxyleucine [2], hydroxyasparagine, N-methyl-isoleucine, D-leucine and the 3-aminodecanoic acid [3].

Laxaphycine B is the main peptide of the laxaphycin family and was characterized by NMR and MS/MS. The stereochemistry of non-natural amino acids was determined by Marfey method. Laxaphycin B was evaluated on different human tumors cell lines in comparison to cisplatin, underlining its cytotoxic potential. In order to confirm its structure and to study the structure/activity relationships of laxaphycin B, we undertook its synthesis.

Results and Discussion

We have developed a strategy to obtain the laxaphycin B based on standard Fmoc solid phase peptide synthesis (SPPS). The method is based on the principle of "head-to-tail" cyclization which requires orthogonal protection for the C-terminus as well as anchoring the first amino acid of the peptide sequence by its side chain. So, our synthesis was realized through the linking of the carboxyl group side chain β -hydroxyaspartic acid to a Rink Amide MBHA LL resin to avoid aggregation issues during the chain elongation of this lipopeptide. The α -carboxyl group of aspartate is protected by the allyl protective group to allow the cyclisation. First, the linear peptide was synthesized using the Liberty One automatic synthesizer and using 2-(1H-7-azabenzotriazol-1-yl)-1,1,3,3-tetramethyluroniumhexafluorophosphate (HATU) as the coupling agent. The quality of coupling is appreciated by the UV monitoring. The cyclisation was performed after the cleavage of allyl protective group with $(\text{PdPh}_3)_4$ using diisopropylcarbodiimide (DIC)/oxyma. The use of oxyma allows for reducing the risk of racemization. After cleavage of the resin and all protective groups of the lateral chains, the cyclic peptide was obtained with a yield of 10% after purification. Several analogues were synthesized with success. In the first phase we synthesized one analogue of laxaphycin B where we had replaced all the non-proteinogenic amino acids with natural amino acids by keeping the stereochemistry of the α carbons (Scheme 1) Then, we progressively introduced each non-proteinogenic amino acid, then the hydrophobic side chain, followed by the

diastereoisomers of hydroxyleucines. To finalize the synthesis of laxaphycin B, we will introduce the recently synthesized N- α -Fmoc-aspartic acid α -allyl ester.



Scheme 1: Laxaphycin (on the left), an analogue (on the right)

Biological activity of analogues

Cytotoxicity assay of two analogues and the laxaphycin B were performed against the melanoma cancer cell line. These results showed the loss of activity of two analogs with IC₅₀ of 41,3 μ M and 42,6 μ M against 0,49 μ M for the laxaphycin B. We have observed that the non-proteinogenic amino acids and their particular spatial disposition confer to this cyclic peptide the ability to create interactions with its biological target. Other studies would have to be conducted in order to confirm if one or more non proteinogenic amino acids are important for the cytotoxic activity.

Acknowledgments

This work was supported by grants of ANR (ANR-2010-BLAN-1533-02), and of Perpignan University (BQR).

References

- [1] Bonnard, I.; Rolland, M.; Salmon, J.M.; Debiton, E.; Barthomeuf, C., Banaigs, B. *J. Med. Chem.* **2007**, *50*, 1266.
- [2] Hale, K.J.; Manaviazar, S.; Delisser, V.M. *Tetrahedron.* **1994**, *50*, 9181.
- [3] Buron, F.; Turck, A.; Ple, N.; Bischoff, L.; Marsais, F. *Tetrahedron Letters.* **2007**, *48*, 4327.

Synthesis and biological studies of 2-naphthylalanine modification of Cyclolinopeptide A

Maria Kinas^a, Krzysztof Kierus^{a,c}, Krzysztof Huben^a, Michał Zimecki^b,
Stefan Jankowski^a, Janusz Zabrocki^{a,c}

^a Institute of Organic Chemistry, Lodz University of Technology, Zeromskiego Str. 116
Łódź, Poland; ^b Institute of Immunology and Experimental Therapy of Polish Academy of
Sciences, R. Weigla 12, 53-114 Wrocław, Poland; ^c Peptaderm inc., Krakowskie
Przedmieście Str. 13, Warsaw, Poland

E-mail: krzysztof.kierus@p.lodz.pl

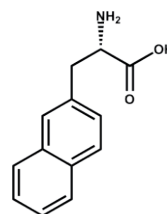
Introduction

Cyclolinopeptide A (CLA), a nonapeptide with a sequence of *cyclo*(Pro-Pro-Phe-Phe-Leu-Ile-Ile-Leu-Val) was first isolated in 1959 from the sediments deposited from crude flaxseed oil [1]. This peptide exhibits potent immunosuppressive activity [2], inhibitory activity towards calcium-dependent activation of T-lymphocyte cell division [3], as well as antimalarial activity [4].

It was postulated that the edge-to-face orientation as well as the distance between Phe aromatic rings is important for the biological activity [5]. To elucidate if the edge-to-face orientation of the two Phe residues of CLA influences its biological activity, analogues with one or both Phe residues substituted by N-benzylglycine were synthesized [6]. Also analogues where one or both aromatic rings of Phe side chain were substituted at position 4 with nitro, amino and acetamido group [7].

In this communication we present linear **1-3** and cyclic **4-6** CLA analogues in which phenylalanine residues in positions 3, 4 and 3 & 4 have been replaced with (2-naphthyl)alanine (**2-Nal**) **7**.

- (1) H-Ile⁶-Ile⁷-Leu⁸-Val⁹-Pro¹-Pro²-Phe³-(2-Nal)⁴-Leu⁵-OH
- (2) H-Ile⁶-Ile⁷-Leu⁸-Val⁹-Pro¹-Pro²-(2-Nal)³-Phe⁴-Leu⁵-OH
- (3) H-Ile⁶-Ile⁷-Leu⁸-Val⁹-Pro¹-Pro²-(2-Nal)³-(2-Nal)⁴-Leu⁵-OH
- (4) c(Pro¹-Pro²-Phe³-(2-Nal)⁴-Leu⁵-Ile⁶-Ile⁷-Leu⁸-Val⁹-)
- (5) c(Pro¹-Pro²-(2-Nal)³-Phe⁴-Leu⁵-Ile⁶-Ile⁷-Leu⁸-Val⁹-)
- (6) c(Pro¹-Pro²-(2-Nal)³-(2-Nal)⁴-Leu⁵-Ile⁶-Ile⁷-Leu⁸-Val⁹-)



7

Results and Discussion

The linear CLA analogs **1-3** were synthesized in 0.2 mmol scale by the manual solid-phase method using chloromethylated Merrifield resin as a solid support. All N-Boc-protected amino acids were obtained from commercial sources. The yields of obtained linear analogues were 77-98% and purity 68-99%. Peptides for biological assays were purified by preparative HPLC as described below for the cyclic analogs.

The crude linear peptides were cyclized by means HOAt/HATU/DIPEA in DMF adding slowly (during 21h) solution of linear peptide and coupling reagents to reaction vessel by syringes pump, to avoid the dimer formation [8]. After evaporation of solvent, crude cyclic peptides **4-6** were purified by preparative reversed-phase HPLC on Kromasil C8 column (21.2x250mm) with a linear gradient 60-100%B 15 min. at a flow rate of 20 ml/min. The yields of the cyclizations calculated for purified compounds were 6-20% and purity was in range 97-99%.

Both series of peptides (linear and cyclic) were tested for biological activity including toxicity of the compounds, effects of the compounds on PHA-induced PMBC proliferation and effects of the peptides on LPS-induced TNF α production by human whole blood cultures. All compounds were devoid of toxicity against PBMC at 1-100 μ g/ml concentration range and did not demonstrate anti-proliferative properties. Only the cyclic peptides were found to inhibit LPS-induced TNF α production and the inhibitory actions for 1, 10 and 100 μ g/ml concentrations were as following: **4** (16, 35 and 47%), **5** (13, 40 and 62%) and **6** (15, 27 and 26%).

Considering the range and degree of TNF α inhibition and lack of toxicity, peptide **5** might be interesting for further research in the in vivo models of inflammation.

Acknowledgments

This work was partially supported by Ministry of Science and Higher Education grand no. N N405 424239

References

- [1] Kaufmann, H. P.; Tobschirbel, A. *Chem. Ber.* **1959**, *92*, 2805-2809.
- [2] Wieczorek, Z.; Bengtsson, B.; Trojnar, J.; Siemion, I. Z. *Pept. Res.* **1991**, *4*, 275-283.
- [3] Gaymes, T. J.; Cebrat, M.; Siemion, I. Z.; Kay, J. E. *FEBS Lett.* **1997**, *418*, 224-227.
- [4] Bell, A.; McSteen, P. M.; Cebrat, M.; Picur, B.; Siemion, I. Z. *Acta Pol. Pharm. Drug Res.* **2000**, *57*, 134-136.
- [5] Zubrzak, P.; Leplawy, M. T.; Kowalski, M. L.; Szkudlińska, B.; Paneth, P.; Silberring, J.; Suder, P.; Zabrocki, J. *Journal of Physical Organic Chemistry* **2004**, *17*, 625-630.
- [6] Leplawy, M. T.; Zubrzak, P.; Olejniczak, B.; Paneth, P.; Smoluch, M.; Silberring, J.; Kowalski, M. L.; Szkudlińska, B.; Grochulska, E.; Zabrocki, J. *Peptides 2000 Proceedings 26th European Peptide Symposium* **2001**, 859-860.
- [7] Kierus, K.; Ciupińska, K.; Waśkiewicz, M.; Grabowska, M.; Kaczmarek, K.; Huben, K.; Jankowski, S.; Zimecki, M.; Zabrocki, J. *J. Pept. Sci.* **2010**, *16*, 59.
- [8] Li, P.; Roller, P. P. *Curr. Top. Med. Chem.* **2002**, *2*, 325-341.

Synthesis and conformational analysis of linear, dimeric and cyclic analogues of the C-terminal hexapeptide of Neurotensin

Constantinos Potamitis¹, Panagiotis Zoumpoulakis¹, Revekka Exarchakou², Vlassios Karageorgios³, Vassiliki Mertziani², Aikaterini Spyridaki³, George Liapakis³, Paul Cordopatis², Vassiliki Magafa^{2*}

¹Laboratory of Molecular Analysis, Institute of Organic and Pharmaceutical Chemistry, National Hellenic Research Foundation, GR-11635 Athens, Hellas; ²Laboratory of Pharmacognosy and Chemistry of Natural Products, Department of Pharmacy, University of Patras, GR-26500 Patras, Hellas; ³Department of Pharmacology, Faculty of Medicine, University of Crete, GR-71003 Heraklion, Hellas
E-mail: exarchakour@upatras.gr; magafa@upatras.gr

Introduction

Neurotensin [(pGlu-Leu-Tyr-Glu-Asn-Lys-Pro-Arg-Arg-Pro-Tyr-Ile-Leu), NT] is a tridecapeptide originally isolated from bovine hypothalamus and later from intestines which displays a wide spectrum of biological actions [1]. The physiological and biochemical actions of NT are mediated through binding to NT receptors (NTS1, NTS2 & NTS3) [2]. All three receptors recognize the same C-terminal hexapeptide fragment of NT [NT(8-13)], which corresponds to the shorter fragment of NT that maintains full biological activities. Although NT(8-13) possesses high receptor binding affinity, it is rapidly degraded by peptidase action. Therefore, it is important to synthesize analogues with stabilized bonds against metabolic deactivation which do not lose binding affinity. Based on literature data and in continuation of our previous work [3], we herein report the synthesis of 5 linear, 3 cyclic and 2 dimeric analogues of NT(8-13) with modifications in the basic structure needed for high affinity binding in order to improve the metabolic stability. The analogues contain D-Arginine or L-Lysine in position 8 or 9, D-Tyrosine(Ethyl) [D-Tyr(Et)] or D-1-Naphthylalanine [D-1-Nal] in position 11 and D-*tert*-Glycine [D-Gly(Bu^t)] in position 12. NMR and Molecular Dynamic simulations have been employed to study the conformational properties of selected peptide analogues in respect to the putative bioactive conformation of the C-terminal region of NT.

Results and Discussion

All analogues shown in **Table 1** were synthesized manually on the 2-chlorotrityl-chloride resin by using standard coupling procedures and Fmoc/Bu^t strategy [4]. The overall yield of the syntheses of the NT analogues was in the range 55-85% (calculated on the amount of linker initially coupled to the resin). Finally, ESI mass spectrometry revealed that the purified peptides were the desired products and their purity determined by analytical HPLC was higher than 98%. A series of NMR spectra including ¹H, 2D TOCSY and 2D NOESY were recorded on a Varian 600 MHz spectrometer in order to elucidate their structure and calculate intramolecular distances from NOEs.

Table 1: Physicochemical properties of the synthesized NT analogues.

Code	Analogues	Yield (%)	HPLC* t_R (min)	TLC**	
				R _{fA}	R _{fB}
NT-1.	cyclo [D-Arg ⁸ , Lys ⁹ , D-Tyr(Et) ¹¹] NT(8-13)	55	11.97	0.56	0.63
NT-2.	cyclo [Lys ⁸ , D-Arg ⁹ , D-Tyr(Et) ¹¹] NT(8-13)	61	11.13	0.54	0.67
NT-3.	cyclo [Lys ⁸ , D-Arg ⁹ , D-Tyr(Et) ¹¹] ₂ NT(8-13)	68	12.92	0.29	0.28
NT-4.	Lys ⁸ [D-Arg ⁹ , D-1-Nal ¹¹] ₂ NT(8-13)	71	14.38	0.59	0.55
NT-5.	[Lys ⁸ , D-Arg ⁹ , D-1-Nal ¹¹] NT(8-13)	82	12.44	0.41	0.73
NT-6.	[D-Arg ⁸ , Lys ⁹ , D-1-Nal ¹¹] NT(8-13)	79	12.39	0.32	0.28
NT-7.	Lys ⁸ [D-Arg ⁹ , D-Tyr(Et) ¹¹] ₂ NT(8-13)	76	12.46	0.55	0.61
NT-8.	[Lys ⁸ , D-Arg ⁹ , D-Tyr(Et) ¹¹ , D-Gly(Bu) ¹²] NT(8-13)	85	11.75	0.53	0.68
NT-9.	[Lys ⁸ , D-Arg ⁹ , D-1-Nal ¹¹ , D-Gly(Bu) ¹²] NT(8-13)	81	12.11	0.54	0.70
NT-10.	[D-Arg ⁸ , Lys ⁹ , D-Gly(Bu) ¹²] NT(8-13)	83	9.76	0.38	0.41

* Linear gradient from 5 to 85% acetonitrile (0.1% TFA) for 30 min, Nucleosil 100 C₁₈ column

** A) butan-1-ol/water/acetic acid/pyridine (4/1/1/2, v/v), B) butan-1-ol/water/acetic acid (4/5/1 v/v, upper phase)

Several efforts have been made to reveal the structure of NT focusing on the C-terminal hexapeptide as it was shown that this region is sufficient for receptor binding and function. Structural information based on previous NMR and molecular modeling experiments, demonstrates that the NT(8-13) fragment presents an extended but slightly bend conformation similar to a β -strand with the important residues of NT (Arg⁹, Try¹¹, Leu¹³) located in space, at the same side of the backbone [5]. Low energy conformers of cyclic peptide NT-2 were determined with MD simulations, using the experimental distances derived from the NOESY spectra. Superimposition between NT-2 and C-terminal part of NT revealed a similar backbone bend of residues 9-12, while Arg⁹ and Leu¹³ side chains adopt the same orientation. A difference is observed with D-Tyr(Et)¹¹ side chain which is oriented at the opposite direction compared to Tyr¹¹.

Acknowledgments

The authors thank the University of Patras for the K. Karatheodoris Research Grant (to V. Magafa_2010_D.156). Part of this work was implemented under the FP7 Regional Potential project “Advancement of Research Capability for the Development of New Functional Compounds” (ARCADE).

References

- [1] Carraway, R.; Leeman, E. S. *J. Biol. Chem.* **1973**, *248*, 6854.
- [2] Vincent, J. P.; Mazella, P.; Kitabgi, P. *Trends Pharmacol. Sci.* **1999**, *20*, 302.
- [3] Exarchakou, R.; Magafa, V.; Manessi-Zoupa, E.; Assimomytis, N.; Georgiadou, M.; Venihaki, M.; Varvounis, G.; Liapakis, G.; Cordopatis, P. In “Peptides 2010”. (M. Lebl, M. Meldal, K. Jensen and T. Hoeg-Jensen, Eds.), Prompt Scientific Publishing, San Diego, **2010**, pp. 446-447.
- [4] Fields, B. G.; Noble, L., R. *Int J Pept. Prot. Res.* **1990**, *35*, 161.
- [5] Coutant, J.; Curmi, P. A.; Toma, F.; Monti, J-P. *Biochemistry*, **2007**, *46*, 4646.

Aggregation and cytotoxic properties of hIAPP17-29 and rIAPP17-29 fragments: A comparative study with the respective full-length parent polypeptides

Flora Marianna Tomasello,^a Alessandro Sinopoli,^b Francesco Attanasio,^b Tiziana Campagna,^b Giuseppe Pappalardo*^b

^a*International PhD Program in Neuropharmacology, University of Catania, Catania, Italy;*

^b*CNR-Institute of Biostructure and Bioimaging, Catania, Italy*

E-mail: giuseppe.pappalardo@cnr.it

Introduction

The onset of type II diabetes mellitus (T2DM) coincides with the deposition of fibrillar material in the islet of Langerhans in the pancreas which is a clinical hallmark of more than 95% of patients suffering this disease [1]. The main component of the pancreatic amyloid deposits is a 37-residues polypeptide hormone called Islet Amyloid Polypeptide (IAPP) or amylin [2]. IAPP from rodents (rIAPP) differs from the human polypeptide at six positions all occurring between residues 17 to 29. Proline substitutions in this region prevent the adoption of a β -sheet conformation by the rIAPP amino acid sequence. The 17–29 region is important because it possesses: 1) the minimum amyloidogenic sequence 23–27 (NFGAIL) found in the human sequence, 2) positions 28–29 in which two prolines of the rat sequence replace two serines in the human one; 3) position 18 at which arginine in the rat sequence is replaced by a histidine in the human sequence. Both hIAPP17-29 and rIAPP17-29 have been shown to recapitulate most of the structural properties of the respective full-length parent polypeptides [3].

Results and Discussion

Far-Uv CD spectroscopy was used to monitor the peptide conformational changes associated with fibril formation. The experiments were carried out at different pH values to verify that, in analogy to what reported for the full-length hIAPP, the protonation state of the His18 imidazole side chain can modulate the aggregation propensity of hIAPP17-29. CD spectra recorded at pH 7.0 (Figure 1A) exhibited an evident conformational polymorphism and a transition from a random coil state to β -sheet peptide structure was observed. Such an occurrence strongly indicates that at this pH value the peptide chain possesses a marked tendency toward self assembly. On the contrary, at pH 4.0 the peptide remains in a random coil conformation during the time course of the experiment while at pH 8.0 hIAPP 17-29 rapidly aggregates and precipitates out from the solution (not shown). Concerning the rat variants, the CD spectra did not changed during the time, which is in agreement with the accepted notion that either full-length rIAPP1-37 or rIAPP17-29 are not prone to aggregation (not shown).

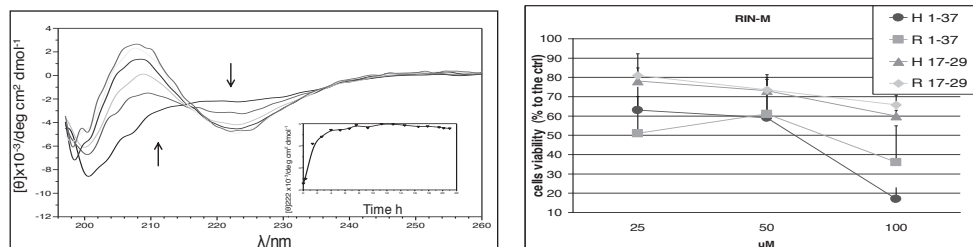


Figure 1. A: CD spectra hIAPP 17-29 pH7, B: MTT assay

The cytotoxic potential of our peptides was also studied by different approaches. Our data suggest that peptides corresponding to the 17-29 sequence of either hIAPP or rIAPP, as found for both 1-37 hIAPP and 1-37 rIAPP, are able to induce cell dysfunctions starting with the disruption of the mitochondrial activity. This means that the cytotoxic potential of the non- β -sheet-forming rat sequences rIAPP1-37 and rIAPP17-29, is comparable to that one of the corresponding human sequences. Similar results were recently reported by Magzoub and Miranker who showed that rIAPP, like hIAPP, is cytotoxic thereby suggesting that β -sheet formation is not a prerequisite for cytotoxicity. By using the ROS's probe DCFHDA, we found increased ROS levels in RIN-M cells cultures in presence of the hIAPP17-29 and rIAPP17-29 peptides. Accordingly N-acetyl-L-cysteine afforded almost complete protection against IAPP-induced cell death. Finally, the sub cellular distribution of the hIAPP peptides was examined by confocal microscopy. Following 20 min incubation, both F-hIAPP1-37 and F-hIAPP17-29 accumulate at specific microdomains on the cell plasma membrane where their uptake follows. Changes in cellular distribution were observed after 1 h of time incubation for both peptides showing a perinuclear localization suggestive of a mitochondrial distribution. Mitochondrial targeting of F-hIAPP17-29 and F-hIAPP 1-37 was confirmed by coinubation with mitotracker. However, few minutes after the F-hIAPP1-37 or the F-hIAPP17-29 targeted the mitochondria, the mitotracker staining was lost as direct result of mitochondrial impairment. Taken together our data suggest that β -sheet conformational transition, generally precluding fibril formation, is not a prerequisite for eliciting toxicity towards pancreatic β -cells. Moreover, we demonstrate that hIAPP1-37 and/or hIAPP17-29 can enter the cell supporting the notion that they might exert their toxic action at mitochondrial level.

Acknowledgments

This work was supported by MIUR, FIRB-MERIT project RBNE08HWLZ.

References

- [1] Clark, A., Wells, C.A., Buley I.D., et. Al., *Diab. Res.*, **1988**, 9, 151-159.
- [2] Westermark, P., Wilander, E., Westermark, G.T., Johnson, K.H., *Diabetologia*, **1987**, 30, 887-892.
- [3] Pappalardo, G., Milardi, D., Magri, A., Attanasio, F., Impellizzeri, G., La Rosa, C., Grasso, D., Rizzarelli, E., *Chemistry Eur. J.*, **2007**, 13, 10202-10215.

Analogues of SFTI-1 as the potential inhibitors of the 20S proteasome

Dębowski Dawid, Mizeria Aneta, Lesner Adam, Łęgowska Anna,
 Rolka Krzysztof

Department of Bioorganic Chemistry, Faculty of Chemistry, University of Gdansk
 Sobieskiego 18, 80-952 Gdansk, Poland
 E-mail: ddebowski@chem.univ.gda.pl

Introduction

A canonical inhibitor of various serine proteases, derived from bovine pancreas (BPTI, 58 amino acids) has been described as the potent inhibitor of chymotrypsin-, trypsin- and caspase-like activities (ChT-L, T-L, C-L, respectively) of rat and porcine 20S proteasome *in vitro* (IC₅₀ lower than 1 μM) and *ex vivo* [1]. Another cyclic peptide *Momordica charantia* trypsin inhibitor I (MCTI-I, 30 amino acids) reduced T-L activity. On the other hand, cyclic sunflower trypsin inhibitor (SFTI-1) composed of only 14 amino acids does not show any inhibitory propensity. BPTI enters the degradation chamber of 20S and blocks active sites stoichiometrically and competitively with the inhibition constant K_i of 2 μM (regarding ChT-L). It was hypothesized that the presence of basic amino acid in P₂' and/or P₃' position of the canonical inhibitor's binding loop determines anti-proteasome activity. To verify this theory, we synthesized a set of monocyclic SFTI-1 analogues with one or two basic residues (Lys or Arg) instead of naturally occurring Ile (P₂') and Pro (P₃') (Table 1). Their effects on human and yeast 20S proteolytic activities were characterized *in vitro*.

Table 1. Primary structures of monocyclic SFTI-1 and its analogues. Positions P₂' and P₃' are underlined, (&) - disulfide bridge.

No.	Analogue	Primary structure
I	SFTI-1	Gly-Arg-Cys(&)-Thr-Lys-Ser-Ile- <u>Pro</u> -Pro-Ile-Cys(&)-Phe-Pro-Asp
II	[Leu ¹ ,Lys ⁸]SFTI-1	Gly-Arg-Cys(&)-Thr-Lys-Ser-Leu-Lys-Pro-Ile-Cys(&)-Phe-Pro-Asp
III	[Arg ³ ,Leu ⁷ ,Lys ⁸]SFTI-1	Gly-Arg-Cys(&)-Thr-Arg-Ser-Leu-Lys-Pro-Ile-Cys(&)-Phe-Pro-Asp
IV	[Arg ⁷ ,Ile ⁸]SFTI-1	Gly-Arg-Cys(&)-Thr-Lys-Ser-Arg-Ile-Pro-Ile-Cys(&)-Phe-Pro-Asp
V	[Arg ⁵ ,Lys ^{7,8}]SFTI-1	Gly-Arg-Cys(&)-Thr-Arg-Ser-Lys-Lys-Pro-Ile-Cys(&)-Phe-Pro-Asp
VI	[Tyr ³ ,Lys ^{7,8}]SFTI-1	Gly-Arg-Cys(&)-Thr-Tyr-Ser-Lys-Lys-Pro-Ile-Cys(&)-Phe-Pro-Asp
VII	[Phe ³ ,Lys ^{7,8}]SFTI-1	Gly-Arg-Cys(&)-Thr-Phe-Ser-Lys-Lys-Pro-Ile-Cys(&)-Phe-Pro-Asp
VIII	[Ala ³ ,Lys ^{7,8}]SFTI-1	Gly-Arg-Cys(&)-Thr-Ala-Ser-Lys-Lys-Pro-Ile-Cys(&)-Phe-Pro-Asp
IX	[Ala ^{7,8}]SFTI-1	Gly-Arg-Cys(&)-Thr-Lys-Ser-Ala-Ala-Pro-Ile-Cys(&)-Phe-Pro-Asp

Results and Discussion

All results are collected in Table 2. The most significant inhibition of ChT-like activity of human, SDS-activated 20S was recorded for analogue **V**. This inhibitor is near 55-times stronger than monocyclic SFTI-1. Its K_i value is only about 3-times higher than that for MG-132 used as the positive control. According to the Lineweaver-Burk plot this inhibition is competitive (Fig.1). Similar results were obtained with the SDS-activated yeast 20S proteasome. In this case, the strongest activities were presented also by analogue **V** and **III**. Their IC₅₀ values were around 50-times lower than that for monocyclic SFTI-1, however, higher than for MG-132. It is noteworthy that the compound **IX** with two Ala residues in positions 7 (P₂') and 8 (P₃') did not display any activity.

Table 2 Inhibitory activities of SFTI-1 analogues against human and yeast 20S.

No.	ChT-like					T-like		C-like	
	Yeast 20S		Human 20S			Human 20S		Human 20S	
	IC ₅₀ [μ M]	K _a $\times 10^5$ [M ⁻¹]	IC ₅₀ [μ M]	K _i [μ M]	K _a $\times 10^5$ [M ⁻¹]	IC ₅₀ [μ M]	K _a $\times 10^5$ [M ⁻¹]	IC ₅₀ [μ M]	K _a $\times 10^5$ [M ⁻¹]
I	51.96 ± 4.90	N/D	51.58 ± 5.22	26.98 *	N/D	>100	N/D	58.19 ± 10.26	N/D
II	2.15 ± 0.10	5.24 ± 2.71	2.66 ± 0.17	1.23 *	3.94 ± 0.99	>100	N/D	6.74 ± 0.37	1.23 ± 0.42
III	1.07 ± 0.01	10.46 ± 4.72	3.36 ± 0.29	1.76 *	3.74 ± 1.18	>100	N/D	2.42 ± 0.04	3.99 ± 1.49
IV	5.36 ± 0.51	1.42 ± 0.28	2.49 ± 0.16	1.31 *	5.00 ± 2.05	60.5 ± 2.2	N/D	2.44 ± 0.43	3.96 ± 1.04
V	1.23 ± 0.06	7.86 ± 2.20	0.94 ± 0.07	0.31 ± 0.04	10.14 ± 2.36	72.16 ± 7.72	N/D	0.61 ± 0.04	15.59 ± 1.39
VI	10.16 ± 0.41	N/D	-	-	-	-	-	-	-
VII	5.34 ± 0.38	2.61 ± 1.16	-	-	-	-	-	-	-
VIII	8.82 ± 0.19	1.66 ± 0.79	-	-	-	-	-	-	-
IX	>100	N/D	-	-	-	-	-	-	-
MG-132	0.26 ± 0.02	38.9 ± 1.2	0.17 ± 0.01	0.10 ± 0.02	65.4 ± 7.1	28.56 ± 3.88	N/D	5.62 ± 0.10	1.82 ± 0.09

*- the K_i values were calculated using the online IC₅₀-to-K_i converter tool (BotDB Database [2]); N/D – not determined (very low activity). The highest activities are in bold. Z-LLL-CHO (MG-132) was used as positive control.

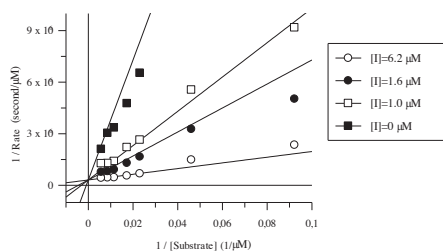


Fig.1 The double reciprocal Lineweaver-Burk plot. The concentration of human SDS-activated 20S was kept constant at 2.7 nM. The substrate Suc-LLVY-amc hydrolysis (AMC release) was recorded in assays with and without inhibitor (analogue V). Assay buffer: 50 mM Tris-HCl (pH 8.1), 0.02% (w/v) SDS.

Analogue V was also the most potent inhibitor of C-like activity of human, SDS-activated 20S. This result is significant because the C-like site must be considered as co-targets (along with ChT-L) of antineoplastic drugs [3]. The T-like activity of latent human 20S was inhibited by all SFTI-1 analogues to a lesser extent. Only for compounds IV and V the IC₅₀ values were lower than 100 μ M.

In summary, our work shows that SFTI-1, although poor 20S proteasome inhibitor itself, can be used as the convenient lead structure to design efficient inhibitors. We confirmed that the presence of at least one basic amino acid residue (Lys or/and Arg) in position P₂' or/and P₃' enhance affinity of monocyclic SFTI-1 analogues towards both, human and yeast proteasome 20S.

Acknowledgments

This work was supported by Polish National Science Center (grant No. UMO-2011/01/D/ST5/02778). We are grateful to Prof. Dr Michael Groll and M. Sc. Phillip Beck (Technische Universität München) for yeast 20S proteasome.

References

- [1] Yabe, K.; Koide, T. *Biochem.* **2009**, *145*, 217.
- [2] Cer, R.Z.; Mudunuri, U.; Stephens, R.; Lebeda, F.J. *Nucleic Acids Res.*, **2009**, *37*, W441.
- [3] Britton, M.; Lucas, M.M.; Downey, S.L.; Screen, M.; Pletnev, A.A.; et al. *Chem. Biol.* **2009**, *16*, 1278.

Angiotensin I metabolism in various kinds of fat tissue- *ex vivo* study in rat model of obesity and insulin resistance

**Beata Bujak-Giżycka¹, Maciej Suski¹, Józef Madej¹, Beata Bystrowska²,
Štefan Zorad³, Lucia Gajdošechova³, Katarína Krskova³,
Rafał Olszanecki¹, Ryszard Korbut¹**

¹*Chair of Pharmacology, Faculty of Medicine* ²*Department of Toxicology, Faculty of Pharmacy, Jagiellonian University Medical College, Krakow, Poland* ;³*Institute of Experimental Endocrinology, Slovak Academy of Sciences, Bratislava, Slovakia*

E-mail: bebujak@gmail.com

Introduction

Over the past two decades, our understanding of renin- angiotensin system (RAS) has experienced remarkable changes [1]. It is well known that obesity is the major risk factor for development of diabetes, premature onset of atherosclerosis and related cardiovascular complications. The traditional view of adipose tissue as a passive reservoir for energy storage is no longer valid. Indeed, in the last decade, adipose tissue has been recognized to be complex and active endocrine organ, which produces cytokines, chemokines, growth factors and other bioactive peptides. Several lines of evidence suggest that adipose tissue could be a rich source of various angiotensins, which may play a multiple roles in regulation of adipose tissue physiology and constitute a link between obesity and cardiovascular disorders [2].

Results and Discussion

Male, 33-weeks of age obese (688,75 ± 17,94 g) and lean (457,33 ± 8,73 g) Zucker rats were killed by decapitation and adipose tissue was quickly removed and weighed. Fragments of periaortic (FP), epididymal (FE), subcutaneous (FS) and retroperitoneal (FR) adipose tissues were incubated with angiotensin I (Ang I; 3µM) with/without ACE inhibitor- perindoprilat (10µM), according to earlier protocol [3]. Separation of angiotensin peptides was performed on a reversed-phase HPLC system [3]. Mass spectrometric detection was performed using a LCQ ion-trap mass spectrometer. For detection, selected ion monitoring (SIM) mode was used [3].

Conversion of Ang I in adipose tissue resulted mainly in formation of Ang-(1-7), Ang-(1-9) and Ang II. In obese rats in every type of fat was observed prevalence of production of Ang-(1-7) over Ang II (Fig.1A). In opposite to obese animals, the main metabolite in lean (control) group was Ang-(1-9) (Fig.1B).

The use of perindoprilat, angiotensin converting enzyme inhibitor, resulted in significant inhibition of Ang II formation. In epididymal fat perindoprilat significantly increased formation of Ang-(1-7).

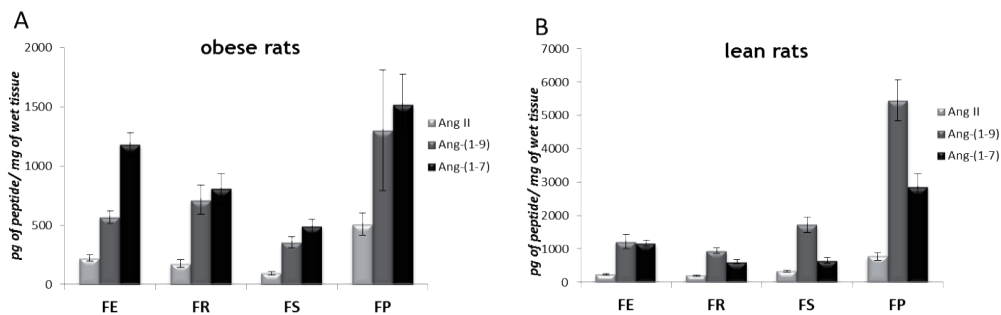


Fig.1. Comparison of levels of main Ang I metabolites produced in various kinds of adipose tissue of obese (A) and lean (B) Zucker rats.

Additionally, qPCR measurements of ACE and ACE-2 mRNA expression in adipose tissue were performed. Expression of ACE mRNA in obese rats was higher than in lean group, however ACE-2 expression was significantly decreased in obese animals compared to control rats (Fig.2). This observation could explain higher production of Ang-(1-9) in adipose tissues of lean animals.

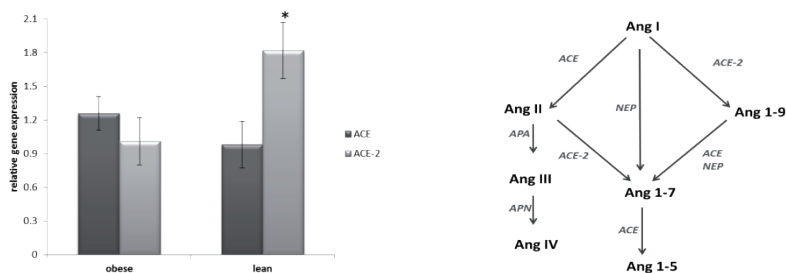


Fig.2. Relative gene expression of ACE and ACE-2 in adipose tissue (left panel) and main pathways of Ang I metabolism (right panel). ACE- angiotensin converting enzyme; ACE-2- angiotensin converting enzyme type 2; NEP- neutral endopeptidase; APA- aminopeptidase A; APN- aminopeptidase N

The quantitative and qualitative description of Ang I metabolism in various kinds of fat tissue in Zucker rats pose the questions about the biological roles of particular peptides both in local regulation of fat tissue functions and in cardiovascular complications of obesity and diabetes.

Acknowledgments

This study was supported by the Polish Ministry of Science and Higher Education co-operation grants 803/N/-Slowacja/2010/0 and 2011/01/M/NZ4/03752 and by grant of Slovak Ministry of Health 2007/27-SAV-02.

References

- [1] Varagic J, Trask A. et al. *J. Mol. Med.* **2008**, *86*, 663.
- [2] Cassis L.A. et al. *Curr. Hypertension Rep.* **2008**, *10*, 93.
- [3] Bujak- Gizycka B., Olszanecki R., Suski M. et al.: *J. Physiol. Pharmacol.* **2010**, *61*, 679.

Assessment of angiotensinogen metabolism in aorta and heart of hypertensive rats

Beata Bujak-Giżycka¹, Beata Bystrowska², Katarzyna Kuś¹,
Rafał Olszanecki¹, Ryszard Korbut¹

¹Chair of Pharmacology, Faculty of Medicine; ²Department of Toxicology, Faculty of Pharmacy, Jagiellonian University Medical College, Krakow, Poland

E-mail:bebujak@gmail.com

Introduction

It is widely recognized that renin-angiotensin system (RAS) plays an important role in the regulation of vessel wall homeostasis. Since 2006, when Nagata [1] et al. have described the new angiotensinogen metabolite- Ang-(1-12) in several rat tissues, our view on RAS has changed. Metabolism of the Ang-(1-12) may represent alternative pathway of Ang II formation, importantly, independent on renin and ACE activity [1,2]. Ahmad et al. [2] have described metabolism of Ang-(1-12) by human atrial tissues and showed that Ang II is formed mainly by chymase. This renin-independent Ang II production could explain the “resistance” regarding use of ACE inhibitors in patients with hypertension or diabetic nephropathy. Noteworthy, the role of Ang-(1-12) in circulation is still unclear and there is no information about possible pharmacological modulation of its metabolism.

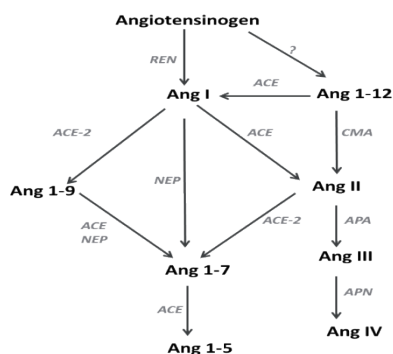


Fig.1. Main pathways of angiotensinogen metabolism. ACE- angiotensin converting enzyme; ACE-2 – angiotensin converting enzyme type 2; APA- aminopeptidase A; APN- aminopeptidase N; CMA- chymase; NEP- neutral endopeptidase; REN- renin

Results and Discussion

Male, 10 months of age, Wistar- Kyoto (WKY) rats (n=6; 385g-411g), and Spontaneously Hypertensive Rats (SHR) (n=6; 353g-399g), were administrated fraxiparine and anaesthetized with thiopentone. Fragments of aorta and hearts were excised through abdominal incision and cut into a suitable number of rings and opened flats. Tissue fragments were incubated with angiotensinogen (fragment 1-14) (Ang-(1-14), 3µM) according to earlier protocol [3]. Separation of angiotensin peptides was performed on a reversed-phase HPLC system [3]. Mass spectrometric detection was performed using a

LCQ ion-trap mass spectrometer. For detection, selected ion monitoring (SIM) mode was used [3].

Conversion of Ang-(1-14) both in aorta and in heart resulted mainly in formation of Ang-(1-12). Ang 1-12 seems to be a prevalent metabolite of angiotensinogen in rat and heart and may serve as a substrate for generation of Ang I, Ang II and other biologically active angiotensin peptides. Ex vivo formation of Ang II was significantly higher in SHR aortas (Fig.2A) as compared to WKY rats but didn't differ in the hearts (Fig.2B).

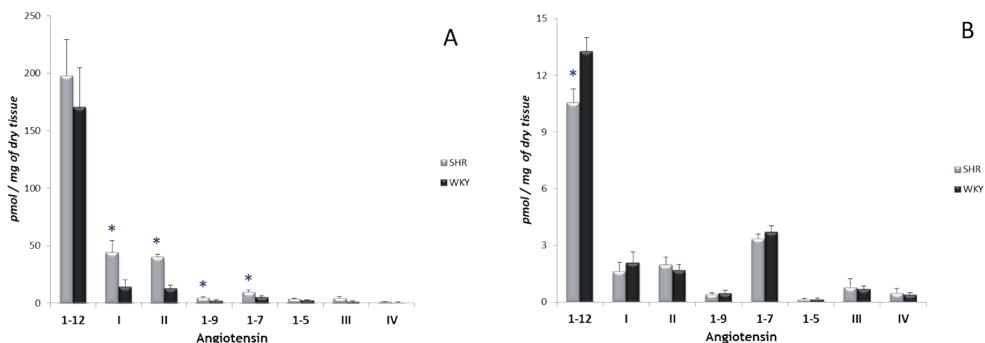


Fig.2. Levels of angiotensin peptides produced by incubation of rats aorta (A) and heart (B) with Ang-(1-14). * $p < 0,05$ vs. WKY (control)

Additionally, qPCR measurements of mRNA expression of main enzymes involved in angiotensinogen metabolism were performed. mRNA expressions of ACE and chymase in SHR aortas were higher compared to WKY. In SHR heart mRNA expression of ACE was twofold lower compared to WKY, but CMA-1 mRNA expression was significantly higher in SHR.

Although ACE mRNA expression in the heart of hypertensive rats was lower, production of Ang II was similar to WKY and it seems to be connected with higher activity of chymase. However the functional consequences of these findings require further investigations.

Acknowledgments

This study was supported by the grant N N401 293939 Polish Ministry of Science and Higher Education.

References

- [1] Nagata, S.; Kato, J.; Sasaki, K. et al. *Biochem. Biophys. Res. Commun.* **2006**, *350*, 1026.
- [2] Ahmad, S.; Simmons, T.; Varagic J.; et al. *PLoS ONE* **2011**, *6*, e28501.
- [3] Bujak-Giżycka, B.; Olszanecki, R.; Suski, M.; et al. *J. Physiol. Pharmacol.* **2010**, *61*, 679.

Design, synthesis and biological evaluation of linear peptide analogs of the A2 subunit (sequence 558-565) of the Factor VIII of blood coagulation

Charis Anastasopoulos, Yiannis Sarigiannis, George Stavropoulos*

Department of Chemistry, University of Patras, 26504 Patras, Greece

e-mail: G.Stavropoulos@chemistry.upatras.gr

Introduction

Blood coagulation is part of an important host defence mechanism, which under pathological conditions results in inappropriate intravascular coagulation when thrombin is produced. Clotting sequence is the result of a cascade of two biochemical pathways, *intrinsic pathway*, so called because all components are present in blood, and *extrinsic pathway*, in which tissue factor is required in addition to circulating components. The activated form of Factor VIII (FVIIIa) is a key component of the fluid phase of the blood coagulation and plays an important role forming a trimolecular complex with Factor IXa, Ca²⁺ and negatively charged phospholipids of the cells membrane. This complex is called *tenase* and participates in activation of prothrombin, which acts on fibrinogen to generate fibrin monomer, polymerized rapidly to form fibrin clot. FVIII is comprised of a heavy (A1-A2-B) and a light (A3-C1-C2) peptide chain, both cleaved by proteases at three sites, resulting in alteration of its covalent structure and conformation. The deficiency of FVIII is known as haemophilia A [1,2].

Results and Discussion

Our research effort is focused on the synthesis and biological evaluation of peptide analogs based on the region in which FVIII interacts with FIX and specifically on the sequence 558-565 of the A2 subunit. The synthesized analogs are examined to inhibit FVIII-FIX interaction resulting in inhibition of blood coagulation [4].

Synthesis

The tested peptides were prepared by Solid Phase Peptide Synthesis protocol (Fmoc/Bu^t methodology) using CLTR-Cl resin as solid support and DIC/HOBt reagents for each coupling cycle. After protected peptide sequence was accomplished a solution of TFE/DCM was used for the cleavage of the protected peptide from the resin. The side deprotection of the protected peptides was achieved using a mixture of TFA/DCM/TES at RT. All the synthesized analogs were purified (RP-HPLC) and identified (ESI-MS). We use the above procedure to synthesize the linear peptides of Table 1, incorporating Asn, Asp, Gln or Glu in position 564. In addition, we substituted Arg⁵⁶² with Lys (analog 3-8) and Gln⁵⁶⁵ with Lys (analog 6-8). Finally, we have synthesized analogs by replacement the Ser⁵⁵⁸ with Phe (7-8).

Biological Assays

The prepared peptides were investigated for their anticoagulant activity by measuring the chronic delay in the activated partial thromboplastin time (aPTT) and also tested for their

ability to reduce the percent activity of FVIIIa, which is generated in samples containing recombinant FVIIIa, *in vitro* [5,6].

Table 1: Biological assays of the synthesized analogs

<i>Analog of the Peptide Sequence Ser⁵⁵⁸-Gln⁵⁶⁵</i>	<i>Δt aPTT (sec)*</i>	<i>Inhibition % of FVIII activity**</i>
1. Ser ⁵⁵⁸ -Val ⁵⁵⁹ -Asp ⁵⁶⁰ -Gln ⁵⁶¹ -Arg ⁵⁶² -Gly ⁵⁶³ -Asn ⁵⁶⁴ -Gln ⁵⁶⁵ -OH	5.8	62.1
2. Ser ⁵⁵⁸ -Val ⁵⁵⁹ -Asp ⁵⁶⁰ -Gln ⁵⁶¹ -Arg ⁵⁶² -Gly ⁵⁶³ - Gln⁵⁶⁴ -Gln ⁵⁶⁵ -OH	3.6	47.5
3. Ser ⁵⁵⁸ -Val ⁵⁵⁹ -Asp ⁵⁶⁰ -Gln ⁵⁶¹ - Lys⁵⁶² -Gly ⁵⁶³ - Asp⁵⁶⁴ -Gln ⁵⁶⁵ -OH	1.5	47.9
4. Ser ⁵⁵⁸ -Val ⁵⁵⁹ -Asp ⁵⁶⁰ -Gln ⁵⁶¹ - Lys⁵⁶² -Gly ⁵⁶³ - Gln⁵⁶⁴ -Gln ⁵⁶⁵ -OH	-1.7	42.5
5. Ser ⁵⁵⁸ -Val ⁵⁵⁹ -Asp ⁵⁶⁰ -Gln ⁵⁶¹ - Lys⁵⁶² -Gly ⁵⁶³ - Glu⁵⁶⁴ -Gln ⁵⁶⁵ -OH	0.6	39.7
6. Ser ⁵⁵⁸ -Val ⁵⁵⁹ -Asp ⁵⁶⁰ -Gln ⁵⁶¹ - Lys⁵⁶² -Gly ⁵⁶³ -Asn ⁵⁶⁴ - Lys⁵⁶⁵ -OH	1.3	40.8
7. Phe⁵⁵⁸ -Val ⁵⁵⁹ -Asp ⁵⁶⁰ -Gln ⁵⁶¹ - Lys⁵⁶² -Gly ⁵⁶³ - Asp⁵⁶⁴ - Lys⁵⁶⁵ -OH	1.8	45.0
8. Phe⁵⁵⁸ -Val ⁵⁵⁹ -Asp ⁵⁶⁰ -Gln ⁵⁶¹ - Lys⁵⁶² -Gly ⁵⁶³ - Glu⁵⁶⁴ - Lys⁵⁶⁵ -OH	1.6	43.7

*Δt aPTT: Divergence of activated partial thromboplastin time (Δt = aPTT_{sample} - aPTT_{control})

**Inhibition (%) of the FVIIIa activity = [(100% value FVIIIa activity control - % value FVIIIa activity sample) / % value FVIIIa activity control] x 100%

Table 1 summarizes the synthesized peptides and their effect on both of the biological assays. The above results show clearly that the native sequence displays the best results in both of the biological assays. It is interesting that analog 4, which incorporates Lys instead of Arg⁵⁶² and Gln instead of Asn⁵⁶⁴, enhances blood coagulation as well even more than the control does, indicative that enhances the FVIIIa-FIXa complex formation. Similar results are received from the other biological assay, showing that the native sequence is the best inhibitor in the interaction of FVIII-FIX. Furthermore, replacement of Arg⁵⁶² with Lys and Asn⁵⁶⁴ with Glu (5) results in a reduced inhibitory activity.

Acknowledgments

This Research Project is co-financed: 80% by European Union – European Social Fund and 20% by General Secretary of Research & Technology (PENED 03ED569).

We also thank SANOFI S.A. Athens-Greece for the financial support.

References

- [1] Fay, P. and Jenkins, V. *Blood Reviews* **2005**, *19*, 15.
- [2] Obergfell, A.; Sturm, A.; Speer, C.; Walter, U. and Grossmann, R *Platelets* **2006**, *17*, 448.
- [3] Bajaj, P.; Schmidt, A.; Mathur, A. *J. Biol. Chem.* **2001**, *276*, 16302.
- [4] Anastasopoulos, C.; Sarigiannis, Y.; Liakopoulou-Kyriakides, M. and Stavropoulos, G. *Peptides 2008 (Proc of the 30th EPS)*, Helsinki, Finland, **2009**, 416
- [5] Barrowcliffe, T.W.; Raut, S. *Seminars in Thrombosis and Haemostasis* **2002**, *28*, 247.
- [6] Minors D., *Anaesthesia and Intensive Care Medicine* **2007**, *8*, 214.

Design, synthesis and biological evaluation of cyclic peptide analogs of the A2 subunit (sequence 558-565) of the Factor VIII of blood coagulation

Charis Anastasopoulos, Yiannis Sarigiannis, George Stavropoulos*

Department of Chemistry, University of Patras, 26504 Patras, Greece

e-mail: G.Stavropoulos@chemistry.upatras.gr

Introduction

The haemostatic mechanism has the crucial role to prevent loss of blood from injured blood-vessels. This loss is prevented by the integrity of the vessel walls, by platelets aggregation or by blood coagulation, which under normal conditions is limited onto the local trauma of the vessel wall. In generally, the mechanism of blood coagulation is important for maintaining vascular integrity and thus for the precaution of an organism from bleeding, which may also occur by blood coagulation caused by thrombin production. The diversion rate of this production leads to an expansion of thrombin to the general blood circulation. Thus, when thrombin generation is not controlled by the mechanisms of inhibition, a widespread undesirable intravascular thrombosis is occurred. The whole process of platelets adhesion requires the presence of clotting factor VIII (FVIII), a necessary for the blood coagulation cascade glycoprotein, which takes part in the *intrinsic pathway* and acts as a coenzyme for the activation of factor IX, a serine protease depended on the thrombin production [1,2]

Results and Discussion

The aim of this project is the synthesis of biologically active cyclic, head to tail, peptides, analogs of the sequence 558-565 of the A2 subunit of FVIII, which are potentially capable to block the formation of FVIIIa-FIXa complex, reducing thrombin production and thus blood coagulation [3].

Synthesis

The tested peptides were prepared by Solid Phase Peptide Synthesis protocol (Fmoc/Bu^t methodology) using CLTR-Cl resin as solid support. The starting linear peptides were assembled using DIC/HOBt procedure for each coupling cycle. After linear protected peptide sequence was accomplished a solution of TFE/DCM (30:70, v/v) was used for the cleavage of the protected peptide from the resin for 1h. Cyclization of the linear protected peptides was achieved by using standard reagents and procedures such as HOBt, TBTU and collidine reacting for ~48h. The side deprotection of the cyclic protected peptides was achieved using a mixture of TFA/DCM/TES (90:5:5) and stirred gently for 3h at RT. All the synthesized analogs were purified (RP-HPLC) and identified (ESI-MS). We use the above procedure to synthesize cyclic, head to tail, peptides incorporating Asn (**I**, **III**) or Asp (**II**, **IV**) at the position 564 of the native linear sequence, while two of them (**III-IV**) correspond to peptoid-peptide analogs (Table 1) by following the submonomer approach and synthesized the N^oPhe residue on the resin.

Biological Assays

The prepared peptides were investigated for their anticoagulant activity by measuring the chronic delay in the activated partial thromboplastin time (aPTT) and also tested for their ability to reduce the % FVIIIa activity, which is generated in samples containing recombinant FVIIIa, *in vitro* [4].

Table 1: Biological assays of the synthesized analogs

<i>Cyclic Analogs of the Peptide Sequence Ser⁵⁵⁸-Gln⁵⁶⁵</i>	<i>At aPTT (sec)*</i>	<i>Inhibition % of FVIII activity**</i>
I. Cyclo[-Ser ⁵⁵⁸ -Val ⁵⁵⁹ -Asp ⁵⁶⁰ -Gln ⁵⁶¹ -Arg ⁵⁶² -Gly ⁵⁶³ -Asn ⁵⁶⁴ -Gln ⁵⁶⁵]	0.9	61.7
II. Cyclo[-Ser ⁵⁵⁸ -Val ⁵⁵⁹ -Asp ⁵⁶⁰ -Gln ⁵⁶¹ -Arg ⁵⁶² -Gly ⁵⁶³ -Asp ⁵⁶⁴ -Gln ⁵⁶⁵]	1.4	63.8
III. Cyclo[-Ser ⁵⁵⁸ -Val ⁵⁵⁹ -Asp ⁵⁶⁰ -Gln ⁵⁶¹ -Arg ⁵⁶² -NPhe ⁵⁶³ -Asn ⁵⁶⁴ -Gln ⁵⁶⁵]	4.7	57.0
IV. Cyclo[-Ser ⁵⁵⁸ -Val ⁵⁵⁹ -Asp ⁵⁶⁰ -Gln ⁵⁶¹ -Arg ⁵⁶² -NPhe ⁵⁶³ -Asp ⁵⁶⁴ -Gln ⁵⁶⁵]	-1.3	50.6

* Δ t aPTT: Divergence of activated partial thromboplastin time ($\Delta t = \text{aPTT}_{\text{sample}} - \text{aPTT}_{\text{control}}$)

**Inhibition (%) of the FVIIIa activity = $[(100\% \text{ value FVIIIa activity control} - \% \text{ value FVIIIa activity sample}) / \% \text{ value FVIIIa activity control}] \times 100\%$

Table 1 summarizes the effect of the synthesized peptides on both of the biological assays. The results indicate that analog **III**, that incorporates NPhe instead of Gly⁵⁶³, is the most active, showing a prolonged aPTT of 4.7 sec whereas analog **I**, the cyclic analog of the native sequence, does not display similar activity (aPTT: 0.9 sec). However, the peptoid-peptide analog **IV**, which incorporates NPhe at the same position as analog **III** and Asp instead of Asn⁵⁶⁴, accelerates clotting formation as well even more than the control does, indicative that enhances the FVIIIa-FIXa complex formation.

Also, the influence of these synthetic peptides on the interaction between FVIIIa and FIXa has been examined as a reduction of the FVIIIa activity by using rFVIIIa in human plasma deficient to FVIII. Analog **II** causes the highest % inhibition of FVIIIa activity (63.8). However, it is interesting that the replacement of Gly⁵⁶³ by NPhe (**IV**), does not afford similar inhibitory activity in comparison with the corresponded cyclic peptide **II**, allowing a reasonable interpretation that its conformation facilitates the interaction between FVIIIa and FIXa.

Acknowledgments

This Research Project is co-financed: 80% by European Union – European Social Fund and 20% by General Secretary of Research & Technology (PENED 03ED569).

We also thank SANOFI S.A. Athens-Greece for the financial support.

References

- [1] Fay, P. and Jenkins, V. *Blood Reviews* **2005**, 19, 15.
- [2] Obergefell, A.; Sturm, A.; Speer, C.; Walter, U. and Grossmann, R; *Platelets* **2006**, 17, 448.
- [3] Anastasopoulos, C.; Sarigiannis, Y.; Liakopoulou-Kyriakides, M. and Stavropoulos, G. *Amino Acids* **2009** 37 (Suppl 1) S-110.
- [4] Barrowcliffe T.W., Raut S. *Seminars in Thrombosis and Hemostasis* **2002** 28, 247.

Development of potent and specific PACE4 inhibitors

Izabela Maluch¹, Anna Kwiatkowska², Christine Levesque², Sophie Routhier², Roxane Desjardins², François D'Anjou², Witold Neugebauer², Bernard Lammek¹, Adam Prahl¹, Robert Day²

¹Institute of Organic Synthesis, Faculty of Chemistry, University of Gdańsk, Gdańsk, Poland; ²Institut de Pharmacologie de Sherbrooke and Département de Chirurgie/Service de Urologie, Université de Sherbrooke, Sherbrooke, Québec, Canada
E-mail: izam@chem.univ.gda.pl

Introduction

The family of proprotein convertases (PCs) consists of seven enzymes that cleave at paired basic residues, namely furin, PC1/3, PC2, PACE4, PC4, PC5/6 and PC7, which are responsible for generating numerous bioactive peptides and proteins [1]. Additionally, PCs are also involved in the development and progression of many diseases [2]. Recently, our research group has demonstrated that PACE4 represents a potential therapeutic target for the treatment of prostate cancer [3]. Moreover, we have developed a potent and selective PACE4 inhibitor (20-fold specificity over furin), known as Multi-Leu (ML) peptide, which has potent antiproliferative effect on prostate cancer cell lines [4]. The potency of this analog was subsequently enhanced by the substitution of Arg in position P1 with a conformationally restricted mimetic – 4-amidinobenzylamine (Amba) [5]. However, the Amba substitution resulted in a reduced selectivity for PACE4. In order to restore this selectivity we have substituted residues in positions P5 and P6 of our ML-peptide analog (ML-Amba, *Fig. 1*) with each of nineteen amino acid residues and verifying its influence on activity and selectivity of these inhibitors.

P8 P7 P6 P5 P4 P3 P2 P1

Ac-Leu-Leu-**Leu-Leu**-Arg-Val-Lys-Amba

Fig.1. Sequence of ML-Amba inhibitor (control peptide).

Results and Discussion

All peptides were prepared by a combination of the solid phase (P9-P2 segments) and solution synthesis (Amba coupling), according to the standard Fmoc strategy on 4-Fmoc-hydrazinobenzoyl AM NovaGel or chloro-(2'-chloro)trityl polystyrene resin using an automatic synthesizer Symphony (Protein Technologies). The inhibitory constants were determined using recombinant human furin and PACE4 in competitive kinetic assay and K_i were calculated according to the tight-binding inhibition kinetics.

Scanning positions P5 and P6 of control peptide provide interesting insights into structure-activity relationships of ML-Amba analogs as potent and selective PACE4 inhibitors. We demonstrated that, peptides containing polar amino acid residues in P5 position are more potent PACE4 inhibitors ($K_i=1.05-2.63$ nM) in comparison with the control analog ($K_i=2.89$ nM). Moreover, we have shown that modification of Leu in position P5 or P6 with basic amino acid residues greatly increased inhibitory potency toward PACE4 and furin ($K_i=0.17-1.89$ nM, and $K_i=0.87-12.42$ nM, respectively). Based on these results, we

combined the most successful modifications to design a several multipoint substituted ML-Amba inhibitors and tested them against PACE4 and furin (Fig. 2).

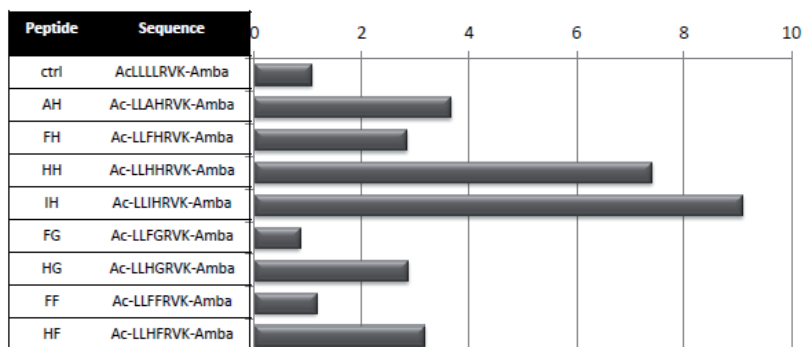


Fig.2. Specificity ratios of inhibitors with general formula Ac-L-L-P6-P5-R-V-K-Amba (peptide ctrl included as a reference)

Among eight designed peptides modified in both scanned positions, the most potent and selective inhibitors are HH (K_i values 0.455 nM and 3.37 nM toward hPACE4 and hfurin, respectively) and IH ($K_i = 0.87$ nM and 7.9 nM, respectively). In conclusion, we have obtained series of potent PACE4 inhibitors, which might serve as a starting point for the development of new anti-prostate cancer agents.

Acknowledgments

This work was awarded by Prostate Cancer Canada and is proudly funded by the Movember Foundation-Grant #2012-951. This work was also supported by the Ministère du Développement Économique, de l'Innovation et de l'Exportation du Québec (MDEIE), the Canadian Institutes of Health Research (CIHR), the Polish Ministry of Science and Higher Education grant no. 1202/B/H03/2010/38, and the European Social Fund in as a part of the project "Educators for the elite – integrated training program for PhD students, post-docs and professors as academic teachers at the University of Gdańsk" within the framework of Human Capital Operational Programme, Action 4.1.1, improving the quality of educational offer of tertiary education institutions. This publication reflects the views only of the author, and the funder cannot be held responsible for any use which may be made of the information contained herein.

References

- [1] Fugère, M.; Day, R. *Trends in Pharmacological Sciences* **2005**, *26*, 294.
- [2] Couture, F.; D'Anjou, F.; Day, R. *Biomol. Concepts*. **2011**, *2*(5), 421.
- [3] D'Anjou, F.; Routhier, S.; Perreault, J.P.; Latil, A.; Bonnel, D.; Fournier, I.; Salzet, M.; Day, R. *Transl. Oncol.* **2011**, *4*(3), 157.
- [4] Levesque, C.; Kwiatkowska, A.; Couture, F.; Desjardins, R.; Routhier, S.; Fugère, M.; Moussette, P.; Prah, A.; Lammek, B.; Appel, J.R.; Houghten, R.A.; D'Anjou, F.; Dory, Y.; Neugebauer, W.; Day, R. submitted to *J. Med. Chem.*
- [5] Kwiatkowska, A.; Couture, F.; Levesque, C.; Beauchemin, S.; Desjardins, R.; Routhier, S.; Dory, Y.; Prah, A.; Lammek, B.; Neugebauer, W.; Day, R. unpublished data

The ability of the peptides to inhibit the supercoiling reaction of DNA gyrase and the relaxation reaction of topo IV was investigated by gel electrophoresis. The minimum concentration that produced complete inhibition of supercoiling or relaxation activities was termed the IC₁₀₀. In the standard supercoiling and relaxation assays at 37°C an initial screening selected *ParELC3*, *ParELC8*, *ParELC10* and *ParELC12* as better gyrase and topo IV inhibitors (complete inhibition at 100 μmol.L⁻¹). Subsequently the IC₁₀₀ for the selected peptides were determined and showed that *ParELC10* was the best topoisomerase inhibitor (Table 1). One possibility to explain the inhibitory activity of the selected peptides is that the core of three-stranded β-sheets that encompasses the residues L61 to F87 is important for interactions with the topoisomerases. Peptides that do not contain any one of the three β-sheets do not inhibit these enzymes.

TABLE 1
Inhibitory activities of peptide analogues of *E.coli* ParE on bacterial topoisomerases

peptide	IC ₁₀₀ (μmol.L ⁻¹) ^a	
	DNA gyrase ^b	topo IV ^b
<i>ParELC3</i>	>20 ^c	10
<i>ParELC8</i>	35	50
<i>ParELC10</i>	20	10
<i>ParELC12</i>	50	25

^a Concentration of the inhibitor required for complete inhibition of topoisomerase activity; ^b From *Escherichia coli*; ^c93% inhibition at 20 μmol.L⁻¹ estimated by ImageJ software .

It is noteworthy that these peptides inhibit preferentially the topo IV relaxation activity, evidence that the interaction mechanism is likely different for these bacterial topoisomerases. The removal of β₄-sheet from *ParELC10* rendered a peptide less active on bacterial topoisomerases but with inhibitory activity on human topoisomerase II. Therefore, the β₄-sheet is not involved in the interactions with human topoisomerase II. These results suggest a new class of molecules with simultaneous inhibitory activity in DNA gyrase and topoisomerase IV. Furthermore, we have obtained the first example of a synthetic peptide from a bacterial toxin with inhibitory activity on human topoisomerase II. Therefore, *ParELC12* peptide has great potential as anticancer drug.

Lastly, preliminary results from intrinsic fluorescence and fluorescence anisotropy assays showed that the inhibition process of the activity of bacterial topoisomerases by ParE must occur by interaction of this toxin with the subunit of the enzyme responsible for DNA binding: GyrA for DNA gyrase and ParC for topo IV.

Acknowledgments

We gratefully acknowledge FAPESP, CAPES and CNPq for financial support.

References

- [1] Jiang, Y.; Pogliano, J.; Helinski, D.R.; Konieczny, I. *Mol. Microbiol.* **2002**, *44*, 971.
- [2] Barbosa, L.C.B.; Garrido, S.S.; Garcia, A.; Delfino, D.B.; Santos, L.N.; Marchetto, R. *Eur. J. Med. Chem.* **2012**, *54*, 591.
- [3] Fiebig, A.; Rojas, C.M.C.; Siegal-Gaskins, D.; Crosson, S. *Mol. Microbiol.* **2010**, *77*, 236.
- [4] Dalton, K.M.; Crosson, S. *Biochemistry*, **2010**, *49*, 2205.
- [5] Barbosa, L.C.B.; Garrido, S.S.; Garcia, A.; Delfino, D.B.; Marchetto, R. *Bioinformatics*, **2010**, *4*, 438.

Ex vivo assessment of angiotensin metabolism in retroperitoneal and periaortic fat tissue of hypertensive rats

**Beata Bujak-Giżycka¹, Maciej Suski¹, Józef Madej¹, Katarzyna Kuś¹,
Štefan Zorad², Rafał Olszanecki¹, Ryszard Korbut¹**

¹Chair of Pharmacology, Jagiellonian University Medical College, Krakow, Poland;

²Institute of Experimental Endocrinology, Slovak Academy of Sciences, Bratislava, Slovakia

E-mail: bebujak@gmail.com

Introduction

The renin-angiotensin system (RAS) has long been recognized as an important regulator of systemic blood pressure and electrolyte homeostasis. Our understanding of RAS has experienced remarkable change over the past two decades. Besides, angiotensin II, the new biologically active peptides [e.g. Ang-(1-7), Ang-(1-12), Ang IV, Ang-(2-10)] and pathways [e.g. angiotensin converting enzyme 2 - ACE2] have been described [1] (Fig.1); some of them, like Ang-(1-7) may oppose many actions of Ang II. Importantly, despite all components of classical RAS are found in adipose tissue [2], the data about fat formation of various angiotensins remain scarce.

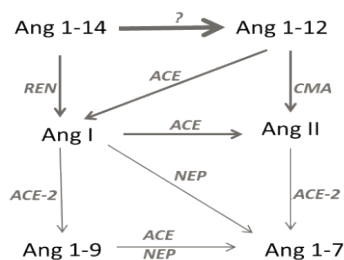


Fig.1. Main pathways of angiotensinogen (fragment 1-14) metabolism. ACE- angiotensin converting enzyme; ACE-2 – angiotensin converting enzyme type 2; CMA- chymase; NEP- neutral endopeptidase; REN- renin.

Results and Discussion

Male, 10 months of age, Wistar- Kyoto (WKY) rats (n=6; 379g-401g), and Spontaneously Hypertensive Rats (SHR) (n=6; 379g-380g), were administrated fraxiparine and anaesthetized with thiopentone. Fragments of periaortic and epididymal fat tissue were excised through abdominal incision and incubated with Ang-(1-14), Ang-(1-12) or Ang I at concentration of 3µM, according to earlier protocol [3]. Separation of angiotensin peptides was performed on a reversed-phase HPLC system. Mass spectrometric detection was performed using a LCQ ion-trap mass spectrometer. For detection, selected ion monitoring (SIM) mode was used [3]. Additionally, qPCR measurements of mRNA expression of main enzymes involved in angiotensinogen metabolism were performed.

Both in the periaortic and epididymal fat, the formation of Ang-(1-7) was higher than production of Ang II. Fat tissue formation of two main Ang I conversion products, Ang II

and Ang-(1-7), differed significantly between SHR and WKY rats. Compared to WKY rats, the formation of Ang-(1-7) in periaortic fat tissue was decreased in SHR. In opposite, in epididymal fat tissue formation of Ang-(1-7) and Ang II was higher in SHR (Fig.2A-C). Higher mRNA expression of ACE and chymase was observed in SHR rats, both in periaortic and epididymal adipose tissue (Fig.2D).

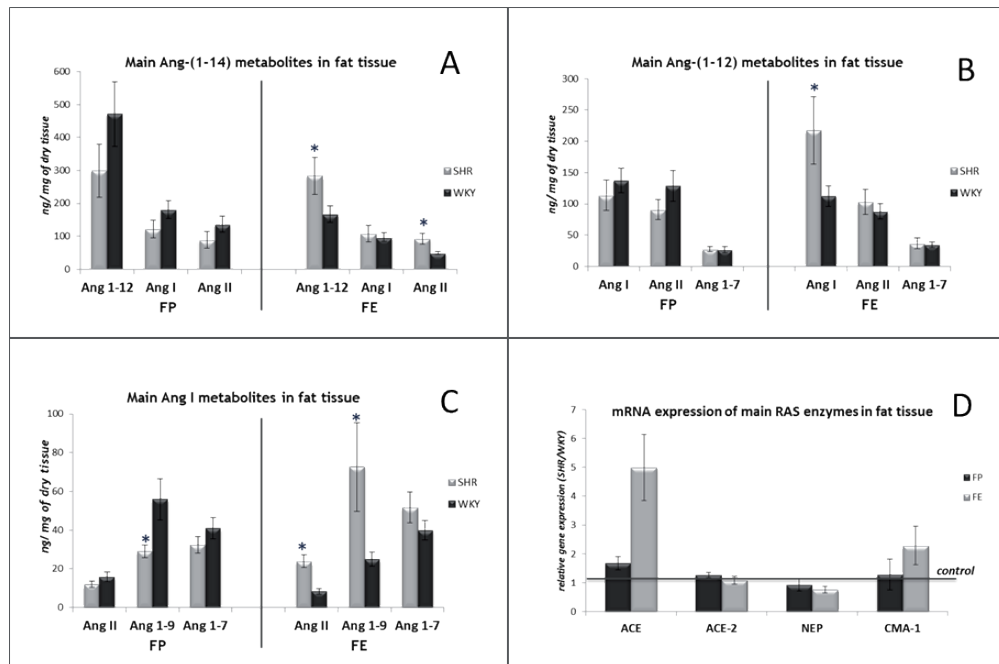


Fig.2. Levels of main angiotensin peptides produced by incubation of periaortic (FP) and epididymal (FE) fat tissue with Ang-(1-14) (A), Ang-(1-12) (B) and Ang I (C). *p<0,05 vs. WKY (control).

Our results suggest that in hypertension visceral fat production of angiotensin peptides is increased, while generation of “beneficial” Ang-(1-7) in periaortic fat is decreased. However, the functional importance of such finding require further investigation.

Acknowledgments

This study was supported by the Polish Ministry of Science and Higher Education grant N N401 293939 and cooperation grant 803/N-Słowacja/2010/0.

References

- [1] Varagic J, Trask A. et al. *J. Mol. Med.* **2008**, *86*, 663.
- [2] Cassis L.A., Police S.B. et al. *Curr. Hypertension Rep.* **2008**, *10*, 93.
- [3] Bujak-Gizycka, B.; Olszanecki, R.; Suski, M.; et al. *J. Physiol. Pharmacol.* **2010**, *61*, 679.

Hydrophobic α -amino acids favour the inhibition of human GIIA phospholipase A₂ by 2-oxoamides

**Sofia Vasilakaki,¹ Efrosini Barbayianni,¹ Thomas M.
Mavromoustakos,¹ Michael H. Gelb,² George Kokotos^{*,1}**

¹*Laboratory of Organic Chemistry, Department of Chemistry, University of Athens,
Panepistimiopolis, Athens 15771, Greece;* ²*Department of Chemistry and Biochemistry,
University of Washington, USA*

E-mail: gkokotos@chem.uoa.gr

Introduction

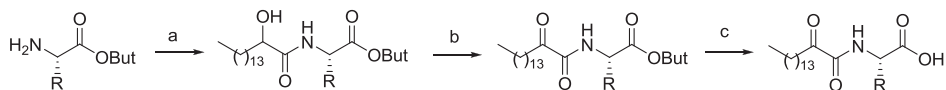
Phospholipases A₂ (PLA₂) are a superfamily of enzymes involved in various biochemical processes -such as arachidonic acid (AA) production- and therefore are pharmaceutical targets. They catalyze the hydrolysis of the *sn*-2 ester bond of glycerophospholipids, producing free fatty acids including arachidonic acid and lysophospholipids.¹ The secreted PLA₂ (sPLA₂) family (groups IB, IIA, IIC, IID, IIE, IIF, III, V, X and XII) are mainly small secreted proteins of 14-18 kDa. GIIA was among the first groups of sPLA₂ identified and was found in the synovial fluid of patients with rheumatoid arthritis. It has also been detected in human atherosclerotic lesions.²

GIIA sPLA₂ contains three long α -helices, two-stranded β -sheets referred as β -wings and a conserved Ca²⁺ binding loop. The active site consists of the catalytic dyad His47/Asp91, the Ca²⁺ ion and a long lipophilic tunnel which tends to enfold the aliphatic parts of substrates when they occur. We have reported that 2-oxoamides derivatives constitute a novel class of inhibitors for cytosolic cPLA₂.³ Most recently, it was found that the long chain 2-oxoamide GK126 based on the amino acid (*S*)-leucine displayed inhibition of human and mouse GIIA sPLA₂ (IC₅₀ 300 nM and 180 nM, respectively).⁴ Here, we present our studies on docking experiments of long chain 2-oxoamide derivatives based on the proteinogenic α -amino acids and the synthesis of the most promising molecules according to the docking results.

Results and Discussion

For simulated docking, the crystal structure of GIIA sPLA₂ was retrieved from the Brookhaven Protein Databank (PDB code: 1KQU). From this structure, water molecules within a distance of 5Å from the active site were set to 'Toggle' and 'Spin' state and all water molecules in a greater distance were deleted. Setting up the active site, all the protein residues within 6.0Å distance of the bound ligand were marked with their charge in physiological pH in order to form sensible interactions with the substrate. The calcium ion was treated in order to have the correct geometry and formal charge. According to the docking results, structures based on non polar amino acids presented promising results and thus we decided to synthesise them. The synthesis of the new 2-oxoamides is depicted in Scheme 1.

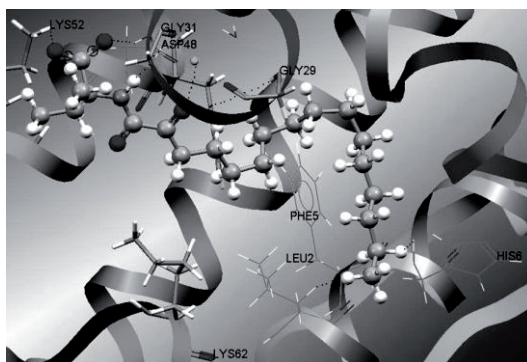
Scheme 1. General method for the synthesis of 2-oxoamide derivatives.



Reagents and conditions: (a) $\text{CH}_3(\text{CH}_2)_{13}\text{CHOHCOOH}$, Et_3N , WSCI , HOBT , CH_2Cl_2 ; (b) NaOCl , AcNH-TEMPO , NaBr , NaHCO_3 , EtOAc , H_2O , toluene, or Dess-Martin, CH_2Cl_2 ; (c) CF_3COOH , CH_2Cl_2 .

The so far *in vitro* results reveal (*S*)-valine derivative GK241 to have a better IC_{50} value than that of (*S*)-leucine derivative GK126. A possible binding mode of GK241 with GIIA sPLA₂ is shown in Figure 1. The key interactions occur between 2-carbonyl group and Gly29/ Ca^{++} and Asp48 with carboxylic acid group and 1-carbonyl group. Carboxylic acid group is also in interaction with Lys52, while valine side chain is located close to Lys52 and the long aliphatic chain is accommodated close to Leu2, Phe5 and His6.

Figure 1. The binding mode of GK241 in the GIIA sPLA₂ active site calculated using GOLD 5.1.



Acknowledgments

This research has been co-financed by the European Union (European Social Fund – ESF) and Greek national funds through the Operational Program "Education and Lifelong Learning" of the National Strategic Reference Framework (NSRF) - Research Funding Program: Heracleitus II. Investing in knowledge society through the European Social Fund.

References

- [1] Dennis, E. A.; Cao, J.; Hsu, Y. H.; Magrioti, V.; Kokotos, G. *Chem. Rev.* **2011**, *111*, 6130.
- [2] Nijmeijer, R.; Meuwissen, M.; Krijnen, P.A.J.; Van Der Wal, A.; Piek, J.J.; Visser, C.A.; Hack, C.E.; Niessen, H.W.M. *Eur. J. Clin. Invest.* **2008**, *38*, 205.
- [3] Six, D. A.; Barbayianni, E.; Loukas, V.; Constantinou-Kokotou, V.; Hadjipavlou-Litina, D.; Stephens, D.; Wong, A. C.; Magrioti, V.; Moutevelis-Minakakis, P.; Baker, S. F.; Dennis, E. A.; Kokotos, G. *J. Med. Chem.* **2007**, *50*, 4222.
- [4] Mouchlis, V. D.; Magrioti, V.; Barbayianni, E.; Cermak, N.; Oslund, R. C.; Mavromoustakos, T. M.; Gelb, M. H.; Kokotos, G. *Bioorg. Med. Chem.* **2011**, *19*, 735.

***In vitro* efficacy of CcdB toxin peptide analogues mediated by drug delivery systems formulation**

**Saulo Santesso Garrido¹, Reinaldo Marchetto¹, Simone Barbosa²,
Pietro Ciancaglini²**

¹UNESP - Univ. Estadual Paulista, Institute of Chemistry - Dept. Biochemistry and Chemistry Technology, Araraquara/SP, Brazil; ²USP - Univ. de São Paulo, Faculty of Philosophy, Sciences and Letters Dept. of Chemistry, Ribeirão Preto/SP, Brazil

saulosantesso@iq.unesp.br

Introduction

Infectious diseases are among the leading causes of deaths of human population. This is due in large part to the emergence of multi-resistant microorganisms to antibiotics. As the development of resistance is a dynamic process and its containment depends on several factors, it is important to the search for natural or synthetic substances that could serve as new drugs for the effective control of those diseases and made this function through alternatives mechanisms comparing with the actually medications [1]. In the search for new therapies, some peptides molecules have attracted the attention of our research group due to their particular properties. The bacterial toxin CcdB is a 11.7 kDa protein with 101 amino acids that with CcdA form a toxin/antitoxin pair involved in a programmed cell death system in *Escherichia coli* [2]. In the CcdA absence, CcdB can kill the cell by an unclear mechanism that involves the interaction of the CcdB C-terminal region (Trp99 - Ile101) with the DNA gyrase and Topoisomerase IV, a pair of bacterial enzymes extremely important in the process of DNA duplication. For several years, our research group is focusing efforts in the developing of a several peptides mimics rationally design based on the primary structure of natural CcdB toxin [3,4], to a better understanding the inhibition mechanism of the activity of this pair of enzymes. However these novel peptides have low ability to cross cell membranes. So the main objective of this data is to show the use of liposome like delivery systems of peptides mimics of CcdB toxin to improve their penetration inside bacterial cells.

Results and Discussion

Some peptide fragments derived from natural CcdB (Fig. 1) was synthesized by solid phase methodology (SPPS) employing the Fmoc linear strategy [5].



Figure 1. Primary structures of synthesized CcdB peptide analogue *CcdBSG-1* and *CcdBSG-2*. (Z = ε-amino hexanoic acid).

The ability of the analogues to inhibit the supercoiling reaction of DNA gyrase and relaxation of topoisomerase IV is evaluated by electrophoresis. It was possible to show that *CcdBSG1* presents a IC₁₀₀ near to 30 μM and 15 μM to *CcdBSG2* (Fig. 2).

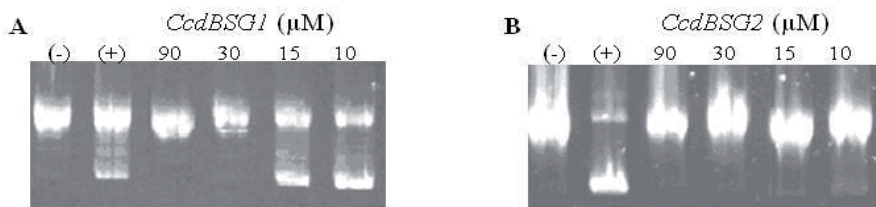


Figure 2. Inhibition assays of DNA supercoiling reactions of DNA gyrase from *E. coli*. (A) CcdBSG1-mediated inhibition and (B) CcdBSG2-mediated inhibition. Controls negative (-) had just the relax DNA and positive (+) with DNA gyrase (3.4 nM).

An IC₁₀₀ equivalent to 15 μM related to CcdBSG2 front DNA gyrase inhibition action is equivalent for 70 μg/mL who is inferior compared to activity by natural CcdB from *Escherichia coli* (100 μg/mL). A similar assay was conducted to evaluate the inhibition of the topoisomerase IV which is involved in the relaxation of DNA. Therefore employing a 15 μM solution we note that both peptides present activity in the inhibition of the DNA relaxation. We have selected the analog CcdBSG2 for later trials by having inhibitory activity on both enzymes in low concentration. The antimicrobial activity of CcdBSG2 was evaluated in liquid medium, using a qualitative technique for detection of bacterial growth. This technique, which is colorimetric, employs the reagent resazurine, component of the Alamar Blue® as an indicator of cell growth. Because of the low ability to cross cell membranes, first the peptide was encapsulated in liposomes prepared by a methodology already described [6] and modified according to the most appropriate lipid composition of liposome fusion to cytoplasmic membrane of bacteria. Large Unilamellares Vesicles (LUV) are made by the extrusion technique using polycarbonate filters of 100 nm in diameter. The particles sizes were determined by measures of distribution of particle size by dynamic light scattering using Beckman Coulter (model N5) equipment. For the microbiology tests solutions containing 100 μM of CcdBSG-2 were encapsulated by liposomes. This peptide was able to inhibit the growth in this condition of *Escherichia coli* 0:157 H: 7 (EHEC) and *Escherichia coli* k100 as representative of Gram negative and *Streptococcus agalactiae* as Gram positive. This fact shows that the transport system promoted by liposomes is very efficient, allowing sufficient permeation through membranes of different composition. The substitution of Ser70 by a Cys probably causes significant growth in the inhibition of the DNA gyrase activity.

Acknowledgments

This work was supported by CNPq in the form of PhD scholarships (Garrido S.S.) and research (Marchetto R.) and FAPESP in the form of travel assistance (2012/11862-0).

References

- [1] Lohner, K.; Staudegger, E. In: LOHNER, K. (Ed.). Development of novel antimicrobial agents: emerging strategies. Horizon Scientific Press: England, **2001**, 1-15.
- [2] Hayes, F. *Science* **2003**, *301*, 1496.
- [3] Trovatti, E.; Cotrim C. A.; Garrido, S. S.; Barros, S. R.; Marchetto, R. *Bioorg. Med. Chem. Lett.* **2008**, *18*, 6161.
- [4] Cotrim, C. A.; Garrido, S. S.; Trovatti, E.; Marchetto, R. *Quim. Nova*, **2010**, *33*(4), 841.
- [5] Stewart, J. M.; Young, J. D. *Solid Phase Peptide Synthesis*. 2nd ed. Rockford: Pierce Chemical Company, **1984**.
- [6] Breukink, E.; Ganz, P.; Kruijff, B.; Seelig, J. *Biochemistry*, **2000**, *39*, 1024.

HslVU, an ancestral form of the 26S proteasome as a potential target for the treatment of parasitoses due to protozoa (*Leishmania*, *Trypanosoma*)

Krishnananda. Samanta,¹ N. Mathy Kebe,² Viviana Apicella,¹ Vincent Lisowski,¹ Andrey Kajava,² Nadine Payrot,¹ Michel Pagès,³ Jean Martinez,¹ Patrick Bastien,³ Olivier Coux², Jean-François Hernandez¹

¹Institut des Biomolécules Max Mousseron (IBMM), UMR5247 CNRS, Universités Montpellier 1 & 2, Faculté de Pharmacie, Montpellier, France; ²Centre de Recherches en Biologie Moléculaire, UMR5237 CNRS, Universités Montpellier 1 & 2, Montpellier, France; ³Department of Parasitology-Mycology, MeBFEA, UMR5090 CNRS – 224 IRD Université Montpellier 1, MIVEGEC, Montpellier, France

E-mail: jean-francois.hernandez@univ-montp1.fr

Introduction

It is urgent to develop less toxic and more efficient treatments for Leishmaniasis and Trypanosomiasis. We propose to target an ancestral form of the proteasome, the HslVU protease, which is present in the parasite's single mitochondrion. It is essential for the growth of these organisms and does not have analogue in the human host. Originally discovered in eubacteria, this protein complex is constituted by two central hexameric HslV protease rings sandwiched between two hexameric HslU ATP-ase rings. As HslV shares a similar enzymatic mechanism with the host proteasome, we propose to inhibit the assembly of the complex in order to be selective. According to studies on bacterial HslVU [1,2], the C-terminal segment of HslU, highly conserved among bacteria and parasites, is essential in HslV activation and in complex assembly, therefore representing a privileged target.

Results and Discussion

We produced recombinant HslV, which is inactive alone, and showed that a synthetic C-terminal HslU peptide (C12-U2 = JMV4733 = H-arg-O2Oc-LQKNVNLAKYLL-OH) was able to induce the digestion by HslV of a fluorogenic substrate that was developed in our laboratory (Z-EVNL-AMC, JMV4482) (Figure 1). Activated HslV was inhibited by classical proteasome inhibitors like peptide boronates or MG132 (not shown).

With this enzymatic test in hands, we started the characterization of the interaction of the C-terminal portion of HslU with HslV. Synthesis of truncated forms and Ala scan based on C12-U2 showed that except Ala⁸, the last 6 C-terminal amino acid residues were essential

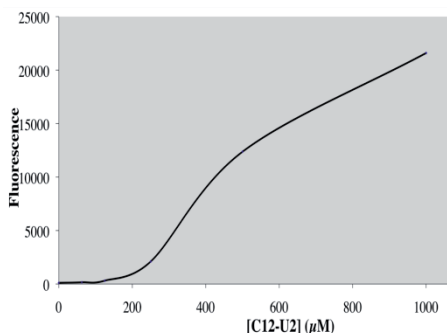


Figure 1. HslV activity in the presence of C12-U2 (HslV, 2 µg; JMV4482, 100 µM; 37°C. Fluorescence at 30 min)

for binding to and activation of HslV (Figure 2). Further analogues incorporating unnatural building blocks at these essential positions to improve affinity will be synthesized.

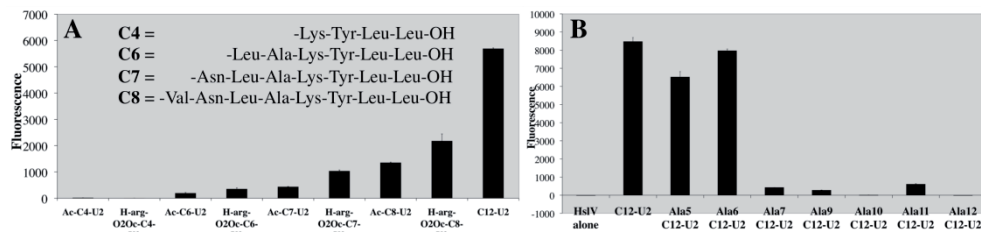
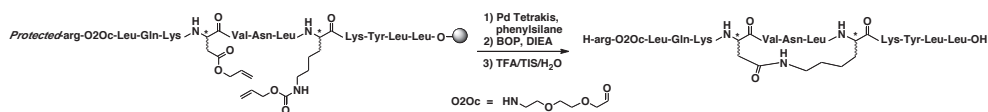


Figure 2. HslV activation by (A) HslU2 Cter peptides of increasing length and (B) Ala scan peptides (peptides, 500 μ M; JMVs4482, 100 μ M; fluorescence at 30 min)

The HslU Cter segment binds to HslV as a partial α -helix. Constraints were introduced to favour this conformation. In particular, cyclic analogues in which Asn⁴ and Ala⁸ of C12-U2 were replaced by an Asp and a Lys of *R* or *S* configuration, respectively, were synthesized. The cyclo[Asp⁴,Lys⁸] analogue showed significantly higher HslV activation potency compared to linear C12-U2. Other analogues with cycle of varying size and various bridges will be prepared and evaluated.



Finally, multivalency was considered to gain affinity. A dimer of C12-U2 was prepared. The length of the spacer (PEG-based) between the two ligands was estimated by molecular modelling. Surprisingly, the resulting HslV activating capacity was only twice that of the monomer. This absence of synergy might be due to the spacer length (63 atoms) that has to be investigated in more details. A trimer analogue is currently under investigation.

In conclusion, this first study opens the way toward more active compounds able to inhibit the interaction between the HslU and HslV rings, essential for protein degradation by the HslVU complex. Their design will be helped by molecular modelling based on known bacterial HslVU 3D structures. Then, the mitochondrial localisation of the target will be considered by exploring the use of mitochondrial penetrating vectors.

Acknowledgments

We thank the Fondation Infectiopôle Sud for supporting K.S.

References

- [1] Ramachandran, R.; Hartmann, C.; Song, H. K.; Huber, R.; Bochtler, M. *Proc. Natl. Acad. Sci. USA* **2002**, *99*, 7396.
- [2] Seong, I. S.; Kang, M. S.; Choi, M. K.; Lee, J. W.; Koh, O. J.; Wang, J.; Eom, S. H.; Chung, C. H. *J. Biol. Chem.* **2002**, *277*, 25976.

***N*- or *C*-terminal biotinylated citrullin containing filaggrin epitope peptides: The effect of biotinylation on the antibody recognition in Rheumatoid Arthritis**

**Fruzsina Babos^{1,4}, Eszter Szarka², György Nagy³, Zsuzsa Majer⁴,
Gabriella Sármay², Anna Magyar¹, Ferenc Hudecz^{1,4}**

¹*Research Group of Peptide Chemistry, Hungarian Academy of Sciences, Eötvös L. University (ELTE), Budapest, Hungary;* ²*ELTE, Department of Immunology, Budapest, Hungary;* ³*Buda Hospital of Hospitaller Brothers of St. John, Budapest, Hungary;* ⁴*ELTE, Department of Organic Chemistry, Budapest, Hungary*

E-mail: babosfruzsi@gmail.com

Introduction

Anti-citrullinated protein antibodies (ACPA) are sensitive and specific markers for diagnosis and prognosis in Rheumatoid arthritis (RA). Antibodies specific for cyclic citrullinated filaggrin peptide (CCP) were detected in RA sera and anti-CCP positivity is widely used for diagnostic purposes. Identification of new epitopes of filaggrin [1] would be useful in the diagnosis of anti-CCP3 seronegative patients. In addition, for optimal antibody recognition of biotinylated epitopes, there is a need to analyse the effect of the position of the labeling moiety in the peptide epitope on the antibody binding. Our aim was to identify new B-cell epitopes of filaggrin and identify the optimal position of biotin in connection with antibody binding properties. These peptides could be then considered as new tools for the detection of ACPA and thus for the early diagnosis of RA by the use of clearly defined epitopes on filaggrin.

Results and Discussion

Previously we have identified by MULTIPIN NCP method a filaggrin region of 19 amino acids (³⁰⁶SHQESTXGX³²⁴SXGRSGRSGS, X= citrulline) and a short pentapeptide (³¹¹TXGRS³¹⁶) as epitope [2]. For the analysis of the effect of label on antibody binding we synthesized *N*- and *C*-terminal biotinylated epitope peptides. To increase the water solubility of the peptides 4,7,10-trioxa-1,13-tridecanediamino succinic acid (Ttds) linker [3] was also used. Selected peptides were synthesised manually by SPPS, according to Fmoc/^tBu strategy and used in indirect ELISA, on NeutrAvidin pre-coated plates. The binding was detected by anti IgG-HRP (Figure 1). We have found that the CCP3+ serum samples specifically recognized the *C*-terminally biotinylated 5-mer filaggrin peptide, while showed no reaction with the *N*-terminally biotinylated ones. In case of the long filaggrin epitope peptides there was no difference in the recognition between the *N*- and *C*-terminal biotinylated analogues.

We have studied the effect of the biotinylation on the secondary structure of the peptides by ECD experiments (Figure 2). The spectra show that the presence and position of the biotin could influence the spectral characteristics mainly of the peptapeptides. No marked differences could be observed in case of the 19-mers by this technique.

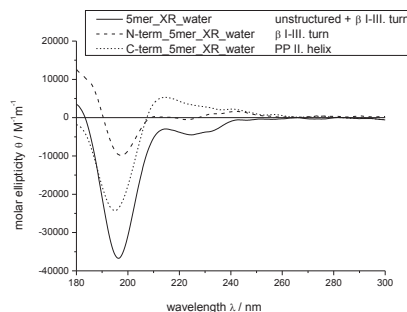
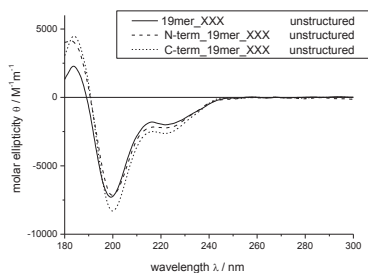
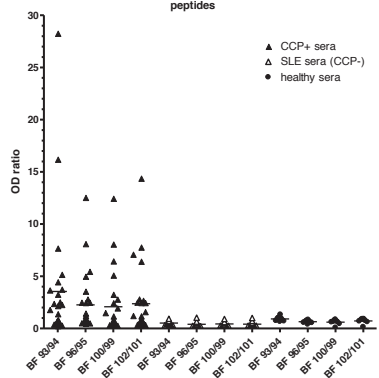
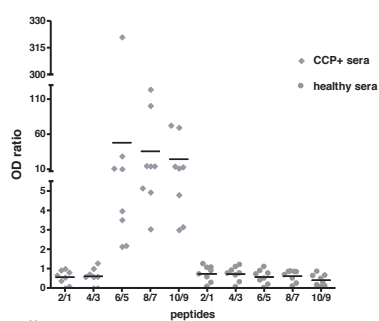


Fig. 2 ECD spectra of 5-mer (right) and 19-mer (left) peptides with N- or C-terminal biotin

1	biotinyl-6-amino-hexanoyl- Filaggrin ³¹¹⁻³¹⁵ RR -NH ₂
2	biotinyl-6-amino-hexanoyl- Filaggrin ³¹¹⁻³¹⁵ XR -NH ₂
3	biotinyl- Filaggrin ³¹¹⁻³¹⁵ RR -NH ₂
4	biotinyl- Filaggrin ³¹¹⁻³¹⁵ XR -NH ₂
5	Ac- Filaggrin ³¹¹⁻³¹⁵ RR -K(biotinyl-6-amino-hexanoyl)-NH ₂
6	Ac- Filaggrin ³¹¹⁻³¹⁵ XR -K(biotinyl-6-amino-hexanoyl)-NH ₂
7	Ac- Filaggrin ³¹¹⁻³¹⁵ RR -K(Ttds-biotinyl)-NH ₂
8	Ac- Filaggrin ³¹¹⁻³¹⁵ XR -K(Ttds-biotinyl)-NH ₂
9	Ac- Filaggrin ³¹¹⁻³¹⁵ RR -Ttds-K(biotinyl-6-amino-hexanoyl)-NH ₂
10	Ac- Filaggrin ³¹¹⁻³¹⁵ XR -Ttds-K(biotinyl-6-amino-hexanoyl)-NH ₂

BF93	biotinyl-6-amino-hexanoyl- Filaggrin ³⁰⁶⁻³²⁴ RRR -NH ₂
BF94	biotinyl-6-amino-hexanoyl- Filaggrin ³⁰⁶⁻³²⁴ XXX -NH ₂
BF95	Ac- Filaggrin ³⁰⁶⁻³²⁴ RRR -K(biotinyl-6-amino-hexanoyl)-NH ₂
BF96	Ac- Filaggrin ³⁰⁶⁻³²⁴ XXX -K(biotinyl-6-amino-hexanoyl)-NH ₂
BF99	Ac- Filaggrin ³⁰⁶⁻³²⁴ RRR -K(biotinyl-6-amino-hexanoyl-Ttds)-NH ₂
BF100	Ac- Filaggrin ³⁰⁶⁻³²⁴ XXX -K(biotinyl-6-amino-hexanoyl-Ttds)-NH ₂
BF101	Ac- Filaggrin ³⁰⁶⁻³²⁴ RRR -Ttds-K(biotinyl-6-amino-hexanoyl)-NH ₂
BF102	Ac- Filaggrin ³⁰⁶⁻³²⁴ XXX -Ttds-K(biotinyl-6-amino-hexanoyl)-NH ₂

Fig. 1 Indirect ELISA with biotinylated peptides, pre-coated with NeutrAvidin

Acknowledgments

This work was supported by grants from the National Scientific Research Fund Hungary (OTKA-A08-CK 80689, OTKA K100720), the RAPEP_09 (OMFB-00135/2010) and by the Foundation for Hungarian Peptide and Protein Research, Budapest, Hungary. TÁMOP 4.2.1./B-09/KMR-2010-0003.

References

- [1] Schellekens, G. A.; de Jong, B. A. W.; van den Hoogen, F. H. J.; van de Putte, L. B. A.; van Venrooij, W. J. *J. Clin. Invest.* **1998**, *101*, 273-281.
- [2] Magyar, A.; Brózik, M.; Hudecz, F. *Collection Symposium Series* **2011**, *13*, 80-84.
- [3] Bartos, Á.; Uray, K.; Hudecz, F. *Peptide Science* **2009**, *92*, 110-115.

New neutrophil serine proteases substrates optimized in prime positions using the combinatorial approach

Jadwiga Popow, Magdalena Wysocka, Adam Lesner,
Krzysztof Rolka

Faculty of Chemistry, Gdansk University, Sobieskiego 18, 80-952 Gdansk, Poland

e-mail: alesner@chem.univ.gda.pl

Introduction

Proteinase 3 (PR3), along with cathepsin G (CG) and neutrophil elastase (HNE), is a neutrophil serine protease localized within azurophilic cytoplasmic granules polymorphonuclear neutrophils (PMNs) [1]. Only recent studies (molecular dynamic simulations and molecular modeling) allowed researchers to characterize the roles of each of the proteases in the development of the lung diseases pathologies and they pointed out that PR3 can have intracellular specific protein substrates, thus resulting in the regulation of intracellular functions such as proliferation or apoptosis [2].

Our project involves chemical synthesis with the combinatorial approach and enzymatic studies of new selective fluorogenic substrates optimized in prime positions for proteinase 3. The general formula of the library is as follows: ABZ-Tyr-Tyr-Abu- X_1' - X_2' - X_3' -Tyr(3-NO₂)-NH₂, where in position X_1' , X_2' and X_3' , the set of all proteinogenic amino acids except Cys was introduced. The ABZ (2-aminobenzoic acid) and Tyr(3-NO₂) (3-nitro-L-tyrosine) at the *N*- and *C*-termini of the sequence substrates were donor / acceptor pair which shows the long-range fluorescence resonance energy transfer (FRET). The library consisting of 6859 octapeptides was synthesized manually on TentaGel S RAM resin as a solid support, using the portioning-mixing method and syringe technology [3,4]. The peptides were synthesized with the *Fmoc* chemistry except the incorporation of aminobenzoic acid (ABZ) which was protected by *tert*-butyloxycarbonyl (*Boc*-) group and introduced into the chain as a dipeptide combined with tyrosine (in position P_3) [5]. Deconvolution of the peptide library was performed by the iterative method in solution using the spectrofluorometer. The excitation and emission wavelengths were 320 nm and 450 nm respectively. Finally, enzyme titration of selected peptide and proteolytic cleavage pattern determination were prepared.

Results and Discussion

This work reports the synthesis of new selective fluorescence substrates of PR3 which are able to distinguish activity between PR3 and HNE. From among amino acids introduced in X_1' we decided to substitute the one which showed the highest fluorescence increase (Thr, data not shown) and the one that most differentiated both enzymes (Asn, Fig. 1A). The same tactics were consistently adopted in further position library screening. This way Glu and Phe residues were selected in position P_2' (when Asn is in position P_1') and Glu and Ser in position P_2' (when Thr is in position P_1' , data not shown). The results of the last step of deconvolution allowed for the emergence of the sequence of the most active PR3 substrate which is as follows: ABZ-Tyr-Tyr-Abu-Asn-Glu-Pro-Tyr(3-NO₂)-NH₂. The

results of the iterative position P₃' screening of the library obtained against PR3 and HNE are presented in Fig. 1.

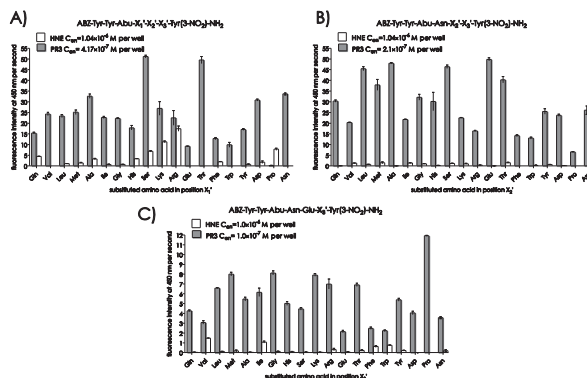


Figure 1. Deconvolution of octapeptides library against human PR3 and HNE.

The cleavage pattern of the most active substrate shows that during the incubation with PR3, the peak with the retention time of approximately 18.6 min in the progress of the digestion is vanishing and only after an hour of reaction new peaks with retention time of 17 min and 10.4 min are appearing while the previous peak has almost completely disappeared. Because PR3 is released from neutrophil accompanied by HNE, we decided to investigate the proteolytic cleavage of ABZ-Tyr-Tyr-Abu-Asn-Glu-Pro-Tyr(3-NO₂)-NH₂ in the presence of this enzyme. Incubation with HNE resulted in very little proteolysis and then only after 48h. In all chromatograms, we see one and the same peak with a retention time of about 18.6 min.

In conclusion, a new selective fluorogenic substrate optimized in prime positions for proteinase 3 (ABZ-Tyr-Tyr-Abu-Asn-Glu-Pro-Tyr(3-NO₂)-NH₂) has been developed using the combinatorial approach. Its outstanding kinetic parameters (K_M 9.8 M⁻¹; k_{cat} 8.93 s⁻¹ and k_{cat}/K_M 932 × 10³ M⁻¹ × s⁻¹) make it excellent tool for determination of PR3 activity.

Acknowledgments

This work was partially supported by the Project contributing to the Development of Young Scientists and PhD students at University of Gdansk under the grant No. 538-8290-1038-12.

References

- [1] Wysocka, M.; Lesner, A.; Guzew, K.; Kulczycka, J.; Łęowska, A.; Wicz, W.; Rolka, K.; *Anal. Chem.* **2010**, 82, 3883-3889.
- [2] Hajjar, E.; Korkmaz, B.; Gauthier, F.; Brandsdal, B. O.; Witko-Sarsat, V.; Reuter, N.; *J. Med. Chem.* **2006**, 49, 1248-1260.
- [3] Houghten, R. H.; Pinilla, C.; Blondelle, S. E.; Appel, J. R.; Dooley, C. T.; Cuervo, J. H.; *Nature* **1991**, 354, 84-90.
- [4] Furka, A.; Sebestyn, F.; Asgedom, M.; Dib, G.; *Int J Pept Protein Res* **1991**, 37, 487-494.
- [5] Schechter, I.; Berger, A.; *Biochem. Biophys. Res. Commun.* **1967**, 27, 157-162.

Peptides in *Xenorhabdus* and *Photorhabdus* spp.

Friederike I. Nollmann, Christina Dauth, Daniela Reimer,
Qiuqin Zhou, Helge B. Bode*

Molekulare Biotechnologie, Institut für Molekulare Biowissenschaften, Goethe Universität
Frankfurt, 60438 Frankfurt am Main

*E-mail: h.bode@bio.uni-frankfurt.de

Introduction

Bacteria of the genus *Xenorhabdus* and *Photorhabdus* are Gram-negative gamma proteobacteria that live in a unique symbiosis with nematodes of the genus *Steinernema* and *Heterorhabditidae*, respectively. Undergoing their complex and partly entomopathogenic life cycle, these bacteria not only produce highly active antibiotics^{[1],[2]} and insecticides^[3] but also a great variety of different small molecular weight compounds and peptides.^[4] Unfortunately, the biological benefits for the most part of these compounds have not been fully understood yet.^[5] With the help of HR-MS, molecular engineering and inverse feeding experiments in addition to NMR we were able to characterize some of these compounds and elucidate their structure.^[6] Since one compound class usually contains a great variety of different derivatives, some of which are only produced in low but not unimportant amounts, there is the need to be able to synthesize (to submit them to continuative testing) and eventually derivatize them.

Results and Discussion

DEPSIPEPTIDES. A fair number of the peptides that have been elucidated in *Xenorhabdus* and *Photorhabdus*, e. g. Szentiamide,^[7] Xenematide^[11] and the Xentrival peptides,^[8] are cyclic depsipeptides which vary in their amino acid composition, their *N*-terminal derivatization and ring size. In the cases of the Xenematide and the Szentiamide biological activities^{[9],[10]} have been discovered. But the Xentrival peptides, which are produced in seventeen different derivatives varying in their quantities from traces to milligram/L amounts, could not be connected to an actual biological activity so far. We tried to establish a synthesis route in order to (1) prove the structure of the derivatives which were produced in too low amounts to be isolated, (2) make these compounds accessible to high throughput screening and (3) obtain photo-reactive and “click”able derivatives in order to shed light on their biological purpose.

CYCLIC PEPTIDES. A compound class which is ubiquitous in the strains of *Photorhabdus* as well as *Xenorhabdus* are the so called GameXPptides.^[6] These peptides are a quite good example for the non-ribosomal peptide synthesis machinery, because they are not only cyclic but also bear a mixture of *L*- and *D*-amino acids as well as further modifications. Due to the fact that we were only able to detect a low bioactivity (in some cases) we are very interested in their actual biological purpose. Therefore, we synthesized photo-reactive and “click”able derivatives, incubated them with insect hemolymph or HeLa cells and submitted them to peptide mass finger print after the reaction with an azido-dye.

METHYLATED PEPTIDES. Another group of peptides which is unique though found in a lot of strains of *Xenorhabdus* as well as *Photorhabdus* is build up of highly methylated

sequences which differ in their amino acid composition or order (usually: valine and leucine), C-terminal amine (phenylethylamine, tryptamine, putrescine and agmatine) and their methylation pattern or degree. Due to the diverse production of these peptides we were only able to isolate a few so far. Since they are quite abundant we are interested in their biological function. We established three different but yet similar synthesis routes according to their methylation pattern and degree. For one the partially methylated peptides which were build up on resin with pre-methylated building blocks (or directly methylated on resin^[11]) followed by the amine condensation in solution.^[12] The permethylated peptides were assembled on resin as well, followed by the methylation^[13] and amination in solution. The highly methylated sequences had to be build up using different pre-synthesized components which then were coupled on resin or in solution. Although there are some methylated peptides known to be synthesized via SPPS^{[12]-[14]} we encountered several problems, e. g. low ability to ionize and dissolve in polar solvents or unwanted side reaction like diketopiperazine formation, which resulted in low yields.

Acknowledgments

The Research leading to these results has received funding from the European Community's Seventh Framework Programme (FP7/2007-2013) under grant agreement no. 223328 and the DFG.

References

- [1] Lang, G.; Kalvelage, T.; Peters, A.; Wiese, J.; Imhoff, J. F. *J. Nat. Prod.* **2008**, *71* (6), 1074.
- [2] Reimer, D.; Pos, K. M.; Thines, M.; Grun, P.; Bode, H. B. *Nat. Chem. Biol.* **2011**, *7* (12), 888.
- [3] Ffrench-Constant, R. H.; Dowling, A.; Waterfield, N. R. *Toxicon* **2007**, *49* (4), 436.
- [4] Reimer, D.; Luxenburger, E.; Brachmann, A. O.; Bode, H. B. *Chembiochem.* **2009**, *10* (12), 1997.
- [5] Bode, H. B. *Curr. Opin. Chem. Biol.* **2009**, *13* (2), 224.
- [6] Bode, H. B.; Reimer, D.; Fuchs, S. W.; Kirchner, F.; Dauth, C.; Kegler, C.; Lorenzen, W.; Brachmann, A. O.; Grun, P. *Chemistry* **2012**, *18* (8), 2342.
- [7] Ohlendorf, B.; Simon, S.; Wiese, J.; Imhoff, J. F. *Nat. Prod. Commun.* **2011**, *6* (9), 1247.
- [8] Zhou, Q. *submitted* **2012**.
- [9] Nollmann, F. I.; Dowling, A.; Kaiser, M.; Deckmann, K.; Grosch, S.; Ffrench-Constant, R.; Bode, H. B. *Beilstein. J. Org. Chem.* **2012**, *8*, 528.
- [10] Hung, K. Y.; Harris, P. W.; Heapy, A. M.; Brimble, M. A. *Org. Biomol. Chem.* **2011**, *9* (1), 236.
- [11] Biron, E.; Chatterjee, J.; Kessler, H. *J. Pept. Sci.* **2006**, *12* (3), 213.
- [12] Li, P.; Xu, J. C. *J. Org. Chem.* **2000**, *65* (10), 2951.
- [13] Bates, R. B.; Brusoe, K. G.; Burns, J. J.; Caldera, S.; Cui, W.; Gangwar, S.; Gramme, M. R.; McClure, K. J.; Rouen, G. P.; Schadow, H.; Stessman, C. C.; Taylor, S. R.; Vu, V. H.; Yarick, G. V.; Zhang, J. X.; Pettit, G. R.; Bontems, R. *Journal of the American Chemical Society* **1997**, *119* (9), 2111.
- [14] Biron, E.; Chatterjee, J.; Ovadia, O.; Langenegger, D.; Brueggen, J.; Hoyer, D.; Schmid, H. A.; Jelinek, R.; Gilon, C.; Hoffman, A.; Kessler, H. *Angew. Chem. Int. Ed Engl.* **2008**, *47* (14), 2595.

Study on the application of furan crosslinking at the protein-DNA interface

Carrette Lieselot L.G.¹, Gattner Michael², Van den Begin Jos¹, Carell Thomas², Morii Takashi³, Madder Annemieke^{1,*}

¹Laboratory for Organic and Biomimetic Chemistry, UGent, Krijgslaan 281 S4, 9000 Gent, Belgium; ²LMU Munich, Butenandstrasse 5-13, D-81377 Munich, Germany; ³Laboratory of Biofunctional Science, Kyoto University, Uji Campus, Uji, Kyoto 611-0011 Japan

E-mail: annemieke.madder@ugent.be

Introduction

The toxicity of furan is known to rely on its selective oxidation in the liver by Cyt P450 enzymes transforming it into the very reactive butenedial, which quickly reacts with proximate nucleophiles of DNA (Figure 1) and proteins. [1] This principle was used in our laboratory to develop a high yielding DNA interstrand crosslinking methodology. [2]

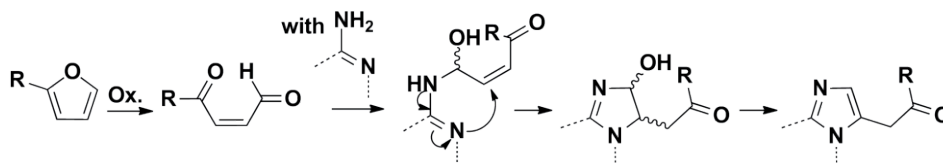


Figure 1. Furan oxidation and reaction with nucleophilic DNA

In view of the demonstrated site-selectivity, the method further holds promise for site-specific crosslinking of proteins to their DNA recognition site, which is highly relevant in the study of transient protein-DNA interactions. Furthermore irreversible DNA binding can be achieved through such a covalent linkage, which is potentially useful for new generation therapeutics. [3]

Results and Discussion

In our previous studies a good major groove binding peptide was found to be prerequisite for such crosslinking experiments to ensure proximity between the reactive enal and the attacking nucleophile. [4] Therefore we chose to work with a miniature transcription factor, to allow for easy modification and analysis. The experiments were carried out with a non-covalent GCN4 mimicking dimer, earlier described by Morii *et al.* (Figure 2). [5]

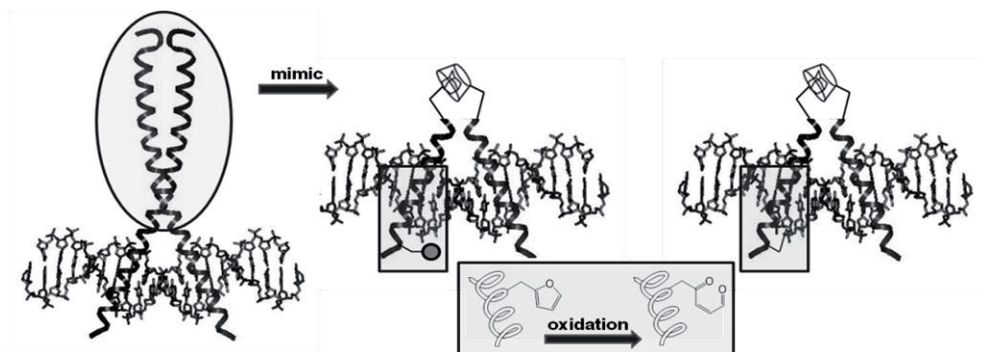


Figure 2. Principle of the crosslinking from furan-modified protein mimic to DNA

Furylalanine was introduced in the peptide by replacing a lysine (K231) or alanine (A239) residue positioned in the major groove, as determined from the crystal structure. [6] Binding of these modified protein mimics was ensured by the generation of heterodimers and verified by EMSA experiments. Optimization of the oxidation conditions was carried out by reaction with hydrazine and monitoring on HPLC. However, furan oxidation in the presence or just before the addition of DNA, did not result in observable crosslink formation. Although unfavorable positioning and/or linking cannot be excluded, we believe that the involvement of the available nucleophilic amine functionalities of the DNA in Watson-Crick basepairing, renders them unreactive towards the crosslinking reaction. This rationale is further supported by the described use of aldehydes for the detection of single stranded regions of DNA [7] and their use to elucidate RNA folding pathways. [8]

We are currently exploring the reverse approach, incorporating the furan moiety into DNA, for further crosslinking to a non-modified protein mimic.

Acknowledgments

J. Goeman is acknowledged for technical support. FWO is acknowledged for an aspirant position. We further acknowledge support from COST action TD0905.

References

- [1] Peterson, L.A. *Drug Metabol. Rev.* **2006**, 38, 615
- [2] Op de Beeck, M., Madder, A., *J. Amer. Chem. Soc.* **2011**, 133, 796
- [3] Verzele, D.; Carrette, L.L.G.; Madder, A. *Drug. Discov. Today: Tech.* **2010**, 7, 115
- [4] Unpublished results of Deceuninck, A. and Madder, A.
- [5] Ueno, M.; Murakami, a.; Makino, K.; Morii, T. *J. Amer. Chem. Soc.* **1993**, 115, 12575
- [6] Keller, W.; König, P.; Richmond, T.J.J. *Mol. Biol.* **1995**, 254, 657
- [7] Murray, V. *Prog Nucleic Acid Res Mol Biol.* **1999**, 63, 367-415
- [8] Mathews, D.H.; Turner, D.H. *Current Protocols in Nucleic Acid Chemistry* **2002**, 11.9.1-11.9.4

Transmembrane channel formation induced by the peptaibol paracelsin from *Trichoderma reesei* (*Hypocrea jecorina*)

Sabine Gelfert-Peukert¹, Günther Boheim¹, Günther Jung²,
Hans Brückner^{3,4}

¹Department of Cell Physiology, Work Group Biophysical Chemistry of Membranes, Ruhr University Bochum, 44780 Bochum, Germany; ²Institute of Organic Chemistry, University of Tübingen, Auf der Morgenstelle 18, 72076 Tübingen, Germany; ³Research Center for BioSystems, Land Use and Nutrition (IFZ), Department of Food Sciences, University of Giessen, Giessen, Germany; ⁴Visiting Professor at the Department of Food Sciences and Nutrition, King Saud University, Riyadh, Kingdom of Saudi Arabia
E-mail: guenther.boheim@web.de

Introduction

The filamentous fungus *Trichoderma reesei* (teleomorph: *Hypocrea jecorina*) and its mutants are of paramount importance owing to their production of cellulases and membrane-active peptide antibiotics [1,2]. We had shown that *T. reesei* QM 9414 produces 20-residue peptaibols named **paracelsin (PC) A-D** [3]. These peptides may be considered as structural analogs of **alamethicins (ALM)** [4] and *vice versa*. The sequences of PC-A and B in comparison to ALM F30 (major component) are shown below (Ac, acetyl; Aib, α -aminoisobutyric acid; Pheol, L-phenylalaninol). Whereas channel-forming activities resulting from shifting Pro¹⁴ to sequential positions 11-17 in synthetic ALM F30 have been analyzed in detail [5], the natural exchange of Pro² in ALM by Ala² in PC-A and B have not yet been analyzed comparatively. The sequences of PC-A, PC-B, and acidic ALM F30 (major sequence) are shown below. Relevant exchange position are in bold letters.

PC-A: Ac-Aib-**Ala**²-Aib-Ala-Aib-Ala-Gln-Aib-**Val**⁹-Aib-Gly-**Aib**¹²- Aib-**Pro**¹⁴-Val-Aib-
Aib-**Gln**¹⁸-Gln-Pheol²⁰

PC-B: Ac-Aib-**Ala**²-Aib-Ala-Aib-Ala-Gln-Aib-**Leu**⁹-Aib-Gly-**Aib**¹²- Aib-**Pro**¹⁴-Val-Aib-
Aib-**Gln**¹⁸-Gln-Pheol²⁰

ALM: Ac-Aib-**Pro**²-Aib-Ala-Aib-Ala-Gln-Aib-**Val**⁹-Aib-Gly-**Leu**¹²-Aib-**Pro**¹⁴-Val-Aib-
Aib-**Glu**¹⁸-Gln-Pheol²⁰

Results and Discussion

The formation and voltage-dependent characteristic single-channel fluctuations of HPLC-purified PC-A and B and the corresponding amplitude histograms formed in bilayer membranes are shown in Figure 1. The homogeneity of the conductance is remarkable and equal at the positive and negative voltage side. This is also evident from the identical peak widths of the latter. The lowest level of conductance in PC-A(B) is 2, amounting to 4(6) at the positive side and 5(6) at the negative side. Exchange of Val⁹ in PC-A against more hydrophobic and bulkier Leu⁹ in PC-B increases the lifetime of the pores. Acidic Glu¹⁸ together with Pro² and Leu¹² in ALM F30 increases the lifetime of the pores notably. This

is in contrast to the exchange of Pro¹⁴ by Ala¹⁴ in a synthetic ALM-analog, altering the current-voltage curves considerably [5]. Similar data were reported for longibrachins [6]. Crucial for the formation of stable pores induced by PC-A and B is, in agreement with ALM, the stereochemistry of the C-terminal part, governed by hydrogen bridges and the bend of about 20 degrees in the helical main axis, induced by the C-terminal Pro¹⁴ residue. The data support the current view that the N-terminal helical conformation of the 20-residue peptaibols with a bend enforced by the crucial Pro¹⁴ in the C-terminal, amphipathic part are optimal for generating membrane-modifying properties in general, including formation of voltage-gated transmembrane channels in lipid bilayer membranes.

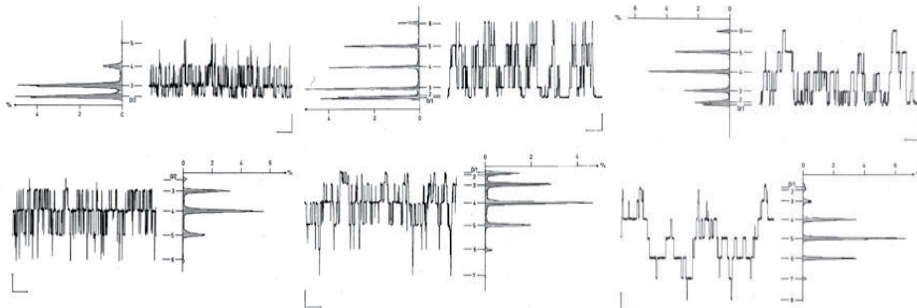


Figure 1. Single-channel fluctuations and corresponding single-channel amplitude histograms induced by pure (HPLC) PC-A (left) and pure PC-B (middle) in comparison to natural, microheterogeneous [3] ALM-F30 (right) ($c = 50 \text{ ng/mL}$) at $\pm 100 \text{ mV}$ (above/below) applied membrane voltage; % refers to statistical probability of current $I = 6 \text{ pA}$; identical scale bars represent 100 pA (vertical transmembrane current scale bar) and 200 ms (horizontal time scale bar). Experimental conditions: planar bilayers were formed from synthetic 1-palmitoyl-2-oleoyl-syn-glycero-3-phosphocholine (1,2-POPC), 1,2-oleoyl-syn-glycero-3-phosphatidylethanolamine (1,2-DOPE), and cholesterol (ratio 87.5 : 10 : 2.5, mol%) by applying a solution of 3.5 mg lipid/ml solvent (hexane – ethanol, 9:1 v/v) on tips of fire-polished patch-clamp glass pipettes. The holes formed were approximately $4.2E-4 \text{ cm}^2$ in area. Measurements were carried out in 1 M KCl/10 mM HEPES buffer (pH 7.3) at $18 \text{ }^\circ\text{C}$. For details of instrumental set up see [7,8]and references cited therein.

References

- [1] Degenkolb, T.; Brückner, H. *Chem. Biodivers.* **2008**, *5*, 1817.
- [2] Irmscher, G.; Jung, G. *Eur. J. Biochem.* **1977**, *80*, 165.
- [3] Brückner, H.; Graf, H.; Bokel, M. *Experientia* **1984**, *40*, 1189.
- [4] Kirschbaum, J.; Krause, C.; Winzheimer, R. K.; Brückner, H. *J. Peptide Sci.* **2003**, *9*, 799.
- [5] Kaduk, C.; Duclohier, H.; Wenschuh, H.; Beyermann, M.; Molle, G.; Bienert, M. *Biophys. J.* **1997**, *72*, 2151.
- [6] Cosette, P.; Rebuffat, S.; Bodo, B.; Molle, G. *Biochem. Biophys. Acta* **1999**, *1461*, 113.
- [7] Boheim, G.; Hanke, W.; Jung, G. *Biophys. Struct. Mech.* **1983**, *9*, 181.
- [8] Boheim, G.; Kolb, H.-A. *J. Membrane Biol.* **1978**, *38*, 99.

Analgesic effects of novel modified with β 2-tryptophan hexapeptide analogues as nociceptin receptor ligands

**A. I. Bocheva¹, H. H. Nocheva¹, N. D. Pavlov^{2,3}, M. Calmès³,
J. Martinez³, P. T. Todorov², E. D. Naydenova²**

¹*Department of Pathophysiology, Medical University of Sofia, Bulgaria;* ²*Department of Organic Chemistry, University of Chemical Technologies and Metallurgy, Sofia, Bulgaria;*

³*Institut des Biomolécules Max Mousseron (IBMM) UMR 5247 CNRS-Université Montpellier 1 et Université Montpellier 2, France*

E-mail: e_naydenova@abv.bg

Introduction

Nociceptin/Orphanin FQ (N/OFQ) is an endogenous ligand of the nociceptin opioid peptide (NOP) receptor, structurally and functionally related to the classical opioid receptors. Via NOP receptor activation N/OFQ modulates several biological actions both at central and peripheral levels [1,2]. It has been found that N/OFQ play a direct role on pain perception. Currently available ligands for the nociceptin (NOP) receptor as hexapeptides and their therapeutic potential in pain have been reviewed. Hexapeptides with Ac-RYYR/KW/IR/K-NH₂ formula have been identified as having the shortest peptide sequence with high NOP-receptor affinity, selectivity and marked analgesic effect. [3]. The aim of the present study was to examine the effects of JTC-801 (a NOP-receptor antagonist) and naloxone (Nal) in the analgesic activity of the newly synthesized hexapeptide analogues.

Results and Discussion

Aiming to develop more potent analgesic substances a new series of β 2-tryptophan modified at 4th and 5th position respectively Ac-RFMWMK-NH₂ and Ac-RYYRWK-NH₂ analogues was synthesized. All the peptides (10 μ g/kg), JTC-801 (0.5mg/kg), and Nal (1mg/kg) were dissolved in saline and intraperitoneally injected in male Wistar rats. Antinociceptive effects were evaluated by two nociceptive tests – the paw-pressure (PP) and the hot plate (HP), and statistically accessed by ANOVA. Pain threshold assessment began 10 min after the intraperitoneal injection of the peptides. Applied alone analogues **1** and **3** showed no statistically relevant differences in pain-perception compared to the referent compounds on PP-test during the hole investigated period. The results showed that analogues **2** and **4** statistically relevant decrease in nociception in comparison to both the referent substances on the 10th min with a decrease in pain threshold on the 20th and 30th min (fig.1A).

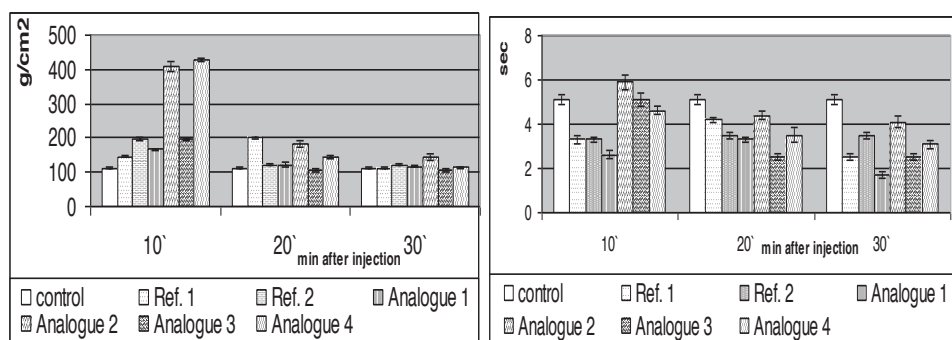
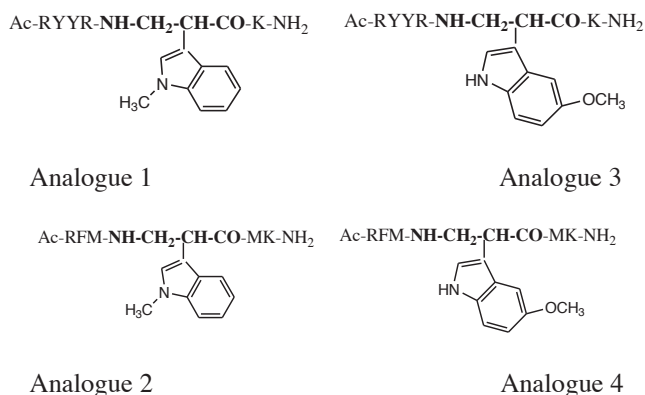


Fig. 1 Effects of newly synthesized analogues estimated by PP-test (A) and HP-test (B). Data are presented as mean \pm S.E.M.

HP-test with analogues **2**, **3**, and **4** showed a statistically relevant increase in pain-threshold compared to the referent substances on the 10th min and analogue **2** holding the highest threshold during the hole investigated period (fig. 1B).

Both JTC-801 injected 10 min before the peptides and Nal injected 20 min before the peptides significantly decreased the analgesic effect of all the investigated peptides.

We suggest that the analgesic effects of newly synthesized hexapeptide analogues are influenced by the nonselective opioid receptors inhibitor and the NOP-receptor inhibitor.

Acknowledgements

The research was supported by Grant DTK 02/61 of the National Research Fund, Bulgaria

References

- [1] Calo G., R. Guerrini, A. Rizzi, S. Salvadori, D. Regoli. *Br. J. Pharmacol.* **2000**, 129(7), 1261.
- [2] Heinricher, M. *Life Sci.* **2003**, 73, 813.
- [3] Dooley, C., Spaeth, C., Berzetei-Gurske, I., et al. *J. Pharmacol. Exp. Ther.* **1997**, 283(2), 735.

Binding, signaling and *in vivo* efficacy of novel peptidic CXCR4 agonists

Marilou Lefrançois¹, Marie-Reine Lefebvre¹, Philip Boulais¹, Jérôme Cabana¹, Christine Mona¹, Étienne St-Louis¹, Pierre Lavigne¹, Richard Leduc¹, Nikolaus Heveker², Emanuel Escher¹

¹Département de Pharmacologie, Université de Sherbrooke, Sherbrooke, Québec;

²Centre de recherche du CHU Ste-Justine, Université de Montréal, Montréal, Québec

E-mail: Emanuel.Escher@USherbrooke.ca

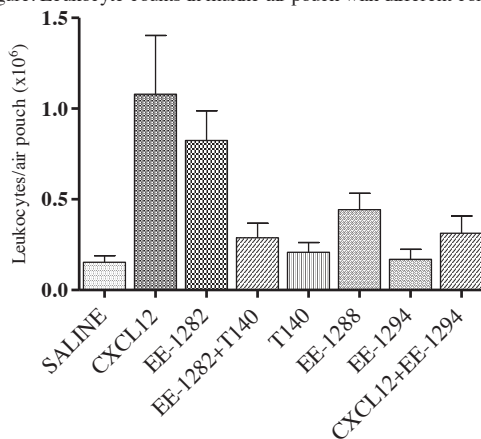
Introduction

Chemokine receptors have become the subject of much attention in recent years as research proved them to be therapeutic targets of great value. CXCR4 in particular, a 7-transmembrane domain receptor, has been identified as a major player not only in AIDS pathogenesis, but also cancer survival, proliferation and metastasis, among other pathologies. However, the implications of this receptor in many normal physiological processes make the clinical use of CXCR4 specific antagonistic drugs a tricky endeavour. Blocking the normal physiological functions of CXCR4 can prove problematic as toxicity may arise. Many antagonistic or inversely agonistic compounds are currently available, but none with agonistic efficacy similar to CXCL12.

Results and Discussion

Our research group has recently [2] discovered high affinity synthetic agonists by combining the inverse agonist T140 [3] to the N-terminal chain of the endogenous ligand CXCL12 (See table). A few chimeric peptides showed full agonist properties in the *in vitro* migration assays, and two have been selected for *in vivo* assays. The mouse assay consists in the subcutaneous injection of sterile air to form an air pouch and, six days later, by the injection of the chemotactic compound to be tested followed (5 hours later) by the collection of the liquid content of the pouch. Sterile saline, EE-1282 and EE-1288, two full agonists at 10 nM *in vitro*, antagonistic compounds T140 and EE-1294 (See figure). Competition assays between CXCL12 and the antagonistic chimeric compound showed that EE-1294 is able to antagonize the chemotactic response induced by CXCL12.

Figure: Leukocyte counts in murine air pouch with different compounds



Compound injected into air pouch (CXCL12: 10 µg, Others: 100 µg)

Table. Structure of the chimeric compounds	
EE-1288	$\begin{array}{c} \text{NH}_2\text{-R-R-Nal-C-Y-R-K-K} \\ \\ \text{HO-K-C-R-R-Y-P} \\ \text{NH}_2\text{KPVLSYRSA} \end{array}$
EE-1282	$\begin{array}{c} \text{NH}_2\text{-R-R-Nal-C-Y-R-K-K} \\ \\ \text{HO-K-C-R-R-Y-P} \\ \text{NH}_2\text{KPBSLSYR} \end{array}$
EE-1294	$\begin{array}{c} \text{NH}_2\text{-R-R-Nal-C-Y-R-K-K} \\ \\ \text{HO-R-C-K-R-R-Y-P} \\ \text{NH}_2\text{KPBSLSYR} \end{array}$
KPVLSYRSA-	N-terminus of CXCL12
B-	<i>p</i> -benzoyl-L-Phe

In order to assess the signalling pathways of EE-1282 and EE-1288, Gi activity was tested and compared to CXCL12 from the reduction of forskolin stimulated cAMP levels in HEK293 human CXCR4 transfected cells. At saturating concentrations, EE-1282 and EE-1288 reduced cAMP levels to a similar degree as CXCL12. This shows that the agonists not only induce *in vitro* chemotaxis, but also signal through the Gi pathway, similarly to CXCL12. In the *in vivo* air pouch assays, we have found that the agonistic chimeric peptides are capable of

inducing a chemotactic response in a mouse model of chemotaxis. These studies confirm that the T140-CXCL12 chimeric peptides connected through position 14 of T140 are able to activate CXCR4 by the same mechanism as the endogenous ligand. We are setting our sights on the binding mode of these compounds to the receptor. Photolabelling studies have allowed us to better understand the chimeric peptides by clarifying that there is indeed a difference in binding sites for the amino-terminal CXCL12-side chain of the agonistic versus the antagonistic peptides.

To conclude, we have found that these agonistic peptides were not only able to induce chemotaxis *in vitro*, but also *in vivo* in a mouse model, whereas such chimeras connected through position 12 of T140 are antagonists of CXCR4. This study as allowed us to observe that the agonists we have discovered that the chimeric agonists act in a similar way as CXCL12 at nanomolar concentrations, showing that the inverse agonist T140 was changed into an agonist by the addition of the CXCL12 N-terminus.

Acknowledgments

Special thanks to Pr Sylvie Marleau for sharing her laboratory's expertise on the air pouch technique. This research was supported by funds from the Canadian Institutes of Health Research.

References

- [1] Heveker, N.; Montes M.; Germeroth L.; Amara A.; Trautmann A.; Alizon M.; Schneider-Mergener J. *Curr. Biol.* **8**(7), 369-376 (1998).
- [2] Lefrançois, M.; Lefebvre MR.; Saint-Onge G.; Boulais PE.; Lamothe S.; Leduc R.; Lavigne P.; Heveker N.; Escher E. *ACS Med. Chem. Lett.*, **2**(8), 597-602 (2011).
- [3] Tamamura, H.; Xu Y.; Hattori T.; Zhang X.; Arakaki R.; Kanbara K.; Omagari A.; Otaka A.; Ibuka T.; Yamamoto N.; Nakashima H.; Fujii N. *Biochem Biophys Res Commun*, **253**(3), 877-82 (1998).

New structural and functional insights in SOCSs/kinases interaction

**P. Brandi¹, D. Marasco^{1,2}, I. De Paola^{1,2}, R. Pastore¹, A. Angelastro¹,
P. L. Scognamiglio^{1,2}**

¹Department of Biological Sciences, University of Naples “Federico II”, Naples, Italy;

²Institute of Biostructures and Bioimaging, National Research Council, Naples, Italy

daniela.marasco@unina.it

Introduction

Suppressor Of Cytokine Signalling (SOCS) proteins are negative feedback regulators of several pathways involved in immune response [1]. SOCS1 and SOCS3 have many similarities as well as some intriguing differences [2]. Both can block signalling by direct inhibition of JAK enzymatic activity yet apparently require different anchoring points within the receptor complex. While the primary SOCS1 interaction is with a critical pY residue within the JAK catalytic loop it interacts also with pY residues in the IFN α R1 and IFN γ R1 subunits in a JAK2-independent manner; the SOCS3–SH2 domain also interacts with Y1007 in JAK2, albeit with slightly lower affinity, but subsequent studies demonstrated a high affinity interaction with pY residues located within receptor subunits [3]. Mutagenesis studies identified small regions at the N-termini of the SOCS1 and SOCS3–SH2 domains, and at the C-terminus of the SOCS3–SH2 domain, which were critical for phosphotyrosine binding. Very recently [4] on the basis of structural and functional investigations a new non competitive inhibitory mechanism of SOCS3 toward JAK2 has been proposed: in it a ternary complex among these two proteins and gp130 occurs. In this complex gp130 phosphopeptide induces a conformational change of the KIR-ESS-SH2 domain of SOCS3 so that the protein can bind to the surface of JAK2. In order to gain insights in molecular discriminants for the interaction of both SOCS1 and SOCS3 toward JAK2 and TYK2 we designed and synthesized several peptides encompassing regions involved in proteins recognition.

Results and Discussion

In preliminary experiments the functional properties of the interaction through SPR technique between KIR region of SOCS proteins and pJAK2 were investigated. Here we confirmed that the interaction of SOCS1-KIR and pJAK2 is in the micromolar range [2]. Then we evaluated the interaction SOCS3-KIR: SOCS3-KIR interacts with pJAK2 with lower affinity respect to SOCS1, since SPR experiments did not reach saturation within the same concentration range used for SOCS1-KIR. Interestingly the addition of ESS residues to KIR region greatly improve this affinity reaching very low micromolar values. Actually experiments involving gp 130 peptides are on going .

To evaluate conformational properties of SOCS3 peptides CD solution analysis was carried as reported in Fig1. In aqueous solution they partially reflects the secondary structures within the whole protein (Fig 1A). In details the sequence KIR-ESS and KIR have similar CD spectra with minima at 199-203 nm and 220-222 nm, while ESS seems to be less

structured lacking of the minimum around 222 nm. We have also performed a TFE titration of KIR-ESS peptide (Fig1.B) that reached the maximum helical content at 20% TFE

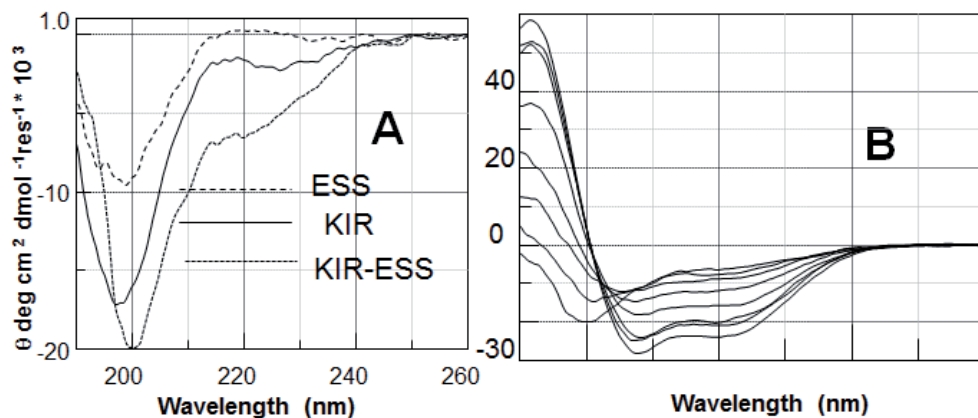


Fig. 1 Overlay of CD spectra of: **A** KIR-ESS, KIR and ESS region of SOCS3, **B** TFE titration of KIR-ESS peptide 0-60 % (v/v)

Actually through an Ala-scanning approach we have identified crucial residues on SOCS3 peptides for the interactions with JAK2, these have been rationally substituted with non-natural analogous amino acids in order to identify more potent sequences as mimetics of SOCS-3[2].

References

- [1] Yoshimura, A., T. Naka, et al. *Nat. Rev. Immunol.* 2007, 7, 454.
- [2] Doti, N., Scognamiglio, P.L., et al. *Biochem J.* 2012, 443, 231-40
- [3] Zeng, B., et al. *Cancer Res* 2008, 68, 5397-404
- [4] Baboon JJ, et al., *Immunity* 2012, 36, 239-250,
- [5] Marasco D, et al. *Curr Protein Pept Sci.* 2008;9:447-67

Elucidation of the structure-activity relationships of Apelin: Influence of unnatural amino acids on binding, signaling and plasma stability

Alexandre Murza^{1,2}, Alexandre Parent², Elie Besserer-Offroy^{1,2}, Nicolas
Beudet², Philippe Sarret², Eric Marsault¹

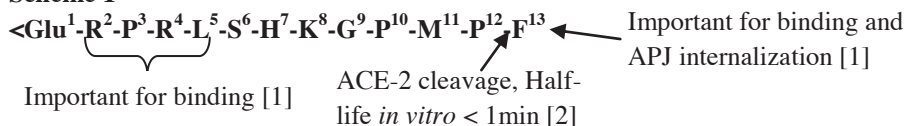
¹Department of Pharmacology; ²Department of Physiology and Biophysics, Faculty of
Medicine and Health Sciences, Université de Sherbrooke, Sherbrooke, QC, Canada

eric.marsault@usherbrooke.ca

Introduction

Apelin is the endogenous ligand of APJ receptor, a member of the G protein-coupled receptor superfamily. There is currently little information on the structure/activity relationship (SAR) of apelin (**Scheme 1**). In an effort to better delineate SAR, we synthesized analogs of apelin-13 modified at selected positions with unnatural amino acids, with a particular emphasis on the C-terminal portion and Pro¹². Analogs were then tested in binding and functional assays by evaluating G_{1/0} mediated reduction in cAMP levels and by assessing β -arrestin2 recruitment to the receptor. The plasma stability of new analogs was also assessed. Several were found to possess increased binding, biased β -arrestin2 signaling and higher stability compared to the parent peptide.

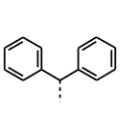
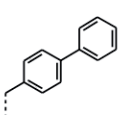
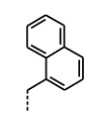
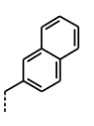
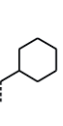
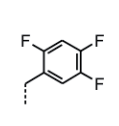
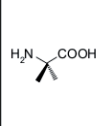
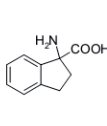
Scheme 1



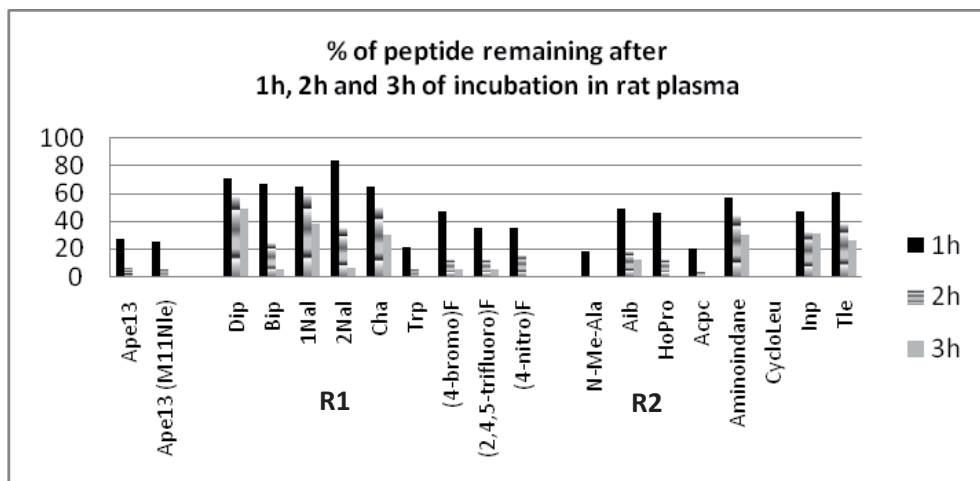
Results and Discussion

The C-terminal Phe¹³ of apelin-13 was replaced by unnatural amino acids (**R1, Table 1**). This set of modifications was performed on the Met11Nle analog which possesses a similar profile in terms of affinity, coupling to second messenger cascades, and stability to that of apelin-13 (IC₅₀ 5.7 nM ; EC₅₀ cAMP 1.9 nM ; EC₅₀ β -arr2 91 nM). Analogs Phe13Dip and Phe13Bip displayed a 10-fold difference in affinity suggesting that the C-terminal binding site is deep rather than wide. Interestingly, Phe13Cha exhibited an affinity comparable to that of apelin-13, indicating that hydrophobic interactions are necessary for binding, but aromatic, π -stacking type interactions are not essential. Phe13-1Nal and Phe13-2Nal showed an interesting trend in the β -arrestin2 pathway. Replacement of Pro¹² by Aib provided a very potent analog, and Pro12Aminoindane exhibited a biased signaling in β -arrestin2 pathway (**R2, Table 1**). Finally, C-terminally modified analogs showed significant improvements in plasma stability over apelin-13, whereas modification of Pro12 displayed more variable results (**Scheme 2**).

Table 1

	R1						R2	
								
	Dip	Bip	1Nal	2Nal	Cha	(2,4,5-trifluoro)F	Aib	Aminoindane
IC ₅₀ (nM)	88 ± 6	7.8 ± 0.4	14 ± 0.9	1.2 ± 0.1	2.3 ± 0.6	0.8 ± 0.2	0.7 ± 0.1	20 ± 1
EC ₅₀ cAMP (nM)	ND	10 ± 3	28 ± 2	20 ± 6	20 ± 8	20 ± 9	30 ± 13	13 ± 4
EC ₅₀ β-arr2 (nM)	630 ± 179	361 ± 64	522 ± 110	70 ± 11	170 ± 32	32 ± 9	46 ± 10	1204 ± 208

Scheme 2



Acknowledgments

Financial support from the Université de Sherbrooke, the Institut de Pharmacologie de Sherbrooke (IPS) and the Centre des Neurosciences de Sherbrooke (CNS).

References

- [1] Medhurst, A.D.; Jennings, C.A.; Robbins, M.J.; Davis, R.P.; Ellis, C.; Winborn, K.Y.; Lawrie, K.W.; Hervieu, G.; Riley, G.; Bolaky, J.E.; Herrity, N.C.; Murdock, P.; Darker, J.G., *J. Neurochem.*, **2003**, *84*, 1162-1172.
- [2] Vickers, C.; Hales, P.; Kaushik, V.; Dick, L.; Gavin, L.; Tang, J.; Godbout, K.; Parsons, E.; Baronas, E.; Hsieh, F.; Tummino, P., *J. Biol. Chem.*, **2002**, *277*, 14838-14843.

Fluorescence spectroscopy as a tool for studying protein-peptide interactions: Evaluation of talin affinity for β_3 integrin derived peptides

**Athina Gkesouli¹, Panagiotis Stathopoulos¹, Aggeliki Psillou²,
Anastasia S. Politou², Vassilios Tsikaris¹**

¹*Department of Chemistry, University of Ioannina, 45110 Ioannina, Greece;* ²*School of Medicine, University of Ioannina, 45110 Ioannina, Greece*

E-mail: btsikari@cc.uoi.gr

Introduction

The platelet receptor $\alpha_{IIb}\beta_3$ plays a critical role in the process of platelet aggregation and thrombus formation. Upon platelet activation the conformation of $\alpha_{IIb}\beta_3$ changes leading to an increased affinity for fibrinogen, which binds and forms bridges between adjacent platelets, assembling them into an aggregate. Importantly, the $\alpha_{IIb}\beta_3$ receptor is involved in the final common pathway for platelet aggregation, independently of the platelet stimulus. Thus, $\alpha_{IIb}\beta_3$ receptor antagonists should provide a wider range of protection against thrombosis compared to the other antiplatelet agents. For this reason antiplatelet therapy with $\alpha_{IIb}\beta_3$ antagonists merits a prominent role in the management of acute coronary syndrome (ACSs). The $\alpha_{IIb}\beta_3$ activation is regulated by “outside-in” and “inside-out” signaling. Among the protein-protein interactions, which contribute to «inside-out» signaling, that of talin with the β_3 cytoplasmic tail (β_3 CT) is the most important [1]. The aim of this research is to investigate the interaction of peptides derived from β_3 CT with talin in order to design a new class of inhibitors of the platelet aggregation, targeting the “inside-out” signaling. The peptide analogues which synthesized are: CF-R⁷³⁶AKWDTANNPLYKE⁷⁴⁹-NH₂, CF-R⁷³⁶AKWDTANNPLTYRKE⁷⁴⁹-NH₂, CF-K⁷¹⁶LLITIHDRKE⁷²⁶-NH₂, K⁷¹⁶LLITIHDRK E⁷²⁶-NH₂.

Results and Discussion

Peptide Synthesis: The peptides were synthesized by solid phase peptide synthesis on a Rink Amide resin using the Fmoc methodology. The coupling reactions were performed using a molar ratio of amino acid/DIC/HOBt/resin 3/3/3/1. The Fmoc deprotection was achieved with 20% piperidine/DMF. The peptides were cleaved from the resin and the protection groups with the mixture TFA/TIS/DMB 92.5/2.5/5 %v/v [2]. The peptides were purified with RP-HPLC and the correct molecular mass was confirmed by ESI-MS.

Fluorescence spectroscopy assays: Talin- β_3 CT binding was followed by: (a) anisotropy fluorescence and (b) by intrinsic fluorescence measurements. In (a) the fluorescence anisotropy of CF-labeled β_3 CT peptide was monitored upon addition of increasing amounts of talin (F2F3 domain) stock solution in PBS buffer. In (b) the intensity of the fluorescence emitted by the single tryptophan residue of talin was recorded upon addition of increasing amounts of β_3 CT peptide. Fluorescence anisotropy was followed at 522nm with an excitation wavelength of 492 nm. Emission spectra were recorded in the range 280-360 nm with an excitation wavelength of 280 nm. All measurements were performed at 20°C.

After each ligand addition, the samples were left to equilibrate for 5 minutes. Table 1 summarize the results obtained from fluorescence spectroscopy binding assays and compare them with the results obtained both of NMR spectroscopy and SRP technique.

Table 1: Fluorescence spectroscopy binding assays

<i>Talin Form</i>	<i>Integrin</i>	<i>Kd (nM)</i>	<i>Technique</i>	<i>Source</i>
Intact talin	β_3	550 \pm 30	SRP	Yan et al,2001 ^[3]
Talin rod	β_3	3400 \pm 500	SRP	Yan et al,2001 ^[3]
Talin head	β_3	92 \pm 4 2500 \pm 300	SRP	Yan et al,2001 ^[3]
Talin F2	β_3	540 \pm 40	SRP	Calderwood et al,2002 ^[4]
Talin F2F3	β_3	130 \pm 10	SRP	Calderwood et al,2002 ^[4]
Talin F2F3	β_3	(223 \pm 5) x10 ³	NMR	Oxley et al,2008 ^[5]
Talin F2F3	β_3 : 736-749	(3490 \pm 47) x10 ³	NMR	Oxley et al,2008 ^[5]
Talin F2F3	β_3 : (736-749)-pTyr	(6530 \pm 140)x10 ³	NMR	Oxley et al,2008 ^[5]
Talin F2F3	β_3 : 736-749	3.9 \pm 1.6	Fluorescence Anisotropy	This work
Talin F2F3	β_3 : (736-749)-pTyr	-	Fluorescence Anisotropy	This work
Talin F2F3	β_3 : 716-726	234 \pm 122	Intrinsic Fluorescence	This work
Talin F2F3	β_3 : 716-726	188 \pm 55	Fluorescence Anisotropy	This work

Conclusions

Both membrane proximal (MP) and membrane distal (MD) β_3 CT peptides bind to talin. Phosphorylation of the MD at Y747 abolishes the binding of talin to β_3 and it appears that isolated MD β_3 CT peptide is more tightly associated with talin than the intact β_3 subunit. This could result from the exposure in the peptide of the binding site that is otherwise partially masked in the context of the intact protein. Finally, these β_3 CT peptides could potentially be used as efficient inhibitors of “inside-out” signaling.

References

- [1] Ma Y.Q.; Qin J.; Plow E.F., *J. Thromb. Haemost.*, **2007**, 5,1345. Review.
- [2] Stathopoulos, P.; Papas, S.; Tsikaris, V. *J. Pept. Sci.* **2006**, 12, 227.
- [3] Yan B.; Calderwood D.A.; Yaspan B.; Ginsberg M.H., *J. Biol. Chem.*, **2001**, 276, 28164.
- [4] Calderwood D.A.; Yan B.; de Pereda J.M.; Alvarez B.G.; Fujioka Y.; Liddington R.C.; Ginsberg M.H., *J. Biol. Chem.*, **2002**, 277, 21749.
- [5] Oxley C.L.; Anthis N.J.; Lowe E.D.; Vakonakis I.; Campbell I.D.; Wegener K.L., *J. Biol. Chem.*, **2008**, 283, 5420.

Functionalized oligoprolines as multivalent scaffolds in tumor targeting

Patrick Wilhelm¹, Carsten Kroll¹, Helmut Mäcke², Helma Wennemers¹

¹ETH Zürich, 8093 Zürich, Switzerland; ²University Hospital Freiburg, Freiburg, Germany

E-mail: helma.wennemers@org.chem.ethz.ch

Introduction

Proline is unique among the proteinogenic amino acids for being not only cyclic but also bearing a secondary amine. This feature is responsible for a significant population of the Xaa-Pro amide bond in a *cis* conformation. Oligoprolines adopt already at short chain lengths of six residues the conformationally well-defined

polyproline II (PPII) helix in aqueous environments.¹ In this highly symmetrical left-handed secondary

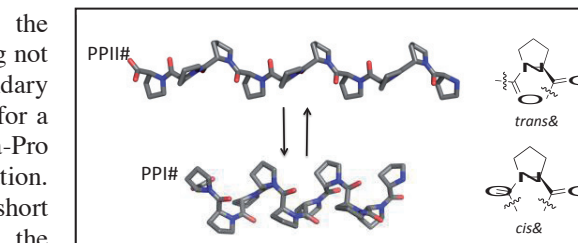
structure every third residue is stacked on top of each other in a distance of about 9.5 Å.¹ Oligoprolines change their conformation from PPII to the more compact right-handed polyproline I (PPI) helix in a more hydrophobic environment. These features remain when 4-azidoproline (Azp) is incorporated into oligoprolines and render such Azp-containing oligoprolines attractive as functionalizable scaffolds.² For example, the introduction of 4-azidoproline (Azp) at every third position lead to functionalizable sites in distances of about 9.5 Å.²

In the present project we are using these functionalizable scaffolds for covalently linking peptidic ligands that are able to bind to regulatory peptide receptors that are overexpressed in numerous human cancers. Use of untemplated radiolabeled analogues of such peptidic ligands is well preceded to localize cancer (Imaging) as well as for peptide receptor radiation therapy (PRRT).³

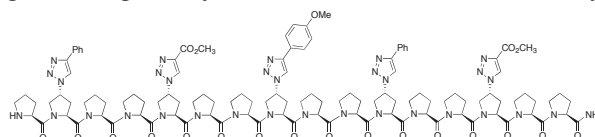
Results and Discussion

Previous studies showed that Azp containing oligoprolines can be functionalized efficiently by either copper(I)-catalyzed Huisgen 1,3-dipolar cycloaddition reactions (CuAAC) by reacting the azides with alkynes or by reduction of the azides to amines and further reaction with carboxylic acids to amides.^{2,4}

Both types of reactions proceed well both in solution phase as well as on-resin and provided the desired product in high yields.



Scheme 1: Models of the PPII helix with *trans* amide bonds (top) and the PPI helix with all *cis* amide bonds (bottom).



Scheme 2: Differentially functionalized oligoprolines by sequential peptide coupling and 'click chemistry' steps on solid phase

We chose to use the click-chemistry approach for this project since it offers benefits such as the functionalization of the oligoproline scaffold with different moieties by alternating peptide coupling and “click-reactions”.²

Recent results showed that a molecule bearing a bombesin-agonist and a bombesin-antagonist on an oligoproline scaffold with a specific spacing between these two recognition elements show a remarkably high tumor uptake *in vitro* and *in vivo* that is superior to not only monovalent analogues but also a divalent agonist with the same spacing between the two ligands.⁵

We are currently expanding this concept to other G-protein coupled receptor (GPCR), for examples, the clinically important Somatostatin receptor (hSst₂).⁴

Acknowledgments

BACHEM and the Swiss National Science Foundation supported this work. We thank the University of Basel where parts of this work were performed.

References

- [1] a) Rabanal, F.; Pons, L.M.; Giralt, E. *Biopolymers* **1993**, *33*, 1019.
b) Kakinoki, S.; Hirano, Y.; Oka, M. *Polym. Bull.* **2005**, *53*, 109.
- [2] a) Kuemin, M; Sonntag, L.-S.; Wennemers, H. *J. Am. Chem. Soc.* **2007**, *129*, 466.
b) Erdmann, R.S.; Kuemin, M.; Wennemers, H. *Chimia*, **2009**, *64*, 19.
c) Nagel, Y.A.; Kuemin, M.; Wennemers, H. *Chimia*, **2011**, *65*, 264.
- [3] a) Reubi, J.C.; Maecke H.R.; Krenning E.P. *J. Nucl. Med.* **2005**, *56*, 67S.
b) Fani, M.; Maecke, H.R.; Okarvi S.M. *Theranostics* **2012**, *2*, 481.
- [4] a) Kuemin, M.; Nagel, Y.A.; Schweizer, S.; Monnard, F.W.; Ochsenfeld, C.; Wennemers, H. *Angew. Chem. Int. Ed.* **2010**, *122*, 6468.
b) Upert, G.; Bouillère, F.; Wennemers, H. *Angew. Chem. Int. Ed.* **2012**, *51*, 4231.
- [5] Kroll, C; Mansi, R.; Braun, F.; Maecke, H.R.; Wennemers, H. *manuscript submitted*.
- [6] For example: a) Maecke, H.R.; Reubi, C.J. *J Nucl Med* **2011**, *52*, 841.
b) Reubi, J.C.; Waser, B. *Eur J Nucl Med Mol Imaging* **2003**, *30*, 781.

Heterofunctional dimer of endothelin ET_A antagonist and ET_B agonist “clicked” N-terminally on resin with second peptide component in solution

WA. Neugebauer,¹ M. Houde,¹ J. Labonté,¹ G. Bkaily,²
 P. D’Orléans-Juste¹

¹Department of Pharmacology; ²Department of Anatomy and Cell Biology, Université de Sherbrooke, Sherbrooke, (Québec), 3001, 12e Avenue Nord, Sherbrooke, J1H 5N4, Québec, Canada

E-mail: Witold.neugebauer@usherbrooke.ca

Introduction

The CuI-catalyzed azide-alkyne addition¹ (CuAAA), the useful variant of "click chemistry," has emerged as a powerful technique for specific addition [1]. That chemistry is also commonly used for conjugation, and cyclization of peptides. It is known that cyclization can increase the metabolic stability of peptides, as well as enhance potency or selectivity. Another useful application of the CuAAA, which we are reporting, is the *N*-terminal crosslink of two synergic peptides to gain their potency. CuAAA reaction is performed on solid phase (Merrifield resin) where one of the peptide components with azido group on the linker is “clicked” with second peptide component in solution, made by Fmoc strategy in partially protected form containing at *N*-terminal side alkyne group. CuAAA coupling is performed in DMF/*t*-BuOH/H₂O with presence of CuI and sodium ascorbate when reacting mixture was degassed. Linked peptides are cleaved finally from resin and purified. As an application example we picked two endothelin active peptide analogues: BQ123 derivative [2] (**Fig.1.**) (a highly potent and selective ET_A antagonist) and IRL-1620 derivative [3] (**Fig.2.**) (a potent and selective ET_B agonist). ET_A analog transformed to “click” component with azido group we kept on the resin while ET_B agonist with *N*-terminal alkyne derivative in solution proceeded to “click” addition. This new heterodimer (**Fig.3.**) has been validated in murine selective ET_A and/or ET_B bioassays. Peptide [I] BQ123NHAcapN3 (**Fig.1.**) was synthesized on Merrifield resin with Boc strategy and cyclized [4] on the resin. Peptide [II] IRL 1620 derivative (**Fig.2.**) was synthesized using continuous flow peptide synthesizer with Fmoc strategy.

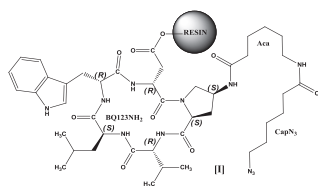


Fig. 1. ET_A component of heterodimer [I].

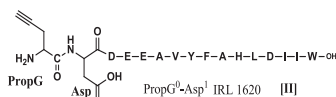


Fig. 2. ET_B component of heterodimer [II].

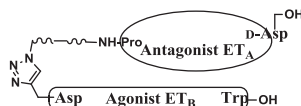
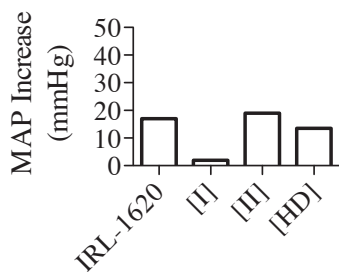


Fig. 3. ET_A antagonist and ET_B agonist heterodimer [HD] “clicked” on *N*-terminals.

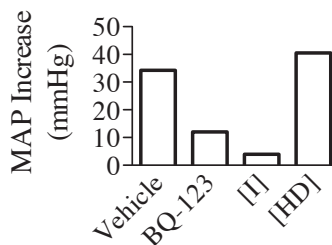
Results and Discussion

The final [HD] product was obtained in poor yield due to the difficult solubility of [II] with Fmoc group on PropG. The benefit of protecting that amino group diminishes the progress of “click” reaction. With another pair of peptides [bradykinin B1 and B2 agonists], the “click” reaction yield was much better. However, peptides [I] and [II] “clicked” in solution and gave a very good yield of the final product [HD]. For this particular example “clicking” those peptides in solution was then a better choice. Modification of both peptides [I] and [II] preserved their original analogues (BQ-123 and IRL-1620) activity. [HD] preserves the ET_B agonism of [II] but does not show ET_A antagonism in our conditions because its ET_B component is 1000-fold more powerful and would be lethal *in vivo* at doses for effective ET_A antagonism. A weaker ET_B agonist in the place of [II] would be required.

Mean Arterial Pressure Increase after
i.v. administration of IRL-1620, [I],
[II] or [HD]



Mean Arterial Pressure Increase elicited by
ET-1 0.5 nmol/kg (i.v.) after the administration of
Vehicle, BQ-123, [I] or [HD]



IRL-1620 : 10 nmol/kg

[I] : 1.7 μ mol/kg

[II] : 10 nmol/kg

[HD] : 20 nmol/kg

BQ-123 : 1.7 μ mol/kg n = 2 for each condition

ET-1 : 0.5 nmol/kg

Vehicle : PBS 0.1 M pH 7.4 + DMSO 10%

Acknowledgments

This work was supported by the Canadian Institutes for Health Research (M.H.)

References

- [1] Tornøe, C.W.; Christensen, C.; Meldal, M. *J. Org. Chem.* **2002**, *67*, 3057-3064.
- [2] Brosseau, J.-P.; Neugebauer, W.A.; Gobeil, F.Jr.; D'Orléans-Juste, P. *Adv. Exp. Med. Biol.* **2009**, *611*, 443-444.
- [3] Takai, M.; Umemura, I.; Yamasaki, K.; Watakabe, T.; Fujitani, Y.; Oda, K.; Urade, Y.; Inui, T.; Yamamura, T.; Okada, T. *Biochem. Biophys. Res. Commun.* **1992**, *184*: 953-959.
- [4] Neugebauer, W.; Gratton, J.-P.; Ihara, N.; Bkaily, G.; D'Orléans-Juste, P. *Peptides*, 1996, Proc. of the 24th EPS Symposium, Eds.:R.Ramage, R. Epton, Mayflower Scientific Ltd., Kingswinford, U.K. **1998**, pp.677-678.

Medicinal chemistry approach for solid phase synthesis of peptide mimetics of viperistatin disintegrin as lead compounds for $\alpha 1/\alpha 2$ integrin receptors

Momic Tatjana,¹ Katzhendler Jehoshua,¹ Marcinkiewicz Cezary,²
Eble A. Johannes,³ Lazarovici Philip^{1*}

¹School of Pharmacy Institute for Drug Research, Faculty of Medicine, The Hebrew University of Jerusalem, Jerusalem, 91120, Israel; ²Department of Biology, Temple University College of Science and Technology; Philadelphia, PA, 19122, USA; ³Center for Molecular Medicine, Department of Vascular Matrix Biology, Frankfurt University Hospital, Excellence Cluster Cardio-Pulmonary System, 60590 Frankfurt, Germany

philipl@ekmd.huji.ac.il

Introduction

A unique anti-cell adhesion peptide was isolated and characterized from *V. palestinae* snake venom, named Viperistatin. Viperistatin is a very potent and selective $\alpha 1\beta 1$ collagen receptor antagonist, blocking the adhesion of cells overexpressing $\alpha 1\beta 1$ integrin receptor to collagen IV with IC_{50} of 0.08 nM. Sequencing of this disintegrin revealed KTS recognition motif required for collagen binding, which was confirmed by a synthetic approach [1]. Since antagonists of $\alpha 1/\alpha 2$ integrin receptors are not available, Viperistatin provides a lead peptide towards synthesis of peptidomimetics with clinical relevance. In this study we investigated the structure-activity relationship (SAR) of over 60 linear peptides with KTS sequence, synthesized by solid phase methodology.

Results and Discussion

For all linear peptides that were synthesized, biological activity was investigated in adhesion assay *in vitro* with K562 cells overexpressing $\alpha 1$ integrin subunit, using the ligand collagen IV. The peptides with highest anti-adhesive activity were classified in four groups (Fig. 1). The most active peptide was L7 (group A), Viperistatin analogue with $K^{21}T^{22}S^{23}$ motif. Peptide L1 (group B), Obtustatin analogue (another closely related disintegrin), which sequence differs from L7 only at $Leu^{24} \rightarrow Arg^{24}$, respectively, had 6-fold decreased activity. This finding is in accordance with the published data for anti-adhesive potency of the above disintegrins [2]. It is proposed that this exchange of amino acid indicates that the positively charged extended side chain of Arg is better suited than alkyl side chain of Leu for establishing productive interaction with residues within the ligand-binding pocket of the $\alpha 1\beta 1$ integrin [2]. In another approach, it was shown that two Cys at the carboxy and amino termini of the L7 have a strong impact on its potency. Upon exchanging the two terminal Cys with two Gly, $\alpha 1$ -mediated anti-adhesive activity of both L8 and L2 peptides decreased drastically 35-fold and 7-fold, respectively. This finding was confirmed in experiments applying peptides with two terminal Gly and modifications in amino acids at the various positions over the sequence (groups A and B). None of the modification recovered anti-adhesive activity of peptides. The loss of anti-adhesive activity upon modification of two

terminal Cys in the linear peptides are further supporting their importance together with other cysteine bridges in disintegrin conformation [3].

Group A															
Peptide	18	19	20	21	22	23	24	25	26	27	28	29	30	IC ₅₀ (nM)	MW (Da)
L7		C	W	K	T	S	R	T	S	H	Y	C		0.105	1371.56
L8		G	W	K	T	S	R	T	S	H	Y	G		3.750	1279.38
L9		G	V	K	T	S	R	T	S	H	Y	G		>4	1192.30
Group B															
L1		C	W	K	T	S	L	T	S	H	Y	C		0.645	1328.54
L2		G	W	K	T	S	L	T	S	H	Y	G		>4	1236.35
L3		G	V	K	T	S	L	T	S	H	Y	G		>4	1149.27
Group C															
L38		G	V	V	G	D	K	T	R	T	S	G	K	0.650	1204.95
L39		V	G	D	K	T	S	R	T	S	K	T	S	>4	1266.37
L41		V	G	D	V	G	D	K	T	S	K	T	S	3.800	1193.28
Group D															
L22		G	W	R	T	S	K	T	R	T	S	G	K	0.700	1364.53
L23		G	V	R	T	S	K	T	R	T	S	G	K	3.800	1277.45
L24		G	V	R	T	S	R	T	R	T	S	G	K	>4	1305.46

Figure 1.

Peptides L38 (group C) and L22 (group D) exhibit anti-adhesive activity similarly to the activity of L1 peptide. In group C we tried to assemble multiple KTS and RTS combined with VGD integrin ligand motifs. It is clear that L38 peptide showed highest anti-adhesive potency in group C. It seems that combination of VGD and RTS sequences is endowing the peptide with the highest potency in the group C compared to peptides containing combination of VGD, RTS and KTS sequences. In group D peptide structures were based on two RTS sequences separated by two amino acids K,T or R,T. It is evident that two RTS sequences separated with K,T are increasing the potency of the peptides (L22 and L23). It is possible that higher potency of peptide with Lys²⁴ is associated with a structure-stabilizing the integrin-binding loop, which supports correct conformational presentation of RTS sequences, in this case to be recognized by $\alpha 1\beta 1$ integrin [2]. From analyzing the SAR of the synthesized linear peptides evaluated in the present study we concluded that the most potent linear peptide of 10-14 units is one with KTS motif, terminating at both ends with Cys and containing Arg at the position 24, generating an IC₅₀ of 0.105 mM (L7). In conclusion: This study provides a basic linear peptide sequence scaffold, containing KTS motif, and propose several requirements for the design of a future lead compound targeting $\alpha 1/\alpha 2$ integrin. We hypothesize that future synthesis addressing bending and cyclization of this lead compound will increase potency and selectivity of L7 derived peptides.

Acknowledgments

We acknowledge the financial support by the German Israeli Foundation (No. 994-3.9/2008), Nofar program of the Office of the Chief Scientist of the Israel Ministry of Industry, Trade and Labor and of Yissum-Translational Office of The Hebrew University of Jerusalem.

References

- [1] Kisiel, D.G.; Calvete, J.J.; Katzhendler, J.; Fertala, A.; Lazarovici, P.; Marcinkiewicz, C. *FEBS Lett.* **2004**, *577*, 478.
- [2] Brown, C.M.; Eble, J.E.; Marcinkiewicz, C. *Biochem J.* **2009**, *417*, 95.
- [3] Calvete, J.J.; Marcinkiewicz, C.; Sanz, L. *Curr. Pharm. Des* **2007**, *13*, 2853.

New antagonists of VEGFR-1: Design, synthesis and biochemical evaluation

**Wang-Qing Liu, Sylvain Broussy, Lei Wang, Nathalie Eilstein,
Marie Reille, Florent Huguenot, Michel Vidal**

*Laboratoire de Synthèse et Structure de Molécules d'Intérêt Pharmacologique UMR 8638
CNRS – Faculté de pharmacie, Université Paris Descartes. 75006 Paris, France*

E-mail: wangqing.liu@parisdescartes.fr

Introduction

Angiogenesis is a key step in the transition of tumors from a dormant state to a malignant state. The vascular endothelial growth factor (VEGF) is a major contributor to tumor angiogenesis. Its pro-angiogenic activity is mainly mediated through binding to two high-affinity tyrosine kinase receptors: VEGFR-1 and VEGFR-2. VEGF binding to these receptors triggers the activation of different signal transduction pathways responsible for the survival, proliferation and migration of endothelial cells^[1]. Consequently, VEGF/VEGFR system constitutes a target to interfere with tumour growth. An attractive approach is the development of peptides, or small-molecules, with a high affinity for the extracellular domain of the receptors to prevent VEGF binding. Based on available X-ray structure of the complex between VEGF and VEGFR-1 d2 region^[2], our laboratory had developed cyclic peptides that had shown VEGFR-1 binding affinities and cellular effects^[3,4,5].

We report here the design, synthesis and biological evaluation of C-terminal modified cyclic peptides and α -helix mimetics as antagonists of VEGF receptors, mimicking VEGF₁₆₅ receptor binding sites.

Results and Discussion

Crystal structure data and mutagenesis studies^[2,6] allowed the identification of two VEGF fragments strongly involved in receptor binding: (1) β 3- β 4 loop Cys⁶¹-Cys⁶⁸ which adopts a pseudocyclic form and interacts with the receptor through hydrophobic and ionic interactions; (2) α 1 helix Lys¹⁶-His²⁷, where F/Y/Y are essential residues for receptor binding. We thus design β 3- β 4 mimetic by modification C-terminus of cyclic peptides developed in our laboratory^[3,5] and α -helix mimetics by insertion of Leu/Aib residues or (d)Pro-Pro motif.

Peptide Synthesis: Linear peptides were synthesized by CEM-Liberty1 synthesizer, with HBTU/DIEA as coupling reagents, 20% piperidine as Fmoc deprotection solution. Coupling was performed for 10 minutes at 50°C and 25W microwave power. Fmoc-deprotection was realized for 3 minutes at 50°C and 25W microwave power. Cyclic peptides were prepared in solution from resin-free linear protected peptides with DIC/HOAt as cyclisation agents. The final peptides were deprotected as usually and purified by semi-preparative HPLC and their molecular weights were checked by ESI mass spectra.

Chemiluminescent VEGF competition assay: The assay was performed as previously described^[7]. Briefly, a fixed amount of biotinylated VEGF₁₆₅ (btVEGF) was incubated with the tested peptide in the presence of recombinant human VEGFR-1 adsorbed on a 96-well microplate. The btVEGF remaining after wash steps was detected by chemiluminescence thanks to HRP-conjugated streptavidin.

Peptide VEGFR1 binding affinity: At the indicated concentration, peptide VEGFR-1 binding affinity is expressed in percentage of btVEGF displaced. Higher is the percentage of btVEGF displaced the better peptides affinity.

β3-β4 mimetic peptide

c[YKDEGLEE]-NH-R

R	100μM (%)	316μM (%)
H ^[4]	17 ± 4	26 ± 5
CH ₂ -Ph	25 ± 4	38 ± 7
(CH ₂) ₂ -Ph	18 ± 5	23 ± 7
(CH ₂) ₂ -Ph(4-OH)	16 ± 5	30 ± 4
CH ₂ -Ph(3,4-diOH)	48 ± 2	58 ± 3
(CH ₂) ₂ -Ph(3,4-diOH)	42 ± 3	56 ± 2
CH ₂ -cyclohexyl	8 ± 2	18 ± 2
CH ₂ -CH(CH ₃) ₂	15 ± 3	33 ± 3
CH ₂ -CH ₂ -OH	24 ± 3	31 ± 6
CH ₂ -CH=CH ₂	27 ± 2	37 ± 4

α-helix mimetic peptide

Sequence	100μM (%)
Ac-KFMDVYQRSY-NH ₂	21 ± 3
FMRKYLEEYLR-NH ₂	18 ± 3
RTFLEEYLRKYLG-NH ₂	34 ± 3
Ac-PTWLEEYLRKYLG-NH ₂	34 ± 4
Ac-PTW-Aib-EEY-Aib-KKY-Aib-G-NH ₂	43 ± 4
c[FMYEY-(d)PP-EGKI]	22 ± 6
c[LQGM-(d)PP-FDYEY]	18 ± 4

C-terminal aromatic rings increase peptide affinity, *especially those carrying OH groups*; A small alkyl chain may increase peptide affinity; Steric hindrance diminish peptide affinity.

Hydrophobic Leu and Aib residues favorite helical conformations confirmed by CD spectra study; Phe residue of the original sequence can be replaced by Trp; dP-P motif containing cyclic peptides maintain peptide affinity.

All these three types of peptides are under further structure modifications and cellular anti-angiogenic effect investigations.

Acknowledgments

This project is financially supported by ANR (project SALSA, grant number ANR-2010-BLAN-1533, France).

References

- [1] Ferrara, N.; Gerber, H. P.; LeCouter, J. *Nat.Med.* **2003**, *9*, 669.
- [2] Wiesmann, C.; Fuh, G.; Christinger, H. W.; Eigenbrot, C.; et al. *Cell* **1997**, *91*, 695.
- [3] Gautier, B.; Goncalves, V.; Coric, P.; et al. *J. Med. Chem.* **2007**, *50*, 5135.
- [4] Goncalves, V.; Gautier, B.; Garbay, C. et al. *J. Pept. Sci.*, **2008**, *14*(6), 767.
- [5] Gautier, B.; Goncalves, V.; Diana, D.; et al. *J. Med. Chem.* **2010**, *53*, 4428.
- [6] Muller, Y. A.; Li, B.; Christinger, H. W.; et al. *Proc Natl Acad Sci U S A* **1997**, *94*, 7192.
- [7] Goncalves, V.; Gautier, B.; Garbay, C.; et al. *Anal. Biochem.* **2007**, *366*, 108.

New polypeptide azemiopsin from *Azemiops feae* viper venom is a selective ligand of nicotinic acetylcholine receptor

Maxim N. Zhmak^{1,2}, Yuri N. Utkin^{1,2}, Christoph Weise³, Igor E.
Kasheverov^{1,2}, Tatyana V. Andreeva², Elena V. Kryukova², Vladislav
G. Starkov², Daniel Bertrand⁴, Victor I. Tsetlin²

¹Syneuro, ul. Miklukho-Maklaya 16/10, 117997, Russia; ²Shemyakin-Ovchinnikov Institute of Bioorganic Chemistry Russian Academy of Sciences, ul. Miklukho-Maklaya 16/10, 117997, Russia; ³Institute of Chemistry and Biochemistry, Freie Universität Berlin, Thielallee 63, D-14 195 Berlin, Germany; ⁴HiQScreen Sàrl, 15, rue de l'Athénée, Case Postale 209, CH-1211 Geneva 12, Switzerland

E-mail: mzhmak@gmail.com

Introduction

Azemiops feae is a fairly rare snake and inhabits South China, North Myanmar, and North Vietnam. Due to limited availability, the venom of *A. feae* is not well studied. In the course of our study of *A. feae* venom, we have isolated a peptide, determined its primary structure and biological activity. Most of the research was carried out by employees of company "Syneuro"[1-3] in the frames of the project "Polypeptides of Burmese vipers *Azemiops feae* - from structure to mechanism of action and application in medicine".

Results and Discussion

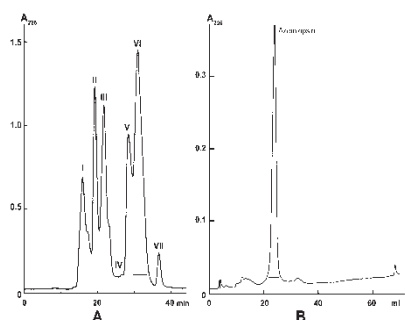


FIGURE 1. Isolation of azemiopsin.

Gel filtration of dried crude *A. feae* venom on Superdex HR75 resulted in seven polypeptide fractions (I–VII, Fig. 1A). The most abundant fraction VI was further separated by reverse-phase HPLC (Fig. 1B). The fractions obtained were analyzed by MALDI MS. The peptide with a molecular mass of 2540 Da (fraction marked by bar in Fig. 1B) was called azemiopsin and used for further study.

Biological activity of azemiopsin was tested in competition experiments using the membranes from the electric organ of *T. californica* as a source of muscle-type nicotinic acetylcholine receptor (nAChR) (IC₅₀ 0.18 μM). On the α7 nAChR azemiopsin was approximately 2 orders of magnitude less active (IC₅₀ 22 μM), and its interaction with acetylcholine-binding proteins (AChBPs) was even less potent (IC₅₀ 63 μM and 230 μM for *L. stagnalis* and *A. californica* proteins, respectively). Azemiopsin displayed pronounced toxicity when injected intraperitoneally into mice. The LD₅₀ was 2.6 mg/kg.

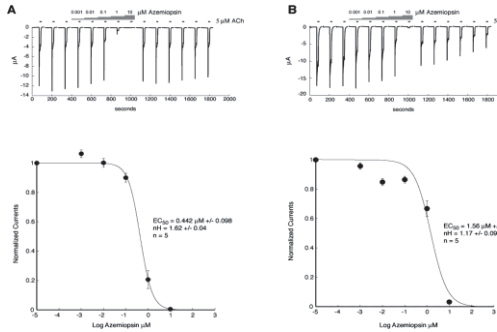


FIGURE 2. Inhibition by azemiopsin of human muscle-type nAChRs expressed in *Xenopus* oocytes.

Conclusion

We have isolated the peptide azemiopsin from *A. feae* venom and demonstrated that it is a potent antagonist at adult muscle-type nAChR, with less activity at $\alpha 7$ nAChR. Although azemiopsin resembles waglerins in the C-terminal part, it is the first natural toxin that blocks nAChR and does not contain disulfide bridges. This lack of disulfide bridges means that azemiopsin will be easier to prepare and handle than other peptides possessing nAChR-blocking activity. It is a better template for molecular design and thus has the potential to be a useful tool in neurotransmitter research and in biomedical applications.

Acknowledgments

This work was supported in part by the Russian Foundation for Basic Research (grant No 12-04-01523) and Ministry of Education and Science of the Russian Federation (state contract no. 16.512.11.2207).

References

- [1] Utkin, Y.N.; Weise, C.; Kasheverov, I.E.; Andreeva, T.V.; Kryukova, E.V.; Zhmak, M.N.; Starkov, V.G.; Hoang, N.A.; Bertrand, D.; Ramerstorfer, J.; Sieghart, W.; Thompson, A.J.; Lummis, S.C.; Tsetlin, V.I. *J. Biol. Chem.* **2012**, *3*, 287(32), 27079.
- [2] Utkin, Y.N.; Weise, C.; Hoang, N.A.; Kasheverov, I.E.; Starkov, V.G.; Tsetlin, V.I. *Dokl. Biochem. Biophys.* **2012**, 442, 33.
- [3] Utkin, Y.N.; Zhmak, M.N.; Andreeva, T.V.; Weise, C.; Kryukova, E.V.; Tsetlin, V.I.; Kasheverov, I.E.; Starkov, V.G. Patent application RU2011143065.

Azemiopsin was tested against the acetylcholine-evoked currents in *Xenopus* oocytes heterologously expressing human muscle-type nAChR and a concentration-dependent blockade was observed. Its affinity for adult $\alpha 1\beta 1\epsilon\delta$ and fetal $\alpha 1\beta 1\gamma\delta$ forms of nAChR was different; it blocked the adult form ($EC_{50} = 0.44 \mu\text{M}$) more potently than the fetal one ($EC_{50} = 1.56 \mu\text{M}$). The toxic effect was readily reversible. After washing out the toxin for 2 min, complete recovery of the response was observed.

Novel neutrophil-activating cryptides hidden in mitochondrial cytochrome *c*

**Yoshinori Hokari¹, Tetsuo Seki¹, Hiroko Nakano², Yuko Matsuo³,
Akiyoshi Fukamizu¹, Eisuke Munekata², Yoshiaki Kiso⁴,
Hidehito Mukai^{2,3,4}**

¹*Graduate School of Life and Environmental Sciences, University of Tsukuba, Tsukuba, Ibaraki 305-8577, Japan;* ²*Institute of Applied Biochemistry, University of Tsukuba, Tsukuba, Ibaraki 305-8572, Japan;* ³*Laboratory of Peptide Biosignal Engineering, Mitsubishi Kagaku Institute of Life Sciences, Machida, Tokyo 194-8511, Japan;* ⁴*Laboratory of Peptide Science, Nagahama Institute of Bio-Science and Technology, Nagahama, Shiga 526-0829, Japan*

E-mail: hmukai-endo@umin.ac.jp

Introduction

While neutrophils infiltrate into damaged sites immediately after tissue injury, endogenous factors which induce their acute transmigration and activation have not been thoroughly elucidated. For the candidates, we recently identified two novel neutrophil-activating cryptides, mitocryptide-1 (MCT-1) and mitocryptide-2 (MCT-2), which were hidden in mitochondrial cytochrome *c* oxidase and cytochrome *b*, respectively [1-5]. In addition, the presence of many unidentified neutrophil-activating peptides other than MCT-1 and MCT-2 was observed [3-5]. These findings suggest that neutrophils are regulated by many unidentified peptides. Here, we further purified a cytochrome *c*-derived neutrophil-activating octadecapeptide from porcine hearts based on the activity to induce β -hexosaminidase release from neutrophilic/granulocytic differentiated HL-60 cells. Structure-activity relationships of the purified peptide on β -hexosaminidase release from the neutrophilic/granulocytic differentiated HL-60 cells were also investigated to elucidate which parts of cytochrome *c* are responsible to induce neutrophilic activation.

Results and Discussion

Neutrophil-activating peptides were extracted and purified based on the activity to induce β -hexosaminidase release from the neutrophilic/granulocytic differentiated HL-60 cells from healthy porcine hearts as described previously with modifications [3, 4]. The amino acid sequences of the substances in the purified fraction were analyzed by automated Edman degradation. The peptide sequence of a substance was revealed as Leu-Glu-Asn-Pro-Lys-Lys-Tyr-Ile-Pro-Gly-Thr-X-Met-Ile-Phe-Ala-Gly-Ile-OH, where X is an unidentified amino acid (Fig. 1). The sequence of this octadecapeptide was indicated to be identical to that of porcine mitochondrial cytochrome *c* (68-85). The synthetic octadecapeptide based on the sequence of cytochrome *c* (68-85) was confirmed to activate neutrophilic/granulocytic differentiated HL-60 cells, demonstrating that the peptide was a neutrophil-activating cryptide produced from cytochrome *c*. We named this neutrophil-activating cryptide as mitocryptide-CYC (MCT-CYC).

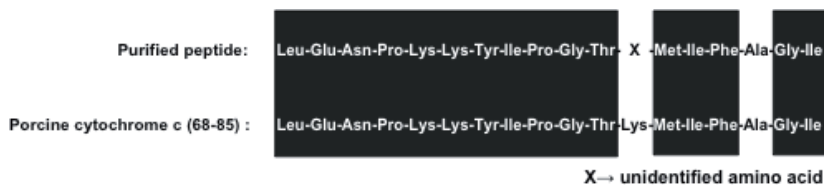


Fig. 1. Amino acid sequences of the purified peptide determined by Edman degradation and porcine cytochrome c (68-85) (MCT-CYC).

We then investigated structure-activity relationships of human cytochrome *c* and its related derivatives on β -hexosaminidase release from neutrophilic/granulocytic differentiated HL-60 cells. The cytochrome *c* (68-104) with a MCT-CYC sequence at its N-terminus was shown to induce β -hexosaminidase release (EC_{50} : cytochrome *c* (68-104), 7×10^{-6} M), even though cytochrome *c* itself did not. MCT-CYC [cytochrome *c* (68-85)] showed approximately two-fold higher efficacy on the induction of β -hexosaminidase release but required higher concentrations for the stimulation than cytochrome *c* (68-104). Moreover, cytochrome *c* (70-85) induced β -hexosaminidase release at 100 times lower concentrations than MCT-CYC [cytochrome *c* (68-85)] with the same maximum response (EC_{50} : cytochrome *c* (70-85), 4×10^{-6} M). In addition, cytochrome *c* (70-88) required higher concentrations than cytochrome *c* (70-85), while exhibiting the same efficacy. These results indicate that peptides derived from the C-terminal side of cytochrome *c* activated neutrophilic/granulocytic cells and that cytochrome *c* (70-85) was the most potent cryptide. Since cytochrome *c* is known to be involved in the apoptotic process, our present results suggest that cryptides produced from cytochrome *c* play an important role in scavenging toxic debris from apoptotic cells by neutrophils.

Acknowledgments

The present study was supported by research grants from the Ministry of Education, Culture, Sports, Science and Technology, Japan (No. 21603014; 40089107) and Nagase Science and Technology Foundation.

References

- [1] Mukai, H.; Hokari, Y.; Seki, T.; Nakano, H.; Takao, T.; Shimonishi, Y.; Nishi, Y.; Munekata, E. *Peptides, The Wave of the Future, Proceedings of the Second International and the Seventeenth American Peptide Symposium*; Lebl, M., Houghten, R. A. Eds.; American Peptide Society: San Diego, **2001**, 1014.
- [2] Mukai, H.; Matsuo, Y.; Kamijo, R.; Wakamatsu, K. *Peptide Revolution: Genomics, Proteomics & Therapeutics, Proceedings of the Eighteenth American Peptide Symposium*; Chorev, M. and Sawyer, T. K. Eds.; American Peptide Society: San Diego, **2003**, 553.
- [3] Mukai, H.; Hokari, Y.; Seki, T.; Takao, T.; Kubota, M.; Matsuo, Y.; Tsukagoshi, H.; Kato, M.; Kimura, H.; Shimonishi, Y.; Kiso, Y.; Nishi, Y.; Wakamatsu, K.; Munekata, E. *J. Biol. Chem.*, **2008**, *283*, 30596.
- [4] Mukai, H.; Seki, T.; Nakano, H.; Hokari, Y.; Takao, T.; Kawanami, M.; Tsukagoshi, H.; Kimura, H.; Kiso, Y.; Shimonishi, Y.; Nishi, Y.; Munekata, E. *J. Immunol.*, **2009**, *182*, 5072.
- [5] Ueki, N.; Someya, K.; Matsuo, Y.; Wakamatsu, K.; Mukai, H. *Biopolymers (Pep. Sci.)*, **2007**, *88*, 190.

N-Terminal modifications of highly potent bradykinin agonists and antagonists for structure activity relationship and cell imaging studies

Lajos Gera,¹ Caroline Roy,² Marie-Thérèse Bawolak,² Xavier Charest-Morin,² Robert S. Hodges,¹ François Marceau²

¹Department of Biochemistry and Molecular Genetics, University of Colorado Denver, Aurora, CO 80045, USA; ²Centre de recherche en rhumatologie, Centre Hospitalier Universitaire de Québec, Québec, QC, Canada G1V 4G2

E-mail: Lajos.Gera@ucdenver.edu

Introduction

The *N*-terminal modification of biologically active peptides is an important research tool because it may have the potential to improve the peptide biostability, hydrophobicity, and activity without adversely affecting other pharmacokinetic properties generally. Fluorophore-acylated peptides are also used in biological studies. We approached this modification to develop potent anti-cancer bradykinins and analogs for cell imaging studies.

Results and Discussion

Acylation and dimerization of peptides can result in an increase of the peptides biological activity. We explored this possibility with our highly potent Bradykinin (BK) antagonist. *N*-terminal modification of B9430 (DArg-Arg-Pro-Hyp-Gly-Igl-Ser-DIgl-Oic-Arg; Igl: α -(2-indanyl)glycine; Oic: octahydroindole-2-carboxylic acid) with a bis-imidate acylating agent, which combined the acylation and the dimerization in one step, provided the highly potent anti-cancer peptide dimer B9870 [Suim-(B9430)₂; suberimidyl] with retained BK-antagonist activity. The recent developed fluorescent kinin agonists and antagonists appear as promising probes to evaluate cell surface expression and subcellular traffic of kinin receptors. We designed and synthesized the full set of fluorescent ligands by extending both our agonist and the antagonist peptides with 5(6)-carboxyfluorescein (CF) and the ϵ -aminocaproyl (ACA) optional spacer. Other carboxylic acid cargos (chlorambucyl: CHB; biotiny: BIO; AlexaFluor-350: AF350; ferrocenoyl: FeC; cetirizine: CTZ) or with fluorescein isothiocyanate: FTC) in part to test the idea of functional cargos targeted to receptors by the peptide structure. The pharmacological evaluation of B₂ receptor (B₂R) ligands with *N*-terminal extensions as compared with the reference agonist (BK, B9972) and antagonist (B9430) is given in Table 1. Synthesis methods (Tab. 1.) are provided as: 1) The peptides were synthesized by solid-phase technology on Merrifield resin using Boc-chemistry. Boc-protected amino acids were coupled using BOP/HOBt/DIEA. The same coupling procedure was used for the *N*-terminal extension with ϵ -ACA, BIO, CHB, and CF as that for the Boc-amino acids. 2) The BK was synthesized on Wang resin using BOP/HOBt/DIEA coupling reagents. The ϵ -ACA-BK was labeled with 1.2 equiv. AF350

Table 1. Pharmacological evaluation of the *N*-terminal modified bradykinins

Peptides	³ H]BK binding IC ₅₀ at B ₂ R (nM) ^a	Human umbilical vein contractility (bioassay for the BK B ₂ R)		Synthesis Methods
		Antagonists: pA ₂	Agonists: contraction EC ₅₀ (nM)	
BK B₂R agonists				
BK	7-11.1 ^a	-	10-19	1
CF-BK	>10,000 ^b	-	Inactive at 6.8 μM	1
CF-ε-ACA-BK	800 ^c	-	>10,000 ^d	1
CHB-BK	66	-	6000	1
CHB-ε-ACA-BK	20	-	6000	1
AF350-ε-ACA-BK	871	-	420	2
CTZ-ε-ACA-BK	125	-	6000	3
FeC-ε-ACA-BK	529	-	3300	3
B9972 ^c	40, 68	-	13	1
FTC-B9972	2205	-	108	4
B₂R antagonists				
B9430	16, 27	7.70	-	1
BIO-B9430	16	-	-	1
CF-ε-ACA-B9430	20	6.83	-	1
FTC-B9430	145	6.96	-	4

^aValues reported were generally obtained in competition with [³H]BK (3 nM) binding to recombinant B₂R-GFP stably expressed in HEK 293 cells, except when indicated otherwise. ^bValues obtained in competition with [³H]BK (3 nM) binding to the population of naturally expressed human B₂R in HEK 293a cells. ^cValues obtained in competition with [³H]BK (3 nM) binding recombinant myc-B₂R transiently expressed in HEK 293a cells ^d21.8% of the maximal BK-induced response at 6.3 μM. IC₅₀: half-maximal inhibitory concentration; EC₅₀: half-maximal effective concentration. ^eBK B₂R agonist (DArg-Arg-Pro-Hyp-Gly-Igl-Ser-Oic-Igl-Arg).

carboxylic acid succinimidyl ester in the presence of HOBt and DIEA. The peptide was cleaved from the resin with TFA:H₂O:TIS (95:2.5:2.5, v/v/v). 3) The ε-ACA-BK was synthesized as above using Fmoc-chemistry. The CTZ and the FeC were activated by BOP/HOBt/DIEA in DMF and coupled separately to the ACA-BK on the resin. 4) The peptides were synthesized on Merrifield resin using Boc-chemistry. The HPLC purified peptides were acylated selectively at the *N*-terminal with fluorescein-5-isothiocyanate. All of the crude peptides were purified by HPLC. These labeling results suggest that our B₂R agonists and antagonist tolerate to a certain level *N*-terminal sequence extension, with the generation of novel structure-activity information, application to cell imaging using ligands conjugated with fluorophores and prospect for functionally active cargoes [1].

Acknowledgements

This presentation is dedicated to the memory of Professor John M. Stewart.

References

[1] Gera, L.; Roy, C; Bawolak, M.T.; Charest-Morin, X.; Marceau, F. *Peptides*. **2012**, 34, 433.

Peptide based artificial receptors for carbohydrate anthrose detection

Andreja Jakas¹, Predrag Cudic², Nina Bionda², Josipa Suć¹, Kristina Vlahoviček-Kahlina¹, Mare Cudic²

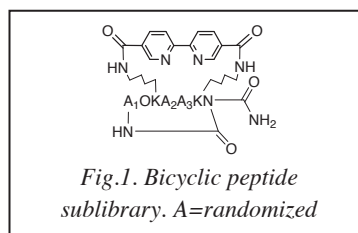
¹Rudjer Boskovic Institute, Zagreb, Croatia; ²Torrey Pines Institute for Molecular Studies, Port St. Lucie, Florida, USA
E-mail:jakas@irb.hr

Introduction

Peptide cyclization represents particularly interesting approach for the design of artificial receptors for carbohydrates, because cyclic peptides provide the possibility of having a spherical lipophilic binding site of appropriate size and shape for a particular carbohydrate substrate.[1] The presence of hydrogen donor/acceptor groups within a three-dimensional structure permits carbohydrate substrates to be encapsulated, thereby allowing their binding in water. Recently, it was found that one of the components of the *B. anthracis* exosporium is a collagen like protein whose carbohydrate portion is composed of the tetrasaccharide with the highly specific monosaccharide upstream terminal, named anthrose.[2] Since anthrose was not found on other bacterial spores, including those closely related to *B. anthracis*, this monosaccharide is an attractive target for the development of new *B. anthracis* detection and identification methods. Considering a typical structure of binding site found in carbohydrate binding proteins such as lectins, we have designed a rigid three-dimensional artificial bicyclic peptide receptor modeled on the cyclic cationic peptide antibiotic polymyxin B, (Fig.1.). In order to identify individual bicyclic peptides displaying both high affinity and selectivity toward anthrose, we have prepared this bicyclic peptide combinatorial library by the process of divide, couple and recombine using standard Fmoc solid-phase peptide synthesis.[3] Prepared combinatorial library is screened for anthrose binding in fluorescence-based assay, and individual bicyclic peptides with enhanced affinity toward anthrose are identified by the positional scanning deconvolution process.[3]

Results and Discussion

We have synthesized 60 sublibrary of bicyclic peptide, 20 for each A position based on the 20 natural amino acids (Fig.1.). Briefly, our synthesis included attachment of the orthogonally protected amino acid Asp *via* side chain to the Rink amide resins (yields 75%-80%), peptide chain elongation using standard Fmoc-chemistry, on-resin head-to-tail cyclization, and in the final step on-resin attachment of the bipyridine dicarboxylate moiety.



Screening for the binding affinity of the bicyclic peptide combinatorial library against synthetic anthrose [4] and control glucose lipidic derivatives (Fig. 2.) was performed in 384 well-plate format. Glucose and anthrose derivatives were immobilized on well surface through hydrophobic interactions. Screening assay is based on the fluorescence

determination of retention of library members to the immobilized sugars after extensive washing with buffer (Fig. 3.).

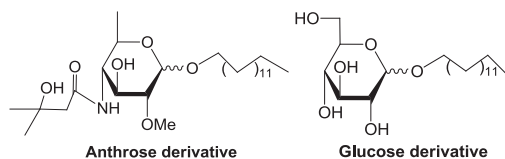


Fig.2. Anthrose and glucose lipidic derivatives for microtiter plate analysis.

The highest affinities and selectivities toward anthrose were obtained for mixtures containing Ala, Phe, Val, Trp, Leu, Asn at position 1, Asp, Cys, Asn, Val, His at position 2 and Met, Phe, His at position 3 of the designed bicyclic heptapeptide (Fig.1). Based on the screening data, we have synthesized 90 individual bicyclic peptides currently undergoing further evaluation for anthrose binding.

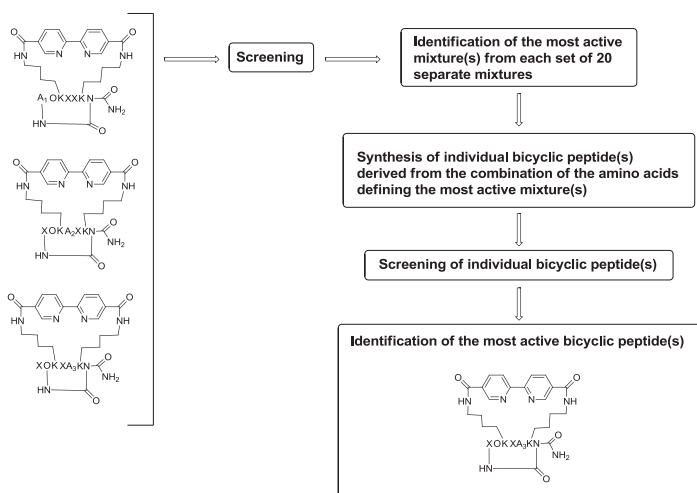


Fig.3. Deconvolution method for library screening.

Acknowledgments

We thank Mrs. Milica Perc for technical assistance. We gratefully acknowledge the financial support of the NATO Public Diplomacy Division, Science for Peace and Security Programme (SfP 983154) and Ministry of Science, Education, Technology and Sport of the Republic of Croatia (098-0982933-2936).

References

- [1] Rodriguez, M. C.; Cudic, P., *Chim. Oggi*, **2011**, *29*, 36-39.
- [2] Daubenspeck, J. M., Zeng, H., Chen, P., Dong, S., Steichen, C. T., Krishana, N. R., Prichard, D. G., Turnbough, C. L., *J. Biol. Chem.* **2004**, *279*, 30945-30953.
- [3] Pinulla, C., Appel, J. R., Houghten, R. A., *Methods in Molecular Biology*, **1996**, *66*, 171-179.
- [4] Dhénin, S. G. Y., Moreau, V., Morel, N., Nevers, M. C., Volland, H., Créminon, C., Djedaini-Pilard, F., *Carbohydr. Res.*, **2008**, *343*, 2101-2110.

Pharmacological activity of new cyclic endomorphin analogs

R. Perlikowska¹, J. Piekialna¹, J. Fichna¹, J.C. do-Rego², A. Janecka¹

¹*Laboratory of Biomolecular Chemistry, Medical University of Lodz, Lodz, Poland;*

²*Service Commun d'Analyse Comportementale (SCAC), Université de Rouen, Rouen, France*

E-mail:renata.perlikowska@umed.lodz.pl

Introduction

Cyclization of linear sequences is a well-known approach used to restrict the flexibility of peptides. Cyclization often increases selectivity of peptides towards one specific receptor type, improved metabolic stability and generally increases lipophilicity, which often improves the blood-brain barrier permeability of peptides.

In our previous study [1] we have reported on the synthesis of a cyclic endomorphin-2 (EM-2) analog, Tyr-c(D-Lys-Phe-Phe-Asp)-NH₂, which elicited analgesia after peripheral administration. Encouraged by the fact that this analog was able to cross the blood-brain barrier we designed and synthesized a new series of cyclic pentapeptides of a general structure:

where: Waa-c(Xaa-Yaa-Zaa-Asp)-NH₂,
 Waa = Tyr or Dmt,
 Xaa = D-Lys or Lys,
 Yaa = Paba, Tic, D-1-Nal, D-2-Nal, Trp, Phe,
 Zaa = Phe, D-2-Nal.

The analogs were obtained by cyclization through an amid bond between the side-chain amino and carboxy groups of the diamino and dicarboxy amino acids introduced into the peptide sequence in positions 2 and 5.

Pharmacological properties of the obtained peptides were characterized *in vitro* and *in vivo*. Their analgesic effect was assessed in the hot-plate test in mice (supraspinally mediated analgesia), after intracerebroventricular (i.c.v.) and intravenous (i.v.) administration.

Results and Discussion

Two of the new cyclic analogs, Dmt-c(D-Lys-D-1-Nal-Phe-Asp)-NH₂ (analog 2) and Dmt-c(D-Lys-D-2-Nal-Phe-Asp)-NH₂ (analog 3), showed very high affinity for the μ -opioid receptor and resistance to enzymatic degradation. As it was shown in the hot-plate test after i.c.v. administration only analog 3 produced a dose-dependent analgesic action, significantly stronger and longer lasting than that of EM-2. The maximal response was observed 30 min after peptide administration for analog 3 and about 8-10 min for EM-2 and lasted about 1 h and 25 min, for these two peptides, respectively. β -Funtaltrexamine (β -FNA) partially reversed analgesic effect of analog 3, indicating that its action was mediated by the μ -opioid receptor. Antinociception after i.v. administration of analog 3 was observed only at high doses showing limited ability of this peptide to enter the central nervous system (CNS) (data not shown).

Taken together, two of the novel cyclic analogs of EM-2, displayed high μ -opioid receptor affinity and possess exceptional metabolic stability, but only one showed supraspinally-mediated analgesia after i.c.v. administration. Analog 3, with Dmt in positions 1 and D-2-Nal in position 3, retained agonist properties of our earlier cyclic peptides of similar structure, what may be optional approach to the development of new drug candidates, but further modifications are necessary to enhance the blood-brain barrier permeability.

Acknowledgments

This work was supported by grants from Polish Ministry of Science and Higher Education No IP2011 040871 (to R.P.), a grant „Start” from the Foundation for Polish Science (to R.P.) and a grant from the Medical University of Lodz No 505-04-003, . The authors wish to thank Jozef Cieslak for his excellent technical assistance.

References

- [1] Perlikowska, R.; do-Rego, J.C.; Cravezic, A.; Fichna, J.; Wyrebska, A.; Toth, G.; Janecka, A. *Peptides* **2010**, *31*, 339.

Conformational properties and energetic analysis of Aliskiren in solution and receptor site

**Aggeliki Politi^{a,b}, Georgios Leonis^b, Haralambos Tzoupis^{a,b}, Dimitrios
Ntountaniotis^c, Manthos G. Papadopoulos^b, Simona Golic
Grdadolnik^{d,e}, Thomas Mavromoustakos^{a,b}**

^a*Department of Chemistry, Laboratory of Organic Chemistry, University of Athens,
Zographou, Athens 15771, Greece;* ^b*National Hellenic Research Foundation, Institute of
Organic and Pharmaceutical Chemistry, 48 Vas. Constantinou, Athens 11635, Greece;*
^c*Department of Chemistry, University of Patras, Patras 26500, Greece;* ^d*Laboratory of
Biomolecular Structure, National Institute of Chemistry Hajdrihova 19, SI-1001 Ljubljana,
Slovenia;* ^e*EN-FIST Centre of Excellence, Dunajska cesta 156, SI-1000 Ljubljana, Slovenia*

E-mail:haralambostz@gmail.com

Introduction

The endocrine renin-angiotensin-aldosterone system (RAAS) is paramount in the regulation of cardiovascular and renal functions. The activation of the RAAS pathway is caused by different signals that trigger the release of renin, which cleaves angiotensinogen to produce decapeptide angiotensin I. Angiotensin I is next converted by angiotensin-converting enzyme (ACE) to the active peptide angiotensin II, which increases the blood pressure. Renin is a highly specific aspartic protease, consisting of 340 amino acids. The cleavage of the Leu10-Val11 amide bond of angiotensinogen to produce angiotensin I, is the rate limiting step in the RAAS cascade. Thus inhibition of this step would be an effective therapeutic scheme against hypertension.

The active site of the protein, as with other members of the aspartic proteases (e.g. HIV-1 protease) consists of two catalytic triads, Asp32/215, Thr33/216, and Gly34/217. Inhibitors bind to the active site of renin adopting an extended conformation. Aliskiren was approved in 2007 by the FDA as the first orally active, direct renin inhibitor for the treatment of hypertension and is a highly potent inhibitor for human renin. Aliskiren has IC₅₀ in the low nM range (0.6 nM) and biological half-life of 24 h[1].

Results and Discussion

MD of Aliskiren in DMSO and Clustering. The cluster analysis on the MD trajectory of aliskiren in DMSO produced 2 major clusters. Cluster 1 (73%) suggested an extended (“open”) conformation for aliskiren, whereas cluster 2 (27%) denoted a “bent” structure. Further QM optimizations and distance calculations showed that of the distances derived from the ab initio methods present similarities with the NMR experimental data. The great structural similarity between the representative conformation of cluster 1 and the crystal structure of aliskiren is denoted by an 1.4 Å RMSD. The NMR and the computational results showed that: (a) aliskiren is a flexible molecule and (b) adopts both “open” and “closed” conformations, however the extended conformer is dominant.

Conformational Properties of Aliskiren in Receptor site. A Ca RMSD calculation with respect to the crystal structure of the complex yielded an average value of $\approx 1\text{\AA}$, suggesting the simulated structure equilibrates towards conformations that resemble the crystal structure. Unbound renin appears more flexible and with a higher deviation from the crystal structure, RMSD $\approx 1.65\text{\AA}$. H-bonding analysis on the complex revealed a strong HB network. At least five HB interactions stabilize aliskiren inside renin in a bound structure. Active site residues Asp32/215 and Gly34 are primarily involved in binding aliskiren inside the cavity, Tyr14, Arg74 and Ser76 further contribute to the strengthening of the interaction. The region around Ser76 (Arg74-Tyr75-Ser76-Thr77-Gly78) forms a loop that lies on top of the active site. The loop remained attached to aliskiren via two HB interactions. Interestingly, in the apo form of renin, the loop appeared increasingly flexible a feature that implicates this region as a modulating factor for the entrance of substrates.

MM-PBSA analysis. Our prediction yielded -12.03 kcal/mol total binding energy for the complex. This value is in fair agreement with the experimental value (-12.64 kcal/mol). The formation of the aliskiren-renin complex is mainly driven by the van der Waals (-35.7 kcal/mol) and the nonpolar contribution to solvation (-28.1 kcal/mol)[2].

Acknowledgments

This work was supported by funding provided by the European Commission for the FP7-REGPOT-2009-1 Project 'ARCADE' (Grant Agreement No. 245866). his research has been co-financed by the European Union (European Social Fund – ESF) and Greek National Funds through the Operational Program “Education and Lifelong Learning” of the National Strategic Reference Framework (NSRF) – Research Funding Program: Heracleitus II. Investing in knowledge society through the EuropeanSocial Fund.

References

- [1] Nussberger, J.; Wuerzner, G.; Jensen, C.; Brunner, HR.; *Hypertension* **2002**, *39*, e1.
- [2] Politi, A.; Leonis, G.; Tzoupis, H.; Ntountaniotis, D.; Papadopoulos, MG.; Grdadolnik, SG.; Mavromoustakos, T.; *Mol. Inf.* **2011**, *30*, 973.

Recognition of adamantyl-anchored mannosylated-tripeptides on liposome surface by Concanavaline A

Štimac¹, S. Šegota², M. Dutour Sikirić², R. Ribić³, L. Frkanec², V. Svetličić², S. Tomić³, B. Vranešić¹, R. Frkanec^{1*}

¹Institute of Immunology, Inc., Rockefellerova 10, 10000 Zagreb, Croatia; ²Ruder Bošković Institute, Bijenička 54, 10 000 Zagreb, Croatia; ³Faculty of Science, University of Zagreb, Horvatovac 102A, 10000 Zagreb, Croatia

rfrkanec@imz.com

Introduction

It is well known that mannose receptors are present on the surface of immunocompetent cells, which plays the key role in recognition and uptake of antigens. The mannosylated liposomes are recognized as attractive drug delivery carriers [1]. We have previously shown the interaction of immunostimulating adamantyltripeptides (D/L-(adamant-2-yl)Gly-L-Ala-D-isoGln (Ad₂TP1 and Ad₂TP2) and phospholipids in liposomal bilayers [2]. The aim of the present study was to investigate the structure of liposomes with encapsulated mannosylated adamantyltripeptides namely (2*R*)-*N*-[3-(α -D-mannopyranosyloxy)-2-methylpropanoyl]-D,L-(adamant-2-yl)glycyl-L-alanyl-D-isoglutamine] (Figure 1), by using dynamic light scattering (DLS) and atomic force microscopy (AFM). Our hypothesis was: if the adamantane molecule penetrates into the lipid core of the bilayer, it might be possible that the hydrophilic part of the mannose molecule could be exposed on the liposome surface. Therefore, if the mannose molecules are exposed on the liposome surface, Con A could bind the liposomes together (Figure 2). As a result the increase in vesicles size could be observed.

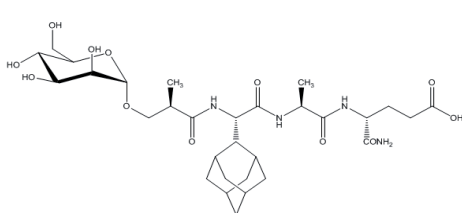


Figure 1. Chemical structure of α -D-Man-(*R*)-OCH₂CH(CH₃)CO-D,L-(adamant-2-yl)Gly-L-Ala-D-isoGln

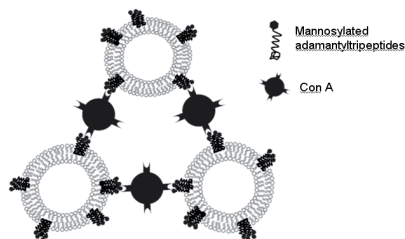


Figure 2. Schematic presentation of Con A interaction with mannosylated adamantyltripeptides anchored via the adamantyl moiety in the lipid bilayer

Results and Discussion

The results revealed that encapsulation of the mannosylated adamantyltripeptides affects the size and structural characteristics of liposomes. The statistically significant increase of the liposome size with encapsulated mannosylated adamantyltripeptides was measured.

After the Con A was added to the liposome preparation, further increase in liposome size and appearance of aggregates has been observed. The enlargement of liposomes was ascribed to the specific binding of the Con A to the mannose molecules present on the surface of the prepared vesicles (Table 1). The AFM analysis revealed that the adamantyltripeptide molecules grouped into small domains that rise above the bilayer surface (Figure 3). The molecule size and molecular geometry, as well as the hydrophilic and hydrophobic surfaces in the structure of mannosylated adamantyltripeptides, are responsible for incorporation and arrangement of molecules in the lipid bilayer. The adamantyl moiety may be considered as a potential membrane anchor for different carbohydrate or other molecules of interest, which could be bound on it and thus exposed on liposome surfaces and as such, used in targeted drug delivery and in the study of specific protein interactions with membrane receptors.

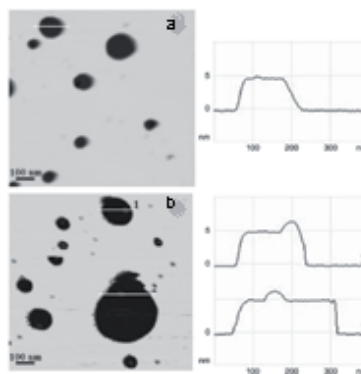


Figure 3. AFM images of (a) Empty liposomes and (b) Liposomes with mannosylated adamantyltripeptides. Images are presented as height data with a vertical profile along indicating lines. Scanned area $1 \mu\text{m} \times 1 \mu\text{m}$ with vertical scale of 15 nm

Table 1. Size distribution of liposome preparations measured by DLS; the results are expressed as average value \pm standard deviation (SD) of three separate experiments

Liposome preparations	Zeta potential/mV	z-average/nm**	PdI
Empty liposomes	-56.0 ± 1.6	166 ± 32^a	0.38 ± 0.03
Liposomes with mannosylated adamantyltripeptides	-52.6 ± 0.46	224 ± 3^b	0.46 ± 0.03
Empty liposomes + Con A	N/A	176 ± 22^a	0.54 ± 0.08
Liposomes with mannosylated adamantyltripeptides + Con A	N/A	267 ± 11^c	0.84 ± 0.03

N/A: not applicable

**_{a,b,c} denote $p < 0.05$, mean values marked with the same letter are not significantly different

Acknowledgments

We thank the Ministry of Science, education and Sports of the Republic of Croatia for its financial support. Projects No. 021-0212432-2431, No. 119-1191344-3121, No. 098-0982934-2744 and No. 098-0982904-2912 are acknowledged.

References

- [1] Espuelas, S., Thuman, C., Heurtault, B., Schuber, F., Frisch, B., *Bioconjugate Chem.* **2008**, *19*, 2385.
- [2] Frkanec, R., Noethig-Laslo, V., Vranešić, B., Miroslavljević, K., Tomašić, J., *Biochim Biophys Acta* **2003**, *1611*, 187.

Synthesis and biological activity of endomorphin-2 analogues containing isoproline, oxopiperadine or oxopyrrolidine ring in position 2

Akihiro Ambo, Mika Tanaka, Motoko Minamizawa, Yusuke Sasaki

Department of Biochemistry, Tohoku Pharmaceutical University, Sendai 981-8558, Japan

E-mail : yasaki@tohoku-pharm.ac.jp

Introduction

Endomorphin-2 (EM2: Tyr-Pro-Phe-Phe-NH₂) is a highly active and selective endogenous μ -opioid receptor ligand [1]. Since Pro² is critical for the proper conformational alignment of two aromatic residues, Tyr¹ and Phe³, at the receptor site, structural modification around Pro² could provide compounds with unique biological properties and improved metabolic stability. We synthesized seven EM2 analogues in which Pro² was replaced with *iso*Pro or with constrained residues containing the oxopiperadine or oxopyrrolidine ring.

Results and Discussion

All peptide analogues were synthesized by solid phase synthesis. Incorporation of the oxopiperadine and oxopyrrolidine ring was achieved using the method of Gellerman *et al.* [2] and Mohamed *et al.* [3], respectively, on the solid support. The receptor binding activity of these analogues for μ and δ receptors was investigated using [³H]DAMGO (μ) and [³H]Deltorphin II (δ) as receptor-selective ligands. Additionally, *in vitro* biological activity was studied using guinea pig ileum (GPI). The results are shown in Table 1. Both diastereoisomers of analogues containing the *iso*Pro residue (**1a** and **1b**) exhibited μ -

Table 1. Opioid receptor binding and biological activity of the synthetic peptides

No.	2nd residue	[³ H]DAMGO		[³ H]DL-II		GPI assay	
		Ki ^{μ} (nM)	R.p.*	Ki ^{δ} (nM)	Ki ^{δ} /Ki ^{μ} ratio	IC ₅₀ (nM)	R.p.*
1a	<i>iso</i> Pro	2.63	58	>3640	>1380	53.6	31
1b	<i>iso</i> Pro	2.13	72	>3640	>1700	1002	1.6
2	c[Met]	2478	0.06	>3640	-	4007	0.41
3	c[D-Met]	8.18	19	2546	311	46.3	35
4	[CH ₂ CH ₂ /Gly]	98.8	1.5	2777	28	2330	0.70
5	[CH ₂ CH ₂ /Ala]	421	0.36	1496	4	>10000	-
6	[CH ₂ CH ₂ /D-Ala]	10.9	14	684	63	190	8.7
	EM2	1.52	100	>3640	>2300	16.4	100

*Relative potency against EM2 (=100).

receptor affinity and selectivity similar to that of EM2, although the biological potencies of these analogues were less than one third that of EM2 in the GPI assay. All the other analogues had significantly lower μ -receptor affinity, with the exception of **3**, which contains an oxopyrrolidine ring formed by cyclization of D-Met at position 2. Compound **3** exhibited relatively high μ -receptor affinity and GPI activity. As shown in Fig. 1, most of the compounds synthesized in this study exhibited markedly high enzymatic stability in a rat brain homogenate compared to EM2 and Met-enkephalin. Therefore, analogues **1a**, **1b** and **3** may serve as lead compounds for the development of novel and enzymatically stable μ -receptor ligands.

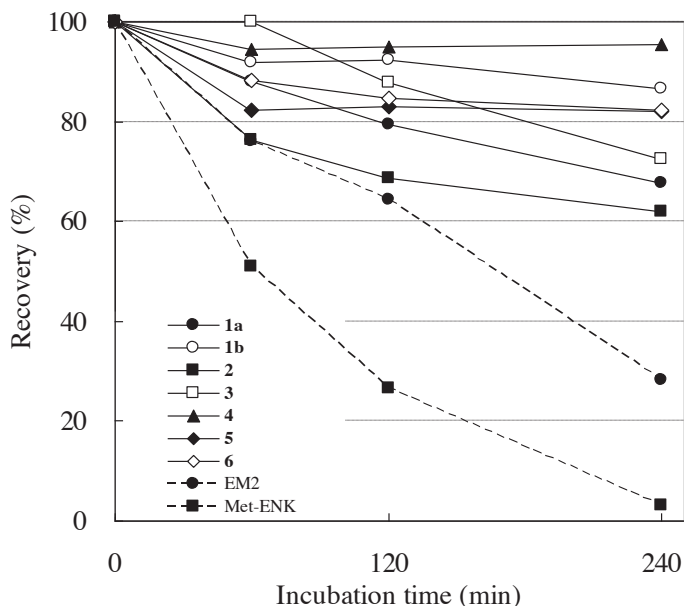


Fig. 1. Stability of synthetic peptides in rat brain homogenate.

References

- [1] Zadina, J. E.; Hackler, L.; Kastin, A. J. *Nature*, **1997**, 368, 499-502.
- [2] Gellerman, G; Hazan, E.; Kovaliov, M.; Albeck, A.; Shatzmiller, S. *Tetrahedron*, **2009**, 65, 1389-1396.
- [3] Mohamed, N.; Bhatt, U.; Just, G. *Tetrahedron Lett.*, **1998**, 39, 8213-8216.

Synthesis of novel modified with β^2 -tryptophan hexapeptide analogues as NOP receptor ligands

**Nikola Pavlov^{1,2}, Petar Todorov¹, Jean Martinez²,
Monique Calmès², Emilia Naydenova^{1*}**

¹*Department of Organic Chemistry, University of Chemical Technologies and Metallurgy, Sofia, Bulgaria;* ²*Institut des Biomolécules Max Mousseron (IBMM) UMR 5247 CNRS-Université Montpellier 1 et Université Montpellier 2, France*

E-mail: e_naydenova@abv.bg

Introduction

Bioactive peptides are important starting structures for the development of potential therapeutic agents. They bind to different receptors (opioid, non-opioid or both) and are involved in the physiological control of various functions, among which nociception is particularly emphasized.

By screening a synthetic peptide combinatorial library, Dooley et al. have isolated and characterized several hexapeptides, including Ac-RFMWMK-NH₂ and Ac-RYYRWK-NH₂, which have high affinity to μ and k_3 opioid receptors, slightly lower affinity for δ receptors, weak affinity for k_1 receptors, and no affinity for k_2 receptors. They were found to be potent μ receptor antagonists in the guinea pig ileum assay and relatively weak antagonists in the mouse vas deferens assay [1]. The hexapeptides with formula Ac-RYYR/KW/IR/K-NH₂ have been identified as shortest peptide sequence with high NOP receptor affinity, selectivity and marked analgesic effect [2]. Therefore, they are used as chemical templates for structure-activity relationship (SAR) studies [3,4].

The aim of the present study was the synthesis and the biological screening of new analogues of Ac-RFMWMK-NH₂ and Ac-RYYRWK-NH₂, modified in position 4 and 5 respectively with newly synthesized β^2 -tryptophan analogues. The synthesis of these new tryptophan analogues has been recently developed in our group via an asymmetric route involving a chiral nitroacrylate [5]. These derivatives incorporated into peptides will result in biologically active materials with enhanced resistance to enzymatic degradation

Results and Discussion

The new hexapeptides containing β^2 -tryptophan analogues at position 4 and 5 respectively (Figure 1) have been synthesized using solid phase peptide synthesis (SPPS) by and standard Fmoc (9-fluorenylmethoxycarbonyl) strategy. Rink-amide MBHA resin and TBTU (2-(1H-benzotriazole-1-yl)-1,1,3,3-tetramethyluronium tetrafluoroborate) were used as solid-phase carrier and condensing reagent. The synthesis of the enantiopure β -tryptophane analogues ((S)-2-indolyl- β -alanines) involves as key step the asymmetric Friedel-Craft alkylation of substituted indoles with a chiral nitroacrylate [5]. This reaction occurs in good yield and high diastereoselectivity (up to 90:10) and provides after reduction of the nitro group, removal of the chiral auxiliary and Fmoc protection the enantiopure β -Tryptophan analogues ready to use in solid-phase peptide synthesis [5].

The newly synthesized hexapeptides have the following sequences:

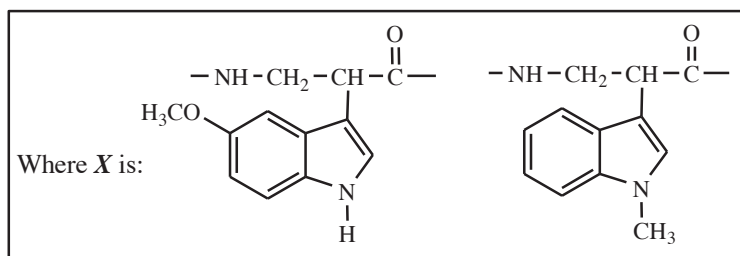
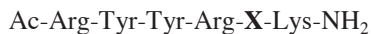


Figure 1. New hexapeptide analogues modified with β^2 -tryptophan.

The crude peptides were purified on a reversed-phase high-performance liquid chromatography (HPLC) and identified by electrospray ionization mass-spectrometry. The effects of these newly synthesized analogues on nociception were studied *in vivo* by tests, involving irritations of mechanoreceptors (*Paw pressure test*) and thermo receptors (*Hot plate test*).

These compounds will be additionally tested *in vitro* for NOP receptor agonistic activity on electrically stimulated smooth-muscle preparations isolated from vas deferens of Wistar rats.

Acknowledgments

The research was supported by Grant DTK 02/61 of the National Research Fund, Bulgaria.

References

- [1] Dooley, C.T.; Chung, N.N.; Schiller, P.W.; Houghten R.A. *Proc. Natl. Acad. Sci. USA*, **1993**, *90*, 10811.
- [2] Dooley, C., Spaeth, C., Berzetei-Gurske, I., et al. *J. Pharmacol. Exp. Ther.* **1997**, *283*(2), 735.
- [3] Naydenova, E.; Todorov, P.; Mateeva, P.; Zamfirova, R.; Pavlov, N.; Todorov, S. *Amino Acids*, **2010**, *39*, 1537.
- [4] Naydenova, E.; Todorov, P. *Journal of UCTM*, **2011**, *46*, 333.
- [5] Pavlov, N.; Gilles, P.; Didierjean, C.; Wenger, E.; Naydenova, E.; Martinez, J.; Calmès, M. *J. Org. Chem.*, **2011**, *76*, 6116.

Tumor cell binding of bombesin-like peptides

Zikos, C., Liolios, C.C., Karachaliou, C.-E., Fragogeorgi, E.A.,
 Durkan, M., Varvarigou, A.D., Paravatou-Petsotas, M., Livaniou, E.

Institute of Radioisotopes & Radiodiagnostic Products, NCSR "Demokritos", Athens,
 Greece

E-mails: liolios@pharm.uoa.gr; livanlts@rrp.demokritos.gr

Introduction

Bombesin (BN) and BN-like peptides are known to recognize the Gastrin-Releasing Peptide - cell receptors (GRPrs), which belong to the G-protein coupled receptor family and are overexpressed in various human tumors^[1]. Radiolabeled derivatives of the above peptides may serve as *in vivo* imaging agents in cancer diagnosis, provided that they retain ability of tumor cell binding.

We have recently presented^[2,3] the results of *in vitro* cell binding studies obtained with PC-3 prostate tumor cells and various BN-like peptides, including peptides which can be radiolabelled with ^{99m}Tc (Table 1). In this study we present the results obtained in the same *in vitro* cell binding system with the BN-like peptides Litorin^[4] (LT) and LT-D, a synthetic LT-peptide bearing the ^{99m}Tc-chelator group, GlyGlyCys- (Table 1). Moreover, we present the results of an "antibody recognition" study obtained with various BN-like peptides - including the LT-peptides - in an in-house developed ELISA system.

Table 1. peptide primary structures

Peptide					1	2	3	4	5	6	7	8	9	10	11	12	13	14	
BN					aa ₁	Q	R	L	G	N	Q	W	A	V	G	H	L	M	
BN-A	G	G	C	R	R	R	Q	R	L	G	N	Q	W	A	V	G	H	L	M
BN-O	G	G	C	aa ₂	aa ₂	aa ₂	Q	R	L	G	N	Q	W	A	V	G	H	L	M
[Lys ¹]BN					K	Q	R	L	G	N	Q	W	A	V	G	H	L	M	
[Tyr ⁴]BN					aa ₁	Q	R	Y	G	N	Q	W	A	V	G	H	L	M	
LT										aa ₁	Q	W	A	V	G	H	F	M	
LT-D								G	G	C	Q	W	A	V	G	H	F	M	

aa₁= pyroglutamic acid, aa₂= ornithine

Results and Discussion

Except LT and LT-D, all the BN-like peptides tested in the PC-3 *in vitro* cell binding system used, exhibited high binding affinity for the tumor cells, similar to that of the control peptide [Tyr⁴]BN (Fig. 1). LT, which is almost identical with the biologically active C-terminal region of BN, BN(7-14), except for a Phe-residue which has replaced Leu¹³ of the BN-sequence, exhibited significantly lower cell binding affinity (Fig. 1). LT-D also exhibited lower tumor cell binding affinity (Fig. 1).

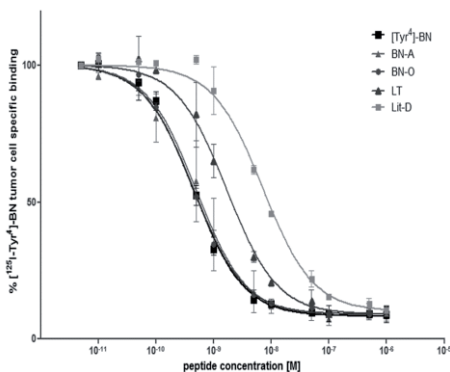


Fig. 1. % Specific binding of [$^{125}\text{I-Tyr}^4$]BN to the GRPrs of PC-3 cells: Inhibition curves obtained with: [Tyr^4]BN, BN-A, BN-O, LT and LT-D

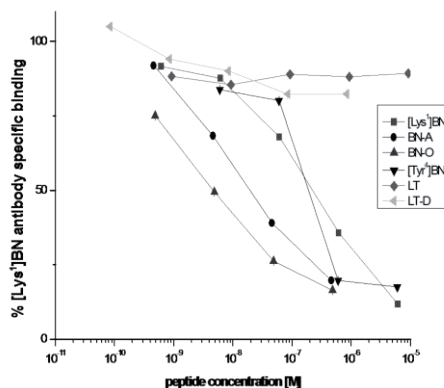


Fig. 2. % Specific binding of [Lys^1]BN to the anti-BN antibody: Displacement curves obtained with: [Lys^1]BN, [Tyr^4]BN, BN-A, BN-O, LT and LT-D

In addition, LT was not recognized by an anti-BN antibody developed by our team against the synthetic peptide [Lys^1]BN^[5] (Fig. 2), which is in accordance with previously reported data^[6]. LT-D was not recognized by the anti-BN antibody, either (Fig. 2). On the other hand, the other BN-like peptides tested, all of which had identical C-terminal regions, were well recognized by the anti-BN antibody, despite their differences in the N-terminal part. This supports the hypothesis that BN contains an epitope located in the C-terminus of the peptide sequence^[7], i.e. at the biologically active part of the molecule^[1] that is recognized by the GRPrs.

In conclusion, LT and LT-D peptides exhibited significantly lower PC-3 cell binding affinity, in comparison with the other BN-like peptides tested, and, at the same time, they were not recognized by the anti-BN antibody in an in-house developed ELISA system. Keeping the above findings in mind, we consider it worthwhile to investigate the possibility of using the above *in vitro* ELISA evaluation system as an additional, non-radioactive, preliminary screening test for selecting the most promising BN-candidates for *in vivo* tumor imaging.

References

- [1] Jensen, R.T.; Battey, J.F.; Spindel, E.R.; Benya, R.V. *Pharmacol. Rev.* **2008**, *60*, 1.
- [2] Fragogeorgi, E.A.; Zikos, C.; Gourni, E.; Bouziotis, P.; Paravatou-Petsotas, M.; Loudos, G.; Mitsokapas, N.; Xanthopoulos, S.; Mavri-Vavayanni, M.; Livaniou, E.; Varvarigou, A.D.; Archimandritis, S.C. *Bioconjugate Chem.* **2009**, *20*, 856.
- [3] Liolios, C.; Fragogeorgi, E.A.; Zikos, C.; Loudos, G.; Xanthopoulos, S.; Bouziotis, P.; Paravatou-Petsotas, M.; Livaniou, E.; Varvarigou, A.D.; Sivolapenko, G.B. *Int. J. Pharm.* **2012**, *430*, 1.
- [4] Durkan, K.; Lambrecht, F.Y.; Unak, P. *Bioconjugate Chem.* **2005**, *18*, 1516.
- [5] Karachaliou, C.-E.; Liolios, C.; Zikos, C.; Durkan, K.; Pirmettis, I.; Papadopoulos, M.; Varvarigou, A.; Livaniou, E. *Abstract Book of the 7th Hellenic Forum of Bioactive Peptides*, **2010**, p. 40.
- [6] Walsh, J.H.; Lechago, J.; Wong, H.C.; Rosenquist, G.L. *Regulatory Peptides* **1982**, *3*, 1.
- [7] Chaturvedi, S.; Parthasarathy, R. *Int. J. Peptide Prot. Res.* **1993**, *41*, 333.

Adapting to substrate requirements: Peptide catalyzed 1,4-addition reactions to α,β -disubstituted nitroolefins

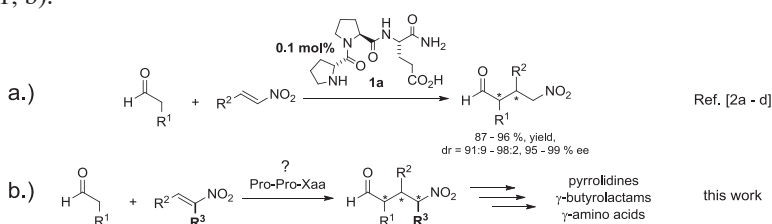
Jörg Duschmalé and Helma Wennemers

Laboratorium für Organische Chemie, D-CHAB, ETH Zürich, Wolfgang-Pauli-Strasse 10,
8093 Zürich, Switzerland

Helma.Wennemers@org.chem.ethz.ch

Introduction

Secondary amine catalyzed conjugate additions of aldehydes to nitroolefins are among the most widely researched organocatalytic reactions, since the resulting γ -nitroaldehydes are versatile intermediates that can be readily transformed into a variety of useful building blocks including chiral γ -amino acids, γ -butyrolactams and pyrrolidines.[1] As a consequence numerous chiral amine based catalysts have been explored in this reaction. Among the most potent catalysts are tripeptides of the type Pro-Pro-Xaa, in which the turn inducing Pro-Pro motif is combined with a C-terminal acidic amino acid (Xaa).[2] Particularly the tripeptide H-D-Pro-Pro-Glu-NH₂ (**1a**) is an exceptionally active and selective catalyst (Scheme 1, a).[2] Examples of addition reactions of carbonyl compounds to nitroolefins, that bear not only a substituent in the α - but also in the β -position, are rare and only a few examples of the addition of aldehydes to these electrophiles have been described in the literature.[3] Challenges in this respect include the remarkably lower reactivity as well as difficulties in controlling the configuration at the carbon bearing the nitro group. Nonetheless, the development of addition reactions of aldehydes to these less reactive nitroolefins is highly desirable, since the resulting γ -nitroaldehydes bear three consecutive stereogenic centers and are therefore valuable intermediates for the synthesis of, for example, chiral pyrrolidines and fully substituted γ -amino acids or γ -butyrolactams (Scheme 1, b).

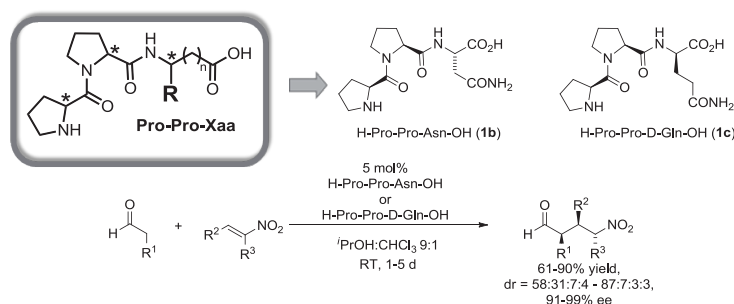


Scheme 1. Peptide catalyzed conjugate addition reactions of aldehydes to a.) β -mono- and b.) α,β -disubstituted nitroolefins.

Results and Discussion

The dramatically lower reactivity of α,β -disubstituted nitroolefins compared to their β -monosubstituted counterparts was exemplified when butanal was reacted with β -methyl- β -nitrostyrene in the presence of 5 mol% H-D-Pro-Pro-Glu-NH₂. The corresponding γ -nitroaldehyde was isolated with good diastereo- and excellent enantioselectivity of the

major diastereoisomer (dr = 67:15:10:8, 98% ee), demonstrating good control over all three stereogenic centers including the one at the carbon bearing the nitro group. However, only 30 % of the nitroolefin was converted after several days. Since this lower reactivity is most likely due to geometric differences between β -mono- and α,β -disubstituted nitroolefins,[4] we hypothesized that a structurally related peptide of the type Pro-Pro-Xaa might be better suited to catalyze reactions of α,β -disubstituted nitroolefins compared to peptide **1a** that was optimized to accommodate β -monosubstituted nitroolefins (Scheme 2). Thus, a small collection of 15 tripeptides of the type Pro-Pro-Xaa was synthesized and tested. All peptides shared the Pro-Pro motif but differed with respect to the stereochemistry of the three amino acid residues as well as the nature of the C-terminal amino acid. Screening of this peptide collection revealed that all peptides were catalytically active. Reactivity as well as selectivity, however, varied significantly. Two peptides, H-Pro-Pro-Asn-OH (**1b**) and H-Pro-Pro-D-Gln-OH (**1c**) were identified that provided the corresponding addition product in reasonable reaction times with good yields and selectivities using only 5 mol% of catalyst.



Scheme 2. Identification of H-Pro-Pro-Asn-OH (**1b**) and H-Pro-Pro-D-Gln-OH (**1c**) as catalysts for the conjugate addition of aldehydes to α,β -disubstituted nitroolefins.

In the presence of H-Pro-Pro-Asn-OH (**1b**) and H-Pro-Pro-D-Gln-OH (**1c**) various combinations of aldehydes and α,β -disubstituted nitroolefins reacted readily providing the corresponding γ -nitroaldehydes in good yields (61-90%) and diastereoselectivities (dr = 58:31:7:4 – 87:7:3:3) as well as excellent enantioselectivities of the major diastereoisomer (92-99% ee, Scheme 2). Furthermore, the synthetic utility of the process was demonstrated by the conversion of the addition products to pyrrolidines as well as fully substituted γ -amino acids and γ -butyrolactams. Mechanistic studies revealed that the configuration at all three stereogenic centers including the one at the carbon bearing the nitro group is induced by the peptidic catalysts.[4]

References

- [1] Vicario, J. *Organocatalytic Enantioselective Conjugate Addition Reactions: A Powerful Tool for the Stereocontrolled Synthesis of Complex Molecules*, RSC, Cambridge, **2010**.
- [2] (a) Wiesner, M.; Revell, J.; Wennemers, H. *Angew. Chem.* **2008**, *120*, 1897. (b) Wiesner, M.; Neuburger, M.; Wennemers, H. *Chem. - Eur. J.* **2009**, *15*, 10103. (c) Wiesner, M.; Upert, G.; Angelici, G.; Wennemers, H. *J. Am. Chem. Soc.* **2010**, *132*, 6. (d) Arakawa, Y.; Wiesner, M.; Wennemers, H. *Adv. Synth. Catal.* **2011**, *353*, 1201.
- [3] (a) Guo, L.; Chi, Y.; Almeida, A. M.; Guzei, I. A.; Parker, B. K.; Gellman, S. H. *J. Am. Chem. Soc.* **2009**, *131*, 16018. (b) Stevenson, B.; Lewis, W.; Dowden, J. *Synlett* **2010**, 672. (c) Wang, Y.; Zhu, S.; Ma, D. *Org. Lett.* **2011**, *13*, 1602. (d) Wang, L.; Zhang, X.; Ma, D. *Tetrahedron* **2012**, *68*, 7675.
- [4] Duschmalé, J.; Wennemers, H. *Chem. – Eur. J.* **2012**, *18*, 1111.

Complex modified silaffin peptides: Versatile tools for efficient enzyme immobilization

Carolyn C. Lechner and Christian F. W. Becker

University of Vienna, Department of Chemistry, Institute of Biological Chemistry,
Währinger Str. 38, 1090 Vienna, Austria

E-mail: christian.becker@univie.ac.at

Introduction

Silaffins are highly posttranslationally modified peptides naturally occurring in diatoms. Besides phosphorylation of the numerous serine residues [1], lysine residues become hydroxylated and phosphorylated at the γ -C-atom and di- and trimethylated or alkylated with exceptional oligo-*N*-methyl-propylenimine units at the ϵ -amino groups [2,3]. In diatoms, silaffins are directly involved in the molecular process leading to the formation of the delicate, nano-patterned silica shells under mild physiological conditions. Deciphering the mechanisms enabling silica biogenesis in diatoms will inspire the development of novel routes for the shape-controlled synthesis of silicon-based materials [4,5] and expand the scope of (bio-)technological applications, e.g. for immobilization of enzymes in silica matrices, imaging applications or use of silica particles for drug delivery.

Results and Discussion

The influence of different posttranslational (peptide **2**, **4** & **5**) and artificial (peptide **3**) modifications of the silaffin R5 sequence (H-SSKKSGSYSGSKGSKRRIL-OH) on silaffin induced silica precipitation was explored with a series of silaffin R5 peptides (Table 1), which were obtained by Fmoc-based SPPS and postsynthetic modification procedures [6].

Table 1. Synthetic silaffin R5 peptides

Sequence	MW [Da]	Yield [%]	Spec. Activity ^a
1 CSSKKSGSYSGSKGSKRRIL	2116.40	49.8	0.82 ± 0.02
2 CSSKKSGSYSGSK(Me) ₃ GSKRRIL ^b	2247.66	18.9	0.94 ± 0.01
3 CSSK(Sp)KSGSYSGSKGSK(Sp)RRIL ^c	2659.18	3.1	0.59 ± 0.03
4 CSSKKSGSYSGSKGpSKRRIL ^d	2196.38	38.8	0.68 ± 0.05
5 CpSpSKKpSGpSYpSGpSKGpSKRRIL ^d	2764.43	0.6	0.10 ± 0.01

^a specific activity in silica precipitation given in pmol Si / nmol peptide * min

^b K(Me)₃ = ϵ -*N,N,N*-trimethyllysine; ^c K(Sp) = ϵ -(4-spermidine) succinyllysine ^d pS = Phosphoserine.

The silica precipitation activity of peptides **1-5** was analyzed with regard to amount of precipitated silica (Table 1) and morphology of the resulting particles (Figure 1) revealing a distinct alteration depending on the particular modifications of the silaffins mainly based on the ability of the peptides to form larger assemblies and on electrostatic interactions between peptide side chains and silicic acid molecules [6]. In addition, we attached the fluorescent dye 7-nitro-1,2,3-benzoxadiazole (NBD) to the N-terminus of the silaffin sequence (peptide **6**, NBD-CSSKKSGSYSGSKGSKRRIL-OH). In this way peptide localization within silica structures can be determined and the capability of silaffin R5 to immobilize covalent attached target molecules during silica precipitation is examined. The

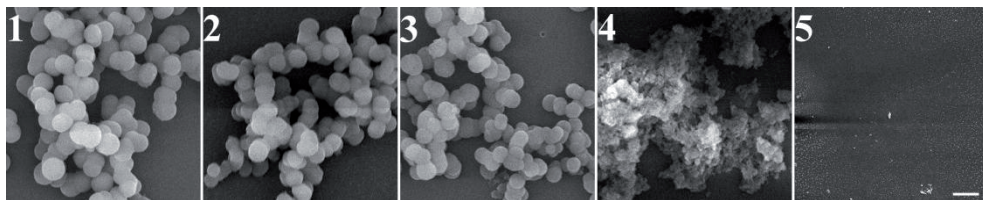


Figure 1. Scanning electron micrographs of silica particles resulting from peptide **1-5**. Scale bar 1 μm .

electron micrograph of silica particles resulting from peptide **6** (Figure 2A) shows that the silaffin peptide variant also leads to spherical silica particles just as the unmodified peptide **1**. Fluorescence micrographs (Figure 2B and C) give evidence that the peptide coprecipitates with the formed silica and is either entrapped in the silica particles or at least tightly associated with the silica material [6].

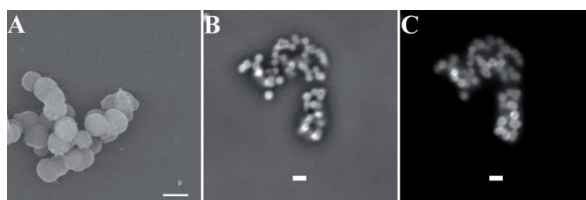


Figure 2. Scanning electron micrograph (A), brightfield micrograph (B) and fluorescence micrograph (C) of silica particles resulting from peptide **6**. Scale bars 1 μm .

These results provide a first explanation for the intricate modifications of silaffin peptides that could be exploited for immobilization of (bio-)technologically interesting proteins. Combining the ability to control the properties of silica materials by usage of synthetic silaffin peptides carrying different modifications with the finding that covalent attachment of target molecules to the peptides does not interfere with silica formation and leads to efficient and homogenous encapsulation paves the way towards novel applications of silaffins as silica precipitation agent and efficient silica anchors for a diverse set of molecules, e.g. fluorescent probes, drugs or enzymes. By N-terminal elongation of the R5-sequence with a non-native cysteine residue a unique thiol function for chemoselective attachment of target molecules is already provided.

Acknowledgments

Financial support from the Wacker Chemie AG and the Institute of Silicon Chemistry at the Technische Universität München is gratefully acknowledged.

References

- [1] Kröger, N.; Lorenz, S.; Brunner, E.; Sumper, M. *Science* **2002**, *298*, 584.
- [2] Kröger, N.; Deutzmann, R.; Sumper, M. *Science* **1999**, *286*, 1129.
- [3] Kröger, N.; Deutzmann, R.; Sumper, M. *J. Biol. Chem.* **2001**, *276*, 26066.
- [4] Mann, S.; Ozin, G. *Nature* **1996**, *382*, 313.
- [5] Parkinson, J.; Gordon, R. *Trends Biotechnol.* **1999**, *17*, 190.
- [6] Lechner, C.C.; Becker, C.F.W. *Chem. Sci.* **2012**, DOI:10.1039/C2SC20687K

Novel ureas based on dipeptide analogues as organocatalysts for the asymmetric aldol reaction

Panagiota Revelou, Christoforos G. Kokotos,
Panagiota Moutevelis-Minakakis*

Laboratory of Organic Chemistry, Department of Chemistry, University of Athens,
Panepistimiopolis, Athens 15771, Greece

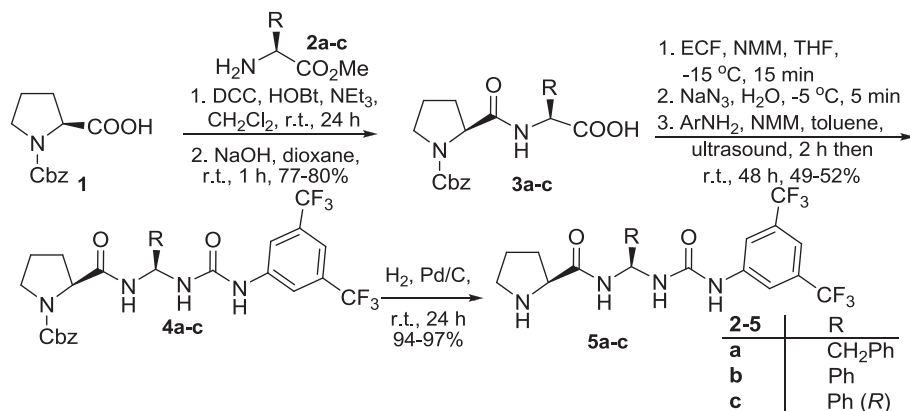
pminakak@chem.uoa.gr

Introduction

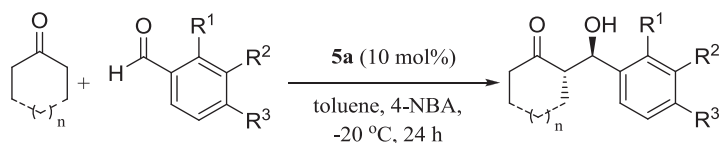
Organocatalysis has met such a great rate of expansion that is nowadays considered the third major branch of modern asymmetric catalysis along with the transition-metal catalysis and biocatalysis. After proline was identified as a catalyst for the enantioselective aldol reaction, it became clear that amino acids and peptides could serve as an abundant pool full of potential to develop novel organocatalytic motives. Organocatalysts combining the prolinamide unit with functionalities able to act as hydrogen bond donors are among the most successful classes of catalysts employed in the aldol reaction [1-4].

Results and Discussion

Herein, we present our study on the catalytic activity of compounds that combine a prolinamide and an urea coupled with a chiral *gem* diamine derived from an amino acid (Scheme 1). (*S*)-Cbz-proline (**1**) was coupled with (*S*)-methyl phenylalaninate (**2a**), (*S*)- or (*R*)-methyl phenylglycinate (**2b** or **2c**). Saponification afforded **3a-c**. The crucial step was a Curtius rearrangement that was accomplished by sonication and the intermediate was treated with an aromatic amine leading to prolinamide-ureas **4a-c** with retention of stereochemistry [5]. Finally, deprotection afforded organocatalysts **5a-c**. Catalyst **5a** proved to be better than catalysts **5b** or **5c** in the reaction between cyclohexanone with 4-nitrobenzaldehyde (entry 1 vs 2-3, Table 1) [6]. Substituted aromatic aldehydes as well as



Scheme 1. Synthesis of organocatalysts **5a-c**.

Table 1. Enantioselective aldol reaction between ketones and aldehydes.

Entry	Ketone	Ar	Yield (%) ^a	dr ^b	ee (%) ^c
1		4-NO ₂ C ₆ H ₄	96	98:2	98
2 ^d		4-NO ₂ C ₆ H ₄	72	99:1	96
3 ^e		4-NO ₂ C ₆ H ₄	65	95:5	91
4	Cyclohexanone	3-NO ₂ C ₆ H ₄	87	96:4	96
5 ^f		2-NO ₂ C ₆ H ₄	90	>99:1	98
6 ^f		4-CF ₃ C ₆ H ₄	77	>99:1	97
7 ^f		3-CNC ₆ H ₄	98	>99:1	97
8	4-Me-cyclohexanone	4-NO ₂ C ₆ H ₄	90	99:1	99
9	cyclopentanone	4-NO ₂ C ₆ H ₄	97	30:70	75 ^g

^aIsolated yield. ^bThe dr was determined by ¹H NMR. ^cThe enantiomeric excess (*ee*) was determined by chiral HPLC. ^dCatalyst **5b** was utilised. ^eCatalyst **5c** was utilised. ^fReaction time 48-72 h. ^g major isomer *syn*: 75% *ee*, minor isomer *anti*: 80% *ee*.

other cyclic ketones were employed successfully (entries 4-9, Table 1).

In conclusion, the synthesis and the evaluation of novel prolinamide compounds bearing an aryl urea moiety was carried out. When a chiral *gem* diamine spacer easily derived from the natural α -amino acid phenylalanine was used, the best results were obtained. This novel organocatalyst provided the products of the reaction between cyclic ketones with aromatic aldehydes in excellent yields and selectivities.

Acknowledgments

Financial support from the EPEAEK program “Organic Synthesis and Applications in Chemical Industry” as well as from the Special Research Account of the University of Athens are highly appreciated.

References

- [1] Tang, Z.; Jiang, F.; Yu, L. T.; Cui, X.; Gong, L. Z.; Mi, A. Q.; Jiang, Y. Z. *J. Am. Chem. Soc.* **2003**, *125*, 5262-5263.
- [2] Gandgi, S.; Singh, V. K. *J. Org. Chem.* **2008**, *73*, 9411-9416.
- [3] Wang, B.; Chen, G.-H.; Liu, L.-Y.; Chang, W.-X.; Li, J. *Adv. Synth. Cat.* **2009**, *351*, 2441-2448.
- [4] Fotaras, S.; Kokotos, C. G.; Tsandi, E.; Kokotos, G. *Eur. J. Org. Chem.* **2011**, 1310-1317.
- [5] Moutevelis-Minakakis, P.; Photaki, I. *J. Chem. Perkin Trans 1* **1985**, 2277-2281.
- [6] Revelou, P.; Kokotos, C. G.; Moutevelis-Minakakis, P; *Tetrahedron* **2012**, *68*, 8732-8738.

Synthesis and a preliminary binding study to a metal surface of peptides characterized by the helicogenic, cyclic disulfide-containing α -amino acid Adt

Karen Wright¹, Edoardo Longo¹, Emanuela Gatto², Mariano Venanzi², Marco Crisma³, Fernando Formaggio³, Claudio Toniolo³

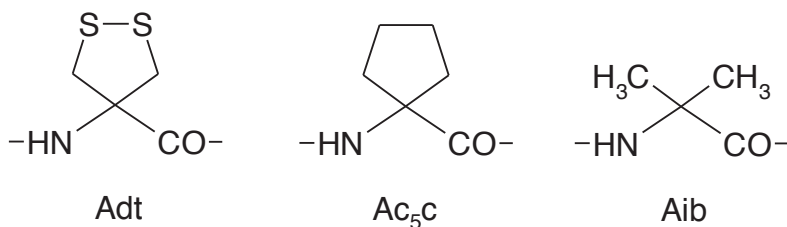
¹ILV, UMR 8180, University of Versailles, 78035 Versailles, France; ²Department of Chemical Sciences and Technologies, University of Rome "Tor Vergata", 00133 Rome, Italy; ³ICB, Padova Unit, CNR, Department of Chemistry, University of Padova, 35131 Padova, Italy

E-mail: wright@chimie.uvsq.fr; claudio.toniolo@unipd.it

Introduction

Peptide self-assembled monolayers are of current interest to study physicochemical properties of modified metal (*e.g.* Au) surfaces. Rigid peptide scaffolds could enhance the interaction between Au surfaces and labels by reducing and precisely monitoring the distance between the supported monolayers and Au. The achiral α -amino acid 4-amino 1,2-dithiolane-4-carboxylic acid (Adt) [1], which contains a cyclic disulfide system, is interesting in this respect because it may allow the *parallel* binding of the peptide helical chain to the metal surface. Adt occurs in Nature [2] and has been utilized in medicinal chemistry [3] and in a model compound of [FeFe] hydrogenase [4].

Adt is a conformationally restricted, helicogenic residue related to the cyclopentane-based Ac₅c and the prototype of their family of C ^{α} -tetrasubstituted α -amino acids Aib [5].



Results and Discussion

We synthesized and fully characterized a series of peptides to the decamer level based on the -Aib-Ala- or the -Ala-Ala- sequence, additionally containing one or two Adt residues. Most part of these peptides was functionalized with spectroscopic [5(6)-fluorescein-NHCS- or 1-pyrenyl-acetyl-] or redox (ferrocenyl-carbonyl) labels. We solved the 3D-structure of Boc-L-Ala-Aib-Adt-L-Ala-Aib-OMe (Figure 1). In the crystal state this pentapeptide folds in a regular 3₁₀-helix, showing that Adt can easily accommodate in this secondary structure. The observed right-handed screw sense is governed by configuration of the two Ala residues. The 1,2-dithiolane ring adopts a ³T₂ (twist) conformation.

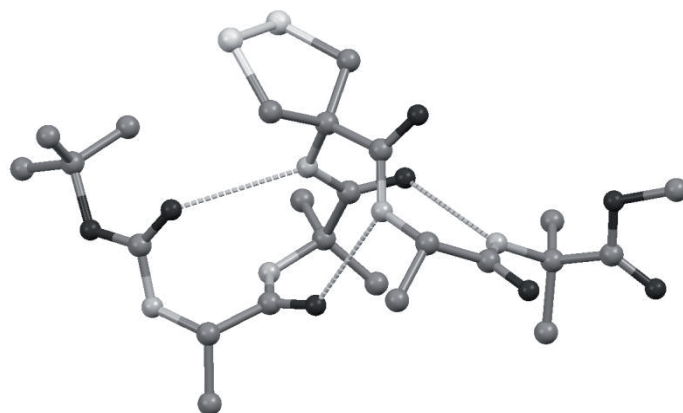


Fig.1. X-Ray diffraction structure of Boc-L-Ala-Aib-Adt-L-Ala-Aib-OMe. The three intramolecular C=O...H-N H-bonds are represented as dashed lines.

In preliminary experiments, binding of these peptides to an Au surface through the Adt dithiolane bridge(s) and their desorption by electrochemical reduction of the Au-S bond were demonstrated to occur.

References

- [1] Morera, E.; Nalli, M.; Mollica, A.; Paglialunga Paradisi, M.; Aschi, M.; Gavuzzo, E.; Mazza, F.; Lucente, G. *J. Pept. Sci.* **2005**, *11*, 104.
- [2] Appleton, D. R.; Copp, B. R. *Tetrahedron Lett.* **2003**, *44*, 8963.
- [3] Morera, E.; Lucente, G.; Ortar, G.; Nalli, M.; Mazza, F.; Gavuzzo, E.; Spisani, S. *Bioorg. Med. Chem.* **2002**, *10*, 147.
- [4] Apfel, U.-P.; Kowol, C. R.; Morera, E.; Görls, H.; Lucente, G.; Keppler, B. K.; Weygand, W. *Eur. J. Inorg. Chem.* **2010**, 5079.
- [5] Toniolo, C.; Crisma, M.; Formaggio, F.; Peggion, C.; *Biopolymers (Pept. Sci.)* **2001**, *60*, 396.

Polymer-supported thiourea catalysts for enantioselective Michael reaction

Stamatis Fotaras, Nicolaos Ferderigos, George Kokotos

Laboratory of Organic Chemistry, Department of Chemistry, University of Athens,
Panepistimiopolis, Athens 15771, Greece

E-mail: gkokotos@chem.uoa.gr

Introduction

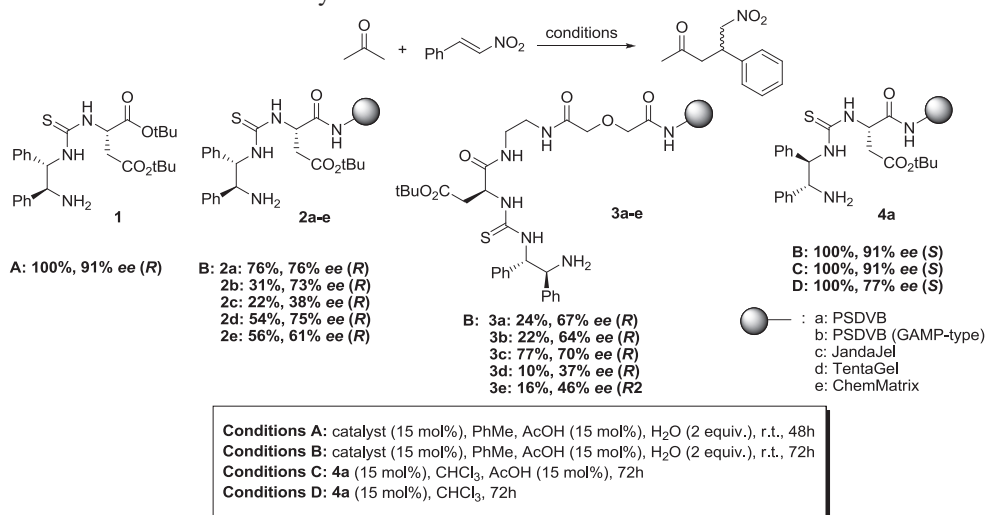
Among the large number of reactions involving the formation of carbon-carbon bond, the addition of ketones to nitroolefins is a powerful tool for the synthesis of γ -nitro-carbonyl compounds, useful intermediates for pharmaceutical industry. Our recently reported primary amine-thioureas based on *tert*-butyl esters of natural amino acids exhibit excellent performance for the Michael reaction of ketones with nitroolefins providing the products quantitatively and almost stereospecifically (>99% *ee*) [1,2]. Using this methodology, enantiopure baclofen and phenibut (analogs of GABA) have been synthesized [2]. Polymer-supported organocatalysts constitute a great challenge for the Michael reaction. In the current study, we report the immobilization of amine-thiourea catalysts containing (1*S*,2*S*)- or (1*R*,2*R*)-diphenylethylenediamine and (*S*)-*tert*-butyl aspartate on various polymer supports, and the evaluation of the resulting supported organocatalysts in the reaction between acetone and *trans*- β -nitrostyrene.

Results and Discussion

Our previously reported primary amine-thiourea (**1**) was initially attached to aminomethylated polymers either directly or by inserting a relatively long spacer unit based on ethylenediamine and 2,2'-oxydiacetic acid, preceded suitable modification of the amino acid segment (Scheme 1). Uniformly-distributed cross-linked polystyrene-divinylbenzene (PSDVB), JandaJel, TentaGel and ChemMatrix resins were used for the immobilization of the catalyst. An aminomethylated PSDVB resin that exhibits a gradual increase of functional groups from the inside to the outside of the polymeric bead (Gradually Aminomethylated Polystyrene Resins, GAMPs) was also used, in order to examine the effect of the enhanced surface-exposed catalytic centers in the reactivity of the supported catalyst.

The activity of all the catalysts that were synthesized was evaluated in the Michael reaction between acetone and *trans*- β -nitrostyrene, under previously reported conditions [1, 2], utilizing toluene or chloroform as the reaction medium and AcOH, H₂O as additives at ambient temperature (Scheme 1). The uniformly-distributed PSDVB-supported catalyst **2a** provides the product in satisfactory yield and enantioselectivity, while the derivative **2b** leads to diminished yield, indicating that the highly shell-functionalized resin, slows down the reaction. The introduction of a longer and more flexible cross-linker than divinylbenzene between polystyrene chains in supported catalyst **2c**, further restricts product formation, while deteriorates the enantioselectivity as well. The insertion of PEG units between the PSDVB matrix and the thiourea catalyst (**2d**) restores the results provided

by the so far optimum supported derivative **2a**, while the ChemMatrix-supported thiourea resin **2e** maintains the yield obtained with the Tentagel resin **2d**, decreasing slightly however the enantioselectivity.



Scheme 1. Polymer-supported primary-amine thiourea catalysts in the Michael reaction.

The insertion of the spacer leads in the case of the **3a** and **3b** derivatives in low product yield in comparison to the directly attached analogues **2a** and **2b**. Compared to derivatives **2d** and **2e**, resins **3d** and **3e** further reduce the yield, while degrade seriously the selectivity of the reaction. The catalyst **3c** exhibits a clear superiority among the thiourea catalysts attached *via* the spacer unit. The replacement of the (1*S*,2*S*)-diphenylethylenediamine unit of the supported catalyst **2a** with the (1*R*,2*R*)-enantiomer in derivative **4a**, leads to quantitative yield, while the opposite enantiomer of the product becomes predominant with high selectivity. Chloroform maintains the results obtained with toluene, while the absence of the acid additive decreases enantioselectivity.

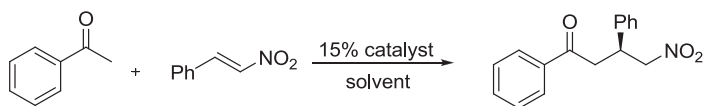
Acknowledgements

This research has been co-financed by the European Union (European Social Fund – ESF) and Greek national funds through the Operational Program "Education and Lifelong Learning" of the National Strategic Reference Framework (NSRF) - Research Funding Program: Heracleitus II. Investing in knowledge society through the European Social Fund.

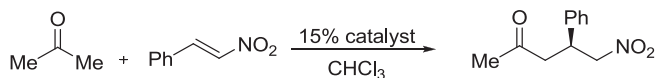
References

- [1] Kokotos, C. G.; Kokotos, G. *Adv. Synth. Catal.* **2009**, *351*, 1355.
- [2] Tsakos, M. C.; Kokotos, C. G.; Kokotos, G. *Adv. Synth. Catal.* **2012**, *354*, 740.

our work on chiral thioureas involving (1*R*,2*R*)-diphenylethylenediamine and various dipeptides. H-Asp(OBu^t)-Asp(OBu^t)-OBu^t, H-Asp(OBu^t)-Val-OBu^t, H-Asp(OBu^t)-Phg-OBu^t, H-Val-Val-OBu^t and H-Phg-Phg-OBu^t were converted to the corresponding isothiocyanates by treatment with thiophosgene and reacted with (1*R*,2*R*)-diphenylethylenediamine to afford the catalysts (Figure 1) used in the present study.



All the thiourea-dipeptide catalysts provided the product of the reaction between acetophenone and *trans*- β -nitrostyrene in high yields (up to 99%) and enantioselectivities (up to 99% ee). Yields ranging from 90% to 99% were observed in CHCl₃, while in water the yields were substantially lower (11-30%), although the enantioselectivities always remained at high level (97-99%).



The product of the reaction between acetone and *trans*- β -nitrostyrene was obtained in high yields (71-99%) and enantioselectivities (92-99% ee). The primary amine-thioureas based on H-Val-Val-OBu^t and H-Phg-Phg-OBu^t proved to be the best catalysts for both the Michael reactions.

In conclusion, we have developed organocatalysts combining the (1*R*,2*R*)-diphenylethylenediamine scaffold with a thiourea based on *tert*-butyl esters of dipeptides. These catalysts are highly effective for the asymmetric Michael addition of acetophenone and acetone to nitroolefins providing the products in high yields and enantioselectivities.

References

- [1] Dalko, P. I. *Enantioselective Organocatalysis: Reactions and Experimental Procedure*; Wiley-VCH: Weinheim, **2007**.
- [2] MacMillan, D. W. C. *Nature* **2008**, *455*, 304.
- [3] Tsogoeva, S. B.; Wei, S. *Chem. Commun.* **2006**, 1451.
- [4] Huang, H.; Jacobsen, E. N. *J. Am. Chem. Soc.* **2006**, *128*, 7170.
- [5] Kokotos, C. G.; Kokotos, G. *Adv. Synth. Catal.* **2009**, *351*, 1355.
- [6] Tsakos, M.; Kokotos, C. G.; Kokotos, G. *Adv. Synth. Catal.* **2012**, *354*, 740.

Primary amino acids as organocatalysts for the asymmetric α -amination of aldehydes

Alexis Theodorou, Giorgos N. Papadopoulos, Christoforos G. Kokotos*

Laboratory of Organic Chemistry, Department of Chemistry, University of Athens,
Panepistimiopolis, Athens 15771, Greece

ckokotos@chem.uoa.gr

Introduction

After List, Lerner and Barbas highlighted that proline can catalyze efficiently the intermolecular aldol reaction between acetone and a variety of aromatic aldehydes, it became evident that amino acids and peptides can afford a plethora of different structural scaffolds for novel catalysts. Organocatalysis has grown to such an extent that now is considered the third major branch of asymmetric catalysis along with transition-metal catalysis and biocatalysis. However, it was only until recently that researchers turned their attention to other amino acids rather than proline. Primary amino acids and peptides have already been applied to a number of transformations with some success [1]. Wennemers and coworkers have utilised a peptide catalyst for the Michael reaction between aldehydes and nitroolefins [2], while Miller and coworkers successfully employed peptide catalysts for the epoxidation of alkenes [3]. We have recently utilised peptide-like catalysts in aldol reactions [4, 5]. We disclose herein our recent studies on the use of simple and cheap primary amino acids and amino acid derivatives, that are either commercially available or easily obtained, as organocatalysts for the asymmetric α -amination of aldehydes.

Results and Discussion

Herein, we report that simple derivatives of primary amino acids can efficiently catalyze this transformation leading to high to quantitative yields and enantioselectivities. In the literature, the non-natural amino acid naphthyl alanine salt (**1**) was recently utilized successfully (Figure 1) [6]. Also, the amino-derivatives of *epi*-quinine were reported to catalyze efficiently this transformation (catalyst systems **2** and **3**, Figure 1) [7, 8]. We have commenced our studies by utilizing a variety of amino acids and other chiral catalysts (Table 1). Proline and proline sulfonamide afforded the desired product after prolonged

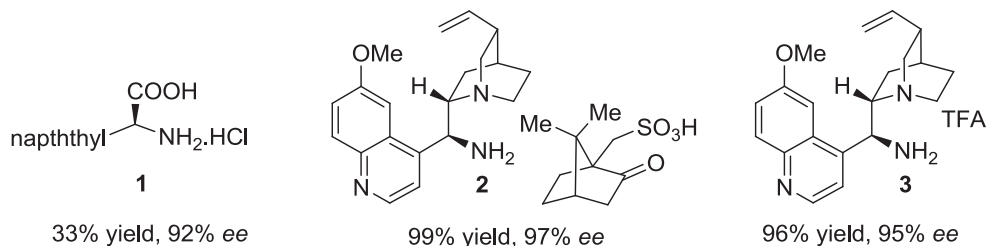
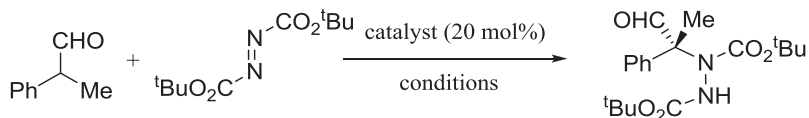


Figure 1. Known organocatalysts for the α -amination of α -branched aldehydes.

Table 1. Enantioselective α -amination of α -branched aldehydes.

Entry	Catalyst	Conditions	Yield (%) ^a	<i>ee</i> (%) ^b
1	H-Pro-OH	CH ₂ Cl ₂ , r.t., 5d	75	65
2	H-Pro-NHSO ₂ Me	CH ₂ Cl ₂ , r.t., 5d	21	66
3	Glucosamine.HCl	CH ₂ Cl ₂ , r.t., 5d	30	51
4	H-His-OH	CH ₂ Cl ₂ , r.t., 5d	traces	-
5	H-Asp-OH	CH ₂ Cl ₂ , r.t., 5d	traces	-
6	H-Asn-OH	CH ₂ Cl ₂ , r.t., 5d	traces	-
7	H-Phe-OH	CH ₂ Cl ₂ , r.t., 18 h	99	66
8	β -Phe	CH ₂ Cl ₂ , r.t., 18 h	92	61
9	H-Asp(OBn)-OH	CH ₂ Cl ₂ , r.t., 72 h	84	78
10	H-Asp(O ^t Bu)-OH	CH ₂ Cl ₂ , r.t., 24 h	99	84
11	H-Asp(O ^t Bu)-OH	THF, 0 °C, 24 h	93	94
11	H-Asp(O ^t Bu)-Val-O ^t Bu	THF, 0 °C, 48 h	98	92

^a Isolated yield. ^b The enantiomeric excess (*ee*) was determined by chiral HPLC.

reaction time (entries 1-2, Table 1). Glucosamine.HCl and naturally occurring amino acids like L-histidine, L-aspartic acid and L-asparagine led to unsatisfactory results after a reaction time of 5 days (entries 3-6, Table 1). On the other hand, phenylalanine and β -phenylalanine led to excellent yields and moderate enantioselectivities (entries 7-8, Table 1). β -Protected aspartic acid provided the best results with β -*tert*-butyl aspartate affording the desired product in 93% yields and 94% *ee* in THF at 0 °C (entries 9-11, Table 1). Finally, dipeptide H-Asp(O^tBu)-Val-O^tBu required longer reaction time to afford the product in similar yield and selectivity (entry 12, Table 1).

In conclusion, the evaluation of amino acids and peptides in the asymmetric α -amination of α -branched aldehydes was performed. From this study, β -*tert*-butyl aspartate proved to be the catalyst of choice affording the desired product in 93% yield and 94% *ee*.

References

- [1] a) Wennemers, H. *Chem. Commun.*, **2011**, 47, 12036-12041; b) Wennemers, H. *J. Pept. Sci.*, **2012**, 18, 437-441.
- [2] Wiesner, M.; Uppert, G.; Angelici, G.; Wennemers H. *J. Am. Chem. Soc.*, **2010**, 132, 6-7.
- [3] Peris, S.; Jakobsche, C. E.; Miller S. J. *J. Am. Chem. Soc.*, **2007**, 129, 8710-8711.
- [4] Fotaras, S.; Kokotos, C. G.; Tsandi, E.; Kokotos G. *Eur. J. Org. Chem.*, **2011**, 1310-1317.
- [5] a) Kokotos, C. G. *J. Org. Chem.*, **2012**, 77, 1131-1135; b) Fotaras, S.; Kokotos, C. G.; Kokotos G. *Org. Biomol. Chem.*, **2012**, 10, 5613-5619.
- [6] Fu, J.-Y.; Yang, Q.-C.; Wang, Q.-L.; Ming, J.-N.; Wang, F.-Y.; Xu, X.-Y.; Wang L.-X. *J. Org. Chem.*, **2011**, 76, 4661-4664.
- [7] Liu, C.; Zhu, Q.; Huang, K.-W.; Lu, Y. *Org. Lett.*, **2011**, 13, 2638-2641.
- [8] Desmarchelier, A.; Yalgin, H.; Coeffard, V.; Moreau, X.; Greck, C. *Tetrahedron Lett.*, **2011**, 52, 4430-4432.

A concise synthesis, docking studies and biological evaluation of *N*-substituted 5-butylimidazole analogues as potent Angiotensin II receptor blockers

George Agelis,^{1,7} Amalia Resvani,^{1,7} Serdar Durdagi,² Tereza Tůmová,³
Jirina Slaninová,³ Panagiotis Giannopoulos,⁴ Katerina Spyridaki,⁴
George Liapakis,⁴ Demetrios Vlahakos,⁵ Thomas Mavromoustakos,⁶
John Matsoukas^{1,7}

¹Department of Chemistry, University of Patras, Patras 26500, Greece; ²Department of Biological Sciences, Institute for Biocomplexity and Informatics, Calgary, Alberta, Canada; ³Institute of Organic Chemistry and Biochemistry, Academy of Sciences of the Czech Republic, Flemingovo nám. 2, 166 10 Prague 6, Czech Republic; ⁴Department of Pharmacology, Faculty of Medicine, University of Crete; ⁵Department of Internal Medicine, "ATTIKON" University Hospital, Athens, Greece; ⁶Department of Chemistry, University of Athens, Athens, Greece; ⁷Eldrug S.A., Patras 26504, Greece

E-mail:aggelisgeorge@hotmail.com; imats@upatras.gr

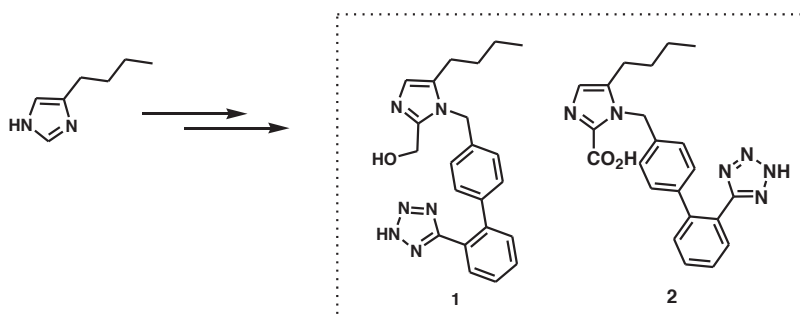
Introduction

The Renin-angiotensin system (RAS) is among the many factors playing role in the pathogenesis of hypertension and cardiovascular disease [1]. Inhibition of RAS has been established as an effective approach for the treatment of several disorders, including hypertension and congestive heart failure. Research efforts over the last decades have focused on the development of highly selective Angiotensin II (ANG II) AT1 receptor blockers (ARBs) which provided a more specific blockade of the RAS. The discovery of potent and orally active ARBs such as losartan has encouraged the development of a large number of similar compounds. Among them, candesartan valsartan, irbesartan, telmisartan, olmesartan and azilsartan [2], which is a newer-generation ARB have been launched. Nearly all of them bear an alkyl-substituted imidazole ring linked to a biphenylmethyl tetrazole moiety. Additionally, a small sized group such as CH₂OH or CO₂H at C-5 of the imidazole as well as a bulky lipophilic, electron-withdrawing substituent, such as a halogen atom seem to favor binding affinity. In this study, we have developed a new synthetic strategy for a series of *N*-substituted 5-butylimidazole analogues, which differ in the orientation of the C-2 and C-5 substituents compared to losartan. Furthermore, the oxidized forms were synthesized leading to the aldehyde and the carboxylic acid **2**. Our synthetic approach included efficient and regioselective reactions in high yield, allowing the facile introduction of the substituents on the imidazole nucleus. The synthesized analogues were tested for their ANG II-antagonistic activity on rat uterus (pA₂) and their AT1 receptor affinity (IC₅₀) using binding assays.

Results and Discussion

A series of *N*-substituted 5-butylimidazole derivatives has been synthesized, via a convenient and facile synthesis and evaluated for their *in vitro* antagonistic activities on

ANG II AT1 receptor. In this series, the most potent analogue was found to be **2** bearing the carboxy group at the C-2 position. Previous work has shown that compound **1** is slightly less potent than losartan and structurally identical except that butyl and hydroxymethyl groups are interchanged though is lacking the chlorine atom [3]. Thus, the polar substituent CH₂OH at the C-2 is favorable for the antagonistic activity. *In vitro* results showed that generally substitution at the C-4 with halogens led to significant decrease of activity. The latter points out that the lipophilic halogen substituents (Cl, Br, I) are unfavorable for the binding affinity for this class of analogues. Molecular docking calculations showed that replacement of a hydrogen atom at the C-4 of the imidazole ring with halogens would have not serious detrimental effect. To follow a similar strategy with losartan, the analogue **2** was synthesized as the oxidized form of **1**. In our case, the antagonistic activity in the uterotonic test of the oxidized compound **2** was similar to losartan [4]. Interestingly, **2** lacks the chlorine atom but still retains equipotency with losartan.



Acknowledgments

This project was financially supported by ELDRUG S.A., Patras Science Park, Greece and pharmaceutical company VIANEX.

References

- [1] Skrbic, R.; Igić, R. *Peptides* **2009**, *30*, 1945-1950.
- [2] (a) Kohara, Y.; Kubo, K.; Imamiya, E.; Wada, T.; Inada, Y.; Naka, T. *J. Med. Chem.* **1996**, *39*, 5228-5235. (b) Baker, W. L.; White, W. B. *Ann. Pharmacother.* **2011**, *45*, 1506-1515.
- [3] Agelis, G.; Roumelioti, P.; Resvani, A.; Durdagi, S.; Androutsou, M-E.; Kelaidonis, K.; Mavromoustakos, T.; Matsoukas, J. *J. Comput.-Aided Mol. Des.* **2010**, *24*, 749-758.
- [4] Agelis, G.; Resvani, A.; Durdagi, S.; Spyridaki, K.; Tůmová, T.; Slaninová, J.; Giannopoulos, P.; Vlahakos, D.; Liapakis, G.; Mavromoustakos, T.; Matsoukas, J. *Eur. J. Med. Chem.* **2012**, *55*, 358-374.

AZT-systemin conjugate translocation throughout tomato plant

Michał Dobkowski^{1,2*}, Rekowski Piotr², Mucha Piotr²

¹Intercollegiate Faculty of Biotechnology University of Gdańsk and Medical University of Gdańsk, Kładki 24, 80-822 Gdańsk, Poland; ²Faculty of Chemistry, University of Gdańsk, Sobieskiego 18, 80-952 Gdańsk, Poland
E-mail:dancer@chem.univ.gda.pl

Introduction

1,3-Dipolar azide alkyne Huisgen cycloaddition (Fig. 1) also called “click chemistry” is a new method of conjugation of biomolecules [1]. Huisgen cycloaddition reaction of alkynes and organic azides has numerous applications in synthetic organic chemistry. This transformation has the advantage of high chemoselectivity since a few functional groups react with azides or alkynes in the absence of other reagents.

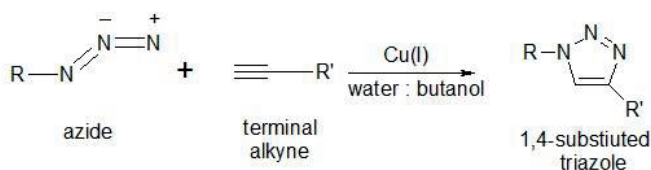


Fig. 1. A scheme of Huisgen cycloaddition

We decided to use Huisgen cycloaddition to synthesize a conjugate of systemin and AZT molecules. Systemin is a plant peptide hormone involved in the wound response in the Solanaceae family. It was the first plant hormone that was proven to be a peptide having been isolated from tomato leaves in 1991. The aim was to determine stability and ability to translocation of systemin and its AZT-conjugate through tomato plant tissues.

Results and Discussion

CD spectrum of systemin shows typical random conformation with a characteristic negative minimum at 200 nm. Conjugation with AZT does not alter systemin's structure. This suggests that biological function and properties of systemin should not be influenced.

To study stability and translocation properties of systemin and its AZT-conjugate, capillary electrophoresis (CE) has been used. A separation of the 3 peptides was easily achieved using phosphate buffer of acidic pH (Fig. 2). The peptide mixture was stable in tomato leaf extract at least for 24 hours.

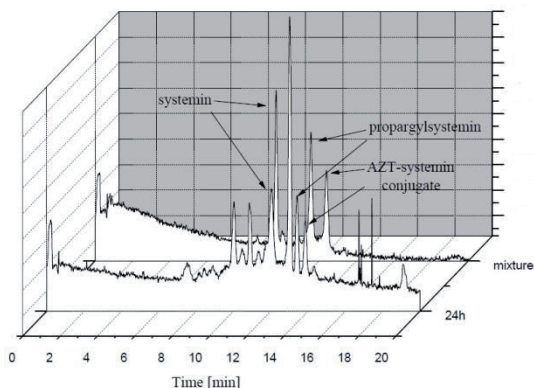


Fig. 2. A time-dependent CE study of systemin analogues stability in tomato leaf extract.

To study the ability of translocation through plant tissues, the mixture of peptides was injected into tomato plant stem at a height of about 80 cm. Then, at regular intervals, small samples, collected 10 cm above the injection site were studied by CE (Fig. 3). The peptides translocation was also studied in tomato leaves. In this experiment, the peptide mixture was injected into the leaf, directly behind the tail. Then, tomato leaf was cut into three equal parts along its long axis.

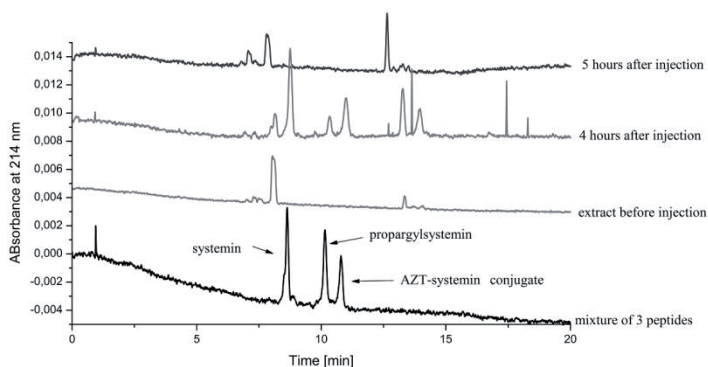


Fig. 3. A time-dependent CE analysis of systemin analogues in tomato stem.

CE experiments showed that systemin's ability to the translocation through plant tissues was retained after conjugation. AZT-systemin conjugate was stable enough to survive in tomato leaf extract at least for 24 hours. It moves easily through tomato stem and leaves. All these facts come to conclusion that systemin can be used as an effective transporter to proliferate cargo (insecticides or herbicides) through plant tissues.

Acknowledgments

This work was supported by the Polish National Science Centre grant no N N204 355540 and UG BN 538-8291-1032-12.

References

- [1] Meldal M, Tornøe C.W., *Chem. Rev.*, **2008**, *108*, 2952-3015.

Click-peptides: Novel 1,2,3-triazole backbone-modified peptidomimetics for tumor targeting

I. E. Valverde,^a A. Bauman,^a C. Kluba,^a A. Mascarin,^a S. Vomstein,^a
M. Walter,^b T. L. Mindt*^a

^aDepartment of Radiology and Nuclear Medicine, Division of Radiological Chemistry, University of Basel Hospital, Basel, Switzerland, ^bUniversitätsklinik für Nuklearmedizin, Inselspital, Bern, Switzerland

Introduction

Regulatory peptides (e.g., somatostatin, bombesin) have been shown to be suitable vectors for the specific delivery of radioactivity to tumors for diagnostic and therapeutic applications in nuclear oncology.[1] A potential drawback of such vectors is their inherent instability *in vivo*. Despite a tremendous effort in the field, new strategies are needed for the stabilization of radiopeptides in order to improve their bioavailability and, consequently, increase their accumulation in the targeted tissue.[2]

It has been suggested that 1,4-disubstituted 1,2,3-triazoles, readily obtained by the well-known copper catalyzed azide alkyne cycloaddition (CuAAC; click chemistry), are suitable amide bond surrogates. Unlike amide bonds, these heterocyclic linkages are resistant to proteolytic degradation.[3] In the present study, we report the synthesis and pharmacological evaluation of radiolabelled analogues of the gastrin releasing peptide receptor (GRPR) targeting peptide bombesin (BBN), in which amide bonds were systematically replaced with 1,2,3-triazoles.

Results and Discussion

In order to investigate the properties of triazole-containing peptide mimics of BBN, we first synthesized the building blocks required for their elongation by solid phase peptide synthesis. Azido derivatives from amino acids were obtained by a copper-catalyzed diazotransfer reaction (Figure 1A).[4] The chiral amino alkynes were prepared by a two-step synthetic procedure including the reduction of the carboxylic acid *via* its Weinreb amide followed by a Seyferth-Gilbert homologation using the Bestmann-Ohira reagent (Figure 1B).[5]

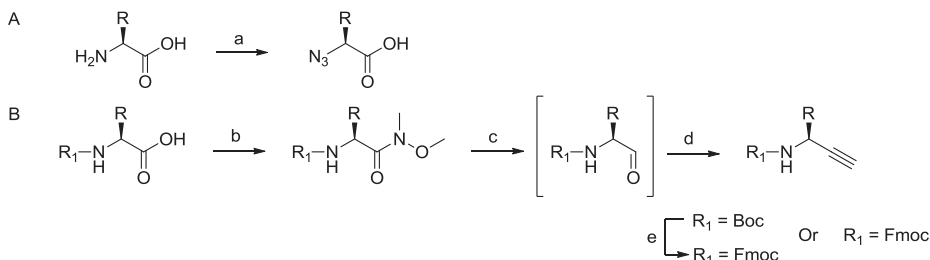


Figure 1. Synthesis of amino acid-derived azides and alkynes a) ImSO_2N_3 , CuSO_4 , K_2CO_3 , MeOH b) MeNHOMe , BOP , DIPEA , CH_2Cl_2 c) DIBAL-H , CH_2Cl_2 d) Bestmann-Ohira reagent, K_2CO_3 , MeOH .

The peptides were assembled by a combination of solid phase peptide synthesis (SPPS) and solid phase CuAAC (Figure 2). The amino acid sequence was elongated N-terminally with a short polyethylene spacer (PEG₄) and conjugated to the universal chelator DOTA. All DOTA-conjugates were obtained in good yields after HPLC purification (10-20%) and their structures were confirmed by mass spectroscopy.

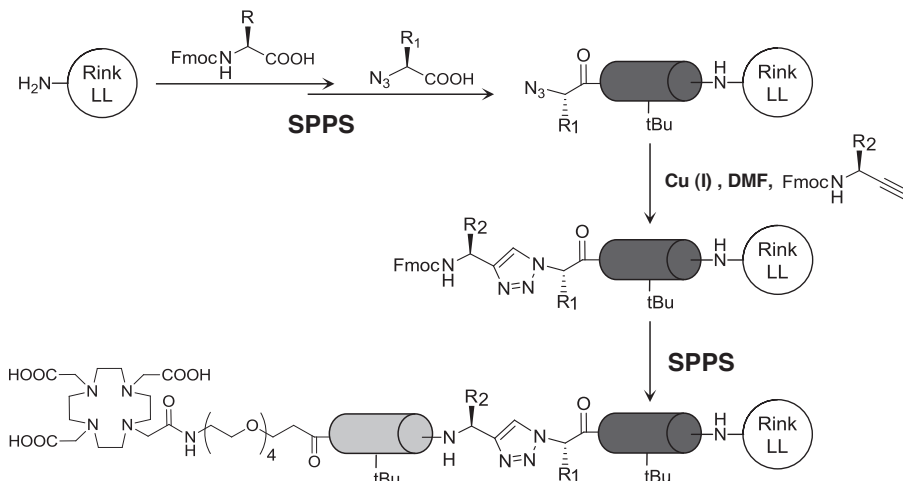


Figure 2. Solid phase synthesis of backbone-modified peptide mimetics

Radiolabeling with $^{177}\text{LuCl}_3$ was performed in ammonium acetate (pH 5.0) at 95°C for 30 min, affording the corresponding radioactive complexes in >95% radiochemical yield and purity. Cell internalization and GRPR binding affinity of the radiotracers were determined by established *in vitro* assays using PC3 cells. Biological half-lives of the compounds were determined by incubation in blood plasma at 37 °C and analysis of samples by radio-HPLC.

In some cases, a single replacement of an amide bond with a 1,2,3-triazole within the amino acid sequence of BBN yielded backbone modified peptidomimetics which retain the single-digit nanomolar receptor affinity and cell internalization properties of the original peptide but exhibit an up-to 5-fold improved stability *in vitro*. Preliminary results *in vivo* with nude mice bearing PC3 xenografts showed an improved tumor uptake of the peptidomimetic. Full evaluation of the novel radiotracers *in vitro* and *in vivo* is currently ongoing.

The methodology presented can be applied to a variety of peptides and thus, holds great potential for the development of novel, stabilized peptide-based (radio)pharmaceuticals.

Acknowledgments

The work was supported by the Swiss National Science Foundation and the Nora van Meeuwen-Häfliger Foundation.

References

- [1] Ambrosini, V.; Fani, M.; Fanti, S. et al. *J. Nucl. Med.* **2011**, *52*, 42S–55S
- [2] Alshoukr, F.; Prignon, A.; Brans, L. et al. *Bioconjugate Chem.* **2011**, *22*, 1374–1385
- [3] Tischler, M.; Nasu, D.; Empting, M. et al. *Angew. Chem. Int. Ed.* **2012**, *51*, 3708–3712.
- [4] Goddard-Borger, E. D.; Stick, R. V. *Org. Lett.* **2007**, *9*, 3797–3800.
- [5] Dickson, H. D.; Smith, S. C.; Hinkle, K. W. *Tetrahedron Lett.* **2004**, *45*, 5597–5599.

Synthesis, biological and structural evaluations of cyclic enkephalins with a diversely substituted guanidine bridge

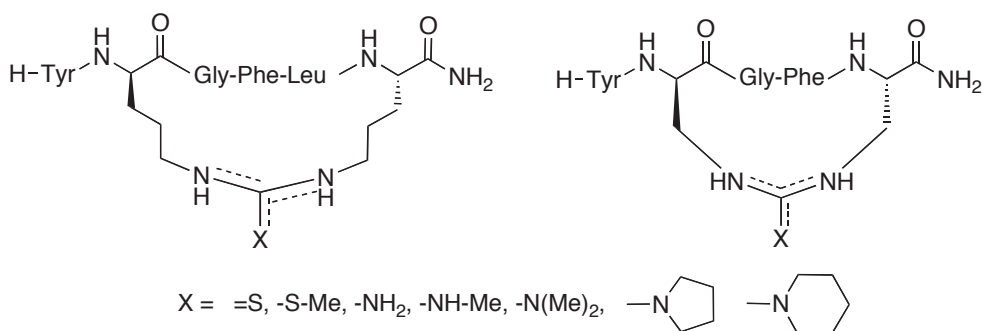
Youness Touati-Jallabe,¹ Engin Bojnik,² Baptiste Legrand,³ Elodie Mauchauffée,¹ Marie-Christine Averlant-Petit,³ Nga N. Chung,⁴ Peter W. Schiller,⁴ Sandor Benyhe,² Jean Martinez,¹ Jean-François Hernandez¹

¹Institut des Biomolécules Max Mousseron (IBMM), UMR5247 CNRS, Universités Montpellier 1 & 2, Faculté de Pharmacie, Montpellier, France. ²Biological Research Center, Institute of Biochemistry, Szeged, Hungary. ³Laboratoire de Chimie Physique Macromoléculaire, UMR7568 CNRS, Université de Lorraine, Nancy, France. ⁴Laboratory of Chemical Biology and Peptide Research, Clinical Research Institute, Montreal, Canada

E-mail: jean-francois.hernandez@univ-montpl.fr

Introduction

We recently described a new type of cyclic peptides possessing a diversely substituted guanidine bridge [1] and showed that the degree of bridge substitution could impact the orientation of the bridge inside the cycle and therefore the peptide conformation. We prepared two series (22 and 15 atoms cycle size) of cyclic enkephalin analogues to assess the potential effect of this kind of bridge on the opioid activity profile.



Results and Discussion

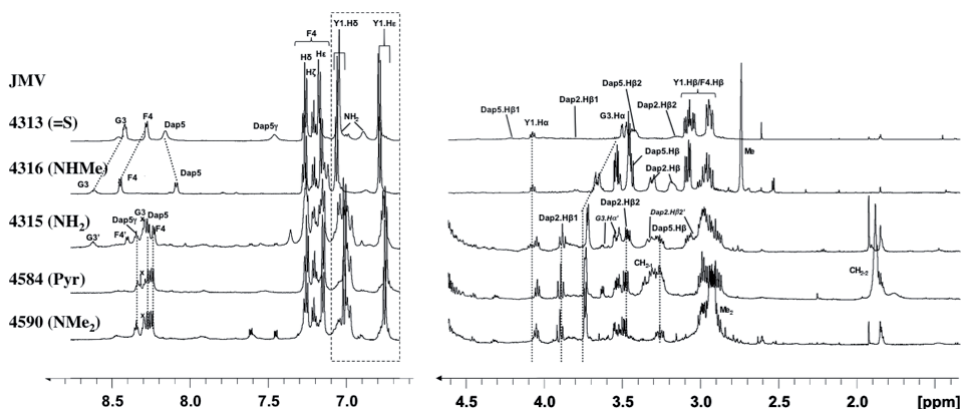
The compounds were synthesized on a solid support via the formation of a thiourea bridge and the variable substituent was introduced in the last step before cleavage [1]. Analogues were tested in μ and δ opioid receptor (MOR, DOR) binding assays and in the functional guinea pig ileum (GPI) and mouse vas deferens (MVD) assays. All compounds were full agonists and were more or less selective for the μ opioid receptor. Whereas only minor variations occurred in the hexapeptide series probably due to their relatively high structural flexibility (not shown), we observed a significant variation in receptor binding affinity and selectivity as a function of the degree of bridge substitution in the shorter series (Table 1).

Table 1. *In vitro* opioid activity profiles of the cyclic pentapeptides

JMV	X	Ki (nM)		δ/μ	GPI		MVD	
		MOR/ [³ H]DAMGO	DOR/ [³ H]DIDI		IC ₅₀ (nM)	Rel. Pot. ^a	IC ₅₀ (nM)	Rel. Pot. ^a
4313	=S	0.4	5.4	13.5	1.76	140	2.37	4.8
4315	-NH ₂	19	739	38.9	244	1	347	0.03
4316	-NHMe	1.5	62	41.3	41.8	5.9	76.5	0.15
4590	-N(Me) ₂	57	738	12.9	-	-	-	-
4584	-Pyrrol.	39	580	14.9	-	-	-	-
4317	-Piper.	107	1097	10.2	398	0.6	306	0.03

^aPotency relative to Leu-Enkephalin. GPI, guinea pig ileum; MVD, mouse vas deferens.

A structural analysis by NMR has been undertaken. The superimposition of 1D spectra showed significant differences between non-, mono- and di-substituted analogues, suggesting variable 3D structural features, which should explain the variations in biological activity. It is noteworthy that the 1D and 2D spectra of the two di-substituted analogues JMV4590 and JMV4584 were similar, suggesting an identical structure, in accordance to their similar activities. The non-substituted peptide JMV4315 showed two series of signals, of which one form had a spectrum comparable to that of JMV4590, while the other one (prime indices) resembled the JMV4316 spectrum, consistent with its intermediate receptor binding affinities. Finally, the NMR spectra of the most potent analogues (thiourea bridge JMV4313 and mono-substituted JMV4316) were clearly different from the others.



These results show that this kind of cyclization could represent a useful tool to easily modulate the conformation and biological activity of a unique peptide sequence.

Acknowledgments

The authors thank Pierre Sanchez for performing mass spectrometry analyses.

References

- [1] Touati-Jallabe Y.; Chiche L.; Hamz  A.; Aumelas A.; Lisowski V.; Berthomieu D.; Martinez J.; Hernandez J.-F. *Chem. Eur. J.* **2011**, *17*, 2566-2570.

Design and synthesis of non peptide mimetics of the immunodominant 83-99 myelin basic protein epitope (MBP₈₃₋₉₉)

Veronika Tsoulougian,¹ Irene Friligou,¹ Efthimia Mantzourani,² Theodore Tselios^{1,*}

¹*Department of Chemistry, University of Patras, GR-265 00, Patras, Greece;* ²*Cardiff School of Pharmacy and Pharmaceutical Sciences, King Edward VII Avenue, Cardiff, CF10 3NB, U.K.*

E-mail: tselios@upatras.gr

Introduction

Multiple Sclerosis (MS) is a chronic inflammatory and demyelinating disease of the central nervous system (CNS), characterized by destruction of the white matter (myelin). MS is believed to be mediated by an autoimmune T-cell response directed at proteins of the myelin sheath such as myelin basic protein (MBP), proteolipid protein (PLP) and oligodendrocyte glycoprotein (MOG). There is evidence that the 83-99 myelin basic protein epitope, is immunodominant for the activated T-cells [1, 2]. The T-cell response is triggered by the formation of the trimolecular complex between the major histocompatibility complex (MHC), the immunodominant myelin basic protein epitope and the T-cell receptor (TCR). In humans, MHC is also called human leukocyte antigen (HLA). For the design of a non peptide mimetic [3, 4], with the ability to block the T-cell activation, a search in several databases was carried out, which led to the identification of an indole ring substituted with specific pharmacophores.

Results and Discussion

Herein we report the synthesis of indole analogues that contain a carboxyl or an ethyl ester group in position C-2 and a phenylamino group in position C-6 of indole. The synthesis of the indole ring was achieved by a Fischer reaction between 3-nitrophenylhydrazine hydrochloride and ethyl pyruvate which gave a mixture of 4- and 6- nitro substituted indole analogues. These analogues were separated by column chromatography and the ethyl 6-nitro-1*H*-indole-2-carboxylate was further used for the synthesis of the final products. Initially the N1- indole position was protected with Boc using di-*tert*-butyl dicarbonate (Boc₂O) in the presence of 4-dimethylaminopyridine (DMAP). Then a catalytic hydrogenation took place in the presence of platinum dioxide (PtO₂-Adams catalyst) for the conversion of the nitro to the corresponding amine group. The amine arylation was achieved with a Chan-Evans-Lam reaction between the protected analogue (6) and phenylboronic acid [PhB(OH)₂]. Copper acetate [Cu(OAc)₂] was used as a catalyst, while pyridine was used as a base in the presence of 4Å molecular sieves for the removal of hydrogen peroxide (H₂O₂) formed during the reaction. The final product (8) was obtained after Boc deprotection with TBAF, whereas the final acid (9) was obtained after basic hydrolysis of the corresponding ethyl ester (8) with a hot ethanolic solution of potassium hydroxide (KOH). The synthesized molecules, as well as their intermediates, were purified

using either column chromatography or High Performance Liquid Chromatography, and they were identified by Mass Spectrometry (ESI-MS) and/or $^1\text{H-NMR}$.

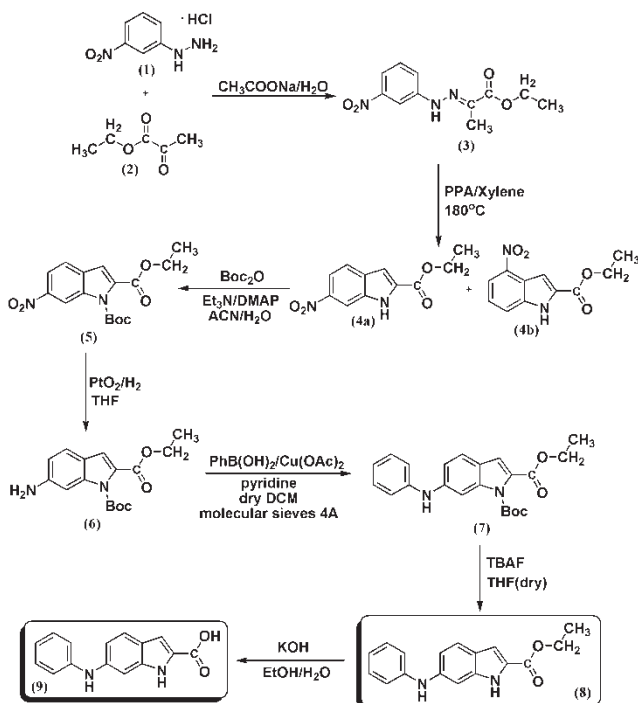


Figure 1: Synthetic procedure of the synthesized indole analogues.

Acknowledgments

This work is financially supported by the “Cooperation” program 09SYN-609-21, (O. P. Competitiveness & Entrepreneurship (EPAN II), ROP Macedonia–Thrace, ROP Crete and Aegean Islands, ROP Thessaly–Mainland Greece–Epirus, ROP Attica).

References

- [1] Mantzourani, E. D.; Platts, J. A.; Brancale, A.; Mavromoustakos, T. M.; Tselios, T. V. *J. Mol. Graph. Model.* **2007**, *26*(2), 471.
- [2] Mantzourani, E. D.; Tselios, T. V.; Grdadolnik, S. G.; Platts, J. A.; Brancale, A.; Deraos, G. N.; Matsoukas, J. M.; Mavromoustakos, T. M. *J. Med. Chem.* **2006**, *49*(23), 6683.
- [3] Spyralanti, Z.; Dalkas, G. A.; Spyroulias, G. A.; Mantzourani, E. D.; Mavromoustakos, T.; Friligou, I.; Matsoukas, J. M.; Tselios, T. V. *J. Med. Chem.* **2007**, *50*(24), 6039.
- [4] Katsara, M.; Deraos, G.; Tselios, T.; Matsoukas, M. T.; Friligou, I.; Matsoukas, J.; Apostolopoulos, V. *J. Med. Chem.* **2009**, *52*(1), 214.

Design and synthesis of small BACE1 inhibitor peptides

Yoshio Hamada^{1,2}, Harichandra D. Tagad², Yoshiaki Kiso^{1,2,3}

¹Faculty of Pharmaceutical Science, Kobe Gakuin University, Kobe, Japan, ²Center for Frontier Research in Medicinal Science, Kyoto Pharmaceutical University, Kyoto, Japan,

³Laboratory of Peptide Science, Nagahama Institute of Bio-Science and Technology, Nagahama, Japan

pynden@gmail.com

Introduction

β -Secretase (BACE1) is a molecular target for developing anti-Alzheimer's disease drugs. Recently, we reported potent penta-peptidic and non-peptidic BACE1 inhibitors containing a substrate transition-state mimic. [1] Previously, we reported potent pentapeptidic BACE1 inhibitors containing a hydroxymethylcarbonyl isostere (HMC) as a substrate transition-state mimic [1,2]. Our BACE1 inhibitor, KMI-429, exhibited potent inhibitory activity in cultured cells and an *in vivo* mouse model [1(e)]. Next we reported small-sized and non-peptidic BACE1 inhibitors that were designed from KMI-429 as a lead compound [1(h-j)]. These inhibitors were substituted with an aromatic moiety at the P₂-P₃ positions of the KMI-compounds and optimized using *in-silico* conformational structure-based design. In this study, we designed a series of small BACE1 inhibitor peptides lacking the P₁-P_{1'} region of KMI-compounds based on *in-silico* conformational structure bound in BACE1.

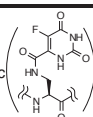
Results and Discussion

Until now, most of the peptidic BACE1 inhibitors possessing a substrate transition-state analogue were designed from the Swedish-mutant APP sequence (EVNL*D) that is cleaved faster than the wild-type APP sequence (EVKM*D) by BACE1. [3] The Km values of the Swedish-mutant and wild-type APP type substrates are similar, suggesting that the affinities for both types of substrates against BACE1 are similar. However, Swedish-mutant type substrates that have very high k_{cat} values exhibited higher catalytic efficiency by BACE1 than wild-type substrates. [3] We speculated that the hydrogen bond interaction between BACE1-Arg235 and the side chain of P₂-Asn of the Swedish-mutant type substrates activate the 'turn-over' of the enzyme, namely improving the k_{cat} value. On the other hand,

Table 1. Peptides and BACE1 inhibitory activity

Compd.	P ₄	P ₃	P ₂	P ₁	P _{1'}	P _{2'}	P _{3'}	P _{4'}	Inhibition % at 2 μ M
1	H-Glu	- Val	- Leu	- Phe	- Ser	- Ala	- Glu	- Phe-OH	6
2	H-Glu	- Val	- Leu	- Phe-D-Ser	- Ala	- Glu	- Phe-OH		28
3	H-Glu	- Val	- Leu	- Phe-D-Ser	- OH				23
4	H-Glu	- Val	- Leu	- Phe-D-Asn	- OH				29
5	H-Glu	- Val	- Leu	- Phe	- OH				8
Compd.	P ₄	P ₃	P ₂	P ₁	P _{1'}				Inhibition % at 2 μ M
6	H-DAP(5FO) ¹	- Val	- Leu	- Phe	- Ser	- OH			85
7	H-DAP(5FO)	- Val	- Leu	- Phe-D-Ser	- OH				94
8	H-DAP(5FO)	- Val	- Leu	- Phe	- Asn	- OH			89
9	H-DAP(5FO)	- Val	- Leu	- Phe-D-Asn	- OH				95
10	H-DAP(5FO)	- Val	- Asn	- Phe	- Asn	- OH			<5
11	H-DAP(5FO)	- Val	- Leu	- Phe	- OH				90
12	H-DAP(5FO)	- Val	- Asn	- Phe	- OH				<5
(KMI-446)	H-DAP(5FO)	- Val	- Leu	- Pns ²	- NH	- C ₆ H ₄	- COOH		99

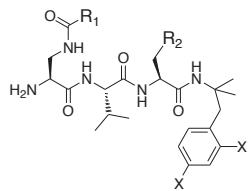
¹DAP(5FO):
 N^{β} -(5-Fluoroorotylyl)-
 L-2,3-diaminopropionic
 acid



²Pns:
 a substrate
 transition-state
 analogue



Table 2. Small BACE1 inhibitor peptides



Compd.	R ₁	R ₂	X	BACE1 inhibition % at 2 μ M
13			-H	70
14			-H	76
15			-H	90
16 (KMI-1608)			-H	92
17 (KMI-1777)			-I	96

we reported that the distances between the guanidino-plane of BACE1-Arg235 and P₂ region of the inhibitors showed similar values of 3 Å in most publicly-available X-ray crystal structures of BACE1-inhibitor complexes, and we suggested that the guanidino-plane of BACE1 interacts with the P₂ region of these inhibitors by a slight force such as σ - π interaction. [1(i)] We speculated that such an interaction at the S₂ site reduces the ‘turn-over’ of the enzyme, and a substrate possessing infinitely small k_{cat} value might turn into an inhibitor. Herein, we designed peptides possessing a P₂-Leu residue and found peptides **1-4** with weak inhibitory activity as shown in Table 1. [4] Next, we designed a series of peptides with a 5-fluoroorotyl moiety at the P₄ position. **6-9** and **11** showed potent inhibitory activity similar to the corresponding inhibitor, KMI-446, with a substrate transition state analogue.

Moreover, we designed small BACE1 inhibitor peptides lacking the P₁-P₁' region using *in-silico* conformational structure-based design as shown in Table 2. [5] Peptides **13-17** possessing two methyl groups at the C-terminus exhibited potent BACE1 inhibitory activity. We considered that the geminal dimethyl effect at the C-terminus stabilized the curved structure around the C-terminus phenyl ring, and the curved structure of peptides could allow for the interaction with S₁ pocket of BACE1. Peptide **17**, with two halogen atoms on the C-terminus phenyl ring, exhibited most potent inhibitory activity. The halogen atoms seemed to have enhanced inhibitory activity by interacting with the hydrophobic S₁ pocket. Although these peptides contain some natural amino acids, they can be lead compounds for developing the practical drugs because of their small molecular sizes.

References

- [1] (a) Shuto, D. *et. al. Bioorg. Med. Chem. Lett.* **2003**, *13*, 4273. (b) Kimura, T. *et. al. Bioorg. Med. Chem. Lett.* **2004**, *14*, 1527. (c) Kimura, T. *et. al. Bioorg. Med. Chem. Lett.* **2005**, *15*, 211. (d) Kimura, T. *et. al. Bioorg. Med. Chem. Lett.* **2006**, *16*, 2380. (e) Asai, M. *et. al. J. Neurochem.* **2006**, *96*, 533. (f) Hamada, Y. *et. al. Bioorg. Med. Chem. Lett.* **2006**, *16*, 4354. (g) Hamada, Y. *et. al. Bioorg. Med. Chem. Lett.* **2008**, *18*, 1649. (h) Hamada, Y. *et. al. Bioorg. Med. Chem. Lett.* **2008**, *18*, 1654. (i) Hamada, Y. *et. al. Bioorg. Med. Chem. Lett.* **2009**, *19*, 2435. (j) Hamada, Y. *et. al. Bioorg. Med. Chem. Lett.* **2012**, *22*, 4640.
- [2] Hamada, Y. *et. al. Expert Opin. Drug Discov.* **2009**, *4*, 391.
- [3] Grüninger-Leitch, F. *et al. J. Biol. Chem.* **2002**, *277*, 4687.
- [4] Hamada, Y. *et. al. ACS Med. Chem. Lett.* **2012**, *3*, 193.
- [5] Hamada, Y. *et. al. Bioorg. Med. Chem. Lett.* **2012**, *22*, 1130.

Design and synthesis of 3'-peptidyl-tRNA analogues – new tools for investigation of the ribosome function

Andrey G. Tereshchenkov,¹ Andrey V. Golovin,² Anna V. Shishkina,³
Natalia V. Sumbatyan,¹ Alexey A. Bogdanov*^{1,3}

¹Chemistry Department; ²Department of Bioengineering and Bioinformatics;
³A. N. Belozersky Institute of Physico-Chemical Biology, Lomonosov Moscow State
University, Moscow, Russian Federation

E-mail: sumbtyan@belozersky.msu.ru

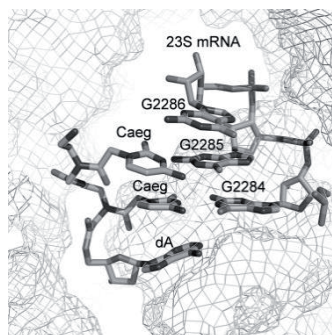
Introduction

Ribosomal tunnel (RT) is located in the large subunit of the ribosome so that its beginning overlaps with the peptidyl transferase center (PTC). The main function of the RT is to provide unhindered exit of newly synthesized polypeptide chain from the ribosome and its delivery to the site of the formation of a complete functional molecule. In the last decade after the appearance of the high-resolution X-ray data [1] detailed studies of the RT are started. This element of the ribosome is unique and fundamentally differs from the currently known channels in the membrane structures responsible for the passage of proteins and peptides. Binding sites of many antibiotics are located in the RT and, as a consequence, the modification of the walls of the RT leads to bacterial resistance to antibiotics [2]. RT is also involved in monitoring the amino acid sequence of a growing polypeptide moving through it. In some cases, peptides strongly interact with the walls of the RT that leads to ribosomal stalling and the arrest of translation [3]. This event is a key point in the regulation of expression of a number of genes.

The low molecular weight synthetic analogues of 3'-peptidyl-tRNA would permit to study the structural aspects of the interaction of the peptide chain with the RT, to identify the chemical nature of specific sites localized in RT which are responsible for interactions with amino acid residues of the nascent polypeptide chain.

Results and Discussion

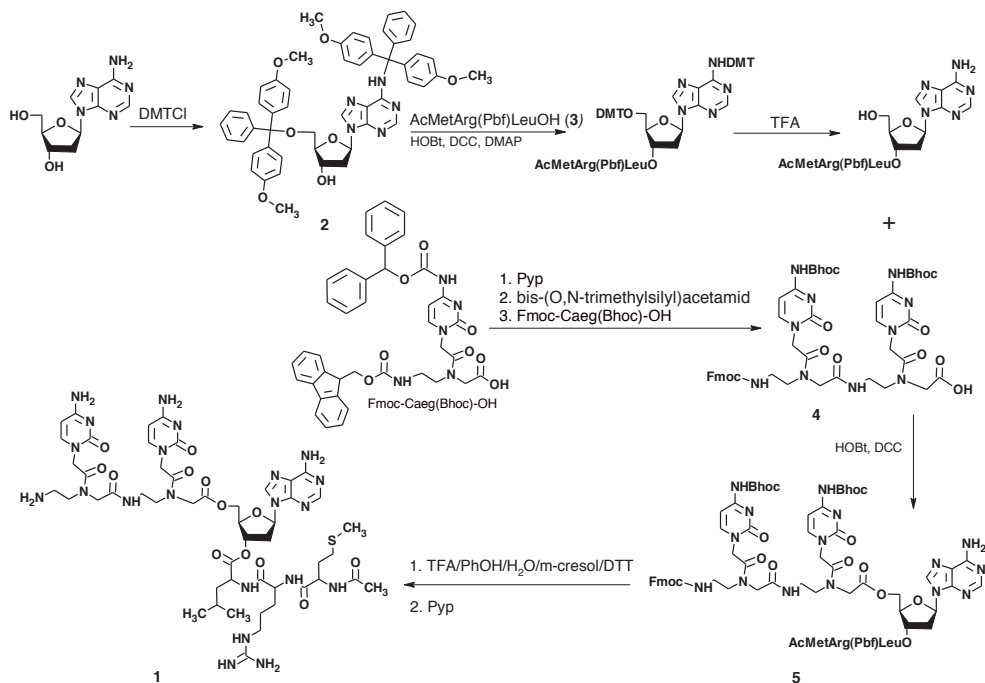
Design and synthesis of new 3'-peptidyl-tRNA analogue were carried out. Conjugate of peptide-nucleic acid (PNA) Caeg-Caeg with 2'-deoxyriboadenosine models 3'-tRNA sequence CCA in designed structure (**Scheme**, compound **1**). Adenosine was introduced in 3'-terminal position of CCA in order to the target compound could react with amino acid residue of aminoacyl-tRNA in A-site of PTC forming peptide bond, i.e., could be "hydrolysable". Peptide moiety of the 3'-peptidyl-tRNA analog is presented by "stop-peptide" MetArgLeu.



Computer simulations of the complexes of different structure CCA with PTC on the base of X-ray data of the complex of *H. marismortui* ribosome with the aminoacyl-tRNA [4] showed the possibility of the formation of

Watson-Crick pairing of the PNA cytosine residues with 23S rRNA nucleotides G2251 and G2252 involved in interactions with peptidyl-tRNA during its specific binding in P site (**Figure**).

Synthesis of “hydrolysable” conjugate included modification of the 3'-hydroxyl of 5'-protected 2'-deoxyadenosine (**Scheme**, compound **2**) by N-blocked “stop-peptide” (**3**), deprotection of the 5'-hydroxyl, its conjugation with N-protected PNA (**4**) and removal of protecting groups from the resulted conjugate (**5**). The target compound (**1**) was purified by HPLC (0-10% acetonitrile in water during 30 min, $\tau = 5,4$ min) and characterized by MALDI-TOF MS, $[M+H]^+$, m/z (found/calculated): 1196,5/1196,5.



Acknowledgments

This study was supported by the Russian Foundation for Basic Research (grants 10-04-01187-a and 11-04-01018-a). We thank Maxim Zhmak (Shemyakin-Ovchinnikov Institute of Bioorganic Chemistry RAS) for the synthesis of the peptide AcMetArg(Pbf)LeuOH.

References

- [1] Hansen, J.L.; Ippolito, J.A.; Ban, N.; Nissen, P.; Moore, P.B.; Steitz, T.A. *Mol. Cell.* **2002**, *10*, 117.
- [2] Starosta, A.L.; Karpenko, V.V.; Shishkina, A.V.; Mikolajka, A.; Sumbatyan, N.V.; Schluenzen, F.; Korshunova, G.A.; Bogdanov, A.A.; Wilson, D.N. *Chem. Biol.* **2010**, *17*, 504.
- [3] Vázquez-Laslop, N.; Ramu, H.; Mankin, A. in: *Ribosomes: Structure, Function and Dynamics*. Eds. Rodnina, M.V.; Wintermeyer, W.; Green, R. Wien, New York: Springer, 2011. P. 377.
- [4] RCSB PDB – 1VQ6.

Design, synthesis and antinociceptive activity of novel Endomorphin-2 and Morphiceptin analogues

Kaloyan Georgiev¹, Tatyana Dzimbova², Hristina Nocheva³, Adriana Bocheva³, Tamara Pajpanova²

¹Medical University of Varna, Varna, Bulgaria; ²Institute of Molecular Biology "Roumen Tsanev", Bulgarian Academy of Sciences, 1113, Sofia, Bulgaria; ³Department of Pathophysiology, Medical University of Sofia, Bulgaria
Email: tamara@bio21.bas.bg

Introduction

Endomorphins (endomorphin-1, EM-1, H-Tyr-Pro-Trp-Phe-NH₂, endomorphin-2, EM-2, Tyr-Pro-Phe-Phe-NH₂) are potent and selective μ -opioid receptor agonists. Furthermore, these tetrapeptides have a strong antinociceptive effect on acute pain, similar to that of morphine, but without some of the undesirable side effects [1, 2].

Morphiceptin (Tyr-Pro-Phe-Pro-NH₂), a tetrapeptide present in the enzymatic digest of bovine β -casein, is a selective ligand of the μ -opioid receptor. Its structure differs from EM-2 only by the amino acids in the fourth position (Pro and Phe, respectively) [3].

A close structural similarity of endomorphin-2 and another atypical opioid peptide, morphiceptin, which both have a Phe residue in the third position, encouraged us to study antinociceptive activity of these two peptides and their analogues.

Results and Discussion

The aromatic amino acids (Tyr1, Phe3, or Phe4) of EM-2 and morphiceptin have been shown to be important structural elements that interact with the opioid receptors besides the proline residue at the second position conferring high selectivity on the μ -opioid receptor [4]. Unfortunately, the exogenous application of these opioid peptides generally met with failure, owing to their biological instability and inability to be transmitted through the blood-brain barrier (BBB) [5].

In order to improve the affinity and chemical stability of these opioid peptides, we have designed, synthesized, and analyzed 9 novel analogues: *EM-2 analogues*: Tyr-D-Pro-Phe-Phe-NH₂ (1); Tyr-Pro-Phe(p-Cl)-Phe-NH₂ (2); Tyr-Pro-Phe(p-F)-Phe-NH₂ (3); Tyr-Pro-Phe-Phe-NH-CH₂-CH₂-NH₂ (4); Tyr-Pro-Phe(p-F)-Phe-NH-CH₂-CH₂-NH₂ (5) and *Morphiceptin analogues*: Tyr-Pro-Phe(p-Cl)-Pro-OH (6); Tyr-Pro-Phe(p-F)-Pro-OH (7); Tyr-Pro-Cav-Pro-OH (8); Tyr-Pro-sArg-Pro-OH (9).

The first modification included EM-2 and morphiceptin analogues, where Phe was replaced with Phe(p-Cl) (2, 6) or Phe(p-F) (3, 7). The peptides were synthesized on a Rink-amide resin using Fmoc-strategy with DIC/HOBt activation.

Next, the analogues 4 and 5 modified at C-terminus with biogenic amines were obtained on a Wang resin using Fmoc-strategy with DCC/HOBt activation. Another important modifying element is non-protein amino acid canavanine (Cav) and its analogue (sArg). It is well documented that Cav and sArg exhibit strong analgesic activity. Two new

morphiceptin analogues were synthesized by introducing Cav and sArg in position 3 (8 and 9). The crude peptides were purified by preparative TLC and their purity was checked by analytical HPLC. The precise molecular mass was confirmed by ESI-MS.

We also studied antinociceptive activity of morphiceptin analogues (8, 9) on the most frequently used models based on tests with thermal (hot plate, tail flick) irritation (Fig. 1).

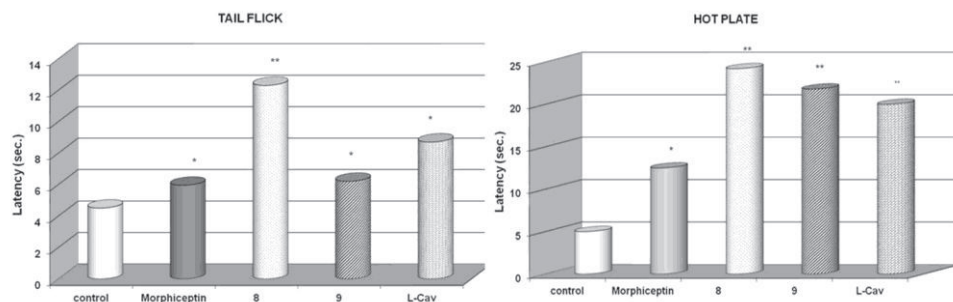


Figure 1. Effects of Morphiceptin and analogues \pm S.E.M.; *P \pm (1 mg/kg, i.p.) on nociception. Data are presented as mean <0.01 , ** P <0.01 versus control; +P <0.01 , ++ P <0.01 versus each of peptides.

Morphiceptin and analogues (all in dose 1 mg/kg) were dissolved in sterile saline solution and were injected i.p. It was found that 8 and 9 exerted antinociceptive effects on hot-plate and tail-flick tests. Stronger was the effect of analogue 8.

Acknowledgments

This work was supported by Bulgarian Ministry of Education and Science, project MY-FS-13/07.

References

- [1] Zadina, J. E.; Hackler, L.; Ge, L. J.; Kastin, A. J. *Nature* **1997**, *386*, 499.
- [2] Hackler, L.; Zadina, J. E.; Ge, L. J.; Kastin, A. J. *Peptides* **1997**, *18*, 1635.
- [3] Chang, K. J.; Su, Y. F.; Brent, D. A.; Chang, J. K. J. *Biol.Chem.* **1985**, *260*, 9706.
- [4] Fichna, J.; do-Rego, J-C.; Kosson, P.; Costentin, J.; Janecka, A. *Biochem. Pharmacol.* **2005**, *69*, 179.
- [5] Fichna, J.; do-Rego, J-C.; Costentin, J.; Chung, N. N.; Schiller, P. W.; Kosson, P.; Janecka, A. *Biochem. Biophys. Res. Commun.* **2004**, *320*, 531.

Facile and efficient syntheses of structurally modified *E*-urocanic acid analogs as potent Angiotensin II receptor blockers

**Amalia Resvani,^{1,5} George Agelis^{1,5} Christos Nikolis,¹ George Liapakis,²
Demetrios Vlahakos,³ Catherine Koukoulitsa,⁴ Dimitris Ntountaniotis,⁴
Thomas Mavromoustakos,⁴ John Matsoukas^{1,5}**

¹*Department of Chemistry, University of Patras, 26500 Patras, Greece;* ²*Department of Pharmacology, Faculty of Medicine, University of Crete;* ³*Department of Internal Medicine, "ATTIKON" University Hospital, Athens, Greece;* ⁴*Laboratory of Organic Chemistry, Department of Chemistry, University of Athens, Panepistimiopolis-Zografou15771, Athens, Greece;* ⁵*Eldrug S.A., Patras 26504, Greece*

E-mail:aggelisgeorge@hotmail.com; imats@upatras.gr

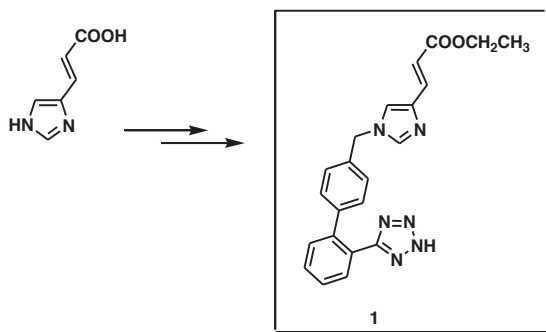
Introduction

The Renin-angiotensin system (RAS) is one of most powerful regulators of blood pressure. Consequently, the RAS has been the prime target for the therapy of cardiovascular diseases and non peptide AT1 receptor antagonists have been developed to specifically block the final site. Research efforts over the last decades have focused on the development of highly selective and strong Angiotensin II (ANG II) AT1 receptor blockers (ARBs) which provided a more specific blockade of the RAS. Losartan potassium was described as the first non-peptide AT1 receptor antagonist and was a drug lead for the development of eight orally active antagonists i.e. candesartan, valsartan, olmesartan, telmisartan which have been established as Angiotensin II AT1 receptor blockers (ARBs). The majority of the ARBs have resulted from the strategy of modifying or replacing several pharmacophore groups of Losartan. Structure Activity Relationship (SAR) studies of ARBs have shown that the lipophilic biphenylmethyl group at the 1-position, a linear alkyl group at the 2-position and an acidic group, like tetrazole, CO₂H, on the biphenylmethyl group are required for antagonistic activity. Furthermore, the DuPont group recommended a small-sized group at the 5-position of the ring such as CH₂OH, CH₂OMe, or CO₂H. In the present study, a series of new 1,5- and 1,4-disubstituted imidazole analogs has been synthesized based on *E*-urocanic acid. In particular, these analogs bear the biphenylmethyl tetrazole moiety at the N-1 of the imidazole ring and the rigid acrylic chain either at C-5 or C-4 which was lengthened by esterification, resulting in the corresponding ethyl ester. The latter was a key precursor for the conversion to the corresponding acrylic alcohol, aldehyde and carboxylic acid. Docking studies and biological evaluation of the synthesized analogs are being undertaken.

Results and Discussion

The present study describes the design and synthesis of a series of new 1,4- and 1,5-disubstituted imidazole analogs based on *E*-urocanic acid [1] as potent ARBs. In particular, the synthesized analogs bear the biphenylmethyl moiety ortho substituted with the tetrazole ring at the N-1 of the heterocycle as well as the acrylic acid side chain substituted either at

the C-4 or C-5 of the ring. Previous work has demonstrated that imidazole 5-acrylic acid ARBs showed high antihypertensive activity leading to Eprosartan, a diacid analog [2]. Furthermore, the rigid acrylic side chain was lengthened by esterification resulting in the corresponding ethyl ester which was the key precursor for further structural modifications. In particular, the resulting ester was readily converted to the anticipated acrylic alcohol, aldehyde and carboxylic acid in order to study the effect of these modifications in binding affinity. Finally, a lipophilic alkyl chain such as the *n*-butyl group was readily introduced at the C-2 position of the imidazole ring which may enhance binding affinity [3]. The synthetic procedure included efficient reactions in high yield, rendering it a general approach for the regioselective structural modifications on an ARB core in a sequential manner. Docking studies and biological evaluation of the synthesized analogs are in progress.



Acknowledgments

This project was financially supported by ELDRUG S.A., Patras Science Park, Greece and pharmaceutical company VIANEX.

References

- [1] Agelis, G.; Resvani, A.; Matsoukas, M. T.; Tselios, T.; Kelaidonis, K.; Kalavrizioti, K.; Vlahakos, D.; Matsoukas, J. *Amino Acids* **2011**, *40*, 411-420.
- [2] Keenan, R. M.; Weinstock, J.; Finkelstein, J. A.; Franz, R. G.; Gaitanopoulos, D. E.; Girard, G. R.; Hill, D. T.; Morgan, T. M.; Samanen, J. M.; Peishoff, C. E.; Tucker, L. M.; Aiyar, N.; Griffin, E.; Ohlstein, E. H.; Stack, E. J.; Wedley, E. F.; Edwards, R. M. *J. Med. Chem.* **1993**, *36*, 1880-1892.
- [3] Agelis, G.; Resvani, A.; Durdagi, S.; Spyridaki, K.; Tümová, T.; Slaninová, J.; Giannopoulos, P.; Vlahakos, D.; Liapakis, G.; Mavromoustakos, T.; Matsoukas, J. *Eur. J. Med. Chem.* **2012**, *55*, 358-374.
- [4] Agelis, G.; Roumelioti, P.; Resvani, A.; Durdagi, S.; Androutsou, M-E.; Kelaidonis, K.; Mavromoustakos, T.; Matsoukas, J. *J. Comput.-Aided Mol. Des.* **2010**, *24*, 749-758.

First synthesis of suitably protected PG-Phe-Ψ[P(S)(OX)CH₂]-Gly-PG' as Thiophosphinyl Dipeptide Isoster (TDI) analog and comparative study for selective deprotection

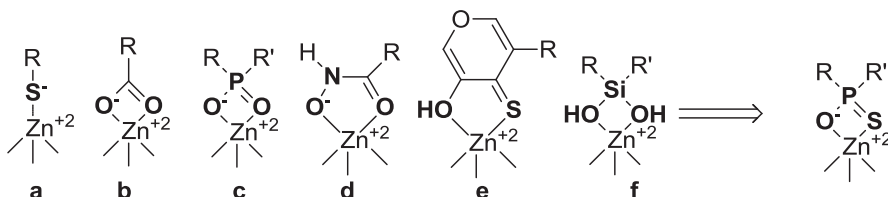
Vassiliou Stamatia

Department of Chemistry, Laboratory of Organic Chemistry, University of Athens,
 Panepistimiopolis Zografou, 15701, Athens, Greece

svassiliou@chem.uoa.gr

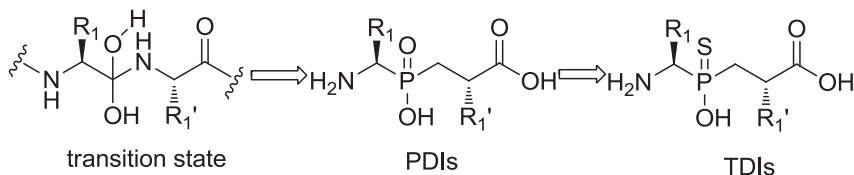
Introduction

The backbone modification of bioactive peptides with replacement of the scissile peptide bond in enzymatic hydrolysis is a well-established strategy for developing protease In particular, for zinc metalloproteases, which contain a zinc atom in their active site, several successful modifications have been reported over the past years (Scheme 1).



Scheme 1. Schematic representation of six zinc-binding groups shown in bold (a: thiolate, b: carboxylate, c: phosphinate, d: hydroxamate, e: hydroxythiopyrone and f: diolsilane) in complex with zinc ion. Possibility for thiophosphinate.

Phosphinyl dipeptide isomers (PDIs), presented as NH₂XaaΨ[P(O)(OH)CH₂]XaaOH, (Scheme 2) are the building blocks for the synthesis of phosphinic pseudopeptides and their chemistry is well documented.¹ In contrast to phosphinyl dipeptide isomers, there is no scientific report concerning thiophosphinyl dipeptide isomers (TDIs).² Herein, we present the first synthesis of fully protected thiophosphinate pseudodipeptides of the general formula PG-Phe-Ψ[P(S)(OX)CH₂]-Gly-OY. The behavior of the protecting groups under several deprotection conditions is investigated in a systematic manner.

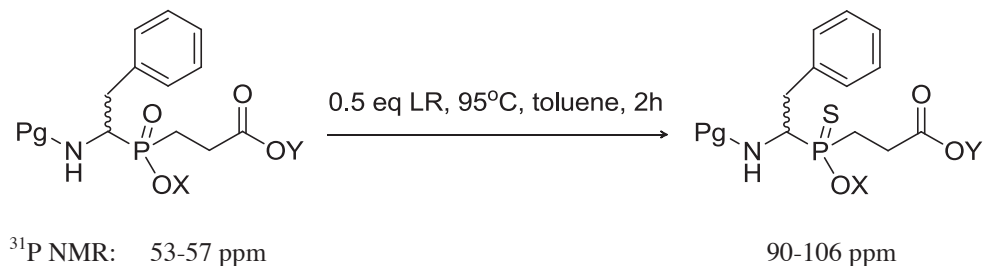


Scheme 2. Similarity between the structure of a peptidic sequence in the so-called tetrahedral-intermediate, a phosphinic dipeptide isomer (PDI) and a thiophosphinic dipeptide isomer (TDI).

Results and Discussion

Starting point of the synthesis was the corresponding phosphinate and Lawesson's reagent was the thionating agent. After detailed experimentation, we found that the optimal reaction conditions were: heating at 95°C, for 2 h in dry toluene using 0.5 equivalents of Lawesson's reagent. The corresponding thiophosphinates were obtained after column chromatography in very good yield with extensive downfield shift in phosphorus NMR.

Table 1. Synthesis of thiophosphinates from the corresponding phosphinates using Lawesson's reagent.



Product	Pg	X	Y	Yield (%)
1	Cbz	Me	Et	89
2	Cbz	Ad	Et	84
3	Fmoc	Me	^t Bu	82
4	Boc	Ad	Et	80
5	Cbz	Me	^t Bu	89
6	Cbz	Me	Allyl	92

Acidic treatment of the thiophosphinates **2** and **4** (TFA/CH₂Cl₂, Tms-Br) in order to remove the thiophosphinyl protecting group resulted in partial or complete S→O exchange. Surprisingly, using 33% HBr/AcOH for the Cbz-group removal in case **1**, didn't affect the thiophosphinyl function. Organic or inorganic volatile bases like NH₃, Et₂NH in methanol slowly demethylated **1** and **5** providing in different ratios, depending on the nucleophilicity and the basicity of the base, the corresponding carboxamide or free carboxylic acid in the case of **1** and quantitatively the *tert*-butyl carboxylic ester in the case of **5**.

References

- [1] Yiotakis, A.; Geogiadis, D.; Matziari, M.; Makaritis, A.; Dive, V. *Curr. Org. Chem.* **2004**, *8*, 1135.
- [2] Vassiliou, S. *Curr. Org. Chem.* **2011**, *15*, 2469.

Fluorescent analogues of SFTI-1 - synthesis and application

Anna Legowska¹, Magdalena Wysocka¹, Adam Lesner¹, Magdalena Filipowicz¹, Adam Sieradzan¹, Michal Pikula², Piotr Trzonkowski², Katarzyna Guzow¹, Krzysztof Rolka¹

¹Faculty of Chemistry, University of Gdansk, Poland; ²Clinical Immunology Division, Medical University of Gdansk, Poland

E-mail: legowska@chem.univ.gda.pl

Introduction

Proteases and their cognate inhibitors are important players in living organisms. Their mutual interactions are essential during the whole life cycle of a single cell starting from fertilization, embryogenesis, hormone processing, blood clotting, digestion to apoptosis [1]. The proteolytic activity is involved in all these pathways. Uncontrolled activity of proteases leads to pathology and disease. In 1999 Luckett *et al.* [2] isolated from sunflower seeds the trypsin inhibitor SFTI-1 (sunflower trypsin inhibitor 1), the smallest and, in addition, the most potent one among inhibitors of the Bowman-Birk family. Its primary structure is shown below:



SFTI-1 is a 14 amino acid circular peptide that was found to be homologous to the much bigger BBI family members. The reactive site P₁-P₁' of the SFTI-1 inhibitor is located between residues Lys⁵-Ser⁶. Owing to its small size and a strong trypsin inhibitory activity,

[(4-NPh₂)Ph]Box-Ala-AEA-[des-Arg²,Phe⁵]SFTI-1

(1) SFTI-1 is considered to be a very attractive template for designing proteinase inhibitors with a potential use as pharmacological agents. We

[2,4,5-(OMe)₃Ph]Box-Ala-AEA-[des-Arg²,Phe⁵]SFTI-1

(2) We have designed and synthesized four monocyclic (with disulfide bridge only) SFTI-1 analogues containing at their N-termini fluorescent moiety attached through bifunctional

[(4-NPh₂)Ph]Box-Ala-AEA-[des-Arg²]SFTI-1

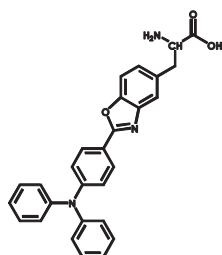
(3) amino-poly(ethyleneglycol)-acids (AEA and/or AEA). The primary structure of these analogues is shown in Fig. 1. These peptides were used as probes for detection of the inhibitor – proteinase complex and also to test their ability to cross cell membranes.

[2,4,5-(OMe)₃Ph]Box-Ala-AEA-[des-Arg²]SFTI-1

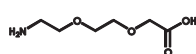
(4)

where:

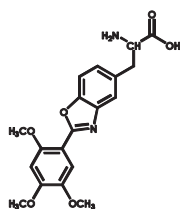
[(4-NPh₂)Ph]Box-Ala



AEA



[2,4,5-(OMe)₃Ph]Box-Ala



AEA

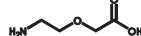


Fig. 1. The chemical structures of obtained SFTI-1 analogues

Results and Discussion

All peptides were synthesized by the solid-phase method using Fmoc chemistry. Fluorescent moieties, synthesized according to the procedure described previously [3], were attached using method applied for other amino acid derivatives. The determined values of the association constants of analogues (1) and (2) with chymotrypsin and (3) and (4) with trypsin indicated that they are potent inhibitors. They were proteolysis-resistant even after a 24 h incubation with the cognate enzyme. In order to monitor an inhibitor – enzyme complex formation, gel filtration on HPLC system equipped with fluorescence detector and acrylamide native gel electrophoresis were applied. The obtained results clearly show that after incubation of SFTI-1 analogues with appropriate proteinase the complexes were formed, as new highly fluorescent peaks on chromatograms or spots on gels corresponding to the complexes appeared. It has been also shown that the analogues do not form complexes with cognate enzymes in the presence of monocyclic SFTI-1 or [Phe⁵]-SFTI-1, which confirms that the interactions between the obtained analogues and trypsin or chymotrypsin are specific.

The fluorescent SFTI-1 analogues were also subjected to cell penetration assay using human fibroblasts cell line. All tested compounds were also able to cross efficiently the cell membrane. The results of 5 min. incubation of inhibitor (1) with human fibroblasts cell line, followed by the extensive PBS wash is presented in Fig. 2. The fluorescence was predominantly localized in the cytoplasmic fraction.

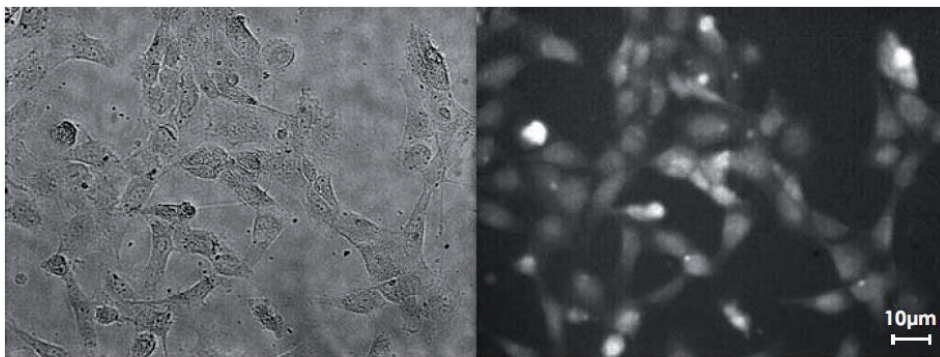


Fig. 2. Fibroblasts cell line + analogue 1; incubation time - 5 minutes.

Acknowledgments

This work was supported by Polish National Science Center (grant No. UMO-2011/01/B/ST5/03772).

References

- [1] Rawlings, N.D.; Barret, A.J. *Method Enzymol.* **1994**, *244*, 19.
- [2] Luckett, S.; Santiago Garcia, R.; Barker, J.J.; Konarev, A.V.; Shewry, P.R.; Clarke, A.R.; Brady, R.L. *J. Mol. Biol.* **1999**, *290*, 525.
- [3] Guzow, K.; Milewska, M.; Wiczak, W. *Spectrochim. Acta, Part A* **2005**, *61*, 1133.

Functional mimicry of protein binding sites: Using CLIPS technology in combination with oxime ligation for the reconstruction of *discontinuous* epitopes

L.E.J. Smeenk^a, H. Hiemstra^a, J.H. van Maarseveen^a, P. Timmerman^b

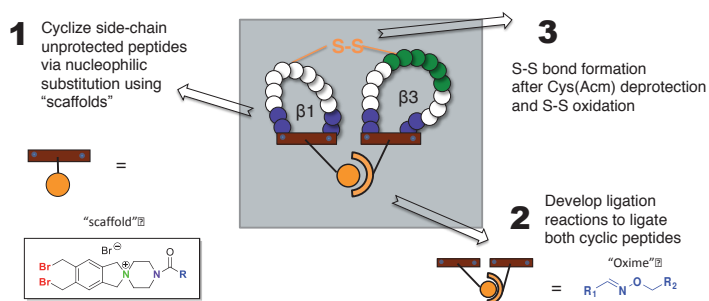
^aUniversity of Amsterdam, The Netherlands; ^bPepscan Therapeutics Lelystad, The Netherlands

E-mail: l.e.j.smeenk@uva.nl

Introduction

The functional reconstruction of folded protein surfaces with peptide-based mimics is an enormous scientific challenge. The majority of proteins show activity through a small area of their folded surface: “the binding site”. However, linear peptides are too flexible and seldomly adopt the correct 3D-structure of the binding site spontaneously. Therefore, they show limited or no activity at all¹. Crucial for activity is to control the secondary (α -helix, β -sheet and/or β -turn) and tertiary structure (relative orientation of subdomain structures).

In this project, peptides are constrained using CLIPSTM technology² (**1** in Figure), followed by oxime ligation (**2** in Figure) and S-S oxidation (**3** in Figure). This technology is applied to the epitope mimicry of three members of the cysteine-knot protein family (FSH, hCG and VEGF) since their epitopes are structurally related. We present the development of a new type of water-soluble scaffolds that have the potential to control both secondary and tertiary structure of discontinuous (*i.e.* double-loop) protein mimics³. Most unique to our approach is the fact that all chemical conversions are performed in aqueous media, using side-chain unprotected peptides. The antigenic activities of these protein mimics are investigated using binding and competition ELISA assays.

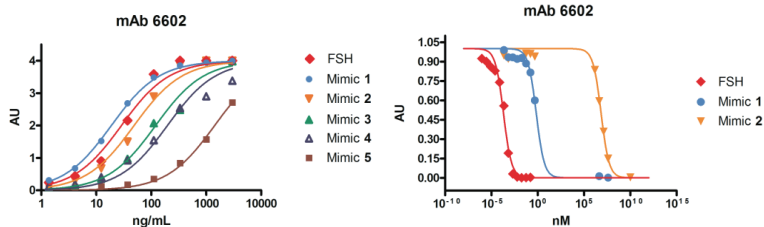


Results and Discussion

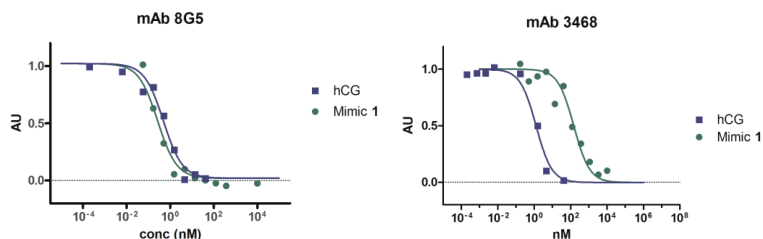
Several structural mimics of the β 1/ β 3-loop binding site on FSH have been synthesized using the protein FSH as a structural model. Amongst these are FSH mimic **1** (native + artificially introduced SS-bond, oxime, *long* β 1/ β 3 peptides), mimic **2** (native SS-bond only, oxime, *long* β 1/ β 3 peptides), mimic **3** (native SS-bond only, oxime, *short* β 1/ β 3

peptides), mimic **4** (no native SS-bond, oxime, *short* β 1/ β 3 peptides) and mimic **5** (only *short* β 3 peptide, no β 1 peptide present). Binding of these mimics (**1-5**) to the anti-FSH mAb 6602 (which specifically recognizes the discontinuous β 1/ β 3 loop) was tested in ELISA and compared to that of the native protein FSH (to which mAb6602 was raised). The importance of the following structural elements to obtain high binding affinities was confirmed:

- Presence of the β 1 peptide in the mimic is essential (mimic **5** vs. mimic **3**)
- Presence of native SS bond (at the top of the β 1/ β 3 loops) improves binding affinity (mimic **3** vs. mimic **4**)
- Longer peptide loops generally improve the binding affinity (mimic **2** vs. mimic **3**)
- Presence of artificially introduced S-S bond at the bottom of the β 3 loop peptide improves further the binding affinity (mimic **1** vs mimic **2**)



The same strategy was also applied to the synthesis of β -hCG mimics. Competition data in ELISA with the anti- β -hCG monoclonal antibodies 3468 and mAb 8G5 showed by far the best results for hCG mimic **1**, which gave an IC_{50} of 150 nM (for 3468) and 0.3 nM (for 8G5) (see below). The binding of mimic **1** to mAb 8G5 is virtually identical to that of β -hCG, which means that mAb 8G5 no longer tells the difference between this mimic and the protein it was derived from. Immunologic and antigenic properties of β -hCG mimic **1** are currently under investigation.



Acknowledgments

We kindly thank the Dutch Foundation for Scientific Research (NWO) for financial support of this research (project nr. ECHO 700.57.017).

References

- [1] For example: Dakappagari, N. K.; Lute, K. D.; Rawale, S.; Steele, J. T.; Allen, S. D.; Phillips, G.; Reilly, R. T.; Kaumaya, P. T. P., *J. Biol. Chem.* **2005**, *280*, 54-63
- [2] Timmerman, P.; Beld, J.; Puijk, W.C.; Meloen, R.H. *ChemBiochem* **2005**, *6*, 821-824
- [3] Smeenk, L.E.J.; Dailly, N.; Hiemstra, H.; Maarseveen, J.H.; Timmerman, P. *Org. Lett.* **2012**, *14*, 1194-1197

Synthesis and purification of enantiomerically pure *N*-amino-imidazolin-2-one dipeptide

Yésica García-Ramos, Caroline Proulx, Christophe Camy,
William D. Lubell

Département de Chimie, Université de Montréal, C.P. 6128, Succursale Centre-Ville,
Montréal, Québec H3C 3J7

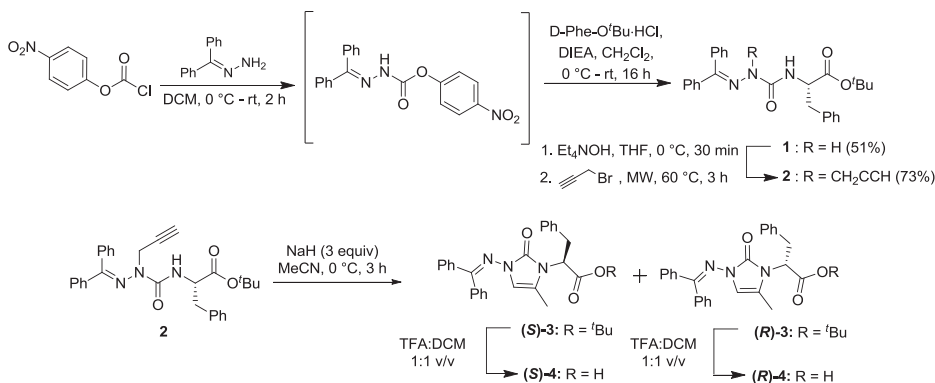
E-mail: william.lubell@umontreal.ca

Introduction

Aza-peptides incorporate a semicarbazide on replacement of an amino acid α -carbon by nitrogen, which favors turn geometry [1]. Similarly, introduction of an *N*-amino-imidazolin-2-one into a peptide restrains conformational liberty as observed by NMR spectroscopic and X-ray crystallographic analyses of 4-methyl *N*-(*p*-methoxybenzamido)imidazol-2-onyl-phenylalanine isopropyl amide, which exhibited turn geometry [2]. In the synthesis of dipeptide building blocks to make such mimics using aza-glycyl-phenylalanine *tert*-butyl ester **1**, racemisation was detected during the alkylation step to make aza-propargylglycinamide **2** and the cyclization step to *N*-amino-imidazol-2-one dipeptide **3** (Scheme). Milder alkylation conditions and a purification method are here reported to procure enantiomerically pure *N*-amino-imidazol-2-one dipeptide **3**.

Results and Discussion

Protected aza-glycyl-phenylalanine *tert*-butyl ester **1** was synthesized by the activation of benzophenone hydrazone with *p*-nitrophenyl chloroformate followed by the addition of *D*-phenylalanine *tert*-butyl ester (Scheme) [3]. Although alkylation of **1** with propargylbromide using *KOt*-Bu caused racemization, the milder base tetraethylammonium hydroxide (300 mol%) was selective such that alkylation at 60 °C under microwave irradiation gave aza-propargylglycinamide **2** in 73% yield and 97% enantiomeric purity [4].



Scheme. Synthesis of aza-propargylglycinamide **2** and imidazol-2-one **3**.

Cyclization of aza-propargylglycinamide **2** was achieved using sodium hydride (300 mol%) in dry acetonitrile for 3 h in 54% yield; however, racemization was detected by SFC analysis. Although conducting the reaction at 0 °C decreased epimerization to give *N*-amino-imidazolin-2-one (*R*)-**3** in 46% enantiomeric excess, a separation technique was necessary to obtain pure enantiomers. Employing supercritical fluid chromatography (SFC), the enantiomers (*R*)-**3** $\{[\alpha_D^{20}] 253 (c 1.06, \text{CHCl}_3)\}$ and (*S*)-**3** $\{[\alpha_D^{20}] -227 (c 0.9, \text{CHCl}_3)\}$ were separated using a preparative column containing a chiral stationary phase [Chiralpak AD-H 50 x 250 mm] and 15% *i*-PrOH in carbon dioxide as eluent with a flow rate of 60 g/min, at 150 bar (Figure).

Enantiomerically pure *N*-amino imidazol-2-ones (*R*)- and (*S*)-**3** were subsequently hydrolyzed with 50% TFA in CH_2Cl_2 for 1 h to furnish the corresponding acids (*R*)-**4** $\{[\alpha_D^{20}] 100 (c 1.15, \text{CHCl}_3)\}$ and (*S*)-**4** $\{[\alpha_D^{20}] -104 (c 1.04, \text{CHCl}_3)\}$, which are currently being introduced into peptides to study the effects of configuration and constraint on conformation and biology.

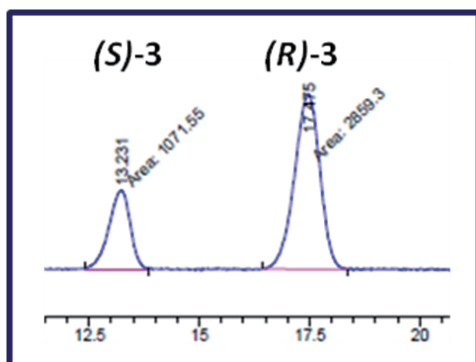


Figure. SFC analytical analysis of (RS)-**3** on a chiral stationary phase [Chiralpak AD-H 4.6 x 250 mm column] with 10% *i*-PrOH in carbon dioxide as eluent (3 mL/min) at 150 bar and 35 °C.

Acknowledgments

The authors thank the Natural Sciences and Engineering Research Council (NSERC) of Canada and the Canadian Institutes of Health Research (CIHR) grant No. TGC-114046. CP is grateful to NSERC and Boehringer Ingelheim for graduate student fellowships.

References

- [1] Proulx, C.; Sabatino, D.; Hopewell, R.; Spiegel, J.; Garcia-Ramos, Y.; Lubell, W. D. *Future Med. Chem.* **2011**, *3*, 1139.
- [2] Proulx, C.; Lubell, W. D. *Org. Lett.* **2012**, *14*, asap.
- [3] Bourguet, C. B.; Sabatino, D.; Lubell, W. D. *Pept. Sci.* **2008**, *90*, 824.
- [4] Garcia-Ramos, Y.; Proulx, C.; Lubell, W. D. *Can. J. Chem.* **2012**, *in press*.

***In vitro* assessment of the cytotoxic effects of novel RGD-mimetics**

Kaloyan Georgiev¹, Anelia Balacheva², Ekaterina Psycheva², Milena Georgieva², Tatyana Dzimbova², Lyubomir Georgiev², Ivan Iliev³, Roumyana Detcheva², George Miloshev², Tamara Pajpanova²

¹Medical University of Varna, Varna, Bulgaria; ²Institute of Molecular Biology "Roumen Tsanev", Bulgarian Academy of Sciences, 1113, Sofia, Bulgaria; ³Institute of Experimental Morphology and Anthropology with Museum, Bulgarian Academy of Sciences, 1113, Sofia, Bulgaria

Email: tamara@bio21.bas.bg

Introduction

Drug design based on the RGD structure may provide new treatments for cancer. We have shown previously [1] that modification of the carboxylic group of RGD with simple esterification increases the cell growth inhibitory effects of the parent compound on tumor cell lines HepG2 and MCF7. In an attempt to look deeper in the details of the observed cytotoxicity in the present work we investigated the genotoxic effect of synthesized by us RGD-mimetics, and their effect on the cell cycle in HepG2 cells as well.

Results and Discussion

In order to characterize the effect of newly synthesized RGD-mimetics and their derivatives HepG2 (liver hepatocellular carcinoma) cell cultures were treated *in vitro* for 17h with increasing concentrations of three compounds. The used concentrations were 0.03, 0.06 and 0.125 mM for RGD; 0.03, 0.06 and 0.125 mM for RGDOME and 0.06 and 0.125 mM for the third compound R(NO₂)GD. After treatment the cells were subjected to Comet assay (CA) to reveal damages in the genomic DNA. The method is a fast, sensitive and amenable tool for detection of genotoxicity at a single-cell level. In our case the Comet assay was applied in its neutral variant [2] with small modifications as in [3].

The results from CA have revealed a well expressed genotoxic activity of all of the tested compounds. The accumulation of DNA damages with the increase of concentration of compounds can be clearly observed in the size and in intensity of the comet tails (Fig.1A). The genotoxic potential of each of the compounds is represented as a percentage of comets in the respective concentrations (Fig.1B). Generally, we observed a well pronounced dose-dependent genotoxic effect of applied compounds. Briefly, Comet assay data confirmed that the three compounds possess certain DNA damaging activity, i.e. genotoxicity. This genotoxic activity could be detected even at the low concentrations (Fig.1A and B). Notably, it was better revealed and was increased with the modifications of the compounds, namely RGDOME and R(NO₂)GD. Thus, the most pronounced effect was observed with R(NO₂)GD at both tested concentrations and a little bit lower activity was detected for RGDOME at 0.06 and 0.125 mM.

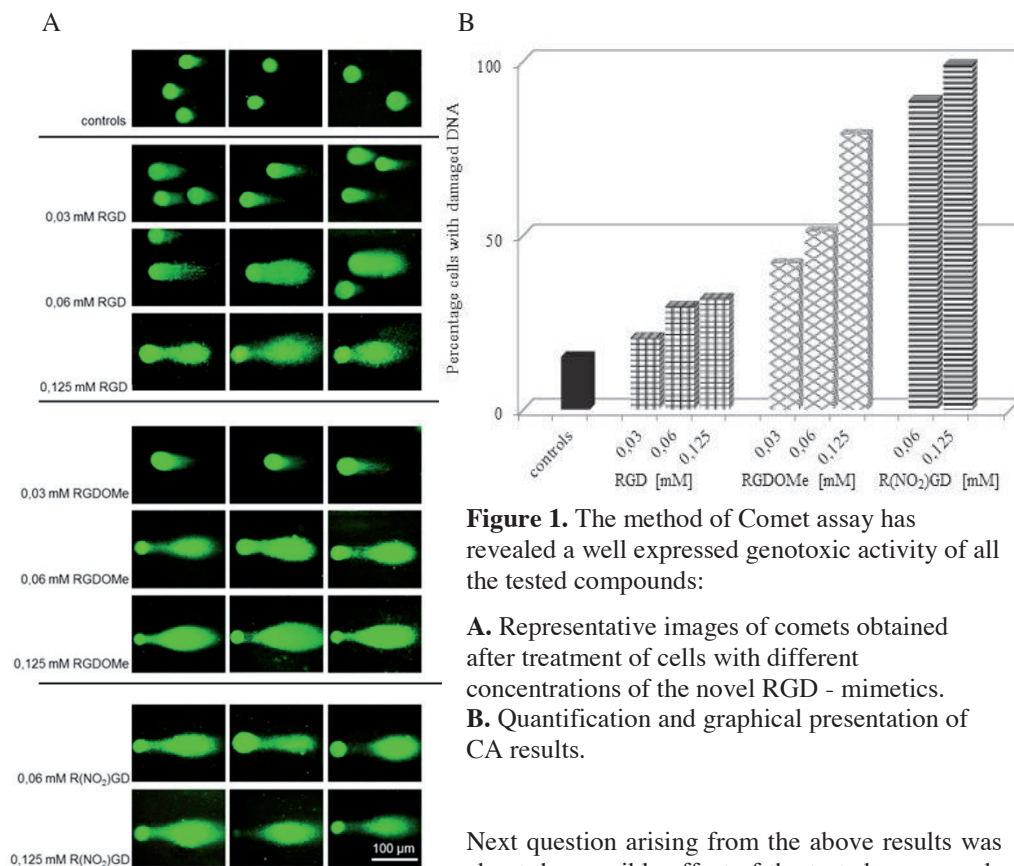


Figure 1. The method of Comet assay has revealed a well expressed genotoxic activity of all the tested compounds:

- A.** Representative images of comets obtained after treatment of cells with different concentrations of the novel RGD - mimetics.
B. Quantification and graphical presentation of CA results.

Next question arising from the above results was about the possible effect of the tested compounds on the cell cycle progression. FACS (Fluorescence Activated Cell Sorting) analysis can be used as a valuable tool for monitoring the progression of cells through different phases of the cell cycle. HepG2 cells were treated likewise in the Comet Assay experiments and were subjected to FACS analysis. The FACS analysis was performed according to [4]. Particularly, FACS histograms did not show any potential of the tested RGD – mimetics to block cells in any phase of the cell cycle (data not shown).

In summary, the results obtained by the Comet assay and FACS analysis show that even strongly pronounced the genotoxic activity of the three compounds is not connected with check-points of the cell cycle, but are rather dependent on their direct action on DNA. The obtained result promotes new ideas for future studying of molecular mechanisms that determine the higher genotoxicity of the novel RGD – mimetics and their derivatives.

Acknowledgments

This work was supported by Bulgarian Ministry of Education and Science, project MY-FS-13/07. E.P. and M.G. are supported by the Bulgarian Science Fund, project DMU 02/8.

References

- [1] Balacheva, A.; Iliev, I.; Detcheva, R.; Dzimbova, T.; Pajpanova, T.; Golovinsky, E. *BioDiscovery*, **2012**, submitted.
- [2] Östling, O.; Johanson, K.J. *Biochem. Biophys. Res. Commun.* **1984**, *123*, 291.
- [3] Peycheva, E.; Georgieva, M.; Miloshev, G. *Biotechnol. & Biotechnol. Eq.* **2009**, *23*, 1090.
- [4] Van Dilla, M. A.; Trujillo, T. T.; Mullaney, P.F.; Coulter, J. R. *Science*, **1969**, *163*,1213.

Microwave assisted solid phase synthesis of urea and urea/amide based foldamers

Karolina Pulka, Céline Douat-Casassus, Gilles Guichard

European Institute of Chemistry and Biology, University of Bordeaux 1 – CNRS UMR
5248, Pessac, France

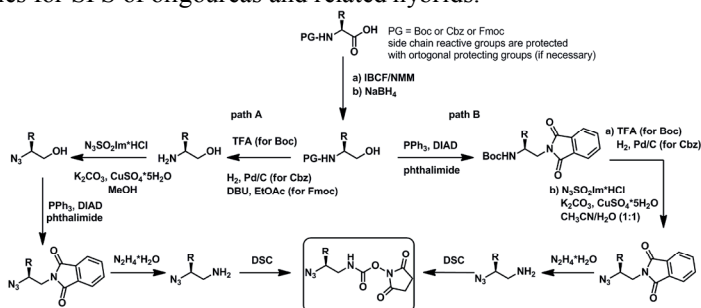
E-mail: g.guichard@iecb.u-bordeaux.fr

Introduction

Foldamers [1] are fully artificial molecules that structurally and functionally mimic variety of biopolymers. Among them, aliphatic *N,N'*-linked oligoureas with proteinaceous side chains can adopt extremely robust helical folds stabilized by intramolecular three-centred H-bonds. Owing to their resistance to the enzymatic degradation, diversity of side chains and structural predictability urea-based foldamers represent unique scaffolds to elaborate functional mimetics of α -polypeptides. Of note, heterogenous oligo(urea/ γ -amides) backbones obtained by substituting NH groups by CH_2 display very similar folding propensities. In the present work we have developed the Solid Phase Synthesis (SPS) of ureas and related hybrids based on the condensation of activated succinimidyl carbamates, under microwave (MW) irradiation.

Results and Discussion

Herein we describe our efforts to improve SPS of oligoureas with the assistance of microwave irradiation. Previously we have applied two strategies involving Fmoc- or Boc-chemistry, but both methodologies suffer some limitations. Fmoc chemistry was not compatible with the MW irradiation, *N*-Fmoc protected monomers (succinimidyl carbamates) were deprotected and oligomerized on resin. On the other hand, excellent results were obtained when *N*-Boc-protected monomers were used, but the final HF cleavage from the resin is impractical for routine use and library production. In search of an alternative to the Fmoc protecting group, we decided to reinvestigate the use of azides as masked amines for SPS of oligoureas and related hybrids.



Scheme 1. General synthetic procedure for the preparation of azido carbamates

The synthesis of 16 new azido succinimidyl carbamate building blocks was performed [2]. They were obtained in 6 steps from α -amino acids (10%–49% overall yield). Two synthetic

routes were developed as outlined in Scheme 1, depending on the nature of the side chain and amino group protection of starting amino acids.

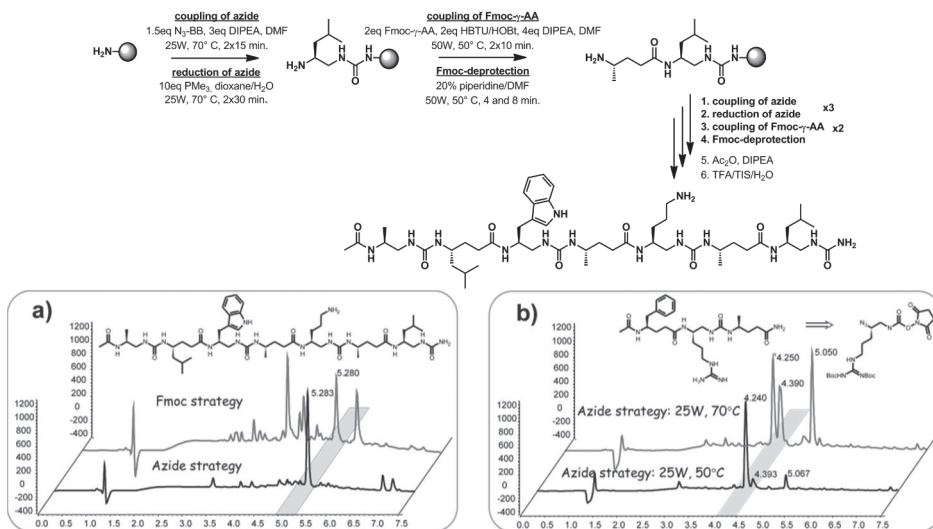


Figure 1. Microwave-assisted SPS of urea/amide hybrid oligomers: a) Comparison of Fmoc and Azide strategies; b) Optimization of the temperature for the synthesis of hybrid oligomers containing Arg-type residue.

With activated monomers in hand, we then investigated the coupling/azide reduction cycle on solid support under MW. Syntheses of oligoureas and hybrids were performed on NovaPEG Rink amide resin, which has high swelling properties in aqueous media, typically used for Staudinger reduction of azide with PMe_3 (Figure 1). To check the efficiency and efficacy of our new methodology, the same sequences were also synthesized via Fmoc method, without microwave irradiation. The purity and the yield of the oligomers were consistently better when we used azide building blocks (Figure 1a).

It is also worth to mention that the temperature under MW irradiation has a strong influence on the purity of oligomers containing Arg-like residue with di-Boc as a protection of the guanidino group (Figure 1b).

In conclusion we have developed the synthesis of azido succinimidyl carbamate monomers and optimized the synthesis of peptidomimetic foldamers under microwave irradiation.

This procedure is likely to facilitate the preparation of libraries of urea-based peptidomimetics for biological evaluation as well as the construction of larger and more sophisticated foldamer architectures.

Acknowledgments

This work was supported by the Centre National de la Recherche Scientifique (CNRS), the Region Aquitaine, the University of Bordeaux and the European Union (Marie Curie PEOPLE-2010-IEF-273224-FOLDAPOP, postdoctoral fellowship to K.P.)

References

- [1] Guichard, G.; Huc, I. *Chem. Commun.* **2011**, *47*, 5933.
- [2] Douat-Casassus, C; Pulka, K.; Claudon, P.; Guichard, G. *Organic Letters* **2012**, *14*, 3130.

Peptide mediated bacterial drug delivery

A mechanistic study of uptake and resistance towards novel antibiotics

Katrine M. Olsen, Thomas Bentin, Peter E. Nielsen

University of Copenhagen, Faculty of Health Sciences, Department of Cellular and Molecular Medicine

kaol@sund.ku.dk

Introduction

Bacteria showing resistance towards multiple antibiotics necessitates development of new types of antibiotics. These antibiotics should have a mechanism different from accessible antibiotics to circumvent existing resistance mechanisms [1]. Previous results have shown that “genetic” antibiotics operating by gene silencing in bacteria may be successful candidates.

Peptide nucleic acids (PNAs) are synthetic mimics of DNA, in which the backbone is replaced with a pseudopeptide backbone to which the nucleobases are linked (Figure 1). PNAs hybridize with complementary DNA, RNA and PNA with high specificity and affinity, because of their uncharged and flexible polyamide backbone. Sequence specific binding of PNAs to RNA make them suited for targeting gene expression at the translational level in an RNA silencing therapy [1].

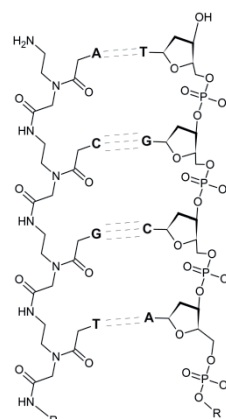


Figure 1: Structure

Efficient silencing requires efficient crossing of cell membranes. This step can be facilitated by cell penetrating peptides (CPPs) as carriers of drug candidates such as PNAs, which have shown promising antibacterial effects, but have poor internalization properties. The exact mechanism by which the PNA-CPP is transported into the cell remains largely unknown [2]. It is hypothesized that after crossing the outer lipopolysaccharide membrane of gram negative bacteria, part of or the entire CPP is cleaved of in the periplasm of the cell. The PNA is then assumed to cross the inner membrane without the carrier peptide or with only a part of the carrier peptide coupled to it. Hence, one aim of this project is enlightening of the fate of the PNA and CPP once inside the cell (Figure 2), which remains to be performed.

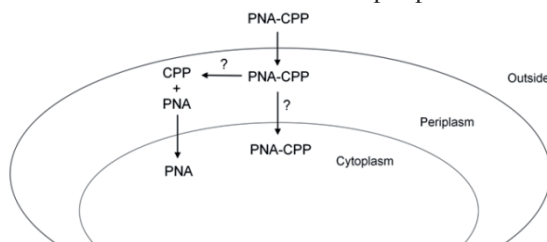


Figure 2: Possible PNA uptake in gram negative bacteria

Furthermore, a simple toxicity screening method is being redesigned using histamine release in rat basophilic leukemia (RBL) 2H3 cells as a quantitatively measure of the allergenicity of PNA-CPPs, in order to pre-screen compounds. The method is based on beta hexosaminidase, which has been found to have identical dose dependent release profile with histamine in RBL 2H3 [3].

Results and Discussion

Initial approaches for development and redesign of a method using histamine release in RBL 2H3 as measure of toxicity of PNA-CPPs has been attempted. Release of histamine from a monolayer of RBL 2H3 cells has been measured after 1 hour of exposure to either PNA2108 or PNA3759 or the positive control used, calcium ionophore (Figure 3). Doses response is observed for the positive control indicating the reliability of the method. The PNA-CPPs tested only cause a minimal of histamine release.

This promising *ex vivo* histamine release screening method is to be further developed and used to test promising PNA-CPPs to avoid features giving rise to systemic toxicity.

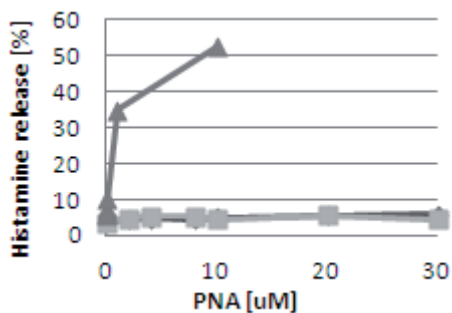


Figure 3: Doses response curve of histamine release in RBL 2H3 cells:

—●— PNA2108: KFFKFFKFFK-CTCATACTCT;
—■— PNA3759: (KFFKFFKFFK)₀-CTCATACTCT
and —▲— calcium ionophore

Acknowledgments

This research is supported by The Danish Council for Independent Research – Medical Sciences and of The Faculty of Health Sciences, University of Copenhagen.

References

- [1] Good, L., Awasthi, S. K., Dryselius, R., Larsson, O., Nielsen, P. E. (2001) *Nat. Biotechnol.* 19, 360-364 .
- [2] Eriksson, M., Nielsen, P. E., Good, L. (2002) *J. Biol. Chem.*,277, 7144-7147.
- [3] Schwartz, L. B., Austen, K. F., Wasserman, S. I. (1979) *J. Immunol.* 123, 1445-1450.

Synthesis of oxytocin-steroid chimeric molecule and its visualization on the rat uterus slices

M. Jurasek^a, P. Skopek^c, M. Flegel^{b,c}, Z. Flegelova^{c,d}, P. Drasar*^a,
M. Lebl^d, T. Kraus^b, S. Hynie^c, V. Klenerova^c

^aInstitute of Chemical Technology, Prague, Czech Republic ^cFirst Faculty of Medicine, Charles University in Prague, Prague, Czech Republic; ^bInstitute of Organic Chemistry and Biochemistry, Czech Academy of Sciences, Prague, Czech Republic; ^dSpyder Institute Prague, Czech Republic

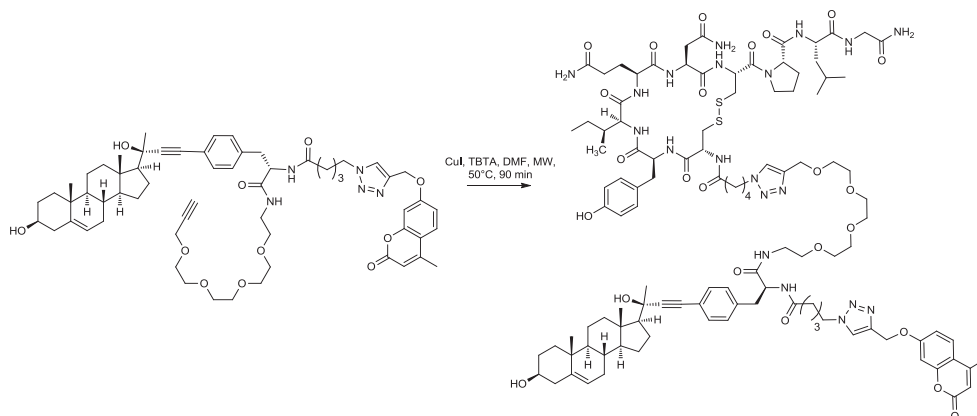
pavel.drasar@vscht.cz

Introduction

Chimeric molecule containing hormones oxytocin, 24-norcholesterol-5-en-22-yn-3 β -ol (pregnenolone derivative) and coumarin as the fluorescent marker was constructed (Scheme 1). The main goal was to prepare the compound recognizing oxytocin receptors on the suitable tissue (uterus, brain). At the same time the proposed structure (steroid increasing lipophilicity) might hopefully lead to better stability of the peptide hormone and enhance its possible penetration through blood brain barrier, for which the similar compounds are considered to be used in future.

Results and Discussion

Click chemistry was used for preparation of the chimeric molecule. Azidovaleric acid was coupled to amino terminus of oxytocin and cross-coupled to the steroid-coumarin hybrid molecule Sonogashira (prepared by coupling of the appropriate building blocks under Sonogashira cross-coupling conditions) [1,2] and functionalized with ethynyl group [3].



Scheme 1. Synthesis of chimeric compound

Fluorescence detection of oxytocin receptors (OTR).

Frozen sections of rat uterus horns (7 μm) were used as a reference tissue containing oxytocin receptors (OTR) with known physiological function. Detection of OTR was performed either with the use of primary polyclonal antibodies (Abcam, UK), diluted 1:250, incubation 4°C overnight, and secondary antibody, which was Alexa Fluor 488 (Invitrogen, CA, USA) 1:600, incubation 2 h, room temperature in the dark, or with the chimeric molecule solution (100 μL , 1 mg/mL, 2 h, r.t.). Immunofluorescence was detected by microscope Leica DM5000 B (Figure 1).

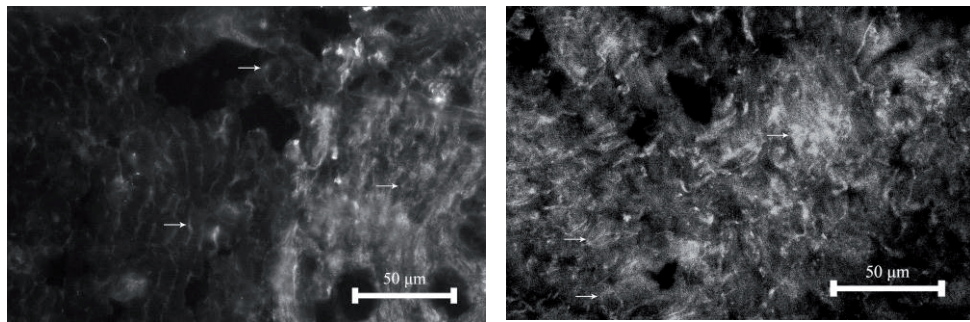


Fig. 1. Immunofluorescence of OTR in the rat uterus horn, detected by the specific anti-OTR antibodies (left panel) and chimeric compound (right panel). The arrows pointing to the circular elements show the receptors on the plasma membranes.

Conclusion

Solution of the synthesized chimeric construction (scheme 1) was successfully used for the visualization of oxytocin receptors (OTR) in the uterus horn. In the next step, this and similar constructs will be used for the OTR depiction on the brain tissue.

Acknowledgments

This work was supported by Grants: GAUK 85210, PRVOUK25/LF1/2, SVV 264514 IOCB RVO: 61388963, 7FP Dinamo grant agreement no: 245122, MŠMT 7E11070

References.

- [1] K. Sonogashira, Y. Tohda and N. Hagihara, *Tetrahedron Letters* 1975, 4467-4470.
- [2] R. Huisgen, *Angewandte Chemie-International Edition* 1963, 75, 604-610.
- [3] a) F.F.Wong, et al., *Tetrahedron* 2010, 66, 4068-4072; b) A. Burger, et al., *Tetrahedron* 1988, 44, 1141-1152.

Rational design, efficient synthesis and biological evaluation of new *N,N'*-symmetrically bis-substituted butylimidazole analogs as potent Angiotensin II receptor blockers

Amalia Resvani,^{1,9} George Agelis,^{1,9} Catherine Koukoulitsa,² Antreas Afantitis,³ Georgia Melagraki,³ Athanasia Sifaka,⁴ Eleni Gkini,⁴ Tereza Tůmová,⁵ Katerina Spyridaki,⁶ Dimitra Kalavrizioti,⁷ Maria-Eleni Androutsou,^{1,9} Jiřina Slaninová,⁵ George Liapakis,⁶ Demetrios Vlahakos,⁸ Thomas Mavromoustakos,² John Matsoukas^{1,9}

¹*Department of Chemistry, University of Patras, 26500 Patras, Greece;* ²*Laboratory of Organic Chemistry, Department of Chemistry, University of Athens, Panepistimiopolis-Zografou15771, Athens, Greece;* ³*Department of Chemoinformatics, NovaMechanics Ltd, John Kennedy, Ave 62-64 Pallouriotissa, Nicosia 1046, Cyprus,* ⁴*Laboratory of Biochemistry, Department of Chemistry, University of Athens, Zografou, 15784 Athens, Greece;* ⁵*Institute of Organic Chemistry and Biochemistry, Academy of Sciences of the Czech Republic, Flemingovo nám. 2, 16610 Prague 6, Czech Republic;* ⁶*Department of Pharmacology, Faculty of Medicine, University of Crete, Voutes, 71003 Heraklion, Crete, Greece;* ⁷*Department of Pharmacology, School of Medicine, University of Patras, 26500 Patras, Greece;* ⁸*Department of Internal Medicine, "ATTIKON" University Hospital, Athens, Greece;* ⁹*Eldrug S.A., Patras 26504, Greece*

E-mail:aggelisgeorge@hotmail.com; imats@upatras.gr

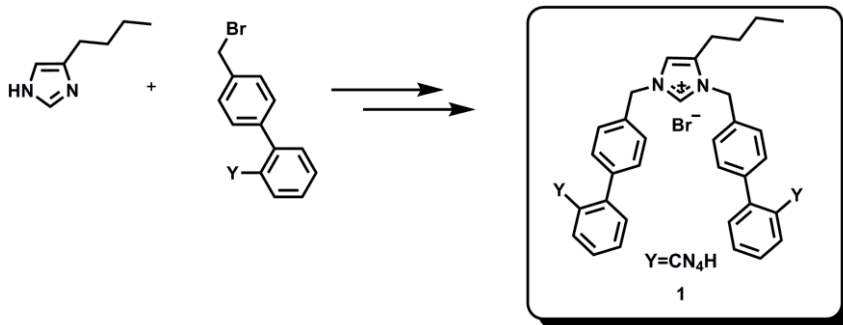
Introduction

The Renin-Angiotensin System (RAS) plays a key role in regulating cardiovascular homeostasis and electrolyte/fluid balance in normotensive and hypertensive subjects. Consequently, research efforts over the last years have been directed toward developing drugs capable of suppressing the RAS at the three different sites of blockades such as non peptide AT1 receptor antagonists [1-3]. In specific, the DuPont group pursued a study in this field and developed Losartan, the first orally effective non-peptide antagonist. Since then, numerous new antagonists have been reported with nine of them in the clinic which have been established as strong AT1 Receptor Blockers (ARBs). The majority of selective ARBs have resulted from the strategy of modifying or replacing several pharmacophore groups of Losartan. Lipophilic substituents, such as the biphenylmethyl group at the N-1 of a heterocycle, a linear alkyl group at the 2-position and an acidic group, like tetrazole, CO₂H, or NHSO₂CF₃ on the biphenylmethyl group are required for antagonistic activity. Furthermore, the DuPont group recommended a lipophilic and electron-withdrawing group, such as iodine or CF₃, as a substituent at the 4-position and a small-sized group at the 5-position, such as CH₂OH, CH₂OMe, or CO₂H. In the present work, a series of new analogs has been synthesized bearing an extra biphenylmethyl moiety at the N-1 and N-3 of the imidazole ring ortho substituted with an acidic functionality such as a tetrazole or its bioisostere carboxy group. The synthesis was based on our Angiotensin II model

conformation [4]. Furthermore, the heterocyclic ring bears the *n*-butyl group either at the C-2 or C-5 as well as the hydroxymethyl group at the C-2 and a halogen atom at the C-4. These unusual analogs were *in vitro* evaluated by means of their binding affinities for the human AT1 receptor, as well as for their ability to inhibit the contractility effect of Angiotensin II in isolated rat uterus, compared to Losartan.

Results and Discussion

The present study refers to the design and syntheses of bis-alkylated 4(5)-butylimidazole analogs as potent ARBs. In particular, a rational design was performed to synthesize a series of *N,N'*-symmetrically bis-substituted imidazole analogs bearing at the N-1 and N-3 two biphenylmethyl moieties ortho substituted either with tetrazole or carboxylate functional groups. The SAR studies demonstrated the importance of the nature and the position of pharmacophores. In particular, the presence of two anionic tetrazole groups along with the lipophilic *n*-butyl group at the C-5 led to the potent analogs **1** ($-\log IC_{50} = 9.46$) compared to Losartan ($-\log IC_{50} = 8.25$). The introduction of the electronegative hydroxymethyl group at the C-2 led to acquisition of affinity ($-\log IC_{50} = 8.37$), while the presence of a halogen atom at the C-4 of the imidazole ring led to an essential decrease in affinity representing poor bioisostere for the tetrazole group. The position of the *n*-butyl group plays a significant role, since reorientation from the C-5 to the C-2 resulted in a sharp drop of affinity. This dramatic loss of activity may be explained by the concealment of the *n*-butyl group between the two biphenyltetrazole moieties.



Acknowledgments

This project was financially supported by ELDRUG S.A., Patras Science Park, Greece and pharmaceutical company VIANEX.

References

- [1] Dagupta, C.; Zhang, L. *Drug Discovery Today* **2011**, *16*(1-2), 22-34.
- [2] Agelis, G.; Resvani, A.; Durdagi, S.; Spyridaki, K.; Tűmová, T.; Slaninová, J.; Giannopoulos, P.; Vlahakos, D.; Liapakis, G.; Mavromoustakos, T.; Matsoukas, J. *Eur. J. Med. Chem.* **2012**, *55*, 358-374.
- [3] Agelis, G.; Roumelioti, P.; Resvani, A.; Durdagi, S.; Androutsou, M-E.; Kelaidonis, K.; Mavromoustakos, T.; Matsoukas, J. *J. Comput.-Aided Mol. Des.* **2010**, *24*, 749-758.
- [4] Matsoukas, J. M.; Hondrelis, J.; Keramida, M.; Mavromoustakos, T.; Makriyannis, A.; Yamdagni, R.; Wu, Q.; Moore, G. J. *J. Biol. Chem.* **1994**, *269*, 5303-5312.

Structure activity relationship study of (+)-negamycin with readthrough-promoting activity for duchenne muscular dystrophy chemotherapy

Akihiro Taguchi¹, Masataka Shiozuka², Yuri Yamazaki¹, Fumika Yakushiji¹, Ryoichi Matsuda², Yoshio Hayashi¹

¹Department of Medicinal Chemistry, Tokyo University of Pharmacy and Life Sciences, Hachioji, Tokyo 192-0392, Japan, ²Department of Life Science, University of Tokyo, Tokyo 153-8902, Japan

E-mail: yhayashi@toyaku.ac.jp

Introduction

Duchenne muscular dystrophy (DMD), characterized by progressive skeletal muscle degeneration, is the most common children's muscular dystrophy, which primarily affects approximately 1 in 3,500 live males birth. A part of this genetic disease is caused by the defect in the muscle protein "dystrophin" by the nonsense mutation, which is a point mutation with a premature termination codon (PTC) in the DNA sequence. Recently, it was reported that both the aminoglycoside antibiotic gentamicin, and the less toxic (+)-negamycin **1** [1] restore dystrophin expression in skeletal and cardiac muscles of *mdx* mice, an animal model of DMD [2]. These compounds are designated as "readthrough compounds" that can skip PTCs, but not of normal termination codons, resulting in the production of full-length proteins. We focused on the dipeptidic antibiotics (+)-**1** (Figure 1) as a promising new therapeutic lead compound for the development of a DMD or other genetic disease drug caused by nonsense mutation.

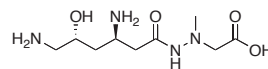


Fig. 1. Structure of (+)-negamycin **1**.

Results and Discussion

We synthesized derivatives to discover new peptidomimetic drug candidates with a suitable readthrough-promoting activity for chemotherapy of DMD. The *in vivo* readthrough-promoting activity of some synthetic derivatives, via our new synthetic route [3] was shown in Table 1 with the ratios of the activity against a positive control gentamicin. A 3-desamino- and glycine-derivative **N3** exhibited a slightly higher readthrough-promoting activity than (+)-**1**, although no antimicrobial activity was observed [4]. In other words, it means that the readthrough-promoting activity could be distinguished from the antimicrobial activity.

To understand the biological effects, the most active **N3** was chosen for further *in vivo* immunohistochemical and biochemical evaluations. **N3** was subcutaneous injected in the abdominal region of *mdx* mice at a dosage of 1 mg for 4 weeks. The serum creatine kinase (CK) level, which is a clinical indicator of muscular dystrophy, was measured. As a result, a significant decrease of the CK level in **N3**-treated mice was observed in comparison to the

controls (saline). This suggests that **N3** protects the muscle tissues collapse in *mdx* mice. In addition, partial dystrophin expression in the skeletal muscle of *mdx* mice was confirmed by the immunohistochemical analysis. Moreover, we examined the acute toxicity of **N3** as compared to (+)-**1** by measuring the body-weight change of *mdx* mice. **N3** exhibited a slight slowing-down of the body weight increase, while (+)-**1** exhibited a marked decrease. Therefore, it can conclude the lower toxic **N3** might have a potential for the long-term treatment for DMD.

We also have performed the other approach focusing on the C5 position of (+)-**1**. 5-*epi*-negamycin **2**, which is an isomer of (+)-**1** with the opposite stereochemistry at the C5 position, exhibited the same activity as (+)-**1** in *in vitro* readthrough assay at 200 μ M (Figure 2). This result prompted us to synthesize 5-dehydro-derivatives. In derivatives, we found 3-*epi*-deoxynegamycin **3**, which is a natural product with the low antimicrobial activity [5], has higher readthrough-promoting activity than (+)-**1** at 200 μ M (Figure 2). This result suggests **3** is more suitable structure than (+)-**1** on readthrough-promoting activity. The SAR study for more potent derivatives is currently under investigation.

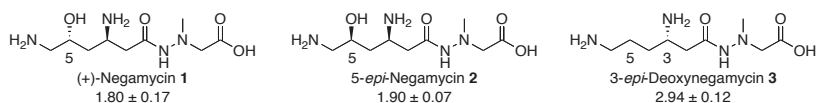


Fig 2. *In vitro* readthrough-promoting activity as compared to control (=1).

Acknowledgments

This research was supported by the Grant-in-Aid for Scientific Research on Priority Areas 20390036 & 23390029 from MEXT (Ministry of Education, Culture, Sports, Science and Technology), Japan and by Intramural Research Grant (23-5) for Neurological and Psychiatric Disorders of NCNP.

References

- [1] Hamada, M.; Takeuchi, T.; Umezawa, H. *et al. J. Antibiot.* **1970**, *23*, 170.
- [2] Arakawa, M.; Shiozuka, M.; Matsuda, R. *et al. J. Biochem.* **2003**, *134*, 751.
- [3] Nishiguchi, S.; Sydnes, M. O.; Taguchi, A.; Regnier, T.; Kajimoto, T.; Node, M.; Yamazaki, Y.; Yakushiji, F.; Kiso, Y.; Hayashi, Y. *Tetrahedron.* **2010**, *66*, 314.
- [4] Taguchi, A.; Nishiguchi, S.; Shiozuka, M.; Nomoto, T.; Ina, M.; Nojima, S.; Matsuda, R.; Nonomura, Y.; Kiso, Y.; Yamazaki, Y.; Yakushiji, F.; Hayashi, Y. *ACS Med. Chem. Lett.* **2012**, *3*, 118.
- [5] Kondo, S.; Yoshida, K.; Ikeda, T.; Iinuma, K.; Honma, Y.; Hamada, M.; Umezawa, H. *J. Antibiot.* **1977**, *30*, 1137.

Table 1. *In vivo* readthrough-promoting activity of negamycin derivatives.

Compound	Structure	Relative Read-through Activity (READ mice)	Anti-microbial Activity
Gentamicin		1.00 ± 0.24	+
N1 (+)-Negamycin		1.00 ± 0.25	+
N2		1.01 ± 0.16	±
N3		1.36 ± 0.14	—
N4		0.83 ± 0.13	—
N5		1.01 ± 0.07	NT

0.1 mg/day/20 g mouse body weight NT = not tested

Studies on a reverse-turn scaffold containing a thiourea functionality

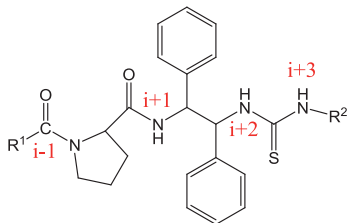
Maria Zervou,¹ Katerina Paschalidou,² Stamatis Fotaras,²
Violetta Constantinou-Kokotou,³ George Kokotos^{1,2,*}

¹Institute of Biology, Medicinal Chemistry and Biotechnology, National Hellenic Research Foundation, Athens, Greece; ²Laboratory of Organic Chemistry, Department of Chemistry, University of Athens, Athens, Greece; ³Agricultural University of Athens, Athens, Greece

E-mail: gkokotos@chem.uoa.gr

Introduction

High interest has been paid to synthetic structural motifs that promote specific conformations because of their importance for the development of new therapeutic peptidomimetics [1]. In addition, such motifs may show catalytic activity for asymmetric organic transformations. During the last two decades, various synthetic structural motifs that promote reverse turns have been studied. Following our interest on chiral prolinamide-thioureas that present interesting organocatalytic activity [2], we have undertaken a combined experimental/computational study to understand the structural features that may stabilize a reverse turn in short length peptidomimetics containing a thiourea functionality. Representative structures from the series, depicted in Scheme 1, were synthesized and studied by NMR spectroscopy (Varian 600 MHz) for the sequential assignment and the exploration of the dipolar connectivities. *In silico* studies included Random Sampling of the conformational space and Molecular Dynamics simulations driven by the calculated from NOE data interatomic distances (Schrodinger Suite 2012).



Scheme 1: Peptidomimetic motif

R¹= Fmoc, Boc or Boc-Ala

R²= Asp(OBut)-OBut or CH₂Ph

Energy refined produced conformers were subsequently modified by applying all the possible combinations of *R* and *S* stereogenic centers in a stepwise manner. The modelled structures were further studied by MD simulations aiming to explore the combinations of heterochiral residues which would promote a folded structure and would favour the potential of a turn motif. The main criteria for choosing the most promising combinations for synthesis consisted of: (1) The populations of folded conformations supporting a β -turn (H-bond between COⁱ⁻¹..NHⁱ⁺²) and/or an α -turn (H-bond between COⁱ⁻¹..NHⁱ⁺³). (2) The stability of the formed H-bonding interactions in the course of the simulation time. (3) The monitoring of sudden changes along the MD trajectories.

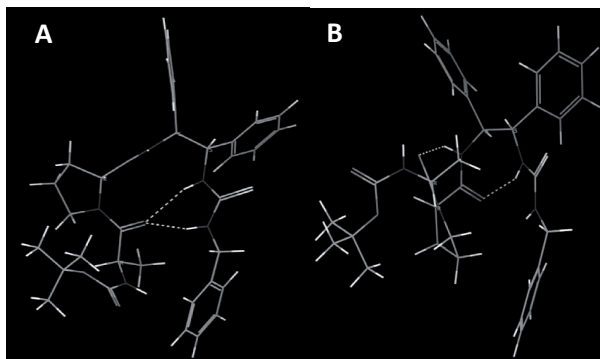
Results and Discussion

In silico studies indicated that: (1) The presence of Boc-(*R* or *S*)-Ala at the (*i*-1)-position could induce stable folded structures in the course of the simulation time, (2) (*R*)-Pro seemed to corroborate better with a turn conformation and (3) The presence of (*R/S*)-Asp(OBut)-OBut or of CH₂Ph at the C-terminal tail could enhance the formation of structured populations.

Compound Boc-(*R*)-Ala-(*R*)-Pro-(1*S*,2*S*)-diphenylethylenediamine-thiourea-CH₂Ph was chosen among the set of the prioritized candidates for synthesis and NMR studies. NMR data indicated the existence of both Pro isomeric forms in a ratio of *trans*:*cis*=3:1.

NOE driven molecular dynamics simulations resulted in the following observations: (1) The *cis* Pro conformer does not contribute to stable folded structures as also confirmed by the lack of indicative NOE signals. (2) Diagnostic NOEs provide evidence for at least two populations bearing Pro in a *trans* conformation. Conformation A potentially prompts to the simultaneous formation of α - and β -turn (H bonds between CO^{*i*-1} - NH^{*i*+3} as well as between CO^{*i*-1} - NH^{*i*+2}) supported by the NOE interactions between the Boc methyl protons on one hand and the C-terminal Ph-H and the preceding methylene group on the other. Besides, the observed NOEs between NH^{*i*+1} vs. NH^{*i*+2} and between Pro α -H and NH^{*i*+1} are also indicative for the formation of a turn structure. The simultaneous observation of dipolar interactions between the backbone CH^{*i*+2} vs. Ala β -H and C-terminal Ph-H vs. Pro δ -H give evidence of the co-existence of conformation B which is stabilized through H bonds between CO^{Pro} - NH^{*i*+2} and CO^{*i*-1} - NH^{*i*+1}.

These results are encouraging and validate the applied combined experimental/computational strategy. The synthesis of related compounds is in progress in an effort to explore the possibility of the stronger stabilization of a reverse turn.



Acknowledgments

This work was implemented under the FP7 Regional Potential project “Advancement of Research Capability for the Development of New Functional Compounds” (ARCADE).

References

- [1] Che, Y.; Marschall, G. R. *Expert Opin. Ther. Targets*, **2008**, *12*, 101.
- [2] Fotaras, S.; Kokotos, C. G.; Tsandi, E; Kokotos, G. *Eur. J. Org. Chem.*, **2011**, *7*, 1310.
- [3] Fotaras, S.; Kokotos, C. G.; Kokotos, G. *Org. Biomol. Chem.*, **2012**, *10*, 5613.

Synthesis and characterization of modified peptidic nucleic acids (PNAs) toward the production of patterned gold surfaces to assist cellular migration

V. Corvaglia,¹ R. Marega,² R. Vulcano,² D. Bonifazi^{1,2}

¹*Department of Chemical and Pharmaceutical Sciences, University of Trieste, Trieste, Italy;* ²*Laboratoire de Chimie Organique et des Matériaux Supramoléculaires, Facultés Universitaires Notre-Dame de la Paix, Namur, Belgium*
E-mail:valecorvaglia@gmail.com

Introduction

Methods to pattern molecules on solid supports have revolutionized the electronics, optics, and photovoltaics fields, and are crucial for many biological applications including the development of model substrates to investigate fundamental issues in cell growth, adhesion, and migration.[1,2] Central to the improvement of these technologies is the nanofabrication of DNA and proteins arrays. More specifically, surface-confined DNA arrays are important in the development of novel DNA sequencing and gene mapping techniques.[3] Most eukaryotic cells sense and respond to the mechanical properties of their surroundings. Several artificial substrates were prepared to better understand the cellular responses to different mechanical and biochemical surface properties,[4,5] such as the unidirectional migration of cells along biochemical gradients,[6] but no one at the present time reported the multidirectional cell movement along a defined substrate. The aim of this project is to produce suitable surface modifications in order to induce multidirectional cellular migration along gold surfaces (Au surfaces). The controlled multidirectional migration along a surface offer several advantages with respect to the monodirectional approach, since the cellular functions can be elicited with spatio-temporal control and in principle recycled. For instance, by the reversible movement of the cells it will be possible to exploit a determined work (expression of a protein, internalization of a pathogen or fluorescent dyes) once the cells reach the target position, and then to recall them back to the starting position. The cellular migration along Au surfaces will occur by generating a chemical gradient of a chemotactic molecule. To this aim self-assembled mono-layers (SAMs) of thiolated DNA chains (DNA-SH) will be produced onto Au surfaces, allowing then for hybridization with complementary modified single-stranded PNAs.[7] PNA has a high biological and chemical stability and it can bind complementary DNA strands with higher affinity than the corresponding DNA sequences.[8] At the beginning, we will use fluorescent PNA chains for characterizing the supramolecular chemical gradient. Subsequently, PNAs bearing a chemotactic agent for inducing the cellular migration will be produced and adopted for biofunctional Au surfaces generation.

Results and Discussion

The first molecular target proposed for cellular migration induction is a peptide composed by the chemotactic IGDQ motif (isoleucine, glycine, aspartic acid and glutamine) and bearing 1-thiol decanoic acid for Au functionalization (Fig. 1). The second target involves

the synthesis of a PNA 12-mer able to bind a complementary DNA-SH and bearing Rhodamine B (Rho) as a fluorescent probe (Fig. 2).

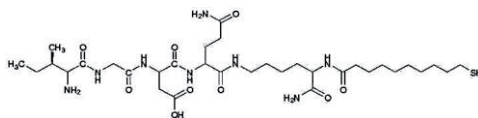


Figure 1.

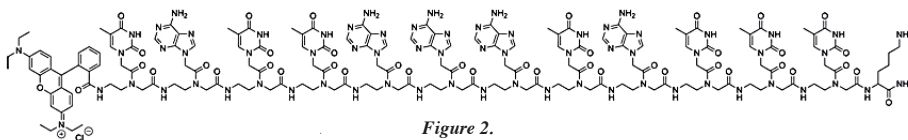


Figure 2.

Peptide IGDQK-SH (Fig. 1) was synthesized by Solid Phase Peptide Synthesis (SPPS) and the chemical gradient was produced by gradually immersing of Au substrates into a diluted peptide solution (1 μM) by a controlled dipping,[9] and subsequent backfilling into a diluted 1-octanethiol solution (3 μM) to promote SAMs formation. IGDQK-SH gradient was characterized by Water Contact Angle (WCA) and Atomic Force Microscopy (AFM), as a function of position along the longitudinal axis of the sample. Both techniques showed the presence of a chemical gradient, due to the increase of the IGDQK-SH molecules adsorbed onto the Au toward the regions that underwent maximum time exposure to the IGDQK-SH solution. For the migration studies, EAhy926 cells were deposited on the Au surfaces, and the cellular migration toward the IGDQK-SH gradient was successfully revealed by optical and fluorescent microscopy imaging. Currently, our work is focused on the synthesis of the fluorescent PNA 12-mer (Fig. 2) able to bind a complementary DNA-SH strand, in order to characterize the supramolecular unidirectional gradient along the Au surfaces through fluorescence microscopy techniques. Once the best conditions of chemical gradient properties will be established, the synthesis of a PNA 12-mer bearing the chemotactic peptide (IGDQ) will be carried out to demonstrate the unidirectional cellular migration. At last, the generation of a bidirectional gradient of DNA-SH/PNA duplexes will be produced and optimized for the bidirectional cellular migration studies.

Acknowledgments

This work was funded by University of Trieste and University of Namur.

References

- [1] Huang, Y.; Duan, X. F.; Wei, Q. Q.; Lieber, C. M. *Science* **2001**, *291*, 630.
- [2] Yousaf, M. N.; Houseman, B. T.; Mrksich, M. *Angew. Chem. Int. Ed.* **2001**, *40*, 1093.
- [3] Li, H.; LaBean, T. H.; Leong, K. W. *Interface Focus* **2011**, *1*, 702.
- [4] Kim, D. H.; Seo, C. H.; Han, K.; Kwon, K. W.; Levchenko, A.; Suh, K. Y. *Adv. Funct. Mater.* **2009**, *19*, 1579.
- [5] Jiang, X. Y.; Bruzewicz, D. A.; Wong, A. P.; Piel, M.; Whitesides, G. M. *Proc. Natl. Acad. Sci. U. S. A.* **2005**, *102*, 975.
- [6] Toh, C. R.; Fraterman, T. A.; Walker, D. A.; Bailey, R. C. *Langmuir* **2009**, *25*, 8894.
- [7] Nielsen, P. E.; Egholm, M.; Berg, R. H.; Buchardt, O. *Science* **1991**, *254*, 1497.
- [8] Egholm, M.; Buchardt, O.; Nielsen, P. E.; Berg, R. H. *J. Am. Chem. Soc.* **1992**, *114*, 1895.
- [9] Morgenthaler, S.; Lee, S. W.; Zurcher, S.; Spencer, N. D. *Langmuir* **2003**, *19*, 10459.

Synthesis of conjugates of muramyl dipeptide and nor-muramyl dipeptide derivatives with adenosine as potential immunosuppressants

M. Samsel,¹ K. Dzierzbicka,¹ P. Trzonkowski²

¹Department of Organic Chemistry, Faculty of Chemistry, Gdansk University of Technology, Gdansk, Poland, ²Department of Clinical Immunology and Transplantology, Medical University of Gdansk, Gdansk, Poland
E-mail:s.monika@wp.pl

Introduction

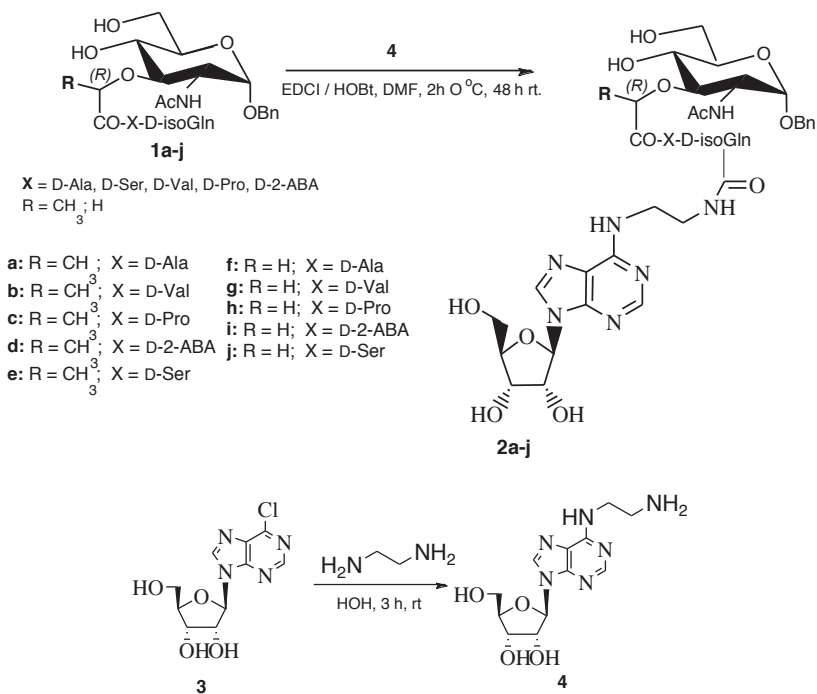
Although many immunosuppressants are in clinical use, they are not free of drawbacks. The problem is not only in toxicity but also in a narrow therapeutic range [1]. In the search of new potential immunosuppressive agents, we synthesized series of MDP(D-D) and nor-MDP(D-D) derivatives linked through an ethyl group to the adenosine.

Muramyl dipeptide (MurNAc-L-Ala-D-isoGln; MDP) is the minimal biological structure of bacterial peptidoglycan that demonstrates adjuvant activity. MDP acts through intracellular NOD2 receptor expressed in immune cells. Structural modifications of MDP, its derivatives and conjugates elicit immunomodulative, antiviral or antitumor activity [2]. Analogues, where D-alanine is replaced with L-amino acid exert immunosuppressive action.

Adenosine is a purine nucleoside that plays an important role in the human body. It acts through the four types of adenosine receptors: A₁, A_{2A}, A_{2B} and A₃, belonging to the G-protein-coupled receptor family. A_{2A} receptors are expressed ubiquitously in the body, but they can be found mainly in the immune system [3]. One of the effects of adenosine acting through A_{2A} receptors is the induction of T-cell anergy [4].

Results and Discussion

In order to achieve compounds that decrease the humoral immune response we modified the peptide part of MDP by replacing Ala with D-amino acid. To amplify the immunosuppressive action an adenosine fragment was attached. Initially, we attempted to couple adenosine directly through an amide bond to the MDP derivative, but the reactivity of a purine amino group at C-6 was insufficient. Therefore, we decided to use a linker between the free carboxyl group of MDP derivatives **1a-j** and the adenosine moiety. 6-Chloropurine riboside **3** was used a substrate to afford N⁶-(2-aminoethyl)adenosine **4** in reaction with 1,2-ethylenediamine as described by Brodelius *et al.* (Scheme 1) [5].



Scheme 1. Synthesis of new conjugates of MDP(D-D) and nor-MDP(D-D) derivatives with adenosine **2a-j**.

Next, the *N*-terminal amino group of **4** was coupled with **1a-j** by means of EDCI (1-ethyl-3-(3-dimethylaminopropyl) carbodiimide) and HOBt (*N*-hydroxybenzotriazole) to yield conjugates **2a-j**. The final products were purified with preparative TLC and their composition was confirmed by ^1H NMR and MALDI-TOF mass analysis. The structure of compounds **2a** and **2g** was confirmed additionally by 2D ROESY and TOCSY ^1H NMR.

Acknowledgments

This work was supported by the Polish National Science Center (NCN) under the Grant No.: N N405 046440.

References

- [1] Yang, Z.; Wang S. *J. Immunol. Methods* **2008**, *336*, 98.
- [2] Ogawa, C.; Liu, Y-J.; Kobayshi, K.S. *Curr. Bioact. Compd.* **2011**, *7*, 180.
- [3] Fredholm, B.B.; Jzerman, A.P.I.; Jacobson, K.A.; Klotz, K.N.; Linden, J. *Pharmacol. Rev.* **2001**, *53*, 527.
- [4] Zarek, P.E.; Huang, C.T. Lutz, E.R.; Kowalski, J.; Horton, M.R.; Linden, J.; Drake, C.G.; Powell, J.D. *Blood*. **2008**, *1*, 251.
- [5] Brodelius, P.; Larsson, P.O.; Mosbach, K. *Eur. J. Biochem.* **1974**, *47*, 81.

Synthesis of CXCR4 specific agonists: SAR studies on the agonist-antagonist transition

Christine Mona¹, Marilou Lefrançois¹, Alexandre Osborne¹, Marie-Reine Lefebvre¹, Nikolaus Heveker², Éric Marsault¹, Emanuel Escher¹

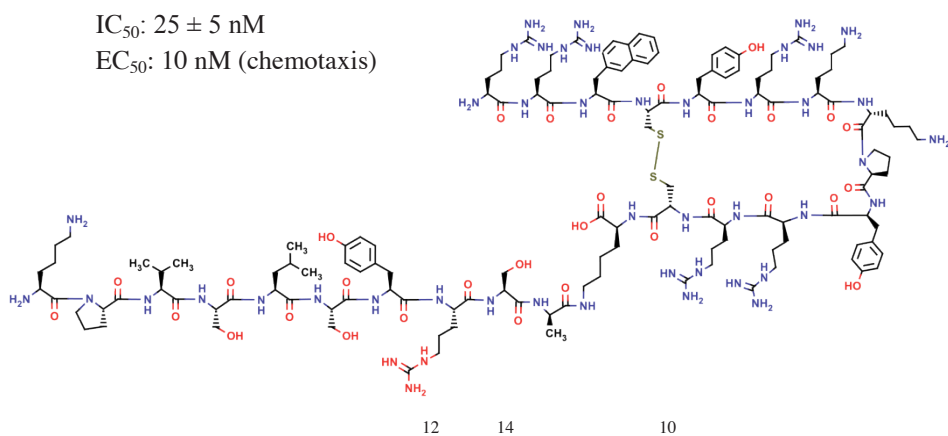
¹Département de Pharmacologie FMSS Université de Sherbrooke, Sherbrooke J1H 5N4,

²Centre de Recherche, Hôpital Sainte-Justine, Montréal H3T 1C5, Canada

Email : emanuel.escher@usherbrooke.ca & eric.marsault@usherbrooke.ca

Introduction

The CXCR4/SDF-1 axis is involved in many biological processes such as hematopoiesis, migration of immune cells, as well as in cancer metastasis. CXCR4 also mediates the infection of T-cells with X4-tropic HIV functioning as a co-receptor for the viral envelope protein gp120. CXCR4, as a pharmaceutical target, is of utmost importance but the lack of synthetic agonists has seriously slowed down drug development. We [1] recently described that grafting the SDF-1 N-terminus onto a side-chain of the inverse agonist T140 [2] provided high affinity synthetic agonists for the chemokine receptor CXCR4.



Scheme 1: T140-Arg¹², Lys¹⁴-ε [SDF1-Ala¹⁰-(1-10)]

To remain stable toward proteases and act as useful pharmaceutical tools, the PK-ADME properties need to be improved with a transition to peptidomimetic structures. In order to improve stability toward proteases, part of the SDF-1 chain was replaced with alanine or unnatural amino acids at different positions. Here, we are studying the substitutions of amino acids in the SDF-1- α N-terminal part.

Results and discussion

Peptides were synthesized using the Fmoc-based solid-phase strategy in a manual reaction vessel; as a first step the synthesis of the (Lys¹⁴[ϵ -DDE]) T140 was completed. The side chain protection of the Lysine in position 14 was selectively removed with hydrazine and the sequences completed. The different peptides were cleaved from the resin, purified on

reverse phase and finally cyclized using in 5% acetic acid and (NH₄)₂CO₃ buffer. Analytical HPLC indicated purity greater than 97%, and molecular weights were confirmed by LC/MS. Competition binding assays were performed on these peptides confirming that they displayed relative affinity for CXCR₄. Moreover, Transwell migration assays on pre-B lymphocytes (REH cells) were performed to elucidate their *in vitro* activity (Table 1).

Compound	Structural Changes in SDF-1 N-terminal graft	Amino-acid sequence	IC ₅₀ (nM)	Max. of Migration (%)
1	Substitution of Valine by :	Bpa	4 ± 1	121
2		Tle	52 ± 11	43
3		Trp	140 ± 65	110
4		2-Nal	22 ± 5	98
5	Substitution of position 5 through 9 : Ala-scan	Leu5 → Ala	168±73	10
6		Ser6 → Ala	170±40	21
7		Arg7 → Ala	91±7	9
8		Tyr8 → Ala	228±68	30
9		Ser9 → Ala	49±11	35

Table 1 : Affinities of T140-SDF-1 chimeras expressed as IC₅₀ and Efficacy relative to SDF-1 (IC₅₀=0.1nM, Max. of migration : 53% of migrated cells normalized to 100%)

Bpa : (*L*)-4-Benzoylphenylalanine ; Tle : (*L*)-*tert*-leucine ; 2-Nal : (*L*)-2-Naphthylalanine

Through this study, we have highlighted several important points for the conservation of the agonistic nature of our chimeras. The Ala scan on the SDF-1 N-terminal part emphasizes the importance of several residues like Leu⁵, Ser⁶ and Tyr⁷ and restricts the transition to peptidomimetic structures. The Tyrosine residue in position 7 appears to govern the agonistic nature since its Ala replacement converts the analogue into an antagonist. The position 3 of our chimeras seems to tolerate hydrophobic structural changes with the ability to make π -stacking. Excessive flexibility or rigidity appears to place the side chain into a less favorable conformation than the one required to induce the activation of the CXCR₄ receptor (data not shown). To conclude, our compounds are able to induce chemotaxis similarly to SDF-1 but at concentrations of 10 to a 100 fold higher than SDF-1.

Acknowledgments

Canadian Institutes of Health Research and *Conseil Régional de la Martinique* for funding

References

- [1] Lefrançois, M. ; Lefebvre, M.R. ; Saint-Onge, G. ; Boulais, P.E.; Lamothe, S. ; Leduc, R.; Lavigne, P. ; Heveker, N. ; Escher, E.; *ACS Med Chem Lett.* **2011** Aug 11;2(8):597-602
- [2] Tamamura, H. ; Fujisawa, M. ; Hiramatsu, K. ; Mizumoto, M. ; Nakashima, H. ; Yamamoto, N. ; Otaka, A. ; Fujii, N. ; *FEBS Lett.* **2004** Jul 2;569(1-3):99-104

The specificity of PNA hybridization was verified using DNA fragment (complementary to synthesized PNA) and capillary electrophoresis (CE) technique. PNA-DNA interaction studies were carried out on a Beckman P/ACE MDQ capillary electrophoresis system using a fused-silica uncoated capillary, running buffer (25 mM phosphate, pH 7), constant voltage 15kV, detection at $\lambda=254$ nm. CE studies confirmed that synthesized PNA fragment bind complementary DNA fragment (Figure 2).

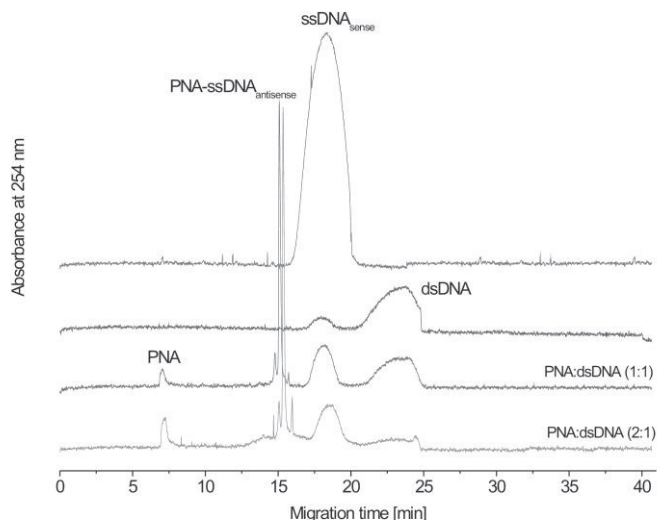


Figure 2. PNA-DNA interaction studies with the use of capillary electrophoresis

Biological studies were performed on Endothelial Cells (ECs) in order to determine localization and optimal delivery conditions of PNA to cells and inhibition of STAT1 expression *in vitro*. PNA cell delivery and localization was visualized using scanning confocal fluorescence microscopy. The fluorescence microscopy studies demonstrated that TAMRA-PTD-4-PNA conjugate was active in permeation of the plasma membrane.

Acknowledgments

This work was supported by the Polish Ministry of Science and Higher Education under grant N N302 016339 and grant UG BN: 538-8291-1031-12.

References

- [1] Leon, A.; Zuckerman, S. *Inflamm Res.* **2005**, *54*, 395-411.
- [2] Hatcher, E.; Balaeff, A.; Keinan, S.; Venkatramani, R.; Beratan, D. N. *J. Am. Chem. Soc.* **2008**, *130*, 11752-11761.

Synthesis of 4-aminotetrolic acid – a part of triazolic nucleic acid monomers

**Michał Dobkowski^{1,2*}, Małgorzata Pieszko², Rekowski Piotr²,
Mucha Piotr²**

¹*Intercollegiate Faculty of Biotechnology University of Gdańsk and Medical University of Gdańsk, Kładki 24, 80-822 Gdańsk, Poland;* ²*Faculty of Chemistry, University of Gdańsk, Sobieskiego 18, 80-952 Gdańsk, Poland*
E-mail:dancer@chem.univ.gda.pl

Introduction

In 2001, M. Meldal group introduced the concept of "click chemistry", which revolutionized modern chemistry. The advantages of using reaction of alkyne and azide group are: versatility, high performance of using a variety of substrates, generating easy to remove by-products without the use of chromatographic methods, regiospecificity, mild reaction conditions, simple substrates and products removed by crystallization or distillation [1]. The cycloaddition of alkyne and azide derivatives with presence of either Cu(I) or complexes Ru(II) may allow for fast, efficient and free from by-products synthesis of the triazolic nucleic acids (TNA) monomers. TNA may be a unique therapeutic tool (along with si- or miRNA), which could be applied clinically in the processes of controlling the flow of genetic information. Due to the specific recognition of nucleic acids and remarkable chemical resistance, TNA may be used both against viruses, bacteria, fungi and other pathogens. Such molecules can block incorrectly synthesized RNA molecules or mutated DNA fragments [2].

Results and Discussion

A new class of nucleic acid - triazolic nucleic acids (TNA) will be synthesized. "Click chemistry" synthesis leads to monomers and then using SPPS protocol TNA polymers will be achieved. Triazolic system is resistant to proteolysis and has a much larger dipole moment than the peptide bond. Probably because of the similarity to the peptide bond and the ability to form hydrogen bonds, peptidomimetics containing triazolic ring show a high biological activity such as antiretroviral, antibacterial and antihistamine.

One of the required reagents, which will be used for synthesis of the monomers is 4-aminotetrolic acid (Fig. 1). It provides greater freedom for the rest of the principles of conformational nucleic acid.

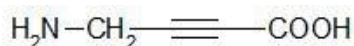


Fig. 1 Structure of 4-aminotetrolic acid.

4-Aminotetrolic acid was synthesized from commercially available reagent of 1,4-dihydroxy-but-2-yn (Fig. 2). Each step of the synthesis was monitored by RP-HPLC.

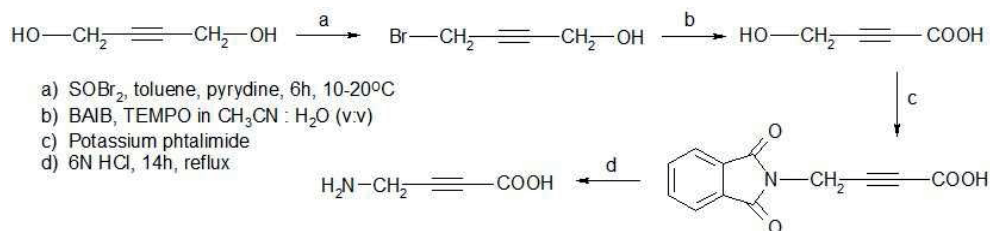


Fig. 2 Synthesis of 4-aminotetrolic acid.

Triazole derivatives obtained by cycloaddition internal alkyne and azide gives nucleic acid monomers. Rhutenium catalyst provides regioselectivity of “click” reaction. The structure of such units is shown in figure 3.

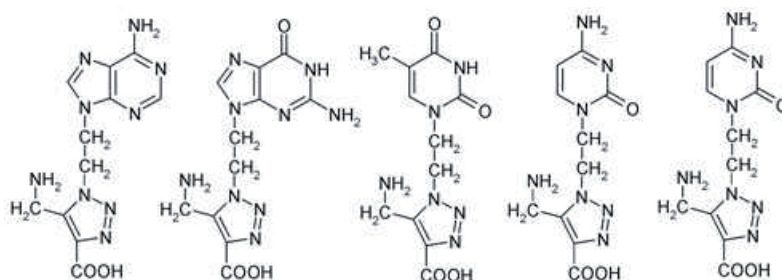


Fig. 3. Triazole modified nucleic bases monomers which will be used for TNA synthesis.

TNA will be synthesized from monomers in the synthesis on a solid support, and therefore complementary to the classical SPPS synthesis. The end result of the project will obtain compounds with inhibitory properties (based on the sequence of peptides selected from phage libraries and triazole structure of nucleic acids (TNA)). They enrich the arsenal of tool used for fight HIV-1.

Acknowledgments

This work was supported by the Polish National Science Centre grant no N N204 355540 and UG BN 538-8291-1032-12.

References

- [1] C. W. Tornøe and M. Meldal, Proc. 17th Am. Pept. Symp., American Peptide Society and Kluwer Academic Publishers, **2001**, 263-264.
- [2] Gil M.V., Arevalo M.J., Lopez O., Synthesis **2007**, 1589-1620.

Synthesis, pharmacological evaluation and conformational investigation of Endomorphin-2 hybrid analogues

**A. Silvani,^{a,*} F. Airaghi,^a G. Balboni,^b E. Bojnik,^c A. Borsodi,^c
T.F. Murray,^d G. Lesma,^a S. Salvadori,^e T. Recca,^a A. Sacchetti^f**

^a*Università degli Studi di Milano, Milano, Italy;* ^b*Università degli Studi di Cagliari, Cagliari, Italy;* ^c*Hungarian Academy of Sciences, Szeged, Hungary;* ^d*Creighton University School of Medicine, Omaha, Nebraska - USA;* ^e*Università degli Studi di Ferrara, Ferrara, Italy;* ^f*Politecnico di Milano, Milano, Italy*
alessandra.silvani@unimi.it

Introduction

In the last years, a new dimension to the field of biomimetic structures has been introduced, through the recognition that the repertoire of polypeptide conformations can be greatly expanded by the creation of structures incorporating β -amino acids. Moreover, the numerous advantages of hybrid (mixed α - and β -) backbone peptidomimetics with respect to homogeneous ones were quite recently outlined.¹

In our ongoing work on the synthesis of peptidomimetic scaffolds² and in the light of the high potential of mixed or “heterogeneous” backbones to expand the structural and functional repertoire of bioactive compounds, we describe here³ the synthesis of various hybrid analogues of the endogenous peptide Endomorphin-2 (H-Tyr¹-Pro²-Phe³-Phe⁴-NH₂, EM-2, Figure), with the aim of evaluating their activity and contributing to SAR understandings.

EM-2 is a highly potent and selective μ -opioid receptor agonist neuropeptide. The opioid system mediates a wide variety of pharmacological and physiological processes, including pain perception and modulation. The amidated tetrapeptide EM-2 has been shown to be μ -opioid receptor (MOR) agonist exhibiting a very high μ -receptor affinity and selectivity. It is an important model in the search towards new analgesics.^{4,5} Structural investigation of EM-2 reveals the high conformational freedom of the Phe side chains and also the inherent flexibility of the peptide backbone, indicating many probable bioactive conformations, ranging from β -turns to extended conformations. The relevant role of the proper spatial orientation of the aromatic rings and in particular of the benzyl side chains at positions 3 and 4 is well established, but not fully clarified.

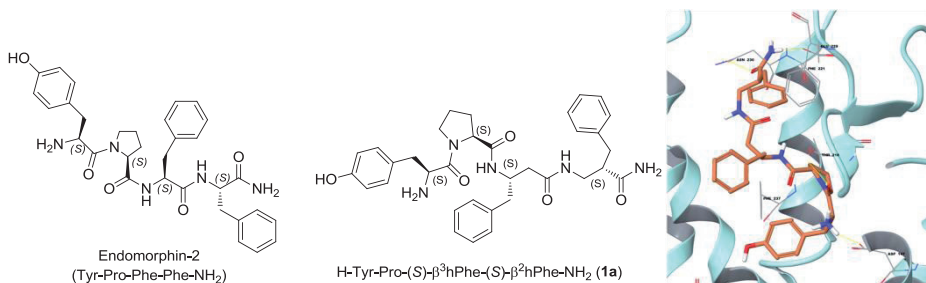
Results and Discussion

We synthesised eleven new EM-2 hybrid analogues, in which both the third and fourth Phe residues (Phe³-Phe⁴) are simultaneously replaced, with the aim of perturbing either the message domain and the address fragment of the reference ligand, by means of backbone elongation.

The new hybrid peptides was evaluated in radioligand receptor binding experiments in cell membranes stably expressing the opioid receptors, ¹H NMR studies, molecular modelling, and molecular docking to a homology MOR model.

Affinity and selectivity for μ and δ opioid receptors have been investigated using rat brain

membranes stably expressing the opioid receptors. Some of them (see compound **1a** as an example, Figure), in spite of the important modifications at their C-termini, maintained a significant nanomolar MOR affinity and a acceptable selectivity.



They are among the few examples of EM-2 analogues in which the C-terminal Phe³-Phe⁴ dipeptide is simultaneously substituted by a peptidomimetic structure with the maintenance of opioid affinity.

Molecular modelling, which was performed taking into account distance restraints from NMR, suggests a high propensity of all analogues for various turn structures. We also performed docking studies in order to elucidate the binding mode for their action. The docking procedure strongly highlights a common binding mode for active compounds, confirming the necessity for specific binding interactions with the MOR model, for instance between Asp 147 and Tyr¹, already identified for EM-2 in recent studies. Additional computational work will be performed in the light of the new context of the quite recent structure elucidation of opioid receptors.⁶ This deepening will be reported in the due course.

References

- [1] (a) Seebach, D.; Gardiner J. *Acc. Chem. Res.* **2008**, *41*, 1366-1375. (b) Wu, Y. D.; Han Y.; Wang D.P.; Gao Y.; Zhao Y.L. *Acc. Chem. Res.* **2008**, *41*, 1418-1427. (c) Horne, W. S.; Gellman S.H. *Acc. Chem. Res.* **2008**, *41*, 1399-1408.
- [2] (a) Sacchetti, A.; Silvani, A.; Lesma, G.; Pilati, T. *J. Org. Chem.* **2011**, *76*, 833-839. (b) Lesma, G.; Landoni, N.; Pilati, T.; Sacchetti, A.; Silvani, A. *J. Org. Chem.* **2009**, *74*, 8098-8105.
- [3] Lesma, G.; Salvadori, S.; Airaghi, F.; Bojnik, E.; Borsodi, A.; Recca, T.; Sacchetti, A.; Balboni, G.; Silvani, A. *Molecular Diversity*, **2012**, accepted.
- [4] (a) Keresztes A.; Borics A.; Toth G. *Chem. Med. Chem.* **2010**, *5*, 1176-1196. (b) Fichna, J.; Janecka, A.; Costentin, J.; Do Rego, J.-C. *Pharmacol. Rev.* **2007**, *59*, 88-123. (c) Leitgeb, B. *Chemistry & Biodiversity* **2007**, *4*, 2703-2724.
- [5] (a) Gentilucci, L.; Tolomelli, A.; De Marco, R.; et al. *ChemMedChem* **2011**, *6*, 1640-1653.
- [6] Manglik A.; Kruse A.C.; Kobliska T.S.; Mathiesen J.M.; Sunahara R.K.; Pardo L.; Weis W.I.; Kobliska B.K.; Granier S. *Nature*. **2012**, *485*, 321-327.

In order to improve the cellular uptake of the PNA oligomers and make sure the PNAs reach their target miR210, we obtained PNAs conjugated at the C-terminus to carrier peptides. Since pre-microRNAs are present both in the nucleus and in the cytoplasm, we choose different peptides for the delivery in both cellular compartments, TAT, NLS, a combination of TAT and NLS, biNLS and K₄. All molecules were entirely obtained by solid phase synthesis, purified by HPLC and characterized by electrospray mass analysis.

In order to assess the viability of our approach we first demonstrated *in vitro* that the PNAs were able to bind the duplex corresponding to the pre-miRNA; we followed the PNA strand invasion by fluorescence experiments employing PNA-peptide oligomers conjugated to the light up probe thiazole orange (TO) [3] and a DNA duplex mimicking pre-miR 210 due to its higher stability as compared to RNA. In all cases an increase in the fluorescence intensity of the TO after invasion was observed, confirming the ability of the PNA to bind to its partner. Next we explored the ability of our molecules to be taken up by cells and to downregulate miRNA expression *in vivo*. Biological studies were carried only on PNA-peptide conjugates complementary to the sense region. Evaluation of the PNA uptake was carried out by FACS using PNA conjugated to fluorescein. PNAs conjugated to carrier peptides as TAT and TAT-NLS display efficient uptake by K562 cells.

The amount of primary miRNA after treatment of the cells with PNA1-TAT was evaluated by quantitative PCR and found reduced. Finally, through quantitative PCR we observed also the reduction of the microRNA-210 amount when cells were treated with the antipre-miR PNA1-TAT.

The use of molecules targeting pre-miRNAs represents a new approach for the interference in miRNA maturation. This has important implications from a theoretical point of view, helping in elucidating miRNA functions and from a practical perspective for the development of new tools for miRNA inhibition

Acknowledgements

This work was partially supported by a grant from MIUR (PRIN2009 *Prot* 20093N774P). RG is granted by TELETHON (GGP10124), by Fondazione Cassa di Risparmio di Padova e Rovigo, by C.I.B. and by Associazione Veneta per la Lotta alla Talassemia.

References

- [1] Alvarez-Garcia, I.; Miska, E. A. *Development* **2005**, *132* (21), 4653-62.
- [2] Gambari, R.; Fabbri, E.; Borgatti, M.; Lampronti, I.; Finotti, A.; Brognara, E.; et al. *Biochem. Pharmacol.* **2011**, *82*, 1416-29.
- [3] Tonelli, A.; Tedeschi, T.; Germini, A.; Sforza, S.; Corradini, R.; Medici, M.C.; et al. *Mol. Biosyst.* **2011**, *7*, 1684-92.

Tetrahydro- β -carboline-based spirocyclic lactam as potential type II' β -turn somatostatine mimetic

**G. Lesma,^{1,*} R. Cecchi,² F. Meneghetti,¹
M. Musolino,¹ A. Sacchetti,³ A. Silvani¹**

¹*Università degli Studi di Milano, Milano, Italy;* ²*Sanofi-aventis - Centro Ricerche Sanofi-Midy - Milano, Italy;* ³*Politecnico di Milano, Milano, Italy*

alessandra.silvani@unimi.it

Introduction

The development of privileged molecular scaffolds efficiently mimicking reverse turn motifs has attracted remarkable interest when structural constraints are exploited to increase both binding and selectivity of model peptides.

One of the successful approaches to restrict peptide conformation is the di-substitution in the α position of an α -amino acid, leading to a conformational constraint and a stereochemically stable quaternary carbon center. In particular, spirocyclic scaffolds are able to provide, upon the attachment of appropriate functional groups, useful high-affinity ligands, relevant to the field of drug discovery.¹

In our ongoing program of identification of peptidomimetic scaffolds of low molecular weight,² we are at present interested into conformationally constrained spirocyclic Tryptophan (Trp) analogues, in order to develop new reverse turn nucleating moieties able to be inserted into pharmacologically relevant peptidomimetic compounds.

Among peptides sharing a Trp-containing β -turn motif of which the Trp residue is critical for binding, we looked at the hormone peptide somatostatin,³ normally expressed as a tetradecapeptide (SRIF-14) and acting in various organ systems as a neuromodulator and a neurotransmitter, as well as a potent inhibitor of various secretory processes and cell proliferation.⁴ Somatostatin and its analogue octreotide (*Sandostatin*® drug, clinically used for the treatment of endocrine tumors and acromegaly) are thought to interact with the sst1-5 receptors mainly by inserting a β -turn substructure, carrying a Lysine (Lys) and a Trp side chain into a pocket of the G protein-coupled somatostatin receptors. SRIF peptidic structure-activity relationship (SAR) studies clearly indicated that the core residues Trp8 and Lys9 (numbering of the residues follows that of native SRIF) are essential binding sites for all somatostatin receptors,⁵ whereas Phe6 is specifically important for activation of subtype sst4, which has been recently recognized as an ideal therapeutic target for Alzheimer's disease.⁶

We report here the preparation and structural characterization of the 1,2,3,4-tetrahydro- β -carboline (THBC)-based spirocyclic lactam **1** (Figure) as type-II' β -turn model compound and the application of its core structure to the synthesis of the somatostatin mimetic **2**, whose biological evaluation is currently underway.

Results and Discussion

Starting from D-Trp, and relying on Seebach's concept of self-reproduction of chirality⁷ for the key Trp α -alkylation step, the synthesis of compounds **1** and **2** was achieved.

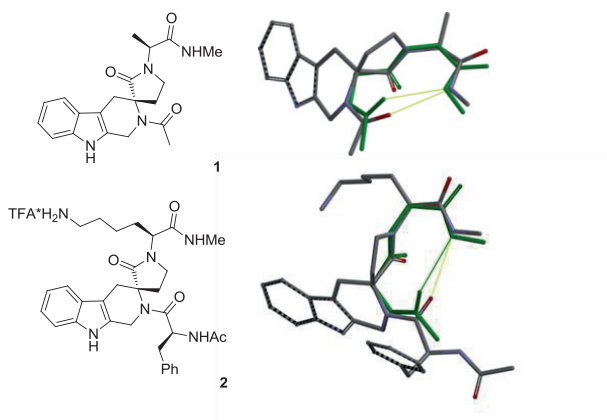


Figure. 1,2,3,4-Tetrahydro- β -carboline (THBC)-based spirocyclic lactam **1** and somatostatin mimetic **2**. Superimposition of the global minimum of compounds **1** and **2** with a ideal type II' β -turn.

With **1** and **2** in hand, we undertook a detailed conformational investigation on their secondary structure, in the solid state by means of X-ray crystallography for **1**, and in solution by means of spectroscopic techniques (NMR and FT-IR), for both **1** and **2**. All structural criteria used to define canonical type-II' β -turns are satisfactorily fulfilled by the peptidomimetic in the solid state, including also the presence of the typical ten-membered intramolecular hydrogen bond. The presence of this last was also fully confirmed by ¹H NMR (by variation of NH proton chemical shift with T, addition of coordinating DMSO, rate of H/D exchange) and IR in diluted solution (2 mM).

The biological evaluation of peptidomimetic compound **2** and of a strictly related analogue is underway.

References

- [1] (a) Pradhan, R.; Patra, M.; Behera, A. K.; Mishra, B. K.; Behera, R. K. *Tetrahedron* **2006**, *62*, 779–828. (b) Van Rompaey, K.; Ballet, S.; Tömböly, C.; DeWachter, R.; Vanommeslaeghe, K.; Biesemans, M.; Willem, R.; Tourwé, D. *Eur. J. Org. Chem.* **2006**, 2899–2911.
- [2] (a) Sacchetti, A.; Silvani, A.; Lesma, G.; Pilati, T.; J. *Org. Chem.* **2011**, *76*, 833–839. (b) Lesma, G.; Landoni, N.; Sacchetti, A.; Silvani, A. *Tetrahedron*, **2010**, *66*, 4474–4478.
- [3] Janecka, A.; Zubrzycka, M.; Janecki, T. *J. Pept. Res.* **2001**, *58*, 91–107.
- [4] Reubi, G. C. *Endocrine Reviews* **2003**, *24*, 389–427 and references cited therein.
- [5] (a) Moller, L. N.; Stidsen, C. E.; Hartmann, B.; Holst, J. J. *Biochim. Biophys. Acta* **2003**, 1616, 1–84. (b) Veber, D. F.; Freidinger, R. M.; Perlow, D. S.; Paleveda, W. J. J.; Holly, F. W.; Strachan, R. G.; Nutt, R. F.; Arison, B. H.; Homnick, C.; Randall, W. C.; Glitzer, M. S.; Saperstein, R.; Hirschmann, R. *Nature* **1981**, *292*, 55–58.
- [6] (a) Crider, A. M.; Witt, K. A. *Mini Rev. Med. Chem.* **2007**, *7*, 213–220.
- [7] Seebach, D.; Fadel, A. *Helv. Chim. Acta* **1985**, *68*, 1243.

The analogues of SFTI-1 modified in the P₁ position by β - and γ -amino acids and *N*-substituted β -alanines

Anna Legowska, Rafal Lukajtis, Magdalena Filipowicz, Monika Legowska, Dawid Debowski, Magdalena Wysocka, Adam Lesner, Krzysztof Rolka

Faculty of Chemistry, University of Gdansk, Poland

E-mail: legowska@chem.univ.gda.pl

Introduction

Serine proteinases are involved in various significant physiological processes, such as: food digestion, fertilization of the ovum, blood clotting or immune response. However, proteolytic enzymes could become a serious threat for living organisms due to their ability to cleave peptide bonds. The inhibitors, that control their activity, are considered the promising class of potential therapeutic agents. One of the proposed templates for the design of new inhibitors is the trypsin inhibitor SFTI-1, the unique member of the Bowman Birk family of inhibitors [1]. Owing to its small size and the well-defined 3D structure, SFTI-1 has been used to design new inhibitors of trypsin, chymotrypsin, cathepsin G, matriptase, β -tryptase, proteinase K or kallikrein-related peptidase [2]. The primary structure of SFTI-1 is presented below:

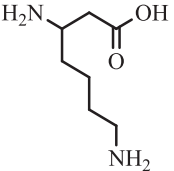
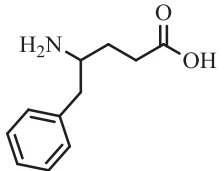
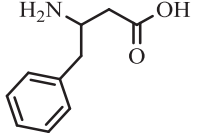
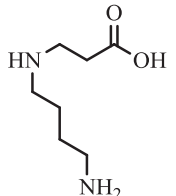
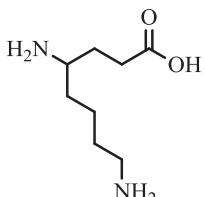
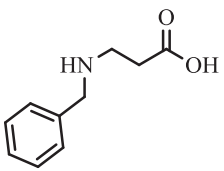


The inherent feature of natural peptides and proteins is their low stability towards proteases which seriously reduces their bioavailability. There is a growing need for development of artificial biopolymers with diverse side chains, capable to mimic peptide function. β - and γ -Peptides are interesting class of peptidomimetics with significant chemical and biological properties. This project is aimed to present, how the single substitution in P₁ position of the primary structure of SFTI-1 with β - or γ -amino acids or *N*-substituted β -alanines (β -peptoid monomers) affects both basic inhibitory features: *in vitro* activity and proteolytic stability. Series of monocyclic analogues of SFTI-1 (with disulfide bridge only) modified in position 5 by mimetics of proteinogenic Lys or Phe were obtained, their primary structures and inhibitory activity expressed association constants (K_a) as are listed in Table 1. All analogues were synthesized manually on solid support using Fmoc/tBu chemistry. β -Peptoid units were introduced into peptide chain using method described by Hamper *et al.* [3].

Results and Discussion

Both SFTI-1 analogues (**I** and **II**) with β -amino acids in the substrate specificity P₁ position, that mimic proteinogenic Lys or Phe residues, retained trypsin and chymotrypsin inhibitory activity. The K_a values determined for these analogues were similar to those obtained for parent inhibitors, and one order of magnitude higher than determined for peptomeric analogues with Nlys and Nphe in discussed position. Further extension of the backbone by insertion of the additional methylene group (analogues **III** and **IV**) resulted in the abolition

Table 1. Analogues of SFTI-1 and building blocks used during synthesis.

Analogue/ K_a [M^{-1}]	The residue in P ₁ position	Analogue/ K_a [M^{-1}]	The residue in P ₁ position
[β^3 hLys ⁵]SFTI-1 (I) 2.5×10^9		[γ^4 hhPhe ⁵]SFTI-1 (IV) NA	
[β^3 hPhe ⁵]SFTI-1 (II) 1.4×10^9		[β hNlys ⁵]SFTI-1 (V) NA	
[γ^4 hhLys ⁵]SFTI-1 (III) NA		[β hPhe ⁵]SFTI-1 (VI) 2.7×10^8	
		[β hPhe ⁵ Abu ^{3,11}]SFTI-1 (VII)* NA	

*linear analogue; NA – not active

of inhibitory activity. Also, the analogue **V** with β -peptoid monomer in P₁ position did not display any activity. Interestingly, similar modification in compound **VI** yielded analogue with strong chymotrypsin inhibitory activity. Unfortunately, elimination of the disulfide bridge from the last analogue gave inactive peptomer **VII**. This is in a good agreement with our previous results indicating that this cyclic element (disulfide bridge) is responsible for proteolytic stability of SFTI-1 analogues and influence strongly observed inhibitory activity. Taking in mind reports considering the high stability of α/β -peptides and α -peptides/ β -peptoids chimeras toward proteolytic degradation, we decided to incubate the active inhibitors with their target enzymes. Analogues **I**, **II** and **VI** were incubated for up to 24 hours with bovine β -trypsin and bovine α -chymotrypsin, respectively. All analogues were resistant *in vitro* to proteolysis.

Acknowledgments

This work was supported by Polish National Science Center (grant No. UMO-2011/01/B/ST5/03772).

References

- [1] Lockett, S.; Santiago Garcia, R.; Barker, J.J.; Konarev, A.V.; Shewry, P.R.; Clarke, A.R.; Brady, R.L. *J. Mol. Biol.* **1999**, *290*, 525.
- [2] Lesner, A.; Legowska, A.; Wysocka, M.; Rolka, K. *Curr. Pharm. Des.* **2011**, *17*, 4317.
- [3] Hamper, B.C.; Kolodziej, S.A.; Scates, A.M.; Smith, R.G.; Cortez, E. *J. Org. Chem.* **1998**, *63*, 708.

Transdermal delivery: New approach in anti-hypertensive therapy

**Michaila Michalatu,¹ Maria-Eleni Androutsou,^{1,3} Theodore Tselios,¹
Amalia Resvani,^{1,3} Pigi Katsougraki,¹ George Agelis,^{1,3}
Dimitrios Vlahakos,² John Matsoukas*^{1,3}**

¹*Department of Chemistry, University of Patras, GR-265 00, Patras, Greece;* ²*Department of Internal Medicine, "Attikon" University Hospital, GR-12462, Athens, Greece;* ³*Eldrug S.A., Pharmaceutical Company, GR-26504, Platani, Patras, Greece*

E-mail: imats@upatras.gr

Introduction

The Renin Angiotensin System (RAS) plays a determinant role in the regulation of blood pressure. Non-peptide Angiotensin II (AII) AT₁ receptor antagonists have been established as an effective treatment of hypertension. Losartan and Valsartan are well known orally active AT₁ antagonists (Sartans). A novel approach for the treatment of hypertension is the transdermal delivery of an antihypertensive drug. Transdermal drug delivery systems (TDDS) offer pharmacological advantages compared to the oral route and improve patient acceptability and compliance. The aim of this study was to achieve the objective of systemic medication of Losartan and Valsartan through topical application and release of drug via skin by developing transdermal drug delivery system. An appropriate analytical method was developed using UPLC/MS for the determination of Losartan concentration in rat plasma.

Results and Discussion

Wistar Rats were weighted and anaesthetized with ketamine/xylazine (3:1) solution. The anaesthetized rats were depilated in a small area and left overnight (in order to avoid the irritation of the skin). The transdermal formulation (30% azone, 30% ethanol, 30% propylene glycol, 10% H₂O, 60 mg of Losartan and Valsartan respectively were dissolved in 300 µL of the above formulation) was applied in the depilated area which was covered with a membrane to avoid the evaporation of the volatile solvents. The rats were placed in a restrainer and their Normal Mean Arterial Blood Pressure (MABP, mmHg) was measured. Then, the Standard Solution (50 µg/kg b.w. AII was dissolved in 0.1 mL Water for Injection, 200µl) was infused subcutaneously and the hypertensive response of the rat was measured (Control AII). Arterial blood pressure signal was monitored in Wistar Rats using a Coda, non-invasive blood pressure system after 3, 6, 8 and 24h of transdermal administration.

	Normal MABP	Control AII	3h after	6h after	8h after	24h after
Valsartan	105.8±11.3	149.7±12.2	118.8±19.0	116.8±21.3	117.1±13.2	116.1±12.4
Losartan	105.2±11.5	150.4±13.0	128.0±23.3	105.6±19.5	107.7±16.2	97.2±13.8

Table 1: Normal Mean Arterial Blood Pressure (MABP, mmHg) of 8 Wistar Rats, the increase of MABP after AII administration (Control AII) and the MABP after 3, 6, 8 and 24h of Sartan transdermal administration

Plasma samples collected from Wistar Rats (n=8) after 3, 6, 8 and 24h of administration. The analysis was carried out on a Waters Acquity UPLC™ system with cooling autosampler and column oven. An Acquity UPLC™ BEH C18 column (150×2.1mm, 1.7µm) was employed for separation with the column temperature maintained at 40°C. The separation was performed using isocratic solution with 60% eluent A (0.1% formic acid in water) and 40% eluent B (0.1% formic acid in acetonitrile) in 5min. A Waters SQD mass spectrometer was used for analytical detection. The ESI source was set in positive ionization mode. Calibration curve were created at the concentration range from 0.9-1000 ng/mL by plotting the peak area ratios of losartan relative to the IS against the various drug concentrations in the spiked plasma standards (R²=0.9995).

Time (h)	Mean Conc. (ng/ml)
3	509.1 ± 193.3
6	1081.3 ± 351.3
8	1643.4 ± 474.3
24	2356.5 ± 1187.4

Table 2: Mean concentration of Losartan in rat plasma (n=8) after 3, 6, 8 and 24h of transdermal administration.

The aim of this investigation was to study the effectiveness of a liquid formulation for the transdermal delivery of two Sartans, Losartan potassium and Valsartan. The primary results demonstrated that both drugs have great potential of transdermal administration, promising an alternative and more effective therapy in hypertension. Further investigations including formulation development and the use of appropriate penetration enhancers are in progress in order to optimize transdermal penetration. Furthermore, polymer selection and design must be considered when striving to meet the diverse criteria for the fabrication of an effective transdermal delivery system. The methodology could be a new generation of anti-hypertensive drug delivery for the better blood pressure regulation.

Acknowledgments

This research has been co-financed by the European Union (European Social Fund – ESF) and Greek national funds through the Operational Program "Education and Lifelong Learning" of the National Strategic Reference Framework (NSRF) - Research Funding Program: Heracleitus II. Investing in knowledge society through the European Social Fund.

We would also like to acknowledge Eldrug S.A., Patras Science Park for the UPLC/MS contribution.

References

- [1] Nishida, N.; Taniyama, K.; Sawabe, T.; Manome, Y. *Int. J. Pharm.* **2010**, *402*, 103.
- [2] Wokovich. A.M. ; Prodduturi. S.; Doub. W.H.; Hussain. A.S.; Buhse. L.F. *Eur. J. Pham. Biopham.* **2006**, *64*, 1.
- [3] Samad, A.; Ullah, Z.; Alam, M.I.; Wais, M.; Shabaz, M.; Shams, S. *Rec. Patent Drug Del. Formul.* **2009**, *3*, 143.

Trehalose conjugated β -sheet breaker peptides as stabilizers of A β monomers

Francesco Attanasio,^a Irina Naletova,^b Vladimir Muronetz,^b Alessandro
Giuffrida,^a Maria Laura Giuffrida,^a Flora Marianna Tomasello,^c
Filippo Caraci,^d Agata Copani,^{a,d} Giuseppe Pappalardo,^a
Enrico Rizzarelli^{a,e}

^aCNR-Institute of Biostructure and Bioimaging, Catania, Italy; ^bBelozersky Institute of
Physico-Chemical Biology, Lomonosov Moscow State University, Moscow, Russia;

^cInternational PhD Program in Neuropharmacology, University of Catania, Catania, Italy;

^dUniversity of Catania, Department of Drug Sciences, Catania Italy; ^eUniversity of Catania,
Department of Chemical Sciences, Catania Italy

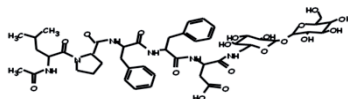
E-mail: giuseppe.pappalardo@cnr.it

Introduction

Alzheimer's Disease (AD) is a progressive neurodegenerative disease affecting more than 15 million people worldwide. The aggregation of amyloid β -peptide (A β) composed of 40-42 amino acid residues is considered to be the crucial step in the etiology of AD.[1]

Notably, A β is nowadays reported as a double-faced biomolecule playing a pivotal role in AD. Indeed, although A β monomers are capable of stimulating neuronal survival via the activation of the IGF1R and the PI3K pathways,[2] the early soluble A β aggregates are toxic as they cause neuronal death.[3] Thus A β self-assembly would be deleterious for two reasons: i) neurotoxic species are formed, ii) neurotrophic factors are cleared. Inhibiting A β self-oligomerization and/or stabilizing A β monomers might, therefore, provide useful approaches to control the pathogenic pathways underlying AD. We have conjugated a trehalose moiety to the known β -sheet breaker pentapeptide LPFFD.[4]

Trehalose has received a special interest because it has been found to be effective in the treatment of neurodegenerative diseases associated with peptide or protein aggregation. Moreover, we have already demonstrated that the glycoside moiety, we covalently linked to the C-terminus of the amino acid sequence, endows the peptide with increased resistance to proteases.[4] Here we show the neuro-protective and neuro-trophic activities of the LPFFD and LPFFD-Th peptides (scheme 1), in addition to experimental evidence indicating a direct interaction of the studied peptides with the monomeric form of A β .



Scheme 1

Results and Discussion

The neuroprotective activity of the LPFFD and LPFFD-Th peptides was tested using two different models of neurodegeneration: the NMDA insult (Figure 1A) and the insulin-

deprivation (Figure 1B). The results indicate that both peptides were neuroprotective at 100nM on mixed neuronal cultures exposed to 300 μ M NMDA for 10 min at room temperature in HEPES-buffered salt solution (Figure 1A). In Figure 1B the ability of LPFFD and LPFFD-Th (100nM) to support neuronal survival in a trophic deprivation model is reported. During this experiment, pure neuronal culture were exposed to peptides in absence of insulin support and maintained for 48 h at 37°C in 5% CO₂.

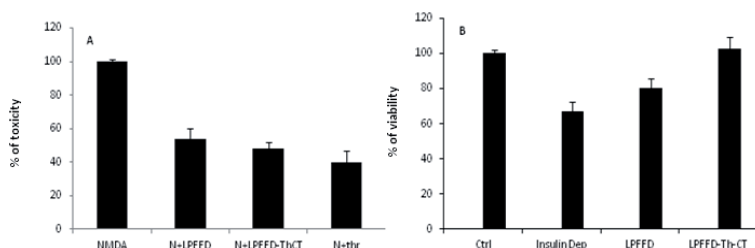


Figure 1. A: NMDA Toxicity; B: MTT Assay.

The neurotrophic action of the pentapeptides may be also explained in terms of their ability to stabilize A β monomers[2,4]. In fact, together with our ESI-MS, fluorescence, DLS and analytical ultracentrifugation data (not shown), it can be hypothesized that both peptides are capable of interacting with the A β monomer. In particular, limited proteolysis LC-MS experiments, carried out on A β samples either in the presence or in the absence of the LPFFD and LPFFD-Th peptides, indicate the 15-20 amino acid region of A β as the recognition site to maintain the fibrillogenic peptide in the monomeric state [5]. To this regard it seems that full comprehension of the molecular factors underlying AD, together with the elucidation of the factors that in vivo contribute to maintain A β in an physiologically benign monomeric conformation, may help to the design of a new generation of therapeutics for AD aiming at preserving the positive action of A β on neurons.[2]

Acknowledgments

This work was supported by MIUR, FIRB-MERIT project RBNE08HWLZ

References

- [1] Hardy, J.; Selkoe, D.J. *Science* **2002**, *297*, 353.
- [2] Giuffrida, M.L.; Caraci, F.; Pignataro, B.; Cataldo, S.; De Bona, P.; Bruno, V.; Molinaro, G.; Pappalardo, G.; Messina, A.; Palmigiano, A.; Garozzo, D.; Nicoletti, F.; Rizzarelli, E.; Copani, A. *J. Neurosci.* **2009**, *29*, 10582.
- [3] Cleary, J.P.; Walsh, D.M.; Hofmeister, J.J.; Shankar, G.M.; Kuskowski, M.A.; Selkoe, D.J.; Ashe, K. H.; *Nat. Neurosci.* **2005**, *8*, 79.
- [4] De Bona, P.; Giuffrida, M.L.; Caraci, F.; Copani, A.; Pignataro, B.; Attanasio, F.; Cataldo, S.; Pappalardo, G.; Rizzarelli, E. *J. Pept. Sci.* **2009**, *15*, 220.
- [5] Giuffrida A.; Attanasio F.; Naletova I.; Muronetz V.; A. Sinopoli A.; Pappalardo G.; Rizzarelli E.; Book of abstracts of XXIII Congresso Della Divisione Di Chimica Analitica Della Società Chimica Italiana **2012**, 194.

Use of substituted oxamide structure in designing pseudo-symmetric HIV protease inhibitors to employ multiple bridging water molecules

**Koushi Hidaka¹, Yuki Toda², Motoyasu Adachi³, Ryota Kuroki³,
Yoshiaki Kiso^{1,4}**

¹*Faculty of Pharmaceutical Sciences, Kobe Gakuin University, Kobe, Japan;* ²*Department of Medicinal Chemistry, Kyoto Pharmaceutical University, Kyoto, Japan;* ³*Molecular Structural Biology Group, Japan Atomic Energy Agency, Tokai, Japan;* ⁴*Peptide Science Laboratory, Nagahama Institute of Bio-Science and Technology, Nagahama, Japan*

E-mail:khida@pharm.kobegakuin.ac.jp

Introduction

Most of HIV protease inhibitors use one bridging water molecule to interact with the flap region. One application to utilize the bridging water is a replacement with carbonyl group in designing cyclic urea inhibitors reported by DuPont Merck [1]. We previously reported allophenylnorstatine-containing HIV protease inhibitors with a hydroxymethylcarbonyl (HMC), proven as an ideal transition state mimic [2]. In our recent report on D-Cys containing HIV protease inhibitors, a sulfonyl derivative showed activity enhancement against drug resistant HIV strains [3]. Interestingly, molecular dynamic (MD) simulations of the inhibitor suggested existence of additional stable bridging water molecules to support the binding with mutated proteases. Later, we confirmed bridging water molecules between sulfonyl moiety of the inhibitor and main chain amide NH groups of HIV-1 protease by X-ray crystallography.

In order to verify our speculation on effect of bridging water molecules, we designed pseudo-symmetric peptides based on HMC combined with hydrazide, that is, “HMC-hydrazide”, which is effective approach to transform substrate-based peptidic inhibitor to pseudo-symmetric peptide [4]. To increase the numbers of bridging water molecules, we replaced amide with sulfonyl and oxamide structures at both terminals.

Results and Discussion

The synthetic pseudo-symmetric compounds were tested against wild-type HIV-1 protease. Derivatives with sulfonyl groups did not exhibit the inhibitory activity (<1%) at 50 nM concentration. On the other hand, derivatives with oxamides showed >20% potency. Especially, compounds with *N*-(2-aminobenzyl)oxamides and *N*-(1-naphthylmethyl)-oxamides exhibited potent activity, 86% and 89%, respectively.

Lopinavir was widely chosen in anti-HIV therapy before the clinical use of darunavir. Therefore, emergence of lopinavir-resistant virus could be a considerable concern. Abbott Laboratories have reported a lopinavir-resistant strain A17 that proliferates in the presence of lopinavir/ritonavir [5]. The mutant clone displayed about 50-fold resistance to lopinavir. To study the resistance further, we prepared a HIV protease variant, A17m5. A17m5 possessed sufficient enzyme activity (K_m 214 μ M, k_{cat} 12 s^{-1}) and low susceptibility to

lopinavir. A17mut could be a novel target for next generation inhibitor development. Inhibitory activities against A17m5 of the two oxamide derivatives were higher (A17m5 17% and 19%, respectively) than that of a pseudo-symmetric analogue without oxamide structures (wild-type 91% and A17m5 8%). MD simulations of one oxamide derivative suggested involvements of four bridging water molecules for the binding (Fig. 1).

In summary, oxamide modifications at both terminals of pseudo-symmetric inhibitors resulted in a moderate activity loss against lopinavir-resistant mutations compared to inhibitors without oxamide. This method to accompany multiple bridging water molecules could be applicable to design protease inhibitors to defeat the drug resistance from amino acid mutations.

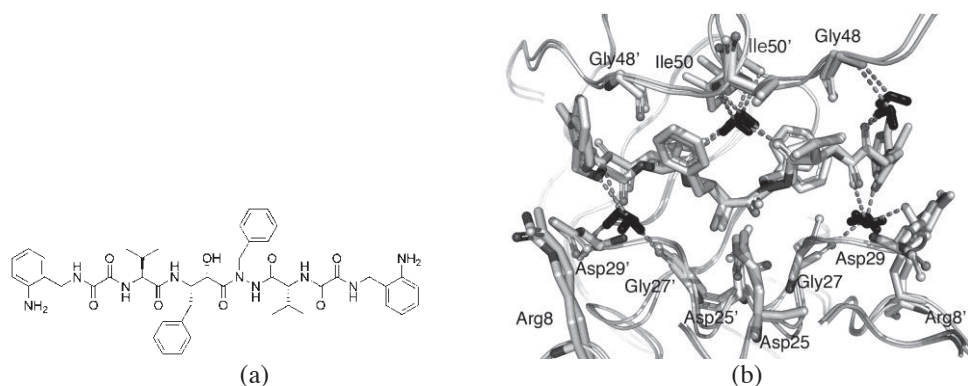


Fig. 1. Structure of oxamide derivative **1** (a) and its MD simulated poses in the active sites of wild-type and A17m5 proteases (b). Bridging water molecules are represented in black.

Acknowledgments

This research was supported by Grant-in-Aid for Young Scientists (B) (No. 23790145) from MEXT of Japan.

References

- [1] Lam, P.Y.; Jadhav, P.K.; Eyermann, C.J.; Hodge, C.N.; Ru, Y.; Bacheler, L.T.; Meek, J.L.; Otto, M.J.; Rayner, M.M.; Wong, Y.N.; Chang, C.-H.; Weber, P.; Jackson, D.A.; Sharpe, T.R.; Erickson-Viitanen, S. *Science*, **1994**, *263*, 380.
- [2] Adachi, M.; Ohhara, T.; Kurihara, K.; Tamada, T.; Honjo, E.; Okazaki, N.; Arai, S.; Shoyama, Y.; Kimura, K.; Matsumura, H.; Sugiyama, S.; Adachi, H.; Takano, K.; Mori, Y.; Hidaka, K.; Kimura, T.; Hayashi, Y.; Kiso, Y.; Kuroki, R. *Proc. Natl. Acad. Sci. USA*, **2009**, *106*, 4641.
- [3] Nakatani, S.; Hidaka, K.; Ami, E.; Nakahara, K.; Sato, A.; Nguyen, J.-T.; Hamada, Y.; Hori, Y.; Ohnishi, N.; Nagai, A.; Kimura, T.; Hayashi, Y.; Kiso, Y. *J. Med. Chem.*, **2008**, *51*, 2992.
- [4] Hidaka, K.; Kimura, T.; Hayashi, Y.; McDaniel, K.F.; Dekhtyar, T.; Colletti L.; Kiso, Y. *Bioorg. Med. Chem. Lett.*, **2003**, *13*, 93.
- [5] Mo, H.; Lu, L.; Dekhtyar, T.; Stewart, K.D.; Sun, E.; Kempf, D.J.; Molla, A. *Antivir. Res.*, **2003**, *59*, 173.

Optimization of the PNA-synthesis using different bases for Fmoc-deprotection

S. Rawer,¹ K. Braun,² R. Pipkorn²

¹Life Technologies, Frankfurter Strasse 129, D-64293 Darmstadt, Germany; ²German
Cancer Research Center, INF 280, D-69120 Heidelberg, Germany

E-mail: stephan.rawer@lifetech.com; k.braun@dkfz.de; r.pipkorn@dkfz.de

Introduction

The promising personalized medicine requires highly sensitive and specific active components which are based on nucleic acids. Because of the sensitivity against natural DNA/RNA nucleases the probes demand modifications. Peptide nucleic acids (PNAs) are not a substrate for cell immanent enzymatic cleavage and therefore they are considered as resistant, highly sensitive and specific tools for antisense strategies especially conjugated with cell penetrating peptides. Shuttle systems individually designed with by SPPS methodologies can be applied in cancer diagnostics and possibly in therapy [1-3]. However it is undisputed, that proper PNAs' syntheses prove to be a challenge for coupling and Fmoc-deprotection. Due to the structure-formation the success of the synthesis strongly depends on parameters, like activator's quality and deprotection kinetics correlating to the length of the PNA polymer SPPS product. Whereas solid phase PNA synthesis's modifications like micro wave [4] and resin matrix [5] optimizing yield and quality are documented the resins physical properties used in the PNA synthesis are critical to a certain extent and required more investigations [6]. Using the new SPPS PNA synthesis' results of the coding sequence of c-myc human Exon II [7], piperidine and pyrrolidine, acting as Fmoc-deprotection reagents as a further example, we compared, analyzed and optimized the PNA synthesis strategy.

Results and Discussion

The diagrams in Figure 1 document the HPLC analysis of the PNA product exemplarily synthesized by SPPS dependent on the used resin specification [8] and the basic capacity of the protection reagent.

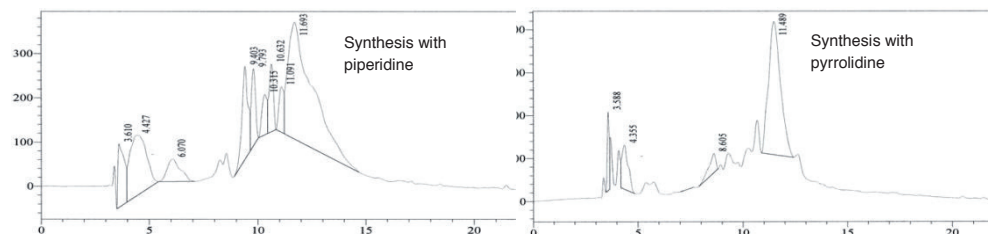


Figure 1 shows the HPLC diagram of the c-myc PNA synthesized on the peptide synthesizer 433A equipped with the special deprotection module with fixed deprotection time. The left picture points out the TentaGel R RAM high swell Rapp Polymers [loading 0.38 mmol/g] deprotected with piperidine and the right picture exhibits the diagram of the pyrrolidine experiment.

The graphs in Figure 2 demonstrate the discrepancies of the deprotection potential as a function of the dissociated PNA building block.

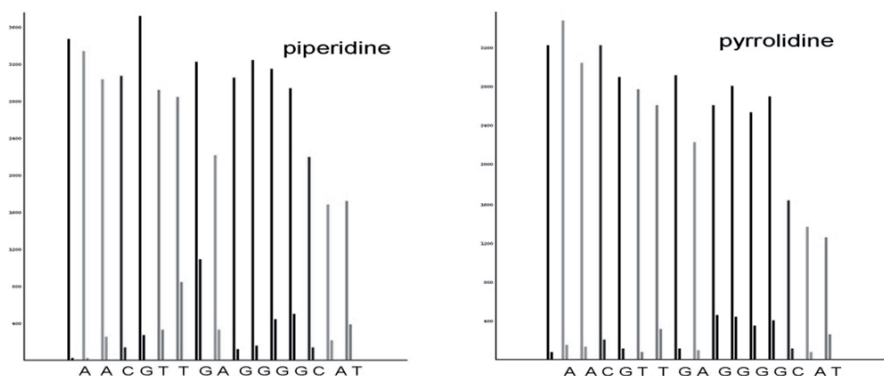


Figure 2 visualizes the deprotection in every coupling step (left bars) and shows a better performance of pyrrolidine in comparison to piperidine in the final step (right bars) in rapid Fmoc deprotection. Each measurement was collected after a base treatment of 2.5 minutes.

Acknowledgments

This work was partially supported by Deutsche Krebshilfe, D-53004 Bonn; Grant Number: 1066335. The authors thank Mario Koch for technical assistance.

References

- [1] Pipkorn, R.; Waldeck, W.; Braun, K. *J. Mol. Recognit.* **2003**, *16* (5), 240-247.
- [2] Pipkorn, R.; Dunsch, L.; Wiessler, M.; Waldeck, W.; Braun, K. *Biopolymers* **2011**, *96* (4), 506.
- [3] Pipkorn, R.; Wiessler, M.; Waldeck, W.; Koch, M.; Braun, K. *Cell Penetrating Peptides 31EPS CPP satellite meeting* **2010**, 10-11.
- [4] Pipkorn, R.; Wiessler, M.; Waldeck, W.; Hennrich, U.; Nokihara, K.; Beining, M.; Braun, K. *Int. J. Med. Sci.* **2012**, *9* (1), 1-10.
- [5] Pugh, K. C.; York, E. J.; Stewart, J. M. *Int. J. Pept. Protein Res.* **1992**, *40* (3-4), 208-213.
- [6] Rawer, S.; Roeder, R.; Henklein, P. Proceedings 29th EPS Symposium. Gdansk, **2006**, p 780.
- [7] Heckl, S.; Pipkorn, R.; Waldeck, W.; Spring, H.; Jenne, J.; von der Lieth, C. W.; Corban-Wilhelm, H.; Debus, J.; Braun, K. *Cancer Res.* **2003**, *63* (16), 4766-4772.
- [8] Amblard, M.; Fehrentz, J. A.; Martinez, J.; Subra, G. *Molecular Biotechnology* **2006**, *33* (3), 239-254.

Alkoxyphenylthio: Novel reducing agent labile cysteine protecting groups

T. M. Postma,^{a,b} M. Giraud,^d F. Albericio^{a,b,c}

^aInstitute for Research in Biomedicine, Barcelona, 08028, Spain; ^bCIBER-BBN, 08028-Barcelona, Spain; ^cDepartment of Organic Chemistry, University of Barcelona, 08028, Barcelona, Spain; ^dLonza Ltd, Visp, VS 3930, Switzerland

E-mail: fernando.albericio@irbbarcelona.org

Introduction

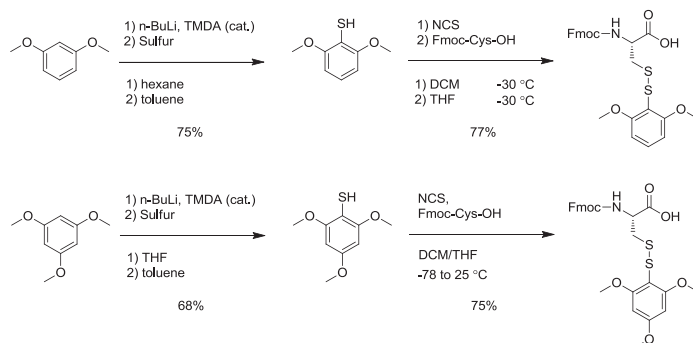
Peptides that contain multiple disulfide bonds are abundant in nature and important from a therapeutic perspective, owing to their potent bioactivities and increased metabolic stability [1]. In order to prepare multiple disulfide containing peptides, orthogonal protecting schemes for cysteine (Cys) need to be employed to achieve the desired disulfide configuration. However, there are few orthogonal Cys protecting groups that can be removed under mild conditions in routine peptide synthesis [2].

Tert-butylthio (StBu) is a commercially available cysteine protecting group compatible with Fmoc/tBu synthesis and orthogonal to all other Cys protecting groups. The StBu protecting group is labile to mild reducing agents and owing to its long deprotection times (4-24 h) cannot be used in routine peptide synthesis. Moreover, in certain cases StBu has been shown impossible to remove and reports of desulfurization due to long exposure to reducing agents, show the significant limitations of this protecting group [3, 4].

Results and Discussion

The concept of Cys protecting groups labile to reducing agents is promising due to orthogonality to other Cys protecting groups and the limitations of StBu, initiated an investigation into novel reductive Cys protecting groups. We started our study with alkoxythiophenol based mixed disulfides. The thiophenols 2,6-dimethoxythiophenol and 2,4,6-trimethoxythiophenol were prepared according to the literature [5]. To prepare mixed disulfides of Fmoc-Cys-OH and an alkoxythiophenol we used a modified method employing *N*-chlorosuccinimide (NCS) [6]. Fmoc-Cys-OH was protected with 2,6-dimethoxyphenylthio (*S*-Dmp) and 2,4,6-trimethoxyphenylthio (*S*-Tmp) (Scheme 1).

To study the functioning of these protecting groups model tripeptides were prepared on a Rink Amide AM resin (Fmoc-Ala-Cys(PG)-Leu-NH₂). The tripeptides containing StBu, *S*-Dmp or *S*-Tmp were screened for lability and stability. All protecting groups were stable to 20% piperidine in DMF and labile to thiols (0.1M *N*-methylmorpholine (NMM) in 20% β-mercaptoethanol / DMF). For quantitative removal of *S*-Dmp and *S*-Tmp a 5 min treatment of the peptidyl-resin with the thiol deprotection mixture was sufficient for the model tripeptide. Whereas, 3 h was needed for quantitative StBu deprotection using the same conditions. This result shows the advantage of using alkoxyphenylthio based protecting groups over StBu, owing to the rapid deprotection times of *S*-Dmp and *S*-Tmp.



Scheme 1: Synthesis of Fmoc-Cys(*S*-Dmp)-OH and Fmoc-Cys(*S*-Tmp)-OH

Subsequently, we prepared linear oxytocin containing StBu, *S*-Dmp or *S*-Tmp on a Rink Amide AM resin. Removal of *S*-Dmp and *S*-Tmp was achieved with a 3x5 min protocol, whereas 8 h was needed to remove StBu. The peptides were oxidized in solution (5% DMSO in H₂O / CH₃CN (3:1) at pH 8.5 for 24 h) and the resulting HPLC traces compared. The best results were obtained with *S*-Tmp in terms of purity compared to StBu (93% to 72%). The best protecting group, *S*-Tmp, was used in the synthesis of the T22 peptide containing 4 Cys residues. The linear peptide was synthesized, the 4 *S*-Tmp residues removed (3x5 min) and cleaved from the resin. The linear peptide was oxidized in solution (5% DMSO in H₂O at pH 8.5 for 24 h) and the product was successfully obtained.

In conclusion, we have developed a highly labile replacement for the difficult to remove StBu Cys protecting group. We recommend *S*-Tmp over *S*-Dmp as it gave the best results.

Acknowledgments

We thank Miriam Góngora-Benítez from the Institute for Research in Biomedicine and Dr. Thomas Bruckdorfer from IRIS Biotech GmbH for fruitful discussions and academic input.

We are grateful to the European community -FP7-PEOPLE-ITN-2008 for financial support.

References

- [1] Livett, B. G.; Gayler, K. R.; Khalil, Z., *Curr. Med. Chem.* **2004**, *11*, 1715-1723.
- [2] Isidro-Llobet, A.; Álvarez, M.; Albericio, F. *Chem. Rev.* **2009**, *109*, 2455-2504
- [3] Góngora-Benítez, M.; Tulla-Puche, J.; Paradis-Bas, M.; Werbitzky, O.; Giraud, M.; Albericio, F. *Peptide Science* **2011**, *96*, 69-80.
- [4] Rijkers, D. T. S.; Kruijtzter, J. A. W.; Killian, J. A.; Liskamp, R. M. J., *Tet. Lett.* **2005**, *46*, 3341-3345.
- [5] Wada, M.; Natsume, S.; Suzuki, S.; Akira, U.; Nakamura, M.; Hayase, S.; Erabi, T., *J. Organomet. Chem.* **1997**, *548*, 223-227.
- [6] Kraus, G. A.; Jeon, I., *Tetrahedron* **2005**, *61*, 2111-2116.

Fast and efficient microwave-assisted monitoring of difficult peptide sequences

**F. Rizzolo,^{a,b,c} C. Testa,^{a,b,c,d} D. Lambardi,^{a,d} M. Chorev,^e M. Chelli,^{a,c}
P. Rovero,^{a,c} A.M. Papini^{a,b,c}**

^aLaboratory of Peptide & Protein Chemistry & Biology - PeptLab - www.peptlab.eu;

^bSOSCO - EA4505 Université de Cergy-Pontoise, 5 mail Gay-Lussac, Neuville-sur-Oise,
Cergy-Pontoise 95031, France; ^c Department of Chemistry "Ugo Schiff", Via della

Lastruccia 3/13, Polo Scientifico e Tecnologico, University of Florence, I-50019 Sesto
Fiorentino, Italy; ^dDepartment of Pharmaceutical Sciences, Via Ugo Schiff 6, Polo
Scientifico e Tecnologico, University of Florence, I-50019 Sesto Fiorentino, Italy;

^eLaboratory for Translational Research, Harvard Medical School, Cambridge, MA 02139,
USA. Department of Medicine, Brigham and Women's Hospital, Boston, MA 02115, USA

fabio.rizzolo@gmail.com

Introduction

Modern solid-phase peptide synthesis (SPPS) protocols allow the assembly of larger and more complex peptides.¹ Unfortunately, the automated synthesizers are generally developed to produce peptides without a real-time monitoring of the progress of the synthesis. Although different methods have been developed for monitoring SPPS, we observed that the use of colorimetric tests or continuous-flow UV absorbance were not informative enough to identify difficult steps in the SPPS. In this study we demonstrated the usefulness of the combination of a microwave (MW) assisted mini-cleavage protocol and the UPLC-ESI-MS/MS analysis for monitoring the quality of the coupling steps in the SPPS. Based on this strategy we monitored the synthesis of PTHrP(1-34)NH₂ (by Fmoc/tBu RT-SPPS, LibertyTM, CEM), characterized by a cluster of sterically hindered arginine residues and hydrophobic amino acid residues in the sequence that present a synthetic challenge.²

Results and Discussion

RT-SPPS of PTHrP(1-34)NH₂ has been performed on Rink-amide NovaSyn[®] TGR resin (0.2 mmol/g, 500 mg). General coupling cycle consists of the removal of *N*-terminal Fmoc-protecting group with a solution of 20% piperidine in DMF. Fresh stock solutions of the Fmoc-protected amino acids (0.2 M, 5 equiv.) and TBTU (0.5 M, 5 equiv.) in DMF, and of DIEA (2 M, 10 equiv.) in NMP were prepared and used as reagents during the SPPS. The PTHrP(1-34)NH₂ synthesis was monitored by UPLC-ESI-MS analysis of MW-assisted mini-cleavages of intermediate resin-bound fragments using Discover[®] S-Class single-mode MW reactor equipped with Explorer-48 autosampler (CEM). A small sample of beads carrying Fmoc-protected resin-bound peptide (10 mg) was weighted into a fritted polypropylene tube and treated twice with a 20% solution of piperidine in DMF (1 ml) each time for 5 min. The beads were then washed with DMF (2×1 ml) and DCM (3×1 ml), dried under vacuum and transferred into a 10 ml glass tube containing the cleavage mixture that was placed into the MW cavity. The mini-cleavages were carried out with 2 ml of TFA/TIS/water solution (95:2.5:2.5 v/v/v) at 45 °C, using 15W for 15 min with external

cooling of the reactor vessel. The reaction mixture was then filtered and the crude peptide was precipitated from the cleavage mixture by addition of ice-cold diethyl ether followed by cooling for 5 min at -20 °C. The product was collected by centrifugation and directly subjected to UPLC-ESI-MS analysis (Table 1).

Table 1. Fmoc/tBu RT-SPPS of PTHrP(1–34)NH₂: list of fragments produced by MW-assisted mini-cleavages of intermediate resin-bound peptides.

Analysed resin-bound sequence	Sequence	Calculated monoisotopic mass	Intact sequences Qtof MS (ESI+) (m/z) found	Deletion sequences Qtof MS (ESI+) (m/z) found	Missing amino acid residues from deletion sequences	Amount of deletion sequences (%)
27-34	H-Leu-Ile-Ala-Glu-Ile-His-Thr-Ala-NH ₂	865.51	866.39 [M + H] ⁺	753.41 [M+H] ⁺	Leu ²⁷	7
25-34	H-His-His-Leu-Ile-Ala-Glu-Ile-His-Thr-Ala-NH ₂	1139.62	1140.90 [M + H] ⁺	1003.95 [M+H] ⁺ 890.93 [M+H] ⁺	His ²⁵ Leu ²⁷ His ²⁸	2 5
22-34	H-Phe-Phe-Leu-His-His-Leu-Ile-Ala-Glu-Ile-His-Thr-Ala-NH ₂	1546.84	1547.41 [M + H] ⁺	1434.44 [M+H] ⁺	Leu ²⁷	8
19-34	H-Arg-Arg-Arg-Phe-Phe-Leu-His-His-Leu-Ile-Ala-Glu-Ile-His-Thr-Ala-NH ₂	2015.15	1008.69 [M + 2H] ²⁺	952.19 [M+2H] ²⁺ 852.72 [M+2H] ²⁺ 774.73 [M+2H] ²⁺	Leu ²⁷ Arg ¹⁹ Arg ²⁰ Arg ¹⁹ Arg ²⁰ Arg ²¹	6 39 51
12-34	H-Gly-Lys-Ser-Ile-Gln-Asp-Leu-Arg-Arg-Arg-Phe-Phe-Leu-His-His-Leu-Ile-Ala-Glu-Ile-His-Thr-Ala-NH ₂	2756.55	1379.24 [M + 2H] ²⁺	1322.29 [M+2H] ²⁺ 1315.26 [M+2H] ²⁺ 1258.81 [M+2H] ²⁺ 1065.43 [M+2H] ²⁺	Leu ²⁷ Gln ¹² Lys ¹³ Leu ²⁷ Gln ¹⁹ Lys ¹³ Gly ¹² Lys-Ser-Ile-Gln-Asp ¹⁷	5 55 3 12

In order to validate the use of microwave irradiation in the mini-cleavage for monitoring the coupling step, we compared the results obtained with the RT- and MW-assisted mini-cleavage protocols. We selected the PTHrP(19-34)NH₂ fragment (synthesised by Fmoc/tBu RT-SPPS, LibertyTM, CEM) that includes a cluster of arginine residues in positions 19-21. The use of microwave-assisted mini-cleavage protocol to monitor the growing peptide chains was useful to optimise deprotection time of multi-arginine containing peptide sequences protected by the N^G-Pbf protecting group. In fact, based on the results obtained by UPLC-ESI-MS, we concluded that 15 and 30 min deprotection steps at RT were not adequate to completely remove the Pbf protecting groups from the arginine side-chain residues. On the contrary, after 1 h at RT, the 19-34 fragment of PTHrP(1-34)NH₂ was cleaved from resin and completely deprotected. Importantly, the MW-assisted mini-cleavage reaction was finished in 15 min, confirming that the use of microwave irradiation in mini-cleavages is an efficient strategy to monitor completion of reaction even in the case of sterically hindered peptide sequences such as Pbf protected multi-arginine containing peptides.

This protocol describes the advantage of combining the use of MW-assisted mini-cleavages with fast and sensitive UPLC-ESI-MS analysis to monitor effectively the progress of difficult peptide synthesis such as in the case of PTHrP(1-34)NH₂. This strategy helps to identify critical coupling steps and therefore prevents formation of deletion sequences and improves the yield and purity of crude peptides. Moreover, this protocol is suitable even in the case of multi-arginine peptides and shortens the reaction time relative to the duration of conventional cleavages.

Acknowledgments

Ente Cassa Risparmio di Firenze and ANR Chaire d'Excellence 2009-2013 PepKit (AMP) are gratefully acknowledged.

References

- [1] Sabatino G.; Papini A. M.. *Curr. Opin. Drug. Discov. Devel.* **2008**, *11*, 762.
- [2] Rizzolo F.; Testa C.; Lambardi D.; Chorev M.; Chelli M.; Rovero P.; Papini A. M.. *J. Peptide Sci.* **2011**, *17*, 708.

Highly efficient infrared (IR) heating method for SPPS in multiple reactors on the Tribute[®] UV-IR peptide synthesizer

James P. Cain, Michael A. Onaiyekan, Christina A. Chantell, Chris Donat, Alex S. Waddell, Robert W. Hensley, Mahendra Menakuru

Protein Technologies, Inc. Tucson, Arizona, 85714

E-mail: info@ptipep.com

Introduction

The application of heat, typically using oil baths, heating elements, or microwaves, has emerged as a useful tool for peptide synthesis [1]. Microwave heating in particular has grown in popularity in recent years, due to the speed with which small volumes can be raised to elevated temperatures. There has been some speculation regarding the existence of a non-thermal “microwave effect”; however, a thorough series of experiments examining the synthesis of both peptides [2] and small molecules [3,4] has shown that observed enhancements in purity can be attributed to purely thermal effects. Apparent discrepancies in the results between microwave and non-microwave heating could be eliminated by careful temperature monitoring and control.

All commercial single-mode microwave reactors currently available allow irradiation of only a single vessel. Thus, it is not possible to perform microwave synthesis of multiple peptides in parallel. Furthermore, limitations in the reaction vessel and mixing options available on microwave synthesizers make scale-up of microwave conditions practically impossible.

A system which could match the advantages of microwave heating (rapid, efficient) while eliminating the disadvantages (serial synthesis, limited scale) would be a powerful new tool at the disposal of the synthetic peptide chemist. To meet this goal, we have developed the first peptide synthesizer with infrared (IR) heating, using the Tribute[®] peptide synthesizer with UV monitoring. Heating with IR is faster than microwaves. Unlike microwave platforms however, multiple reaction vessels can be heated with IR simultaneously, allowing parallel synthesis. Vortex mixing (or vortex mixing with nitrogen bubbling) ensures that a homogeneous temperature distribution is maintained.

To illustrate the efficiency of IR heating, we have synthesized two peptides originally prepared using microwave conditions (Figure 1). The first is the 65-74 fragment of the acyl

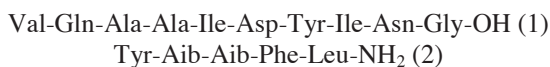


Fig. 1. Structures of peptides synthesized using IR heating on the Tribute[®] UV-IR.

carrier peptide (⁶⁵⁻⁷⁴ACP), a well-known difficult sequence commonly used to test the efficacy of various synthesis protocols. The second peptide contains two adjacent sterically hindered Aib residues in place of the glycines found in native leucine enkephalin [5]. Peptides containing sterically hindered residues such as Aib are notoriously difficult to synthesize, and are also often used to test the efficacy of different synthesis protocols.

Results and Discussion

The results show the two heating methods generated peptides with very similar crude purities (Table 1).

Table 1. Crude % purities for peptides synthesized using infrared (IR) or microwave heating.

Peptide	Crude % Purity	
	Infrared (IR) Heating	Microwave Heating
⁶⁵⁻⁷⁴ ACP	92	87
Tyr-Aib-Aib-Phe-Leu-NH ₂	89	92

⁶⁵⁻⁷⁴ACP was synthesized using infrared heating on the Tribute[®] UV-IR with a crude purity of 92% [6] (Figure 2). This value is very similar to the purity of 87% reported for the microwave synthesis [7]. Tyr-Aib-Aib-Phe-Leu-NH₂ was synthesized using infrared heating on the Tribute[®] UV-IR with a crude purity of 89% [8] (Figure 2). This value is very similar to the purity reported for the microwave synthesis [5]. LC-MS analysis confirmed that the correct peptides were synthesized (data not shown).

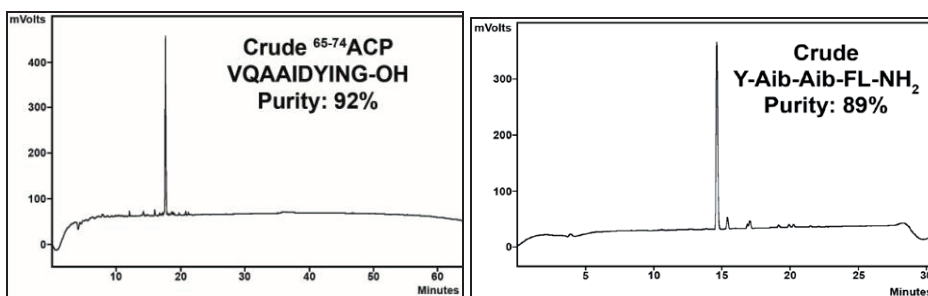


Fig. 2. Crude HPLC traces of peptides synthesized with infrared (IR) heating on the Tribute[®].

References

- [1] Pedersen, S.L.; Tofteng, A.P.; Malik, L.; Jensen, K.J. *Chem. Soc. Rev.* **2012**, *41*, 1826-1844.
- [2] Bacsa, B.; Horvati, K. *et al. J. Org. Chem.* **2008**, *73*, 7532-7542.
- [3] Hosseini, M.; Stiasni, N.; Barbieri, V.; Kappe, C.O. *J. Org. Chem.* **2007**, *72*, 1417-1424.
- [4] Herrero, M.A.; Kremsner, J.M.; Kappe, C.O. *J. Org. Chem.* **2008**, *73*, 36-47.
- [5] Subiros-Funosas, R.; Acosta, G.A.; El-Faham, A.; Albericio, F. *Tetrahedron Lett.* **2009**, *50*, 6200-6202.
- [6] Cain, J.P.; Onaiyekan, M.A.; Chantell, C.A.; Donat, C.; Waddell, A.S.; Hensley, R.W.; Menakuru, M. *PharmaChem* **2012** pending publication.
- [7] Microwave Synthesis of ACP 65-74, Application Note BIO-0001, CEM Corp. (Matthews, NC).
- [8] Cain, J.P.; Onaiyekan, M.A.; Chantell, C.A.; Donat, C.; Waddell, A.S.; Hensley, R.W.; Menakuru, M. *PharmaChem* **2012**, May/June, 2-3.

In-water solid-phase peptide synthesis using nanoparticulate Fmoc-amino acids with microwave irradiation

**Keiko Hojo, Asaki Hara, Mare Onishi, Hideki Ichikawa,
Yoshinobu Fukumori**

*Faculty of Pharmaceutical Sciences & Cooperative Research Center of Life,
Kobe Gakuin University, Kobe 650-8586, Japan*

E-mail: hojo@pharm.kobegakuin.ac.jp

Introduction

The consumption of organic solvent is extremely large in chemical peptide syntheses due to the multiple condensation steps. The toxic and volatile nature of organic solvents poses a serious risk of environmental pollution. There is now a compelling need to develop new peptide synthesis technologies that will reduce the damage to the environment. Until recently, peptide synthesis in aqueous solution has remained largely unexplored. This is because the most common building blocks are sparingly soluble in water and are considered inappropriate for in-water peptide synthesis. We have developed a method for solid-phase peptide synthesis (SPPS) in water, which utilizes water-insoluble Fmoc-amino acids that are converted to water-dispersible nanoparticles [1-3]. In this way, the solubility problem is overcome. However, there are two main problems with this nanoparticle approach; (i) slow reaction rates (ii) poor yields for long peptides because of their chain aggregation in water. MW assisted SPPS is particularly attractive including automated peptide synthesizers equipped with MW capability. The main advantages of MW assisted chemistry are shorter reaction times and higher yields. Since water is polar in nature, it has good potential to absorb microwaves and convert them to heat energy, thus accelerating the reactions in an aqueous medium. A trial of MW assisted in-water solid-phase synthesis of 5-residue peptide using non-disperse Boc-amino acids has been reported by Albericio previously [4]. Currently, Fmoc-amino acids are routinely used as building blocks for SPPS. Fmoc-amino acids are sparingly soluble in water and have greater hydrophobic characteristics than Boc-amino acids. With this in mind, we have developed a microwave irradiation procedure aimed at reducing reaction time and increasing reaction yield for in-water solid-phase synthesis using water-dispersible Fmoc-amino acid nanoparticles.

Results and Discussion

First, we tested and evaluated the coupling efficiency of the solid-phase microwave reaction between the Fmoc-Phe-OH nanoparticles with H-Gly-Rink amide-TentaGel resin using several different coupling methods. WSCI, DMTMM and combination of several types of additive, HOSu, HONB and sulfo-HOSu were examined. Reaction temperature was 70°C using a power of 70 W. The coupling reaction using WSCI combination with sulfo-HOSu was completed within 3 min. Surprisingly, in the case of DMTMM, the reaction was completed in only 1 min. These reactions were smoother than expected, suggesting that the reaction time between an aqueous nanocolloid and a solid support is dramatically reduced by MW radiation in high polar water-based solvent.

To evaluate the advantage of the in-water coupling reaction with MW radiation, we also applied the microwave radiation to the in-water solid phase synthesis of Leu-enkephalinamide (Tyr-Gly-Gly-Phe-Leu-NH₂) using Fmoc chemistry. The reaction was carried out in aqueous solution with MW irradiation. Results of the HPLC analysis for Leu-enkephalinamide afforded a single peak. The presence of only one peak in the chromatogram of crude peptides suggested the absence of diastereomeric compounds. Thus, there is no significant racemization during the MW assisted coupling reaction.

Difficult sequences peptides are problematic to synthesize using a conventional method due to the aggregation of protected peptide chain on the resin. MW irradiation is useful in breaking up the aggregation of a peptide chain. To further evaluate this MW assisted in-water synthesis method, we demonstrated

the synthesis of ACP (65-74) peptide, Val-Gln-Ala-Ala-Ile-Asp-Tyr-Ile-Asn-Gly-NH₂, which is a well-known difficult sequences. Using a combination of MW irradiation and water-dispersible nanoparticles, we synthesized ACP (65-74) peptide on the Rink amide-TentaGel resin according to the same in-water protocol. All the coupling steps were performed by double coupling reactions. Figure 1 shows the HPLC analysis profile of the ACP (65-74) peptide synthesized in water by this methodology. Clearly, the data shows a main peak. Even though all the synthetic processes were carried out in aqueous media, ACP (65-74) peptide was obtained in satisfactory purity.

We have demonstrated that MW radiation can be successfully applied to the rapid synthesis of oligopeptides in high yield and purity. This is the first documented example of in-water solid-phase synthesis of peptides with difficult sequences. Therefore, this protocol should be generally applicable to a wide range of peptides, including sequences that are otherwise difficult to synthesize.

Acknowledgments

This work supported by a "Strategic Research Foundation" at Private Universities matching fund subsidy from the Japanese Ministry of Education, Culture, Sports Science and Technology, 2012-2016.

References

- [1] Hojo, K.; Ichikawa, H.; Maeda, M.; Kida, S.; Fukumori, Y.; Kawasaki, K. *J. Peptide Sci.* **2007**, *13*, 49..
- [2] Hojo, K.; Ichikawa, H.; Fukumori, Y.; Kawasaki, K. *Int. J. Peptide Res. Ther.* **2008**, *14*, 373.
- [3] Hojo, K.; Hara, A.; Kitai, H.; Onishi, M.; Ichikawa, H.; Fukumori, Y.; Kawasaki, K. *Chemistry Central J.* **2011**, *5*, 49.
- [4] Galanis, A. S.; Albericio, F.; Grötli, M. *Org. Lett.* **2009**, *20*, 4488.

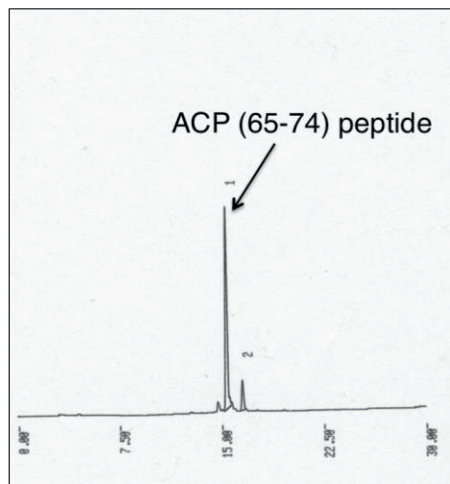


Figure 1. Analytical HPLC profiles of ACP (65-74) peptide obtained by MW assisted solid phase synthesis in water using nanoparticles.

Novel Liquid Phase Peptide Synthesis (LPPS) technology: Elongation using Organic Solvent Nanofiltration (OSN)

Wenqian Chen^{1,2}, Michele Cristau¹, Andrew G. Livingston²

¹Lonza Ltd, Lonzastrasse, 3930 Visp, Switzerland; ²Department of Chemical Engineering,
Imperial College London, South Kensington Campus, London SW7 2AZ, UK

E-mail: wenqian.chen@lonza.com

Introduction

Organic Solvent Nanofiltration (OSN) is integrated into Liquid Phase Peptide Synthesis (LPPS) in order to offer faster isolation as compared to the conventional liquid phase techniques (i.e. extraction and precipitation)¹⁻². The conventional Fmoc chemistry is applied for peptide synthesis with the target peptide grown on an anchor which is soluble in common organic solvents³. The ideal anchor must be completely retained by the OSN membranes, which in turn should allow other reagents such as amino acid, activator and racemisation suppressor to pass through. After each reaction (i.e. deprotection and coupling), diafiltration is performed to obtain the growing peptide in solution by washing off other reagents with pure solvents. This method is designed to overcome the disadvantages of traditional LPPS, yet retain the benefits of lower cost. Furthermore, it should give higher peptide quality as compared to Solid Phase Peptide Synthesis (SPPS).

A typical constant volume diafiltration system is shown in Figure 1.. When operated at high pressure, a portion of the feed tank solution permeates through the membranes and the membranes retain large molecules (i.e. the valuable compound), while allowing small molecules (i.e. contaminants) to pass through. In order to keep a constant feed tank volume, fresh solvent is pumped into the system to compensate the loss of solvent through the permeate stream.

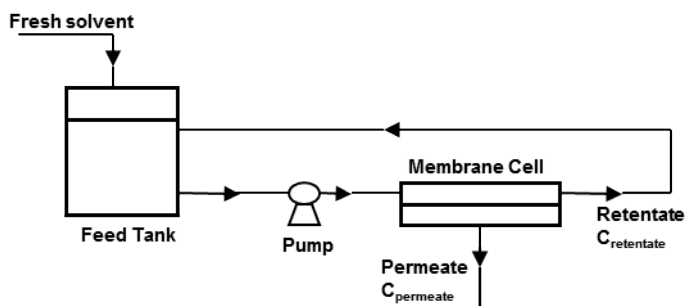


Figure 1. Schematic of a Constant Volume Diafiltration system.

Ceramic membranes Inopor 450 and Inopor 750 are used in the experiments. For the purpose of peptide synthesis, the membranes are characterised by 1.0 wt% Fmoc-Ala-OH/THF solution as Fmoc-Ala-OH is one of the smallest amino acid and THF is a common solvent for peptide synthesis. The rejection data of Inopor 450 and 750 are shown in the Results and Discussion section below (see Table 1).

The rejection of two soluble anchors with molecular weights between 1776 and 1949 g/mol, as shown in Figure 2, were tested.



(a) Anchor A

(b) Anchor B

Figure 2. Soluble Anchors

Results and Discussion

Although Inopor 450 is supposed to be a tighter membrane than Inopor 750, it has a lower rejection of Fmoc-Ala-OH than Inopor 750. Nevertheless, both membranes have similar rejections for the two anchors. As the anchors have high rejections (i.e. more than 90%), they are suitable for LPPS with OSN.

Table 1. Rejection data of ceramic membranes

	Fmoc-Ala-OH in THF	Anchor A in THF	Anchor B in DMF
Inopor 450	32.7 ± 1.4%	93.9 ± 0.3%	97.3 ± 0.2%
Inopor 750	49.4 ± 1.7%	93.8 ± 0.7%	95.1 ± 0.3%

Acknowledgments

The research leading to these results has received funding from the European Community's Seventh Framework Programme ([FP7/2007-2013] under grant agreement n° 238291).

In addition, we would like to thank Lonza Ltd and Imperial College London.

References

- [1] So, S.; Peeva, L.G.; Tate, E.W.; Leatherbarrow, R.J.; Livingston, A.G. *Chem. Commun.* **2012**, 46, 2808-2810
- [2] So, S.; Peeva, L.G.; Tate, E.W.; Leatherbarrow, R.J.; Livingston, A.G. *Org. Process. Res. Dev.* **2010**, 14(6), 3113-1325
- [3] Fischer, P.M.; Zheleva, D.I. *J. Pept. Sci.* **2002**, 8(9), 529-542

Return of cotton as a carrier for solid phase synthesis

Michal Lebl, Zuzana Flegelova

Spyder Institute Praha, Czech Republic

E-mail: michallebl@gmail.com, zuzana.flegelova@centrum.cz

Introduction

Cotton was shown as a convenient solid phase support earlier [1-3], but did not find wide acceptance by the peptide community. We decided to try its application as (i) a support of choice for the synthesis driven by combination of capillary forces and gravity, (ii) support for synthesis utilizing *in situ* neutralization Boc based protocol, (iii) support for combinatorial synthesis based on easy labeling and physical separability of cotton substrate, and (iv) support for multisupport synthesis.

Results and Discussion

We have built a simple synthesizer in which the cotton carrier (functionalized thread, 0.2 $\mu\text{mol}/\text{cm}$) is placed inside the capillary tubing and the appropriate reagents are introduced by connecting the inlet with appropriate reagents. The speed of “pumping” the reagents is driven by the difference between the elevation of the inlet and outlet of the capillary tubing.

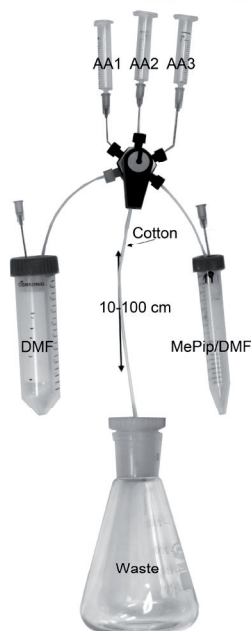


Figure 1. Scheme of the capillary cotton synthesizer.

A scheme of this synthesizer utilizing the six-way distribution valve is shown in Figure 1 and the synthesizer used for the syntheses described here was shown elsewhere in this proceedings [4]. To compare the performance of this “synthesizer” with the normal procedure, we have used the same amount of the modified cotton thread loaded into the polypropylene tubing (the best way to introduce the thread into the tube is the application of the vacuum) and into the polypropylene syringe. In the syringe we actually tested several different types of the cotton threads at the same time, since it is easy to separate the threads at the end based on their different lengths. We have used the Fmoc amino acids activated by DIC/HOBt in DMF. Coupling time was 1 hour and deprotection 20 min. The flow through the tubing had to be adjusted by elevation of the waste reservoir (end of the tubing) for each reagent so that the appropriate exposure time is achieved. Products were deprotected by 50% TFA and cleaved from the cotton threads (after separation into individual eppendorf vials) by 1M NaOH. HPLC analysis has shown that products (model sequences YGGFLG) were almost identical.

We have shown that Boc solid phase synthesis utilizing *in situ* neutralization is compatible with cotton substrate and provides high quality products. Combining with the fact that cotton by itself [5] acts as the self-association breaking agent, makes

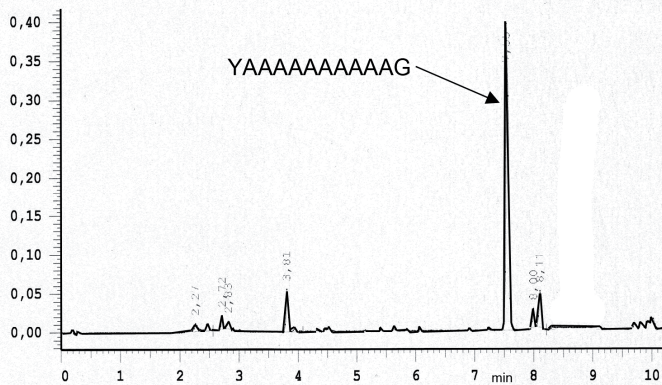


Figure 2. HPLC of crude product (Symmetry C18 4.6x75mm, 0-90% ACN/0.05%TFA in 10 min).

2x, 100% TFA 90 sec, wash DMF and 5% DIEA/DMF, coupling Boc-Ala/TCTU/HOBt/DIEA 5 min) and the sequence was assembled in 2 hours. The product was deprotected and cleaved from the support by 1M NaOH and HPLC trace is shown in Figure 2. The yield from 50 cm of thread was 6.6 mg.

Labeling of individual solid support particles can be easily based on the length of the cotton thread pieces, number and positions of knots, or their attachment to a secondary carrier. In addition, it is possible to synthesize peptides differing by the partial structure (alternative linkers, terminal modifications, etc.) in a mixture of classical resin with labeled cotton carriers, which are easily separable at the end of the synthesis. We have used this technique in the analysis of the synthetic problems of the sequence SFRNGVSGVKKTSFRRAKQ (neuropeptide S), which according to the prediction by Peptide Companion shows difficulties at position 9 and 10, and which by classical Fmoc synthesis results in a complex mixture. In repeated synthesis we added a labeled 10 cm piece of cotton string on which we have already assembled simple pentapeptide in couplings 6, 8, 10, 12, 14 and 16. These cotton pieces contained one to six knots and at the end of the synthesis were separated from the rest of the resin. Due to the different attachment to the solid carrier, the contamination of the threads by resin particles (Rink resin) did not interfere with alkaline cleavage of cotton peptides. In this way we obtained 10 to 20 mers and we could analyze whether the synthetic complication were caused by the carboxy or amino terminal sequence. We could conclude that the amino terminal sequence is not problematic and that the problem is caused (as predicted) by SGVK sequence.

References

- [1] Eichler, J.; Bienert, M.; Stierandova, A.; Lebl, M. *Peptide Res.* **1991**, *4*, 296-307.
- [2] Lebl, M.; Eichler, J. *Peptide Res.* **1989**, *2* (4), 297-300.
- [3] Rinnova, M.; Jezek, J.; Malon, P.; Lebl, M. *Peptide Res.* **1993**, *6* (2), 88-94.
- [4] Lebl, M., *Peptides 2012*, pp 22-23.
- [5] Lebl, M.; Stierandova, A.; Eichler, J.; Bienert, M. In *Peptides 90, Proc.21.EPS*, Giralt, E., Andreu, D., Eds.; ESCOM: Leiden, 1991; pp 153-155.

cotton a suitable carrier for synthesis of "difficult" sequences. As the first model sequence we used an easy peptide YGGFAG to test the behavior of cotton under conditions of the *in situ* neutralization. The favorable result prompted us to synthesize well known difficult sequence YAAAAAAAAAAG. We achieved 10 min cycle time (DMF wash

Simplifying native chemical ligation with an N-acylsulfonamide linker

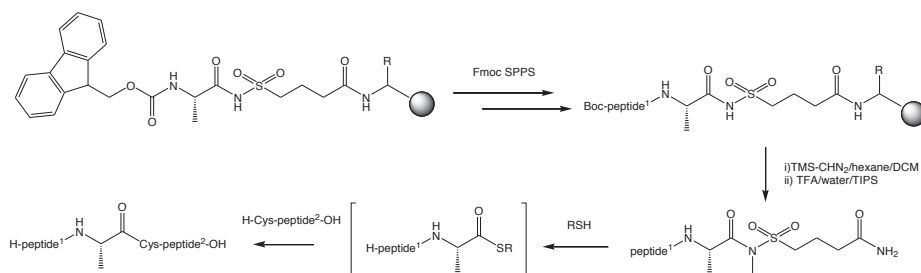
F. Burlina,^a C. Morris,^b R. Behrendt,^c P. White,^{*,d} J. Offer^{*,b}

^aUPMC Univ Paris 06, CNRS, ENS, 75005 Paris, France ; ^bMRC National Institute for Medical Research, London, NW7 1AA UK; ^cMerck & Cie, 8200 Schaffhausen, Switzerland;
^dMerck Chemicals, Beeston, Notts, NG9 2JR UK
e-mail: peter.white@merckgroup.com

Introduction

The use of native chemical ligation (NCL) has revolutionized the synthesis and semi-synthesis of small proteins.[1]. Key to the reaction is the exquisite selectivity of the reaction of C-terminal thioester of the N-fragment with the N-terminal cysteinyl thiol of the C-fragment. Whilst peptide thioesters are readily accessible by Boc SPPS, they cannot be made directly by Fmoc SPPS owing to the instability of thioesters to piperidine. Therefore, many ingenious indirect approaches have been developed to generate the required thioester peptide,[2-4] of which the sulfonamide method as described by Pessi and co-workers [5] remains the most frequently used. It involves displacement of the peptide fragment with a thiol from an alkylated peptidyl-sulfamylbutyryl resin. The sulfonamide method, whilst popular, has been plagued by notoriously low yields. These originate from incomplete acylation of the resin-bound sulfonamide with the C-terminal residue; incomplete alkylation of the sulfonamide; and incomplete thiolysis. We describe here the development of a novel dual linker strategy is described, involving anchoring of the sulfonamide linker to a standard acid-labile resin.[6] This approach overcomes the limitations of the sulfonamide method and provides a simple and robust strategy for Fmoc SPPS-based NCL (Figure 1).

Fig. 1: Dual linker strategy.



Results and discussion

The utility of our dual linker strategy was demonstrated in the preparation of BPTI, a 58 residue, small protein containing a full range of side chain functional groups. Its length is more typical of peptides used for NCL. The strategy of Lu and co-workers [7] was selected for the preparation of BPTI, involving the ligation of two fragments: BPTI (1-37) and BPTI (38-58).

BPTI (38-58) was assembled using a CS Bio 336 automated synthesizer by Fmoc SPPS using DIPCDI/HOBt activation. BPTI (1-37) was assembled in a similar manner on Fmoc-Gly-sulfamylbutyryl Sieber Amide resin. Methylation of the linker was effected by treatment with 2M TMS-CHN₂ in hexane/DCM (1:1) for 18 hours.

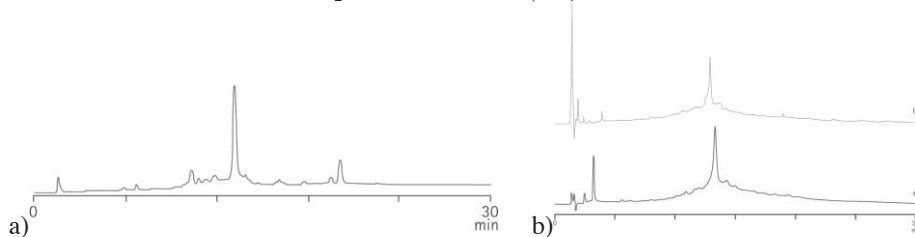


Fig. 2: HPLC profiles of a) N-BPTI (1-37)-sulfamylbutyramide & b) N-BPTI (1-37)-N-methylsulfamylbutyramide.

Following purification by RP-HPLC, the two fragments were ligated (Fig. 3) using low millimolar fragment concentration. N-BPTI (1-37)-N-methylsulfamylbutyramide (10 mg, 2 μ mol) and BPTI (38-58) (5.8 mg, 2 μ mol) were dissolved in 1 mL of degassed 0.2 M sodium phosphate buffer pH 7.5, containing 6 M guanidine·HCl, 2 mM EDTA, 50 mM TCEP, 60 mM MPAA. The solution was heated at 40 °C. The reaction was allowed to stir under Ar for 8 h. HPLC purification yielded linear BPTI (2.6 mg, 16% yield). The product was characterized by MALDI-TOF MS in positive linear mode using CHCA matrix: m/z = 6517.9 [M+H]⁺ (calc: 6517.6). Figure 3 shows the monitoring by HPLC of a preliminary sample scale ligation reaction. The reaction was almost complete in 8 h, a time comparable to that observed by Lu and co-workers [7] with classical NCL using a preformed thioester.

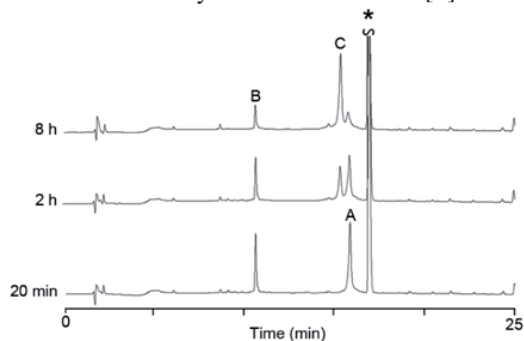


Fig. 3: HPLC profiles of monitoring of a preliminary ligation reaction. N-BPTI(1-37)-N-methylsulfamylbutyramide (A), BPTI(38-58) (B); BPTI(1-58) (C); *MPAA.

References

- [1] Kent, S. B. (2009) *Chem. Soc. Rev.* **2009**, 38, 338.
- [2] Kang, J., Macmillan, D. *Org. Biomol. Chem.* **2010**, 8, 1993.
- [3] Mende, F., Seitz, O. *Angew. Chem. Int. Ed.* **2011**, 50, 1232.
- [4] N. Ollivier, Dheur, J., Mhidia, R., Blanpain, A., Melnyk, O. *Org. Lett.* **2010**, 12, 5238.
- [5] Ingenito, R., Bianchi, E., Fattori, D., Pessi, A. *J. Am. Chem. Soc.* **1999**, 121, 11369.
- [6] Burlina, F., Morris, C., Behrendt, R., White, P., Offer, J. *Chem. Comm.*, **2012**, 48, 2579.
- [7] Lu, W., Starovasnik, M. A., Kent, S. B. H. *FEBS Lett.* **1998**, 429, 31.

Solid phase synthesis and biological evaluation of novel bifunctional opioid agonist – neurokinin-1 antagonist peptidomimetics

Karel Guillemyn¹, Isabelle Van den Eynde¹, Attila Keresztes², Eva Varga², Josephine Lai², Frank Porreca², Emeric Miclet³, Isabelle Correia³, Nga N. Chung⁵, Carole Lemieux⁵, Jozef Vanden Broeck⁴, Peter W. Schiller⁵, Dirk Tourwé¹, Steven Ballet¹

¹Department of Organic Chemistry, Vrije Universiteit Brussel, Brussels, Belgium;

²Department of Pharmacology, University of Arizona, Tucson AZ, U.S.A.; ³Laboratoire des Biomolécules, Université Pierre et Marie Curie, UMR 7613, Paris, France; ⁴Animal Physiology and Neurobiology Department, Katholieke Universiteit Leuven, Leuven, Belgium; ⁵Department of Chemical Biology and Peptide Research, Clinical Research Institute of Montreal, Montreal, Canada

E-mail: sballet@vub.ac.be

Introduction

We have developed and refined several methodologies to prepare amino-tetrahydro-azepinone derivatives as conformationally constrained aromatic residues. These were successfully used as central scaffolds for the preparation of ligands for different G protein-coupled receptors and their use as ‘privileged templates’ has been validated.¹ Herein, the 4-amino-1,2,4,5-tetrahydro-2-benzazepin-3-one (Aba) building block was used to develop new chimeric opioid agonist/neurokinin-1 antagonists. It has been shown that bifunctional peptides that combine these activities show enhanced antinociceptive potency in acute pain states and prevention of tolerance that is induced by chronic opioid intake has been illustrated.²

The high affinity μ/δ ligand tetrapeptide Dmt-D-Arg-Aba-Gly-NH₂ (**1**) was combined with the NK1 antagonist Ac-Aba-Gly-NMe-3',5'-Bn(CF₃)₂ (**2**) to obtain Dmt-D-Arg-Aba-Gly-NMe-3',5'-(CF₃)₂-Bn (**3**), a chimeric peptide mimetic with overlapping pharmacophores (Fig. 1).¹

Results and Discussion

In this study structure-activity relationships in **3** were derived by substitution or removal of several functional groups (Figure 1). The glycine moiety was substituted by a β -Ala residue. The trifluoromethyl groups were removed and the side chain charge of D-Arg was replaced by substitution with D-Cit. The role of the conformational constraint (Aba) was examined via a ring opening of Aba-Gly to Phe-Sar and the importance of the cis-trans equilibrium at the level of the C-terminal amide bond was evaluated by introduction of a *N*-*i*Bu substituent.

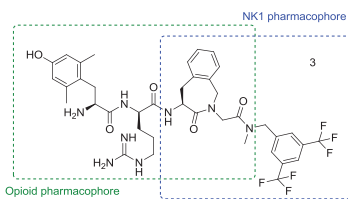


Fig. 1: Bifunctional ligand (**3**).

The solid-phase synthesis of the dual ligands was carried out on 2-Cl-trityl resin. After coupling of the first amino acid, a reductive amination was executed with Phth-*o*-formyl-Phe (**5**). Cyclisation with TBTU yielded the Aba-residue (**7**). Further standard SPPS protocols, cleavage from the resin, final coupling with the benzylamines in solution and full deprotection yielded the desired dual ligands.

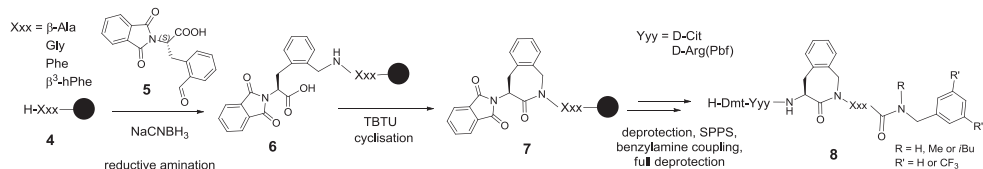


Fig. 2: Solid phase synthesis of the bifunctional opioid-NK1 ligands.

During the synthesis, problems were encountered in the reductive amination step. Using β-Ala as Xxx (Fig. 2), the synthesis went smoothly, but with Gly double reductive amination could not be avoided. Moreover, partial racemisation was observed when α-substituted amino acids were used. Alternatively, alkylation of the Xxx amino terminus with Phth-*o*-bromomethyl-Phe-OH was tried (not shown), but double alkylation could not be avoided. Although the solid phase method is a fast and easy method to obtain peptides which contain the Aba-β-Ala dipeptide constraint, optimisation is still needed using α-amino acids.

Introduction of the β-Ala residue yielded products with very good opioid affinity (K_i^{μ} : 0.08 nM, K_i^{δ} : 2.1 nM), but a decrease of binding at the NK1 receptor (K_i : 0.5 → 13 nM). The removal of the trifluoromethyl groups generally lowers the NK1R affinity (K_i : 0.5 → 1529 nM). Removal of the side chain charge of D-Arg does not affect opioid agonism, but NK1 affinity is greatly influenced (K_i : 13 → 3000 nM). By substitution of the *N*-Me group with *N*-*i*Bu, the binding to the NK1R drops (K_i : 13 → 308 nM). The Aba-constraint is essential for NK1 antagonism (K_i : 0.5 → 734 nM), while opioid agonism is maintained. Best overall results were obtained with the ligand Dmt-D-Arg-Aba-β-Ala-NMe-Bn: pA_2^{NK1} : 6.4 nM, K_i^{NK1} : 13 nM, K_i^{μ} : 0.08 nM and K_i^{δ} : 0.3 nM.

Hence, it was possible to synthesize new bifunctional peptides with subnanomolar opioid affinity and moderate nanomolar affinity for the NK1 receptor. Future efforts are focused on the recovery of the NK1R binding, while maintaining the opioid potency.

Acknowledgements

We thank the Fund for Scientific Research-Flanders (FWO), the Ministère du Développement Economique, de l'Innovation et de l'Exportation (MDEIE) du Québec and the Canadian Institutes of Health Research (CIHR, MOP-89716, to PWS) for the financial support.

References

- [1] Ballet, S.; Feytens, D.; Buysse, K.; Chung, N. N.; Lemieux, C.; Tumati, S.; Keresztes, A.; Van Duppen, J.; Lai, J.; Varga, E.; Porreca, F.; Schiller, P. W.; Broeck, J. V.; Tourwé, D. *J. Med. Chem.* **2011**, *54*, 2467 and references therein.
- [2] Largent-Milnes, T.M.; Yamamoto, T.; Nair, P.; Moulton, J.W.; Hruby, V.J.; Lai, J.; Porreca, F.; Vanderah, T.W. *Br. J. Pharmacol.* **2010**, *161*, 986.

A combined biological and theoretical study of prolyl peptides as inhibitors of angiotensin I converting enzyme

B. Yakimova, M. Rangelov, D. Petkova, B. Tchorbanov, I. Stoineva

Institute of Organic Chemistry with Centre of Phytochemistry - Bulgarian Academy of Sciences, 1113 Sofia, Bulgaria

E-mail: istoineva@yahoo.com

Introduction

The ectoenzyme - angiotensin I converting enzyme (ACE) is an integral part of the renin-angiotensin system, which is a critical regulator of blood pressure and fluid homeostasis. There are two identically significant isoforms of ACE in human tissue- somatic and testicular. Somatic ACE has two structurally homologous domains (N-and C-), while testicular ACE exists as a single domain glycoprotein identical to the C-domain of somatic ACE. Recent results show unexpected differences in substrate and inhibitory selectivity between the N-domain and C-domain of human, rat and mouse ACE. Knowing the role of each ACE domain is important for developing ACE domain specific inhibitors for the treatment of hypertension and for better understanding of the physiological consequences of ACE action. Many short peptide inhibitors isolated from milk, corn and fish protein sources, can be used as a novel alternative to synthetic antihypertensive drugs.

The aim of this study was to find a relationship between biological activity of short prolyl peptides as inhibitors of ACE and their binding to the active site by means of docking simulations.

Results and Discussion

H-Val-Pro-OH (VP), H-Val-Pro-Pro-OH (VPP) and H-Val-Pro-Pro-Pro-OH (VPPP) were synthesized by classical and solid phase peptide methods [1]. An original HPLC method was applied for ACE activity determination, and rabbit serum was used as enzyme source. The inhibitory potency of prolyl peptides were compared with the well known ACE inhibitors: Lisinopril and Fosinoprilat.

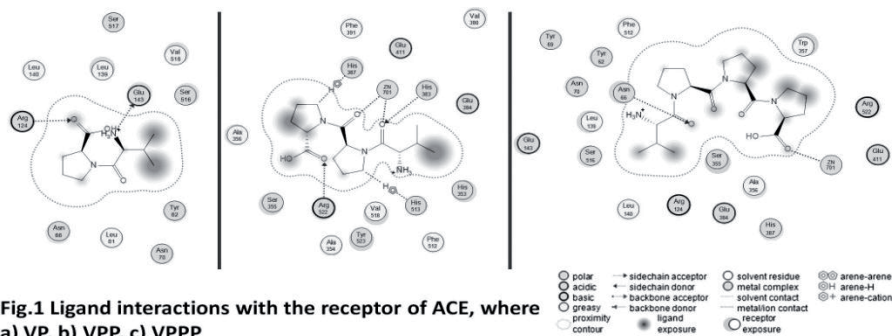
The IC_{50} and IC_{100} values were determined by non-linear regression analysis of enzyme activity/inhibitor concentrations curves using software package GraphPad Prism 5.0.

The highest inhibitory activity was manifested by VPP with IC_{50} about 9 μ M, followed by VPPP (IC_{50} -0.51 mM), and VP (IC_{50} -0.9 mM).

The docking simulation was performed with MOE2011 [2], "Induced Fit" protocol was used. The placement was performed by "triangle matcher" and retain poses were optimized and rescored by MMFF94x Force Field (FF). FF optimization was performed on the ligands and near residues of receptor. To select the best matches was used force field energy. For some of the visualizations we used VMD [3]. The interactions between the different ligands and the active site of ACE are shown on Fig. 1.

Comparing the results it can be seen that VPP has more electrostatic interactions than VP and VPPP. It is apparent that the tripeptide forms two bonds with the Zn^{2+} anion, which is

the one of the strongest interactions. VPP is involved in two hydrogen bonds with His³⁸³ and Arg⁵²², the same as VP (Glu¹⁴³ and Arg¹²⁴), while in VPPP hydrogen bond is only one-with Asn⁶⁶. VPP is also forming 2 π hydrogen bonds with His³⁸⁷ and His⁵¹³. In all of the cases the peptide is oriented with the most lipophilic parts toward the solvent (H₂O).



The different type of interactions between the most active tripeptide and the active site of ACE are presented on Fig. 2 by equipotential sections (-2 and 2 kcal/mol).

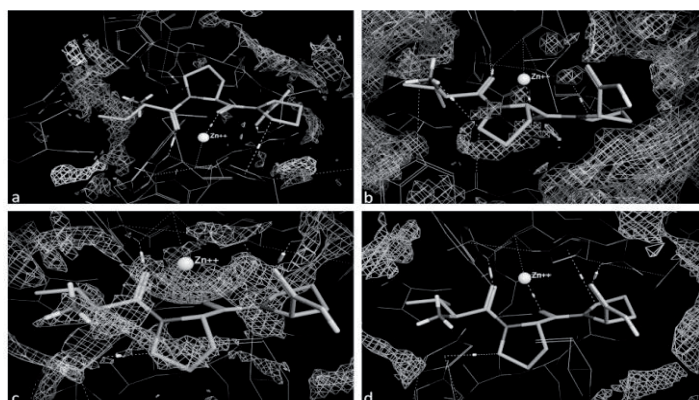


Fig. 2 Interactions between VPP and active site of ACE, where a) are the electrostatic interactions, b) interactions between the ligand and the receptor in the terms of ΔG ; c) solvent accessible parts of the structure and d) hydrophobic interactions.

The observed best inhibitory potency of VPP is in agreement with the results obtained by the docking simulation. This tripeptide binds to the enzyme active site in the most effective way due to hydrophobic, electrostatic and p hydrogen interactions.

References

- [1] Naydenova E., Bratovanova E., Marinova M., Stoineva I. and Tchormanov B., *J Pept. Sci.*, **2007**, 676-677.
- [2] Molecular Operating Environment (MOE), **2011.10**; *Chemical Computing Group Inc.*, 1010 Sherbooke St. West, Suite #910, Montreal, QC, Canada, H3A 2R7, 2011.
- [3] Humphrey, W., Dalke, A. and Schulten, K., "*VMD - Visual Molecular Dynamics*", *J. Molec. Graphics*, **1996**, vol. 14, pp. 33-38.

A platform technology for the emergency response to outbreaks of novel enveloped viruses

Antonello Pessi,¹ Annunziata Langella,² Elena Capitò,³ Silvia Ghezzi,⁴ Elisa Vicenzi,⁴ Guido Poli,⁴ Thomas Ketas,⁵ Cyrille Mathieu,⁶ Branka Horvat,⁶ Anne Moscona,⁵ Matteo Porotto⁵

¹*PeptiPharma, Pomezia (RM) Italy;* ²*Merck Serono, Guidonia (RM) Italy;* ³*BASF Italia, Pontecchio Marconi (BO) Italy;* ⁴*San Raffaele Scientific Institute, Milano, Italy;* ⁵*Weill Medical College of Cornell University, New York, NY;* ⁶*INSERM U758 Ecole Normale Supérieure de Lyon, France*

E-mail: a.pessi@peptipharma.it; map2028@med.cornell.edu

Introduction

Over the past decade, the global effort to meet the challenge of emerging viral pathogens has resulted in a greatly enhanced ability to identify and genetically fingerprint causative agents, often with extraordinary speed. However, our ability to quickly acquire genetic information on the causative agents of infectious diseases is not matched by our ability to develop suitable treatments. Genetic information does not readily translate into new therapies, since drug discovery typically requires information beyond simple knowledge of the viral genome.

We propose here that for enveloped viruses, a major class of emerging pathogens, a platform technology is available that would enable preparation and shelving of specific inhibitors designed on the basis of genetic information only.

Results and Discussion

Fusion between the viral and cell membranes is an obligatory step for all enveloped viruses. Viral fusion is driven by proteins which, although specific to each virus, act through a common mechanism: formation of a complex between two heptad repeat (HR) regions. HR-derived peptides can block this process, and fusion inhibitors (FI) represent a clinically validated therapeutic strategy. The characteristic sequence pattern of HR enables their identification directly from genomic information, providing an opportunity for a rapid therapeutic response to emerging viral pathogens, as shown in the recent SARS outbreak, where FI were developed before the fusion protein structure became available.

However, the potency of HR-derived peptides differs considerably among viruses, and for weak inhibitors it must be increased by peptide engineering strategies – a time-consuming process which negates emergency use. We propose a different approach, which increases antiviral activity without changing the native HR sequence.

Our technology consists in derivatizing the FI with a cholesterol group (“cholesterol-tagging”). Cholesterol drives FI enrichment in the lipid raft compartment of the membrane, where viral fusion occurs, thus dramatically increasing its antiviral potency, as shown so far for HIV [1], influenza virus [2], parainfluenza virus (HPIV) [3], and the emerging Nipah virus (NiV), fatal in humans[3-4]. An additional advantage of cholesterol tagging is that it

prolongs the half-life of the peptide in vivo [1, 4], endowing the peptide with pharmacokinetic properties compatible with a once-daily self-injectable therapeutic.

In a further development of this strategy, we have combined cholesterol-tagging with dimerization [5]. Dimerization works by reducing the k_{off} of the inhibitor-fusion protein complex formation, while cholesterol tagging facilitates the encounter of the peptide with the viral target protein, increasing the k_{on} for complex formation. Accordingly, we have shown that cholesterol-tagged dimeric FI are highly efficacious in preventing or curtailing HPIV, NiV, and HIV replication in vitro and in vivo [5].

An outline of a rapid-response strategy to an outbreak of a viral pathogen is shown in Figure 1. Notably, this process could be activated in anticipation, rather than as a consequence, of a viral outbreak, with stockpiling of a defined number of doses.

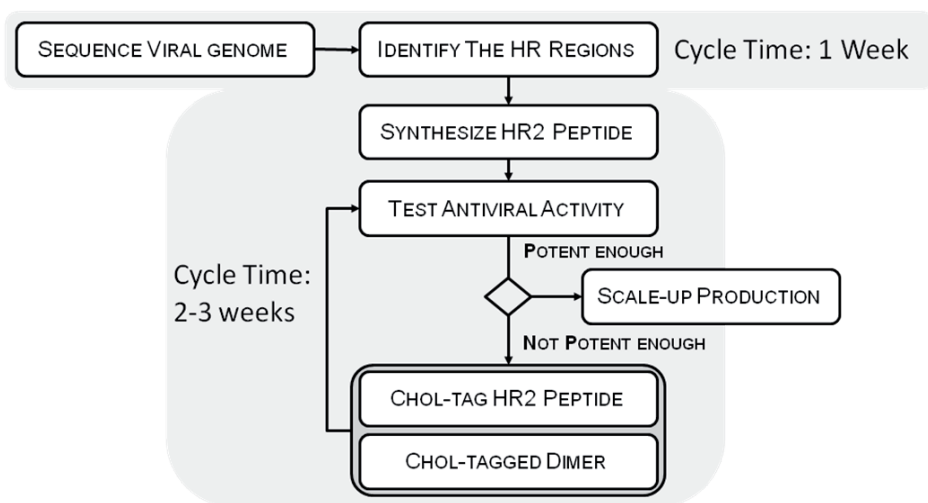


Figure 1. Outline of a rapid-response strategy to outbreaks of emerging viral pathogens, based on cholesterol-tagging of peptides derived from the pathogen fusion protein.

A ready-to-use first-generation therapeutic may be subsequently substituted by second-generation molecules, either of similar nature, e.g. sequence-optimized cholesterol-tagged FI, or resulting from antibody libraries or small-molecule medicinal chemistry efforts.

We are currently probing the scope of our strategy by pursuing cholesterol-tagged inhibitors for a variety of enveloped viruses.

References

- [1] Ingallinella, P.; Bianchi, E.; Ladwa, N. A.; Wang, Y.-J.; Hrin, R.; Veneziano, M.; Bonelli, F.; Ketas, T. J.; Moore, J. P.; Miller, M. D.; Pessi, A., Proc. Natl. Acad. Sci. U.S.A. 2009, 106, 5801.
- [2] Lee, K. K.; Pessi, A.; Gui, L.; Santoprete, A.; Talekar, A.; Moscona, A.; Porotto, M., J. Biol. Chem. 2011, 286, 42141.
- [3] Porotto, M.; Yokoyama, C. C.; Palermo, L. M.; Mungall, B.; Aljofan, M.; Cortese, R.; Pessi, A.; Moscona, A., J. Virol. 2010, 84, 6760.
- [4] Porotto, M.; Rockx, B.; Yokoyama, C. C.; Talekar, A.; DeVito, I.; Palermo, L. M.; Liu, J.; Cortese, R.; Lu, M.; Feldmann, H.; Pessi, A.; Moscona, A., PLoS Pathog. 2010, 6, e1001168.
- [5] Pessi, A.; Langella, A.; Capitò, E.; Ghezzi, S.; Vicenzi, E.; Poli, G.; Ketas, T.; Mathieu, C.; Cortese, R.; Horvat, B.; Moscona, A.; Porotto, M., PLoS One 2012, 7, e36833.

A stable gonadotropin releasing hormone analogue for the treatment of endocrine disorders and prostate cancer

**T. Katsila¹, E. Balafas², G. Liapakis³, P. Limonta⁴, M. M. Marelli⁴,
K. Gkountelias³, T. Tselios⁵, N. Kostomitsopoulos²,
J. Matsoukas⁵, C. Tamvakopoulos¹**

¹Division of Pharmacology-Pharmacotechnology, BRFAA, Athens, Greece; ²Center for Experimental Surgery, BRFAA, Athens, Greece; ³Department of Pharmacology, University of Crete, Crete, Greece; ⁴Department of Endocrinology, Physiopathology and Applied Biology, Università degli Studi di Milano, Milano, Italy; ⁵Department of Chemistry, University of Patras, Patras, Greece

E-mail: imats@upatras.gr

Introduction

Gonadotropin-releasing hormone (GnRH) receptor agonists have wide clinical applications (prostate cancer, endocrine disorders) on the basis of their superiority, when compared to the native hormone (GnRH) in terms of potency (high receptor affinity) and improved proteolytic stability. However, GnRH analogues are still susceptible to the action of proteolytic enzymes and have limited absorption and low bioavailability. As a consequence, these peptides are administered intramuscularly or subcutaneously and as depot formulations compromising efficacy (being dependent on patient compliance). Therefore, the development of novel peptide analogues with enhanced *in vivo* stability could potentially provide therapeutic alternatives.

Taking into account the importance of hormonal therapy for the treatment of prostate cancer and endocrine disorders as well as the current needs for improved therapeutic approaches, we focused on efforts to discover pharmacokinetically superior and possibly equipotent novel GnRH peptide analogues. Although superagonists have well-established clinical benefits, it is true that their *in vivo* stability remains a limiting factor that most likely prevents them from exerting any direct effects on tumors (extrapituitary) or causing rapid desensitization of the GnRH-I receptor. Herein, we report our findings regarding analogue 1, [Des- Gly10,Tyr5(OMe),D-Leu6,Aze-NHEt9]GnRH, a molecule with the conformational features required for agonistic activity and enhanced *in vitro* and *in vivo* stability compared with leuprolide.

Results and Discussion

In vitro (kidney mouse membranes) and *in vivo* (clinically relevant pharmacokinetic mouse model) bioassays were coupled to liquid chromatography-tandem mass spectrometry. Analogue 1, an agonist of the GnRH-I receptor with a binding affinity in the nanomolar range, caused testosterone release in mice that was acutely dose-dependent, an effect blocked by cetrorelix.

Repeated dosing studies in mice demonstrated that analogue 1 was well tolerated and had potency similar to that of leuprolide, based on plasma and testis testosterone reduction and histopathological findings.

Analogue 1 also shared with leuprolide similar significant antiproliferative activity on androgen-dependent prostate cancer (LNCaP) cells.

Although analogue 1 has reduced binding affinity on the GnRH-I receptor compared with leuprolide, repeated dosing studies in mice demonstrated that analogue 1 was well tolerated and had potency similar to that of leuprolide. Analogue 1 was also endowed with significant anti-proliferative activity on prostate cancer cells (LNCaP), similar to that exerted by leuprolide (drug in the clinic). On the basis of its pharmacokinetic advantages, it is likely that the peptide analogue in question or analogues based on this new design will be therapeutically advantageous for the treatment of endocrine disorders or prostate cancer. Such pharmacokinetic advantages can be particularly valuable with respect to local/direct extrapituitary effects that will be essential for more effective treatment of cancer.

References

- [1] Katsila, T.; Balafas, E.; Liapakis, G.; Limonta, P.; Montagnani-Marelli, M.; Gkountelias, K.; Tselios, T.; Kostomitsopoulos, N.; Matsoukas, J.; Tamvakopoulos, C. *J Pharmacol Exp Ther.* **2011**, 336, 613

Anti-peptide antibodies to synthetic fragments of alpha7-subunit acetylcholine receptor or prion protein protect cells against beta-amyloid toxicity

**A.V. Kamynina¹, K.M. Holmstrom², D.O. Koroev¹, O.M. Volpina¹,
A.Y. Abramov²**

¹*Shemyakin-Ovchinnikov Institute of Bioorganic Chemistry, Russian Academy of Science, Moscow, Miklukho-Maklaya street, 16/10, 117997, Russia;* ²*Department of Molecular Neuroscience, UCL Institute of Neurology, Queen Square, London WC1N 3BG, UK*

E-mail: anes.kamynina@gmail.com

Introduction

One of the hypotheses of Alzheimer's disease neuropathology involves beta-amyloid (A β) binding with proteins on neuronal cell surface which leads to cell lysis and amyloid plaque formation. According to the latest data α 7-type of the nicotinic acetylcholine receptor (AChR) and the prion protein can be the target for beta-amyloid toxicity [1,2]. Aggregated A β causes many pathological changes in cultures of mixed neurons and astrocytes such as sporadic cytoplasmic intracellular Ca²⁺-signal, activation of reactive oxygen species (ROS) production and cell death. We suggested that specific antibodies to fragment 173-193 of α 7-subunit of the AChR (AChRabs) or to fragment 95-123 of the prion protein (PrPabs) would protect cells from β A induced cell death via modulation of either Ca²⁺-signal or ROS production.

Results and Discussion

We examined the effect of a 24 hr exposure of hippocampal cultures of neurons and astrocytes to A β 25–35 on cell viability and found that, remarkably, 30.2 \pm 2.1% of cells died during this period. 20 min pre-incubation of primary co-culture with 20 μ g/ml of either AchRabs or PrPabs significantly reduced cell death of hippocampal neurons and astrocytes to 15.75 \pm 1.53% and 18.6 \pm 1.5% dead cells respectively, $p < 0.05$).

Application of the A β peptide fragment 25-35 to rat cortical neurons and astrocytes in co-culture causes sporadic increases in intracellular calcium ([Ca²⁺]_i) in astrocytes but not in neurons [3]. We therefore investigated whether either AchRabs or PrPabs can modify the A β -induced calcium signal. In agreement with our the previous publications A β 25-35 induced dramatic [Ca²⁺]_i signals in astrocytes. However, 1 hour pre-incubation of the co-culture of cortical neurons and astrocytes with AchRabs or PrPabs (20 μ g/ml) did not alter the ability of A β 25-35 induce calcium signal in astrocytes. Thus, incubation of the neurons and astrocytes with either AchRabs or PrPabs did not alter effect of A β 25-35 on [Ca²⁺]_i.

One of the most profound effects of A β on brain cells is the action of the peptide on production of ROS. We have found that application of A β 25-35 fragment (50 μ M) significantly enhanced the rate of ROS production in hippocampal astrocytes. Pre-incubation of neurons and astrocytes with 20 μ M inhibitor of NADPH oxidase, AEBSF, almost completely blocked the effect of A β on ROS production, suggesting that most of the

A β -induced free radicals are generated by the NADPH oxidase. Interestingly, pre-incubation of cortical co-culture of neurons and astrocytes for 20 min with 20 μ g/ml either AchRabs or PrPabs also reduced the rate of A β -induced ROS production. This would suggest that application of the antibodies to AChR or to the prion protein modulates activity of the NADPH oxidase in astrocytes. This effect cannot be explained solely by the induction of a calcium signal because the antibodies did not change A β -induced calcium signal.

To investigate the mechanism of action of the antibodies to AChR α 7-type on NADPH oxidase, we stimulated the cortical astrocytes with an activator of NOX2 (1mg/ml phorbol 12-myristate 13-acetate, PMA) which induced a 8 -fold increase in the rate of HET fluorescence in the cells. This effect was significantly blocked in the presence of the inhibitor of NADPH oxidase AEBSF (20 μ M). PMA-induced ROS production in astrocytes was also partially inhibited by AchRabs. Thus, pre-incubation of the primary co-cultures with the antibodies affected NADPH oxidase activation. Pre-incubation of the cells with acetylcholine (Ach) significantly reduced ROS production by NADPH oxidase in cortical astrocytes. Furthermore, the inhibitor of α 7 nAChRs α -bungarotoxin inhibited the effect of PMA on ROS production which suggests a role for AChR α 7-type in activation of the NADPH oxidase.

A β can trigger the cell death cascade by activation of caspase 3. To investigate the effect of antibodies on A β -induced caspase 3 activation we used NucView 488 caspase 3 substrate which allows the visualization of the activation of this enzyme in real time. Application of A β 25-35 induced a rapid activation of caspase 3 in neurons and astrocytes. Pre-incubation of the cells with either AchRabs or PrPabs significantly reduced the rate of caspase 3 activation and the number of cells with activated caspase 3. Importantly, α -bungarotoxin, which is toxic by itself, protected cells significantly against A β -induced caspase 3 activation.

The observed positive effect of antibodies to α 7-type AchR or to the prion protein gives an additional explanation regarding the involvement of these proteins in AD pathology and provides new approach into an anti-AD vaccine design.

Acknowledgments

Supported by RAS program FSN-2012 and RFBR grant 10-04-01256.

References

- [1] Wang, H.Y., Lee, D.H., D'Andrea, M.R., Peterson, P.A., Shank, R.P., Reitz, A.B. *Biol. Chem.* **2000**, 275, 5626-5632.
- [2] Lauren, J., Gimbel, D.A., Nygaard, H.B., Gilbert, J.W., Strittmatter, S.M. *Nature*. **2009**, 457, 1128-1134.
- [3] Ionov, M., Burchell, V., Klajnert, B., Bryszewska, M., Abramov, A.Y. *Neurosci.* **2011**, 180, 229-237.

Autoantibodies to N-glycosylated peptide sequons in Rett syndrome: The first insight to disclose an autoimmune mechanism

F. Nuti,^{a,b} F. Real-Fernandez,^{a,b,c} G. Rossi,^{a,d} S. Pandey,^{a,b} G. Sabatino,^{a,b} C. Tiberi,^{a,b} M. Larregola,^{a,e} S. Lavielle,^f J. Hayek,^g C. De Felice,^h P. Rovero,^{a,c,d} A. M. Papini^{a,b,c,e}

^aLaboratory of Peptide & Protein Chemistry & Biology - PeptLab - www.peptlab.eu;

^bDepartment of Chemistry "Ugo Schiff", Via della Lastruccia 3/13, Polo Scientifico e Tecnologico, University of Florence, I-50019 Sesto Fiorentino, Italy; ^cToscana Biomarkers S.r.l. Via Fiorentina, I-53100 Siena; Italy; ^dDepartment of Pharmaceutical Sciences, Via Ugo Schiff 6, Polo Scientifico e Tecnologico, University of Florence, I-50019 Sesto Fiorentino, Italy; ^eSOSCO-EA4505, University of Cergy-Pontoise, F-95031, France; ^fLaboratory of BioMolecules, Université Pierre et Marie Curie-CNRS-ENS, F-75005 Paris, France; ^gChild Neuropsychiatry Unit, University Hospital AOUS of Siena, Siena, Italy; ^h Neonatal Intensive Care Unit, University Hospital AOUS of Siena, Siena, Italy

nuti.francesca@gmail.com

Introduction

Rett syndrome (RTT) is a relatively rare clinical form of autistic pervasive disorders affecting almost exclusively females, with a frequency of about 1:10,000 worldwide. RTT is specifically characterized by loss of acquired purposeful hand skills, loss of acquired spoken language, gait dyspraxia and stereotypic hand movements. RTT natural history progresses throughout 4 clinical stages: neurological regression (stage I); autistic-like (stage II); pseudo stationary (stage III); the "wheelchair" phase (stage IV). Besides the typical cases (*ca.* 76%) at least 3 major Variants are recognized: early seizure (ESV), preserved speech (PSV), and congenital (CV). Up to 95% of typical RTT cases are caused by mutations in the methyl-CpG binding protein 2 (MeCP2) [1], a gene located in the Xq28 region of the human genome that encodes a protein whose full list of functions still remains unknown. Up to now the pathogenetic mechanism leading from gene mutation to disease expression remains to be clarified. However, RTT may be a multifactorial disorder triggered by different factors acting on a genetically programmed substrate. Few immunological studies have been reported in the literature on RTT, highlighting a possible pathogenetic role of immunological dysregulation. Nevertheless, elevated neopterin concentration in urines (usually occurring in autoimmune disorders), the presence of antineuronal antibodies in serum or cerebrospinal fluid (CSF), and the dysfunction of microglia (small glial cells that participate in brain's immune response) have been described. Microglia have also the role to clean up normal cellular debris in brain by phagocytosis. Recently Kipnis [2] discovered that when microglia lack properly functioning of MeCP2, they are unable to perform this crucial duty efficiently. Therefore derangement of microglia immune responsiveness might be likely to occur in RTT patients, as both neuro-inflammation and phagocytosis are powerful modulators of the CNS immune system.

RTT has recently been proposed as a model of Multiple Sclerosis (MS), a severe neurological progressive disease. In fact, in Rett mouse models Glatiramer acetate, an immunomodulator with proven safety and efficacy in MS, induced elevation of brain BDNF levels [3].

To explore the hypothesis of a devastating CNS immune dysregulation that up to now is fatal for most of Rett children, we took advantage of our previous experience in identifying autoantibodies as biomarkers of disease activity in MS. In fact, aberrant glycosylation of CNS antigens could be a common feature to neoantigens produced in inflammatory conditions arising either as a consequence of neuronal disruption or a variety of environmental events such as bacterial and/or viral exposure. The idea is to identify pathogenic antibodies in RTT as in MS by specific probes i.e., short β -hairpin peptide sequences, containing the N-glycosylated moiety Asn(Glc) [4].

Results and Discussion

Aberrant modifications of proteins components of organs or tissues target of immune-mediated diseases can contribute to create neo-antigens, producing autoantibodies to the neoepitopes. Autoantibodies can be important biomarkers of disease activity but they are often characterised by a low binding affinity affecting their reliable identification. This is possibly because of the lower molecular weight of the epitope compared to the protein antigen. To explore the potentiality of the multivalent interaction to increase the binding affinity, the Multivalent Asn(Glc)-Epitope (MEp), CT35 [5], was designed and synthesized. The new Mep CT35 was tested in SP-ELISA on sera of 183 RTT patients and compared to 72 autistic children as controls.

CT35 is able to detect specific IgM Abs in a statistically significant number of RTT patients' sera, but only in very few cases IgG Abs. The Rett patients developing IgGs Abs are in the group of the rare survivors (age 5-30, 12/187).

This is the first time that anti-N-glycosylated peptide antibodies have been discovered in children affected by Rett Syndrome with MECP2 gene mutation and not in Autistic children with no MECP2 gene mutation. The new selected N-glycosylated multivalent peptide-based immunoassay can offer interesting future applications as important prognostic tool for monitoring Rett syndrome and guiding a possible therapeutic treatment, up to now undiscovered for this devastating rare disease.

Acknowledgments

We thank for the financial support by Ente Cassa di Risparmio di Firenze and the ANR Chaire d'Excellence 2009-2013 PepKit (France) to AMP.

References

- [1] Amir R.E., et al. *Nat. Genet.* **1999**, 23, 185–188.
- [2] Kipnis J., Nature 484, 105–109. *Nature* (05 April 2012).
- [3] Ben-Zeev B., et al., *Medical Hypotheses* **2011**, 76, 190–193.
- [4] Lolli, F. et al., *Proc. Natl. Acad. Sci.* **2005**, 102, 10273–10278; Lolli F., et al. *J. Neuroimmunol.* **2005**, 167(1-2), 131–137, Papini A.M., *J. Pept. Sci.* **2009**, 15 621–628.
- [5] Hayek J., et al. Italian Patent n FI2012A000107.

Synthesis and formulation design of PEGylated vasoactive intestinal peptide derivative with high metabolic stability

Satomi Onoue^{a*}, Masashi Kato^a, Takuya Matsui^a, Takahiro Mizumoto^b, Baosheng Liu^c, Liang Liu^c, Shizuo Yamada^a

^a*School of Pharmaceutical Sciences, University of Shizuoka, 52-1 Yada, Suruga-ku, Shizuoka 422-8526, Japan;* ^b*ILS Inc., 1-2-1, Kubogaoka, Moriya, Ibaraki 302-0104, Japan;* ^c*American Peptide Company, 777 East Evelyn Ave. Sunnyvale, CA, 94086, U.S.A.*

E-mail: onoue@u-shizuoka-ken.ac.jp

Introduction

Vasoactive intestinal peptide (VIP) acts as the major peptide transmitters in the central and peripheral nervous systems [1]. Although VIP has been thought to be promising drug candidates for airway inflammatory diseases, the therapeutic potential of VIP is highly limited because of rapid metabolic degradation and systemic side effects. Previously, our group developed a VIP derivative, [Arg^{15,20,21}, Leu¹⁷]-VIP-GRR (IK312532), with improved metabolic stability [2], and respirable powder (RP) formulation of IK312532 (IK312532-RP) for pulmonary administration [1]. These attempts successfully led to enhanced efficacy of IK312532 in the airway system and reduced systemic exposure; however, further chemical modification of IK312532 with a focus on metabolic stability might provide better clinical outcome of inhalation therapy [3,4]. Currently, covalent adduction of therapeutic peptides/proteins with poly(ethylene glycol) (PEG) has become a widely used drug delivery approach, the major purposes of which are to prolong half-life and to reduce immunogenicity. Conjugation of VIP and its derivatives with PEG might be a viable option for enhanced metabolic stability, thereby prolonging the duration of action; however, far less is known about the feasibility and pharmacological outcomes of new PEGylated VIP derivatives. The major purposes of the present study were (i) to design a new VIP derivative through conjugation of IK312532 with PEG with a molecular weight of 5,000 Da (P5K), and (ii) to apply it to the RP system for treatment of airway inflammation.

Results and Discussion

In the present study, Cys-coupled IK312532, [Arg^{15,20,21}, Leu¹⁷]-VIP-GRRC, was chemically synthesized with a yield of 6%, and selective PEGylation (5,000 Da) at the thiol group of Cys was achieved using PEG-maleimide. Thus, IK312532/P5K, a PEGylated VIP derivative, was successfully obtained with a peptide purity of 99.4%, and the overall yield of IK312532/P5K was ca. 3%. To elucidate the possible influence of PEGylation on the secondary structure, the secondary structures of IK312532 and IK312532/P5K in 50% MeOH/20 mM Tris-HCl (pH7.4) were evaluated by CD spectral analysis. Both VIP derivatives exhibited typical spectral patterns for an α -helical structure, showing a positive band at <200 nm and two intense negative bands at 209 nm and 222 nm. IK312532 and IK312532/P5K were estimated to contain ca. 60% and 52% α -helical structure, respectively, suggesting that PEGylation at the C-terminus would not affect the secondary structure of IK312532. Receptor-binding activity of IK312532/P5K was also assessed using L2 cells

expressing VPAC2 receptor, and both VIP derivatives could compete with [¹²⁵I]VIP in a concentration-dependent manner, and their inhibitory effects (IC₅₀ value) were calculated to be 2.8±0.9×10⁻⁹ (IK312532) and 81.7±29.6×10⁻⁹ (IK312532/P5K) M. There appeared to be ca. 30-fold reduction in the receptor-binding affinity of IK312532 after PEGylation at the C-terminus, although the secondary structure did not vary. The PEGylated molecules intermolecularly block the attachment of neighboring molecules, causing an apparent reduction of association rate, although the PEGylated molecules might eventually bind to the receptor. To clarify the stabilizing effect of conjugated PEG against enzymatic degradation, IK312532 and IK312532/P5K were incubated in bronchoalveolar lavage fluid (BALF) for 2.0 h at 37°C and subjected to RP-HPLC analysis. The kinetic degradation constants were calculated to be 0.42±0.05 h⁻¹ for IK312532 and 0.16±0.01 h⁻¹ for IK312532/P5K. Thus, the metabolic stability of IK312532 was found to be 2.6-fold improved by the PEGylation approach, and enhanced metabolic stability could provide prolonged duration of action.

For the *in vivo* studies, IK312532/P5K-RP, an inhalable formulation of IK312532/P5K, was firstly prepared with a jet-milling system since the RP formulation would offer direct targeting of airway systems with rapid onset and reduced adverse effects [5,6]. Based on laser diffraction and cascade impactor analyses, the IK312532/P5K-RP exhibited high dispersibility and inhalation performance. To elucidate the therapeutic potential of the IK312532/P5K-RP, anti-inflammatory effects of insufflated IK312532/P5K-RP in the lung were assessed using a rat model of acute airway inflammation. Antigen challenge led to marked increase of granulocytes in the bronchial epithelium and interstitium, followed by epithelial hyperplasia. In addition to the lung tissue, the insufflated antigen caused marked recruitment of inflammatory cells in BALF as evidenced by 8.4-fold increase of total cell numbers, mainly consisting of monocytes and neutrophils. On the contrary, these antigen-evoked airway inflammatory events were significantly attenuated by pretreatment with IK312532/P5K (150 µg of IK312532/P5K). In the lung tissue, there were no significant differences in the numbers of recruited granulocytes between control and antigen-exposed rats with IK312532/P5K-RP treatment, and antigen-stimulated epithelial hyperplasia was also attenuated by ca. 61%. At 24 h after the last antigen challenge, treatment of antigen-exposed rats with IK312532/P5K-RP led to significant reduction of inflammatory cells in BALF by 78% for total cells, 86% for macrophages, and 78% for neutrophils. Neutrophilia-related biomarkers, such as myeloperoxidase and lactate dehydrogenase, in pulmonary tissues were also indicative of the potent immune-modulating effects of IK312532/P5K-RP. From these findings, with the aid of the RP formulation approach, the C-terminally PEGylated IK312532 might be a promising agent for treatment of airway inflammatory diseases.

References

1. Onoue, S.; Yamada, S.; Yajima, T. *Peptides* **2007**, *28*, 1640.
2. Onoue, S.; Misaka, S.; Yamada, S. *Naunyn Schmiedebergs Arch. Pharmacol.* **2008**, *377*, 579.
3. Onoue, S.; Matsui, T.; Kuriyama, K.; Ogawa, K.; Kojo, Y.; Mizumoto, T.; Karaki, S.; Kuwahara, A.; Yamada, S. *Peptides* **2012**, *35*, 182.
4. Onoue, S.; Misaka, S.; Ohmori, Y.; Sato, H.; Mizumoto, T.; Hirose, M.; Iwasa, S.; Yajima, T.; Yamada, S. *Eur. J. Pharm. Biopharm.* **2009**, *73*, 95.
5. Onoue, S.; Misaka, S.; Kawabata, Y.; Yamada, S. *Expert Opin. Drug Deliv.* **2009**, *6*, 793.
6. Onoue, S.; Hashimoto, N.; Yamada, S. *Expert Opin. Ther. Patents.* **2008**, *18*, 429.

Design and synthesis of potent linear and cyclic Dirucotide analogues

Kyriaki Mavridaki¹, Georgios Deraos^{1,3}, Spyros Deraos¹, Pigi Katsougraki¹, Panagiotis Plotas^{2,3}, Theodore Tselios¹, Athanasia Mouzaki², John Matsoukas^{1,3}

¹*Department of Chemistry, University of Patras, Patras, Greece;* ²*School of Medicine, University of Patras, Greece;* ³*Eldrug S.A., Pharmaceutical Company, GR-26504, Platani, Patras, Greece*

Introduction

Multiple sclerosis (MS) is a CD4⁺ T cell mediated chronic inflammatory disease of the central nervous system (CNS) characterized by discrete areas of inflammation followed by demyelination and paralysis. Myelin basic protein (MBP) is one of the major autoantigens defined in MS, with encephalitogenic T cell epitopes a major one being MBP₈₇₋₉₉. One approach, involves the design and use of cyclic peptide analogs of disease-associated myelin epitopes to modify T-cell responses. Mutated peptides (altered peptide ligand, APL), with amino acid mutations at TCR contact residues, to alter immune responses from Th1 dominant to Th2 dominant, is a novel approach to the immunotherapy of autoimmune diseases such as MS. Dirucotide, was used for the treatment of MS. Administration of this APL was suspended and stopped approximately midway during phase II study because of a systemic hypersensitivity-type reaction in several MS. A new approach is the introduction of rationally designed cyclic peptides, or a non-peptide-mimetic drug molecule resembling in the pharmacophore groups that NMR studies and molecular modeling results in a study with the receptor complex. Both are more resistant to proteolytic enzymes. Moreover, the cyclic molecules are able to be administrated orally due to increased bioavailability, resulting in a better pharmacological profile. These results and of ours overwhelmingly justify our studies with cyclic MBP analogues. The design and synthesis of mutated peptide analogs, APL (antagonists), from self-antigens of the myelin sheath constitute promising approaches for the treatment of MS. In this study two analogues linear and Cyclic MBP₈₂₋₉₈(Ala⁹¹) were synthesized in order to study their effect in MS patient's peripheral blood cells, towards new therapeutic agents in MS.

Results and Discussion

In this study we design and synthesized a linear and cyclic analogue of Dirucotide analogue 82-98 sequence of the Myelin Basic Protein. The peptides were synthesized in solid phase, using 2-chlorotrityl-chloride resin and Fmoc protected amino acids by Fmoc/tBu methodology. Cyclization was achieved using O-benzotriazol-1-yl-N,N',N'-tetramethyluronium tetrafluoroborate (TBTU) and 1-hydroxy-7-azabenzotriazole, 2,4,6 collidine allowing fast reaction and high yield cyclization product. Results indicate that HOAt, a 4-nitrogen containing variant, is a very effective coupling additive, more efficient than HOBt for solution or solid phase synthesis. The cyclization reaction was monitored using the ninhydrin test and analytical HPLC. The reaction mixture was resolved by thin layer chromatography using a n-butanol/acetic acid/water (4/1/1) solvent system. The

protected cyclic analog was then deprotected with 65% trifluoroacetic acid (TFA) + 3% TES, anisole, water in DCM. The purification was achieved using HPLC reversed-phase chromatography and the peptide purity, 99% was assessed by analytical HPLC and mass spectrometry (ESI-MS).

The final peptide analogues are under evaluation in School of Medicine, University of Patras for their ability to induce Th2 cytokine profile in PBMCs of MS patients. Furthermore, conformational studies will be made for linear and cyclic MBP(82-98)(Ala⁹¹) using NMR techniques by National Hellenic Research Foundation.

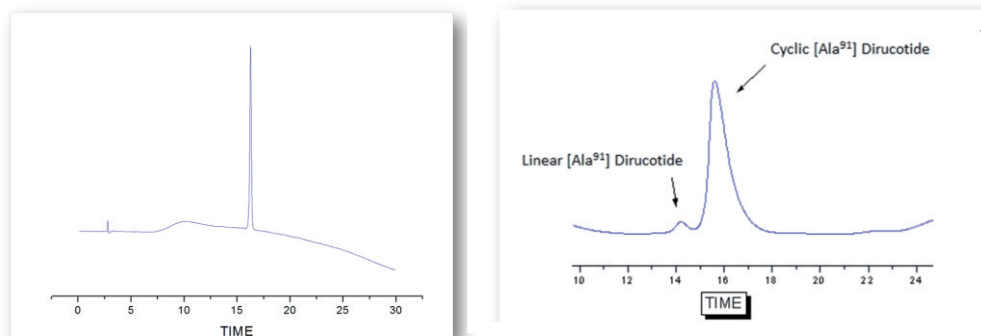


Figure 1: RP-HPLC lyophilized Cyclic [Ala⁹¹] MBP(82-98)(Ala⁹¹) analogue and monitoring of protected peptide after cyclization procedure. [Nucleosil C18, 250x4,6mm, 5µm. TR: 15,7min. Conditions: 5%(B) to 100%(B) in 35min, Flow rate: 1ml/min, (A):TFA solution in H₂O 0,08%(v/v), (B):TFA solution in AcN 0,08%(v/v)]

Acknowledgments

This work is financially supported by the “Cooperation” program 09SYN-609-21, (O. P. Competitiveness & Entrepreneurship (EPAN II). We are grateful to VIANEX S.A. for supporting this work.

References

- [1] Matsoukas J.; Apostolopoulos V.; Kalbacher H.; Papini AM.; Tselios T.; Chatzantoni K.; Biagioli T.; Lolli F.; Deraos S.; Papathanassopoulos P.; Troganis A.; Mantzourani E.; Mavromoustakos T.; Mouzaki A.; *J Med Chem* **2005** 48(5): 1470-1480.
- [2] Katsara M.; Yuriev E.; Ramslund PA.; Tselios T.; Deraos G.; Lourbopoulos A.; Grigoriadis N.; Matsoukas J.; Apostolopoulos V.; *Immunology*. **2009 Dec**;128(4):521-33.
- [3] T. Tselios.; V. Apostolopoulos.; I. Daliani.; S. Deraos.; S. Grdadolnik.; T. Mavromoustakos.; M. Melachrinou.; S. Thymianou.; L. Probert.; A. Mouzaki.; J. Matsoukas. *Journal of Medicinal Chemistry*, **2002**, 45, 275-283.
- [4] Deraos G.; Chatzantoni K.; Matsoukas MT.; Tselios T.; Deraos S.; Katsara M.; Papathanasopoulos P.; Vynios D.; Apostolopoulos V.; Mouzaki A.; Matsoukas J.; *J Med Chem*. 2008 Dec 25;51(24):7834-42.

Design of CXCR4 ligands for diagnostic and therapeutic applications

**O. Demmer,^{a,b} I. Dijkgraaf,^c E. Gourni,^c M. Schottelius,^c A. O. Frank,^a
F. Hagn,^a L. Marinelli,^d S. Cosconati,^e R. Brack-Werner,^f S. Kremb,^f U.
Schumacher,^g H.-J. Wester,^c H. Kessler^{b,h}**

^a Institute for Advanced Study at the Department, Chemie, Technische Universität München, Lichtenbergstraße 4, 85748 Garching, Germany, ^b current address: Zealand Pharma A/S, Smedeland 36, 2600 Copenhagen, Denmark; ^c Lehrstuhl für Pharmazeutische Radiochemie Walter-Meißner-Str. 3, D-85748 Garching, Germany, ^d Dipartimento di Chimica Farmaceutica e Tossicologica, Università di Napoli "Federico II", Via D. Montesano 49, 80131 Napoli, Italy, ^e Dipartimento di Scienze Ambientali, Seconda Università di Napoli, Via Vivaldi 43, 81100 Caserta, Italy, ^f Helmholtz Zentrum München, Institute of Virology, Ingolstädter Landstr. 1, D-85764 Neuherberg/München, Germany, ^g Institute for Anatomy II: Experimental Morphology, Universitätsklinikum Hamburg-Eppendorf, Martinistrasse 52, 20246 Hamburg, Germany, ^h Chemistry Department, Faculty of Science, King Abdulaziz University, P.O. Box 80203, Jeddah 21589, Saudi Arabia

ode@zealandpharma.com

Introduction

The chemokine receptor subtype CXCR4 belongs to the G-protein coupled receptors (GPCRs) and is, together with its natural ligand CXCL12 (or SDF-1), a central part of the signaling system in the human body. Its functions range from stem cell trafficking during embryogenesis over cardiovascular, hematopoietic and brain development to signaling in the nervous and immune system. Furthermore, CXCR4 is one of two major co-receptors used by the human immunodeficiency virus (HIV) for cell entry and CXCR4-using viruses are critical for the pathogenesis of AIDS. Hence, CXCR4 represents a valuable therapeutic option for multiple diseases such as inflammation, cancer and HIV/AIDS. Our aim was to use CXCR4 ligands in an approach for personalized medicine especially for cancer by developing **diagnostics** to identify the relevant patient subgroup and accompanying **therapeutics** to treat these patients in a better way.

Results and Discussion

We chose the highly stable, cyclic pentapeptide FC131 developed by Fujii et al. as starting point for our optimization because of its excellent CXCR4 affinity.^[1] Additionally FC131 is selective for CXCR4 without binding CXCR7 and has as inverse agonist a potentially better side-effect profile over partial agonists, as for example, AMD3100.

To develop high affinity CXCR4 ligand for molecular imaging we modified FC131 in four SAR rounds with more than 60 peptides.^[2,3] Therein, we found an anchoring point for prosthetic groups, investigated the optimal side chain lengths and the best spacing group.

Finally, we introduced a *N*-methylated D-amino acid next to the tyrosine as this was shown to improve affinity.^[4]

We chose DOTA as a complexing moiety as its cyclen scaffold is also found in the CXCR4 drug AMD3100, and we hypothesized that we could gain receptor affinity as chelates of AMD3100 have shown to have superior affinity. The type and length of spacer between the peptide and DOTA was optimized in more than 25 compounds. We used gallium and indium chelates as these ions are relevant for imaging purposes. Our ⁶⁸Ga-labeled CXCR4 PET imaging probe of the most affine compound shows excellent *in vivo* distribution and binding characteristics in tumor bearing mice that recommend the further clinical evaluation of this compound.^[2,3]

In addition to a diagnostic tool there was still the need for a highly active CXCR4 antagonist as therapeutic. We used the knowledge that the peptide backbone of *cyclo*-(D-Tyr-[NMe]-D-Arg-Arg-Nal-Gly-) (Nal=L-3-(2-naphthyl)alanine) exhibits two conformations in solution and tried to enforce a single active one.^[4]

Both conformations of the *N*Me-D-Orn analog were elucidated in water by NMR followed by distance geometry and molecular dynamic calculations.^[5] In both structures the Tyr and Orn side chains are oriented towards each other. The hydrophobic interaction between them has a stabilizing effect for both the *trans* and the *cis* conformation. We hypothesized that using a peptoid motif by exchanging the *N*-methyl group and the aminoalkyl side chain leads to a single conformation. Therein only the *trans* conformer is stabilized as both side chains are closer to each other while the *cis* conformer is destabilized as both residues are oriented away from each other.

The introduction of the peptoid motif in this position showed increased CXCR4 affinity for all investigated compounds. Elucidation of the most active compound showed that we succeeded in restricting the conformation into a single active one by using the peptoid motif. By introducing a guanidino group at the aminoalkyl chain the binding affinity was optimized into the picomolar range to be 400 to 1500-fold higher than compounds currently under clinical development, such as KRH-1636 or AMD3100.^[5] Additional evaluation by Polyphor Ltd. confirmed the very high antagonistic CXCR4 activity of this compound in a chemotaxis assay and showed favorable *in vitro* ADMET.

Acknowledgments

We thank Dr. Daniel Obrecht, Dr. Barbara Romagnoli, Dr. Steffen Weinbrenner, and Dr. Françoise Jung from Polyphor Ltd. for additional evaluation of OD001.

References

- [1] Fujii, N.; Oishi, S.; Hiramatsu, K.; Araki, T.; Ueda, S.; Tamamura, H.; Otaka, A.; Kusano, S.; Terakubo, S.; Nakashima, H.; Broach, J. A.; Trent, J. O.; Wang, Z. X.; Peiper, S. C. *Angew. Chem. Int. Edit.* **2003**, *42*, 3251.
- [2] Demmer, O.; Gourni, E.; Schumacher, U.; Kessler, H.; Wester, H.-J. *ChemMedChem* **2011**, *6*, 1789.
- [3] E. Gourni, O. Demmer, M. Schottelius, C. D'Alessandria, S. Schulz, I. Dijkgraaf, U. Schumacher, M. Schwaiger, H. Kessler, H.-J. Wester, *J. Nucl. Med.* **2011**, *52*, 1803.
- [4] S. Ueda, S. Oishi, Z.-X. Wang, T. Araki, H. Tamamura, J. Cluzeau, H. Ohno, S. Kusano, H. Nakashima, J. O. Trent, S. C. Peiper, N. Fujii, *J. Med. Chem.* **2007**, *50*, 192.
- [5] O. Demmer, A. O. Frank, F. Hagn, M. Schottelius, L. Marinelli, S. Cosconati, R. Brack-Werner, S. Kremb, H.-J. Wester, H. Kessler *Angew. Chem. Int. Edit.* **2012**, *51*, 8110.

Development of new anti-prostate cancer agents through SAR studies of potent PACE4 inhibitor

Anna Kwiatkowska, Christine Levesque, Frederic Couture, Roxane Desjardins, Sophie Routhier, Xue-Wen Yuan, François D'Anjou, Witold Neugebauer, Robert Day

Institut de pharmacologie de Sherbrooke (IPS) et département de chirurgie/service d'urologie, Faculté de médecine et des sciences de la santé (FMSS), Université de Sherbrooke, Sherbrooke, Québec, Canada

E-mail: anna.kwiatkowska@usherbrooke.ca

Introduction

Prostate cancer (PCa) is the most common cancer diagnosed in North American men and the second leading cause of male cancer deaths. Recently, we have demonstrated that PACE4 represents a potential therapeutic target for the treatment of prostate cancer [1]. Moreover, we have developed potent and relatively selective PACE4 inhibitor (20-fold specificity over furin), known as Multi-Leu (ML) peptide, which has potent antiproliferative effect on prostate cancer cell lines. Having in mind that peptides as drug candidates may be limited by poor metabolic stability and low bioavailability, we decided to evaluate various substitutions that could improve the pharmacokinetic properties of our ML inhibitor. Our studies (unpublished data) have demonstrated, that the substitution of position P8 of ML inhibitor with D-amino acids (D-Leu or D-Nle) increased plasma stability of the resulting analogues. Furthermore, the recent study has shown, that introduction of the decarboxylated and conformationally restricted arginine mimetic (Amba) in the position P1 of furin inhibitor significantly improved its potency [2]. Continuing our research, we have designed and synthesized new analogues of ML inhibitor having various chemical modifications (PEGylation, fatty acid acylation, P1 and/or P8 position substitution) in order to improve its pharmacokinetic properties.

Results and Discussion

All peptides were obtained by solid phase peptide synthesis or a combination of solid phase peptide synthesis and solution synthesis (Amba analogues), according to standard coupling procedures and Fmoc/tBu strategy. The inhibitory constants (Figure 1) were determined using recombinant human furin and PACE4 by competitive kinetic assay. For analogues modified with Amba, K_i were calculated according to the tight-binding inhibition kinetics. The substitution of the Arg residue in position P1 with its conformationally restricted mimetic – Amba significantly improved inhibitory potency towards PACE4 (7-fold) and furin (130-fold) of our leading compound. However, the specificity towards PACE4 was greatly reduced by this modification. Furthermore, we determined the antiproliferative activity of our analogues using MTT assay on prostate cancer cell lines. The peptide modified with Amba or additionally substituted with D-Leu showed the highest activity on both LNCaP ($IC_{50} = 84\mu\text{M}$ or $35\mu\text{M}$, respectively) and DU-145 ($IC_{50} = 86\mu\text{M}$ or $61\mu\text{M}$, respectively) cell lines (Figure 2).

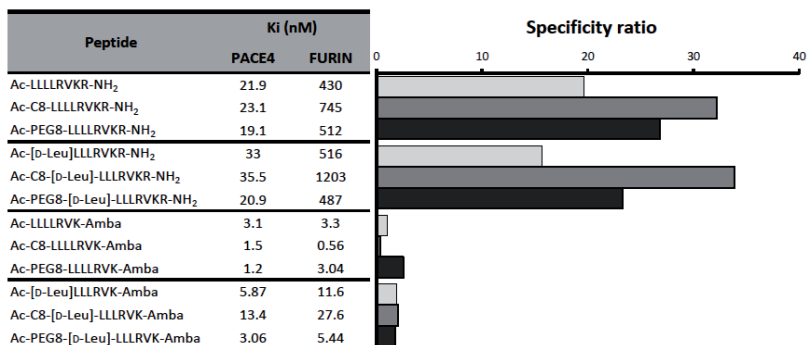


Figure 1. Inhibitory potency and specificity of Multi-Leu analogues.

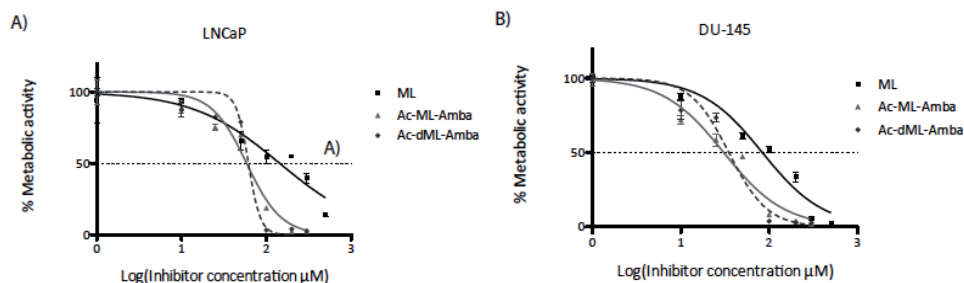


Figure 2. Antiproliferative activity of selected Multi-Leu inhibitors on prostate cancer A) DU-145 and B) LNCaP cell lines using MTT assay.

Our study provides interesting insights into structure-activity relationships of Multi-Leu analogues. We demonstrated that, *N*-terminal extensions (C8 or PEG8) do not affect the activity of our inhibitors. Moreover, we have shown that potency and antiproliferative activity of Multi-Leu analogues can be greatly improved by the incorporation of the Amba modification. The combination of substitutions used in the present study, increased potency and antiproliferation effects of our Multi-Leu peptide, thus providing better pharmacological properties for the development of potential anti-prostate cancer agents.

Acknowledgments

This work was awarded by Prostate Cancer Canada and is proudly funded by the Movember Foundation-Grant #2012-951. This work was also supported by the Ministère du Développement Économique, de l'Innovation et de l'Exportation du Québec (MDEIE) and the Canadian Institutes of Health Research (CIHR).

References

- [1] D'anjou, F.; Routhier, S.; Perreault, J.P.; Latil, A.; Bonnel, D.; Fournier, I.; Salzet, M., Day, R. *Transl. Oncol.* **2011**, *4*, 157–172.
- [2] Becker, G.L.; Sielaff, F.; Than, M.E.; Lindberg, I.; Routhier, S.; Day, R.; Lu, Y.; Garten, W.; Steinmetzer, T. *J. Med. Chem.* **2010**, *53*, 1067-75

Development of the first orally active NPFF-R antagonist capable of reversing opioid-induced hyperalgesia in rodents

F. Bihel,¹ S. Schneider,¹ M. Schmitt,¹ J.P. Humbert,² K. Elhabazi,² E. Laboureyras,³ G. Simonnet,³ E. Schneider,⁵ B. Petit-Demouliere,⁴ F. Simonin,² J.J. Bourguignon¹

¹LIT, UMR7200, Strasbourg Univ., Illkirch, France; ²UMR7242, IREBS, Strasbourg Univ., Illkirch, France; ³UMR5287, Bordeaux II Univ., Bordeaux, France; ⁴Inst. Clinique de la Souris, Strasbourg Univ., Illkirch, France; ⁵Phenopro, Illkirch, France

Introduction

The development of drugs that can more effectively and safely treat both acute and chronic pain (resulting from post-operative surgery, cancer, neuropathies, etc) remains a major unmet challenge in pharmaceutical industry. Opiate analgesics, such as morphine or fentanyl, continue to be the cornerstone medication for treating moderate to severe pain, but their use upon chronic administration suffers from important side-effects such as opioid-induced tolerance, addiction and hyperalgesia. Several anti-opioid systems have been reported as valuable targets for blocking opioid-induced hyperalgesia. Among them the NPFF receptors belonging to the GPCR family were recently identified as one of the keystone of the opioid-induced hyperalgesia. In a first approach, we developed the first NPFF-receptor antagonist (**RF9**), and its co-administration with opioids (fentanyl) led to block the delayed and long lasting paradoxical opioid induced-hyperalgesia and prevented the development of associated tolerance. However the dipeptidic nature of RF9 limited its application to subcutaneous or intravenous administration [1]. The objective of this project was to develop a novel orally-active NPFF-R antagonist, exhibiting anti-hyperalgesic effects similar to those observed with RF9.

Results and Discussion

Starting from **RF9** (Fig.1A), we first performed an optimization of the N-terminus part of the dipeptide, by synthesizing more than 80 compounds. The replacement of the bulky adamantane by the sterically hindered 2-phenylbenzene moiety (**RF213**) led to a strong increase in affinity by about two orders of magnitude towards NPFF1-R ($K_i = 0.32$ nM), similar to the affinity of the endogenous octapeptidic NPFF1-R ligand NPVF (VPNLPQRF-NH₂). Interestingly, compound **RF213** exhibits over 3 orders of magnitude in selectivity for NPFF1 versus NPFF2 receptor ($K_i = 590$ nM). Then, we proceeded to the deletion of the C-terminal amide function of the dipeptide **RF213**, leading to the arginine derivative **RF272**. This deletion had almost no impact towards NPFF2-R ($K_i = 250$ nM), but dramatically decreased the affinity towards NPFF1-R ($K_i = 310$ nM). Nethertheless, **RF272** was not anymore a peptide, but was still keeping a submicromolar affinity towards both NPFF-R. The guanidine group is rich of H-bond donor, which is considered as a negative parameter to cross the blood-brain-barrier through passive diffusion. Then, we decided to switch the arginine residue by a non-natural N,N-dialkylated ornithine (e.g. piperidine analog **RF313** – Fig1A), allowing keeping cationic moiety without any H-bond donor. Starting from Fmoc-Glu(tBu)-OH, we established an efficient synthetic pathway

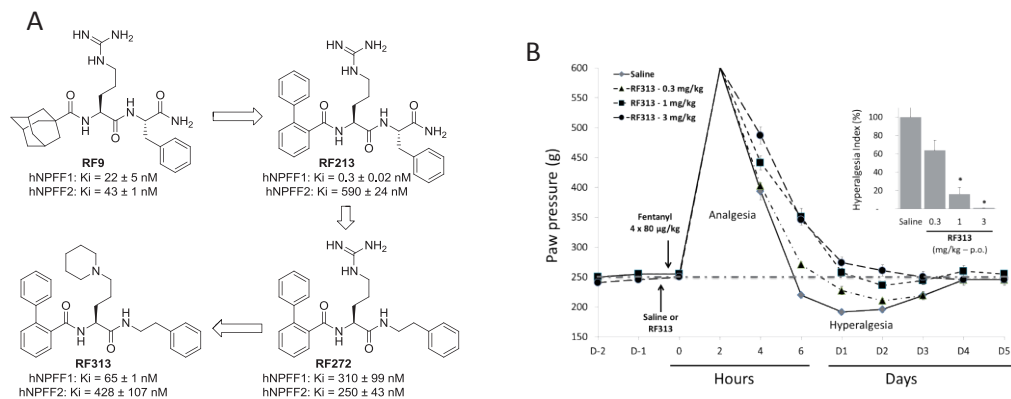


Figure 1. A) Structural evolution of the dipeptide **RF9** to the non-natural amino acid derivative **RF313**, and their pharmacological activities towards both NPPF1 & 2 receptors. B) Preventive effect of **RF313** on fentanyl-induced hyperalgesia. On day 0 (D0), fentanyl (80 µg/kg) injection was performed every 15 min for 1 hour, resulting in a total dose of 320 µg/kg. **RF313** (0.3, 1 and 3 mg/kg) or saline was orally administered 30 min before the first administration of fentanyl. Nociceptive threshold was measured by the paw-pressure test. *Inset* : Hyperalgesic index (HI) is the area between the baseline and the curve for nociceptive threshold on the days after fentanyl administration, normalized to control. Values are expressed as the mean \pm SD. * Dunnett test $P < 0.001$ for comparison between saline group and Compound **RF313** group.

leading to **RF313** in 7 steps (41% global yield). The non-peptidic **RF313** appeared slightly more selective toward NPPF1 ($K_i = 64$ nM) vs NPPF2 ($K_i = 428$ nM). Oral administration of the highly water-soluble **RF313** to rats at low doses (0.3 to 3 mg/kg) in a paw-pressure vocalization test exhibited a potent *in vivo* preventive effect on opioid-induced hyperalgesia. Moreover, screened at 1 µM, **RF313** did not show any affinity towards about 40 protein-targets including (α , β , D, M, μ , δ , κ , Y, 5HT, hERG, etc). Chronic administration of **RF313** to mice (30 mg/kg, i.p.) did not exhibit any toxicity, side effects, or any negative impact on muscular strength, motricity or weight evolution.

RF313 is the first orally-active NPPF antagonist capable of reversing opioid-induced hyperalgesia at low dose. Moreover, the good pharmacological profile in terms of anti-OIH efficacy, selectivity and clinical observations, allows to identify **RF313** as a potential pre-clinical candidate in the treatment of acute and chronic pain.

Acknowledgments

This work was supported by grants from Agence Nationale de la Recherche (ANR-06-Neuro-041-01, ANR-08-EBIO-014-01), Alsace BioValley (Conectus, Pharmadol), Conseil Régional d'Alsace (Pharmadol), Communauté Urbaine de Strasbourg (Pharmadol), ICFRC (Pharmadol), OSEO (Pharmadol), Direction Générale des Entreprises (Pharmadol).

References

- [1] Simonin, F.; Schmitt, M.; Laulin, J. P.; Laboureyras, E.; Jhamandas, J. H.; MacTavish, D.; Matifas, A.; Mollereau, C.; Laurent, P.; Parmentier, M.; Kieffer, B. L.; Bourguignon, J. J.; Simonnet, G., *Proc. Natl. Acad. Sci. U.S.A.* **2006**, *103* (2), 466-71.

Enhanced stability and biological properties of rationally designed cyclic analogues of Luteinizing Hormone – Releasing Hormone

Despina Laimou^{a,‡}, Theodora Katsila^{b,‡}, John Matsoukas^{a,*}, Andrew Schally^d, Kostas Gkountelias^c, George Liapakis^c, Constantin Tamvakopoulos^b, Theodore Tselios^{a,*}

^aDepartment of Chemistry, University of Patras, 26500 Patras, Greece; ^bDivision of Pharmacology-Pharmacotechnology, Biomedical Research Foundation, Academy of Athens, Athens 11527, Greece; ^cDepartment of Pharmacology, Faculty of Medicine, University of Crete, Heraklion, Crete, Greece; ^dVeterans Affairs Medical Center and Departments of Pathology and Medicine, Division of Hematology/Oncology, University of Miami Miller School of Medicine, Miami, FL 33125, USA

E-mail: tselios@upatras.gr, imats@chemistry.upatras.gr

Introduction

Luteinizing Hormone - Releasing Hormone, LHRH (A.V. Schally, R.Guillemin Nobel Prize 1977) was first isolated from mammalian hypothalami as the decapeptide (pGlu-His-Trp-Ser-Tyr-Gly-Leu-Arg-Pro-Gly.NH₂)¹. LHRH is synthesized by gonadotropic cells of the hypothalamus and is the central regulator of the reproductive system. LHRH interacts with high affinity the G-protein-coupled receptor localized on anterior pituitary gland and cancer cells stimulating the biosynthesis and the releasing of luteinizing (LH) and follicle-stimulating (FSH) hormones.

Many diseases, such as prostate and breast cancer, endometriosis and uterine leiomyomas, are stimulated by steroid hormones. LHRH agonistic analogues, Leuprolide², Triptorelin, Buserelin, Goserelin, Nafarelin and Histrelin, have achieved widespread clinical use for the control of reproduction³. Following the elucidation of the amino acid sequence of LHRH native hormone, modifications to the sequence were developed in the expectation of greater potency and improved receptor-binding.

This study reports⁴ a novel cyclization strategy for the design and synthesis of novel Leuprolide analogues, cyclized at the C- and N- terminal, retaining the basic backbone sequence of leuprolide. The analogues synthesized were: cyclo(1-10)[Pro¹, DLeu⁶, BABA¹⁰]LHRH (**1**), cyclo(1-10)[Pro¹, Tyr(OMe)⁵, DLeu⁶, Aze⁹, BABA¹⁰]LHRH (**2**), cyclo(1-11)[Pro¹, DLeu⁶, BABA¹⁰, Acp¹¹]LHRH (**3**), cyclo(1-11)[Pro¹, Tyr(OMe)⁵, DLeu⁶, BABA¹⁰, Acp¹¹]LHRH (**4**), cyclo(1-10)[Pro¹, Tyr(OMe)⁵, DTrp⁶, Aze⁹]LHRH (**5**). The rationale of our approach is that novel LHRH peptide analogues with a profound pharmacokinetic advantage that is particularly valuable with respect to local/direct effects can serve as therapeutic alternatives for the treatment of endocrine disorders and hormone – dependent cancers.

Results and Discussion

The binding affinities ($-\log IC_{50}$) of the novel cyclic LHRH analogues reported for the human LHRH - I receptor were determined from competition experiments performed under equilibrium conditions in membranes from HEK 293 cells stably expressing the human LHRH receptor and using [^{125}I -DTyr⁶, His⁵] LHRH as the radioligand. Leuprolide served as a control. In this study, all analogues evaluated bound to the human LHRH - I receptor in a dose - dependent manner (**Table 1**).

Table 1: Amino acid sequence, $-\log IC_{50}$ values and peptide stability data for the novel cyclic LHRH analogues reported.

Peptides	Aminoacid Sequence	$-\log IC_{50}$	Peptide Stability at t = 30 min
LHRH	Pyr-His-Trp-Ser-Tyr-Gly-Leu-Arg-Pro-Gly-NH ₂		highly unstable
Leuprolide	(Des-Gly ¹⁰ , D-Leu ⁶ , Pro-NHET ⁹) LHRH	9.12 ± 0.19	3%
(1)	cyclo(1-10)[Pro¹, D-Leu⁶, BABA¹⁰] LHRH	6.17 ± 0.15	100%
(2)	cyclo(1-10)[Pro ¹ , Tyr(OMe) ⁵ , D-Leu ⁶ , Aze ⁹ , BABA ¹⁰] LHRH	5.82 ± 0.15	90%
(3)	cyclo(1-11)[Pro ¹ , D-Leu ⁶ , BABA ¹⁰ , Acp ¹¹] LHRH	5.31 ± 0.02	72%
(4)	cyclo(1-11)[Pro ¹ , Tyr(OMe) ⁵ , D-Leu ⁶ , BABA ¹⁰ , Acp ¹¹] LHRH	5.54 ± 0.26	90%
(5)	cyclo(1-10)[Pro ¹ , Tyr(OMe) ⁵ , D-Trp ⁶ , Aze ⁹] LHRH	5.58 ± 0.25	68%

Peptide stability was evaluated both in vitro and in vivo. In vitro stability data were acquired following the incubation of the analogues **1 - 5** as well as the native hormone (LHRH) with mouse kidney membrane preparations on the basis that kidney is the major site for the metabolism of LHRH and the analogues. After extraction and detection by the novel LC - MS/MS methodology developed, the peak areas for the analogues **1 - 5** and LHRH were set as 100% at t = 0. The native decapeptide LHRH showed an extensive in vitro degradation within 30min of incubation. Following 30min of incubation with mouse kidney membranes, only 3% of leuprolide remained intact. All cyclic analogues tested were significantly more stable compared to leuprolide and/or the native hormone. In particular, 90% of analogues **2** and **4** remained intact at t = 30 min, compared to 72 % and 68 % of **3** and **5** (at t = 30 min), respectively.

Acknowledgments

Despina Laimou was financially supported by the University of Patras (Karatheodoris Grant). The authors would like to thank the A.G. Leventis Foundation for funding of the Dr C. Tanvakopoulos' lab in the Biomedical Research Foundation of the Academy of Athens. Also, we would like to thank Dr N Kostomitsopoulos and Mr E Balafas for assistance with the in vivo studies.

References

- [1] Schally, A.V.; Arimura, A.; Baba, Y. et al., 1971 *Biochem. Biophys. Res. Commun.* **1971**, *43*, 393.
- [2] Laimou D. K.; Katsara M.; Matsoukas M. I.; Apostolopoulos V.; Troganis A.N.; Tselios T. V. *Amino acids* **2010**, *39(5)* 1147.
- [3] Laimou D., Katsila T., Matsoukas J., Schally A., Gkountelias K., Liapakis G., Tamvakopoulos C. and Tselios T., *European Journal of Medicinal Chemistry*, Submitted

Enhancement of the antiplatelet activity of novel synthetic peptides in animals receiving low doses of aspirin, in an experimental model of arterial thrombosis

Vassilios Moussis¹, Constantinos V. Englezopoulos², Kleopatra Rousouli¹, Nikolaos D. Papamichael³, Vassiliki D. Roussa³, Christos S. Katsouras³, Katerina K. Naka³, Alexandros D. Tselepis¹, Lambros K. Michalis³, Vassilios Tsikaris¹

¹Chemistry Department, University of Ioannina, Ioannina, Greece; ²Michaelidion Cardiac Center, Medical School, University of Ioannina, Ioannina, Greece; ³Cardiology Department, University Hospital of Ioannina, Ioannina, Greece

E-mail: btsikari@cc.uoi.gr

Introduction

Glycoprotein IIb/IIIa receptors (integrins α IIb β 3) are the most prominent member of adhesion receptors that mediate platelet aggregation mainly by binding to fibrinogen. The platelet activation and the resultant aggregation have a key role in the pathogenesis of cardiovascular and cerebrovascular events and their inhibition has been proven crucial for the treatment of acute coronary syndromes. The α IIb β 3 human platelet integrin primarily interacts with its ligands through a common tripeptide sequence, the RGD (Arg-Gly-Asp) sequence. Our research group has previously identified the 313-332 sequence of the α IIb subunit of the human platelet integrin α IIb β 3 being crucial for the binding of fibrinogen and therefore inducing platelet aggregation. Peptide analogues of this sequence have demonstrated antiaggregatory effects on human platelets *in vitro*. The most potent *in vitro* inhibitory effects on platelet aggregation of human platelets were exhibited by the peptide YMESRADR that corresponded to the residues 313-320 of the α IIb subunit of the α IIb β 3 integrin. Administration of multiple antiplatelet agents has become the mainstay in the treatment of acute coronary syndromes in everyday clinical practice. We have previously reported significant antiplatelet effects of novel synthetic peptides' single administration on experimental carotid artery thrombosis in rabbits [1]. In the present study we sought to investigate the peptides' effects when administered in marginally effective doses (significantly lower than those utilized in the past), in animals that had previously received low doses of aspirin.

Results and Discussion

The peptides when co-administered with aspirin preserved the carotid artery's blood flow, in contrast to the total artery occlusion observed in animals receiving aspirin and placebo. Blood flow at 90 min after electrical stimulation was reduced to 56.7 \pm 7.9% and 33.2 \pm 0.3% in the YMESRADR and (S,S) PSRCDCR-NH₂ groups respectively (p<0.001 vs aspirin and control). Thrombus weight was significantly reduced in animals receiving YMESRADR and (S,S) PSRCDCR-NH₂ versus aspirin and control (3.9 \pm 0.3mg and 3.1 \pm 0.4mg, vs 7.8 \pm 2.2mg and 5.7 \pm 0.8mg respectively, p<0.05). Platelet aggregation was significantly

inhibited in the YMESRADR and (S,S) PSRCDCR-NH₂ groups by 36.0±14.1% and 45.0±12.0% for ADP (p<0.05 vs aspirin and control), and 35.5±6.3% and 54.2±5.6% for AA (p<0.05 vs aspirin and control), respectively. Blood loss did not significantly differ among the various groups. Administration of novel synthetic peptides, even at marginally effective doses, in animals previously treated with low doses of aspirin results in enhanced antiplatelet effects in an experimental model of arterial thrombosis.

References

- [1] Roussa, V.D.; Stathopoulou, E.M.; Papamichael, N.D.; Englezopoulos, C.V.; Rousouli, K.I.; Trypou, P.; Moussis, V.; Tellis, C.C.; Katsouras, C.S.; Tsikaris, V.; Tselepis, A.D.; Michalis, L.K. *Platelets* **2011**, *22*, 361.

HIV-1 epitopes localizing to the membrane proximal external region (MPER) of gp41 and to the V3 loop of gp120: Synthesis and immunization assays

**Ioanna Kostoula,¹ Mingkui Zhou,² Maria Hertje,² Eugenia Panou,¹
Ursula Dietrich,² Maria Sakarellos-Daitsiotis¹**

¹*Section of Organic Chemistry and Biochemistry, Department of Chemistry, University of Ioannina, Greece;* ²*Georg-Speyer-Haus, Institute for Biomedical Research, Paul-Ehrlich-Str. 42-44, 60596 Frankfurt, Germany*

E-mail: ioanna.kws@gmail.com

Introduction

The HIV-1 epidemic continues spreading around the world with many new infections per day and more than 70 million people living with HIV-1 [1]. Development of an effective vaccine is still an urgently needed priority in AIDS. Elite controllers (EC) is a subgroup of long term non progressors, which are persons controlling the infection over decades without any antiviral therapy. However most of the efforts undertaken have failed so far as the virus has evolved numerous mechanisms to protect its functionally important entry domains from the immune system.

Peptide mimics of epitopes for pathogen-specific antibodies present in patient sera can be selected based on the phage display technology. Such mimotopes potentially represent vaccine candidates in case they are able to induce neutralizing antibodies (nAbs) upon vaccination. The induction of nAbs is a major goal in the development of a preventive HIV-1 vaccine, as several animal studies have shown their decisive role in protective immunity. Despite the fact that a handful of broadly nAbs (b12, 2G12, 2F5, 4E10) is known for many years, including structural information of their target epitopes, attempts to induce nAbs upon vaccination have largely failed. Recently, some additional exceptionally broad neutralizing antibodies have been identified from chronically HIV-1 infected patients. These antibodies have been cloned based on sorting and cloning of single B cells from patients with broad neutralizing activity using engineered Env constructs. The new nAbs recognize quaternary structures in the context of the native envelope spike and show features of extensive affinity maturation and adaptation during the course of the infection.

Epitopes for HIV-specific antibodies in EC, encompassing segments of the membrane proximal external region (MPER) of gp41 and the tip of the V3 loop of gp120 were identified using the phage display technology [2]. Synthetic epitopes of HIV were conjugated to an artificial sequential oligopeptide carrier (SOC₄), or to the palmitoyl group and used in immunization experiments, for the induction of neutralizing antibodies.

Results and Discussion

Based on the phage display technology, three epitopes for HIV specific antibodies in EC sera were identified and synthesized. Peptide synthesis was carried out by the stepwise solid-phase synthesis procedure (SPPS) on a Rink Amide resin using the Fmoc

methodology. Palmitoyl group was incorporated in the α -amino terminal group of the first epitope (EC26-2A4) as adjuvant. All three epitopes were coupled to a Sequential Oligopeptide Carrier Ac-(Lys-Aib-Gly)₄, SOC₄, in two copies, by chemoselective ligation [3].

ELISAs were performed with patient IgG affinity purified with EC26-2A4 so as to prove the reactivity of the synthesized peptide conjugates with the original patient antibodies. Mice were immunized with both Palm-EC26-2A4 and SOC-EC26-2A4. Immunization experiments for the induction of neutralizing antibodies and the formulation of vaccine candidates are currently in progress for the second and third epitope.

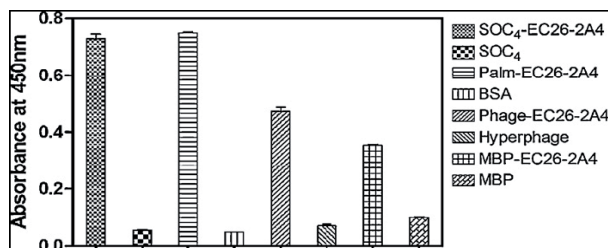


Figure 1: Reactivity of different epitope conjugates and controls (conjugates alone) with antibody affinity purified from patient EC26 plasma. Hyperphage corresponds to a wildtype phage without peptide inserts.

Eliciting broadly nAbs against HIV-1 is a key issue in the development of a successful prophylactic vaccine. It was found that the EC26-2A4 MPER epitope is a promising candidate for vaccine development. In particular, due to the absence of crossreactivity with cardiolipin associated with other potent MPER mAbs like 2F5. Immunization studies in larger animals have now to be performed in order to obtain sufficient amounts of sera to analyze the breadth of neutralization with a panel of different HIV-1 isolates.

References

- [1] Berkley, S. *Lancet* **2003**, 362, 992.
- [2] Humbert, M.; Antoni, S.; Brill, B.; Landerz, M.; Rodes, B.; Soriano, V.; Wintergerst, U.; Knechten, H.; Staszewski, S.; von Laer, D.; Dittmar, M.T.; Dietrich, U. *Eur. J. Immunol.* **2007**, 37, 501-515.
- [3] Zhou, M.; Kostoula, I.; Brill, B.; Panou, E.; Sakarellos-Daitsiotis, M.; Dietrich, U. *Vaccine* **2012**, 30, 1911-1916.

Identification of novel anti-thrombotic cadherin derived peptides

K. Golla,¹ I. Stavropoulos,² D. C. Shields,² N. Moran¹

¹*Molecular & Cellular Therapeutics, Royal College of Surgeons in Ireland;* ²*Complex and Adaptive Systems Laboratory University College of Dublin*

E-mail:kalyangolla@rcsi.ie

Introduction

The main role of platelets is to survey the blood vessels for evidence of damage. At sites of blood vessel damage, platelets react by rapidly activating and forming a localized thrombus. Activated platelets secrete ADP to recruit more platelets to the damaged site in order to prevent excessive blood loss. In cardiovascular disease, platelets can form thrombi in intact blood vessels at sites of atherosclerosis. This is called thrombosis. There is an ongoing search for pharmaceutical agents to inhibit these thrombotic events. Previous studies in our laboratory have identified cell permeable peptides derived from platelet cell adhesion molecules, such as cadherins, that behave as platelet function modifiers ¹.

Cadherins are single pass trans-membrane calcium dependent cell adhesion molecules present at most adherence junctions. In this study, we explore the possible role of cadherins in platelet function. In addition, we design, synthesize and characterize a panel of peptides derived from important functional regions of cadherin intracellular domains. Our aim is to determine if such peptides can modulate platelet function thereby identifying them as potential therapeutic antithrombotic agents.

Results

We have identified Cadherin 5 and Cadherin 6, but not cadherin 1 or 2 in human platelets by using western blot and Mass spectroscopic techniques. Overlapping peptides derived from juxta-membrane region of the Cadherin 1, 2, 5 and 6 were designed, synthesized and analyzed in a high throughput platelet ADP secretion assay.(Figure 1; 50 μ M). In our assays, platelet secretion of ADP is measured by luminometry, in the presence and absence of a potent platelet activator such as the thrombin receptor activating peptide (TRAP). All the peptides derived from cadherins significantly inhibited platelet activation. In contrast, some peptides, e.g. Cad 1-1 & 5-1 significantly induced platelet activation in the absence of TRAP. Dose dependent studies suggested that 25 μ M is the minimum peptide concentration that can have an effect. The critical residues responsible for inhibitory activity were analysed by deleting amino acids from N- and C-termini of each peptide. Deletion studies suggested that the charge-rich, membrane proximal region of each peptide was crucial for activity and also highlighted that a short motif, KEPLLP, is a potent inhibitor of platelet function. This KEPLLP motif had previously been identified as the dynamic binding site for p120-catenin in the Cadherin juxta-membrane region ². Structure-activity relationship (SAR) analysis identified Lysine (K) and the first leucine (L) residues of KEPLLP as crucial for inhibitory activity.

Discussion

In this study we have been identified Cadherin-5 and Cadherin-6 protein in human platelets. Overlapping peptides derived from juxta-membrane region of Cadherins inhibited platelet function. Therefore, Cadherin derived peptides may facilitate the development of a therapeutic agent for the treatment of cardiovascular disease. However, the mechanism of inhibitory activity of these peptides still needs to be elucidated.

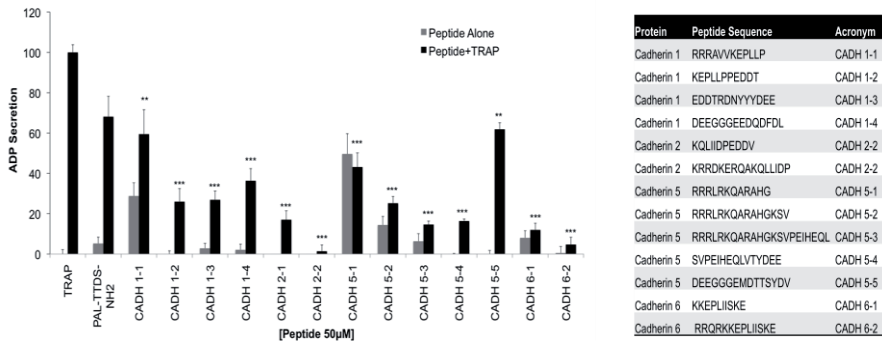


Figure 1: Platelet ADP secretion response is modified by peptides derived from Cadherins 1,2,5 and 6: Peptides were synthesized with N-terminus palmitoylation and C-terminus amidation. Peptides were analysed in a high throughput platelet ADP secretion assay¹ in the presence (black bars) or absence (grey bars) of the platelet agonist TRAP. The results were normalized to maximum response to TRAP as 100% and response to buffer as 0%.. Data represents the Mean \pm standard error mean (SEM) of N=6 individual donors. **P<0.001 and ***P<0.0001. Cadherin peptide sequences are listed in the table.

Acknowledgments

This work supported by Science Foundation Ireland (SFI) Grant No. 08/IN.1/B1864

References

1. Edwards, R. J.; Moran, N.; Devocelle, M.; Kiernan, A.; Meade, G.; Signac, W.; Foy, M.; Park, S. D.; Dunne, E.; Kenny, D.; Shields, D. C. *Nat Chem Biol* 2007, 3 (2), 108-12.
2. Ishiyama, N.; Lee, S. H.; Liu, S.; Li, G. Y.; Smith, M. J.; Reichardt, L. F.; Ikura, M. *Cell* 2010, 141 (1), 117-28.

Improved antiproliferative activity of desmopressin analogs assessed by Ala-scanning

**María Pastrian¹, Fanny Guzmán², Giselle Ripoll³, Juan Garona³,
Marina Pifano³, Osvaldo Cascone¹, Graciela Ciccía⁴, Fernando
Albericio^{5,6,7}, Daniel Gómez³, Daniel Alonso³, Nancy Iannucci^{1,4}**

¹*School of Pharmacy and Biochemistry, University of Buenos Aires, Argentina;*

²*Biotechnology Nucleus, Pontifical Catholic University of Valparaiso, Chile;* ³*Laboratory of Molecular Oncology, Quilmes National University, Buenos Aires, Argentina;*

⁴*Therapeutic Peptides Research and Development Laboratory, Chemo-Romikin, Buenos Aires, Argentina;* ⁵*Institute for Research in Biomedicine, Barcelona Science Park, Spain;*

⁶*CIBER-BBN, Networking Centre on Bioengineering, Biomaterials and Nanomedicine, Barcelona Science Park, Spain;* ⁷*Department of Organic Chemistry, University of Barcelona, Spain*

E-mail: iannucci@ffyb.uba.ar

Introduction

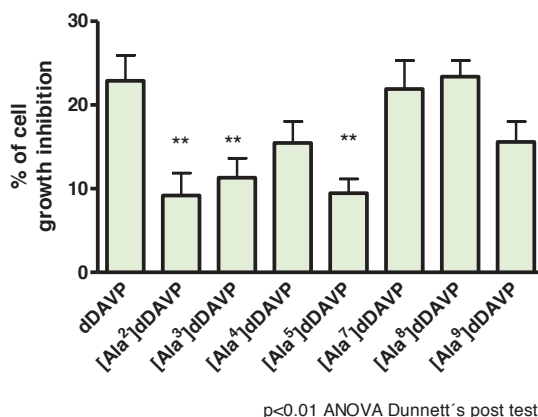
Desmopressin (dDAVP), a synthetic analog of the vasopressin (AVP) hormone, has been extensively used in the treatment of water balance related diseases and some haemostatic disorders. This analog has been modified in order to enhance its specificity and half life. The biological activity of dDAVP is mediated through its interaction with the V2 receptor (V2R) of renal collecting ducts and endothelium cells. Many authors have reported the presence of V2R in some tumor cells [1]. Our previous work described the advantages of dDAVP application at the perioperative window during mammary tumor surgery [2]. We have also reported that 2 substitutions at positions 4 and 5 in dDAVP enhance the antiproliferative activity of the resultant analog assayed in MCF7, a V2R expressing human breast carcinoma cell [3]. The aim of this work was to identify other key positions involved in the antiproliferative activity of dDAVP, by performing the Ala-scanning analysis of the peptide. Positions 1 and 6, involved in disulphide bridge formation, were not Ala-substituted in order to maintain the cyclic feature of the analogs.

Results and Discussion

Two V2R expressing human breast carcinoma cells were assayed, MCF7 and MDA-MB-231. The antiproliferative effect of dDAVP on MDA-MB-231 cells was stronger than on MCF7 cells at high concentration, thus the Ala-scanning was performed on MDA-MB-231 cells at 1000 nM peptide dose.

Ala-scanning results showed the relevance of the amino acids located at the loop of dDAVP for the antiproliferative activity (Fig. 1). The activity was reduced between 30-60% when amino acids 2-5 were substituted, while the activity was conserved when amino acids Pro⁷ and D-Arg⁸ were substituted. Finally the activity was reduced 30% when Gly⁹ was substituted.

Fig. 1: Ala-scanning analysis of dDAVP on MDA-MB-231 cells at 1000 nM peptide dose for 72 h.



In accordance with these results, we classified the analogs into three groups:

Group	Residue	Feature
I	2, 3, 5	Crucial for antiproliferative activity
II	4, 9	Tolerant to substitution
III	7, 8	Unrelated to antiproliferative activity

The structure-antiproliferative activity relationship of dDAVP on MDA-MB-231 cells assessed by Ala-scanning highlights the role of the amino acids located at the loop of the peptide. Amino acids 2, 3 and 5 might be crucial for the activity display; in the analog previously described a conservative substitution at position 5 was introduced [3]. Residues 4 and 9 result tolerant to Ala-substitution because the activity was reduced 30%. Finally, residues 7 and 8 resulted indifferent to Ala-substitution, becoming our future targets for designing novel analogs with enhanced antiproliferative activity.

Acknowledgments

GR, OC, DG, DA and NI are researchers from CONICET. Authors thank Chemo Romikin peptide synthesis facilities, and funds from ANPCyT (PAE 37011 PICT 063).

References

- [1] North WG. *Exp. Physiol.* **2000**, *85*, 27.
- [2] Alonso D.; Ripoll G.; Garona J.; Iannucci N.; Gomez D. *Curr. Pharm. Biotech.*, **2011**, *12*, 1974.
- [3] Iannucci N.; Ripoll G.; Garona J.; Cascone O.; Ciccia G.; Gomez D.; Alonso D. *Future Med. Chem.* **2011**, *3*, 1987.

Kinetic investigations on amide analogues of isoform 3 of antistasin

**R. Raykova¹, D. Danalev^{1*}, D. Marinkova¹, L. Yotova¹, S. Tchaoushev²,
N. Mahmoud¹**

¹*University of Chemical Technology and Metallurgy, Biotechnology Department, 8 Blvd. Kliment Ohridski, Sofia 1756, Bulgaria;* ²*University of Chemical Technology and Metallurgy, Department of Chemical Engineering, 8 Blvd. Kliment Ohridski, Sofia 1756, Bulgaria*

E-mail: dancho.danalev@gmail.com

Introduction

Blood coagulation cascade plays a crucial role in human homeostasis. During the process of thrombus formation two serine proteinases play a key role - Factor Xa and thrombin. They are therefore prime targets for development of new drugs for the prevention and treatment of haemostatic disorders.

Many of the strongest natural anticoagulants are isolated from bloodsucking animals and they were found in the saliva of different types of leeches. Antistasin is one of the most powerful anticoagulants discovered in 1987 by Tuszynski et al. [1]. Previously we reported for the synthesis of hybrid structures between antistasin isoform 2 and 3 and different tripeptide sequences which are well known serine proteinase inhibitors [2]. Herein we report on our kinetic investigation of newly synthesized peptide amides, analogues of isoform 3 of ATS.

Results and Discussion

Our objectives were as following:

1. To define the kinetic parameters of enzyme catalyzed reactions in presence of substrate BAPNA with model enzyme trypsin.
2. To define the type of inhibition of the serine proteinases thrombin, plasmin and factor Xa;
3. To determine if any selectivity according to the place of inhibition of thrombus formation is available.
3. To calculate K_i and V_{max} values of the investigated reactions.

To determine the amidase activity the investigation was done with one of enzymes (Factor Xa, thrombin or plasmin) and four different substrate concentrations: $9,2 \cdot 10^{-4}$ M (S1), $4,6 \cdot 10^{-4}$ M (S2), $1,8 \cdot 10^{-4}$ M (S3) и $0,9 \cdot 10^{-4}$ M (S4) in the presence of inhibitors: I_1 – Tyr-Ile-Arg-Pro-Lys-Arg-NH₂, I_2 – Phe- Ile-Arg-Pro-Lys-Arg-NH₂, I_3 – Arg-Pro-Lys-Arg-NH₂ with concentrations $1,87 \cdot 10^{-4}$ M.

The obtained results are presented in the following tables (1-3):

Table 1. Kinetic relevance of factor Xa without/with inhibitors I₁, I₂, I₃

Factor Xa	Without inhibitor	in presence of I ₁	in presence of I ₂	in presence of I ₃
K _m ·10 ⁻⁴ , [M]	9,02	9,15	9,10	9,14
V _{max} , [μmol/min.mg]	0,033	0,019	0,013	0,025

Table 2. Kinetic relevance of thrombin without/with inhibitors I₁, I₂, I₃

Thrombin	Without inhibitor	in presence of I ₁	in presence of I ₂	in presence of I ₃
K _m ·10 ⁻⁴ , [M]	9,14	9,17	9,22	9,16
V _{max} , [μmol/min.mg]	0,051	0,029	0,019	0,043

Table 3. Kinetic relevance of plasmin without/with inhibitors I₁, I₂, I₃

Plasmin	Without inhibitor	in presence of I ₁	in presence of I ₂	in presence of I ₃
K _m ·10 ⁻⁴ , [M]	8,79	9,14	9,13	9,08
V _{max} , [μmol/min.mg]	0,022	0,014	0,010	0,017

In a short conclusion we revealed:

1. According to the calculated kinetic parameters for all enzymes V_{max} value decreases in the presence of inhibitor. K_m is constant in the absence/presence of inhibitor.
2. The observed kinetics of the reactions with enzymes tripsin, thrombin, plasmin and factor Xa, in absence/presence of inhibitor show noncompetitive type of inhibition. Our investigation reveals very interesting relationship between structure of inhibitors and determined type of inhibition: the natural antistasin is competitive inhibitor. Its C-terminal forms behave as pseudo-competitive inhibitors and the amide analogues of antistasin are noncompetitive inhibitors.

Acknowledgments

We would like to thank of Erasmus-Mundus program for financial support which giving us the opportunity to participate in the 32th EPS. We would like also to thank to UCTM Scientific Fund for financial support (project 10984).

References

- [1] Tuszyński G.P.; Gasić T.B.; Gasik G.J. *J.Biol.Chem.* **1987**, 262, 9718.
- [2] Danalev D. L.; Vezekov L. T. *Bulg. Chem. Commun.*, Proceeding of the 5-th Bulgarian Peptide Symposium, **2009**, 41 (2), 99.

Lebetin peptides: Chemical synthesis, biological activity and structure activity relationships

Mosbah, A.^{1,4,5}, Marrakchi, N.², Ganzalez, M.J.³, Giralt, E.³, El Ayeb, M.², Bertin, D.¹, Baudy-Floc'h, M.,⁵ Gignes, D.,¹ Darbon, H.,⁴ Mabrouk, K.¹

¹Institut de Chimie Radicalaire, Organique et Polymères de Spécialité. Campus de Saint Jérôme, 13397 Marseille; ²Laboratoire des Venins et Toxines, Institut Pasteur de Tunis, Tunisie; ³Departement of organic chemistry, University of Barcelona, E-08028, Barcelona, Spain; ⁴AFMB, UMR 6098 CNRS et Universités Aix-Marseille I et II, Campus de Luminy, Marseille, France; ⁵UMR CNRS 6226, Université de Rennes 1, 263 Avenue du Général Leclerc, 35042 Rennes Cedex, France

amor.mosbah@univ-rennes1.fr

Introduction

Lebetin 2 forms a new family of platelet aggregation inhibitors lacking RGD sequence. It is composed of two classes of peptide analogs: lebetin 2 α (G1-G38) and lebetin 2 β (D2-G38). To evaluate the relative anti-platelet aggregation activities of each peptide, the lebetins were chemically synthesized and fully characterized. Here we described the solution structure of lebetin G1-G38 from the venom of *Vepera lebetina* by ¹H bidimensional NMR. This peptide has been demonstrated to be associated with a potent anti-platelet aggregating activity. The G1-G38 three dimensional structures consists in a compact β -bulged hairpin core from which emerge one loop and the C- and N-terminus.

Results and Discussion

Peptide synthesis and purification: G1-G38 and D2-G38 were assembled automatically using Fmoc/*t*-Bu strategy. The crude lebetin 2 (sL2) peptides were oxidized by exposure to air and purified by preparative HPLC. The folding process was independent of peptide concentration and was rapid as the oxidized peptide was detected within 1h and the reduced disappeared completely in less than 2h. The synthetic product was indistinguishable from native material as the synthetic lebetin 2 peptides were eluted with the natural lebetin 2 isoforms. The M.W. was determined by ESI mass spectrometry (found 3.943 \pm 0.4, 3.886 \pm 0.3 Da, 3.943 and 3.886 Da for lebetin 2 α and D2-G38 respectively).

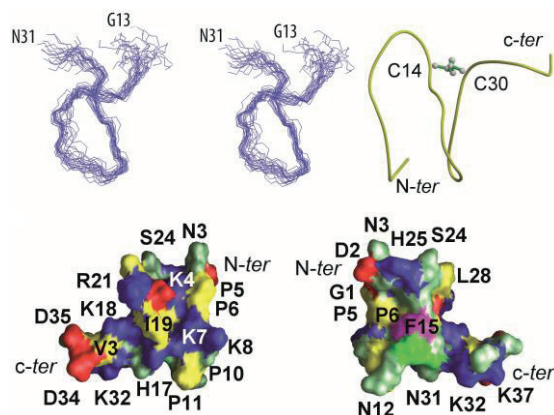
Inhibition of platelet aggregation by lebetin 2 synthetic peptides: The rabbit platelet aggregation was inhibited by both G1-G38 and D2-G38, with IC₅₀ values from 0.2 nM to 0.9 nM and 80% inhibition was obtained at peptide concentration of 0.95 and 1.5 nM respectively. Lebetin 2 α and lebetin 2 β inhibited human platelet aggregation with IC₅₀ of 2.5 nM, with 98% inhibition at 30 nM. G1-G38 and D2-G38 inhibit aggregation of rabbit and human platelet by a factor of 10 to 230 greater than those of lebetin 1[1]. This result suggests that the C-terminus disulfide-bonded sequence (Cys 14 to Gly 38) is involved in this higher level of inhibition.

Structure Calculation : Sequential assignment was obtained by the standard method first described by Wüthrich [2]. At the end of the sequential assignment procedure, almost all

protons were identified and their resonance frequency determined. The structure of G1-G38 was determined by using 301 NOE-based distance restraints. The best-fit superimposition of backbone atoms for 24 models gives RMSD values of 1.4 ± 0.31 Å for backbone atoms and 2.74 ± 0.65 Å if all non-hydrogen atoms are included between the region enclosed Cys14 and Cys30. The correlation with the experimental data shows no NOE-derived distance violation greater than 0.16 Å and the analysis of the Ramachandran plot shows (in PROCHECK software nomenclature) 88% of the residues in the most favoured, 12% in the additional, none in the generously allowed regions, nor in the disallowed regions.

Structure description: The structure of the central portion (C14-C30) of G1-G38 has been classified as bulged β -hairpin conformation, which contains a 4.3.1 loop according to the classification of Baldomero [3]. The turn is centred on the sequence Ser24 to Ser26. The *C-termini* (N31-G38) of the G1-G38 were well defined locally and adopt the same conformation in all of the 10 final refined structures and the *N-termini* (G1-N13) was in disordered conformation.

Protein surface: The surface of the G1-G38 peptide is predominantly covered by hydrophilic amino acids. However, a few hydrophobic residues, especially of L28, C14, C30, F15, G16 and G29 lie on the surface of the G1-G38 peptide with a total solvent accessible surface of 50 \AA^2 . All the polar residues are exposed to the solvent, although no well-defined salt bridges can be detected on the surface of the protein. In the complete bundle of NMR solutions, it appears that most of these surface side chains are mobile. Atomic coordinates of the best G1-G38 structures have been deposited with RSCB Protein Data Bank as entry 1Q01 and all parameters have been deposited in the Bio Mag Res Bank (BMRB) BMRB-8546.



Top: Left: Stereo view of the 10 best molecular G1-G38 structures (only $C\alpha$ atoms are displayed) superimposed for best fit. Right: Molscript ribbon drawing of the averaged minimised G1-G38 structure. The disulfide bridge are in balls and sticks and numbered.

Bottom: Molecular surface of G1-G38.

References

- [1] Barbouche R, Marrakchi N, Mabrouk K, Krifi MN, Van Rietschoten J, Fenouillet E, El Ayeb M, Rochat H. *Toxicon* : official journal of the International Society on Toxinology 1998; 36(12):1939-1947
- [2] Guntert P, Braun W, Wuthrich K. *Journal of molecular biology* 1991;217(3):517-530.
- [3] Oliva B, Bates PA, Querol E, Aviles FX, Sternberg MJ. *Journal of molecular biology* 1997;266(4):814-830.

Ligands that stabilize the amyloid β -peptide in a helical conformation reduces A β toxicity

Jyotirmoy Maity¹, Dmytro Honcharenko^{1*}, Partha P. Bose¹, J. Johansson², Roger Strömberg^{1*}

¹Department of Biosciences and Nutrition; ²Department of Neurobiology, Care Sciences and Society, Karolinska Institute, Novum, S-14183 Huddinge, Sweden

E-mail: Dmytro.Honcharenko@ki.se; Roger.Strömberg@ki.se

Introduction

There is indication that prefibrillar soluble aggregates, such as soluble A β oligomers, may play a significant role in the development of AD [1]. A β is generated by cleavage of the membrane associated amyloid β precursor protein (A β PP) [2], and it initially harbours α -helices which are strongly predicted to form β -strands [3]. Inhibition of formation of β -sheet fibrils or A β oligomers could prevent occurrence or progression of AD. Targeting of A β in an elongated, β -strand-like conformation with a range of inhibitors prevents its aggregation [4]. The disadvantages of this strategy are the lack of specificity of low molecular mass compounds and potential accumulation of cytotoxic soluble, non-fibrillar A β aggregates [5]. Prevention of β -sheet structure formation could be achieved by targeting and stabilization of the α -helical structure of A β in a state similar to its native structure in membrane embedded APP.

Results and Discussion

Recently we reported on inhibition of A β aggregation *in vitro* and reduction of its toxicity *in vivo* [6]. By using low molecular weight molecules designed to target and stabilize the A β central helix (residues 13–26) in an α -helical conformation the A β aggregation and accumulation of cytotoxic species was delayed. Oral administration of these inhibitors in *Drosophila melanogaster* expressing human A β ₁₋₄₂ in the central nervous system resulted in prolonged lifespan, decrease of locomotor dysfunction and reduction of neuronal damage.

Stabilization of the central A β α -helix appears to counteract polymerization into toxic assemblies and indicates that this approach holds promise for the development of orally available compounds against AD. Additional support for the concept comes from recent molecular dynamics simulations that also uncover details of the mechanism of unfolding of the A β central helix [7] as well as retardation of the folding in presence of ligands designed to interact with the native helical conformation [8].

Encouraged by the initial biological data we are currently developing a new generation of ligands in order to improve binding affinity to A β . This involves synthesis of various novel unnatural amino acids which then will be incorporated into short peptoid ligands. Methodology for the synthesis of novel triamino acid monomers comprises suitable protection for the solid-phase peptide synthesis (SPPS) (Figure).

The synthesis procedure is based on reaction of protected Fmoc-glycinal **2** with α -Boc-protected diamino acids. Compound **2** is made from 3-aminopropane-1,2-diol **1** with Fmoc-

OSu followed by treatment with NaIO₄ in THF [9]. Then reductive amination reaction between α -Boc-protected diamino acids and **2** were done in presence of NaBH₃CN. The secondary amine present in the triamino acids **3a-c** was protected with Boc to obtain the final monomeric building blocks **4a-c**.

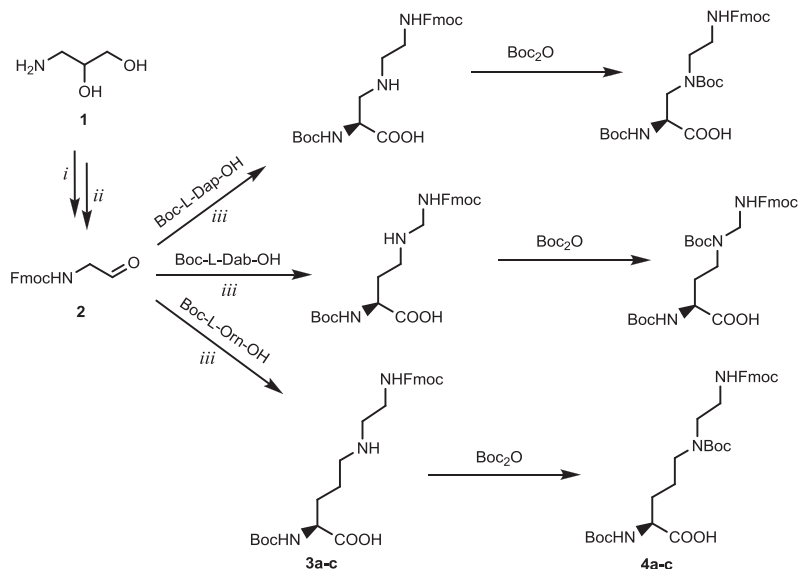


Figure. Synthesis of the novel triamino acid building blocks. *i*) FmocOSu *ii*) NaIO₄ *iii*) NaBH₃CN

The new triamino acid building blocks will be used to produce a set of new compounds, and their properties and ability to inhibit A β aggregation will be tested.

Acknowledgments

We gratefully acknowledge financial support from The Swedish Science Research Council, The Knowledge Foundation and AlphaBeta AB.

References

- [1] Walsh, D. M.; Klyubin, I.; Fadeeva, J. V.; Cullen, W. K.; Anwyl, R.; Wolfe, M. S.; Rowan, M. J.; Selkoe D. J. *Nature* **2002**, *416*, 535.
- [2] Esler, W. P.; Wolfe, M. S. *Science* **2001**, *293*, 1449.
- [3] Kallberg, Y.; Gustafsson, M.; Persson, B.; Thyberg, J.; Johansson, J. *J. Biol. Chem.* **2001**, *276*, 12945.
- [4] Mason J. M.; Kokkoni N.; Stott K.; Doig A. J. *Curr. Opin. Struct. Biol.* **2003**, *13*, 526.
- [5] Cohen F. E.; Kelly J.W. *Nature* **2003**, *426*, 905.
- [6] Nerelius, C.; Sandegren, A.; Sargsyan, H.; Raunak, R.; Leijonmarck, H.; Chatterjee, U.; Fisahn, A.; Imarisio, S.; Lomas, D. A.; Crowther, D. C.; Strömberg, R.; Johansson, J. *PNAS* **2009**, *106*, 9191.
- [7] Ito, M.; Johansson, J.; Strömberg, R.; Nilsson, L. *PLOS ONE*, **2011**, *6*, e17587.
- [8] Ito, M.; Johansson, J.; Strömberg, R.; Nilsson, L. *PLOS ONE*, **2012**, *7*, e30510.
- [9] Matsumori, N.; Masuda, R.; Murata, M. *Chemistry Biodiversity*, **2004**, *1*, 346.

Novel non-covalent staple peptides

Rubí Zamudio Vázquez,^{a,b} Judit Tulla Puche,^{a,b} Fernando Albericio^{a,b,c}

^a*Institute for Research in Biomedicine, Barcelona Science Park, Barcelona, Spain;*

^b*CIBER-BBN, Networking Centre on Bioengineering, Biomaterials and Nanomedicine, Barcelona, Spain;* ^c*Department of Organic Chemistry, University of Barcelona, Barcelona, Spain*

E-mail: fernando.albericio@irbbarcelona.org

Introduction

Triostins (A, B and C) are well-known natural products with antibiotic and antitumor activities. They belong to the family of quinoxaline antibiotics and were isolated from several *Streptomyces* strains.[1-3]

Since they are DNA bisintercalators,[4,5] higher binding affinity can be expected over monofunctional derivatives[6] and they might be used at lower concentrations thereby reducing the incidence of unwanted side effects. Nonetheless, very significant increase in binding is rarely achieved because of steric and entropic constraints.[7]

Herein, a library of twelve simplified Triostin A analogues has been synthesized and evaluated for its antiproliferative activity against four human cancer cell lines. It is demonstrated that having the peptide in the staple form that bisintercalator cyclic (depsi)peptides adopt when binding to DNA[8,9] improves its biological activity.

Results and Discussion

We designed and synthesized a small library of staple peptides defined by a β -hairpin motif, in which two antiparallel strands are connected by a two-residue loop (*D*-Pro-Gly) with two quinoxalines attached to both ends.

The chosen approach to synthesize the peptide scaffold was the Solid Phase Peptide Synthesis (SPPS) with the introduction of the 2-quinoxalinecarboxylic acids and the side-chains deprotection as the final stages carried out in solution. The aromatic groups are thought to be oriented in parallel to interact with two adjacent DNA base pairs.

The synthesized compounds were evaluated for their antiproliferative activities against four human cancer cell lines: cervical adenocarcinoma HeLa cells, lung carcinoma A-549 cells, breast adenocarcinoma SK-BR-3 cells and colon adenocarcinoma HT-29 cells. Most of our compounds are cytotoxic (Figure 1) and some of them show a lower IC₅₀ value than Triostin A.

HeLa cells were incubated with the most active compound (Comp 2) [5 μ M] at 37 °C, in 5% CO₂ for 5 min and visualized by confocal microscopy. Our drug entered rapidly to the cells by diffusion and stained intensely the nucleoli, thus DNA affinity was corroborated.

We used the ApoTox-Glo™ Triplex Assay (Promega) to assess viability, cytotoxicity and caspase activation events after treating HeLa cells. We observed caspase-3/7 activation without previous loss of cell membrane integrity, which indicates that our compound causes apoptosis.

UV Circular Dichroism spectroscopy (CD) was used to investigate the secondary structure of compound 2. The expected β -sheet conformation was corroborated.

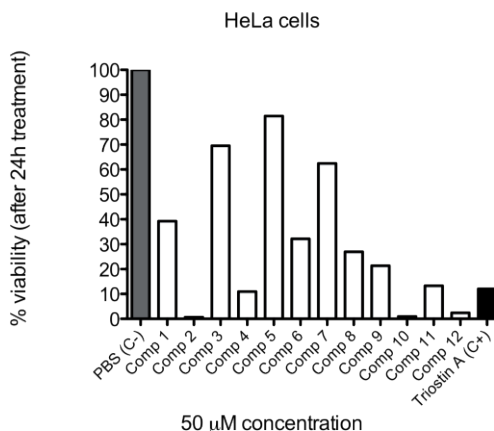


Figure 1. Antiproliferative activity of the synthesized Triostin A analogues against cervical adenocarcinoma cells.

Acknowledgments

R.Z.V. thanks "la Caixa" Foundation and IRB Barcelona for a PhD fellowship.

References

- [1] Shoji, J. I.; Katagiri, K. *J. Antibiotics Ser. A*. **1961**, *14*, 335.
- [2] Kuroya, M.; Ishida, N.; Katagiri, K.; Shoji, J.; Yoshida, T.; Mayama, M.; Sato, K.; Matsuura, S.; Niinome, Y.; Shiratori, O. *J. Antibiotics Ser. A*. **1961**, *14*, 324.
- [3] Matsuura, S. *J. Antibiotics Ser. A*. **1965**, *18*, 43.
- [4] Wang, A. H.; Ughetto, G.; Quigley, G. J.; Hakoshima, T.; van der Marel, G. A.; van Boom, J. H.; Rich, A. *Science* **1984**, *225*, 1115.
- [5] Sheldrick, G. M.; Heine, A.; Schmidt-Base, K.; Pohl, E.; Jones, P. G.; Paulus, E.; Waring, M. J. *Acta Crystallogr., Sect. B* **1995**, *51*, 987.
- [6] Antonini, I.; Santoni, G.; Lucciarini, R.; Amantini, C.; Sparapani, S.; Magnano, A. *J. Med. Chem.* **2006**, *49*, 7198.
- [7] Martínez, R.; Chacón-García, L. *Curr. Med. Chem.* **2005**, *12*, 127.
- [8] Boger, D. L.; Chen, J. H.; Saionz, K. W.; Jin, Q. *Bioorg. Med. Chem.* **1998**, *6*, 85.
- [9] Negri, A.; Marco, E.; García-Hernández, V.; Domingo, A.; Llamas-Saiz, A. L.; Porto-Sanda, S.; Riguera, R.; Laine, W.; David-Cordonnier, M-H.; Bailly, C.; García-Fernández, L. F.; Vaquero, J. J.; Gago, F. *J. Med. Chem.* **2007**, *50*, 3322.

On the mechanism of degradation of oxytocin and its analogues in aqueous solutions - part II

**Kazimierz Wiśniewski, Jens Finnman, Marion Flipo, Robert Galyean,
Claudio D. Schteingart**

Ferring Research Institute, Inc, San Diego, CA 92121, USA

E-mail: Kazimierz.Wisniewski@ferring.com

Introduction

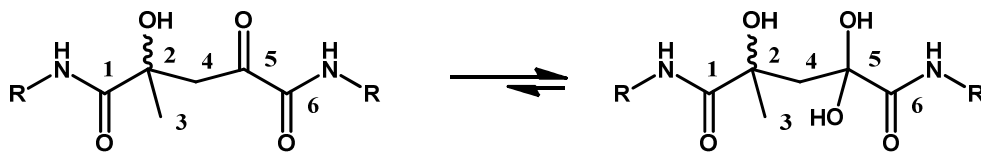
The cyclic nonapeptide oxytocin (OT) is extensively used for induction of labor by intravenous administration of an aqueous formulation [1]. Surprisingly, little is known about its mechanism of degradation in solution or the structure of the degradation products. Recent studies have identified monomeric polysulfides and dimeric products, postulated to derive from β -elimination followed by deamidation and dimerization [2, 3].

We have previously reported on the degradation of OT and its analogues in aqueous solutions [4], and also observed monomeric polysulfides with up to 6 sulfur atoms. However, we found that the dimeric degradants generated from various N-terminally modified OT analogues were identical, indicating that the N-terminal groups were lost in the process. We hypothesized a dimerization mechanism starting with β -elimination via cleavage of the C-S bond of Cys¹ to produce a [Δ Ala¹]OT intermediate that could be hydrolyzed to an N-pyruvoyl (N-Pyv) linear peptide with loss of the N-alkyl group [5]. This intermediate would subsequently dimerize with the formation of a new C-C bond, possibly through an aldol-type condensation, and formation of a disulfide bond between Cys⁶ of both monomers, after loss of one or two sulfur atoms.

To provide evidence for our proposal, the OT analogues [Pyv¹,Cys⁶]OT, [Pyv¹,Ala⁶]OT, [[¹³C₃]Pyv¹,Cys⁶]OT and [[¹³C₃,¹⁵N]Cys¹]OT were synthesized, incubated at pH 7.4, and the degradation products analyzed by HPLC, LCMS, and ¹³C NMR. Based on these studies we propose a mechanism of OT degradation in slightly acidic to neutral solutions as well as the structures of the dimeric degradants.

Results and Discussion

Incubation of OT, [Pyv¹,Cys⁶]OT and ([Pyv¹,Cys⁶]OT)₂ led to identical dimeric degradation products, strongly suggesting that [Pyv¹,Cys⁶]OT is an intermediate in the OT degradation process. Treatment of the dimers with DTE resulted in compounds with molecular weights increased by 2 a.m.u., indicating the dimers are held by one disulfide bridge and another, non-reducible linkage. The formation of this linkage may require that the intermolecular disulfide bridge is formed first, as the non-cysteine analogue [Pyv¹,Ala⁶]OT showed negligible dimerization. The observed ¹³C NMR chemical shifts of the two major ¹³C enriched dimers (Table) and ¹³C-¹³C COSY NMR spectrum of the slower running dimer are in good agreement with the connectivity shown in the Table:



Compound	Chemical shifts (ppm)					
	C1	C2	C3	C4	C5	C6
Faster dimer (observed)	176.8	72.7	24.0	47.9	88.4	172.0
Slower dimer (observed)	178.1	72.9	24.5	45.9	88.0	171.6
ChemDraw predicted for left structure, R=H	176.2	77.2	23.8	39.7	197.6	163.2
ChemDraw predicted for right structure, R=H	176.2	70.2	24.2	48.8	100.1 ^a	172.3

Table. ¹³C NMR chemical shifts in D₂O of carbon atoms involved in the formation of aldol-type linkage. The chemical shifts of C-2, 4, and 5 indicate preference for the hydrated form in water. ^a Chemical shift for hydrated carbonyl in pyruvic acid is ~94 ppm.

Based on the above we propose the revised structures of dimeric products of OT degradation shown in Fig. 1.

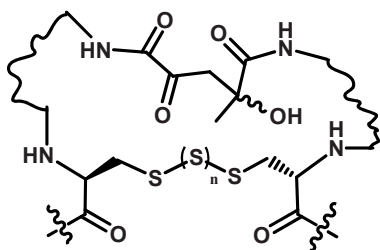


Fig. 1. Proposed structures of dimeric products of OT degradation: major ($n = 0$) and minor ($n = 1$). The portions of OT molecule that don't participate in the process are represented by irregular lines.

We suggest the following mechanism of OT degradation in near-neutral solutions: The process begins with a C-S bond cleavage within the Cys¹ residue by β -elimination yielding a putative linear persulfide [Δ Ala¹,Cys(S)⁶]OT. This intermediate donates a sulfur atom to an intact OT molecule or an OT polysulfide to produce higher OT polysulfides and converts to [Pyv¹,Cys⁶]OT via hydrolysis of the Δ Ala residue. The pyruvoyl peptide dimerizes by the formation of a new disulfide bridge between the Cys⁶ residues and a second C-C bond via a non-stereospecific aldol-type condensation. Alternatively, the persulfide intermediate hydrolyses to [Pyv¹,Cys(S)⁶]OT and reacts with [Pyv¹,Cys⁶]OT to yield the minor, trisulfide dimers (Fig. 1, $n=1$). The mechanism outlined here may be general for cyclic peptides containing an N-terminal Cys residue forming an intramolecular disulfide bridge, although the reaction rate may depend strongly on the ring size.

References

- [1] Trissel, L. A.; Zhang, Y.; Douglass, K.; Kastango, E. *Int. J. Pharm. Comp.* **2006**, *10*, 156.
- [2] Hawe, A.; Poole, R.; Romeijn, S.; Kasper, P.; van der Heijden, R.; Jiskoot, W. *Pharm. Res.* **2009**, *26*, 1679.
- [3] Avanti, C.; Permentier, H. P.; Dam, A.; Poole, R.; Jiskoot, W.; Frijlink, H. W.; Hinrichs, W. L. *Mol. Pharm.* **2012**, *9*, 554.
- [4] Wisniewski, K.; Finnman, J.; Flipo, M.; Galyean, R.; Schteingart, C. D. In *Peptides. Building Bridges: Proceedings of the 22nd American Peptide Symposium*. M. Lebl (Ed), Prompt Scientific Publishing, San Diego 2011, pp 60-61
- [5] Patchornik, A.; Sokolovsky, M. *J. Am. Chem. Soc.* **1964**, *86*, 1206.

Peptide inhibitors of integrin $\alpha_{IIb}\beta_3$ activation

**Vassilios Moussis¹, Klytaimnistra Kiouptsi¹, Alexia Gourogianni¹,
Vassiliki Koloka¹, Marion Egot², Christilla Bachelot-Loza², Eugenia
Panou-Pomonis¹, Maria Sakarellos-Daitsiotis¹,
Demokritos C. Tsoukatos¹, Vassilios Tsikaris¹**

¹*Department of Chemistry, University of Ioannina, Ioannina, Greece;* ²*INSERM U765
Paris, France*

E-mail: btsikari@cc.uoi.gr

Introduction

$\alpha_{IIb}\beta_3$, the major expressed on platelet membrane integrin, plays a critical role in haemostasis by mediating between platelet to platelet and platelet to matrix protein interactions. Physiological platelet agonists activate transduction pathways (inside-out signalling) leading to the conversion of $\alpha_{IIb}\beta_3$ from a 'low' to a 'high' affinity state, which allows the integrin to become competent to bind adhesive proteins, such as fibrinogen and von Willebrand factor. Following ligand engagement, $\alpha_{IIb}\beta_3$ triggers transduction events (outside-in signalling) which, co-ordinated with other signals and activated by other platelet receptors, lead to platelet aggregation. They are important signalling molecules which mediate the above bi-directional transfer of information from the extra-cellular matrix to the cytoplasm and vice versa. The conformational change, responsible for the bi-directional signalling is thought to be initiated at the cytoplasmic domain and then propagated via the trans-membrane segments to the extra-cellular part of $\alpha_{IIb}\beta_3$. Platelet integrin $\alpha_{IIb}\beta_3$ contains an acidic membrane distal motif, ¹⁰⁰⁰LEEDDEEGE¹⁰⁰⁸, in the cytoplasmic domain of the α_{IIb} subunit. We have recently reported that a lipid-modified peptide corresponding to the above region, palmitoyl-K-LEEDDEEGE (pal-K-1000-1008), is platelet permeable, has inhibited platelet aggregation induced by thrombin and by pal-KVGF¹⁰⁰⁰FKR, fibrinogen and PAC-1 binding to activated platelets [1]. Regarding the mechanism of the above inhibition we reported recently that the peptide inhibited the association of talin with $\alpha_{IIb}\beta_3$. Moreover, we have reported that a peptide corresponding to the extra-cellular sequence YMESRADR (313–320) of the α_{IIb} subunit plays an important role in platelet activation by taking the place of a clasp between the head domains of the two subunits [2]. This peptide also inhibited fibrinogen binding and $\alpha_{IIb}\beta_3$ -mediated outside-in signalling. The aim of the present study was to investigate the cooperativeness of the intra- and extra-cellular peptides on platelet aggregation inhibition and their effect on the phosphorylation of the signalling molecules focal adhesion kinase FAK and extracellular regulated kinase ERK.

Results and Discussion

Pal-K-1000-1008 together with the extracellular YMESRADR peptide, at concentrations lower than their IC₅₀ values, showed cooperative inhibition of platelet aggregation. The peptide combination inhibited also fibrinogen and PAC-1 binding to activated platelets. FAK phosphorylation is a post-aggregation event related to outside-in activation of the receptor. The combination of peptides inhibited FAK phosphorylation. ERK phosphorylation is independent from platelet aggregation, and is enhanced by RGD-peptide

inhibitors. The combined peptides inhibited ERK2 phosphorylation. Pathological thrombosis is leading to occlusion and irreversible tissue damage or infarction in diseased vessels. Because of the importance of $\alpha_{IIb}\beta_3$ integrin in platelet aggregation, it has become an attractive pharmacological target for the prevention of ischemic cardiovascular events. Strategies to inhibit its function still include RGD analogs. The above inhibitors have presented clinical problems also due to their integrin activating properties [3, 4]. The results of the present work, using intracellular in combination with extra-cellular peptide inhibitors, with a non RGD like mechanism of action, may provide an alternative pharmacological approach.

Acknowledgements

This work was supported by the Joint Research and Technology program Platon France-Greece.

References

- [1] Koloka, V.; Christofidou, E.; Vaxevelis, S.; Dimitriou, A.A.; Tsikaris, V.; Tselepis, A.D.; Panou-Pomonis, E.; Sakarellos Daitsiotis, M.; Tsoukatos, D.C. *Platelets* **2008**, *19*, 502.
- [2] Mitsios, J.V.; Tambaki, A.P.; Ampatzis, M.; Biris, N.; Sakarellos-Daitsiotis, M.; Sakarellos, C.; Soteriadou, K.; Goudevenos, J.; Elisaf, M.; Tsoukatos, D.C.; Tsikaris, V.; Tselepis, A.D. *E. J. Biochem.* **2004**, *271*, 855.
- [3] Du X.P., Plow E.F., Frelinger A.L., O'Toole T.E., Loftus J.C., Ginsberg M.H. *Cell* **1991**, *65*, 409.
- [4] Peter K., Schwarz M., Ylanne J, Kohler B., Moser M., Nordt T., Salbach P., Kubler W., Bode C. *Blood* **1998**, *92*, 3240.

A proteomic approach to investigate the mechanism of action of anticancer peptides

Filippo Genovese¹, Alessandra Gualandi^{1,2}, Laura Taddia¹, Monica Caselli¹, Glauco Ponterini¹, Stefania Ferrari, Gaetano Marverti¹, Remo Guerrini³, Michela Pelà^{1,3}, Giorgia Pavesi¹, Claudio Trapella³, Maria Paola Costi¹

¹*University of Modena and Reggio Emilia, Modena, Italy;* ²*CRBA, S. Orsola University Hospital, Bologna, Italy;* ³*University of Ferrara, Ferrara, Italy*

E-mail: mariapaola.costi@unimore.it

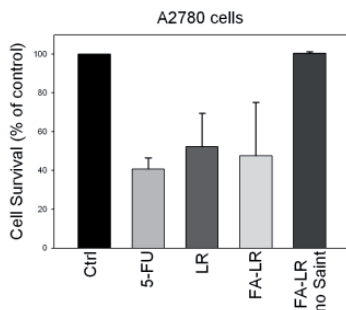
Introduction

Many efforts to improve survival of patients affected by Ovarian Cancer (OC) have focused on more effective systemic therapies and on the search for new therapeutic targets. One of the molecular targets for OC is human Thymidylate Synthase (hTS), a homodimeric enzyme essential for DNA biosynthesis. The main goal of our research is to identify compounds able to inhibit hTS by interfering with its dimerization, without causing its over-expression and the onset of cellular drug resistance against the traditional hTS-targeted compounds. We have recently discovered some peptides which specifically target the hTS dimer interface and inhibit the enzyme by stabilizing its di-inactive form [1]. These molecules have been recently investigated for their SAR profile. LR, our lead compound, inhibits the intracellular enzyme in both cisplatin (cDDP)-sensitive and -resistant ovarian cancer cells without causing protein overexpression, thus showing a potential for overcoming the limits of OC chemotherapy. This work aims at setting up a proteomic approach able to provide information on the changes in the protein expression profile induced in OC cells by treatment with LR with respect to a well-known folate antimetabolite, Pemetrexed (PTX) and identify key proteins that are involved in its mechanism of action.

Results and Discussion

The biological activity of the peptides has been tested in two cDDP-sensitive OC cell lines, 2008 and A2780, and their resistant counterparts, C13* and A2780/CP, in order to display and study possible different responses modulated by cDDP resistance. The cell growth inhibitory effect of the peptides has been compared to that of the classic, catalytic-pocket binding folate-cycle inhibitor 5-fluorouracil (5-FU). The cytotoxicity of LR versus the four cell lines was comparable to or lower than that of 5-FU, in particular when it was transfected into cells by means of a peptide delivery system [2]. To improve internalization of the peptide by folate receptor molecules, which are abundant in cancer-cell membranes, the N-terminus was engineered with a folic acid (FA) derivative; the FA-LR conjugate showed a comparable cytotoxic effect against these ovarian cell lines, as shown in Figure 1. The best activity of FA-LR was observed when protease inhibitors were associated with the delivery of the conjugate supporting the already observed peptide liability.

LR effectiveness is only partially affected by cisplatin-resistance phenotype particularly when the latter is bound to FA, since little differences were observed between 2008 or A2780 cells and their respective resistant counterparts, as cell growth inhibition achieved was about 40-50% in all cell lines.



Effects of the peptide LR on growth of cisplatin-sensitive A2780 cells. 24 h after seeding, cells were treated for 72 h with 10 μ M 5-FU or 10 μ M LR transfected into cells alone or conjugated to FA by means of a peptide delivery system (Saint PhD).

In order to investigate the effects of hTS-interface-mimicking peptides at a cellular level, we started a parallel study in which the cellular behavior of the LR peptide was investigated in combination with the proteomic differential analysis of the cytoplasmatic proteins of treated vs. untreated OC cells. The same experiment was performed with PTX. The bioinformatic analysis of the effects of our peptide drug

candidate indicates that deregulations can be mainly assigned to modulation of translational initiation, termination of RNA Pol-II transcription, transport, and protein catabolic events. Although apparently folate pathway members are not directly altered at a protein level, as the selection of ions to be sequenced is stochastic and biased towards abundant peptides, the bioinformatic analysis of LR-modulated proteins suggested cellular investigations on the proteins of the folate-associated genes showing the largest number of dependencies to the species of the core set, *e.g.*, deoxycytidine kinase (DCK), which is required for the phosphorylation of several deoxyribonucleosides and nucleoside analogues. Comparison with the PTX-modulated proteins shows that some proteins of the proteasome complex and ribonucleoproteins are involved in both cases. These differences suggest that the two compounds may show a different mechanism of action which is in agreement with the hypothesized pharmacological model. Detailed cellular proteins profile based on the inferred roles of the identified proteins will further clarify the biological effects.

Acknowledgments

This work is supported by AIRC-DROC IG10474; www.unimore.airc-droc.it.

References

- [1] Cardinale, D. et al. *PNAS* **2011**, *108*, E542.
- [2] van der Gun, B.T. et al. *J. Control. Release* **2007**, *123*, 228.

Ribavirin-Cell Penetrating Peptides hybrid molecules a promising alternative as inhibitors of multienzyme systems

**R. Raykova¹, D. Danalev*¹, L. Yotova¹, N. Lubin-Germain², J. Uziel²,
N. Mahmoud¹, B. Hristova^{1,2}**

¹*University of Chemical Technology and Metallurgy, Biotechnology Department, 8 Blvd. Kliment Ohridski, Sofia 1756, Bulgaria;* ²*Université de Cergy-Pontoise, Laboratoire SOSCO EA 4505, 5 Mail Gay-Lussac, Neuville sur Oise, 95031 Cergy-Pontoise cedex, France*

E-mail: dancho.danalev@gmail.com

Introduction

Hepatitis C is a liver disease provoked by a virus known as HCV. The disease is insidious. HCV causes anorexia, nausea, vomiting, fever, fatigue and jaundice. In about 40% of sufferers the disease is short, but others become chronic. In the chronic form in about 20% of cases the final result is cirrhosis of the liver and in the remaining 20% it leads to liver cancer. HCV is a very serious problem today. About 3% of people infected with HCV worldwide, i.e. about 4 million are residents of Europe. 170 million people carry the disease as a chronic illness with the potential to develop into cancer in their liver. All these people represent a "reservoir" for storage and distribution of HCV.

Ribavirin, the nucleoside analog 1- β -D-ribofuranosyl-1,2,4-triazole-3-carboxamide, known by the trade name Virazole (also known as Rebetron in combination with interferon- α), exhibits antiviral activity against a variety of RNA viruses (paramyxoviruses, flaviviruses, etc) as well as some DNA viruses. In humans ribavirin is currently used in combination with interferon- α to treat HCV infections. This lack of strict specificity and a broad spectrum of activity are due to its multifunctional mechanism of action against viruses. These characteristics have made ribavirin a drug of substantial research interest. Unfortunately, ribavirin shows a significant toxicity, causing bleeding in accumulation [1].

The process of introducing drugs into cells has always proved a major challenge for research scientists and for the pharmaceutical industry. The cell membrane is selectively permeable and supports no generic mechanism for their uptake. A drug must be either highly lipophilic or very small to stand a chance of cellular internalization. These restrictions mean that the repertoire of possible drug molecules is limited. The existing methods for delivery of macromolecules, such as viral vectors and membrane perturbation techniques, can result in high toxicity, immunogenicity and low delivery yield. However, in 1988 the remarkable ability of a peptide to traverse a cell's plasma membrane independent of a membrane receptor was revealed. They cause changes in the membranes leading to their permeability. This type of peptide molecules is called cell penetrating peptides (CPP) [2]. A well know member of this group of peptides, with proven membrane-penetrating properties, is so called "sweet arrow peptide" (SAP) (VRLPPP)₃ described by Fernandez-Carneado et al. in 2004 [3].

Herein, we report on the synthesis of four SAP analogues replacing Leu residue with Asp, Glu, Asn and Gln in order to incorporate ribavirin in the CPP molecule.

Results and Discussion

We chose to replace Leu residue of SAP with the amino acids Asp, Glu, Asn and Gln and to synthesise the following products: H-Val-Arg-Asp (ribavirin)-Pro-Pro-Pro-OH; H-Val-Arg-Glu (ribavirin)-Pro-Pro-Pro-OH; H-Val-Arg-Asn-Pro-Pro-Pro-ribavirin; H-Val-Arg-Gln-Pro-Pro-Pro-ribavirin. These amino acids were chosen because of its adequate structure to provide us the necessary additional functional groups in their side chains for bonding of the drug molecules. This decision was also framed by the idea of using two strategies for the synthesis of CPP-drug molecule. For the synthesis of aim CPP we used conventional SPPS (solid phase peptide synthesis) by Fmoc-strategy.

Strategy I

Here suitably modified ribaverin molecule was previously linked to the carboxyl function of the side chain of Asp or Glu. For this purpose, two acidic amino acids were used as allyl esters on α COOH group. On every stage, this function was unblocked by treatment with tetrakis / Pd, allowing the extension of the main chain. Additionally, during this strategy we used chlorotrytyl resin as a solid phase support. Thus, we synthesized the first two peptide H-Val-Arg-Asp(OAll)-Pro-Pro-Pro-OH and H-Val-Arg-Glu(OAll)-Pro-Pro-Pro-OH. Since in our opinion the incorporation of drug molecule in the middle of the peptide fragment could lead to distortions of secondary and tertiary structure of the peptide, and hence the loss of its membrane penetrating properties, we decided to realize the synthesis of these peptides, but linking drug molecules to their C-terminus. For this purpose, we used the following strategy II.

Strategy II.

Like in the first strategy we replaced the amino acid Leu in the structure of SAP with Gln and Asn using an original strategy for the synthesis of Gln and Asn-containing peptides previously created by us, assuming adequately protected Glu and Asp and connect them to the Rink amide resin [4]. For this purpose the connection of peptide and resin is made by COOH functions in a side chain of Glu and Asp. Typical of Rink amide resin is that the final peptide unblocking leads to the amides obtaining. Thus using Glu and Asp as starting amino acids, in the final peptides they become to Gln and Asn.

We synthesized 4 new peptides analogues of SAP with potential cell penetrating properties. A new interesting strategy for synthesis of Gln and Asn containing peptides starting form Glu and Asp and using Rink amide resin was applied for the synthesis of two of the target peptides. The connection of ribavirin on the newly synthesized CPP is under progress.

Acknowledgments

We would like to thank of Erasmus-Mundus program for financial support which giving us the opportunity to participate in the 32th EPS. We would like also to thank to National Fund Scientific investigations of Bulgaria for financial support (project DOO2-296).

References

- [1] Crotty S.; Cameron C.; Andino R. *J. Mol. Med.* **2002**, *80*,86.
- [2] Vezekov L. L. ; Maynadier M. ; Hernandez J.-F.; Averlant-Petit M.-C.; Fabre O.; Benedetti E.; Garcia M.; Martinez J.; Amblard M. *Bioconjugate Chem.* **2010**, *21*, 1850.
- [3] Fernandez-Carneado J.; Kogan M.J.; Castel S.; Giralt E.; *Angew. Chem. Int. Ed.* **2004**, *43*, 1811.
- [4] Minchev I.; Danalev D.; Vezekov L., Nikolaeva-Glomb L., Galabov A., *Inter. J. Pept. Res. Therap.* **2010**, *16*, 233.

Sequences of ACE-inhibitory precursor peptides from bacterial fermented milk of *Camelus dromedarius*

Omar A. Alhaj^{1*}, Hans Brückner^{2,3}, Abdulrhman S. Al-Khalifa¹

¹Department of Food Science and Nutrition, College of Food and Agricultural Sciences, King Saud University (KSU), Riyadh, Kingdom of Saudi Arabia, PO Box 2460, Riyadh 11451; ²Research Center for BioSystems, Land Use and Nutrition (IFZ), Department of Food Sciences, Justus-Liebig University of Giessen, 65392 Giessen, Germany; ³Visiting Professor at ¹KSU, Riyadh, Kingdom auf Saudi Arabia

E-mail: oalhaj@ksu.edu.sa

Introduction

Hypertension is recognized as a serious risk factor for cardiovascular diseases. Since the vasoactive octapeptide angiotensin II is converted enzymatically from its precursor peptide angiotensin I, hypertension can be treated by drugs having angiotensin I converting enzyme (ACE) inhibitory activities. Peptides showing such activities have been isolated from various food proteins including fermented milk products [1-3]. Few data are available from lactic fermented milk of dromedaries (*Camelus dromedarius* L.), commonly referred to as 'camels'. We treated camel milk with bacterial starter cultures and analyzed the peptides released (see Table 1) for sequences containing ACE-inhibitory peptides.

Results and Discussion

Milk was from dromedaries of the 'Majaheim' breed from a farm located in Al-Jawf, an oasis town in northwestern Saudi Arabia. The milk was sterilized and inoculated with bacterial starter cultures, *Lactobacillus helveticus* (LMG 11445) or *Lactobacillus acidophilus* (LMG 11430), and incubated anaerobically at 37 °C for 127 and 112 h, respectively. Samples were filtered through 3 kDa cutoff dialysis membranes [4], analyzed by HPLC-MALDI-TOF MS and identified by searching the SwissProt database with the Mascot search algorithm. Seven potential ACE-inhibitory peptides were characterized resulting from the action of *Lactococcus helveticus* and two peptides from *Lactobacillus acidophilus*. All peptides originated from camel milk β -casein [5] and contained C-terminal sequences that could be correlated with peptides of established ACE-inhibitory activity [6] (Table 1).

Conclusions

It is hypothesized that the active, C-terminal peptides from the precursor peptides identified will be released by digestive enzymes of the gastrointestinal tract of the human body. Since Saudi Arabia is the world's second largest producer of camel milk, amounting to 93.015 metric tons in 2009, and consumption of camel milk is common in Arab countries as well as in Pakistan, India and China, regular consumption of lactic fermented camel milk might assist in reducing cardiovascular diseases resulting from hypertension.

Table 1. Selected sequences of (a) ACE-inhibitory peptides of established activity released from milk proteins [6] in comparison to (b) relevant peptides characterized in bacterial fermented milk of camel. Sequences of potentially ACE-inhibitory peptides encrypted in (b) are underlined. Amino acid sequence positions in camel β -casein [5] are given.

(a) Established ACE-inhibitory peptides [6]	(b) Identified peptides in fermented camel milk	Camel [5] β -casein	Starter culture
KVLPVP	LSLSQF <u>KVLPVP</u> Q	155-167	1
	SLSQF <u>KVLPVP</u> Q	156-167	1
	SQF <u>KVLPVP</u> Q	158-167	1
LHLPLP	TDLEN <u>LHLPL</u> PL	119-131	1
	DLEN <u>LHLPL</u> PL	120-131	1
	LEN <u>LHLPL</u> PL	121-131	1
KVLPVP	<u>KVLPVP</u> QQMVPYPQ	161-174	1
AVPYQR	KVLPVPQQM <u>VPYP</u> Q	161-174	1
AVPYP	KVLPVPQQM <u>VPYP</u> Q	161-174	1
PYP	KVLPVPQQM <u>VPYP</u> Q	161-174	1
YQEPVLQPV R	VLPFQEPVPD <u>PVR</u> G	182-195	2
	FQEPVPD <u>PVR</u>	185-194	2
1 <i>Lb. helveticus</i>			
2 <i>Lb. acidophilus</i>			

Acknowledgments

This research is supported by ‘The National Plan for Science & Technology’ (NPST) of the King Saud University, Riyadh (project number 11-AGBR 1603-02).

References

- [1] Alhaj, O. A.; Al Kanhal, H. *Int. Dairy J.* **2010**, *20*, 811.
- [2] Li, G. H.; Le, G. W.; Shi, Y. H.; Shrestha, S. *Nutrition Res.* **2004**, *24*, 469.
- [3] López-Fandiño R.; Otte, J.; van Camp, J. *Int. Dairy J.* **2006**, *16*, 1277.
- [4] Brückner, H.; Schieber, A. *Eur. Food Res. Technol.* **2000**, *210*, 330.
- [5] Kappeler, S.; Farah, Z.; Puhan, Z. *J. Dairy Res.* **1998**, *65*, 209.
- [6] Meisel, H.; Walsh, D. J.; Murray, B.; FitzGerald, R. J. In *Nutraceutical Proteins and Peptides in Health and Disease*; Mine Y. and Shahidi, F., Eds.; CRC Press, Boca Raton, FL, USA, 2006, Vol. 4, pp. 269- 315.

Short bioactive peptides against *Plasmodium gallinaceum*

Adriana Farias Silva,¹ Ceres Maciel,² Margareth Lara Capurro,²
Antonio de Miranda,³ Vani Xavier de Oliveira Junior¹

¹Universidade Federal do ABC, Santo André, Brazil; ²Universidade de São Paulo, São Paulo, Brazil; ³Universidade Federal de São Paulo, São Paulo, Brazil

adriana.silva@ufabc.edu.br

Introduction

Malaria is an acute febrile infectious disease caused by protozoa of the *Plasmodium* genus and is transmitted by mosquitoes of the genus *Anopheles*. The World Health Organization has reported that 250-500 million people contract malaria annually, resulting around 800 thousand deaths [1]. However, efforts to control this disease are hampered by drug resistance in parasites, insecticide resistance in mosquitoes, and the lack of an effective vaccine [2]. Recently, we have reported a research, which showed the angiotensin II (AII) action against mature sporozoites of *Plasmodium gallinaceum* [3]. In an attempt to establish the smallest amino acid sequence to biological activity and analyze its hydrophobic cluster influence, we synthesized and tested a series of AII analogues.

Results and Discussion

AII analogues were synthesized using solid phase method on chloromethylated resin, cleaved from the resin using TFMSA/TFA mixture, purified by RP-HPLC and characterized by mass spectrometry. The conformational studies were performed by circular dichroism (CD) (Data not shown). Lytic activity assays (*in vitro*) were performed using mature sporozoites, collected from salivary glands of *A. aegypti* infected. The sporozoites were incubated with peptides at 37°C for 1 hour, and the cell membrane integrity was monitored by fluorescence microscopy - Figure 1.

The CD studies suggest that the active analogues adopt a β -fold conformation similar to obtained for the native AII, which have been related in several techniques as NMR and X-Ray diffraction [4,5]. The results showed that the hydrophobic cluster formed by Tyr-Ile-His has influence in the antimalarial activity.

The results were divided in three distinct analogues groups: analogues (2, 3 and 4) that presented a reduction among 15% to 30% of the AII biological activity; equipotent analogues (1, 5 and 6), among them the short analogues 5 and 6, and the group formed by analogue 7, that presented lower lytic activity.

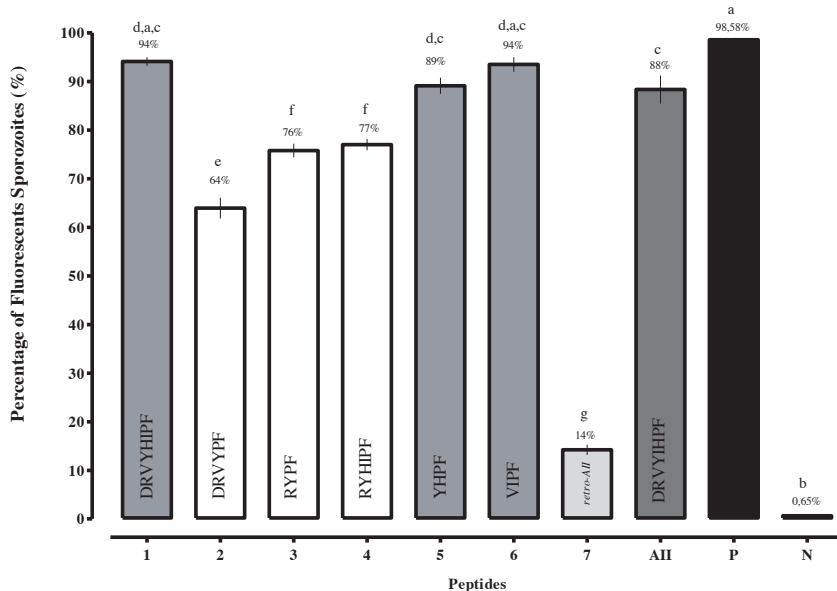


Figure 1. Effects of the AII analogues on membrane permeability expressed as the percent of fluorescent mature sporozoites. Data are presented as mean \pm standard deviation of fluorescent sporozoites percentage/blade ($n=9$). Different letters indicate significant difference between the groups treated with AII, peptide analogues and positive control group (P, treated with digitonin and PBS) and negative (N, treated with PBS), respectively (ANOVA followed by Tuckey test, $p<0,001$).

In summary, short peptides may provide a significant antiplasmodial activity on *Plasmodium gallinaceum* and that ability to rupture the membrane is related to hydrophobic cluster or hydrophobic amino acid residues in the structure of these compounds. Our approach is helpful to understand the contribution of this analogues opening new perspectives towards the design of new chemotherapeutic agents.

Acknowledgments

This research was supported by FAPESP and CNPq

References

- [1] Lundqvist, J.; Larsson, C.; Nelson, M.; Andersson, M.; Bergstrom, S.; Persson, C. *Infect. Immun.* **2010**, *78*, 1924.
- [2] Ito, J.; Ghosh, A.; Moreira, L. A.; Wimmer, E. A.; Jacobs-Lorena, M. *Nature* **2002**, *417*, 452.
- [3] Maciel, C.; Oliveira, V. X.; Fázio, M. A.; Nacif-Pimenta, R.; Miranda, A.; Pimenta, P. F.; Capurro, M. L. *PLoS ONE* **2008**, *3*, e3296.
- [4] Carpenter, K. A.; Wilkes, B. C.; Scheller, P. W. *Eur. J. Biochem.* **1998**, *251*, 448.
- [5] Tzakos, A. G.; Bonvin, A. M. J. J.; Troganis, A.; Cordopatis, P.; Amzel, M. L.; Gerothanassis, I. P.; van Nuland, N. A. J. *Eur J Biochem* **2003**, *270*, 849.

Synthesis and anticancer activity of new analogs of Vapreotide and RC-121

Svetlana Staykova¹, Emilia Naydenova², Diana Wesselinova³,
Lyubomir Vezenkov⁴

¹University of Chemical Technology and Metallurgy, Department of Organic Chemistry
Blvd. 8 Kl. Ohridski, 1756 Sofia, Bulgaria; ²Institute of Experimental Morphology,
Pathology and Anthropology with Muzeum, Bulgarian Academy of Sciences, Acad. G.
Bonchev Street, Bl. 25, 1113 Sofia, Bulgaria
e_naydenova@abv.bg

Introduction

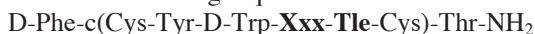
Somatostatin (SST), a cyclic tetradecapeptide hormone is widely distributed in the body, being found in high concentrations in the hypothalamus, in other areas of the brain, and in the gastrointestinal tract. It has a broad range of biological actions that include inhibition of releasing of growth hormone, insulin, glucagon and other hormones, also inhibition of the proliferations of a large variety of cells [1]. The dual actions of natural somatostatins made them logical candidates as anticancer drugs, as well as for the treatment of neuroendocrine disorders. However, the short half-lives of the native somatostatin peptides presented a barrier to further therapeutic development [2]. The synthetic derivatives of somatostatin as RC-160 (Vapreotide: D-Phe-c(Cys-Tyr-D-Trp-Lys-Val-Cys)-Trp-NH₂) and RC-121 (D-Phe-c(Cys-Tyr-D-Trp-Lys-Val-Cys)-Thr-NH₂) have similar activity to native SST, but a longer half-life [3,4]. They have shown *in vitro* and *in vivo* antitumor activity in different studies. Vapreotide is applied in the treatment of acute esophageal variceal bleeding (EVB) in patients with cirrhotic liver disease and AIDS-related diarrhea [5].

In our previous investigation we demonstrate that new synthesized modified C-amide analogs of the SST analog Octreotide (SMS 201-995) exert cytotoxic activity against some tumor cells [6].

The aim of the present study was the synthesis and the biological screening of new octapeptide analogs of RC-160 (Vapreotide, D-Phe-c(Cys-Tyr-D-Trp-Lys-Val-Cys)-Trp-NH₂) and RC-121(D-Phe-c(Cys-Tyr-D-Trp-Lys-Val-Cys)-Thr-NH₂).

Results and Discussion

The new octapeptides have the following sequences:



where:

XXX: Dab (compound **1T**), Dap (compound **2T**), Lys (compounds **3T**) and Orn (compound **4T**).

The Val at position 6 was replaced by the steric restricted amino acid Tle (t-leucine) (compounds **1T-4T**) to stabilize the desired conformation necessary for biological activity. In order to elucidate the influence of the length of the side chain of Lys at position 5 it was substituted by Orn, Dab and Dap.

The peptides were prepared with good yield by solid phase peptide synthesis - Fmoc (9-fluorenylmethoxycarbonyl) - strategy. Rink-amide MBHA resin and TBTU (2-(1H-

benzotriazole-1-yl)-1,1,3,3-tetramethyluronium tetrafluoroborate) were used as solid-phase carrier and condensing reagent. The direct disulfide bond formation has been employed on the solid phase with $\text{Ti}(\text{CF}_3\text{CO}_2)_3$ in DMF. The peptide purity was checked by LC-electrospray ionization mass spectrometry and the optical rotation was measured in water. The data are summarized in Table 1.

Table 1. Structures and characteristics of the synthesized analogs:

No	STRUCTURE	GF	Exact Mass	[MH] ⁺ observed	RT [min]	α_{546}^{20} *
1T	D-Phe-c(Cys-Tyr-D-Trp-Dab-Tle-Cys)-Thr-NH ₂	C ₄₉ H ₆₅ N ₁₁ O ₁₀ S ₂	1031.4357	1032.25	5.26	-62.5
2T	D-Phe-c(Cys-Tyr-D-Trp-Dap-Tle-Cys)-Thr-NH ₂	C ₄₈ H ₆₃ N ₁₁ O ₁₀ S ₂	1017.4201	1018.25	5.23	-36.36
3T	D-Phe-c(Cys-Tyr-D-Trp-Lys-Tle-Cys)-Thr-NH ₂	C ₅₁ H ₆₉ N ₁₁ O ₁₀ S ₂	1059.467	1060.4778	14.06	-66.67
4T	D-Phe-c(Cys-Tyr-D-Trp-Orn-Tle-Cys)-Thr-NH ₂	C ₅₀ H ₆₇ N ₁₁ O ₁₀ S ₂	1045.4514	1046.4572	8.7	-70.59

*Optical rotation in H₂O (c 0.25) at 20°C

The cytotoxic activity of the compounds **1T** - **4T** was measured *in vitro* by the MTS-dye reduction assay for cell viability against the MDA-MB-231 (human breast cancer cell line), HT-29 (human colorectal cancer cell line), HeLa (cervical cancer cell line) and Hep G-2 (human hepatocellular carcinoma cell line) [7]. Cells were cultivated with different amounts of the substances at concentration from $4 \cdot 10^{-3}$ - $4 \cdot 10^{-8}$ M for 24 h. The new analog **3T** following by **1T** and **4T** exert the most pronounced inhibition of the cell vitality at higher concentrations. It is important to mention that IC₅₀ calculations of all substances revealed best inhibitory effect towards the MDA-MB-231, HeLa and HepG2. The compound **4T** exerted the most pronounced antiproliferative effect against the HeLa with IC₅₀ 30 μM. This findings are important because each of these compounds may find its application on some tumor cells.

Acknowledgments

This work was supported by Grant 10917 from the University of Chemical Technology and Metallurgy.

References

- [1] Murray, R. D.; Kim, K.; Ren, S.G.; Chelly, M.; Umehara, Y., Melmed, S. *J. Clin. Invest.* **2004**, 114, 349
- [2] Dinnendahl, V.; Fricke, U.; *Arzneistoff-Profil.* 8 (23 ed.), Govi Pharmazeutischer Verlag: Eschborn, Germany, **2010**
- [3] Zou, Y.; Xiao, X.; Li, Y.; Zhou, T. *Oncol. Reports*, **2009**, 21, 379
- [4] Cai, R.-Z.; Szoke, B.; Lu, R.; Fu, D.; Redding, T. W.; Shally A. V. *Proc. Natl. Acad. Sci. USA*, **1986**, 83, 1896.
- [5] <http://www.drugbank.ca/drugs/DB04894>
- [6] Staykova, S.; Naydenova, E.; Wesselinova, D.; Kalistratova, A.; Vezenkov, L., *Protein and Peptides Letters*, in press
- [7] CellTiter 96 Non-Radioactive Cell proliferation assay, Technical Bulletin #TB112, Promega Corporation USA. Revised 12/99.

Synthesis and biological evaluation of creatinyl amino acids

Sergey Burov¹, Maria Leko¹, Marina Dorosh¹, Olga Veselkina²

¹*Institute of Macromolecular Compounds RAS, St-Petersburg, Russia;*

²*Closed Joint-Stock Company "Vertex", St-Petersburg, Russia*

E-mail: burov@hq.macro.ru

Introduction

Creatine (Cr), a small molecule synthesized in the kidney, liver and pancreas plays an essential role in the cellular energy metabolism. Cr possesses neuroprotective activity in experimental models of brain stroke and related diseases [1]; however it has poor ability to penetrate the blood-brain barrier (BBB) without specific carrier protein (CRT). Thus, synthesis of stable hydrophobic derivatives capable of crossing the BBB by alternative pathway is of great importance for the treatment of different neurological diseases including hereditary CRT deficiency. Vennerstrom and Miller suggested Cr esterification as a convenient method for the prevention of intramolecular cyclization to creatinine (Cn) [2]. Although Cr esters are less polar as compared to natural molecule and can penetrate the BBB, recently it was shown that their enzymatic or non-enzymatic cleavage resulted in Cn formation instead of expected free Cr [3, 4]. Here we describe the synthesis and biological activity of new hybrid compounds – creatinyl amino acids (Cr-AA).

Results and Discussion

Preparation of Cr derivatives with neuroprotective properties encounters several common problems including low Cr solubility in water and organic solvents, its propensity for cyclization and strong influence of any structural modifications on biological activity. To avoid solubility limitations and exclude the possibility of intramolecular cyclization, in our initial experiments synthesis of Cr-AA was performed by the guanidinylation of sarcosyl peptides [5]. To elucidate the influence of attached amino acid on physico-chemical properties and stability of Cr derivatives, we prepared a set of analogues, shown in Table 1. According to HPLC analysis extent of sarcosyl peptide conversion was about 90-100%, however the yield of purified product was only 40-60% due to its partial loss in the course of IEC and subsequent crystallization. To simplify the synthetic procedure we investigated the possibility of direct amino group acylation by anhydrous Cr or Cr hydrate. In our experience, application of p-TSA counterion ensures Cr solubility and significant suppression of intramolecular cyclization. While our attempts to prepare Cr active esters failed, both DCC and MA methods resulted in the formation of desired product. The treatment of crude product can be simplified by using of anion-exchange resin at the stage of p-TSA removal. The application of IRA-67 in free-base form resulted in significant decomposition of Cr-Gly-OEt accompanied by Cn formation, while the resin in acetate form does not influence the product stability. Commonly, the crude product obtained after IEC contains about 5-10% of Cn. Its content can be reduced up to 3-5% by crystallization from MeCN, followed by the dissolution of Cr-Gly-OEt in ethyl alcohol and removal of precipitated Cn.

It was shown that stability of Cr derivatives is strongly dependent on the structure of

Table 1. List of creatinyl amino acids and peptides			
Cr-containing compounds	Yield ^a (%)	ESI MS	
		MW	[M+H] ⁺
1a Cr-Gly-OEt	22(1), 25(2)	216.12	217.15
1b Cr-Gly-OH	12(1)	188.09	189.11
1c Cr-Gly-NHEt	29(1), 18(2) ^b	215.14	216.16
1d Cr-Gly-OBzl	21(1)	278.14	279.14
1e Cr-Gly-OiPr	20(2)	230.14	231.15
2a Cr-Phe-OEt	22(1)	306.17	307.18
2b Cr-Phe-NH ₂	46(1), 10(2) ^b	277.15	278.17
2c Cr-Phe-OH	20(1)	278.14	279.15
3a Cr-Tyr-NH ₂	38(1)	293.15	294.16
3b Cr-Tyr-OH	16(1)	294.13	295.15
4 Cr-GABA-OEt	29(1)	244.15	245.18
5 H-Lys(Cr)-OEt	26(1), 6(2) ^b	287.20	288.16
6 Cr-Gly-Gly-OEt	15(2)	273.14	274.16
7 Cr-Glu-Arg-OEt	24(1) ^c	444.24	445.26
8 Cr-Phe-Arg-Gly-OEt	37(1) ^c	519.29	520.33

^a Total yield of products, obtained using different synthetic approaches: (1) guanidinylation of sarcosyl peptides; (2) acylation by Cr p-toluensulfonate. ^b Significant loss of product at the stage of crystallization. ^c Yields were calculated starting from sarcosyl peptides

adjacent amino acid residue, the kind of counterion and pH of solution. Creatinyl-glycine esters seem to be less stable as compared to other analogues. These data can be explained by the assumption that the degradation mechanism comprises intramolecular cyclization resulted in cleavage of amide bond and Cn formation. However, it should be mentioned that surprisingly high stability of Cr-GABA-OEt remains unclear.

The neuroprotective activity of Cr-AA was tested *in vivo* using two different models: NaNO₂-induced hypoxia (mice) and ischemic stroke (rats). All tested compounds were administered *i.p.* at doses of 100-500 mg/kg. It was shown that efficacy of antihypoxic action depends on the structure of amino acid moiety. Thus, Cr-Phe-NH₂ and Cr-GABA-OEt possessed moderate activity, while Cr-Tyr-NH₂ and Cr-Gly-OEt increase life span of experimental animals about two times. Similar results were obtained using ischemic brain injury model. *I.p.* administration of Cr-GABA-OEt (1 mM/kg) and Cr-Phe-NH₂ reduces the size of necrotic zone by 25% in contrast to more than 50% in the case of *i.v.* Cr-Gly-OEt injection 1 h before or after ischemia. These data evidenced that creatinyl amino acids possess pronounced neuroprotective properties. The mechanism of their biological action and potential synergistic effect of attached amino acid residue are under investigation.

References

- [1] Klivenyi, P.; et.al. *Nat. Med.* **1999**; 5, 347.
- [2] Vennerstrom, J.L.; Miller, D.W. *WO/2002/022135*. 21.03.2002.
- [3] Giese, M.W.; Lecher, C.S. *Int. J. Sports Med.* **2009**; 30, 766.
- [4] Giese, M.W.; Lecher, C.S. *Biochem. Biophys. Res. Commun.* **2009**; 388, 252.
- [5] Burov, S.V.; Khromov, A.N. *Russian Patent 2354645*, Nov. 21, 2007.

Synthesis and evaluation of SARS 3CL protease inhibitors using the serine template

Daiki Takanuma¹, Kenichi Akaji², Hiroyuki Konno¹

¹Department of Biochemical Engineering, Graduate School of Science and Technology,
Yamagata University, Yonezawa, Japan; ²Department of Medicinal Chemistry, Kyoto
Pharmaceutical University, Yamashina-ku, Kyoto, Japan

E-mail:konno@yz.yamagata-u.ac.jp

Introduction

Severe acute respiratory syndrome (SARS) is a contagious respiratory disease to human which is caused by the SARS coronavirus (SARS-CoV). The key enzyme in the processing of polyproteins translated by viral RNA genome of SARS-CoV is a 33kDa protease called 3C-like protease (3CL protease). SARS 3CL protease is a cysteine protease containing a Cys-His catalytic dyad, and cleaves precursor poly proteins at as many as 11 conserved site involved a conserved Gln at the P1 position and a small amino acid (Ser, Ala, or Gly) at the P'1 position. Due to its functional importance in the viral life cycle, SARS 3CL protease is considered to be an attractive target for drug design against SARS. Recently, we found tetrapeptide aldehyde, Ac-Thr-Val-Cha-His-H, showed high inhibitory activity with IC₅₀ value of 98 nM toward 3CL-R188I mutant protease^{1,2}.

To compare the inhibitory activity of small compounds with those containing active functional groups, we synthesized serine-derivatives within the essential functional groups and evaluated its inhibitory activity (Fig. 1).

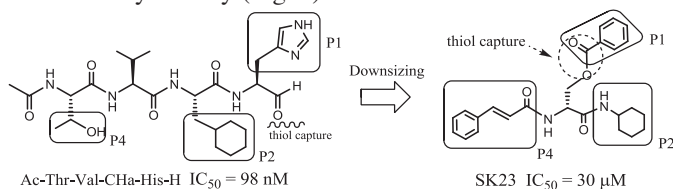
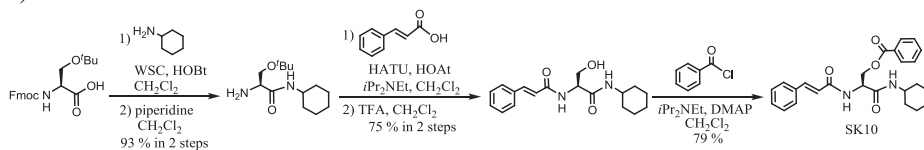


Fig. 1 Design of SARS 3CL protease inhibitors

Results and Discussion

The synthetic scheme was started from Fmoc-Ser(*t*Bu)-OH, following modification of C-terminal carboxyl group with P2 position, N-terminal amine with P4 position and side chain alcohol with P1 position functionalities. 5 steps overall reaction led to obtain the novel serine derivatives for the small molecular inhibitors against SARS 3CL protease (Scheme 1).



Scheme 1. Synthesis of SK10

The assay with 3CL R188I mutant protease was examined to evaluate the inhibitory activity of the synthetic serine derivatives (Table 1). At the modification of P4 position, SK50 which has trimethoxy cinnamoyl derivative shows inhibitory activity with IC_{50} value of 74 μ M. 2-methyl-6-nitrobenzoate derivative, SK14 with IC_{50} value of 65 μ M was effective. SK42 with IC_{50} value of 180 μ M suggested that the length of the P2 position between nitrogen and cyclic group might be required to need at least one carbon. In construct, there is no significant difference between L- and D- forms of serine derivative inhibitors.

Subsequently, molecular docking study of complex of 3CL protease with the ligand was carried out. Docking simulation experiment with R188I (PDB ID: 3AW0) and SK23, which has the best activity in the serine derivatives to date, indicated that P1 position fitting S1' pocket. At the result of assay, P1, P2 and P4 positions of the inhibitor should be modified by benzoyl group, cyclohexyl group and cinnamoyl group, respectively (Fig. 2).

Table 1. Results of assay

P4			P1			P2			D-form		
Structure	MW CLogP	IC_{50}	Structure	MW CLogP	IC_{50}	Structure	MW CLogP	IC_{50}	Structure	IC_{50} MW CLogP	
	438.22 4.1691	>3200 μ M		316.39 2.2319	1500 μ M		434.22 4.7483	650 μ M		408.47 4.2546	>1600 μ M
	436.24 4.7461	155 μ M		392.49 4.8223	380 μ M		448.65 5.2265	120 μ M		408.45 3.4908	1200 μ M
	436.24 4.7461	98 μ M		358.43 3.1285	400 μ M		446.54 5.2841	85 μ M		434.63 5.4451	180 μ M
	480.23 4.4840	145 μ M		420.50 4.8261	125 μ M		421.49 3.4821	180 μ M		428.48 4.6161	255 μ M
	510.24 4.1262	74 μ M		479.53 4.8781	65 μ M		427.49 2.1167	>1600 μ M		446.54 5.2841	340 μ M
				623.84 6.0861	550 μ M		509.60 1.4847	>3200 μ M		428.48 4.6161	225 μ M
										434.63 5.4451	430 μ M

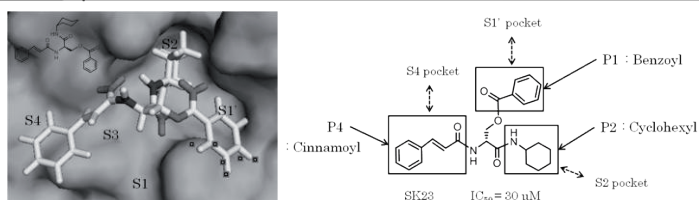


Fig. 2 Result of Docking simulation

In conclusion, 48 novel small molecular inhibitors were synthesized and evaluated against SARS 3CL protease. SK23 with IC_{50} value of 30 μ M is the best active compound at this time. Toward the creation of further reasonable inhibitors, SAR study will be progress in due course.

References

- [1] Akaji K.; Konno H.; Onozuka M.; Makino A.; Saito H.; Nosaka K. *Bioorg. Med. Chem.* **2008**, 16, 9400-9408.
- [2] Akaji K.; Konno H.; Mitsui H.; Teruya K.; Shimamoto Y.; Hattori Y.; Ozaki T.; Kusunoki M.; Sanjoh A. *J. Med. Chem.* 2011, 54(23), 7962-7973.

The influence of N-terminal extremity in the antiplasmodial activity of Angiotensin II

Marcelo Der Torossian Torres,¹ Adriana Farias Silva,¹ Mayra Chamlian,¹ Alexandre Jesus Barros,² Clovis Ryuichi Nakaie,² Antonio Miranda,² Margareth Lara Capurro,³ Vani Xavier de Oliveira Junior¹

¹*Universidade Federal do ABC, Santo André, Brazil;* ²*Universidade Federal de São Paulo, São Paulo, Brazil;* ³*Universidade de São Paulo, São Paulo, Brazil*

marcelo.torres@ufabc.edu.br

Introduction

Malaria is a disease that affects over 500 million people every year. Among the natural molecules used in treatments, some are peptides, as the angiotensin II (AII) [1]. In an attempt to increase its activity against malaria sporozoites some conformationally constrained analogues scanning the whole AII sequence, with lactam bridge, were synthesized and tested. The analogues with higher antimalarial activity presented the lactam bridge proximal to the N-terminal extremity. Based on these peptides, this work present new analogues, using different bridgehead elements and different scaffold sizes derivative of lactam ring scan in the N-terminal extremity.

Results and Discussion

The cyclic analogues that contained i-(i+2) and i-(i+3) lactam bridge, scaffold using Asp and Lys residues, presented higher antiplasmodial activity when the bridge was inserted next to N-terminal extremity, among them, the most active was DRDVKYIHPF (76%) [1]. The insertion provides conformational changes in the molecule and in its hydrophobic cluster formed by Tyr, Ile and His [2], which may have influence in the peptide-membrane interaction. Thus, new analogues were synthesized with a lactam bridge next to the N-terminal portion, using Glu/Asp/Orn/Lys residues as bridgeheads components in i-(i+4) lactam bridge scaffolds (Table 1).

The analogues which contained the Glu residue presented higher antiplasmodial activity (81%), suggesting that the scaffold size has direct affecting the biological action. Therefore, new restrict peptides by i-(i+2) and i-(i+3) lactam bridge were designed, using Glu residue as bridgehead element, but the same effect was not verified, getting a maximum of 65% of bioactivity. The biological results indicate that activity can be influenced by displacement of the amide group inside the lactam ring, probably due to intra/intermolecular interactions changes, and it is also dependent of the bridge size.

On the other hand, an increase in the hydrophobic character of AII sequence was promoted by replacing the Asp residue for Fmoc-Glu and Asp(O^tFm), in order to improve the interaction in the sporozoite membrane. However, the replacement by Fmoc-Glu provided a decrease of activity, while that Asp(O^tFm) kept the AII activity, because of changes in the peptide charge, which may have modified the conformation in physiological medium.

Table 1. Effects on membrane permeability of mature sporozoites of AII analogues.

Peptide	Sequence	FM ^a (%)	HPLC Purity (%) ^b	Calcd Mass (Da) ^c	Obsvd Mass (m/z) ^c
1	<u>EDRVOYI</u> HPPF	81	100	1270,7	1272
2	<u>DDRVKYI</u> HPPF	54	99	1270,7	1272
3	<u>EDRVKYI</u> HPPF	14	99	1284,7	1285
4	<u>DDRVOYI</u> HPPF	77	100	1256,7	1255
5	<u>DREVKYI</u> HPPF	50	100	1284,7	1286
6	<u>DREVOYI</u> HPPF	47	98	1270,7	1272
7	(Fmoc)ERVYIHPF	54	99	1281,6	1282
8	(OFm)DRVYIHPF	77	98	1267,6	1269
9	<u>DERVKYI</u> HPPF	65	99	1284,7	1285

^aFluorescence microscopy (FM): used to monitor the integrity of the cell membrane, the sporozoites were incubated with AII and its analogues for 1 hour at 37°C. Ormithine = O.

^bHPLC: Column Supelcosil C18 (4.6 x 150 mm), 60 Å, 5 µm; Solvent System: A (0.1% TFA/H₂O) and B (0.1% TFA in 60% ACN/H₂O) ; Gradient: 5 – 95% B in 30 minutes, Flow: 1.0 mL/min; λ = 220 nm; Injection Volume: 50 µL and Sample Concentration: 1.0 mg/mL.

^cLC/ESI-MS: Micromass instrument, model ZMD coupled on a Waters Alliance, model 2690 system. Conditions of mass measurements: positive mode; range between 500 and 2000 m/z; nitrogen gas flow: 4.1 L/h; capillary: 2.3 kV; cone voltage: 32 V; extractor: 8 V; source heater: 100 °C; solvent heater: 400 °C; ion energy: 1.0 V and multiplier: 800 V.

The introduction of conformational restrictors can potentiate the pharmacological activity, reducing the enzymatic degradation by elimination of the metabolized forms. Moreover, it can enhance selectivity by lowering the number of bioactive conformers. The formation of these bridges leads to a stabilized conformation, providing a turn in the molecule that may increase the action of antimicrobial peptides in the disruption of lipid membranes [3].

Acknowledgments

This work has been supported by grants and fellowships from FAPESP, CAPES and CNPq.

References

- [1] Maciel, C.; Oliveira, V. X.; Fázio, M. A.; Nacif-Pimenta, R.; Miranda, A.; Pimenta, P. F.; Capurro, M. L. *PLoS ONE* **2008**, *3*, e3296.
- [2] Zhang, W. J.; Nikiforovich, G. V.; Pérodin, J.; Richard, D. E.; Escher, E.; Marshall, G. R. *J. Med. Chem.* **1996**, *39*, 2738-2744.
- [3] Tzakos, A. G.; Bonvin, A. M. J. J.; Troganis, A.; Cordopatis, P.; Amzel, M. L.; Gerothanassis, I. P.; van Nuland, N. A. J. *European Journal of Biochemistry* **2003**, *270*,849-860.

Analogs of RGD as anti-angiogenic compounds

**T. Thi Phan,^{1,2} S. Abbour,¹ F. Jouan,² Y. Arlot-Bonnemains,²
M. Baudy-Floc'h¹**

¹ICMV, UMR CNRS 6226, University of Rennes 1, F-35042 Rennes Cedex, France; ²UMR
CNRS 6290-IGDR, University of Rennes 1, Rennes, France

E-mail: michele.baudy-floch@univ-rennes1.fr

Introduction

Angiogenesis depends on the adhesive interactions of vascular cells. The adhesion receptor integrin $\alpha_v\beta_3$ was identified as a marker of angiogenic vascular tissue. The $\alpha_v\beta_3$ integrin receptor plays an important role in human metastasis and tumor-induced angiogenesis, mainly by interacting with matrix proteins through recognition of an Arg-Gly-Asp (RGD) motif [1,2]. Inhibition of the $\alpha_v\beta_3$ -integrins with a cyclic RGD peptide impairs angiogenesis, growth and metastasis of solid tumours in vivo [3,5]. The aim of this study was to investigate the effects of replacement of α -amino acids by aza- β^3 -amino acids in cyclic RGD-peptides as $\alpha_v\beta_3$ -integrin antagonist on angiogenesis, microcirculation, growth and metastasis formation of a solid tumour in vivo.

Results and Discussion

One peptide and four cyclic pseudopeptides were prepared using Fmoc/*t*Bu SPPS strategy on a microwave peptide synthesizer (Liberty, CEM). Cyclisation was performed on resin, for that a Fmoc-Lys-Oallyl or a Fmoc-aza- β^3 Lys-Oallyl were first anchored to the CTC resin, after elongation of peptide chain removal of the allyl ester protecting group from the carbonyl function with Pd(PPh₃)₄ in the presence of PhSiH₃ was done. Then removal of the Fmoc group from the N-terminal amino acid of the peptidic chain can allow the on-resin cyclization using PyBOP/HOBt. Then side chain deprotection and cleavage of the cyclic pseudopeptide from the solid support were performed. Finally, pseudopeptides were purified by reversed-phase HPLC (RP-HPLC). Integrity of the peptide was assessed by MALDI-TOF analysis. The purity of peptides and pseudopeptides was obtained by reversed-phase HPLC.

PP1: c[Arg-Gly-Asp-DPhe-Lys] (23%)

PP2: c[Arg-aza- β^3 -Gly-Asp-aza- β^3 -Phe-Lys] (12%)

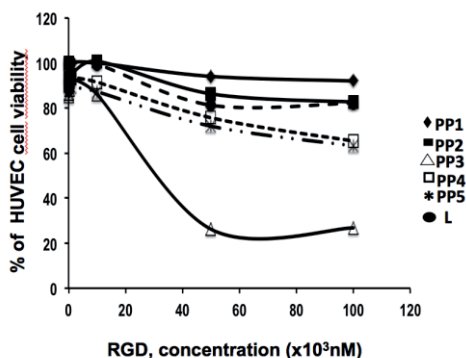
PP3: c[Arg-Gly-Asp-aza- β^3 -Phe-Lys] (25%)

PP4: c[Arg-Gly-Asp-aza- β^3 Phe-aza- β^3 Lys] (50%)

PP5: c[aza- β^3 Arg-Gly-aza- β^3 -Asp-Phe-Val] (60%)

The two cells lines 786-0 (renal tumor cell-A) and HUVEC (human umbilical vascular endothelial cell-B) were cultivated in the presence of different concentration of the modified RGD (PP2, PP3, PP4, PP5 and L) and were compared to RGDfK (PP1). The cell viability and proliferation were evaluated by the MMT assay after 48 hours of incubation.

RGD nM	PP1	PP2	PP3	PP4	PP5	L
0	100	100	100	100	100	100
1	84	86	91	87	87	79
5	79	88	88	85	87	79
10	70	66	80	75	81	73
100	48	49	60	68	61	69
500	48	51	56	64	49	65



Effect of RGD onto the 786-0 cells viability (%)

All the tested RGD, excepted PP4 and linear product, slightly affect cell proliferation of the 786-0 tumour cell (A). A concentration of 10nM of PP2 induces a decrease of 40% of cell viability. In contrast, all the compounds tested onto the HUVEC cell lines (B) are efficient in affecting cell proliferation. The PP3 induces a decrease of 80% of cell proliferation at a concentration of 50 μ M. (IC₅₀ for the PP3 is 30 μ M). A magnitude x1000 was observed between the effective concentrations onto the two cell lines.

Conclusions

We report the development of efficient solid-phase method for the synthesis of cyclic aza- β^3 RGD peptides for constructing potent $\alpha_v\beta_3$ receptor antagonists. The RGD analogs develop an antiproliferative activity against the kidney tumor cells (786-0) with a IC₅₀ of 95 nM for PP2 similar to PP1, the Kessler's peptide. The other pseudopeptides are less efficient to inhibit the proliferation of these tumor cells. In contrast, only PP3 is able to inhibit the proliferation of the endothelial cells (HUVEC) in range concentration x100 times higher than for inhibiting the 786-0 proliferation. The IC₅₀ of PP3 is of 30 μ M for the HUVEC. These results are in accordance with the fact that aza- β^3 -Phe side chain, which is beared by a chiral nitrogen with non configuration, can adopt the right configuration to interact with the receptor and contributes in both PP2 and PP3 to the activity of the RGD pseudopeptides on both cell lines. The aza- β^3 -Gly monomer increases the antiproliferative activity in tumor cells probably due to the formation of a N-N turn mimicking the γ -turn, which is important to get the best affinity and selectivity towards the receptor.

References

- [1] Gottschalk, K.-E.; Kessler, H. *Angew. Chem. Int. Ed.* **2002**, *41*, 3767.
- [2] Haubner, R, Schmitt, W., Hölzemann, G., Goodman, S.L., Jonczyk, A. and Kessler, H. *J. Am. Chem. Soc.* **1996**, *118*, 7881 and references therein.
- [3] Marinelli, L., Lavecchia, A., Gottschalk, K.-E., Novellino, E., Kessler, H. *J. Med. Chem.* **2003**, *46*, 4393.
- [4] Dechantsreiter, M.A.; Planker, E.; Mathä, B.; Lohof, E.; Hölzemann, G.; Jonczyk, A.; Goodman, S.L.; Kessler, H. *J. Med. Chem.* **1999**, *42*, 3033.
- [5] Haubner, R., Finsinger, D., Kessler, H. *Angew. Chem.* **1997**, *36* 1374.

[¹¹¹In/¹⁷⁷Lu]JMV4168 in the diagnosis and therapy of GRPR-positive tumors

Theodosia Maina^a, Pantelis J. Marsouvanidis^a, Linda M. van der Graaf^b, Jean A. Fehrentz^c, Bouchra Hajjaj^c, Luc Brunel^c, Berthold A. Nock^a, Eric P. Krenning^b, Jean Martinez^c, Marion de Jong^b

^aMolecular Radiopharmacy, IRRP, NCSR "Demokritos", Athens, Greece; ^bDepartment of Nuclear Medicine, Erasmus MC, Rotterdam, The Netherlands; ^cFaculté de Pharmacie, CNRS-Universités de Montpellier 1 et 2, Montpellier, France

E-mail:maina_thea@hotmail.com

Introduction

The high density expression of GRPRs (gastrin-releasing peptide receptors) in frequently occurring human cancers (e.g. breast and prostate cancer) provides the opportunity to use radiolabeled GRPR-seeking bombesin (BBN) analogs for cancer diagnosis and treatment [1]. So far, agonists have been preferred for such applications due to their capacity to internalize after binding to their receptor. Recent evidence, however, indicates that antagonist-radioligands may show a superior *in vivo* profile despite their inability to internalize [2-4]. In this work we present JMV4168, generated by coupling the chelator DOTA to the GRPR-antagonist JMV594 [5,6] via a (β Ala)₂-spacer (DOTA-(β Ala)₂-D-Phe-Gln-Trp-Ala-Val-Gly-His-Sta-Leu-NH₂) for stable binding of useful radiometals, such as ¹¹¹In (SPECT imaging) and ¹⁷⁷Lu (radionuclide therapy). The synthesis, ¹¹¹In/¹⁷⁷Lu-labeling and biological properties of the new tracer in GRPR⁺-cells and animal models are reported.

Results and Discussion

The affinity of JMV4168 (IC₅₀ = 8.2±0.7 nM) determined during competition binding assays against [¹²⁵I-Tyr⁴]BBN in human prostate cancer PC-3 cells expressing the GRPR was comparable to [Tyr⁴]BBN (IC₅₀ = 1.8±0.2 nM). Both radiotracers slowly degraded after entry in the blood stream of healthy Swiss albino mice, with >60% of [¹¹¹In]JMV4168 remaining intact at the first critical 5 min pi (Fig. 1) and >50% of [¹⁷⁷Lu]JMV4168 at 10 min pi.

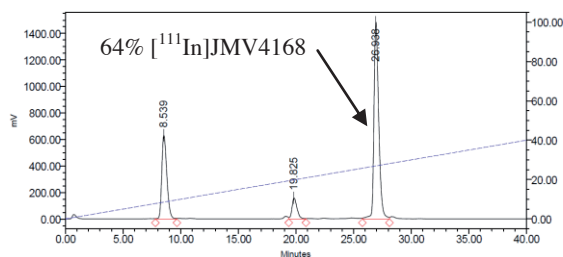


Figure 1: RP-HPLC analysis of mouse blood collected 5 min after injection of [¹¹¹In]JMV4168 in mice revealing 64% intact radioligand in the blood stream.

After injection in SCID mice bearing human PC-3 xenografts (1-2 μ Ci, 10 pmol peptide), [¹¹¹In]JMV4168 and [¹⁷⁷Lu]JMV4168 displayed similar biodistribution patterns (Fig. 2, A –

B). They localized efficiently and specifically in the GRPR-expressing PC-3 xenografts at 4 h pi (17.0%ID/g ^{111}In ; 18.4%ID/g ^{177}Lu , both $<1.5\%$ ID/g during GRPR-blockade by coinjection of 40 nmol $[\text{Tyr}^4]\text{BBN}$). Radioactivity cleared rapidly from background tissues, including the kidneys and the GRPR⁺-pancreas; in contrast, washout from the tumor was much slower with significant tumor uptake still documented at 96 h pi (Fig. 2, B).

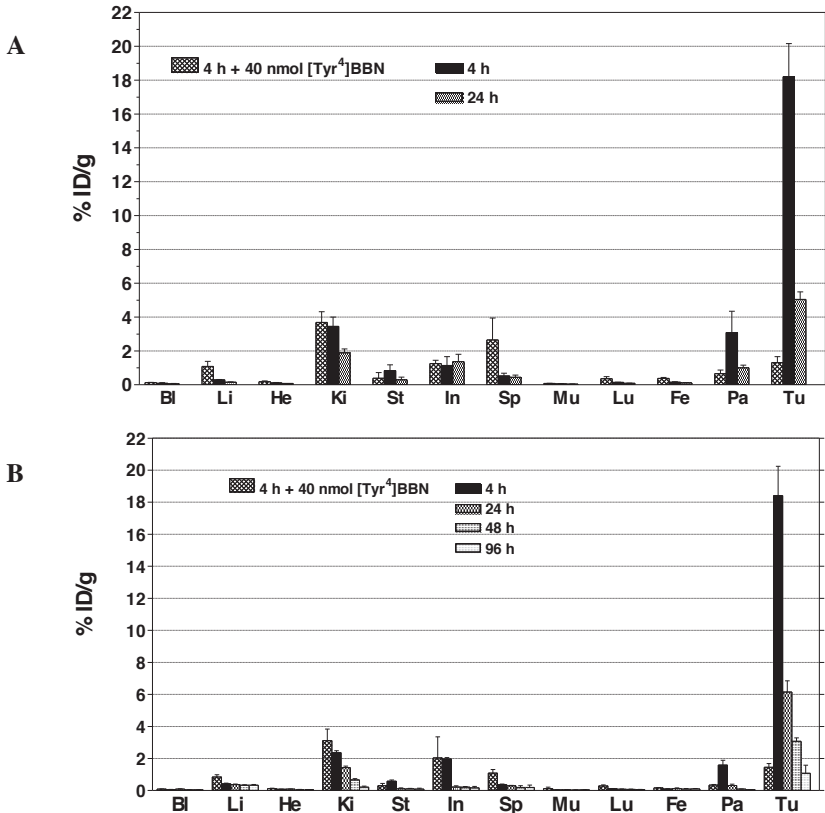


Figure 2: Biodistribution of (A) ^{111}In]JMV4168 and (B) ^{177}Lu]JMV4168 in PC-3 tumor-bearing SCID mice, as %ID/g (mean \pm SD, n= 4); Bl= blood, Li= liver, He= heart, Ki= kidneys, St= stomach, In= intestines, Sp= spleen, Mu =muscle, Lu= lungs, Fe= femur, Pa= pancreas, Tu= PC-3 tumor.

^{111}In]JMV4168 and ^{177}Lu]JMV4168 show a very promising profile for further validation as a diagnostic/therapeutic pair in the treatment of GRPR-expressing tumors in man.

References

- [1] Reubi, J.C. *Endocr. Rev.* **2003**, 24(4), 389.
- [2] Ginj, M.; Zhang, H.; Waser, B.; et al. *PNAS* **2006**, 103(44), 16436.
- [3] Cescato, R.; Maina, T.; Nock, B.A.; et al. *J. Nucl. Med.* **2008**, 49, 318.
- [4] Mansi, R.; Wang, X.; Forrer F.; et al. *Clin. Cancer Res.* **2009**, 15(16), 5240.
- [5] Azay, J.; Nagain, C.; Llinares, M.; et al. *Peptides* **1998**, 19(1), 57.
- [6] Tokita, K.; Katsuno, H.; Hocart, S.V.; et al. *J. Biol. Chem.* **2001**, 276, 36652.

[¹¹¹In]AT5S & [¹¹¹In]AT6S: Two novel bis-disulfide bridged SS-14 radiopeptides with diverging biological profiles

Aikaterini Tatsi^{a,b}, Renzo Cescato^c, Theodosia Maina^a, Beatrice Waser^c,
Eric P. Krenning^d, Marion de Jong^d, Jean-Claude Reubi^c,
P. Cordopatis^b, Berthold A. Nock^a

^aMolecular Radiopharmacy, IRRP, NCSR "Demokritos", Athens, Greece; ^bDepartment of Pharmacy, University of Patras, Greece; ^cInstitute of Pathology, University of Bern, Bern, Switzerland; ^dDepartment of Nuclear Medicine, Erasmus MC, Rotterdam, The Netherlands

E-mail: ktatsi19@gmail.com

Introduction

The five sst₁₋₅ subtypes are expressed together and in various combinations in many human tumors [1-3]. Therefore, the development of radiolabeled somatostatins binding to all five sst₁₋₅ is expected to broaden the clinical indications of sst₂-preferring radioligands and to increase uptake in lesions with multi-sst expression. In a previous study, [¹¹¹In-DOTA⁰,DTrp⁸]SS-14 ([¹¹¹In]AT2S) showed a pansomatostatin behavior but a poor *in vivo* stability [4]. Aiming toward a higher metabolic stability, we have introduced a second disulfide bridge to the AT2S motif generating either an extra 6-amino acid (AA) (AT5S) or an extra 8-AA ring (AT6S) (Fig. 1). *In vitro* and *in vivo* characterization of the bicyclic analogs and their respective ¹¹¹In-radioligands is reported herein.

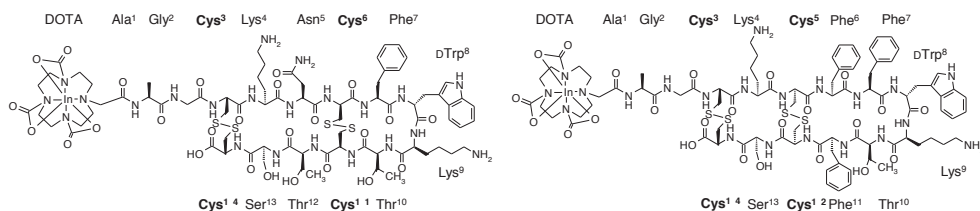


Figure 1: Chemical structure of [¹¹¹In]AT5S (left) and [¹¹¹In]AT6S (right)

Results and Discussion

The orthogonally protected sequences were assembled on the solid support; deprotection and release from the resin was achieved by TFA. The first cyclization (Cys⁶-Cys¹¹ – in AT5S, or Cys⁵-Cys¹² – in AT6S) was performed in 1% DMSO, while the second (Cys³-Cys¹⁴) was completed by iodine oxidation; the products were purified by semi-preparative RP-HPLC. ESI-MS and analytical RP-HPLC confirmed their formation in >94% purity.

The affinity of AT5/6S for the human sst₁₋₅ was determined by receptor autoradiography during competition binding against the universal radioligand [¹²⁵I]LTT-SS-28 [4,5]. Results (IC₅₀s in nM) summarized in Table 1 reveal the total loss of AT5S affinity to all sst₁₋₅; in contrast, AT6S displayed a typical pansomatostatin binding profile. Concordant with this finding, only AT6S stimulated sst₂-internalization during an immunofluorescence-based receptor internalization assay, showing agonistic properties for the sst₂.

Table 1: Affinity profile of AT5S and AT6S for the $hsst_{1-5}$

Analog, #AA in ring(s)	$hsst_1$	$hsst_2$	$hsst_3$	$hsst_4$	$hsst_5$
SS14 (12)	2.1 ± 0.4	0.6 ± 0.1	3.9 ± 1.3	1.9 ± 0.6	11.0 ± 3.5
AT2S (12)	14 ± 2.4	1.5 ± 0.3	2.4 ± 0.5	3.7 ± 0.7	12.0 ± 1.9
AT5S (6/12)	> 1000	616 ± 148	> 1000	> 1000	> 1000
AT6S (8/12)	12 ± 3.3	6.3 ± 0.6	9.7 ± 3.6	5.4 ± 0.8	26 ± 7.0

Both peptides were easily labeled with ^{111}In affording the respective radioligands (Fig. 1) in >97% radiochemical purity and yield. RP-HPLC analysis of blood samples collected 5 min after injection of [^{111}In]AT5S or [^{111}In]AT6S (100 μL , ≈ 1 mCi, 3 nmol) in Swiss albino mice revealed that >98% of the radioligands remained intact.

Biodistribution was performed in rat sst_2^+ AR4-2J and HEK293- $hsst_3$ tumor-bearing SCID mice 4 h post injection (pi) of [^{111}In]AT6S (100 μL , 2 μCi , 10 pmol). Comparative data of [^{111}In]AT6S vs. [^{111}In]AT2S as reference [4] in AR4-2J and HEK293- sst_3 tumors and kidneys at 4 h pi is presented in Fig. 2. The metabolically stabilized [^{111}In]AT6S exhibited equal uptake in the AR4-2J tumors, but a higher uptake in the HEK293- $hsst_3$ tumors and in the kidneys compared to [^{111}In]AT2S (control).

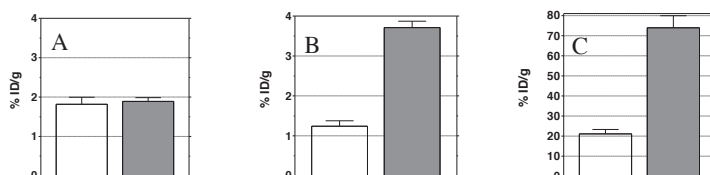


Figure 2: Uptake of [^{111}In]AT6S ■ vs. [^{111}In]AT2S □ in (A) $rsst_2^+$ AR4-2J tumors, (B) in HEK293- $hsst_3$ tumors and (C) kidneys in SCID mice at 4 h pi (%ID/g, mean \pm sd, n=4).

The present study has shown that introduction of an extra disulfide bridge in the AT2S motif confers high metabolic stability on the resulting radioligands. AT6S, with a double 8/12-member ring, showed a pansomatostatin profile, while [^{111}In]AT6S exhibited higher uptake in HEK293- $hsst_3$ tumors in mice than [^{111}In]AT2S (reference). At the same time the elevated renal uptake of [^{111}In]AT6S shows that further structural interventions are required to improve the *in vivo* profile. Interestingly, the 6/12-member ring combination in AT5S led to total loss of sst_{1-5} affinity; the structural parameters leading to such an effect are currently investigated by NMR conformational studies.

References

- [1] Patel, Y.C.; Greenwood, M.T.; Panetta, R.; et al. *Life Sci.* **1995**, *57*, 1249.
- [2] Patel, Y.C. *Front. Neuroendocrinol.* **1999**, *20*, 157.
- [3] Reubi, J.C.; Waser, B.; Schaer, J.C.; Laissue, J.A. *Eur. J. Nucl. Med.* **2001**, *28*, 836.
- [4] Tatsi, A.; Maina, T.; Cescato, R.; et al. *Eur. J. Nucl. Med. Mol. Imaging Res.* **2012**, *2*, 25.
- [5] Cescato, R.; Schulz, S.; Waser, B.; et al. *J. Nucl. Med.* **2006**, *47*, 502.

Determination of antiviral activity of test compounds in CPE (cytopathic effect)-inhibitory assays (Schmidtke et al. *J Virol Meth* 2001, 95:133-43) [2]

Cells and viruses: MDCK cells and influenza virus A/Hongkong/68

The replication of influenza viruses in MDCK cells induces the complete destruction of host cells, a distinct cytopathic effect (CPE). The virus-induced CPE can be inhibited by addition of antiviral compounds (100 μl /well; 2 parallels/concentration, dilution factor 2). Untreated (virus control) and compound-treated confluent monolayers of test cells were infected with a multiplicity of infection that induces a complete CPE in virus control 24 h after virus addition. Thereafter, adherent cells were fixed and stained with a crystal violet/formalin solution. After elution of the stain, inhibition of virus-induced CPE was quantified by optical density (OD) determination in a Dynatech microplate reader. The percentage of antiviral activities of test compounds was calculated. Based on the mean dose response curve of at least 2 assays, the 50 % CPE inhibitory concentration (IC₅₀) was calculated (Table 1).

Table 1. Cytotoxicity and anti-influenza activity in MDCK cells

Compound	CC50 [$\mu\text{g}/\text{ml}$]	MTD [$\mu\text{g}/\text{ml}$]	IC 50 [$\mu\text{g}/\text{ml}$]	IS
1	50	3.6	not active	455
2	50	9.7	0.11	
3	23.7	8.8	not active	
4	36.6	13.6	not active	

Novel rimantadine (1, 2) and amantadine (3, 4) analogues have been synthesized with amino acids containing thiazole and thiazolyl-thiazole rings and their activity on the Influenza virus A/Hongkong/68 have been explored.

The results in our investigations showed that derivative of rimantadine containing thiazolyl-thiazole ring inhibited markedly the influenza virus-induced cytopathic effect at non cytotoxic concentrations (selectivity index = 455).

Acknowledgments

For the support of this work we are grateful to the National Found for Scientific Research of Bulgaria (Contracts DMU-03/2), South-West University "Neofit Rilski" Bulgaria (SRP-A4/12).

References

- [1] J.C. Watts, P. Marvin, *U.S. Patent*, **1967**, 3, 310, 469.
- [2] Schmidtke et al. *J Virol, Meth*, **2001**, 95:133-43.

Chemical stability of esters of acyclovir with amino acid and cholic acids

Kiril Chuchkov, Radoslav Chayov, Ivanka G. Stankova

South-West University "Neofit Rilski", Blagoevgrad, Bulgaria

E-mail:chuchich@abv.bg

Introduction

The discovery of the guanine analogue of acyclovir (9-[(2-hydroxyethoxy)methyl]guanine), ACV, set the stage for a new generation of antiviral agents [1, 2]. Along with its high specificity, ACV demonstrates low aqueous solubility and low bioavailability by oral administration (14%). To overcome this problem, several acyclovir amino acid esters have been synthesized. Valacyclovir, the valine ester of ACV, was found to metabolise easily by oral administration and possess four-fold higher bioavailability than acyclovir.

In our previous work, we synthesized esters of acyclovir with (4-F-phenylalanine **1**) and bile acids (deoxycholic **2** and chenodeoxycholic **3** acids) (Figure 1.) and studied their antiviral activity against HSV-1, HSV-2 and EBV. Under the particular experimental conditions the most promising anti-EBV candidate compounds is (DCh-ACV) **2**, for which the toxicity:activity index (MNC:MIC) is the highest among the compounds tested and as high as the one for acyclovir.

The object of this study was to assess the chemical stability of some of the synthesized acyclovir esters with peptidomimetics at pH 1.0 and pH 7.4 at 37°C. An HPLC method was used for quantification of the ester concentrations [3, 4].

Results and discussion

The chemical stability of acyclovir esters: 4-F-phenylalanylacyclovir (R,S) (4-F)-Phe-ACV) **1**, acyclovirdeoxycholol (DCh-ACV) **2** and acyclovirchenodeoxycholol (CCh-ACV) **3** was studied under experimental conditions of biological relevance, i.e. at pH 1 and pH 7.4, at a temperature of 37°C. The structures of the compounds under investigation are presented in Fig. 1. During analysis each sample was directly analyzed by HPLC.

It was established that, under the described experimental conditions, some esters are underwent decomposition by hydrolysis. The hydrolysis followed apparent first order kinetics, and the rate constants (K) were obtained as slopes from the semi-logarithmic plots of the unchanged ester concentration versus time. The chemical stability was assessed by means of the decomposition half-lives $t_{1/2}$:

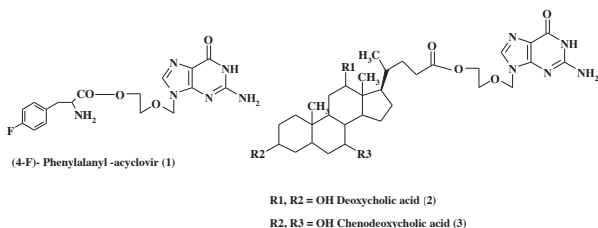


Fig. 1. Structures of new acyclovir analogues

Table 1. The rate constants k and $t_{1/2}$ values of the examined compounds at pH=7.4

Compound	k [1/mol.s]	$t_{1/2}$ [min]	$t_{1/2}$ [h]
1.(4-F)-Phe-ACV)	0.00022	3176.04	52.9
2.(DCh-ACV)	0.00009	7419.9	123.7
3.(CCh-ACV)	0.00016	4463.31	74.4

Table 2. The rate constants k and $t_{1/2}$ values of the examined compounds at pH=1.0

Compound	k [1/mol.s]	$t_{1/2}$ [min]	$t_{1/2}$ [h]
1.(4-F)-Phe-ACV)	0.00645	107.49	1.8
2.(DCh-ACV)	0.00032	2176.05	36.3
3.(CCh-ACV)	0.00028	2439.6	40.7

The chemical stability experiments revealed that the examined amino acid ester of acyclovir were relatively unstable in acidic pH, but bile acid ester is stable in the same pH (Fig. 2). In pH 7,4 all of tested drugs are more stable than valacyclovir ($t_{1/2} = 13$ h) – the first effective prodrug of acyclovir. In acidic pH DCh-ACV and CCh-ACV are more stable than valacyclovir.

The compounds DCh-ACV and CCh-ACV with appreciable effect against HSV-1 exhibited satisfying chemical stability. Acyclovirchenodeoxycholol **3** is the most promising anti-EBV prodrug candidate with high activity and satisfying chemical stability.

Acknowledgments

For the support of this work we are grateful to the National Found for Scientific Research of Bulgaria (Contracts DMU-03/2), South-West University "Neofit Rilski" Bulgaria (SRP-A4/12).

References

- [1] Elion, G.B.; Furman, P.A.; Fyfe, J.A.; de Miranda, P.; Beauchamp, L.; Schaeffer, H.J. *Proc Nat Acad Sci USA*. **1977**, *74*, 5716–5720.
- [2] De Clercq, E.; Field, H.J. *Br J Pharmacol*. **2006**, *147*, 1–11.
- [3] Zacchigna, M.; Di Luca, Maurich G.V.; Boccu, E. *Farmaco*. **2002**, *57*, 207–214.
- [4] Zhivkova, Zv.; Stankova, I. *Int J Pharm*. **2000**, *200*, 181–185.

Comparative evaluation of [¹¹¹In-DOTA]GRP analogs as candidates for GRPR⁺-tumor imaging: Preclinical results

Pantelis I. Marsouvanidis^a, Theodosia Maina^a, Eric P. Krenning^b,
Marion de Jong^b, Berthold A. Nock^a

^aMolecular Radiopharmacy, I/R-RP, NSCR "Demokritos", Athens, Greece; ^bDepartment of Nuclear Medicine, Erasmus MC, Rotterdam, The Netherlands

E-mail: pmarsouvanidis@yahoo.gr

Introduction

Gastrin-releasing peptide receptors (GRPR) have attracted much attention owing to their expression in many frequently occurring human cancers, such as in prostate, breast and lung cancer. So far, radiopeptides derived from the amphibian tetradecapeptide bombesin (BBN) have been proposed for diagnostic imaging and radionuclide therapy of GRPR-expressing tumors [1-4]. Instead, we have designed a series of analogs based on the mammalian 27-mer GRP, truncated at positions 13/14 or at positions 17/18. All analogs carry the chelator DOTA at the N-terminus for stable binding of medically useful radiometals (e.g. ¹¹¹In) and comprise: SAR-G2= DOTA-GRP(14-27); SAR-G3= DOTA-GRP(13-27); SAR-G4= DOTA-GRP(17-27); and SAR-G5= DOTA-GRP(18-27). We were especially interested to investigate potential effects of positively charged Arg¹⁷ and/or Lys¹³ on the biological performance of resulting radioligands.

Results and Discussion

Based on affinity, as determined during competition binding assays against [¹²⁵I-Tyr⁴]BBN in GRPR-expressing prostate cancer PC-3 cell membranes, compounds can be ranked as follows: SAR-G3 > SAR-G2 > SAR-G4 >> SAR-G5 (Fig. 1). Thus, the GRP(13/14-27) analogs show superior GRPR-affinity than their shorter GRP(17/18-27) counterparts. Furthermore, the basic amino acids Lys¹³ and Arg¹⁷ enhance the affinity of SAR-G3 and SAR-G4, respectively, for the GRPR.

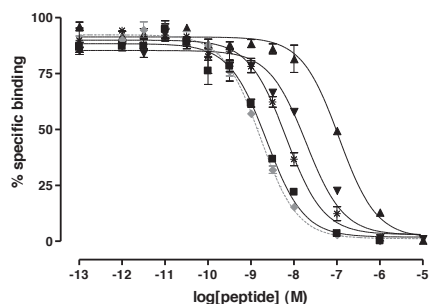


Figure 1: Comparative competition binding data of SAR-Gs in PC-3 cell membranes. * SAR-G2 (6.6±0.2 nM), ■ SAR-G3 (2.3±0.2 nM), ▼ SAR-G4 (19.2±2.9 nM), ▲ SAR-G5 (112±16 nM), ◆ [Tyr⁴]BBN (1.6±0.1 nM).

Results of RP-HPLC analysis of blood collected 5 min after injection of [¹¹¹In]SAR-Gx (100 µL, 0.8-0.9 mCi, ≈3 nmol peptide) in healthy Swiss albino mice is summarized in Table 1. During this period 20-30% of parent [¹¹¹In]SAR-Gx survived, except for [¹¹¹In]SAR-G2 which was almost totally consumed (<5% intact).

Table 1: [¹¹¹In]SAR-Gx found intact in the blood of mice 5 min after radioligand injection.

Radiopeptide	Formula	%intact [¹¹¹ In]SAR-Gx
[¹¹¹ In]SAR-G2	[¹¹¹ In-DOTA ⁰]GRP(14-27)	4
[¹¹¹ In]SAR-G3	[¹¹¹ In-DOTA ⁰]GRP(13-27)	20
[¹¹¹ In]SAR-G4	[¹¹¹ In-DOTA ⁰]GRP(17-27)	27
[¹¹¹ In]SAR-G5	[¹¹¹ In-DOTA ⁰]GRP(18-27)	22

Comparative biodistribution data at 4 h and 24 h after injection of [¹¹¹In]SAR-Gx (100 μL, 2 μCi, 10 pmol total peptide) in ♀SCID mice bearing human PC-3 xenografts is summarized in Fig. 2. All radiopeptides displayed specific uptake in the PC-3 tumor, as shown by the lower tumor values attained in the animal groups treated with excess (40 nmol) [Tyr⁴]BBN (4 h block). Interestingly, the positive Lys¹³-containing [¹¹¹In]SAR-G3, displayed a twice as high tumor targeting than the rest members of the group, consistent with its higher *in vitro* affinity. The high tumor uptake was, however, compromised by an undesirably high renal accumulation. The latter may be effectively reduced by kidney protection strategies currently applied [5].

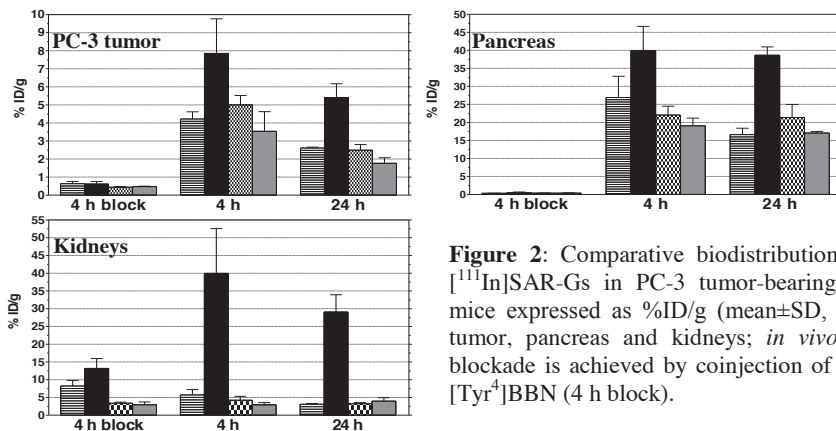


Figure 2: Comparative biodistribution data of [¹¹¹In]SAR-Gs in PC-3 tumor-bearing ♀SCID mice expressed as %ID/g (mean±SD, n=4) for tumor, pancreas and kidneys; *in vivo* GRPR-blockade is achieved by coinjection of 40 nmol [Tyr⁴]BBN (4 h block).

In conclusion, human GRP-based radioligands can target GRPR-expressing tumors *in vivo* as effectively as their amphibian BBN homologs providing a supplementary platform for innovative structural interventions. Both peptide chain length and the presence of basic amino acids greatly affect GRPR-affinity, metabolic stability and *in vivo* profile of SAR-G radioligands, especially tumor, pancreas and renal uptake.

References

- [1] Gugger, M.; Reubi, J.C. *Am. J. Pathol.* **1999**, *155*, 2067.
- [2] Reubi, J.C. *Endocr. Rev.* **2003**, *24*(4), 389.
- [3] Maina, T.; Nock, B.; Mather, S. *Cancer Imaging*, **2006**, *6*, 153.
- [4] Sancho, V.; Di Florio, A.; Moody, T.W.; Jensen, R.T. *Curr. Drug Deliv.* **2011**, *8*(1), 79.
- [5] Gotthardt, M.; van Eerd-Vismale, J.; Oyen, W.J.; et al. *J. Nucl. Med.* **2007**, *48*(4), 596.

Synthesis of a cyclic CPP by on-resin side chain-to-side chain cyclisation via CuAAC click chemistry

Florian Reichart and Ines Neundorf

Institute of Biochemistry, University of Cologne, Cologne, 50674, Germany

E-mail: ines.neundorf@uni-koeln.de

Introduction

Cell-penetrating peptides (CPPs) are delivery vectors that are supposed to circumvent the problem of limited transport of bioactive molecules into their target cells. During the last years they have been used for the intracellular transport of a number of different bioactive substances [1]. Recently, we demonstrated that the CPP sC18, which is made up of the residues 106–121 of the C-terminal region of the cationic antimicrobial cathelicidin peptide, CAP18, is an effective carrier peptide for the cellular transport of small organic substances like fluorophors and toxic peptide sequences [2,3]. However, the general limitation of this strategy for future in vivo applications is the only poor proteolytic stability of peptides. In general, linear peptides are more susceptible to degradation by endogenous peptidases than their cyclic analogs [4]. Aim of this study is to cyclise a sC18 variant on-resin by side chain-to-side chain cyclisation by means of CuAAC click chemistry.

Results and Discussion

The linear precursor peptide for cyclisation was derived from the peptide CAP18(106-117) (sequence: G¹⁰⁶LRK¹⁰⁹RLRKFRNK¹¹⁷-NH₂) with Gly¹⁰⁶ and Lys¹⁰⁹ substituted by the clickable amino acids L-propargylglycine (Pra) in position 106 and L-(ε-azido-)lysine (Lys(N₃)) in position 109, respectively. This linear peptide – (Pra¹⁰⁶, Lys(N₃)¹⁰⁹)-CAP18(106-117) (**1**) – was synthesised via standard Fmoc solid phase peptide synthesis (SPPS) with Oxyma Pure and DIC as activation and coupling reagents, carried out in double coupling steps for each amino acid on Rink amide AM polystyrene resin as solid support. After completion of the synthesis a sample cleavage of the peptide from the solid support with subsequent HPLC and MALDI-MS/MS analysis confirmed the identity of the linear peptide (**1**) with 65 % purity due to HPLC peak area (Figure 1).

Peptide cyclisation was done on-resin without previous purification by means of copper-mediated azide-alkyne cycloaddition (CuAAC) reaction via side-chain to side-chain cyclisation. Therefore, Cu(I) was introduced equimolar to the peptide as CuBr, which shows sufficient solubility in a solution of MeCN/H₂O 1:1 (v/v) that further provides satisfactory swelling properties for the applied polystyrene resin. Despite thorough degassing of the solvent, argon covering and sealing of the reaction vessel, the use of sodium ascorbate is recommended as reducing agent for emerging Cu(II), to keep sufficient amounts of Cu(I) available. DIPEA was added as weak base to reach pH 8, and 2,6-lutidine as ligand for Cu(I). The cyclisation was stopped after 24 h by simple washing off the reaction mixture and removal of residual copper ions with a saturated EDTA solution.

After cyclisation the peptide was cleaved from the solid support accompanied by concomitant full deprotection of the amino acid side chains to give the cyclic peptide cyclo-

(Pra¹⁰⁶, Lys(N₃)¹⁰⁹)-CAP18(106-117) (**2**) with 55 % yield due to HPLC peak area. Since there is no change in the molecular mass observable before and after cyclisation, the products were identified by their RP-HPLC peak retention time and MALDI-MS/MS fragmentation. The collected HPLC fractions confirmed the linear or cyclic nature of the peptides. Due to the insusceptibility of cyclic moieties to complete fragmentation any amino acid cleavage during MS/MS-fragmentation is only expected to occur in the linear part of the peptide, leaving the cyclic part untouched. This results in the selective appearance of certain corresponding b- and y-fragments allowing to distinguish between the linear and cyclic form.

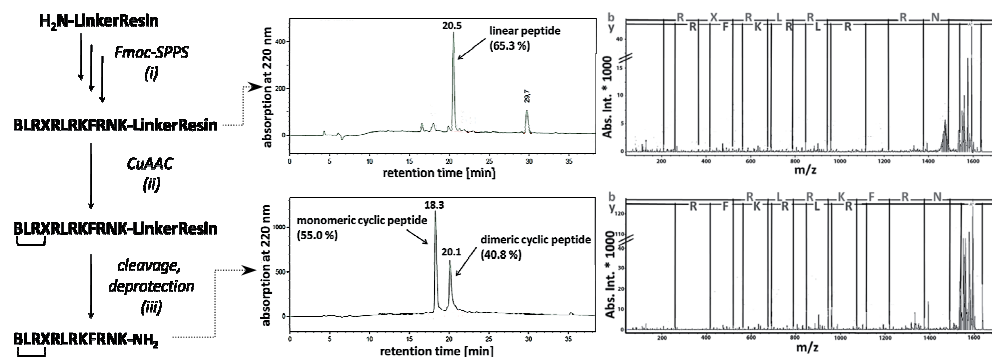


Figure 1. (left-) Synthesis procedure for (**2**); (i) Fmoc-solid-phase peptide synthesis based on Rink amide AM polystyrene resin; (ii) CuBr (1 eq), Na-ascorbate (3 eq), DIPEA (10 eq), 2,6-lutidine (10 eq) in MeCN/H₂O (1:1), argon, pH~8, rt, 24 h; (iii) TFA/TIS/H₂O 95:2.5:2.5 (v/v/v), rt, 3 h. (center-) RP-HPLC-analysis of sample cleavage before (above) and after cyclisation (below). (right-) MALDI-MS/MS fragmentation pattern of linear (**1**) (above) and cyclic monomeric peptide (**2**) (below); b- and y-fragments are indicated on top. (B: L-propargylglycine, X: L-(*ε*-azido-)lysine)

Beside the monomeric cyclic peptide, also the corresponding dimeric species occurred in the course of cyclisation to an extent of 41%. For suppression of the dimer formation peptide cyclisation could be carried out on low loading resins with high swelling properties for pseudo dilution effects. Additionally, performing the reaction in solution allowing higher peptide dilution would be an alternative since dimerisation is known to be highly dependent on the peptide concentration [5].

In conclusion, the linear cell-penetrating peptide CAP18(106-117) was successfully cyclised on-resin via side-chain to side-chain cyclisation using CuAAC reaction. Currently, we are working on the optimisation of this reaction to synthesise additional sC18 CPP variants with a cyclic peptide backbone and on investigating their structural and biological properties.

References

- [1] Langel, U., Cell-penetrating peptides: Processes and Applications, CRC Press, Boca Raton, 2002.
- [2] Neundorf, I. et al. *Pharmaceuticals* **2009**, 2, 49.
- [3] Splith, K. et al. *Bioconjugate Chem.* **2010**, 21, 1288.
- [4] Mandal, D. et al. *Angew. Chem. Int. Ed.* **2011**, 50, 9633.
- [5] Choi, W.J. et al. *Bioorg Med Chem Lett.* **2006**, 16(20), 5265.

Neurotensin and oligo-branched peptides decorating liposomes for selective doxorubicin delivery

Diego Tesauro,¹ Antonella Accardo,¹ Chiara Falciani,² Ilenia Brunetti,² Barbara Lelli,² Luisa Bracci,² Giancarlo Morelli¹

¹*Dept. Biological Sciences, CIRPeB, Univ. of Naples "Federico II", IBB CNR, Via Mezzocannone 16, 80134 Naples, Italy;* ²*Dept. Molecular Biology, Univ. of Siena, Via Fiorentina 1, 53100 Siena, Italy*

E-mail:dtesauro@unina.it

Introduction

Nanoparticles play a crucial role in medicine for their potential application as in vivo carriers of active principles [1]. Liposomes display unique pharmacokinetic properties slowly releasing drugs loaded in the inner aqueous cavity. This would allow the reduction of undesired effects on non target organs and the increase of therapeutic efficacy on the desired tissues [2]. Drug delivery procedures, aimed at achieving this goal, have been investigated particularly for the treatment of cancer. In the last years we have developed supramolecular aggregates labeled by bioactive peptides able to recognize overexpressed receptors on tumor cells membrane delivering doxorubicin chemiotherapeutic drug [3].

We previously studied the use of tetrabranch peptides that contain the sequence of the human regulatory peptide neurotensin (NT) or a truncated form (NT8–13) as tumor targeting agents. NT receptor type1(NTS1) is overexpressed in severe malignancies such as small cell lung cancer and colon, pancreatic, and prostate carcinomas [4].

Here we report the results achieved delivering doxorubicin specifically by neurotensin decorating liposome toward overexpressing neurotensin receptors cells. Liposomes were obtained by co-aggregation of the DOPC phospholipid with a new synthetic amphiphilic molecule NT4Lys(C18)₂. The peptide based monomer contains a lysine scaffold derivatized with a lipophilic moiety and with a tetra-branched neurotensin (NT1-13) peptide or a truncated form (NT8–13) able to recognize overexpressed receptors.

Results and Discussion

The NT4Lys(C18)₂, amphiphilic molecules were designed in order to form mixed liposome with phospholipids exposing on surface NT sequences able to recognize receptors. To achieve this goal two oxoethylene (H-AhOH-OH) residues, acting as spacers, and a hydrophobic moiety based on two C18 alkyl chains were linked to C terminal of the three-lysine branched core. Further on N- terminals of the core four copies of NT1-13 or NT 8-13 peptide were tethered.. Chemical synthesis of NT4Lys(C18)₂ was carried out on solid phase following modified protocols of the Fmoc/t-Bu-based procedures for solid-phase peptide synthesis (SPPS) with step-by-step peptide chain elongation. The orthogonally-protected lysine (DdeLys(Fmoc)-OH) residue was anchored to the Rink amide resin. After removal of the Fmoc lysine side chain protecting group, two H-AhOH-OH linkers and the hydrophobic moiety with two C18 chains were sequentially introduced. Dde deprotection of the lysine N-terminal amine allows the synthesis of the branched NT tetramers. The

peptide derivatives were collected in good yield after HPLC–RP purification and were analyzed by mass spectrometer. Liposomes were formulated following well assessed procedure adding the NT4Lys(C18)₂ peptide monomers to DOPC in ratio 5:95. The size of liposome was determined by Dynamic light scattering measurements which indicate a value for the hydrodynamic radius (RH) of 88.3 ± 4.4 nm.

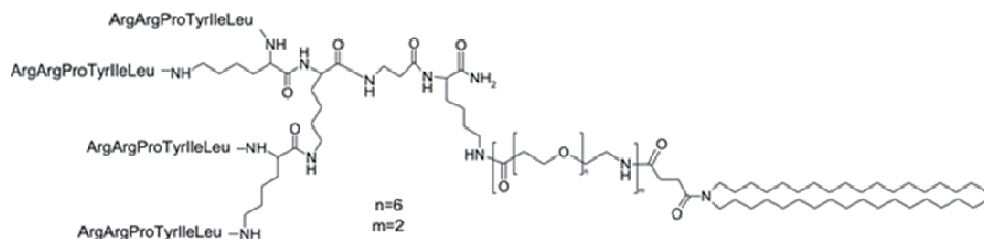


Figure Schematic representation of (NT8-13)₄Lys(C18)₂ amphiphilic monomer.

Liposomes were loaded with doxorubicin by using the pH gradient method. The selective internalization and cytotoxicity of neurotensin labeled liposomes as compared to pure DOPC liposomes, were tested in HT29 human colon adenocarcinoma and TE671 human rhabdomyosarcoma cells, both of which express neurotensin receptors. FACS analysis indicates an increase in fluorescence signal of the (NT8-13)₄-liposomes, in both cell lines and the cytotoxicity is increased four-fold with respect to DOPC. These effects could be ascribed to the higher rate of internalization for DOPC-(NT8-13)₄Lys(C18)₂-DOXO liposomes, due to stronger binding driven by a lower dissociation constant of the NT4-liposomes that bind the membrane onto a specific protein, in contrast to DOPC liposomes, which approach the plasma membrane unselectively. Similar results were achieved testing (NT1-13)₄Lys(C18)₂ containing liposomes.

Acknowledgments

The authors thank the MIUR for financial support (PRIN 2009WCNS5C).

References

- [1] Torchilin V.P. *Nat Rev drug* **2005**, *4*, 145.
- [2] Langer, R.. *Nature*, **1998**,, 392, 5.
- [3] Accardo, A.; Morisco, A.; Tesaro, D.; Pedone, C.; Morelli G. *Therapeutic Delivery* **2011**, *2*, 235.
- [4] Falciani, C.; Fabbrini, M.; Pini A.; Lozzi, L.; Lelli, B.; Pileri, S.; Brunetti, J.; Bindi, S.; Scali,S.; Bracci, L. *Mol. Cancer Ther.* **2007**, *6*, 2441.

Non-toxic delivery of siRNA by amphiphilic peptides and silencing of hTERT

Masayuki Fujii* and Shutaro Fujiaki

Department of Biological & Environmental Chemistry, Kinki University, 11-6 Kayanomori,
Izuka, Fukuoka 820-8555, Japan

E-mail:mfujii@fuk.kindai.ac.jp

Introduction

Recently, small interfering RNA (siRNA), one kind of RNA interference (RNAi) technology represent the most common and, to date, the most effective method to inhibit target gene expression in human cells. It is also a common recognition that non-toxic delivery of siRNA is an urgent problem for the therapeutic application of siRNA. For the efficient gene silencing *in vivo*, prolonged circulation of siRNA, non-toxic cellular uptake and resistance against enzymatic degradation are indispensably required.¹ Telomerase activity has been regarded as a critical step in cellular immortalization and carcinogenesis and because of this, regulation of telomerase represents an attractive target for anti-tumor specific therapeutics.

Results and Discussion

In this paper, we present the efficient and non-toxic cellular uptake of siRNA using novel amphiphilic peptides (Pfect β) and the application to silencing of hTERT in human cancer cell lines.

As shown in Figure 1, the complex of siRNA and a specific amphiphilic peptide (Pfect β 7) was taken up into cells more effectively than those of siRNA and the currently commercial lipofection reagents. Spectroscopic observations suggested that the peptide Pfect β bound to dsDNA and dsRNA forming an antiparallel β -sheet structure in the minor or major groove of double stranded nucleic acids and consequently the surface of the complex became lipophilic and the complex could easily penetrate into cells.

Silencing effect of siRNA targeting hTERT mRNA were also evaluated in HeLa cells and the results were summarized in Figure2. The complex also showed a high silencing effect against hTERT mRNA.

siRNA-Pfect β 7 complex was completely non-toxic against human cancer cells and the half-life time of siRNA was largely extended to over 48h in the complex (data not shown).

Thus shown above, siRNA-Pfect β 7 complex could be effectively taken up into cells, showed a high silencing effect against hTERT mRNA, showed almost no cyto-toxicity and protected siRNA against nuclease digestion. We believe that the therapeutic application of these siRNA-amphiphilic peptides complex is very promising.

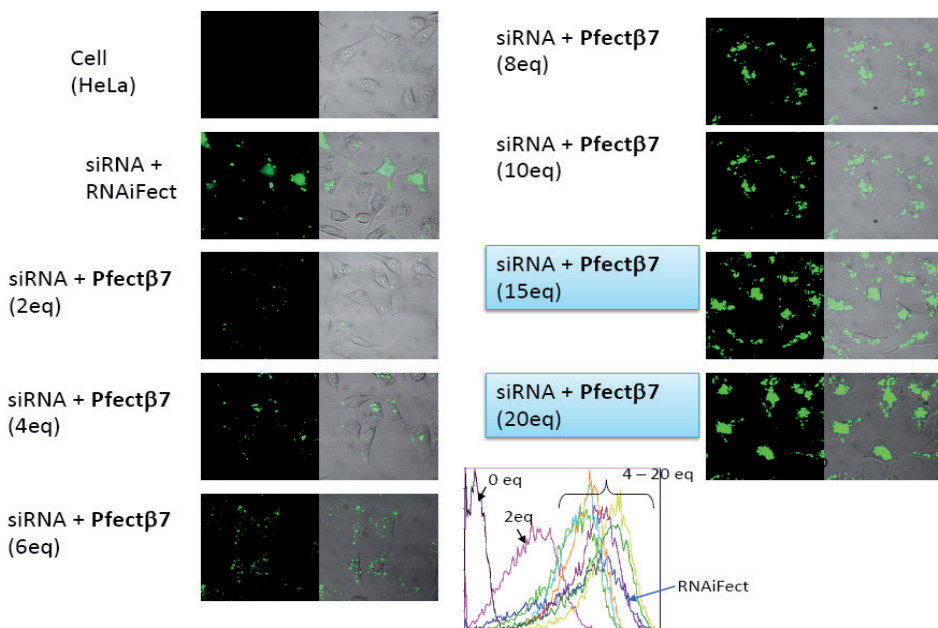


Figure 1. Cellular Uptake of siRNA –Pfectβ7 Complex.

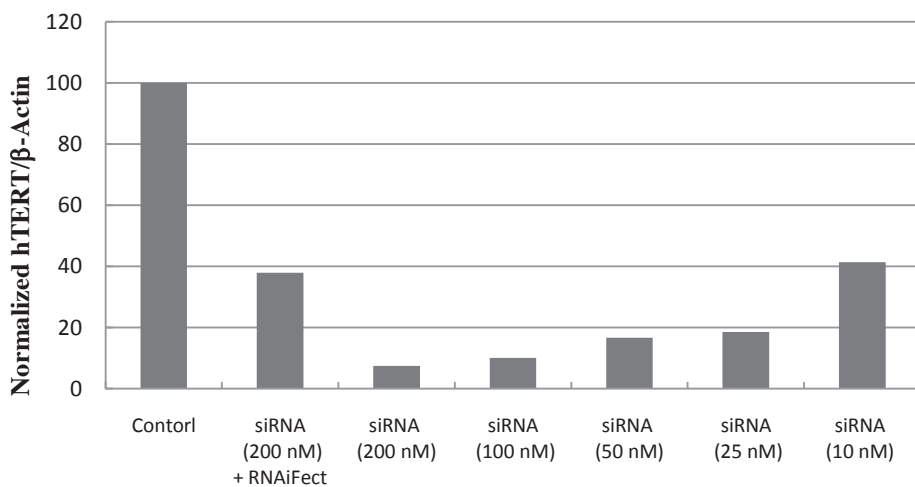


Figure 2. Silencing of hTERT by siRNA-Pfectβ7 Complex

References

- [1] Gaynor, J. W., Campbell, B. J., Cosstick, R., *Chem. Soc. Rev.*, (2010), **39**, 4169-4184.

Botulinum enzyme retargeted using SNARE protein stapling is capable of selectively silencing neuroendocrine cells

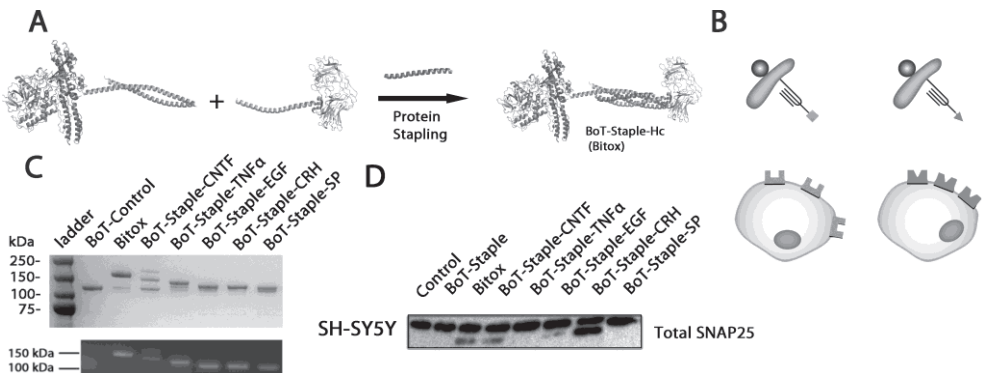
Jason Arsenault, Enrico Ferrari, Dhevahi Niranjana, Bazbek Davletov*

Laboratory of Molecular Biology, Medical Research Council, Neurobiology division,
Cambridge, UK

*E-mail: bazbek@mrc-lmb.cam.ac.uk

Introduction

A number of pathologies involving a dysregulation of exocytosis are capable of wreaking havoc on hormonal homeostasis. Recently, we have developed SNARE based protein stapling, which enables a fast throughput assembly of novel protein chimeras for long term cell silencing [1]. Using peptide sequences implicated in the irreversible parallel tetrahelical coiled-coil motif, we are able to fuse together enzymatic subunits with targeting domains in a “lego” like manner. These targeted domains are attached to the N or C terminal of our SNARE motif peptides expressed recombinantly or by solid phase peptide synthesis [1-3]. This stapling method permits us to assemble the translocation and enzymatic domains of botulinum neurotoxin type A (BoNT/A) that can inhibit exocytosis once internalized, with various receptor-binding domains to target cells selectively. To assay these targeting domains certain cell models were chosen such as two neuroblastoma (Neuro2A and SH-SY5Y), an insulinoma (Min6), a pheochromocytoma (Pc-12), and a pituitary adenoma (AtT-20) cell lineages. These cells can display hypersecretory pathologies if present in animals and patients. Furthermore, to ascertain cell selectivity in a heterologous cell population, *ex vivo* cortical cells were used. Figure 1 shows the tri component SNARE assembly process (A) to exploit the cell surface receptor expression (B). The SDS-resistant complexes can be visualized on gel and illuminated by the use of a fluorescent staple peptide in the complex (Fig 1C) [1-2]. Cleaved SNAP25 was visualized in western blotting by the appearance of a smaller band at 24 kDa below the normal 25 kDa band (Fig 1D). BoT designates the Botulinum neurotoxin’s enzymatic and translocation domain. Bitox designates the functionally reassembled native-like toxin [1,3].



Results and Discussion

Through this study over fifty different polypeptide targeting domains, whose sequences have been taken from native hormones, growth factors, neurotransmitters and cytokines were tested on each of the aforementioned cell types. Among the identified functional targeting domains Vasoactive intestinal peptide (VIP), Ciliary neurotrophic factor (CNTF), Epidermal growth factor (EGF), and Corticotrophin releasing hormone (CRH) were capable of driving internalization into certain cell lineages. SNAP25 cleavage indicates that the VIP targeting domain could be internalized into Neuro2A and Pc-12 and to a lesser degree in SH-SY5Y cells (exemplified in figure 1D). The CNTF domain could internalize the enzyme into Neuro2A and SH-SY5Y cells. The EGF moiety could internalize the complex into Pc-12 and Min6 cells and to a lesser degree into Neuro2A and SH-SY5Y. The CRH domain was able to internalize abundantly into AtT-20, Neuro2A and SH-SY5Y cells. Pharmacological competitions with an excess of VIP antagonist, human CNTF, and human EGF could reduce the SNAP25 cleavage of their homologous toxin assemblies, which were applied on the susceptible cells. Once internalized, the enzyme's cleavage of intracellular SNAP25 inhibits vesicle fusion at the plasma membrane, thus reducing exocytosis rates as observed by inhibition of ³H-norepinephrine release in Pc-12 and SH-SY5Y cells, and a reduction of adrenocorticotrophin releasing hormone and insulin in AtT-20 and Min6 cells respectively as measured by corresponding immunoassay. To visualize population differences, *ex vivo* rat cortical cells were observed by confocal microscopy using an anti-Map2ab antibody to label dendrites of mature neurons and an antibody capable of recognizing only BoNT/A-cleaved SNAP25. Colocalization measurements showed that the native BoNT/A was indiscriminate in its cellular targeting affecting both Map2ab+ and - cells. In contrast, the EGF targeting domain directed the enzyme almost exclusively towards immature Map2ab- cells while the CNTF directed the enzyme towards Map2ab+ cells. These results thus indicate that our assemblies are biologically valid for reducing exocytosis rates and are able to target specific populations within a heterologous culture. Furthermore, our complexes can be assembled using a fluorescent staple to monitor internalization and localization [1-2]. Since the staple can also be functionalized, multiple targeting domains can be assembled on the same toxin complex. Combinations of homo- and hetero- targeting domains together with other diverse functionalities enable a "swiss army knife" applications of protein assembly for multiple biotechnological and medical purposes.

Acknowledgments

The Medical Research Council of the United Kingdom funded this research. We would like to thank John O'Brien for microscopy advice and Chunjing Gu and Yvonne Valis for help with animal tissue experimentation.

References

- [1] Darios, F., Ferrari, E., et al., *PNAS*, **2010**, 107(42), 18197-201.
- [2] Ferrari, E., Soloviev, M., et al., *Bioconjug Chem*, **2012**, 23(3), 479-84.
- [3] Ferrari, E., Maywood E.S., et al., *Toxins (Basel)*, **2011**, 3(4), 345-55.

Short-chain fatty acid acylated daunorubicin-GnRH-III bioconjugates with enhanced cellular uptake, *in vitro* and *in vivo* antitumor activity

**Rózsa Hegedüs^{1,2}, Marilena Manea^{3,4}, Erika Orbán¹, Ildikó Szabó¹, Éva
Sipos⁵, Gábor Halmos⁵, Bence Kapuvári⁶, Ákos Schulcz⁶,
József Tóvári⁶, Gábor Mező¹**

¹Research Group of Peptide Chemistry, Hungarian Academy of Sciences, Eötvös Loránd
University, 1117 Budapest, Hungary; ²Department of Organic Chemistry, Eötvös L.
University, 1117 Budapest, Hungary; ³Laboratory of Analytical Chemistry and Biopolymer
Structure Analysis, Department of Chemistry, University of Konstanz, 78457 Konstanz,
German; ⁴Zukunftskolleg, University of Konstanz, 78457 Konstanz, Germany; ⁵Department
of Biopharmacy, Medical and Health Science Center, University of Debrecen, 4032
Debrecen, Hungary; ⁶National Institute of Oncology, 1122 Budapest, Hungary

E-mail: rozsa.hegedus@gmail.com

Introduction

Cancer is one of the leading causes of death worldwide. Besides lung, stomach, liver and breast cancer, colorectal cancer is still a major health problem and one of the most common causes of cancer death in the developed countries (WHO) [1]. It has been shown that a fiber and complex carbohydrate rich diet could be preventive for colon cancer. Depending on the source, the major products are linear (acetate, propionate, butyrate, valerate, hexanoate) and branched (isobutyrate, isovalerate) short chain fatty acids (SCFAs), that exert a tumor growth inhibitory effect [2]. Therefore, SCFAs may be an important component of drug delivery systems for targeted cancer chemotherapy.

Tumor targeting with gonadotropin-releasing hormone (GnRH) analogs is based on the discovery that GnRH receptors are highly expressed in many tumor cells, compared with their expression in normal tissues [3,4]. Using these peptides as targeting moieties in a bioconjugate with chemotherapeutic agents can increase the selectivity and reduce the toxic side effects of the anticancer drugs. In particular, GnRH-III (<EHWSHDWKPG-NH₂) is suitable as a targeting moiety due to its antiproliferative effect and weak endocrine activity in mammals.

In the present work, we report on the synthesis and biochemical characterization (enzymatic stability, cellular uptake, *in vitro* and *in vivo* antitumor activity as well as GnRH-receptor binding affinity) of novel daunorubicin-GnRH-III bioconjugates in which Ser in position 4 was replaced by Lys acylated on its ϵ -amino group with SCFAs of different length (Glp-His-Trp-Lys(X)-His-Asp-Trp-Lys(Dau=Aoa)-Pro-Gly-NH₂, where Glp is pyroglutamic acid, Aoa is aminoxyacetyl, Dau is daunorubicin, and X: propionyl, *n*-butyryl, isobutyryl, valeryl, isovaleryl, crotonyl, caproyl and myristyl groups) in order to enhance the antitumor activity, cellular uptake and enzymatic stability of the bioconjugates.

Results and Discussion

The peptides were synthesized by SPPS (Fmoc/tBu) using orthogonal protecting groups (ivDde and Mtt) for lysine. The SCFAs and aminooxyacetyl group were attached to the peptide chain on the solid support, while the chemical ligation (oxime bond formation) of daunorubicin was carried out in solution (0.2 M NH₄OAc buffer, pH 5.0) [5].

Replacement of ⁴Ser by Lys(X) enhanced the *in vitro* cytostatic effect and cellular uptake of the oxime bond-linked Dau-GnRH-III bioconjugates on MCF-7 (human breast) and HT-29 (human colon) cancer cell lines. The highest *in vitro* cytostatic effect was determined in case of bioconjugates GnRH-III(⁴Lys(iBu), ⁸Lys(Dau=Aoa)) (IC₅₀(μM): 2.2±0.0 (MCF-7) and 2.0±0.6 (HT-29)) and GnRH-III(⁴Lys(nBu), ⁸Lys(Dau=Aoa)) (IC₅₀(μM): 0.7±0.2 (MCF-7) and 2.2±0.6 (HT-29)). These two compounds were also the most effectively taken up by both tested cell lines. Almost 100% of the cells were Dau positive at 20 μM concentration.

All bioconjugates were digested by α-chymotrypsin (the cleavage site was at the peptide bond ³Trp-⁴Lys(X)) and the degradation rate strongly depended on the type of fatty acid. Except GnRH-III(⁴Lys(iBu), ⁸Lys(Dau=Aoa)), the stability of bioconjugates was increased compared to GnRH-III(⁴Lys(Ac), ⁸Lys(Dau=Aoa)) [6] that has been so far the most efficient bioconjugate developed in our laboratories (e.g., 64% intact bioconjugate could be detected after 6 h in case of *n*-butyrylated and 33% in case of acetylated compound). In the presence of rat liver lysosomal homogenate, in all cases, the smallest identified drug containing metabolite was H-Lys(Dau=Aoa)-OH, that can bind to DNA [7]. Fragments without SCFAs were also identified by LC-MS suggesting the release of free fatty acids. However, no free daunorubicin release was observed.

Comparing the investigated bioconjugates containing GnRH-III derivatives as targeting moieties, GnRH-III(⁴Lys(nBu), ⁸Lys(Dau=Aoa)) showed the highest affinity to the GnRH receptors both on human pituitary (IC₅₀(nM): 9.03±0.78) and human prostate cancer tissue (IC₅₀(nM): 7.41±0.55) in a radioligand binding assay.

No macroscopic metastases were observed in any of the investigated groups in the *in vivo* experiment on NSG HT-29 colon cancer bearing female mice. In contrast to the treatment with free daunorubicin, the bioconjugate GnRH-III(⁴Lys(nBu), ⁸Lys(Dau=Aoa)) had a positive effect on the interaction between the tumor and the surrounding tissues, which made the tumor easily operable. Moreover, the bioconjugate was less toxic.

Acknowledgments

This work was supported by grants from the Hungarian National Science Fund (OTKA NK 77485, OTKA K81596), TAMOP 4.2.1/B-09/1/KONV-2010-0007 and University of Konstanz (Zukunftskolleg, Project 879/08; AFF and Young Scholar Fund, Project 435/11).

References

- [1] Sauer, J.J.; Richter, K.K.; Pool-Zobel, B.L. *Nutr. Biochem.* **2007**, *18*, 736.
- [2] Beyer-Sehlmeyer G.; Gleis, M.; Hartmann, E.; *et al. Br. J. Nutr.* **2003**, *90*, 1057.
- [3] Mezö, G.; Manea, M. *Exp. Opin. Drug Deliv.* **2010**, *7*, 79.
- [4] Emons, G.; Sindermann, H.; Engel, J.; *et al. Neuroendocrinology* **2009**, *90*, 15.
- [5] Hegedüs, R.; Manea, M.; Orbán, E.; *et al. Eur. J. Med. Chem.* **2012**, *56*, 155.
- [6] Manea, M.; Leurs, U.; Orbán, E.; *et al. Bioconjug. Chem.* **2011**, *22*, 1320.
- [7] Orbán E.; Mezö, G.; Schlage, P.; *et al. Amino Acids* **2011**, *41*, 469.

Stability and biodistribution of three ¹¹¹In-labeled CCK2R-targeting peptides – A comparative study in mice

Aikaterini Kaloudi^a, Pantelis J. Marsouvanidis^a, Aikaterini Tatsi^a, Eric P. Krenning^b, Marion de Jong^b, Berthold A. Nock^a, Theodosia Maina^a

^aMolecular Radiopharmacy IRRP, NCSR “Demokritos”, Athens, Greece; ^bDepartment of Nuclear Medicine, Erasmus MC, Rotterdam, The Netherlands

E-mail: katerinakaloudi@yahoo.gr

Introduction

Radiolabeled minigastrin (MG) and cholecystokinin (CCK) analogs have been proposed for application in the diagnostic imaging and radionuclide therapy of CCK2R⁺ human tumors, like medullary thyroid cancer (MTC) [1-5]. Radiolabeled DOTA-MGs containing poly-Glu sequences, despite their excellent affinity to CCK2R and their high metabolic stability, have shown unfavorably high kidney accumulation [6]. This property limits their potential for CCK2R-targeted radionuclide therapy. In this study we have coupled the chelator DOTA at the N-terminus of Gastrin I (GI)-related sequences creating the following analogs: Sargastrin1 (SG1= [(DOTA)Gln¹,Nle¹⁵]GI), Sargastrin2 (SG2= [(DOTA)Gln¹,D¹⁰Glu⁶⁻¹⁰,Nle¹⁵]GI) and MG11 ([DOTA]D¹⁰Glu¹⁰]GI(10-17)). In SG2 the (Glu)₅-chain of the original peptide has been replaced by (D¹⁰Glu)₅, a modification reported to reduce kidney values in DOTA-MG radioligands [7]. MG11 is totally lacking the (Glu)₅-moiety and has shown poor stability and low renal uptake after injection in man [8]. Comparative data of the ¹¹¹In-labeled analogs retrieved from CCK2R-expressing animal models is presented herein.

Results and Discussion

Comparative biodistribution data for [¹¹¹In]MG11, [¹¹¹In]SG1 and [¹¹¹In]SG2 in SCID mice bearing CCK2R⁺ AR4-2J tumors is summarized in Fig. 1. [¹¹¹In]MG11 and [¹¹¹In]SG2 displayed significantly reduced kidney uptake (1.8±0.3 %ID/g and 46.3±9.8 %ID/g vs. 104.4±15.7 %ID/g of [¹¹¹In]SG1 at 4 h pi), but also lower uptake in the CCK2R⁺ implanted tumors and in the stomach.

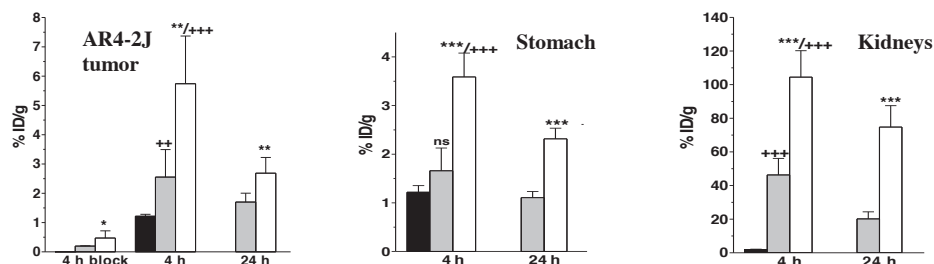


Figure 1: Comparative biodistribution (%ID/g) for [¹¹¹In]MG11 ■, [¹¹¹In]SG2 ■ and [¹¹¹In]SG1 □ in AR4-2J tumor-bearing SCID mice. Statistically significant differences (*) between [¹¹¹In]SG1 and (+) between [¹¹¹In]MG11 and the other radiopeptides: ns= non-significant, *⁺P<0.05 (significant), **/+⁺P<0.01, ***/+⁺P<0.001 (very significant).

As shown in Fig. 2, during RP-HPLC analysis of mouse blood collected 5 min after injection of test radioligand, [¹¹¹In]MG11 was found to be the least stable (only 4% of parent peptide detected) followed by [¹¹¹In]SG1 (≈20%), while [¹¹¹In]SG2 was the most stable (>40%).

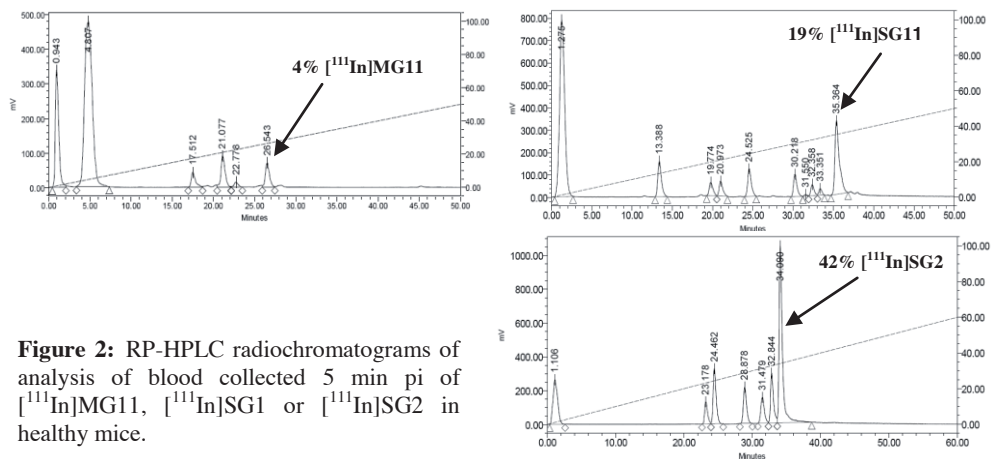


Figure 2: RP-HPLC radiochromatograms of analysis of blood collected 5 min pi of [¹¹¹In]MG11, [¹¹¹In]SG1 or [¹¹¹In]SG2 in healthy mice.

Substitution of Glu⁶⁻¹⁰ by dGlu⁶⁻¹⁰ in GI-derived radiopeptides enhanced stability and reduced renal uptake by ~2.5 fold. On the other hand, removal of the (Glu)₅-sequence in MG11 suppressed kidney accumulation but undermined stability. Both modifications, however, compromised tumor targeting, demonstrating that more efficacious structural changes in the GI motif are warranted to improve the *in vivo* profile of resulting radioligands.

Acknowledgments

This study was performed in the framework of COST Action BM0607: “Targeted Radionuclide Therapy”.

References

- [1] Reubi, J.C. *Curr. Top. Med. Chem.* **2007**, 7, 1239.
- [2] Behr, T.M.; Jenner, N.; Radetzky, S.; Béhé, M.; et al. *Eur. J. Nucl. Med.* **1998**, 25, 424.
- [3] Béhé, M.; Behr, T. M. *Biopolymers* **2002**, 66, 399.
- [4] Nock, B.A.; Maina, T.; Béhé, M.; et al. *Eur. J. Nucl. Med. Mol. Imaging* **2005**, 46, 1727.
- [5] Fröberg, A.C.; de Jong, M.; Nock, B.A.; et al. *Eur. J. Nucl. Med. Mol. Imaging* **2009**, 36, 1265.
- [6] Good, S.; Walter, M.A.; Waser, B.; et al. *Eur. J. Nucl. Med. Mol. Imaging* **2008**, 35, 1868.
- [7] Laverman, P.; Joosten, L.; Eek, A.; et al. *Eur. J. Nucl. Med. Mol. Imaging* **2011**, 38, 1410.
- [8] Breeman, W.A.P.; Fröberg, A.C.; de Blois, E.; et al. *Nucl. Med. Biol.* **2008**, 35, 839.

Synthesis and characterization of a ^{99m}Tc-labeled rhodamine-conjugated angiotensin peptide as a potential cardiac function imaging agent

Subhani M. Okarvi

Cyclotron and Radiopharmaceuticals Department, King Faisal Specialist Hospital
and Research Centre, MBC-03, PO Box 3354, Riyadh 11211, Saudi Arabia

E-mail: sokarvi@kfshrc.edu.sa

Introduction

Angiotensin II (Ang II) is an 8-amino acid peptide that has been known to play a vital role in cardiovascular system. The actions of Ang II have been implicated in many cardiovascular conditions, such as coronary heart disease and heart failure [1]. In an attempt to develop a single-photon emission computed tomography (SPECT)-based cardiac agent with enhanced targeting efficiency, we linked Ang II to rhodamine (Rh), a lipophilic cation (like ^{99m}Tc-MIBI), that specifically accumulates in the myocardium. Rhodamine is a cationic fluorescent dye that accumulates in mitochondria of the living cells and also in cardiac muscle cells [2, 3]. Rhodamine dyes share several properties with ^{99m}Tc-MIBI, the most commonly used myocardial perfusion agent, suggesting that radiolabeled Rh might prove useful for heart imaging [1, 2]. The Rh conjugated Ang II after radiolabeling with ^{99m}Tc was evaluated for its potential as a heart imaging agent. In addition to its usefulness as a heart imaging agent, this mitochondria-specific dye has been examined as a potential chemotherapeutic agent because of its retention in a variety of cancer cells for about 2 to 5 days, whereas, normal cells release it within 1 to 6 h [4]. It has been shown that Rh is relatively non-toxic to the normal cells but it selectively kills certain cancer cells both *in vitro* and *in vivo*. It is assumed that the inhibition of protein synthesis and oxidative phosphorylation in mitochondria by Rh may be responsible for its action. It is also believed that cancer cells in comparison to the normal epithelial cells may have a higher mitochondrial or plasma transmembrane potential; Rh crosses these barriers because of the net positive charge on the molecule. The high specificity for mitochondria and low toxicity to the healthy cells coupled with selective accumulation in carcinoma cells suggest that Rh when radiolabeled with Tc-^{99m} radionuclide may prove to be a new selective cancer diagnostic agent through non-invasive tools.

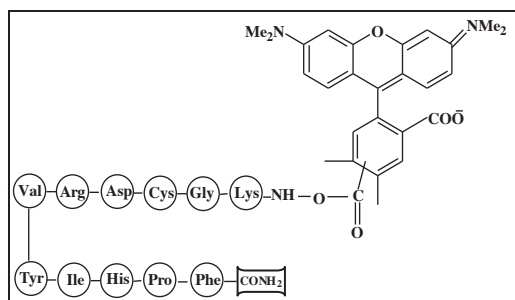


Figure 1. Structure of rhodamine-angiotensin II conjugate.

Rh-Lys-Gly-Cys-Asp-Arg-Val-Tyr-Ile-His-Pro-Phe-CONH₂ (Figure 1) was prepared by solid-phase peptide synthesis according to Fmoc/HBTU methodology. NHS-Rh was attached to the Ang II peptide via the free amino group of Lys residue by manual synthesis. Rh-Ang II conjugate was purified by HPLC and radiolabeled with ^{99m}Tc by the stannous-tartrate exchange labeling method. *In vitro* stability was determined in human plasma and in excess of cysteine. *In vivo* biodistribution and biokinetics were performed in Balb/c mice and Sprague Dawley rats at 30 and 60-min post-injection

Results and Discussion

The Rh-Ang II conjugate was successfully prepared by Fmoc-based solid-phase peptide synthesis. The conjugate radiolabeled efficiently (>75% labeling efficiency) with ^{99m}Tc via Cys-Gly-Lys chelating sequence. ^{99m}Tc-Rh-Ang II exhibited good radiochemical stability against cysteine transchelation and sufficient metabolic stability in human plasma *in vitro*. The cell-binding ability of the ^{99m}Tc-Rh-Ang II was determined on various human breast cancer cell lines (MDA-MB-231, MCF-7, T47D) and compared with clinically-used cardiac agent, ^{99m}Tc-MIBI. As can be seen in Figure 2, the cell uptake pattern of ^{99m}Tc-Rh-Ang II was found to be comparable with ^{99m}Tc-MIBI, indicating the potential of hybrid compound for targeting of breast cancer cells. In mice, the radioconjugate displayed efficient clearance from the blood and excreted mainly through the renal route with some excretion by the hepatobiliary pathway. The uptake in the heart was 1.8±0.5% ID/g as early as 30 min post-injection; whereas, the uptake in the lungs, liver, stomach and kidneys varied between 1–10% ID/g. In rats, ^{99m}Tc labeled conjugate displayed relatively better pharmacokinetic characteristics than mice, with low uptake in the major organs (<4% ID/g). The uptake in the heart (1.7±0.4% ID/g) was found to be higher than the uptake in the blood and muscle, resulting in good heart-to-blood and heart-to-muscle uptake ratios.

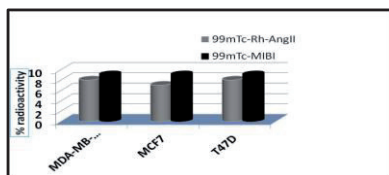


Figure 2. %Cell-uptake of ^{99m}Tc-Rh-Ang II in various human breast cancer cell lines.

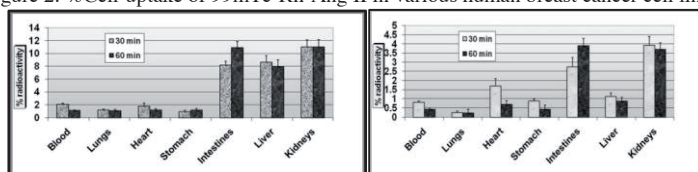


Figure 3. *In vivo* biodistribution of ^{99m}Tc-Rh-Ang II conjugate in mice (left) and rats (right) at 30 and 60 min post-injection. Data are expressed as % injected dose/gram (%ID/g).

In conclusion, this initial study towards the development of an effective cardiac imaging agent advocates that the use of hybrid conjugates appears to hold a great promise as a new and attractive approach for rapid and efficient imaging of cardiac system.

References

- [1] De Gasparo, M.; Catt, K. J.; Inagami, T. *Pharmacol. Rev.* **2000**, *52*, 415.
- [2] Lacerda, S. H.; Abraham, B.; Stringfellow, T. C. *Photochem. Photobiol.* **2005**, *81*, 1430
- [3] Heinrich, T. K.; Gottumukkala, V.; Snay, E. *Appl. Radiat. Isotopes* **2010**, *68*, 96.
- [4] Harapanhalli, R. S.; Roy, A. M.; Adelstein, S. J. *J. Med. Chem.* **1998**, *41*, 2111.

Synthesis and *in vitro* antitumor activity of new GnRH-II conjugates

Ildikó Szabó¹, Erika Orbán¹, Szilvia Bősze¹, Beatriz Garcia de la
Torre², David Andreu², Gábor Mező¹

¹Research Group of Peptide Chemistry, Hungarian Academy of Sciences, Eötvös L.
University, Pázmány P. s. 1/A, H-1117 Budapest, Hungary; ²Proteomics and Protein
Chemistry Unit, Department of Experimental Health Sciences, University of Pompeu
Fabra, Barcelona, Spain
E-mail:szaboi8@gmail.com

Introduction

In humans two isoforms of GnRH exist, GnRH-I (<EHWSYGLRPG-NH₂, where <E is pyroglutamic acid) and GnRH-II (<EHWSHGWYPG-NH₂). It was indicated that GnRH-II derivatives have more potent antiproliferative activity on human endometrial and ovarian cancer cells *in vitro* than GnRH-I analogs. tumor cells (e.g. breast, colon) produce GnRH-I and GnRH-II, and express GnRH receptors. GnRH-II analogs, both agonists and antagonists, induce apoptosis in many different cell types [1-2]. The success of chemotherapy depend on suppression of resistance to anticancer drug and the prevention of side effects [3]. In several cancers, Bcl-2 or Bcl-XL overexpression has been shown to correlate with chemotherapy and radiation resistance as well as with poor clinical prognosis. Short synthetic peptides corresponding to the minimal sequence of BH3 domain when bound to the antiapoptotic Bcl-2 family proteins; suppress the cellular antiapoptotic defense [4]. The practical use of BH3 peptides is limited by its low rate permeation into cancer cells. Thus delivery systems could be utilized to promote its delivery into cancer cells [3]. In the regulation of apoptosis, not only the pro- and antiapoptotic proteins [5], but other molecules play a role (e.g. CK2, casein kinase II enzyme) [6].

Our aim was to design and prepare new GnRH-II derivatives and conjugates, which contains proapoptotic peptide and anticancer drug . *In vitro* cytotoxic effect of the new bioconjugates was determined on MCF-7 and HT-29 cells.

Results and Discussion

Synthesis of GnRH-II agonists [D-Lys⁶]GnRH-I and [D-Lys⁶]GnRH-II, their proapoptotic peptide (Bak) or casein kinase inhibitor (CK2i) containing conjugates was carried out on solid phase using Fmoc/^tBu strategy. In case of the synthesis of CK2i containing peptide analogs, special cleavage mixture (20% piperidine, 0.1M HOBt in DMF) was used to remove the Fmoc-protecting group, which could prevent the succinimide ring formation. The crude peptides were used for the conjugation with daunomycin (Dau). Dau was coupled to the peptide directly in solution (0.2M NaOAc-buffer, pH 5.2) *via* oxim bond formation. Conjugates were purified by semipreparative RP-HPLC and characterized by analytical RP-HPLC and ESI-MS.

Cytotoxicity of GnRH-I and GnRH-II conjugates and the free drug was analysed *in vitro* by MTT-assay on MCF-7 and HT-29 cells using 72 hr incubation then IC₅₀ values were determined (Table 1.).

Table 1. *In vitro* cytotoxic effect of the GnRH conjugates

	MCF-7	HT-29
	IC ₅₀ values +/- SD (μM)	
Bak (H-MGQVGRQLAIIIGDDINRRY-NH ₂)	35.5±12.3	62.0±23.7
[D-Lys ⁶]GnRH-I	77.0±10.2	50.3±8.7
[D-Lys ⁶]GnRH-I-Bak	40.4±7.5	34.5±3.5
[D-Lys ⁶ (Dau=Aoa)]GnRH-I	0.1±0.04	1.1±0.1
[D-Lys ⁶ (Dau=Aoa)]GnRH-I-Bak	0.3±0.2	0.8±0.2
[D-Lys ⁶]GnRH-II	37.4±15.1	35.2±18.7
[D-Lys ⁶]GnRH-II-Bak	33.1±13.5	85.0±6.5
[D-Lys ⁶ (Dau=Aoa)]GnRH-II	0.3±0.03	1.4±0.5
[D-Lys ⁶ (Dau=Aoa)]GnRH-II-Bak	2.6±0.9	0.9±0.05
Daunomycin	0.4±0.05	0.4±0.08
CK2i (H-RRRDDDADDD-OH)	67.9±10.6	62.1±4.5
[D-Lys ⁶]GnRH-I-CK2i	61.5±10.2	38.7±9.0
[D-Lys ⁶]GnRH-II-CK2i	50.9±10.2	58.4±12.6
[D-Lys ⁶ (Dau=Aoa)]GnRH-I-CK2i	2.1±0.7	1.9±0.7
[D-Lys ⁶ (Dau=Aoa)]GnRH-II-CK2i	1.3±0.4	1.8±0.3

We observed that the conjugation of GnRH peptides ([D-Lys⁶]GnRH-I, [D-Lys⁶]GnRH-II) or their chimera versions (Bak and CK2i) with daunomycin increased the *in vitro* cytotoxic activity at least with one order of magnitude. No significant difference was observed between the Bak or CK2i peptide containing conjugates. It is interesting to note that in some cases the Dau-peptide conjugates (e.g. [D-Lys⁶(Dau=Aoa)]GnRH-I-Bak) were as effective as the free drug ((IC₅₀: 0.3 μM vs IC₅₀: 0.4μM on MCF-7 cells).

Our results suggest, that the combination of GnRH as targeting moiety, Bak or CK2i fragment as proapoptotic or enzyme inhibitory peptide and Dau, as anticancer drug could result in highly potent multifunctional therapeutic agents.

Acknowledgments

This work was supported by grants from the Hungarian National Science Fund (OTKA NK 77485) and Hungarian-Spanish Tét (NKTH Tét ES-20/2008).

References

- [1] Kim K.Y., et al. *J. Clin. Endocrinol. Metab.* **2004**, 89, 3020.
- [2] Hong I.S., et al. *J. Clin. Endocrinol. Metab.* **2008**, 93, 3179.
- [3] Dharap S.S., et al. *J. Controlled Release.* **2003**, 91, 61.
- [4] Minko T., et al. *Dis. Management Clin. Outcomes* **2001**, 3, 48.
- [5] Lutz R.J. *Biochem. Sci. Trans.* **2000**, 28, 51.
- [6] Montenarch M. *Cell Tissue Res.* **2010**, 342, 139.

Synthesis and *in vitro* characterization of peptide conjugates containing new drug candidates effective against *Mycobacterium tuberculosis* H₃₇Rv

Zsuzsa Baranyai¹, Kata Horváti¹, Nóra Szabó², Gábor Mező¹, Donát Schnöller³, Csanád Péntzes³, Éva Kiss³, Ferenc Hudecz^{1,4}, Szilvia Bősze¹

¹Research Group of Peptide Chemistry, Hungarian Academy of Sciences, Eötvös Loránd University, Budapest, Hungary; ²Laboratory of Bacteriology, Korányi National Institute for Tuberculosis and Respiratory Medicine, Budapest, Hungary; ³Laboratory of Interfaces and Nanostructures, Institute of Chemistry, Eötvös Loránd University, Budapest, Hungary;

⁴Department of Organic Chemistry, Institute of Chemistry, Eötvös Loránd University, Budapest, Hungary

E-mail: baranyaizsuzs@gmail.com

Introduction

Tuberculosis (TB) is a bacterial infection mainly caused by *Mycobacterium tuberculosis*. TB remains a major public health problem worldwide and the first cause of mortality attributable to a single intracellular pathogen. The cellular uptake of the antituberculars by infected host cells is limited. It is a possible approach to enhance the uptake of the antituberculars by receptor mediated delivery. The host cell specific delivery of the active compounds could increase the intracellular concentration [1]. In this study macrophage – as main host cell – related tuftsin receptor [2] specific conjugates were synthesized and *in vitro* characterized. The membrane penetration ability of a free drug and its peptide conjugate was compared.

Results and Discussion

Tuftsin is a tetrapeptide (human: TKPR, canine: TKPK) produced by enzymatic cleavage of the Fc-domain of the heavy chain of IgG [3]. Oligotuftsins derivatives ($[TKPKG]_2(OT10)$, $TKPR-[TKPKG]_2$) were applied as carriers and targeting moieties [2, 4, 5]. The molecules of a database (ZINC8 [6]), that consists eight million moieties, were docked to the dUTPase enzyme, which plays a key role in the metabolism of the bacteria [7]. Two of these new *in silico* identified and optimized antitubercular compounds (TB803, TB823) were conjugated to oligotuftsins derivative peptide carriers through oxime bond [8]. The following peptide conjugates were prepared: TB803=Aoa-OT10, $TKPR[TKPK(Aoa=TB823)G]_2$; where Aoa is aminoxyacetyl entity. The conjugates were characterized by RP-HPLC, mass spectrometry and amino acid analysis (data not shown).

Minimal inhibitory concentration (MIC) of the conjugates, the free drugs and carriers were determined on *M. tuberculosis* H₃₇Rv in Sula liquid medium (pH 6.5) after 4 weeks of incubation. In order to confirm the growth inhibition colony forming unit (CFU) was determined by subculturing from the Sula medium onto drug-free Löwenstein-Jensen solid medium. Samples were incubated for 4 weeks. We observed that the antitubercular activity of the free TB803 and TB823 was essentially preserved after conjugation to peptide carriers through oxime bond (Table 1.).

Compound	MIC ($\mu\text{g/ml}$)	CFU
isoniazid (control)	0.16	12
TB803	1.0	3
TB823	0.5	11
TB803=Aoa-OT10	6.9	10
TKPR[TKPK(Aoa=TB823)G] ₂	4.8	3

Table 1. The minimal inhibitory concentration (MIC) and the colony forming unit (CFU) values of the compounds, conjugates. Isoniazid (a first line antitubercular drug) was used as control. Oligo(u)tsin carriers have no antimicrobial effect.

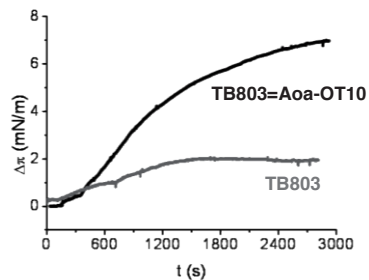


Figure 1. Increase of surface pressure due to penetration of the free TB803 and its conjugate, TB803=Aoa-OT10 into a DPPC monolayer.

The cellular uptake of the free TB803 and the TB803-conjugate was determined by flow cytometry and fluorescent microscopy on MonoMac6 human monocytic cell culture. Both compounds, TB803 and its conjugate are fluorescent. The conjugation of TB803 drug candidate markedly enhanced the *in vitro* cellular uptake.

Lipid Langmuir monolayer was used as membrane model. The ability of penetration of the free TB803 and its peptide conjugate into the Langmuir monolayer of dipalmitoyl-glycero-phosphocoline (DPPC) was determined. Aqueous solution of the drug or the conjugate was injected below the compressed lipid layer to obtain a final drug concentration of 2×10^{-6} M in the subphase. The change in surface pressure ($\Delta\pi$) as the indicator of drug penetration into the monolayer was recorded as a function of time for one hour at 24°C [9]. TB803 showed lower affinity to the lipid monolayer, while its conjugate possessed enhanced penetration indicating high degree of membrane affinity (Figure 1.). This might be connected to the structure and amphiphilic character of the peptide conjugate.

Acknowledgments

This work was supported by the Hungarian National Science Fund (OTKA 68358, 68120), National Office for Research and Technology (NKFP_07_1-TB_INTER-HU), and ELTE TÁMOP-4.2.2/B-10/1-2010-0030.

References

- [1] Horváti, K.; Bacsa, B.; Szabó, N.; Dávid, S.; Mező, G.; Grolmusz, V.; Vértessy, B.; Hudecz, F.; Bősze, Sz. *Bioconjugate Chem.* **2012**, *23*(5), 900-907.
- [2] Mező, G.; Kalászi, A.; Reményi, J.; Majer, Zs.; Hilbert, Á.; Láng, O.; Köhidai, L.; Barna, K.; Gaál, D.; Hudecz, F. *Biopolymers* **2004**, *73*(6), 645-656.
- [3] Najjar, V. A. *Adv. Exp. Med. Biol.* **1979**, *121*, 131-147.
- [4] Fridkin, M.; Najjar, V. A. *Crit. Rev. Biochem. Mol. Biol.* **1989**, *24*(1), 1-40.
- [5] Siemion, I. Z.; Kluczyk, A. *Peptides* **1999**, *20*(5), 645-674.
- [6] Irwin, J. J.; Shoichet, B. K. *J. Chem. Inf. Model.* **2005**, *45*(1), 177-182.
- [7] Sasseti, C. M.; Boyd, D. H.; Rubin, E. J. *Mol. Microbiol.* **2003**, *48*(1), 77-84.
- [8] Shao, J.; Tam, J. P. *J. Am. Chem. Soc.* **1995**, *117*(14), 3893-3899.
- [9] Schnöller, D.; Péntes, Cs. B.; Horváti, K.; Bősze, Sz.; Hudecz, F.; Kiss, É. *Prog. Colloid Polym. Sci.* **2011**, *138*, 131-138.

Synthesis of GSH-linked tyrosinase-activated melanoma prodrugs

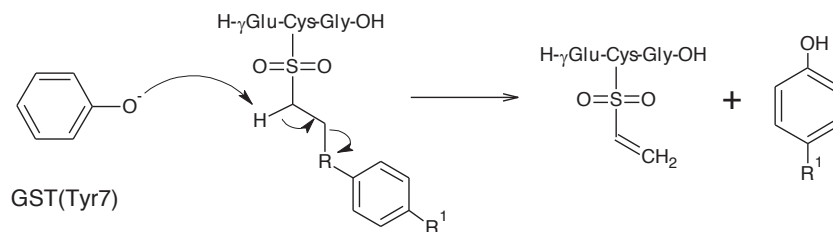
Paolo Ruzza,¹ Andrea Calderan,¹ Alberto Nassi,² Luigi Quintieri²

¹CNR Institute of Biomolecular Chemistry, Padua Unit, Padua, Italy; ²Dept. of Pharmaceutical and Pharmacological Sciences, University of Padua, Padua, Italy

E-mail: paolo.ruzza@cnr.it

Introduction

Melanoma is the most deadly skin cancer with an increasing incidence. Its therapy continues to be a challenge since, regardless of the treatment used, long-term survival is quite uncommon. Melanoma cells are characterized by high levels of glutathione S-transferase P1-1 (GSTP1-1). This enzyme is also highly expressed in solid tumors as well as in drug-resistant cells, where a role for this protein in the regulation of cell proliferation has been described [1]. Structure and mechanistic studies showed that in the GST-GSH complex, the GST Tyr residue placed near the S atom of the Cys in GSH, is in the phenoxide form to facilitate the deprotonation of the sulfhydryl group in GSH, making it able to react with electrophilic species [2, 3]. Glutathione (GSH)-linked anticancer prodrugs could be activated by physiological concentration of GSTs through a β -elimination reaction that cleaves the prodrug into an active drug and a glutathione analogue according the scheme of figure 1. By taking advantage of this active-site geometry, we designed and synthesised compounds **1-3**, where two tyrosinase activated melanoma prodrugs (4-methoxyphenol and N-acetyl-4-S-cysteaminyphenol) were linked to GSH by either an ethoxy or an ethoxycarbonyl. In this way the Tyr phenoxide would be able to abstract one of the acidic methylene protons linked to the sulfone moiety, releasing the tyrosinase-activated melanoma prodrugs.



Compound	R	R ¹
1	O	OCH ₃
2	OC(O)O	OCH ₃
3	OC(O)O	S-(CH ₂) ₂ -NHC(O)CH ₃

Figure 1. Proposed GST activations of synthesized compounds **1-3**.

Results and Discussion

GSH was synthesized by SPPS starting from Fmoc-Gly-Wang-Resin, using the Fmoc/HBTU chemistry in 0.06-molar scale. The Cys sulfhydryl group was protected by the Mmt group, which was removed from peptide anchored to the resin by treatment with 1% TFA in DCM containing 5% TIS, and then treated with the Br-derivatives. Sulfur was oxidized to sulfone by treatment with H₂O₂ and peracetic acid. Crude peptide analogues were purified by preparative HPLC and characterized by ESI-MS analysis.

Preliminary studies were carried out to investigate whether compounds **1-3** are stable at 37°C in 0.1 M phosphate buffer at pH 7.2 or 8.5. HPLC analysis show clearly that compound **1**, containing the ethoxy linker, is stable at both tested pHs (data not shown). On the contrary compounds **2** and **3**, containing the ethoxycarbonyl moiety, are degraded in a pH-depend manner.

Thereafter, compounds **1-3** have been incubated at 37°C in 0.1 M phosphate buffer, pH 7.4, either in the absence or the presence of rat liver or kidney cytosolic fractions as source of GST enzymes. While compound **1** concentration did not decrease with time neither in the absence nor in the presence of rat liver or kidney cytosolic fractions, indicating the stability of ethoxy linker to cleavage by cytosolic GSTs, both compounds **2** and **3** degraded in a time dependent manner releasing the corresponding tyrosinase substrate in all the three incubation conditions. A comparison of the disappearance rates revealed that compounds **2** and **3** were cleaved much more quickly in incubates containing a cytosolic fraction than in phosphate buffer. The difference observed in hydrolysis rates between incubates containing liver or kidney fractions probably arise from a different tissue expression pattern of GSTs.

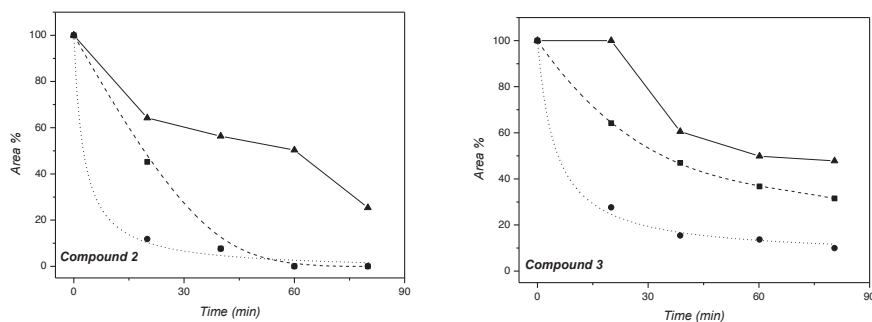


Figure 2. Time-course of enzyme catalyzed degradation of compounds **2** and **3** incubated at 37°C in 0.1 M phosphate buffer, pH 7.4, either in the absence (solid line) or the presence of rat liver (dot lines) or kidney (dash line) cytosolic fractions.

References

- [1] Ruzza, P.; Rosato, A.; Rossi, C. R.; Floreani, M.; Quintieri, L. *Anticancer Agents Med. Chem.* **2009**, *9*, 763.
- [2] Satyam, A.; Hocker, M. D.; KaneMaguire, K. A.; Morgan, A. S.; Villar, H. O.; Lyttle, M. H. *J. Med. Chem.* **1996**, *39*, 1736.
- [3] Kong, K. H.; Takasu, K.; Inoue, H.; Takahashi, K. *Biochem. Biophys. Res. Commun.* **1992**, *184*, 194.

Synthesis, *in vitro* and *in vivo* evaluation of new ^{99m}Tc-labeled cyclic RGDfK peptide monocationic complexes

Andrea Calderan,¹ Cristina Bolzati,² Barbara Biondi,¹ Fiorenzo Refosco,^b Nicolò Morellato,³ Nicola Salvatore,³ Paolo Ruzza¹

¹CNR Institute of Biomolecular Chemistry, Padua Unit, Padua, Italy; ²CNR Institute of Inorganic Chemistry and Surface, Padua, Italy; ³Department of Pharmaceutical and Pharmacological Sciences, University of Padua, Padua, Italy

E-mail: andrea.calderan@cnr.it

Introduction

Synthetic peptides represent first choice biomolecules, with respect to proteins and mAb, for the monitoring the population variability and receptor functionality associated to a tumor pathology due to their favorable pharmacokinetic profile. It has been demonstrated that the surface molecule integrin alpha-V beta-3 could be an ideal target for the interaction with radiolabeled peptides. This integrin is indeed overexpressed both in tumor cells and in tumor vessels endothelium, while it is not expressed in the majority of normal tissues. Cyclic peptides with the sequence Arg-Gly-Asp (RGD), are known to bind the integrin alpha-V beta-3 with high affinity and selectivity and could conveniently radiolabelled to target tumor cells for teragnostic purposes [1]. Recently, we have demonstrated that the cyclic RGDfK peptide interacts with high affinity to A375 human melanoma cells [2]. The aim of this work was to label with ^{99m}Tc the RGDfK peptide by using the [^{99m}Tc(N)(PNPn)]²⁺ moiety (where PNPn stands for [(CH₃)₂PCH₂CH₂]₂NCH₂CH₂OCH₃ or [(HOCH₂)₂PCH₂CH₂]₂NCH₂CH₂OCH₃) to obtain a radiolabeled peptide useful for melanoma imaging [3,4]. To this purpose a Cys-peptide conjugate (NS-RGDfK) was synthesized and used for preparation of monocationic [^{99m}Tc(N)(NS-RGDfK)(PNPn)]⁺ complexes. *In vitro* stability and transchelation studies with cysteine and glutathione of radiolabeled complexes were investigated as well as their pharmacokinetic profiles in healthy rats.

Results and Discussion

Peptide was prepared by SPPS starting from Fmoc-L-Asp(Wang-Resin)-OAll. Peptide was assembled using the Fmoc/HBTU chemistry in 0.06-molar scale by manual solid-phase. HBTU/HOBt activation employed a three-fold molar excess of Fmoc-amino acids in DMF solution for each coupling cycle. After on-resin cyclization, ivDde protecting group was removed from Lys side-chain to allow the coupling of the cysteine residue that will act as bidentate ligand coordinated to the metal centre in the final complexes.

The monocationic [^{99m}Tc(N)(Cys-N,S)(PNPn)]⁺ dissymmetrical nitrido compounds, was prepared according to Figure1. The two step reaction requires the simultaneous addition of aminodiphosphine and Cys-peptide to a the mixture of ^{99m}Tc(N)-intermediates produced in the first step. Radiolabelled compounds were obtained in good radiochemical yield (RCY).

The use of the cysteine residue determines the formation of two diastereoisomers upon coordination onto the $[\text{TcN}(\text{PNP})]^{2+}$ moiety, depending on the orientation (*syn* or *anti*) of the cysteine side-chain towards the $\text{Tc}\equiv\text{N}$ unit.

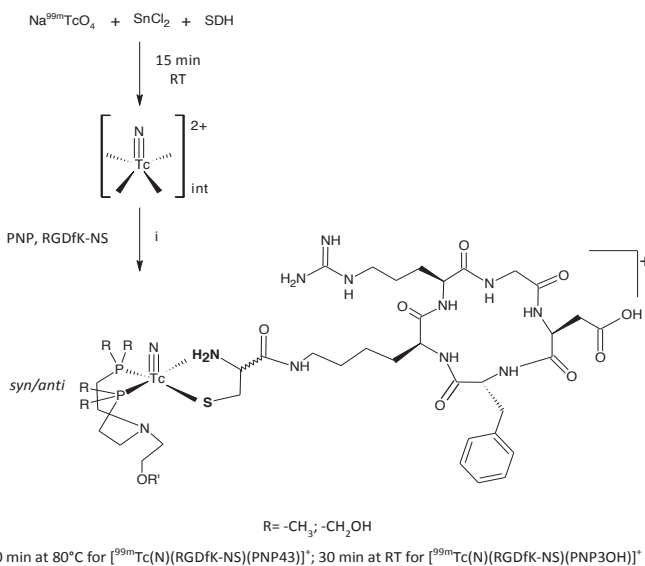


Figure 1. The two steps procedure to obtain monocationic complexes.

Complexes evidenced a good stability in rat and human sera as well as in rat liver and rat kidney homogenates. Rat biodistribution studies were performed to investigate the organ uptake and excretion pathways. Complexes present an extremely fast elimination from the blood and from significant organs; the renal excretion was extremely rapid and the activity was mainly eliminated through the urinary tract.

The introduction in the PNP ligand of more hydrophilic groups with respect to bulkier substituents [5] allows modifying the biodistribution profile reducing the hepatic uptake and favoring the renal elimination of the radio-compound. These results make these compounds good candidates for studies in animals bearing tumors.

Acknowledgments

This work was supported by the Italian MIUR grant PRIN 2008.

References

- [1] Mas-Moruno, C.; Rechenmacher, F.; Kessler, H. *Anticancer Agents Med. Chem.* **2010**, *10*, 753.
- [2] Ruzza, P.; Marchiani, A.; Nassi, A.; Rondina, M.; Rosato, A.; Rossi, C.R.; Mammi, S.; Floreani, M.; Quintieri, L. *J. Pept. Sci.* **2008**, *14*, 159.
- [3] Bolzati, C.; Boschi, A.; Uccelli, L.; Tisato, F.; Refosco, F.; Cagnolini, A.; Duatti, A.; Prakash, S.; Bandoli, G.; Vittadini, A. *J. Am. Chem. Soc.* **2002**, *124*, 11468.
- [4] Bolzati, C.; Refosco, F.; Marchiani, A.; Ruzza, P. *Curr. Med. Chem.* **2010**, *17*, 2656.
- [5] Decristoforo, C.; Santos, I.; Pietzsch, H.J.; Kuenstler, J.U.; Duatti, A.; Smith, C.J.; Rey, A.; Alberto, R.; Von Guggenberg, E.; Haubner, R. *Q. J. Nucl. Med.* **2007**, *51*, 33.

The influence of HIV-1 Tat protein sequences on platelet activation

**Panagiotis Stathopoulos, Andromaxi A. Dimitriou, Eleni Malisiova,
Vasilios G. Chantzichristos, Aikaterini Gatsiou, Alexandros D. Tselepis,
Vassilios Tsikaris**

Chemistry Department, University of Ioannina, 45110, Greece

E-mail: btsikari@cc.uoi.gr

Introduction

Several reports have evidenced an increased incidence of thrombotic events in HIV-infected patients, especially after an antiretroviral therapy. In these cases activation of the platelets has been observed. However, the exact mechanism by which HIV-1 infection leads to platelet activation is not fully understood. It has been proposed that significant role in the pathogenesis of AIDS-associated diseases may play the HIV-1 Tat (trans-acting transcriptional activator) protein. The HIV-1 Tat protein is an 86-101 amino acids polypeptide which can be released by HIV-infected cells. Recently, Wang, J. et al. have investigated the effect of HIV-1 Tat protein on platelet activation [1]. They reported that Tat protein interacts directly with platelets through the chemokine CCR3 and β_3 -integrin receptors and induces the activation of platelet. The attachment of Tat protein to $\alpha_v\beta_3$ integrin occurs through the RGD motif in Tat's C-terminal domain (Tat₇₈₋₈₀) [2]. In this work, using flow cytometry assays, we proposed that the sequence located between amino acids 48-60 of Tat protein play a significant role in platelet activation. The Tat₄₈₋₆₀ (G⁴⁸RKKRRQRRRPPQ⁶⁰-NH₂) cationic peptide is a well-known Cell Penetrating Peptide (CPP) [3] which has been successfully used in numerous studies to deliver bioactive molecules such as proteins, peptides, nanoparticles, and liposomes into cells. Moreover, in order to investigate the influence of Tat R⁷⁸GD⁸⁰ region on platelet activation we designed, synthesized and tested for the inhibitory activity on platelet aggregation the PRGDP, QPRGDP, QPRGDPTG, PRGDPTG HIV-1 Tat derived peptide analogues.

Results and Discussion

Peptides synthesis

Peptides were synthesized manually by solid-phase peptide synthesis on a Rink Amide resin, using the Fmoc strategy. Coupling reactions of Fmoc amino acids were performed in DMF using a molar ratio of amino acid/HBTU/HOBt/DIEA/resin (3:3:3:6:1) and Fmoc deprotection steps were carried out with 20% piperidine in DMF (v/v) for 15 min. The peptides were cleaved from the resin with 95% TFA in the presence of TIS and DMB as scavengers [4]. All peptides were purified by RP-HPLC and their identification was confirmed by ESI-MS.

Biological assays

Platelet aggregation in PRP: Inhibition of the platelet aggregation was measured using Human Platelet Rich Plasma (PRP) to a final platelet concentration of 250.000 platelets/ μ l. The tested peptide was added (final concentration of 500 or 1000 μ M) to 500 μ l of PRP.

After 1 min of incubation, ADP was added to a final concentration of 5 or 2 μM . Inhibition effect was determined on the basis of the light transmittance changes.

P-selectin exposure and PAC-1 binding: Platelets were incubated in the presence or in the absence of the peptides with or without ADP for 1 or 15 min at 37°C. Platelets were then stained with PAC-1-FITC or CD62P-PE and left for 20 min in the dark. After that platelets diluted (1:5, v/v) with 10mM PBS at pH 7.4 and immediately analyzed by flow cytometry.

The stimulatory effect of Tat₄₈₋₆₀ (G⁴⁸RKKRRQRRRPPQ⁶⁰-NH₂) peptide was investigated by flow cytometry assays measuring the expression and the binding of well-known platelet activation markers such as P-selectin and PAC-1 antibody. P-selectin is stored in α -granules of platelets and translocate to the platelet membrane after their activation and PAC-1 is a monoclonal antibody that recognizes an epitope on $\alpha_{\text{IIb}}\beta_3$ expressed only in its activated state. In particular, the membrane P-selectin expression and PAC-1 binding in inactivated platelets (Median Fluorescence Intensity, MFI: 7 \pm 2 and 5 \pm 3) was significantly increased after their incubation with Tat₄₈₋₆₀ peptide (MFI: 110 \pm 11 and 36 \pm 10) at a final peptide concentration of 500 μM . These results indicate that the Tat48-60 peptide activate human platelets. However, the exact mechanism by which Tat₄₈₋₆₀ peptide leads to platelet activation is under investigation. There are two possible mechanisms which could explain this effect of the Tat₄₈₋₆₀ peptide on platelet activation. According to this aspect Tat₄₈₋₆₀ peptide either interacts directly with platelet receptors stimulating them via an outside-in signaling activating pathway or the above cationic peptide acts as CPP inside the platelets, activating various intracellular signal transduction pathways which lead to their activation. On the other hand the PRGDP, QPRGDP, QPRGDPTG and PRGDPTG HIV-1 Tat derived peptide analogues which include the -R⁷⁸GD⁸⁰- sequence, did not act as RGD like analogues, since they didn't show appreciable inhibitory activity in PRP aggregation assays, at a final concentration of 1mM (inhibition < 20%). This behavior of the RGD HIV-1 Tat based analogues could be attributed to the nature of the residues adjacent to the RGD sequence. The above results suggest that the 76-83 HIV-1 Tat RGD containing sequence is not recognized by $\alpha_{\text{IIb}}\beta_3$ platelet receptor and probably doesn't participate through this way to platelet aggregation. Constructively, the stimulatory activity of Tat48-60 peptide on platelets activation must be taking into account if it has to be used as a CPP.

Acknowledgments

This study was supported by the Regional Operational Programme (ROP) of Thessaly-Mainland Greece- Epirus within the frame of National Strategic Reference Framework for the period 2007-2013 (ESPA 2007-13).

References

- [1] Wang, J.; Zhang, W.; Nardi, M.A.; Li, Z. *Journal of Thrombosis and Haemostasis* **2010**, *9*, 562.
- [2] Urbinati, C.; Mitola, S.; Tanghetti, E.; Kumar, C.; Waltenberger, J.; Ribatti, D.; Presta, M.; Rusnati, M. *Arteriosclerosis, Thrombosis, and Vascular Biology*, **2005**, *25*, 2315.
- [3] Dimitriou, A.A.; Stathopoulos, P.; Mitsios, J.V.; Sakarellos-Daitsiotis, M.; Goudevenos, J.; Tsikaris, V.; Tselepis, A.D. *Platelets*, **2009**, *20*, 539.
- [4] Stathopoulos, P.; Papas, S.; Tsikaris, V. *J. Pept. Sci.* **2006**, *12*, 227.

***trans*-4-Hydroxyproline analogues of cyclolinopeptide A: Synthesis, conformation and biology**

**Joanna Katarzyńska¹, Agnieszka Wyczalkowska¹, Krzysztof Huben¹,
Michał Zimecki², Stefan Jankowski¹, Janusz Zabrocki^{1,3}**

¹ Institute of Organic Chemistry, Lodz University of Technology, 90-924 Łódź, Poland;

² Institute of Immunology and Experimental Therapy, Polish Academy of Sciences, 53-114
Wrocław, Poland; ³ Peptaderm Inc., Krakowskie Przedmieście 13, 00-071 Warszawa,
Poland

E-mail: joanna.katarzynska@p.lodz.pl

Introduction

Nonproteinogenic amino acids have been tools to modify the structures of natural peptides since a long time [1]. Many bioactive peptides involved in a physiological and biochemical processes cannot be applied in the therapy because of their instability in physiological conditions. That's why the synthesis of their stable active analogues is a challenge for medicinal chemistry now a days.

trans-4-Hydroxyproline (Hyp) is an important building block of natural collagen. It is responsible for the stabilization of collagen super helix, forcing the *trans* amide bonds configuration with preceding amino acids. Some hypothesis invokes a hyperconjugative ability and stereoelectronic effect by which the electronegative oxygen atom of the hydroxyl group reorganizes the main chain in the proper conformation for triple-helix formation. On the other hand the alternative hypothesis suggests that a network of water molecules links by hydrogen bond the Hyp hydroxyl group and main chain carbonyl group [2].

At the same time the impact of the synthetic *trans*-4-hydroxyproline on the conformation other than the collagen peptide chains of biologically important compounds is little known.

Results and Discussion

Now we present synthesis, conformation and biological activity of new analogues of cyclolinopeptide A (CLA), containing *trans*-4-hydroxyproline instead of proline residues in position 3 or 4. It is known that immunosuppressive activity of CLA is comparable with cyclosporine A and is associated with the presence of the tetrapeptide fragment Pro-Pro-Phe-Phe containing Pro-Pro *cis* amide bond [3]. We expected that inserting the hydroxyl group into the pyrrolidine ring might influence on the biological activity and conformation of the native peptide due to its hydrophilic character and hydrogen bonding ability.

c (Leu ¹ - Val ² - Hyp ³ - Pro ⁴ - Phe ⁵ - Phe ⁶ - Leu ⁷ - Ile ⁸ - Ile ⁹)	CLA[Hyp ³]
c (Leu ¹ - Val ² - Pro ³ - Hyp ⁴ - Phe ⁵ - Phe ⁶ - Leu ⁷ - Ile ⁸ - Ile ⁹)	CLA[Hyp ⁴]
c (Leu ¹ - Val ² - Hyp ³ - Hyp ⁴ - Phe ⁵ - Phe ⁶ - Leu ⁷ - Ile ⁸ - Ile ⁹)	CLA[Hyp ^{3,4}]

The linear precursors of modified CLA analogues were prepared manually by standard solid-phase procedure "step by step" on Wang resin using Fmoc/tBu strategy and TBTU as coupling reagent. The cyclizations of linear peptides have been made under high dilution

conditions by means of EDC/HOBt coupling reagents. Structures of all compounds were characterized by MS and NMR spectroscopy.

NMR-studies

The one- and two-dimensional ^1H NMR spectra of CLA analogues containing one 4-hydroxyproline residue were recorded in CDCl_3 (CLA[Hyp³] and CLA[Hyp⁴]) or DMSO-d_6 (CLA[Hyp^{3,4}]) on a Bruker Avance II Plus spectrometer at 700 MHz at 300 K. Proton assignments were based on TOCSY, ROESY and ^1H - ^{13}C HSQC experiments. Spectra exhibited broad signals characteristic for the conformational flexibility. However, the inspection of ^1H NMR spectra of CLA[Hyp³] and CLA[Hyp⁴] revealed the presence of one isomer for both CLA analogues. For peptide CLA[Hyp³] all *cis* geometry of peptide bonds were found and for CLA[Hyp⁴] the *trans* geometry of Hyp-Pro peptide bond was identified. The analysis of the NH region for doubly modified peptide CLA[Hyp^{3,4}] revealed the presence of two isomers due to *cis-trans* isomerization of Hyp-Hyp peptide bond. The ratio of isomers was estimated as 45:55 on the basis of integrations of OH signals. The assignment of the Hyp-Hyp peptide bond geometry for each isomer was impossible due to overlapping of diagnostic signals.

Biology

The presented compounds were assayed for inhibition of phytohemagglutinin A (PHA) – stimulated human peripheral mononuclear blood cells (PMBC) proliferation. CLA[Hyp⁴] and CLA[Hyp^{3,4}] analogues showed similar activities in the proliferation assay (85% and 81% inhibition, respectively at 100 $\mu\text{g/ml}$), while CLA[Hyp³] analogue was more potent (24% inhibition at 10 $\mu\text{g/ml}$ and 93% at 100 $\mu\text{g/ml}$).

Moreover the compounds were tested for their potential toxicity in 24h culture of PBMC. The cell survival was determined by MTT colorimetric method and control cultures were contained appropriately diluted DMSO in culture medium. CLA[Hyp⁴] and CLA[Hyp^{3,4}] analogues were not toxic at the 1-100 $\mu\text{g/ml}$ concentration range. On the other hand CLA[Hyp³] analogue demonstrated small toxicity at 1-10 $\mu\text{g/ml}$ and a quite significant one (53%) at 100 $\mu\text{g/ml}$.

The effects of the compounds on lipopolysaccharide (LPS)-induced tumor necrosis factor alpha ($\text{TNF}\alpha$) production in the whole blood cell cultures were moderate and did not increase with compounds concentration. The inhibitory effects on the cytokine production in this assay were the following: CLA[Hyp³] – 67% and 45%, CLA[Hyp⁴] – 42% and 45% and CLA[Hyp^{3,4}] – 46 and 43% (at 1 $\mu\text{g/ml}$ and 50 $\mu\text{g/ml}$ concentrations).

To sum up the compounds (despite of CLA[Hyp³] because of its high toxicity) may be considered as markedly inhibitory at 1 $\mu\text{g/ml}$ concentration in $\text{TNF}\alpha$ inhibition assay and may show promising actions in *in vivo* experimental models of inflammation.

Acknowledgments

This work was supported by National Science Centre, grant N N405 424239.

References

- [1] Goodman, M.; Zhang, J.; *Chemtracts-Organic Chemistry* **1997**, *10*, 629.
- [2] Berisio, R.; De Simone, A.; Ruggiero, A.; Importa, R.; Vitagliano, L.; *J. Pept. Sci.* **2008**, *15*, 131 and references cited herein.
- [3] Siemion, I. Z.; Pędyczak, A.; Strug, I.; Wiczorek, Z.; *Arch. Immunol. Ther. Exp.* **1994**, *42*, 459.

An NMR method to discriminate between the 2.0₅-helix and the 3₁₀-helix of a spacer peptide

Cristina Peggion, Marco Crisma, Fernando Formaggio,
Claudio Toniolo

ICB, Padova Unit, CNR, Department of Chemistry, University of Padova, 35131 Padova,
Italy

E-mail: cristina.peggion@unipd.it

Introduction

The ideal fully-extended, peptide conformation, also known as 2.0₅-helix, is characterized by the $\varphi = \psi = \omega = 180^\circ$ torsion angles. The repeating motif of this foldamer is a pentagonal (pseudo)cyclic structure (called C₅), stabilized by an intraresidue H-bond. Typically, the N-H and C=O groups in the 2.0₅-helix are not involved in intermolecular H-bonds. Multiple C₅ conformations were observed in homo-peptides made up of C^{α,α}-dialkylated glycines with both side chains longer than a methyl. This is the case for C^{α,α}-diethylglycine (Deg) (Figure 1), the residue studied in this work. It is known that Deg homo-peptides can adopt the 2.0₅-helix [1] or the 3₁₀-helix depending on environmental factors (*e.g.* solvent polarity) and the N- and/or C-terminal moieties [2,3].

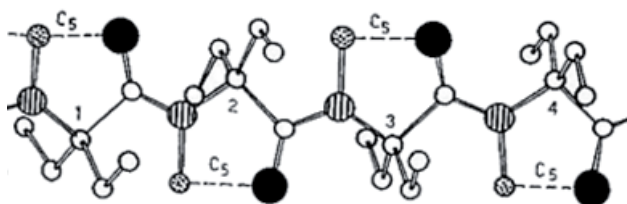


Fig.1. Representation of a segment of four Deg residues in the 2.0₅-helix structure.

Results and Discussion

In this communication, we introduce an NMR method to discriminate between the 2.0₅-helix and the 3₁₀-helix based on the observation of cross-peak intensities in the NOESY spectrum of a -(Deg)₄- homo-peptide [4]. A NH(i)→βCH(i-1) cross peak more intense than the NH(i)→βCH(i) cross peak is observed when the peptide adopts the 2.0₅-helical conformation. By contrast, an opposite trend of intensities of the same NOE cross peaks indicates the occurrence of a 3₁₀-helical conformation (Figure 2).

By using this method, we were also able to determine that polar solvents, such as MeCN or MeOH, may induce a 3₁₀-helical structure in Deg homo-peptides which otherwise adopt the 2.0₅-helix conformation in CDCl₃. This finding allows us to rapidly switch this series from "short" (3₁₀-helix) to "long" (2.0₅-helix) peptides by changing the solvent only, thus making them extremely attractive tools.



Fig.2. Models for Deg homo-peptides. Left: right-handed 3_{10} -helical conformation ($\phi, \psi = -57^\circ, -30^\circ$)[1]. The pro-S and pro-R side chains are in the trans and g^+ dispositions, respectively, as commonly observed in the crystal state. Right: fully-extended conformation ($\phi, \psi = 180^\circ, 180^\circ$), with the pro-S and pro-R side chains in the g^+ and g^- dispositions, respectively.

References

- [1] Toniolo, C.; Crisma, M.; Formaggio, F.; Peggion, C. *Biopolymers (Pept. Sci.)* **2001**, *60*, 396.
- [2] Formaggio, F.; Crisma, M.; Peggion, C.; Moretto, A.; Venanzi, M.; Toniolo, C. *Eur. J. Org. Chem.* **2012**, 167.
- [3] Formaggio, F.; Crisma, M.; Ballano, G.; Peggion, C.; Venanzi, M.; Toniolo, C. *Org. Biomol. Chem.* **2012**, *10*, 2413.
- [4] Peggion, C.; Crisma, M.; Toniolo, C.; Formaggio, F. *Tetrahedron* **2012**, *68*, 4429.

Anti-Freeze Peptides for potential applications in the food industry: Molecular modelling, chemical synthesis and analytical studies

Ho Zee Kong,¹ Clive Evans,² Conrad Perera,¹ Vijayalekshmi Sarojini^{1*}

¹School of Chemical Sciences and ²School of Biological Sciences, The University of Auckland, Private Bag 92019, Auckland, New Zealand

*E-mail: v.sarojini@auckland.ac.nz

Introduction

Naturally occurring antifreeze proteins (AFPs) enable organisms like polar fish to survive the freezing temperatures of their natural habitat [1]. As well as being cryoprotective, many AFPs exhibit properties of ice-recrystallization inhibition [2]. The ability of AFPs to influence the size, morphology and aggregation of ice crystals can be used in food technology, where the growth of ice crystals in frozen foods is of primary concern [3]. Tailor made analogues of naturally occurring AFPs were synthesized and their potential applications in the preservation of frozen food products were investigated.

Results and Discussion

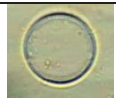
Synthesis and antifreeze effects: Two analogues (AFP1 and AFP2) of the naturally occurring winter flounder AFP (AFPW) were designed, where multiple salt bridges (i+3,4 type) were introduced into the natural sequence. It was hypothesized that these salt bridges would contribute to extra stability of the peptide helices in extremes of pH and temperatures. The peptides (Figure 1) were synthesized by manual Solid Phase Peptide Synthesis (SPPS). Antifreeze activity (thermal hysteresis) studies of the peptides were carried out using a nanoliter osmometer (Otago Osmometers) attached to a microscope. Results are summarised in table 1. Both AFPW and AFP2 modified ice crystal growth, forming classic bipyramidal crystals. AFPW displayed greater thermal hysteresis (0.95°C) than AFP2 (0.08°C). AFP1 did not show any antifreeze activity, but it bound to ice and modified crystal growth. Molecular modelling (data not shown) revealed that the salt bridge residues in AFP1 were too far apart in space, preventing salt bridge formation.

DTASD AAAAA ALTAA NAKAA AELTA ANAAA AAAAT AR (AFPW)
DTASD **ARAAD** ELTAA NAKAA AELTA ANARA **ADEAT** AR (AFP1)
DTASD AEDAA **RLTAA** NAKAA AELTA ANAED **AARAT** AR (AFP2)

Figure 1: Sequences of anti-freeze peptides used in this study (salt bridge residues in bold)

None of the AFPs formed perfect α -helices in water as observed by circular dichroism (data not shown). However, AFP2 showed some evidence of increased stability under extreme pH conditions as determined by changes to the ratio of the molar ellipticity values [$\theta_{222}/\theta_{208}$].

Table 1. Antifreeze activity of winter flounder AFP (AFPW) and its analogues

Sample	Water	AFP1	AFP2	AFPW
Concentration (mg/mL)	-	0.01	0.01	0.01
Thermal hysteresis (°C)	-	0.02	0.08	0.95
Ice morphology				

Effects on frozen agar gels: The ability of the AFPs to preserve the structure and texture of frozen material after repeated freezing and thawing cycles was evaluated using agar gel blocks as models. AFPs were incubated with 1% agar gel, the agar gels were frozen at -27°C overnight and thawed at 22°C. Both active AFPs (AFPW and AFP2) minimised the growth of large ice crystals on agar gels during freezing and enabled the overall gel structure to be maintained on thawing (Figure 2).

Sample	Control (no AFP)		AFPW		AFP2	
		Mass (g)		Mass (g)		Mass (g)
Frozen at -27°C		0.9443		0.9434		0.8490
Thawed at 22°C for 60 min.		0.3643		0.7784		0.6410

Figure 2: Preservation of 1% agar gel structure by AFPs after freezing and thawing.

In conclusion, both AFPW and AFP2 showed thermal hysteresis (antifreeze) activity and both altered ice crystal morphology, although to different extent. Both also had effects on preserving the texture of frozen agar gels. The ability of the APFs to preserve gel structure after freezing and thawing holds promise for their use as potential cryoprotective agents in frozen food products. However, factors such as allergenicity will need to be carefully evaluated before these molecules gain acceptance as cryoprotectants in the food industry.

Acknowledgments

We gratefully acknowledge support from The University of Auckland Faculty Research Development Fund (Grant No 3700349).

References

- [1] DeVries, A.L.; Wohlschlag, D.E. *Science*. **1969**, *163*, 1073-5.
- [2] Feeney, R.E.; Burcham, T.S.; Yeh, Y. *Annu Rev Biophys Bio*. **1986**, *15*, 59-78.
- [3] Feeney, R.E.; Yeh, Y. *Trends Food Sci Tech*. **1998**, *9*, 102-6.

Conformational analysis of liposomal A β 1-15 derived lipopeptides by Attenuated Total Reflectance Infrared (ATR-IR) spectroscopy

Maria Pilar Lopez Deber*, Dorin Mlaki, David T. Hickman,
Pedro Reis, Andrea Pfeifer, Andreas Muhs

AC Immune SA, PSE-B, EPFL, 1015 Lausanne, Switzerland

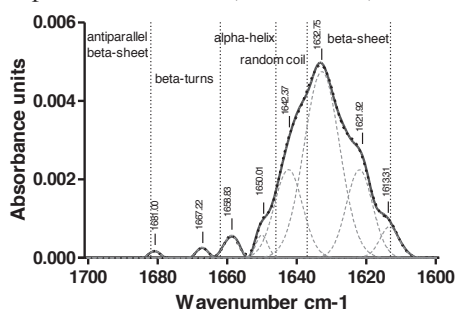
E-mail: andreas.muhs@acimmune.com

Introduction

We have previously shown that active immunization with N- and C-terminus di-palmitoylated A β 1-15 peptide embedded in liposomes (ACI-24) was capable of eliciting a conformation-specific strong immune response in mice [1]. The antigenic peptide was shown to mimic the aggregated β -sheet conformation of the pathological A β 42 peptide on the surface of the liposomes by CD, ssNMR and ThT assay. We have also reported the modulation of the conformation of A β 1-15 derived sequences by means of different lipidation patterns, lipid chain lengths and peptide net charge. Here we present the characterization of this panel of liposomal peptide constructs by ATR-IR and correlate the results with previous studies by CD.

Results and Discussion

Scaffold adopts an aggregated β -sheet structure: Liposomal Palm1-15 amide I band IR spectra showed the characteristic absorbance maximum around 1633 cm⁻¹ of an extended conformation (Figure below) in accordance with reported CD [1]. Estimation of the % of each structural component was done by curve fitting procedures, confirming that the β -sheet components are the predominant ones (75% in total).



Fatty acid chain length correlates with % β -sheet: Liposomal constructs of A β 1-15 acylated with shortened lipid chains (C12, C8 and C4) instead of palmitic acid (C16), showed also predominant β -sheet conformations with % increasing with increasing hydrocarbon chain length, as seen by CD [1].

Dominant β -sheet conformation after multi-lipidation: All lipidated A β 1-15 derived constructs (Table 1) adopted on the liposomal bilayer a dominant β -sheet conformation as

showed by the higher intensity peaks in the region around 1620 and/or 1635 cm^{-1} , in agreement with CD spectra [1]. The exception was liposomal Palm 1-15(1C) with higher intensity peaks in the region of random coil (1645 cm^{-1}) and α -helix (1651 cm^{-1}). This mixed profile from β -sheet, random coil and α -helix contributions, was also observed in its CD spectrum [1].

Table 1

Liposomal construct	Peptide Sequence	β -sheet	random coil	α -helix	turns
		%area	%area	%area	%area
Palm1-15	H-K(Palm)-K(Palm)-A β 1-15-K(Palm)-K(Palm)-OH	75	19	4	1
Palm1-15(4C)	H-A β 1-15-K(Palm)-K(Palm)-K(Palm)-K(Palm)-OH	87	8	0	5
Palm1-15(1N1C)	H-K(Palm)-A β 1-15-K(Palm)-OH	68	0	25	5
Palm1-15(2C)	H-A β 1-15-K(Palm)-K(Palm)-OH	77	17	0	6
Palm1-15(1C)	H-A β 1-15-K(Palm)-OH	40	34	17	9

Induction of β -sheet conformation independent of peptide length and sequence: Palmitoylated A β 1-15 derived sequences with shortened length (Palm1-9) or different amino acid order (reverse Palm15-1 and scrambled scPalm1-15) adopted all β -sheet type structures when incorporated into liposomes, as seen by CD (Table 2). The threshold in peptide length was determined by the shortest construct analyzed: Palm1-5 adopted the mixed conformation with the highest % of disordered component, as shown by CD and ATR-IR.

Table 2

Liposomal construct	Peptide Sequence	β -sheet	random coil	α -helix	turns
		%area	%area	%area	%area
Palm1-15	DAEFRHDSGYEVHHQ	75	19	4	1
Palm1-9	DAEFRHDSG	39	22	0	39
Palm1-5	DAEFR	58	39	0	4
scPalm1-15	GHEAYHSVERFDQH	56	14	13	18
Palm15-1	QHHEVYGSDFRFEAD	87	4	1	8
Palm1-15 (E3K,D7K,E11K)	DAKFRHKSGYKVVHHQ	44	11	29	15
Palm1-15 (E3K,D7K)	DAKFRHKSGYEVHHQ	58	8	18	16
Palm1-15 (E3A,D7K)	DAEFRHKSGYEVHHQ	66	4	17	12
Palm1-15 (D7K)	DAEFRHKSGYEVHHQ	64	8	17	11
Palm1-15	DAEFRHDSGYEVHHQ	75	19	4	1

Peptide net charge influence on β -sheet conformation: ATR-IR qualitative and quantitative analysis of mutant sequences from the liposomal scaffold peptide (Table 2) confirmed the predominant extended conformation, with the % β -sheet component increasing with the net negative charge, as previously seen by CD.

In summary, the results obtained from the ATR-IR secondary structure analysis of a panel of liposomal amyloid-derived lipopeptides were in accordance with *in solution* CD published data. This *solid state* IR technique showed to be more powerful than CD for the quantification of conformational components (specially β -sheet elements) without the requirement of subtracting the signal of empty liposomes. In conclusion, the presented strategy to control the conformation of liposomal peptide immunogens could be applied to the rational design of vaccines against a range of protein misfolding diseases, such as Alzheimer's disease.

References

- [1] Hickman, D.T.; Lopez-Deber, M. P.; Mlaki Ndao, D.; Silva, A. B.; Nand, D.; Pihlgren, M.; Giriens, V.; Madani, R.; St-Pierre, A.; Karastaneva, H.; Nagel-Steger, L.; Willbold, D.; Riesner, D.; Nicolau, C.; Baldus, M.; Pfeifer, A.; Muhs, A. *J. Biol. Chem.* **2011**, *286*, 13966.

Conformational similarities and differences of Angiotensin II (AII): AII acetate vs AII TFA salt in solution

Constantinos Potamitis¹, Eftichia Kritsi¹, Amalia Resvani^{2,3}, Maria-Eleni Androutsou^{2,3}, Panagiotis Plotas³, Pigi Katsougraki², George Agelis^{2,3}, Maria Zervou¹, Panagiotis Zoumpoulakis^{1*}, John Matsoukas^{2,3*}

¹*Institute of Biological, Medicinal Chemistry and Biotechnology, National Hellenic Research Foundation, Athens, Greece;* ²*Laboratory of Organic Chemistry, Biochemistry and Natural Products, Department of Chemistry, University of Patras, Rio, Greece;* ³*Eldrug SA, Patras Science Park, Greece*
E-mail: pzoump@eie.gr; imats@upatras.gr

Introduction

Angiotensin II (AII) (Asp1-Arg2-Val3-Tyr4-Ile5-His6-Pro7-Phe8) is an octapeptide hormone produced by the rennin-angiotensin cascade, directly correlated to hypertension. It is formed by the action of the angiotensin converting enzyme (ACE) which cleaves the C-terminal part (-His-Leu) of the decapeptide Angiotensin I. AII is a vasoconstrictor and plays a central role in the regulation of blood pressure and electrolyte homeostasis [1]. The solution structural models of AII have been previously studied [2] emphasizing on the side-chain orientation of aromatic residues Tyr4, His6, Phe8, which constitute a biologically relevant hydrophobic core. The ring cluster conformation of AII was the basis for the design of peptide mimetics [3]. In this work, the conformational properties of AII of acetate salt which is the active form of the octapeptide have been studied in comparison with AII-Trifluoroacetic acid (TFA) salt in an amphoteric (DMSO) solvent, in order to simulate the membrane environment.

Results and Discussion

NMR ¹H assignment and ROE constrains

The assignment of both AII acetate and TFA salt in *d*₆-DMSO solution was achieved by 2D TOCSY and ROESY NMR spectra, acquired in a 600 MHz Varian spectrometer. The most important ROE correlations were converted into intramolecular distances and were used as constraints at Molecular Dynamics (MD) simulations.

Molecular Dynamics simulations

MD simulations were performed under the calculated constrain distances using Macromodel module of Schrodinger Suite 2012 under OPLS 2005 force field, at simulation temperature 300 K, time step 1 fs, equilibration time 2000 ps and simulation time 15 ns. 1000 conformations were sampled and clustered in 10 groups according to the torsional RMSD of their phi, psi and omega dihedrals. The final step was the energy minimization using PRCG algorithm under constraints.

Two representative, energy minimized conformations of AII acetate salt were derived after MD simulations in accordance with the ROE distances, sharing some common conformational characteristics. The C-terminal residues His6-Pro7-Phe8 form a backbone bend implied by the ROE correlation between the H5 of His6 and β H of Phe8. Another bend is observed at the backbone of Tyr4-Ile5-His6 due to the spatial vicinity of Tyr4 α H and His6 NH. The major difference lies on the orientation of Arg2 side chain. The first one (light grey in Fig. 1a) is energetically favoured (Potential Energy=107.8 kJ/mol) possibly due to the side chain stabilization by the H-bond between the Arg2 guanidine group and His6 heterocyclic ring, while the other one (dark grey in Fig. 1a) orients the side chain in opposite direction. The flexibility of Arg2 induces a different bending at the N-terminus of AII (Fig. 1a). Despite this flexibility, the ROE calculated distance between the Arg2 δ H and one aromatic proton of Tyr4 is satisfied in both cases.

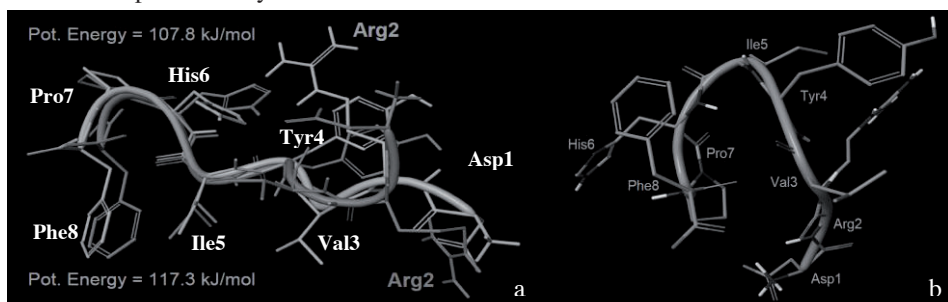


Figure 1. (a) Superimposition of the two representative conformations of AII acetate salt from MD simulations depicting the flexibility of Arg2. (b) Representative conformation of AII in accordance with the ROE distances of AII TFA salt after MD simulations.

In the case of the more acidic environment of TFA salt, AII adopts a less extended conformation, dominated by a large backbone bend (Tyr4-Ile5-His6-Pro7). The observed ROE signals between Tyr4 - His6 and Ile5 β H - Pro δ H induce this folded conformation of AII after the MD simulations (Fig. 1b).

Even though AII acetate and TFA salt have major conformational differences in DMSO solution, both of them present a similar backbone bend at the C-terminal residues (His6 - Phe8). This finding is important since the C-terminus of AII is crucial for binding the AT1 receptor thus exhibiting its vasoconstrictive action.

Acknowledgments

This work was implemented under the FP7 Regional Potential project “Advancement of Research Capability for the Development of New Functional Compounds” (ARCADE).

References

- [1] Mavromoustakos, T.; Kolocouris, A.; Zervou, M.; Roumelioti, P.; Matsoukas, J.; Weisemann, R. *J. Med. Chem.* **1999**, 42, 1714.
- [2] Matsoukas, J.; Hondrelis, J.; Keramida, M.; Mavromoustakos, T.; Makriyannis A.; Yamdagni, R.; Wu, Q.; Moore, G. *J. Biol. Chem.* **1994**, 269, 5303.
- [3] Agelis, G.; Resvani, A.; Durdagi, S.; Spyridaki, K.; Tůmová, T.; Slaninová, J.; Giannopoulos, P.; Vlahakos, D.; Liapakis, G.; Mavromoustakos, T.; Matsoukas, J. *Eur. J. Med. Chem.* **2012**, 55, 358-374.

Consequence of Pro→Ala point mutations for peptide structure and flexibility based on the SAA protein (86-104) fragment mutants

Martyna Maszota, Paulina Czaplewska, Natalia Karska, Marta Spodzieja, Jerzy Ciarkowski, Sylwia Rodziewicz-Motowidło

Department of Chemistry, University of Gdańsk, ul. Sobieskiego 18/19, 80-952, Gdańsk, Poland

E-mail: martynam@chem.univ.gda.pl

Introduction

Human serum amyloid A (SAA) is a highly conserved apolipoprotein produced by the liver under inflammatory conditions accompanying e.g. atherosclerosis, cancer and amyloidosis [1]. It is also known that SAA1 α isoform has the amyloidogenic properties [2]. The C-terminal sequence of SAA contains three proline residues, which probably are responsible for the unordered structure. Recent in vitro studies involving SAA and human cystatin C (hCC) revealed direct interactions between the (86-104) fragment of SAA and the (93-120) sequence of hCC. The NMR studies for the wild (86-104) of SAA protein sequence found an unordered structure in phosphate buffer. Based on these data we decided to check how the point mutations Pro→Ala in (86-104) SAA fragment could influence the peptide's structures. We synthesized four peptides with Pro→Ala point mutations (P(92,97)A; P(92,101)A; P(97,101)A; P(92,97,101)A) and we analyze the solution structures of these peptides using 2D NMR supported with the molecular dynamics.

Results and Discussion

The peptides were synthesized according to the published method [3] using the standard solid-phase synthesis technique. Peptides were synthesized using 9-fluorenylmethoxycarbonyl (Fmoc) chemistry. Peptides were analyzed by matrix-assisted laser desorption/ionization time-of-flight (MALDI-TOF) mass spectrometry (MS). Purity of peptide was confirmed by analytical HPLC. Proton resonance assignments were achieved using the standard Wüthrich procedure [4]. The interproton distances were calculated based on NOE intensities picked up from the NOESY spectra with the mixing time of the 200 ms by the CALIBA algorithm of the CYANA [5] program. The mutants structures were calculated using the Simulated Annealing algorithm in the CYANA package. MD simulations were also carried out with the AMBER force field in AMBER 8.0 package [6]. The time-averaged MD (TAV) utilizing the distance derived from the NMR spectra was made. The MD simulations were carried out at 305 K with the particle-mesh Ewald procedure. The time step was 2 fs, total duration of the run was 2 ns. Molecular structures were drawn and analyzed with PYMOL [7]. For all mutations about 300 inter-residue constrains and 100 intra-residue constrains were found. A strong $d_{\text{NN}(i, i+1)}$ connectivities suggesting α -helical conformation were found for (8-11) region of SAA(86-104) P(97,101)A mutant. Furthermore in SAA(86-104) P(97,101)A mutant the presence of diagnostic medium range $d_{\text{H}\alpha\text{-NH}(i, i+3)}$, $d_{\text{H}\alpha\text{-H}\beta}(i, i+3)$ NOE effects in the (8-11) fragment points to a well-defined helical conformation. All calculated in CYANA and AMBER structures

has unordered N- and C-terminal fragments. The CYANA SAA(86-104) P(92,101)A mutant forms bends in (5-8) and (13-17) fragments. For SAA(86-104) P(92,97)A mutant all calculated structures has similar bends in (3-17) fragment with helix-like (7-9) region. The SAA(86-104) P(92,97,101)A mutant tend to form 3.10 helix in (2-6) fragment and bend structure in (8-14) region. The SAA(86-104) P(97,101)A mutant has the most well defined secondary structure - bends in (3-6) and (12-17) fragments and α -helix in (8-11) region. The structures of SAA (86-104) mutants obtained by MD simulation are as follows: the SAA(86-104) P(92,97)A, SAA(86-104) P(92,97,101)A and SAA(86-104) P(97,101)A mutants creates a bends in (3-17) fragment which forms helix-like conformation. Structures of these mutants are very similar to the structures obtained in the CYANA (see Figure 1). In the least structured mutant, SAA(86-104) P(92,101)A, bend in only (13-17) fragment was found. Comparing these results to the native structure we have to conclude that Pro97 residue highly destabilizes the secondary structure of SAA(86-104) peptide and is critical for this peptide ordered structure formation.

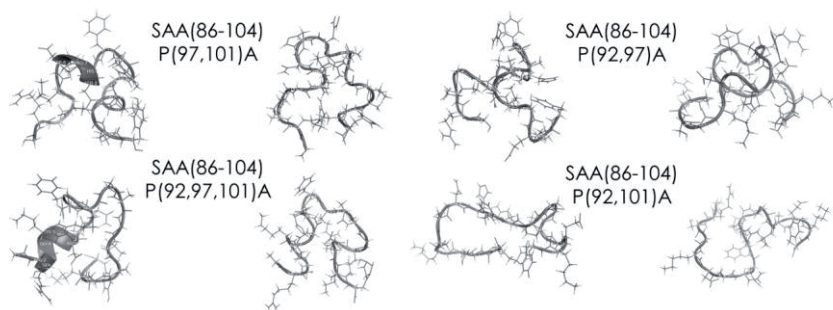


Figure 1: The mean structure of the SAA (86-104) Pro \rightarrow Ala mutants obtained during the Simulated Annealing simulations in the CYANA (left) and the time-averaged MD (right).

Acknowledgments

Acknowledgements: This work is financially supported by the grant from Polish Ministry of Higher Education 1264/B/H03/2009/37 and European FP7 Bio-NMR project.

References

- [1] Uhlar, C.M.; Whitehead, A.S. *Eur. J. Biochem.* **1999**, *265*, 501–523.
- [2] Baltz, M.L.; Rowe, I.F.; Caspi, D.; Turnell, W.G.; Pepys, M.B. *Clin. Exp. Immunol.* **1986**, *66*(3), 701–708.
- [5] Atherton, E.; Sheppard, R. C. *Solid Phase Peptide Synthesis: A Practical Approach*; Oxford University Press: Oxford, **1989**
- [6] Wüthrich, K. *NMR of Proteins and Nucleic Acids*, John Wiley & Sons, New York **1986**
- [7] Güntert, P.; Mumenthaler, C.; Wuthrich, K. *J. Mol. Biol.* **1997**, *273*, 283.
- [8] Case, D.T.; Darden, T.A.; Cheatham ,T.E. III; Simmerling, C.L.; Wang, J.; Duke, R.E.; Luo, R.; Merz, K.M.; Pearlman, D.A.; Crowley, M. AMBER8, University of California, San Francisco **2004**
- [9] The PyMOL Molecular Graphics System, Version 1.3 Schrödinger, LLC

How ionic liquids interact with peptides

Carmen Mrestani-Klaus, Annkathrin Richardt, Frank Bordusa

Institute of Biochemistry and Biotechnology, Martin-Luther-University Halle-Wittenberg,
Halle, Germany

E-mail: mrestani-klaus@biochemtech.uni-halle.de

Introduction

In spite of the broad use of ionic liquids (ILs) for chemical reactions, studies of their influence on the structure of peptides and proteins have an exceedingly short history.

We could successfully use ILs as reaction additives in the protease-mediated ligation of cleavage-sensitive peptide and protein fragments [1]. Furthermore, in our studies on purely chemical acylation reactions of peptides with nucleophilic side chain functionalities, which usually lead to multiple acylation patterns, a surprising regioselectivity-inducing effect of ILs has been found [2]. To explain both findings based on a hypothetical effect of ILs on the spatial structure of the biocatalyst or peptide/protein targets, the impact of ILs on the *cis/trans* ratio of Xaa-Pro peptide bonds as a sensitive and IL-compatible probe for conformational changes in peptides was studied. Using solvent jump experiments we could prove this hypothesis demonstrating indeed a remarkable influence of ILs in the IL-water mixtures on the native *cis/trans* equilibrium – a finding which represents the first experimental proof of a general impact of ILs on the conformation of peptides [2]. We hypothesized direct and unique interactions between those biomolecules and ILs as the molecular reason for this IL-mediated structural effect. To verify this, we performed systematic investigations using solution and in particular high-resolution magic angle spinning (HR-MAS) NMR spectroscopy as the central tool for analyzing structural phenomena on a molecular level [3,4]. Successful proton resonance assignments of both the ILs and, most importantly, the dissolved peptides enabled the analysis of proton chemical shift changes of peptide signals upon dissolving in the respective IL-water mixture.

Results and Discussion

In accordance with the solvent jump experiments, we included in our studies peptides of the type Suc-Ala-Xaa-Pro-Phe-pNA (Xaa = Gly, Lys) as well as the highly water and IL soluble tetrapeptides Ala-Xaa-Pro-Phe (Xaa = Ala, Asp, Glu, Gly, Lys, Phe). Both types of peptides represent excellent proline-containing model compounds. Initially, we performed proton NMR measurements on the peptides and on different *N,N'*-dialkylated imidazolium-based ionic liquids in aqueous solution separately. To visualize peptide/IL interactions, high-resolution ¹H HR-MAS NMR measurements on peptide/D₂O/IL mixtures were carried out. The measurements were performed in 70% IL/30% D₂O (v/v). Further increase in IL concentration led to decreased resolution of the peptide signals. We obtained highly resolved one- and two-dimensional proton HR-MAS spectra in sufficiently high quality for an almost complete assignment of both IL and peptide proton signals. We then extracted the ¹H NMR chemical shifts from the spectra as a basis for determination of the chemical shift differences between the reference systems in aqueous peptide solution and the IL/D₂O/peptide systems. Ratios of the *cis/trans* peptide isomers were determined by

integration of well-resolved signals in the 1D proton spectra of the different solvent systems used here.

The remarkable peptide chemical shift differences arise from direct IL/peptide interactions and IL-induced conformational changes in certain peptide regions. The type and extent of both are mainly affected by the individual Xaa as well as the IL's anion moieties. Significant downfield shifts indicate strong interactions between the ILs and the peptide backbone, which can be attributed to hydrogen bonding with the IL anions. On the other hand, remarkable upfield shifts obtained in the presence of charged and aromatic amino acids as well as proline point to hydrophobic interactions and stacking effects with the IL imidazolium ring. Measurements with varying water/IL ratio (10%, 30%, 50% and 70% IL) showed that at IL contents below 50% (v/v), the chemical shift differences are significantly smaller for a large number of peptide protons, they apparently rise at 50% IL (v/v) and increase further at 70% IL content. This might be a hint that in pure ILs these differences should increase as well. In order to characterize the prominent influence of IL anions on IL/peptide interactions in more detail and to clarify how different ILs as both H-bond donors and acceptors modulate the chemical shift difference values, we performed additional experiments with different anionic species, such as [Et₂PO₄], [Me₂PO₄], [CF₃CO₂], [OAc], [SCN], [Cl], [Br] and [Tos], and the fixed cation [EMIM]. It turned out that ILs with different anions led to different peptide chemical shift amplitudes with SCN⁻ showing the maximum downfield shifts and OAc⁻ the maximum upfield shifts. The question whether the studied ILs can be classified according to their preferential interaction, with respect to water, with the exposed surface of dissolved peptides in correlation to the well-known Hofmeister series requires further investigations. In fact, for organic salts the information on ion stabilizing properties is essentially limited. In this respect, it was of great importance to perform comparative investigations using inorganic salts. We found that ILs (organic salts) and inorganic salts behave different regarding the type and strength of their interactions with peptides. In addition, inorganic salts have no influence on the *cis/trans* equilibrium in contrast to ILs that clearly favor the *trans* isomer. Moreover, different chemical shift changes, strikingly at position Xaa, were observed for *cis*- and *trans*-configured peptide isomers dissolved in aqueous ILs based on direct conformer-specific IL/peptide interactions. The results suggest that the strong IL salt effect on the structure and conformation of peptides turned out to be unique for ionic liquids.

Acknowledgments

The authors thank the Deutsche Forschungsgemeinschaft (DFG) for funding within the priority program SPP 1191, grants BO 1770/4-1 and BO 1770/4-2.

References

- [1] Wehofsky, N.; Wespe, C.; Cerovsky, V.; Pech, A.; Hoess, E.; Rudolph, R.; Bordusa, F. *ChemBioChem* **2008**, *9*, 1493.
- [2] Wespe, C. *Ph.D. thesis*, Martin-Luther-University Halle-Wittenberg, Halle, **2009**.
- [3] Richardt, A.; Mrestani-Klaus, C.; Bordusa, F. in M. Lebl, M. Meldal, K. J. Jensen, T. Hoeg-Jensen (Eds.), *Peptides: Tales of Peptides* **2010** (Proc. 31st Eur. Peptide Symp.) Prompt Scientific Publishing, San Diego, 16.
- [4] Mrestani-Klaus, C.; Richardt, A.; Wespe, C.; Stark, A.; Humpfer, E.; Bordusa, F. *ChemPhysChem* **2012**, *13*, 1836.

Short-chain fatty acid acylated daunorubicin-GnRH-III bioconjugates with enhanced cellular uptake, *in vitro* and *in vivo* antitumor activity

Rózsa Hegedüs^{1,2}, Marilena Manea^{3,4}, Erika Orbán¹, Ildikó Szabó¹, Éva Sipos⁵, Gábor Halmos⁵, Bence Kapuvári⁶, Ákos Schulcz⁶,
József Tóvári⁶, Gábor Mező¹

¹Research Group of Peptide Chemistry, Hungarian Academy of Sciences, Eötvös Loránd University, 1117 Budapest, Hungary; ²Department of Organic Chemistry, Eötvös L. University, 1117 Budapest, Hungary; ³Laboratory of Analytical Chemistry and Biopolymer Structure Analysis, Department of Chemistry, University of Konstanz, 78457 Konstanz, German; ⁴Zukunftskolleg, University of Konstanz, 78457 Konstanz, Germany; ⁵Department of Biopharmacy, Medical and Health Science Center, University of Debrecen, 4032 Debrecen, Hungary; ⁶National Institute of Oncology, 1122 Budapest, Hungary

E-mail: rozsa.hegedus@gmail.com

Introduction

Cancer is one of the leading causes of death worldwide. Besides lung, stomach, liver and breast cancer, colorectal cancer is still a major health problem and one of the most common causes of cancer death in the developed countries (WHO) [1]. It has been shown that a fiber and complex carbohydrate rich diet could be preventive for colon cancer. Depending on the source, the major products are linear (acetate, propionate, butyrate, valerate, hexanoate) and branched (isobutyrate, isovalerate) short chain fatty acids (SCFAs), that exert a tumor growth inhibitory effect [2]. Therefore, SCFAs may be an important component of drug delivery systems for targeted cancer chemotherapy.

Tumor targeting with gonadotropin-releasing hormone (GnRH) analogs is based on the discovery that GnRH receptors are highly expressed in many tumor cells, compared with their expression in normal tissues [3,4]. Using these peptides as targeting moieties in a bioconjugate with chemotherapeutic agents can increase the selectivity and reduce the toxic side effects of the anticancer drugs. In particular, GnRH-III (<EHWSHDWKPG-NH₂) is suitable as a targeting moiety due to its antiproliferative effect and weak endocrine activity in mammals.

In the present work, we report on the synthesis and biochemical characterization (enzymatic stability, cellular uptake, *in vitro* and *in vivo* antitumor activity as well as GnRH-receptor binding affinity) of novel daunorubicin-GnRH-III bioconjugates in which Ser in position 4 was replaced by Lys acylated on its ϵ -amino group with SCFAs of different length (Glp-His-Trp-Lys(X)-His-Asp-Trp-Lys(Dau=Aoa)-Pro-Gly-NH₂, where Glp is pyroglutamic acid, Aoa is aminoxyacetyl, Dau is daunorubicin, and X: propionyl, *n*-butyryl, isobutyryl, valeryl, isovaleryl, crotonyl, caproyl and myristyl groups) in order to enhance the antitumor activity, cellular uptake and enzymatic stability of the bioconjugates.

Results and Discussion

The peptides were synthesized by SPPS (Fmoc/tBu) using orthogonal protecting groups (ivDde and Mtt) for lysine. The SCFAs and aminooxyacetyl group were attached to the peptide chain on the solid support, while the chemical ligation (oxime bond formation) of daunorubicin was carried out in solution (0.2 M NH₄OAc buffer, pH 5.0) [5].

Replacement of ⁴Ser by Lys(X) enhanced the *in vitro* cytostatic effect and cellular uptake of the oxime bond-linked Dau-GnRH-III bioconjugates on MCF-7 (human breast) and HT-29 (human colon) cancer cell lines. The highest *in vitro* cytostatic effect was determined in case of bioconjugates GnRH-III(⁴Lys(iBu), ⁸Lys(Dau=Aoa)) (IC₅₀(μM): 2.2±0.0 (MCF-7) and 2.0±0.6 (HT-29)) and GnRH-III(⁴Lys(nBu), ⁸Lys(Dau=Aoa)) (IC₅₀(μM): 0.7±0.2 (MCF-7) and 2.2±0.6 (HT-29)). These two compounds were also the most effectively taken up by both tested cell lines. Almost 100% of the cells were Dau positive at 20 μM concentration.

All bioconjugates were digested by α-chymotrypsin (the cleavage site was at the peptide bond ³Trp-⁴Lys(X)) and the degradation rate strongly depended on the type of fatty acid. Except GnRH-III(⁴Lys(iBu), ⁸Lys(Dau=Aoa)), the stability of bioconjugates was increased compared to GnRH-III(⁴Lys(Ac), ⁸Lys(Dau=Aoa)) [6] that has been so far the most efficient bioconjugate developed in our laboratories (e.g., 64% intact bioconjugate could be detected after 6 h in case of *n*-butyrylated and 33% in case of acetylated compound). In the presence of rat liver lysosomal homogenate, in all cases, the smallest identified drug containing metabolite was H-Lys(Dau=Aoa)-OH, that can bind to DNA [7]. Fragments without SCFAs were also identified by LC-MS suggesting the release of free fatty acids. However, no free daunorubicin release was observed.

Comparing the investigated bioconjugates containing GnRH-III derivatives as targeting moieties, GnRH-III(⁴Lys(nBu), ⁸Lys(Dau=Aoa)) showed the highest affinity to the GnRH receptors both on human pituitary (IC₅₀(nM): 9.03±0.78) and human prostate cancer tissue (IC₅₀(nM): 7.41±0.55) in a radioligand binding assay.

No macroscopic metastases were observed in any of the investigated groups in the *in vivo* experiment on NSG HT-29 colon cancer bearing female mice. In contrast to the treatment with free daunorubicin, the bioconjugate GnRH-III(⁴Lys(nBu), ⁸Lys(Dau=Aoa)) had a positive effect on the interaction between the tumor and the surrounding tissues, which made the tumor easily operable. Moreover, the bioconjugate was less toxic.

Acknowledgments

This work was supported by grants from the Hungarian National Science Fund (OTKA NK 77485, OTKA K81596), TAMOP 4.2.1/B-09/1/KONV-2010-0007 and University of Konstanz (Zukunftskolleg, Project 879/08; AFF and Young Scholar Fund, Project 435/11).

References

- [1] Sauer, J.J.; Richter, K.K.; Pool-Zobel, B.L. *Nutr. Biochem.* **2007**, *18*, 736.
- [2] Beyer-Sehlmeyer G.; Gleis, M.; Hartmann, E.; et al. *Br. J. Nutr.* **2003**, *90*, 1057.
- [3] Mező, G.; Manea, M. *Exp. Opin. Drug Deliv.* **2010**, *7*, 79.
- [4] Emons, G.; Sindermann, H.; Engel, J.; et al. *Neuroendocrinology* **2009**, *90*, 15.
- [5] Hegedüs, R.; Manea, M.; Orbán, E.; et al. *Eur. J. Med. Chem.* **2012**, *56*, 155.
- [6] Manea, M.; Leurs, U.; Orbán, E.; et al. *Bioconjug. Chem.* **2011**, *22*, 1320.
- [7] Orbán E.; Mező, G.; Schlage, P.; et al. *Amino Acids* **2011**, *41*, 469.

Investigating the structural determinants of neuropeptide 26RFa required for the activation of the receptor GPR103

**Amélie Marotte¹, Laure Guilhaudis¹, Ganesan², Cindy Neveu³,
Benjamin Lefranc³, Jérôme Leprince³, Hubert Vaudry³,
Isabelle Ségalas-Milazzo¹**

¹UMR 6014 CNRS, "Analysis and Modeling team", Université de Rouen, IRIB; ²School of pharmacy, University of East Anglia, Norwich, NR4 7TJ; ³U982 INSERM, Université de Rouen, IRIB

amelie.marotte@etu.univ-rouen.fr

Introduction

26RFa, a neuropeptide of the RFamide family, has been recently discovered by three different teams and has been shown to be the ligand of GPR103, a G-protein coupled receptor [1]. This peptide, composed of 26 amino acids, possesses the C-terminal signature of the RFamide family, the motif Arg-Phe-NH₂. Consistent with the localization of 26RFa and its precursor in hypothalamic nuclei involved in feeding behavior, intracerebroventricular administration of 26RFa has been found to induce a dose-dependent increase in food consumption in rodents [2]. In methanol, the peptide encompasses an α -helix between P⁴ and R¹⁷, surrounded by two unstructured regions [3]. Structure/activity relationship studies revealed that the deletion of nine amino acids from the N-terminal region of 26RFa did not markedly affect the biological activity while the suppression of three more amino acids led to less potent peptides [4]. The decrease of the biological activity observed along the truncation suggests that suppressed residues could be implied in a structuration required to maintain the biological activity. We decided to investigate the 3D structures of fragments which possess different sequence lengths in the N-terminal region in order to determine the impact of the deletions on the structuration.

This analysis will give us some clues to highlight the structural determinants required to maintain the biological activity. In line with obtained results, analogues of 26RFa will be synthesized to obtain new potent ligands of GPR103.

Results and Discussion

We analyzed the 3D structure of 26RFa₇₋₂₆, 26RFa₁₁₋₂₆ and 26RFa₁₃₋₂₆ by NMR (Bruker avance III, 600MHz, CPTXI probe) and molecular modeling (Felix, CNS, Charmm22). We observed that the longest fragment (26RFa₇₋₂₆) possesses a stabilized helix, the medium length fragment (26RFa₁₁₋₂₆) possesses a nascent helix while the shortest fragment (26RFa₁₃₋₂₆) has no helical structure. This structural analysis shows that the diminution of the length of the N-terminal region leads to a destabilization of the helical structure. The decrease of the biological activity could thus be due to the loss of structuration in the N-terminal region.

According to these observations, we decided to study the importance of a stabilized helix on the biological activity by stabilizing the nascent helix of 26RFa₁₁₋₂₆ and nucleating the helix in 26RFa₁₃₋₂₆.

Among the diversity of helix stabilizing strategies, we chose the Hydrogen Bond Surrogate (HBS) method as it allows preserving the amino acid side chains [5]. HBS strategy stabilizes the helix by replacing the main hydrogen bond (NH → O=C(R)NH) in (i,i+4) position by a hydrazone link (N=N=CH-CH₂-CH₂) (Fig. 1). We synthesized two analogues, one of 26RFa₁₁₋₂₆ and the second of 26RFa₁₃₋₂₆, but only the analogue of 26RFa₁₁₋₂₆ was obtained.

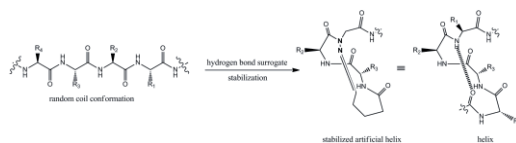


Fig. 1 : HBS principle. R₁, R₂, R₃ and R₄ symbolise the amino acid side chains

The biological activity of 26RFa₁₁₋₂₆ hydrazone linked analogue is inferior to 26RFa₁₁₋₂₆. In order to explain this result, we analyzed the 3D structure of the molecule using NMR and molecular modeling. This structural study revealed that the 26RFa₁₁₋₂₆ hydrazone linked analogue possesses a stabilized helix which is longer than in the original peptide (26RFa₁₁₋₂₆). These results lead us to suggest that the decrease of the biological activity could be due to a too long and/or a too much stabilized helix. We propose the synthesis of news analogues possessing the following modifications: (1) lengthening the hydrazone link by adding a -CH₂ group in order to slightly destabilize the helix, (2) replacing a glycine at the end of the desired length helix by a sarcosine in order to avoid the formation of a hydrogen bond and to shorten the helix.

This second series of analogues is being synthesized. Their structural analysis will allow us to elucidate the role of the helix length and of the helix stability on the biological activity and to propose new modifications in order to improve the potency of our analogues.

Acknowledgments

This work is supported by the IS:CE-Chem project, which was selected under the European cross-border cooperation programme Interreg IV A France-(Channel)-England, co-funded by the ERDF.

References

- [1] Chartrel, N.; Dujardin, C.; Anouar, Y.; Leprince, J.; Decker, A.; Clerens, S.; Do-Rego, J. C.; Vandesande, F.; Llorens-Cortes, C.; Costentin, J.; Beauvillain, J. C.; Vaudry, H. *Proc. Natl. Acad. Sci. USA* **2003**, *100*, 15247-15252; Jiang, Y.; Luo, L.; Gustafon, E. L.; Yadav, D.; Laverty, M.; Murgolo, N.; Vassileva, G.; Zeng, M.; Laz, T. M.; Behan, J.; Qiu, P.; Wang, L.; Wang, S.; Bayne, M.; Greene, J.; Monsma, F.; Zhang, F. L. *J. Biol. Chem.* **2003**, *278*, 27652-27657; Fukusumi, S.; Yoshida, H.; Fujii, R.; Maruyama, M.; Komatsu, H.; Habata, Y.; Shintani, Y.; Hinuma, S.; Fujino, M. *J. Biol. Chem.* **2003**, *278*, 46387-46395.
- [2] Do-Rego, J. C.; Leprince, J.; Chartrel, N.; Vaudry, H.; Costentin, J. *Peptides* **2006**, *27*, 2715-2721.
- [3] Thuau, R.; Guilhaudis, L.; Ségalas-Milazzo, I.; Chartrel, N.; Oulyadi, H.; Boivin, S.; Fournier, A.; Leprince, J.; Davoust, D.; Vaudry, H. *Peptides* **2005**, *26*, 779-789.
- [4] Le Marec, O.; Neveu C.; Lefranc B.; Dubessy, C.; Boutin, J. A.; Do-Régo, J. C.; Costentin, J.; Tonon, M. C.; Tena-Sempere, M.; Vaudry, H.; Leprince, J. *J. Med. Chem.* **2011**, *54*, 4806-4814.
- [5] Cabezas, E.; Satterthwait, A. C. *J. Am. Chem. Soc.* **1999**, *121*, 3862-3875.

Local control of the peptide backbone geometry using trifluoromethylated pseudoprolines

Feytens Debby,¹ Chaume Grégory,² Chassaing Gérard,¹ Lavielle Solange,¹ Brigaud Thierry,² Byun Byung Jin,³ Kang Young Kee,^{3,*} Emeric Miclet^{1,*}

¹Laboratoire des BioMolécules, UMR 7203, Ecole Normale Supérieure, UPMC Paris 06, 4, Place Jussieu, 75005 Paris, France ; ²Laboratoire SOSCO, Université de Cergy-Pontoise, EA 4505, 5 mail Gay Lussac, 95000 Cergy-Pontoise, France; ³Department of Chemistry, Chungbuk National University, Cheongju, Chungbuk 361-763, Republic of Korea

E-mail: ykkang@chungbuk.ac.kr, emeric.miclet@upmc.fr

Introduction

The cyclic nature of the proline residue gives rise to some unique conformational properties of the peptide backbone. First, it induces a constraint by restricting the ϕ -dihedral angle to values around 60°. Second, the Xaa-Pro peptide bond is subject to *cis/trans* isomerization characterized by an increased *cis* population and an activation energy that is low when compared to the other amino acids. Besides, the five-membered ring of the Pro residue can adopt two main distinct conformations (up-puckered or down-puckered) that are almost equally abundant in peptides and proteins. A variety of mimics and analogs have been designed in order to control the conformation of the peptide backbone and/or to alter the *cis/trans* ratios and the rotational barriers for *cis-trans* isomerization [1]. In this presentation, NMR studies and theoretical calculations have been performed on model peptides 1, 2, and 3 [2] in chloroform, DMSO, and water, allowing a precise description of unique conformational properties (Figure 1).

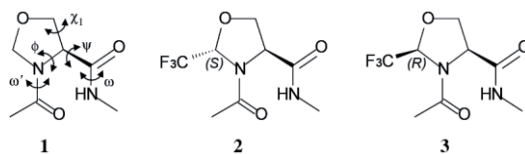


Figure 1 : Structure of model peptides 1-3

Results and Discussion

It is shown that trifluoromethyl C^δ-substitutions of oxazolidine-based pseudoprolines can strongly influence the *cis-trans* rotational barriers with only moderate effects on the *cis/trans* population ratio. Replacing the prolyl residue by the C^δ-(R)-CF₃ oxazolidine **3** within a pseudotriptide sequence was accompanied with a 4 kcal/mol decrease of the *cis-trans* energy barrier. Such an enhancement of the interconversion rate may be very valuable for tuning the biological processes that rely on this molecular switch. Moreover, the CF₃ group allowed a tight control of the ψ -dihedral angle. In CHCl₃, C^δ-(R)-CF₃ **3** significantly stabilized a γ -turn like conformation, whereas C^δ-(S)-CF₃ **2** stabilized PPI/PPII-like backbone conformations (Figure 2). These same PP conformations were highly dominating

in water (>90%), whatever the C^δ-CF₃ configuration. The proline effect is therefore greatly enhanced using trifluoromethylated pseudoproline since the PPI/PPII-like population in water is only ~50% for the natural prolyl residue [3]. Finally, the C^δ-CF₃ configuration can be used to efficiently constrain the ring puckering without affecting the *cis/trans* population ratio. The down-puckering was always associated with the C^δ-(*S*)-CF₃ oxazolidine (**2**), whereas the up-puckering was associated with the C^δ-(*R*)-CF₃ oxazolidine **3** (Figure 2).

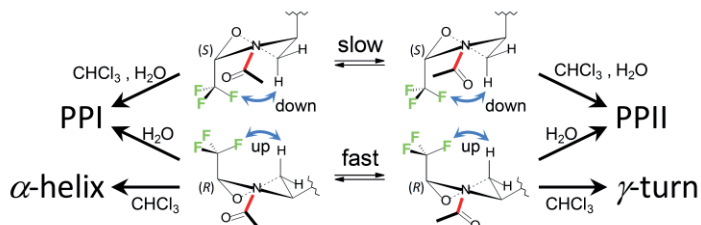


Figure 2 : Solvent effect on peptide conformation

Minimized structures have proven that both electrostatic interactions and hyperconjugations involving the CF₃ group were responsible for these unique structural properties [4]. Favored electrostatic interactions were found between the negatively charged F atoms and a positively charged H^B for the down (respectively up) puckering of the C^δ-(*S*)-CF₃ oxazolidine (respectively C^δ-(*R*)-CF₃ oxazolidine). In addition, the C^e-F antibonding orbitals were involved in two hyperconjugations that stabilized the down (respectively up) puckering in peptide **2** (respectively **3**). Analysis of the transition states have shown that the favorable F⁻---H^N electrostatic contact observed in peptide **3** was replaced by an unfavorable H^α---H^N contact in peptide **2**, providing a rationale for the low *cis-trans* energy barrier observed in peptide **3** (Figure 3).

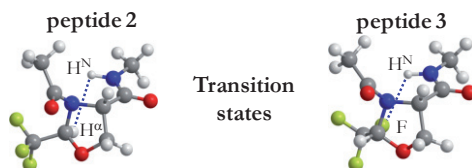


Figure 3 : Electrostatic contacts in the transition states of peptides **2** and **3**

Acknowledgments

Debby Feytens is a postdoctoral researcher of the Fund for Scientific Research Flanders (FWO-Vlaanderen). Thierry Brigaud thanks Central Glass Co. for financial support.

References

- [1] See works from Lubell, W. D.; Mutter, M.; Raines, R. T.; Wennemers, H. and collaborators.
- [2] Chaume, G.; Barbeau, O.; Lesot, P.; Brigaud, T. *J. Org. Chem.* **2010**, *75*, 4135-4145.
- [3] Kang, Y. K. *J. Mol. Struct. (Theochem)* **2004**, *675*, 37-45.
- [4] Feytens, D.; Chaume, G.; Chassaing, G.; Lavielle, S.; Brigaud, T.; Byun, B. J.; Kang, Y. K.; Miclet, E. *J Phys Chem B.* **2012**, *116*, 4069-79.

Model of angiotensin II bound to the AT1 receptor in the lipid bilayer environment

Minos-Timotheos Matsoukas, Theodore Tselios

Department of Chemistry, Section of Organic Chemistry, Biochemistry and Natural Products, University of Patras, 26500 Patras, Greece

E-mail: tselios@upatras.gr

Introduction

The Renin-Angiotensin System (RAS) plays a major role in blood pressure regulation. A sequence of enzyme reactions leads to the release of angiotensin II which interacts principally with the type-1 angiotensin II receptor (AT1), a 359-residue receptor, which belongs to the G protein-coupled receptor family. Angiotensin II (AngII) is the natural hormone (8 residue peptide) that activates the receptor, mediating intracellular pathways that lead to increase of blood pressure.

On this basis, the crystal structure of bovine rhodopsin, (pdb code 1U19), was used as a 3D template and the GROMACS software was utilized for molecular dynamics simulations in order to evaluate the binding mode of Angiotensin II according to previous methods reported by the group [1]. Moreover, newest information on the role of the 2nd extracellular loop [2] were implemented on the model, therefore we propose the contribution mechanism of the residues F170–Q187 in the binding of Angiotensin II to the AT1 receptor.

Results and Discussion

The construction of the receptor was performed by means of the Modeller program taking into consideration the two disulfide bonds between C18 and C274 as well as between C101 and C180 in the extracellular domain. The AMBER99SB force field was used for the protein and peptide, and the Berger force field for the lipids.

Angiotensin II was manually docked into the receptor's binding site taking into account several parameters: i) the interaction of the C-terminal of the peptide and K199^{5,42} as an initial guide, ii) avoiding steric clashes between the binding site and AngII and iii) known interactions between AngII and specific residues of the receptor. Through the MD simulation, the positioning of the K199^{5,42} side chain was monitored as it plays a major role in agonist and antagonist binding due to its positive charge. Also, the rmsd's of the protein and the peptide were examined to determine whether a stable interaction is formed as well if the whole system is stable through the dynamics simulation. According to the rmsd values, the system was considered as stabilized after the 22th ns of the simulation.

Concluding, we have constructed a 3D model of the AT1 receptor interacting with AngII, based on the crystal structure of rhodopsin. The important amino acids of the binding site identified by mutagenesis studies were taken into consideration during the docking procedure. The main observations of this process were: i) The C-terminal is seen to interact with the K199^{5,42}, N200^{5,43} and S109^{3,33} residues forming several hydrogen bonds (fig. 1), ii) His⁶ of AngII has its imidazole group placed between the two hydrophobic residues I288^{7,39} and H256^{6,51}, iii) Tyr⁴ interacts through pi-pi interactions with F28, while the N_α atom

forms a hydrogen bond with N174 of the extracellular loop 2 and iv) Arg², due to the large and flexible side chain, forms a few H-bonds with E185, S186, N174 και N176 residues of the EL2 as well. Also, the role of the EL2 aromatic residues appears very important, especially the one of Y184 which makes several interactions with the peptide.

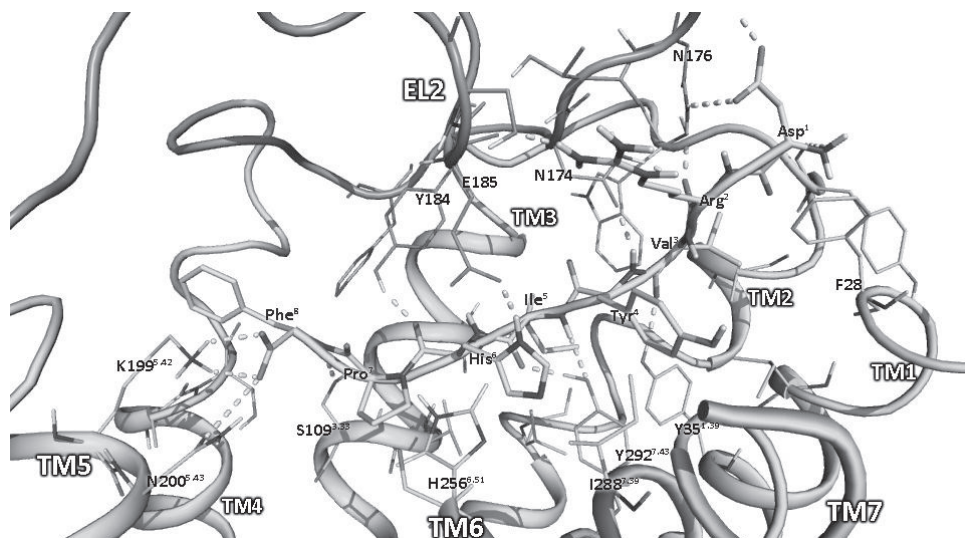


Figure 1. Detailed interactions of the AT1 receptor with angiotensin II. AngII and AT1 are displayed in gray color, whereas the important extracellular loop is displayed in dark grey.

Acknowledgments

This work was financially supported by the “Cooperation” program 09SYN-609-21, (O. P. Competitiveness & Entrepreneurship (EPAN II), ROP Macedonia - Thrace, ROP Crete and Aegean Islands, ROP Thessaly – Mainland Greece – Epirus, ROP Attica).

References

- [1] Matsoukas M. T.; Zoumpoulakis P.; Tselios T. *J. Chem. Inf. Model.* **2011**, 51, 2386.
- [2] Unal, H.; Jagannathan, G.; Bhat, M. B.; Karnik, S. S. *J. Biol. Chem.* **2010**, 285, 16341

Molecular modeling of the Kyotorphin analogues, containing unnatural amino acids

Nicolay Dodoff, Tatyana Dzimbova, Tamara Pajpanova

Acad. Roumen Tsanev Institute of Molecular Biology, Bulgarian Academy of Sciences,
Acad. G. Bonchev Str. Block 21, 1113 Sofia, Bulgaria

E-mail: tamara@bio21.bas.bg

Introduction

The dipeptide kyotorphin (Tyr-Arg, Kyo) plays a role in pain modulation in the mammalian central nervous system (CNS), and is one of the most investigated neuropeptides. The Tyr-Arg motif exists widely throughout the brain not only as Kyo, but also as the *N*-terminal part of several endogenous analgesic peptides [1, 2]. Our special interest concerns the synthesis of Kyo analogues using non-protein amino acid norsulfoarginine (NsArg) as a structural analogue of arginine. In our previous *in vivo* experiments we demonstrated that these analogues exerted a strong-reversible analgesic effect, more pronounced than that of Kyo [3, 4]. The conformational features of these dipeptides are of particular interest, both from theoretical and pharmacological points of view. Since no single-crystal X-ray diffraction data for the compounds are available until now, we undertook a quantum-chemical modelling of their structure. Here we present our preliminary computational results for Kyo, NsArg-Tyr and Tyr-NsArg.

Results and Discussion

The initial conformational search for each molecule was performed at Molecular Mechanics level (HyperChem 7.5 programme [5], MM+, force field; bond charges; Directed search, RMS gradient < 0.009). The lowest-energy conformation (LEC) for each diastereomer was further minimized with the same force field (RMS < 0.001). The LECs thus obtained were subjected to Hartree-Fock (HF) *ab initio* optimization in gas phase and in water medium with 3-21G* basis set [6]. Maximum gradient < $1 \cdot 10^{-4}$ Hartree/Bohr (< $9 \cdot 10^{-4}$ for NsArg-Tyr-E-W and NsAr-Tyr-Z-W). The HF calculations were performed on a personal computer, as well as on a HPC Cluster Platform Express 7000 (Institute of Parallel Processing, BAS) using the Firefly [7], and GAMESS [8] quantum chemistry packages, respectively. The most important computational results are illustrated and summarized in Figure 1 and Table 1. The *zwitter*-ionic forms of the sulfo-analogues, upon HF optimization in gas phase, were found to converge to the corresponding non-ionic diastereomers. In water medium, however, equilibrium conformations were indeed obtained (NsArg-Tyr-E-*zw*-W, NsArg-Tyr-Z-*zw*-W, Tyr-NsArg-E-*zw*-W and Tyr-NsArg-Z-*zw*-W). For all three peptides, all the LECs adopt a *scorpion*-like conformation with close proximity of the guanidino group and phenolic residue. This finding clearly demonstrates that the molecules of the artificial isomeric dipeptides NsArg-Tyr and Tyr-NsArg are indeed sterically similar to that of kyotorphin. In all the three cases, H-bonding plays an important role (Fig. 1).

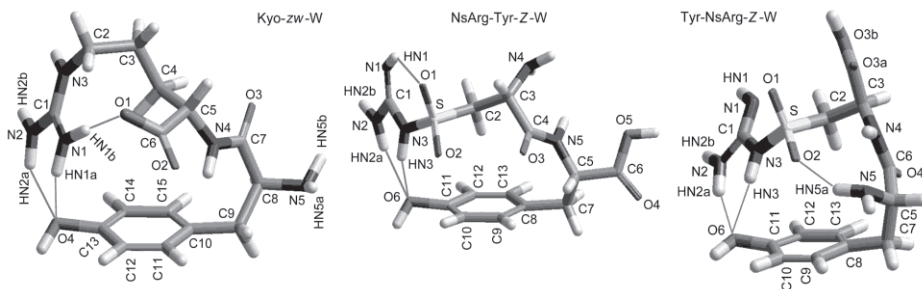


Figure 1. View of the HF optimized lowest-energy forms of Kyo, NsArg-Tyr and Tyr-NsArg with the atom numbering and hydrogen bonds. For the notations see the footnotes to Table 1.

Table 1. Energies (Hartree) of the HF optimized Kyo, NsArg-Tyr and Tyr-NsArg diastereomers (*E* and *Z*) in neutral and *zwitter-ionic* (*zw*) form in gas phase and water medium (*W*).

Kyo- <i>E</i> ^a	Kyo- <i>E-W</i> ^a	Kyo- <i>Z</i> ^a	Kyo- <i>Z-W</i> ^a	Kyo- <i>zw</i> ^a	Kyo- <i>zw-W</i> ^a
-1146.8892	-1146.9279	-1146.9059	-1146.9396	-1146.8886	-1146.9473
NsArg-Tyr- <i>E</i> ^b	NsArg-Tyr- <i>E-W</i> ^b	NsArg-Tyr- <i>Z</i> ^b	NsArg-Tyr- <i>Z-W</i> ^b	NsArg-Tyr- <i>E-zw-W</i> ^b	NsArg-Tyr- <i>Z-zw-W</i> ^b
-1613.7592	-1613.8090	-1613.7567	-1613.8109	-1613.7611	-1613.7570
Tyr-Nsarg- <i>E</i> ^b	Tyr-NsArg- <i>E-W</i> ^b	Tyr-NsArg- <i>Z</i> ^b	Tyr-NsArg- <i>Z-W</i> ^b	Tyr-Nsarg- <i>E-zw-W</i> ^b	Tyr-Nsarg- <i>Z-zw-W</i> ^b
-1613.7843	-1613.8204	-1613.7829	-1613.8240	-1613.7909	-1613.7956

^a*E* and *Z* denote the configuration of the N1=C1 bond with respect to N3-C2 bond.

^b*E* and *Z* denote the configuration of the N1=C1 bond with respect to N3-S bond.

Acknowledgments

The work is financially supported by Bulgarian Ministry of Higher Education and Science (Grant MY-FS-13/07). It is part of European FP7 HP-SEE Project (Contract No RI-261499) and of the bilateral cooperation between the Bulgarian Academy of Sciences and the Aristotle University of Thessaloniki (2012-14).

References

- [1] Fukui, K.; Shiomi, H.; Takagi, H.; Hayashi, K.; Kiso, Y. Kitagawa K. *Neuropharmacology* **1983**, *22*, 191.
- [2] Amano, H.; Morimoto, Y.; Kaneko, S.; Takagi H. *Neuropharmacology* **1984**, *23*, 395.
- [3] Dzimbova, T., Pajpanova, T.; Golovinsky E. *Bulg. Chem. Commun.* **2006**, *38*, 45.
- [4] Bocheva A.; Dzambazova-Maximova E.; Dzimbova T.; Pajpanova T., Golovinsky E. *Compt. Rend. Acad. Bulg. Sci.* **2006**, *59*, 219.
- [5] Hypecube, Inc., HYPERCHEM Release 7.52, **2002**.
- [6] EMSL Basis Set Exchange Library; <https://bse.pnl.gov/bse/portal>.
- [7] Granovsky A. A., Firefly Version 7.1.G, **2009**;
<http://classic.chem.msu.edu/gran/firefly/index.html>.
- [8] GAMESS Version 25 Mar 2010 (R2); Schmidt M. W.; Baldrige K. K.; Boatz J. A.; Elbert S. T.; Gordon M. S.; Jensen, J. H.; Koseki, S.; Matsunaga, N.; Nguyen, K. A.; Su, S.; Windus, T. L.; Dupuis M.; Montgomery, J. A., Jr. *Comput. Chem.*, **1993**, *14*, 1347.

Monitoring peptide folding in membrane-active peptides: A time-resolved spectroscopic study

**E. Gatto,^{1*} S. Lopez,² L. Stella,¹ G. Bocchinfuso,¹ A. Palleschi,¹
C. Serpa,² F. Formaggio,³ C. Toniolo,³ M. Venanzi¹**

¹*University of Rome Tor Vergata, Department of Chemical Sciences and Technologies, 00133-Rome, Italy;* ²*University of Coimbra, Coimbra Chemistry Center, 3004-535-Coimbra, Portugal;* ³*ICB, Padova Unit, CNR, Chemistry Department, University of Padova, 35131-Padova, Italy*

**emanuela.gatto@uniroma2.it*

Introduction

Trichogin GA IV is an antimicrobial peptide characterized by a high content of the nonproteinogenic C^{α,α}-disubstituted glycine Aib (α -aminoisobutyric acid). Owing to the gem-dimethyl substitution on the C^α atom, Aib exhibits a strong propensity to induce 3_{10} / α -helical conformations in peptides. We have already reported on a fluorescent trichogin GA IV analogue [1,2]. The primary structure (and acronym) of the peptide investigated was:

Fmoc-Aib-Gly-Leu-Aib-Gly-Gly-Leu-TOAC-Gly-Ile-Leu-OMe (**F0T8**)

where Fmoc is fluorenyl-9-methyloxycarbonyl, Aib is α -aminoisobutyric acid, TOAC is 2,2,6,6-tetramethylpiperidine-1-oxyl-4-amino-4-carboxylic acid, and OMe is methoxy.

Experimental and computational results indicated that the structural and dynamical properties of **F0T8** are characterized by transitions between an elongated helical conformation and a more compact structure mimicking a helix-turn-helix motif. To further investigate the role of the Gly5-Gly6 central motif in trichogin conformation and dynamics we have synthesized a new trichogin analogue having the Gly6 residue substituted by Aib

Fmoc-Aib-Gly-Leu-Aib-Gly-**Aib**-Leu-TOAC-Gly-Ile-Leu-OMe (**F0A6T8**)

This replacement is expected to stiffen the peptide backbone, reducing the flexibility around the crucial -Gly5-Gly6- dipeptide unit. Also in this case the double substitution of an energy donor (Fmoc) and an acceptor (TOAC) pair in the trichogin sequence enables us to make use of time-resolved optical spectroscopies, spanning from the nanosecond to the microsecond time regime, to investigate the conformational propensity and the dynamical features of **F0A6T8**.

Results and Discussion

All spectroscopic measurements (CD, steady-state and time-resolved fluorescence, and nanosecond transient absorption) were carried out in acetonitrile.

The CD spectra reveal that also the **F0A6T8** analogues predominantly populate helical conformations. However, the ratio of the molar ellipticities measured at 222 and 208 nm, is

0.40 for **F0T8** and 0.54 for **F0A6T8**, suggesting that the latter peptide has a larger α -helical content than the former. Increasing the temperature from 10°C up to 60°C, both peptides showed a decrease in their helical content.

Time-resolved fluorescence experiments show that the emission of **F0A6T8**, like that of **F0T8**, is described by a bi-exponential decay. This result suggests that also in this case two different conformers are mainly populated, the longer and more abundant being associated with a helical conformation. This assignment is confirmed by the observation that, by increasing the temperature, there is a decrease in the long lifetime population, paralleling the decrease in the helical content observed at the CD.

Laser flash photolysis measurements allowed us to measure the triplet decay rate constant (k_T) of the fluorene probe, which is determined by the peptide dynamics. Fmoc triplet quenching by TOAC occurs almost instantaneously, once the two probes attain short separation distances [1]. This allows us to use intramolecular triplet-quenching experiments to determine the rate of contact formation between the two probes in the peptides. The conformational interconversion that brings the TOAC group at a very close distance to the fluorene moiety occurs in the microsecond time scale. The relative higher rigidity of **F0A6T8** is supported by the measured k_T value, that is smaller by a factor of two with respect to the triplet decay rate constant measured for **F0T8**. Therefore, by laser flash photolysis measurements we can determine the conformational interconversion rate constants, which have been found to be 0.7 ms for the **F0A6T8** peptide and 0.3 ms for the **F0T8** trichogin analogue.

Molecular mechanics calculations support our experimental results, suggesting that the **F0A6T8** peptide shows two minimum-energy conformers. One is an extended helical conformation, the other is a bent structure, characterized by a compact 3D arrangement, where two helical segments are connected by a turn involving the Gly5-Aib6 residues. The theoretical quenching efficiencies are in very good agreement with the experimental values. In conclusion, spectroscopic techniques ranging from the nanosecond to the microsecond time range and molecular mechanics calculations have been employed for the investigation of a fluorescent trichogin analogue, having the Gly6 residue substituted by Aib, in order to investigate the structural and dynamical role of the Gly5-Gly6 central motif. Our results indicate that this replacement stiffens the peptide backbone, reducing the flexibility around the crucial -Gly5-Gly6- dipeptide unit.

Acknowledgments

This work was funded by the grant PRIN 2008 (MIUR of Italy) and the European Community's Seventh Framework Programme (grant agreement n° 228334).

References

- [1] Venanzi, M., Gatto, E., Bocchinfuso, G., Palleschi, A., Stella, L., Formaggio, F. and Toniolo, C. *ChemBioChem* **2006**, *7*, 43–45.
- [2] Venanzi, M., Gatto, E., Bocchinfuso, G., Palleschi, A., Stella, L., Baldini, C., Formaggio, F. and Toniolo, C. *J. Phys. Chem. B* **2006**, *110*, 22834–22841.

Pharmacophore model of cysteine-based $\alpha 4\beta 1$ integrin ligands based on conformational solution studies

Maria Zervou^{a*}, Constantinos Potamitis^a, Panagiotis Zoumpoulakis^a,
Charalambos Fotakis^a, Evangelia Papadimitriou^b, Paul Cordopatis^b,
Vassiliki Magafa^{b*}

^aInstitute of Biology, Medicinal Chemistry and Biotechnology, National Hellenic Research Foundation, Athens, Greece; ^bDepartment of Pharmacy, University of Patras, Patras, Greece

E-mail: mzervou@ie.gr; magafa@pharmacy.upatras.gr

Introduction

The antigen $\alpha 4\beta 1$, a member of the integrin family, is involved in the migration of lymphocytes through endothelium to the site of inflammation [1]. Thus, $\alpha 4\beta 1$ antagonists may be useful compounds for the treatment of various inflammation disorders such as asthma and inflammatory arthritis. In addition, recent studies indicate that $\alpha 4\beta 1$ integrin promotes angiogenesis by allowing the invasion of myeloid cells into tumors, while $\alpha 4\beta 1$ antagonists prevent monocyte-induced angiogenesis, macrophage colonization of tumors and tumor angiogenesis [2]. Aiming to the discovery of novel $\alpha 4\beta 1$ antagonists, a series of new peptide analogues cyclized through cysteine disulphide bonds were synthesized and tested *in vivo* against angiogenesis in chicken embryo chorioallantoic membrane (CAM model) [3].

SAR results indicated that: YR-c(CDPC)-CONH₂ (**GD1S**) promoted angiogenesis at the higher studied concentration and showed slight inhibition at the lower one, Sal-R-c(CDPC)-OH (**GD5S**) showed important inhibition of angiogenesis at dose-dependent manner, YR-c(CDPC)-OH (**GD4S**) and Sal-YR-c(CDPC)-OH (**GD9S**) both showed no activity on angiogenesis.

NMR spectroscopy was applied for the sequential assignment as well as for the elucidation of specific conformational features. Experimental NOE data were further imposed as distance constraints to a thorough conformational search by applying Molecular Dynamics simulations. Energy refined conformers were used as template for the **generation of the pharmacophore model associated with the antagonistic activity**. Such studies are intended to drive a rationalized design and development of this class of inhibitors.

Results and Discussion

NOE driven MD simulations indicated the distinct conformational characteristics of the **inhibitor GD5S** mapping the **proximity of the Sal aromatic ring to the Pro moiety and the distal arrangement of the Arg side chain from the cyclized part of the peptide**. The Pro-aromatic interaction (C-H \cdots π) cannot be sustained when Sal is mutated by the longer side chain and more flexible Tyr residue of the **promoter GD1S** and the conformation is stabilized through the H-bond interaction between the guanidine group and the Asp side-chain carboxyl group (Fig.1). These conformational properties led to the generation of a **pharmacophore hypothesis** with the following features: a) a cluster of three H-bond

donors from the NH groups of Arg, Cys1 and Cys2, b) two H-bonds acceptors from the hydroxyl group of Sal and the carbonyl of Asp, c) two negatively charged regions due to the Asp and the terminal carboxyl moieties, d) a positively charged region from the Arg guanidino group, e) a hydrophobic area caused by the Arg side chain and f) an aromatic feature due to the Sal phenyl ring stacking against the pyrrolidine ring of Pro (Fig.2).

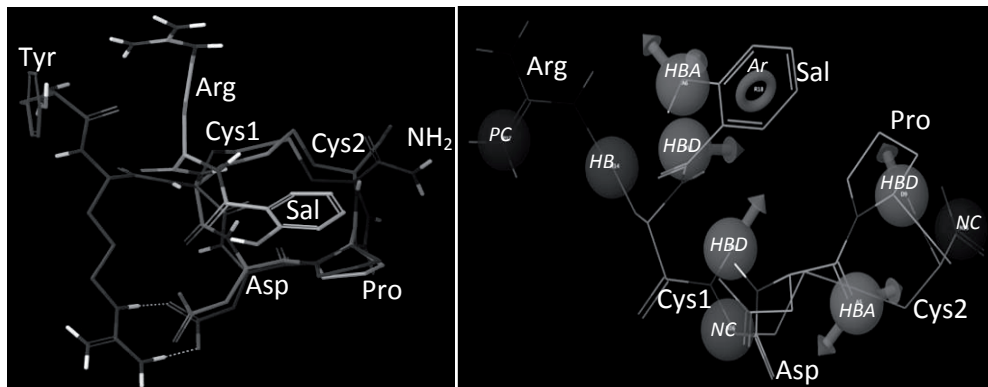


Figure 1(Left): Superimposition of the promoter **GD1S** (dark grey) with the inhibitor **GD5S** (light grey) derived from MD simulations.

Figure 2(Right): Pharmacophore model associated with the antagonistic activity. The abbreviations used are, HBD: H-bond donors, HBA: H-bond acceptors, NC / PC: Negatively / Positively charged regions, HB: Hydrophobic areas and Ar: Aromatic rings.

The **inactive analog GD4S** folds the Tyr aromatic ring towards the cyclic peptide backbone stabilized by H bonding interaction between Tyr-OH and Cys1 carboxyl group. This interaction though, shifts the Tyr ring away from Pro thus disrupting the aromatic-prolyl interaction. The **inactive analog GD9S** stabilizes its conformation by forming H-bonds between the guanidino group of Arg and the side-chain carboxyl group of Asp as well as an H-bond network involving Cys1 amide, Sal-OH and Arg amide. These interactions cluster the three residues preceding the cyclization in a distal arrangement from the cyclized backbone thus the peptide fails to position an aromatic moiety (Tyr or Sal ring) towards the Pro ring. These observations further confirm our suggestion that a conformation stabilized by a C-H \cdots π interaction might be associated with antagonistic activity.

Acknowledgments

This work was implemented under the FP7 Regional Potential project “Advancement of Research Capability for the Development of New Functional Compounds” (ARCADE).

References

- [1] Hynes, R.O. *Cell*, **1992**, *69*, 11.
- [2] Jin, H.; Su, J.; Garmy-Susini, B.; Kleeman, J.; Varner, J. *Cancer Res.* **2006**, *66*, 2146.
- [3] Daletos, G.K.; Lamprou, M.; Zoumpoulakis, P.; Zervou, M.; Assimomytis, N.L.; Geronikaki, A.; Papadimitriou, E.; Magafa, V.; Cordopatis, P. In “*Peptides 2010*” (M. Lebl, M. Meldal, K. Jensen and T. Hoeg-Jensen, Eds.), *Prompt Scientific Publishing, San Diego*, pp. 444-445 (2010).

Probing alpha-synuclein molecular binding sites and their effects on aggregation by NMR spectroscopy

A. Byrne,¹ M. Bisaglia,² L. Bubacco,² N. Andersen¹

¹Chemistry Department, University of Washington, Seattle, WA 98195, U.S.A.; ²Dept. of Biology, University of Padova, Padova 35121, Italy

E-mail: andersen@chem.washington.edu

Introduction

We have established that designed hairpin peptides interfere with the amyloidogenesis of both human pancreatic amylin and α -synuclein (α -syn), two polypeptides associated with human diseases [1]. In the case of α -syn, the most potent ‘amyloid inhibitors’ appeared to act by diverting α -syn to non-amyloid aggregates. In the present report, we examine the early stages of α -syn aggregation, with and without added peptides, by NMR spectroscopy.

Results and Discussion

The peptide ‘inhibitors’ examined herein are hairpins: WW2 (KKLTVW-**I**pGK-WITVSA) and cyclo-WW2 (the cyclic form of **p**KKLTVW-**I**pGK-WITVSIP), **p** = D-Pro. As it turned out, amyloid fibril formation from α -syn was slow under NMR conditions (100 - 400 μ M α -syn) so long as the solutions were cold (< 293 K). Amyloid formation can be induced by the addition of 1.5 – 4 vol-% HFIP, with warming and stirring in most cases. HFIP addition also accelerated the formation of non-amyloid aggregates in samples containing hairpin WW2. 2:1 WW2/ α -syn samples (150 μ M α -syn) afforded non-amyloid precipitate in 6 h with additional precipitation upon HFIP addition. In a parallel experiment with cyclo-WW2, aggregate precipitation occurred within 20 min. Thus, even though the mechanism of amyloid fibril inhibition is completely different for hAM and α -syn, rigidification of the hairpin conformation by cyclization increases potency. *The hairpin binding hypothesis stands confirmed for both of these amyloidogenic species.*

An NMR monitored WW2/ α -syn titration experiment afforded an insight into the nature of the non-amyloid aggregate. As the precipitate forms the signals due to WW2 disappear with none present in the filtrate after aggregation is complete: the ‘inhibitor’ is incorporated in the non-amyloid aggregate that forms.

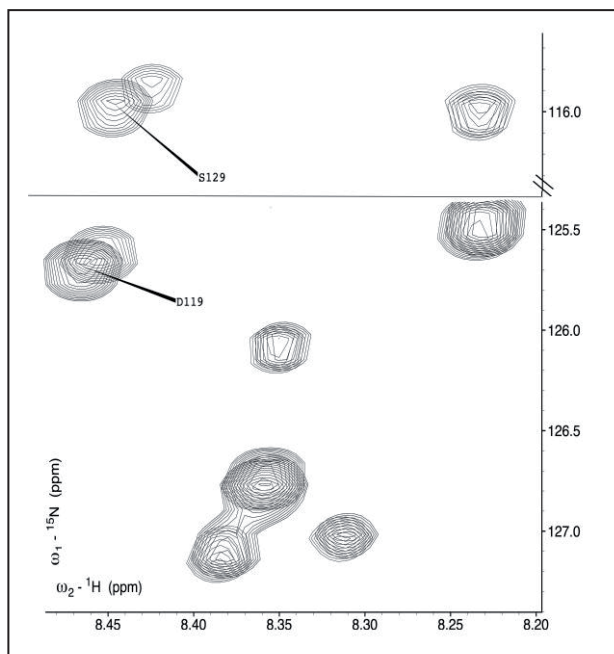
We turned to NMR studies of ¹⁵N-labeled α -syn (100 and 400 μ M) to examine the changes that result at the early stages of uninhibited amyloid formation and modifications to this that occur in the presence of added peptides. In a variety of buffers (with and without the addition of 1.5 vol-% HFIP), the initial ¹⁵N-HSQC spectra reproduced the results reported by Bodner et al. [2], and fully 75 % of the signals were sufficiently resolved for assignment by analogy. As a control, the spectral changes for an uninhibited 100 μ M α -syn sample with 1.5 vol-% HFIP present throughout were followed over a 12-hr period. Most of the peaks broadened to the extent that they disappeared from the spectra. The peaks that were absent at 6 h were due to L8, T92, N103 and most of the residues in the two ‘amyloidogenic patches’ (V⁶⁶G⁶⁷GAVVTA⁷³ and V⁷⁷AQKTV⁸²) that have been the basis

of previous sequence-related inhibitor designs. By the 12-hour point, the only sharp peaks remaining that could be firmly assigned were in the C-terminus: E105 – A140. This segment appears to retain random-coil flexibility in the pre-amyloid oligomeric state. The solution was still transparent at the 12 hour point indicating the absence of mature fibrils, which precipitated from the solution at longer times.

The sequence of peak disappearances was altered by the addition of hairpin WW2 and some of the peaks showed changes in chemical shifts. The shifts due to peptide binding to monomeric α -syn were more readily observed at higher concentrations (400 μ M α -syn) in the absence of added HFIP. HSQC spectra were recorded as the ‘inhibitor’ concentration was serially increased to: 120, 240, 600 μ M. In the case of hairpin WW2, substantial titration shifts were observed at V118, D119, D121, N122, S129, and G132. Two of these shifts are illustrated in the Figure.

Figure – Segments of the HSQC spectra recorded with 0.6 and 1.5 equivalents of WW2 added to α -syn are overlaid.

No comparable shifts were observed N-terminal to these. This leads us to suggest that the formation of the non-amyloid aggregates that we observe with WW2 results from a binding-induced structuring transition in the random coil C-terminus of α -syn. This C-terminal binding event may also result in a conformational changes in the amyloidogenic N-terminal region that retard the formation of pre-amyloid oligomers.



Solution-state NMR, which detects only monomeric and small oligomeric species, appears well suited for examining the earliest stages of amyloidogenesis; these probably include the generation of the toxic species associated with amyloid diseases.

Acknowledgments

Initial studies were supported by a grant from the U.S. National Institutes of Health (3R01-GM-059658-08S1).

References

- [1] Huggins, K.; Bisaglia, M.; Bubacco, L.; Tatarek-Nossol, M.; Kapurniotu, A.; Andersen, N. *Biochemistry* **2011**, *50*, 8202-8212.
- [2] Bodner C.; Maltsev A.; Dobson C.; Bax A. *Biochemistry* **2010**, *49*, 862-71.

Synthesis and *in vitro* activity examinations of 1,4-disubstituted-[1,2,3]triazolyl-containing cyclopeptides, analogs of MT-II, obtained via i to i+5 intramolecular side chain to side chain azide-alkyne cycloaddition

Chiara Testa,^{1,2,3,4} Debora D'Addona,^{1,3} Mario Scrima,⁵ Anna Maria D'Ursi,⁵ Marvin L. Dirain,⁶ Michael Chorev,^{7,8} Carrie Haskell-Luevano,^{6,9} Paolo Rovero,^{1,2} Anna Maria Papini^{1,3,4}

¹Laboratory of Peptide & Protein Chemistry & Biology, Polo Scientifico e Tecnologico, University of Florence, 50019 Sesto Fiorentino (FI), Italy; ²Department of Pharmaceutical Science, Polo Scientifico e Tecnologico, University of Florence, 50019 Sesto Fiorentino (FI), Italy; ³Department of Chemistry "Ugo Schiff", University of Florence, 50019 Sesto Fiorentino (Fi), Italy; ⁴Laboratoire SOSCO – EA4505 Université de Cergy-Pontoise Neuville-sur-Oise, 95031 Cergy-Pontoise, France; ⁵Department of Pharmaceutical Science, Salerno, 84084, Italy; ⁶Departments of Pharmacodynamics, University of Florida, Gainesville, FL 32610, USA; ⁷Laboratory for Translational Research, Harvard Medical School, Cambridge, MA 02139, USA; ⁸Department of Medicine, Brigham and Women's Hospital, MA 02115, USA; ⁹Department of Medicinal Chemistry, University of Minnesota, Minneapolis, MN 55455, USA

Chiara.testa1@gmail.com

Introduction

MT-II, Ac-Nle⁴-c[Asp⁵-D-Phe⁷-Lys¹⁰]αMSH₄₋₁₀-NH₂ is a long acting, non-selective super-agonist of melanocortin G protein-coupled receptors, (GPCR-MCRs) [1]. This homodetic peptide is characterized by a lactam bridge between residues i and i+5, stabilizing the pharmacophore containing sequence His⁶-D-Phe⁷-Arg⁸-Trp⁹ in a type-II β-turn [2]. The recently introduced Cu^I-catalyzed azide-alkyne 1,3-dipolar Huisgen's cycloaddition (CuAAC), presents a promising opportunity to develop a new paradigm for an orthogonal bioorganic and intramolecular side chain-to-side chain cyclization. Herein we report the design, synthesis, biological activity and conformational analysis of a series of i-to-i+5 1,4- and 4,1-disubstituted [1,2,3]triazole-bridged cyclopeptides derived from MT-II.

Results and Discussion

In the present study we report a systematic structure-activity-conformation relationship study in which we demonstrate that side chain-to-side chain conformational stabilization of β turn by triazolyl bridged structures led to cyclic peptides able to enhance *in vitro* potency and subtype receptor selectivity. In this study we demonstrate that the linear peptides (I'÷X') containing pairwise modifications consisting of ω-azido- and ω-alkynyl-side chains at positions i and i+5, are in general less potent than or equipotent to the original MT-II. On the other hand the cyclic peptides (I÷X) are more potent than their linear precursors, confirming that conformational stabilization in the form of side chain-to-side chain cyclization enhances *in vitro* potency (Table 1). Of interest is the emergence of mMC5R selectivity (cyclopeptides III, VIII, IV and X). Moreover, the triazolyl-containing

cyclopeptides (I÷X) showed similar potency compared to the parent lactam-containing MT-II analogs, indicating that these types of side chain modifications are a promising alternative to the lactam types of cyclizations.

Table 1. (A) Adenylate cyclase activity (EC_{50}) of linear peptide precursors (I'÷X') and (B) triazolyl-containing cyclopeptides (I÷X.)

A						B					
Peptide		mMC1R	mMC3R	mMC4R	mMC5R	Peptide		mMC1R	mMC3R	mMC4R	mMC5R
ide	nXaa, mYaa	EC_{50} (nM)	EC_{50} (nM)	EC_{50} (nM)	EC_{50} (nM)	ide	nXaa, mYaa	EC_{50} (nM)	EC_{50} (nM)	EC_{50} (nM)	EC_{50} (nM)
I'	1yl, 4az	0.46±0.11	2.19±0.45	1.50±0.69	3.22±0.92	I	c[1yl, 4az]	5.18±0.54	3.14±0.25	1.62±0.57	1.93±0.07
V'	4az, 1yl	0.24±0.08	1.92±0.45	0.81±0.32	1.90±0.51	V	c[4az, 1yl]	0.85±0.07	3.70±0.36	0.58±0.14	1.76±0.37
II'	2yl, 3az	0.72±0.15	3.27±0.88	2.22±1.06	5.33±1.65	II	c[2yl, 3az]	0.11±0.029	0.29±0.1	0.22±0.06	0.34±0.09
VI'	3az, 2yl	0.83±0.26	3.66±1.16	2.15±0.81	5.04±1.59	VI	c[3az, 2yl]	0.71±0.11	1.91±0.73	0.85±0.36	1.88±0.70
III'	3yl, 2az	0.82±0.12	0.91±0.22	0.13±0.01	0.13±0.009	III	c[3yl, 2az]	0.1±0.009	0.21±0.038	0.051±0.006	0.042±0.005
VII'	2az, 3yl	0.36±0.09	0.86±0.2	0.098±0.017	0.086±0.013	VII	c[2az, 3yl]	0.074±0.02	0.20±0.006	0.048±0.007	0.045±0.004
IV'	4yl, 1az	1.24±0.027	1.58±0.2	0.19±0.04	0.18±0.049	IV	c[4yl, 1az]	0.087±0.029	0.2±0.002	0.041±0.001	0.035±0.007
VIII'	1az, 4yl	0.53±0.13	1.32±0.16	0.14±0.009	0.13±0.006	VIII	c[1az, 4yl]	0.53±0.14	0.60±0.04	0.14±0.02	0.13±0.015
IX'	2yl, 2az	1.98±0.50	2.33±0.31	0.29±0.009	0.23±0.002	IX	c[2yl, 2az]	0.32±0.097	0.63±0.13	0.14±0.029	0.15±0.02
X'	2az, 2yl	0.25±0.09	0.44±0.06	0.058±0.006	0.051±0.007	X	c[2az, 2yl]	0.20±0.023	0.29±0.07	0.067±0.004	0.07±0.004

The introduction of the triazolyl moiety between residues i and i+5 allowed us to obtain a type I β turn bioactive conformation [Figure 1 (A), (C), and (E)].

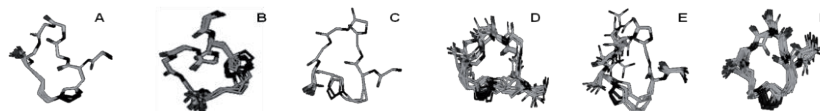


Figure 1. Best 20 NMR calculated structure bundles of: cyclopeptide I (A) and (B) [(A) is the most abundant conformer and (B) is the less abundant one]; cyclopeptide V (C); X (D); IV (E); II (F).

The conformational data confirm once again [3] that the size of the cycle and the position of the triazolyl ring play a key role in regulating the conformational preferences of the triazolyl bridged cyclopeptides. In fact we demonstrated that i-to-i+5 side chain-to-side chain bridged [1,2,3]triazolyl containing-cyclopeptides can successfully replace the classical β -turn stabilizing the corresponding lactam containing cyclopeptides.

In conclusion these studies support our previous hypothesis and extend the proof-of-concept introduced with the PTHrP model peptide that it is possible to enhance bioactivity *in vitro* stabilizing specific secondary structures induced by side chain-to-side chain triazolyl containing cyclopeptides [3-5].

Acknowledgments

This work was granted by "Programme de cotutelle internationale de thèse de doctorat soutenu par la région Ile-de-France" (CT), ANR Chaire d'Excellence 2009-2013 (AMP) and by Fondazione Ente Cassa di Risparmio di Firenze.

References

- [1] Al-Obeidi, F.; de Lauro Castrucci, A.M.; Hadley, V.J. *J. Med Chem.* 1989, 32, 2555.
- [2] Ying, J.; Köver, K.E.; Gu, X.; Han, G.; Trivedi, D.B.; Kavarana, M.J.; Hruby, V.J. *Biopolymers*, 2003, 71, 696.
- [3] Scrima, M.; Le Chevalier-Isaad, A.; Rovero, P.; Papini, A.M.; Chorev, M.; D'Ursi, A.M. *Eur. J. Org. Chem.* 2010, 446
- [4] Cantel, S.; Le Chavelier Isaad, A.; Scrima, M.; Levy, J.J.; DiMarchi, R.D.; Rovero, P.; Halperin, J.A.; D'Ursi, A.M.; Papini, A.M.; Chorev M. *J. Org. Chem.* 2008, 73, 5663.
- [5] Le Chevalier Isaad, A.; Papini, A.M.; Chorev M.; Rovero, P. *J. Pept. Sci.*, 2009, 15, 451.

Scaffold discovery by phylomers: A novel CD40L specific scaffold derived from glycyl tRNA synthetase

Shane R. Stone¹, Katrin Hoffmann^{1,2}, Nadia Milech^{1,2}, Paula T, Cunningham¹, Maria Kerfoot¹, Scott Winslow¹, Yew-Foon Tan¹, Mark Anastasas¹, Clint Hall¹, Marie Scobie¹, Paul Watt², Richard Hopkins^{1,2}

¹*Drug Discovery Technology Unit, Telethon Institute for Child Health Research, 100 Roberts Road, Subiaco, 6008, Western Australia;* ²*Phylogica Pty Ltd, 100 Roberts Road, Subiaco, 6008, Western Australia*

E-mail: sstone@ichr.uwa.edu.au

Introduction

The CD40-CD40L pathway is a key component within the immune system [1] and has been the focus of antibody-based treatments for a variety of cancers [2] but with varying degrees of success due to complications arising from Fc effector functions [3]. It is believed that small protein and peptide-based inhibitors of this pathway may provide more attractive therapeutic alternatives to antibodies [3]. In this paper we present, as a case study, our results from targeting CD40L using phylomer libraries [4] and the discovery of a novel CD40L-specific scaffold derived from the glycyl tRNA synthetase family.

Results and Discussion

Biopanning of phylomer phage display libraries against human CD40L yielded a cluster of six, highly specific, overlapping peptide fragments corresponding to the conserved catalytic domain from the $G\alpha 2\beta 2$ family of Glycyl tRNA synthetases. Structural analysis of the Glycyl tRNA synthetase family showed that the overlapping peptide fragments described a scaffold consisting of a central β -sheet, comprising 4 anti-parallel β -strands, flanked by N- and C-terminal α -helices. Further structural analysis revealed that these key structural features, which also encompass the crucial ATP-binding motifs of the catalytic domain, are conformationally conserved across both tetrameric $G\alpha 2\beta 2$ and dimeric $G\alpha 2$ Glycyl tRNA synthetases, yet importantly, there is only limited sequence conservation across these classes [5].

Given the identical function of the described domain and its structural conservation, we postulated that members of the dimeric $G\alpha 2$ class would display similar CD40L specific binding as the tetrameric $G\alpha 2\beta 2$ class, despite the sequence dissimilarity. To test this hypothesis, structurally equivalent peptide fragments of representative bacterial, archaeal and eukaryotic genomes comprising both the dimeric $G\alpha 2$ and tetrameric $G\alpha 2\beta 2$ classes were tested for binding and specificity to human CD40L.

Figure 1. Comparison of Specificity and Potency for *B. pertussis* and *H. sapiens* 1064 ortholog sequences

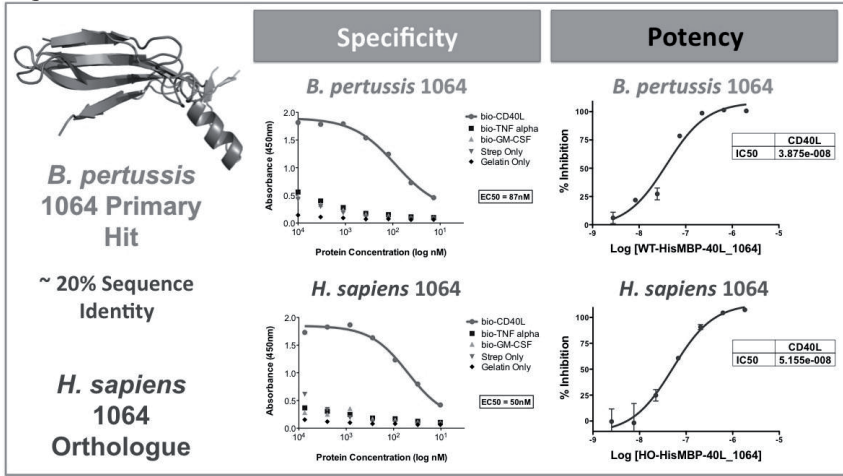


Table 1. CD40-CD40L Inhibition IC50s for selected Glycyl tRNA Synthetase 1064 Orthologues

Organism	Sub-Class	IC ₅₀ (nM)
<i>B. pertussis</i>	Gα2β2	39
<i>S. typhimurium</i>	Gα2β2	10
<i>S. aureus</i>	Gα2	143
<i>B. burgdorferi</i>	Gα2	71900*
<i>C. tepidum</i>	Gα2	210
<i>P. horikoshi</i>	Gα2	30
<i>H. sapiens</i>	Gα2	52

Our experimental results showed that both archaeal (*P. horikoshii*) and eukaryotic (*H. sapiens*) structurally equivalent peptides bound to CD40L with reasonable specificity and activity, inhibiting the CD40-CD40L interaction with comparable IC₅₀'s to the primary Gα2β2 class sequences. Similar results were also observed for the representative bacterial Gα2 class peptides. Together this data strongly suggests that this is a unique scaffold with exquisite specificity for CD40L. Further, that the sequentially diverse orthologous peptides display CD40L specific binding has important implications to the affinity enhancement strategies to develop the scaffold as a therapeutic agent, and in improving its “drug-like” properties.

References

- [1] Daoussis, D., Andonopoulos, A.P., Liossis, S.N., *Clin. Diag. Lab. Immun.* **2004**, 11 (4): 635-41
- [2] Elgueta, R., Benson, M.J., de Vries, V.C., Wasiuk, A., Guo, Y., Noelle, R.J., *Immun. Rev.* **2009**, 229 (1): 152-72
- [3] Deambrosis, I., Lamorte, S., Giaretta, F., Tei, L., Biancone, L., Bussolati, B., Camussi, G., *J. Mol. Med.*, **2009**, 87 (2): 181-97
- [4] Watt, P.M., *Nature Biotech.*, **2006**, 24 (2): 177-83
- [5] Tang, S.-N. and Huang, J.-F., *FEBS Lett.*, **2005**, 579(6), 1441-1445

Structural studies of nucleophosmin 1 helical peptides

**C. Di Natale¹, L. De Rosa², M. Leone², P.L. Scognamiglio^{1,2},
L.Vitagliano², D. Marasco^{1,2}**

¹*University of Naples "Federico II", Naples, Italy;* ²*Institute of Biostructures and
Bioimaging National Research Council, Naples, Italy*

daniela.marasco@unina.it

Introduction

The definition of the molecular basis of human diseases is one of the most important goals of structural biology. Nucleophosmin, NPM1, physiologically, despite its nucleolar localization, shuttles constantly across nucleolar, nucleoplasmic and cytoplasmic compartments. This shuttling activity of NPM1 is critical for most of its functions, including regulation of ribosome biogenesis and control of centrosome duplication [1]. Deregulation of NPM1 is implicated in the pathogenesis of several human malignancies. Indeed, NPM1 has been described both as an oncogene and as a tumor suppressor depending on the cell type. It is important to note that mutations involving the NPM1 gene are the most frequent molecular alterations in acute myeloid leukemia (AML) accounting for about 60% of cases (i.e. one-third of adult AML) [2]. This protein has a modular structure; the N-terminal domain is the oligomerization domain, the C-terminal region contains the structural elements responsible for RNA/DNA recognition [1]. NMR investigations have shown that the last 53 C-terminal residues fold in a 3-helix bundle [1, 3]. Here, we have further investigated the structural determinants of the folding process of the C-term NPM1 domain by the designing several peptides covering the three helices. Their conformational properties were investigated by CD and NMR spectroscopy.

Results and Discussion

To evaluate the conformational properties of sequences covering regions H1, H2 and H3, that belong to the C-terminal 3-helix bundle domain, separately, we have investigated the peptides reported in Table 1 through circular dichroism spectroscopy. These sequences were designed on the basis of secondary structure elements of the native protein and, for each, several mutations were introduced to enhance helical propensity or evaluate conformational effects of diseases-associated substitutions. H1 and H3 peptides show a clear tendency to adopt helical structures, while the behavior of H2 peptide is quite different. The CD spectrum of a freshly prepared solution of H2 shows a broad Cotton effect still referred to a prevalent helical conformation but, a time dependent variation of CD spectrum occurs, and after 2h a typical β -sheet spectrum can be recorded. Then, while all helical peptides show an unusual thermal stability, they were completely denaturated upon UREA addition (0-8M), among them, H2 shows the higher level of CD signal variation upon temperature, even if not cooperative.

Confirming CD analysis, NMR experiments carried out on H1 and H3 (Table 1) indicated propensities of these peptides to adopt helical conformations. On the contrary, NMR analysis of H2 peptide resulted rather difficult due to the presence of a few duplicated spin systems in the spectra and the occurrence of changes in chemical shifts over time. These

phenomena are likely connected to severe aggregation processes as further supported by high increase in sample viscosity after a few hours.

Table 1: Cterm NPM1-derived sequences investigated in this study

NAME	SEQUENCE
H1	²⁴² SSVEDIKAKMQASIEKAH ²⁵⁹
H1 ARTI	LT ²⁴² SSVEDIKAKMQASIEKAH ²⁵⁹ KGI
H1 KGG	²⁴² SSVEDIKAKMQASIEK GG ²⁵⁹
H2	²⁵⁹ GSLPKVEAKFINYVK C FR ²⁷⁷
H2 CS	²⁵⁹ GSLPKVEAKFINYVK S FR ²⁷⁷
H3	²⁷⁹ TDQEAIQDLWQWRKSL ²⁹⁴
H3 MUT a	²⁷⁹ TDQEAIQDLCLAVEEVSLRK ²⁹⁸
H3 MUT e	²⁷⁹ TDQEAIQDLWQSLAQVSLRK ²⁹⁸

In order to evaluate the thermodynamic effects of each protein region on the conformations of others, CD and ITC assays on ternary complexes are under investigation. These experiments will help to understand the molecular basis of the folding and unfolding mechanism of the region directly involved in aberrant expression levels during disease and will assist the structure-based design of molecules that may rescue pathological NPM1 mutants by stabilizing the native-like state.

References

- [1] Scaloni, F., Federici, L., et al. Proc Natl Acad Sci USA. 2010, 107, 5447-52.
- [2] Falini, B., Bolli, N., et al. Leukemia. 2009, 23,1731-43.
- [3] Marasco, D., et al, submitted.

Structurally diverse cyclisation linkers impose different backbone conformations in bicyclic peptides

Shiyu Chen,¹ Julia Morales-Sanfrutos,¹ Alessandro Angelini,¹
Brian Cutting,² Christian Heinis*¹

¹ Institute of Chemical Sciences and Engineering, Ecole Polytechnique Fédérale de Lausanne, CH-1015 Lausanne, Switzerland; ² Pharmacenter, University of Basel, CH-4056 Basel, Switzerland

*E-mail: christian.heinis@epfl.ch

Introduction

Cyclic peptides are conformationally more constrained than linear analogues, a property that offers a number of advantages, such as better binding affinities, higher target specificity and improved stability in biological fluids. Recently, cysteine-rich peptides displayed on phage were cyclized with the thiol-reactive linker tris(bromomethyl)benzene (A, TBMB) [1] and potent bicyclic peptide binders could be isolated [2].

In this work [3], we developed two new linkers, (B) 1,3,5-triacryloyl-1,3,5-triazinane (TATA) and (C) N,N',N''-(benzene-1,3,5-triyl)tris(2-bromoacetamide) (TBAB) to generate bicyclic peptides. The structurally diverse linkers imposed entirely different backbone conformations in bicyclic peptides. The linkers might be applied to generate combinatorial libraries of structurally diverse macrocycles.

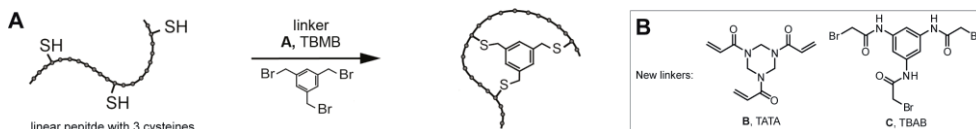


Figure 1. (A) Generate bicyclic peptides. (B) New linkers developed in this work.

Results and Discussion

Reactivity of linkers with a linear peptide: Peptide cyclisation with different linkers was tested with the peptide PK15 (H-ACSDRFRNCPAD EALCG-NH₂; previously isolated in phage selections against the human serine protease plasma kallikrein when cyclized with TBMB) [2]. PK15 at a concentration of 2 μM can be quantitatively modified with 2.5 μM TBMB, 10 μM TATA and 2.5 μM TBAB (Figure 2).

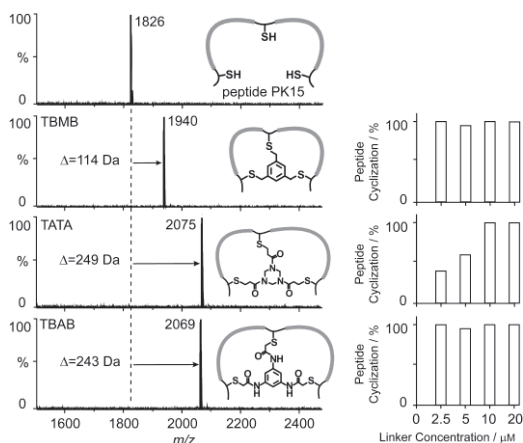


Figure 2. Modify peptide with different linkers

Inhibitory activity of bicyclic peptides with different linkers: Peptide PK15 cyclized with TATA or TBAB inhibited human plasma kallikrein about 1000-fold weaker (IC_{50} s of 3.61 μ M and 4.92 μ M, respectively) compared to the TBMB conjugate which had a strong inhibitory activity (IC_{50} of 2.82 nM as described previously [2]). This dramatic loss in potency indicated that the new linkers provide an entirely different environment to the peptide.

Conformations of bicyclic peptides by solution NMR: The NOESY spectra of peptide PK15 cyclized with TBMB (Figure 3 A), TATA (B) and TBAB (C) are assigned and the regions of the amide and α -protons resonances are shown with different chemical shifts. The inter-residual resonances of the peptides also vary with the linkers. The NOESY spectrum of the peptide PK15 - TBMB contained only 6 medium range and no long range interactions as reported previously [2]. In contrast, peptide PK15 - TBAB contained 39 medium range and 6 long range interactions. The inter-amino acids NOE constraints in the two bicyclic peptides suggest substantially different peptide backbone conformations.

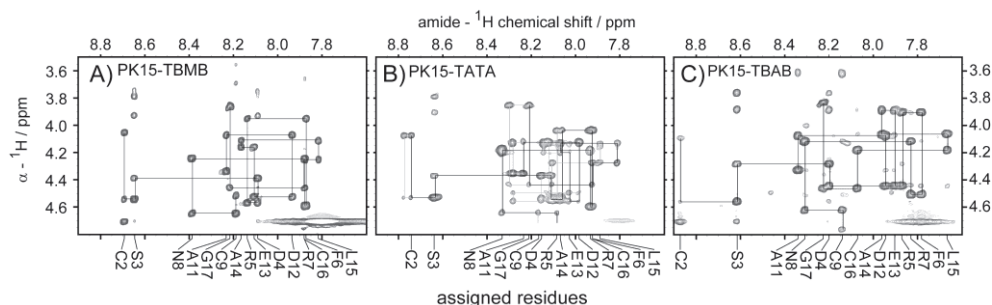


Figure 3. Peptide PK15 modified with different linkers shown varied amide proton chemical shifts.

In summary, we have developed structurally diverse cyclisation reagents that are able to impose unique peptide backbone conformations in bicyclic peptides. The strong structural impact of the relatively small linkers on the peptide was not necessarily expected considering the flexible cysteine side chains that tether the peptides to the linkers. The dominant effect of the linker may be explained by its central location forming the branching point of the bicyclic peptide. The variations in the IC_{50} s obtained for same peptide with different linkers, suggests that combining different linkers with random libraries could be a promising strategy to generate repertoires of highly structurally diverse macrocycles.

Acknowledgments

We thank Sir Greg Winter for fruitful discussions, helpful advice and comments on the manuscript. The financial contribution from the Swiss National Science Foundation (SNSF Professorship PP00P3_123524/1 to C.H.) is gratefully acknowledged. J.M.S. is supported by a fellowship of the Ministerio de Educacion del Gobierno de Espana.

References

- [1] Timmerman P.; Beld J.; Puijk W.C.; Muelen R.H. *ChemBiochem* **2005**, *6*, 821.
- [2] Heinis C.; Rutherford T.; Freund S.; Winter G. *Nat. Chem. Biol.* **2009**, *5*, 502.
- [3] Chen S.; Morales-Sanfrutos J.; Angelini A.; Cutting B.; Heinis C. *ChemBiochem*. **2012**, *13*, 1032.

Study of peptide structural modifications induced by controlled gamma ray irradiation experiments

Renata F. F. Vieira¹, Daniela T. Nardi¹, Nanci Nascimento²,
Jose C. Rosa³, Clovis R. Nakaie¹

¹Department of Biophysics, Federal University of Sao Paulo, Sao Paulo, 04044020, Brazil;

²Nuclear and Energy Research Institute (IPEN), University of Sao Paulo, Sao Paulo, 05508000, Brazil;

³Protein Chemistry Center and Department of Molecular and Cell Biology, School of Medicine of Ribeirao Preto, University of Sao Paulo, Ribeirao Preto, 14049900, Brazil

E-mail:cnakaie@unifesp.br

Introduction

The oxidation by free radicals of several macromolecules, mainly affecting protein structures is known to govern several processes within cells, and is implicated in some illness such as cancer, diabetes, Alzheimer's and Parkinson's diseases, etc [1,2]. In some cases, strong electromagnetic radiation causes irreversible changes in protein conformation [3]. We have initiated [4, 5] an investigation related to the effect of radical species upon structures of some peptide segments. In the proposed experimental protocol, aqueous peptide solution was submitted to gamma ray irradiation in controlled 1-15 kGy doses. The generation of peptide analogues, possibly induced by reactive oxygen species (ROS) were examined by electrospray triple-quadrupole tandem mass spectrometry (collision induced dissociation approach – CID-MS/MS) and amino acid analysis of crude and/or purified by-products.

Results and Discussion

Noteworthy, the gamma irradiation process induced, regardless of the peptide sequence, a non-linear and progressive degradation of all peptides assayed. Figure 1 shows for example, the time-course degradation process of *Ang-(1-7)*(DRVYIHP) and *BKRB₂'s* (305-325) fragment ((LVYVIVGKFRFRKKSREVYQAI), respectively. Furthermore, these peptides could be classified in some different classes according to their half-life dose. For instance, the vasoactive angiotensin II (AngII), Ang-(1-7), bradykinin (BK) and some related peptides were more stable than the melanocyte-stimulating hormone α -MSH, Substance P or the BK's B2 receptor above mentioned. Usually, the most prominent derivatives generated from this experimental protocol revealed that they are likely induced by oxidation process, yielding a variation of +16 Da in their molecular weight. The main source of peptide modifications seems to lie either on the Phe (hydroxyl group insertion at *o*-, *m*- or *p*- positions of its aromatic side chain) or Met oxydation. In the former case, only Phe⁸ and not Phe⁵ is oxidized in the BK structure [5] whereas Substance P generates an analogue bearing Met-sulfoxide without modifying its Phe^{7,8} residues.

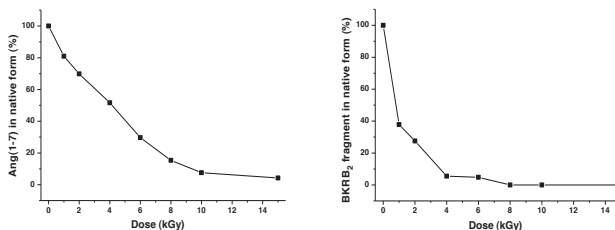


Figure 1: Remaining Ang-(1-7) (a) and BKRFB₂ fragment (b) quantities (in percentage) as a function of the gamma irradiation dose.

Using the CID-MS/MS technique, it was possible to monitor sequentially the entire fragmentation pattern of this latter peptide. According to these data, the gamma radiation affected only the Met residue in its structure, thus pointing to a different oxidation potential for this hydrophobic amino acid when compared with Phe residue. The ion fragmentation data of Substance P is compatible with oxidized Met, indicated by the presence of the y1 ion with respect to m/z 165.065 and is also compatible with the presence of both intact Phe residues by b7, b8 and b9 ions with m/z 882.4, 1029.5 and 1086.5 (RPKPQQFFG), respectively (Figure 2).

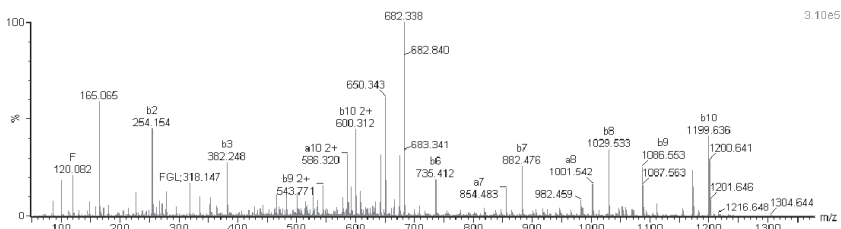


Figure 2: CID-MS/MS ion fragmentation data compatible with oxidized Met in Substance P sequence. $[M + 2H^+] = 682.3$

Of relevance, one can stress that even in small peptide structures, this experimental protocol applying strong electromagnetic radiation seems to induce a clear residue- and sequence-dependent effect in the peptide backbone. Thus, collectively, these findings clearly stress the complexity of factors involved in peptide structural modifications induced by gamma ray-type strong electromagnetic irradiation experiment. An additional target of this approach lies indeed, in the production of unusual peptides for further structure-function investigations.

Acknowledgments

We thank for CNPq and FAPESP for financial support.

References

- [1] Opara, E. C. *J. Investig. Med.* **2004**, *52*, 19.
- [2] Simic, M. G. *Cancer Research (Suppl.)*. **1994**, *54*, 1918s.
- [3] Lee, Y. and Song, K. B. *J. Biochem. Mol. Biol.* **2002**, *35*, 590.
- [4] Nardi, D. T.; Casare, M. S.; Teixeira, L. G. D.; Nascimento, N.; Nakaie, C. R. *Int. J. Radiat. Biol.* **2008**, *84*, 937.
- [5] Nardi, D. T.; Rosa, J. C.; Jubilot, G. N.; Miranda, A.; Nascimento, N.; Nakaie, C. R.. *Int. J. Pept. Res. Ther.* **2010**, *16*, 71.

Temperature dictates the conformational preference of “RGD” in peptide sequence “RIPRGDMP” from kistrin and selects the bio-active conformation

Sanjay K. Upadhyay¹, Diana Writer¹, Y. U. Sasidhar^{2*}

¹*Department of Biosciences and Bioengineering IIT Bombay, Powai, Mumbai - 400076;* ²*Department of Chemistry IIT Bombay, Powai, Mumbai -400076, India*

*E-mail: *sasidhar@chem.iitb.ac.in; sanjay23@iitb.ac.in*

Introduction

α IIb β 3 is integrin receptor present on the surface of blood platelets including megakaryocytes and play a crucial role in platelets physiology. It specifically binds with the fibrinogen and enable blood clotting during vascular injury. Therefore, the drugs that inhibit fibrinogen binding with α IIb β 3 receptors are effective for treating coronary thrombosis. Literature suggests that constrained RGD peptides have increased activities in comparison to their linear counterpart for receptor α IIb β 3. Furthermore, the antagonist property of RGD ligands also depends on C α -C α and C β -C β distances between R and D residues [1]. To determine the bioactive conformation required to bind with receptor α IIb β 3, the peptide sequence “RIPRGDMP” from Kistrin was inserted into CDR 1 loop region of REI protein (REI-RGD34) to restrict the conformational sampling of peptide. The activity of REI-RGD34 was studied; and it was found that as the temperature increased REI-RGD34 showed a higher affinity towards receptor [2]. The proposed mechanism for the increased activity of REI-RGD34 at higher temperature could be explained in two ways. One, the modified complex forces the restricted peptide to adopt a bioactive conformation or second, it unfolds the peptide in a way that opens its binding surface with high affinity for receptor. In this communication we model the conformational preferences of “RGD” sequence in octapeptide “RIPRGDMP” at two different temperatures at 25^oC and 42^oC using multiple MD simulations and discuss the results.

Results and Discussion

MD simulations are performed using GROMACS package 4.0.4 and all atom OPLS-AA/L force field. The peptide sequence ⁴⁶RIPRGDMP⁵³ was taken from kistrin (1N4Y). Starting structures for the simulated peptides were set to be extended with backbone dihedral angles for all residues as 180^o, except for proline where Φ was kept as -60^o. Productive simulation was done under NPT conditions for 300 ns at each temperature totaling to 600 ns.

Temporal variation of radius of gyration (Rg, Rgh), RMSD and end to end distance with respect to time are calculated for the peptide at both the temperatures (25^oC and 42^oC) and shown in Fig. 1(a,b,c,d). A transition from extended conformation (Rg \sim 0.8 \pm 0.07 nm) to a more compact conformation (Rg \sim 0.55 \pm 0.05 nm) with respect to time around \sim 210 ns was observed at 42^oC. The DSSP plot is prepared for the simulated systems at both temperatures with respect to time and shown in Fig. 1.

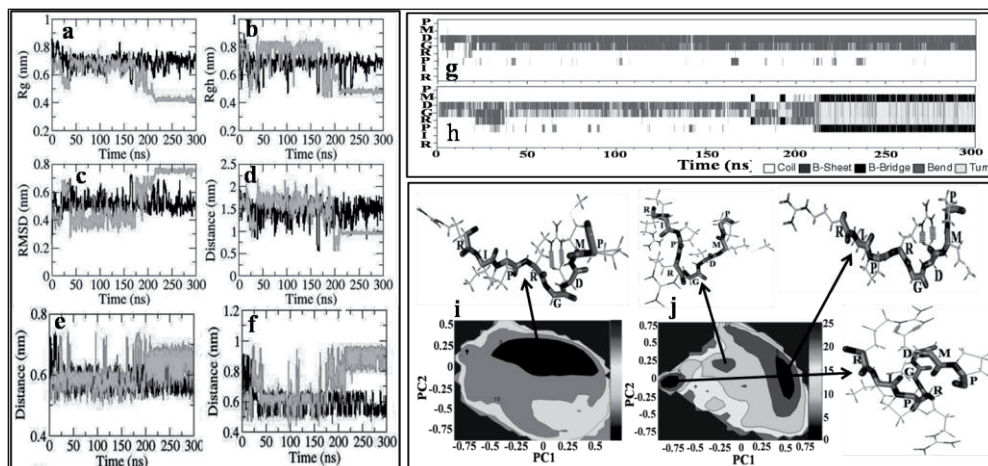


Figure 1. a, b, c, d, e and f show the variation of Rg, Rgh, RMSD, end-to-end distances, R4C α -D6C α and R4C β -D4C β vs. time respectively (Dark gray: 25°C and light gray: 42°C). DSSP plots vs. time at 25°C and 42°C shown in g and h respectively. Free energy landscape along PC1 and PC2 at 25°C and 42°C is shown in i and j respectively.

The receptor recognition sequence ‘RGD’ is present at 4th, 5th and 6th position in the peptide “RIPRGDMP”. At 25°C sampling of residues ‘RGD’ dominated by *bends* and *coil* conformations (Fig.1g). However a transition from *bend* to *turn* conformation was observed around ~ 210 ns for sequence ‘RGD’ at 42°C; followed by the simultaneous transition from *coil* to β -bridges for flanking residue PRO-3 and MET-7 from N and C terminal respectively (Fig.1h). The free energy landscape along eigenvector 1 and 2 also shows two well defined minima at 42°C with *bend* and *turn* conformations (Fig. 1j). The distance between C α atoms of ARG-4 and ASP-6 as a function of time changes from an average value of $\sim 0.58 \pm 0.06$ nm to $\sim 0.7 \pm 0.03$ with concomitant change from *bend* to *turn* conformation at 42°C (Fig. 1e). Subsequently the distance between C β of ARG-4 and ASP-6 also vary from an average value of $\sim 0.6 \pm 0.04$ nm to $\sim 0.98 \pm 0.03$ nm (Fig.1f). A comparison of pharmacophoric distances and angles of recognition sequence ‘RGD’ in *turn* conformation with natural potent inhibitor kistrin suggests that sampled *turn* conformation at 42°C temperature could be the bio-active conformation. Thus, the temperature dependent activity of the octapeptide “RIPRGDMP” when inserted in to the loop region of REI can be explained by the presence of the *turn* conformation at higher temperature.

Acknowledgments

We thank ICMR for SRF; DST and IIT Bombay for travel grants to attend EPS meeting.

References

- [1] Peishoff, C.E.; Ali, FE.; Bean, JW.; Calvo, R. et al. *J Med Chem.* **1992**, 35(21), 3962.
- [2] Zhao, B.; Helms, LR.; Desjarlais, RL.; Abdel-Meguid, SS.; Wetzel, R. *Nat Struct Biol.* 1995, 2(12), 1131.

The crystal structure of the 14-residue peptaibol trichovirin at atomic resolution

Renate Gessmann¹, Danny Axford², Robin L. Owen², Hans Brückner^{3,4},
Kyriacos Petratos¹

¹Institute of Molecular Biology and Biotechnology, Foundation of Research and
Technology Hellas (IMBB-FORTH), N. Plastira 100, Heraklion, Crete 70013, Greece;

²Diamond Light Source Ltd, Harwell Science and Innovation Campus, Didcot OX11 0DE,
England; ³Research Center for BioSystems, Land Use and Nutrition (IFZ), Department of
Food Sciences, Justus-Liebig University Giessen, 35392 Giessen, Germany; ⁴Visiting
Professor at Department of Food Science and Nutrition, College of Food and Agricultural
Sciences, King Saud University, Riyadh 11450, Kingdom of Saudi Arabia

E-mail: petratos@imbb.forth.gr

Introduction

Natural trichovirin (TV) is a mixture of microheterogeneous polypeptide antibiotics isolated from the filamentous fungus *Trichoderma viride* NRRL 5343. TV belongs to the group of peptaibiotics that are characterized by the presence of high proportions of the characteristic, non-proteinogenic and helix-inducing amino acid α -aminoisobutyric acid (Aib) [1-4]. The subgroup named peptaibols contains a C-terminal bound β -amino alcohol. This group of membrane-active peptides is of interest because of its broad range of biocidal activities and its unique feature to form voltage-gated transmembrane channels in lipid bilayer membranes. Conventional segment condensation provided the uniform 14-residue component named trichovirin I-4A of the sequence: Ac-Aib¹-L-Asn-L-Leu-Aib-L-Pro-L-Ala-L-Val-Aib-L-Pro-Aib-L-Leu-Aib-L-Pro-L-Leuol¹⁴ (Ac, acetyl; Leuol, leucinol). This synthetic peptide was used for the present X-ray analysis. The crystal structures of the protected C-terminal 8- and 12-residue segments used for the synthesis of TV have been reported previously [3].

Results and Discussion

Crystals from synthetic TV were obtained from a methanol-acetonitrile-water mixture as colorless, hair-like objects with a smallest dimension of about 30 μm . Crystals were mounted by hand onto MicromeshTM sample supports. Diffraction data were collected at 100 K at the Diamond Light Source using the microfocus beamline I24. The X-ray beam (wavelength = 0.7469 \AA) was focused to a size of 10 μm full-width-half-maximum using two pairs of Kirkpatrick-Baez mirrors. A dataset of 1500 images, covering 375 degree rotation, was collected to 0.9 \AA resolution from a single TV crystal. Two independent molecules (mol-A and mol-B) were located in the crystal's asymmetric unit. Both chains adopt a curved 3_{10} -helical conformation comprising 4 complete turns stabilized by intramolecular hydrogen bonds. A stereo view of the superposition of mol-B (dark grey) on mol-A (light grey) is shown in Figure 1 together with the 3_{10} -helical wheel projection of TV in comparison to a putative, modeled α -helix of TV. From the data it is hypothesized that during the embedment of TV in a lipid-bilayer membrane a structural change should occur

from 3_{10} - to α -helix [5]. Recently, the mainly 3_{10} -helical crystal structure of the trichovirin-related natural 15-residue peptaibol samarosporin I (= emerimicin IV) has also been determined at atomic resolution [6]. This peptide, besides Aib, contains *trans*-4-hydroxy-L-Pro as well as the non-proteinogenic D-isovaline (Iva).

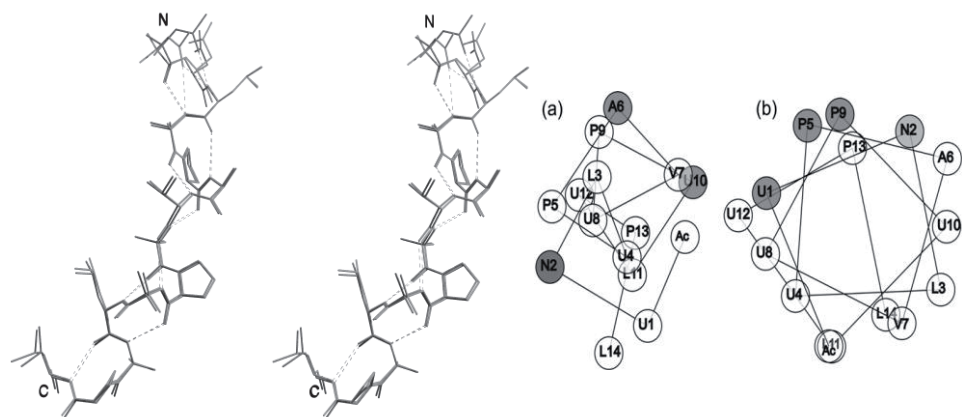


Fig. 1. Left: stereo view of the superposition of mol-B (dark grey) on mol-A (light grey) of trichovirin. Hydrogen bonds are shown as dashed lines. N and C denote the amino- and reduced (amino alcohol) carboxyl-termini of the molecules. Right: real helical wheel projections of the 3_{10} -helical crystal structure of trichovirin (a) and of a modeled α -helix (b). Gray shaded residues indicate carbonyl and/or polar side chain groups that are not involved in intramolecular hydrogen bonding. The N-terminal NH groups and the C-terminal CH_2OH -groups, which potentially form intermolecular hydrogen bonds, are not shaded. (Produced with WHEEL perl script kindly provided by L. S. Vermeer, Department of Biochemistry, University of Oxford, England).

References

- [1] Toniolo, C.; Brückner, H. (Eds). Topical Issue Peptaibiotics. *Chem. Biodivers.* **2007**, *4*, 1021-1412.
- [2] Toniolo, C.; Benedetti, E. *Trends Biochem. Sci.* **1991**, *16*, 350.
- [3] Gessmann, R.; Benos P.; Brückner, H.; Kokkinidis, M. *J. Peptide Sci.* **1999**, *5*, 83.
- [4] Gessmann, R.; Brückner, H.; Petratos, K. *J. Peptide Sci.* **2003**, *9*, 753.
- [5] Gessmann, R.; Axford, D.; Owen, R.L.; Brückner, H.; Petratos, K. *Acta Crystallogr.* **2012**, D68, 109.
- [6] Gessmann, R.; Axford, D.; Evans, G.; Brückner, H.; Petratos, K. *J. Peptide Sci.* **2012**, in press.

The fully-extended peptide conformation as a molecular bridge: A fluorescence investigation

Fernando Formaggio¹, Marco Crisma¹, Gema Ballano¹, Cristina Peggion¹, Mariano Venanzi², Claudio Toniolo¹

¹ICB, Padova Unit, CNR, Department of Chemistry, University of Padova, 35131 Padova, Italy ; ²Department of Chemical Sciences and Technologies, University of Rome "Tor Vergata", 00133 Rome, Italy

E-mail: wright@chimie.uvsq.fr; claudio.toniolo@unipd.it

Introduction

The fully-extended peptide conformation (2.0_5 -helix) (Figure 1) is the longest possible for a single α -amino acid as it is characterized by an axial translation per residue of about 3.85 Å. Therefore, it is extremely attractive for its application as a molecular bridge [1,2]. However, it is known that the stability of this type of helical structure (relative to the competing, much shorter 3_{10} -helix) appears to be dramatically governed by the choice of the C-terminal functionality (esters, not amides, seem to be appropriate) [3].

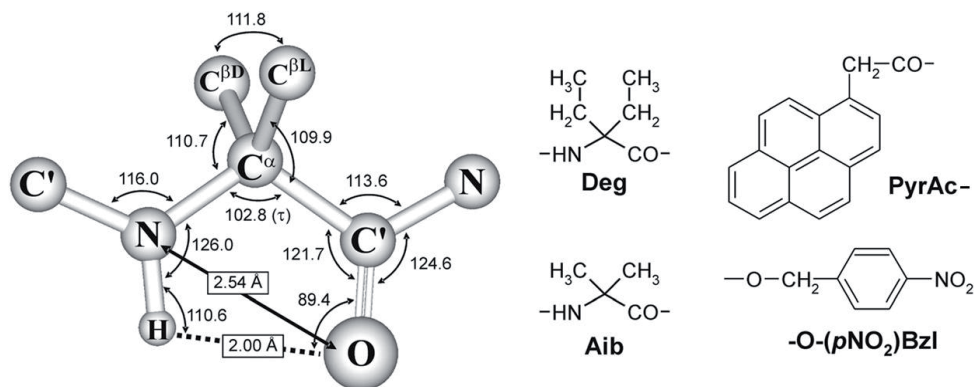


Fig.1. Average geometrical parameters for the fully-extended, intramolecularly H-bonded, C_5 conformation from a statistical analysis of the published X-ray diffraction structures [1,2]. In addition, the chemical formulas of Deg, Aib, PyrAc, and $O-(pNO_2)Bzl$ are shown.

Results and Discussion

In this work, we examined the series PyrAc-(Deg)_n-O-(pNO_2)Bzl [where PyrAc is the fluorophore 1-pyrenylacetyl, Deg is $C^{\alpha,\alpha}$ -diethylglycine, $n=1-5$, and $O-(pNO_2)Bzl$ is *para*-nitrobenzoxy] (Figure 1), with the Deg homo-peptides as fully-extended bridges, in a static fluorescence study. To perform a very stringent comparison with our FT-IR absorption and NMR results, the solvent used was $CHCl_3$. The quenching efficiencies for the shortest members of the series, the (Deg)₁₋₃ peptides, steadily decrease from 0.97 ($n=1$) to 0.89 ($n=2$), and 0.64 ($n=3$) (Figure 2). This finding is compatible with the conclusion that these three peptides are all essentially fully-extended in $CHCl_3$ solution. However, the quenching

efficiencies for the longest Deg homo-peptides, 0.68 for $n=4$ and 0.65 for $n=5$, are not further reduced. The inevitable conclusion is that the tetra- and pentapeptides populate at least two different conformations (most probably, the 2.0_5 -helix and the 3_{10} -helix) in which the probe dyads are located at different distances. Notably, these results fit well with those extracted from our FT-IR absorption and NMR studies in the same solvent of low polarity. We conclude that a combination of terminally aromatic groups, as in the Deg homo-peptide series investigated in this work, is not eligible for the fabrication of a robust fully-extended conformation despite the presence of an ester C-terminal functionality.

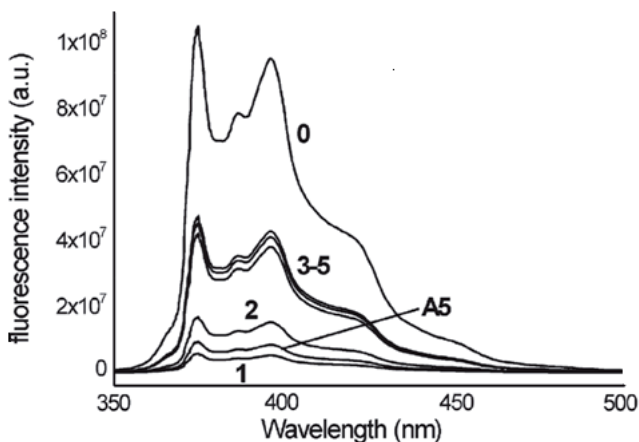


Fig.2. Fluorescence spectra of the blank PyrAc–OH (**0**), the Deg derivative and homo-peptides PyrAc-(Deg) $_n$ -O-(pNO $_2$)Bzl ($n = 1-5$) (**1-5**), and the 3_{10} -helical Aib homo-peptide PyrAc-(Aib) $_5$ -O-(pNO $_2$)Bzl (**A5**) in CHCl $_3$ solution (concentration: 10^{-7} M).

References

- [1] Toniolo, C.; Crisma, M.; Formaggio, F.; Peggion, C.; Broxterman, Q. B.; Kaptein, B. *Biopolymers (Pept. Sci.)* **2004**, *76*, 162.
- [2] Crisma, M.; Formaggio, F.; Moretto, A.; Toniolo, C. *Biopolymers (Pept. Sci.)* **2006**, *84*, 3.
- [3] Formaggio, F.; Crisma, M.; Peggion, C.; Moretto, A.; Venanzi, M.; Toniolo, C. *Eur. J. Org. Chem.* **2012**, 167.
- [4] Formaggio, F.; Crisma, M.; Ballano, G.; Peggion, C.; Venanzi, M.; Toniolo, C. *Org. Biomol. Chem.* **2012**, *10*, 2413.

Vasopressin and vasotocin - NMR studies in a membrane-mimicking environment

Emilia A. Lubecka, Emilia Sikorska, Franciszek Kasprzykowski,
Dariusz Sobolewski, Jerzy Ciarkowski

Faculty of Chemistry, University of Gdansk, 80-952 Gdansk, Poland

E-mail:emilial@chem.univ.gda.pl

Introduction

In this paper, the conformations of arginine-vasopressin (CYFQNCPRG-NH₂, **AVP**) and arginine-vasotocin ([Ile³]AVP, **AVT**) in mixed dodecylphosphocholine (DPC) and sodium dodecylsulfate (SDS) micelles using NMR spectroscopy and molecular modeling methods have been studied. **AVP** controls resorption of water by the distal tubules of the kidney and regulates the osmotic pressure of blood in mammals, while **AVT** exhibits both oxytocin and vasopressin activities [1]. It is believed that micelles may partially restrict conformational freedom of the peptides and probably induce a conformation, which is supposed to be bound to the receptor. DPC micelles are considered good models of eukaryotic cell membrane while the addition of some SDS would introduce a slight negative charge typical of cell membranes of eukaryotic organisms [2].

Results and Discussion

The three-dimensional structures of both peptides were determined in AMBER 11.0 [3] force field using the time-averaged molecular dynamics. The calculations were performed in an *explicit* DPC-SDS micelle during 8 ns long MD. The conformations obtained during the last 2 ns of simulation were considered in further analyses. As a result, the sets of 500 conformations for both peptides were obtained.

AVP adopts very stable β -turns at positions 3,4 and 4,5 (IV and II', respectively) during the entire MD simulation. A low temperature coefficient of an amide proton of Cys⁶ of **AVP** (-2.7 ppb/K) suggests that the 4,5 β -turn is stabilized by the HN⁶-CO³ hydrogen bond. MD suggests also some tendency to adopt unstable β -turn type IV at position 6,7. This β -turn seems to be typical of ~26% conformations from the final ensemble. In turn, **AVT** exhibits a strong tendency to adopt 4,5 β IV-turn. The β -turn at this position is typical of vasopressin-like peptides. Moreover, **AVT** reveals same tendency to adopt β -turn at position 2,3 (~22% conformations from the final ensemble), which, in turn, is characteristic of oxytocin-like peptides. The C-terminal part of **AVT** exhibits large conformational freedom and does not create any stable β -turns. The structures of both peptides are displayed in the Figure 1.

The analysis of interactions of both peptides with DPC-SDS micelle shows that **AVP** is more deeply immersed into the micelle core than **AVT** (Fig. 2). The consequence of this may be a lower flexibility of **AVP** than **AVT**.

In both peptides, the side chain of residue at position 3 is immersed into the micelle core. Moreover, the low temperature coefficient of the amide protons of Phe/Ile³ may indicate

that they are shielded from solvent. In turn, polar residues, Gln⁴ and Asn⁵ are exposed to the aqueous phase (Fig. 2). However, some difference in the slope of both peptides to the micelle surface is observed. Thus, AVT is located more parallel to the surface of the micelles than AVP.

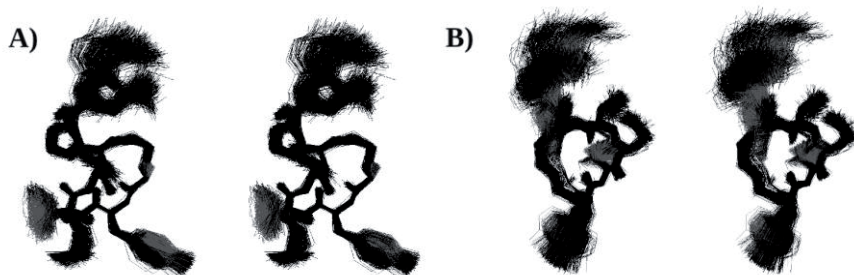


Figure 1. Stereoviews of the of the final 500 conformations of (A) AVP and (B) AVT. RMSD=0.164 and 0.304 Å for backbone atoms of cyclic part, respectively.

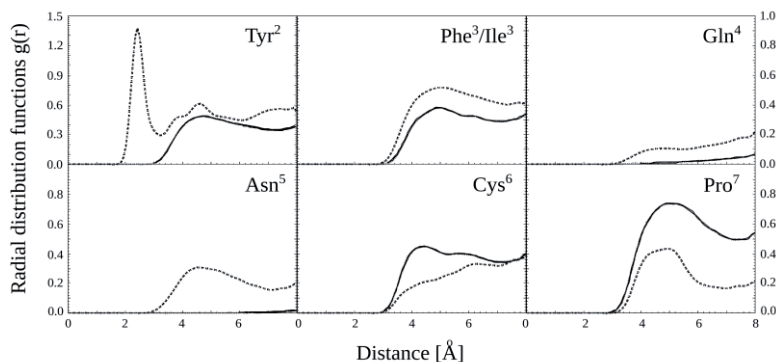


Figure 2. Radial distribution functions $g(r)$ between the hydrophobic micelle core and the side chain (heavy atoms) of residues 2-7 of AVP (dotted line) and AVT (solid line). The r parameter defines the distance in Å. Note different scale for residue 2.

Our results suggest that mixed dodecylphosphocholine (DPC) and sodium dodecylsulfate (SDS) micelles make a very good environment to analyze structure of vasopressin- and oxytocin-like peptides.

Acknowledgments

This work was supported by the Polish National Science Centre Grant No. 2011/01/N/ST4/05175. The calculations were carried out in the Academic Computer Centre (TASK) in Gdansk, Poland. Partial funding was also provided by the University of Gdansk, DS. 8453-4-0169-11 and DS. 8370-4-0136-12. E. Lubecka is additionally the recipient of the Travel Grant from the Organising and Scientific Committees of the 32nd EPS 2012.

References

- [1] Acher, R.; Chauvet, J.; Chauvet, M. *Adv. Exp. Med. Biol.* **1995**, 395, 615.
- [2] Wymore, T.; Gao, X.F.; Wong, T.C. *J. Mol. Struct.* **1999**, 485, 195.
- [3] Case, D.; Darden, T.; et al. **2010**, *AMBER 11*, University of California, San Francisco.

β -Phenylproline: Effect of the β -phenyl substituent on the β -turn propensity and pyrrolidine puckering

Paola Fatás, Ana I. Jiménez, M. Isabel Calaza, Carlos Cativiela

Department of Organic Chemistry, ISQCH, CSIC–University of Zaragoza, 50009
Zaragoza, Spain

anisjim@unizar.es

Introduction

Proline exhibits a high propensity to induce β -turns, where it occupies the $i+1$ corner position [1]. Incorporation of substituents into the pyrrolidine ring generates proline analogues provided with new side-chain functionality. Such proline analogues are expected to retain the conformational properties of the parent amino acid, yet the new substituent added could interfere with the capacity to induce β -turns. We synthesized the *cis* and *trans* stereoisomers of β -phenylproline [2], *L-cis*(β Ph)Pro and *L-trans*(β Ph)Pro, that is, the proline analogues that bear a phenyl substituent attached to the β pyrrolidine carbon either *cis* or *trans* to the carbonyl moiety. In this work, we have compared the conformational properties of *L-cis*(β Ph)Pro and *L-trans*(β Ph)Pro to that of the parent amino acid (*L-Pro*) when occupying the $i+1$ position of dipeptide sequences [3].

Results and Discussion

Terminally blocked dipeptides containing *L-cis*(β Ph)Pro or *L-trans*(β Ph)Pro at the $i+1$ position and *L*- or *D*-Phe at $i+2$ (Figure 1) were synthesized by standard methods in solution [3]. Their conformational propensities have been studied in the solid state by X-ray diffraction analysis and in solution by NMR and IR spectroscopy [3], and compared to those of the reference peptides incorporating unmodified proline, *L-Pro* [4].

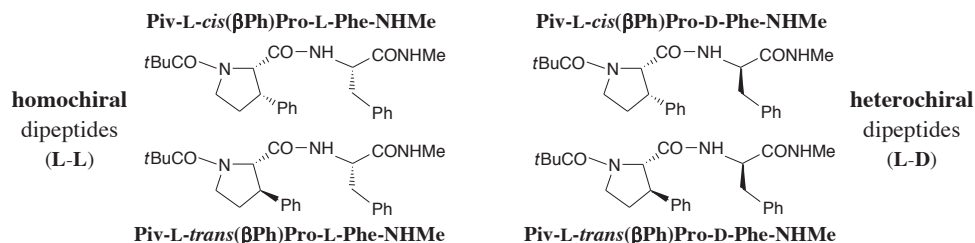


Figure 1. Structure of the four (β Ph)Pro-containing dipeptides studied.

In the solid state, the four peptides in Figure 1 adopt a β -turn of type II, as do the parent peptides containing *L-Pro* [4]. Intramolecular interactions between the phenyl ring of (β Ph)Pro and that of the contiguous *L*- or *D*-Phe residue are observed in all crystallized (β Ph)Pro-containing peptides, with parallel or perpendicular arrangements of the interacting aromatic moieties (see, for example, Figure 2 left).

In chlorinated solvents, the β -turn is maintained although significant differences are observed. Thus, for the homochiral dipeptides in Figure 1, a small percentage of molecules

adopt a conformation different from a β -turn, as indicated by the weak IR absorption bands of the Piv-CO and NHMe groups at frequencies typical of non-hydrogen-bonded sites. A similar behavior is observed for the reference L-Pro-L-Phe and L-Pro-D-Phe sequences [4]. In contrast, the two heterochiral peptides in Figure 1 adopt exclusively a β -turn.

The NMR and IR data indicate that the intramolecular Ar \cdots Ar interaction observed in the solid state for all (β Ph)Pro-containing peptides is maintained in solution only for the heterochiral peptides. This interaction seems to be responsible for the stabilization of the β -turn conformation observed for these peptides. The interaction involving the phenyl ring of D-Phe and that of L-*cis*(β Ph)Pro or L-*trans*(β Ph)Pro in solution occurs for a perpendicular arrangement of the aromatic moieties (Figure 2, right). This involves a modification of the orientation of the D-Phe side chain with respect to that observed in the solid state (χ^1 moves from near 60° in the crystal to about -60° in CDCl₃ solution, Figure 2).

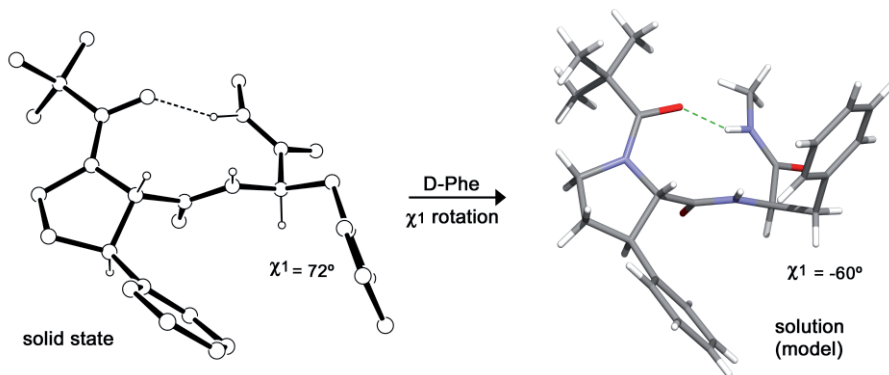


Figure 2. Conformation adopted by Piv-L-*trans*(β Ph)Pro-D-Phe-NHMe in the solid state (X-ray diffraction analysis, left) and CDCl₃ solution (model, right). The phenyl groups involved in an Ar \cdots Ar intramolecular interaction adopt a quasi-parallel or a perpendicular arrangement, respectively.

The pyrrolidine conformation is greatly affected by the presence of the β -phenyl group. The puckering modes that alleviate most the steric hindrance introduced by the bulky phenyl substituent are preferred. The L-*cis*(β Ph)Pro residue shows a marked propensity for the C γ -*endo*/C β -*exo* half-chair arrangement whereas the *trans* derivative exhibits a higher flexibility, with different pyrrolidine shapes being energetically accessible.

Acknowledgments

Ministerio de Ciencia e Innovación-FEDER (grant CTQ2010-17436; FPU fellowship to P.F.); Gobierno de Aragón-FSE (research group E40).

References

- [1] (a) MacArthur, M. W.; Thornton, J. M. *J. Mol. Biol.* **1991**, *218*, 397. (b) Rose, G. D.; Gierasch, L. M.; Smith, J. A. *Adv. Protein Chem.* **1985**, *37*, 1.
- [2] Fatás, P.; Gil, A. M.; Calaza, M. I.; Jiménez, A. I.; Cativiela, C. *Chirality*, in press (doi: 10.1002/chir.22101).
- [3] Fatás, P.; Jiménez, A. I.; Calaza, M. I.; Cativiela, C. *Org. Biomol. Chem.* **2012**, *10*, 640.
- [4] (a) Bardi, R.; Piazzesi, A. M.; Toniolo, C.; Sen, N.; Balam, H.; Balam, P. *Acta Cryst., Sect. C* **1988**, *44*, 1972. (b) Aubry, A.; Cung, M. T.; Marraud, M. *J. Am. Chem. Soc.* **1985**, *107*, 7640. (c) Jiménez, A. I.; Cativiela, C.; Aubry, A.; Marraud, M. *J. Am. Chem. Soc.* **1998**, *120*, 9452.

4-Methoxybenzyloxymethyl group as a thiol protecting group for cysteine to suppress base-catalyzed racemization in Fmoc chemistry

Hajime Hibino¹, Yuji Nishiuchi^{1,2}

¹SAITO Research Center, Peptide Institute, Inc., Ibaraki, Osaka 567-0085, Japan;

²Department of Chemistry, Graduate School of Science, Osaka University, Toyonaka, Osaka 560-0043, Japan

E-mail:hibino@peptide.co.jp

Introduction

In Fmoc chemistry the Trt and Acn groups are widely accepted as a protecting group for Cys. Upon incorporation of these Cys derivatives onto the growing peptide chain, however, considerable base-catalyzed racemization of Cys is known to always occur at the activating and coupling steps with phosphonium or uronium reagents such as PyBOP or HBTU, respectively. Therefore, the carbodiimide-mediated coupling method has been recommended to reduce the racemization rate to acceptable levels (<1.0%) although the DIC/HOBt method is considered to have no advantage in terms of coupling efficiency over that using PyBOP or HBTU [1]. In order to find an *S*-protected Cys derivative applicable for Fmoc chemistry that can efficiently suppress racemization of Cys on activating and coupling processes, we introduced the 4-methoxybenzyloxymethyl (MBom) group into the thiol function of Cys.

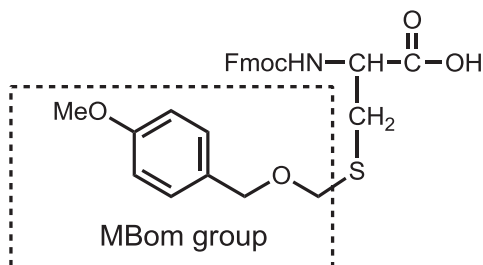


Fig. 1. Structure of Fmoc-Cys(MBom)

Results and Discussion

The suppressive effect of the MBom group on racemization during incorporation of Cys was evaluated by synthesizing a model peptide, Gly-Cys-Phe-NH₂, in the conventional and the microwave (MW)-assisted SPPS. Fmoc-Cys(MBom) was found to be accompanied by an acceptable level of racemization (0.4%) on the activating and coupling steps in the conventional SPPS compared with Fmoc-Cys(Trt) and Fmoc-Cys(Acn) (8.0% and 4.8%, respectively). Even in the case of the MW-assisted SPPS performed at 50°C/80°C, Fmoc-Cys(MBom) caused significant reduction in the level of racemization (0.8/1.3%) while

Fmoc-Cys(Trt) and Fmoc-Cys(Acm) led to a considerable extent (10.9/26.6% and 8.8/15.3%, respectively) (Table 1).

Table 1. Racemization during incorporation of the Cys derivatives^a

Temperature (°C)	Racemization (%) ^b		
	MBom	Trt	Acm
rt ^c	0.4	8.0	4.8
50 ^d	0.8	10.9	8.8
80 ^d	1.3	26.6	15.3

^aCoupling conditions: Fmoc-amino acid/HCTU/6-Cl-HOBt/DIEA (4/4/4/8 equiv, 1-min preactivation) in DMF. ^bGly-D-Cys-Phe-NH₂/Gly-L-Cys-Phe-NH₂ x 100. ^cConventional SPPS. ^dMW-assisted SPPS on a Discover SPS (CEM Corp., Matthews, NC).

As for racemization of the C-terminal Cys esterified to a Trt-type resin, the Bz-Ser(*t*Bu)-Cys(X)-NovaSynTGT resin was exposed to 20% piperidine/DMF for a given period of time to estimate the racemization rate arising during the repetitive Fmoc deprotection reactions. The products prepared using Cys(Trt) and Cys(Acm) contained significant amounts of isomers in that order. However, a much lower rate of racemization (6.4%) was detected even after a 6-h treatment with 20% piperidine/DMF when Cys(MBom) was used (Fig. 2).

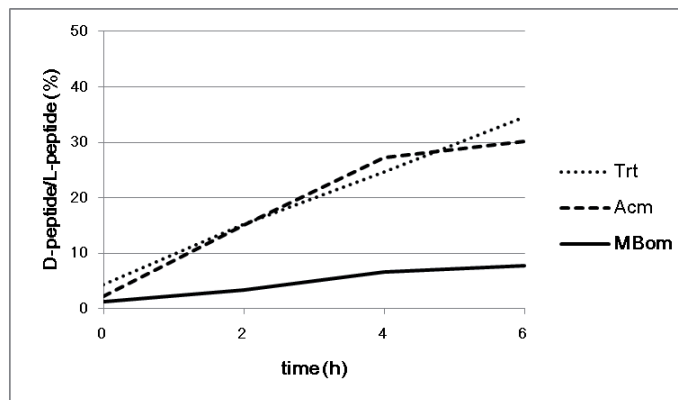


Fig. 2. Racemization of the C-terminal Cys linked to Trt resin

In summary, the MBom group on Cys was demonstrated to effectively prevent racemization of Cys during its incorporation mediated even by phosphonium or uronium reagents as well as that of the C-terminal Cys esterified to the solid support during repetitive base treatment. The use of Fmoc-Cys(MBom) can facilitate the avoidance of ambiguities in the quality of the synthesized Cys-rich peptides.

References

- [1] Han, Y.; Albercio, F.; Barany, G. *J. Org. Chem.* **1997**, 62, 4307-4312.

Synthesis of various peptides using DIC/HOBt and preactivation on the Overture™ robotic peptide library synthesizer

**James P. Cain, Christina A. Chantell, Michael A. Onaiyekan,
Mahendra Menakuru**

Protein Technologies, Inc. Tucson, Arizona, 85714

E-mail: info@ptipep.com

Introduction

Diisopropylcarbodiimide (DIC) is a classical peptide coupling reagent, most commonly used in combination with hydroxybenzotriazole (HOBt) to form an active ester of an amino acid which subsequently reacts with the free amine of a growing peptide chain. Most typically, the incoming protected amino acid is “preactivated” by mixing with HOBt and DIC for a pre-determined time before addition to the resin.

The 96-channel Overture™ is the first commercially available robotic peptide library synthesizer to offer preactivation. With the preactivation option, up to 48 channels may be used as preactivation chambers for the remaining 48 reactors. This new innovation allows the Overture™ to synthesize up to 48 peptides in parallel with preactivation.

To demonstrate this functionality, we have synthesized the following peptides:

- (1) **ACP (65-74):** VQAAIDYING-OH
- (2) **G-LHRH:** GHWSYGLRPG-NH₂
- (3) **Terlipressin (linear):** GGGCYFQNCPKG-NH₂
- (4) **CCK-7:** YMGWMDF-NH₂
- (5) **Angiogenin (108-123):** ENGLPVHLDQSIFRRP-OH
- (6) **Substance P:** RPKPQQFFGLM-NH₂
- (7) **Dynorphin A (1-11):** YGGFLRRIRPK-NH₂

Fig. 1. Peptide sequences synthesized using DIC and preactivation on the Overture™

Results and Discussion

A conservative protocol, using seven minute preactivation times and two one hour couplings, was employed. LC/MS analysis indicated that the correct peptide was made in each case (data not shown). Purity was determined using RP-HPLC. In all cases the desired peptide was produced with excellent purities (Figure 2).

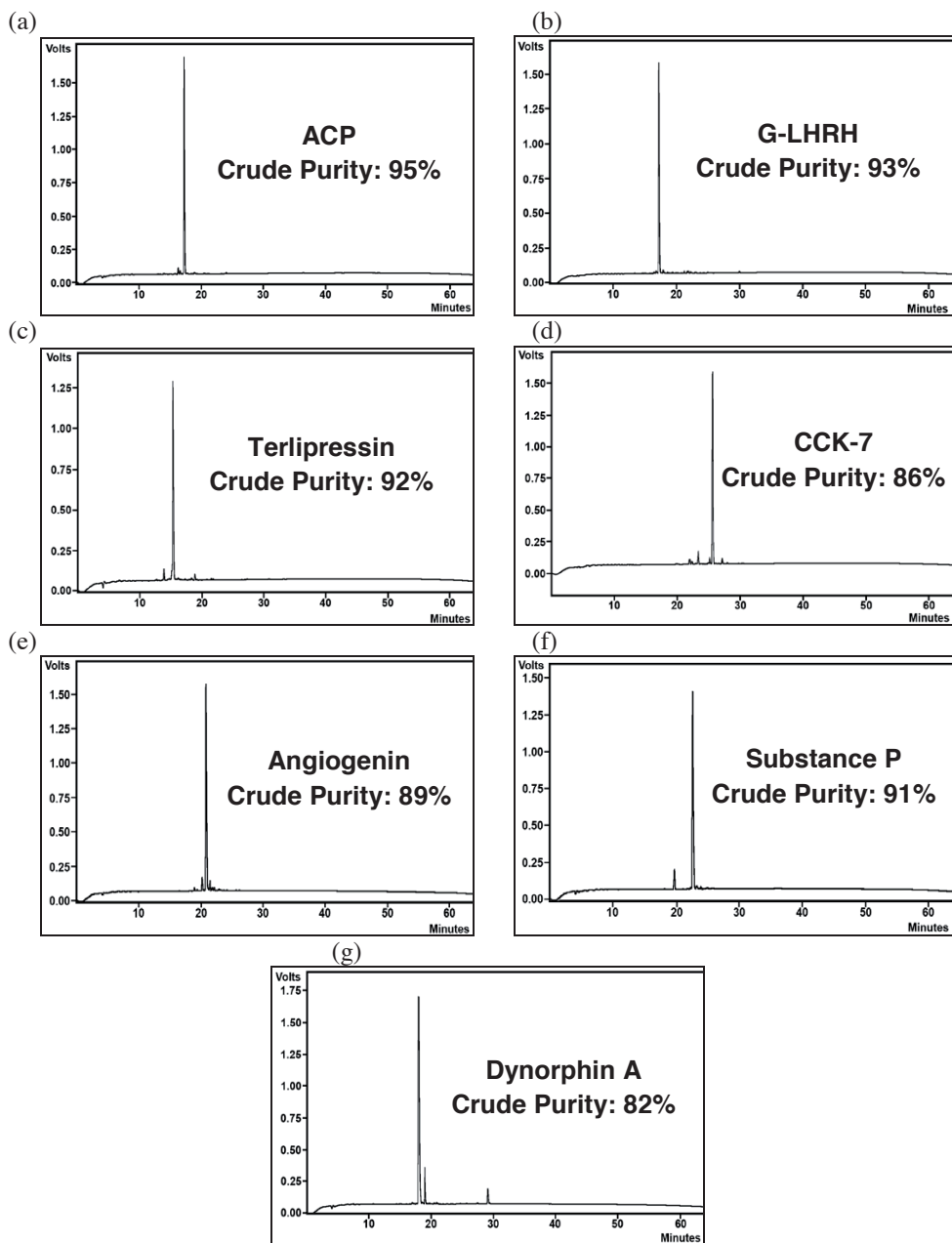


Fig. 2. HPLC trace of a) ACP; b) G-LHRH; c) Terlipressin; d) CCK-7; e) Angiogenin; f) Substance P; g) Dynorphin A

A convenient [2+2] cycloaddition-cycloreversion reaction for the synthesis of colorful peptides as new imaging chromophores

Nikki Kramer, Rob M. J. Liskamp, Dirk T. S. Rijkers*

*Medicinal Chemistry & Chemical Biology, Utrecht Institute for Pharmaceutical Sciences,
Department of Pharmaceutical Sciences, Faculty of Science, Utrecht University, P.O. Box
80.082, 3508 TB Utrecht, The Netherlands*

D.T.S.Rijkers@uu.nl

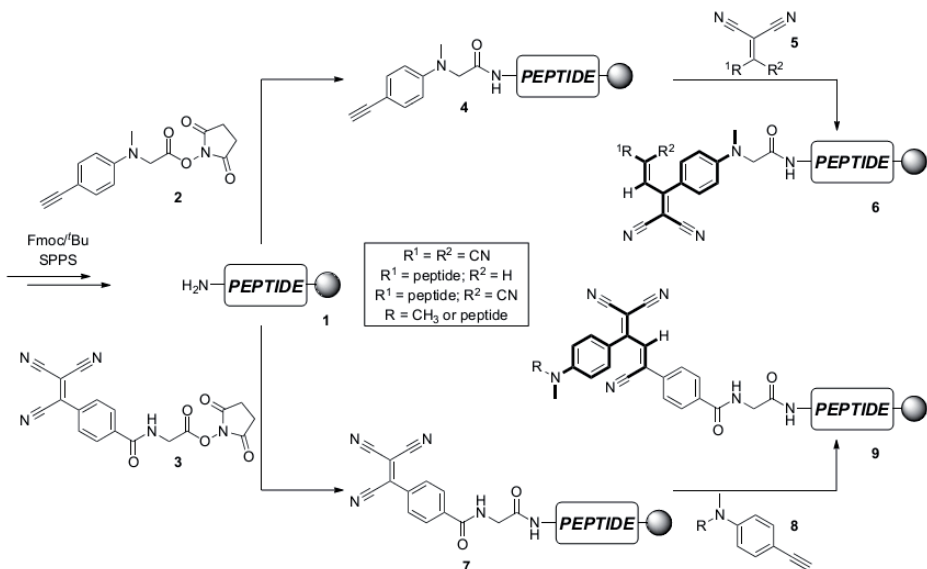
Introduction

Labeled peptides are important tools in chemical biology to obtain information on their biological function in, for example, cellular communication processes as well as to study the molecular basis of disease. The functionalization of bioactive peptides with biophysical reporter groups like strongly absorbing chromophores, is most often performed via post-synthetic chemoselective bioconjugation reactions, involving amino, thiol, or azide specific reactions. An alternative approach for the installation of intense chromophoric organic molecules is the coupling of non-chromophoric precursor molecules to obtain chromophoric properties in the final product. Recently, we have shown that the [2+2] cycloaddition-cycloreversion reaction between peptide-functionalized electron-rich alkynes and electron-deficient cyanovinyl derivatives results in the formation of a new class of π -conjugated peptidic donor-acceptor chromophores [1]. Herein we describe the synthesis of the versatile building blocks *N*- α -(4-ethynylphenyl)-*N*- α -(methyl)-glycine (**2**) and *N*- α -(4-(1,2,2-tricyanovinyl)benzoyl)-glycine (**3**) to functionalize peptides (**1**) with D- π -A chromophore precursor molecules (**6** and **9**) (Scheme 1).

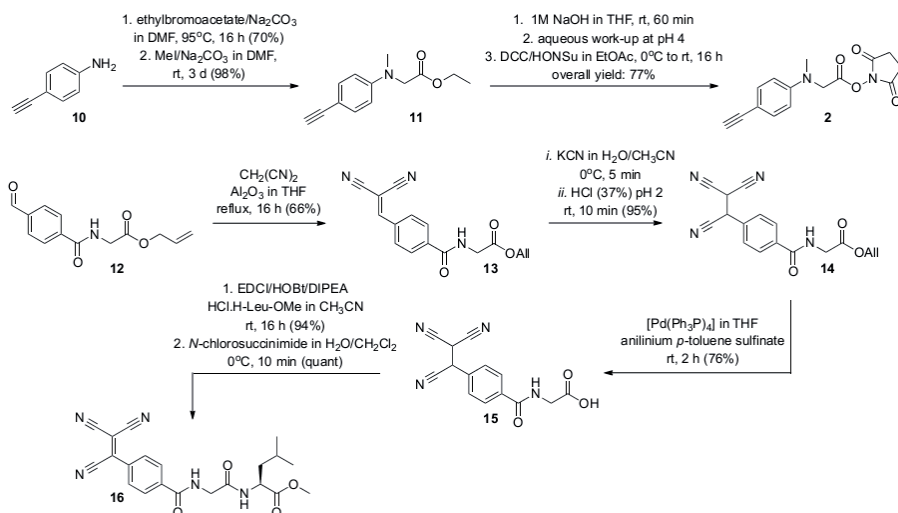
Results and Discussion

The concept of the [2+2] cycloaddition-cycloreversion reaction between a peptide-functionalized electron-rich alkyne **4** (with **5** to give **6**), or an electron-deficient cyanovinyl derivative **7** (with **8** to give **9**) is shown in Scheme 1. To obtain D- π -A chromophore functionalized peptides (e.g. **6**), alkyne **2** is required, and its synthesis is shown in Scheme 2 and previously described in reference 1a. On the other hand, the synthesis of peptide derivative **7** was more challenging due to the presence of the electron-deficient tricyanovinyl moiety as a reactive Michael acceptor, while a nucleophilic substitution-addition-elimination (S_{AE}) on the carbonyl of the ONSu active ester **3** will give the compound of interest. Therefore, it was decided to develop a synthesis route for acid **15** which can be coupled to amines in a well-defined manner, since its tricyanoalkane moiety will not interfere with the mild amide formation reaction conditions. Thus, aldehyde **12** underwent an Al_2O_3 -catalyzed Knoevenagel condensation with malononitrile to give dicyanovinyl derivative **13**. Subsequently, **13** was treated with KCN/HCl in aqueous CH_3CN to install the tricyanoalkane moiety, and compound **14** was obtained in an excellent yield of 95%. Then, the allyl ester was deprotected via a Pd-catalyzed allyl transfer in the presence of anilinium *p*-toluene sulfinate as scavenger. It turned out that the choice of the

scavenger was most critical, since a too strong base resulted in *C*-allylation of the tricyanoalkane moiety. Finally, **15** was efficiently coupled to HCl·H-Leu-OMe with EDCI/HOBt, and the corresponding dipeptide was treated with *N*-chlorosuccinimide to oxidize the tricyanoalkane moiety to obtain quantitatively tricyanovinyl derivative **16**.



Scheme 1. The push-pull substituted buta-1,3-diene scaffold results in colorful peptides.



Scheme 2. Synthesis of synthons **2** and **15** to arrive at D- π -A functionalized peptides.

References

- [1] (a) Rijkers, D.T.S.; Diederich, F. *Tetrahedron Lett.* **2011**, 52, 4021; (b) Rijkers, D.T.S.; de Prada López, F.; Liskamp, R.M.J.; Diederich, F. *Tetrahedron Lett.* **2011**, 52, 6963.

Access to all β -phenylproline stereoisomers in enantiomerically pure form

Paola Fatás, Ana M. Gil, Ana I. Jiménez, M. Isabel Calaza,
Carlos Cativiela

Department of Organic Chemistry, ISQCH, CSIC–University of Zaragoza, 50009
Zaragoza, Spain

cativiela@unizar.es

Introduction

Due to its cyclic structure, proline is the coded amino acid with a more restricted conformational flexibility. The incorporation of additional groups into the pyrrolidine ring is a useful means to produce new amino acids that combine the conformational properties of proline with side-chain functionality. This is the case of β -phenylproline, (β Ph)Pro (Figure 1), that can be regarded as a proline-phenylalanine hybrid in which the orientation of the aromatic substituent is dictated by the conformation of the five-membered ring and the *cis* or *trans* configuration of the phenyl group relative to the carbonyl moiety [1].

We have developed synthetic procedures for the preparation of all four stereoisomers of (β Ph)Pro (two *cis* and two *trans* enantiomers, Figure 1) in optically pure form and suitably protected for use in peptide synthesis [2]. The methodology is based on the preparation of racemic precursors and their subsequent HPLC resolution on chiral columns.

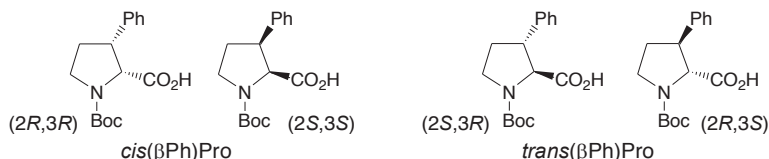


Figure 1. Structure of the four (β Ph)Pro stereoisomers synthesized in enantiopure form.

Results and Discussion

First, we synthesized racemic precursors of the desired amino acids [2], namely racemic *cis* and *trans* *N*-Boc- β -phenylproline methyl esters (*cis*-**2** and *trans*-**2**, Figure 2). The route started with the preparation of **1** as previously reported [3], which was transformed into a *cis/trans* mixture of the target compounds (**2**). Separation of *cis/trans* isomers was then achieved by selective saponification. Thus, only the less hindered ester moiety in *trans*-**2** reacted with sodium hydroxide to give the corresponding carboxylic acid, which was easily separated from unreacted *cis*-**2**. The *trans* carboxylic acid isolated was esterified to obtain pure *trans*-**2**. Importantly, *N*-Boc protection is essential to achieve a completely selective saponification.

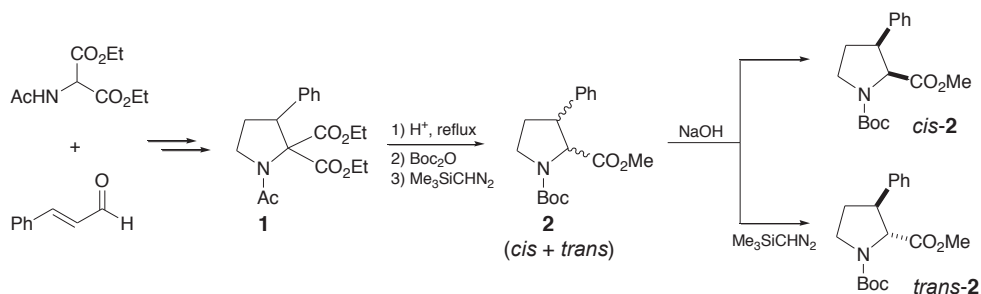


Figure 2. Synthesis of *cis*- and *trans*-(β Ph)Pro in racemic form.

Racemic *cis*-2 and *trans*-2 were then submitted to chiral HPLC resolution [2] (Figure 3). Semi-preparative columns (250 mm \times 20 mm) containing chiral stationary phases derived from amylose (Chiralpak® IA) and cellulose (Chiralpak® IC) were used, respectively, for the resolution of *cis*-2 (5.40 g) and *trans*-2 (3.0 g). Both enantioseparation processes were very efficient with above 95% of the racemic material injected being recovered in enantiomerically pure form after a single passage through the column. The four enantiopure *N*-Boc- β -phenylprolinates isolated were transformed into the corresponding *N*-Boc amino acids. Thus, the four (β Ph)Pro stereoisomers shown in Figure 1 were obtained in enantiomerically pure form and gram-scale quantities.

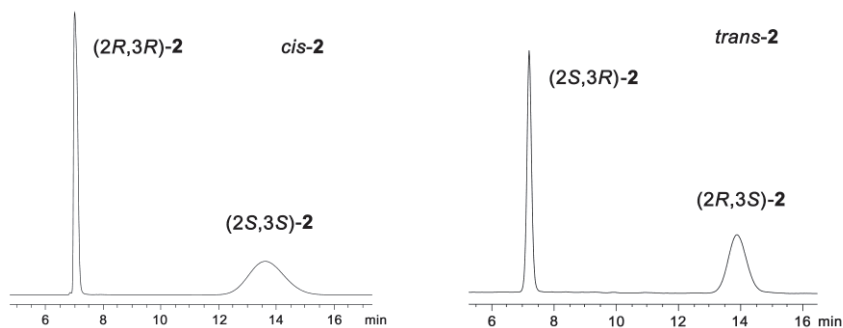


Figure 3. Profiles of the analytical HPLC resolution of *cis*- and *trans*-(β Ph)Pro. *Cis*-2: Chiralpak® IA, *n*-hexane/2-propanol 90:10. *Trans*-2: Chiralpak® IC, *n*-hexane/2-propanol/chloroform 75:15:10.

Acknowledgments

Ministerio de Ciencia e Innovación-FEDER (grant CTQ2010-17436; FPU fellowship to P.F.); Gobierno de Aragón-FSE (research group E40).

References

- [1] Fatás, P.; Jiménez, A. I.; Calaza, M. I.; Cativiela, C. *Org. Biomol. Chem.* **2012**, *10*, 640.
- [2] Fatás, P.; Gil, A. M.; Calaza, M. I.; Jiménez, A. I.; Cativiela, C. *Chirality*, in press (doi: 10.1002/chir.22101).
- [3] (a) Chung, J. Y. L.; Wasicak, J. T.; Arnold, W. A.; May, C. S.; Nadzan, A. M.; Holladay, M. W. *J. Org. Chem.* **1990**, *55*, 270. (b) Cox, D. A.; Johnson, A. W.; Mauger, A. B. *J. Chem. Soc.* **1964**, 5024.

Access to cyclic or branched peptides using bis(2-sulfanylethyl)amido side-chain derivatives of Asp and Glu

Emmanuelle Boll, Julien Dheur, Hervé Drobecq, Oleg Melnyk

UMR CNRS 8161, Univ. Lille Nord de France, Pasteur Institute of Lille, France

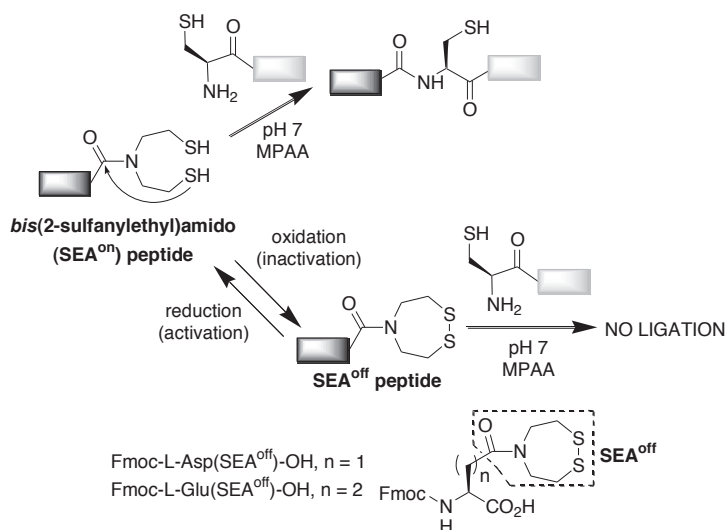
oleg.melnyk@ibl.fr

Introduction

The importance of peptide cyclization for studying peptide conformation, creating new structures, or for developing peptide therapeutics is well established. In particular, side-chain lactam bridges linking two amino acid residues that are several residues apart in the linear sequence or backbone peptide cyclization enable rigidification of the structure and improvement of in vivo stability.

Native Chemical Ligation (NCL) is now an established method for producing backbone-cyclized peptides or proteins. The application of NCL to the synthesis of side-chain cyclized peptides is less frequent. Head-to-side-chain cyclization by ligating a C-terminal thioester with a Cys residue located on a lysine side-chain was used by few authors. In contrast, tail-to-side-chain amide cyclization linking the N-terminus of the peptide to the side-chain carboxylic acid group of Asp or Glu residues is rare. This is probably due to the difficulty of installing a thioester group on amino acid side-chains such as aspartic or glutamic acids using Fmoc-SPPS.

The reaction of a bis(2-sulfanylethyl)amido (SEA^{on})[1] group with an N-terminal cysteine residue in water and at neutral pH results in the formation of a native peptide bond. Oxidation of SEA^{on} results in a cyclic disulfide called SEA^{off} having a 1,2,5-dithiazepan-5-carbonyl structure. SEA^{off} is a self-protected form of SEA^{on}. [2] SEA^{off} and SEA^{on} can be easily interconverted by reduction/oxidation. We show here that SEA^{off} derivatives of Asp



and Glu can be easily prepared. Interestingly, SEA^{off} group is stable during the repetitive piperidine treatments used for removing the Fmoc group during Fmoc-SPPS. This property led us to consider the utility of side-chain SEA^{off} derivatives of Asp and Glu for accessing branched or tail-to-side-chain cyclic peptides using Fmoc-SPPS and intermolecular or intramolecular SEA native peptide ligation.[3]

Results and Discussion

The synthesis of Fmoc-Asp(SEA^{off})-OH and Fmoc-Glu(SEA^{off})-OH is straightforward. First, *bis*({2-[triphenylmethyl)sulfonyl]ethyl})amine was coupled to the side-chain of Boc-Asp-*Ot*Bu or Boc-Glu-*Ot*Bu using PyBOP/DIEA activation. Formation of the cyclic disulfide using iodine was followed by removal of the Boc group in TFA and then by the reaction of the α -amino group with Fmoc-OSu.

Fmoc-Asp(SEA^{off})-OH and Fmoc-Glu(SEA^{off})-OH derivatives are fully compatible with standard Fmoc-SPPS. This enabled the synthesis of model peptides Ac-Asp(SEA^{off})XLKEPVHGA-NH₂ (with X = Ile, Ala) and Ac-Glu(SEA^{off})ILKEPVHGA-NH₂ which were used for the synthesis of branched peptides by intermolecular SEA ligation with model Cys peptide H-CILKEPVHGV-NH₂. Ligation proceeded successfully either at pH 5.5 or 7.3 at 37°C in the presence of MPAA as catalyst. For example ligation of Ac-Asp(SEA^{off})ALKEPVHGA-NH₂ with the model Cys peptide at pH 5.5 furnished branched peptide Ac-Asp(CILKEPVHGV-NH₂)ALKEPVHGA-NH₂ (84 % after RP-HPLC purification) with no aspartimide formation.

Synthesis of model peptides featuring an N-terminal Cys residue and a C-terminal Asp(SEA^{off}) or Glu(SEA^{off}) residue, i.e. H-C(StBu)ILKEPVHGAAsp(SEA^{off})-NH₂, was also undertaken, and enabled tail-to-side chain cyclization by intramolecular SEA ligation. Here again cyclization proceeded successfully with no side-product formation and led to the isolation of the cyclic peptides with 31% (Asp) or 49% (Glu) yields.

Acknowledgments

We acknowledge financial support from Cancéropôle Nord-Ouest, Région Nord Pas de Calais, ANR grant "click-unclick" and the European Community.

References

- [1] (a) Ollivier, N.; Dheur, J.; Mhidia, R.; Blanpain, A.; Melnyk, O. *Org. Lett.* **2010**, *12*, 5238.
- [2] (a) Ollivier, N.; Vicogne, J.; Vallin, A.; Drobecq, H.; Desmet, R.; El-Mahdi, O.; Leclercq, B.; Goormachtigh, G.; Fafeur, V.; Melnyk, O. *Angewandte. Chem. Int. Ed.* **2012**, *51*, 209. (b) Raibaut, L.; Ollivier, N.; Melnyk, O. *Chem. Soc. Rev.*, in press, **2012**, DOI:10.1039/C2CS35147A.
- [3] Boll, E.; Dheur, J.; Drobecq, H.; Melnyk, O. *Org Lett* **2012**, *14*, 2222.

Unprecedented side reactions in the SPPS of Cys-containing peptides

**Panagiotis Stathopoulos, Serafim Papas, Charalambos Pappas,
Vassilios Mousis, Nisar Sayyad, Andreas Tzakos, Vassilios Tsikaris**

Chemistry Department, University of Ioannina, 45110, Greece

E-mail: btsikari@cc.uoi.gr

Introduction

Decomposition of the resin linkers upon the TFA cleavage of the peptides in the Fmoc strategy is a common and well-documented phenomenon. This was observed to be the case both for the Rink amide resin, resulting in C-terminal alkylated amide by-products [1], as well as for the Wang resin, resulting in side chain alkylation of indole ring of Trp-containing peptides [2]. To our knowledge, such side products have not been reported for cysteine-containing peptides, although are prone to oxidation and alkylation by cations produced during the cleavage process. Cys-containing peptides are very important biomolecules due to the inherent reactivity of the thiol group, allowing them to participate in an array of processes ranging from redox reactions, metal ion binding, post-translational modifications, disulfide bond formation, to name some. In our laboratory, using the Wang resin for the synthesis of various Cys-containing peptides with the Fmoc strategy, we observed both the expected peptide and a by-product formation, similar to the case of Trp-containing peptides. The percentage of this by-product varied up to 35%. This finding prompted us to investigate the nature of the formed side product, the influence of the Cys position in the peptide sequence and the possibility of minimizing its formation changing resin substitution and composition of the cleavage mixture.

Results and Discussion

Identification of side product formation in a Cys-containing peptide model

To probe the nature of the Cys-containing byproducts we synthesized the cysteine-containing peptide model Ac-Ala-Arg-Cys-OH (peptide 1). The synthesis occurred on Wang resin using Fmoc based methodology. The side-chains of cysteine and arginine residues were protected by trityl and Pbf groups, respectively. After the final TFA cleavage using the standard cleavage mixture (94% TFA, 2.5% EDT, 2.5% TIS, 1% H₂O) of peptide from the solid support and HPLC purification we isolated both the desired peptide and a by-product, which exhibited an increased mass by 106 *Amu* in respect to the target peptide. Moreover, this by-product exhibited an absorbance at 280 nm in the UV detector despite the absence of aromatic residues in the peptide sequence. By the use of ESI-MS we found that the relative percentage of side product was ~19.0 (Table 1). In order to unambiguously determine the identity of the formed byproduct we used NMR spectroscopy. On the basis of the recorded ¹H NMR spectrum a p-hydroxy benzyl group was found to be covalently attached on the thiol-group of Cys, similarly to the case of Trp-containing peptides. The accessibility of Cys containing peptides for such alkylation was further validated by the synthesis of the Ac-Ala-Arg-OH peptide that did not result in any byproduct formation.

Influence of cysteine position on the S-alkylated side product formation

In order to evaluate the influence of cysteine position on the by-product formation we synthesized and studied the Ac-Arg-Cys-Ala-OH (peptide 2) and Ac-Cys-Arg-Ala-OH (peptide 3), changing the position of cysteine from the C- to the N-terminal end of the initial peptide model (peptide 1). The experimental conditions used for the synthesis of the peptide analogues 2 and 3 were similar with those of the peptide model 1. As showed in Table 1, alkylation of Cys-containing peptides with the p-hydroxy benzyl group seems to be sensitive to the position of Cys in the peptide sequence. More specifically, the highest tendency of side product formation was observed when the cysteine residue occupied the C-terminus of the peptide (entries 1, 3 and 4).

Influence of the Wang resin substitution on the S-alkylated side product formation

To probe the influence of the resin substitution on the byproduct formation, cleavage experiments were performed for peptide analogues 1 and 3, having cysteine residue at the C- and the N-terminus (Ac-Ala-Arg-Cys-OH and Ac-Cys-Arg-Ala-OH) respectively. In these experiments the cleavage mixture was constant (94%TFA, 2.5%H₂O, 2.5%EDT, 1%TIS), while the Wang resin substitution was varied. As showed in Table 1, when the resin substitution was increased, the yield of the S-alkylated side product formation was also increased (entries 1, 2 and 4, 5 respectively).

Influence of the cleavage mixtures on the S-alkylated side product formation

Evaluation of the cleavage conditions that could minimize the percentage of the S-alkylated by-product was estimated by using various cleavage mixtures. Table 1 summarized some of the results obtained from these experiments. From entries 5-10 of Table 1 we conclude that the presence of EDT in the cleavage mixture is crucial for suppression of S-alkylated side product formation, while DMB (1,3-dimethoxybenzene) and H₂O don't prevent significantly cysteine alkylation.

Table 1: Percentage of S-alkylated side product (SP) depending on the resin substitution, cysteine position and cleavage mixtures

Entry	Peptide analogues	Substitution	Cleavage mixture (3h)	SP (%) ^a
1	Ac-Ala-Arg(Pbf)-Cys(Trt)-Wang	0.75	94%TFA, 2.5%H ₂ O, 2.5%EDT, 1%TIS	19.1
2	Ac-Ala-Arg(Pbf)-Cys(Trt)-Wang	0.32	94%TFA, 2.5%H ₂ O, 2.5%EDT, 1%TIS	11.6
3	Ac-Arg(Pbf)-Cys(Trt)-Ala-Wang	0.6	94%TFA, 2.5%H ₂ O, 2.5%EDT, 1%TIS	9.2
4	Ac-Cys(Trt)-Arg(Pbf)-Ala-Wang	0.79	94%TFA, 2.5%H ₂ O, 2.5%EDT, 1%TIS	4.3
5	Ac-Cys(Trt)-Arg(Pbf)-Ala-Wang	0.4	94%TFA, 2.5%H ₂ O, 2.5%EDT, 1%TIS	3.9
6	Ac-Cys(Trt)-Arg(Pbf)-Ala-Wang	0.4	89%TFA, 2.5%H ₂ O, 2.5%EDT, 1%TIS, 5%DMB	2.0
7	Ac-Cys(Trt)-Arg(Pbf)-Ala-Wang	0.4	92.5%TFA, 2.5%TIS, 5%DMB	25.7
8	Ac-Cys(Trt)-Arg(Pbf)-Ala-Wang	0.4	90%TFA, 2.5%TIS, 2.5%H ₂ O, 5%DMB	18.5
9	Ac-Cys(Trt)-Arg(Pbf)-Ala-Wang	0.4	95%TFA, 2.5%TIS, 2.5%H ₂ O	70.6
10	Ac-Cys(Trt)-Arg(Pbf)-Ala-Wang	0.4	95%TFA, 2.5%TIS, 2.5%EDT	3.3

^a The percentages represent the relative peak intensities estimated from the related ESI-MS spectra

References

- [1] Giraud, M.; Cavelier, F.; Martinez, J. *J Pept Sci.* **1999**, *5*, 457
- [2] Stathopoulos, P.; Papas, S.; Tsikaris, V. *J. Pept. Sci.* **2006**, *12*, 227.

Amides of antiviral drug oseltamivir with antioxidant active aminoacids: Synthesis and biological activities

Maya Chochkova,¹ Galya Ivanova,² Angel Galabov,³ Tsenka Milkova¹

¹South-West University "Neofit Rilski", Blagoevgrad, Bulgaria; ²REQUIMTE, Departamento de Química, Faculdade de Ciências, Universidade do Porto, 4169-007 Porto, Portugal; ³The Stephan Angeloff Institute of Microbiology, Bulgarian Academy of Sciences, Sofia, Bulgaria

E-mail:mayabg2002@yahoo.com

Introduction

Annually, influenza infects approximately 600,000,000 people and causes epidemics and pandemics all over the world [1]. Influenza viruses belong to the family *Orthomyxoviridae* and have negative-sense, single-stranded RNA genome [2]. According to the antigenic difference in their nucleoproteins and matrix proteins, the viruses are divided into three genera: A, B and C [3]. To date, two strategies for combating influenza: vaccines and drugs are applied. The rapidly spreading influenza viruses and their mutation lead to limitation of protection through vaccination; therefore there is a great need to develop novel anti-influenza drugs.

Currently, four antiviral drugs have been approved by the Food and Drug Administration: aminoadamantanes (rimantadine and amantadin), known as M2 channel blockers and neuraminidase inhibitors (Zanamivir [Relenza] and Oseltamivir [Tamiflu]), belonging to the second generation anti-flu agents. Lately, the majority of research efforts are focused on the influenza neuraminidase, that is essential for virus replication and infectivity. This enzyme has become an attractive target for the development of new neuraminidase inhibitors, which have activity against both influenza viral types A and B.

Many investigators have shown that oxidative stress is important in the pathogenesis of pulmonary damage during influenza virus infections. Therefore, antioxidant could be one potential approach to chemotherapy for human influenza infection. The application of combination therapy of antioxidants with antiviral drugs could reduce the complications and lethal effects, caused by an influenza virus [4].

Results and Discussion

In our study, antiviral drug oseltamivir (Os) was conjugated to antioxidant active amino acid derivatives of cysteine, histidine and tyrosine, in order to indicate a possible advantage of chemically combining the two treatments during severe influenza infection. The C-terminus of the amino acids was converted to amide (**1a-c**) using EDC/ HOBt method (**Fig. 1a**). Initially, we evaluated the antioxidative activities (% RSA) of oseltamivir amides (**1a-c**) by use of the 1, 1-diphenyl-2-picrylhydrazyl (DPPH) radical scavenging test [5]. The effect of the tested activities was illustrated in **Fig. 1b**. The results were expressed as: % RSA = [Abs516 nm (t=0)-Abs516nm (t=t')]/Abs516 nm (t=0) x 100. It was established that conversion of amino acid derivatives into their Os analogues significantly decreased the DPPH scavenging abilities compared with positive control like *N*-Acetyl cysteine (ACC).

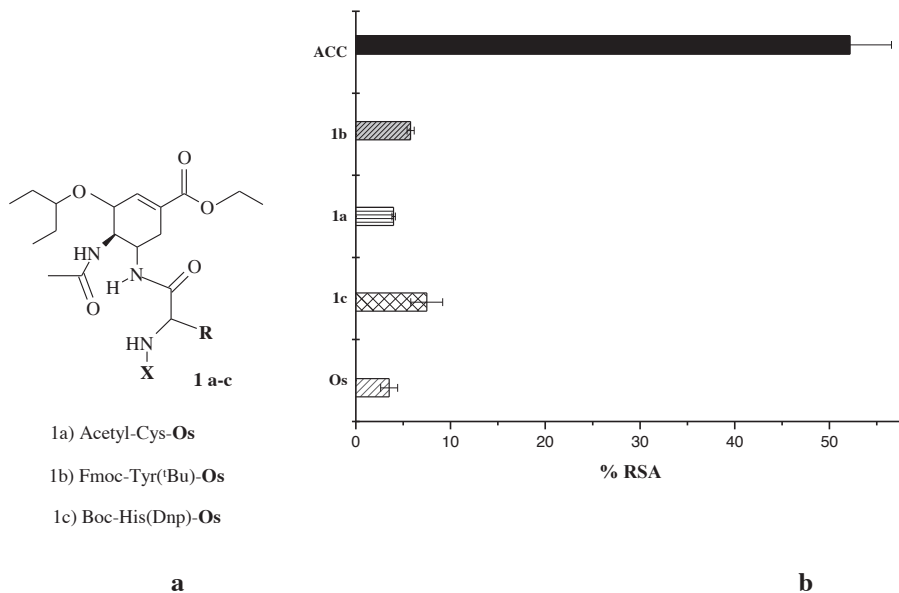


Fig. 1.

Although DPPH assay has been widely used to conveniently test for determination of the free radical scavenging activity of compounds, the method is only chemical relevance and the system used is a homogenous solution. It has been known that the antioxidant activity in homogenous solutions may not parallel that in heterogeneous media (e.g. human red blood cells). Therefore, to evaluate the influence of microenvironment on antioxidative effect, the tested amides will be investigated in other antioxidant model.

Acknowledgments

For the support of this work we are grateful to the National Found for Scientific Research of Bulgaria (Contracts DMU-03/2), South-West University "Neofit Rilski" Bulgaria (SRP-A4/12).

References

- [1] Englund, J. A. *Semin. Pediatr. Infect.Dis.* **2002**, *13*, 120.
- [2] Lamb, R. A.; Krug, R. M. Orthomyxoviridae: the viruses and their replication. In *Fields Virology*; Fields, B. N.; Knipe, D. M.; Howley, P. M., Eds, Philadelphia: Lippincott-Raven, 2001; Vol. 1; p 1487.
- [3] Palese, P.; Young, J.F. *Science* **1982**, *215*, 1468.
- [4] Uchide, N.; Toyoda, H. *Molecules* **2011**, *16*, 2032.
- [5] Nenadis, N., Tsimidou, M.; *JAOCs* **2002**, *79*, 1191.

An expedient synthesis of guanidine-bridged cyclopeptides

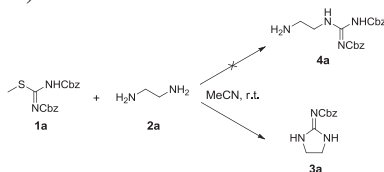
Xiaoxiao Yang, Hao Lin, Dexin Wang

Institute of Materia Medica, Chinese Academy of Medical Sciences and Peking Union
Medical College

E-mail: yangxx@imm.ac.cn

Introduction

Guanidine is a very important alkaline pharmacophore. Recently, referred to reported method for synthesis of aminoalkylguanidine[1], we planed to synthesize **4a** by reacting **1a** [2] with ethylenediamine (**2a**). However, an unexpected compound was found as the only product of the reaction. By analyzing mass spectrum and NMR data, the product turned out to be a cyclic guanidine **3a** which has been reported by Rapoport[3] with 3.7 % yield using benzyl chloroformate(Cbz-Cl) and 2-imino-imidazolidine as reaction materials (Scheme 1).

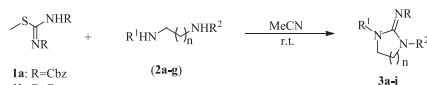


Scheme 1

This result inspired us to develop a simple and convenient synthetic method of compound **3a** and then try to apply it to prepare other substituted five-membered or six-membered cyclic guanidine derivatives. Then we tried to apply this mechanism to synthesize two types of guanidine-bridged cyclopeptides — *N*-terminus local cyclo-guanidine peptide which was accomplished and backbone guanidine-bridged marco-cyclic peptide which is still under investigation.

Results and Discussion

For synthesis of aliphatic cyclic guanidine derivatives, we introduced two guanidinyllating reagents **1a** and **1b** to react with aliphatic diamine **2a–g** at ambient temperature to afford corresponding 2-alkyloxycarbonyliminoimidazolidine derivatives **3a–I**. The yields ranged from moderate to high depending on the structure of the aliphatic diamine. For diamine with two primary amino (ethylenediamine **2a** and 1, 3-propylenediamine **2e**), the reaction condition was mild, and usually the product **3a** and **3e** could be precipitated gradually during reaction (acetonitrile as solvent) with high yield. However, for diamines with single or two secondary amino groups (entry 3, 7–9), the yields were improved while the reaction time being extended or the reaction proceeding at 70 °C. We found that *tert*-butoxycarbonyl (Boc)-protected group was less beneficial for this reaction than benzyloxycarbonyl(Cbz)-protected group (entry 8, 9).



Entry	Diamine 2	n	R ¹	R ²	Compound 1	R	Product 3	Yield (%)	Mp (°C)
1	a	1	H	H	a	Cbz	a	91	180-182
2	b	1	H	CH ₃	a	Cbz	b	73	55-57
3	c	1	H	CH ₂ CH ₃	a	Cbz	c	58, 79 ^b	52-54
4	d	1	CH ₃	CH ₃	a	Cbz	d	70	- ^c
5	e	2	H	H	a	Cbz	e	90	192-194
6	f	2	H	CH ₃	a	Cbz	f	72	39-41
7	g	2	CH ₃	CH ₃	a	Cbz	g	56, 76 ^b	56-58
8	a	1	H	H	b	Boc	h	54, 86 ^b	205 ^d
9	e	2	H	H	b	Boc	i	57, 89 ^b	176 ^d

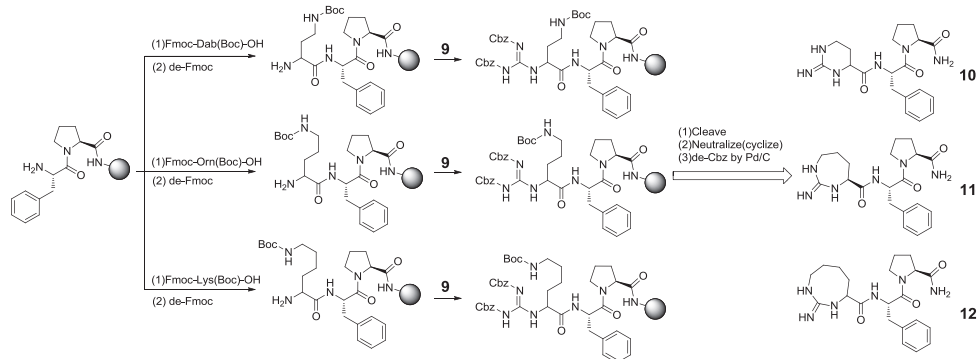
^a Reaction condition: 1 mmol of diamine was reacted with 0.5 mmol of compound 1 in MeCN at ambient temperature.

^b The yields were improved by heating at 70 °C for 2 h after stirring for 2h at room temperature.

^c The compound was achieved as colourless oil.

^d The compound decomposed at this temperature.

We utilize this mechanism to synthesize macrocyclic guanidine peptide, including localized macrocyclic guanidine peptide. N, N'-orthogonal protected diamino acids such as diaminobutyric acid (Dab), ornithine (Orn) and Lysine (Lys) were introduced to provide side chain amino group to react with other guanidinylated amino group. Since the synthesis of backbone cyclopeptide is still under investigation right now, here we could only demonstrate synthesis of N-terminus macrocyclic guanidine peptide for sure. Since nucleophilicity of α -NH₂ is too low to attack the guanidine carbon to proceed second 1,4-nucleophilic addition-elimination reaction, it should be guanidinylated firstly to form bis-Cbz protected guanidine intermediate. In order to guanidinylate α -NH₂, bis-Cbz protected amidinopyrazole (**9**) was used as guanidinyating reagents instead of methylisothiourea **1a**. Three N-terminus local macrocyclic peptides (**10-12**) derived from neuroendocrine TRH-like tripeptide (Pyr-Phe-Pro-NH₂)[4] were successfully synthesized and characterized by HRMS.



Acknowledgments

We would like to thank project 81001366 by NSFC funding this research work.

References

- [1] D. Castagnolo, F. Raffi, G. Giorgi, et al. *Eur. J. Org. Chem.* **2009**, 3, 334;
- [2] X. Wang, J. Thottathil. *Tetrahedron Asym.* **2000**, 11, 3665.
- [3] K. Matsumoto, H. Rapoport, *J. Org. Chem.* **1968**, 33, 552.
- [4] P.J.Gkonos et al., *Peptides.* **1994**, 15, 1281.

Aryl hydrazine resin as a tool in the synthesis of C-terminal modified peptides – optimization of oxidation conditions

Izabela Maluch¹, Aleksandra Walewska¹, Anna Kwiatkowska²,
Bernard Lammek¹, Robert Day², Adam Prahl¹

¹Institute of Organic Synthesis, Faculty of Chemistry, University of Gdańsk, Gdańsk, Poland; ²Institut de Pharmacologie de Sherbrooke, Université de Sherbrooke, Sherbrooke, Québec, Canada

E-mail:izam@chem.univ.gda.pl

Introduction

Recently, Kwon et. al. [1] presented a novel and straightforward strategy to synthesize peptides with p-nitroanilides and other anilide analogues using aryl hydrazine resin. The resin is also a multipurpose tool for the synthesis of carboxylic acids, esters and thioesters [2-4]. When the synthesis is completed, the fully protected peptide hydrazide resin is oxidized with either *N*-bromosuccinimide (NBS) or copper(II) acetate in pyridine. The resulting acyl diazene resin is then cleaved by peptide displacement at the C-terminus with amine. In our approach, we used a 4-Fmoc-hydrazinobenzoyl AM NovaGel resin to synthesize a peptide-substituted amide in the C-terminus.

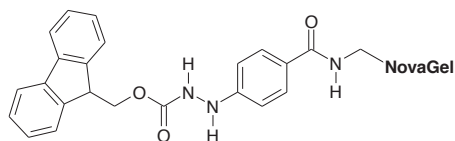


Fig.1. Structure of 4-Fmoc-hydrazinobenzoyl AM NovaGel resin linker

After synthesis of peptides using standard Fmoc-protocols, we used $\text{Cu}(\text{OAc})_2$ to oxidize the peptidyl resin and protected 4-amidinobenzylamine (Amba) that could mimic the C-terminal residue. We tried to improve the yields of this reaction by changing its conditions, e.g. concentration of $\text{Cu}(\text{OAc})_2$, time of oxidation and quality of Amba. Moreover, we conducted the study to check whether during coupling of 4-amidinobenzylamine to the C-terminus of the peptide chain, it is necessary to protect its amidino group, which can be competitive for the free amino group.

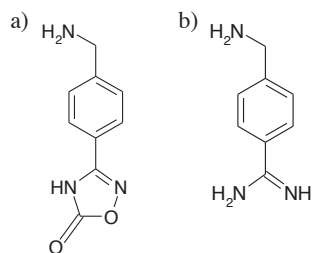


Fig. 2. Structures of (a) protected and (b) unprotected Amba

All peptides were synthesized with an automatic synthesizer Symphony (Protein Technologies), purified by reversed-phase HPLC (Waters, Shimadzu) and identified by LCMS ESI-IT-TOF (Shimadzu).

Results and Discussion

First, the oxidative cleavage was carried out with NBS in pyridine and protected 4-aminobenzylamine. However, the yield of the reaction was insufficient, even after attempts of optimizing the conditions. In the next step, we applied copper(II) acetate in the presence of pyridine and protected Amba. Following optimization, the efficiency of the process was significantly improved. The best results were observed in case of prolonged reaction time (24 hours), higher amount of $\text{Cu}(\text{OAc})_2$ (0.7 eq) and purified protected Amba. These conditions are needed to obtain a reasonably high efficiency of the oxidative cleavage in the synthesis of our C-terminal modified peptides using the aryl hydrazine resin linker.

To the implementation of the second part of this project, we synthesized two analogues with identical sequences, but using two different forms of Amba (protected and unprotected one). Afterwards, we proved with HPLC, that these two peptides have similar profiles. Moreover, preliminary kinetic assays confirmed that both of synthesis methods rise to the same final product (inhibition constants K_i of synthesized peptides toward hPACE4 and h-furin amount 0.2nM and 3.45nM respectively).

Data obtained by realization of described experiments expanded our knowledge of the possible methods for modifying the peptide chain at the C-terminus and enabled to select the most effective and convenient procedure of the synthesis of our peptide inhibitors.

Acknowledgments

This work was supported by the University of Gdańsk (DS/8453-4-0169-2) and the European Social Fund in as a part of the project "Educators for the elite – integrated training program for PhD students, post-docs and professors as academic teachers at the University of Gdańsk" within the framework of Human Capital Operational Programme, Action 4.1.1, Improving the quality of educational offer of tertiary education institutions.

This publication reflects the views only of the author, and the funder cannot be held responsible for any use which may be made of the information contained therein.

References

- [1] Kwon, Y.; Welsh, K.; Mitchell, R.M.; Camarero, J.A. *Org. Lett.* **2004**, *6*, 3801.
- [2] Peters, C.; Waldmann, H. *J. Org. Chem.* **2003**, *68*, 6053.
- [3] Woo, Y.H.; Mitchell, A.R.; Camarero, J.A. *Int. J. Pept. Res. Ther.* **2007**, *13*, 181.
- [4] Camarero, J.A.; Hackel, B.J.; de Yoreo, J.J.; Mitchell, A.R. *J. Org. Chem.* **2004**, *69*, 4145.

Catalytic conversion of tertiary amides of amino acids to amines

Efrosini Barbayianni, George Kokotos*

Laboratory of Organic Chemistry, Department of Chemistry, University of Athens,
Panepistimiopolis, Athens 15771, Greece

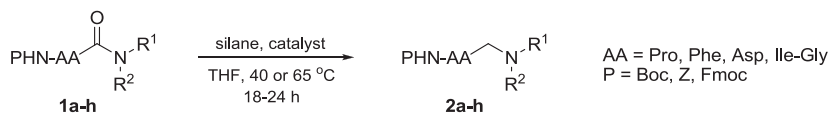
E-mail: gkokotos@chem.uoa.gr

Introduction

The catalytic reduction of carboxylic acid derivatives, including amides, has been widely developed over recent years.¹⁻⁴ The so-called metal-catalyzed hydrosilylation is a mild and chemoselective tool for useful transformations in Organic Synthesis. The purpose of our study was to investigate the application of zinc-catalyzed hydrosilylation in amino acid tertiary amides, and herein we report our results to produce several useful organic compounds and building blocks.

Results and Discussion

Testing a variety of *N*-protected amino acid tertiary amides, namely piperidine, pyrrolidine, morpholine, as well as Weinreb amides, we found that either triethoxysilane [(EtO)₃SiH] at 40 °C or diethoxymethylsilane [(EtO)₂MeSiH] and 1,1,3,3-tetramethyldisiloxane (TMDS) at 65 °C, in the presence of a catalytic amount of zinc acetate [Zn(OAc)₂] or chloroplatinic acid (H₂PtCl₆·6H₂O), may selectively reduce them to the corresponding tertiary amines (Scheme 1). Some indicative results are depicted in Table 1.

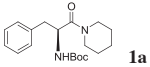
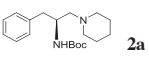
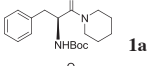
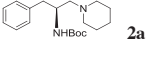
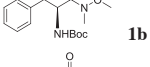
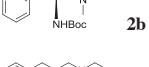
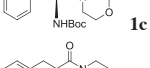
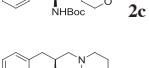
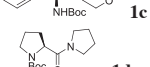
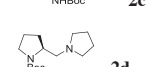
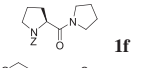
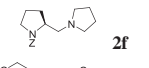
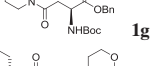
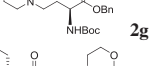
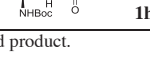
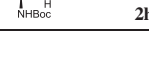
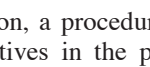
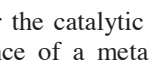


Scheme 1. Metal-catalyzed reduction of amino acid tertiary amides.

Piperidine amide of Boc-phenylalanine (**1a**) was used as a model compound to find out the optimum reaction conditions. Thus, it occurred that **1a** provided the diamine **2a** in medium yield using (EtO)₃SiH in the presence of 20% Zn(OAc)₂ (entry 1, Table 1). A slight decrease in yield was observed using (EtO)₂MeSiH and 10% Zn(OAc)₂ (entry 2, Table 1). Morpholine amide **1c** afforded the corresponding diamine **2c** (entry 4, Table 1), the deprotected derivative of which has been used successfully as an organocatalyst in asymmetric aldol reaction.⁵ As a general remark, it appeared that (EtO)₂MeSiH was less effective than (EtO)₃SiH towards the zinc-catalyzed reduction of the above mentioned compounds. Pyrrolidine amide of Boc-proline (**1d**) yielded in high yield the amine **2d** (entry 6, Table 1), whose unprotected form is an efficient organocatalyst for various asymmetric organic transformations. Morpholine amides of appropriately protected aspartic acid (**1g**) and isoleucine-glycine dipeptide (**1h**) were subjected to (EtO)₃SiH or (EtO)₂MeSiH/Zn(OAc)₂ reductive conditions, however their conversion to the tertiary amines was very low. The desired diamines **2g**, a useful building block for cobicistat,⁶ and

2h, a chiral ligand for the catalytic asymmetric addition of alkylzinc reagents to aldehydes⁷ were therefore obtained in moderate isolated yields by applying the TMDS/H₂PtCl₆·6H₂O reductive protocol (entries 8 and 9, Table 1).

Table 1. Metal-catalyzed reduction of amino acid tertiary amides.

Entry	Amide	Diamine	Silane	Catalyst	% [mol]	Yield (%) ^a
1	 1a	 2a	(EtO) ₃ SiH	Zn(OAc) ₂	20	57
2	 1a	 2a	(EtO) ₂ MeSiH	Zn(OAc) ₂	10	51
3	 1b	 2b	(EtO) ₃ SiH	Zn(OAc) ₂	10	56
4	 1c	 2c	(EtO) ₃ SiH	Zn(OAc) ₂	10	84
5	 1c	 2c	(EtO) ₂ MeSiH	Zn(OAc) ₂	10	55
6	 1d	 2d	(EtO) ₃ SiH	Zn(OAc) ₂	10	82
7	 1f	 2f	(EtO) ₃ SiH	Zn(OAc) ₂	10	68
8	 1g	 2g	TMDS	H ₂ PtCl ₆ ·6H ₂ O	1	41
9	 1h	 2h	TMDS	H ₂ PtCl ₆ ·6H ₂ O	1	34

^aYield of isolated product.

In conclusion, a procedure for the catalytic hydrosilylation of tertiary amides of α -amino acid derivatives in the presence of a metal catalyst was investigated. The method was applied for the synthesis of the organocatalyst pyrrolidinylmethylpyrrolidine, a chiral diamine metal ligand, and a building block for the investigational drug cobicistat.

References

- [1] Addis, D.; Das, S.; Junge, K.; Beller, M. *Angew. Chem. Int. Ed.* **2011**, *50*, 6004.
- [2] Das, S.; Addis, D.; Zhou, S.; Junge, K.; Beller, M. *J. Am. Chem. Soc.* **2010**, *132*, 1770.
- [3] Das, S.; Addis, D.; Junge, K.; Beller, M. *Chem.-Eur. J.* **2011**, *17*, 12186.
- [4] Hanada, S.; Tsutsumi, E.; Motoyama, Y.; Nagashima, H. *J. Am. Chem. Soc.* **2009**, *131*, 15032.
- [5] Kumar, A.; Singh, S.; Kumar, V.; Chimni, S. S. *Org. Biol. Chem.* **2011**, *9*, 2731.
- [6] Xu, L.; Liu, H.; Murray, B. P.; Callebaut, C.; Lee, M.S.; Hong, A.; Strickley, R.; Tsai, L. K.; Stray, K. M.; Wang, Y.; Rhodes, G. R.; Desai, M. C. *ACS Med. Chem. Lett.*, **2010**, *1*, 209.
- [7] Sprout, C. M.; Seto, C. T. *J. Org. Chem.* **2003**, *68*, 7788.

Chemical stability and structure – activity relationship studies of novel cyclic NGR peptides

**Gábor Mező¹, Kata Enyedi^{1,2}, András Czajlik³, Ildikó Szabó¹,
Rózsa Hegedüs^{1,2}, Zsuzsa Majer², Eszter Lajkó⁴, László Kőhidai⁴,
András Perczel²**

¹*Research Group of Peptide Chemistry, Hungarian Academy of Sciences, Eötvös Loránd University, 1117 Budapest, Hungary;* ²*Institute of Chemistry, Eötvös Loránd University, 1117 Budapest, Hungary;* ³*Faculty of Information Technology, Pázmány Péter Catholic University, 1083 Budapest;* ⁴*Department of Genetics, Cell and Immunobiology, Semmelweis University, 1089 Budapest, Hungary*

E-mail: gmezo@elte.hu

Introduction

NGR peptides received particular interest when phage display libraries were used to identify non-RGD integrin binding motifs. Among the non-RGD peptides, the NGR tripeptide motif was the most frequent one showing integrin binding properties. Recently, it has been found that isoDGR peptides formed by deamidation through succinimide ring formation possess integrin binding properties. Furthermore, NGR peptides bind to Aminopeptidase N (APN or CD13), a membrane-bound metallopeptidase that is overexpressed on angiogenic blood vessels on tumor tissues, similarly to integrin receptors [1]. This observation suggests CD13 as a selective target for targeted delivery of drugs and nanoparticles to tumor neovasculature using NGR peptides as homing motif [2].

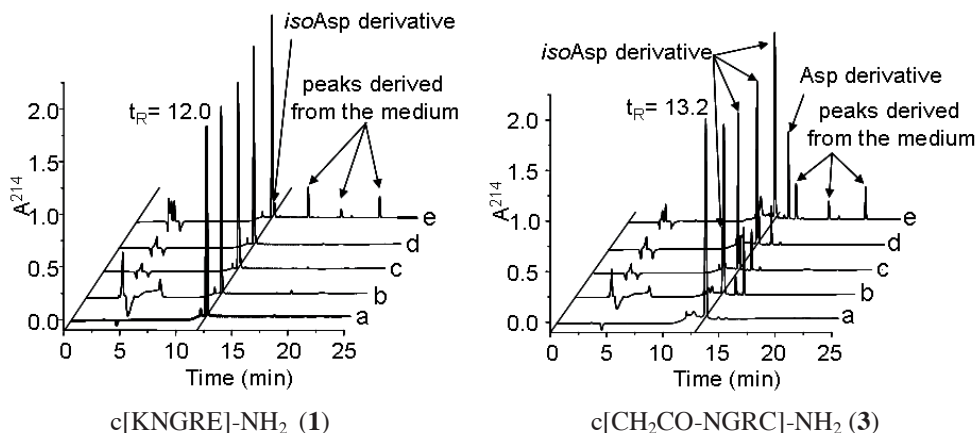
In our work, new cyclic-NGR peptides containing a thioether linkage were prepared. The influence of their structure on the succinimide ring formation and deamidation was evaluated and compared with the data on cyclic-NGR derivatives containing amide bond or disulfide bridge in the cycle (c[KNGRE]-NH₂ and Ac-c[CNGRC]-NH₂) [3,4].

Results and Discussion

The linear precursor peptides were prepared by solid phase peptide synthesis using Fmoc/tBu strategy, while cyclization reactions were performed in solution. The c[KNGRE]-NH₂ (**1**) with amide bond in the 17 atom-member cycle was formed with good yield from H-Lys(CIZ)-Asn-Gly-Arg-Glu-NH₂ semiprotected peptide in the presence of BOP/HOBt/DIEA coupling agents in DMF. CIZ group was removed using liquid HF afterwards. In case of disulfide bond formation (Ac-c[CNGRC]-NH₂ (**2**)), the oxidation of Ac-Cys(Acm)-Asn-Gly-Arg-Cys(Acm)-NH₂ with Tl(tfa)₃ under acidic conditions led to better results than the air oxidation from unprotected peptide in Tris buffer (pH 8.1). Under basic conditions, deamidation was observed that increased with time. Cyclic-NGR peptides containing a thioether bond were obtained from N-terminal haloacylated peptides containing cysteine or homocysteine at the C-terminus. The cyclization of ClCH₂CO-Asn-Gly-Arg-*h*Cys-NH₂ and ClCH₂CO-Asn-Gly-Arg-*h*Cys-NH₂ was ready in Tris buffer in 3 h with good yields resulting in 15 or 16 atom-member cyclic peptides (c[CH₂CO-NGRC]-NH₂ (**3**) and c[CH₂CO-NGR*h*C]-NH₂ (**5**)). However, a low amount of deamidated

derivatives was detected that was more pronounced in case of Cys derivative. Cyclic-NGR peptide with 16 atom-member ring ($c[\text{CH}_2\text{CH}_2\text{CO-NGRC}]\text{-NH}_2$ (**4**)) could be prepared from $\text{BrCH}_2\text{CH}_2\text{CO-Asn-Gly-Arg-Cys-NH}_2$, but the 17 atom-member cyclic peptide ($c[\text{CH}_2\text{CH}_2\text{CH}_2\text{CO-NGRC}]\text{-NH}_2$) could not be efficiently prepared by this procedure.

The deamidation was studied in plain water (**a**), 0.2 M NH_4OAc buffer (pH 5.0) (**b**), PBS solution (pH 7.4) (**c**), 0.1 M Tris buffer (pH 8.1) (**d**) at RT for 48 h and in cell culture medium (pH 7.3) (**e**) at 37°C for 24 h. The decomposition was followed by RP-HPLC. The compounds were stable under storage conditions at 4°C for longer time and in plain water. Further results indicated that the elevation of the pH and temperature increased the deamidation. The cyclic peptides with larger ring size were more stable. The order of the stability of the compounds in all circumstances was as follows: **1** > **2** > **4** > **5** > **3** (Figure).



According to the NMR studies, the cyclic peptides were quite flexible, but the predominant structures were inverse γ -turn for compound **1**, γ -turn and distorted β -turn for compounds **2** and **5**, while in case of compound **3** two turns (inverse γ -turn, γ -turn) were identified in the molecule. Compound **4** showed several structures (two inverse γ -turns, distorted β -turn and atypical) with similar possibilities. Only compound **1** had short distance between carbonyl oxygen of the side chain of Asn and NH in amide bond between Asn and Gly suggesting a possible hydrogen bond. This hydrogen bond might stabilize the H atom in amide bond that can prevent the deprotonation as the initial step of deamidation. This can explain the increased stability of the $c[\text{KNGRE}]\text{-NH}_2$ cyclic peptide.

Acknowledgments

This work was supported by grants from the Hungarian National Science Fund (OTKA NK 77485, K 81596 and K 100720).

References

- [1] Pasqualini, R.; Koivunen, E.; Kain, R.; *et al. Cancer Res.* **2000**, *60*, 722.
- [2] Wickström, M.; Larsson, R.; Nygren, P.; Gullbo, J. *Cancer Sci.* **2011**, *102*, 501.
- [3] Negussie, A.H.; Miller, J.L.; Reddy, G.; *et al. J. Control. Release* **2010**, *143*, 265.
- [4] Curnis, F.; Arrigoni, G.; Sacchi, A.; *et al. Cancer Res.* **2002**, *62*, 867.

Clickable peptides and their attachment to oligonucleotides

M. Hocharenko*, M. Alvira, P. Steunenberg, R. Strömberg*

*Karolinska Institutet, Department of Biosciences and Nutrition, Novum SE-141 83
Huddinge, Sweden*

E-mail: Roger.Stromberg@ki.se; Malgorzata.Honcharenko@ki.se

Introduction

Delivery is a seriously limiting factor for antisense, siRNA and gene therapy *in vivo*. [1,2] One approach to enhance nucleic acid uptake into cells is to utilize cell penetrating peptides (CPPs) either in the form of covalent conjugates, which also protects from digestion by intracellular enzymes. [3] Conjugation of peptides with oligonucleotides with copper (I) catalyzed 1,3-dipolar cycloaddition between an azide and an alkyne, commonly referred to as click chemistry [4,5] appear to be a suitable approach if convenient synthesis of building blocks and efficient conjugation can be achieved.

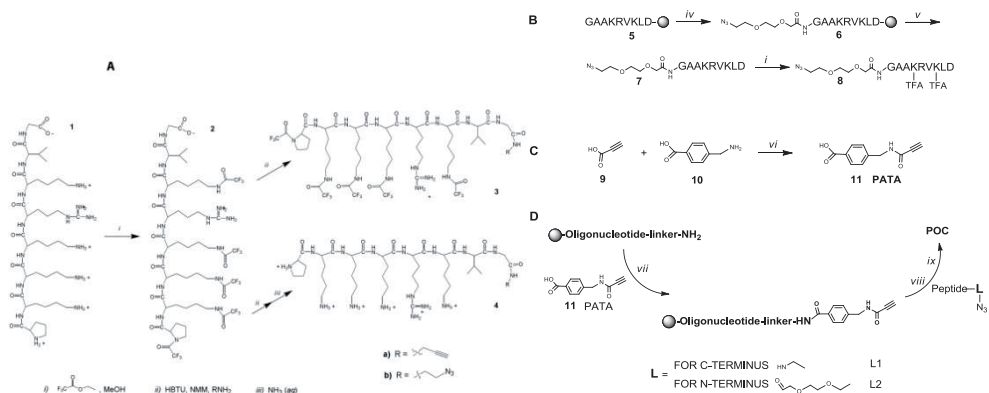
Results and Discussion

We have developed a convenient method for conversion of commercially available peptides into protected derivatives that can be readily used in 1,3-dipolar cycloaddition (click chemistry). To achieve this we have converted the peptides into alkyne and azide derivatives at the carboxyterminus with side chain amino groups either protected or deprotected (path A below). [6]

In addition the N-terminus can be conveniently azido-functionalized while still attached to solid support (path B). [7]

The azido-peptides were shown to be useful for synthesis of peptide-oligonucleotide conjugates where an efficient conjugation at room temperature and low millimolar concentration is enabled by an activated alkyne linker (PATA). [7]

Non-supported fully deprotected peptides can be purchased and converted into azido derivatives by intermediate TFA protection and subsequent attachment of an azide containing linker. Side chain and α -amino groups were converted into trifluoroacetamides and subsequent coupling to 2-azidoethylamine (or propargylamine) was performed to obtain the desired clickable peptides, from which a deprotected derivative could also be made. An N-terminal azido derivatized (**7**) peptide was readily made from a solid supported peptide (**5**) by condensation with 2-(2-azidoethyl)ethoxyacetic acid to give **6**. Cleavage from support and reaction with ethyl trifluoroacetate then gave **8**. To increase the efficiency of the click reaction at room temperature and low mM concentration we developed a linker with an activated triple bond donor, α -(N-propynoylamino)-*p*-toluic acid (PATA). For the synthesis of POCs we used DNA and locked nucleic acid (LNA) as well as 2'-O-methyl RNA oligonucleotides, purchased still attached to CPG or polystyrene PS support. A 2-(aminoethoxy)ethyl phosphate linker was attached with H-phosphonate chemistry whereupon PATA was coupled on to the aminolinker-oligonucleotide. Cu(I) catalyzed cycloaddition with the peptide azides then gave excellent conversion into the corresponding peptide-oligonucleotide conjugates. [7]



Scheme . A-B: Synthesis of alkyne or azido-functionalized peptides **C:** Synthesis of active alkyne linker, PATA. **D:** Scheme for POC conjugate synthesis on solid support using commercial oligonucleotides with aminolinkers. *iv*) 2-(2-azidoethoxy)ethoxyacetic acid, HBTU/ NMM/DMF; *v*) 90% TFAA, 4% TIS, 4% H₂O, 2% 3,5-dioxo-1,8-octanedithiol; *vi*) DCC/MeCN; *vii*) HBTU/NMM/DMF; *viii*) 1.2 eq. CuSO₄, 3 eq. sodium ascorbate, 2 eq of peptide-azide; *ix*) NH₃, aq. sat. 55° C.

The methodology should be highly suitable for parallel synthesis of libraries of POCs in which either or both components are varied. Use of the 1,3-dipolar cycloaddition with an activated alkyne should also make the approach suitable for conjugation with other biomolecules or labels thus enabling the use of a single type of conjugation method in synthesis of different conjugates.

Acknowledgments

This work was supported by grants from The Swedish Science Research Council, VINNOVA and EU (FP7:ITN-2008-238679).

References

- [1] Akhtar, S., Hughes, M.D., Khan, A., Bibby, M., Hussain, M., Nawaz, Q., Double, J. and Sayyed, P. *Advanced Drug Delivery Reviews*, **44**, 3-21, (2000).
- [2] Lebleu, B., Moulton, H.M., Abes, R., Ivanova, G.D., Abes, S., Stein, D.A., Iversen, P.L., Arzumanov, A.A. and Gait, M.J. *Advanced Drug Delivery Reviews*, **60**, 517-529, (2008).
- [3] Frederic, H., May Catherine, M. & Gilles, D., *British Journal of Pharmacology*, **157**, 195-206, 2009
- [4] Kolb, H.C., Finn, M.G. & Sharpless, K.B. (2001) *Angew. Chem., Int. Ed.*, **40**, 2004-2021; Kolb, H.C. & Sharpless, K.B. *Drug Discovery Today*, **8**, 1128-1137, (2003).
- [5] Meldal, M. & Tornøe, C.W., *Chem. Rev.*, **108**, 2952-3015, (2008); Tornøe, C.W., Christensen C. & Meldal, M., *J. Org. Chem.* **67**, 3057-3064, (2002)
- [6] Steunenberg, P., Wenska M., Strömberg R. *Nature Protocols*, DOI: 10.1038/nprot.2010.94.
- [7] Wenska, M., Alvira, M., Steunenberg, P. Stenberg, Å., Murtola, M., and Strömberg, R., *Nucleic Acid Research*, 2011, 39(20); 9047-9059

Comparison of alternative deprotection reagents to piperidine for the synthesis of a poly-alanine peptide on the Tribute[®] peptide synthesizer

**Michael A. Onaiyekan, James P. Cain, Christina A. Chantell,
Mahendra Menakuru**

Protein Technologies, Inc. Tucson, Arizona, 85714

E-mail: info@ptipep.com

Introduction

In peptide synthesis, piperidine is a common agent for Fmoc removal. However, piperidine is a controlled substance which requires special handling and cannot be used in some countries. Therefore, it would be useful to identify alternative deprotection reagents to piperidine for Fmoc removal. Peptides containing poly-alanine tracts have been associated with several human diseases and malformations [1] and have been used to form model beta sheet systems for studying Alzheimer's disease [2,3]. Due to their high propensity to aggregate after the fifth residue, these sequences are extremely difficult to synthesize by conventional Fmoc solid phase peptide synthesis. In this application, (A)₁₀K-OH was synthesized using the Tribute[®]'s Intellisynth UV monitoring and Feedback System to compare the efficiency of Fmoc removal by piperidine vs. three alternative bases (pyrrolidine, cyclohexylamine, and *tert*-butylamine) in the last 5 cycles of the synthesis.

Results and Discussion

HPLC results and UV data for the last five cycles of (A)₁₀K-OH synthesized with each deprotection reagent are shown in Figure 1. Mass analysis data confirmed the identity of the (A)₁₀K-OH product peak at an elution time of ~8.2 minutes (*m/z* = 856), and the Fmoc-(A)₆K-OH impurity peak (*m/z* = 794) at an elution time of ~24.8 minutes (data not shown). Percent purities and total deprotection repeats and times are shown in Table 1. Pyrrolidine produced the highest purity product (46.020%) with the fewest number of deprotection repeats (14 repeats) and shortest total deprotection time (14 minutes) even compared to piperidine (40.846% purity, 19 repeats, 29 minutes). Cyclohexylamine and *tert*-butylamine both performed less efficiently than piperidine with product purities of only 24.432% and 11.877%, respectively, and 35 or more deprotection repeats and total deprotection times of 88 minutes or more. Based on these results, it appears that pyrrolidine is the only viable candidate for replacing piperidine during the synthesis of difficult peptides like poly-alanines.

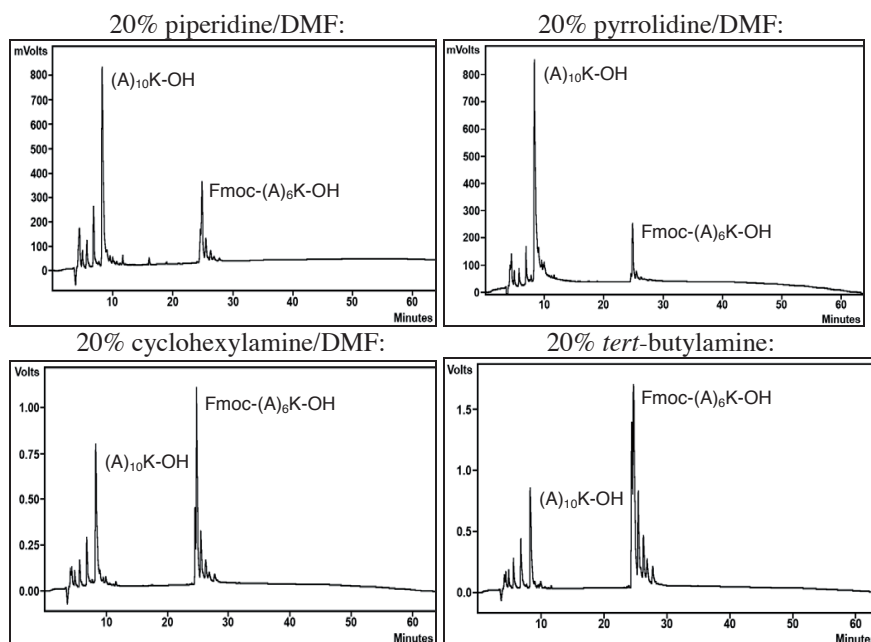


Fig. 1. HPLC results and UV data from the last five cycles of crude (A)₁₀K-OH synthesized on the Prelude[®] and Tribute[®] with UV-monitoring.

Table 1. HPLC percent purities for product (A)₁₀K-OH and Fmoc-(A)₆K-OH peaks and total deprotection repeats and times for the deprotection reagents used in this study.

Deprotection Reagents	A ₁₀ K-OH % Purity	Fmoc-A ₆ K-OH % Purity	Total Dep Reps	Total Dep Time
Piperidine	40.846	13.911	19	29
Pyrrolidine	46.020	9.033	14	14
Cyclohexylamine	24.432	28.522	35	88
<i>tert</i> -Butylamine	11.877	30.586	40	107

20% pyrrolidine produced a higher purity product with fewer repetitions and shorter deprotection times than piperidine. It was the only deprotection reagent in this study proven through UV-monitoring data to be as or even more efficient than piperidine. Based on these results, pyrrolidine may be an effective substitute for piperidine when controlled substances cannot be used.

References

- [1] Brown, L.Y.; Brown, S.A. *TRENDS in Genetics* **2004**, *20*, 51-58.
- [2] Forood, B.; Prez-Pay, E.; Houghten, R.A.; Blondelle, S.E. *Biochem. Biophys. Res. Comm.* **1995**, *211*, 7-13.
- [3] Blondelle, S.E.; Forood, B.; Houghten, R.A.; Prez-Pay, E. *Biochemistry* **1997**, *36*, 8393-8400.

Cyclolinopeptide A analogs modified with pipercolic acid

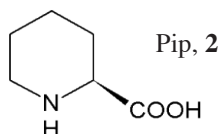
J.Olejniak¹, P. Kossakowska¹, K.Huben¹, J. Artym², M. Zimecki²,
J. Zabrocki^{1,3}, S. Jankowski¹

¹Institute of Organic Chemistry, Faculty of Chemistry, Lodz University of Technology,
Żeromskiego 116, 90-924 Łódź, Poland; ²Institute of Immunology and Experimental
Therapy, Polish Academy of Sciences, R. Weigla 12, 53-114 Wrocław, Poland; ³Peptaderm
Inc., Krakowskie Przedmieście Str.13, Warsaw, Poland

e-mail: stefan.jankowski@p.lodz.pl

Introduction

Immunosuppressors, such as Cyclosporine A (CsA) and Tacrolimus^R, are routinely used in prevention of graft rejection after organ transplantation and in therapy of some autoimmune diseases, including skin inflammation. A naturally occurring in linseed oil Cyclolinopeptide A (CLA, c(-Pro-Pro-Phe-Phe-Leu-Ile-Ile-Leu-Val) **1** [1] possesses a strong immunosuppressive activity, comparable at low doses with that of CsA [2], but is much less toxic. It has been suggested that the tetrapeptide sequence **Pro-Pro-Phe-Phe** is responsible for the interaction of the CLA molecule with the proper cellular receptor [3]. We synthesized new linear **1L**, **2L** and cyclic **1C**, **2C** CLA analogues, containing instead of one proline residue its six-membered mimics, pipercolic acid (Pip, **2**).



1C (-Leu-Ile-Ile-Leu-Val-**Pip**⁶-Pro-Phe-Phe)
2C (-Leu-Ile-Ile-Leu-Val-Pro-**Pip**⁷-Phe-Phe)
1L Leu-Ile-Ile-Leu-Val-**Pip**⁶-Pro-Phe-Phe
2L Leu-Ile-Ile-Leu-Val-Pro-**Pip**⁷-Phe-Phe

Results and Discussion

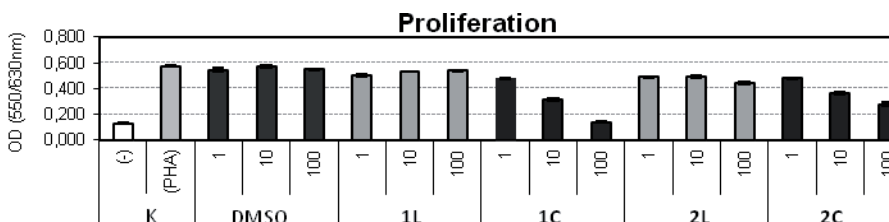
The linear peptides **1L**, **2L** were synthesized by the manual solid-phase method using chloromethylated Merrifield resin as a solid support. Standard N-Boc-protected amino acids and Boc-L-homoproline **2** were obtained from commercial sources. Starting with 0.2 mmol (0.65 mg/mol Boc-Phe-P) of resin the protected amino acids were added in a stepwise fashion to the growing peptide chain. Amino acids were coupled in a 3-fold excess using TBTU/HOBt (or HATU/HOAt) in the presence DIPEA in DCM. Removal of the Boc-protecting group was 50% (v/v) TFA in DCM. The peptides were cleaved from the resin with TFMSA/TFA with anisole added as scavenger. The resin was filtered and washed with TFA and the peptides were precipitated with anhydrous ethyl ether.

The crude linear peptides obtained in solid form by lyophilization from acetic acid were cyclized (HATU/HOAt/DIPEA) in DMF [4,5] with using an infusion pump.

Crude cyclic peptides **1C**, **2C** were purified by preparative reversed phase HPLC on Kromasil C8 column. The purity of the linear and cyclic peptides were checked by analytical HPLC (purity >98 %) and their structures were confirmed by MALDI-MS.

The peptides were devoid of toxicity up to 100µg/ml with regard to human peripheral blood mononuclear cells PBMC, and did not inhibit TNF-α production in blood cell culture at

the 1-25 μ g/ml concentration range. **1C** exhibited dose-dependent, anti-proliferative actions for PHA-activated PBMC (45% and 75% inhibition at 10 μ g/ml and 100 μ g/ml, respectively). **2C** was less inhibitory (13% and 49% inhibition, respectively). **1L** and **2L** had, in turn, no significant effects on PHA-induced cell proliferation. Because of its strong anti-proliferative activity **1C** was tested for growth inhibition of L-1210 lymphatic leukemia. The peptide was found to strongly inhibit the cell growth even at low concentration (63% inhibition at 5 μ g/ml).



Conclusions: **1C** compound might be of interest as a strong anti-proliferative agent (transplantation, anti-cancer therapy).

The one- and two-dimensional ^1H NMR spectra were recorded in DMSO- d_6 on a Bruker Avance II Plus spectrometer at 700 MHz within the temperature range 300 – 340 K. Proton assignments were based on TOCSY, ROESY, ^1H - ^{13}C and ^1H - ^{15}N HSQC experiments.

The different temperature effects on ^1H NMR spectra of **1C** and **2C** were found. Spectrum of **1C** at 300 K exhibited broad signals characteristic for the conformational flexibility. Signals became narrower when temperature increased and at 340 K well resolved spectrum was recorded. The opposite temperature effect was observed for peptide **2C**.

The inspection of the NH region revealed the presence of one isomer **1C** or two isomers **2C**. For peptide **1C** all *trans* geometry of peptide bonds were found. Peptide **2C** is a mixture of two isomers due to *cis-trans* isomerisation of Pro-Pip peptide bond: isomer *trans* (63%) and *cis* (37%). The low temperature coefficients (<3 ppb/K) of NH protons shifts, characteristic for the presence of intramolecular hydrogen bonds, were found only for peptide **1C** (NH (Leu⁵, Ile⁶ and Val⁹)).

Conclusions: CLA analogue **2C** containing pipercolic acid in position 7 is more flexible than **1C** peptide, which is additionally stabilized by three intramolecular hydrogen bonds $\text{NH}\cdots\text{O}=\text{C}$. For **2C** any hydrogen bonding was detected.

Peptide **1C** consist one isomer with all *trans* peptide bonds. Peptide **2C** exists as a mixture of two isomers due to *cis/trans* isomerization of the Pro-Pip peptide bond (*trans* -67%).

Acknowledgement

This project was supported by National Science Center grant N N405 424239.

References

- [1] Kaufmann H. R.; Tobschirbel A.; *Chem.Ber.* **1959**, 92, 2805
- [2] Wieczorek Z.; Bongtsson B.; Trojnar J.; Siemion I. Z.; *Pept. Res.* **1991**, 4, 275
- [3] Siemion I. Z.; Pędyczak A.; Strug I.; Wieczorek Z.; *Arch. Immunol. Ther. Exp.* **1994**, 42, 459
- [4] Vojkovsky T.; *Pept.Res.* **1995**, 8, 236
- [5] Li P.; Roller P. P.; *Curr. Top. Med.* **2002**, 2, 325.

Synthesis of the first Multivalent Epitope containing *N*^ε-(1-deoxy-D-fructosyl)lysyl as diagnostic tool for diabetes

O. Monasson,^{1,2} F. Rizzolo,^{1,2,3} P. Traldi,⁴ A. Lapolla,⁵ M Chorev,⁶
P.Rovero,^{1,3} A.M. Papini^{1,2,3}

¹Laboratory of Peptide & Protein Chemistry & Biology - PeptLab - www.peptlab.eu; ²SOSCO - EA4505 Université de Cergy-Pontoise, 5 mail Gay-Lussac, Neuville-sur-Oise, Cergy-Pontoise 95031, France; ³ Department of Chemistry "Ugo Schiff", Via della Lastruccia 3/13, Polo Scientifico e Tecnologico, University of Firenze, I-50019 Sesto Fiorentino, Italy; ⁴CNR ISTM, Corso Stati Uniti 4, I-35127 Padova, Italy; ⁵University of Padova, Dipartimento Sci. Med. & Chirurg., Via Giustiniani 2, I-35128 Padova, Italy, ⁶ Laboratory for Translational Research, Harvard Medical School, Cambridge, MA 02139, USA. Department of Medicine, Brigham and Women's Hospital, Boston, MA 02115, USA

E-mail:Olivier.monasson@u-cergy.fr

Introduction

Advanced Glycation Endproducts (AGEs) result of a sequence of chemical reactions following the initial non-enzymatic glycation on sequence specific free amino terminal or *N*^ε-amino groups of Lys/Arg side chains (Figure 1). AGEs are prevalent in the diabetic vasculature and contribute to the development of vascular complications, such as atherosclerosis, retinopathy, and nephropathy particularly in the autoimmune type 1 diabetes.[1] AGEs are known to play a role as proinflammatory mediators as well as in gestational diabetes, possibly by contributing to the formation of cross-links causing permanent damages in proteins affecting irreversibly their physiological role.

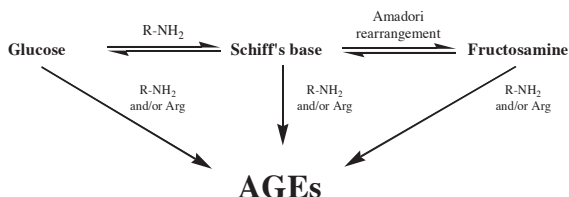


Figure 1. Pathways for AGEs formation.

Moreover, proteins modified by AGEs can generate neoantigens, which are recognised by the immune system as non-self. As a consequence, autoantibodies to non-self AGE-cross-linked proteins could play a role in vascular complications of diabetes. Our goal is to develop fully characterised Multivalent Epitopes (MEps) mimicking specific AGEs to detect anti-AGEs autoantibodies in sera of diabetic patients. The higher affinity of the MEps toward specific autoantibodies can pave the way for using the latter as potential biomarkers for diagnosis, treatment monitoring and prognosis of vascular complications in diabetes.

Results and Discussion

We synthesized MEp 1 by SPPS integrating the building block N^α -Fmoc-Lys[N^ϵ -(2,3:4,5-di-*O*-isopropylidene-1-deoxyfructopyranosyl), N^ϵ -Boc]-OH (Figure 2).[2]

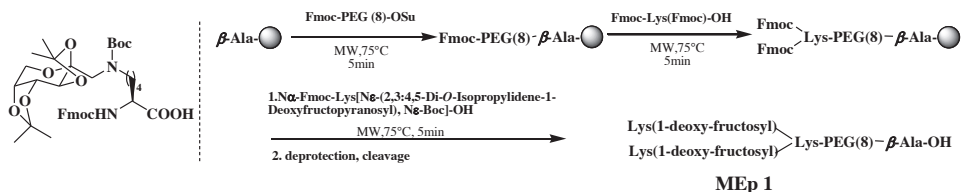


Figure 2. Synthesis of MEp 1.

Synthesis of MEp 1 was performed on preloaded Fmoc- β Ala-Wang resin (0.23 mmol/g, 500 mg) previously swelled in DMF for 30 min. During the coupling cycle, the N-terminal Fmoc-protecting group was removed at room temperature with 20% piperidine in DMF. After coupling Fmoc-PEG(8)-OSu (2.5 equiv) with TBTU (2.5 equiv) in DMF (3mL) and DIPEA (5 equiv), we performed a single coupling of Fmoc-Lys(Fmoc)-OH (2.5 equiv) by TBTU (2.5 equiv) in DMF (3mL) and DIPEA (5 equiv). Finally we introduced the building block N^α -Fmoc-Lys[N^ϵ -(2,3:4,5-di-*O*-isopropylidene-1-deoxyfructopyranosyl), N^ϵ -Boc]-OH (2.5 equiv) activated with TBTU (2.5 equiv) in DMF (3mL) and DIPEA (5 equiv). All the couplings were performed on a SyroWave (Biotage) at 75°C, 20 Watts for 5 minutes. The final MEp 1 was cleaved from the resin by treatment with TFA/TIS/water solution (2.5 mL, 95:2.5:2.5, v/v/v) for 2 h at room temperature and purified by LC/MS Waters (column Kinetex C18, 2.6 mm 100×3 mm, Phenomenex; 0.8 mL/min 5-50% B (A: H₂O, 0.1% TFA; B: ACN, 0.1% TFA in 5 min; R_t: 4,6 min, m/z: calculated 1220.7, found 1222.7). We obtained 13 mg (9%) of the pure MEp 1.

Purified MEp 1 will be tested by SP-ELISA for its capacity to bind autoantibodies from sera of diabetic patients.

Acknowledgments

This work was supported by ANR Chaire d'Excellence 2009-2013 (AMP).

References

- [1] Ahmed N, Mirshekar-Syahkal B, Kennish L, Karachalias N, Babaei-Jadidi R, Thornalley PJ. *Mol Nutr Food Res* **2005**; 49: 691-699.
- [2] Carganico S, Rovero P, Halperin H.A, Papini A.M., Chorev M. *J.Pept.Sci.* **2009**, 15, 67-71.

Enantiopure trifluoromethylated pseudoprolines: Synthesis and incorporation in small peptides

Julien Pytkowicz, Julien Simon, Nathalie Lensen, Evelyne Chelain,
Grégory Chaume, Thierry Brigaud*

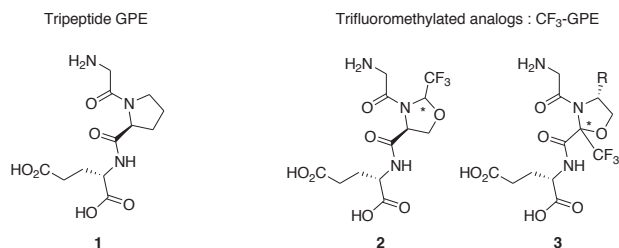
Laboratoire SOSCO, Université de Cergy-Pontoise, 5, mail Gay Lussac, 95000 Cergy-
Pontoise, France

E-mail: julien.pytkowicz@u-cergy.fr

Introduction

The endogenous tripeptide GPE **1** also named “Glypromate” is made up by the three *N*-terminal residues (glycine-proline-glutamate) of the insulin-like growth factor 1 (IGF1). This tripeptide is a partial glutamate antagonist and showed good results in different neuroprotective *in vitro* and *in vivo* experiments.[1,2] GPE also binds to glial cells regulating neurotransmitter levels in the brain.[3,4] However, GPE suffers from poor lipophilicity and a short half-life *in vivo*. That’s why there is a need for more lipophilic and protease resistant analogues of GPE.

We present here the synthesis of the trifluoromethylated analogues **2** and **3** based on the 2 or 5-CF₃-pseudoproline residues.



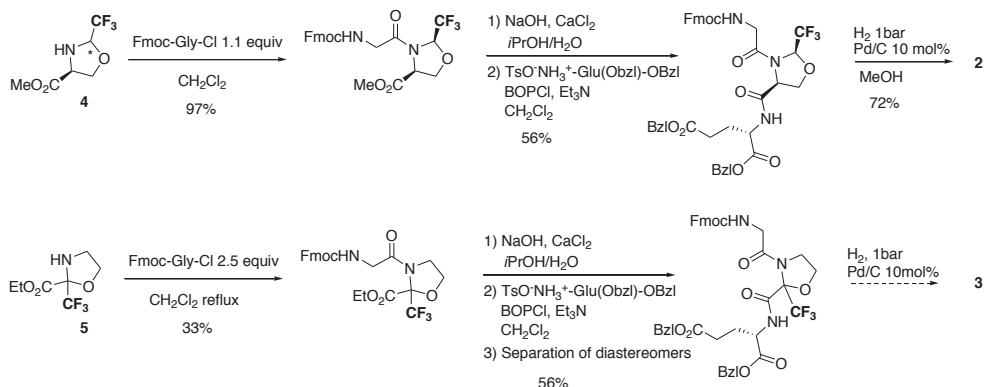
Introduction of fluorine atoms on bioactive compounds is known to deeply modify their physico and biochemical properties increasing lipophilicity and resistance to protease.[5] Thus, developing a trifluoromethylated analogues, we intend to increase the bioavailability of GPE, keeping the benefit of its neuroprotective properties.

Our research team is strongly involved in the synthesis of trifluoromethylated alpha-amino acids. Recently we published the synthesis of 2-trifluoromethyl-1,3-oxazolidines derived from fluoral and (*L*)-serine and we demonstrated that these five membered ring 5-CF₃-pseudoprolines are hydrolytically stable and can be considered as proline analogues.[6] That’s the reasons why we are interested to replace the proline residue of GPE by those trifluoromethylated compounds.

Results and Discussion

CF₃-pseudoproline **4** was readily synthesized from commercially available fluoral hemiacetal and boc-protected serine methyl ester. The heterocycle was obtained as a

mixture of two diastereomer used without separation in the subsequent coupling reaction. The strongly deactivated nitrogen of the pseudoproline necessitated the activation of the Fmoc-protected glycine by the formation of its acylchloride. Optimized base free conditions led to the single *cis* diastereomer of the pseudo-dipeptide in excellent yield. After a smooth saponification of the methyl ester to avoid the deprotection of the Fmoc-protecting group, the benzyl-protected glutamate was coupled using standard reagents. A complete deprotection of the pseudo-tripeptide was finally performed using catalytic hydrogenolysis. Starting from racemic 2-CF₃-pseudoproline **5**, derived from ethanolamine and ethyl trifluoropyruvate, the same sequence led to the formation of two diastereomer of the protected pseudo-tripeptide. Hopefully, these two diastereomer could be separated by standard silica-gel chromatography. The deprotection conditions used for **2** should give us soon the free pseudo-tripeptide **3**.



In vitro and *in vivo* biological studies will now be conducted on these trifluoromethylated GPE analogues to precise the role of such a fluorinated functionality toward lipophilicity and protease resistance.

Acknowledgments

The authors thank Central Glass Company for the generous gift of fluoral and financial support and J-B Pytkowicz for the optimization of the tripeptide synthesis.

References

- [1] Saura, J.; Curatolo, L.; Williams, C. E.; Gatti, S.; Benatti, L.; Peeters, C.; Guan, J.; Dragunow, M.; Post, C.; Faull, R. L. M. *Neuroreport*. **1999**, *10*, 161-164.
- [2] By Guan, J.; Waldvogel, H. J.; Faull, R. L. M.; Gluckman, P. D.; Williams, C. E. *Neuroscience*. **1999**, *89*, 649-659.
- [3] Sizonenko, S. V.; Sirimanne, E. S.; Williams, C. E.; Gluckman, P. D. *Brain Res*. **2001**, *922*, 42-50.
- [4] Guan, J.; Thomas, G. B.; Lin, H.; Mathai, S.; Bachelor, D. C.; George, S.; Gluckman, P. D. *Neuropharmacology* **2004**, *47*, 892-903.
- [5] Begue, J.-P., Bonnet-Delpon, D., Eds. *Bioorganic and Medicinal Chemistry of Fluorine*; Wiley: New York, **2008**.
- [6] Chaume, G.; Barbeau, O.; Lesot, P.; Brigaud, T. *J. Org. Chem.* **2010**, *75*, 4135-4145.

FastBoc synthesis of ACP (65-74) using preactivation on the Overture™ robotic peptide library synthesizer

James P. Cain, Christina A. Chantell, Michael A. Onaiyekan,
Mahendra Menakuru

Protein Technologies, Inc. Tucson, Arizona, 85714

E-mail: info@ptipep.com

Introduction

FastBoc chemistry (or *in situ* neutralization in Boc solid-phase peptide synthesis) was first popularized in 1992 by Kent and Alewood as a way to perform up to 3 couplings an hour or 75 couplings a day [1]. It did this by removing the extra washing and pre-coupling neutralization steps, using high reagent concentrations for shorter reaction times, and flow washes. The use of a single-solvent (DMF) throughout the synthesis maximized the solvation of the peptide-resin, resulting in higher reaction efficiencies best observed during difficult couplings. The original work produced one peptide manually, or using a single-channel automated peptide synthesizer, custom-modified to perform this chemistry but not available commercially in this configuration. The 96-channel Overture™ is the first commercially available robotic peptide library synthesizer to offer preactivation. With the preactivation option, up to 48 channels may be used as preactivation chambers for the remaining 48 reactors. This new innovation allows the Overture™ to perform FastBoc chemistry (which relies on preactivation of the incoming amino acid with coupling agent and base) on up to 48 reaction vessels at a time. In this poster, we demonstrate how just one block pair of 16 reaction vessels can perform ~3 x 16 couplings an hour, or an unprecedented 64 x 16 couplings per day.

To demonstrate FastBoc chemistry on the Overture™, we have synthesized the well-known difficult sequence ACP (65-74) one of the peptides reported in the first description of *in situ* neutralization chemistry (Figure 1).

Val-Gln-Ala-Ala-Ile-Asp-Tyr-Ile-Asn-Gly-OH

Fig. 1. Difficult sequence synthesized using in situ neutralization Boc chemistry with preactivation on the Overture™ Robotic Peptide Library Synthesizer

Results and Discussion

ACP (65-74) was synthesized on an Overture™ Robotic Peptide Library Synthesizer using the FastBoc *in situ* neutralization protocol and preactivation. Sixteen peptides were synthesized using 2 minute deprotection times and 10 minute coupling times resulting in a cycle time of 22.5 minutes and a total synthesis time of ~3.3 hours. The resulting crude peptides had an average purity of 73% and all displayed the correct molecular mass found by LC-MS, demonstrating the efficiency of this protocol even for a relatively difficult sequence like ACP (65-74). HPLC profiles of several representative crude peptides resulting from synthesis, HF cleavage, and lyophilization are shown in Figure 2. These

results are comparable to those previously demonstrated for Fmoc protocols using 20 minute double coupling and highly efficient activators such as HATU (80%), COMU (78%), or HDMC (76%) [2]. The favorable results, despite using a 10 minute single coupling and the less active HBTU, may in part be attributed to the enhancement of peptide-resin solvation in the TFA salt form.

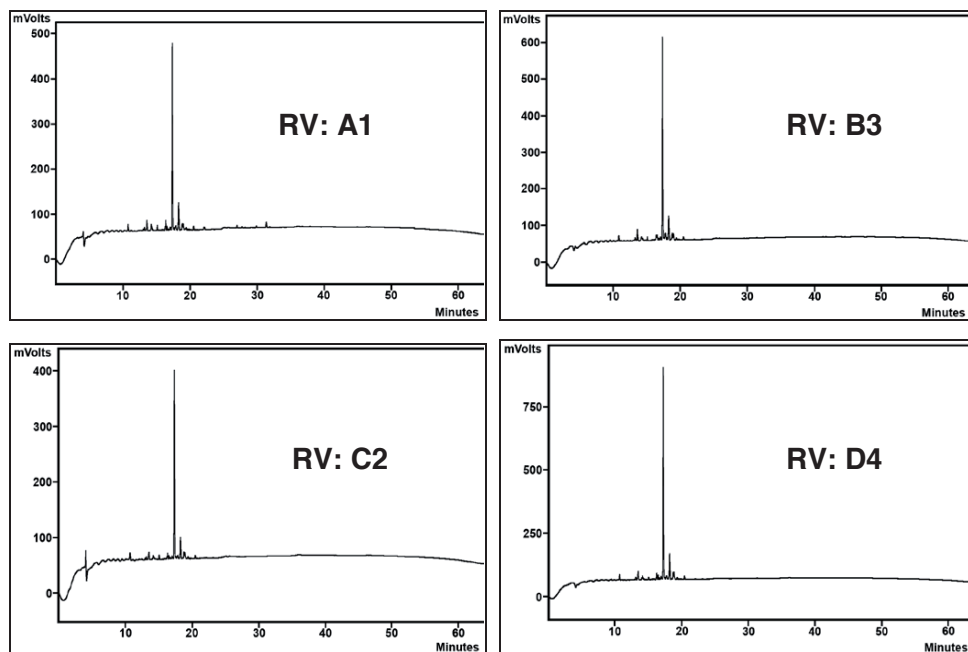


Fig. 2. HPLC traces of several representative crude ACP (65-74) peptides.

Acknowledgments

The authors would like to gratefully acknowledge Dr. Nabila Brabez and Dr. Victor Hruby of the University of Arizona Department of Chemistry for their gracious assistance with the HF cleavage of the peptide.

References

- [1] Schnolzer, M.; Alewood, P.; Jones, A.; Alewood, D.; Kent, S.B.H. *Int. J. Pept. Prot. Res.* **1992**, *40*, 180-193.
- [2] Chantell, C.A.; Onaiyekan, M.A.; Menakuru, M. *J. Pept. Sci.* **2012**, *18*, 88-91.

Resin via click chemistry to apply in SPPS

Vida Castro,^{a,b} Hortensia Rodriguez,^{a,b} Fernando Albericio^{a,b,c,d}

^aInstitute for Research in Biomedicine, 08028-Barcelona, Spain. ^bCIBER-BBN, Networking Centre on Bioengineering, Biomaterials and Nanomedicine, PCB, 08028-Barcelona, Spain;

^cDepartment of Organic Chemistry, University of Barcelona, 08028-Barcelona, Spain;

^dSchool of Chemistry, University of KwaZulu- Natal, South Africa

E-mail : vida.castro@irbbarcelona.org

Introduction

Solid-phase linkers for the preparation of peptides and other organic molecules are based mostly on the presence of alkoxy phenyl moieties. At the end of the synthetic process, these resins are treated with TFA to release the target molecules, thereby rendering carboxylic acids or amides. However, this acid treatment could cause extra cleavages through the amide bond used to anchor the linker to the solid support and/or through the phenoxy moiety present in the linker. These side-products can be difficult to remove from the crude product or, worse still, can back-alkylate the cleaved peptide at sensitive residues, such as Trp or Tyr. This back-alkylation, in addition to jeopardizing the purification, decreases the final yield. To circumvent this problem, some non-acid degradable linkers have been developed. These linkers are characterized by activation of the benzyl alcohol by a non-cleavable electron-donating group in either the *ortho* or *para* position,[1] and by two phenyl rings attached by a Suzuki reaction.[2] On the other hand, copper-catalyzed azide-alkyne cycloaddition (CuAAC) assisted Solid Phase Synthesis (SPS) has been used to obtain cyclic peptides,[3] triazolyl aminoacyl (peptidyl) penicillins,[4] and aldehyde-functionalized resins.[5] Peptides with a triazole moiety inside their structures are less susceptible to attack by hydrolytic enzymes and esterases, and can be assessed against different pharmacological targets.[3,4] Also, the CuAAC strategy has been used as a modular method for attaching Cell-Penetrating Peptides (CPPs) to bioactive peptides and for immobilizing the first generation MacMillan catalyst onto a polystyrene resin and Fe₃O₄ magnetic nanoparticles.[6]

Here we report a novel concept linker be used in SPS This linker has two unique features, namely methoxy groups are the only activating groups of the phenyl ring and the linker is anchored to the solid support through a triazol scaffold via Click chemistry (CuAAC).

Results and Discussion

We developed a resin through copper-catalyzed azide-alkyne cycloaddition (CuAAC) via Click Chemistry reaction and applied it to SPPS. The previous transformation and the Click Chemistry reaction progress were followed by IR spectrometry. This resin is more acid stable than Wang resin, avoiding side alkylation reaction reported to the Wang resin.[2] Moreover, this resin was more efficient than Wang resin for SPPS. We synthesized three model peptides. The results show higher yields and similar purities in comparison with the same peptides synthesized on Wang resin.

In conclusion, we have developed novel resin via Click Chemistry reaction and applied to SPPS.

Acknowledgments

This work was partially supported by Fellowship Marie Curie Initial Training Networks (ITN) MEMTIDE Project: FP7-PEOPLE_ITN08, the Institute for Research in Biomedicine (IRB) and the Barcelona Science Park (PCB).

References

- [1] Gu, W.; Silverman, R., B. *Org. Lett.* **2003**, *5*, 415.
- [2] Colombo, A.; De la Figuera, N.; Fernández, J., C.; Fernández-Fornier, D.; Albericio, F.; Forns, P. *Org. Lett.* **2007**, *9*, 4319.
- [3] Metaferia, B., B.; Rittler, M.; Gheeya, J., S.; Lee, A.; Hempel, H.; Plaza, A.; Stetler-Stevenson, G.; Bewley, C., A.; Khan, J. *Bioorg. Med. Chem. Lett.* **2010**, *20*, 7337.
- [4] Cornier, P., G.; Boggáin, D., B.; Mata, E., G. *Tetrahedron Lett.* **2012**, *53*, 632.
- [5] Lober, S.; Rodríguez-Loaiza, P.; Gmeiner, P. *Org. Lett.* **2003**, *5*, 1753.
- [6] Riente, P.; Yadav, J.; Pericàs, M., A. *Org. Lett.* **2012**, *14*, 3668.

Fully automated click cyclization of a cancer-targeting peptide on the Prelude[®] peptide synthesizer

James P. Cain, Michael A. Onaiyekan, Christina A. Chantell,
Mahendra Menakuru

Protein Technologies, Inc. Tucson, Arizona, 85714

E-mail: info@ptipep.com

Introduction

The copper-catalyzed azide-alkyne cyclization (CuAAC), the most commonly recognized variant of “click chemistry,” has emerged as a powerful technique for ligation, conjugation, and cyclization reactions of peptides. It is known that cyclization can increase the metabolic stability of peptides, as well as enhancing potency or selectivity by stabilizing an active conformation. One application of the CuAAC that has generated interest is the use of this reaction to replace a disulfide bridge with the product triazole, which among other complementary properties may prevent *in vivo* redox chemistry. In a recent example, a novel cyclic NGR peptide analogue was synthesized on resin via click chemistry [1]. Small peptides containing the NGR motif have generated interest in drug delivery research, as ligands containing this sequence seem to bind preferentially to a CD13 isoform expressed in tumor vasculature rather than normal tissue [2]. In this application, we synthesize a new analogue of the cyclic cancer-targeting peptide CNGRC where we replace the disulfide bond with a triazole linkage using click chemistry (Figure 1) and a fully automated, on-resin method using the Prelude[®] peptide synthesizer. We modified a convenient method that has been described for performing the cyclization, using 20% piperidine in DMF as the only base in the reaction mixture [3].

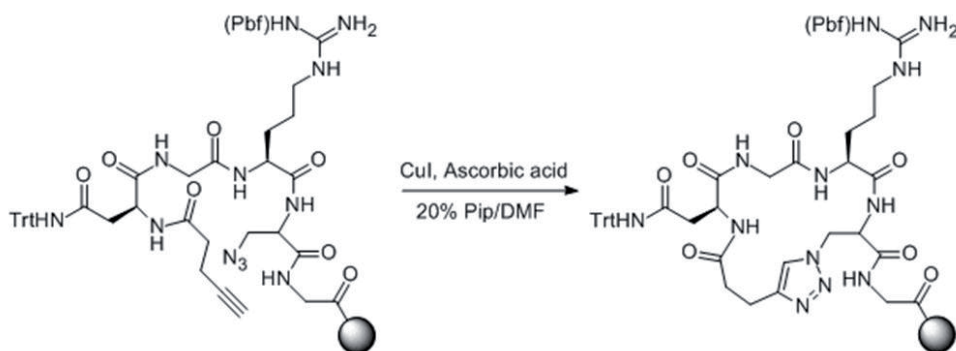


Fig. 1. Click Reaction

Results and Discussion

The linear NGR peptide, flanked by pentynoic acid at the N-terminus and azidoalanine-glycine at the C-terminus, was synthesized using an unoptimized protocol in 78% purity. After treating the peptidyl-resin with CuI and ascorbic acid in 20% piperidine/DMF

solution, a clear shift in the retention time of the major peak from 10.1 min to 6.9 min was observed in the HPLC trace (Figure 2), indicating that the cyclization reaction was successful. The product was found with 76% purity.

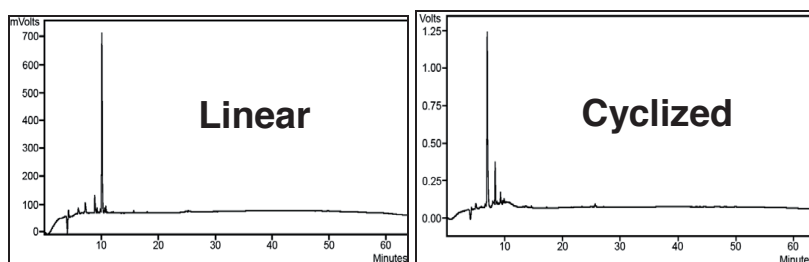


Fig. 2. HPLC traces of the linear and cyclized peptide.

We have demonstrated that the CuAAC click reaction can be fully automated by synthesizing a novel cyclic cancer-targeting NGR peptide containing a triazole linkage on the Prelude[®] peptide synthesizer. The Prelude[®]'s Single-Shot[™] delivery feature was used to deliver expensive special monomers and reagents without priming or wasting a drop.

References

- [1] Metaferia, B.B. *et al. Bioorg. Med. Chem. Lett.* **2010**, *20*, 7337-7340.
- [2] Corti A.; Cumis F.; Arap W.; Pasqualini R. *Blood* **2008**, *112*, 2628-2635.
- [3] Zhang Z.; Fan E. *Tetrahedron Lett.* **2006**, *47*, 665-669.

Manufacture of optically active D-allo-threonine from L-threonine by ARCA technology

**Eui Sung Jeong,¹ Juwan Maeng,¹ Yun Soo Ahn,² Mi-ran Kim,²
Kwan Mook Kim,³ Heungsik Yoon,¹ Hyunil Lee^{*,1}**

¹*Aminologics R&D Center, Unit 1102 Sicox Tower, 513-14 Sangdaewon-Dong, Jungwon-Gu, Seongnam-Si, Gyunggi-Do, Korea;* ²*Aminolux R&D Center, Unit 1101 Sicox Tower, 513-14 Sangdaewon-Dong, Jungwon-Gu, Seongnam-Si, Gyunggi-Do, Korea;* ³*Department of Chemistry and Nano Science (BK21), Ewha Womans University, Seoul 120-750, Korea*

** corresponding author. E-mail:hilee@aminologics.co.kr*

Introduction

Unnatural amino acids including D-amino acids are manufactured mainly by the enzymatic process. However, one enzyme can produce only one amino acid due to its high specificity and it takes a long time and lots of expenses to develop the appropriate enzyme itself. ARCA (Alanine Racemase Chiral Analogue) is an organic catalyst¹ which can overcome these drawbacks and can produce almost all kinds of amino acids efficiently.

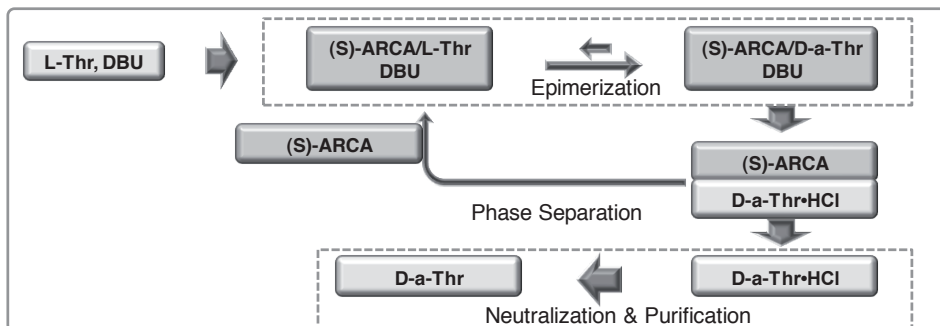
D-allo-threonine is one of four stereoisomers of threonine, which is useful for the syntheses of biologically active compounds^{2a-d} - depsipeptides or peptides, but there are a few methods³ to synthesize it. Using ARCA technology, D-allo-threonine can be easily manufactured from L-threonine. The amine functionality of L-threonine is freely reacted with the aldehyde group of ARCA to form the corresponding imine, which is easily epimerized in the presence of organic base due to the acidity of the α -proton of imine. The difference in the stability between the imines of the optical epimers rendered them to be shifted to D-allo-threonine derivative dominantly. Once the epimerization reaction reached equilibrium, the reaction mixture was hydrolyzed under acidic condition to give D-allo-threonine and ARCA, which could be recycled repeatedly without significant loss in yield or purity to produce more D-allo-threonine from L-threonine in excellent yields. Optimization of the reaction conditions with various bases and solvents is discussed and mass production of optically active D-allo-threonine including optical purification is described. The manufacturing process for the preparation of ARCA will be shared as well.

Results and Discussion

Synthesis of (S)-ARCA : (S)-ARCA was synthesized by the five step reactions from 3-hydroxy-2-naphthoic acid and 2-naphthol in 14% yield. The purity of (S)-ARCA was over 99% and 99.5%ee. All the intermediates and product are easily purified by recrystallization in an appropriate solvent. All the processes are scalable and the yields are moderate to good.

Synthesis of D-allo-threonine : L-Threonine can be easily converted to D-allo-threonine by the reaction with (S)-ARCA in the presence of organic base. The solution of L-threonine, (S)-ARCA and organic base in dichloromethane (DCM) is stirred to form corresponding schiff base, and epimerization is occurred simultaneously. The resulting schiff base is mainly converted to that of D-allo-threonine. Then the schiff base is hydrolyzed with

aqueous HCl solution, and the resulting amino acid is transferred to aqueous layer. Aqueous layer is separated and followed by neutralization & purification to give enantiomerically pure D-allo-threonine (>99.5%ee). Organic layer can be recovered and reused repeatedly without any other purification. The organic base, amount of solvent and the purification process was optimized.



The most effective and economic organic base was 1,8-diazabicycloundec-7-ene (DBU) considering the reaction rate and D ratio of the corresponding shift base. And the optimum volume of the solvent was 15 mL/g based on the amount of (S)-ARCA. Also, the molar equivalents of L-threonine between 0.8 and 0.95 were compared and 0.9eq was optimum amount. After hydrolysis with aq. HCl, the aqueous layer was separated and neutralized with 50% aq. NaOH to adjust pH = 6. Methanol as an antisolvent, was added and crude D-allo-threonine was precipitated in 72% yield (optical purity > 99.5%ee). To remove the incorporated inorganic salt, the crude product was suspended in the mixture of water and methanol (7/10, 17 mL/g based on the crude product), refluxed for 1h and cooled to room temperature, followed by filtration to give pure D-allo-threonine in 90% yield.

The manufacturing process of D-allo-threonine by ARCA technology is simple and scalable, which is composed of epimerization, phase separation and recrystallization. The synthetic parameters were optimized suitable for large scale production. Using this process, 760 Kg of D-allo-threonine was produced with high purity (>99%, 99.8%ee) in 54% yield. The recyclability of (S)-ARCA was confirmed by reusing 30 times.

Acknowledgments

This Research was financially supported by WPM (World Premier Materials) program from Korean MKE (Ministry of Knowledge Economy)

References

- [1] a) Park, H.; Kim, K.M. ; Lee, A. ; Ham, S. ; Nam, W. ; Chin, J. *J. Am. Chem. Soc.* **2007**, *129*, 1518. b) Kim, K.M. ; Park, H. ; Kim, H.-J. ; Chin, J. ; Nam, W. *Org. Lett.*, **2005**, *7* (16), 3525.
- [2] a) Cruz, L.J. ; Luque-Ortega, J.R. ; Rivas, L. ; Albericio, F. *Mol. Pharmaceutics* **2009**, *6* (3), 813. b) Zlatopolskiy, B.D. ; Meijere, A. *Chem. Eur. J.* 2004, *10*, 4718. c) Okanoya, J.F. ; Kolasa, T. ; Miller, M.J. *J. Org. Chem.* **1995**, *60*, 1932. d) Walker, S. ; Chen, L. ; Hu, Y. ; Rew, Y. ; Shin, D. ; Boger, D.L. *Chem. Rev.* **2005**, *105*, 449
- [3] Shiraiwa, T. ; Fukuda, K. ; Kubo, M. *Chem. Pharm. Bull.* **2002**, *50*(2) 287.

Methodological study of the peptide coupling of *N*-deactivated proline surrogate trifluoromethylated pseudoprolines

Grégory Chaume,¹ Debby Feteyns,² Philippe Lesot,³ Emeric Miclet,²
Solange Lavielle,² Gérard Chassaing,² Thierry Brigaud¹

¹Laboratoire SOSCO, EA 4505, Université de Cergy-Pontoise, 95000 Neuville/Oise,
France; ²Laboratoire des BioMolécules, UMR 7203, Université Pierre et Marie Curie,
75005 Paris, France; ³RMN en Milieu Orienté, ICMMO, UMR CNRS 8182, Université
Paris Sud 11, 91405 Orsay, France

E-mail: gregory.chaume@u-cergy.fr

Introduction

Incorporation of proline derivatives is known to restrict the Xaa-Pro *cis/trans* isomerization, to limit the protein folding and consequently to modulate the biological activity of peptides. Based on these observations, Mutter's group introduced pseudoproline building blocks (Ψ Pro) into a peptide sequence as reversible protecting groups for Ser, Thr and Cys [1]. Ψ Pro proved to be a versatile tool for overcoming the aggregation encountered during SPPS and to induce β -turns containing predominantly *cis*-amide bond [2]. Our group develops efficient synthetic routes for the preparation of enantiopure α -trifluoromethylated amino acids (α -Tfm-AAs) [3] and their incorporation into a peptide chain [4]. α -Tfm-AAs are very attractive compounds for the design of biologically active molecules, particularly peptides, due to the unique properties impart by the CF₃ group [5]. In the course of our study, we developed an efficient preparation of various CF₃- Ψ Pro [6] and we recently reported their ability to control both the *cis/trans* isomerization and the backbone dihedral angles on tripeptide mimics [7]. Here, we present a methodological study allowing the incorporation of CF₃- Ψ Pro in peptide chains.

Results and Discussion

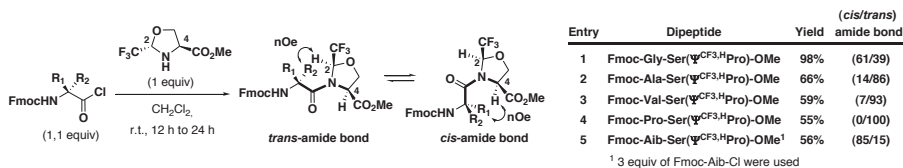
We first studied the experimental conditions allowing the peptide coupling reaction at the C-position. Starting from CF₃- Ψ Pro methyl esters, a saponification followed by a peptide coupling reaction using standard reagents afforded the corresponding dipeptides in moderate to good yields depending of the stereochemistry of the CF₃- Ψ Pro (Scheme 1). As already reported, no protection of the CF₃- Ψ Pro amino group is required since the presence of the neighboring CF₃ group decreased the nucleophilicity of the amine function [4].



Scheme 1 : Peptide coupling reaction at the C-position of CF₃- Ψ Pro

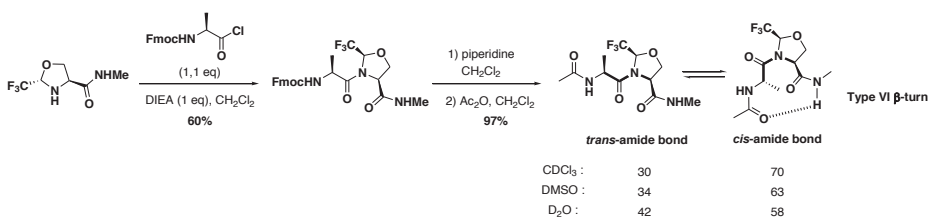
Peptide coupling reactions at *N*-position of CF₃- Ψ Pro required substantial activation to offset the low nucleophilicity of the amino group. The use of a stoichiometric amount of

various Fmoc-amino acid chlorides in base free condition afforded the corresponding dipeptides with a complete epimerization at C₂ center (Scheme 2). Increase of the steric hindrance of the alkyl chain of the amino acid decreased both the yield and the *cis/trans* amide bond ratio (entry 1-3). Coupling of proline or amino isobutyric acid (Aib) residue gave respectively a complete *trans*-amide bond (entry 4) and *cis*-amide bond (entry 5) in moderate yields.



Scheme 2 : Peptide coupling reaction at the N-position of CF₃-ΨPro

In order to study the local control of the *cis/trans* isomerization in peptide, we synthesized a CF₃-ΨPro containing tetrapeptide mimic. This model peptide was prepared in two step starting from pseudoproline methyl amide and NMR study showed a type VI β-turn conformation (Scheme 3).



Scheme 3 : NMR study of the *cis/trans* isomerization of model tetrapeptide

Acknowledgments

Debby Feytens is a postdoctoral researcher of the Fund for Scientific Research Flanders (FWO-Vlaanderen). Thierry Brigaud thanks Central Glass Co. for financial support.

References

- [1] Tuhscherer, G.; Mutter, M. *J. Peptide Sci.* **2005**, *11*, 278-282.
- [2] Dumy, P.; Keller, M.; Ryan, D. E.; Rohwedder, B.; Wöhr, T.; *J. Am. Chem. Soc.* **1997**, *119*, 918-925.
- [3] (a) Simon, J.; Nguyen, T. T.; Chelain, E.; Lensen, N.; Pytkowicz, J.; Chaume, G.; Brigaud, T. *Tetrahedron: Asymmetry* **2011**, *22*, 309-314; (b) Caupène, C.; Chaume, G.; Ricard, L.; Brigaud, T. *Org. Lett.* **2009**, *11*, 209-212; (c) Chaume, G.; Van Severen, M.-C.; Marinkovic, S.; Brigaud, T. *Org. Lett.* **2006**, *8*, 6123-6126; (d) Chaume, G.; Van Severen, M.-C.; Ricard, L.; Brigaud, T. *J. Fluorine Chem.* **2008**, *129*, 1104-1109.
- [4] Chaume, G.; Lensen, N.; Caupène, C.; Brigaud, T. *Eur. J. Org. Chem.* **2009**, 5717-5724.
- [5] Kocsch, B.; Sewald, N.; Hofmann, H.-J.; Burger, K.; Jakubke, H.-D. *J. Pept. Sci.* **1997**, *3*, 157-167.
- [6] Chaume, G.; Barbeau, O.; Lesot, P.; Brigaud, T. *J. Org. Chem.* **2010**, *75*, 4135-4145.
- [7] Feytens, D.; Chaume, G.; Chassaing, G.; Lavielle, S.; Brigaud, T.; Byun, B. J.; Kang, Y. K.; Miclet, E. *J. Phys. Chem. B* **2012**, *116*, 4069-4079.

New functionalized aza- β^3 -amino acids for click-chemistry

Shoukri Abbour, Michèle Baudy-Floc'h

UMR CNRS 6226, Université de Rennes 1, Rennes, France

shoukri.abbour@univ-rennes1.fr, michele.baudy-floch@univ-rennes1.fr

Introduction

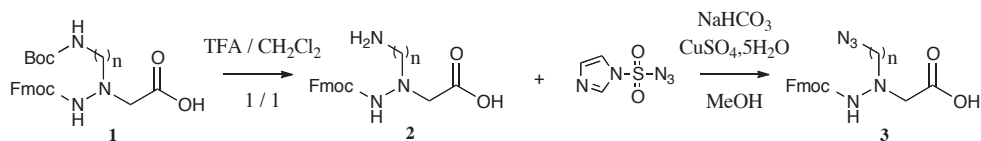
Aza- β^3 -peptides represent an exciting type of peptidomimetics [1]. The aza- β^3 -amino acids are analogs of β^3 -aminoacids in which the CH_α is replaced by a nitrogen atom conferring a better flexibility to the pseudopeptide due to the side chain beared on a chiral nitrogen with non-fixed configuration. The non-natural oligomers have an extended conformational space and are supposed to adopt non-canonical secondary structures [2]. In addition, the backbone modification makes these molecules more stable towards proteolytic degradation [3,4].

The majority of proteins in nature are post-translationally modified, and the most abundant modification is the protein glycolysation, which introduces wide structural variety to proteins. Glycoproteins have an important role in the biological recognition process, such as immunodifferentiation, cell adhesion, cell differentiation and regulation cell growth [5].

New aza- β^3 -amino acids bearing either an azide instead of amine on Lys and Orn chain or an alkyne function will be described in the goal to perform reactions of click chemistry either to cyclize aza- β^3 -peptides or to obtained glycopseudopeptides.

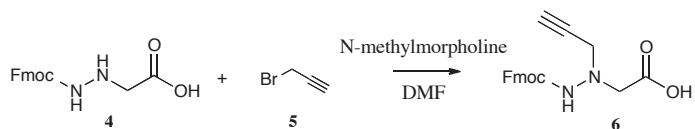
Results and Discussion

We have previously reported a method to prepare N^β -Fmoc-aza- β^3 -amino acids via reductive amination of glyoxylic acid and Fmoc-hydrazine [6]. Taking account of this previous method, it seems interesting to introduce new side-chains with azide or alkyne functions. For that, selective deprotection with trifluoroacetic acid (TFA) of Fmoc-aza- β^3 -Orn(Boc)-OH (**1**, $n=3$) and Fmoc-aza- β^3 -Lys(Boc)-OH (**1**, $n=4$) [6], gave Fmoc-aza- β^3 -Orn-OH (**2**, $n=3$) and Fmoc-aza- β^3 -Lys-OH (**2**, $n=4$) in 90% yield. A diazo-transfer reaction with imidazole-1-sulfonyl azide chloride [8] on the crude amine in presence of CuSO_4 , $5\text{H}_2\text{O}$, NaHCO_3 in methanol afforded respectively Fmoc-aza- β^3 -Orn (N_3)-OH (**3**; $n=3$) or Fmoc-aza- β^3 -Lys (N_3)-OH (**3**; $n=4$) in 40% yield (Scheme 1).



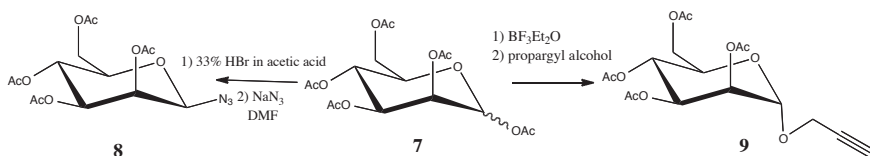
Scheme 1: Fmoc-aza- β^3 -Orn(N_3)-OH (**3**, $n=3$) and Fmoc-aza- β^3 -Lys(N_3)-OH (**3**, $n=4$)

Nucleophilic substitution of propargyl bromoacetate **5** by Fmoc-aza- β^3 -Gly-OH **4** [7] in the presence of *N*-methyl-morpholine in DMF from -15°C to room temperature during 3 days led to Fmoc-aza- β^3 -Pra-OH (**6**) in 54% yield (Scheme 2).



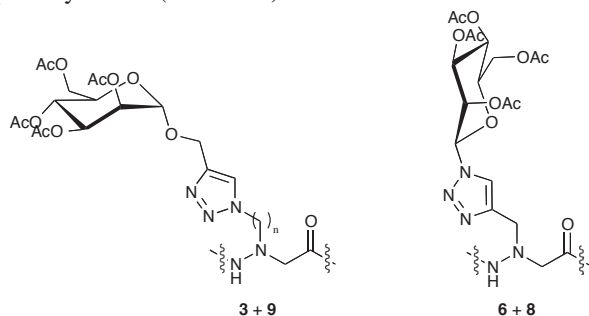
Scheme 2: Fmoc-aza- β^3 -Pra-OH **6**.

On the other hand, two functionalized D-mannose derivatives have been prepared starting from the per-*O*-acetylated D-mannose **7**: compound **8** with the azido group directly attached on the anomeric position of the tetra-acetylated D-mannose and analogs **9** with an acyl function on the anomeric position. The syntheses of these analogs are summarized in Scheme 3, according to strategies described in the literature [9, 10].



Scheme 3: Synthesis of azido and acyl D-mannose

These carbohydrates **8** or **9** could be linked by click chemistry to **6** or **3** respectively either before or after peptide synthesis (Scheme 4).



Scheme 4: Click chemistry between aza- β^3 -amino acids and Functionalized D-Mannose

References

- [1] Busnel, O.; Bi, L.; Dali, H.; Cheguillaume, A.; Chevance, S.; Bondon, A.; Muller, S.; Baudy-Floc'h, M. *J. Org. Chem.* **2005**, *70*, 10701-10708.9
- [2] Cheguillaume, A.; Salaün, A.; Sinbandhit, S.; Potel, M.; Gall, P.; Baudy-Floc'h, M.; Le Grel, P. *J. Org. Chem.* **2001**, *66*, 4923-4929.
- [3] Dali, H.; Busnel, O.; Hoebeker, J.; Bi, L.; Decker, P.; Briand J.P.; Baudy-Floc'h, M.; Muller, S. *Mol. Immunol.* **2007**, *44*, 3024-3036.
- [4] Neveu, C.; Lefranc, B.; Tasseau, O.; Do-Rego, J. C.; Bourmaud, A.; Chan, P.; Bauchat, P.; Le Marec, O.; Chuquet, J.; Guilhaudis, L.; Boutin, J. A.; Ségalas-Millazo, I.; Costentin, J.; Vaudry, H.; Baudy-Floc'h, M.; Vaudry, D.; Leprince, J. *J. Med. Chem.* **2012**, in press.
- [5] Dwek, R. A. *Chem. Rev.* **1996**, *96*, 683-720.
- [6] Busnel, O.; Bi, L.; Baudy-Floc'h, M. *Tetrahedron Lett.* **2005**, *46*, 7073-7075.
- [7] Busnel, O.; Baudy-Floc'h, M. *Tetrahedron Lett.* **2007**, *48*, 5767-5770.
- [8] Tanaka, T.; Nagai, H.; Noguchi, M.; Kobayashi, A.; Shoda, S. *Chem. Commun.* **2009**, 3378-3379, and ref cited.
- [9] Touaibia, M.; Wellens, A.; Shiao, T. C.; Wang, Q.; Sirois, S.; Bouckaert, J.; Roy, R. *ChemMedChem* **2007**, *2*, 1190-1201.

N-Oligoethyleneglycol cyclic peptides

Ana I. Fernández-Llamazares,¹ Jan Spengler,¹ Fernando Albericio^{1,2}

¹ Institute for Research in Biomedicine (IRB Barcelona), Barcelona Science Park, Baldiri Reixac 10, 08028 Barcelona, Spain; ² Department of Organic Chemistry, University of Barcelona, Martí i Franqués 1-11, 08028 Barcelona, Spain

e-mail : anna-iris.fernandez@irbbarcelona.org, fernando.albericio@irbbarcelona.org

Introduction

The potential of peptides as drug candidates is often limited by their pharmacokinetic properties [1]. An approach to increase the bioavailability of peptides is PEGylation, which consists in the covalent attachment of a polyethylene glycol (PEG) chain to a derivatizable functionality of the peptide [2]. Conjugation of peptides with PEG is typically performed at the *N*-terminal, at the *C*-terminal or at certain side-chain functional groups. However, in several bioactive cyclic peptides such attachment sites do not exist.

We have investigated the use of backbone amide groups as an attachment site for oligoethylene glycol (OEG). Herein we report the synthesis of several *N*-OEG analogs of two bioactive cyclic peptides.

Results and Discussion

Our synthetic strategy to prepare *N*-OEGylated cyclic peptides relies on the use of Fmoc-protected *N*-OEG amino acids or dipeptides. These building blocks are prepared by reductive alkylation of the *N*-terminal with a monodisperse oligoethylene glycol aldehyde and then employed in the SPPS of the linear peptide precursor, which is cleaved from the solid support for subsequent cyclization in solution. The challenging step of the synthesis is the coupling to the *N*-substituted residue, which is hampered by steric hindrance.

First, we performed a full *N*-OEG₂ scan of the Sansalvamide A peptide [*N*-OEG₂ = *N*-CH₂CH₂-(OCH₂CH₂)₂-OCH₃]. The *N*-OEG₂ group was incorporated by using an *N*-OEG₂ amino acid as building block during the SPPS of the linear pentapeptide precursor. As expected, solid-phase couplings to the *N*-OEG₂ residues required special conditions. Such difficult couplings were achieved via the corresponding amino acid chloride, which was generated *in situ* with triphosgene [3] and left to react overnight. After cleavage from the solid support, the linear pentapeptides were efficiently cyclized in solution. All the compounds synthesized were tested for their cytotoxicity against three cancer cell lines: GLC-4, MDA-MB-231 and SW-480. Some of the *N*-OEG analogs exhibited cytotoxicity within the same range of the Sansalvamide A peptide and the corresponding *N*-Me analogs, which were also synthesized as a control. This suggests that backbone amide groups may be useful *N*-OEGylation sites in bioactive cyclic peptides.

Next, we evaluated up to which length of an OEG chain the SPPS of *N*-OEG peptide analogs is possible. Cilengtide was selected as model peptide and several analogs were prepared in which the *N*-Me group of valine was replaced by monodisperse OEG chains of different length [*N*-OEG₂ = *N*-CH₂CH₂-(OCH₂CH₂)₂-OCH₃, *N*-OEG₁₁ = *N*-CH₂CH₂CH₂-(OCH₂CH₂)₁₁-OCH₃, *N*-OEG₂₃ = *N*-CH₂CH₂CH₂-(OCH₂CH₂)₂₃-OCH₃]. These

cyclopentapeptides were obtained from their linear precursors, which were synthesized in solid phase and then cyclized and deprotected in solution. In the case of *N*-OEG₂-Cilengitide, an *N*-substituted valine was used as building block and the solid-phase coupling to the *N*-OEG₂ residue was efficiently performed using an amino acid chloride, which was generated *in situ* with triphosgene [3]. In the case of *N*-OEG₁₁-Cilengitide and *N*-OEG₂₃-Cilengitide, the use of triphosgene did not enable efficient coupling to the *N*-substituted peptidyl-resin. This problem could be circumvented by forming the Phe-Val(*N*-OEG) bond in solution and using an *N*-substituted dipeptide as a solid-phase building block, but the coupling of such dipeptide takes place with considerable epimerization at the *C*-terminal. The target pentapeptides are obtained as a mixture of diastereomers which, after cyclization and deprotection, can be separated by RP-HPLC purification.

Acknowledgments

This work was partially supported by CICYT (CTQ2009-07758), the Generalitat de Catalunya (2009SGR 1024), the Institute for Research in Biomedicine and the Barcelona Science Park. Ana I. Fernández-Llamazares thanks Ministerio de Educación y Ciencia for a FPU fellowship. We thank the Cancer Cell Biology Research group for their support for the cytotoxicity assays and we thank Barcelona Science Park (Mass Spectrometry Core Facility, Nuclear Magnetic Resonance Unit) for the facilities.

References

- [1] Chatterjee, J.; Gilon, C.; Hoffman, A.; Kessler, H. *Acc. Chem. Res.* **2008**, 41, 1331-1342.
- [2] Harris, J. M.; Chess, R. B. *Nat. Rev. Drug Discovery*, **2003**, 2, 214-221.
- [3] Falb, E.; Yechezkel, T.; Salitra, Y.; Gilon, C. *J. Pept. Res.*, **1999**, 53, 507-517.

Peptidyl-vinylketones as a novel class of inhibitors of the cysteine protease caspase-3

Kai Holland-Nell, Jörg Rademann

Institut für Molekulare Pharmakologie, Robert-Rössle-Str. 10, D-13125 Berlin, Germany;
Institut für Pharmazie, Universität Leipzig, Brüderstr. 34, D-04103 Leipzig, Germany

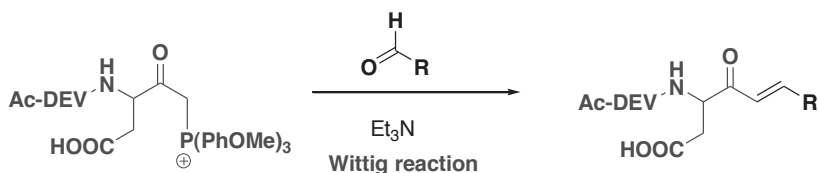
rademann@uni-leipzig.de

Introduction

The effect of peptidic enzyme inhibitors is often based on the modification of the natural substrates at the cleavage site [1]. Replacement of the scissile peptide bond by peptide isosters is a common technique to disfavor cleavage and to inhibit the activity of proteases. Thereby, the recognition site of the peptide should remain unchanged guaranteeing high specificity of the inhibitor. In order to proof the potential of vinylketones as peptide bond isosters, an efficient synthesis towards such compounds was developed. This concept was applied to the cysteine protease caspase-3, which functions as an important enzyme in the apoptosis cascade.

Results and Discussion

The synthesis towards peptidyl-vinylketones started with coupling of bromo-acetyl bromide to a common Wang resin. This allowed for the introduction of a phosphorane at the C-terminus of the peptide [2]. Deprotonation to the phospho-ylide and subsequent coupling of the first amino acid generated the basis for peptide synthesis. The peptide was extended by standard SPPS. Acidic cleavage removed all protecting groups and provided soluble peptidyl-phosphoranes. This intermediate product was finally transferred into the peptidyl-vinylketone by the use of Wittig chemistry. The phosphorane was easily deprotonated to the ylide by triethylamine. The reaction with an aldehyde created the desired vinylketone function at the C-terminus of the peptide. This very mild reaction was performed in acetonitrile/water mixtures at room temperature. A variety of peptide inhibitors could be formed by choosing different aldehydes.



This strategy was applied to caspase-3 inhibitors. Using the commonly known Ac-DEVD motif, the C-terminal Ac-DEVD-phosphorane was synthesized in yields of 32% (after HPLC-purification). The reaction with a set of six aliphatic and aromatic aldehydes led to the corresponding vinylketones (yields in Tab.1). Interestingly, two products with the expected mass of the peptidyl-vinylketone were formed in each reaction and could be isolated by HPLC. Closer NMR analysis revealed for both of the products an *E*-conformation at the double bond. Differences were monitored instead for the NH_α , CH_α ,

CH_β protons of ¹Asp and ²Val indicating an epimerization at the C_α centre of the first amino acid. This effect has also been reported for peptide-aldehydes [3].

In order to test the activity of the 12 peptidyl-vinylketones, a caspase-3 inhibition assay was performed. The K_i-values of the compounds ranged from 18.6 down to 1.0 nM (Tab.1). Particularly, the aromatic inhibitors and that with an extended aliphatic chain were able to fill the hydrophobic cavity at the S1'-site and showed a better performance than the standard inhibitor Ac-DEVD-aldehyde (K_i 3.8 nM). In comparison to analogous inhibitors missing the double bond, the presented compounds show activity on the same level [4].

The variable introduction of different residues at the C-terminus enables a library approach in order to find optimal residues filling the S1'-site and providing a more effective inhibition. Thereby, the peptidyl-vinylketones circumvent some of the disadvantages of peptide-aldehydes, particularly the instability of the aldehyde function. In addition, the vinyl group renders a couple of subsequent modifications possible, e.g. nucleophilic addition and epoxidation. The presented method opens a convincing synthesis route towards such peptidyl-vinylketones. The combination of SPPS on phosphorylated resins with the Wittig reaction allows for an easy and general transfer of this method to other peptidic protease inhibitors.

inhibitor	structure	yield	inhibition in nM	
			IC ₅₀	K _i
standard	Ac-DEVD - H	- -	23.5	3.8
1	- propene	28	41.1	6.7
2		49	114.6	18.6
3	- butene	20	34.2	5.6
4		15	28.3	4.6
5	- pentene	15	12.8	2.1
6		24	30.8	5.0
7	- hexene	19	15.6	2.5
8		20	13.9	2.3
9	- phenylethene	39	21.5	3.5
10		33	13.3	2.2
11	- toulylethene	29	6.5	1.1
12		24	6.1	1.0

Table 2: Yields and activities of the synthesized Ac-DEVD-vinylketone inhibitors in comparison to the standard inhibitor Ac-DEVD-aldehyde.

References

- [1] Venkatesan, N.; Kim, B.H.; *Curr Med Chem.* **2002**, *9*(24), 2243-2270.
- [2] Ahsanullah; Al-Gharabli, S.I.; Rademann, J.; *Org. Lett.* **2012**, *14* (1), 14-17.
- [3] Moulin, A.; Martinez, J.; Fehrentz, J.A.; *J. Pept. Sci.* **2007**, *13*, 1-15.
- [4] Goode, D.R.; Sharma, A.K.; Hergenrother, P.J.; *Org. Lett.* 2005, *7* (16), 3529-3532.

Ring-closing metathesis of astressin-derived peptides as novel corticotropin releasing factor antagonists

Abbas H. K. Al Temimi, Rob M. J. Liskamp, Dirk T. S. Rijkers*

Medicinal Chemistry & Chemical Biology, Utrecht Institute for Pharmaceutical Sciences,
Department of Pharmaceutical Sciences, Faculty of Science, Utrecht University, P.O. Box
80.082, 3508 TB Utrecht, The Netherlands

D.T.S.Rijkers@uu.nl

Introduction

Cyclization of peptides is a well-accepted approach to increase their biostability and bioactivity. This is especially true for a series of peptides that display strong corticotropin releasing factor (CRF) antagonistic activity. Seminal studies by Rivier *et al.* have shown that the incorporation of a lactam bridge in an *N*-terminally truncated CRF-sequence resulted in an enormous increase in CRF-antagonistic activity and potency, due to the stabilization of the bioactive α -helical conformation of the peptide; and the newly designed peptide was called astressin [1]. Based on the astressin sequence, we started an extensive truncation and deletion study to arrive at astressin analogs with a reduced size but still remain active as CRF antagonists [2]. This study resulted in the smallest CRF antagonist, astressin(30-41), which sequence was further optimized by Yamada *et al.* [3], to arrive at **1**, and was found to be equipotent as full length astressin (Figure 1). In the present study, peptide **1** was used to explore other covalent constraints to stabilize the α -helical conformation. It was decided to replace the glutamic acid/lysine residues, which form the lactam-bridge via their side chains, by alkene-substituted amino acid residues to form an alkene-bridge featuring ring-closing metathesis (RCM).

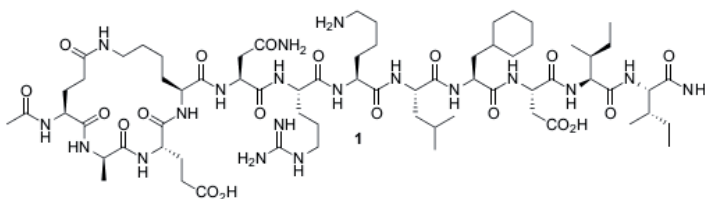


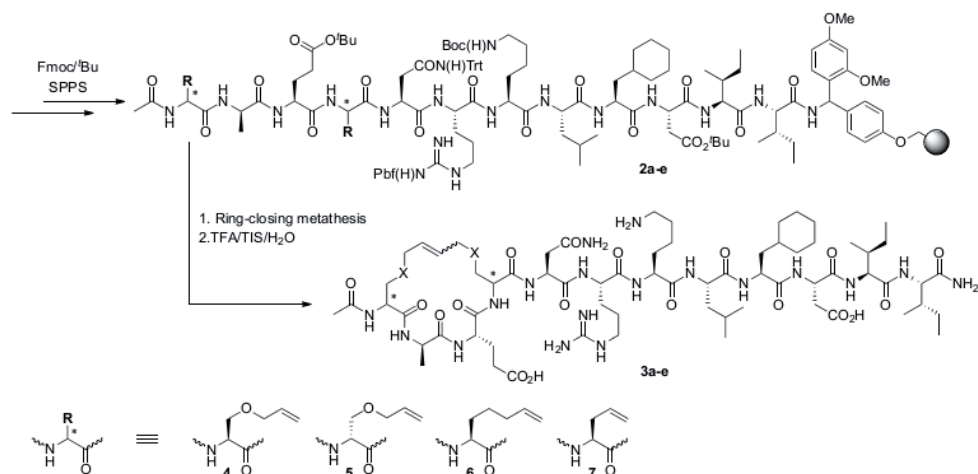
Figure 1. Structural formula of the CRF antagonist as described by Yamada *et al.*[3]

Results and Discussion

The RCM-precursor peptides **2a-e** were synthesized via Fmoc/^tBu SPPS protocols, in which four different alkene-functionalized amino acids were incorporated, *e.g.* L-serine(*O*-prop-2-enyl): L-Ser(All) **4**, D-serine(*O*-prop-2-enyl): D-Ser(All) **5**, (*S*)-2-aminohept-6-enoic acid **6**, and (*S*)-allylglycine **7**, respectively, as shown in Scheme 1. RCM was performed on the solid support and it turned out that microwave irradiation was essential, as reported previously by Robinson *et al.*[4] Under these conditions peptides **2d** (containing (*S*)-2-aminohept-6-enoic acid **6**) and **2e** (containing (*S*)-allylglycine **7**), smoothly underwent

RCM in the presence of the ruthenium-based 2nd generation Grubbs catalyst. After cleavage from the resin, peptides **3d-e** were obtained in good yield and were analyzed by HPLC and characterized by mass spectrometry.

Unfortunately, however, these RCM reaction conditions did not result into the desired cyclic peptides **3a-c**. Mass spectrometry indicated the presence of fully deprotected RCM-precursor peptides. Apparently, the metathesis catalyst functioned as an olefin isomerization/migration agent in which the *O*-prop-2-enyl moiety was converted into its *O*-prop-1-enyl congener. This explains the presence of the linear peptides since *O*-prop-1-enyl moiety is unreactive during RCM but also acid labile and is cleaved off during the TFA treatment. The isomerization can be effectively suppressed by adding 1,4-benzoquinone [5], and after careful optimization, peptides **2a-c** (**2a**: L-Ser(All)/L-Ser(All), **2b**: L-Ser(All)/D-Ser(All), **2c**: D-Ser(All)/L-Ser(All)) could efficiently converted into **3a-c** by using the following reaction conditions: 15 mol-% Hoveyda-Grubbs catalyst/1,4-benzoquinone (5 equiv over resin loading) in 0.4 M LiCl in dimethylacetamide/CH₂Cl₂ at 100°C (microwave irradiation) during 75 min.



Scheme 1. Synthesis of aestressin-derived peptides **3a-e** via ring-closing metathesis.

References

- [1] Gulyas, J.; Rivier, C.; Perrin, M.; Koerber, S.C.; Sutton, S.; Corrigan, A.; Lahrichi, S.L.; Craig, A.G.; Vale, W.; Rivier, J. *Proc. Natl. Acad. Sci. USA* **1995**, *92*, 10575.
- [2] Rijkers, D.T.S.; Kruijtzter, J.A.W.; van Oostenbrugge, M.; Ronken, E.; den Hartog, J.A.J.; Liskamp, R.M.J. *ChemBioChem* **2004**, *5*, 340.
- [3] Yamada, Y.; Mizutani, K.; Mizusawa, Y.; Hantani, Y.; Tanaka, M.; Tanaka, Y.; Tomimoto, M.; Sugawara, M.; Imai, N.; Yamada, H.; Okajima, N.; Haruta, J.-i. *J. Med. Chem.* **2004**, *47*, 1075.
- [4] Robinson, A.J.; Elaridi, J.; van Lierop, B.J.; Mujcinovic, S.; Jackson, W.R. *J. Pept. Sci.* **2007**, *13*, 280.
- [5] Hong, S.H.; Sanders, D.P.; Lee, C.W.; Grubbs, R.H. *J. Am. Chem. Soc.* **2005**, *127*, 17160.

Simple and efficient solid-phase preparation of azido-peptides

Morten B. Hansen, Theodorus H. M. van Gulp, Jan C. M. van Hest,
Dennis W. P. M. Löwik*

Radboud University Nijmegen, Institute for Molecules and Materials (IMM),
Heyendaalseweg 135, 6525 AJ Nijmegen, The Netherland

E-mail: D.Lowik@science.ru.nl

Introduction

Azido-peptides are usually prepared by incorporation of azide containing residues or azide functionalization of aldehyde resins affording C-terminal azido-peptides.[1] Alternatively, the N-terminus can be converted into an azide via a Cu(II)-catalyzed diazotransfer reaction using triflyl azide.[2] Recently, a number of safer, shelf-stable and easily prepared diazotransfer reagents have been developed, of which imidazole-1-sulfonyl azide has been used to introduce azide moieties in proteins under copper-free conditions. Typically, it has not been reported to be used on the solid phase.[3] In order to acquire more knowledge on such solid phase approach we decided to examine the scope of this reaction. For this exploration we focused on a PEG-based resin because of its very good swelling characteristics in a wide range of solvents including water,[4] which is of particular interest as imidazole-1-sulfonyl azide is usually used in polar solvents. To study the solid phase diazotization of peptides using imidazole-1-sulfonyl azide hydrochloride, a model peptide ALYKAG was prepared by standard solid phase peptide synthesis on a NovaPEG Rink resin. This resulted in a quick, easy and copper-free protocol to N-terminal azido-peptides.

Results and Discussion

It was found that the diazotransfer reaction is very fast as it reaches a maximum conversion of around 95% already after 10 minutes (Fig. 1). Surprisingly, Cu(II) does not seem to have a favourable effect on this conversion; neither on the rate nor on the overall conversion. Hence, Cu(II) can be left out of the reaction. The diazotization efficiency was studied using 1, 3 or 5 equivalents of the diazotransfer reagent. One equivalent gives less conversion than three equivalents, which again gives less than five. Repeated treatment with transfer reagent did not lead to full conversion as only 98% conversion was observed.

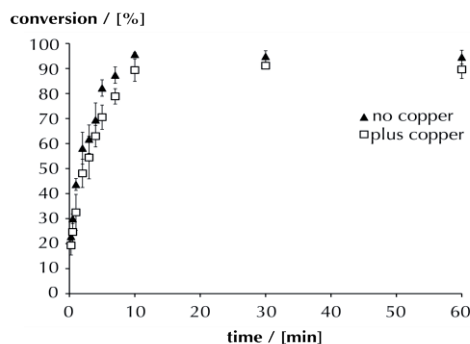


Figure 1. Kinetics of the diazotization of ALYKAG on solid support. The conversion of amino-ALYKAG to azido-ALYKAG.

To study the scope of the reaction with respect to the N-terminal amino acid that was diazotized we test the reaction on XLYKAG (where X = all natural side-chain protected amino acids except Pro). Only Cys(Trt) and Met did not produce clear amine to azide conversions. Met showed reasonable conversions, but suffered from oxidation. All others gave clear conversions up to 97% within 30 minutes.

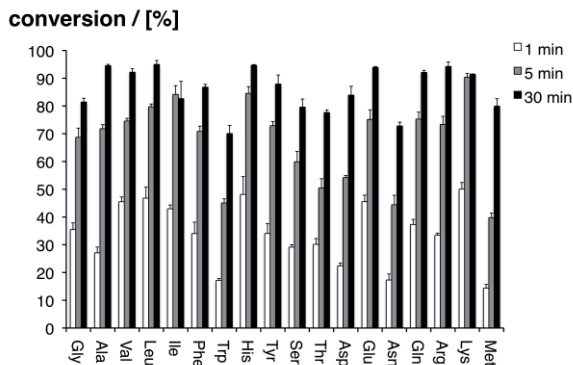


Figure 2. Variation of the N-terminal amino acid.

Next, a polystyrene (PS) resin was compared with the PEG based one to perform the diazotization reaction on. On both the PS and PEG resin, with K_2CO_3 as a base, a poor conversion was observed in DMF. Employing DIPEA as a base led to better conversions. Nevertheless, under these conditions PS resin performed best.

Finally, we also established the effect of the solvent on the transfer reaction (on the PEG resin) which was found to have a strong influence on the efficiency of the diazotransfer reaction. After 30 min. in dichloromethane only 5% conversion was observed. Changing to methanol gave a modest conversion of 40%. Clearly these solvents are worse than DMF and water which yielded an 82% and 97% conversion respectively. The trend that seems to manifest is that increasing solvent polarity leads to increased conversion efficiency. Solvent proticity seems to be less important to reach high conversions as DMF (non-protic) was better than methanol (protic solvent).

In summary, imidazole-1-sulfonyl azide hydrochloride was used to transform the N-terminus of a model peptide on solid phase into an azide moiety. It was found that this conversion could be accomplished within 30 min with high efficiency under aqueous conditions on a NovaPEG resin or in DMF on polystyrene beads without the need for Cu(II) as a catalyst as optimal conditions.[5].

References

- [1] Ten Brink, H. T.; Meijer, J. T.; Geel, R. V.; Damen, M.; Löwik, D. W. P. M.; van Hest, J. C. M., *J. Pept. Sci.* **2006**, *12*, 686.
- [2] a) Rijkers, D. T. S.; van Vught, H. H. R.; Jacobs, H. J. F.; Liskamp, R. M. J., *Tet. Lett.* **2002**, *43*, 3657; b) Angelo, N. G.; Arora, P. S., *J. Org. Chem.* **2007**, *72*, 7963; c) Papadopoulos, A.; Shiao, T. C.; Roy, R., *Mol. Pharm.* **2012**, *9*, 394.
- [3] a) Goddard-Borger, E. D.; Stick, R. V., *Org. Lett.* **2011**, *13*. Schoffelen, S.; van Eldijk, M. B.; Rooijackers, B.; Raijmakers, R.; Heck, A. J. R., *Chem. Sci.* **2011**, *2*, 701-705; b) Hansen, M. B.; Verdurmen, W. P. R.; Leunissen, E. H. P.; Minten, I.; van Hest, J. C. M.; Brock, R.; Löwik, D. W. P. M., *ChemBioChem* **2011**, *12*, 2294
- [4] a) García-Martín, F.; Quintanar-Audelo, M.; García-Ramos, Y.; Cruz, L. J.; Gravel, C.; Furic, R.; Côté, S.; Tulla-Puche, J.; Albericio, F. *J. Comb. Chem.* **2006**, *8*, 213; b) Hansen, M. B.; Rademann, J.; Grötli, M.; Meldal, M.; Bock, K. *JACS* **1999**, *121*, 5459; c) Meldal, M. *Tet. Lett.* **1992**, *33*, 3077.
- [5] Hansen, M.B.; van Gorp T.H.M.; van Hest, J.C.M.; Löwik; D.W.P.M, *Org. Lett.*, **2012**, *14*, 9, 2330.

SPPS of N-glycosylated Multivalent Epitopes to detect autoantibodies in Multiple Sclerosis patients' sera

**Caterina Tiberi,^{1,2} Giuseppina Sabatino,^{1,3} Margherita Di Pisa,^{1,2}
Giada Rossi,^{1,4} Paolo Rovero,^{1,4} Anna Maria Papini^{1,2,5}**

¹Laboratory of Peptide & Protein Chemistry & Biology - PeptLab - www.peptlab.eu;

²Department of Chemistry "Ugo Schiff", University of Florence, Via della Lastruccia 3/13, I-50019 Sesto Fiorentino (FI), Italy; ³Espikem Srl, I-59100 Prato, Italy; ⁴Department of Pharmaceutical Sciences, Polo Scientifico e Tecnologico, University of Florence, Sesto Fiorentino (FI), Italy; ⁵SOSCO-EA4505, University of Cergy-Pontoise, F-95031, France

caterina.tiberi@gmail.com

Introduction

Multiple Sclerosis (MS) is the most known chronic, inflammatory, demyelinating disease of the central nervous system, caused by an autoimmune response to self-antigens in genetically susceptible individuals. MS has not been yet characterized, thus resulting in difficult evaluation of prognosis and diagnosis. In the last few years, the role of autoantibodies in MS has been reevaluated, and, therefore, their identification as specific biomarkers is a relevant target [1]. Autoantibodies fluctuating in biological fluids can be detected by diagnostic immunoassays using native autoantigens. However, aberrant post-translational modifications may affect the immunogenicity of self-protein antigens, triggering an autoimmune response and creating neo-antigens. In this case, post-translationally modified peptides are more valuable tools with respect to isolated or recombinant proteins. In fact, synthetic peptides can be specifically modified to mimic neo-epitopes able to detect specific antibodies with higher affinity compared to proteins. The previously defined "Chemical Reverse Approach" was successfully developed to select synthetic peptides bearing specific post-translational modifications to set up diagnostic/prognostic assays of some autoimmune diseases [2]. In particular, an N-glycosylated type I β -turn peptide structure was demonstrated to accurately measure IgM and IgG antibodies in sera of a statistically significant patients' population. The β -turn structure seems to optimally expose the minimal epitope Asn(Glc) in the ELISA solid-phase conditions [3].

Results and Discussion

All classes of antibodies have multiple equivalent receptor sites. Polyvalent binding in antigen-antibody recognition seems to be an ubiquitous characteristic of immune recognition. Therefore, polyvalency could be responsible for high-affinity binding to epitopes present in different structures (proteins, glycolipids, etc.). It is accepted that free antibodies in solution do not activate an immune response; however, multiple copies of antibodies can strongly interact with multiple receptors triggering an internal immune signal. Therefore, it appears fundamental the design of multivalent ligands, bearing multiple copies of minimal epitopes, i.e., Asn(Glc) [4]. With this idea in mind, we synthesized a collection of lysine branched structures, e.g. Multiple Epitopes (MEPs), with

spacers of different length anchoring peptide sequences surrounding the minimal epitope. MEps have been synthesized introducing Fmoc-L-Asn(GlcAc4)-OH as a building-block [5] in an optimized Fmoc/tBu SPPS. We synthesized six MEps based on a lysine tetrameric core bearing the different spacers β -Alanine, Fmoc-3,6-dioxa-octanoic acid (Fmoc-HN-(CH₂-CH₂-O)₂-CH₂-COOH; Fmoc-Ado-OH) or Fmoc-1,13-diamino-4,7,10-trioxatridecan-succinamic acid (Fmoc-HN-(CH₂)₃-(O-CH₂-CH₂)₃-CH₂-HN-CO-(CH₂)₂-COOH; Fmoc-TTDS-OH), and specific peptide sequences, e.g. a β -hairpin N-glycosylated pentapeptide (CT32, CT33), an N-glycosylated hexapeptide (CT34) and an N-glycosylated consensus sequence (CT38). All the MEps were cleaved from the resin, purified by preparative HPLC (Waters 600), and further characterized by HPLC ESI-MS. MEp structures and analytical data are summarized in Table 1.

Table 1. Sequences and analytical data of the synthesized MEps

MEp [6]	MEp structure	ESI-MS (m/z)	
		calculated	found
CT21	(Ac-N(Glc)- β A) ₄ -K ₂ -K- β A	1017.98	1016.42 [M+2H] ²⁺
CT35	(Ac-N(Glc)-spacer _{TTDS}) ₄ -K ₂ -K- β A	1480.28	1479.35 [M+2H] ²⁺
CT32	(Ac-E-R-N(Glc)-G-H-spacer _{Ado}) ₄ -K ₂ -K- β A	1418.12	1416.63 [M+3H] ³⁺
CT33	(Ac-E-R-N(Glc)-G-H-spacer _{TTDS}) ₄ -K ₂ -K- β A	1220.87	1219.93 [M+4H] ⁴⁺
CT34	(Ac-E-R-N(Glc)-G-H-S) ₄ -K ₂ -K- β A	1339.28	1338.81 [M+3H] ³⁺
CT38	(Ac-N(Glc)-H-T-spacer _{TTDS}) ₄ -K ₂ -K- β A	1306.35	1304.38 [M+3H] ³⁺

IgG antibody titers to the six MEps were measured by solid-phase ELISA in 16 MS patients positive to the original N-glycosylated type I β -turn peptide structure and compared to 14 negative healthy blood donors. In particular, SP-ELISA absorbance values for patients and blood donors let us to select CT35 as the most valuable tool. We also investigated antibody affinity of CT35 in a competitive ELISA compared to the N-glycosylated type I β -turn peptide coated on a polystyrene microplate. As an example, in one MS positive serum, CT35 was able to inhibit IgG antibodies with an IC₅₀ of 8,88 μ M. In conclusion, this study reports for the first time that MEps, e.g. synthetic multivalent ligands, can be very efficient antigenic probes increasing detection affinity of autoantibodies in MS.

Acknowledgments

We thank for the financial support Ente Cassa di Risparmio di Firenze and the ANR Chaire d'Excellence 2009-2013 PepKit (France) to AMP.

References

- [1] Roland P. *et al. Clin. Pharmacol. Ther.*, **2003**, 73, 284-291; Baker M. *Nature Biotech.*, **2005**, 23, 297-304.
- [2] Papini A. M., *J. Pept. Sci.* **2009**, 15 621-628.
- [3] Lolli F. *et al. J. Neuroimmunol.* , **2005**, 167, 131-137; Lolli F. *et al. Proc Natl Acad Sci USA*, **2005**, 102, 10273-10278; Papini A. M., *Nat Med*, **2005**, 11, 13.
- [4] Mammen M. *et al. Angew. Chem. Int. Ed.* **1998**, 37, 2754-2794; Gestwicki J.E. *et al. JACS* **2002**, 124, 14922-14933.
- [5] Nuti F. *et al. Biopolymers*, **2010**, 94(6), 791-799.
- [6] Hayek J. *et al. Italian Patent n FI2012A000107*.

Synthesis and preliminary characterization of a nitronyl nitroxide α -amino acid

Karen Wright¹, Joseph Scola², Antonio Toffoletti³, Fernando Formaggio³, Claudio Toniolo³

¹ILV, UMR 8180 and ²GEMAC, UMR 635, University of Versailles, 78035 Versailles, France; ³ICB, Padova Unit, CNR, Department of Chemistry, University of Padova, 35131 Padova, Italy

E-mail:claudio.toniolo@unipd.it

Introduction

Nitronyl nitroxides are members of a class of stable free radicals that have attracted considerable interest as spin probes and as organic magnetic materials. Peptides have previously been rarely labeled with nitronyl nitroxides (*via* side chain substitution or with a His analogue [1,2]).

Incorporation of the nitronyl nitroxide functionality into a peptide enables one to assess the environment of a single functional group resulting from the 3D-structure of the molecule. EPR spectroscopy is ideal in this respect as this radical-containing function may be observed without interfering signals.

Results and Discussion

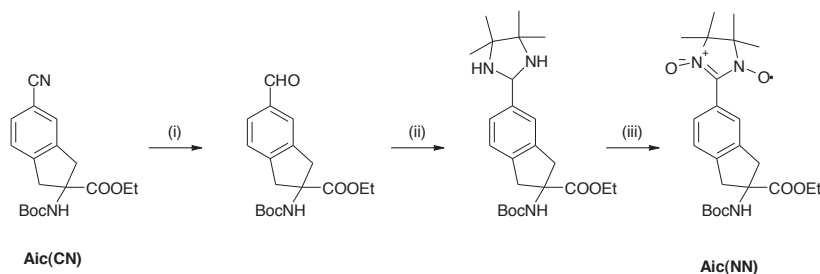


Fig. 1. Synthesis of the terminally protected Aic(NN) from its precursor Aic(CN). (i) Raney-Ni, NaH_2PO_2 , pyridine/AcOH/ H_2O , 40 °C; (ii) 2,3-diamino-2,3-dimethylbutane, CHCl_3 , 60 °C; (iii) a) *m*CPBA, $\text{CH}_2\text{Cl}_2/\text{NaHCO}_3$ aq., b) NaIO_4 aq., 0 °C.

The synthesis of the nitronyl nitroxide, C ^{α} -tetrasubstituted α -amino acid Aic(NN) (a sterically restricted amino acid that promotes formation of peptide β -turns and helical structures [3]) was achieved by derivatization of racemic 2-amino-5-cyano-indan-2-carboxylic acid [Aic(CN)] (Figure 1).

Racemic, terminally protected Aic(NN) was prepared by *bis*(alkylation) of ethyl isocyanoacetate under phase-transfer conditions with 3,4-(*bis*)bromomethyl benzonitrile as alkylating agent, followed by acidic hydrolysis, N ^{α} -Boc protection, and saponification of the ester function. Optical resolution was achieved through formation of the diastereomeric

amides of (*S*)-phenylglycinol followed by chromatographic separation and mild acidic hydrolysis. Reduction of the nitrile group to an aldehyde was carried out with Raney-nickel in the presence of sodium hypophosphite. Condensation with 2,3-diamino-2,3-dimethylbutane gave the corresponding tetramethylimidazolidine, which was oxidized with 3-chloroperbenzoic acid (mCPBA) to the desired nitronyl nitroxide.

The UV-Vis absorption and EPR spectra (the latter are shown in Figure 2) of this amino acid were recorded and its magnetic properties were examined.

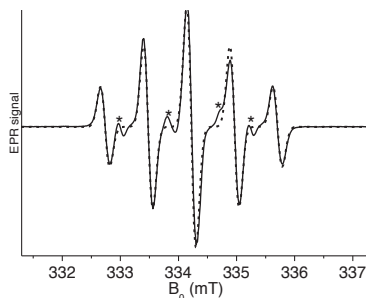


Fig. 2. The full line is the experimental EPR spectrum of a 1 mM toluene solution of Boc-Aic(NN)-OEt at $T = 290$ K. The intensity ratios in the multiplet are 1:2:3:2:1, as expected for hyperfine coupling with two equivalent ^{14}N nuclei. The dashed line is the spectrum calculated with the following parameters: hyperfine coupling constant $a_{\text{N}} = 0.743$ mT; $g_{\text{iso}} = 2.0065$. The small lines marked by asterisks are due to a different radical species which produces slowly, likely as a consequence of light exposure. The a_{N} and g_{iso} values are very close to those reported for similar nitronyl nitroxides [4].

References

- [1] Zhang, J., Zhao, M., Cui, G., Peng, S. *Bioorg. Med. Chem.* **2008**, *16*, 4019.
- [2] Weinkam, R. J., Jorgensen, E. C. *J. Am. Chem. Soc.* **1971**, *93*, 7033.
- [3] Toniolo, C., Crisma, M., Formaggio, F., Peggion, C. *Biopolymers (Pept. Sci.)* **2001**, *60*, 396.
- [4] Ullman, E., Osiecki, J., Boocock D., Darcy, R. *J. Am. Chem. Soc.* **1972**, *94*, 7049.

Synthesis of a protected derivative of (2R,3R)- β -hydroxyaspartic acid suitable for Fmoc-based solid phase peptide synthesis

F. Boyaud, B. Viguiet, N. Inguibert

Laboratoire de Chimie des Biomolécules et de l'Environnement-EA4215 Centre de
Phytopharmacie, 58 avenue Paul Alduy 66860 Perpignan

E-mail: nicolas.inguibert@univ-perp.fr

Introduction

The laxaphycin B is a cyclic lipopeptide [1] with interesting cytotoxic activities, but as for a lot of marine natural products accessing to the natural source is not always simple, isolation process is time consuming and despite the hard work performed for the structure determination this last one need to be confirmed by synthesis. Furthermore, as most of the cyclolipopeptides originating from the sea the laxaphycin B contain numerous non ribosomal amino acids. One of this is the (2R,3R)- β -hydroxy aspartic acid which we want to use as the first amino acid to be anchored to the resin in order to develop a solid phase peptide synthesis of this peptide. In this strategy the amino acid would be bound to the resin via its lateral chain, therefore we need to protect the amino function with a Fmoc and the carboxylic one with an allyl group.

Results and Discussion

As previously reported the different stereoisomers of the β -hydroxyaspartic acid are accessible using various synthesis [2] [3]. By applying the method reported by Chavignon [4] et al the fully unprotected (2R,3R)-beta-hydroxy aspartic acid could be obtained in multigram scale. Representatives of this derivate usable in SPPS are scarcely reported [5], and no one bear the protection we needed. Therefore, at this stage it was necessary to develop a strategy to introduce the required protections (Figure 1).

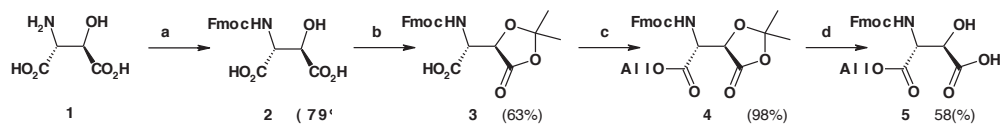


Figure 1: Synthesis of protected β -hydroxyaspartic **5**. a) 10% Na_2CO_3 , FmocOSu, dioxane, 25°C; b) $(\text{CH}_3\text{O})_2\text{C}(\text{CH}_3)_2$, AcOEt, 70°C, 24h; h) AllylBr, Cs_2CO_3 , DMF, 25°C; i) TFA, H_2O , 70°C.

Fmoc group was classically introduced on compound **1** allowing the production of compound **2**. Next, the differentiation of the two carboxylic functions was accomplished by the use of 2,2-dimethoxypropane under acidic catalysis (*p*-TsOH), leading to the formation of **3**. The allyl ester was introduced using cesium carbonate and excess of allyl bromide, followed of the deprotection of **4** in mild acidic condition to form **5**.

In the normal conditions of solid phase peptide synthesis (SPPS), the hydroxyl function should be protected and attempts were pursued to protect it by the tert-butyldimethylsilyl group, but this led to unsatisfactory yields and moreover the target compound decomposes over time even if stored at 4°C. Therefore, compound **8** was used directly on solid phase without protecting the hydroxyl function for the synthesis of an analogue of laxaphycin B (Figure 2). First, the compound **8** was anchored on the rink amide resin and the elongation of peptide realized with HATU as the coupling agent. The cyclization was performed after deprotection of the allyl protecting group.

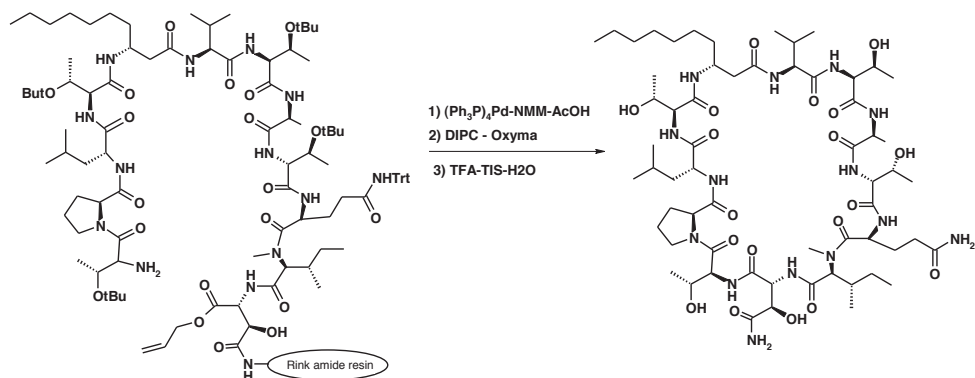


Figure 2: Cyclization of a laxaphycin B analog.

The cyclic peptide was obtained with yield of 8%. Furthermore, we observed an absence of acetylation on the hydroxyl function despite a capping of the residual amine group of the resin after the first step of the SPPS. Thus the steric hindrance of the resin plays the role of protecting group for the hydroxyl function. Our study allowed for the first time the synthesis in multi-grams scale of (2R,3R)-3-(((9H-fluoren-9-yl)methoxy)carbonylamino)-4-oxo-4-(prop-2-en-1-yloxy)butanoic acid **5** in a 10% overall yield starting from dimethyltartrate and this compound is useful as building block at least for the synthesis of laxaphycin B derivatives thus allowing to begin a relation structure activity study of this peptide.

Acknowledgments

This work was supported by grants of ANR (ANR-2010-BLAN-1533-02), and of Perpignan University (BQR).

References

- [1] Bonnard, I.; Rolland, M.; Salmon, J.M.; Debiton, E.; Barthomeuf, C.; Banaigs, B. *J. Med. Chem.* **2007**, *50*, 1266.
- [2] Cardillo, G.; Gentilucci, L.; Tolomelli, A.; Tomasini, C.; *Synlett* **1999**, *11*, 1727-1730.
- [3] Khalaf, J.K.; Datta, A.; *Amino Acids*, **2008**, *35*, 507-510. And reference cited therein.
- [4] Burgat Charvillon, F.; Amouroux, R.; *Synthetic Comm.* **1997**, *27*, 395-403
- [5] Bionda, N.; Cudic, M.; Barisic, L.; Stawikowski, M.; Stawikowska, R.; Binetti, D.; Cudic, P.; *Amino Acids*, **2012**, *42*, 285-293. And reference cited therein.

First synthesis of both pure diastereomeric N^6 -(1,2-dithiolane-(3*R* or *S*)-pentanoyl)- N^2 -Fmoc-*L*-Lys-OH for Fmoc/tBu SPPS

**C. Rentier,^{1,2,3} F. Nuti,^{1,2} M. Chelli,^{1,2} G. Pacini,^{1,4} P. Rovero,^{1,4}
C. Selmi,⁵ A. M. Papini^{1,2,3}**

¹Laboratory of Peptide & Protein Chemistry & Biology - PeptLab - www.peptlab.eu;

²Department of Chemistry "Ugo Schiff", Via della Lastruccia 3/13, Polo Scientifico e Tecnologico, University of Florence, I-50019 Sesto Fiorentino, Italy; ³SOSCO – EA4505, University of Cergy-Pontoise, Neuville-sur-Oise, 95031 Cergy-Pontoise, France;

⁴Department of Pharmaceutical Sciences, Via Ugo Schiff 6, Polo Scientifico e Tecnologico, University of Florence, I-50019 Sesto Fiorentino, Italy; ⁵Department of Translational Medicine, IRCCS-Istituto Clinico Humanitas, University of Milan, Milan, Italy

E-mail:cedric.rentier@gmail.com

Introduction

Primary Biliary Cirrhosis (PBC) is an autoimmune chronic cholestatic liver disease characterized by destruction of intrahepatic small bile ducts, ultimately leading to liver failure. PBC is usually characterized by the presence of antimitochondrial antibodies (AMA) circulating in blood. In fact, AMA are positive in 90-95% of patients long before the first clinical symptoms and appear to be directed against a family of the 2-oxo acid dehydrogenase (2-OADC) complexes located in the inner mitochondrial membrane. More specifically, up to now the pyruvate dehydrogenase E2 complex (PDC-E2) has been recognised as the major autoantigen. The common feature of the putative autoantigens seems to be the lipoylated moiety. Indeed, it has been previously reported that self reactivity in PBC could be induced by xenobiotics responsible of aberrant post-translational modifications of proteins breaking immune tolerance [1].

We previously reported that the use of synthetic peptides mimetics of neoantigens, i.e., PDH(44-63) and a type I' β -turn peptide structure [2], modified by the racemic N^6 -(1,2-dithiolane-3-pentanoyl)- N^2 -Fmoc-*L*-Lys-OH were able to detect autoantibodies in sera of PBC patients [3].

Results and Discussion

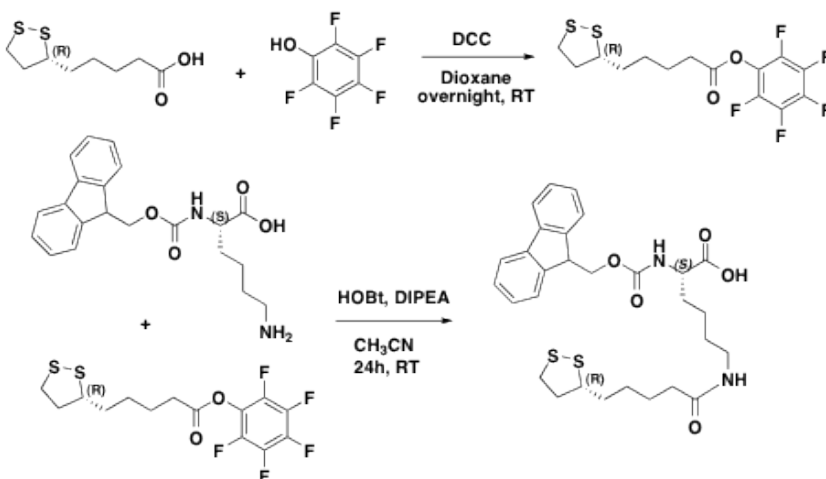
Lipoic acid possesses an asymmetric center at its C6. In nature, (*R*)-(+)- α lipoic acid is preferred to the (*S*)-enantiomer as an essential cofactor of four mitochondrial complexes [4].

In order to understand the possible role of the lipoic moiety chiral center in detecting autoantibodies, we successfully performed the first synthesis of the two diastereomeric lipoyl-lysine building blocks useful for Fmoc/tBu SPPS, i.e., N^6 -(1,2-dithiolane-(3*R*)-

pentanoyl)-*N*²-Fmoc-*L*-Lys-OH and *N*⁶-(1,2-dithiolane-(3*S*)-pentanoyl)-*N*²-Fmoc-*L*-Lys-OH.

The synthesis was performed in two steps starting from the two pure enantiomers of the lipoic acid. After i) activation of the lipoic acid as pentafluorophenylester, ii) coupling to Fmoc-*L*-Lys-OH side-chain by HOBt and DIPEA in CH₃CN at rt., we obtained *N*⁶-(1,2-dithiolane-(3*R*)-pentanoyl)-*N*²-Fmoc-*L*-Lys-OH (25% overall yield) and *N*⁶-(1,2-dithiolane-(3*S*)-pentanoyl)-*N*²-Fmoc-*L*-Lys-OH (16% overall yield) in hundred-milligram scale (Scheme 1).

Both diastereomers were characterized by NMR (¹H and ¹³C-NMR, DEPT 135, COSY, HETCOR), HPLC-MS, and optical rotations [*R*_t = 4.20 min for the (3*R*)-diastereomer; *R*_t = 4.08 for the (3*S*)-diastereomer; performed on C18 column (Phenomenex Jupiter C18 250x5mm) with a gradient 50-100% MeCN/0.1% TFA in water/0.1% TFA over 5 min at 0.6 mL/min]; [α]_D = -31° for the (3*R*)-diastereomer and [α]_D = +22° for the (3*S*)-diastereomer, at 22°C].



Scheme 1: Synthetic pathway to *N*⁶-(1,2-dithiolane-(3*R*)-pentanoyl)-*N*²-Fmoc-*L*-Lys-OH.

Acknowledgments

ANR Chaire d'Excellence PeptKit 2009-2013 (AMP) is gratefully acknowledged for its financial support.

References

- [1] a) Selmi, C.; *et al. Hepatology*, **2003**, 38, 1250-1257; b) Rieger R.; *et al. J. Autoimmun.*, **2006**, 27, 7-16.
- [2] Lolli, F. *et al., PNAS*, **2005**, 102(29), 10273-10278.
- [3] Innocenti, E.; *et al. Peptides 2008: Chemistry of Peptides in life science, technology and medicine. The Proceedings of the 30th European Peptide Symposium Helsinki*, **2009**, 470-471.
- [4] Raddatz, G.; *et al. Journal of Biotechnology*, **1997**, 58, 89-100.

Synthesis and polymerization of silaproline targeting PPII structure

Charlotte Martin, Jean Martinez, Florine Cavalier

Institut des Biomolécules Max Mousseron (IBMM) UMR 5247 CNRS-Universités
Montpellier 1 et 2, Place Eugène Bataillon, 34093 Montpellier, France

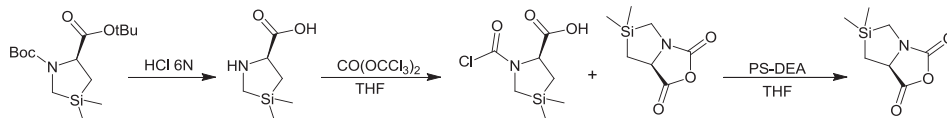
florine@univ-montp2.fr

Introduction

Silaproline[1] (Sip) is a silicon-containing analogue of proline, which exhibits similar conformational properties[2]. The presence of dimethylsilyl group confers to silaproline a higher lipophilicity as well as an improved resistance to biodegradation. Silaproline was synthesized successfully via asymmetric synthesis following the Schollkopf procedure[1]. More recently, a racemic synthesis was carried out allowing the gram scale preparation of enantiomerically pure Sip, requiring enantiomer resolution by chiral high performance liquid chromatography[3] (HPLC).

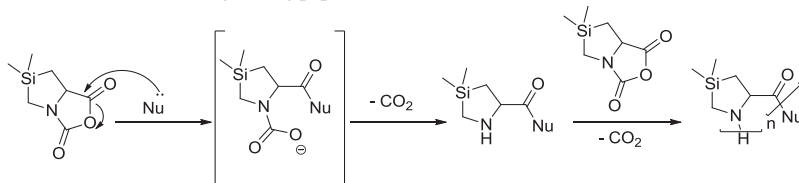
Polyprolines are attracting polymers due to their folding property into PPII structure, their significance in protein/protein interactions and their potential as new therapeutic targets. In this context, our aim was to change the physico-chemical properties of polyproline polymers retaining PPII structure. We investigated the synthesis of homopolypeptides by polymerization of silaproline *N*-carboxyanhydride.

Results and Discussion



Scheme 1 : Synthesis of Sip *N*-carboxyanhydride (Sip-NCA)[4]

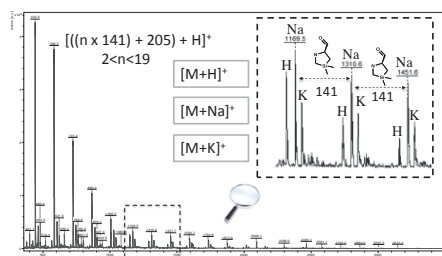
Synthesis of homopolypeptides was performed by ring opening polymerization (ROP) with a normal amine mechanism (NAM)[5].



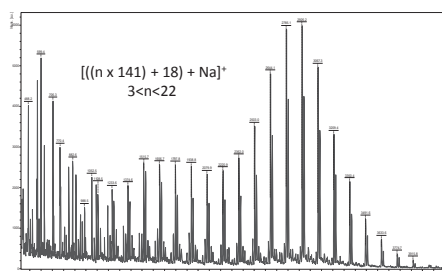
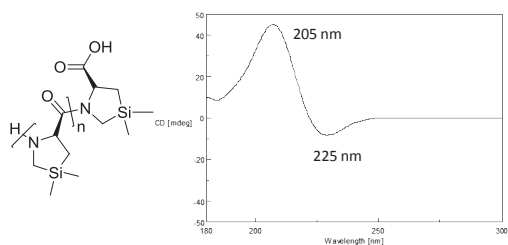
Scheme 2 : Sip-NCA Polymerization

Two types of initiators were tested, water and proline benzyl ester, that yielded homopolypeptides with different termination. These two homopolypeptides were characterized with MALDI-TOF and circular dichroism.

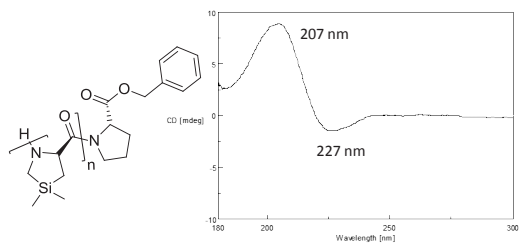
MALDI-TOF



CIRCULAR DICHROISM



HCCA matrix



0.1 mg/mL in HFIP

Figure 7 : Characterization of homopolypeptides with MALDI-TOF and circular dichroism

Silaproline was successfully synthesized by means of polystyrene-supported tertiary amines, allowing direct polymerization into homopeptides. The Sip-NCA has been obtained for the first time and was fully characterized. Polymerization of the lipophilic silaproline resulted in non water-soluble peptides, which did not desorb properly for MALDI analysis. However, circular dichroism of homopolysilaproline compared to homopolyproline confirmed the PPII structure.

Acknowledgments

The authors thank the “Ministère de l'Éducation Nationale” for MENRT grant of Charlotte Martin. We are grateful to Mathieu Dupré for MALDI spectra.

References

- [1] Vivet, B.; Cavelier, F.; Martinez, J., *Eur. J. Org. Chem.* 2000, 5, 807-811.
- [2] Cavelier, F.; Vivet, B.; Martinez, J.; Aubry, A.; Didierjean, C.; Vicherat, A.; Marraud, M., *J. Am. Chem. Soc.* 2002, 124, 2917-2923.
- [3] Martin, C.; Vanthuyne, N.; Miramon, H.; Martinez, J.; Cavelier, F., *Amino Acids* 2012, 43, 649-655.
- [4] Gulín, O. P.; Rabanal, F.; Giralt, E., *Org. Lett.* 2006, 8, 5385-5388.
- [5] Hadjichristidis, N.; Iatrou, H.; Pitsikalis, M.; Sakellariou, G., *Chem. Rev.* 2009, 109, 5528-5578.

Design and synthesis of cross-linked peptide probes for the development of an in vitro diagnostics for Coeliac Disease

**Margherita Di Pisa,^{1,2} Giuseppina Sabatino,^{1,2,3} Simona Pascarella,^{1,4}
Mario Chelli,^{1,2} Paolo Rovero,^{1,3,4} Anna Maria Papini^{1,2,5}**

¹Laboratory of Peptide & Protein Chemistry & Biology - PeptLab - www.peptlab.eu;

²Department of Chemistry "Ugo Schiff", Via della Lastruccia 3/13, Polo Scientifico e Tecnologico, University of Florence, I-50019 Sesto Fiorentino, Italy; ³Espikem Srl, I-59100 Prato, Italy; ⁴Department of Pharmaceutical Sciences, University of Florence, I-50019 Sesto Fiorentino, Italy; ⁵Laboratoire SOSCO - UMR 8123 Université de Cergy-Pontoise, Neuville-sur-Oise, F-95031 Cergy-Pontoise, France

margherita.dipisa@unifi.it

Introduction

Coeliac Disease (CD) is an autoimmune enteropathic condition triggered in genetically susceptible individuals, by the gliadin fraction of wheat gluten and similar alcohol soluble proteins (prolamines). The main autoantigen is the Ca²⁺-dependent intracellular enzyme tissue Transglutaminase (tTG) [1]. This enzyme promotes in its active site protein cross-links via transamidation reaction and can recognise gliadin peptide epitopes. Untreated CD patients have high levels of circulating IgAs and IgGs anti-tTG, anti-gliadin, anti-tTG-gliadin adducts, and anti-endomysium. Their presence strongly correlates with the gluten dietary intake [2,3]. Transamidation can be considered an aberrant post-translational modification triggering autoantibodies in Coeliac Disease. Therefore, cross-linked peptides between Lys- and Glu side-chains of tTG and α -Gliadin peptide epitopes could be innovative tools to develop peptide-based in vitro diagnostics for Coeliac Disease.

Results and Discussion

Following our "Chemical Reverse Approach" [4], we selected three tTG peptide epitopes, e.g., tTG(I), tTG(II), and tTG(III) and three α -Gliadin peptide epitopes, e.g., α Glia(61-69), α Glia(63-71), and α Glia(68-76) [5,6], previously identified as autoantigens in CD4+ T cell extracts. Nine peptides containing cross-links between Lys- and Glu side-chains in tTG and α Glia linear fragments respectively, were synthesized by Fmoc/tBu SPPS. The target Lys side-chains in tTG peptide sequences were protected by Dde that was orthogonally removed to react regioselectively with the Glu side chains in α -Glia peptide fragments. Coupling reactions were performed in heterogeneous phase with the tTG fragments still anchored on the resin, and α -Glia peptides coupled in solution. The cross-linked peptide probes were tested in direct ELISA on sera of newly diagnosed coeliac patients to evaluate IgA and IgG antibody titre in 24 CD sera and 18 healthy blood donors (DS) as controls.

Cross linked Peptide	tTG-Gliadin fragments	Sequence	ESI-MS [M+2H] ²⁺ (m/z) Calc (obs.)	HPLC (Rt,min)	HPLC Purity
I	tTGI- αGli2(61-69)	Ac-XXXXXXXXXXKXX-NH ₂ Ac-PFPOPELPY-NH ₂	1271.1 (1272.02)	3.31 ^a	95%
II	tTGI- αGli2(63-71)	Ac-XXXXXXXXXXKXX-NH ₂ Ac-POPELPYPQ-NH ₂	1271.61 (1272.4)	2.11 ^a	90%
III	tTGI- αGli2(68-76)	Ac-XXXXXXXXXXKXX-NH ₂ Ac-PYPOPELPY-NH ₂	1279.1 (1280.02)	2.86 ^a	95%
IV	tTGII- αGli2(61-69)	Ac-XXXXXXXXXXKXX-NH ₂ Ac-PFPOPELPY-NH ₂	1327.2 (1327.6)	3.99 ^a	>98%
V	tTGII- αGli2(63-71)	Ac-XXXXXXXXXXKXX-NH ₂ Ac-POPELPYPQ-NH ₂	1317.71 (1318.2)	2.75 ^a	95%
VI	tTGII- αGli2(68-76)	Ac-XXXXXXXXXXKXX-NH ₂ Ac-PYPOPELPY-NH ₂	1335.21 (1336.2)	3.51 ^a	95%
VII	tTGIII- αGli2(61-69)	Ac-XXXXXXXXXXKXX-NH ₂ Ac-PFPOPELPY-NH ₂	914.50 (915.19)	3.46 ^a	>98%
VIII	tTGIII- αGli2(63-71)	Ac-XXXXXXXXXXKXX-NH ₂ Ac-POPELPYPQ-NH ₂	905.01 (905.67)	3.51 ^b	95%
IX	tTGIII- αGli2(68-76)	Ac-XXXXXXXXXXKXX-NH ₂ Ac-PYPOPELPY-NH ₂	922.50 (923.22)	4.01 ^b	>98%

Table 1. Cross-linked peptides tested in SP-ELISA. Cross-linked peptides were characterized by RP-HPLC ESI-MS (Waters Alliance 2695 equipped with a diode array detector) using a Phenomenex Kinetex C-18 column 2.6µm (100 × 3.0 mm) 0.6 ml/min. The solvent systems used were: A (0.1% TFA in H₂O MilliQ) and B (0.1 % TFA in CH₃CN); with different gradients at 0.6 ml/min in 5 min., ^a30-70% B, ^b20-60% B.

Peptide II appears to contain the most reactive epitope being able to recognize, in preliminary tests, IgGs in newly diagnosed coeliac patients' sera. Therefore, Peptide II will be selected as the most promising candidate to develop a new peptide-based ELISA helping to characterize with higher sensitivity CD patients in an early phase of the disease onset.

Acknowledgments

This work has been supported by Ente Cassa di Risparmio di Firenze and the ANR Chaire d'Excellence 2009-2013 PepKit (France) to AMP.

References

- [1] Dieterich, W.; Ehnis, T.; Bauer M.; Donner, P.; Volta, U.; Riecken, E.O.; Schuppan, D. *Nat Med*, **1997**, *3*, 797-801.
- [2] Halttunen, T.; Mäki, M., *Gastroenterol*, **1999**, *116*, 566-572.
- [3] Matthias, T.; Not, T.; Selmi, C. *Clinic Rev Allerg Immunol*, **2010**, *38*, 298-301.
- [4] Le Chevalier Isaad, A.; Papini, A.M.; Chorev, M.; Rovero., P. *J. Pept.Sci.*, **2009**, *15*, 451-454.
- [5] Fleckenstein, B.; Qiao, S.W.; Larsen, M.R.; Jung, G.; Roepstorff, P.; Sollid, L. M.; *J Biol Chem*, **2004**, *279(17)*, 17607-17616.
- [6] Dørum, S.; Qiao, S.W.; Sollid, L.M.; Fleckenstein, B. *J Prot Res*, **2009**, *8*, 1748-1755.

Synthesis of O-glycopeptides using *N,N'*-isopropylidene dipeptide derivatives

Hiroki Kobayashi¹ and Toshiyuki Inazu*^{1,2}

¹Department of Applied Chemistry, School of Engineering, & ²Institute of Glycoscience, Tokai University, 4-1-1 Kitakaname, Hiratsuka, Kanagawa 259-1292 Japan

E-mail: inz@keyaki.cc.u-tokai.ac.jp

Introduction

Glycoconjugates such as glycoproteins and glycolipids have important roles in cell functions. In order to study the structure–function relationship, synthesis of these glycoconjugates is essential. Glycoproteins and glycopeptides are classified into two categories: N- and O-glycosylated derivatives. The *N*-acetyl- α -D-galactopyranosylated Ser or Thr derivatives [Ser/Thr(α -D-GalNAc)] are important intermediates for O-glycopeptide synthesis. However, the synthesis of Ser/Thr(α -D-GalNAc) derivatives by chemical glycosylation is difficult because of the decreased nucleophilicity of hydroxy function in the glycosyl acceptor due to an unfavorable hydrogen-bonding pattern between the OH and α -NH groups [1]. Several approaches to overcome this problem have been reported [1, 2]. In addition, the O-glycosidic bond is cleaved easily in acidic conditions.

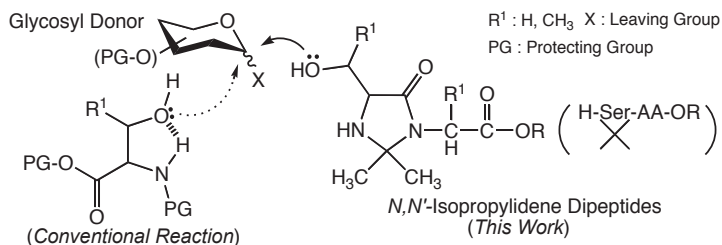


Fig. 1. Mechanism of O-glycosylated amino acid synthesis.

We assumed that the formation of a cyclic structure containing an α -NH group would increase the reactivity of OH function. Thus, we focused on the *N,N'*-isopropylidene derivatives of Ser/Thr containing dipeptides. To the best of our knowledge, there have been only a few reports regarding *N,N'*-isopropylidene dipeptides since the first report in 1965 [3]. Recently, a solid phase synthesis using *N,N'*-isopropylidene dipeptides as acyl components and deprotection of the *N,N'*-isopropylidene group using ytterbium (III) trifluoromethanesulfonate (Yb(OTf)₃) was reported [4]. In this paper, we studied the glycosidation of *N,N'*-isopropylidene dipeptides with the new deprotecting conditions for the *N,N'*-isopropylidene group of the glycosylated derivative.

Results and Discussion

First, we studied the glycosidation of *N,N'*-isopropylidene peptides **1** and **2**, which were synthesized according to the literature [3, 4]. We chose 2,3,4,6-tetra-*O*-benzyl-D-mannopyranosyl trichloroacetimidate (**3**) as the glycosyl donor because it has high reactivity, broad utility, and a simple structure. The reaction of mannopyranosyl

Synthetic approaches for the development of cell penetrating conjugates linked through thioether or disulfide bond

Sereti Evaggelia, Papas Serafim, Dimitriou Andromaxi, Papadopoulos Christos, Moussis Vassilios, Tselepis D. Alexandros, Tsikaris Vassilios

Department of Chemistry, University of Ioannina, 45110, Greece

E-mail: btsikari@cc.uoi.gr

Introduction

One of the biggest challenges of the scientific world in our days is to develop transport models for targeting delivery of biological molecules and drugs. Cell Penetrating Peptides (CPPs) are small molecules with the ability to enter the cell membrane. They have been successfully used for cellular uptake of biologically active cargoes, such as proteins, peptides, plasmids, liposomes, oligonucleotides, organic moieties and drugs, which do not go through the cell membrane by themselves. Taking advantage of the accumulated knowledge in our laboratory concerning the functionalities of a class of carriers formed by the repetitive (Lys-Aib-Cys), we report on synthetic approaches for the formation of conjugates with intermolecular thioether or disulfide bonds. As bioactive molecule we selected the R⁹⁹⁷PPLEED¹⁰⁰³ sequence derived from the intracellular part of the α_{IIb} -platelet integrin receptor. This region is critically involved in platelet aggregation and is a target of intervention for developing antithrombotic agents [1]. The Ac-[Lys-Aib-Cys(CH₂CO- α_{IIb} 997-1003)]₄-NH₂ and Ac-[Lys-Aib-Cys(Cys- α_{IIb} 997-1003)]₄-NH₂ conjugates were synthesized and examined for their ability to inhibit platelet aggregation (figure 1).

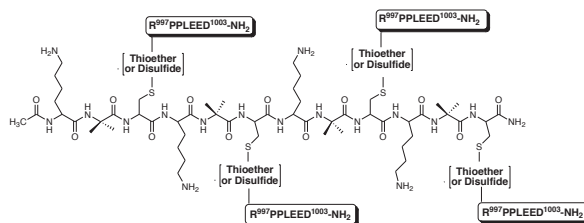


Figure 1. The general formula of the conjugates.

Results and Discussion

Peptide Synthesis

Both carrier and the bioactive molecule were synthesized stepwise on a Rink amide resin by the solid-phase peptide synthesis methodology using the Fmoc/*t*Bu strategy. The simultaneous deprotection of the side chains and cleavage of the peptides from the resin were performed by applying Reagent I (92.5% TFA/2.5% TIS/5% DMB) [2]. The identification and the purification was done with LC-MS with HPLC respectively.

Thioether Formation

The reaction was carried out in liquid phase. The IAc-R⁹⁹⁷PPLEED¹⁰⁰³-NH₂ was dissolved in a mixture of 0.2M Tris buffer in Acetonitrile 1/1 (v/v) at pH=8. The carrier was added

slowly at solid phase under Ar atmosphere. After 4 hours the final product was purified and identified with analytical HPLC and MS respectively.

Disulfide Formation

To do so, two different approaches have been used:

1. Activation of the four Cys residues of the carrier. The activation was performed in both solid and liquid phase using 2,2 dithiobis (5nitropyridine) (DTNP) or 2,2 dithiodipyridine (DTP). In all cases, the reaction with the Ac-Cys –R⁹⁹⁷PPLEED¹⁰⁰³-NH₂ which performed in aqueous solution of acetic acid pH=4) under Ar atmosphere, had many side-reactions and the final product was isolated in small yields (approx. 13%).

2. Activation of the Cys containing bioactive molecule. The use of the DTP in liquid phase was found to be the most efficient. The conjugation with the carrier took place in aqueous solution of acetic acid (pH=4) under Ar atmosphere. The carrier was added slowly in solid phase and final product was purified and identified with analytical HPLC and MS respectively.

Biological assays

Inhibition of the platelet aggregation measured with aggregometer using Platelet Rich Plasma (PRP). The conjugate concentration was 500μM. After one minute of incubation, ADP was added to a final concentration of 5μM. Table 1 is summarized the biological results.

Conjugate	IC ₅₀ (μM)
Ac-[Lys-Aib-Cys(CH ₂ CO-α _{IIb} 997-1003)] ₄ -NH ₂	212
Ac-[Lys-Aib-Cys(Cys-α _{IIb} 997-1003)] ₄ -NH ₂	279
*Pal-α _{IIb} 997-1003	445
α _{IIb} 997-1003	n.a

*Pal: Palmitoyl group

Conclusions

The Cell Penetrating Sequential Carrier is proper to transport bioactive cargo into platelets. The most efficient way to form four disulfide bonds with the CPSC is in liquid phase, by activation of the Cys-containing bioactive cargo. Attempts to activate the four Cys of the carrier gave many byproducts and intramolecular disulfide bonds. Both the CPSC conjugates exhibited higher anti- aggregatory activity compared to Pal-α_{IIb}997-1003.

Acknowledgements

This study was supported by the Regional Operational Programme (ROP) of Thessaly-Mainland Greece- Epirus within the frame of National Strategic Reference Framework for the period 2007-2013 (ESPA 2007-13).

References

- [1] Koloka, V.; Christofidou, E. D.; Vaxevelanis, S.; Dimitriou, A. A.; Tsikaris, V.; Tselepis, A. D.; Panou-Pomonis, E.; Sakarellos-Daitsiotis, M.; Tsoukatos, D. C. *Platelets*. **2008**, *19*, 502.
- [2] Stathopoulos, P.; Papas, S.; Tsikaris, V. J. *Pept. Sci.* **2006**, *12*, 227.

Synthetic study of Callipeltin B analogues and its cytotoxicity

Mari Kikuchi¹, Yoshihisa Watanabe², Masaki Tanaka², Kenichi Akaji³,
Hiroyuki Konno¹

¹Department of Biochemical Engineering, Graduate School of Science and Technology,
Yamagata University, Yonezawa, Yamagata 992-8510, Japan; ²Department of Basic
Geriatrics, Graduate School of Medical Science, Kyoto Prefectural University of Medicine,
Kamigyo-ku, Kyoto 602-8566, Japan; ³Department of Medicinal Chemistry, Kyoto
Pharmaceutical University, Yamashina-ku, Kyoto 607-8412, Japan

E-mail:konno@yz.yamagata-u.ac.jp

Introduction

Callipeltin B (**1**) is cyclic depsipeptide isolated from marine sponge *Callipelta* sp. by Zampella group in 1996¹. The molecule was reported to exhibit broad-spectrum cytotoxicity against the tumor cell lines. Although callipeltin B (**1**) contained the novel β -MeOTyr, Lipton *et al.* reported the synthesis and cytotoxicity of desmethoxycallipeltin B (**2**), in which substitution of D-Tyr for β -MeOTyr did not substantially affect the cytotoxicity of callipeltin B (**1**)². However, structure-activity relationship study of callipeltin B (**1**) has not been shown to date in detail. In the course of our recent research regarding the synthetic study of cyclic depsipeptides, we have conducted studies on the synthesis of callipeltin B (**1**) suppose to be efficient structures for the anti-cancer drugs (Fig. 1).

In the present study, we report the synthesis of cyclic depsipeptides of callipeltin B analogues consisting of L-, D-amino acids and/or unusual amino acids for structure-activity relationship study of callipeltin B (**1**) against HeLa cells.

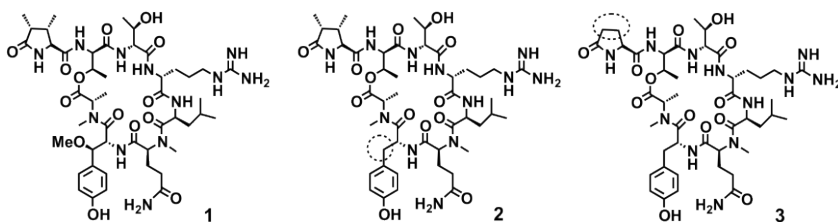


Fig. 1. Structure of callipeltin B (**1**), desmethoxycallipeltin B (**2**) and its analogue (**3**).

Results and Discussion

Callipeltin B (**1**) consists of 8 amino acids, almost of unusual amino acids. Prior to the synthesis of cyclic depsipeptide, we synthesized Fmoc-*N*-MeAla-OH (**4**), Fmoc-*N*-MeGln-OH (**5**), Fmoc-(2*R*, 3*R*)- β -MeOTyr(MEM)-OH (**6**), Fmoc-D-*allo*Thr(*t*Bu)-OH (**7**) and diMepyroGlu (**8**) which were necessary unusual Fmoc-amino acids for the constructing of callipeltin B (**1**) (Fig. 2). **4** and **5** were prepared from Fmoc-Ala-OH and Fmoc-Gln(*Trt*)-OH via the oxazolidine intermediates, respectively. **6** was synthesized using Lewis acid mediated the aziridine ring-opening reaction. D-*allo*Thr was prepared through the

epimerization of α -proton of L-Thr and then the side chain was protected with *t*Bu group to give desired **7**. DiMePyroGlu (**8**) was obtained by diastereoselective hydrogenation and alkylation starting from Garner's aldehyde.

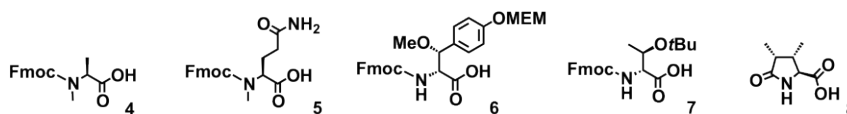
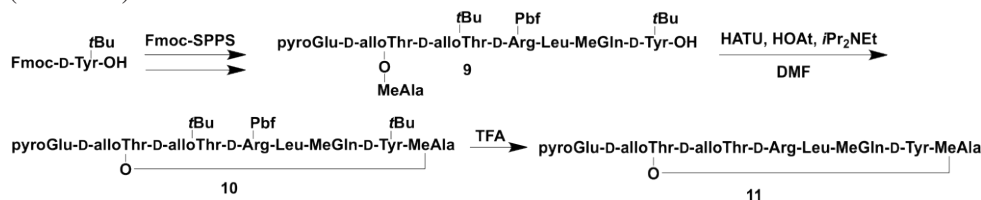


Fig. 2. Synthesized unusual amino acids with protecting groups.

For the synthesis of the cyclic depsipeptides, the route via intramolecular amide bond formation with Tyr-MeAla was selected. Coupling conditions on solid support were optimized to use PyBOP or HATU and esterification was employed MSNT/MeIm condition. After completion of the chain assembly, the resin was treated with HFIP/CH₂Cl₂ to give the linear peptide (**9**). The intramolecular amide linkage with Tyr-MeAla in the presence of HATU/HOAt yielded the corresponding protected cyclic depsipeptide (**10**), followed by final deprotection using TFA to afford the desired *cyclo*[-O-D-alloThr(pyroGlu)-D-alloThr-D-Arg-Leu-MeGln-D-Tyr-MeAla-] (**11**). Callipeltin B analogues containing several unusual amino acids were synthesized by similar methods (Scheme 1).



Scheme 1. Synthesis of cyclic depsipeptide (**11**).

These synthetic peptides were assayed for cytotoxicity against HeLa cells. As the results, all of the synthesized peptides were not exhibited potent activity. These results suggested that diMePyroGlu residue was needed to show potent cytotoxic activities against HeLa cells³. Structure-activity relationship study of cytotoxic depsipeptides will be reported in due course.

Acknowledgments

This work was supported in part by the Japan Science Society (23-324) in Japan. M. K. is grateful for Japan Society for the Promotion of Science Fellowships for young scientists (8696).

References

- [1] D' Auria, M. V.; Zampella, A.; Paloma, L. G.; Minale, L. *Tetrahedron* **1996**, *52*, 9589-9596.
- [2] Krishnamoorthy, R.; Richardson, B. L.; Lipton, M. A. *Bioorg. Med. Chem. Lett.* **2007**, *17*, 5136-5138.
- [3] Kikuchi, M.; Watanabe, Y.; Tanaka, M.; Akaji, K.; Konno, H. *Bioorg. Med. Chem. Lett.* **2011**, *21*, 4865-4868.

Templating cyclic β -tripeptides: Combination of inhibitor and recognition motifs with fluorescence labeling and cell penetrating units

Hanna Radzey, Frank Stein, Ulf Diederichsen

*Institut für Organische und Biomolekulare Chemie, Georg-August-Universität Göttingen,
Tammannstraße 2, 37077 Göttingen, Germany and Cluster of Excellence 171 of the DFG
Research Center for Molecular Physiology of the Brain (CMPB)*

E-mail: udieder@gwdg.de

Introduction

The recent expansion of high resolution imaging techniques offers new possibilities to gather information about biological processes and their location *in vitro*. Herein, we describe two methods to image the signal transducer and activator of transcription 3 (STAT3) protein using a specific inhibitor linked to the fluorophore and a cell penetrating peptide via a cyclic β -tripeptide on the one hand, and on the other hand sodium channels using conotoxins linked directly to a fluorophore.

STAT3 imaging requires three different properties comprised in one single molecule, since the inhibitor is not cell-penetrating. The combination of different properties in one single molecule with predefined topology can be accomplished using templates as described by Mutter *et al.* within the concept of template assembled synthetic proteins (TASP).[1] The concept describes the covalent attachment of artificial secondary structure building blocks to a template that reinforces and directs the folding of the newly designed molecule into a predetermined topology. We were interested in a template that arranges three different units, a cell-penetrating peptide, a fluorophore and an inhibitor unit, combined in one single molecule providing a certain topology, such as the three units not overlapping or sterically hinder each other. Cyclic β -tripeptides were used as templates forming very rigid structures with three defined topological sides providing the β -amino acid property of being quite resistant to proteolytic degradation.[2] For sodium channel imaging as second application, fluorophore and inhibitor were directly linked without using a template.

Results and Discussion

In the first approach STAT3 was the target. Proteins of the STAT group belong to a family of latent cytoplasmatic transcription factors, each having its unique function to transduce extracellular signals and directly modulate transcription. STAT3, which has been described as oncogenic, can be addressed using the peptide sequence Y(p)LKTKF, that targets the SH2 domain of STAT3 and thereby inhibits the dimerization of two STAT3 proteins leading to no nuclear translocation and no DNA binding.[3,4] The inhibitor sequence was synthesized on a chlorotrityl resin using the standard SPPS Fmoc protocol. The peptide was equipped with an alkyne moiety being able to react via Huisgen [2+3]-cycloaddition. Additionally, the inhibitor sequence was incorporated into the inhibitor loop of the cystine knot microprotein oMCoTI-II, which can be attached to the scaffold via an alkyne moiety as well. oMCoTI-II forms very rigid and well defined structures due to the cystine knot

motif.[5] Hence, the inhibitor is stable against proteolytic degradation or high temperatures. As a fluorophore 5(6)-TAMRA was used due to its stability within peptide coupling steps. In the first approach a cell penetrating unit is needed, therefore penetratin from the *Antennapedia homeobox* sequence was utilized, which was synthesized on a chlorotrityl resin using the standard SPPS Fmoc protocol. Cleavage from the resin was accomplished using mild acidic conditions yielding a completely protected peptide with a free C-terminus. These three units were combined on a cyclic β -tripeptide template.[6] The syntheses of the β^3 -amino acids, incorporating the Fmoc- or CBz-protecting group or an azide, were accomplished utilizing Arndt-Eistert homologation to form the diazoketone followed by conversion into β -amino acids via Wolff rearrangement using silver salts. The cyclic β -tripeptide was synthesized on solid support applying an oxidation labile aryl hydrazide linker. Following different cleavage and coupling steps two cell penetrating labeled inhibitors were synthesized on the basis of the cyclic β -tripeptide.

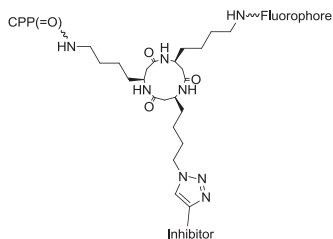


Figure 1: Structure of the cyclic β -tripeptide used as the scaffold

In the second approach sodium channels were addressed being the key players of electrical signal integration, action potential generation and propagation in neurons. An alkyne modified μ -conotoxin was used as the inhibitor synthesized on MBHA-rink amide resin using the SPPS Fmoc protocol. Successful folding was achieved in a buffer using EDTA and oxidized and reduced glutathione. Furthermore the alkyne modified μ -conotoxin will be linked to Alexa Fluor® 647 azide using click chemistry followed by a detailed analysis with advanced single molecule imaging.[7]

These accomplishments will be a starting point for the development of new labeling units, linking different inhibitor sequences to the cyclic β -tripeptide or different folded conotoxins to a fluorophore, and thereby, addressing different ion channels.

Acknowledgments

The work was performed with financial support by the Cluster of Excellence 171 of the DFG Research Center for Molecular Physiology of the Brain (CMPB).

References

- [1] Tuchscherer, G; Mutter, M. *J. Biotechnol.* **1995**, *41*, 197-210.
- [2] Seebach, D.; Gardiner, J. *J. Acc. Chem. Res.* **2008**, *41*, 1366-1375.
- [3] Bromberg, J. F.; Wrzeszczynska, M. H.; Deygan, G.; Zhao, Y.; Pestell, R. G.; Albanese, C.; Darnell, J. E. *Cell* **1999**, *98*, 295-303.
- [4] Ren, Z.; Cabell, L. A.; Schaefer, T. S.; McMurray, J. S. *Bioorg. Med. Chem. Lett.* **2003**, *13*, 633-636.
- [5] Hernandez, J. F.; Gagnon, J.; Chiche, L.; Nguyen, T. M.; Andrieu, J. P.; Heitz, A.; Hong, T. T.; Pham, T. T.; Nguyen, D. L. *Biochemistry* **2000**, *39*, 5722-5730.
- [6] Stein, F.; Mehmood, T.; Plass, T.; Zaidi, J. H.; Diederichsen, U. *Beilstein J. Org. Chem.* **2012**, accepted.
- [7] Enderlein, J.; Toprak, E.; Selvin, P. R. *Opt. Express* **2006**, *14*, 8111-8120.

Three-component synthesis of neoglycopeptides using a Cu(II)-triggered aminolysis of peptide hydrazide resin and azide-alkyne cycloaddition sequence

Jean-Philippe Ebran, Nabil Dendane, Oleg Melnyk*

CNRS UMR 8161, Univ. Lille Nord de France, Institut de Biologie de Lille, 1 rue du Pr. Calmette, 59021 Lille, France

jean-philippe.ebran@ibl.fr, oleg.melnyk@ibl.fr

Introduction

Principle of Three-Component Reaction

Multicomponent reactions (MCRs) represent a chemical process involving at least three reactants for the formation of several covalent bonds in one operation.¹ Since its discovery reported by Meldal² and Sharpless³, the copper(I)-catalyzed Huisgen 1,3-dipolar cycloaddition of organic azides and terminal alkynes (CuAAC) has been playing an outstanding role in various fields of chemistry and biochemistry.

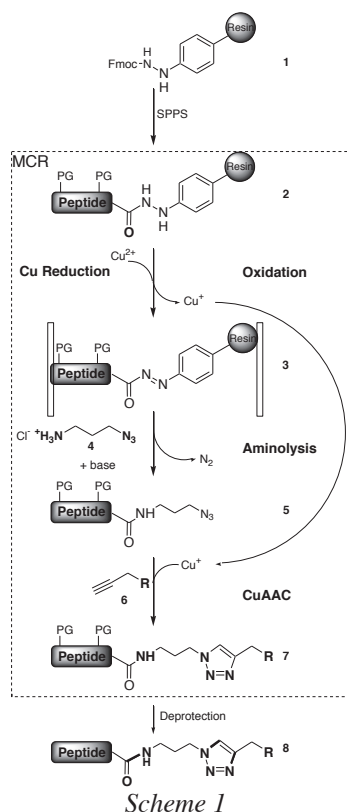
Only few reports describe the implementation of CuAAC in MCRs. Here we describe a novel three-component reaction based on a Cu(II)-triggered aminolysis of peptide hydrazide resin and an azide-alkyne cycloaddition sequence.⁴ (Scheme 1)

One of the components of the MCR is the protected peptidyl resin **2**, which is obtained from arylhydrazine resin **1** using standard solid phase peptide synthesis.

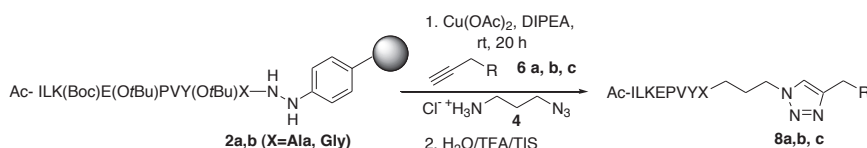
The catalyst of CuAAC, i.e. Cu(I), is generated in situ during oxidation of arylhydrazine resin **2** by Cu(II).

Aminolysis of resin **3** by azido amine **4** releases the protected peptide **5**. Cu(I) formed during oxidative aminolysis catalyzes the CuAAC between azido peptide **5** and alkyne **6** giving protected triazole **7**.

Overall, this MCR encompasses four chemical transformations: **oxidation** of hydrazide **2**, **reduction** of Cu(II) into Cu(I), diazene **aminolysis** and finally **CuAAC**.



Results and Discussion



Oxidative aminolysis of hydrazide **2** requires 2 equivalents of Cu(II). Optimizations of experimental conditions were performed using protected peptide hydrazide resin **2a** (X=Ala), 2 equiv of ammonium salt **4**, 2 eq. of 4-phenyl-1-butyne **6a** and 2.5 eq. of Cu(OAc)₂ in presence of DIPEA. The influence of different solvents on the MCR efficiency was first examined

(Table 1). Dichloromethane (entry 3) proved to be superior to THF and DMF (entries 1 and 2). In each case unreacted C-terminal azido peptide was identified as a major side product (~30% by RP-HPLC). By using a pyridine-dichloromethane mixture, yield of MCR target peptide **8a** was improved (entry 4) while proportion of side product was decreased 2-fold. Replacing Cu(OAc)₂ by Cu(OAc), 1,2,3-triazole product **9** formed from cycloaddition of alkyne **6a** and azide **4** was isolated with 84 % yield (entry 5). This experiment shows importance of Cu(II) to trigger the MCR. The MCR was applied to the synthesis of novel C-terminal neoglycopeptides using quinic and shikimic derivatives as mannose mimics.⁵

RP-HPLC chromatogram highlights the good purity of the crude neoglycopeptide **8b** released during the MCR. Similar result was obtained for MCR involving resin **2b** (X=Gly) and quinic derivative.

In summary, a novel Cu(II)-triggered MCR based on an oxidative aminolysis 1,3-cycloaddition sequence has been developed. The MCR process implies a peptide hydrazide resin, an amino azide linker and an alkyne resulting in the formation of amino 1,2,3-triazole linker modified peptides. MCR was applied to the synthesis of a novel family of C-terminal neoglycopeptides.

Acknowledgments

We thank financial support from CNRS, Région Nord-Pas-de-Calais, ImaBioTech and Endotis Pharma Inc. We acknowledge CSB platform (<http://csb.ibl.fr>) for technical support.

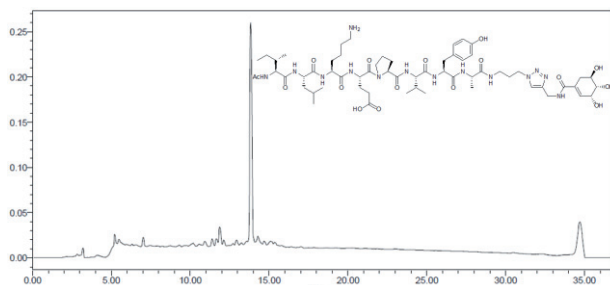
References

- Multicomponent Reactions*; J. Zhu, H. Bienaymé, Eds.; Wiley-VCH: Weinheim, 2005.
- W. Tornøe, C. Christensen, M. Meldal *J. Org. Chem.* 2002, 67, 3057-3064.
- V. V. Rostovtsev, L. G. Green, V. V. Folkin, K. B. Sharpless *Angew. Chem. Int. Ed.* 2002, 41, 2596-2599.
- J.-P. Ebran, N. Dendane, O. Melnyk *Org. Lett.* 2011, 13, 4336-4339.
- a) C. Grandjean, G. Angyalosi, E. Loing, E. Adriaenssens, O. Melnyk, V. Pancré, C. Auriault, H. Gras-Masse *ChemBioChem.* 2001, 2, 747-757. b) C. Grandjean, H. Gras-Masse, O. Melnyk *Chem. Eur. J.* 2001, 7, 230-239. c) G. Angyalosi, C. Grandjean, M. Lamirand, C. Auriault, H. Gras-Masse, O. Melnyk *Bioorg. Med. Chem. Lett.* 2002, 12, 2723-2727.

Entry	Resin 2 X	Alkyne 6	Solvent	Metal	Product	Yield (%) ^a
1	2a, Ala ^b		THF	Cu(OAc) ₂	8a	6
2	2a, Ala ^b		DMF	Cu(OAc) ₂	8a	13
3	2a, Ala ^b		CH ₂ Cl ₂	Cu(OAc) ₂	8a	14
4	2a, Ala ^b		CH ₂ Cl ₂ /pyridine (5 eq.)	Cu(OAc) ₂	8a	18
5	2a, Ala ^b		CH ₂ Cl ₂ /pyridine (5 eq.)	Cu(OAc)	9	84
6	2a, Ala ^b		CH ₂ Cl ₂ /pyridine (5 eq.)	Cu(OAc) ₂	8b	14
7	2b, Gly ^c		CH ₂ Cl ₂ /pyridine (5 eq.)	Cu(OAc) ₂	8c	11

^a Overall isolated yield (%). ^b 2 eq. of amine **4**. ^c 1.5 eq. of amine **4**.

Table 1. Results for the MCR



Total chemical synthesis of calstabin 2 protein

**M. Jullian,^a O. Melnyk,^b G. Ferry,^c J.A. Boutin,^c L. Ronga,^{*a†}
K. Puget^{a†}**

^aGENEPEP SA, Saint Jean de Vedas, France; ^bCNRS UMR 8161, Université Lille Nord de France, Institut Pasteur de Lille, Lille, France ; ^cInstitut de Recherches Servier, Croissy-sur-Seine, France ; [†] equal contribution

*E-mail:luisa.ronga@genepep.com

Introduction

Peptidyl prolyl cis/trans isomerases (PPIs) form 3 small families of proteins to which belong FKBP and cyclophilin. These proteins are folding helper proteins. Together with chaperones, they form receptor complexes. They catalyze the isomerization of prolyl peptide bonds in various folding states of target proteins. Indeed, their role has been implicated in refolding of denatured proteins or folding of de novo synthesized proteins [1].

Among them, the FKBP subclass comprises the small PPI calstabin 1 and 2. It is of interest to try to understand the way those proteins act, in order to help the overexpression of various types of membrane proteins, aiming at the renaturation, purification and crystallization attempts of receptors. We chose to work on calstabin 2 because this short (107 aa) protein has been described as a sub-family comprising 4 isoforms (from ~30 to ~100 aminoacids), some of them not being fully described to date. The relative shortness of those proteins together with the fact that the two higher molecular weight ones are catalytically active as prolyl isomerases, facilitate the characterization of the synthetic proteins.

Results and Discussion

In order to obtain the full length calstabin 2, a native chemical ligation (NCL) approach was chosen [2]. An optimized stepwise elongation allowed the obtention of the 86-mer C-terminal segment up to the Cys 22. Moreover, several methods were compared for the synthesis of peptide 1-21 opportunely functionalized at its C-terminus for the NCL.

Firstly, we tested the in situ thioesterification of fully protected fragment 1-21 carboxylate synthesized on 2-chlorotrityl chloride resin [3]. The desired peptide 1-21 thioester was obtained together with a side-product probably due to the additional thioesterification of a side chain carboxylate deprotected during 1% TFA cleavage.

Then, we synthesized the 1-21 fragment on 3-(Fmoc-amino)-4-aminobenzoyl (Dbz) resin in order to obtain this peptide with a C-terminal N-acyl-benzimidazolone functionality (Nbz) which undergoes rapid thiolysis, enabling thioester peptide to be generated before purification or in situ during a native chemical ligation [4]. The 1-21 Nbz fragment was obtained by suppressing the acetylation step after each peptide coupling which initially caused the acetylation of the second Dbz amine. Unfortunately, the purification of our Nbz peptide before NCL failed due to the hydrolysis of Nbz favored by RP-HPLC conditions.

Finally, the peptide 1-21 featuring a C-terminal bis(2-sulfanylethyl)amido (SEA) group was synthesized on an innovative solid support [5] and obtained in good overall yield and purity.

The 1-21 SEA fragment was employed for the chemoselective and regioselective reaction with the 22-107 cysteinyl peptide in the presence of 4-mercaptophenylacetic acid and tris(2-carboxyethyl)phosphine in a phosphate buffer (pH 7) at 40°C. This ligation at Thr site afforded the full length calstabin 2 in good yield (Figure 1).

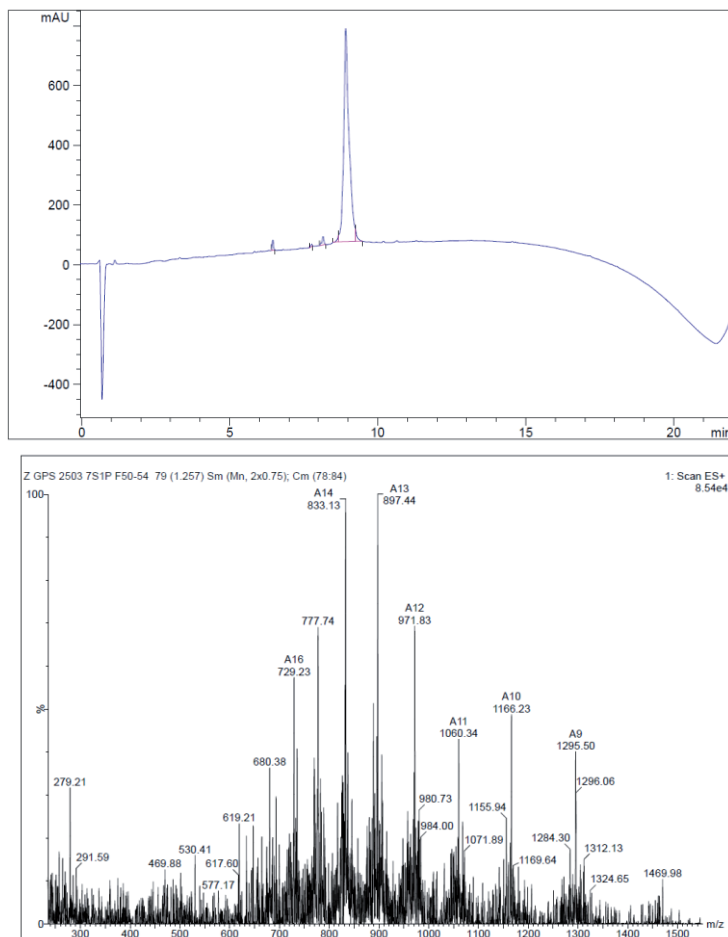


Figure 1. RP-HPLC and ESI spectrum of full length calstabin 2

References

- [1] Schiene-Fischer, C. and Yu, C. FEBS Lett. 2001, 495, 1.
- [2] Dawson, P.E.; Muir, T.W.; Clark-Lewis, I.; Kent, S.B. Science 1994, 266, 776.
- [3] Flemer, S. Jr. J Pept Sci. 2009, 15, 693.
- [4] Blanco-Canosa, B. and Dawson, P. E. Angew Chem Int Ed Engl. 2008, 47, 6851.
- [5] Ollivier, N.; Dheur, J.; Mhidia, R.; Blanpain, A.; Melnyk, O., Org. Lett. 2010, 12, 5238.

Statistical analysis of amino acid fingerprint to characterize protein binders in works of art

G. Sabatino,^{a,b} F. Di Pisa,^a M. Potenza,^b L. Rosi,^b L. Dei,^b
A.M. Papini^{a,b}

^a Laboratory of Peptide & Protein Chemistry & Biology - PeptLab - www.peptlab.eu;

^b Department of Chemistry "Ugo Schiff", Via della Lastruccia 3/13, Polo Scientifico e Tecnologico, University of Florence, I-50019 Sesto Fiorentino, Italy

giuseppina.sabatino@gmail.com

Introduction

Historically three types of proteinaceous materials (egg, animal glue, milk, and casein) were used as binders for pigments and as adhesives or protective/consolidating coatings in easel and wall paintings. Their identification is extremely useful for the deep knowledge of original ancient painting techniques, to adequately select and apply the most appropriate conservation procedures.

Ultra Performance Liquid Chromatography (UPLC) is a highly sensitive and suitable technique for accurate analysis of limited amounts of samples contained in original ancient works of art. Therefore, efficient molecular diagnostics of protein-based binders is a relevant topic in the field of chemical sciences applied to the conservation and safeguard of cultural heritage. Protein identification is a challenge because of degradation from aging, contamination effects, and possible presence of paint media based on mixtures as "*tempera grassa*".

Recently, we reported the amino acid analysis by AccQ•Tag™ UPLC (Waters) of standard binders (ovalbumin, whole egg, egg white) and model specimens. The UPLC analysis was compared to dot-ELISAs [1]. In particular, after hydrolysis of the samples (24 h, 114 °C, 0.6 M HCl), amino acid derivatization was performed by 6-aminoquinoly1-N-hydroxysuccinimidyl carbamate.

Results and Discussion

Herein, we report the use of our methodology to selected standard binders, e.g. milk, casein, rabbit, and fish glue, to obtain a reproducible fingerprint taking into account the complexity of the mixture. Moreover, we propose to extrapolate an innovative multivariate statistical analysis of the standard binders fingerprints obtained by AccQ•Tag™ UPLC to models and works of art samples. Principal Component Analysis (PCA) is mainly employed to elaborate data in complex mixtures. The standards are X1=Egg, X2=Glue, X3=Milk. Each one is characterized with a fingerprint reporting the retention times and the average peak area of 18 amino acids (H, S, R, G, D/N, E/Q, T, A, P, C, K, Y, M, V, I, L, F, HyP). In Table 1 we describe the results of our preliminary study. Statistical Model A was elaborated starting from standard ovoalbumin, casein, and rabbit glue and statistical Model B was elaborated starting from whole egg, milk, and rabbit glue. To verify the reliability of the statistical models, we used, as controls, painting layer samples (M) prepared in accordance with traditional painting procedures. A layer of tempera from different types of

protein material and red ochre pigment was applied to a mortar surface. Finally the statistical models A and B were applied to real samples of ancient panel paintings (RS).

Table 1. Results of UPLC analysis reported as average peak area for Real Samples (RS) and Model Samples (M)

		Ovalbumin	Casein	Rabbit Glue	Ratio
Statistical Model A	Sample	Estimate	Estimate	Estimate	
	RS182	0.170	-	0.936	1:5.5
	RSOro	-	-	7.492	-
	RSCroce	-	-	6.455	-
	M 3 (glue)	-	0.023	0.653	1:28
	M 12 (glue)	0.011	-	0.044	1:4
	M 8 (yolk + milk)	0.191	0.043	-	4.4:1
	M 9 (barium caseinate)	-	0.103	-	-
	M 4 (glue)	-	-	0.976	-
	M 5 (milk)	-	0.036	-	-
M 6 (egg)	0.226	-	-	-	
M 7 (glue)	-	-	2.081	-	
		Whole egg	Milk	Rabbit Glue	Ratio
Statistical Model B	Sample	Est	Estimate	Estimate	
	RS182	0.1769	-	0.937	1:5.3
	RSOro	-	-	7.492	-
	RSCroce	-	-	6.455	-
	M 3	-	0.0163	0.669	1:41
	M 12	-	-	0.043	-
	M 8 (yolk + milk)	0.1273	0.1086	-	1.2:1
	M 9 (barium caseinate)	-	0.116	-	-
	M 4 (glue)	-	-	0.976	-
	M 5 (milk)	-	0.038	-	-
M 6 (egg)	0.2206	-	-	-	
M 7 (glue)	-	-	2.081	-	

The data reported in Table 1 demonstrate, for the first time, that our Statistical Models A and B based on PCA are reliable for painting layer samples used as controls (M). Therefore, we were able to characterize the presence of egg and glue in the *RS 182* and rabbit glue in *RS Oro* and *RS Croce*.

Acknowledgments

The authors express their gratitude to Prof. Guido Botticelli for the careful preparation of the model samples. Ente Cassa di Risparmio di Firenze and from Regione Toscana PAR-FAS SICAMOR PROJECT (decreto n. 155 del 13/01/10) are gratefully acknowledged.

References

- [1] Potenza, M.; Sabatino, G.; Giambi, F.; Rosi, L.; Dei, L.; and Papini, A. M. *Anal Bioanal Chem*, **2012** DOI 10.1007/s00216-012-6049-9.

Use of internal references for the quantitative HPLC-UV analysis of solid-phase reactions

**Jan Spengler,^{a,b*} Ana I. Fernández-Llamazares,^{a,b}
Fernando Albericio^{a,b,c*}**

^aInstitute for Research in Biomedicine, Barcelona Science Park, Baldori Reixac 10, 08028-Barcelona, Spain; ^bCIBER-BBN, Networking Centre on Bioengineering, Biomaterials and Nanomedicine, Barcelona Science Park; ^cDepartment of Organic Chemistry, University of Barcelona, Martí i Franqués 1-11, 08028-Barcelona, Spain

E-mail: jan.spengler@irbbarcelona.org; fernando.albericio@irbbarcelona.org

Introduction

Reactions performed on solid supports are commonly monitored by HPLC-UV after cleaving off the products from a resin sample. However, UV-absorption coefficients may differ from compound to compound, and therefore, the relation of the area percentage values of the peaks may not directly reflect the molar concentrations of the corresponding compounds. For example, in solid-phase peptide synthesis it is for this reason difficult to calculate the yield of the coupling of a Fmoc-amino acid or the removal of the Fmoc-group due to its high absorbance.

Furthermore, it is not practical to compare HPLC spectra from different resin samples (e.g., before and after reaction) directly. A direct comparison by analyzing same (mg) amounts of resin would involve a tedious sample preparation extremely error prone and would not make much sense because factors resulting from the increase or decrease of the molecular weight of the resin-bound compounds may have a significant influence on the results.

Results and Discussion

The use of internal reference compounds allows a rapid assessment of reactions performed on solid phase. The internal reference compound is bound to the resin together with the substrate and cleaved off with the products after the reaction has been performed. Commercially available compounds can be used for this purpose. The peak integration of the reference compound in the HPLC-UV spectra can be correlated directly to those of the rest of compounds present in the reaction mixture and therefore a quantitative interpretation of the spectra with respect to conversion and yield is possible. The proof of principle as well as the accuracy of this method is demonstrated.

Acknowledgments

Peter Fransen (IRB Barcelona, for proposing the use of 1-pyreneacetic acid as internal reference), Brigitte Morales (MIT, Internship 2011), Isidro Casals (PCB). The work has been partially financed by CICYT (CTQ2009-07758), the Generalitat de Catalunya (2009SGR 1024), the Institute for Research in Biomedicine Barcelona (IRB Barcelona), and the Barcelona Science Park.

β_2 -Microglobulin: A “difficult” protein

Sabine Abel, Michael Beyermann

Leibniz-Institut für Molekulare Pharmakologie (FMP), Robert-Roessle-Str. 10, 13125
Berlin, Germany

E-mail: abel@fmp-berlin.de

Introduction

β_2 -Microglobulin (β_2 M) constitutes the light, non-covalently bound chain of the main histocompatibility complex.^[1] It causes in hemodialysis patients dialysis related amyloidosis by formation of amyloidal fibers.^[2, 3]

By now, the mechanism of the formation of the amyloidal fibers is still unknown. For the investigation of this process by infrared (IR)-spectroscopy,^[4] particularly local changes of key positions, such as tyrosine-66 and tyrosine-78, ¹³C-labeled β_2 M has to be synthesized.

Results and Discussion

β_2 M, a 99-residue protein, is difficult to produce by automated solid-phase peptide synthesis (SPPS). More promising is a strategy involving the native chemical ligation (NCL) for which cysteines within the protein are used. β_2 M contains cysteines in positions 25 and 80.^[1] This allows a three segment strategy utilizing automated SPPS for preparing the peptides, followed by two NCLs, disulfide formation and protein folding (Figure 1).

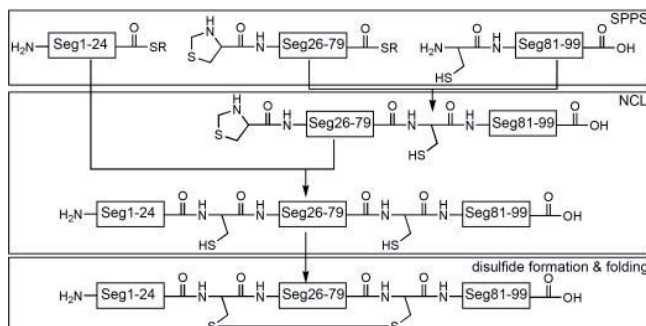


Figure 1: Synthesis strategy

After the final deprotection of the peptide segments, mainly, two complications had to be eliminated. Trifluoroacetylation which occurs at serine and threonine was removed by hydrolysis and *S-tert*-butylsulfonation of methionine in the C-terminal peptide segment was removed by stirring for one hour at 60°C in water and subsequent lyophilisation.^[8]

The first NCL between the middle and the C-terminal segments proceeded smoothly, although it went along with the formation of disulfide and internal thioester.

For the second NCL a dramatic loss of N-terminal segment was found due to side reactions. Further investigation revealed internal cyclisation reactions to be responsible for the loss, namely, lactame and oxazolone formation. Optimized ligation conditions suppressed the formation of these products.

In order to synthesize pure β_2 M problems observed for SPPS of the segments had to be eliminated. Difficulties due to peptide aggregation were avoided by using pseudo-prolines.^[5, 6] 20% piperidine-0.1 M formic acid was applied for Fmoc-removal to avert the formation of aspartimide and further side products.^[7]

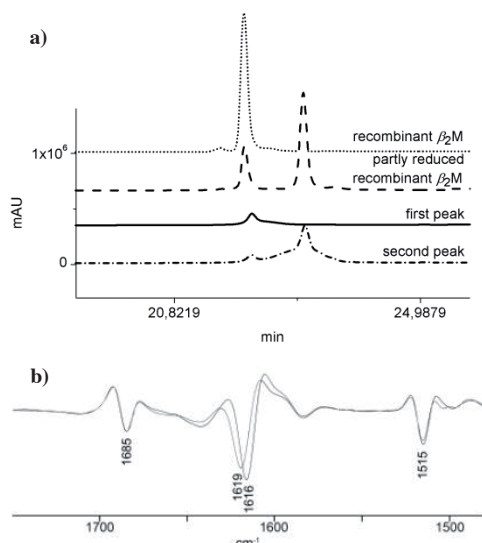


Figure 2 a): RP-HPLC comparison of isolated products & recombinant β_2M

Figure 2 b): IR-spectra of synthesized (grey) & recombinant (black) β_2M exhibit different β -sheet structures

synthesized β_2M folding product showed the same behaviour just as the isolated β_2M in SEC and RP-HPLC.

In conclusion, our approach to obtain β_2M demonstrates the scope but also limitations of the chemosynthesis of proteins. In particular it points to problems of producing pure peptide segments by SPPS, side reactions during native chemical ligation, misfolding and characterisation of proteins.

Acknowledgments

We would like to thank Dr. Heinz Fabian from the Robert Koch Institute (Berlin, Germany) for the infrared spectroscopic measurements.

References

- [1] Bjorkman, P. J.; Saper, M., A.; Samraoui, B.; Bennett, W. S., Strominger, J. L.; Wiley, D. C. *Nature* **1987**, *329*, 506.
- [2] White, H. E.; Hodgkinson, J. L.; Jahn, T. R.; Cohen-Krausz, S.; Gosal, W. S.; Mueller, S.; Orlova, E. V.; Radford, S. E.; Saibil, H. R. *J. Mol. Biol.* **2009**, *389*, 48.
- [3] Yamamoto, S.; Kazama, J. J.; Narita, I.; Naiki, H.; Gejyo, F. *Bone* **2009**, *45*, S39.
- [4] Fabian, H.; Gast, K.; Laue, M.; Misselwitz, R.; Uchanska-Ziegler, B.; Ziegler, A.; Naumann, D. *Biochemistry* **2008**, *47*, 6895.
- [5] Haack, T.; Mutter, M. *Tetrahedron Lett.* **1992**, *33*, 1589.
- [6] Woehr, T.; Wahl, F.; Nefzi, A.; Rohwedder, B.; Sato, T.; Sun, X.; Mutter, M. *J. Am. Chem. Soc.* **1996**, *118*, 9218-9227.
- [7] Doelling, R.; Beyermann, M.; Haenel, J.; Kernchen, F.; Krause, E.; Franke, P.; Brudel, M.; Bienert, M. *J. Chem. Soc., Chem. Commun.* **1994**, 853.
- [8] Bienert, M.; Klauschenz, E.; Nikolics, K.; Niedrich, H. *Int. J. Peptide Res.* **1982**, *19*, 310.

The product of the second NCL showed two peaks in RP-HPLC. By means of mass spectrometry the proof of their identity was unsuccessful. After isolation, the identity was verified by a comparison with recombinant β_2M in terms of RP-HPLC (Figure 2 a). However, the cyclic β_2M of the chemosynthesis (first peak) exhibited different properties in size exclusion chromatography (SEC) and IR-spectroscopy as well (Figure 2 b), interpreted as an exceeded molecular shell for the synthesized β_2M compared to the isolated β_2M and maybe reflecting a different β -sheet structure compared to that of recombinant β_2M , respectively.

Assuming a different folding for the crude product of the chemosynthesis, we totally reduced it. The folding proceeded this time under exactly the same conditions as for the recombinant β_2M . Carefully following these conditions the chemically

A synthetic 83 amino acid long peptide corresponding to the minimal metacaspase catalytic domain induces cell death in *Leishmania major*

Servis Catherine , Zalila Habib* , Gonzalez Iveth, Lozano Leyder, Fasel Nicolas

Department of Biochemistry, University of Lausanne, Epalinges, Switzerland

** Corresponding author: habib.zalila@unil.ch*

Introduction

Leishmania, a single-celled protozoan parasite, causes a spectrum of diseases with significant morbidity and mortality in developing countries, affecting millions of people worldwide. Current treatments carry noxious side effects and are proving increasingly ineffective against a rising population of resistant parasite strains. New approaches such as activating a cell death program could be interesting alternatives.

Metacaspases are distant orthologues of metazoan caspases and are restricted to yeast, plants, fungi and protozoans [1]. Despite an increasing interest in recent years, very little is known about metacaspase function other than their link to cell death, as shown in plants [2], yeast and protozoan parasites [3] and a role in cell cycle or proliferation [4].

At the biochemical level, metacaspases cleave substrates with basic residues at P1 position (mainly arginine and to a lesser extent lysine) [5]. A library screen revealed the VRPR tetrapeptide to be the most suitable recognition motif for plant metacaspase [6]. VRPR motif is also cleaved by *Plasmodium* [3] and *Leishmania* metacaspases.

Leishmania major expresses a 435 amino acids long polypeptide with a central catalytic domain containing the catalytic dyad H147/C202. We have shown that *L. major* metacaspase (LmjMCA) is able to replace the yeast metacaspase in mediating oxidative stress-induced apoptosis [5]. More recently, we characterized the role of LmjMCA in cell death under various stress-conditions. LmjMCA shows extensive processing into a cytoplasmic catalytic domain and impairs mitochondrial function when either the full length or the catalytic domain of LmjMCA (aa117-298) are overexpressed [7]. The LmjMCA precursor polypeptide is processed in several cd-LmjMCA (LmjMCA catalytic domain) peptides ranging between 10 and 35 kDa [7] upon the induction of cell death using various triggers. In this study, we investigated the enzymatic activity of a peptide representing a shortened form of the catalytic domain and exploited its physiological relevance in cell death to kill *Leishmania* parasites and to investigate whether LmjMCA could participate in a specific cell death program.

Results and Discussion

In this work we showed that, in stress conditions, LmjMCA precursor forms were extensively processed into soluble forms containing the catalytic domain and this domain

was sufficient to enhance sensitivity of parasites to hydrogen peroxide by impairing the mitochondrion function. We tested different lengths of LmjMCA catalytic domain and found that the overexpression of the polypeptide corresponding to amino acids 136-218 was sufficient to sensitize *L. major* mitochondria to oxidative stress. These findings were used to synthesize an 83aa long peptide corresponding to the minimal metacaspase catalytic domain (aa136-218) (Fig 1).

Fig 1. Sequence of the synthetic peptide corresponding to the minimal catalytic domain (CD136-218) was synthesized by automated Fmoc solid phase peptide synthesis

¹³⁵PGDVLFFHFSGHGGQAKATRDSEEKYDQCLIPLDHVKNGSILDDDLFLMLVAPL
PSGVRMTCVFDCCHSHASMLDLFPSYVAPR²¹⁸

Sequence of the catalytically inactive version (CD136-218 H147A/C202A).

This peptide has been characterized as having the specific metacaspase activity in vitro and is currently used to investigate its activity on possible target proteins, which have been identified in a yeast two-hybrid screen. Identifying proteins involved in the metacaspase signaling pathway will shed light on the understanding of CD in *Leishmania* and in lower eukaryotes.

Acknowledgments

This work was funded by the grants FNRS N° 3100A0-116665/1, IZ70Z0-131421 and by the Swiss Secretariat for Education and Research in the framework of the COST action BM0802.

References

- [1] Uren, A. G.; K. O'Rourke, et al. (2000). *Molecular Cell* **6** (4): 961-967.
- [2] Coll, N. S.; D. Vercammen, et al. (2010). *Science* **330** (6009): 1393-1397.
- [3] Meslin, B.; H. Zalila, et al. (2011). *Parasites & vectors* **4**: 26.
- [4] Ambit, A.; N. Fasel, et al. (2008). *Cell death and differentiation* **15** (1): 113-122.
- [5] Gonzalez, I. J.; C. Desponds, et al. (2007). *International journal for parasitology* **37** (2): 161-172.
- [6] Vercammen, D.; W. Declercq, et al. (2007). *The Journal of Cell Biology* **179** (3): 375-380.
- [7] Zalila, H.; I. J. Gonzalez, et al. (2011). *Molecular microbiology* **79** (1): 222-239.

Condensation of peptides with dienophiles

Leonid Sklyarov, Igor Nazimov, Rustam Ziganshin, Vladimir Zaikin,
Sergey Andreev

NRC Institute of Immunology, Moscow, Russia

E-mail: lsklyarov@yandex.ru

Introduction

The condensation reaction of acylated amino acids and peptides (Fig. 1) with unsaturated compounds is the simplest method of synthesis of such heterocyclic compounds, such as derivatives of pyridoxine, nicotinic and isonicotinic acids, and substituted pyrroles [1]. Significant polyfunctionality and reactivity of these derivatives allows using them for the synthesis of more complex compounds: multiplet peptides, porphyrins and dendrimers which are objects of supramolecular chemistry and nanotechnology. High fluorescence activity, absorption and the stability of the modified peptide bond (incorporated into the heterocycle) to electron impact in mass spectrometry of the peptide-dienophiles condensation products can be used for sequencing of peptides. Their acidolysis and hydrolysis leads to fragmentation of the peptide chain. Amino acid or mass-spectrometric analysis of the resulting fragments may restore the original sequence.

Results and Discussion

The polyfunctionality of 3-aminopyridines and pyridoxine for the first time creates an approach to synthesis of dendrimeric multiplet peptides (MP).

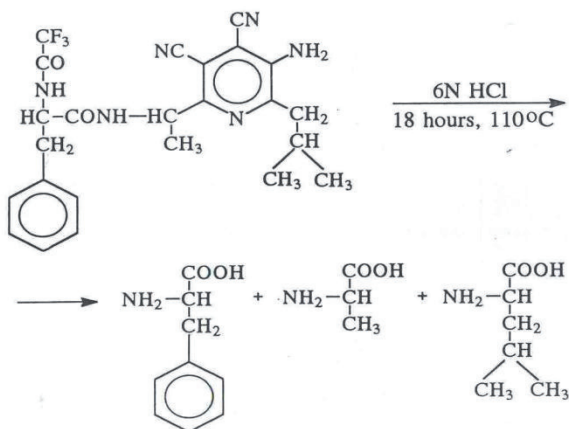
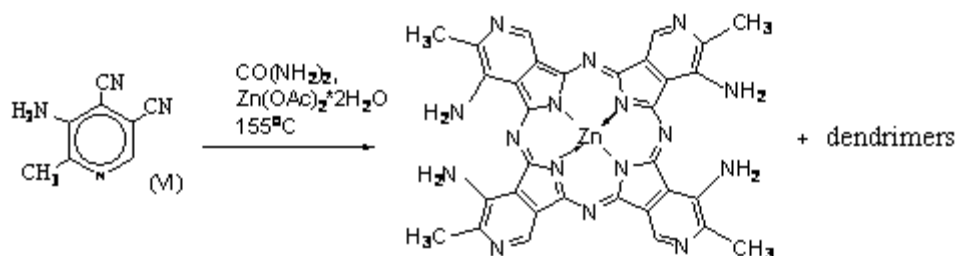


Fig 1. EL- fragmentation and hydrolysis of peptidylpyridine. M -486 M -243, M-,372, M-000, M-000, The ratio of amino acids Phe:Ala:Ile is 10:1,2:1

Template reaction of dendrimerization of substituted nonsymmetrical dicyanopyridines (easily forming by condensation of amino acids or peptides to a fumaric acid nitrile^[1]), led to multiple porphyrines derivatives (porphyrazines) with a molecular mass about 40 kDa. (Fig 2) Template synthesis of porphyrine isomers and their dendrimer derivatives is likely controlled by metal ions capable to complex to the external functional groups. Commonly, for the synthesis of porphyrines the starting compounds are symmetrical complexation group-free structures. The reactivity of nitrile groups in positions 4 and 5 for 3-amino-3-hydroxypyridine is very different. This should lead to the interaction of the type "head to tail". Hence, if the reaction proceeds in the presence of urea, ammonia and metal ions forming urea derivatives or a stable complex with external functional groups (hydroxyl, amino group in the position 6 of pyridine ring), it is then perhaps the formation of symmetrical isomers.



Dendrimerization has resulted in 4-fold molecular weight increase, obviously due to adduction of two pyridines to monotetraporphyrin and subsequent quaterization. Initial step of this process (in case of 2-methyl-3-amino - 4,5 - dicyanopyridine) can be monitored mass spectrometrically: m/z 158 (initial pyridine), m/z 634-637 (monoporphyrins), m/z 785-798 (+1 pyridine core), m/z 950-1016 (+2 pyridine cores), m/z 3920-4030 (1 dendrimer), m/z 4910-4930 (1 dendrimer + porphyrin + 2 pyridines), etc. Such reactions may results in valuable products: highly immunogenic multiple peptides, adjuvants, transfection agents, dendrimeric fluorescent tags. Valuable physical and chemical properties of the resulting compounds, strong absorption and fluorescence in the red spectral region, the ability to multi-point interaction (especially with biopolymers) and relatively high solubility in aqueous media makes them promising for use in biotechnology and medicine. Fluorescence of tetraporphyrin multiplet derivatives in a wide range (400-900 nm) allowed to observe binding of these compounds to cell lines by flow cytometry with various excitation sources. High fluorescence activity and absorption of the peptide-dienophiles condensation products can be use for sequencing of peptides (Fig 1). The reaction is carried out in the presence of anhydrides and acid chlorides, and peptide oxazole derivatives leads to acylation, decarboxylation and condensation. Their acidolysis leads to fragmentation of the peptide chain. Amino acid or mass-spectrometric analysis of the resulting fragments may restore the original sequence. The process is facilitated by a modification of the N-terminal amino acids, for example, by diazotization of peptides.

References

- [1] Sklyarov, L. Yu.; Kochetkova G.G. *Patent U.S.S.R.* 1976, № 618940.

Development of a novel structural vaccinology strategy for epitope discovery for the *Burkholderia pseudomallei* OppA antigen

Alessandro Gori, Claudio Peri, Renato Longhi, Giorgio Colombo

Istituto di Chimica del Riconoscimento Molecolare, Consiglio Nazionale delle Ricerche,
20131 Milano, Italy

E-mail: a.gori@insm.isti.cnr.it ; g.colombo@icrm.cnr.it

Introduction

Structure based vaccine design is a promising and attractive strategy towards the development of fully synthetic vaccine candidates, as well as in the discovery of new biomarkers.^[1] We present here a multi-disciplinary approach where the crystal structure of Oligopeptide-binding protein A (OppA_{Bp}) from the Gram-negative pathogen *Burkholderia pseudomallei*, the etiological agent of melioidosis, was used as the basis for the application of a computational strategy combining Matrix of Local Coupling Energies (MCLE) and Electrostatic Desolvation Profiles (EDP) methods to predict consensus epitopes that were realized in the form of peptides (COMP 1-3, Fig. 1).^[2,3] Parallel experimental epitope mapping based on proteolytic digestion and immunocapturing was performed generating three more peptide candidates (EXP 4-6, Fig. 1). All peptides were conjugated to carrier protein HSA and underwent immunogenicity evaluation in healthy patients, giving promising feedbacks.

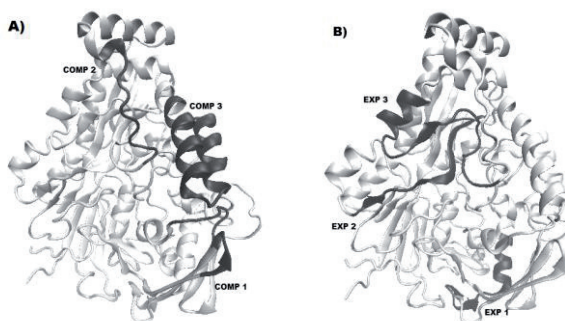


Figure 1. OppA crystal structure and A) Epitope candidates resulting from Theoretical prediction (COMP 1-3); B) Epitope candidates from Experimental mappings (EXP 4-6).

Results and Discussion

Although the results of theoretical and experimental epitope mapping differed in their sequences, they mapped closely in their 3D locations. To allow scarcely accessible regions to be identified as possible antibody binding sites our computational methods were integrated with a domains decomposition *ab initio* approach, resulting in improved agreement with the experimentally mapped epitopes.^[3] To evaluate the immunogenicity of the synthetic peptides, these were coated onto ELISA plates, probed with diluted plasma

samples from healthy controls, *i.e.* seropositive (S+) and seronegative (S-) individuals and recovered melioidosis subjects (R), and quantified by indirect ELISA (Fig.2). Control experiments were run using *B.pseudomallei* antigen extract and recombinant OppA.

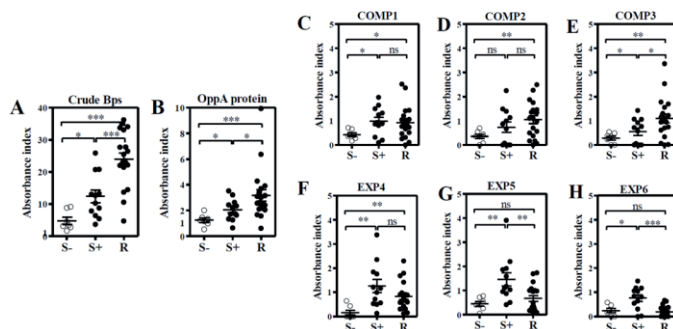


Figure 2. Antibody response to *B. pseudomallei* antigens in plasma of healthy and recovered melioidosis subjects.

All of the peptide epitope candidates were selectively recognized by the plasma antibodies, thus confirming the reliability of the computational prediction. Notably, reactivity against COMP 1-3 peptides was generally higher in the R group in comparison with the S- one and, in particular, the reactivity of COMP 3 was significantly diverse among the three groups, highlighting its potential as diagnostic tool. Moreover, human plasma antibodies to EXP 5-6 peptides were significantly higher in the S+ group than S- or R melioidosis groups, suggesting that these peptides might be used to discriminate between asymptomatic vs. clinical melioidosis. Overall, results from computational predictions nicely complement data from experimental mapping. Furthermore, predictions from protein domains decomposition strategy may lead to additional good new candidates. It is also worth noting that recovered melioidosis patients with the history of recurrent infection had anti-OppA levels lower than those without recurrent infection. This is indicative that a partial protection against *B. pseudomallei* infection may arise from an OppA derived epitopes vaccination strategy. According to this, protective experiments in infection models using OppA derived epitopes are following next.

Acknowledgments

We thank the Cariplo Progetto Vaccini for financial support. We are grateful to Prof. Martino Bolognesi, Dr. Patricia Lassaux, Dr. Louise Gourlay (Crystallography – University of Milan), to Prof. Xavier Daura, Dr. Mario Ferrer-Navarro, Dr. Oscar Conchillo Solé (Experimental epitope mapping – Universidad Autonoma de Barcelona) and to Prof. Ganjana Lertmemongkolchai, Dr. Darawan Rinchai (Immunoreactivity assays – Khon Kaen University).

References

- [1] Purcell, A.W.; McCluskey, J.; Rossjohn, J. *Nature Rev. Drug Disc.* **2007**, *6*, 404-414.
- [2] Wiersinga, W.J.; van der Poll, T. et al. *Nature Rev. Microbiol.* **2006**, *4*, 272-282.
- [3] Scarabelli, G.; Morra, G.; Colombo, G. *Biophys J.* **2010**, *98*, 1966-1975.
- [4] Genoni, A.; Morra, G.; Colombo, G. *J. Phys. Chem.* **2012**, *116*, 3331-3343.

Development and validation of a UPLC- MS analytical method for the control of the conjugation of [Lys-Gly]₅-MOG₃₅₋₅₅ with mannan

Maria-Eleni Androutsou,¹ Irene Friligou,^{1,2} John Matsoukas,² Theodore Tselios²

¹*Department of Chemistry, University of Patras, GR-265 00, Patras, Greece;* ²*Eldrug S.A., Pharmaceutical Company, GR-26504, Platani, Patras, Greece*

E-mail: tselios@upatras.gr

Introduction

Multiple Sclerosis (MS) is a slowly progressive, immunologically mediated disease of the central nervous system (CNS), characterized by inflammation and demyelination of white matter in the brain and spinal cord^{1,2}. MS is generally considered to be an autoimmune disease involving CD4⁺ and CD8⁺ T lymphocytes and B cells. This is strongly supported by the strong association of the MHC class II gene with disease and the ability of TH1 and Th17 CD4⁺ T lymphocytes to drive disease in an animal model for MS named experimental autoimmune encephalomyelitis (EAE)^{1,2}. Modern approaches for the treatment of MS involve the design and synthesis of peptide analogues of immunodominant Myelin epitopes in order to regulate the immune response. Mannan has successfully been used as a carrier to target T cell antigens to the mannose receptor of dendritic cells leading to the induction of Th1 or Th2 immune responses regarding its form (oxidized or reduced respectively). The ability of mannan to induce different T cell cytokine profiles depending on the mode of conjugation with the peptide analogue^{3,4}. The Mannan-[Lys-Gly]₅-MOG₃₅₋₅₅ (Ap-MOG) conjugation presents an important molecule for the immunotherapy of MS^{2,3}. In this report, a sensitive, selective and rapid UPLC-MS method was developed for the determination of the [Lys-Gly]₅-MOG₃₅₋₅₅ peptide in order to control the conjugation of mannan with the [Lys-Gly]₅-MOG₃₅₋₅₅ peptide.

Results and Discussion

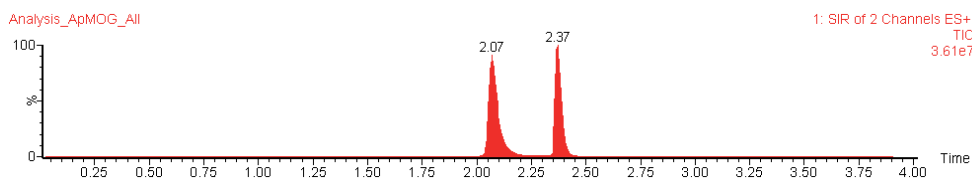
The analysis was carried out on a Waters Acquity UPLCTM system with cooling autosampler, column oven and a sample manager. A Waters SQD mass spectrometer was used for analytical detection. Stock solutions of [Lys-Gly]₅-MOG₃₅₋₅₅ and angiotensin II (IS) were prepared in water at the concentration of 1mg/ml. Stock solutions were used to prepare calibration samples (STDs) and quality controls (QCs). Working solution of IS was made at the concentration of 0.2 mg/mL in water.

Standard samples of 20, 40, 50, 60, 70, 80, 90 µg/ml were prepared from stock solution in water. Quality control (QC) samples were used to determine accuracy and precision of the method, and were independently prepared at low (25 µg/mL), medium (55 µg/mL) and high (85 µg/ml) concentrations. IS concentration was 12 ng/mL.

An Acquity UPLCTM BEH C18 column (150×2.1mm, 1.7µm) was employed for separation with the column temperature maintained at 40°C. The separation was performed using

gradient solution with 95% eluent A (0.1% formic acid in water) and 5% eluent B (0.1% formic acid in acetonitrile) in 3min. Initially 0.0 min = 5% B; 3 min = 50% B curve 6; 3.3 min = 100% B curve 6; 3.4 min = 5% B curve 8; 3.7 min = 5% B curve 6. For MS detection, ESI was used in positive mode applying for capillary 3.5 kV and for cone voltage 30 V. The molecular weight of [Lys-Gly]₅-MOG₃₅₋₅₅ (ApMOG) was 3508.07 Daltons. Mass fragment monitored for ApMOG and Angiotensin II (IS) were 502.54 and 524.10 respectively.

Calibration curve based on peak area ratio was linear at the concentration range of 20 – 90 µg/ml, with a detection limit of 5 µg/ml. Limit of quantification (LOQ) was considered as the lowest STD level of the calibration curve. Limit of detection (LOD) was defined by the concentration that yields a signal to-noise ratio of 3.



Scheme 1: Typical Chromatograms of [Lys-Gly]₅-MOG₃₅₋₅₅ expressed in minutes, $t_R = 2.07 \pm 0.02$ for [Lys-Gly]₅-MOG₃₅₋₅₅ and 2.37 ± 0.02 for Angiotensin II (IS).

Table 1: Quality controls (QCs) concentrations (µg/ml) for the analyte

QC Concentration (µg/ml)	Accuracy (%)	Precision (RSD%) Intra-day	Precision (RSD%) Inter-day
25 (low)	92,81	8,84	9,21
55 (medium)	102,29	6,25	7,03
85 (high)	98,35	5,42	6,21

The method showed satisfactory reproducibility and confirmed the entire conjugation between oxidized mannan and peptide sequence.

Acknowledgments

This work is financially supported by the “Cooperation” program 09SYN-609-21, (O. P. Competitiveness & Entrepreneurship (EPAN II), ROP Macedonia - Thrace, ROP Crete and Aegean Islands, ROP Thessaly – Mainland Greece – Epirus, ROP Attica).

References

- [1] Mantzourani, E.D.; Mavromoustakos, T.M.; Platts, J.A.; Matsoukas, J.M.; Tselios, T.V. *Cur. Med. Chem.* **2005**, *12(13)*, 1569.
- [2] Katsara, M.; Deraos, G.; Tselios, T.; Matsoukas, M. T.; Friligou, I.; Matsoukas, J.; Apostolopoulos, V. *J. Med. Chem.* **2009**, *52(1)*, 214.
- [3] Katsara, M.; Yuriev, E.; Ramslund, P.A.; Tselios, T.; Deraos, G.; Lourbopoulos, A.; Grigoriadis, N.; Matsoukas, J.; Apostolopoulos, V. *Immunology.* **2009**, *128*, 521.

Cell–Penetrating Peptide mimetics with 1,2-fused isoxazoles and phthalazines as anchor heterocycles of α - or β -peptide sequences

Petros G. Tsoungas¹, George N. Pairas², Paul Cordopatis²

¹*Dept. of Biochemistry, Hellenic Pasteur Institute;* ²*Dept of Pharmacy, Univ. of Patras*
pacord@upatras.gr

Introduction

Peptides, despite their potential, have seen limited use as clinically viable drugs, particularly those derived from α -natural amino acids, mainly because of their rapid proteolysis, low membrane permeability, pharmacodynamics, bioavailability and toxicity [1]. A chemically induced modification of a peptide structure and subsequently its conformation gives rise to a peptide mimic with improved performance on the aforementioned functions [2] or introduces biological and chemical properties associated with effective drug action [3].

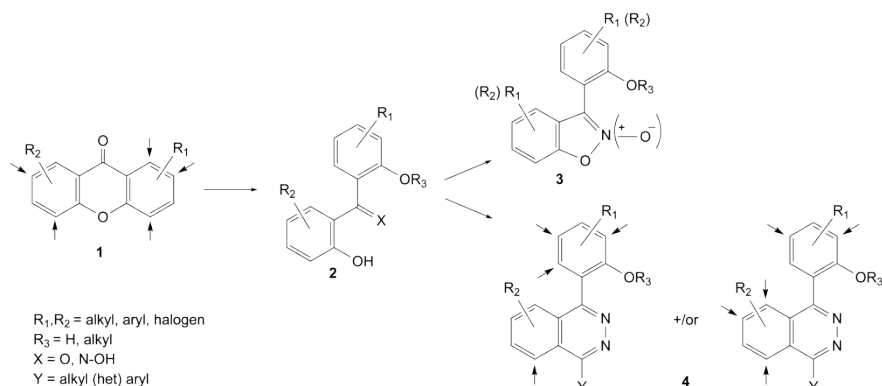
Peptides penetrating the cell membrane, known as Cell Penetrating Peptides (CPPs) or Protein Transduction Domains (PTD), as well as their mimics have been reported in the past few years [4]. They are typically short sequences of 15-20 amino acids, frequently charged. CPPs have been characterized and optimized as delivery agents to cells by two distinct routes (i) an energy-dependent vesicular one and (ii) a translocation of the lipid bilayer. Some CPPs are natural sequences while others are artificial constructs, designed to capture the features of natural formations. CPPs are particularly important in the delivery of peptides, proteins, nucleic acids, small molecule drugs or imaging agents. Appended ones enhance the activity of peptide-based drugs [4].

Heterocycle-based CPP mimics exhibit conformational constraints and / or latent reactivity related to the hetero-cycle's structural profile and are, thus, promising candidates for therapeutics [5]. The heterocycle can enter either at the beginning or at the end of the synthetic scheme. 5- and 6-membered N,O- and N,N-heterocycles are included in the most commonly employed ones. 1,2-fused isoxazoles (or their N-oxides) **3** and phthalazines **4** figure prominently among them.

Results and Discussion

The contiguous arrangement of N and O atoms in an aromatic ring and fusion of the latter to another one affect the conformation of the structures, mainly their planarity and rigidity. Suitable substitution generates anchor structures onto which peptide sequences can be attached.

(A)symmetric regioselective substitution patterns of **3** and **4** are obtained by the xanthone-based approach [6,7], having a C-O to C-C oxidative domino rearrangement as the key reaction [8] (Scheme 1).



Scheme 1

Amide, bromine or carboxyl appendices are anchor sites for coupling to any desired peptide chain (Fig.1). The latter can be effected through (a) transamidation [9] and/or a Hartwig-Buchwald coupling [10] or (b) a Ballini reaction [11] followed by an Umpolung approach [12].

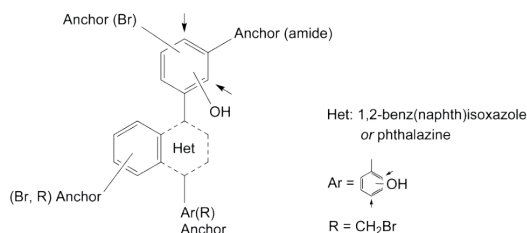


Fig.1

References

- [1] Frackenpohl, J.; Arvidsson, P.I.; Sreiber, J.V.; Seebach, D. *ChemBioChem*, **2001**, 2, 445.
- [2] Seebach, D.; Gardiner, J. *Acc.Chem.Res.*, **2008**, 41(10),1366.
- [3] Jeng, A.Y; Savage, P.; Beil, M.E.; Brusco, W.; Hoyer, D.; Fink, C.A.; Trapani, A.J. *Clin.Sci.*, **2002**, 103, Suppl.48, 98.Abell, A. (Ed.), *Advances in Amino Acid Mimetics and Peptidomimetics*, JAI Press, Greenwich 1, **1999**.
- [4] Khafagy, El Sayed; Morishita, M. *Adv. Drug Deliv.Rev.*, **2012**, 64(6), 531. Stewart, K.M.; Horton, K.L.; Kelley, A.O. *Org.Biomol.Chem.*, **2008**, 6, 2242.
- [5] Sebbage, V.; *Biosci.Horizons*, **2009**, 2(1),64.
- [6] Odrowaz-Sypniewsky, M.; Tsoungas, P.G.; Varvounis, G.; Cordopatis, P. *Tetrahedron Lett.*, **2009**, 50, 5981.
- [7] Gardikis, Y.; Tsoungas, P.G.; Potamitis, C; Zervou, M; Cordopatis, P. *Heterocycles*, **2011**, 83(5), 1077. Gardikis, Y.; Tsoungas, P.G.; Potamitis, C.; Zervou, M.; Pairas, G.; Cordopatis, P. *ibid*, **2011**, 83(6), 1291.
- [8] (a) Kotali A. and Tsoungas, P. G. *Tetrahedron Lett.*, **1987**, 28, 4321, (b) Kotali, A. Paulidou.; G. Glaveri, U.; Tsoungas, P. G. *Synthesis*, **1990**, 1172.
- [9] Bhadury P. S.; Song B.-A.; Yang S.; Hu D.-Y.; Xue,W. *Curr. Med. Chem.*, **2009**, 6, 380. Doyle, A.G.; Jacobsen, E. N. *Chem. Rev.*, **2007**, 107, 5713. Pellissier, H. *Tetrahedron*, **2007**, 63, 9267.
- [10] Hartwig, J.F. *Acc. Chem. Res.*, **2008**, 41, 1534.
- [11] Ballini, R.; Barboni, L.; Giarlo, G. *J.Org.Chem.*, **2004**, 69, 6907.
- [12] Shen, B.; Makley, D.M.; Johnston, J.N. *Nature*, **2010**, 465, 1027.

Keratin and collagen models as a tool in the deterioration of works of art

Evmorfia Fotou,¹ Ioanna Kostoula,¹ Stella Zevgiti,¹ Eugenia Panou-Pomonis,¹ Georgios Panagiaris,² Maria Sakarellos-Daitsiotis¹

¹*Section of Organic Chemistry and Biochemistry, Department of Chemistry, University of Ioannina, 45110 Ioannina, Greece;* ²*Department of Conservation of Antiquities and Works of Art, T.E.I of Athens, 12210 Egaleo, Greece*

E-mail: evi-fotou@hotmail.com

Introduction

Among the materials constituting cultural heritage, proteinaceous materials such as wool, leather and silk, are the most susceptible to damage and decay due to the influence of environment, temperature, humidity, air pollutants and light. Identification of proteins is essential to understand ancient technologies, determine the extent of decay and help in future restoration and preservation processes [1,2].

Aiming at contributing to the development of a reliable and reproducible immunoassay for the evaluation of the keratin and collagen based on the decay of works of art, three polypeptides YRSGGGFGYRSGGGFGYRS- β Ala-NH₂, [Pro-Cys(Acm)-Gly]_n and [Pro-Ser-Gly]_n were synthesized as models of keratin and collagen fragments. The obtained sera will be used to evaluate the decay of keratin and collagen in artificial and natural samples.

Results and Discussion

The polypeptide [Pro-Cys(Acm)-Gly]_n was synthesized by polymerization of the pentachlorophenyl ester, while synthesis of the peptide YRSGGGFGYRSGGGFGYRS- β Ala-NH₂ was performed by the Fmoc/tBu strategy on a Rink Amide AM resin. Coupling reactions were performed using a molar ratio of amino acid/HBTU/HOBt/DIEA/resin 3/3/3/6/1. All residues were introduced as Fmoc-protected amino acids and Fmoc-groups were removed using 20% piperidine in DMF. The N-terminal part of the peptide was acetylated. Cleavage of the peptide from the resin, as well as all the protective groups, was carried out with the mixture TFA/TIS/H₂O 95/2.5/2.5 v/v. The purity was checked by analytical HPLC and the correct molecular mass was confirmed by ESI-MS. The conformational study of the polymer [Pro-Cys(Acm)-Gly]_n was performed with circular dichroism spectroscopy (Figure 1).

The polypeptide YRSGGGFGYRSGGGFGYRS- β Ala-NH₂ was used to immunize New Zealand white rabbits. The animals received, firstly, an injection of 1.5mg of peptide in 750 μ l H₂O and 750 μ l Complete Freund's adjuvant and then repeated injections of 0.75mg of peptide in 750 μ l H₂O and 750 μ l Incomplete Freund's adjuvant. Blood was collected from the ear of the animal 7 days after each injection [3]. The collected sera of the rabbits were tested for the presence of antibodies against the polypeptide by ELISA (Figure 2). The immunization experiments of the polymers [Pro-Cys(Acm)-Gly]_n and [Pro-Ser-Gly]_n are in progress.

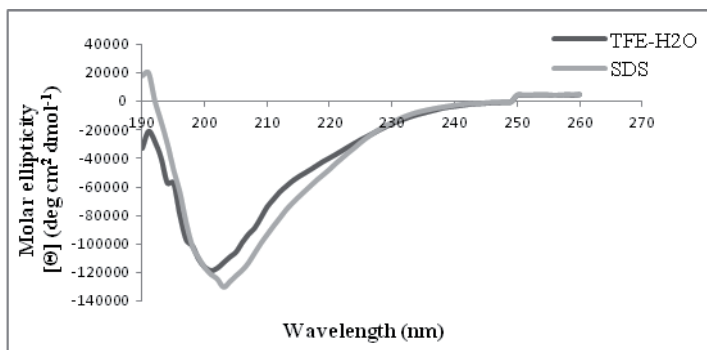


Figure 1: CD spectra of [Pro-Cys(Acm)-Gly]_n in TFE/H₂O 50:50 v/v and SDS 8mM.

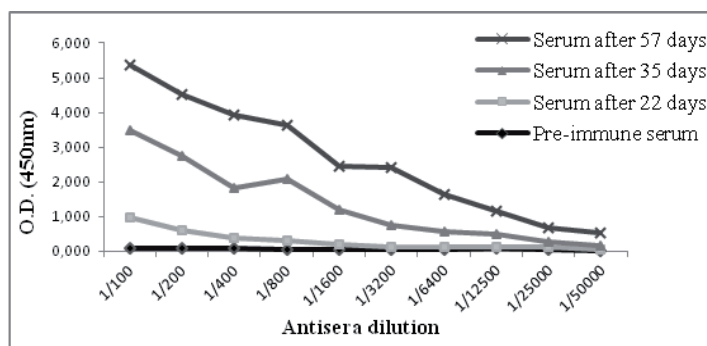


Figure 2: Binding of rabbit antisera to the polypeptide YRSGGGFGYRSGGGFGYRS-βAla-NH₂ at dilutions from 1:100 to 1:50.000.

Acknowledgment

This research has been co-financed by the European Union (European Social Fund – ESF) and Greek national funds through the Operational Program "Education and Lifelong Learning" of the National Strategic Reference Framework (NSRF) - Research Funding Program: *THALES. Reinforcement of the interdisciplinary and/or inter-institutional research and innovation with the possibility of attracting high standard researchers from abroad through the implementation of basic and applied excellence research.*

References

- [1] Deselnicu D.C. *Rev. J. Leather and Footwear*. **2010**, *10*, 13-30.
- [2] Baranski, A.; Lagan, J.M.; Lojewski, T. *e-Preservation Sci*. **2006**, *3*, 1-4.
- [3] Zevgiti, S.; Sakarellos, C.; Sakarellos-Daitsiotis, M.; Ioakimoglou, E.; Panou-Pomonis, E. *J. Pep. Sci*. **2007**, *13*, 121-127.

New biphasic solvent systems for the purification of non-ionic synthetic hydrophobic peptides by Centrifugal Partition Chromatography

**Nassima Amarouche^a, Leslie Boudesoque^a, Matthieu Giraud^b,
Alessandro Butte^b, Francesca Quattrini^b, Jean-Hugues Renault^{a*}**

^a*ICMR UMR CNRS 7312, SFR Cap-Santé Université de Reims Champagne-Ardenne, Bât. 18, Moulin de la Housse, B.P. 1039, 51687 Reims cedex 2, France;* ^b*Lonza AG, Valais Works, Rottenstrasse 6, 3930 Visp, Switzerland*

nassima.amarouche@etudiant.univ-reims.fr

Introduction

Protected synthetic non-ionic peptides, which are for example synthetic intermediates for the production of API's, are often very hydrophobic and not soluble in most common solvents. They are thus difficult to purify by preparative RP-HPLC, classically used for industrial production. It is then challenging to develop alternative purification chromatographic processes using suitable solvents and providing good yields, high purity and sufficient productivity. The technique of support free liquid-liquid chromatography, including both its hydrostatic (Centrifugal Partition Chromatography or CPC) and its hydrodynamic (Counter-Current Chromatography or CCC) declensions, are mainly involved in phytochemical studies [1] but has also been applied to peptide purification [2]. The previously developed biphasic solvent systems are not adapted to the purification of highly hydrophobic protected peptides. This is a specific problem that may require development of some new biphasic systems for large scale protected peptides purification. In the course of the purification of some protected synthetic peptides, intermediates for the production of API's, sparingly soluble in most of the solvents used with CPC, we initiated the use of two new scales of biphasic solvents systems composed of heptane-tetrahydrofuran-acetonitrile-dimethylsulfoxide-water and heptane-N-methyl tetrahydrofuran – N-methyl pyrrolidone-water, as well as a ternary biphasic solvent system composed of cyclopentyl methyl ether-dimethyl formamide-water. It is the goal of this work to present those generally useful biphasic systems for separating protected peptides and their characterization.

Results and Discussion

Since the goal of CPC is preparative rather than analytical, the choice of solvents is mainly guided by the solubility of the compounds. Building a system around good solvents of the sample, ensure a maximum solubility in the final system, and a better method capacity. Due to their low solubility in water and the common solvents used in CPC, solvent systems for protected peptides should be built around strong solvents such as dimethyl formamide, N-methyl pyrrolidone (NMP), acetonitrile, dimethyl sulfoxide (DMSO) and other similar organic solvents, ensuring maximum solubility of the sample in the system. The type 0 ternary system composed of water, DMSO, and THF, known for its powerful solvating properties [3] is unsuitable for the purification of hydrophobic protected synthetic peptides

as those peptides, insoluble in water, tend to partition preferentially in the THF and DMSO rich upper phase. A modification of the system by introducing heptane and acetonitrile facilitate their transition to the aqueous lower phase. The new quinquenary resulting biphasic system composed of heptane, THF, acetonitrile, DMSO and water may be then adapted to the particular case of purification protected non-ionic peptides. The system was efficiently tested on the purification of a protected synthetic 39 mer exenatide, a glucagon-like peptide-1 agonist, drug used in the treatment of some cases of diabetes (Figure1).

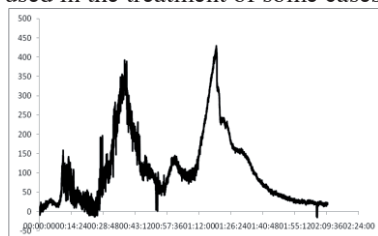


Figure 1: CPC chromatogram of 2g of a 81% initial purity 39mer protected exenatide: biphasic system, Hept/THF/MeCN/DMSO/W (15:35:15:20:15, v/v); HPLC analysis of pic 4 shows 98.57% exenatide purity.

A modification of the new developed quinquenary biphasic system by introducing the two new solvents 2-methyltetrahydrofuran (2-MeTHF) and N-Methyl-2- pyrrolidone (NMP) lead to the simpler new quaternary system Heptane/ 2-MeTHF/NMP/ W. A substitution of Me-THF by Cyclopentyl methyl ether (CPME) and NMP by dimethylformamide (DMF) in the system leads to the new type 1 ternary system CPME/DMF/W. The new systems Heptane/MeTHF/NMP/W and CPME/DMF/W were efficiently used on the purification of a 8mer partially protected peptide intermediate of bivalirudin synthesis (Figure 2).

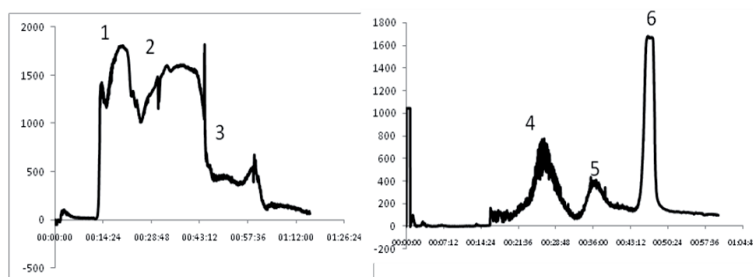


Figure 2: CPC chromatogram of 1g of a 68% initial purity 8mer protected peptide intermediate of bivalirudin synthesis, left: biphasic system, Heptane/ Me-THF/NMP/water (7:50:23:20, v/v), right: biphasic system CPME/DMF/W (7:5 : 1, v/v), HPLC analysis of pics 2 and 6 shows purities of 98% and 99.05% respectively

In order to allow a quick finding of the suitable solvent system composition for a successful fractionation, new scales covering a broad range of polarities by gradually varying the ratio of each solvent in the mixture were built for the quinquenary and the ternary developed systems. A ternary diagram was built for the new ternary built system.

References

- [1] Pauli G. F.; Pro S. M.; Friesen J. B. *J. Nat. Prod.* **2008**, *71*, 1489.
- [2] Knight M., *J. Chromatogr. A.* **2007**, *148*, 1151.
- [3] Foucault A. P; Durand P.; Camacho Frias E.; Le Goffic F., *Anal. Chem.* **1999**, *65*, 2150.

Spectroscopic investigation of the interaction of curcumin with the β -amyloid peptide of Alzheimer's disease

D. Benaki,¹ K. Stamatakis,¹ L. Leondiadis,² E. Mikros,³ M. Pelecanou¹

Institutes of ¹Biology and ²Radioisotopes & Radiodiagnostic Products, NCSR
«Demokritos», Athens, Greece; ³Div. of Pharmaceutical Chemistry, Univ. of Athens,
Panepistimiopolis Zografou, Athens, Greece

E-mail: pelmar@bio.demokritos.gr

Introduction

Curcumin (diferuloylmethane), is the major (2-8% by weight) polyphenolic pigment of the turmeric root (*Curcuma longa*), belonging to the *Zingiberaceae* family. For over 6000 years curcumin has been used in traditional Indian and Chinese medicine to treat various common ailments including stomach upset, flatulence, dysentery, ulcers, jaundice, arthritis, sprains, wounds, acnes, skin and eye infections. Extensive research within the past two decades has shown that curcumin has potential therapeutic value against neurodegenerative, cardiovascular, pulmonary, metabolic, auto-immune, and neoplastic diseases [1] with well documented beneficial antioxidative, anti-inflammatory, and antitumorigenic effects against cancer and other chronic diseases. The pleiotropic activities of curcumin related to its high ability to affect various signaling pathways are attributed to the presence of many functional groups in its structure including the α , β -unsaturated β -diketone moiety, carbonyl and enolic groups of the β -diketone moiety, methoxy and phenolic hydroxyl groups, and phenyl rings, all suitable for interaction with other macromolecules.

Recent experimental findings provide evidence that curcumin may play a role in the treatment of Alzheimer's Disease (AD). Curcumin selectively labels amyloid plaques and blocks aggregation as well as fibril formation *in vitro*. Most importantly when injected peripherally into animal model of the AD pathology, it was shown to cross the blood-brain barrier, to label plaques, and to reduce amyloid levels and plaque-amyloid burden *in vivo* [2]. In the current work CD, NMR, and Fluorescence spectroscopy were used as biophysical tools to investigate the interaction of curcumin with the β -AP (1-40) under various experimental conditions. Studies were performed in aqueous solution and in various v/v% of methanol as co-solvent in order to increase the solubility of curcumin in the aqueous environment.

Results and Discussion

Methanol 100%: The NMR spectrum of curcumin in 100% methanol is characterized by resonances with short line widths and nOe cross peaks orientated antiphase compared to the diagonal, as expected from its molecular weight. The connectivities observed are in agreement with the free rotation of the phenyl groups around the bond connecting them to the dienic bridge and the presence of *syn* and *anti* conformers depending on the orientation of the substituents on the phenyl group relative to the β -diketone oxygens. The presence of β -AP(1-40) in solution has two effects on the spectrum of curcumin: (a) the nOes reverse sign, become in-phase with the diagonal, indicative of the association with a macromolecular entity, and (b) only the conformer with both methoxy groups orientated

anti to oxygens of the β -diketone moiety is present, implying that this structure favors interaction with β -AP(1-40).

Methanol/Water 50%: In 50% methanol noticeable changes in the NMR lineshape and width indicate that curcumin exists in a different solution state. This is further described by the sign of the nOe correlation peaks being in-phase with the diagonal, probably related to the formation of a higher order structure dictated by the hydrophobic nature of curcumin. The presence of β -AP(1-40) results in great broadening of the curcumin resonances suggesting its interaction with a higher order (oligomeric or polymeric) β -AP(1-40) species not visible in the spectrum. The interaction of the β -AP(1-40) with curcumin in 50% methanol is also clearly evidenced by fluorescence through an intensity enhancement and a blue shift of 22 nm compared to the spectrum of plain curcumin (Figure 1), findings that usually denote the change of the microenvironment of the fluorophore to more hydrophobic.

Aqueous solution: Curcumin is sparingly soluble in water and the interaction with β -AP(1-40) was investigated only through CD spectropolarimetry for which concentrations of the range of μ M are required. Curcumin is a symmetric molecule and has no CD spectrum in all UV region. However, in the presence of β -AP(1-40) an induced near-UV CD spectrum of curcumin is observed (Figure 2), attributed to direct interaction with β -AP(1-40) and consequent loss of symmetry. This observation is further confirmed by a notable retardation of the β -AP(1-40) aging, in the presence of curcumin, suggesting an inhibitory role for curcumin on the aggregation of the β -AP(1-40) peptide.

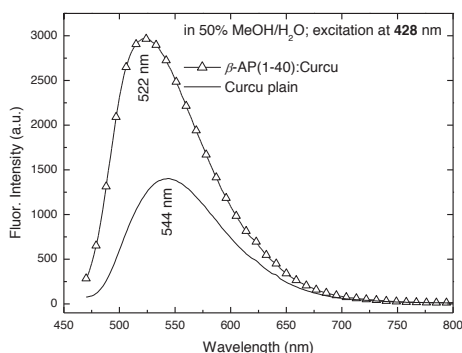


Figure 1. Fluorescence spectra of plain curcumin and its mixture with β -AP(1-40) in 50% methanol.

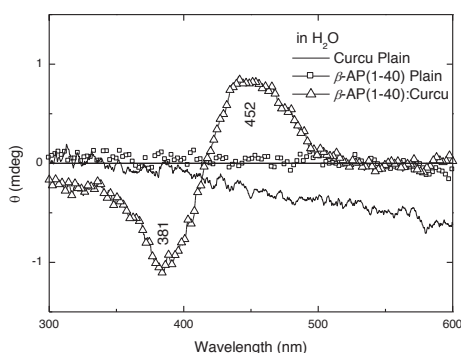


Figure 2. Near UV spectra of aqueous solutions of plain β -AP(1-40), plain curcumin and their mixture.

Our experimental findings support the direct interaction of β -AP(1-40) with curcumin and establish its importance as a potential aggregation inhibitor of β -AP.

References

- [1] Agarwal, B.B.; Harikumar, K.B. *Int. J. Biochem. Cell Biol.* **2009**, *41*, 40.
- [2] Yang, F.; Lim, G.P.; Begum, A.N.; Ubada, O.J.; Simmons, M.R.; Ambegaokar, S.S.; Chen, P.P.; Kayed, R.; Glabe, C.G.; Frautschy, S.A.; Cole, G.M. *J. Biol. Chem.* **2005**, *280*, 5892.

Synthesis and anticancer activities of lipophilic somatostatin derivatives

Hitomi Inazumi¹, Tai-jiro Suyama¹, Daisuke Takami¹, Koushi Hidaka¹,
Anna Miyazaki^{1,2}, Toshio Yokoi¹, Isoko Kuriyama³, Hiromi Yoshida³,
Yoshiyuki Mizushima^{2,3}, Yuko Tsuda^{1,2}

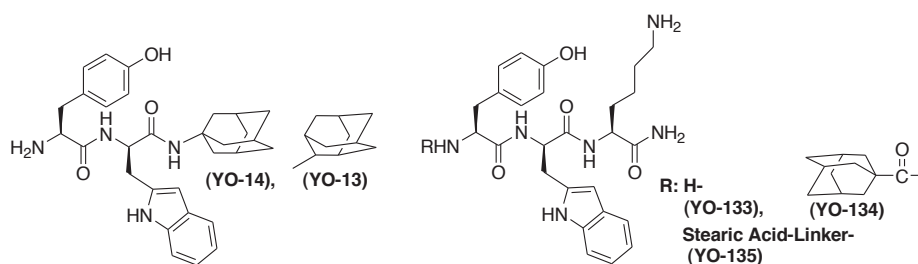
¹Faculty of Pharmaceutical Sciences; ²Cooperative Research Center of Life Sciences;

³Department of Nutritional Science, Kobe Gakuin University, Kobe 650-8586, Japan

E-mail: tsuda@pharm.kobegakuin.ac.jp

Introduction

Somatostatin (SS-14) is a cyclic tetradecapeptide and known as an anti-tumor agent as well a potent suppressor of secretion of growth hormone, insulin, glucagon and so on. A lot of efforts have been made to develop SS-14 analogues with clinically useable anti-tumor activity. Keri *et al.* reported that TT-232 [H-D-Phe-c(Cys-D-Trp-Lys-Cys)-Thr-NH₂] exhibited a potent antiproliferative activity without antiseecretory action mediated through SS-14 receptors (SSTRs) [1]. Based on its sequence, we synthesized H-Tyr-D-Trp-NH-1-Ada (adamantane) (YO-14) and H-Tyr-D-Trp-NH-2-Ada (YO-13) and reported they had potent antiproliferative activity in cancer cells (A-430 and SW480), which were comparable to TT-232 and cycloheximide [2]. A structure-activity relationship analysis revealed that the lipophilicity of YO-14 and -13 could be responsible for their antiproliferative activity. Now, we described 1) replacement of Tyr of YO-14/-13 with Tyr(Bzl), Phe, 1-Nal(1-naphthylalanine), and 2-Nal (2-naphthylalanine); 2) incorporation of stearic acid (a C18 lipophilic moiety) and 1-adamantanecarboxylic acid on the N-terminus of H-Tyr-D-Trp-Lys-NH₂, the TT-232 fragment; and 3) investigation of their physicochemical properties and biological activities.



Scheme 1. Structure of synthetic somatostatin derivatives.

Results and Discussion

Protected peptides were synthesized by a solution method using Boc-chemistry except YO-135, which was assembled by a standard Fmoc solid phase peptide synthesis (SPPS) on Fmoc-amide resin (Applied Biosystems Inc.). Final products were identified by analytical HPLC, MALDI (ESI)-TOF mass spectrometry and elemental analysis.

Table 1. Analytical data of YO-compounds.

Compound	Retention time ^{a)} (min)	Hydrophobicity ^{b)} ϕ_o	TOF-MS: m/z [M+H] ⁺	
			Found	Clacd
YO-14	24.6	49.5	501.7	501.6
YO-13	24.2		501.5	501.6
YO-89	30.4	51.6	591.7	591.6
YO-90	29.9	51.1	591.6	591.7
YO-91	21.3	/	592.6	592.7
YO-92	21.1	/	592.4	592.7
YO-109	41.1	55.6	485.9	485.6
YO-110	41.6	55.1	485.9	485.6
YO-111	44.3	58.5	535.3	535.6
YO-112	43.3	59.6	535.5	535.6
YO-113	45.5	59.9	535.3	535.6
YO-114	44.6	55.9	535.4	535.6
YO-115	39.1	51.6	529.3	529.6
YO-116	38.4	48.9	529.4	529.6
YO-133	14.9	/	495.2	495.2
YO-134	32.8	/	657.3	657.3
YO-135	62.1	/	1108.6	1108.6

^aExperimental conditions: Waters model 600E; column, COSMOSIL C18-AR-II (4.6 x 250 mm); solvent system (A) 0.05% TFA in water, (B) 0.05% TFA in CH₃CN, runs from A (90) :B (10) to A (10) :B (90) in 80 min. ^bValue was determined according to the literature (Anal. Chem. **1998**, 79, 4228).

The critical micelle concentration (CMC) of the surfactant was determined by measuring a change the fluorescence emission spectrum of pyrene monomers as a function of the surfactant [3]. The CMC (1.1×10^{-5} M) in aqueous YO-135 solutions was obtained, suggesting that YO-135 can form small colloidal particles (micelles) under these conditions. Among the YO-14/-13 related compounds, YO-113 and -114 exhibited not only the highest lipophilicity but also the strongest antiproliferative activity on HCT116 cells at 100 μ M in addition to an inhibition of DNA polymerase. These activities were greater than those of YO-14 and -13. YO-133 (H-Tyr-D-Trp-Lys-NH₂) showed neither anticancer nor DNA polymerase inhibitory activities. On the other hand, YO-135, in which a stearic acid bound to the TT-232 fragment (Tyr-D-Trp-Lys) through a linker, showed both antiproliferative activity on HCT116 cells and DNA polymerase inhibition at 100 μ M. Those findings suggest that lipophilicity correlates well with the antiproliferative activity on HCT116 cells and inhibition of DNA polymerase. Further structure-activity relationship studies are progressing in our group.

Acknowledgments

We are grateful to Dr. Lawrence H. Lazarus (NHEHS) for critical reading of the manuscript. The work was supported in part by a Grand-in-Aid for Scientific Research (C) (No. 22590111) from MEXT.

References

- [1] Keri, G.; Erchegeyi, J.; *et al. Proc. Natl. Acad. Sci. USA*, **1996**, 93, 12513.
- [2] Miyazaki, A.; Tsuda, Y.; *et al. J. Med. Chem.* **2008**, 51, 5121.
- [3] Dominguez, A.; Fernandez, A.; *et al. J. Chem. Edu.* **1997**, 74, 1227.

Synthesis of an anthraquinone type compound conjugated to the immunodominant 35-55 myelin oligodendrocyte glycoprotein (MOG₃₅₋₅₅)

I. Friligou, A. Tapeinou, J. Matsoukas, T. Tselios*

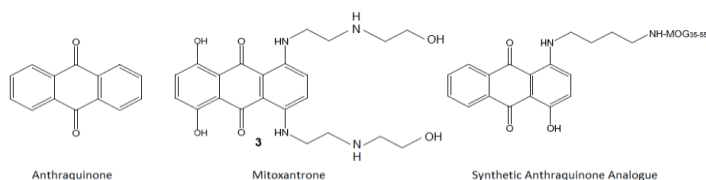
Department of Chemistry, Section of Organic Chemistry, Biochemistry and Natural Products, University of Patras, 265 00, Patras, Greece

E-mail: atapeinou@upatras.gr

Introduction

Multiple Sclerosis (MS) is a chronic autoimmune disease of the central nervous system (CNS)^{1,2}. Our aim was to immunologically control the attack of the myelin sheath in MS patients without the total suppression of the immune system. Anthraquinones (Mitoxantrone, Ametantrone) are widely used in cancer therapy as immunosuppressants. Mitoxantrone is also used to treat several forms of advancing MS, including secondary progressive MS, progressive relapsing MS, and advanced relapsing-remitting MS³. More specifically, Mitoxantrone is an inhibitor of the type II topoisomerase, which disrupts DNA synthesis and DNA repair in both healthy cells and cancer cells. Herein, we report the synthesis of an anthraquinone type compound conjugated to the immunodominant 35-55 myelin oligodendrocyte glycoprotein (MOG₃₅₋₅₅) for the selective immunosuppression of the encephalitogenic T cells in MS patients.

The anthraquinone was synthesized by a Friedel-Crafts acylation of hydroquinone from phthalic anhydride, followed by reduction of the resulted quinizarine to its leuco form, addition of the appropriate diamine and air oxidation. The synthesized molecules were purified using liquid chromatography, and they were identified by mass spectrometry and ¹H-NMR. The synthesis of the MOG₃₅₋₅₅ was performed under microwave irradiation⁴ and its conjugation with the anthraquinone was performed in solution. The final analogue was purified by RP-HPLC and identified by ESI-MS.



Results and Discussion

Synthesis of the anthraquinone type compound

In this study, an anthraquinone type compound was synthesized by a Friedel-Crafts acylation of hydroquinone from phthalic anhydride in the presence of molten salts

$\text{AlCl}_3\text{-NaCl}$. The reaction took place at 200-200°C for 30min. The precipitated product was of high purity and it was identified by $^1\text{H-NMR}$. The resulting quinizarin was dissolved in MeOH and it was reduced to its leuco form by refluxing it for 2h in the presence of Zn and AcOH. The obtained leuco-quinizarin was of high purity and it was identified by $^1\text{H-NMR}$. Its reaction with N-Boc-ethylenediamine took place at 50-55°C for 1h, and air oxidation followed for further 4h to give a mixture of products. Boc deprotection was achieved with 65% trifluoroacetic acid (TFA) in DCM in the presence of anisole as scavenger for 2h at RT. The final products were purified by semi-PREP RP-HPLC and they were identified by $^1\text{H-NMR}$.

Synthesis of the immunodominant 35-55 myelin oligodendrocyte glycoprotein (MOG₃₅₋₅₅)

The synthesis of MOG₃₅₋₅₅ was performed under microwave irradiation on Liberty™ Microwave Peptide Synthesizer (CEM), since microwave energy represents a fast and efficient way to enhance both the deprotection and coupling reactions overcoming chain aggregation. The resin utilized was CLTR-CL which is combined with Fmoc/ tBu methodology. The synthesized peptide analogue was characterized by ESI-MS.

Coupling MOG₃₅₋₅₅ to anthraquinone

The coupling of MOG₃₅₋₅₅ to the anthraquinone type compound was performed in solution by *in situ* activation with the uronium salt reagent TBTU in the presence of DIPEA. The reaction was completed after 12h. The deprotection of product was achieved with 65% trifluoroacetic acid (TFA) in DCM in the presence of triethylsilane (TES), anisole and water as scavengers for 5h at RT. The solvent was removed on a rotary evaporator and the obtained oily product was precipitated from cold diethylether as a white solid. The purity of the crude product was 23% according to RP-HPLC analysis, while the high purity of the final product was verified by RP-HPLC and its identification was achieved by ESI-MS.

Acknowledgments

This work was financially supported by the “Cooperation” program 09SYN-609-21, (O. P. Competitiveness & Entrepreneurship (EPAN II), ROP Macedonia - Thrace, ROP Crete and Aegean Islands, ROP Thessaly – Mainland Greece – Epirus, ROP Attica).

References

- [1] Spyranti, Z.; Dalkas, G. A.; Spyroulias, G. A.; Mantzourani, E. D.; Mavromoustakos, T.; Friligou, I.; Matsoukas, J. M.; Tselios, T. V. *J. Med. Chem.* **2007**, 50(24), 6039-6047.
- [2] Katsara, M.; Deraos, G.; Tselios, T.; Matsoukas, M. T.; Friligou, I.; Matsoukas, J.; Apostolopoulos, V. *J. Med. Chem.* **2009**, 52(1), 214-218.
- [3] Fox, E. *J. Clin. Ther.* **2006**, 28, 461-474.
- [4] Friligou, I.; Papadimitriou, E.; Gatos, D.; Matsoukas, J.; Tselios, T. *Amino Acids* **2010**, 40, 1431-1440.

Design and synthesis of N-methyl derivatives of urotensin-II

Francesco Merlino¹, Salvatore Di Maro¹, Ali Munaim Yousif¹, Pietro Campiglia², Stefania Meini³, Paolo Santicioli³, Carlo A. Maggi³, Ettore Novellino¹, Paolo Grieco¹

¹Dept. Pharmaceutical and Tox. Chemistry, University of Naples Federico II, Italy; ²Dept. of Pharmaceutical Sciences, University of Salerno, Italy; ³Dept. of Pharmacology, Menarini Ricerche, S.p.A., Florence, Italy

E-mail:paolo.grieco@unina.it

Introduction

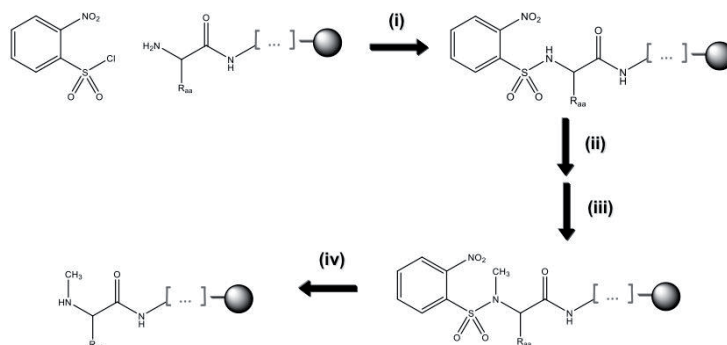
Human Urotensin-II is an undecapeptide (hUT-II, H-Glu-Thr-Pro-Asp-c[Cys-Phe-Trp-Lys-Tyr-Cys]-Val-OH) which was identified as a potent vasoconstrictor that binds with high affinity at UT receptor. The cysteine-linked cyclic region, hUT-II(4-11), is responsible for the biological activity and has been widely used to elucidate the Structure-Activity Relationship of hUT-II. With the aim to investigate the role of hydrogen bond and the effects of a peptide backbone constraint on binding affinity and biological activity, we have designed and synthesized new analogues by multiple N-Methylation of hUT-II(4-11) backbone amide bonds. All the peptides were performed by a novel synthetic approach, in which the introduction of N-methyl groups occur during regular solid-phase peptide synthesis (Table 1). On these new ligands we evaluated the binding affinity and biological activity at the UT receptor.

Table 1. Structures and Biological Activity of synthesized peptides

Code	Structure	pD ₂ (± SEM)	pK _a /pK _i (± SEM)
hUT-II(4-11)	H-Asp-c[Cys-Phe-Trp-Lys-Tyr-Cys]-Val-OH	8.20 ± 0.01	8.34 ± 0.08
Me5	H-Asp-c[(NMe)Cys-Phe-Trp-Lys-Tyr-Cys]-Val-OH	8.26 ± 0.03	8.53 ± 0.08
Me6	H-Asp-c[Cys-(NMe)Phe-Trp-Lys-Tyr-Cys]-Val-OH	6.36 ± 0.04	6.64 ± 0.10
Me7	H-Asp-c[Cys-Phe-(NMe)Trp-Lys-Tyr-Cys]-Val-OH	8.50 ± 0.05	8.76 ± 0.07
Me8	H-Asp-c[Cys-Phe-Trp-(NMe)Lys-Tyr-Cys]-Val-OH	4.91 ± 0.18	=5
Me9	H-Asp-c[Cys-Phe-Trp-Lys-(NMe)Tyr-Cys]-Val-OH	5.25 ± 0.07	=5
Me10	H-Asp-c[Cys-Phe-Trp-Lys-Tyr-(NMe)Cys]-Val-OH	8.31 ± 0.08	8.45 ± 0.05

Results and Discussion

We developed this small library of compounds to observe the conformational behavior and the effects in the binding to hUT receptor by N-methylation. Peptides were synthesized using a conventional Fmoc-based solid-phase strategy in a manual reaction vessel. The site-selective N-methylation of peptides was carried out on the solid support during the peptide synthesis by chemical approach developed by Fukuyama and Miller, and then optimized by Kessler et al. The direct N-methylation of the desired amino acid consists in three-step procedure involving amine activation by introduction of *o*-nitrobenzenesulfonyl group (*o*-NBS), followed by methylation and deprotection of the *o*-NBS group (Scheme 1).



Scheme 1.

Disulfide bridge was obtained on solid phase. Once the linear peptide was synthesized, the S-Trt group was removed by dilute TFA and the oxidation of thiols was carried out by using I₂ (10 eq) and DIEA (5 eq). The purification of final products was achieved using a semipreparative RP-HPLC. Binding on human UT receptor and functional assays in the rat isolated thoracic aorta were performed and the results are reported in Table 1. The compounds Me5, Me7 and Me10 resulted to be the more interesting peptides for their ability to preserve UT activation. In particular, the compound Me7 resulted to be a little more active respect to the UT(4-11) used as reference. The introduction of multiple N-methyl group in the hUT-II(4-11) sequence represents the next step to investigate the effects of this modification in the conformation and modulation of bioactivity into this cyclic peptide. These new ligands will be used in preliminary NMR conformational studies to define structural requirements to improve receptor affinity.

Acknowledgments

The Authors would like to thank the Menarini Ricerche for the valuable support.

References

- [1] Grieco, P.; Carotenuto, A.; Campiglia, P.; Marinelli, L.; Lama, T.; Petacchini, R.; Santicioli, P.; Maggi, C.A.; Rovero, P.; Novellino, E. *J. Med. Chem.* 2005, 48, 7290-7297.
- [2] Chatterjee, J.; Gilon, C.; Hoffman, A.; Kessler, H. *Accounts of chemical Research* 2008, 41, 1331-1342.

Peptide-epitope mapping and reactivity of the autoantigen Aquaporin-4

**H. Alexopoulos, E. I. Kampylafka, H. M. Moutsopoulos, M. C. Dalakas,
A. G. Tzioufas**

*Department of Pathophysiology, Faculty of Medicine, National and Kapodistrian
University of Athens, Greece*

e-mail:halexo@med.uoa.gr

Introduction

Neuromyelitis optica (NMO or Devic's Disease) is a rare autoimmune inflammatory demyelinating syndrome of the Central Nervous System (CNS) that preferentially targets the optic nerves and spinal cord ¹. Its course is usually relapsing, but without marked remission between relapses, leading to rapid accumulation of irreversible deficits ². The studies by Lennon et al ³ have provided unequivocal evidence that a specific autoantibody (NMO-IgG) against aquaporin-4 (AQP4) is a marker for the disease and differentiates neuromyelitis optica from multiple sclerosis ¹. Despite the fact that anti-AQP4 antibodies have an established role in the pathogenesis of neuromyelitis optica, their specificity regarding antigenic epitopes has not yet been determined.

Results

We used sera from 21 patients positive for NMO IgG/anti-AQP4 antibodies, as detected by indirect immunofluorescence on mouse brain tissue ³ (21/21 positive) and by a cell based assay. Sera from 28 healthy subjects were used as normal controls. The disease control group comprised of 23 patients with Systemic Lupus Erythematosus (SLE) and 23 patients with primary Sjögren's Syndrome (pSS), without neurological involvement. Eleven peptides, in the form of peptide dendrimers (multiple antigenic peptides, MAP) were synthesized. All patients and controls were evaluated for the presence of autoantibodies against the 11 peptides by ELISA assays. Homologous inhibition experiments were performed, in order to evaluate the specificity of the potential epitopes.

Peptides AQPp1, AQPp4 and AQPp8 contained the epitopes that were mostly recognized by the NMO positive sera, reaching reactivity levels of 42.9%, 33.3% and 23.8% of patients, respectively. The 3 most reactive peptides (AQPp1, AQPp4 and AQPp8), are part of the intracellular regions of the molecule (*Figure 1*). These peptides were further tested against 23 SLE and 23 pSS disease controls, in order to assess the specificity of their recognition. The identification of the 3 most reactive peptides, which are therefore potential linear antigenic epitopes of the AQP4 molecule, enabled the search of protein databases to identify similar sequences with other unrelated proteins. A 73% sequence similarity was observed between AQPp8 (amino acids 257-271) EFKRRFKEAFSKAAQ, and the [aa219-233] domain of the human protein TAX1BP1 (EFKKRFSDATSKAHQ), which is involved in the replication of the HTLV-1 virus, the etiological agent of HTLV-1-associated myelopathy/ tropical spastic paraparesis (HAM/TSP).

Discussion

All 3 B-cell epitopes identified in our study were surprisingly located in the intracellular domains of the molecule. This observation is in agreement with the recent finding of intracellular AQP4 T-cell epitopes. The mechanisms of recognition of intracellular epitopes are more complex, and to a great extent unknown. Many autoantibodies directed against intracellular antigens, including anti-U1RNP, anti-dsDNA, anti-Ro/SSA, anti-La/SSB, anti-Hu and others, have the potential to penetrate cells ^{4,7}, *in vivo* ^{8,9}. Our study does not address the conceivable pathogenic role of these specific antibodies but rather raises important questions about the generation of the immune response. One of the 3 epitopes identified in our study, presents high similarity with the human TAX1BP1 protein, which is involved in the pathogenesis of HAM/TSP, a disease that shares common clinical features with neuromyelitis optica. Future studies in our laboratory aim to determine the pathogenic relevance of these findings.

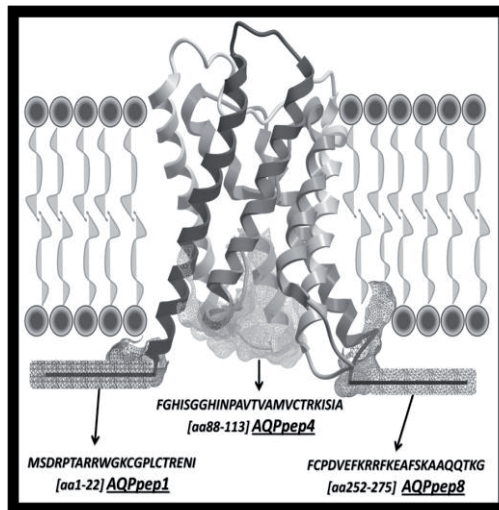


Figure 1: Dominant linear epitopes are located in the intracellular regions of the molecule.

References

- [1] Wingerchuk, D. M.; Lennon, V. A.; Pittock, S. J.; Lucchinetti, C. F.; Weinshenker, B. G. *Neurology* 2006, 66, 1485-9.
- [2] Jarius, S.; Paul, F.; Franciotta, D.; Waters, P.; Zipp, F.; Hohlfeld, R.; Vincent, A.; Wildemann, B. *Nat Clin Pract Neurol* 2008, 4, 202-14.
- [3] Lennon, V. A.; Wingerchuk, D. M.; Kryzer, T. J.; Pittock, S. J.; Lucchinetti, C. F.; Fujihara, K.; Nakashima, I.; Weinshenker, B. G. *Lancet* 2004, 364, 2106-12.
- [4] Alarcon-Segovia, D.; Llorente, L.; Ruiz-Arguelles, A. *J Autoimmun* 1996, 9, 295-300.
- [5] Hormigo, A.; Lieberman, F. *J Neuroimmunol* 1994, 55, 205-12.
- [6] Lisi, S.; Sisto, M.; Soleti, R.; Saponaro, C.; Scagliusi, P.; D'Amore, M.; Saccia, M.; Maffione, A. B.; Mitolo, V. *J Oral Pathol Med* 2007, 36, 511-23.
- [7] Ruiz-Arguelles, A.; Rivadeneyra-Espinoza, L.; Alarcon-Segovia, D. *Curr Pharm Des* 2003, 9, 1881-7.
- [8] Deng, S. X.; Hanson, E.; Sanz, I. *Int Immunol* 2000, 12, 415-23.
- [9] Ehrenstein, M. R.; Katz, D. R.; Griffiths, M. H.; Papadaki, L.; Winkler, T. H.; Kalden, J. R.; Isenberg, D. A. *Kidney Int* 1995, 48, 705-11.

Spectroscopic studies and *in vitro* functional effect of the chiral complexes of dinuclear rhodium

Zsuzsa Majer¹, Gábor Szilvágyi¹, Tamás Sipőcz¹, Norbert Szoboszlai²,
Erika Orbán³, Szilvia Bősze³

¹Eötvös Loránd University, Institute of Chemistry, Laboratory for Chiroptical Structure Analysis H-1117 Pázmány Péter sétány 1/A Budapest, Hungary; ²Eötvös Loránd University, Institute of Chemistry, Laboratory of Environmental Chemistry and Bioanalytics, Budapest, Hungary; ³Research Group of Peptide Chemistry, Hungarian Academy of Sciences, Budapest, Hungary

E-mail: majer@chem.elte.hu

Introduction

Dinuclear rhodium(II) complexes have attracted great attention because of their chemical reactivity, high catalytic activity, cytostatic properties [1] and potential applications as anticancer agents [2]. Dirhodium tetraacetate can accept both mono- and bidentate ligands: it can easily exchange one or more of its acetate units with a different type of ligands, as amines, alcohols, carboxylic acids, amino acids, etc. Axial ligands most commonly donor solvent molecules, are present in the majority of “paddlewheel” dirhodium complexes [3].

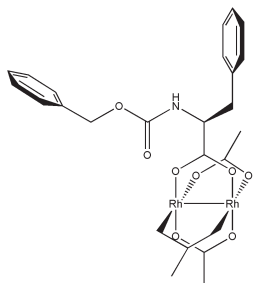
This work is aimed at the structure elucidation of the adduct of Rh₂(OAc)₄ with N-methyl-D-phenylalanine (NMe-phe-O⁻, adduct Rh₂M₂) and study of the *in vitro* functional effect of our earlier described amino acid containing chiral dirhodium complexes.

Results and Discussion

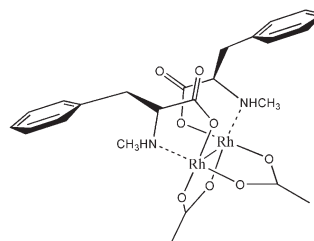
The adducts of Rh₂(OAc)₄ with chiral amino acid derivatives, as N-benzyloxy-carbonyl-L-phenylalanine (Z-Phe-O⁻, adduct Rh₂L_n, n=1-4) and N-acetyl-L-phenylalanine (Ac-Phe-O⁻ adduct Rh₂K_n, n=1-4) [4]; as well as N-methyl-D-phenylalanine (NMe-phe-O⁻, adduct Rh₂M₂) were prepared, separated and characterized by multiple spectroscopic methods (ECD, FTIR, VCD) supported by quantum chemistry (geometry optimization, conformer search, simulation of ECD and VCD spectra) at *ab initio* DFT-level.

We identified two different structures of the dirhodium complexes: (1) a “typical” paddlewheel with carboxylate bridging-type structure [4], where the acetate ligands of Rh₂(OAc)₄ were exchanged for protected amino acids, e.g. Z-Phe-O⁻ (Rh₂L_{1,4}), Ac-Phe-O⁻ (Rh₂K_{1,4}); (2) a “non-typical” paddlewheel structure, where the amino acid ligands are coordinated to the rhodium core by bidentate chelating mode, when the ligand was NMe-phe-OH (see Figures).

We have determined the cytostatic activity of the compounds *in vitro* and expressed as IC₅₀ values on HT-29 human colorectal adenocarcinoma cultures. Therefore cells were treated with the compounds at 10⁻⁴ to 5·10² μM concentration range and the activity of the compounds was determined by MTT-assay [5]. Intracellular rhodium content of the cells was measured by TXRF (total reflection X-ray fluorescence) method as described by Polgári et al. [6].



"typical" paddlewheel structure
(Rh_2L_1 adduct, where $L = Z\text{-Phe-O}^-$)



bidentate chelate type bonding
(Rh_2M_2 adduct, where $M = NMe\text{-phe-O}^-$)

Compound $Rh_2(OAc)_4$ exhibited significant cytostatic effect (IC_{50} : 16.8 μM) on HT-29 cell culture. Among the protected amino acid containing derivatives compounds RhL_1 , RhL_2 and RhL_3 with $Z\text{-Phe-O}^-$ proved to be the more active on tumor cells. The IC_{50} values of their cytostatic effects were measured as 20.2 μM , 4.5 μM and 58.5 μM , respectively. In the case of the $Ac\text{-Phe-O}^-$ containing Rh_2K_1 , Rh_2K_2 , Rh_2K_3 and Rh_2K_4 derivatives the *in vitro* antitumor activity was gradually diminished as increasing number of ligands were incorporated (IC_{50} values: 45.2 μM , 98.2 μM , 121.0 μM and > 200 μM , respectively).

It is worth to emphasize that the presence of the $NMe\text{-phe-O}^-$ moiety as ligand destroyed the *in vitro* cytostatic activity ($IC_{50} > 500 \mu M$).

Our results also indicate that the cellular uptake rate and *in vitro* cytostatic activity depend on (i) the structure/geometry of the complex and (ii) the number of the ligands. The dirhodium complexes, Rh_2L_1 and Rh_2L_2 were determined as the most effective compounds (IC_{50} values are 20.2 μM and 4.5 μM , respectively). So the growing number of ligands ($n=2,3$) or the blocked axial position of dirhodium core, reduce their efficacy and indicate that the presence of a "free" place for binding of a newer molecule (open coordination site) is highly important for their cytostatic activity *in vitro*.

Acknowledgments

This work was supported by the Hungarian Scientific Research Fund (OTKA K81175 and K100720). The participation on the conference was sponsored by the Foundation for the Hungarian Peptide and Protein Research.

References

- [1] Erck, A.; Rainen, L.; Whileyman, J.; Chang, I.-M.; Kimball, A. P.; Bear, J. L. *Proc. Soc. Exp. Biol. Med.* **1974**, *145*, 1278.
- [2] Chifotides, H. T.; Dunbar, K. R. *Acc. Chem. Res.*, **2005**, *38*, 146.
- [3] Cotton, F. A.; Walton, A. R. *Multiple Bonds Between Metal Atoms*; Clarendon Press: Oxford, **1993**.
- [4] Szilvgyi, G.; Hollosi, M.; Tolgyesi, L.; Frelek, J.; Majer, Zs. *Tetrahedron Asymm.* **2008**, *19*, 2594.; Szilvgyi, G.; Majer, Zs.; Vass, E.; Hollosi, M. *Chirality* **2011**, *23*, 294.
- [5] Liu, Y B; Peterson, D A; Kimura, H; Schubert, D. J. *Neurochem.* **1997**, *69*, 581.
- [6] Polgari, Zs.; Ajtony, Zs.; Kregsamer, P.; Strel, C.; Mihucz, V.G.; Reti, A.; Budai, B.; Kralovanszky, J.; Szoboszlai, N.; Zaray, Gy. *Talanta* **2011**, *85* 1959.

Chiroptical spectroscopic investigation on diamide peptide models

**Krisztina Knapp¹, Marcin Górecki², Miklós Hollósi¹, Elemér Vass¹,
Zsuzsa Majer¹**

¹*Eötvös Loránd University, Institute of Chemistry, Department of Organic Chemistry, 1518
Budapest 112, P.O. Box 32, Hungary;* ²*Institute of Organic Chemistry, Polish Academy of
Sciences, ul. Kasprzaka 44/52, 01-224 Warsaw, Poland*

E-mail:knkriszta@chem.elte.hu

Introduction

The continuously growing interest in the understanding of peptide folding led to the conformational investigation of methylamides of N-acetyl- α -amino acids. These amino acid derivatives are the simplest compounds which include the essential structural elements (“dipeptide unit”) of a polypeptide backbone and have been the subject of extensive spectroscopic (FTIR, VCD, ECD, NMR) and theoretical analysis [1-3]. Despite numerous experimental and computational studies the conformational arrangement of dipeptide units is still not clear in all details. It is of advantage to extend the series of the diamide peptide models with β -amino acid containing diamide compounds.

This work reports a detailed conformational analysis of N'-methylamides of N-acetyl-L- α - and β -amino acids (Ala, Pro, Phe) by chiroptical spectroscopic methods and theoretical calculations.

Results and Discussion

Diamide peptide models were prepared from the corresponding N-Boc- α -amino acids in solution phase, characterized with ESI-MS. The β -amino acids were synthesized by the Arndt-Eistert homologation reaction and Wolff rearrangement [4].

VCD spectra at a resolution of 4 cm⁻¹ were recorded in ACN-d₃ or DMSO-d₆ solutions with a Bruker Equinox 55 FT-IR spectrometer combined with a PMA37 VCD module and equipped with an MCT detector. ECD spectra in CH₃CN (c~0.5 mg/ml) and KCl (0.06-0.08 mg compounds/100 mg KCl) were recorded with Jasco J-810 and J-815 spectropolarimeters, respectively.

Quantum chemical calculations were performed by the Gaussian 09 program package [5]. VCD spectra of the individual conformers were calculated at B3LYP/6-31++G** level of theory, using a polarizable continuum model (IEF-PCM) for ACN or DMSO. ECD spectra of the lowest-energy conformers were computed by using the TD-DFT method at the B3LYP/6-311++G** DFT level of theory combined with the corresponding IEF-PCM solvent model for ACN or without solvent model.

In this paper only six spectra of three compounds are shown, namely the experimental and computed spectra of Ac-Pro-NHCH₃, Ac- β h-Ala-NHCH₃ and Ac-Phe-NHCH₃ (Figure 1.).

The calculated ECD spectrum of conformer *t-P-1* agrees with the experimental ECD spectrum of Ac-Pro-NHCH₃ obtained in KCl (Fig. 1. A). Presumably mainly conformer *t-P-1* exists in solid state. In the experimental and calculated ECD spectra of Ac-βh-Ala-NHCH₃ obtained in ACN (Fig. 1. B) overlapping transitions (π - π^* and n - π^*) are seen. Although the calculated spectrum is slightly red shifted compared to the measured spectrum, the calculated population-averaged ECD spectrum of conformer *B1* agrees with the experiment. In the amide I region (1600-1700 cm⁻¹) the VCD spectrum of Ac-Phe-NHMe obtained in ACN (Figure 1. C) the computations and the observations do not agree well. Possible explanations for the discrepancy (positive couplet for $\beta_L(a)$ conformer and negative couplet in the measured spectrum) are (i) the two amide I bands of $\beta_L(a)$ result from intensive nonrobust VCD modes according to the calculations [6], (ii) the solvent may be coordinated in a specific alignment, therefore not the lowest-energy conformer $\beta_L(a)$ but the second conformer $\beta_L(g^-)$ is predominant.

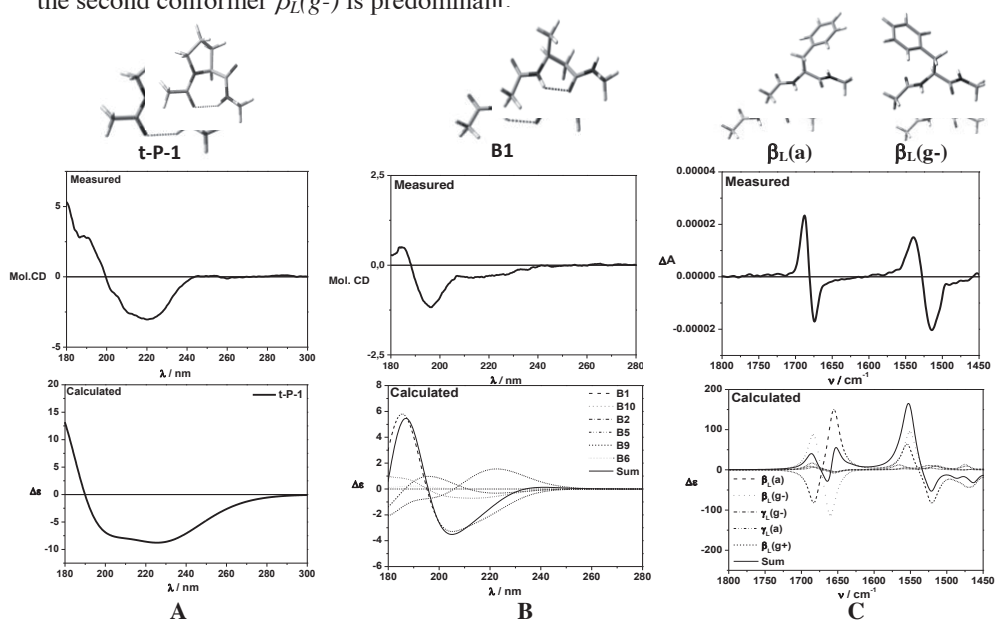


Figure 1. Experimental and calculated ECD spectra of Ac-Pro-NHCH₃ in KCl (A) and Ac-βh-Ala-NHCH₃ in ACN (B) and VCD spectrum of Ac-Phe-NHCH₃ in ACN (C)

Acknowledgments

This work was supported by the Hungarian Research Fund (OTKA K81175), Hungarian Academy of Sciences and Polish Academy of Sciences (nu 17) the Social Renewal Operational Programme (TÁMOP-4.2.2/B-10/1-2010-0030) and the Central Hungarian Operational Programme (KMOP-4.2.1/B-10-2011-0002).

References

- [1] Dungan, J. M., III and Hooker; T., Jr. *Macromolecules* **1981**, *14*, 1812.
- [2] Gerhards, M.; Uterberg, C.; Gerlach, A.; Jansen, A. *Phys. Chem. Chem. Phys.*, **2004**, *6*, 2682.
- [3] Flores-Ortega, A.; Jiménez, A. I.; Cativiela, C., et. al. *J. Org. Chem.*, **2008**, *73*, 3418.
- [4] Müller, A.; Vogt, C.; Seewald, N. *Synthesis*, **1998**, *6*, 837.
- [5] Frisch, M. J. et. al. Gaussian 09, Revision B.01, Gaussian, Inc., Wallingford CT, **2010**.
- [6] Góbi, S.; Magyarfalvi, G. *Phys. Chem. Chem. Phys. Communication*, **2011**, *13*, 16130.

Role of cation- π interaction in the photolysis of disulphide bridge containing cyclic model peptides

Eszter Illyés¹, Krisztina Knapp¹, Gabriella Csík², Zsuzsa Majer¹

¹*Eötvös Loránd University, Institute of Chemistry, Laboratory for Chiroptical Structure Analysis, H-1117 Pázmány Péter sétány 1/A Budapest, Hungary;* ²*Semmelweis University, Department of Biophysics and Radiation Biology, H-1094 Budapest, Tűzoltó utca 37-47, Hungary*

E-mail: illyes@elte.hu, majer@chem.elte.hu

Introduction

Cation- π interactions make a significant contribution to the overall stability of most proteins [1]: it is a structure-stabilizing electrostatic interaction between a cation and a polarizable π electron cloud of an aromatic ring. This interaction mainly exists when the cationic moieties are 6.0-10 Å distance to the face of an aromatic ring [2]. Such interactions occurs by peptides, proteins e.g. when the aromatic side chain of Trp, Tyr or Phe interact with the cationic moieties of Arg, Lys side chain. According to Protein Data Bank overall every 77th amino acid residue interacts with cations. This type of interaction should be considered alongside the more conventional hydrogen bonds, salt bridges, and hydrophobic effects in any analysis of protein structure. They can also contribute significantly to intermolecular contacts and interactions with ligands. This work reports the study of cation- π interactions by models on Trp-mediated photolysis, which are small disulfide bridged cyclic model peptides containing aromatic amino acid and some of them have Arg or Lys in the sequences. The Trp-mediated photolysis of disulfide bridges has also a structural criteria [3,4] and the optimal models fulfill the both criteria. After modeling the cyclic peptides, we synthesized and characterized the compounds, where the distance between aromatic ring and cationic moiety is optimal. We tested whether the Arg, Lys side chain has an influence on the disulfide bridge splitting in models.

Results and Discussion

The modeling was directed by Molecular Mechanics calculations (MM; HyperChem 6.0 in vacuum, Molecular Mechanics Force Field: Amber 96) to find the ideal model where the distance in small peptide models between the CE2 atom of Trp and the disulfide bridge is 5-10 Å and between the centroid of aromatic ring of Trp, Tyr and the cationic side chain of Arg and Lys is 6-10 Å (see in Table). The peptides were synthesized on Rink Amide MBHA resin using conventional Fmoc chemistry [5]. The crude peptide (purity >80 %) was cyclized by air oxidation in water at pH 7.8-8 (NH₄HCO₃) and the cyclization was followed by RP-HPLC. After the purification the cyclic peptides were identified by ESI-MS. Determination of the evolved thiols generated during illumination of peptides were quantified using the reaction of thiol group with 7-diethylamino-3-(4'-maleimidylphenyl)-4-ethylcoumarine (CPM) and the fluorescence increase of peptide-CPM adduct was measured at the CPM emission maximum at $\lambda = 476$ nm.

The smallest energy conformer	-SS- /Trp or Tyr distance (Å)	Trp-Lys/ –Arg distance (Å)	SH $\mu\text{M}/\%$ after 1 hour illumination	
			280nm	290nm
Ac-c(CWAGC)-NH ₂	9.61117	-	0	0.197/0.6
Ac-c(CWGAC)-NH ₂	9.67964	-	-	-
Ac-c(CWAKC)-NH ₂	9.08829	7.6070	0	0.599/1.7
Ac-c(CWKAC)-NH ₂	7.91659	7.5510	0	0.640/1.8
Ac-c(CWARC)-NH ₂	9.88286	11.8784	-	-
Ac-c(CWRAC)-NH ₂	9.75967	11.4623	0	0.277/0.8
Ac-c(CWYGC)-NH ₂	9.4650/12.1387	-	0	0

In summary: cation- π interaction was studied on Trp mediated photolysis, where simple models /Ac-c(CWAGC)-NH₂, Ac-c(CWGAC)-NH₂/ were compared with their Arg and Lys containing analogues. Illuminated the Trp models at $\lambda = 290$ nm after 1 hour the amount of evolved thiols was the following: Ac-c(CWKAC)-NH₂, Ac-c(CWAKC)-NH₂ > Ac-c(CWRAC)-NH₂ >> Ac-c(CWAGC)-NH₂ while illumination at $\lambda = 280$ nm we didn't measured any evolved thiols. Interestingly, if Trp and Tyr are nearby each other in models, no detectable evolved thiols.

We can say as a conclusion, both Lys and Arg promote the cleavage of S-S bridges through the cation- π effect. However, at the Trp-Lys containing models the amount of thiols is higher than in Trp-Arg models and this is in good agreement with measured distance of the models (see the Table).

Acknowledgments

This work was supported by the Hungarian Scientific Research Fund (OTKA K10072).

References

- [1] Dougherty, D.A. *Science* **1996**, 271,163.
- [2] Gallivan, J.P.; Dougherty, D.A.; *Proc. Natl. Acad. Sci. USA*, **1999**, 96, (17), 9459.
- [3] Ioerger, T.M.; Du, C.; Linthicum, D.S. *Molec. Immunology* **1999**, 36, 373.
- [4] Vanhooren, A.; De Vriendt, K.; Devreese, B.; Chedad, A.; Sterling, A.; Van Dael, H.; Van Beeumen, J.; Hanssens, I. *Biochemistry*, **2006**, 45, 2085.
- [5] Albericio, F. *Solid-Phase Synthesis: A Practical Guide (1 ed.)*. Boca Raton: CRC Press. **2000**, 848.

Antimicrobial peptides as novel delivery vehicles for genetic antibiotics

Gitte Bonke Seigan¹, Henrik Franzyk¹, Peter E. Nielsen²

University of Copenhagen, Faculty of Health and Medical Sciences, ¹Department of Drug Design and Pharmacology and ²Department of Cellular and Molecular Medicine.

E-mail:gbs@sund.ku.dk

Introduction

Major health problems arising from increased bacterial resistance towards existing antibiotics have made discovery of new antibacterial drugs without known resistance issues a research field of utmost importance.

Proof of concept for an antimicrobial approach, using the DNA mimic peptide nucleic acid (PNA) antisense targeting of essential bacterial genes, was obtained a decade ago [1], and later in vivo activity was demonstrated [2]. However, this technology is still limited by suboptimal carriers that facilitate effective bacterial delivery and confer optimal pharmacokinetic properties to the prospective drugs [3-4], because the large hydrophilic PNA molecules are not readily taken up by bacteria. Therefore it is necessary to devise suitable conjugates of the antisense PNA oligomers in order to obtain sufficiently potent antibacterial activity. So far, a few cell-penetrating peptides, known to act on human cells, have been investigated as potential vehicles for bacterial delivery, although the originally employed synthetic bacterial membrane-active peptide, (KFF)₃K, remain among the most efficient delivery vehicles [2]. However, a non-essential membrane-associated transporter is required for bacteria to be susceptible to this peptide [5], and thus its use is not a general approach.

In the past two decades, parallel efforts of exploiting natural antimicrobial peptides (AMPs) as drugs have been made. The cationic AMP subclass appears to be directly involved in the innate immune response towards microbial infections. Moreover, such AMPs are known to exhibit activity against both Gram-positive and -negative bacteria [6-8]. Typically AMP sequences comprise 10-40 amino acid residues, and positive charges together with a high content of hydrophobic residues are characteristic features. Surprisingly, cationic AMPs with an internal target appear not to have been investigated for bacterial delivery of antibiotics. The present study addresses this possibility.

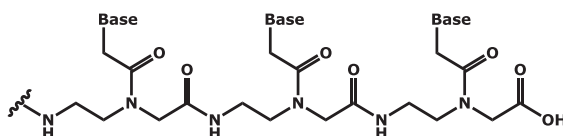


Figure 1: Peptide nucleic acid (PNA). Base = adenine, guanine, thymine or cytosine.

Results and Discussion

From the literature we chose a number of AMPs reported to act via intracellular targets, which implies that these AMPs must possess an inherent ability to permeate bacterial cell

membranes without directly killing of the bacteria. This property indicates that they might well function as delivery vehicles for PNA in order to improve the silencing efficacy on targeted bacterial genes.

The selected AMPs were synthesised by using SPPS, and they were purified by preparative HPLC. The AMPs were coupled to a well-characterized antibacterial PNA oligomer, targeting the essential bacterial *ftsZ* gene, and subsequently the PNA-AMP conjugates were tested *in vitro* for antibacterial activity in *E. coli*.

Table 1: Minimal inhibitory concentrations (MIC) for peptide nucleic acid-antimicrobial peptide (PNA-AMP) conjugates and the AMPs alone.

PNA-AMP conjugate	MIC (μM)	AMP	MIC (μM)
PNA-SMCC-Cys-Pep-1-K	3	Pep-1-K	3
PNA-SMCC-Cys-K ₆ L ₂ W ₃	3	K ₆ L ₂ W ₃	3
PNA-SMCC-Cys-Oncocin	0.9	Oncocin	3
PNA-SMCC-Cys-IsCT- <i>p</i>	3	IsCT- <i>p</i>	10
PNA-SMCC-Cys-NLS-Gb3	3	NLS-Gb3	10
PNA-eg1-Cys-(KFF) ₃ K	0.9		

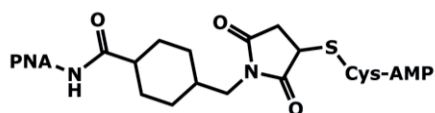


Figure 2: General formula representing the PNA-SMCC-Cys-AMP conjugates. PNA = peptide nucleic acid. SMCC = Succinimidyl-4-[N-maleimidomethyl]-cyclohexan-1-carboxylate. Cys = cysteine. AMP = antimicrobial peptide.

Three AMPs were found to have a higher minimal inhibitory concentration (MIC) than the corresponding PNA-AMP conjugate. This indicates that the PNA is transported into the bacteria by the AMP and silences the gene without the AMP itself inhibiting the bacteria. Two AMPs exhibit a MIC equal to that of the PNA-AMP conjugate thereby suggesting that the AMP part may be solely responsible for the observed inhibition of the bacterial growth. Therefore it can be concluded that some AMPs could be interesting delivery vehicles for possible future PNA antibiotics.

References

- [1] Good, L.; Awashti, S. K.; Dryselius, R.; Larsson, O.; Nielsen, P. E. *Nat. Biotechnol.* **2001**, *19*, 360-364.
- [2] Tan, X-X.; Actor, J. K.; Chen, Y. *Antimicrob. Agents Chemother.* **2005**, *49*, 3203-3207.
- [3] Mellbye, B. L.; Puckett, S. E.; Tilley, L. D.; Iversen, P. L.; Geller, B. L. *Antimicrob. Agents Chemother.* **2009**, *53*, 525-530.
- [4] Ghosal, A.; Nielsen, P. E. *Nucleic Acid Ther.* (in press).
- [5] Ghosal, A.; Vitali, A.; Stach, J. E. M.; Nielsen, P. E. (submitted).
- [6] Brown, K. L.; Hancock R. E. W. *Curr. Opin. Immunol.* **2006**, *18*, 24-30.
- [7] Zasloff, M. *Nature* **2002**, *415*, 389-395.
- [8] Hancock, R. E. W.; Stahl, H.-G. *Nat. Biotechnol.* **2006**, *24*, 1551-1557.

Solid-phase syntheses of galanins [GALs] and their fragments with different strategies, analytical controls, conformations and new biological studies

Lajos Balásperi^{a*}, János Tóth^b, Gábor Blazsó^c, Zsuzsanna Majer^d, Gábor K.Tóth, Eszter Lajkó^e, László Kőhidai^e, Ilona Szabó^f, Gábor Mező^f, László Virág^g, Gyula Papp^g, András Varró^g

^aDepartment of Medical Chemistry, University of Szeged; ^bDepartment of Internal Medicine, Central County Hospital, Kecskemét; ^cDepartment of Pharmacodynamics & Biopharmacy, University of Szeged; ^dDepartment of Organic Chemistry, Eötvös Lóránd University, Budapest; ^eDepartment of Genetics, Cell- and Immunobiology, Semmelweis University, Budapest; ^fResearch Group of Peptide Chemistry of the Hungarian Academy of Sciences, ELTE, Budapest; ^gDepartment of Pharmacology & Pharmacotherapy, University of Szeged, Hungary

Introduction

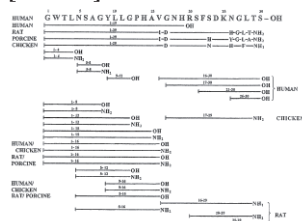
Galanins [GALs] are widely distributed 29/30-amino acid neuropeptides, [neuroendocrine and neuromodulating] peptides with multiple biological effects, present in the periphery, in the endocrine system and the central nervous system [CNS]. The first GAL, the bovine GAL was discovered in intestinal extracts in 1985 by Mutt [1]. The name galanin originated from the first and last amino acids of the porcine sequence. The amino acid sequences of different species are very conserved with [almost 90%] identity in the known 18 various sequences. Most of them were synthesised by different, excellent synthetic groups. The first human GAL was prepared in 1991 [2]. GAL is cleaved from a 123 amino acid long prepropeptide, along with a 59 amino acid long GAL message-associated peptide [GAMP]. The GAL-like-peptide [GALP] was discovered and synthesised by a combination of recombinant DNA technology. The immunoreactivity of this peptide has been observed in the Glia and in activated microglia and in cortex. The most important full endogenous GALs are the human, bovine, rat, porcine and chicken species. We have prepared these full GALs [Table 1], the galantid [M15] antagonist and 26 further N- and C-terminal fragments. Our aims were to work out the best synthesis and preparing and controlling sufficiently pure peptides for our biological partners, who are interested in GALs studies.

GWTLNSAGYLLGPHA VGNHRFSFDKNGLTS-OH	human	GAL[1-30]-OH
GWTLNSAGYLLGPHA VGNH-OH	human	GAL[1-19]-OH
GWTLNSAGYLLGPHA LDSHRSFQDKHGLA-NH ₂	bovine	GAL[1-29]-NH ₂
GWTLNSAGYLLGPHA IDNHRFSFDKHGLA-NH ₂	rat	GAL[1-29]-NH ₂
GWTLNSAGYLLGPHA IDNHRSFHDKYGLA-NH ₂	porcine	GAL[1-29]-NH ₂
GWTLNSAGYLLGPHA VDNHRSFNDKH GFT-NH ₂	chicken	GAL[1-29]-NH ₂
GWTLNSAGYLLGPQQFFGLM-NH ₂	galantid	[1-20]-NH ₂

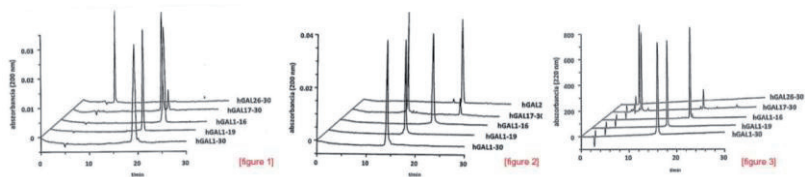
[Table 1]

Results and Conclusions

[Table 2]



The 32 GAL peptides and their fragments were synthesised [Table 2] by solid-phase synthesis on MBHA or TentaGel S-NH₂ resins, using Boc- or Fmoc- α -protecting groups and strategies. Removing from resins, all crude peptides were purified by semipreparative RP-HPLC on a 25x2.5 cm column [YMC Co., Japan]. The pure peptides were analytically controlled by analytical RP-HPLC column [YMSCo.,Japan] A [water-0.1% TFA] against B [acetonitrile] [Figure 1] by RP-CZE, MEK [Figure 2] and by FAB-MS, EIMS [Figure 3], in some cases with an amino acid analyzer.

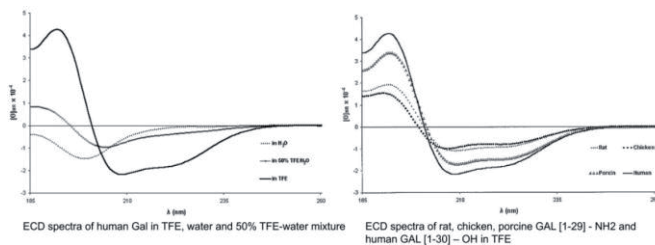


Sequences, helix cont. [%] λ 222

Human GAL (1-30)-OH	78	H.GAL[1-30]-OH	14.25	98	14.30	3157.9	3157.7
Rat GAL (1-29)-NH ₂	44	H.GAL[1-19]-OH	14.41	97	15.48	1964.2	1964.5
Porcine GAL (1-29)-NH ₂	69,5	H.GAL[1-15]-OH	15.67	97	16.80	1571.8	1572.2
Chicken GAL (1-29)-NH ₂	38,5	H.GAL[1-16]-OH	15.63	96	16.80	1669.9	1669.9
Human GAL (1-19)-OH	11	H.GAL[1-12]-OH	14.26	94	--	1251.42	1251.39
Human GAL (1-16)-NH ₂	17						
Porcine/rat GAL (1-16)-NH ₂	20						
Porcine/rat GAL (1-16)-OH	11						
Human GAL (1-12)-OH	10						
Human GAL (16-30)-OH	29						

[table 4]

[table 3]



Conformation studies

By CD-spectra [ECD spectroscopy in aqueous solution and in 30% TFE-water] were measured for almost all our peptides and fragments [Table 4]. In water, the full GALs exhibited an unordered conformation [strong negative band at 200 nm], while in the TFE an ordered structure, mainly helical. GALs ECD spectra show in water unordered, while in TFE ordered structure. The helical content of the full GALs increased in the sequence human GAL[1-30]-OH > porcine GAL[1-29]-NH₂ > rat GAL[1-29]-NH₂ ~ chicken GAL[1-29]-NH₂. The different helix content can explain with the changes in sequences which caused structural heterogeneity. The human GAL[1-19]-OH is a classical sample of an ordered type I(III) β -turn conformation transition. The shorter sequences of N-terminal GAL[1-12]-OH and GAL[5-12]-OH are flexible and show in TFE a conformer population containing a β -turn structure [broad weak, negative band at ~205 nm and a shoulder at ~220nm]. Similar studies were performed with FT-IR spectra D₂O and ¹H-NMR studies [DQF-COSY, TOCSY and ROESY] were carried out. FT-IR data on these GALs in aqueous solution indicated a completely random coil peptide. ¹H-NMR data in structural terms suggest that in TFE GAL[1-30]-OH is predominantly helical, while in water it does not adopt a fixed conformation. Conformational analysis of the 3-dimensional structures of GALs in aqueous solution indicated that they do not adopt a fixed conformation.

Biological studies

Physiological, biological and pharmacological investigations are on going anti-inflammatory effects, smooth muscle effects, cell adhesions of GALs and fragments, GALs effects on oxytocin and vasopressin, effects of GALs and fragments on ACh release and electrophysiological studies with human GAL[1-30]-OH have been performed. It has become evident that GALs and their N-terminal fragments inhibit glucose-stimulated insulin secretion *in vitro*.

References

- [1]. Tatemoto K, A.Rökkaeus, H.Tornwell, T.J. McDonald, & Victor Mutt. **1983** FEBS Lett. **1984** 124-128.
- [2]. Schmidt W.E., H.Kratzin, K. Eckart et al. **1991** Proc. Natl. Acad. Sci. USA **88** 11435-11439.

Proceedings of the
Thirty-Second European Peptide Symposium
September 2-7, 2012
Athens, Greece

Author Index

A

Abbour Shoukri 482, 610
Abdelhamid Muhammad E. 220
Abel Sabine 648
Abramov A. Y. 430
Accardo Antonella 496
Acerra Nicola 86
Adachi Motoyasu 44, 404
Afantitis Antreas 376
Agelis George 342, 358, 376, 400, 526
Ahmad Fuaad A. A. H. 114
Ahn Yun Soo 606
Aikawa Haruo 98
Airaghi F. 392
Ait-Mohand Samia 228
Akaji Kenichi 44, 478, 636
Al Temimi Abbas H. K. 616
Albericio Fernando 136, 158, 408, 452,
460, 602, 612, 646
Alenowicz Magda 388
Alexopoulos H. 672
Alhaj Omar A. 470
Al-Khalifa Abdulrhman S. 470
Alonso Daniel 452
Alves I. D. 172
Alvira M. 590
Amar S. 102
Amarouche Nassima 50, 662
Ambo Akihiro 322
Amso Zaid 40
Anastasas Mark 550
Anastasopoulos Charis 264, 266
Andersen N. 70, 546
Anderson J. 70
Andrä Jörg 38, 160
Andreev Sergey 652
Andreeva Tatyana V. 308
Andreu David 508
Androutsou Maria-Eleni 26, 376, 400,
526, 656
Ang Yi Li 122
Angelastro A. 294
Angelini Alessandro 554

Apicella Viviana 278
Argyriou Aikaterini 58
Arlot-Bonnemains Y. 482
Arsenault Jason 500
Artym Jolanta 52, 594
Assimomytis Nikos L. 146, 238
Attanasio Francesco 256, 402
Averlant-Petit Marie-Christine 348
Avitabile C. 394
Axford Danny 560

B

Babos Fruzsina 246, 280
Babu M. Madan 134
Bachelot-Loza Christilla 464
Baçhor Remigiusz 82
Balacheva Anelia 368
Balafas E. 428
Balásperi Lajos 682
Balboni G. 392
Baleux Françoise 92
Ballano Gema 562
Ballet Steven 422
Balliu Alexandra 154
Bamm Vladimir V. 134
Banaigs B. 250
Banères Jean-Louis 112
Bang Jeong-Kyu 156
Bánóczy Z. 100
Baranyai Zsuzsa 510
Barbayanni Efrosini 274, 586
Barbosa Luiz Carlos B. 270
Barbosa Simone 276
Barrère-Lemaire Stéphanie 42
Barros Alexandre Jesus 480
Bastien Patrick 278
Batta Gyula 184
Batzloff M. R. 114
Bauab T. M. 178
Baudy-Floc'h Michèle 456, 482, 610
Bauman A. 346
Bawolak Marie-Thérèse 312
Beaudet Nicolas 240, 296

Bechara C. 172
 Bechinger B. 170
 Becker Christian F. W. 330
 Bédard François 188
 Bednářová Lucie 174
 Behrendt R. 420
 Benaki Dimitra 242, 664
 Bentin Thomas 372
 Bentrop Detlef 58
 Benyhe Sandor 246, 348
 Berg Albrecht 208
 Bertin D. 456
 Bertrand Daniel 308
 Besserer-Offroy Elie 296
 Beyermann Michael 28, 648
 Bianchi Elisabetta 108
 Bianchi N. 394
 Bihel F. 442
 Bindi Stefano 78
 Bionda Nina 314
 Biondi Barbara 150, 176, 192, 514
 Biron Eric 188, 194
 Bisaglia M. 546
 Bkaily G. 302
 Blayo Anne-Laure 112
 Blazsó Gábor 682
 Blond Alain 72, 182
 Bluijssen Hans 388
 Bobone S. 138, 166
 Bocchinfuso G. 138, 166, 170, 542
 Bocharov Eduard V. 54
 Bocheva Adriana I. 290, 356
 Bode Helge B. 284
 Bode Jeffrey W. 134
 Bode S. A. 172
 Bogdanov Alexey A. 354
 Boheim Günther 288
 Boisguerin Prisca 42
 Bojnik E. 246, 392
 Bojnik Engin 348
 Boll Emmanuelle 20, 576
 Bolzati Cristina 514
 Bonifazi D. 382
 Bonke Seigan Gitte 680
 Bonnaffé David 92
 Bonnard I. 250
 Bordusa Frank 530
 Borisov Yurii A. 54
 Born Ilona 244
 Borovičková Lenka 230, 238
 Borsodi A. 246, 392
 Bose Partha P. 458
 Bősze Szilvia 236, 508, 510, 674
 Bouayad-Gervais Samir H. 18
 Boudesoque Leslie 50, 662
 Boulais Philip 292
 Bourguignon J. J. 442
 Boutin J. A. 642
 Boyaud F. 250, 624
 Boynik E. 246
 Brabez N. 126
 Bracci Luisa 78, 94, 496
 Bracke Nathalie 104
 Brack-Werner R. 438
 Brandenburg Klaus 160
 Brandi P. 294
 Braun K. 406
 Bregant S. 172
 Breitling Reinhard 118
 Briasoulis Evangelos 230
 Brigaud Thierry 536, 598, 608
 Brognara E. 394
 Broussy Sylvain 306
 Brückner Hans 168, 204, 208, 288, 470, 560
 Brunel Luc 142, 484
 Brunetti Ilenia 78, 94, 496
 Bubacco L. 546
 Bujak-Giżycka Beata 260, 262, 272
 Burlina F. 172, 420
 Burov Sergey 476
 Burvenich Christian 104
 Butte Alessandro 50, 662
 Buyst Dieter 202
 Byk Gerardo 24
 Byrne A. 70, 546
 Bystrowska Beata 260, 262
 Byun Byung Jin 536

C

- Cabana Jérôme 292
Cabral F. R. 222
Cai Hui 128
Cai Lifeng 14
Cai Minying 106
Cain James P. 144, 412, 570, 592, 600, 604
Calaza M. Isabel 566, 574
Calderan Andrea 512, 514
Calmès M. 290, 324
Campagna Tiziana 256
Campbell J. H. 68
Campiglia Pietro 670
Camy Christophe 366
Cantel S. 142
Capitò Elena 426
Capurro Margareth Lara 472, 480
Caraci Filippo 402
Carell Thomas 286
Carrette Lieselot L. G. 286
Caruso Mario 66
Carvalho L. A. C. 180
Cascone Osvaldo 158, 452
Caselli Monica 466
Castro Vida 602
Cativiela Carlos 566, 574
Cavelier Florine 240, 628
Cecchi R. 396
Cellucci Antonella 108
Čeřovský Václav 174, 190
Cescato Renzo 120, 486
Chamlian Mayra 480
Chan L. Y. 68
Chantell Christina A. 144, 412, 570, 592, 600, 604
Chantzichristos Vasilios G. 516
Charest-Morin Xavier 312
Chasapis Christos T. 58
Chassaing Gérard 126, 172, 536, 608
Chaume Grégory 536, 598, 608
Chayov Radoslav 490
Chelain Evelyne 598
Chelli Mario 410, 626, 630
Chen Shiyu 554
Chen Wenqian 416
Chinen Takumi 34
Chochkova Maya 580
Chorev Michael 186, 410, 548, 596
Chrudimská Tereza 190
Chubb Anthony J. 62
Chuchkov Kiril 488, 490
Chung Nga N. 348, 422
Ciancaglini Pietro 276
Ciarkowski Jerzy 528, 564
Ciccia Graciela 452
Cilli E. M. 178
Ciossek Thomas 12
Clark R. J. 68
Clayette Pascal 92
Clemmer David 12
Coïc Yves-Marie 92
Colomb-Delsuc Mathieu 84
Colombo Giorgio 654
Connell Bridgette 92
Constantinou-Kokotou Violetta 380
Copani Agata 402
Corbani M. 246
Cordopatis Paul 120, 146, 230, 238, 254, 486, 544, 658
Correia Isabelle 422
Corvaglia V. 382
Cosconati S. 438
Costi Maria Paola 466
Couture Frederic 440
Coux Olivier 278
Covinhas Aurélie 42
Craik David J. 2, 68
Crisma Marco 192, 334, 520, 562
Cristau Michele 416
Crooks Richard O. 86
Csík Gabriella 678
Cudic Mare 314
Cudic Predrag 314
Čujová Sabína 174
Cunningham Paula T. 46, 550
Cutting Brian 554

Cydzik Marzena 82
Czajlik András 588
Czaplewska Paulina 528
Czaplewski Cezary 214

D

D' Andrea L. D. 394
D'Addona Debora 548
D'Anjou François 268, 440
D'Orléans-Juste P. 302
D'Ursi Anna Maria 548
Dadayan Alexander K. 54, 90
Dailly Nicolas 46
Dalakas M. C. 672
Daly N. L. 68
Damian Marjorie 112
Danalev D. 454, 468
Darbon H. 456
Darji Ayub 110
Dauth Christina 284
Davey Norman E. 62
Davletov Bazbek 500
Day Robert 268, 440, 584
De Felice C. 432
de Jong Marion 120, 484, 486, 492, 504
de la Torre Beatriz Garcia 508
de Miranda Antonio 472
de Oliveira Junior Vani Xavier 472, 480
De Paola I. 294
de Planque Maurits R. R. 134
De Poli Matteo 176
De Rosa L. 552
De Spiegeleer Bart 104
De Zotti Marta 138, 150, 166, 176, 192
Dębowski Dawid 258, 398
Dedek Matt M. 106
Degenkolb Thomas 204, 208
Dei L. 644
Deigin Vladislav 36
Demange Luc 112
Demmer O. 438
Dendane Nabil 640
Denoyelle Séverine 112
Depaul Lorenzo 94

Deraos Georgios 26, 134, 436
Deraos Spyros 436
Derreumaux P. 60
Desai Kunal 108
DeSilva C. 126
Desjardins Roxane 268, 440
Desmet Rémi 212
Detcheva Roumyana 368
Devocelle Marc 62
Dheur Julien 20, 576
Di Marco Annalise 108
Di Maro Salvatore 670
Di Natale C. 552
Di Pisa F. 644
Di Pisa Margherita 620, 630
Diederichsen Ulf 30, 638
Dietrich Ursula 110, 448
Dijkgraaf I. 438
Dimitriou Andromaxi A. 516, 634
Diness Frederik 10
Dioni I. 16
Dirain Marvin L. 548
Dobkowski Michał 344, 390
Dodoff Nicolay 540
Dókus L. E. 100
Domingues T. M. 162
Donat Chris 412
do-Rego J. C. 316
Dörfelt Heinrich 208
Dorosh Marina 476
Douat-Casassus Céline 370
Drasar P. 374
Drobecq Hervé 212, 576
Du Xiaobing 108
Dubuisson Jean 90
Ducasse Rémi 72, 182
Duffy Fergal J. 62
Dumulon-Perreault Veronique 228
Durdagi Serdar 342
Durkan M. 326
Duschmalé Jörg 328
Dutour Sikirić M. 320
Dzierzbicka Krystyna 164, 384
Dzimbova Tatyana 232, 356, 368, 540

E

Eberle Alex N. 8
Eble A. Johannes 304
Ebran Jean-Philippe 640
Edwards Richard J. 62
Eglin David 136
Egot Marion 464
Eilstein Nathalie 306
El Ayeb M. 456
El Shazely Baydaa 190
Elhabazi K. 442
Elia Elena 230
Emeric Miclet 536
Englezopoulos Constantinos V. 446
Enjalbal C. 142
Enyedi Kata 588
Erdmann Frank 74
Escher Emanuel 292, 386
Evans Clive 522
Exarchakou Revekka 146, 238, 254

F

Fabbri E. 394
Falciani Chiara 78, 94, 496
Farrotti A. 138, 166, 170
Fasel Nicolas 650
Fatás Paola 566, 574
Fathi Haleh 176
Fehrentz Jean-Alain 112, 484
Feinäugle P. 224
Ferderigos Nicolaos 336
Fernández-Llamazares Ana I. 612, 646
Ferrari Enrico 500
Ferrari Stefania 466
Ferry G. 642
Feteyns Debby 536, 608
Fichna J. 316
Fields G. B. 102
Filipowicz Magdalena 362, 398
Finnman Jens 462
Fischer Gunter 74
Flegel Martin 200, 374

Flegelova Zuzana 200, 374, 418
Flipo Marion 462
Formaggio Fernando 66, 138, 150, 166,
176, 192, 334, 520,
542, 562, 622
Fotakis Charalambos 544
Fotaras Stamatis 336, 380
Fotou Evmorfia 660
Fraczyk Justyna 234
Fragneto G. 138
Fragogeorgi E. A. 326
Franck Alicia 42
Frank A. O. 438
Fransen Peter 136
Franzyk Henrik 680
Friedrich P. 100
Friligou Irene 350, 656, 668
Frkanec L. 320
Frkanec R. 320
Fučík Vladimír 190
Fujiaki Shutaro 498
Fujii Masayuki 498
Fujita Yoshio 196
Fukamizu Akiyoshi 310
Fukumori Yoshinobu 414
Fukuoka Satoshi 160
Funikov Sergei 90

G

Gagne Didier 112
Gajdošechova Lucia 260
Galabov Angel 488, 580
Galgóczi László 184
Galyean Robert 462
Gambari R. 394
Ganesan 534
Ganzalez M. J. 456
García-Ramos Yésica 18, 366
Garona Juan 452
Garrido Saulo S. 270, 276
Gatsiou Aikaterini 516
Gattacceca F. 250
Gattner Michael 286

Gatto Emanuela 66, 334, 542
Gelb Michael H. 274
Gelfert-Peukert Sabine 288
Genovese Filippo 466
Georgiev Kaloyan 356, 368
Georgiev Lyubomir 368
Georgiev Rumen 488
Georgieva Milena 368
Gera Lajos 312
Gerelli Y. 138
Gerotheranassis Ioannis P. 134
Gessmann Renate 560
Gevaert Bert 104
Ghezzi Silvia 426
Giannopoulos Panagiotis 342
Giannopoulou Efstathia 238
Gigmes D. 456
Gil Ana M. 574
Gillies R. J. 126
Giordano L. 166
Giralt E. 456
Girard Anick 194
Giraud Matthieu 50, 408, 662
Giuffrida Alessandro 402
Giuffrida Maria Laura 402
Gkesouli Athina 298
Gkini Eleni 376
Gkountelias Kostas 428, 444
Gobbo Maria 150
Golla Kalyan 62, 450
Golovin Andrey V. 354
Gómez Daniel 452
Gonzalez Iveth 650
González Rodrigo 158
Good M. F. 114
Górecki Marcin 676
Gori Alessandro 654
Goulard Christophe 72, 182
Gourni E. 438
Gourogiani Alexia 464
Govorun V. M. 64
Graham Bim 220
Grdadolnik Simona Golic 318

Grieco Paolo 670
Gross Michael 12
Gross Stephanie 38
Grubhoffer Libor 190
Gsponer Joerg 134
Gualandi Alessandra 466
Guérin Brigitte 228
Guerrini Remo 466
Guichard Gilles 370
Guilhaudis Laure 534
Guillemin Karel 422
Guittet Eric 72, 182
Gunaekera S. 68
Gutsmann Thomas 160
Guyon F. 60
Guzmán Fanny 158, 452
Guzow Katarzyna 362

H

Hagn F. 438
Hahn K.-S. 166
Hajjaj Bouchra 484
Hall Clint 550
Halmos Gábor 96, 502, 532
Hamada Yoshio 352
Hansen Morten B. 618
Hara Asaki 414
Harauz George 134
Haskell-Luevano Carrie 548
Haslam Niall J. 62
Havard Thierry 140
Hayashi Yoshio 34, 378
Hayek J. 432
Hegedüs Rózsa 502, 532, 588
Heinbockel Lena 160
Heinis Christian 554
Hemmerich Peter 118
Hengerer Bastian 12
Henklein Petra 28
Henriques S. T. 68
Hensley Robert W. 412
Hernandez Jean-François 278, 348
Hertje Maria 448

Heveker Nikolaus 292, 386
Hibino Hajime 568
Hickman David T. 524
Hidaka Koushi 44, 404, 666
Hiemstra H. 364
Hocharenko M. 590
Hodges Robert S. 312
Hoffmann Katrin 550
Hojo Keiko 414
Hokari Yoshinori 310
Holland-Nell Kai 614
Hollósi Miklós 676
Holmstrom K. M. 430
Holton Therese 62
Honcharenko Dmytro 458
Hoogewijs Kurt 202
Hopkins Richard 46, 550
Horvat Branka 426
Horváti Kata 510
Houde M. 302
Howl John 116
Hristova B. 468
Hruby Victor J. 106, 126
Huang Zhi-Hua 128
Huben Krzysztof 52, 252, 518, 594
Hudecz Ferenc 100, 280, 510
Huguenot Florent 306
Humbert J. P. 442
Hynie S. 374

I

Iannucci Nancy 158, 452
Ichikawa Hideki 414
Iliev Ivan 368
Illyés Eszter 678
Inazu Toshiyuki 632
Inazumi Hitomi 666
Ingallinella Paolo 108
Inguibert N. 250, 624
Inomata Tatsuji 48
Ivanov V. T. 64
Ivanova Galya 580
Iversen Anita 204, 208

J

Jahn Reinhard 30
Jahreis Günther 74
Jakas Andreja 314
Jaklitsch Walter M. 204, 208
Janecka A. 316
Jankowski Stefan 52, 252, 518, 594
Jee Joo-Eun 122
Jensen Knud J. 4
Jeong Eui Sung 606
Ježek Rudolf 152
Jia Z. 114
Jiménez Ana I. 566, 574
Johansson J. 458
Jones Sarah 116
Josan J. 126
Jouan F. 482
Jullian M. 642
Jung Günther 288
Jurasek M. 374

K

Kaca Wiesław 234
Kaconis Yani 160
Kad Neil M. 86
Kajava Andrey 278
Kalavrizioti Dimitra 376
Kalofonos Haralabos P. 238
Kaloudi Aikaterini 504
Kamiński Zbigniew J. 234
Kampylafka E. I. 672
Kamynina A. V. 430
Kang Young Kee 536
Kapel Romain 50
Kapunári Bence 96, 502, 532
Karachaliou C.-E. 326
Karageorgios Vlassios 254
Kárpáti Sarolta 236
Karreman Christiaan 12
Karska Natalia 528
Kasheverov Igor E. 308
Kasprzykowski Franciszek 564

- Katagiri Fumihiko 248
 Katarzyńska Joanna 52, 518
 Kato Masashi 434
 Katsila Theodora 428, 444
 Katsougraki Pigi 26, 400, 436, 526
 Katsouras Christos S. 446
 Katzhendler Jehoshua 304
 Kebe N. Mathy 278
 Kele Zoltán 184
 Keller Andrea-Anneliese 118
 Keresztes Attila 422
 Kerfoot Maria 46, 550
 Kessler H. 438
 Ketas Thomas 426
 Khaldi Nora 62
 Khandadash Raz 24
 Kielmas Martyna 198
 Kier B. 70
 Kierus Krzysztof 52, 252
 Kijewska Monika 198
 Kikuchi Mari 636
 Kim Kwan Mook 606
 Kim Mi-ran 606
 Kimonyo Anastase 168
 Kinas Maria 252
 Kiouptsi Klytaimnistra 464
 Kiso Yoshiaki 44, 310, 352, 404
 Kiss Éva 510
 Klenerova V. 374
 Kluba C. 346
 Kluczyk Alicja 82
 Knapp Krisztina 676, 678
 Knaute Tobias 76
 Kobayashi Hiroki 632
 Kóhidai László 588, 682
 Kokotos Christoforos G. 226, 332, 338, 340
 Kokotos George 274, 336, 338, 380, 586
 Kokotou Maroula G. 226
 Kolesanova Ekaterina 90
 Kolesińska Beata 234
 Koloka Vassiliki 464
 Kong Ho Zee 522
 Konieczna Iwona 234
 Konno Hiroyuki 80, 478, 636
 Kopylov Arture T. 54
 Korbut Ryszard 260, 262, 272
 Koroev D. O. 430
 Kossakowska P. 594
 Kostomitsopoulos N. 428
 Kostomoiri Myrta 242
 Kostoula Ioanna 448, 660
 Koukkou Anna-Irini 154
 Koukoulitsa Catherine 358, 376
 Kounnis Valentinos 230
 Kowapradit J. 114
 Kramer Nikki 572
 Kraus T. 374
 Kremb S. 438
 Krenning Eric P. 120, 484, 486, 492, 504
 Kritsi Eftichia 526
 Kroll Carsten 300
 Kroneislová Gabriela 152
 Krskova Katarína 260
 Kryukova Elena V. 308
 Kukavica-Ibrullj Irena 188
 Kukowska Monika 164
 Kunz Horst 128
 Kuriyama Isoko 666
 Kuroki Ryota 44, 404
 Kuś Katarzyna 262, 272
 Kwiatkowska Anna 268, 440, 584
 Kwinkowski Marek 234

L

- Labonté J. 302
 Laboureyras E. 442
 Lai Josephine 422
 Laimou Despina 444
 Lajkó Eszter 588, 682
 Lambardi D. 410
 Lameiras Pedro 50
 Lammek Bernard 244, 268, 584
 Langella Annunziata 426
 Langridge James 12
 Lapidus Dmitrijs 214
 Lapolla A. 186, 596

Larregola M. 186, 432
Latter E. 138
Laufer Ralph 108
Lavielle Solange 126, 172, 432, 536, 608
Lavigne Pierre 292
Lazarovici Philip 304
Le S. J. 68
Lebel Rejean 228
Lebl Michal 22, 200, 374, 418
Lebleu Bernard 42
Lechner Carolin C. 330
Leclercq Bérénice 212
Lecorché P. 172
Leduc Richard 292
Lee Hyunil 606
Lee Su Seong 122
Lefebvre Marie-Reine 292, 386
Lefranc Benjamin 534
Lefrançois Marilou 292, 386
Łęgowska Anna 258, 362, 398
Legowska Monika 398
Legrand Baptiste 348
Leist Marcel 12
Leko Maria 476
Lelli Barbara 78, 94, 496
Lemieux Carole 422
Lensen Nathalie 598
Leondiadis L. 664
Leone M. 552
Leonis Georgios 318
Lepage Martin 228
Leprince Jérôme 534
Lescop Ewen 72, 182
Lesma G. 392, 396
Lesner Adam 258, 282, 362, 398
Lesot Philippe 608
Leurs Ulrike 96
Levesque Christine 268, 440
Lévesque Roger C. 188
Li Yan-Mei 128
Li Yanyan 72, 182
Liapakis George 254, 342, 358, 376,
428, 444

Liepina Inta 214
Lim Jaehong 122
Limnios Dimitris 338
Limonta P. 428
Lin Hao 582
Lindner Kathrin 12
Liolios C. C. 326
Liskamp Rob M. J. 572, 616
Lisowski Vincent 278
Lissy E. 218
Liu Baosheng 434
Liu Junyang 32
Liu Keliang 14
Liu Liang 434
Liu Wang-Qing 306
Livaniou Evangelia 242, 326
Livingston Andrew G. 416
Liwo Adam 214
Lloyd G. Kenneth 34
Lombardi Federica 62
Longhi Renato 654
Longo Edoardo 216, 334
Lopez Deber Maria Pilar 524
Lopez S. 542
Lorenzón E. N. 178
Lorkowski Stefan 118
Lortat-Jacob Hugues 92
Lovas Sándor 56
Lovecká Patra 152
Löwik Dennis W. P. M. 618
Lozano Leyder 650
Lozzi Luisa 78, 94
Lubecka Emilia A. 564
Lubell William D. 18, 140, 366
Lubin-Germain N. 468
Luchinat Claudio 134
Lukajtis Rafal 398
Lukanowska Monika 116
Lygina Antonina 30
Lyubchenko Yuri L. 56

M

M'Kadmi Céline 112
Maaroufi Halim 188

Mabrouk K. 456
 Macek Tomáš 148, 152
 Machini M. T. 180
 Machtey Victoria 24
 Maciel Ceres 472
 Mäcke Helmut 300
 Macková Martina 148, 152
 Macůrková Anna 152
 Madder Annemieke 202, 286
 Madej Józef 260, 272
 Maeng Juwan 606
 Magafa Vassiliki 146, 230, 238, 254, 544
 Maggi Carlo A. 670
 Magyar Anna 246, 280
 Mahmoud N. 454, 468
 Maina Theodosia 120, 484, 486, 492, 504
 Maity Jyotirmoy 458
 Majer Zsuzsa 280, 588, 674, 676, 678, 682
 Malakoutikhah Morteza 84
 Malavolta L. 222
 Malešević Miroslav 74
 Malisiova Eleni 516
 Małuch Izabela 268, 584
 Mancin Fabrizio 216
 Manea Marilena 96, 502, 532
 Mann David 210
 Mantzourani Efthimia 350
 Marasco D. 294, 552
 Marc Ivan 50
 Marceau François 312
 Marchetto Reinaldo 270, 276
 Marcinkiewicz Cezary 304
 Marega R. 382
 Marelli M. M. 428
 Marianou Asimina 154
 Marie Jacky 112
 Marinelli L. 438
 Marinkova D. 454
 Marotte Amélie 534
 Marrakchi N. 456
 Marsault Eric 296, 386
 Marsh Donald J. 108
 Marsouvanidis Pantelis 484, 492, 504
 Martin Charlotte 628
 Martin Lisandra L. 220
 Martinez Jean 112, 142, 240, 278, 290,
 324, 348, 484, 628
 Martins José 202
 Martins O. P. 222
 Marverti Gaetano 466
 Mary Sophie 112
 Maryasov Alexander G. 150
 Mascarin A. 346
 Mason Jody M. 86
 Maszota Martyna 528
 Mata Alvaro 136
 Mathieu Cyrille 426
 Matsoukas John 26, 134, 342, 358, 376, 400,
 428, 436, 444, 526, 656, 668
 Matsoukas Minos-Timotheos 538
 Matsuda Ryoichi 378
 Matsui Takuya 434
 Matsuo Yuko 310
 Mattei B. 162
 Mauchauffée Elodie 348
 Maupetit J. 60
 Mavridaki Kyriaki 436
 Mavromoustakos Thomas M. 274, 318, 342,
 358, 376
 Meini Stefania 670
 Melagraki Georgia 376
 Meldal Morten 10
 Melnyk Oleg 20, 212, 218, 576, 640, 642
 Menakuru Mahendra 144, 412, 570, 592,
 600, 604
 Meneghetti F. 396
 Merlino Francesco 670
 Mertziani Vassiliki 146, 254
 Meyenberg Karsten 30
 Mező Gábor 96, 502, 508, 510, 532,
 588, 682
 Mhidia R. 20
 Michalatou Michaila 400
 Michalis Lambros K. 446
 Miclet Emeric 422, 608
 Mikros E. 664
 Milanov Peter 232

Milech Nadia 550
Milkova Tsenka 580
Miller Chris 40
Miloshev George 368
Milov Alexander D. 150
Minamizawa Motoko 322
Mindt T. L. 346
Miranda Antonio 162, 480
Miyazaki Anna 666
Mizeria Aneta 258
Mizumoto Takahiro 434
Mizushina Yoshiyuki 666
Mlaki Dorin 524
Moisa Alexandr 90
Momic Tatjana 304
Mona Christine 292, 386
Monasson O. 186, 596
Monincová Lenka 174
Monteagudo Edith 108
Monteiro M. J. 114
Mooney Catherine 62
Morales-Sanfrutos Julia 554
Moran Niamh 62, 450
Morellato Nicolò 514
Morelli Giancarlo 496
Moretto Alessandro 216
Morii Takashi 286
Morris C. 420
Morse D. 126
Mosbah A. 456
Moscona Anne 426
Moulin Aline 112
Moussis Vassilios 446, 464, 578, 634
Moutevelis-Minakakis Panagiota 332
Moutsopoulos H. M. 672
Mouzaki Athanasia 436
Mrestani-Klaus Carmen 530
Mucha Piotr 344, 390
Muguruma Kyouhei 34
Muhs Andreas 524
Mukai Hidehito 310
Munekata Eisuke 310
Muronetz Vladimir 402
Murray T. F. 392

Murza Alexandre 296
Musolino M. 396
Mussbach Franziska 118
Myasoedov Nikolay F. 54

N

Nagulapalli Malini 134
Nagy György 280
Naka Katerina K. 446
Nakaie Clovis R. 222, 480, 556
Nakano Hiroko 310
Naletova Irina 402
Nan Yong Hae 156
Nardi Daniela T. 556
Narumi Tetsuo 98
Nascimento Nanci 556
Nassi Alberto 512
Naydenova E. 290, 324, 474
Nazimov Igor 54, 652
Neubauerová T. 148
Neugebauer Witold 228, 268, 302, 440
Neundorf Ines 494
Neuteboom Saskia 34
Neveu Cindy 534
Nguyen Thi Thuy An 188
Niarchos Athanassios 146
Nielsen Kristian Fog 204, 208
Nielsen Peter E. 372, 680
Nielsen Thomas 10
Nikolis Christos 358
Niranjan Dhevahi 500
Nishiuchi Yuji 568
Nocheva H. 290, 356
Nock Berthold A. 120, 484, 486, 492, 504
Nogueira L. G. 178
Nollmann Friederike I. 284
Nomizu Motoyoshi 248
Nomura Wataru 98
Novellino Ettore 670
Nowicki Łukasz 164
Ntountaniotis Dimitrios 318, 358
Nuti F. 186, 432, 626
Nuzillard Jean-Marc 50

O

O'Brien Kevin 62
O'Mullane Anthony P. 220
O'Toole Ronan 40
Oancea Simona 176
Offer J. 420
Ogunkoya Ayodele O. 132
Okarvi Subhani M. 124, 506
Olejnik Jadwiga 52, 594
Ollivier Nathalie 20, 212
Olsen Katrine M. 372
Olszanecki Rafał 260, 262, 272
Onaiyekan Michael A. 144, 412, 570, 592,
600, 604
Onishi Mare 414
Onoue Satomi 434
Oon Jessica 122
Orbán Erika 96, 502, 508, 532, 674
Orioni B. 138
Orlandin Andrea 216
Osborne Alexandre 386
Otsuki Yusuke 80
Otto Sijbren 84
Owen Robin L. 560

P

Pacini G. 626
Padilla A. 60
Pagès Michel 278
Pairas George 238, 658
Pajpanova Tamara 356, 368, 540
Palladino Michael 34
Palleschi A. 138, 166, 170, 542
Panagiaris Georgios 660
Pandey S. 16, 432
Panou-Pomonis Eugenia 110, 154, 448,
464, 660
Papadimitriou Evangelia 544
Papadopoulos Christos 634
Papadopoulos Giorgos N. 340
Papadopoulos Manthos G. 318
Papadopoulos Minas 242

Papamichael Nikolaos D. 446
Papas Serafim 578, 634
Papini Anna Maria 16, 186, 410, 432, 548,
596, 620, 626, 630, 644
Papini Emanuele 192
Papp Gyula 682
Pappalardo Giuseppe 256, 402
Pappas Charalambos 578
Paravatou-Petsotas Maria 242, 326
Parent Alexandre 296
Parigi Giacomo 134
Park Y. 166
Pascarella Simona 630
Paschalidou Katerina 380
Pastore R. 294
Pastrian María 452
Pattabiraman Vijaya R. 132
Pavesi Giorgia 466
Pavlov Nikola 290, 324
Pawlowski Nikolaus 76
Payrot Nadine 278
Peggion Cristina 176, 192, 520, 562
Peier Andrea M. 108
Pelà Michela 466
Pelecanou Maria 242, 664
Pencheva Nevena 232
Penfold J. 138
Pénzes Csanád 510
Perczel András 588
Peremans Kathelijne 104
Perera Conrad 522
Perez K. R. 162
Peri Claudio 654
Perlikowska R. 316
Pernodet Jean-Luc 72, 182
Peroni E. 16
Pessi Antonello 108, 426
Pethő Lilla 96
Petit-Demouliere B. 442
Petkova D. 424
Petratos Kyriacos 560
Petre Alina 12
Peycheva Ekaterina 368
Peyralans Jerome J.-P. 84

Pfeifer Andrea 524
Piantavigna Stefania 220
Piekielna J. 316
Pierson Nick 12
Pieszko Małgorzata 390
Pifano Marina 452
Pikula Michal 362
Pini Alessandro 78, 94
Pipkorn Ruediger 28, 406
Pirmettis Ioannis 242
Plotas Panagiotis 26, 436, 526
Pocai Alessandro 108
Poli Guido 426
Polis Ingeborg 104
Politi Aggeliki 318
Politou Anastasia S. 298
Pons Miquel 270
Ponterini Glauco 466
Popow Jadwiga 282
Porotto Matteo 426
Porreca Frank 422
Postma T. M. 408
Potamitis Constantinos 254, 526, 544
Potenza M. 644
Potts Barbara 34
Poulas Konstantinos 146
Prahl Adam 244, 268, 584
Prell Erik 74
Proulx Caroline 18, 366
Prozorovsky Vladimir 90
Przybylski Michael 12
Psillou Aggeliki 298
Puget K. 642
Pulido Daniel 136
Pulka Karolina 370
Pyndyk Nadezhda 90
Pytkowicz Julien 598

Q

Qian Ying 108
Qiu Yibo 130
Qu Xiaohu 220
Quattrini Francesca 50, 662
Quintieri Luigi 512

R

Rademann Jörg 614
Radulska Adrianna 228
Radzey Hanna 638
Raibaut L. 20, 218
Rangelov M. 424
Rao Tara 86
Rapp Wolfgang 28
Ravenni Niccolò 94
Rawer Stephan 28, 406
Raykova R. 454, 468
Real-Fernandez F. 432
Rebuffat Sylvie 72, 182
Recca T. 392
Refosco Fiorenzo 514
Reichart Florian 494
Reille Marie 306
Reimer Daniela 284
Reimer Ulf 76
Reis Pedro 524
Reissmann Siegmund 118
Rekowski Piotr 344, 388, 390
Relich Inga 234
Remuzgo C. 180
Renault Jean-Hugues 50, 662
René Adeline 240
Rentier C. 186, 626
Resvani Amalia 342, 358, 376, 400, 526
Reubi Jean-Claude 120, 486
Revelou Panagiota 332
Ribić R. 320
Richardt Annkathrin 530
Rijkers Dirk T. S. 572, 616
Ripoll Giselle 452
Riske K. A. 162
Rizzarelli Enrico 402
Rizzolo F. 410, 596
Rodriguez Hortensia 602
Rodriguez-Cabello José Carlos 66
Rodziewicz-Motowidło Sylwia 528
Röhrich Christian R. 204, 208
Rolka Krzysztof 258, 282, 362, 398
Romanelli A. 394

Ronga L. 642
Rosa Jose C. 556
Rosi L. 644
Rossi Giada 432, 620
Rössle Manfred 160
Rothemund Sven 28
Rousouli Kleopatra 446
Roussa Vassiliki D. 446
Routhier Sophie 268, 440
Rovero Paolo 16, 186, 410, 432, 548,
596, 620, 626, 630
Roversi D. 166
Roy Caroline 312
Royo Miriam 136
Ruczyński Jarosław 388
Rudowska Magdalena 82
Rustanti L. 114
Ruzza Paolo 512, 514

S

Saavedra Scott S. 106
Sabatino Giuseppina 432, 620, 630, 644
Sacchetti A. 392, 396
Sagan S. 172
Sakarellos-Daitsiotis Maria 110, 154, 448,
464, 660
Sakka Marianna 154
Salvadori S. 392
Salvarese Nicola 514
Samanta Krishnananda 278
Samsel Monika 164, 384
Šanda M. 148
Santicioli Paolo 670
Santos Laura N. 270
Sapundzhi Fatima 232
Sarigiannis Yiannis 264, 266
Sármay Gabriella 280
Sarojini Vijayalekshmi 40, 522
Sarret Philippe 240, 296
Sasaki Yusuke 322
Sasidhar Y. U. 558
Saviano M. 394
Sayyad Nisar 578

Scali Silvia 78
Schaaper Wim 46
Schaefer Buerk 118
Schally Andrew 444
Schildknecht Stefan 12
Schiller Peter W. 348, 422
Schlage Pascal 96
Schmitt M. 442
Schnatbaum Karsten 76
Schneider E. 442
Schneider S. 442
Schnöller Donát 510
Schottelius M. 438
Schreier Verena Natalie 96
Schteingart Claudio D. 462
Schulcz Ákos 96, 502, 532
Schumacher U. 438
Schutkowski Mike 76
Scian M. 70
Scobie Marie 550
Scognamiglio P. L. 294, 552
Scola Joseph 622
Scrima Mario 548
Sebastiani F. 138
Seelbach Ryan 136
Seelig J. 162
Ségalas-Milazzo Isabelle 534
Šegota S. 320
Seki Tetsuo 310
Selmi C. 626
Senesi R. 138
Sereti Evaggelia 634
Serpa C. 542
Servis Catherine 650
Seznec Janina 76
Shechter David 76
Shen Y. 60
Shi Lei 128
Shi Weiguo 14
Shields Denis C. 62, 450
Shin Song Yub 156
Shiozuka Masataka 378
Shishkina Anna V. 354

Siafaka Athanasia 376
Sieradzan Adam 362
Sikorska Emilia 564
Sikorski Krzysztof 388
Silló Pálma 236
Silva Adriana Farias 472, 480
Silvani A. 392, 396
Simon Julien 598
Simonin F. 442
Simonnet G. 442
Sinopoli Alessandro 256
Sipőcz Tamás 674
Sipos Éva 502, 532
Sklyarov Leonid 652
Skopek P. 374
Skwarczynski M. 114
Slaninová Jiřina 174, 190, 230, 238, 342, 376
Śleszyńska Małgorzata 244
Smeenk L. E. J. 364
Smietana M. 142
Sobolewski Dariusz 244, 564
Spanou Danai 338
Spengler Jan 612, 646
Spiccia Leone 220
Spodzieja Marta 528
Spyridaki Aikaterini 254, 342, 376
Spyroulias Georgios A. 58
Stalmans Sofie 104
Stamatakis K. 664
Stankova Ivanka G. 488, 490
Starkov Vladislav G. 308
Stathopoulos Panagiotis 298, 516, 578
Stavropoulos George 264, 266
Stavropoulos I. 62, 450
Staykova Svetlana 474
Stefanowicz Piotr 82, 198
Stein Frank 638
Stella L. 138, 166, 170, 542
Steunenberg P. 590
Štimac A. 320
St-Louis Étienne 292
Stoineva I. 424
Stone Shane R. 46, 550

Strömberg Roger 458, 590
Stuart Marc C. A. 84
Suć Josipa 314
Sumbatyan Natalia V. 354
Sumikura Makiko 34
Sun Zhan-Yi 128
Suski Maciej 260, 272
Suyama Tai-jiro 666
Svetličić V. 320
Szabados Hajnalka 236
Szabó Ildikó 502, 508, 532, 588
Szabó Ilona 682
Szabó Nóra 510
Szarka Eszter 280
Szelağ Małgorzata 388
Szewczuk Zbigniew 82, 198
Szilváygi Gábor 674
Szoboszlai Norbert 674

T

Taddia Laura 466
Tagad Harichandra D. 352
Taguchi Akihiro 378
Taguchi Hiroaki 196
Takahashi Daisuke 48
Takami Daisuke 666
Takanuma Daiki 478
Tam James P. 130
Tamamura Hirokazu 98
Tamvakopoulos Constantin 428, 444
Tan Yew-Foon 46, 550
Tanaka Hironari 34
Tanaka Masaki 636
Tanaka Mika 322
Tanaka Tomohiro 98
Tantos Á. 100
Tapeinou A. 668
Tate Edward W. 210
Tatsi Aikaterini 120, 486, 504
Tavano Regina 192
Tchaoushev S. 454
Tchorbanov B. 424
Tedesco A. C. 222

Vaudry Hubert 534
Venzani Mariano 66, 334, 542, 562
Ventura Salvador 214
Verbeken Mathieu 104
Veselkina Olga 476
Vezenkov Lyubomir 474
Vicenzi Elisa 426
Vicogne Jérôme 212
Vidal Michel 306
Vieira Renata F. F. 556
Viguier B. 624
Vijay Vaishnavi 62
Vilcinskas Andreas 204, 208
Virág László 682
Vitagliano L. 552
Vlad Camelia 12
Vlahakos Demetrios 342, 358, 376, 400
Vlahoviček-Kahlina Kristina 314
Voburka Zdeněk 148, 190
Voglmayr Hermann 204, 208
Volpina O. M. 430
Vomstein S. 346
Voronina Olga L. 88
Vranešić B. 320
Vulcano R. 382

W

Waddell Alex S. 412
Walewska Aleksandra 584
Walrant A. 172
Walter M. 346
Wang Chao 14
Wang Dexin 582
Wang Kun 14
Wang Lei 32
Wang Lei 306
Waser Beatrice 120, 486
Watanabe Yoshihisa 636
Watt Paul 550
Weise Christoph 308
Weiss Aryeh 24

Wennemers Helma 224, 300, 328
Wenschuh Holger 76
Wesoły Joanna 388
Wesselinova Diana 474
Wester H.-J. 438
White P. 420
Wilczek Carola 76
Wildemann Dirk 76
Wilhelm Patrick 300
Winslow Scott 550
Wiśniewski Kazimierz 462
Witczak A. 250
Wojciechowska Monika 388
Wojewska Dominika 82
Wong Clarence T. T. 130
Worth N. F. 68
Wright Karen 334, 622
Writer Diana 558
Wu Boqian 10
Wyczałkowska Agnieszka 518
Wynendaele Evelien 104
Wysocka Magdalena 282, 362, 398

X

Xu Zhangshuang 32

Y

Yakimova B. 424
Yakushiji Fumika 34, 378
Yamada Shizuo 434
Yamazaki Yuri 34, 378
Yang Xiaoxiao 582
Yasui Hiroyuki 34
Ye Tao 32
Yokoi Toshio 666
Yoon Heungsik 606
Yoshida Hiromi 666
Yotova L. 454, 468
Yousif Ali Munaim 670
Yuan Jing 134
Yuan Xue-Wen 440

Z

Zabala Juliana Gonzalez 110
Zabrocki Janusz 52, 252, 518, 594
Zagoriti Zoi 146
Zaikin Vladimir 652
Zalila Habib 650
Zaman M. 114
Zamudio Vázquez Rubí 460
Zamyatnin Alexander A. 88, 206
Žďárek Jan 190
Zervou Maria 380, 526, 544
Zerweck Johannes 76
Zevgiti Stella 110, 660
Zhang Han 106
Zhang Yuliang 56
Zhao Chuan 220
Zhmak Maxim N. 308
Zhou Mingkui 448
Zhou Qiuqin 284
Ziganshin R. H. 64
Ziganshin Rustam 652
Zikos Christos 242, 326
Zimecki Michał 52, 252, 518, 594
Ziora Z. M. 114
Zirah Séverine 72, 182
Zolotarev Yurii A. 54, 90
Zorad Štefan 260, 272
Zoumpoulakis Panagiotis 254, 526, 544
Zriba Rriadh 228
Zytko Karolina 108



ISBN 978-960-466-121-3